

# Strategies Toward Nucleophilic Additions to $\eta^2$ -Bound Arenes

Jacob Anthony Smith

Brighton, Michigan

B.S.; Chemistry, The University of Chicago 2014

A Dissertation presented to the Graduate Faculty of the University of  
Virginia in Candidacy for the Degree of Doctor of Philosophy

Department of Chemistry

University of Virginia

April 2020

## Dissertation Abstract

Chapter 1 details the concepts of aromaticity and the importance of aromatic molecules in a variety of industrial and medicinal contexts. Speculation is included with regard to the potential value of aromatic molecules as a largely untapped source in drug development given the difficulties in realizing dearomatized manifolds. Common dearomatization methodologies are examined and the development of dihapto-coordinate enabled dearomatization is discussed. Existing limitations of dearomatization methodologies promoted by electron-rich metals are presented, particularly within the context of aromatics with electron withdrawing groups (EWGs) and in the dearomatization of benzene itself.

Chapter 2 investigates the protonation of benzene itself once bound to the tungsten scaffold. An estimate of the pKa of the resulting tungsten benzenium is provided and the selectivity of the initial protonation is examined. The selective formation of 1,3-cyclohexadiene and cyclohexene is presented and mechanistic considerations are presented. Importantly, the success and stability of the dearomatized benzene enables comparison to other heavy metal analogs with data consistent with the postulation that the tungsten fragment is the most activating of developed dearomatization scaffolds.

Chapter 3 details how the dearomatization of benzene can be used to generate regio- and stereo-specific isotopologues of cyclohexene. This is an extension of the mechanistic work presented in Chapter 2 and details the synthesis of novel cyclohexene isotopologues (including those of substituted cyclohexenes). Support for the resulting stereochemical assignments is supported through NMR and molecular rotational resonance (MRR) spectroscopic techniques along with neutron diffraction.

Chapter 4 continues to investigate the nuances of the complex  $WTp(NO)(PMe_3)(\eta^2\text{-cyclohexene})$ . Topics include the ability to distinguish isomerization mechanisms operative for



isotopologues, inferring mechanisms by products determined by molecular rotational resonance spectroscopy (MRR) and attempts derivatize the dihapto-bound alkene bond. Attempts to access agostic complexes and the potential to recycle the tungsten dearomatization fragment is also presented.

Chapter 5 reports on the ability of molybdenum to bind the first substituted benzene ( $\alpha,\alpha,\alpha$ -trifluorotoluene). Much of this work was initially pioneered by Dr. Jeffery Myers. The resulting molybdenum-trifluorotoluene complex can be synthesized via direct reduction and optimized conditions are presented. The substituted benzene is exceptionally labile and readily undergoes substitution reactions with a variety of unsaturated ligands. The kinetics of this process are investigated and a proof of concept is detailed to show the substitution route to a dihapto-coordinate molybdenum benzene complex. This is the first isolatable monomeric molybdenum benzene complex of which we are aware.

Chapter 6 looks to examine the compatibility with molybdenum and tungsten scaffolds together with electron deficient arenes. A survey of aromatics with  $\pi$ -bond containing EWGs supports concerns that dihapto coordination of the EWG pre-empts coordination of the aromatic ring. While  $-\text{CF}_3$  groups appear to be compatible with both systems, aryl C-F bonds are only tolerated by the molybdenum scaffold. Energies and isomerization dynamics of the resulting dearomatized  $\pi$ -ligands are investigated.

Chapter 7 looks to generate exceptionally electron-deficient  $\pi$ -ligands from the double protonation of anisole once bound to the potent tungsten  $\pi$ -base. The resulting dicationic fragment is moderately stable in solution and reacts with a variety of weak aromatic nucleophiles. The resulting substituted oxonium containing ligands can be treated with a range of reagents and provide a synthetic route to a series of novel 1,4-cyclohexene complexes.

Chapter 8 extends the methodology of double protonation to benzene which can be enabled by complexation to either the tungsten or molybdenum dearomatization agents. The resulting electrophilic organometallic scaffolds can then be treated with weak aromatic nucleophiles. An examination in the selectivity of the addition process is analyzed, as well as the ability for the metal to direct both of the initial protonations.

Chapter 9 details the development of the tri-n-butyl-phosphine ligand (P(n-Bu)<sub>3</sub>) as a cost efficient alternative to the PMe<sub>3</sub> ligand initially developed on the tungsten scaffold. We report on the ability of the {WTPNO P(n-Bu)<sub>3</sub>} synthon to form dihapto-coordinate complexes with a variety of unsaturated ligands. Notably, for molecules highly stabilized by aromaticity (i.e benzene and benzene derivatives), a significant amount of C-H activated product is shown to be in equilibrium with the  $\eta^2$ -isomer. Extensive computational work is presented to evaluate the mechanisms associated with this novel equilibrium, investigating the intermediates between the oxidative addition and reductively eliminated products. The computational work was done in collaboration with Anna Schouten and Professor Daniel Ess from Brigham Young University.

## Copyright Information

**Chapter 3** is a modified version of a published work that has been approved for publication by *Nature* and its reprinting is in accordance with Springer Nature Author Reuse Guidelines.

**Smith, Jacob A.**; Wilson, Katy B.; Sonstrom, Reilly E.; Kelleher, Patrick; Welch, Kevin, D.; Pert, Emmitt K.; Westendorff, Karl S.; Wang, Xiaoping.; Dickie, Diane A.; Pate, Brooks H.; Harman, W. *Nature*

**Chapter 6** is a draft of a publication to be submitted to *Organometallics*.

**Smith, Jacob A.**; Simpson, Spenser R.; Westendorff, Karl S.; Weatherford-Pratt, Justin.; Myers Jeffrey A.; Wilde, Justin H.; Dickie, Diane A.; Harman, W. D. “Dearomatization of Electron Deficient Arenes with Group 6 Dearomatization Agents”

**Chapter 9** is a draft of a publication to be submitted to the *Journal of the American Chemical Society*.

**Smith, Jacob A.**; Schouten, Anna; Wilde, Justin H.; Westendorff, Karl S.; Dickie, Diane A.; Ess, Daniel H.; Harman, W. D. “The  $\eta^2$ -Benzene/Phenyl-Hydride Equilibrium on an Early Transition Metal”

## Acknowledgements

There are innumerable people who have either taught me something interesting, put me in a position to succeed or who have provided encouragement. I will have to omit most of you because I am quite tired of writing and will have to focus on those who have directly impacted my chemical education or been an integral part of my graduate school experience.

I read an article once that correlated the probability of obtaining a degree in a STEM field with a strong secondary school teacher. My high school chemistry teacher Rick DesJardins is living proof of this, and multiple tenure-holding PIs at R1 institutes no doubt owe some debt to him for enabling generations of productive graduate students. He made intro-level chemistry intelligible (not always a given) and probably maintained the most college-like class I had in my high school career. Most impressively, many of the things he taught have actually withstood my graduate education. I most appreciate as well him opting to go along with my classroom antics and not sending me to the principal's office.

When I had an inkling I may have been interested in chemistry I was fortunate to work with Dr. (now Professor) Heidi Phillips (now Hendrickson) in the group of Professor Barry Dunitz at the University of Michigan. They were a computational lab, and while I have since lost any kind of true intuition for computational work, their instruction on the physical chemistry side of things probably helped me more than I know. Heidi was exceptionally generous, offering to mentor a very low value 19 year old for several months (forsaking a good amount of research time I am sure). She was a great teacher and proof that Hillsdale College (her alma mater) in Michigan has probably the most underrated chemical education program in the country.

In college I had exposure to more than a dozen world-class chemists at UChicago. They are not all however worldclass educators. I am very thankful then that two of the rare examples of

being able to be a good researcher and a good chemical educator (both pale in comparison to Dean, more later) were both organometallic chemists. That seems to be a running theme now that I think about it. I had actually just switched back from Tibetan (don't ask) to the chemistry major after a rough stint in organic chemistry when I took Rich Jordan's organometallic class. For the first time in a while, things had started to piece together. The "memorization" I had relied on to barely squeak by in undergraduate organic was replaced with the tendrils of chemical intuition and reasoning. I'm sure he has no idea who I am because I had adamantly/stupidly resolved to never go to a professor's office hours. I did however, surprisingly attend all of his classes. In grad school, his lab website has been a very useful resource for scorpionate chemistry, NMR kinetics and a myriad of other information. There are several personal connections to several successful PhDs from his lab that illustrate his effectiveness as a teacher and mentor.

The next class that I had true fun in was the advanced inorganic lab class by Michael Hopkins. Professor Hopkins, apart from being an effective teacher, also somehow graciously wrote me a recommendation that I am sure I would not have gotten into UVA without. I also now have a talking point whenever I meet a faculty member from Pittsburgh (has been a useful talking point more than one would expect). In the lab class he taught, he and his graduate students had nicknamed me and my lab partner "Team Disaster" due to our creativity in causing problems for our TAs to deal with. The chemical scarring on my hand (from a tungsten complex no less!) is a nice reminder of those times.

Despite the effective teachings of Professors Hopkins and Jordan, I had entirely renounced more schooling. I was ready to make money man and had accepted a chemist position with a US Steel contractor in Detroit (Zug Island)! What they don't tell you is that the bigger paycheck of a B.S. (compared to grad student) comes at the cost of a job that is much, much harder to find roles

to actively think. This may not be the case for all BS-level positions (just in case an aspiring undergrad picks this up and is torn on grad school or working) but man, this one was mind-numbing. That being said, the people I was able to work were 1) great people and 2) introduced me to working with a wide variety of people and personalities across a myriad of ages and backgrounds. My lab supervisor and initial trainer Josh Franklin truly trained my first lab skills in a rigorous way and embodied the true power of multi-tasking. It was incredibly useful being able to do 14 hours of lab work in an 8-10 hours shift. I will say that one area of lab I am often complemented on (not that there are many) is my lab multitasking skills (the secret is to build-up a lot of aerobic endurance with a coffee IV shoved into your arm). But I tell you what, Josh Franklin is probably the best “lab skills” chemist (not researcher, don’t get too worried guys) I have had the pleasure to work with. He would probably laugh in my face if he’s seen how slow I’ve gotten since grad school.

Now for the great chemical educators at UVA. Professor Brent Gunnoe’s inorganic class was amazingly informative and helpful in preparing me for the work I’d pursue in the Harman Lab. I still actively refer back to his notes, he is a very effective communicator and teacher. Professor Michael Hilinski’s organic III course is by far the most comprehensible organic class I’ve taken (not that I claim proficiency). He made a subject that had historically been beyond my reach relatively sensible.

A great “go-to” source of chemical information is Professor Kevin Welch. His weakness is that he has to come into the lab for coffee, that’s when you attack with a question (and Kevin is all too curious to not deign with a response). He has done well in his role as the “Fun Uncle” of the lab and I appreciate his guidance and also for his part in getting Dean excited about mechanistic/deuterium work.

That brings me to Dean Harman. Dean is a great chemical educator, innovative and insightful chemical researcher who does an excellent job in fostering an ideal environment to learn and grow. His patience may in fact be endless (I remember a stern but measured response after I told him of my multigram synthesis of a diazonium salt). Even more important than his effectiveness as a chemistry mentor, Dean is a good man. I am very thankful I found my way into his lab (my initial plan was to suck his funding dry then defect to the Gunnoe Lab). It was a happy accident that I fell in love with his lab's chemistry. This has been echoed over many years, but I probably would not have finished my PhD in another PIs lab. I am grateful to Dean for being an excellent mentor and letting me run relatively wild for my first 2-3 years here. Perhaps more important than the chemical knowledge he was able to convey, he also helped me how to "think like a chemist", which is just another way of saying "Dean taught me how to think". I also thank him for ultimately enabling a degree of freedom and opportunity that few people are fortunate to experience.

The research support staff in the UVA chemistry department is incredible. Dr. Earl Ashcroft, Dr. Jeff Ellena and Dr. Diane Dickie are great, great people who really make UVA a great place to work and conduct research. The stockroom crew (Mike, Debbie, Danny) are another great trio that do a great job in a sometimes very difficult position. Special credit is due to Diane in her initial travels to ORNL. Somehow, that project got the happy ending it deserved (getting a crystal for neutron diffraction was probably the research equivalent of waiting to do a paper the night before it is due and getting an A+). Gratitude is express as well to Dr. Xiaoping Wang for taking a chance on our chemistry and using his "personal" allotment time on the TOPAZ instrument.

Now for what I'll call the "older Harmanites". Ben, Bri, Phil were advanced grad students when I first joined who I appreciate their forwardness, patience and reception to some of my initial

questions about Harman Lab chemistry (and chemistry in general). Special acknowledgment to Phil especially who was my cubby mate and fell most victim to my initial questions (which hopefully became more and more intelligible over time).

Next of course, is Dr. Jeff Myers. Jeff is an excellent researcher and enviably hard-working. I appreciate his time and patience as I struggled to get a handle on molybdenum chemistry. He was an effective trainer who taught me more in my first month of grad school than I had learned in probably four years of undergraduate coursework. His work ethic, leadership and selflessness really set a shining example of how to be an effective grad student. As I've gotten older I also have grown to appreciate what I would have originally deemed his "hang-ups" about the lab. I am looking forward to when our paths cross again.

Next on the list is Dr. Katy Wilson. Katy is a good friend, astute researcher and was a great "cubbie-mate" over the past two years. She somehow found time to nearly always deal with my often rabbit-hole leading chemical questions. I can't tell you how her curiosity has made me a better chemical researcher and student. She made it ok again to not know things which is a severely underestimated dynamic that should be in every lab. I also greatly, greatly appreciate all of her work with generating deuterated trifluoromethyl-cyclohexenes. She was a great guide as I started to explore tungsten-chemistry. Without her the isotopologue paper would be in a much poorer spot than it is.

Dr. Steven Dakermanji was another senior lab member who, amazingly enough, broke ground in catalysis in our lab. Steven is a selfless worker and I am glad he let me to infringe a bit on his catalysis chemistry (still a pipe dream for me). You could always count on running into Steven on the weekend in the lab.. I am sorry for the hard time I gave you in New Orleans but really, but really, there was nothing to worry about! I always enjoyed lording being older (age)



over Steven.

I was unable to work with Dr. Mahendra Chordia for very long but I am grateful for his guidance and extensive knowledge, not just about chemistry but about science in general. Mahendra really helped start to think like an organic chemist for the couple months I was able to work with him, and brought in a fresh wave of techniques and ideas into the lab. I also owe him for really pushing me to think about the “next steps” of my career.

Now, onto my “peer” (more superior) of (recently) Dr. Justin Wilde. Justin was a great colleague to have and really pushed me to be a better chemist/thinker. Apart from being a great resource for organic chemistry, Justin has a keen eye for detail and is also able to essentially quadruple the scale of any reaction his touches. He was amazingly resilient with developing some pretty spectacular pyridine chemistry and managed to bring together a lot of excellent research that had been tangentially developed over the years. I lament not being able to work directly with Justin on a more constant basis, I feel that his idea for a deuterated analog of propylhexadrine would have been a great project for us to have pursued.

Now for the “young un’s” (more or less). Spenser is a very determined chemist who, despite his organic-leaning tendencies, found some really really cool organometallic chemistry with his PhCN and PhSO<sub>2</sub>R complexes with tungsten. I think he also has a track record for uncovering some of the most unlikely/unlucky findings with his complexes (C-H activation of a methyl group, elimination of his EWG, a metal-arenium that doesn’t immediately isomerize, 5 (!) tungsten-arene isomers of PhCN). His burgeoning leadership in the lab is definitely appreciated as well as his expertise on the “new” chromatography instrumentation. I think he will fit very well in the new organic-focused paradigm in the lab and appreciate his help on the EWG paper, without which we would not have shown the ability to “do anything” with those complexes.

I was very, very fortunate to have been able to have “trained” Justin Weatherford-Pratt. I’m not sure he really needed my “training” but appreciate him listening to my over-inflated spiels in any case. Justin has really pushed the tungsten-anisole chemistry in directions I never would have even thought to have went and am very excited to see what he is able to develop. He also does a great job at pushing against traditional “wisdom”. I too wish I had more time to develop some of the anisole chemistry with him. His chemistry knowledge has probably surpassed mine months ago and he has enough of a physical chemistry expertise that he actually knows what is going on.

Jonathan Dabbs has been another great colleague to work with. He is taking on the formidable task of continuing the pyridine-dearomatization and I am sure will rise up to it spectacularly. Jon has the uncanny ability to talk and present like a well-polished 5<sup>th</sup> year graduate student, a skill I am still working on developing. He has an intense curiosity and motivation that will serve him well. I appreciate him entertaining my thoughts on pyridines, even if the validness of them wasn’t always there.

Mary Shindler was my newest protégé and again, I wish I was able to work longer with her. Mary’s calm demeanor masks an uncanny memory and great attention to detail. In the couple months of our working she was able to uncover some great, great mysteries with more tungsten-benzene chemistry and she is another one I am happy to hand off one of “my” projects to. It will be very exciting to see what she is able to do. I also appreciate her guidance about Manassas.

Megan Woodland is another new graduate student that I lament having fairly limited time to spend with. We were able to bond quite nicely (too short-lived) over being fellow citizens of Bachelor Nation. She too seems a promising researcher to add to the work dearomatizing pyridines.

Eric Hunt was brave enough to jump ship to a synthetic lab and has a firm understanding of

fundamental organic concepts. It will be great to see the extensions to the work that Katy was able to lay the foundation with.

Now for the undergraduates. Karl Westendorff is a bright, aspiring chemist who someone has managed to do research full time in two different laboratories (while taking a rigorous ChemE schedule). Karl's innate curiosity and academic rigor have already won him a Goldwater Scholarship even in spite of his Marxist-leanings (talk about irony!). He really brought a much needed level of rigor and detail to the burgeoning computational work in our lab and, while I'm sure that's where his eventual studies will take him, he is a strong synthetic chemist in his own right. It will be very exciting to keep track of his whereabouts.

Another talented undergrad that I was able to work alongside was Alex Heyer. Dean is particularly devious, as he is able to recruit the highest performing undergraduate students (who eventually eclipse their graduate counterparts at the end) and put them to good use. Alex is a living embodiment of that and was able to take a struggling system and really do some great, structural/pure inorganic based work in conjunction with the Machan Lab. He has been a great resource in terms of entertaining unconventional questions (a common theme for most Harmanites).

Other undergraduates I was lucky enough to work alongside were Hannah Nedzbala, Emmit Pert, Andrew Chung and Thomas Miller. Again, all of these kind folks display the exact qualities you would want in a scientist and have entertained my questions (however poorly thought out) and one time or another.

I would like to thank the more interpersonal connections as well in the form of Ann, Joe and Jackie (who will probably never read this). Their antics and experience of being "real adults" (i.e. mid 20-somethings not in grad school) was a great dynamic to be apart of and I appreciate

their friendships.

I would be nowhere near the opportunities I have available without the support of my family. Mom, Dad, Nick and Olivia I cannot thank you enough for providing guidance, support, opportunity and for entertaining my scientific curiosities at a young age. My family was a source of love and support that has really given me a myriad of opportunities that others simply don't have access to. They really embodied in me that if you want to raise your status or give yourself opportunity, essentially the only way forward is through education and hard-work.

I would also like to thank my (new) in-laws. Jenny, Joey, Andy, Sophia, Gabriel and "V" I could not ask for a better family to join. Trips to NOVA or Lexington were welcome breaks and I am very excited to be closer geographically to the majority of you.

Finally, to Bella. I am absolutely sure I would not be the person who I am or have the amazing opportunities I have somehow fallen into without you, and I am so happy that you've been able to be with me nearly every step of the way. Your love, support, humor and kindness have helped me grow as a person and I am so happy to be able to continue on my life journey with you as my wife. You are amazingly resourceful, a great scientist in your own right and have been my best friend. Bella and I met as we were both TAing the same chemistry class and hit it off within a month. Little could I have suspected that the hilarious, wise-cracking TA in the Wednesday section would become so important to me (and I could not be happier about it). From midnight outings for chicken nuggets to cross-country road trips to Sante Fe (and a weekend trip to Niagara Falls! That was fun one but a tough on) I sincerely value your friendship. I am excited to continue our adventure together. I love you.

## Table of Contents

|                              |              |
|------------------------------|--------------|
| <b>Abstract</b>              | <b>2-4</b>   |
| <b>Copyright Information</b> | <b>5</b>     |
| <b>Acknowledgements</b>      | <b>6-14</b>  |
| <b>Table of Contents</b>     | <b>15</b>    |
| <b>List of Abbreviations</b> | <b>16-17</b> |
| <b>List of Figures</b>       | <b>18-20</b> |
| <b>List of Schemes</b>       | <b>20-24</b> |
| <b>List of Tables</b>        | <b>25</b>    |
| <b>Concluding Remarks</b>    | <b>332</b>   |
| <b>Appendix</b>              | <b>335</b>   |

## List of Abbreviations

- 9-BBN** 9-Borabicyclo(3.3.1)nonane
- API** Active Pharmaceutical Ingredient
- BTX** Benzene, Xylenes, Toluene
- DMAP** 4-Dimethylaminopyridine
- CDA** Current Density Analysis
- COSY** Correlation Spectroscopy
- Cp** Cyclopentadienyl
- CV** Cyclic Voltammetry
- DBU** 1,8-Diazabicyclo[5.4.0]undec-7
- DFT** Density functional theory
- DPhAT** Diphenyl ammonium hydride
- EtCN** Propionitrile
- Et<sub>2</sub>O** Diethyl ether
- EWG** Electron Withdrawing Group
- FTIR** Fourier Transform Infrared
- HOMO** Highest Occupied Molecular Orbital
- HOTf** Trifluoromethanesulfonic Acid
- HMBC** Heteronuclear Multiple-Bond Correlation
- HSQC** Heteronuclear Single Quantum Correlation
- IR** Infrared
- LiAlH<sub>4</sub>** Lithium Aluminum Hydride
- LUMO** Lowest Unoccupied Molecular Orbital

**MeCN** Acetonitrile

**MeIm** N-Methyl-Imidazole

**MMR** Molecular Rotational Resonance

**MTAD** N-methyl-1,2,4-triazine-3,5-dione

**MTDA** Methyl Trimethylsilyl Dimethylketene Acetal

**NaBH<sub>4</sub>** Sodium borohydride

**nBuLi** n-Butyl Lithium

**NMR** Nuclear Magnetic Resonance

**NOESY** Nuclear Overhauser Effect Spectroscopy

**NCIR** Nucleus-Independent Chemical Shift

**SMPO** Styrene Monomer Propylene Oxide

**SOMO** Singly Occupied Molecular Orbital

**TBAF** Tetrabutylammonium Fluoride

**TBAH** Tetrabutylammonium Hydride

**TBAI** Tetrabutylammonium Iodide

**TBSOTf** Tert-Butyldimethylsilyl Trifluoromethanesulfonate

**TEA** Triethylamine

**THF** Tetrahydrofuran

**Trp** Trispyrazoylborate

**UV** Ultraviolet

## List of Figures

|                    |   |           |
|--------------------|---|-----------|
| <b>Figure 1.1.</b> | Electron Delocalization and Resonance Structures of Benzene   | <b>30</b> |
| <b>Figure 1.2.</b> | Example of molecules stabilized by aromatic character   | <b>32</b> |
| <b>Figure 1.3.</b> | Access to a biologically active molecule from the dearomatization of benzene  | <b>34</b> |
| <b>Figure 1.4.</b> | Comparing Aromatic Reactivity Enabled by $\eta^6$ -coordination vs. $\eta^2$ -coordination  | <b>40</b> |
| <b>Figure 1.5.</b> | Depicting $\pi$ -backbonding interactions in the dihapto-coordination of benzene  | <b>41</b> |
| <b>Figure 1.6.</b> | Osmium and ruthenium pentaamine complexes stabilized by $\pi$ -backbonding  | <b>41</b> |
| <b>Figure 1.7.</b> | Matching electrochemical potential across dihapto-based dearomatization agents  | <b>45</b> |
| <b>Figure 1.8.</b> | Synthesis of discrete cyclohexene isotopomers from dearomatization of benzene   | <b>49</b> |
| <b>Figure 2.1</b>  | Distortions of benzene upon complexing to electron-rich dearomatization agents  | <b>56</b> |
| <b>Figure 2.2</b>  | Addition of carbon electrophiles to third row metal-benzene complexes   | <b>57</b> |
| <b>Figure 2.3</b>  | Fluctuational behavior the tungsten-benzene complex   | <b>61</b> |
| <b>Figure 2.4</b>  | Spin saturation exchange of $\text{WTP}(\text{NO})(\text{PMe}_3)(\text{H})(\text{Ph})$ and $\text{WTP}(\text{NO})(\text{PMe}_3)(\eta^2\text{-benzene})$ | <b>63</b> |
| <b>Figure 2.5</b>  | DFT Studies of the dearomatization of benzene and cyclohexadiene isomers  | <b>65</b> |
| <b>Figure 2.6</b>  | Spin saturation exchange of two tungsten-benzenium isomers  | <b>69</b> |
| <b>Figure 2.7</b>  | Mechanism accounting for the isomerization process between two tungsten-benzenium isomers   | <b>70</b> |
| <b>Figure 2.8</b>  | Establishing relative energies of tungsten-benzenium isomers with DFT studies   | <b>71</b> |
| <b>Figure 2.9</b>  | $^1\text{H}$ NMR showing deuterium incorporation into a tungsten-benzenium complex  | <b>72</b> |
| <b>Figure 2.10</b> | $^1\text{H}$ NMR Comparing 1,3- and 1,4-cyclohexadiene complexes of tungsten  | <b>78</b> |
| <b>Figure 3.1</b>  | Methods for deuterium integration into small molecules and a tungsten-dearomatization fragment.   | <b>92</b> |
| <b>Figure 3.2</b>  | Sequential reduction of benzene to cyclohexene.   | <b>94</b> |



|                   |  |            |
|-------------------|--|------------|
| <b>Figure 3.3</b> | Synthesis of isotopologues of cyclohexene.   | <b>97</b>  |
| <b>Figure 3.4</b> | Isotopologues of functionalized cyclohexene complexes.   | <b>103</b> |
| <b>Figure 4.1</b> | Illustrative differences in the electrochemical behavior of tungsten-olefin and tungsten-arene complexes.                                | <b>127</b> |
| <b>Figure 4.2</b> | Conformations of cyclohexene once bound to the tungsten dearomatization fragment.  | <b>129</b> |
| <b>Figure 4.3</b> | Differences in the moment of inertia as a result of different weight distributions during rotation.                                      | <b>131</b> |
| <b>Figure 4.4</b> | Spectroscopic evidence for a ring-flip of the cyclohexene ring on a tungsten complex.  | <b>132</b> |
| <b>Figure 4.5</b> | Theorized hydrogen-bonding interactions between a metal nitrosyl ligand and methanol.  | <b>136</b> |
| <b>Figure 4.6</b> | Proposed complexation of a Lewis acid to the tungsten-cyclohexene complex.   | <b>140</b> |
| <b>Figure 5.1</b> | Fluctional behavior of the molybdenum-PhCF <sub>3</sub> complex.   | <b>169</b> |
| <b>Figure 5.2</b> | Proposed intrafacial ring-walk mechanism of the Mo-PhCF <sub>3</sub> complex.  | <b>170</b> |
| <b>Figure 5.3</b> | Proposed ligand substitution mechanism and accompanying rate expression under pseudo-first order conditions.                             | <b>172</b> |
| <b>Figure 5.4</b> | Pictorial representation of assumptions underlying the connection between substitution rate and bond dissociation energy.                | <b>173</b> |
| <b>Figure 5.5</b> | Development of the molybdenum-benzene- <i>d</i> <sub>6</sub> complex in benzene- <i>d</i> <sub>6</sub> .                                 | <b>175</b> |
| <b>Figure 6.1</b> | SC-XRD determination of a tungsten 1,2-trifluoromethyl-xylenes complex   | <b>195</b> |
| <b>Figure 6.2</b> | SC-XRD determination of molybdenum 1,2- and 1,3-bistrifluoromethyl xylene complexes.   | <b>197</b> |
| <b>Figure 7.1</b> | Comparison of the <sup>1</sup> H NMR spectra of various tungsten-ally complexes.   | <b>232</b> |
| <b>Figure 7.2</b> | Resolution of the chiral-at-metal tungsten center and resulting NMR of the tungsten-allyl complex following the addition of β-estradiol. | <b>236</b> |
| <b>Figure 7.3</b> | Crystal structure of a tungsten-iminium complex.   | <b>241</b> |
| <b>Figure 7.4</b> | Crystal structure of a 4H-anisolum complex.  | <b>242</b> |

|                   |  |            |
|-------------------|--|------------|
| <b>Figure 8.1</b> | Different contributing resonance structures for the resulting structure after the double protonation of the tungsten-benzene complex.                  | <b>280</b> |
| <b>Figure 9.1</b> | Spin saturation exchanges between an $\eta^2$ -benzene complex on tungsten and the C-H activated phenyl hydride isomer.                                | <b>297</b> |
| <b>Figure 9.2</b> | Ground state, intermediate and transition state structure of isomers of the tungsten-benzene complex.  | <b>301</b> |
| <b>Figure 9.3</b> | Molecular orbital interactions between various tungsten-benzene complexes.   | <b>302</b> |
| <b>Figure 9.4</b> | Reaction coordinate diagram for the interfacial and intrafacial ring isomerizations of a tungsten-anisole complex.                                     | <b>308</b> |
| <b>Figure 9.5</b> | SC-XRD structure determination of a tungsten-PhCF <sub>3</sub> complex.  | <b>311</b> |
| <b>Figure 9.6</b> | Van't Hoff Plot of the temperature dependence on the $\eta^2$ -PhCF <sub>3</sub> and phenyl-hydride isomer equilibrium on a tungsten-phosphinecomplex. | <b>312</b> |

#### List of Schemes

|                     |   |           |
|---------------------|---|-----------|
| <b>Scheme 1.1.</b>  | Reactivity of alkene complexes  | <b>31</b> |
| <b>Scheme 1.2.</b>  | Friedel-Crafts Reaction   | <b>32</b> |
| <b>Scheme 1.3.</b>  | Heck Reaction   | <b>33</b> |
| <b>Scheme 1.4.</b>  | The Birch Reduction   | <b>35</b> |
| <b>Scheme 1.5.</b>  | The Asahi Process   | <b>36</b> |
| <b>Scheme 1.6.</b>  | Value-Added Products derived from cyclohexene   | <b>36</b> |
| <b>Scheme 1.7.</b>  | Dearomatization via an arenophile cycloaddition adduct  | <b>37</b> |
| <b>Scheme 1.8.</b>  | Dearomatization products realized via hexahapto metal coordination  | <b>38</b> |
| <b>Scheme 1.9.</b>  | Double nucleophilic addition to a cationic manganese complex  | <b>39</b> |
| <b>Scheme 1.10.</b> | Reduction of an osmium-pentaammine triflate complex to various aromatic complexes.                              | <b>43</b> |
| <b>Scheme 1.11.</b> | The selective deuteration of pentaammine osmium-benzene to pentaamine osmium-cyclohexene- <i>d</i> <sub>4</sub> | <b>44</b> |

|                     |   |            |
|---------------------|---|------------|
| <b>Scheme 1.12.</b> | Synthesis of a novel 1,4-cyclohexadiene product from the tungsten-enabled dearomatization of benzene  | <b>46</b>  |
| <b>Scheme 1.13.</b> | Contrasting the reactivity of {MoTp(NO){DMAP}} and {WTP(NO)(PMe <sub>3</sub> )} with fluorinated arenes   | <b>47</b>  |
| <b>Scheme 1.14.</b> | The double protonation of a tungsten-aniline complex and extensions to the double protonation of anisole and benzene complexes of tungsten                    | <b>48</b>  |
| <b>Scheme 2.1.</b>  | Synthesis of a novel 1,4-cyclohexadiene complex from the tungsten-enabled dearomatization of benzene  | <b>58</b>  |
| <b>Scheme 2.2.</b>  | Ligand substitution of metal-benzene complexes and coordination of other aromatics  | <b>59</b>  |
| <b>Scheme 2.3.</b>  | Proposed selective formation of 1,3-cyclohexadiene from a tungsten-benzenium synthon  | <b>59</b>  |
| <b>Scheme 2.4.</b>  | Proposed decomposition pathway of tungsten-benzene to the complex WTP(NO)(PMe <sub>3</sub> )(C <sub>6</sub> H <sub>9</sub> ) <sup>+</sup> (OTf <sup>-</sup> ) | <b>67</b>  |
| <b>Scheme 2.5.</b>  | Protonation of tungsten-benzene to form two tungsten-benzenium isomers  | <b>68</b>  |
| <b>Scheme 2.6.</b>  | Proposed mechanisms responsible for <i>endo</i> protonation involving a hydroxyimido ligand   | <b>71</b>  |
| <b>Scheme 2.7.</b>  | Addition of acetone's enolate to the tungsten-benzenium complex   | <b>74</b>  |
| <b>Scheme 2.8.</b>  | Proposed mechanism leading to a tungsten $\kappa^1$ -acetonitrilium complex   | <b>75</b>  |
| <b>Scheme 4.1</b>   | Proposed investigation into the behavior of a tungsten-cyclohexene complex.   | <b>126</b> |
| <b>Scheme 4.2</b>   | Synthesis of the tungsten-cyclohexene complex.  | <b>128</b> |
| <b>Scheme 4.3</b>   | Evidence for the interfacial ring-flip of cyclohexene on the tungsten complex.  | <b>130</b> |
| <b>Scheme 4.4</b>   | Potential mechanisms that could result in ring-isomerization and deuterium scrambling.  | <b>137</b> |
| <b>Scheme 4.5</b>   | Theorized tandem addition reaction sequence on the tungsten-cyclohexene complex.  | <b>139</b> |
| <b>Scheme 4.6</b>   | Decomplexation of various cyclohexene ligands via acidolysis.   | <b>140</b> |

|                    |   |            |
|--------------------|---|------------|
| <b>Scheme 4.7</b>  | The O-H activation of methanol promoted by a tungsten complex.  | <b>140</b> |
| <b>Scheme 4.8</b>  | Theoretical C-H activated olefin complexes via Lewis Acid coordination.   | <b>142</b> |
| <b>Scheme 4.9</b>  | Nitrosyl methylation of the tungsten-cyclohexene complex and reactivity with a hydride  | <b>144</b> |
| <b>Scheme 4.10</b> | Methylation of a tungsten complex of 1,4-cyclohexadiene   | <b>146</b> |
| <b>Scheme 4.11</b> | Generation of a tungsten-cyclohexanone complex from tungsten-cyclohexene.   | <b>147</b> |
| <b>Scheme 4.12</b> | The synthesis of cyclohexene oxide and its unintended polymerization  | <b>148</b> |
| <b>Scheme 4.13</b> | Synthesis of 1,2-trans-dibromocyclohexane from the bromination of a tungsten cyclohexene complex.   | <b>149</b> |
| <b>Scheme 4.14</b> | Recycling of the tungsten dearomatization scaffold using DMA as a ligand.   | <b>151</b> |
| <b>Scheme 5.1</b>  | Optimization of a molybdenum dearomatization synthon.   | <b>164</b> |
| <b>Scheme 5.2</b>  | Synthesis of a molybdenum-triflate complex.   | <b>166</b> |
| <b>Scheme 5.3</b>  | Ligand substitution reactions using the molybdenum-PhCF <sub>3</sub> complex.   | <b>174</b> |
| <b>Scheme 6.1</b>  | Incorporation of electron-withdrawing group functionalities in benzenerings.  | <b>189</b> |
| <b>Scheme 6.2</b>  | Dearomatization of electron-deficient benzenes promoted by tungsten.  | <b>192</b> |
| <b>Scheme 6.3</b>  | Synthesis of a tungsten-benzoate complexes.   | <b>193</b> |
| <b>Scheme 6.4</b>  | Dearomatization of substituted trifluorotoluenes with tungsten.   | <b>194</b> |
| <b>Scheme 6.5</b>  | Dearomatization and protonation of 3-trifluoromethyl-N,N-dimethylaniline  | <b>195</b> |
| <b>Scheme 6.6</b>  | Molybdenum-promoted dearomatization of substituted trifluorotoluenes.   | <b>196</b> |
| <b>Scheme 6.7</b>  | Molybdenum-promoted dearomatization of fluorobenzenes.  | <b>198</b> |
| <b>Scheme 6.8</b>  | Divergent isomerization pathways between tungsten and molybdenum aromatic complexes.  | <b>201</b> |
| <b>Scheme 7.1</b>  | Previous work showing the double protonation of an aniline derivative enabled by tungsten and extensions for the double protonation of anisole. | <b>223</b> |
| <b>Scheme 7.2</b>  | Synthesis of oxadecalin structures from tungsten-dearomatization of anisole.  | <b>224</b> |

|                    |   |            |
|--------------------|---|------------|
| <b>Scheme 7.3</b>  | The double protonation of anisole enabled by a tungsten dearomatization agent.  | <b>225</b> |
| <b>Scheme 7.4</b>  | Generation of a $\kappa^1$ -N-acetonitrilum complex on tungsten.  | <b>226</b> |
| <b>Scheme 7.5</b>  | Successful addition of weak aromatic nucleophiles to the tungsten-anisole derived electrophile.                                     | <b>227</b> |
| <b>Scheme 7.6</b>  | Speculated complexes that account for the identity of a second complex that also shows integration of a weak aromatic nucleophile.  | <b>228</b> |
| <b>Scheme 7.7</b>  | Generation of a tungsten-cyclohexadiene complex.  | <b>230</b> |
| <b>Scheme 7.8</b>  | Synthesis of tungsten-allyl complexes.  | <b>231</b> |
| <b>Scheme 7.9</b>  | Proposed mechanism detailing the deprotonation of tungsten-allyl complexes.   | <b>233</b> |
| <b>Scheme 7.10</b> | Nucleophile scope for C-C bond formation with an electron-deficient $\pi$ -ligand derived from tungsten.                            | <b>234</b> |
| <b>Scheme 7.11</b> | Synthesis of various tungsten-allyl complexes.  | <b>238</b> |
| <b>Scheme 7.12</b> | Reactivity of the oxo-carbenium functionality with amines, iodide and cyanide sources.  | <b>240</b> |
| <b>Scheme 7.13</b> | Proposed mechanism for iminium formation by treating the oxo-carbenium complex with an amine.                                       | <b>241</b> |
| <b>Scheme 7.14</b> | The proposed, two electron electrochemical reduction of an oxo-carbenium functionality and reactivity with hydrogen-bond donors.    | <b>242</b> |
| <b>Scheme 7.15</b> | Single and double protonation of a tungsten-6-methoxy-tetralin complex.   | <b>244</b> |
| <b>Scheme 8.1</b>  | Double nucleophilic additions to benzene promoted by arene coordination to electron-deficient metal complexes.                      | <b>277</b> |
| <b>Scheme 8.2</b>  | The double protonation of benzene with $\pi$ -donor groups and extending this methodology to the double protonation of benzene.     | <b>278</b> |
| <b>Scheme 8.3</b>  | The successful double protonation of benzene enabled by a tungsten-dearomatization fragment.  | <b>279</b> |
| <b>Scheme 8.4</b>  | Regioselectivity of the addition of thiophene to an electrophile derived from the double protonation of benzene.                    | <b>280</b> |
| <b>Scheme 8.5</b>  | Substrate scope of aromatics capable of undergoing electrophilic aromatic substitution with an electron deficient tungsten complex. | <b>281</b> |

|                    |   |            |
|--------------------|---|------------|
| <b>Scheme 8.6</b>  | The synthesis of a tungsten-benzene- <i>d</i> <sub>6</sub> complex and selectivity in the subsequent protonations and nucleophilic addition.                          | <b>282</b> |
| <b>Scheme 8.7</b>  | One pot synthesis feature a double protonation and double nucleophilic addition to the tungsten-benzene complex.  | <b>282</b> |
| <b>Scheme 8.8</b>  | Large-scale optimization of the molybdenum-benzene complex.   | <b>284</b> |
| <b>Scheme 8.9</b>  | Addition of a weak aromatic nucleophile to the molybdenum-benzene complex, speculated to occur on the $\pi$ -ligand resulting from the double protonation of benzene. | <b>284</b> |
| <b>Scheme 9.1</b>  | Typically proposed linear sequence for the oxidative addition of benzene.   | <b>295</b> |
| <b>Scheme 9.2</b>  | Synthesis of a tungsten-benzene complex with PBU <sub>3</sub> as the ancillary ligand.  | <b>296</b> |
| <b>Scheme 9.3</b>  | Isomerization and spin-saturation exchange for the observed tungsten-benzene isomers.   | <b>298</b> |
| <b>Scheme 9.4</b>  | Gibbs landscape for intermediates involved in the tungsten- $\eta^2$ -arene and tungsten-phenyl-hydride isomerization   | <b>301</b> |
| <b>Scheme 9.5</b>  | Trajectory connections between transition states involving the tungsten-benzene complex.  | <b>304</b> |
| <b>Scheme 9.6</b>  | The isomerization of a tungsten-anisole complex and purported isomerization mechanism.  | <b>306</b> |
| <b>Scheme 9.7</b>  | The oxidative addition the OH functionality of HFIP on a tungsten complex.  | <b>310</b> |
| <b>Scheme 9.8</b>  | Mechanistic divergence in the isomerization pathways of PhCF <sub>3</sub> ligand on electron-rich molybdenum and tungsten metals.                                     | <b>311</b> |
| <b>Scheme 9.9</b>  | Comparison of C-F activated products on tungsten scaffolds supported by PMe <sub>3</sub> and PBU <sub>3</sub>   | <b>313</b> |
| <b>Scheme 9.10</b> | Synthesis of a substituted trifluoromethylated cyclohexadiene from the dearomatization of PhCF <sub>3</sub> .   | <b>316</b> |

### List of Tables

|                  |   |            |
|------------------|---|------------|
| <b>Table 4.1</b> | Experiments evaluating isotopologue distributions of cyclohexene- <i>d</i> <sub>1</sub> through NMR and MRR analysis. | <b>133</b> |
|------------------|---|------------|

|                   |  |            |
|-------------------|--|------------|
| <b>Table 4.2</b>  | Estimates of isotopic purity with NMR, MRR, HRMS and neutron diffraction for tungsten cyclohexene- $d_n$ complexes and the free organics of cyclohexene- $d_n$ . | <b>134</b> |
| <b>Table 4.3</b>  | Structural differences between a neutral tungsten-cyclohexene complex and a cationic tungsten-cyclohexene complex that has been methylated at the nitrosyl.      | <b>135</b> |
| <b>Table 5.1</b>  | Ligand substitution reactions of the molybdenum- $\alpha$ -pinene complex.   | <b>167</b> |
| <b>Table 5.2</b>  | Electrochemical properties and substitution rates for various molybdenum- $\pi$ -ligand complexes.   | <b>171</b> |
| <b>Table 5.3</b>  | Comparison of properties between the molybdenum-PhCF <sub>3</sub> and molybdenum-PhH complexes.  | <b>176</b> |
| <b>Table 6.1</b>  | DFT calculations comparing the relative binding energies of electron-deficient benzenes.   | <b>190</b> |
| <b>Table 6.2</b>  | Coordination diastereomer ratios and electrochemical data of electron-deficient benzenes on tungsten.  | <b>197</b> |
| <b>Table 6.3</b>  | DFT calculations for various isomers of a molybdenum-fluorobenzene complex.  | <b>199</b> |
| <b>Table 8.1</b>  | Comparison of properties for tungsten and molybdenum benzene complexes.  | <b>283</b> |
| <b>Table 9.1</b>  | Solvent dependence on the arene/aryl hydride equilibrium.  | <b>309</b> |
| <b>Table 9.2</b>  | Coordination of various unsaturated ligands and percentages of dihapto-coordinate and C-H activated isomers.   | <b>314</b> |
| <b>Table 9.3</b>  | SC-XRD structural determination of tungsten cyclohexene complexes supported by PMe <sub>3</sub> and PBU <sub>3</sub> .   | <b>315</b> |
| <b>Table 9.4</b>  | Comparison of tungsten PhH, PhOMe and PhCF <sub>3</sub> complexes.   | <b>316</b> |
| <b>Chapter 1:</b> | <b>Introduction</b>  | <b>29</b>  |
| 1.1               | Introduction   | <b>30</b>  |
| 1.2               | Defining Aromaticity   | <b>31</b>  |
| 1.3               | Aromatic Molecules: A Survey of “Traditional” Aromatic Reactivity  | <b>32</b>  |
| 1.4               | Aromatics as Starting Materials for Medicinal Chemistry  | <b>34</b>  |
| 1.5               | The Birch Reduction  | <b>35</b>  |
| 1.6               | The Asahi Process  | <b>36</b>  |
| 1.7               | Dearomatized Products via Cycloadditions with Arenophiles  | <b>37</b>  |
| 1.8               | Aromatic Reactivity Enabled by Electron Deficient Metal Complexes  | <b>37</b>  |
| 1.9               | $\Pi$ -Backbonding   | <b>40</b>  |

|  |   |            |
|--|---|------------|
| 1.10   | Dearomatization via Dihapto-Coordination  | 42         |
| <b>Chapter 2: Studies of WTp(NO)(PMe<sub>3</sub>)(η<sup>2</sup>-benzene)</b>   |   | <b>55</b>  |
| 2.1  | Introduction  | 56         |
| 2.2  | Fluclional Behavior of WTp(PMe <sub>3</sub> )(NO)(η <sup>2</sup> -benzene) via NMR Studies  | 59         |
| 2.3  | DFT Studies Estimating Dearomatization Across 3rd Row Dearomatization Agents  | 64         |
| 2.4  | Synthesis of WTp(PMe <sub>3</sub> )(NO)(η <sup>2</sup> -benzenium) (OTf-)   | 66         |
| 2.5  | Dynamic Behavior of WTp(PMe <sub>3</sub> )(NO)(η <sup>2</sup> -benzenium) in Solution   | 69         |
| 2.6  | Reactivity WTp(PMe <sub>3</sub> )(NO)(η <sup>2</sup> -benzenium)  | 72         |
| 2.7  | pKa Determination of WTp(PMe <sub>3</sub> )(NO)(η <sup>2</sup> -benzenium)  | 74         |
| 2.8  | Synthesis of WTp(PMe <sub>3</sub> )(NO)(η <sup>2</sup> -1,3-cyclohexadiene)   | 75         |
| 2.9  | Synthesis and Reactivity of WTp(PMe <sub>3</sub> )(NO)(η <sup>2</sup> -1,4-cyclohexadiene)  | 77         |
| 2.10   | Conclusion  | 79         |
| <b>Chapter 3: The Regio- and Stereoselective Preparation of Cyclohexene Isotopologues and Stereoisotopomers from Benzene</b> |   | <b>90</b>  |
| 3.1  | Introduction  | 91         |
| 3.2  | The Protonation of Benzene and Cyclohexadiene Complexes of Tungsten   | 93         |
| 3.3  | Deuterium Studies   | 95         |
| 3.4  | Methods to Determine Isotopic Purity  | 98         |
| 3.5  | Mechanistic Considerations  | 99         |
| 3.6  | Comparison to Other Systems and Considerations of Absolute Stereocontrol  | 100        |
| 3.7  | Isotopologues of Substituted Cyclohexenes   | 102        |
| 3.8  | Conclusion  | 104        |
| <b>Chapter 4: Investigations of WTp(NO)(PMe<sub>3</sub>)(η<sup>2</sup>-cyclohexene)</b>                                      |   | <b>125</b> |
| 4.1  | Introduction  | 126        |
| 4.2  | Synthesis and Conformations of WTp(PMe <sub>3</sub> )(NO)(η <sup>2</sup> -cyclohexene)  | 128        |
| 4.3  | Evidence for Interfacial Isomerization for WTp(PMe <sub>3</sub> )(NO)(η <sup>2</sup> -cyclohexene)  | 129        |
| 4.4  | Liberation of Cyclohexene Isotopologues from Tungsten for Analysis by Molecular Rotational Resonance Spectroscopy (MRR)                           | 132        |
| 4.5  | Decomplexation of the η <sup>2</sup> -Bound Cyclohexenes with Acid Sources  | 138        |
| 4.6  | Nitrosyl Modulation Studies   | 140        |
| 4.7  | Methylation of WTp(NO)(PMe <sub>3</sub> )(η <sup>2</sup> -1,2-cyclohexene) and WTp(NO)(PMe <sub>3</sub> )(η <sup>2</sup> -1,2-1,4-cyclohexadiene) | 144        |
| 4.8  | Functionalization of the Tungsten-Alkene Bond   | 147        |
| 4.9  | Efforts Toward Tungsten Recyclability   | 149        |
| 4.10   | Conclusion  | 152        |



|  |            |
|--|------------|
| <b>Chapter 5: Optimized Synthesis of MoTp(NO)(4-DMAP)(<math>\eta^2</math>-3,4-<math>\alpha,\alpha,\alpha</math>-trifluorotoluene): An Exceptionally Labile Synthron for Molybdenum-Promoted Dearomatization, Including Access to MoTp(NO)(4-DMAP)(<math>\eta^2</math>-benzene)</b> | <b>163</b> |
| 5.1 Introduction   | 164        |
| 5.2 Synthesis of a Molybdenum Triflato Complex   | 165        |
| 5.3 Labile $\pi$ -Ligands and Molybdenum Dearomatization   | 167        |
| 5.4 Studies of MoTp(NO)(DMAP)( $\eta^2$ - $\alpha,\alpha,\alpha$ -trifluorotoluene)  | 171        |
| 5.5 Synthesis of MoTp(NO)(DMAP)( $\eta^2$ -benzene)  | 175        |
| 5.6 Conclusion   | 177        |
| <b>Chapter 6: Dearomatizing Electron Deficient Arenes with Group 6 Dearomatization Agents</b>  | <b>188</b> |
| 6.1 Introduction   | 189        |
| 6.2 Studies of $\pi$ -EWGs on Benzenes and Molybdenum and Tungsten Fragments   | 190        |
| 6.3 Benzenes with Sulfur-Based EWGs  | 191        |
| 6.4 Accessing EWGs with $\pi$ -Bonds   | 193        |
| 6.5 Substituted Trifluoromethylated Benzenes   | 195        |
| 6.6 Properties of Electron Deficient Benzenes on {WTP(NO)(PMe <sub>3</sub> )}  | 196        |
| 6.7 Dihapto-Coordination of Aryl Halides.  | 200        |
| 6.8 Dynamic Behavior of Electron Deficient Benzenes on Tungsten and Molybdenum   | 201        |
| 6.9 Conclusion   |            |
| <b>Chapter 7: The Double Protonation of Anisole Upon Coordination to the {WTP(NO)(PMe<sub>3</sub>)} Fragment: A Versatile Electrophile</b>   | <b>222</b> |
| 7.1 Introduction   | 223        |
| 7.2 The Double Protonation of Anisole  | 224        |
| 7.3 Initial Nucleophilic Additions to a Double-Protonated Anisole Complex  | 226        |
| 7.4 Synthesis of Substitued Tungsten-Allyl Complexes   | 230        |
| 7.5 Double Protonating an Alternate Diastereomer of a Tungsten-Anisole Complex   | 234        |
| 7.6 Triple Nucleophilic Additions to Anisole   | 237        |
| 7.7 Alternative Reactivity of the Oxo-Carbenium Functionality  | 239        |
| 7.8 Electrochemical Behavior of Tungsten-Oxo-Carbnium Complexes  | 242        |
| 7.9 Double Protonation of Substitued Anisoles  | 243        |
| 7.10 Conclusion  |            |
| <b>Chapter 8: The Double Protonation of Aromatics Enabled by Group 6 Dearomatization Agents</b>  |            |
| 8.1 Introduction   | 277        |
| 8.2 The Double Protonation of Benzene  | 279        |
| 8.3 Nucleophilic Additions to a Double Protonated Benzene Complex  | 280        |
| 8.4 Deuterium Studies  | 281        |
| 8.5 Nucleophilic Addition of Beta-Estradiol  | 282        |
| 8.6 Double Protonation of Benzene on Molybdenum and Nucleophilic Additions   | 285        |

## 8.7 Conclusions

|  |            |
|--|------------|
| <b>Chapter 9: Experiments and Direct Dynamics Simulations Reveal Network of Reaction Pathways for WTp(NO)(PR<sub>3</sub>)(η<sup>2</sup>-arene) to Aryl Hydride Equilibrium</b> | <b>293</b> |
| 9.1 Introduction   | 294        |
| 9.2 Synthesis and Equilibrium Studies  | 296        |
| 9.3 Static DFT landscape for η <sup>2</sup> -benzene and phenyl hydride equilibrium  | 298        |
| 9.4 Quasiclassical direct dynamics simulations   | 303        |
| 9.5 Equilibrium Dynamics of Anisole  | 306        |
| 9.6 Solvent Dependence on Equilibrium and O-H Activation   | 309        |
| 9.7 Electron Deficient Benzenes on {WTp(NO)(P(n-Bu) <sub>3</sub> )}  | 310        |
| 9.8 Coordination of Aromatic and Unsaturated Ligands   | 313        |
| 9.9 Synthetic implications.  | 316        |
| 9.10 Conclusions   | 317        |

# **Chapter 1**

## **Introduction**

## 1.1 Introduction

Aromaticity is a chemical phenomenon that synthetic and theoretical chemists alike have sought to define since Faraday's discovery of benzene in 1825. Molecules possessing aromatic character are often reluctant to undergo chemical transformations. This diminished reactivity is in marked contrast to other unsaturated molecules (olefins, alkynes, ketones) which readily engage in a plethora of chemical reactions. Due to their exceptional stability, aromatic molecules are readily found in nature. Aromatic frameworks are common structural motifs of natural products and of molecules synthesized by the human body, and aromatic molecules can even be found in the interstellar medium.<sup>1-2</sup>

Synthetic chemists have utilized aromatic molecules as starting materials for medicines, natural products, petrochemical additives and other value-added products.<sup>3-9</sup> The majority of these reactions result in the formation of aromatic substitution products. However, harsh reaction conditions are often needed to engender reactivity on otherwise inert aromatic molecules. These demanding reaction conditions prohibit the use of many functional groups. Consequently, this curtails the diversity of accessible molecules that can be derived from aromatic precursors.

Within the context of drug development, aromatic molecules could serve as attractive precursors to bioactive small molecules. The multiple alkene bonds within an aromatic

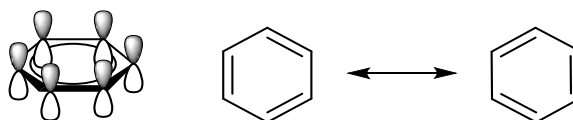


**Figure 1.1:** Depiction of in-phase p-orbitals involved in delocalization of the  $\pi$ -electrons on benzene (left). The net result is a molecule with two equally contributing resonance structures (right).

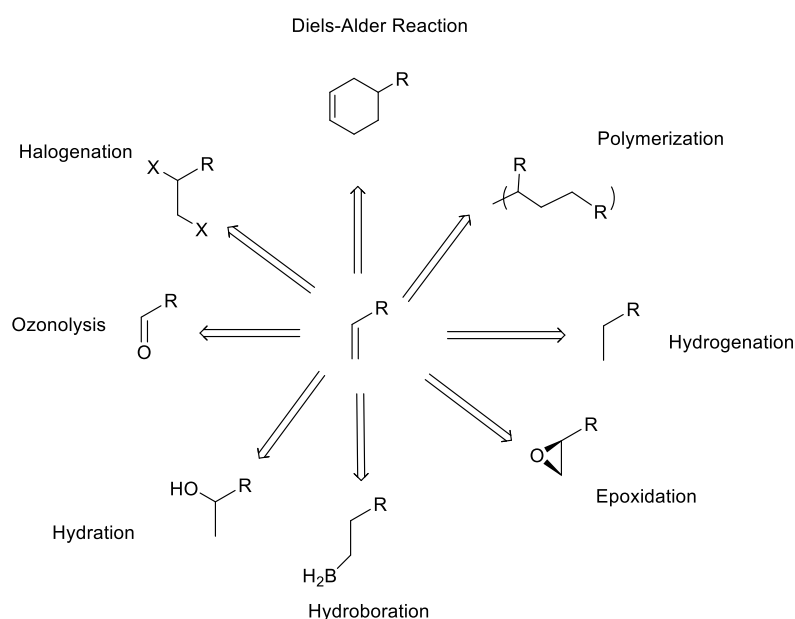
framework afford opportunities for chemical elaboration. Many aromatics contain heteroatoms or other functionalities that are often associated with an increase in the efficacy of the active pharmaceutical ingredients (APIs) of a drug.<sup>8, 11</sup> A robust synthetic methodology that could effectively dearomatize aromatic molecules, thereby promoting chemical transformations under

mild conditions, would be a valuable tool to the medicinal chemist.

## 1.2 Defining Aromaticity

Aromatic molecules are characterized by arrays of delocalized electrons conjugated across a planar molecule. This terminology (aromaticity) is usually applied to systems with alternating  $\pi$ -bonds. Traits associated with aromatic molecules often include high resonance stabilization energies and downfield resonance shifts in the  $^1\text{H}$  and  $^{13}\text{C}$  nuclear magnetic resonance (NMR) spectra of these compounds due to ring anisotropy.<sup>8, 13</sup>

One theoretical treatment of aromatic molecules suggests that differences between the predicted and observed diamagnetic susceptibility of a molecule should serve as the criterion of aromaticity.<sup>14-15</sup> Computational investigations to quantify aromaticity such as current density analysis (CDA) and nucleus-independent chemical shift (NICS)



**Scheme 1.1:** Sampling of reactions available to alkene structures. Analogous reactivity with aromatic molecules is often not observed or requires more demanding reaction conditions.

have been pursued as more rigorous descriptors of aromatic character.<sup>13</sup> Additionally, aromaticity is often associated with delocalization of electron density associated with alternating  $\pi$ -bonds of a planar ring. However, aromaticity arising from conjugated  $\sigma$ -,  $\delta$ - and even  $\phi$ -bond symmetries has also been proposed.<sup>16-18</sup> For instance, aromatic character stemming from d-orbital interactions has been invoked for molybdenum and tungsten oxide clusters.<sup>19</sup> New synthetic methods developed around aromatic molecules could inform theoretical treatments of aromaticity.

### 1.3 Aromatic Molecules: A Survey of “Traditional” Aromatic Reactivity

This thesis seeks to report on activating traditionally inert aromatic molecules toward novel reactivity. As such, a few descriptors should suffice as a working definition of aromaticity. Aromatic molecules are those that have a planar, cyclic structure with alternating single and double bonds. The planarity and conjugation of  $4n + 2\pi$ -electrons (Hückel’s rule)

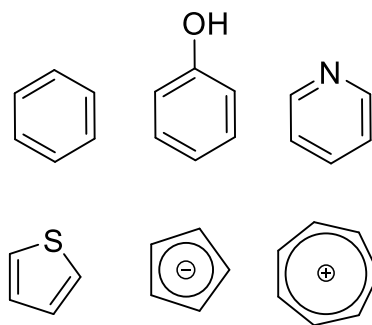


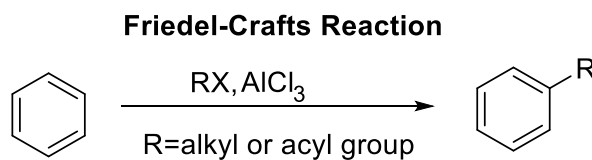
**Figure 1.2:** Examples of molecules that are stabilized by aromatic character.

results in a net delocalization of electron density around the aromatic ring. A consequence of this charge delocalization is the ability of the aromatic molecule to retain its aromatic character, even under reaction conditions where non-aromatic alkene bonds would react (**Scheme 1.1**).

The heat of hydrogenation of benzene, the quintessential aromatic, is  $\sim 36$  kcal/mol less than would be expected from a non-aromatic “cyclohexatriene” molecule.<sup>8</sup> The difference between the theoretical (as the “triene”-molecule) and experimentally determined heat of hydrogenation for benzene is attributed to aromatic stabilization.<sup>8</sup>

Benzene is often a component of crude oil, and substituted benzenes are omnipresent in nature as well. Phenolic moieties are present in naturally occurring steroids. Fused benzenes (naphthalene, anthracene, phenanthrene) represent additional classes of aromatic molecules and are components of crude oil or wood tars.

Heteroatom-containing aromatics (pyridine) and five-member ring aromatics (pyrrole, thiophene, furan) represent additional classes of aromatic molecules with their own associated reactivity.



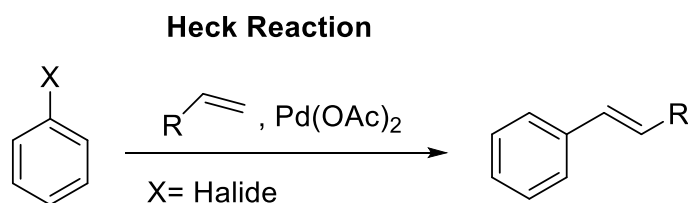
**Scheme 1.2:** Industrially relevant electrophilic aromatic substitution reaction (Friedel-Crafts) that generates substituted benzenes as value added products.

Some classes of aromatic molecules are presented in **Figure 1.2**.

Aromaticity can be used to explain the stabilization and geometry of the tropylium cation (**Figure 1.2**). This cationic species is exceptionally stable as its six  $\pi$ -electrons are part of a conjugated network. Cyclopentadiene features methylene protons that are relatively acidic ( $\text{pK}_a \sim 15$ ) compared to other aliphatic protons. The conjugate base of this complex, the cyclopentadienyl anion, also follows Hückel's rule of aromaticity with six conjugated  $\pi$ -electrons. In these examples, aromaticity is a concept that rationalizes chemical stability.

Industrially relevant processes that utilize aromatic substrates include the Friedel-Crafts alkylation and acylation reactions; which generate substituted alkyl or acyl benzenes respectively. Shell's styrene monomer propylene oxide (SMPO) process generates styrene (a precursor to polystyrene), and the methylation of toluene generates valuable derivatives of xylene.<sup>20</sup> The benzene, toluene, xylenes (BTX) chemical series is important to a wide range of petrochemical processes, with millions of metric tons of these chemicals produced annually.<sup>21-22</sup>

Halogenated benzenes are often employed in various coupling methodologies which have proven valuable to small molecule development, in academic research and



**Scheme 1.3:** Example of a widespread coupling reaction (Heck) that is able to couple halogenated aromatic substrates to alkenes with a palladium catalyst.

even in industrial applications.<sup>23</sup> One notable example includes the Heck Reaction depicted in **Scheme 1.3**, though other notable cross-coupling reactions utilizing palladium are known (Negishi, Suzuki, Sonogashira, Buchwald-Hartwig).<sup>23</sup> A recent example by Buchwald and co-workers has shown improved functional compatibility in C-N coupling reactions with the stoichiometric use of palladium.<sup>24</sup> We note that this study shows the power of chemical transformation promoted by the stoichiometric use of a metal to promote reactivity upon organic substrates.

Substitution and coupling methodologies utilizing aromatics are valuable in generating structural complexity. However, widespread chemical transformations that would selectively result in partially saturated molecules (i.e. cyclohexene, cyclohexadienes) from aromatic precursors are significantly lacking in comparison. The efficient, controlled integration of functionalities to an aromatic ring would represent a paradigm shift in synthetic methodology. This would couple the ability to introduce widespread functionality while generating three-dimensional molecules from planar aromatic substrates.

#### 1.4 Aromatics as Starting Materials for Medicinal Chemistry

Within the context of medicinal chemistry, the aromatic framework represents an attractive target for functionalization. The sites of unsaturation (alkene bonds) in an aromatic molecule represent potential points of chemical elaboration. General strategies that aim to synthesis dearomatized adducts from aromatic molecules can be broadly classified as “dearomatization”. Dearomatization would enable the formation of multiple  $sp^3$ -hybridized carbons from aromatic precursors in a regio- and stereoselective manner. Ideally, structural features associated with the dearomatized product would include a limited number of rotatable bonds, increased saturation in the molecule and the formation of multiple stereocenters. These molecular properties have been correlated with greater degrees of success in pharmaceutical trials compared to molecules that are more “flat” or two-dimensional in their molecular topology.<sup>11</sup>

Additionally, many aromatics have built-in biologically compatible functional groups (i.e. fluorine, sulfur, nitrogen). Starting from a substituted benzene and building complexity around a biologically compatible group would

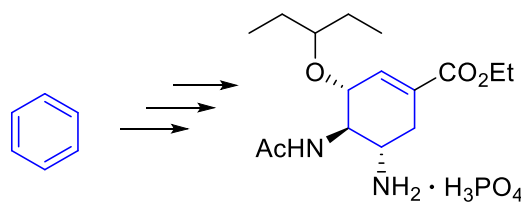


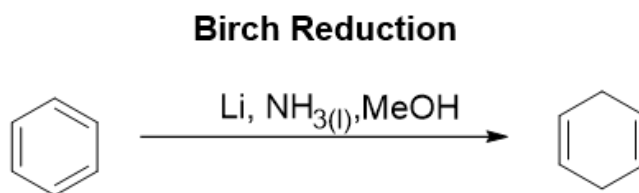
**Figure 1.3:** Theoretical access to a biologically relevant molecule (antiviral Tamiflu) from the selective addition of functionalities to a benzene ring.



offer an alternative to “late-stage” incorporation of these functional groups.<sup>25-26</sup> For example, late-stage incorporation of fluoro- or trifluoromethyl-groups is an active research area given the benefits of fluorinated drugs. These fluorinated molecules display increased lipophilicity and enhanced stability to deleterious metabolism pathways compared to non-fluorinated analogs.<sup>27-29</sup> The dearomatization of fluorine-containing benzenes and building molecular complexity around an existing fluorine functionality would represent a complementary synthetic strategy to late-stage methodologies.

### 1.5 The Birch Reduction

The Birch reduction is effective in converting benzene to dienes. This reaction is an example of how aromatic stability can be overcome. In the case of benzene, treatment with a dissolved alkali metal (i.e. lithium, sodium) in ammonia followed by a protic solvent (i.e. methanol, isopropanol) selectively generates a 1,4-cyclohexadiene product. Despite its discovery more than 70 years ago, modifications of the Birch Reduction are still being developed.<sup>30-31</sup> One recent example is an ammonia-free Birch Reduction that utilizes sodium metal solubilized with various crown ethers in anhydrous THF.<sup>32</sup> The resulting electride salts promote the reduction of benzene to the 1,4-cyclohexadiene product without the need for lithium or liquid ammonia. Despite this advance, the requirement of a strong reducing agent limits the available substrate scope. Additionally, no stereocenters are formed in this reaction, even in cases where substituted benzenes are used.

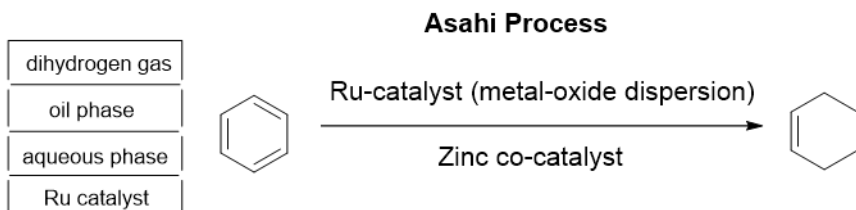


**Scheme 1.4.** The selective reduction of benzene to 1,4-cyclohexadiene.

## 1.6 The Asahi Process

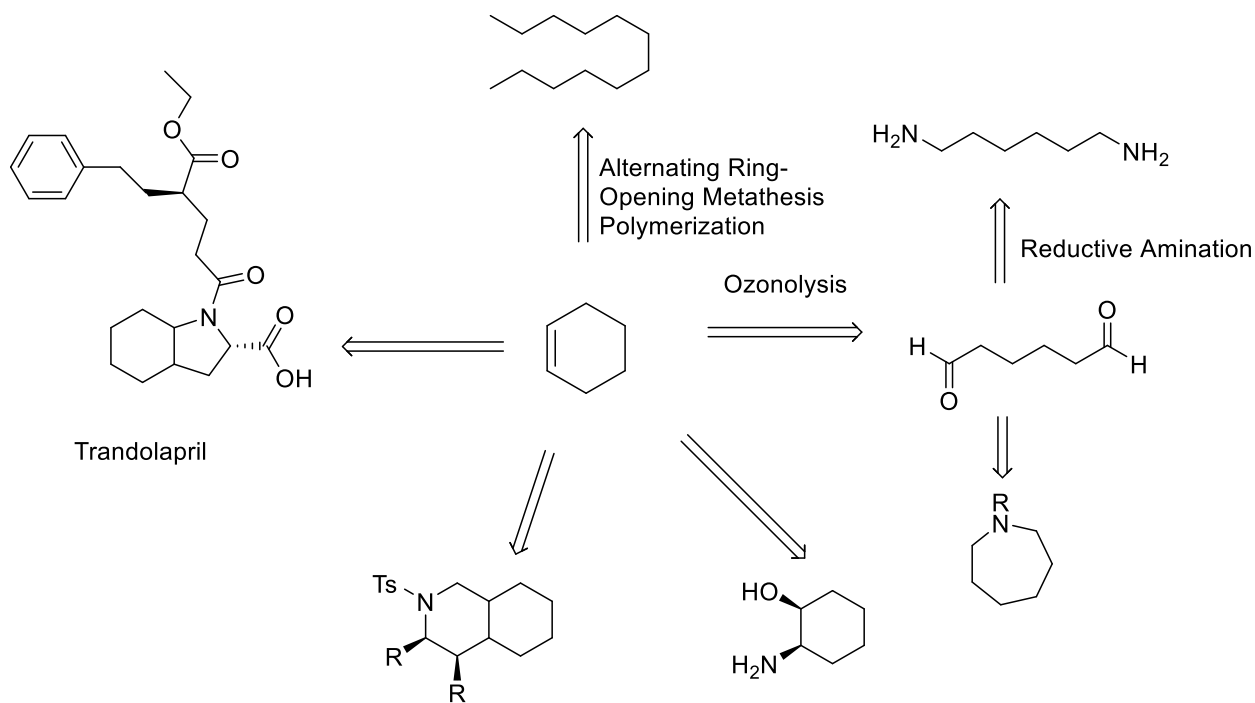
The only industrially employed process that synthesizes cyclohexene from benzene is the Asahi

Process (Scheme 1.5).<sup>7</sup>



**Scheme 1.5:** Catalytic, partial hydrogenation of benzene to cyclohexene with a ruthenium catalyst. The remaining alkene functionality represents an accessible site of further elaboration.

Cyclohexene serves as a useful chemical building block for various value-added molecules as depicted in Scheme 1.6. The Asahi Process reaction relies on a heterogeneous ruthenium catalyst with a zinc co-catalyst. The stability of the ruthenium catalyst is bolstered by the solid-site support (metal oxides), and reaction conditions employ a four-phase mixture: a phase of gaseous hydrogen, an oil phase, an aqueous phase, and the solid phase that includes the ruthenium catalyst.<sup>33-39</sup> The zinc co-catalyst helps to avoid over-reduction to cyclohexane.



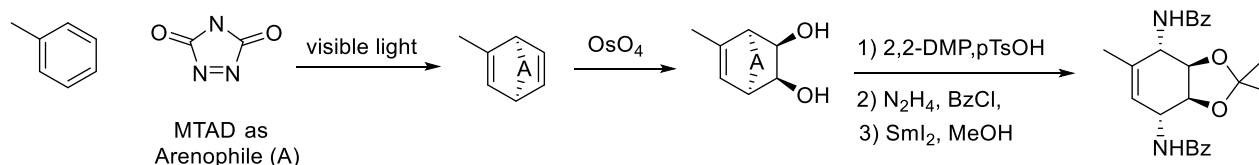
## 1.7 Dearomatized Products via Cycloaddition with Arenophiles

Traditionally, the ability to use aromatic molecules as substrates for cycloaddition reactions requires the use of ultraviolet (UV) light. The high energy UV wavelengths required for the resulting chemical transformation can degrade the desired organic product. However, recent work by the Sarlah Group out of the University of Illinois at Urbana-Champaign has led to classes of “arenophiles” that can be activated by exposure to visible light.<sup>8</sup>

A detailed description of this burgeoning methodology is beyond the scope of this chapter. However, the following example illustrates the potential value of this synthetic strategy.<sup>40</sup> Activation of N-methyl-1,2,4-triazine-3,5-dione (MTAD) with visible light results in a high energy species whose SOMO is able to add to the LUMO group orbitals on an aromatic ring (i.e. toluene). The net result is a cycloaddition adduct featuring a 1,4-cyclohexadiene motif as depicted in **Scheme 1.7**. The resulting, unsubstituted double-bond (in the case of toluene) can form a vicinal diol product with high levels of diastereoselectivity upon treatment with osmium tetroxide. This can then be readily converted into a functionalized 1,4-diaminocyclohexene product.

## 1.8 Aromatic Reactivity Enabled by Electron Deficient Metal Complexes

A common methodology in activating aromatic molecules is through hexahapto-coordination to an electron deficient metal center. Common transition metal systems used in this methodology include  $\{\text{Cr}(\text{CO})_3\}$ ,  $\{\text{Mo}(\text{CO})_3\}$ ,  $\{\text{Mn}(\text{CO})_3\}^+$ ,  $\{\text{Mn}(\text{CO})_2(\text{NO})\}^{2+}$  and  $\{\text{FeCp}\}^+$  among others.<sup>6</sup> Here, metals are often coordinated to ligands that have strong  $\pi$ -acceptor properties

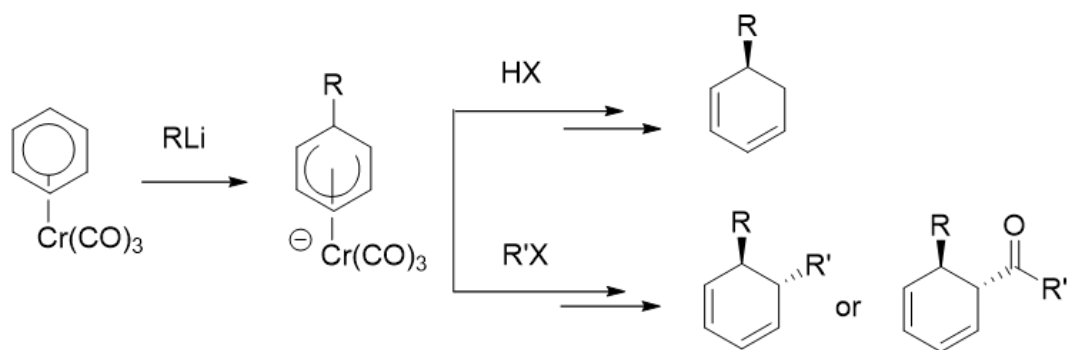


**Scheme 1.7:** Activating the arenophile N-methyl-1,2,4-triazine-3,5-dione (MTAD) with visible light. The resulting 1,4-cyclohexadiene product can then be further functionalized and here is shown to readily undergo a selective hydroxylation reaction to generate a 1,2-vicinal diol product followed by di-amination.

(i.e. carbonyl, nitrosyl ligands). Additionally, several of these complexes are overall cationic in nature. Such metal complexes, being exceptionally electron deficient, are able to bind aromatic ligands in an  $\eta^6$ -coordination mode. Here, donation of the electron density from the aromatic's  $\pi$ -cloud to the electron-deficient metal center generates a stable metal-arene complex.

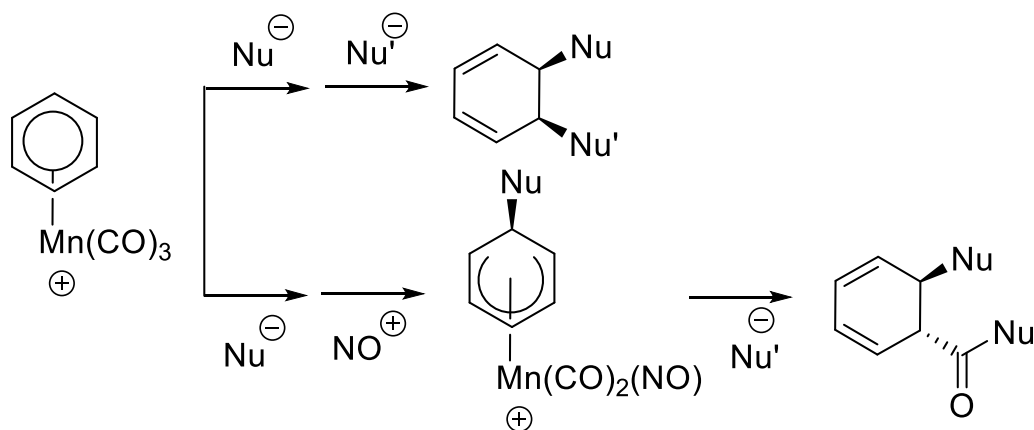
Once coordinated to the metal, the aromatic is primed for nucleophilic addition and nucleophilic aromatic substitution reactions. In the case of  $\text{Cr}(\text{CO})_3(\eta^6\text{-arene})$ , dearomatization is achieved by treatment with a strong nucleophile (i.e. organolithium or Grignard reagents).<sup>6</sup> The resulting product is an anionic chromium-supported cyclohexadienyl species. This intermediate can then react with acid to generate a 1,3-cyclohexadiene product with a newly formed stereocenter. Alternatively, treatment of the cyclohexadienyl intermediate with a carbon electrophile generates a trans-substituted 1,3-cyclohexadiene product. If electrophilic addition instead occurs on one of the carbonyl ligands, resulting carbonyl insertion into the cyclohexadienyl adduct results in a ketone-incorporated product (**Scheme 1.8**).<sup>6</sup>

The  $\{\text{Mn}(\text{CO})_3\}^+$  fragment is more electrophilic than its neutral, chromium analog. As such, aromatics bound to these complexes can undergo a *double* nucleophilic addition. The first nucleophile is generally a very reactive and “hard” nucleophile (i.e. organolithiums such as MeLi or a hydride from  $\text{LiAlH}_4$ ).<sup>6</sup>



**Scheme 1.8:** Dearomatization promoted by hexahapto-coordination of benzene to an electron deficient metal center.

In some cases, after the initial nucleophilic addition, the metal center can undergo ligand substitution of a carbonyl for a cationic nitrosyl ligand. The resulting cationic complex now includes a nitrosyl ligand, which is an even better  $\pi$ -acceptor ligand than a carbonyl. As such, the resulting product is even *more* reactive than the original  $\{\text{Mn}(\text{CO})_3\}^+$  species and can be treated with a wider range of nucleophiles. Examples of successful nucleophiles include phosphorous and nitrogen nucleophiles, as well as hydrides, enolates, Grignards and organolithium reagents.<sup>6</sup> In the cases of phenyl and methyl organolithium reagents, nucleophilic attack can occur on a carbonyl ligand. Insertion of the resulting acyl group into the cyclohexadienyl ligand gives trans-1,2-substituted cyclohexadiene products (**Scheme 1.9**).



**Scheme 1.9:** Double nucleophilic addition to benzene enabled by an exceptionally electron-deficient, cationic manganese complex. Nitrosylation of the metal after the initial addition can activate the bound  $\pi$ -ligand to react with even weaker nucleophiles.

The activation of aromatic compounds toward nucleophiles through hexahapto-coordination to an electron deficient metal complex is a powerful methodology in accessing various dearomatized products. Even so, several limitations exist. One is that the nucleophiles used (often Grignards or other organo-metal reagents) must be anionic and highly reactive in nature. In many cases, only a single alkene bond of the aromatic molecule is functionalized. Finally, chiral auxiliaries need to be utilized in order to access enantioenriched products.

An alternative dearomatization methodology using transition metals utilizes electron-rich metal fragments that engage in  $\eta^2$ -coordination with the aromatic molecule. This bonding motif depends on the ability of the metal to  $\pi$ -backbond to the aromatic ligand, and offers complementary reactivity to electron-deficient, metal-enabled transformations (**Figure 1.4**).

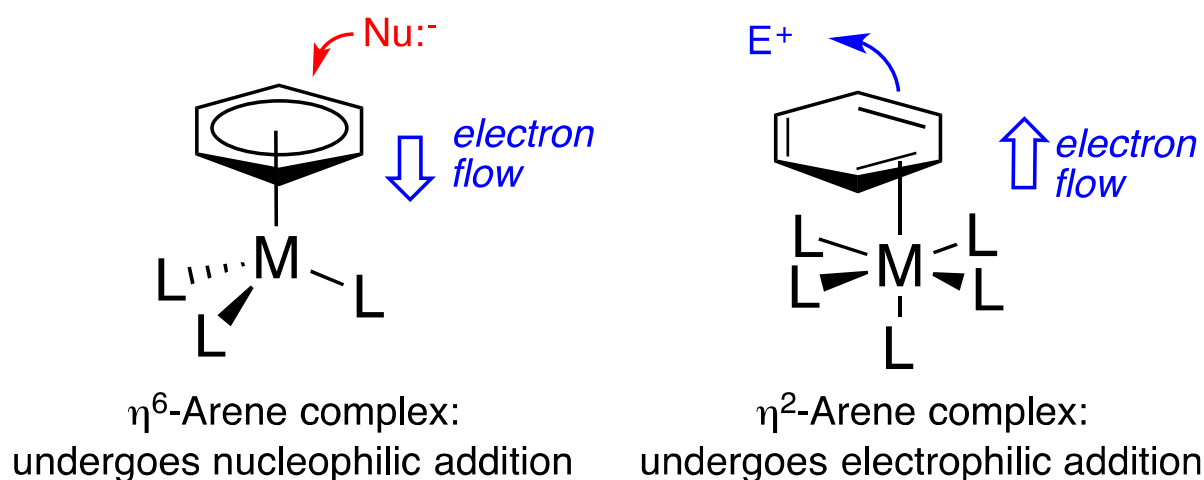


**Figure 1.4:** Comparison of reactivity engendered from the hexahapto-coordination of benzene to an electron deficient metal (left) and the effects of dihapto-coordination enabled by  $\pi$ -backbonding from an electron-rich transition metal scaffold.

## 1.9 $\pi$ -Backbonding

The phenomenon of  $\pi$ -backdonation is a central concept in organometallic chemistry. In this bonding interaction, a metal utilizes filled  $d\pi$ -orbitals to donate into a symmetry appropriate anti-bonding orbital of a ligand.  $\pi$ -backdonation strengthens the metal-ligand bond at the expense of populating anti-bonding orbitals on the coordinated ligand. This bonding interaction is prevalent in the coordination chemistry between transition metals and carbonyl and nitrosyl ligands.

With a sufficiently electron-rich metal,  $\pi$ -backdonation has proved to be a crucial interaction in the activation of small molecules (i.e.  $N_2$ ,  $H_2$ ,  $CH_4$ ) and has even been invoked in certain metal-halide bonds. In the case of the latter, back-donation is postulated to occur from metal  $d\pi$ -orbitals to the symmetry correct d-orbitals of the halogen.<sup>41</sup> In the case of dinitrogen

complexes,  $\pi$ -backbonding plays a pivotal role in stabilizing various dinitrogen adducts given the poor  $\sigma$ -donation ability of the dinitrogen ligand. The first structurally characterized monomeric dinitrogen complex was of  $\text{Ru}(\text{NH}_3)_5(\text{N}_2)^{2+}$ , with the bond between metal and dinitrogen significantly fortified by a  $\pi$ -backbonding interaction.<sup>42-43</sup> Notably, the influences of  $\sigma$ -donation and  $\pi$ -backbonding are synergistic; donation

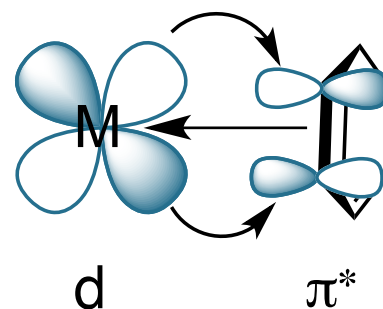


**Figure 1.5:** Generalized schematic detailing  $\pi$ -backbonding from metal to aromatic ligand

from ligand to metal results in a more electron-rich metal that is then able to act as a better  $\pi$ -base.

It should be then of little surprise that the third row congener,  $\{\text{Os}(\text{NH}_3)_5\}^{2+}$  could serve even more potent  $\pi$ -base than its ruthenium analog. This pentaammineosmium fragment forms a stable dinitrogen complex with the dinitrogen bond slightly elongated (1.12 Å upon coordination vs. 1.09 Å as free dinitrogen).<sup>44</sup> In this case, osmium binds  $\kappa^1$ -to the dinitrogen ligand, analogous to its ruthenium predecessor (**Figure 1.6**).

The discovery of the first ruthenium dinitrogen complex was unintentional and an overview of the developments that led to its discovery are documented elsewhere.<sup>43</sup> In the vein of serendipitously discovering unusual coordination complexes, reduction of  $\text{Os}(\text{NH}_3)_5(\text{OTf})^{3+}$  with magnesium in the presence of acetone led to a thermally stable  $\eta^2$ -acetone complex.<sup>45</sup> In this coordination mode the pentaammineosmium fragment is bound to the carbonyl of acetone in a

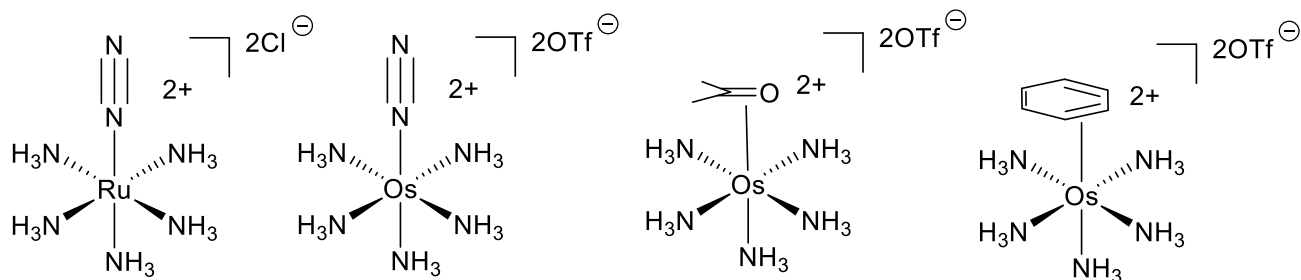


**Figure 1.6:** Series of metal-complexes where coordination of the ligand (dinitrogen, acetone, benzene) is supported by large degrees of  $\pi$ -backbonding from metal to ligand.

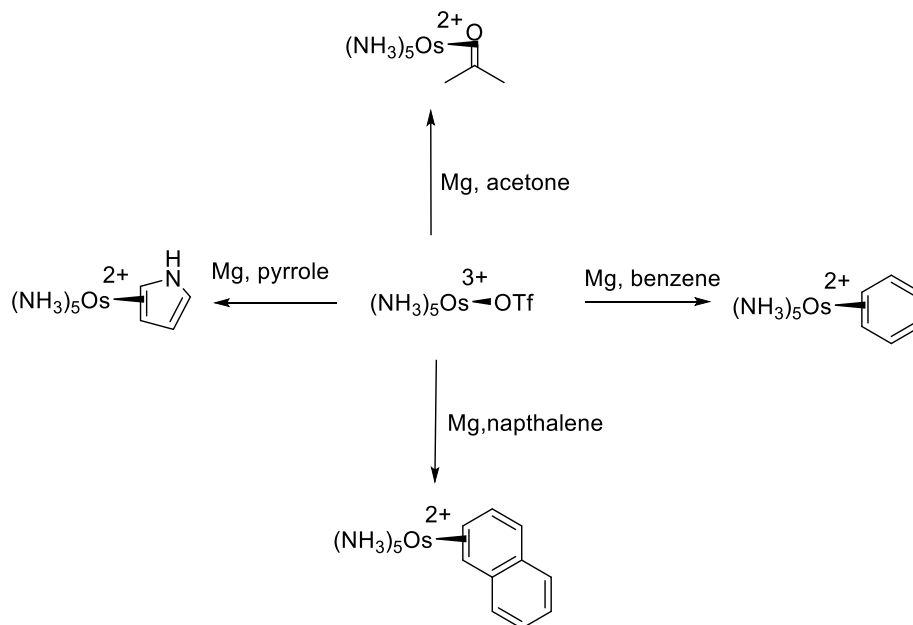
dihapto-fashion. At its discovery, it was one of the only thermally stable  $\eta^2$ -coordinated ketone complexes known and its discovery ushered in a new paradigm of thermally stable coordination modes.<sup>45</sup>

### 1.10 Dearomatization via Dihapto-Coordination

Starting from the initial discovery of dihapto-coordinated acetone, it was found that the pentaammineosmium fragment reacts with a wide array of unsaturated ligands including ketones, aldehydes, esters and even aromatics to form thermally stable  $\eta^2$ -complexes.<sup>46</sup> While there is  $\sigma$ -donation from the filled  $\pi$ -bond in these ketone-containing ligands (donation to the symmetry correct orbitals on the metal), the major bonding interaction is that of  $\pi$ -backdonation from the metal into the  $\pi^*$ -orbitals of the  $\pi$ -acceptor ligand.

The  $\{\text{Os}(\text{NH}_3)_5^{2+}\}$  fragment is significantly  $\pi$ -basic to form thermally stable dihapto-coordinate arene complexes.<sup>47</sup> In dihapto-based dearomatization, the metal-aromatic bonding ligand interaction is localized on a single alkene bond. Dearomatization by  $\eta^2$ -coordination makes the bound aromatic more electron-rich. Subsequently, the aromatic ligand displays reactivity similar to that of an electron-rich diene and readily reacts with an array of electrophiles. This is complementary to the activation enabled by hexahapto-coordination, which engenders reactivity with nucleophiles. A common synthetic scheme to accessing dihapto-coordinated aromatic molecules is shown in **Scheme 1.10** and relies on using magnesium to reduce the osmium(III) species. The resulting osmium(II) species is now electron-rich enough to engage in the  $\eta^2$ -coordination mode with unsaturated molecules.





**Scheme 1.10:** Reduction of an osmium-triflate complex in the presence of various aromatics

In the case of benzene, once coordinated to  $\{\text{Os}(\text{NH}_3)_5^{2+}\}$ , the benzene ring distorts significantly due to population of its  $\pi^*$ -orbitals. The alkene bond to which the metal is bound is significantly lengthened compared to uncomplexed benzene (1.46 Å vs 1.40) and the resulting, unbound alkenes are shortened in length. Additionally, the hybridization of the  $\eta^2$ -bound carbons are more  $sp^3$  in character. These features are all consistent with a dearomatized adduct. The geometrical distortions are in contrast to those reported for other dihapto-coordinate aromatics to silver or copper. In the latter case, the aromatic  $\pi$ -ligand often features little to no distortion of the aromatic ring.<sup>48-50</sup> here, the metal-arene bonding interactions rely on mostly non-covalent Van der Waals forces. Such bonding interactions are observed only with crystal structure data, and the aromatic ligand readily decomplexes from the metal once the complex is in solution.

The degree of distortion in the benzene molecule suggests significant dearomatization of the benzene ring and indeed, multiple reports investigating the reactivity of the bound benzene ring to pentaammineosmium(II) show enhanced reactivity.<sup>10, 47</sup> Elegant chemistry was then extended to other aromatic scaffolds including phenol, aniline, anisole, naphthalene among others, wherein the

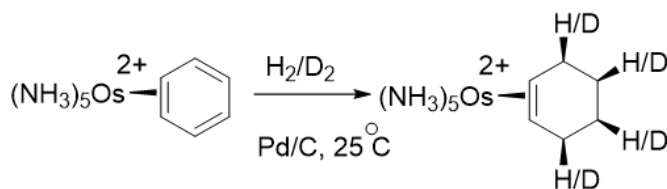
aromatic core was elaborated into more complicated alicyclic structures.<sup>51-55</sup>

A relevant example of osmium-engendered reactivity for this thesis is the stereoselective deuteration of benzene to a single *d*<sub>4</sub>-isotopologue of

cyclohexene. Once coordinated to the electron rich pentaammineosmium fragment, the benzene ligand readily undergoes a net reduction to cyclohexene in the presence of hydrogen or deuterium gas at ambient temperatures upon exposure to a palladium on carbon catalyst.<sup>10</sup> Experiments with deuterium gas show exclusive addition of the deuterium “exo” relative to the metal, with deuterium addition occurring on the face of the aromatic opposite to the face coordinated to the metal. This results in the stereoselective formation of a *d*<sub>4</sub>-isotopologue (3,4,5,6-tetra-deuterio-cyclohexene) osmium complex of cyclohexene.

Despite the activating nature of the {Os(NH<sub>3</sub>)<sub>5</sub>}<sup>2+</sup> fragment, the substantial cost and potential toxicity of the osmium system were limitations that prompted investigation into alternative dihapto-coordinate based dearomatization metal complexes. The π-basic fragment {ReTp(MeIm)(CO)} (Tp= trispyrazoylborate, MeIm= N-methyl-midazole) was ultimately developed by matching the electrochemical potential of its osmium precursor.<sup>56-57 58</sup> Both of these complexes are highly reducing and feature a relatively innocuous steric profile around the metal center.<sup>59</sup>

A notable feature of the rhenium system is the use of the trispyrazoylborate ligand (Tp) originally developed by Trofimenko.<sup>60</sup> This tridentate “scorpionate” ligand reinforces the octahedral geometry of the metal complex, thereby suppressing the formation of seven-coordinate



**Scheme 1.11:** The selective hydrogenation of benzene to cyclohexene enabled by dihapto-coordination of an electron rich osmium complex to benzene. A selective *d*<sub>4</sub>-isotopologue of cyclohexene can be generated with this methodology, with the steric demand associated with the metal directing exclusive deuteration “exo” relative to the metal.

species that would result from an oxidative addition. Such a product would strain the angle between the pyrazole rings established by pyrazole bonding to the boron.

Another important element of the rhenium system is the absence of an internal mirror plane within the molecule. An elegant strategy in resolving the chiral-at-metal complex allows for the synthesis of rhenium-arene complexes where the aromatic ligand is bound to only a single hand of the dearomatization agent. Once coordinated to a single enantiomer of the metal, addition reactions to the aromatic ring would occur enantioselectively. Here, the chirality of the metal is transferred to the chirality of the resulting organic ligand. Many features of the rhenium system (i.e. chirality, Tp ligand) were transferred to the development of later generations of  $\pi$ -basic dearomatization fragments.<sup>59, 61-63</sup>

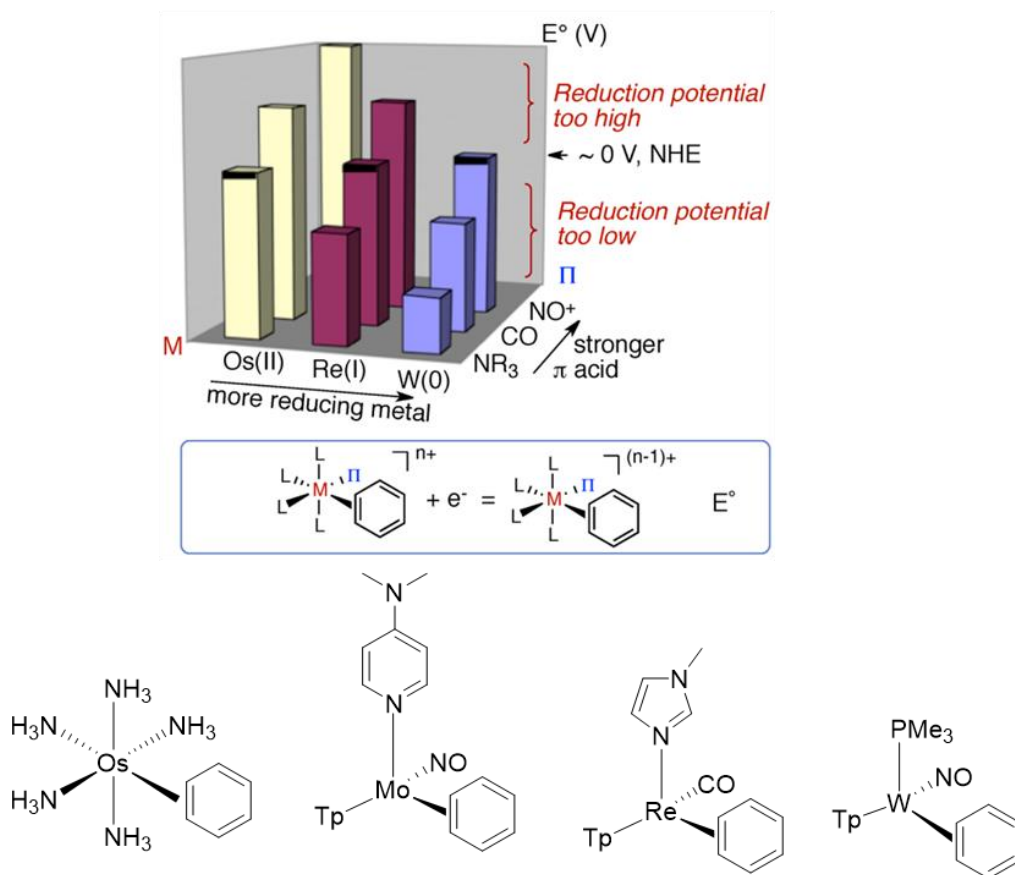
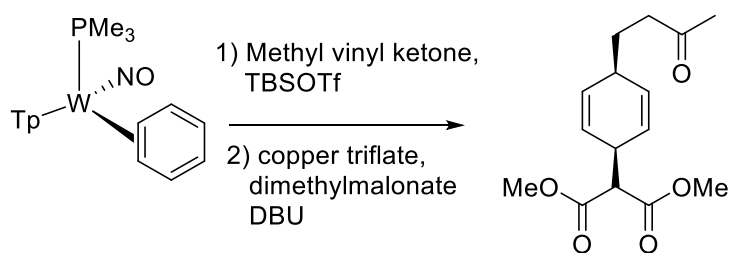


**Figure 1.7:** Classes of electron-rich dearomatization agents and the dihapto-coordination of benzene. Careful matching of electrochemical potentials to the original pentaamine osmium fragment through ligand substitution enables the synthesis of multiple metals capable of  $\eta^2$ -based dearomatization.

Eventually dearomatization agents based off of Group 6 metals were developed in the forms of  $\{\text{MoTp}(\text{DMAP})(\text{NO})\}$  (DMAP= 4-dimethylaminopyridine) and  $\{\text{WTP}(\text{PMe}_3)(\text{NO})\}$ . Analogous to the development of the rhenium system, these Group 6 dearomatization agents were made possible by matching their electrochemical parameters to those of previous systems (**Figure 1.7**). These complexes are more cost effective than their rhenium and osmium forbearers.<sup>61</sup> The reactivity of Group 6-based complexes with polycyclic aromatic hydrocarbons, arenes with electron donating groups and heterocycle aromatics has been investigated extensively.<sup>64-68</sup>

In contrast to the well documented reactivity with fused benzene systems and electron-rich aromatics, the ability of molybdenum and tungsten dearomatization fragments

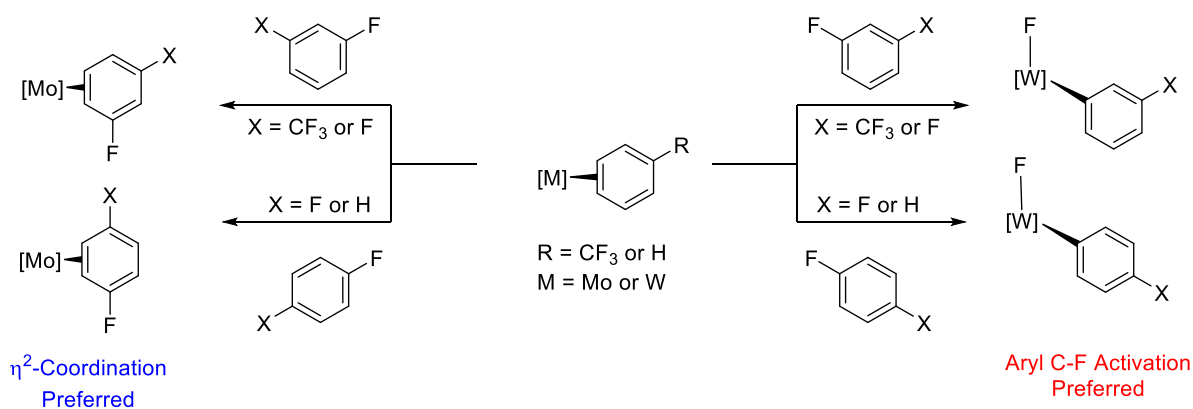


**Scheme 1.12** A low-yielding tandem addition product enabled by the tungsten-promoted dearomatization of benzene before a thorough report by Wilson et al in 2019.

to promote reactivity on benzene or electron deficient benzene derivatives is relatively unexplored. For the complex  $\text{WTP}(\text{PMe}_3)(\text{NO})(\eta^2\text{-benzene})$ , the benzene ligand is electron rich and capable of undergoing Diels-Alder reactions. However, exposure to electrophiles largely resulted in deleterious oxidation of the metal center.<sup>69</sup> Although a versatile exchange synthon, only a single low-yielding 1,4-cyclohexadiene product had been realized by the tungsten promoted dearomatization of benzene until a report by Dr. Katy Wilson in 2019 (**Scheme 1.12**).<sup>70-71</sup> Preliminary data for the molybdenum complex indicated that the second row dearomatization agent would be insufficiently  $\pi$ -basic to form a thermally stable  $\eta^2$ -bond with benzene.<sup>58</sup> The development of molybdenum and tungsten-enabled dearomatization of benzene will be examined in this work. The ability for tungsten and molybdenum to bind benzene and promote novel reactivity is presented in Chapters 2, 3, 5 and 8.

Another under-investigated class of aromatics in the context of dihapto-based dearomatization are benzenes with electron withdrawing groups (EWGs). The initial reluctance to explore the reactivity of electron deficient arenes developed around concerns that the deactivating nature of the EWG on the aromatic ring would be at odds with the electron donation properties of the metal. Furthermore, many EWGs feature  $\pi$ -bonds which could compete with metal coordination of the aromatic ring.<sup>72</sup> Additionally, an earlier investigation of the tungsten-based fragment with fluorinated aromatics found that the tungsten often preferentially activates aryl-C-F bonds over dihapto-coordination.<sup>73</sup> While mechanistically interesting, such complexes are not amenable to dihapto-based dearomatization after the oxidative addition has occurred (**Scheme 1.13**).

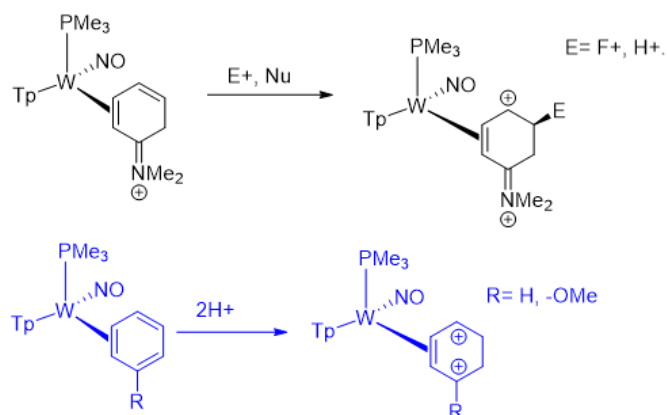
An important exception to this is in the ability of trifluorotoluene to form stable dihapto-coordinate adduct with both tungsten and molybdenum scaffolds. This coordination mode was exploited by both Dr. Jeffery Myers and Dr. Katy Wilson in the molybdenum and tungsten-enabled dearomatization of trifluorotoluene to generate novel trifluoromethylated cyclohexadiene and cyclohexene products.<sup>74-75</sup> This success led us to query what other EWGs could be tolerated by either the molybdenum or tungsten fragments. This chemistry is presented in Chapter 6.



**Scheme 1.13:** Propensity of  $\{\text{WTp}(\text{NO})(\text{PMe}_3)\}$  to oxidatively add across aryl C-F bonds. Exposing the same aromatics with  $\{\text{MoTp}(\text{NO})(\text{DMAP})\}$  results in exclusive dihapto-coordinate arene complexes.

The ability for tungsten to form stable complexes with a variety of electron-deficient species prompted us to query whether or not an electron-rich arene would be able to support a double protonation to generate a dicationic  $\pi$ -ligand. This reactivity was observed previously with exceptionally electron-rich complexes of *N,N*-dimethylaniline (**Scheme 1.14**).<sup>76</sup> Reports on extending this methodology for tungsten-anisole complexes are presented in Chapter 7. The double protonation of benzene is presented in Chapter 8.

Finally, Chapter 9 details the development of the  $P(n\text{-Bu})_3$  ligand as a cost-efficient alternative to the  $\text{PMe}_3$  ligand initially developed on the tungsten scaffold. We report on the ability of the  $\{\text{WTp}(\text{NO})\text{P}(n\text{-Bu})_3\}$  synthon to form dihapto-coordinate complexes with a variety of unsaturated ligands. The



**Scheme 1.14:** The double protonation of an aniline derivative enabled by coordination to an electron-rich metal scaffold (top) and proposed reactivity to extend the double protonation to anisole and benzene (bottom).

resulting metal-arene complexes are destabilized compared to their  $\text{PMe}_3$ -supported analogs.

Notably, for molecules highly stabilized by aromaticity (i.e. benzene,  $\alpha, \alpha, \alpha$ -trifluorotoluene, anisole), a significant amount of C-H activated product is shown to be in equilibrium with the  $\eta^2$ -isomer. The prevalence of C-H activated species appears to decrease as the associated aromatic character of the ligand decreases. These results are consistent with a previous report detailed by Jones and co-workers on the  $\eta^2$ :aryl hydride equilibrium associated with an electron rich rhodium fragment.<sup>77</sup> Extensive computational work by Anna Schouten under the guidance of Dr. Daniel Ess at Brigham Young University is presented that evaluates the mechanisms associated with this novel equilibrium; which investigates the intermediates between

the oxidative addition and reductive elimination products.

In essence, the heart of this thesis demonstrates that the molybdenum and tungsten scaffolds are more potent  $\pi$ -bases than originally thought and that novel reactivity can be realized by systematic alteration of reaction conditions.

The success with the double protonation of

benzene and anisole suggests that double-

protonation may serve as a general procedure for

a wide variety of aromatic ligands. Additionally,

the metal is able to selectively control the

integration of electrophilic and nucleophilic

reagents with markedly high degree of control.

An excellent illustration is the selective reduction

of benzene to cyclohexene using sequential sources of cationic and anionic deuterium sources.

This reaction was extensively examined with deuterium studies and extended to the synthesis of novel cyclohexene isotopologues and is presented in Chapter 3 (**Figure 1.8**).

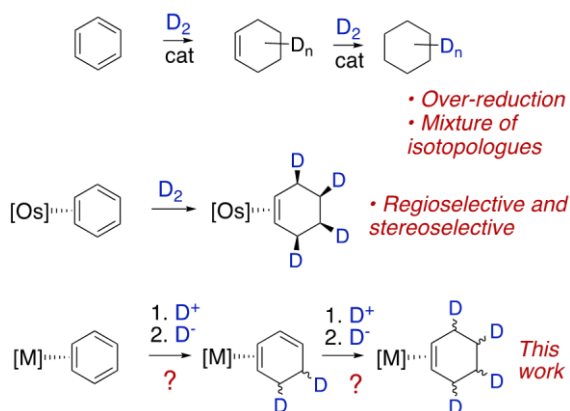


**Figure 1.8:** The generation of isotopologues of cyclohexene and existing limitations regarding chemo-control and selectivity (top), scope (middle) and a proposed investigation with  $M = \text{WTp}(\text{NO})(\text{PMe}_3)(\eta^2\text{-benzene})$  (bottom).<sup>10,12</sup>

## References

1. McGuire, B. A.; Burkhardt, A. M.; Kalenskii, S.; Shingledecker, C. N.; Remijan, A. J.; Herbst, E.; McCarthy, M. C., Detection of the aromatic molecule benzonitrile ( $\text{C}_6\text{H}_5\text{CN}$ ) in the interstellar medium. *Science* **2018**, *359* (6372), 202.
2. Smith, K. T., A specific interstellar aromatic molecule. *Science* **2018**, *359* (6372), 172.
3. Bingham, T. W.; Hernandez, L. W.; Olson, D. G.; Svec, R. L.; Hergenrother, P. J.; Sarlah, D., Enantioselective Synthesis of Isocarbostyryl Alkaloids and Analogs Using Catalytic Dearomatative Functionalization of Benzene. *Journal of the American Chemical Society* **2019**, *141* (1), 657-670.
4. Chen, J.; Nielsen, R. J.; Goddard, W. A.; McKeown, B. A.; Dickie, D. A.; Gunnoe, T. B., Catalytic Synthesis of Superlinear Alkenyl Arenes Using a Rh(I) Catalyst Supported by a "Capping Arene" Ligand: Access to Aerobic Catalysis. *Journal of the American Chemical Society* **2018**, *140* (49), 17007-17018.
5. Giustra, Z. X.; Ishibashi, J. S. A.; Liu, S.-Y., Homogeneous metal catalysis for conversion between aromatic and saturated compounds. *Coordination Chemistry Reviews* **2016**, *314*, 134-181.
6. Kündig, E. P.; Pape, A., Dearomatization via  $\eta^6$ -Arene Complexes. In *Transition Metal Arene  $\pi$ -Complexes in Organic Synthesis and Catalysis*, Kündig, E. P., Ed. Springer Berlin Heidelberg: Berlin, Heidelberg, 2004; pp 71-94.
7. Nagahara, H.; Ono, M.; Konishi, M.; Fukuoka, Y., Partial hydrogenation of benzene to cyclohexene. *Applied Surface Science* **1997**, *121-122*, 448-451.
8. Wertjes, W. C.; Southgate, E. H.; Sarlah, D., Recent advances in chemical dearomatization of nonactivated arenes. *Chemical Society Reviews* **2018**, *47* (21), 7996-8017.
9. Jia, X.; Foley, A. M.; Liu, C.; Vaughan, B. A.; McKeown, B. A.; Zhang, S.; Gunnoe, T. B., Styrene Production from Benzene and Ethylene Catalyzed by Palladium(II): Enhancement of Selectivity toward Styrene via Temperature-dependent Vinyl Ester Consumption. *Organometallics* **2019**, *38* (19), 3532-3541.
10. Harman, W. D.; Taube, H., The selective hydrogenation of benzene to cyclohexene on pentaammineosmium(II). *Journal of the American Chemical Society* **1988**, *110* (23), 7906-7907.
11. Lovering, F.; Bikker, J.; Humblet, C., Escape from Flatland: Increasing Saturation as an Approach to Improving Clinical Success. *Journal of Medicinal Chemistry* **2009**, *52* (21), 6752-6756.
12. Joannou, M. V.; Bezdek, M. J.; Chirik, P. J., Pyridine(diimine) Molybdenum-Catalyzed Hydrogenation of Arenes and Hindered Olefins: Insights into Precatalyst Activation and Deactivation Pathways. *ACS Catalysis* **2018**, *8* (6), 5276-5285.
13. Gershoni-Poranne, R.; Stanger, A., Magnetic criteria of aromaticity. *Chemical Society Reviews* **2015**, *44* (18), 6597-6615.
14. Dauben, H. J.; Wilson, J. D.; Laity, J. L., Diamagnetic susceptibility exaltation as a criterion of aromaticity. *Journal of the American Chemical Society* **1968**, *90* (3), 811-813.
15. von Schleyer, P. R.; Jiao, H., What is aromaticity? In *Pure and Applied Chemistry*, 1996; Vol. 68, p 209.
16. Li, Z.-H.; Moran, D.; Fan, K.-N.; Schleyer, P. v. R.,  $\sigma$ -Aromaticity and  $\sigma$ -Antiaromaticity in Saturated Inorganic Rings. *The Journal of Physical Chemistry A* **2005**, *109* (16), 3711-3716.



17. Tsipis, A. C.; Kefalidis, C. E.; Tsipis, C. A., The Role of the 5f Orbitals in Bonding, Aromaticity, and Reactivity of Planar Isocyclic and Heterocyclic Uranium Clusters. *Journal of the American Chemical Society* **2008**, *130* (28), 9144-9155.
18. Zhai, H.-J.; Averkiev, B. B.; Zubarev, D. Y.; Wang, L.-S.; Boldyrev, A. I.,  $\delta$  Aromaticity in [Ta<sub>3</sub>O<sub>3</sub>]<sup>-</sup>. *Angewandte Chemie International Edition* **2007**, *46* (23), 4277-4280.
19. Huang, X.; Zhai, H.-J.; Kiran, B.; Wang, L.-S., Observation of d-Orbital Aromaticity. *Angewandte Chemie International Edition* **2005**, *44* (44), 7251-7254.
20. Buijink, J. K. F.; Lange, J.-P.; Bos, R.; Horton, A. D.; Niele, F. G. M., Propylene Epoxidation via Shell's SMPO Process. 2008; pp 355-371.
21. Cypres, R.; Braekman-Danheux, C.; Delaunois, C.; Halloin, V., Aromatisation of 1,3-butadiene under pressure. *Thermochimica Acta* **1991**, *179*, 99-107.
22. Pop, G.; Musca, G.; Maria, G.; Straja, S.; Mihail, R., Selective methanol conversion to BTX. *Industrial & Engineering Chemistry Product Research and Development* **1986**, *25* (2), 208-213.
23. Biffis, A.; Centomo, P.; Del Zotto, A.; Zecca, M., Pd Metal Catalysts for Cross-Couplings and Related Reactions in the 21st Century: A Critical Review. *Chemical Reviews* **2018**, *118* (4), 2249-2295.
24. Uehling, M. R.; King, R. P.; Krska, S. W.; Cernak, T.; Buchwald, S. L., Pharmaceutical diversification via palladium oxidative addition complexes. *Science* **2019**, *363* (6425), 405.
25. Campbell, M. G.; Ritter, T., Late-Stage Fluorination: From Fundamentals to Application. *Organic Process Research & Development* **2014**, *18* (4), 474-480.
26. Yerien, D. E.; Bonesi, S.; Postigo, A., Fluorination methods in drug discovery. *Organic & Biomolecular Chemistry* **2016**, *14* (36), 8398-8427.
27. Gillis, E. P.; Eastman, K. J.; Hill, M. D.; Donnelly, D. J.; Meanwell, N. A., Applications of Fluorine in Medicinal Chemistry. *Journal of Medicinal Chemistry* **2015**, *58* (21), 8315-8359.
28. Alonso, C.; Martínez de Marigorta, E.; Rubiales, G.; Palacios, F., Carbon Trifluoromethylation Reactions of Hydrocarbon Derivatives and Heteroarenes. *Chemical Reviews* **2015**, *115* (4), 1847-1935.
29. Furuya, T.; Kamlet, A. S.; Ritter, T., Catalysis for fluorination and trifluoromethylation. *Nature* **2011**, *473* (7348), 470-477.
30. Birch, A. J., 117. Reduction by dissolving metals. Part I. *Journal of the Chemical Society (Resumed)* **1944**, (0), 430-436.
31. The Birch Reduction of Aromatic Compounds. In *Organic Reactions*, pp 1-334.
32. Lei, P.; Ding, Y.; Zhang, X.; Adijiang, A.; Li, H.; Ling, Y.; An, J., A Practical and Chemoselective Ammonia-Free Birch Reduction. *Organic Letters* **2018**, *20* (12), 3439-3442.
33. Pham, H. Q.; Marks, M. J.
34. Shim, S. C.; Doh, C. H.; Kim, T. J.; Lee, H. K.; Kim, K. D., A new and convenient synthesis of N-substituted perhydroazepines from adipaldehyde and primary amines with tetracarbonylhydridoferrate, HFe(CO), as a selective reducing agent. *Journal of Heterocyclic Chemistry* **1988**, *25* (5), 1383-1385.
35. Zawilska, J. B., Methoxetamine – a novel recreational drug with potent hallucinogenic properties. *Toxicology Letters* **2014**, *230* (3), 402-407.
36. Sopko, M. A.; Ehret, M. J.; Grgas, M., Desvenlafaxine: Another “Me Too” Drug? *Annals of Pharmacotherapy* **2008**, *42* (10), 1439-1446.
37. Song, A.; Parker, K. A.; Sampson, N. S., Synthesis of Copolymers by Alternating ROMP (AROMP). *Journal of the American Chemical Society* **2009**, *131* (10), 3444-3445.

38. Sarkar, N.; Banerjee, A.; Nelson, S. G., [4 + 2] Cycloadditions of N-Alkenyl Iminium Ions: Structurally Complex Heterocycles from a Three-Component Diels–Alder Reaction Sequence. *Journal of the American Chemical Society* **2008**, *130* (29), 9222-9223.
39. Ungureanu, I.; Klotz, P.; Mann, A., Phenylaziridine as a Masked 1,3 Dipole in Reactions with Nonactivated Alkenes. *Angewandte Chemie International Edition* **2000**, *39* (24), 4615-4617.
40. Okumura, M.; Sarlah, D., Visible-Light-Induced Dearomatizations. *European Journal of Organic Chemistry* **2019**, n/a (n/a).
41. Zietlow, T. C.; Hopkins, M. D.; Gray, H. B., Electrochemistry of quadruply bonded molybdenum dimers. Evidence for metal-to-halide back-bonding. *Journal of the American Chemical Society* **1986**, *108* (26), 8266-8267.
42. Bottomley, F.; Nyburg, S. C., Molecular nitrogen as a ligand: the crystal structure of nitrogenpentaamineruthenium(II) dichloride. *Chemical Communications (London)* **1966**, (24), 897-898.
43. Senoff, C. V., The discovery of  $[\text{Ru}(\text{NH}_3)_5\text{N}_2]^{2+}$ : A case of serendipity and the scientific method. *Journal of Chemical Education* **1990**, *67* (5), 368.
44. Taube, H., Chemistry of ruthenium(II) and osmium(II) amines. In *Pure and Applied Chemistry*, 1979; Vol. 51, p 901.
45. Harman, W. D.; Fairlie, D. P.; Taube, H., Synthesis, characterization, and reactivity of the (.eta.2-acetone)pentaammineosmium(II) complex. *Journal of the American Chemical Society* **1986**, *108* (26), 8223-8227.
46. Harman, W. D.; Sekine, M.; Taube, H., Redox-promoted linkage isomerizations of aldehydes and ketones on pentaammineosmium. *Journal of the American Chemical Society* **1988**, *110* (8), 2439-2445.
47. Harman, W. D.; Taube, H., Reactivity of pentaammineosmium(II) with benzene. *Journal of the American Chemical Society* **1987**, *109* (6), 1883-1885.
48. Smith, H. G.; Rundle, R. E., The Silver Perchlorate-Benzene Complex,  $\text{C}_6\text{H}_6 \cdot \text{AgClO}_4$ , Crystal Structure and Charge Transfer Energy<sup>1</sup>. *Journal of the American Chemical Society* **1958**, *80* (19), 5075-5080.
49. Álvarez, M.; Urbano, J.; Fructos, M. R.; Álvarez, E.; Pérez, P. J., Copper(I)-Arene Complexes with a Sterically Hindered Tris(pyrazolyl)borate Ligand. *European Journal of Inorganic Chemistry* **2018**, *2018* (19), 2026-2030.
50. Dias, H. V. R.; Wang, Z.; Jin, W., Synthesis and Chemistry of [Hydrotris(3,5-bis(trifluoromethyl)pyrazolyl)borato]silver(I) Complexes. *Inorganic Chemistry* **1997**, *36* (27), 6205-6215.
51. Cordone, R.; Harman, W. D.; Taube, H., .pi.-Heterocyclic complexes of pentaammineosmium(II) and the metal-induced cycloaddition of pyrrole and maleic anhydride. *Journal of the American Chemical Society* **1989**, *111* (15), 5969-5970.
52. Harman, W. D.; Schaefer, W. P.; Taube, H., The regio- and stereospecific selective hydrogenation of .eta.2-coordinated arenes. *Journal of the American Chemical Society* **1990**, *112* (7), 2682-2685.
53. Harman, W. D.; Sekine, M.; Taube, H., Substituent effects on .eta.2-coordinated arene complexes of pentaammineosmium(II). *Journal of the American Chemical Society* **1988**, *110* (17), 5725-5731.
54. Harman, W. D.; Taube, H., Redox-coupled linkage isomerizations with .eta.2-coordinated anilines. *Journal of the American Chemical Society* **1988**, *110* (16), 5403-5407.

55. Myers, W. H.; Sabat, M.; Harman, W. D., Enamine character of a 2,3-eta<sup>2</sup>-coordinated pyrrole. *Journal of the American Chemical Society* **1991**, *113* (17), 6682-6683.
56. Chordia, M. D.; Smith, P. L.; Meiere, S. H.; Sabat, M.; Harman, W. D., A Facile Diels–Alder Reaction with Benzene: Synthesis of the Bicyclo[2.2.2]octene Skeleton Promoted by Rhenium. *Journal of the American Chemical Society* **2001**, *123* (43), 10756-10757.
57. Meiere, S. H.; Brooks, B. C.; Gunnoe, T. B.; Sabat, M.; Harman, W. D., A Promising New Dearomatization Agent: Crystal Structure, Synthesis, and Exchange Reactions of the Versatile Complex TpRe(CO)(1-methylimidazole)(η<sup>2</sup>-benzene) (Tp = Hydridotris(pyrazolyl)borate). *Organometallics* **2001**, *20* (6), 1038-1040.
58. Surendranath, Y.; Harman, W. D., The role of electrochemistry in the development of π-basic dearomatization agents. *Dalton Transactions* **2006**, (33), 3957-3965.
59. Brooks, B. C.; Brent Gunnoe, T.; Dean Harman, W., Dihapto binding of aromatic molecules by π-basic transition metal complexes: development of alternatives to the {Os(NH<sub>3</sub>)<sub>5</sub>}<sup>2+</sup> fragment. *Coordination Chemistry Reviews* **2000**, *206-207*, 3-61.
60. Trofimenko, S., Boron-Pyrazole Chemistry. *Journal of the American Chemical Society* **1966**, *88* (8), 1842-1844.
61. Liebov, B. K.; Harman, W. D., Group 6 Dihapto-Coordinate Dearomatization Agents for Organic Synthesis. *Chemical Reviews* **2017**, *117* (22), 13721-13755.
62. Meiere, S. H.; Keane, J. M.; Gunnoe, T. B.; Sabat, M.; Harman, W. D., Binding and Activation of Aromatic Molecules by a Molybdenum π-Base. *Journal of the American Chemical Society* **2003**, *125* (8), 2024-2025.
63. Ha, Y.; Dilsky, S.; Graham, P. M.; Liu, W.; Reichart, T. M.; Sabat, M.; Keane, J. M.; Harman, W. D., Development of Group 6 Dearomatization Agents. *Organometallics* **2006**, *25* (21), 5184-5187.
64. Strausberg, L.; Li, M.; Harrison, D. P.; Myers, W. H.; Sabat, M.; Harman, W. D., Exploiting the o-Quinodimethane Nature of Naphthalene: Cycloaddition Reactions with η<sup>2</sup>-Coordinated Tungsten–Naphthalene Complexes. *Organometallics* **2013**, *32* (3), 915-925.
65. Myers, J. T.; Shivokevich, P. J.; Pienkos, J. A.; Sabat, M.; Myers, W. H.; Harman, W. D., Synthesis of 2-Substituted 1,2-Dihydronaphthalenes and 1,2-Dihydroanthracenes Using a Recyclable Molybdenum Dearomatization Agent. *Organometallics* **2015**, *34* (14), 3648-3657.
66. Kosturko, G. W.; Graham, P. M.; Myers, W. H.; Smith, T. M.; Sabat, M.; Harman, W. D., Tungsten-Promoted Diels–Alder Cycloaddition of Pyridines: Dearomatization of 2,6-Dimethoxypyridine Generates a Potent 2-Azadiene Synthone. *Organometallics* **2008**, *27* (17), 4513-4522.
67. Todd, M. A.; Sabat, M.; Myers, W. H.; Harman, W. D., [2+2] Cycloaddition Reactions with a Tungsten-Stabilized 2H-Phenol. *Journal of the American Chemical Society* **2007**, *129* (36), 11010-11011.
68. Surendranath, Y.; Welch, K. D.; Nash, B. W.; Harman, W. H.; Myers, W. H.; Harman, W. D., Tungsten-Promoted Dearomatization of Heterocycles: Uncovering the Latent 2-Azadiene Character of Pyrimidines. *Organometallics* **2006**, *25* (25), 5852-5853.
69. Graham, P. M.; Meiere, S. H.; Sabat, M.; Harman, W. D., Dearomatization of Benzene, Deamidization of N,N-Dimethylformamide, and a Versatile New Tungsten π Base. *Organometallics* **2003**, *22* (22), 4364-4366.
70. Ding, F.; Harman, W. D., Stereoselective Tandem 1,4-Addition Reactions for Benzenes: A Comparison of Os(II), Re(I), and W(0) Systems. *Journal of the American Chemical Society* **2004**, *126* (42), 13752-13756.

71. Wilson, K. B.; Smith, J. A.; Nedzbala, H. S.; Pert, E. K.; Dakermanji, S. J.; Dickie, D. A.; Harman, W. D., Highly Functionalized Cyclohexenes Derived from Benzene: Sequential Tandem Addition Reactions Promoted by Tungsten. *The Journal of Organic Chemistry* **2019**, *84* (10), 6094-6116.
72. Lis, E. C.; Delafuente, D. A.; Lin, Y.; Mocella, C. J.; Todd, M. A.; Liu, W.; Sabat, M.; Myers, W. H.; Harman, W. D., The Uncommon Reactivity of Dihapto-Coordinated Nitrile, Ketone, and Alkene Ligands When Bound to a Powerful  $\pi$ -Base. *Organometallics* **2006**, *25* (21), 5051-5058.
73. Liu, W.; Welch, K.; Trindle, C. O.; Sabat, M.; Myers, W. H.; Harman, W. D., Facile Intermolecular Aryl-F Bond Cleavage in the Presence of Aryl C-H Bonds: Is the  $\eta^2$ -Arene Intermediate Bypassed? *Organometallics* **2007**, *26* (10), 2589-2597.
74. Myers, J. T.; Smith, J. A.; Dakermanji, S. J.; Wilde, J. H.; Wilson, K. B.; Shivokevich, P. J.; Harman, W. D., Molybdenum(0) Dihapto-Coordination of Benzene and Trifluorotoluene: The Stabilizing and Chemo-Directing Influence of a CF<sub>3</sub> Group. *Journal of the American Chemical Society* **2017**, *139* (33), 11392-11400.
75. Wilson, K. B.; Myers, J. T.; Nedzbala, H. S.; Combee, L. A.; Sabat, M.; Harman, W. D., Sequential Tandem Addition to a Tungsten-Trifluorotoluene Complex: A Versatile Method for the Preparation of Highly Functionalized Trifluoromethylated Cyclohexenes. *Journal of the American Chemical Society* **2017**, *139* (33), 11401-11412.
76. Salomon, R. J.; Todd, M. A.; Sabat, M.; Myers, W. H.; Harman, W. D., Single and Double Electrophilic Addition Reactions to the Aniline Ring Promoted by a Tungsten  $\pi$ -Base. *Organometallics* **2010**, *29* (4), 707-709.
77. Chin, R. M.; Dong, L.; Duckett, S. B.; Partridge, M. G.; Jones, W. D.; Perutz, R. N., Control of  $\eta^2$ -coordination vs. carbon-hydrogen bond activation by rhodium: the role of aromatic resonance energies. *Journal of the American Chemical Society* **1993**, *115* (17), 7685-7695.

# Chapter 2

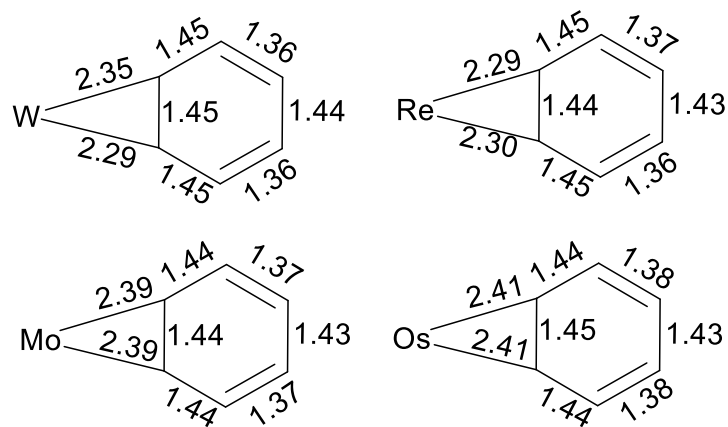
## Studies of $\text{W Tp}(\text{NO})(\text{PMe}_3)(\eta^2\text{-benzene})$

## 2.1 Introduction

Electron-rich metal complexes based on osmium, rhenium and tungsten have dearomatized benzene.<sup>1-4</sup> Structural data obtained from single crystal X-Ray diffraction (SCXRD) shows significant distortion of the benzene ring upon its complexation to the metal fragments {Wtp(PMe<sub>3</sub>)(NO)}, {ReTp(MeIm)(CO)} and {Os(NH<sub>3</sub>)<sup>2+</sup>} (Figure 2.1). Some of these changes include elongation of the metal-bound alkene carbons and distortion of the dihapto-bound carbons to become more sp<sup>3</sup>-like in character. Additionally, the resonances associated with the bound benzene carbons observed via <sup>13</sup>C NMR spectra are shifted upfield (~ 60-70 ppm) compared to that observed for free benzene (128 ppm).

The resonances in the <sup>1</sup>H NMR spectra corresponding to the protons attached to the metal-bound carbons are significantly shifted upfield as well. These spectroscopic features can be attributed to disruption of ring-

anisotropy for the metal-bound alkene carbons. Alternatively, these atoms may be shifted upfield in the NMR spectra as



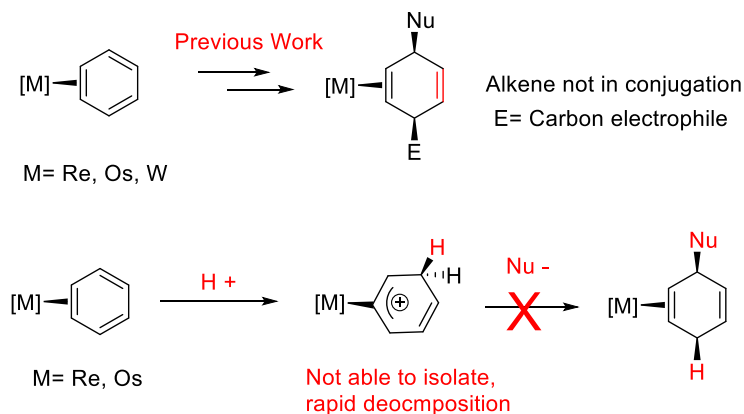
a result of significant electron donation from metal to the  $\eta^2$ -bound carbons (shielding).

Once dearomatized, the benzene ring behaves similarly to an electron-rich diene. Various cycloaddition products have been synthesized after treating these heavy metal benzene complexes

**Figure 2.5:** Distortions of benzene observed upon complexation to various dearomatization scaffolds. Distances derived from X-ray diffraction for the osmium, rhenium and tungsten complexes. For molybdenum, numbers are from DFT calculations. Here W = {Wtp(PMe<sub>3</sub>)(NO)}, Re = {ReTp(MeIm)(CO)}, Mo = {MoTp(4-DMAP)(NO)}, Os = {Os(NH<sub>3</sub>)<sub>5</sub>}<sup>2+</sup>.

with dienophiles.<sup>1,5</sup> The ability to perform tandem addition reactions (sequential addition of electrophiles and nucleophiles) on the benzene ring has been more difficult to attain.

The higher oxidation state  $\{\text{Os}(\text{NH}_3)_5(\eta^2\text{-benzene})\}^{2+}$  complex has difficulty sustaining protonation on the benzene ring. Its conjugate acid,  $\{\text{Os}(\text{NH}_3)_5(\eta^3\text{-benzenium})\}^{3+}$ , decomposes at temperatures above -40



°C. Upon exposure to nucleophiles, the osmium-benzenium deprotonates or otherwise undergoes oxidative decomposition.<sup>6-7</sup> Studies utilizing various acid sources give an approximate pKa ~ -8 for  $\{\text{Os}(\text{NH}_3)_5(\eta^3\text{-benzenium})\}^{3+}$ .

**Figure 6.2.** Limitations of previously reported tandem addition reaction on various heavy metal benzene complexes. Here W =  $\{\text{WTp}(\text{PMe}_3)(\text{NO})\}$ , Re =  $\{\text{ReTp}(\text{MeIm})(\text{CO})\}$ , Mo =  $\{\text{MoTp}(4\text{-DMAP})(\text{NO})\}$ , Os =  $\{\text{Os}(\text{NH}_3)_5\}^{2+}$ .

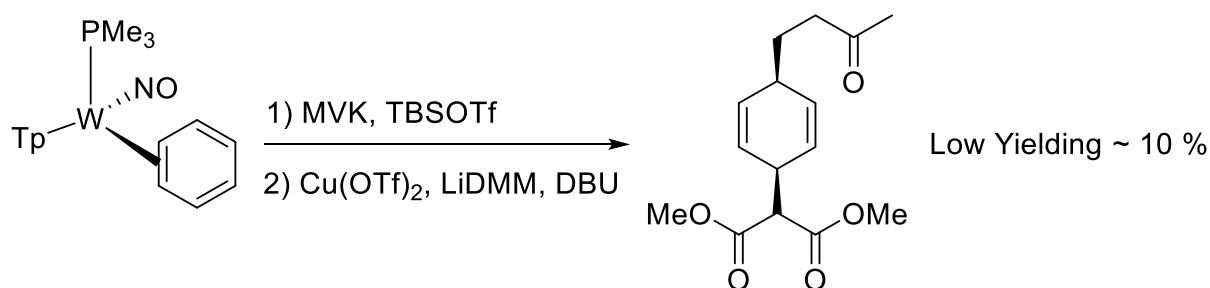
The  $\text{ReTp}(\text{BuIm})(\text{CO})(\eta^2\text{-benzene})$  system is better able to support protonation on the benzene ring. <sup>1</sup>H NMR data of  $\text{ReTp}(\text{BuIm})(\text{CO})(\eta^2\text{-benzene})$  dissolved in a methanesulfonic acid (pKa ~ -2.6) solution and recorded at -20 °C suggested the formation of an  $\eta^2$ -benzenium complex.<sup>6</sup> However, upon warming the solution to 20 °C, the only diamagnetic species observed was the  $\eta^2$ -allyl species  $\{\text{ReTp}(\text{BuIm})(\text{CO})(\eta^2\text{-C}_6\text{H}_9)^+\}$  (OTf<sup>-</sup>). The formation of this species was accompanied by the concomitant release of free benzene, indicating oxidative decomposition of the complex. Similar to the osmium system, treating rhenium-benzene with nucleophiles led to deprotonation or oxidative decomposition.

The tungsten-analog  $\text{WTp}(\text{PMe}_3)(\text{NO})(\eta^2\text{-benzene})$  (**1**) decomposes in an analogous manner to  $\text{ReTp}(\text{BuIm})(\text{CO})(\eta^2\text{-benzene})$  when treated with a strong acid. That is, if **1** is treated with HOTf in

CH<sub>3</sub>CN at -40 °C, the  $\eta^2$ -allyl complex {WTp(PMe<sub>3</sub>)(NO)( $\eta^2$ -C<sub>6</sub>H<sub>9</sub>)<sup>+</sup>} (OTf<sup>-</sup>) (**2**) is the only observed diamagnetic species.<sup>8</sup> Speculation for this mechanism is provided *vide infra*.

The ability to protonate and add nucleophiles to the benzene ring with various classes of 3<sup>rd</sup> row dearomatization agents was originally unsuccessful.<sup>9</sup> However, treating benzene complexes of osmium and rhenium with carbon electrophiles proved to be more promising. In these cases, carbon electrophiles followed by a nucleophile (tandem addition) led to diverse 1,4-cyclohexadiene products in moderate to good yield.<sup>9</sup> After this addition sequence however, the remaining alkene bond, no longer in conjugation with the metal, was unable to undergo further metal-mediated reactivity (**Figure 2.2**).

In contrast to the results with Re and Os, reactions of the tungsten analog **1** with carbon electrophiles were largely unsuccessful. Only a single, low-yielding 1,4-cyclohexadiene product was realized and its synthesis required use of an oxidant (**Scheme 2.1**).<sup>9</sup> The unproductive reactivity of the tungsten-benzene complex with carbon electrophiles may be attributed to the more negative oxidation potential of the tungsten-benzene complex, compared to its rhenium and osmium forbearers.<sup>1</sup> As such, the addition of carbon electrophiles to the tungsten-benzene complex is still an unmet challenge.



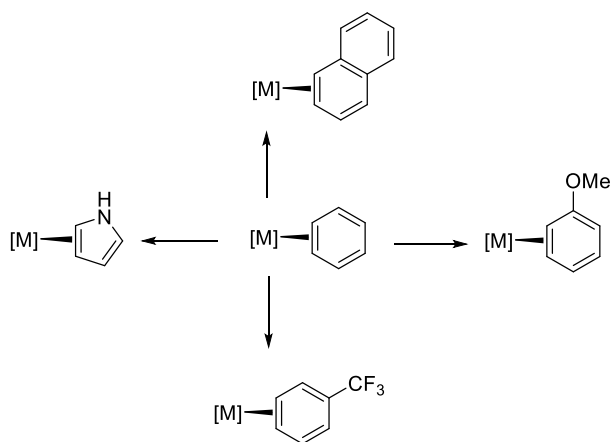
**Scheme 2.1.** Low-yielding process synthesizing a novel 1,4-cyclohexadiene derivative from the tungsten-enabled dearomatization of benzene.

Until recently, the main synthetic utility of **1** was in accessing a labile aromatic ligand that could readily undergo ligand substitution reactions. Allowing **1** to stir with a variety of unsaturated ligands



leads to disassociation of the benzene and coordination of the new  $\pi$ -ligand (**Scheme 2.2**).<sup>1-3</sup>

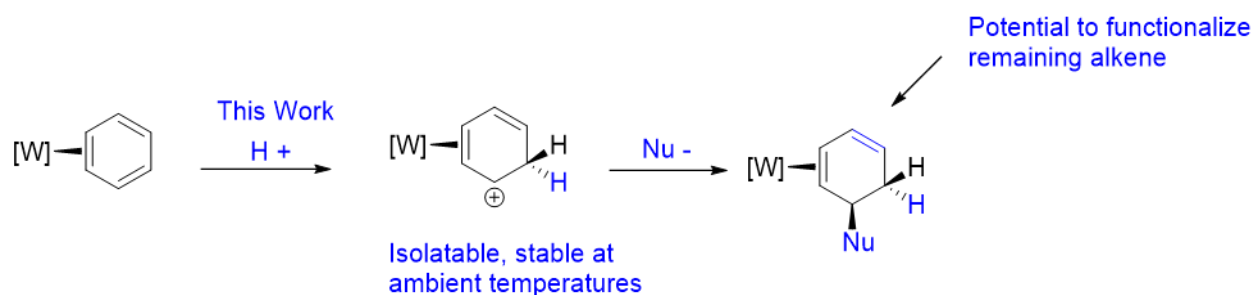
<sup>10</sup> The mild conditions needed for ligand substitution allow for the coordination of aromatic ligands whose functionalities would be incompatible with sodium. Sodium is needed to reduce the dearomatization synthon  $\text{WTP}(\text{NO})(\text{PMe}_3)(\text{Br})$  to a tungsten (0)



**Scheme 2.2.** Here  $M = \{\text{WTP}(\text{PMe}_3)(\text{NO})\}$ ,  $\{\text{ReTP}(\text{MeIm})(\text{CO})\}$  or  $\{\text{Os}(\text{NH}_3)_5\}^{2+}$ .

oxidation state, which is then capable of dihapto-coordinating aromatic molecules upon dissociation of the labile bromide ligand. Similar ligand substitution methodologies have been employed to expand the substrate scope for osmium and rhenium-enabled dearomatization.

There are many facets of the tungsten system that suggest it may be an even more activating  $\pi$ -base than rhenium or osmium. Studies that attempt to establish various metrics of  $\pi$ -basicity are presented below. Additionally, the synthesis of an electron-deficient benzenium ligand derived from **1** is explored in this chapter.



**Scheme 2.3.** Generation of a 1,3-cyclohexadiene ligand from the tungsten-mediated dearomatization of benzene.

## 2.2 Fluxional Behavior of $\text{WTP}(\text{PMe}_3)(\text{NO})(\eta^2\text{-benzene})$ via NMR Studies

Initial data suggested that **1** is more electron-rich than its rhenium and osmium-benzene counterparts. The oxidation potential associated with **1**, determined by cyclic voltammetry (sweep rate 100 mV/s), is more negative than that of  $\text{Os}(\text{NH}_3)_5(\eta^2\text{-benzene})^{2+}$  or  $\text{ReTP}(\text{MeIm})(\text{CO})(\eta^2\text{-$

benzene).<sup>10</sup> Additionally, both the tungsten and rhenium-benzene complexes are able to undergo cycloaddition reactions with N-methylmaleimide (NMM). The rate of cycloaddition associated with **1** however is ~ four times faster than for the rhenium-analog. The osmium-benzene adduct is unable to engender analogous reactivity. Taken together, these data suggest that the fragment {WTP(NO)(PMe<sub>3</sub>)} is a more activating  $\pi$ -base than either the osmium or rhenium fragments.

The benzene ligand of osmium, rhenium and tungsten complexes can undergo ligand substitution with another aromatic ligand on a practical synthetic timeframe (1-2 days).<sup>2,5</sup> The substitution half-life ( $t_{1/2}$ ) associated with benzene dissociation for **1** is ~ 1.1 hours in acetone solution under pseudo-first order conditions at ambient temperatures. The substitution rate of the rhenium-benzene complex is  $t_{1/2} = 2$  hours and osmium-benzene  $t_{1/2} = 8$  hours under analogous conditions.<sup>1</sup>

These data initially appear contradictory to the order of claimed  $\pi$ -basicity ( $W > Re > Os$ ). That is, if the metal-benzene bond is primarily contingent on  $\pi$ -back-donation from metal to benzene, then the superior  $\pi$ -base would result in a more stable metal-arene bond. This fortified bonding interaction would lead to a less labile benzene ligand. We propose that for the higher oxidation state complexes of rhenium and osmium, the  $\sigma$ -bonding component (donation from the  $\pi$ -bond of the aromatic to the metal) is a more significant stabilizing interaction for metal-ligand bonding than for the tungsten analog. The different steric profiles across these third-row systems may play a significant role as well, though a rigorous treatment of these steric parameters is not pursued here.

In order to assess another metric that could be a more reliable indicator of  $\pi$ -basicity, dynamic NMR experiments were pursued to determine the  $\Delta G^\ddagger$  for the ring-walk process observed for **1**. Evidence for such a process is apparent in <sup>1</sup>H NMR spectra of **1** at ambient temperatures. These spectra reveal six broadened proton resonances associated with the benzene ring, indicating that a

fluctuational process is operative on the timescale of the NMR experiment. Variable temperature experiments show the impact of temperature on this process and the results are illustrated in **Figure 2.3**.

Dynamic  $^1\text{H}$  NMR techniques were utilized and the barrier to the ring-walking process associated with **1** is estimated to be  $\sim 15.1$  kcal/mol. This is a higher barrier to isomerization ( $\Delta G^\ddagger$ ) than that measured for  $\text{ReTp}(\text{NO})(\text{MeIm})(\text{benzene})$  (14.5 kcal/mol) and  $\text{Os}(\text{NH}_3)_5(\eta^2\text{-benzene})^{2+}$  (12.5 kcal/mol).<sup>4, 10</sup> Credit is given to Mary Shingler for successfully reproducing these variable temperature experiments on **1**. Tangentially, analogous experiments were performed on the recently realized molybdenum-benzene adduct (the synthesis of which is detailed in Chapter 5). These experiments reveal a  $\Delta G^\ddagger$  for ring walk isomerization of 13.8 kcal/mol for the molybdenum-benzene adduct.<sup>4</sup>

Taken together, initial electrochemical measurements and the lower oxidation state of the tungsten fragment suggest that it could be a superior  $\pi$ -base to the osmium or rhenium analogs. In terms of reactivity, the benzene ligand is activated toward reactivity with dienophiles once bound to the tungsten metal. An apparent discrepancy arises in the enhanced substitution rate of the benzene ligand once bound to tungsten compared to rhenium and osmium.

To rationalize discrepancies in observed substitution rates, the role of  $\sigma$ -donation from benzene to metal potentially conflates the ability of substitution rates to act as a metric of  $\pi$ -basicity.

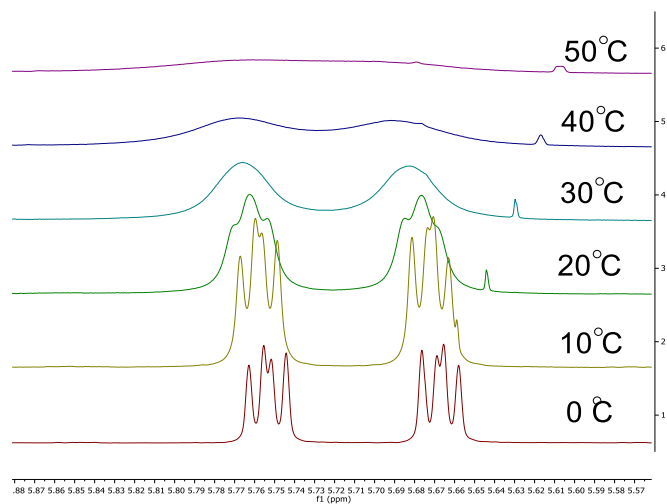


**Figure 2.3:** Fluctuational behavior displayed by two benzene proton resonances of **1** at temperatures ranging from 0 to 50 °C.

Additionally, the use of electrochemistry in glean information about the sensitivity of these metal-benzene complexes toward oxidation is limited due to the chemically irreversible nature of the oxidation process. That is, the chemically irreversibility fails to maintain the equilibrium conditions of the Nernst Equation, and thus the observed  $E_{p,a}$  for all of these metal-benzene complexes are more positive than their theoretical  $E_{1/2}$  values.<sup>11</sup>

Given these limitations, the  $\Delta G^\ddagger$  associated with ring isomerization may be a better metric in establishing a relative order of  $\pi$ -basicity. We postulate that the stabilization of the dihapto-bound benzene due to  $\pi$ -backdonation is reflected in these barriers. A slower isomerization rate therefore correlates better to the role of  $\pi$ -basicity of the metal fragment.

With these data, the  $\Delta G^\ddagger$  to ring isomerization follows the order W>Re>Mo>Os. As mentioned *vide supra*, we propose that this is a better metric with which to gauge the  $\pi$ -basicity of these different dearomatization systems. In the case of the third row heavy metal systems, this trend is also reflected for pKa estimates of the conjugate acids of these metal-benzene adducts as will be seen *vide infra*.<sup>6</sup>

In addition to the differences in the  $\Delta G^\ddagger$  associated with ring isomerization, the complex **1** is also in equilibrium with a small amount of the tungsten hydride species WTp(PMe<sub>3</sub>)(NO)(H)(Ph) (**1H**). The population of this species is temperature and solvent dependent, but in general represents < 10% of the total isomer composition of **1** observed in solution. The formation of analogous metal-hydride species derived from benzene is not observed for the related osmium, rhenium or molybdenum benzene complexes.

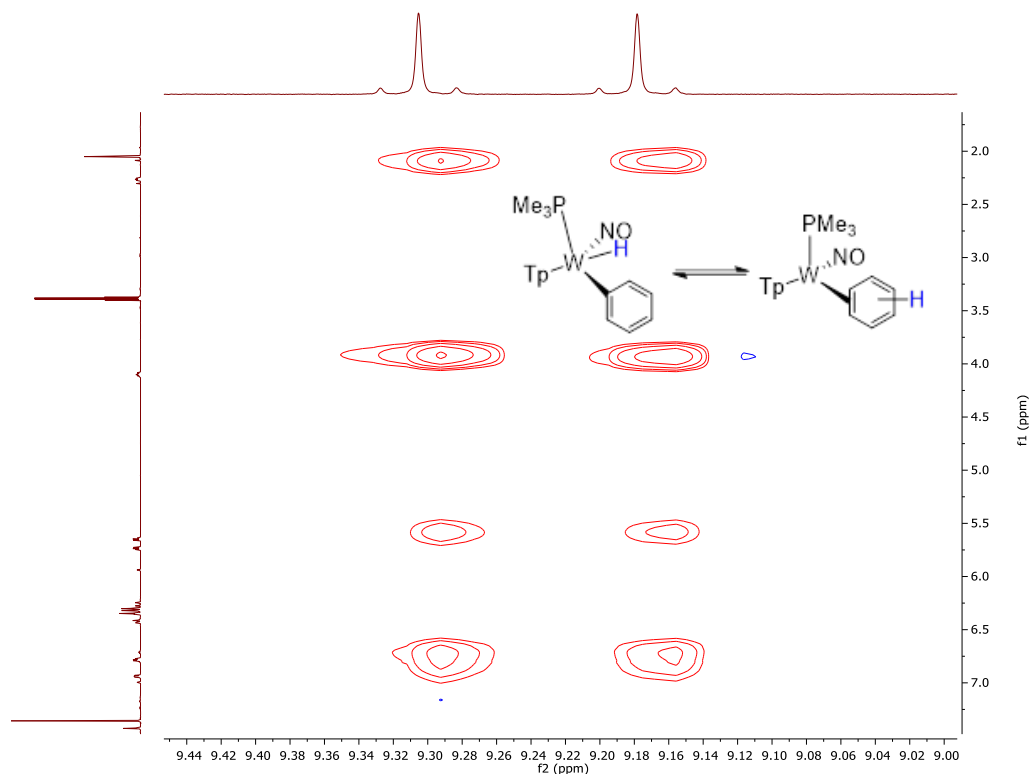


**Figure 2.4.** Fluctional behavior that shows proton exchange between the tungsten-hydride resonance of **1H** and the protons on the dihapto-coordinate form **1** on the timescale of an NOESY NMR experiment at 0 °C. Here the red resonances indicated the proton exchange and the resonances are split by the  $^{31}\text{P}$  nuclei of the phosphine ligand.

NOESY experiments at reduced temperatures (0 °C) reveal a dynamic process where the tungsten-hydride resonance of **1H** is able to exchange with every proton position on the dihapto-coordinate isomer form on the timescale of the NMR experiment. This suggests that one possible mechanism for ring isomerization involves sequential C-H activation of the metal-bound carbons. Upon C-H activation to generate **1H**, rotation about the newly formed metal-phenyl  $\sigma$ -bond can occur. Subsequent reductive elimination would lead to the regeneration of **1** (an overall “ring-flip” mechanism).

These data do not rule out another isomerization mechanism where the metal performs an intrafacial ring-wizzer without undergoing oxidative addition. The symmetry of the benzene ring makes these two potential mechanisms indistinguishable, and it is possible that both processes may

operative on the timescale of the NMR experiment. Intensive DFT studies pursued by Anna Schouten under the guidance of Professor Dan Ess at Brigham Young University examine these pathways in Chapter 9.

### 2.3 DFT Studies Estimating Dearomatization Across 3<sup>rd</sup> Row Dearomatization Agents

DFT studies were pursued to model the partial hydrogenation of benzene to form 1,3- and 1,4-cyclohexadienes. The energies of these molecules were compared with that of benzene and an equivalent of dihydrogen. The relative energies of these species were then evaluated upon complexation to various 3<sup>rd</sup> row dearomatization agents in silico. The summaries of these calculations are presented in **Figure 2.5**.

Unless otherwise specified, all DFT calculations in this chapter use optimized geometries calculated with the B3LYP method. The LANL2DZ basis set was used to describe the tungsten atom, and the 6-31G(d) basis set was utilized for all other “light” atoms. This combination has proved to be reliable for Os, Mo, Re, and W systems for binding energies, charge transfer processes, and optimized geometries.<sup>6, 12-13</sup> The energies of these models are the electronic energies associated with the system unless otherwise noted.

In cases where benzene and dihydrogen are modeled, the two chemical entities are enforced to being 15 angstroms apart in the in silico model to minimize non-covalent interactions. Notably, the energies associated with the formation of the free cyclohexadienes are nearly 6 kcal/mol higher in energy than an equivalent of benzene and dihydrogen (**Figure 2.5**). The higher energy associated with these systems is attributed to the aromatic resonance stability of the free benzene ring. Tangentially, we note that the 1,3- and 1,4-cyclohexadiene isomers are nearly degenerate in energy despite conjugation of the  $\pi$ -system in the 1,3-cyclohexadiene isomer. Previous reports have proposed that hyper-conjugation in the 1,4-cyclohexadiene isomer plays a significant role in

stabilizing the overall energy of this molecule.<sup>14</sup>

Modeling the third row metal-benzene adducts with an equivalent of dihydrogen was then pursued. The equivalent of dihydrogen was also constrained to being 15 angstroms away from the metal atom center. Further computational modeling was performed for various metal-cyclohexadiene complexes (**Figure 2.5**).

Modeling partial hydrogenation of the benzene while bound to the metal yields metal-cyclohexadiene complexes.

These complexes are lower energy systems than the partial hydrogenation of free benzene to either 1,3- or 1,4-

cyclohexadiene. That is, upon complexation to any of the electron rich metal, the electronic energy associated with the resulting cyclohexadiene complex (regardless of isomer) is lower than that of the metal-benzene complex and the equivalent of dihydrogen. This result is consistent with significant loss of aromatic stability associated with the benzene ring upon complexation to any of the third row dearomatization agents.

Modeling the metal-1,3-cyclohexadiene complexes of osmium, rhenium and tungsten illustrates differences in the  $\pi$ -backbonding ability between these metal systems. Namely, when the unbound alkene is in conjugation with the metal system, the tungsten complex

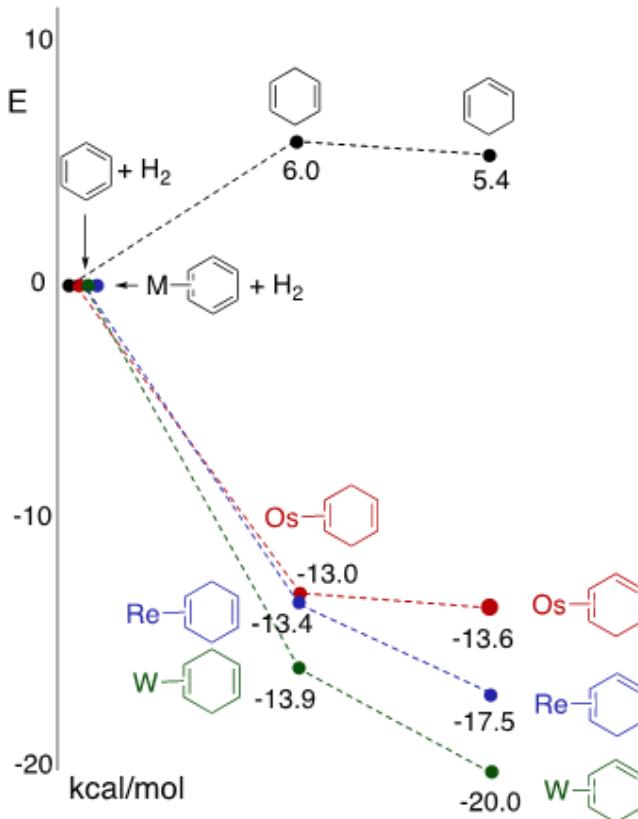


**Figure 2.5.** Comparison of relative energies showing the effects of partial hydrogenation of benzene as a free ligand (top) and once complexed to various 3<sup>rd</sup> row dearomatization metals. Here W={WTp(PMe<sub>3</sub>)(NO)}, Re = {ReTp(MeIm)(CO)} and Os = {Os(NH<sub>3</sub>)<sub>5</sub>}<sup>2+</sup>.

WTP(PMe<sub>3</sub>)(NO)( $\eta^2$ -1,3-cyclohexadiene) (**3**) is now the *relative* lowest energy system, followed by rhenium and osmium complexes of 1,3-cyclohexadiene. The tungsten metal is better able to  $\pi$ -backbond into the conjugated alkene bond compared to its rhenium and osmium counterparts *because it is a superior  $\pi$ -base*. This could also explain why complexation of the 1,4-cyclohexadiene isomer to tungsten, rhenium and osmium metals yields similar energies (a range of  $\sim 1$  kcal/mol) with WTP(PMe<sub>3</sub>)(NO)( $\eta^2$ -1,2-1,4-cyclohexadiene) (**4**) being the lowest energy isomer. Without an extended  $\pi$ -system to back-bond into, differences between the relative stabilities of these metal complexes are less pronounced.

While we do not rigorously address the steric factors that could attribute to the enhanced stability observed for the tungsten-benzene complex, a qualitative treatment can be made. Namely, the ammonia ligands associated with the osmium complex are probably less sterically demanding than the Tp or ancillary ligands (PMe<sub>3</sub>, methylimidazole) associated with the tungsten and rhenium complexes. Additionally, the cone-angle of the PMe<sub>3</sub> ligand is potentially more sterically encumbering than the planar methyl-imidazole (MeIm) ligand of rhenium. It is reasonable to extrapolate that the ligand set on tungsten may in fact be the most sterically demanding across all three systems. The fact that the tungsten-cyclohexadiene adduct is still more stable (determined by DFT methods) is a testament to the exceptional  $\pi$ -basicity of the tungsten fragment.

#### 2.4 Synthesis of WTP(PMe<sub>3</sub>)(NO)( $\eta^2$ -benzenium) (OTf-)

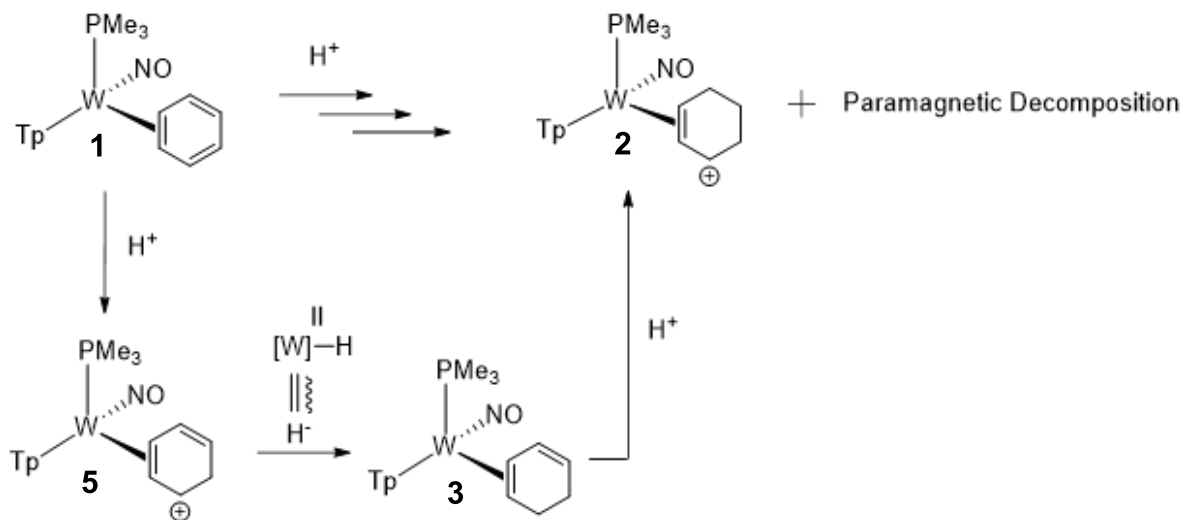
As mentioned *vide supra*, efforts to protonate **1** to generate WTP(PMe<sub>3</sub>)(NO)( $\eta^2$ -benzenium) (**5**) with strong acids were unsuccessful. The highly reducing metal center is sensitive to oxidation pathways that would pre-empt protonation of the benzene ring. Indeed, treatment of tungsten-benzene with strong acids (HOTf, methanesulfonic acid) even at reduced temperatures yields **2** in low yields. A proposed decomposition pathway is given in **Scheme 2.4** which would



account for the generation of **2**.

We speculate that after the initial protonation of the benzene ligand of **1** to generate the benzenium complex **5**, a hydride source adds to speculated intermediate **5** which ultimately leads to the tungsten-cyclohexadiene complex **3** after a presumable hydride addition. A hydridic proton source could arise from the in situ generation of a tungsten-hydride species that would arise from the formal two electron oxidation of the metal center.

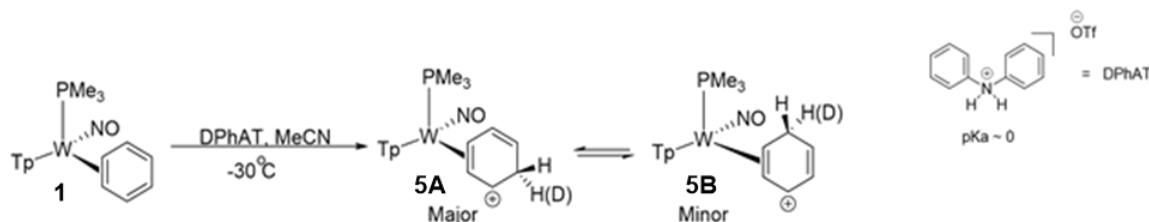
After the hydride addition, this would result in the transient formation of the tungsten-cyclohexadiene complex **3** which would be even more reactive toward protonation than the tungsten-benzene complex (enhanced  $\pi$ -backbonding from metal to the metal-cyclohexadiene  $\pi$ -ligand). Subsequent protonation would yield the tungsten-allyl complex **2**. The low mass recovery of the diamagnetic species **2** associated with this process (< 10%) can be explained by metal oxidation that generates an in situ derived hydride complex. After hydride delivery to **5**, the metal decomposes to paramagnetic material.



**Scheme 2.4.** Proposed decomposition pathway of **1** to **2** under acidic conditions. Mass recovery of **2** is generally low (< 10%) and significant paramagnetic decomposition accompanies its formation.

Following these results, **1** was treated with a series of weaker acid sources at variable temperatures (-30 °C to 25 °C). Gratifyingly, when **1** was treated with diphenylammonium triflate (DPhAT) in acetone-*d*<sub>6</sub> at -30 °C, frozen in N<sub>2</sub>(l) and observed at 0 °C by <sup>1</sup>H NMR, signals consistent with the formation of **5** were observed. A key spectral feature supporting protonation of the benzene ring geminal protons at 4.2 and 4.1 ppm which display strong coupling to one another (*J* = ~ 28 Hz). Repeating this experiment in MeCN-*d*<sub>3</sub> and DCM-*d*<sub>2</sub> showed similar features. Two benzenium isomers are observed in solution as depicted in **Scheme 2.5**.

Upon warming to room temperature in either DCM-*d*<sub>2</sub> or acetone-*d*<sub>6</sub>, rapid decomposition to uncharacterized paramagnetic materials was observed along with the concomitant release of free benzene. When a solution of the tungsten-benzenium **5** in MeCN-*d*<sub>3</sub> was warmed to room temperature however, signals consistent with **5** persisted for ~ 30 minutes. Characterization of **5** by <sup>1</sup>H, <sup>13</sup>C and multidimensional NMR spectroscopy in MeCN-*d*<sub>3</sub> allows for full assignment of the protons and carbons associated with this complex. Using chilled diethyl ether as a precipitating solvent, **5** can be isolated from dichloromethane in 86% yield on a 1.9 gram scale. As a solid, no decomposition is observed over a timescale of weeks if the complex is stored at reduced temperatures (-30 °C).



**Scheme 2.5.** Successful conditions that lead to the formation of two isomers of a tungsten-benzenium species.

Analysis by FTIR measurements and low temperature cyclic voltammetry were pursued to gauge the electronic parameters of **5**. The nitrosyl stretching frequency of **5** is measured to be  $\nu_{\text{NO}}$ =

1637  $\text{cm}^{-1}$  by solid state FTIR. By cyclic voltammetry, the oxidation potential of **5** was determined to be  $E_{p,a} = 0.70$  V (sweep rate of 100 mV/s). These data support that **5** is a significantly more electron deficient species than **1** ( $\nu_{\text{NO}} = 1564$   $\text{cm}^{-1}$  and  $E_{p,a} = -0.16$  V).

## 2.5 Dynamic Behavior of $\text{WTP}(\text{PMe}_3)(\text{NO})(\eta^2\text{-benzenium})$ in Solution

Analysis of complex **5** reveals two isomers that exist in a 10:1 ratio as detailed in **Figure 2.6**. The major isomer (**5A**) is formed with the metal binding two internal carbons of the  $\pi$  system and with the newly formed  $\text{sp}^3$  carbon distal to the  $\text{PMe}_3$  ligand. The minor isomer (**5B**) is bound at a terminus of the  $\pi$  system with the  $\text{sp}^3$  carbon proximal to the phosphine ligand.  $^1\text{H}$  and  $^{13}\text{C}$  NMR data of the benzenium complexes **5A** and **5B** suggest that the charge of the complex is localized at the carbon distal to the  $\text{PMe}_3$  ligand.

The chemical shifts for **5A** are similar with those observed for



The  $\eta^2$ -benzenium complexes **5A** and **5B** interconvert on the NMR timescale: NOESY data indicate spin saturation transfer for *seven* pairs of protons between the two benzenium isomers, *but no other exchanges* (**Figure 2.6** and **Figure 2.7**). Thus the 10:1 ratio represents a thermodynamic equilibrium between the two isomers, occurring through a mechanism

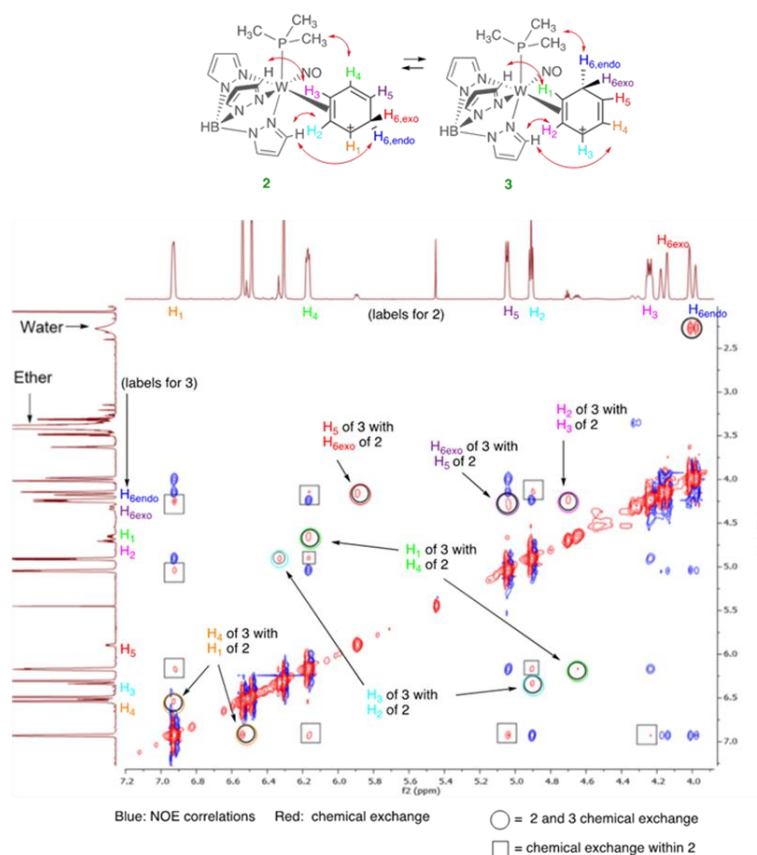


**Figure 2.6.** Partial NOESY spectra of the tungsten-benzenium complexes **5A** and **5B**. Blue signals indicate through space NOE interactions while red signals indicated chemical exchange of proton resonances on the timescale of the NMR experiment.

involving deprotonation of the acidic H<sub>6endo</sub> proton. This is followed by a ring-walk and subsequent re-protonation (vide infra).

By DFT calculations the electronic energies of the two lowest isomers correspond to the observed isomers by NMR spectroscopy (**Figure 2.8**). Notably, these calculated tungsten-benzenium species show features consistent with an “ $\eta^2$ -allyl complex”. Features of this distortion include two carbons that display a strong bonding interaction with the metal center. The carbon distal to the phosphine ligand has a localized positive charge and displays a weaker metal-carbon bonding

interaction than those designated as the  $\eta^2$ -bound carbons. This is evidenced by an elongated metal-carbon distance (2.73 Å as determined by DFT calculations). This distortion has been investigated previously for simple allyl complexes of {Wtp(NO)} and has been attributed to the asymmetry of the  $d\pi$ -orbitals of the metal center in both rhenium and tungsten. In the case of tungsten, this distortion is purported to arise from breaking of the degeneracy of the  $d\pi$ -orbital by interaction with the double-faced NO  $\pi$ -acid and subsequent orbital distortion of the HOMO associated with the metal arising from pyrazole ring interactions  $d$ -orbitals of tungsten. The energies associated with various tungsten-benzenium species that localize the cationic charge on other carbons are significantly destabilized as shown in **Figure 2.8**.

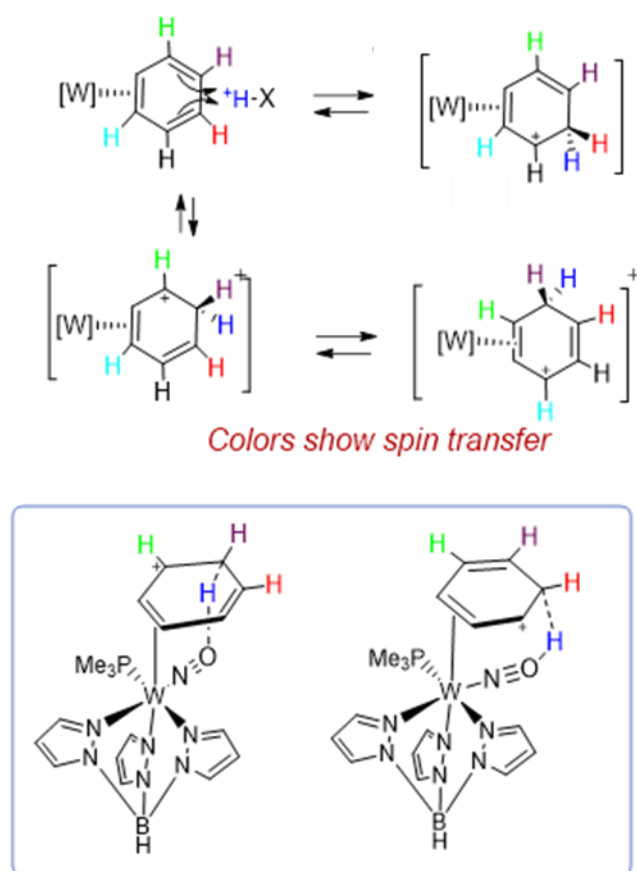


**Figure 2.7.** Spin transfer observed between protons of **5A** and **5B** (top). Purported role of the nitrosyl ligand in achieving selective “endo”-protonation (bottom).

When **1** is treated with DPhAT- $d_2$  a significant decrease for the proton resonance is observed associated with the geminal proton that is on the same face that the metal is bound to (“endo” relative to the metal). In the fully proteated form, this resonance displays a strong NOE correlation to the Tp3A proton. This correlation is not observed for the other methylene proton which we ascribe as the “exo” proton. Deuteration of rhenium and osmium benzenes complexes gave results that were consistent with direct-exo protonation of the benzene ring.<sup>6</sup>

While endo-protonation has been observed for a number of other  $\pi$ -ligands supported by transition metal complexes, the location of protonation (regiochemistry) is at odds with the product one would expect that would occur upon direct protonation of the metal followed by proton transfer.<sup>15</sup> That is, such a process would result in protonation at the alpha or beta carbons of the dihapto-bound benzene ring. In principle, protonation of the  $\eta^2$ -benzene ligand of **1** could occur at any one of the six carbons.

Rather, we propose a mechanism in which the nitrosyl ligand first is protonated to form a hydroxylimido

ligand, similar to that reported by Legzdins et al.<sup>16</sup> This would be followed by a concerted proton transfer in which a gamma carbon of the benzene is protonated simultaneously with release of electron density back into the tungsten through the NO group (**Scheme 2.6**). This would stabilize the emerging benzenium ligand by minimizing charge separation in the associated transition state.

An analogous protonation at the other gamma carbon would lead to the minor isomer **5B**. DFT calculations pursued by Emmitt Pert indicate that the  $\eta^2$ -benzenium complex **5** is only 2.4

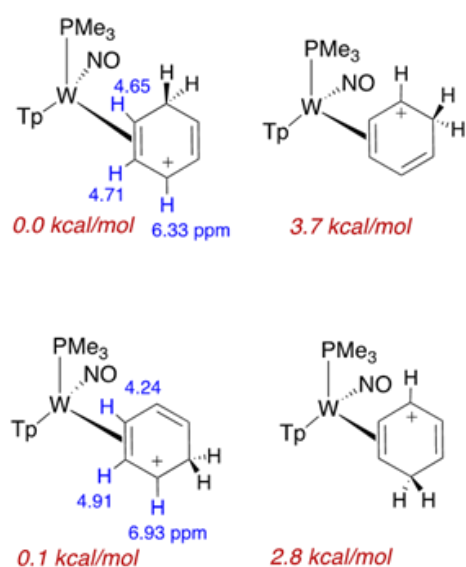


**Figure 2.8.** Relative stabilities of various isomers of a tungsten-benzenium complex. All energies are electronic energies and are given relative to the lower energy isomer (set to 0 kcal/mol). The two lowest energy isomers are those observed in solution.

kcal/mol lower in energy than the protonated nitrosyl complex, and the activation barrier for this process is only ~12 kcal/mol. The transition state calculations performed here utilize the B3LYP method and SDD basis set for all atoms. The role of nitrosyl ligands in intramolecular proton transfer has been previously documented.<sup>17, 16, 18</sup>

## 2.6 Reactivity of $\text{WTP}(\text{PMe}_3)(\text{NO})(\eta^2\text{-benzenium})(\text{OTf}-)$

Dr. Katy Wilson showed that **5** could serve as a potent electrophile for a variety of nucleophilic reagents (amines, enolates, Grignards, cyanide, phosphines).<sup>19</sup> The resulting 1,3-cyclohexadiene adducts, arising from the initial protonation and nucleophilic addition of benzene, could then be elaborated further by a sequential tandem addition sequence to generate novel cyclohexene products. This work excellently illustrates the stereo- and

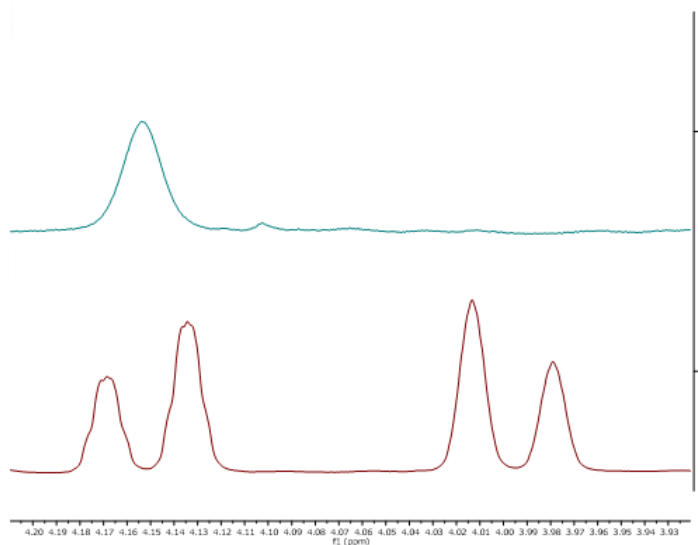


**Figure 2.9:** Partial  $^1\text{H}$  NMR spectra of **5** showing methylene protons (bottom). The resonance at 4.00 corresponds to the proton resonance that is on the same side of the ring that the metal is bound to (“endo” relative to the metal) and use of an appropriate  $\text{D}^+$  source results in significant suppression ( $> 95\%$ ) of the proton resonance (top).

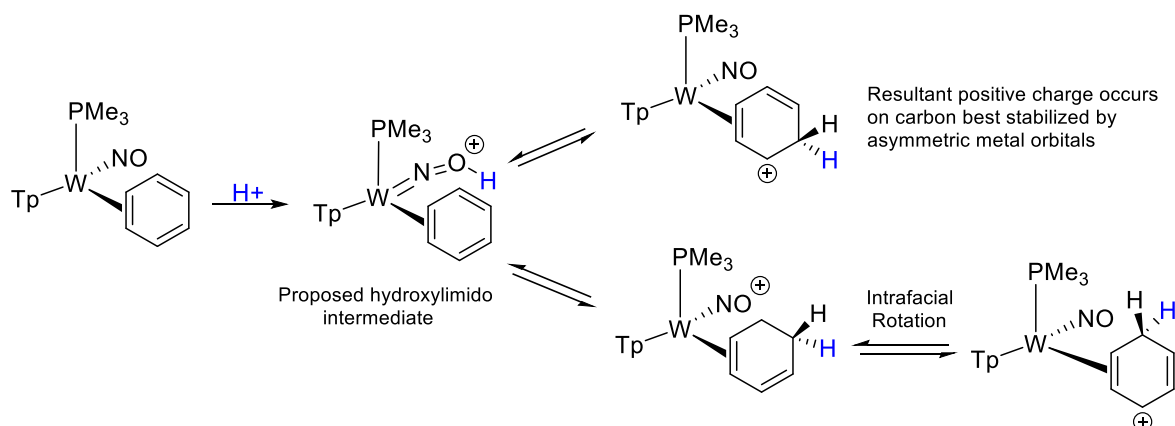
regioselective directing power of the metal center. The reactivity observed is highly selective even in the absence of substituents on the benzene ring.

While a full discussion of this chemistry is beyond the scope of this chapter and detailed more efficiently elsewhere, several comments on the reactivity of **5** deserve comment.<sup>19</sup> Notably, when exposing **5** to nucleophiles, low temperatures can be utilized to pre-empt deprotonation and give only the desired nucleophilic addition product. While a formal treatment of these competing processes has not been pursued, empirically we observe that addition tends to predominate over

deprotonation at lower temperatures. Given that the resulting adducts from either process (deprotonation and nucleophilic addition) are generally irreversible, it must be the case that the relative rates of formation of nucleophilic addition versus deprotonation are strongly temperature dependent. While lowering the temperature would slow the rate of each reaction pathway, *the rate of deprotonation must be more sensitive to changes in temperature than that of addition.*

As a case in point, when a solution of **5** in acetone is treated with nBuLi, a new diamagnetic species is observed,  $\text{WTp}(\text{PMe}_3)(\text{NO})(\eta^2\text{-2,3-(S)-1-(cyclohexa-2,4-dien-1-yl)propan-2-one})$  (**6**). This result is consistent with deprotonation of acetone with nBuLi in situ to generate acetone's enolate (**Scheme 2.7**). Nucleophilic addition of this enolate to complex **5** would lead to the generation of **6**. Apparently this process, the deprotonation of acetone and the addition of its enolate to **5**, is faster than deprotonation of **5** by nBuLi.

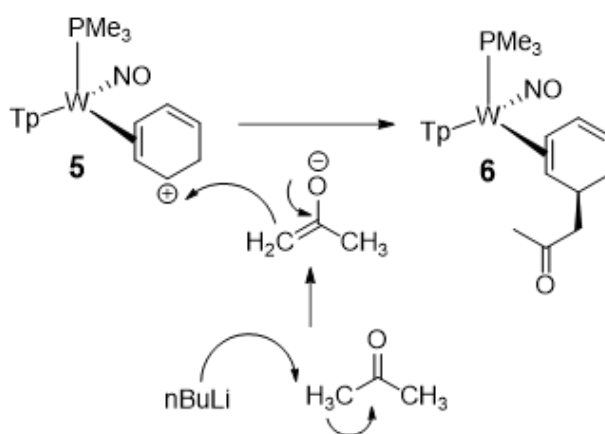
To confirm the identity of **6**, repeating the experiment in acetone- $d_6$  results in loss of the methylene set associated with the acetone enolate addition adduct ( $^1\text{H}$  resonances at 2.75 ppm and 2.56 ppm as determined by  $^1\text{H}$  NMR spectroscopy) as well as a methyl group at 2.01 ppm. Additionally, HRMS analysis of **6** reveals an isotopic pattern consistent with a  $m/z$  ratio of the  $\text{M}+\text{H}$



**Scheme 2.6.** A proposed hydroxylimido intermediate that plays a key role in enabling proton delivery to the bound benzene ring. An intrafacial ring isomerization would account for the structure determined for **5B**.

enolate adduct. Further synthetic investigation of this complex was not pursued, though insight by Justin Wilde proposes that this adduct could be a precursor to propylhexedrine, a nasal decongestant. The ability to prepare enolates in situ with strong bases could be utilized to generate a wide scope of nucleophiles not commercially available. Efforts to extend this methodology to generate nucleophiles from asymmetric ketones (i.e. 1,1,1-trifluoroacetone, 4-acetylphenol and 4-acetylaniline) or to fluorinated aliphatic substrates (Vertrel XF) were unsuccessful.

Treatment of **5** in MeCN-*d*<sub>3</sub> with HOTf in an attempt to deliver a second proton to the benzene ring did not result in any reactivity. Presumably, HOTf leveled in MeCN-*d*<sub>3</sub> is not acidic enough to generate a double protonation adduct of benzene. However, oxidative decomposition is not observed, implying that **5** is resistant to degradative oxidation pathways. This is also



**Scheme 2.7.** Proposed mechanism showing the in situ deprotonation of acetone to generate acetone's enolate which can then act as a nucleophile for **5** to generate **6**.

reflected in a low temperature (0 °C) cyclic voltammetry experiment performed on **5** in MeCN which shows an  $E_{p,a} = 0.70$  V (100 mV/s sweep rate). Attempts to double protonate **1** under different solvent conditions proved to be more productive and those results are presented in Chapter 8.

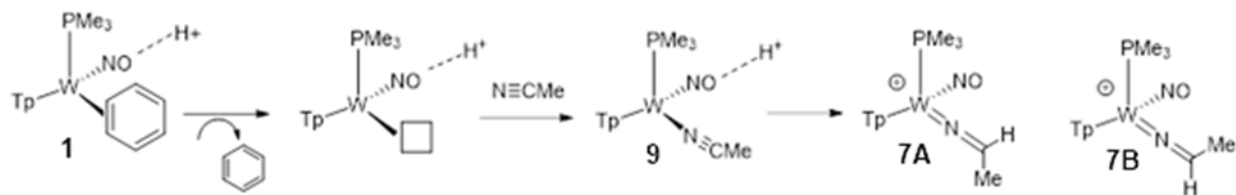
## 2.7 pKa Determination of WTp(PMe<sub>3</sub>)(NO)(η<sup>2</sup>-benzenium)(OTf-)

Attempts to estimate the pKa of **5** were pursued by treating **1** with a range of acid sources weaker than DPhAT (pKa ~ 0). Conditions were pursued that had previously led to the successful protonation of **1** with DPhAT in situ. A solution of **1** was prepared in MeCN-*d*<sub>3</sub> at -30 °C, treated with a solution of excess acid dissolved in MeCN-*d*<sub>3</sub> which was also cooled to -30 °C. The resulting reaction mixture was transferred to an NMR tube. This solution was then frozen in N<sub>2(l)</sub>, taken to an



800 MHz NMR spectrometer where the frozen solution was allowed to thaw before a  $^1\text{H}$  NMR experiment was performed at 0 °C.

Treating **1** with various acid sources in  $\text{MeCN-}d_3$  such as 3-trifluoromethyl anilinium (pKa  $\sim$  3), pyridinium triflate (pKa  $\sim$  5), di-isopropylammonium triflate (DPAT, pKa  $\sim$  11), and L-dibenzoyltartaric acid (pKa  $\sim$  12) did not yield **5** or the decomposition species **2**. The latter of these species is observed upon protonation of **1** with strong acid (HOTf or methanesulfonic acid) in  $\text{MeCN-}d_3$ . Rather, over time the formation of a new diamagnetic complex **7** is observed. There is a correlation between the strength of the acid source and the rate of formation of **7**. Treatment of **1** with stronger acids form species **7** within minutes. Weaker acids (DiPAT, L-DBTA) generate **7** over the course of several hours. During this process the concomitant release of the benzene ligand is observed. Analysis of this complex by  $^{31}\text{P}$  NMR shows a species with a  $J_{\text{WP}} = 333$  Hz at -9.8 ppm. Comparison of the resulting proton spectra with one reported by Lis et al reveals that **7** is the complex  $\text{WTp}(\text{PMe}_3)(\text{NO})(\kappa^1\text{-N-acetonitrilium})(\text{OTf-})$ .<sup>20</sup>



**Scheme 2.8.** Proposed mechanism for the enhanced dissociation of benzene and the generations of a  $\kappa^1$ -acetonitrilium complex under acidic conditions.

Conditions which are not sufficiently acidic to protonate the benzene complex also seem to preclude the formation of the tungsten-allyl complex **2**. Rather, an unknown mechanism enables enhanced substitution of the benzene for the acetonitrile ligand (**Scheme 2.8**). The complex  $\text{WTp}(\text{PMe}_3)(\text{NO})(\eta^2\text{-acetonitrile})$  (**8**) can be readily protonated in the presence of weak acids.<sup>20</sup> Additionally, **8** is predicted to be more stable than the  $\text{WTp}(\text{PMe}_3)(\text{NO})(\kappa^1\text{-N-acetonitrile})$  (**9**) isomer by more than 8 kcal/mol from DFT calculations. Given that only **7** is observed, the

mechanism that leads to its formation most likely precludes the formation of the  $\eta^2$ -acetonitrile complex **8**. Under these conditions, enhanced substitution rate is speculated to generate the  $\kappa^1$ -acetonitrile complex **9** from the tungsten-benzene complex **1**. The formation of **9** is then followed by protonation to generate the  $\kappa^1$ -acetonitrilium complex **7** at a rate faster than the isomerization of **9** to form **8**.

Alternatively, the electronic changes which allow for accelerated substitution of the benzene ligand could involve either transient protonation or enhanced hydrogen bonding interactions between the acidic proton and nitrosyl ligand. This would increase the ability of the nitrosyl to act as an even better  $\pi$ -acceptor ligand, resulting in an overall more electron deficient-metal center. Consequently, this would reduce  $\pi$ -backbonding from the metal to the benzene ligand, enabling accelerated ligand substitution where the benzene falls off and acetonitrile is able to rapidly coordinate in a  $\kappa^1$ -fashion to generate **9**. If the metal is insufficiently  $\pi$ -basic to support the dihapto-coordinate acetonitrile adduct **8** due to the enhanced  $\pi$ -acceptor properties of the protonated nitrosyl ligand, **9** would persist long enough to be protonated, resulting in the observed  $\kappa^1$ -acetonitrilium **7**. The identification of **7** complex is useful as its presence has been observed in other reaction conditions which utilize acid or electrophiles and acetonitrile as a solvent. Presumably, other nitrile based solvents (propionitrile, benzonitrile) could engage in similar reactivity.

The net result of these pKa measurements suggest that the pKa of **5** is similar to that of DPhAT ( $\sim 1$ ). This approximation is supported as **5** can be isolated in chilled diethyl ether without noticeable deprotonation on the timescale of the experiment. These results imply that excess diethyl ether is not sufficient to appreciably deprotonate **5**. The acidity of protonated diethyl ether is estimated to be pKa  $\sim -3$ .

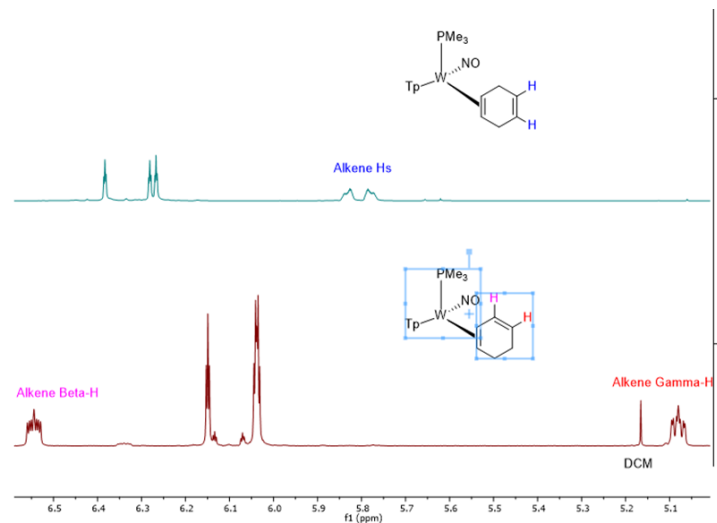
## 2.8 Synthesis of WTp(PMe<sub>3</sub>)(NO)( $\eta^2$ -1,3-cyclohexadiene)

As has been discussed, **5** can serve as an effective electrophile for a wide array of nucleophilic reagents. Initial investigations using hydride as a nucleophile in an attempt to generate the seemingly pedestrian tungsten-cyclohexadiene complex **3** proved difficult. Instead, over-reduction to WTp(PMe<sub>3</sub>)(NO)( $\eta^2$ -cyclohexene) (**10**) was often observed, even when one equivalent of an acid source was used. This was often accompanied with varying ratios of **1** and **3**.

Presumably, after the initial hydride addition to the tungsten-benzenium complex **5** to generate the **3**, the resulting cyclohexadiene complex would be even more reactive to protonation compared to the tungsten-benzene adduct **1**. As such, any acid or amount of **5** that had not yet reacted with the hydride source would be acidic enough to protonate **3** and generate the tungsten-allyl species **2**. This complex could then readily react with excess hydride to yield the resulting cyclohexadiene complex. One equivalent of NaBH<sub>4</sub> has the potential to serve as a source of four equivalents of hydridic protons.

Investigation into different hydride strengths found that weaker hydride sources actually led to enhanced degrees of over-reduction to generate complex **10**.<sup>21</sup> A correlation was found between the solubility (and therefore concentration) of the hydride source in solution and the ratios of the desired adduct **3** and the over-reduced product **10**. For example, treating an acetonitrile solution of **5** at -30 °C with the organic soluble nBu<sub>4</sub>NBH<sub>4</sub> reducing agent gives a ratio of tungsten-cyclohexadiene (**3**): tungsten-cyclohexene (**10**) of 2:1. Using NaBH<sub>4</sub> under analogous conditions shows only the formation of **10**. Unfortunately, attempts to pre-dissolve hydride sources with “hard” cations such as sodium in various crown ethers (15-crown-5, 18-crown-6) and treating these hydride sources with **5** led to predominant deprotonation of **5** to regenerate **1**. Stronger hydride sources (LiAlH<sub>4</sub> and 9-BBN lithium hydride) often led to mixtures of **1** and **3**.

In these cases, a correlation between hydride reactivity and the ability to quench sources of acid (either excess free acid or reaction with **5** species) would suppress formation of **2**, a key intermediate in the generation of **10**. Additionally, temperature plays a key role in this process in determining the distribution of observed products. Optimized conditions were realized by adding solutions of **5** (prepared in situ) to frozen solutions of MeOH/NaBH<sub>4</sub> that would then be allowed to thaw at -60 °C and further details are presented in the



Experimental Section of this chapter. In no instance however is the product

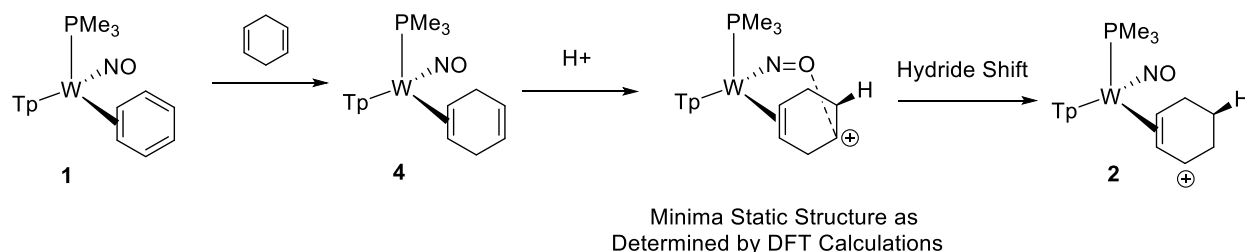
**Figure 2.10.** Illustrative differences in the <sup>1</sup>H NMR spectra between the 1,3-cyclohexadiene tungsten-adduct (**3**) and that of a tungsten-1,4-cyclohexadiene complex (**4**).

WTP(Me<sub>3</sub>)(NO)(η<sup>2</sup>-1,4-cyclohexadiene) (**4**) observed. This illustrates the remarkable regioselectivity of cyclohexadiene adducts derived from **5**.

## 2.9 Synthesis and Reactivity of WTP(Me<sub>3</sub>)(NO)(η<sup>2</sup>-1,4-cyclohexadiene)

Authentic samples of **4** were derived from ligand exchange with **1** and 1,4-cyclohexadiene. Illustrative differences in the <sup>1</sup>H NMR spectra for the unbound alkene protons in **3** and **4** are presented in **Figure 2.10**. As mentioned *vide supra*, the generation of 1,4-cyclohexadiene complexes were often regarded as a synthetic “dead end” in the case of osmium and rhenium-promoted reactions on aromatic molecules. The resulting unbound alkene was not in conjugation with the metal. In contrast to this, when a solution of **4** in MeCN is treated with DPhAT, clean conversion to **2** is observed (**Scheme 2.11**). Analogous reactivity for the osmium and rhenium supported 1,4-cyclohexadiene scaffolds has not been observed.

DFT calculations were pursued in an attempt to elucidate a potential mechanism that enables the formation of the tungsten-allyl complex **2** from the protonation of **4**. A minimum static structure, **2H**, shows significant distortion of the nitrosyl ligand to generate a bent nitrosyl ligand (**Figure 2.11**). Here the nitrosyl oxygen lone pair forms a formal O-C bond with the carbon that stabilizes the concomitant positive charge after protonation of the alkene bond. To rationalize the formation of **2**, we invoke a symmetry allowed 1,2-hydride transfer which would lead to the successful generation of **2** after the initial protonation of **4**. These data suggest that the nitrosyl ligand may be able play a more dynamic role in modulating organic chemistry on various  $\pi$ -ligands bound to the tungsten fragment. This also suggests that metal-directed chemistry could be realized from 1,4-cyclohexadiene structural motifs.



**Scheme 2.9.** Proposed “nitrosyl-assist” pathway that enables access to **2** from the protonation of **4**. After the initial protonation, a 1,2-hydride shift would lead to the formation of **2**.

## 2.10 Conclusion

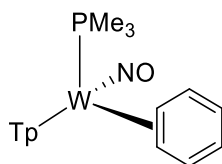
The protonation of **1** to yield the tungsten-benzenium complex **5** allowed access to a variety of functionalized tungsten-cyclohexadiene and tungsten-cyclohexene complexes.<sup>19</sup> Mechanisms responsible for the fluctational behavior of **1** and **5** have been presented that are supported by NOESY NMR experiments. The stability of the tungsten-benzenium complex **5** has also been investigated and compared to the osmium and rhenium-supported benzenium ligands. Holistically, a comparison between osmium, rhenium and tungsten benzene complexes was made through DFT, dynamic NMR and pKa studies. Results from these studies suggest that tungsten is the most  $\pi$ -basic of the third row dearomatization agents.

Initial deuterium labeling experiments showed that treating **1** with an appropriately acidic deuterium source results in a single isotopomer of **5**. The deuteration occurs in a highly regio- and stereospecific manner with a high degree of isotopic purity (> 95 %). A previous report showed the ability of  $[\text{Os}(\text{NH}_3)_5(\eta^2\text{-benzene})]^{2+}$  to generate a selective  $d_4$ -isotopologue of cyclohexene from the dearomatization of benzene.<sup>22</sup> Consequently, there is an open-ended question as to whether tungsten could enable complementary reactivity to generate a series of novel isotopologues of cyclohexene. In this case, deuterium would be sequentially introduced utilizing appropriate cationic (deuteron) and anionic (deuteride) sources of deuterium into the benzene ring. The result would be different isotopologues of cyclohexene, which could be used as deuterated building blocks for medicinal chemists. A full investigation on this methodology and the mechanistic details of this process will be examined in Chapter 3. Extensions in generating substituted cyclohexene isotopologues will also be presented.

## Experimental

**General Methods.** NMR spectra were obtained on 500, 600 or 800 MHz spectrometers. Chemical shifts are referenced to tetramethylsilane (TMS) utilizing residual  $^1\text{H}$  signals of the deuterated solvents as internal standards. Chemical shifts are reported in ppm and coupling constants ( $J$ ) are reported in hertz (Hz). Chemical shifts for  $^{19}\text{F}$  and  $^{31}\text{P}$  spectra were reported relative to standards of hexafluorobenzene (164.9 ppm) and triphenylphosphine (-6.00 ppm). Infrared Spectra (IR) were recorded on a spectrometer as a solid with an ATR crystal accessory, and peaks are reported in  $\text{cm}^{-1}$ . Electrochemical experiments were performed under a nitrogen atmosphere. Most cyclic voltammetric data were recorded at ambient temperature at 100 mV/s, unless otherwise noted, with a standard three electrode cell from +1.8 V to -1.8 V with a platinum working electrode, acetonitrile (MeCN) solvent, and tetrabutylammonium (TBAH) electrolyte (~1.0 M). All potentials are reported versus the normal hydrogen electrode (NHE) using cobaltocenium hexafluorophosphate ( $E_{1/2} = -0.78$  V, -1.75 V) or ferrocene ( $E_{1/2} = 0.55$  V) as an internal standard. Peak separation of all reversible couples was less than 100 mV. All synthetic reactions were performed in a glovebox under a dry nitrogen atmosphere unless otherwise noted. All solvents were purged with nitrogen prior to use. Deuterated solvents were used as received from Cambridge Isotopes and were purged with nitrogen under an inert atmosphere. When possible, pyrazole (Tp) protons of the (trispyrazolyl) borate (Tp) ligand were uniquely assigned (e.g., “Tp3B”) using two-dimensional NMR data (see Fig. S1). If unambiguous assignments were not possible, Tp protons were labeled as “Tp3/5 or Tp4”. All  $J$  values for Tp protons are 2 ( $\pm 0.4$ ) Hz.

### Synthesis of $\text{WTp}(\text{NO})(\text{PMe}_3)(\eta^2\text{-benzene})$ (2)

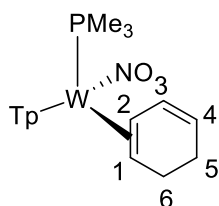


### Alternative Procedure

First a 1 L round bottom flask was dried in a 150 C oven along with a 350 mL coarse porosity fritted disc which was  $\frac{3}{4}$  filled with silica. After 4 h the glassware was removed from the oven and brought into an inert atmosphere glovebox. The 1L round bottom flask was then charged with anhydrous benzene (800 mL) followed by  $\text{WTp}(\text{NO})(\text{PMe}_3)(\text{Br})$  (12.28 g, 21.1 mmol) followed by an excess of 30-35% by weight sodium dispersion in toluene solution (14.41 g, ~ x mmol). The sides of the round bottom flask were rinsed with another wash of benzene (200 mL) and the resulting heterogeneous green reaction mixture was allowed to rapidly stir over a course of 16 h. The next day the reaction mixture had turned to a dark brown/black color and the solution was first filtered through a 150 mL medium porosity fritted disc that was filled  $\frac{1}{2}$  way with Celite and set in benzene. The resulting eluent was then loaded onto the a 350 mL coarse porosity fritted disc which was  $\frac{3}{4}$  filled with silica and set in benzene. The eluent was then loaded onto the column and allowed to drip filter until separation occurred between a green band that developed at the front of the column followed closely by a vibrant orange band. When all of the reaction mixture had been loaded the column was rinsed with a 3:1 solution of benzene: diethyl ether (~ 3 x 300 mL). At this point vacuum was cautiously applied to the column until the majority of the green band had eluted through the column. The resulting green filtrate was then discarded and the resulting orange band was allowed to filter slowly through. The initial filtrate was discarded again and the column was then rinsed with diethyl

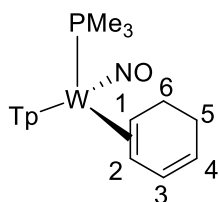
ether (2 L total) to elute all of the orange colored band which appears a homogeneous yellow coloration in solution. The 2 L of diethyl ether was subjected to dynamic vacuum in vacuo until ~ 300 mL of solution remained. Next hexanes (1 L) was added to induce further precipitation and generate a golden yellow suspension. This heterogeneous yellow solution was then eluted through a 150 mL fine porosity fritted disc to isolate a vibrant yellow solid. The solid was washed with hexanes (2 x 50 mL) and to dessicatted over a period of 6 h before a mass was taken of the vibrant yellow solid (5.31 g, 43.4%). Characterization has been reported previously.<sup>1</sup>

### Synthesis of WTp(NO)(PMe<sub>3</sub>)(η<sup>2</sup>-1,2-1,3-cyclohexadiene) (3P)



To a 4-dram vial was added 2 mL of MeCN and **1** (0.200 g, 0.344 mmol) to generate a heterogeneous yellow reaction mixture. This solution was then cooled to -30°C. DPhAT was added to this reaction mixture and the solution was allowed to stand at -30°C. Over 15 min a homogeneous red reaction mixture develops indicating the formation of **2** in solution. Separately a solution of 2 mL of MeOH was chilled to -30°C and to this solution NaBH<sub>4</sub> (0.030g, 0.79 mmol) was added. The NaBH<sub>4</sub>/MeOH solution was then added to a dewar of liquid nitrogen and the solution was frozen. The homogenous red reaction mixture of **2** was then added to this frozen solution of MeOH and NaBH<sub>4</sub> and the reaction mixture was allowed to thaw while sitting at -30°C. After one hour the reaction mixture had turned to a homogenous orange color. A 60 mL coarse fritted porosity disc was filled with ~ 5 cm of neutral alumina and set in Et<sub>2</sub>O. The homogeneous orange solution was then filtered through the neutral alumina column and a light yellow band was eluted with 100 mL of Et<sub>2</sub>O. The solvent was removed in vacuo until a pale yellow solid remained. This was re-dissolved in 2 mL of DCM and added to a 4-dram vial that contained 15 mL of sitting hexanes. This homogeneous yellow solution was subsequently allowed to cool at -30°C for 16 h. After being allowed to cool a light green crystalline product had developed on the sides of the vial. The organic layer was decanted and the product was then dried with N<sub>2</sub> (g) and allowed to desiccate for 8 h before a mass was taken of the resultant light yellow crystalline product (0.162 g, 81%). Characterization has been reported previously.<sup>8</sup>

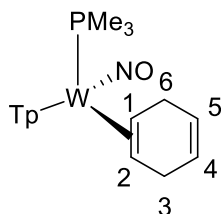
### Synthesis of WTp(NO)(PMe<sub>3</sub>)(η<sup>2</sup>-1,2-1,3-cyclohexadiene) (3D)





A mixture of complexes **3P** and **3D** (0.298 g, 0.511 mmol) were dissolved in 2 mL of DME and allowed to cool to -30 °C over a period of 15 min. To this homogeneous light yellow solution was added HOTf (0.198 g, 1.311 mmol) and the reaction mixture turned to a homogeneous orange color. This reaction mixture was allowed to sit at -30 °C for 5 min and then subsequently added to 15 mL of standing ether at room temperature. A dark brown solid congregated on the bottom of the flask, and the organic layer was decanted before the solid was re-dissolved in 2 mL of DCM and again precipitated into 50 mL of stirring ether to generate a light yellow heterogeneous mixture. This solid was then dried under dynamic vacuum in a desiccator for two hr and its identity as **4** was confirmed by NMR. This solid was then dissolved in DCM (2 mL) and allowed to sit at -30 °C. In a separate 4-dram vial was added DBU (0.582g, 3.82 mmol) along with DCM (1 mL) and this solution was also cooled to -30 °C over a course of 15 min. The DBU/DCM solution was then added to the DCM solution of **4** and upon addition a homogeneous pink reaction mixture develops. This reaction mixture was allowed to stand for 5 min at room temperature and then loaded onto a coarse 60 mL fritted disc that had been filled with ~ 3 cm of basic alumina and set in ether. The pink band was eluted with 60 mL of ether and the solvent was then removed in vacuo. A light yellow film coats the bottom of the filter flask, this was re-dissolved in DCM (2 mL) and added to standing pentane (15 mL) and was allowed to sit at -30 °C for 16 hr. The next day a yellow crystalline material had formed at the sides of the vial. The organic layer was then decanted and the vial was dried under dynamic vacuum for 6 hr to yield a fine yellow powder (0.102 g, 34%). Characterization has been reported previously.<sup>8</sup>

#### Synthesis of WTp(NO)(PMe<sub>3</sub>)(η<sup>2</sup>-1,2-1-4-cyclohexadiene) (**4**)

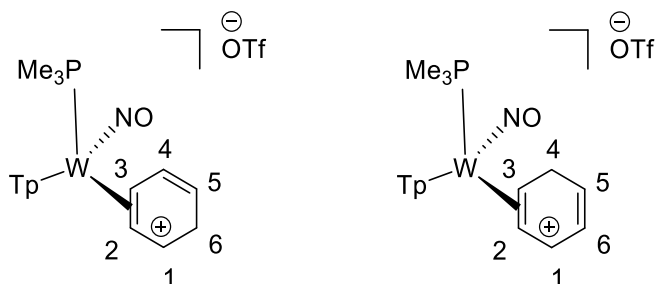


A 4-dram vial was charged with 1 mL of DME, complex **1** (0.301 g, 0.518 mmol) and 1,4-cyclohexadiene (2.00g, 24.9 mmol) and this heterogeneous yellow reaction mixture was allowed to stir. After 50 h the homogeneous purple reaction mixture was slowly added to 30 mL of stirring pentanes that had been chilled to -30 °C. Upon addition a light pink solid precipitates out of solution. This light pink solid was collected on a 30 mL fine porosity fritted disc and subsequently washed with 3 x 5 mL of chilled pentane. The collected product was then desiccated for 2 h to yield a fine pink powder (0.191 g, 63%).

CV (MeCN):  $E_{p,a} = +0.27$  V (NHE). IR:  $\nu(\text{BH}) = 2481$  cm<sup>-1</sup>,  $\nu(\text{NO}) = 1553$  cm<sup>-1</sup>. <sup>1</sup>H-NMR (acetone-*d*<sub>6</sub>,  $\delta$ , 25 °C): 8.25(1H, d, Tp3A), 8.08 (1H, d, Tp3B), 7.92 (1H, d, Tp5B), 7.88 (1H, d, Tp5C), 7.80 (1H, d, Tp5A), 7.49 (1H, d, Tp3C), 6.38 (1H, t, Tp4B), 6.28 (1H, t, Tp4A), 6.27 (1H, t, Tp4C), 5.83 (1H, m, H4) 5.78 (1H, m, H5), 3.55 (1H, m, H6-*exo*), 3.45 (2H, overlap, H3-*exo* and H3-*endo*), 3.10 (1H, d,  $J = 17.8$ , H6-*endo*), 2.83 (1H, m, H1), 1.34 (1H, m, H2), 1.21 (9H, d,  $J = 8.2$ , PMe<sub>3</sub>). <sup>13</sup>C-NMR (acetone-*d*<sub>6</sub>,  $\delta$ , 25 °C). 144.0 (Tp3/5), 142.8 (Tp3/5), 141.5 (Tp3/5), 137.3 (Tp3/5), 136.7 (Tp3/5), 136.6 (Tp3/5), 127.7 (C4/5), 127.6 (C4/5), 107.1 (Tp4), 106.7 (Tp4), 106.2

(Tp4), 51.7 (C1, d,  $J_{PC} = 11.9$ ), 51.4 (C2), 30.1 (C3, buried under acetone), 29.2 (C6, buried under acetone), 13.6 (PMe<sub>3</sub>, d,  $J_{PC} = 27.4$ ). <sup>31</sup>P-NMR (CDCl<sub>3</sub>, δ, 25 °C): -8.9 ( $J_{WP} = 292$ , PMe<sub>3</sub>). Anal. Calcd for C<sub>18</sub> H<sub>27</sub> BN<sub>7</sub> OPW: C, 37.08; H, 4.67; N, 16.82. Found: C, 37.35; H, 4.58; N, 16.69.

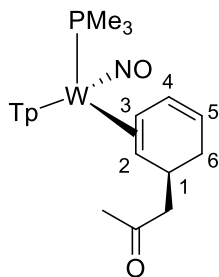
### Synthesis of WTp(NO)(PMe<sub>3</sub>)(η<sup>2</sup>-2,3-benzenium) (5A) and WTp(NO)(PMe<sub>3</sub>)(η<sup>2</sup>-1,2-benzenium) (5B)



A 4-dram vial was charged with 5 mL of DCM and chilled to -30°C for 15 min. **1** (1.52 g, 2.61 mmol) was then added, resulting in a heterogeneous yellow reaction mixture. Diphenylammonium triflate (DPhAT) (0.909 g, 2.84 mmol) was added to the reaction mixture at -30°C resulting in the formation of a homogenous red solution. This solution was allowed to stand at -30°C for 20 min. This reaction solution was then added to stirring Et<sub>2</sub>O that had been chilled to -30°C (60 mL) to yield a dull yellow precipitate. The yellow solid was collected on a 30 mL fine porosity fritted disc and washed with chilled Et<sub>2</sub>O (2 x 20 mL). The isolated yellow solid was then desiccated for two h yielding **2A** and **2B** (1.63 g, 2.24 mmol, 86% yield) in a 10:1 ratio.

CV (MeCN at -6 °C)  $E_{p,a} = +0.70$  V (NHE). IR:  $\nu(\text{BH}) = 2520$  cm<sup>-1</sup>,  $\nu(\text{NO}) = 1637$  cm<sup>-1</sup>. **Complex 2A** (major): <sup>31</sup>P NMR (CD<sub>3</sub>CN, δ): -7.44 ( $J_{WP} = 274$ ). <sup>1</sup>H NMR (CD<sub>3</sub>CN, δ, 0°C): 8.33(1H, d, Tp3B/5B), 8.03 (1H, d, Tp3A), 8.02 (1H, d, Tp5C), 7.97 (1H, d, Tp3C), 7.94 (1H, d, Tp3B/5B), 7.80 (1H, d, Tp5A), 6.93 (1H, broad singlet, H1), 6.54 (1H, t, Tp4C), 6.49 (1H, t, Tp4B), 6.31 (1H, t, Tp4A) 6.17 (1H, m, H4), 5.04 (1H, m, H5), 4.91 (1H, t,  $J = 7.2$ , H2), 4.24 (1H, m, H3), 4.16 (1H, d,  $J = 28.3$ , H6-*exo*), 4.00 (1H, d,  $J = 28.3$ , H6-*endo*), 1.18 ((H, d,  $J = 9.9$ , PMe<sub>3</sub>). <sup>13</sup>C NMR (CD<sub>3</sub>CN, δ, 0°C): 147.9 (Tp3A), 146.7 (Tp5C), 145.7 (C1), 143.0 (Tp3/5), 139.4 (Tp3/5), 139.3 (2C, Tp3/5), 126.1 (C4), 119.5 (C5), 109.2 (Tp4B), 108.7 (Tp4C), 107.8 (Tp4A), 95.1 (C2), 64.5 (C3), 30.7 (C6), 13.1 (PMe<sub>3</sub>, d,  $J = 34.2$ ). **Complex 2B** (minor): <sup>1</sup>H NMR (CD<sub>3</sub>CN, δ, 0°C): 8.31 (1H, d, Tp3/5), 8.11 (1H, d, Tp3/5), 8.01 (1H, d, Tp3/5), 7.92 (1H, d, Tp3C), 7.81 (1H, d, Tp3/5), 6.55 (1H, buried, H4), 6.52 (1H, t, Tp4), 6.49 (1H, buried, Tp4), 6.34 (2H, overlapping, Tp4 & H3), 5.89 (1H, m, H5), 4.71 (1H, t,  $J = 7.5$ , H2), 4.65 (1H, m, H1), 4.34 (1H, d,  $J = 25.8$ , H6-*exo*), 3.36 (d,  $J = 25.8$ , 1H, H6-*endo*), 1.11 (9H, buried, PMe<sub>3</sub>). Attempts at elemental analysis were not successful due to the unstable nature of the complex at ambient temperatures.

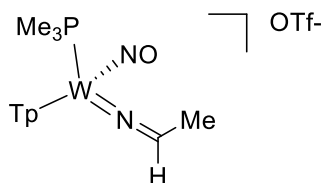
### Synthesis of WTp(PMe<sub>3</sub>)(NO)(η<sup>2</sup>-2,3-(S)-1-(cyclohexa-2,4-dien-1-yl)propan-2-one) (6)



To a 4-dram vial chilled a solution of **1** (0.250 g, 0.430 mmol) in acetone (10 mL) to  $-30\text{ }^{\circ}\text{C}$ . DPhAT (0.198g, 0.617 mmol) was then added to the solution. The reaction mixture goes from a homogeneous yellow color to a homogeneous red solution over a course of 15 min. Next triphenylphosphine (0.658 g, x mmol) was added and to this solution was add a 1.6 M solution of nBuLi in hexanes (1 mL, 1.6 mmol). The resulting solution was allowed to sit at  $-30\text{ }^{\circ}\text{C}$  over a period of three days. A coarse porosity 30 mL fritted disc was filled with 3 cm of silica and set in diethyl ether and the reaction mixture was eluted through. A light yellow band was eluted with diethyl ether ( $\sim 80\text{ mL}$  total) and the solvent was removed in vacuo until a minimal amount of solid remained. Pentane (50 mL) was then added to the solution to induce precipitation of the yellow solid. This solid was caught on a fine 15 mL porosity fritted disc and washed with pentane (3 x 5 mL) before the resulting yellow solid was allowed to dry in vacuo. A yellow solid was recovered (mass recovery 0.162 g, excess phosphine observed).

$^{31}\text{P}$  NMR ( $\text{CD}_3\text{CN}$ ,  $\delta$ ): -12.8 ( $J_{\text{WP}} = 284$ ).  $^1\text{H}$  NMR ( $\text{CD}_3\text{CN}$ ,  $\delta$ ,  $25^{\circ}\text{C}$ ): 8.05 (1H, d, Tp3/5), 8.03 (1H, d, Tp3/5), 7.84 (1H, d, Tp3/5), 7.77 (1H, d, Tp3/5), 7.36 (1H, d, Tp3/5), 6.46 (1H, m, H), 6.35 (1H, t, Tp4), 6.30 (1H, t, Tp4), 6.25 (1H, t, Tp4), 4.87 (1H, m, H5), 3.11 (1H, q,  $J = 6.8$ , H1), 2.84 (1H, m, H3), 2.75 (1H, dd,  $J = 7.0, 15.0$ , methylene of enolate), 2.69 (1H, m, H6'), 2.56 (1H, dd,  $J = 6.7, 15.0$ , methylene of enolate), 2.01 (3H, s, methyl of enolate), 1.68 (1H, m, H6'), 1.22 (9H, d,  $J_{\text{PH}} = 8.52$ ,  $\text{PMe}_3$ ), 0.93 (1H, buried, H2).  $^{13}\text{C}$  NMR ( $\text{CD}_3\text{CN}$ ,  $\delta$ ,  $25^{\circ}\text{C}$ ): 210.8 (carbonyl), 144.3 (Tp3/5), 142.8 (Tp3/5), 141.7 (Tp3/5), 137.8 (Tp3/5), 137.1 (Tp3/5), 137.0 (Tp3/5), 132.3 (C4, d,  $J_{\text{PC}} = 2.8$ ), 117.0 (C5), 107.3 (Tp4), 107.1 (Tp4), 106.8 (Tp4), 60.7 (C2), 54.5 (methylene of enolate), 49.7 (C3, d,  $J_{\text{PC}} = 10.1$ ), 33.6 (C1), 30.7 (methyl), 28.9 (C6), 13.8 ( $\text{PMe}_3$ , d,  $J_{\text{PC}} = 28.7$ ). HRMS Data Theoretical, Observed: 638.1939 (84.69%), 638.1946 (x%), 639.1966 (79.84%), 639.1979 (x%), 640.1964 (100%), 640.1980 (100%), 641.2006 (42.4%), 641.2018 (x%), 642.2008 (x%), 642.1996 (84.3%).

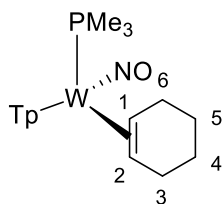
### Synthesis of $\text{WTP}(\text{PMe}_3)(\text{NO})(\kappa^1\text{-N-acetonitrilium})$ (**7**)



Observation of **7** occurred originally in situ when a solution of **1** in  $\text{MeCN-d}_3$  was prepared at  $-30\text{ }^{\circ}\text{C}$  with pyridinium triflate and allowed to warm to  $0\text{ }^{\circ}\text{C}$  in the NMR. Signs consistent with the formation of **7** appeared during the initial timepoint.<sup>20</sup>

Alternatively, 4-dram vial was charged with **1** (0.100 g, 0.164 mmol) along with MeCN (1mL) at -30 °C. The reaction mixture is initially a homogeneous yellow color and upon addition of pyridinium triflate turns to a homogeneous red color .allowed to warm to room temperature over a course of 10 minutes. Over this period the reaction mixture turns to a homogeneous green/teal coloration. This solution was then added to a solution of -30 °C chilled diethyl ether (10 mL) to generate a light green tinted solid. This solution was allowed to sit at -30 °C over a course of 16 h to induce precipitation. The next day the organic layer was decanted and the resulting solid, an off green color, was dried with a stream of N<sub>2(g)</sub> and allowed to dry under dynamic vacuum for 30 min before analysis by <sup>1</sup>H NMR to confirm the identity of the product.<sup>20</sup> A mass of the product was not taken.

### Synthesis of WTp(NO)(PMe<sub>3</sub>)(η<sup>2</sup>-1,2-cyclohexene) (**10**)



A 4-dram vial was charged with 1 mL of DME, complex **1** (0.200 g, 0.344 mmol) and cyclohexene (2.00g, 24.3 mmol) and this heterogenous yellow reaction mixture was allowed to stir. After 27 h the now homogenous purple reaction mixture was added to a 250 mL filter flask and the solvent was removed in vacuo. The resulting pink solid was re-dissolved in 2 mL of DCM and slowly added to 30 mL of stirring pentanes that had been chilled to -30°C. Upon addition a light pink solid precipitates out of solution. This light pink solid was collected on a 30 mL fine porosity fritted disc and subsequently washed with 3 x 5 mL of chilled pentane. The collected product was then desiccated for 2 h to yield a fine light pink powder (0.083 g, 41%).

### Alternative Synthesis of WTp(NO)(PMe<sub>3</sub>)(η<sup>2</sup>-1,2-cyclohexene) (**5**)

To a 4-dram vial **4** (0.107 g, 0.136 mmol) was dissolved in 1 mL of MeOH and chilled to -30°C. To this was added NaBH<sub>4</sub> that had been dissolved and chilled in a -30°C MeOH solution. The solution of **4** was then added to the NaBH<sub>4</sub>/MeOH solution and the resulting reaction mixture was allowed to sit at -30°C for 16 h. The reaction mixture was then eluted through a silica column on a fine 15 mL fritted disc and a light yellow band was eluted with ether. The solvent was then removed in vacuo and picked up in 1 mL of DCM. This was then added to 15 mL of sitting hexanes and allowed to sit at -30°C for 2 h during which a light yellow solid had precipitated from solution. This solid was then isolated on a fine 15 mL fritted disc, washed with 2x5 mL of hexanes to yield an off-white solid (0.058 g, 67%).

CV (MeCN):  $E_{p,a} = +0.28$  V (NHE). IR:  $\nu(\text{BH}) = 2482$  cm<sup>-1</sup>,  $\nu(\text{NO}) = 1554$  cm<sup>-1</sup>. <sup>1</sup>H-NMR (CDCl<sub>3</sub>,  $\delta$ , 25 °C): 8.28 (1H, d, Tp3A), 8.08 (1H, d, Tp3B), 7.69 (1H, d, Tp5B), 7.64 (1H, d, Tp5C), 7.60 (1H, d, Tp5A), 7.24 (1H, d, Tp3C), 6.28 (1H, t, Tp4B), 6.20 (1H, t, Tp4A), 6.13 (1H, t, Tp4C), 3.00 (1H, m, H6<sub>exo</sub>) 2.92 (2H, overlap, m, H4-*endo/exo*), 2.71 (1H, m, H1), 2.64 (1H, m, H6-*endo*), 1.75 (2H, overlap, m, H6-*endo/exo*), 1.46 (2H, overlap, m, H5-*endo/exo*), 1.38 (1H, m, H2), 1.21 (9H, d,  $J_{\text{PH}} = 8.1$ , PMe<sub>3</sub>). <sup>13</sup>C-NMR (CDCl<sub>3</sub>,  $\delta$ , 25 °C). 143.4 (Tp3B), 142.9 (Tp3A),

140.1 (Tp3C), 136.2 (Tp5), 135.6 (Tp5). 135.4 (Tp5), 106.3 (Tp4B), 105.6 (Tp4), 105.5 (Tp4), 53.8 (C2), 53.6 (C1, d,  $J_{PC} = 10.6$ ), 30.0 (C6, d,  $J_{PC} = 4.2$ ), 29.4 (C3), 24.9 (C4/5), 24.8 (C4/5), 14.0 (PMe<sub>3</sub>, d,  $J_{PC} = 27.5$ ). <sup>31</sup>P-NMR (CDCl<sub>3</sub>, δ, 25 °C): -9.1 ( $J_{WP} = 291$ , PMe<sub>3</sub>). Anal. Calcd for 20C<sub>18</sub>H<sub>29</sub>BN<sub>7</sub>OPW·DCM: C, 36.79; H, 4.98; N, 16.76. Found: C, 37.35; H, 4.58; N, 16.69.

#### Characterization in MeCN-*d*<sub>3</sub>

<sup>1</sup>H-NMR (MeCN-*d*<sub>3</sub>, δ, 25 °C): 8.21 (1H, d, Tp3A), 8.03 (1H, d, Tp3B), 7.85 (1H, d, Tp5B), 7.78 (1H, d, Tp5C), 7.75 (1H, d, Tp5A), 7.35 (1H, d, Tp3C), 6.36 (1H, t, Tp4B), 6.27 (1H, t, Tp4A), 6.21 (1H, t, Tp4C), 3.04 (1H, m, H6*exo*), 2.93 (1H, m, H3-*exo*), 2.86 (1H, m, H3-*endo*), 2.72 (1H, m, H1), 2.63 (1H, m, H6-*endo*), 1.69 (1H, m, H4-*endo*), 1.66 (1H, m, H5-*endo*), 1.42 (2H, overlap, m, H4/H5-*exo*), 1.16 (1H, m, H2), 1.10 (9H, d,  $J_{PH} = 8.2$ , PMe<sub>3</sub>). <sup>13</sup>C-NMR (MeCN-*d*<sub>3</sub>, δ, 25 °C): 144.2 (Tp3B), 143.3 (Tp3A), 141.7 (Tp3C), 137.6 (Tp5), 136.9 (overlapping Tp5), 107.4 (Tp4B), 106.9 (Tp4A), 106.6 (Tp4C), 53.5 (2C, overlapping C1 and C2), 30.7 (C6), 30.2 (C3), 25.6 (2C, overlapping C4/C5), 25.4 (2C, overlapping C4/C5), 13.8 (PMe<sub>3</sub>, d,  $J_{PC} = 27.5$ ).

## References

1. Graham, P. M.; Meiere, S. H.; Sabat, M.; Harman, W. D., Dearomatization of Benzene, Deamidization of N,N-Dimethylformamide, and a Versatile New Tungsten  $\pi$  Base. *Organometallics* **2003**, *22* (22), 4364-4366.
2. Harman, W. D.; Taube, H., Reactivity of pentaammineosmium(II) with benzene. *Journal of the American Chemical Society* **1987**, *109* (6), 1883-1885.
3. Meiere, S. H.; Brooks, B. C.; Gunnoe, T. B.; Sabat, M.; Harman, W. D., A Promising New Dearomatization Agent: Crystal Structure, Synthesis, and Exchange Reactions of the Versatile Complex  $\text{TpRe}(\text{CO})(1\text{-methylimidazole})(\eta^2\text{-benzene})$  (Tp = Hydridotris(pyrazolyl)borate). *Organometallics* **2001**, *20* (6), 1038-1040.
4. Myers, J. T.; Smith, J. A.; Dakermanji, S. J.; Wilde, J. H.; Wilson, K. B.; Shivokevich, P. J.; Harman, W. D., Molybdenum(0) Dihapto-Coordination of Benzene and Trifluorotoluene: The Stabilizing and Chemo-Directing Influence of a  $\text{CF}_3$  Group. *Journal of the American Chemical Society* **2017**, *139* (33), 11392-11400.
5. Chordia, M. D.; Smith, P. L.; Meiere, S. H.; Sabat, M.; Harman, W. D., A Facile Diels–Alder Reaction with Benzene: Synthesis of the Bicyclo[2.2.2]octene Skeleton Promoted by Rhenium. *Journal of the American Chemical Society* **2001**, *123* (43), 10756-10757.
6. Keane, J. M.; Chordia, M. D.; Mocella, C. J.; Sabat, M.; Trindle, C. O.; Harman, W. D., Transition Metal-Stabilized Arenium Cations: Protonation of Arenes Dihapto-Coordinated to  $\pi$ -Basic Metal Fragments. *Journal of the American Chemical Society* **2004**, *126* (21), 6806-6815.
7. Winemiller, M. D.; Kopach, M. E.; Harman, W. D., Protonation of Unactivated Aromatic Hydrocarbons on Osmium(II): Stabilization of Arenium Cations via Unprecedented  $\eta^2$ - and  $\eta^3$ -Coordination. *Journal of the American Chemical Society* **1997**, *119* (9), 2096-2102.
8. Harrison, D. P.; Nichols-Nielander, A. C.; Zottig, V. E.; Strausberg, L.; Salomon, R. J.; Trindle, C. O.; Sabat, M.; Gunnoe, T. B.; Iovan, D. A.; Myers, W. H.; Harman, W. D., Hyperdistorted Tungsten Allyl Complexes and Their Stereoselective Deprotonation to Form Dihapto-Coordinated Dienes. *Organometallics* **2011**, *30* (9), 2587-2597.
9. Ding, F.; Kopach, M. E.; Sabat, M.; Harman, W. D., Tandem 1,4-Addition Reactions with Benzene and Alkylated Benzenes Promoted by Pentaammineosmium(II). *Journal of the American Chemical Society* **2002**, *124* (44), 13080-13087.
10. Liebov, B. K.; Harman, W. D., Group 6 Dihapto-Coordinate Dearomatization Agents for Organic Synthesis. *Chemical Reviews* **2017**, *117* (22), 13721-13755.
11. Elgrishi, N.; Rountree, K. J.; McCarthy, B. D.; Rountree, E. S.; Eisenhart, T. T.; Dempsey, J. L., A Practical Beginner's Guide to Cyclic Voltammetry. *Journal of Chemical Education* **2018**, *95* (2), 197-206.
12. Harman, W. D.; Trindle, C., Charge donation to and dearomatization of benzene attending complexation: DFT estimates of binding energies of  $\text{TpMXO}(\text{L})$  with benzene, for Tp = hydridotris(pyrazolyl) borate, MXO = MoNO, ReCO, and WNO, and L = ammonia, N-methylimidazole, pyridine, phosphine, methyl isocyanide, and carbon monoxide. *Journal of Computational Chemistry* **2005**, *26* (2), 194-200.

13. Liu, W.; Welch, K.; Trindle, C. O.; Sabat, M.; Myers, W. H.; Harman, W. D., Facile Intermolecular Aryl–F Bond Cleavage in the Presence of Aryl C–H Bonds: Is the  $\eta^2$ -Arene Intermediate Bypassed? *Organometallics* **2007**, *26* (10), 2589-2597.
14. Mulliken, R. S.; Rieke, C. A.; Brown, W. G., Hyperconjugation\*. *Journal of the American Chemical Society* **1941**, *63* (1), 41-56.
15. Leong, V. S.; Cooper, N. J., Electrophilic activation of benzene in [Cr( $\eta^4$ -C<sub>6</sub>H<sub>6</sub>)(CO)<sub>3</sub>]<sub>2</sub>. *Journal of the American Chemical Society* **1988**, *110* (8), 2644-2646.
16. Sharp, W. B.; Legzdins, P.; Patrick, B. O., O-Protonation of a Terminal Nitrosyl Group To Form an  $\eta^1$ -Hydroxylimido Ligand. *Journal of the American Chemical Society* **2001**, *123* (33), 8143-8144.
17. Hsieh, C.-H.; Ding, S.; Erdem, Ö. F.; Crouthers, D. J.; Liu, T.; McCrory, C. C. L.; Lubitz, W.; Popescu, C. V.; Reibenspies, J. H.; Hall, M. B.; Darensbourg, M. Y., Redox active iron nitrosyl units in proton reduction electrocatalysis. *Nature Communications* **2014**, *5* (1), 3684.
18. Timmons, A. J.; Symes, M. D., Converting between the oxides of nitrogen using metal–ligand coordination complexes. *Chemical Society Reviews* **2015**, *44* (19), 6708-6722.
19. Wilson, K. B.; Smith, J. A.; Nedzbala, H. S.; Pert, E. K.; Dakermanji, S. J.; Dickie, D. A.; Harman, W. D., Highly Functionalized Cyclohexenes Derived from Benzene: Sequential Tandem Addition Reactions Promoted by Tungsten. *The Journal of Organic Chemistry* **2019**, *84* (10), 6094-6116.
20. Lis, E. C.; Delafuente, D. A.; Lin, Y.; Mocella, C. J.; Todd, M. A.; Liu, W.; Sabat, M.; Myers, W. H.; Harman, W. D., The Uncommon Reactivity of Dihapto-Coordinated Nitrile, Ketone, and Alkene Ligands When Bound to a Powerful  $\pi$ -Base. *Organometallics* **2006**, *25* (21), 5051-5058.
21. Heiden, Z. M.; Lathem, A. P., Establishing the Hydride Donor Abilities of Main Group Hydrides. *Organometallics* **2015**, *34* (10), 1818-1827.
22. Harman, W. D.; Taube, H., The selective hydrogenation of benzene to cyclohexene on pentaammineosmium(II). *Journal of the American Chemical Society* **1988**, *110* (23), 7906-7907.

## **Chapter 3**

# **Preparation of Cyclohexene Isotopologues and Stereoisotopomers from Benzene**



### 3.1 Introduction

The hydrogen isotopes deuterium (D) and tritium (T) have become essential tools of chemistry, biology, and medicine.<sup>1</sup> Beyond their widespread use in spectroscopy, mass spectrometry, and mechanistic and pharmacokinetic studies, there has been considerable interest in incorporating deuterium into the active pharmaceutical ingredient (API) of drugs.<sup>1</sup> The deuterium kinetic isotope effect (DKIE), which compares the rate of a chemical reaction for a compound to its deuterated counterpart, can be dramatic.<sup>1-3</sup>

Consequently, the strategic replacement of hydrogen with deuterium can affect both the rate of metabolism and distribution of metabolites for a compound,<sup>4</sup> improving the efficacy and safety of the drug. As an example, Deutetrabenazine, a promising treatment for Huntington's disease,<sup>5</sup> recently became the first deuterated drug to win FDA-approval. Significantly, the pharmacokinetics of a deuterated compound depends on the location(s) where the deuterium/hydrogen replacement has occurred. While methods currently exist for deuterium incorporation at both early and late stages of a drug's synthesis,<sup>6-7</sup> these processes are often unselective and the stereoisotopic purity can be difficult to measure.<sup>7-8</sup> A systematic method for the preparation of pharmacologically active compounds as discrete stereoisotopomers could improve pharmacological and toxicological properties of drugs and provide new mechanistic information related to their distribution and metabolism in the body.

Herein we describe a new approach toward the preparation of stereoselectively deuterated "building blocks" for pharmaceutical research. We demonstrate proof of concept through a four-step conversion of benzene to cyclohexene, as bound to a tungsten complex. Using different combinations of deuterated and protected acid and hydride reagents, positions of deuterium incorporation can be precisely controlled on the cyclohexene ring. In total, 52 unique

stereoisotopomers of cyclohexene are available, in the form of ten different isotopologues. This concept can be extended to prepare discrete stereoisotopomers of functionalized cyclohexenes that can be incorporated into drug design.

Our longstanding interest in opening new pathways of reactivity for aromatic molecules through their *dihapto-coordination* to transition metal complexes<sup>9</sup> prompted us to query whether it would be possible to carry out

the deuteration of benzene regio-

and stereoselectively to form various isotopomers of cyclohexene. Typically, hydrogenation of

benzene using D<sub>2</sub> gas leads to isotopologue mixtures of cyclohexane.<sup>10-12</sup> However, Taube et al.

demonstrated that the complex [Os(NH<sub>3</sub>)<sub>5</sub>(η<sup>2</sup>-benzene)]<sup>2+</sup> could be deuterated to form a single stereoisotopomer of [Os(NH<sub>3</sub>)<sub>5</sub>(η<sup>2</sup>-cyclohexene-*d*<sub>4</sub>)]<sup>2+</sup> using D<sub>2</sub> and a Pd/C catalyst.<sup>13</sup> We posited

that benzene bound in this manner could also be converted to cyclohexene using four well-defined

additions of “ionic hydrogen” (H<sup>+</sup>, H<sup>-</sup>, H<sup>+</sup>, and H<sup>-</sup>), passing through an η<sup>2</sup>-1,3-cyclohexadiene

intermediate (**Figure 3.1**). If these reactions could be performed regio- and stereoselectively, one

could access a diverse set of isotopologues and even stereoisotopomers of cyclohexene using

various combinations of protected and deuterated reagents.

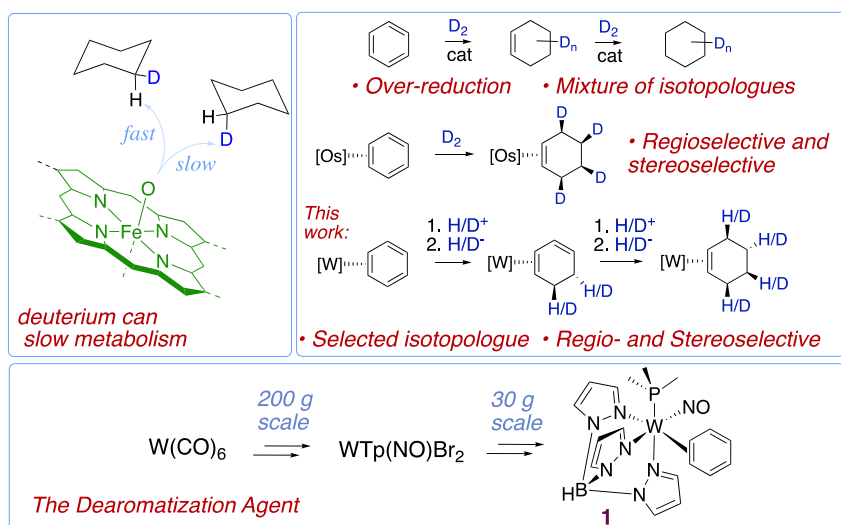


**Figure 3.1.** Deuterium kinetic Isotope effect (DKIE; left), methods for the selective deuteration of benzene (right), and the dearomatized benzene complex WTP(NO)(PMe<sub>3</sub>)(η<sup>2</sup>-benzene) (bottom).

### 3.2 The Protonation of Benzene and Cyclohexadiene Complexes of Tungsten

The dearomatization agent {WTp(NO)(PMe<sub>3</sub>)} is considerably more activating than its osmium predecessor.<sup>9</sup> Strong  $\pi$ -backbonding renders arene and diene complexes of this system highly nucleophilic, and resistant to substitution.<sup>9</sup> Furthermore, this system displays significant electronic asymmetry, and the benzene complex WTp(NO)(PMe<sub>3</sub>)( $\eta^2$ -benzene) (**1**) can be prepared on a multi-gram scale,<sup>14</sup> and in enantioenriched form.<sup>15</sup> Treatment of an acetone-*d*<sub>6</sub> solution of **1** with diphenylammonium triflate (DPhAT, pK<sub>a</sub> ~ 0) at -30 °C affords its clean conversion to the  $\eta^2$ -benzenium complex [WTp(PMe<sub>3</sub>)(NO)( $\eta^2$ -C<sub>6</sub>H<sub>7</sub>)](OTf) (**2**; **Figure 3.2**). Using chilled diethyl ether as a precipitating solvent, **2** can be isolated from dichloromethane in 86% yield (1.9 g). As an acetonitrile solution, the  $\eta^2$ -benzenium complex **2** is moderately stable at room temperature but soon decomposes (*t*<sub>1/2</sub> ~ 6 min). At 0°C, however, **2** exists in equilibrium with its diastereomer **3** in a 10:1 ratio (**Figure 2**) and persists for three hours without significant decomposition.

The major isomer (**2**) is formed with the metal binding two internal carbons of the five-carbon  $\pi$ -system, and with the newly formed sp<sup>3</sup> carbon distal to the PMe<sub>3</sub> ligand. The minor isomer (**3**) is bound at a terminus of the  $\pi$ -system with the sp<sup>3</sup> carbon proximal to the phosphine. Proton NMR data and DFT calculations (Chapter 3 Appendix; **Figures S1-S3**) of these  $\eta^2$ -benzenium complexes (**2**, **3**) suggest that they are similar in structure to complexes of the form [WTp(NO)(PMe<sub>3</sub>)( $\eta^2$ -allyl)]<sup>+</sup>,<sup>16</sup> where the allyl ligand is tightly bound to the metal through only two carbons. A third carbon, *weakly* associated to the metal, resembles a carbocation, and is indicated as such in figures herein (**Figure 3.2**).

Combining cold solutions of **2** and tetrabutylammonium borohydride generates WTp(PMe<sub>3</sub>)(NO)( $\eta^2$ -1,3-cyclohexadiene) exclusively (**4**). Despite the coexistence of the allyl conformer **3** in solution, the WTp(PMe<sub>3</sub>)(NO)( $\eta^2$ -1,4-cyclohexadiene) complex (**8**) is undetected

(**Figure 3.2**) in the reaction mixture.<sup>16</sup> The  $\eta^2$ -diene complex **4** was then treated with either DPhAT or HOTf/MeOH acids to generate the  $\eta^2$ -allyl complex (**6**).<sup>16</sup> When **6** was subjected to base, it deprotonated to form **5**, a stereoisomer of **4**,<sup>16</sup> in which the uncoordinated double bond is now distal to the  $\text{PMe}_3$ .<sup>16</sup> Combining the allyl complex **6** with a hydride source produced the desired  $\eta^2$ -cyclohexene complex **7** (67%). Crystals suitable for X-ray structure determinations were grown for complexes of cyclohexadiene **4**, allyl complex **6**, and cyclohexene **7**, and a rendering of these structures, along with key NOE

interactions are provided in supplementary material (Chapter 3 Appendix, **Figure S4**). An overlap of signals in the  $^1\text{H}$  NMR spectrum of cyclohexene complex **7** precluded unambiguous stereochemical assignments of some of the ring proton signals.

However, by methylating the nitrosyl ligand of **7** ( $\text{CH}_3\text{OTf}$ ) to generate  $[\text{WTP}(\text{NOMe})(\text{PMe}_3)(\eta^2\text{-C}_6\text{H}_{10})\text{OTf}]$  (**9**),<sup>17</sup> the chemical shifts of the cyclohexene ring separated to the point that each proton could be assigned with high confidence (Chapter 3 Appendix). An X-ray structure determination of **9** provided conclusive evidence for methylation of the nitrosyl oxygen (**Figure 3.2**), analogous to

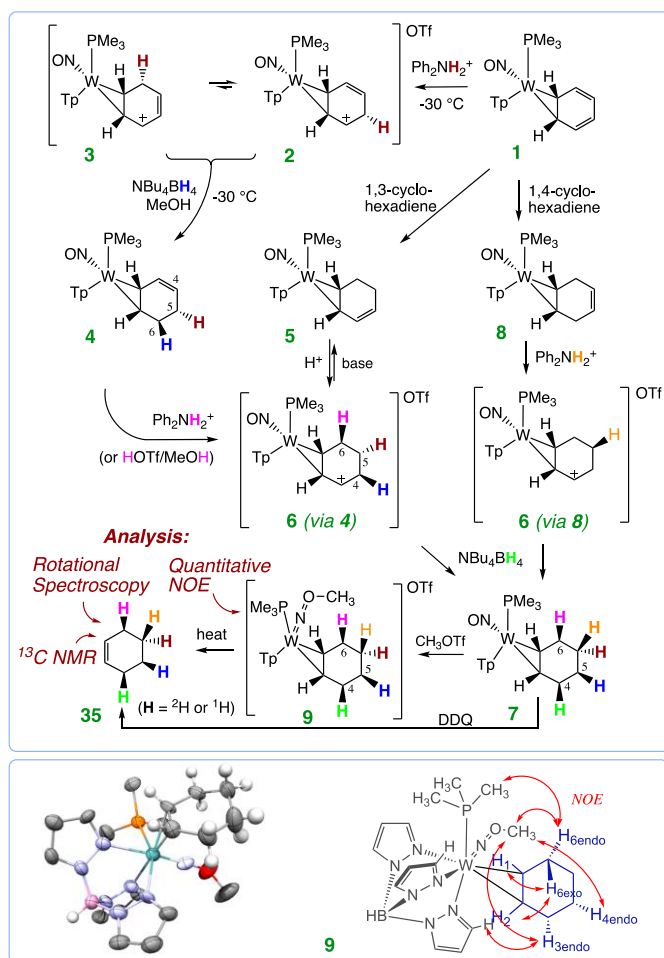


**Figure 3.2.** The sequential reduction of benzene to cyclohexene bound to tungsten. inset: Molecular structure determination and relevant NOE interactions (red arrows) for methylated cyclohexene complex, **9** ( $\text{Ph}_2\text{NH}_2^+$  as OTf salt).

earlier literature reports.<sup>18</sup> Strong NOE interactions between the ring endo protons and the methylated nitrosyl ligand further facilitated these assignments and quantitative NOE experiments were carried out that support the stereochemical assignments of all diastereotopic protons on the cyclohexene ring (Chapter 3 Appendix, section H).

### 3.3 Deuterium Studies

With all hydrogen resonances for the methylated  $\eta^2$ -cyclohexene complex **9** fully assigned, we embarked on a series of deuteration experiments to investigate the regio- and stereochemical fidelity of the reaction sequence (**Figure 3.3**). When the  $\eta^2$ -benzenium complex **11** is prepared from **1** using  $[\text{MeOD}_2^+]\text{OTf}$ , a loss of signal intensity is observed corresponding to the methylene endo proton. This indicates that protonation of the  $\eta^2$ -benzene occurs *endo* relative to the metal (red, **Figure 3.3**). A complementary experiment was next performed starting with the fully deuterated benzene complex, **17**, in which  $\text{MeOH}^+$  was used as the acid source. In this case, protonation led to a single broad proton resonance for the deuterated  $\eta^2$ -benzenium complex **18**. This proton signal is  $\sim 0.03$  ppm upfield from its proteo counterpart, consistent with a primary H/D isotopic shift.<sup>19</sup> The endo-selective protonation of the benzene ligand in **1** is in stark contrast to the addition of carbon and heteroatom electrophiles, which have been observed to add *exo* to  $\eta^2$ -arene and  $\eta^2$ -diene ligands of tungsten complexes.<sup>9</sup> When  $\eta^2$ -benzenium complexes **11** and **18** were treated with  $\text{NaBD}_4$  or  $\text{NaBH}_4$ , respectively, the complementary cyclohexadiene complexes **12** and **19** were formed (**Figure 3.3**). A comparison of NOESY data for all three isotopologues of the cyclohexadiene complex (**4**, **12**, **19**) confirms that the proton delivered from the borohydride reagent is *exo* relative to the metal (blue H; **Figure 3.3**). The cyclohexadiene complexes **12** and **19** were then taken forward to their  $\pi$ -allyl analogs **13**, **15**, and **20** (**Figure 3.3**). This time, in contrast

to protonation of the  $\eta^2$ -benzene ligand of **1**, the acidic hydrogen was delivered predominantly *exo* to the metal (pink, **Figure 3.3**).

Of note, the resulting  $\eta^2$ -allyl complexes (**13**, **15**, **20**) have undergone a conformational change (“allyl shift”) such that the second proton added becomes H<sub>6<sub>exo</sub></sub> (conversion of **4** to **6**, **Figure 3.2**), while the first proton added is now H<sub>5<sub>endo</sub></sub>. For allyl complexes **13** and **20**, full stereoselective protonation was achieved. However, with the preparation of **15** or **26** we experienced difficulties in achieving full deuterium incorporation, owing to an unusually large DKIE ( $k_H/k_D \sim 37$  at -30 °C for the deuteration of **12** or **4**). This DKIE was determined for **4** as the average value from three separate experiments in which **26** was generated from acidic solutions with differing H/D ratios (Chapter 3 Appendix, SI, section K). This DKIE could be decreased by raising the temperature to 22 °C, however such action compromised the stereofidelity of the resulting deuterated product (**15**), with endo deuteration of the  $\eta^2$ -diene **12** now competing with exo deuteration. Consequently, stereoselective deuterium incorporation at the H<sub>6<sub>exo</sub></sub> position of cyclohexene (i.e., **16**, **33-35**, **41**, **44**, **49**, **51**; pink D, **Figure 3.3**) could not be achieved above ~75-80%. A similar outcome was observed when we tried to convert the d<sub>6</sub>-isotopologue, diene **19** to allyl **30**.

Finally, as before, treatment of **13**, **15**, or **20** with a hydride or deuteride source confirmed that the corresponding  $\eta^2$ -cyclohexene products (**14**, **16**, **21**) are formed by nucleophilic addition *anti* to the metal (**Figure 3.3**). Similar to the 1,3-diene complex **4**, its isomer **5** undergoes exo protonation to form the allyl complex **24**. Remarkably, treatment of the 1,4-cyclohexadiene complex (**8**) with D<sup>+</sup> (D<sub>2</sub>NPh<sub>2</sub><sup>+</sup> in MeOD) also undergoes direct exo protonation (Figure 3), this time providing allyl **25**. The direct exogenous protonation of the *unconjugated* C=C bond in **8** appears to result in a carbocation that DFT calculations reveal can be stabilized by the participation

of the nitrosyl ligand. A subsequent [1,2]-hydride shift results in the formation of the allyl complex **25** (Chapter 3 Appendix, **Figure S5**). Unambiguous assignment of the deuterated hydrogen atom in **25** comes from its conversion to **9-*d*<sub>1</sub>** (via **39**; **Figure 3.3**).

In order to demonstrate regio- and stereocontrol of deuterium incorporation, additional deuterated isotopomers of the allyl complex were prepared from the monodeuterated dienes **22** and **23**, and from the benzene-*d*<sub>6</sub>-derived allyls **30** and **31** (**Figure 3.3**). The allyl complexes **24-31** were then combined with deuteride or hydride to form 18 additional cyclohexene complexes **32-46**, **49-51**. In principle, one can *selectively* make 10 different isotopologues of the cyclohexene complex using the procedures outlined above (*d*<sub>0</sub>-*d*<sub>4</sub>; *d*<sub>6</sub>-*d*<sub>10</sub>), eight of which (**7**, **16**, **32-38**) are reported herein.

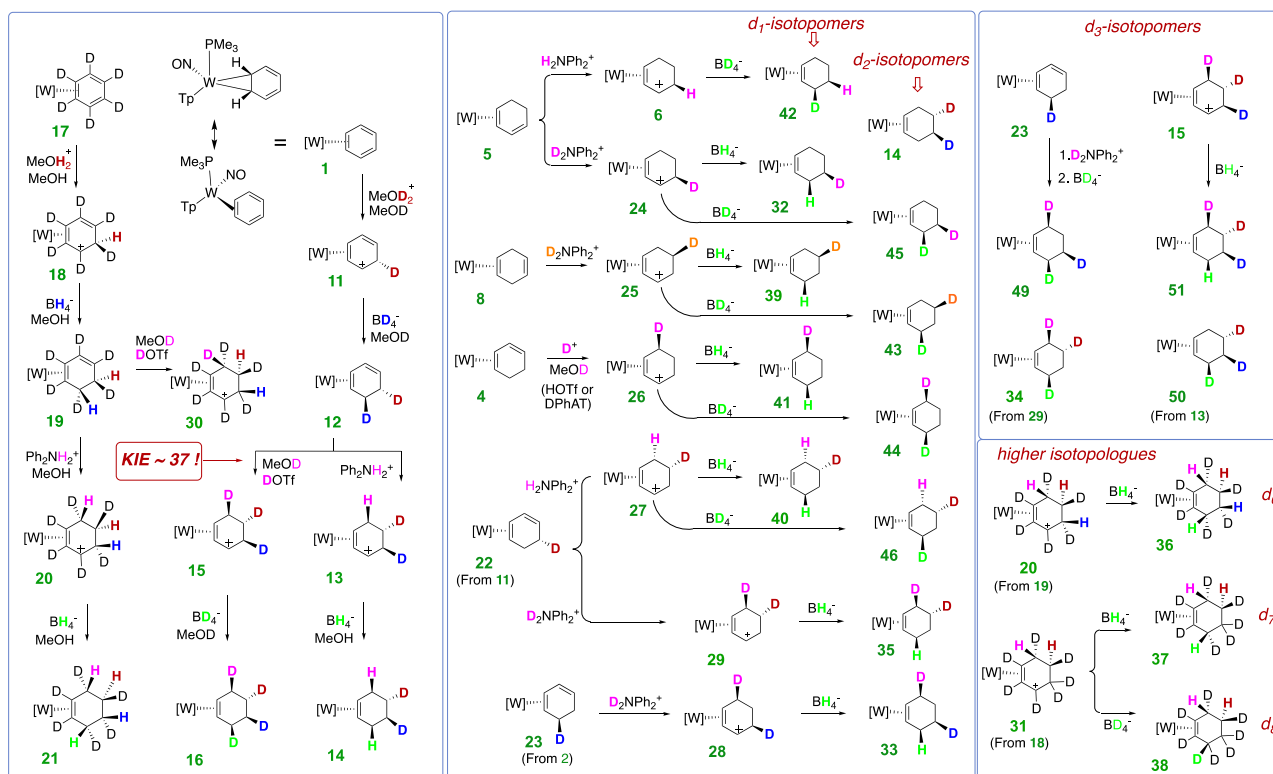


**Figure 3.3.** Synthesis of isotopologues and stereoisotopomers of the cyclohexene complex **7**.

### 3.4 Methods to Determine Isotopic Purity

Levels of isotopic purity for the cyclohexene ligand isotopologues were determined by recording HRMS data for the corresponding complexes as their methylated adducts (**Figure 3.2. 9- $d_n$** ), in order to create a suitable cation for ESI mass analysis. Using the isotope envelope of **9- $d_0$**  as a reference (Chapter 3 Appendix, **Figure S6**), the isotopic purity of **7**, **16**, and **32-38** (as converted to **9- $d_n$** ) was estimated to be >90%, with the exception of **16** (79%), for which the high DKIE of the second protonation prevented complete deuteration at the H<sub>6exo</sub> position (vide supra). Finally, as a demonstration of how the {WTP(NO)(PMe<sub>3</sub>)} system precisely governs both the stereochemistry and regiochemistry of protonation and hydride addition, a series of five monodeuterated (**32, 39-42**), seven dideuterated (**14, 33, 35, 43-46**), and four trideuterated (**34, 49-51**) isotopomers of the cyclohexene complex were prepared from these methods (**Figure 3.3**).

Oxidation of the tungsten complex **7** with DDQ releases the free cyclohexene (**Figure 3.2; 10**). Such action on **32, 42, 45, and 46** confirmed the expected regiochemistry of these  $d_1$  and  $d_2$  isotopomers of cyclohexene via <sup>13</sup>C NMR. Of note, introduction of a single deuterium in 3-deuterocyclohexene or 4-deuterocyclohexene allows one to distinguish all six of the carbons in the <sup>13</sup>C NMR spectrum, owing to isotopic shifting of the now asymmetric cyclohexene carbons (Chapter 3 Appendix, **Figure S7**). Alternatively, solvent-free heating of various isotopologues of the methylated complex **9** effected the release of the cyclohexene ligand for analysis by MRR spectroscopy (Chapter 3 Appendix, section L).<sup>20</sup> These experiments determined that 1) over-deuteration is exceedingly low (< 2%). 2) the stereoselectivity is excellent when assessed by observation of undesired cis/trans isomers, which in the worst case is 22:1 and in other cases it is 40:1 or higher. 3) The dominant stereoisotopomers in all cases are those predicted by <sup>1</sup>H NMR data. As a final check of stereochemical assignments, the locations of the deuterium atoms were



confirmed for complex **45** by neutron diffraction at Oak Ridge National Lab (Chapter 3 Appendix, SI section I; TOPAZ at ONRL).

### 3.5 Mechanistic Considerations

The reaction of **1** with  $D^+$  to form **11** results in deuterium incorporation exclusively endo to the metal, but this does not definitively show which carbon is initially protonated (**Figure S8**). Given that the endo proton of the benzene ligand in **1** completely preempts protonation from an exogenous acid (exo), we propose that the protonation must be concerted-- that *C-H bond formation is intramolecular and simultaneous with electronic changes at the metal*, which could lower the activation barrier for this process relative to protonation by an external acid. Such a mechanism could occur via a hydride intermediate, but this seems sterically untenable. Rather, we propose a mechanism (Chapter 3 Appendix, section M; **Figure S8**) in which the nitrosyl ligand first is protonated to form a hydroxylimido ligand analogous to that reported by Legzdins et al.<sup>21</sup> This action is followed by a concerted proton transfer in which a gamma carbon of the benzene is protonated simultaneously with release of electron density back into the tungsten through the NO group. The role of nitrosyl ligands in intramolecular proton transfer has been previously documented.<sup>22</sup> In contrast, the stereochemistry and kinetics of  $\eta^2$ -diene protonation (e.g., **4**, **Figure 3.2**) indicates the hydrogen is delivered exogenously, anti to the tungsten (**Figure 3.1**). We speculate that while endo protonation may still be accessible for these 1,3-cyclohexadiene complexes, the less-delocalized diene ligand is most likely more basic than its  $\eta^2$ -benzene predecessor, and its direct exo protonation apparently preempts the purported endo mechanism at -30 °C.

### 3.6 Comparison to Other Systems and Considerations of Absolute Stereocontrol

Transition metal promoted protonation of benzene was observed in the  $\eta^4$ -benzene complexes  $\text{Cr}(\text{CO})_3(\eta^4\text{-benzene})^-$  and  $\text{Mn}(\text{CO})_3(\eta^4\text{-benzene})^-$  by Cooper et al,<sup>23-24</sup> and was proposed to occur via hydride intermediates.<sup>23-24</sup> More recently, Chirik et al have explored the molybdenum-catalyzed reduction of benzene and cyclohexadiene, with  $\text{D}_2$  (g), which resulted in mixtures of isotopologues of cyclohexane.<sup>12</sup> However, reduction of cyclohexene with  $\text{D}_2$  produced a single cis isotopomer of 1,2-dideuterocyclohexane using the molybdenum catalyst.

The high stereoselectivity enabled by the tungsten system provides unprecedented control over the preparation of specific isotopologues and isotopomers of cyclohexene, starting from either benzene complex **1** or its deuterated analog **17**, and utilizing either proteated or deuterated sources of acids and hydrides (Chapter 3 Appendix, **Table S1**). As illustration, consider the  $d_2$ -isotopologue of the cyclohexene complex, **7-d<sub>2</sub>**. Given that the  $\{\text{WTp}(\text{NO})(\text{PMe}_3)\}$  system is available in enantioenriched form,<sup>15</sup> one has access to 14 different isotopomers (individual enantiomers of **14**, **33**, **35**, **43-46**; Chapter 3 Appendix, **Table S2**). The cyclohexene- $d_2$  ligand of these complexes, once removed from the metal by oxidative decomplexation, would be available as 11 individual isotopomers: both enantiomers of *cis*-3,4-, *trans*-3,4-, *cis*-3,5-, *trans*-3,5-, *trans*-4,5-, and the meso compound *cis*-3,6-dideuterocyclohexene. Similarly, 11 distinct isotopomers of cyclohexene- $d_8$  should be available from this methodology starting from benzene- $d_6$ . Regarding cyclohexene complex **7-d<sub>3</sub>** and **7-d<sub>7</sub>**, 8 isotopomers of each would be available, and all 16 of these complexes would yield a unique, chiral cyclohexene (8 cyclohexene- $d_3$ , and 8 cyclohexene- $d_7$ ). All totaled, (Chapter 3 Appendix, **Table S2**) the methodology outlined herein could provide access to 52 unique isotopomers of cyclohexene, as derived from benzene and benzene- $d_6$ . For reference, the total number of isotopomers for cyclohexene is 528.

The ability of {WTP(NO)(PMe<sub>3</sub>)} to be optically resolved on a practical scale and to retain its stereochemical configuration, even when undergoing ligand displacement,<sup>15</sup> also makes it a valuable tool for determining the isotopic pattern of cyclohexene H/D isotopomers produced by other methods.<sup>8</sup> Consider for example a scenario in which an unknown isotopomer of cyclohexene-*d*<sub>1</sub> is combined with the resolved form of benzene complex (*R*)-**1** in solution and allowed to undergo ligand exchange. Even though the two faces of the cyclohexene ring will bind to tungsten with equal probability, the <sup>1</sup>H NMR spectrum will be unique for each of the five possible isotopomers (Chapter 3 Appendix , SI; **Figure S11**). A similar approach could be taken for any cyclic alkene (e.g., dehydropiperidines, pyrrolines, cyclopentenes) for which an <sup>1</sup>H NMR spectrum of a fully deuterated species can be fully assigned (*vide supra*).

The development of deutetribenzazine, is considered by many as a prelude to a new generation of medicines and therapies that incorporate deuterium into the active pharmaceutical ingredient.<sup>5</sup> Given that *each stereoisotopomer of a biologically active substance will have its own unique pharmacokinetic profile*, the ability to stereoselectively deuterate cyclohexene or other medchem building blocks could enable the development of new probes, fragment libraries, and leads for medicinal chemists, as well as providing a new tool for organic and organometallic mechanistic studies. Cyclohexene can be readily converted into perhydroindoles,<sup>25</sup> perhydroisoquinolines,<sup>26</sup> and azepines.<sup>27</sup> However, the inability to chemically differentiate the two alkene carbons or the enantioface of the deuterated cyclohexene limits its potential. But by replacing the benzene ligand in Figure 2 with a substituted benzene, or utilizing a non-hydrogenic nucleophile in the conversion of **6** to **7** (**Figure 3.2**), one can envision a series of 3-substituted cyclohexenes with highly defined isotopic patterns.

### 3.7 Isotopologues of Substituted Cyclohexene

As proof of concept, we prepared the tungsten-trifluorotoluene complex  $\text{WTp}(\text{NO})(\text{PMe}_3)(\eta^2\text{-CF}_3\text{Ph})$ ,<sup>28</sup> which can be elaborated into a 3-(trifluoromethyl)cyclohexene complex (**47**) analogous to the cyclohexene complex **7** (Chapter 3 Appendix, **Figure S14**). Liberation of the cyclohexene from  $\{\text{WTp}(\text{NO})(\text{PMe}_3)\}$  can be accomplished by a one-electron oxidant such as DDQ, Fe(III), or  $\text{NOPF}_6$  in yields ranging from 70-75%.<sup>28</sup> Oxidation of **47** would generate a cyclohexene that has been previously shown to undergo diastereoselective epoxidation, and would therefore be an attractive building block for medicinal chemistry.<sup>29</sup> Repeating the synthesis of **47** with deuteride in the final step yields the *cis*-6-deutero-3-(trifluoromethyl)cyclohexene complex **52** in 95% yield.

Various other isotopologues of **47** and **52** were also prepared (**47**, **52**, **53**, **54**), and the reaction pattern was found to be similar to that observed for benzene. Prepared compounds are summarized in **Figure 3.4**, with synthetic details provided in the experimental section of this chapter. Notably, in the syntheses of **47**, **52**, **53**, **54**, protonation at the carbon bearing the  $\text{CF}_3$  group ultimately occurs endo to the metal, allowing the  $\text{CF}_3$  group to assume an exo stereochemistry. However, if the purported diene intermediate is protonated under kinetic control, exo protonation forces the  $\text{CF}_3$  group endo, and the result after a second hydride reduction is the cyclohexene complex **55**. Exploiting this reactivity feature, we were able to prepare other isotopologues of **55** with inversion of the stereocenter bearing the  $-\text{CF}_3$  substituent (**Figure 3.4**, **56**, **57**; Chapter 3 Appendix, **Figure S14**).

As further demonstration of the ability of this methodology to selectively prepare isotopomers of functionalized cyclohexenes, we have prepared the tungsten complex of *cis,trans*-3-cyano-4,5-dideuterocyclohexene (**58**) by the addition of cyanide to the allyl intermediate **13** (57%; dr > 98%;

**Figure 3.4.**) Other d<sub>1</sub>-isotopologues were also prepared (Chapter 3 Appendix, **Figure S15**) and the stereochemistry could again be controlled with the sequence of nucleophiles. For example, **58**, **59** and **60** could be prepared by generating the appropriate isotopologue of the tungsten-allyl complex and then treating with NaCN (Chapter 3 Appendix, **Figure S16**).

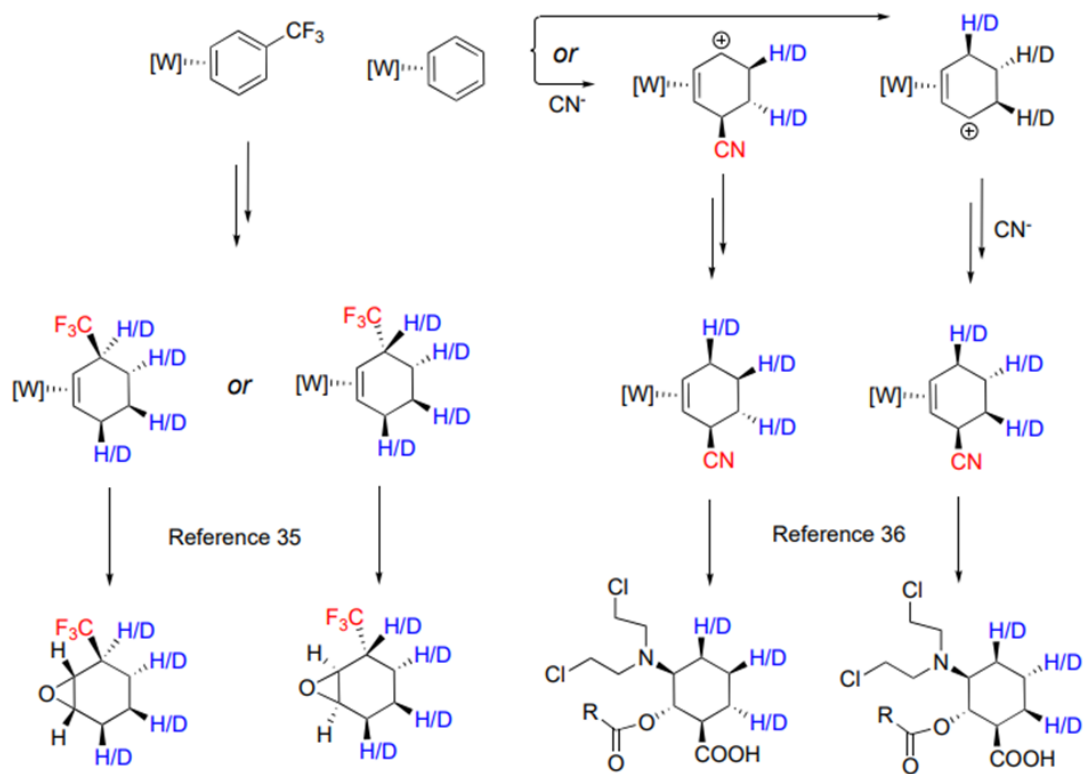


**Figure 3.4.** Examples of functionalized cyclohexene isotopomer complexes.

Conversely, treating the benzenium **2** with NaCN leads to a cyano-substituted cyclohexadiene that can subsequently be combined with acid and hydride source to generate other cyclohexene isotopomers (**61-63**). 3-cyanocyclohexene (proteo form) has been previously used as a precursor to cytotoxic mustards that are of interest in cancer research.<sup>30</sup> Allyl-substituted cyclohexenes theoretically exist as 1024 different H/D isotopomers (512 for each enantiomer). Using the tungsten dearomatization methodology, the CF<sub>3</sub>- and CN-substituted cyclohexenes are accessible as 64 and 60 unique isotopomers respectively. We further note that a full range of both carbon and nitrogen nucleophiles has now been demonstrated to add to tungsten benzenium and allyl tungsten complexes,<sup>31</sup> which demonstrates the broad scope of compounds that can now be prepared as various deuterioisotopomers.

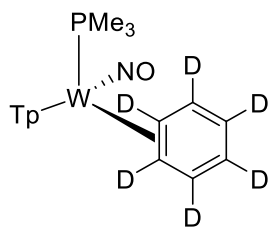
### 3.8 Conclusion

In conclusion, we show that complexation of benzene to {WTP(NO)(PMe<sub>3</sub>)} activates the arene toward a four-step reduction sequence by which deuterium can be selectively incorporated into various positions of the cyclohexene core. This approach provides direct access to 52 unique isotopomers of the organic cyclohexene, and can be adapted to provide substituted cyclohexenes that also can be prepared with excellent isotopomeric control.

## Experimental

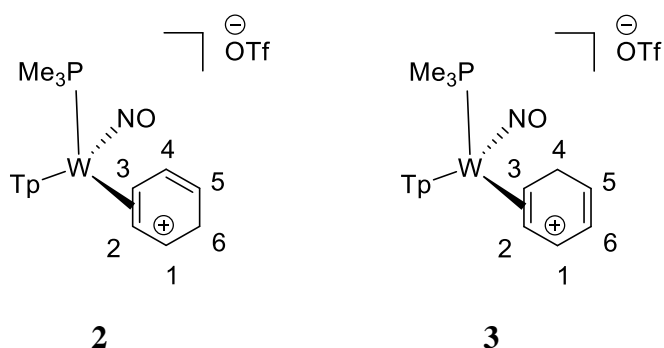
**General Methods.** NMR spectra were obtained on 500, 600 or 800 MHz spectrometers. Chemical shifts are referenced to tetramethylsilane (TMS) utilizing residual  $^1\text{H}$  signals of the deuterated solvents as internal standards. Chemical shifts are reported in ppm and coupling constants ( $J$ ) are reported in hertz (Hz). Chemical shifts for  $^{19}\text{F}$  and  $^{31}\text{P}$  spectra were reported relative to standards of hexafluorobenzene (164.9 ppm) and triphenylphosphine (-6.00 ppm). Infrared Spectra (IR) were recorded on a spectrometer as a solid with an ATR crystal accessory, and peaks are reported in  $\text{cm}^{-1}$ . Electrochemical experiments were performed under a nitrogen atmosphere. Most cyclic voltammetric data were recorded at ambient temperature at 100 mV/s, unless otherwise noted, with a standard three electrode cell from +1.8 V to -1.8 V with a platinum working electrode, acetonitrile (MeCN) solvent, and tetrabutylammonium (TBAH) electrolyte (~1.0 M). All potentials are reported versus the normal hydrogen electrode (NHE) using cobaltocenium hexafluorophosphate ( $E_{1/2} = -0.78$  V, -1.75 V) or ferrocene ( $E_{1/2} = 0.55$  V) as an internal standard. Peak separation of all reversible couples was less than 100 mV. All synthetic reactions were performed in a glovebox under a dry nitrogen atmosphere unless otherwise noted. All solvents were purged with nitrogen prior to use. Deuterated solvents were used as received from Cambridge Isotopes and were purged with nitrogen under an inert atmosphere. When possible, pyrazole (Tp) protons of the (trispyrazolyl) borate (Tp) ligand were uniquely assigned (e.g., “Tp3B”) using two-dimensional NMR data (see Fig. S1). If unambiguous assignments were not possible, Tp protons were labeled as “Tp3/5 or Tp4”. All  $J$  values for Tp protons are 2 ( $\pm 0.4$ ) Hz.

### Synthesis of $\text{WTP}(\text{NO})(\text{PMe}_3)(\eta^2\text{-}d_6\text{-benzene})$ (17)



In an oven-dried 50 mL round bottom flask 25.0 g (297 mmol) of freshly degassed benzene- $d_6$  was added with a Teflon-coated magnetic stir bar. This solution was stirred and **1** (0.404 g, 1.44 mmol) was added resulting in a homogeneous yellow reaction mixture which was allowed to stir for 18 h. The reaction mixture was then added to 100 mL of pentane and the solvent volume was reduced *in vacuo* until half of the original solvent volume had been evaporated. Upon the evaporation of solvent, a golden-yellow colored solid precipitated out of solution. This yellow solid was collected on a fine 15 mL fitted disc and washed with 2 x 15 mL of pentane to yield a yellow solid that was allowed to desiccate for six h. A yellow solid was recovered (0.241 g, 59%).  $^1\text{H}$  NMR features matched those reported previously for **1** with the absence of protons on the benzene ring.

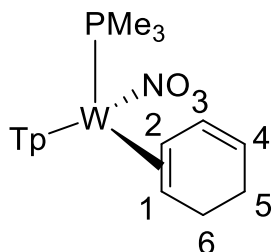
### Synthesis of $\text{WTP}(\text{NO})(\text{PMe}_3)(\eta^2\text{-}2,3\text{-benzenium})$ (2) and $\text{WTP}(\text{NO})(\text{PMe}_3)(\eta^2\text{-}1,2\text{-benzenium})$ (3)



A 4-dram vial was charged with 5 mL of DCM and chilled to  $-30^{\circ}\text{C}$  for 15 min. **1** (1.52 g, 2.61 mmol) was then added, resulting in a heterogeneous yellow reaction mixture. Diphenylammonium triflate (DPhAT) (0.909 g, 2.84 mmol) was added to the reaction mixture at  $-30^{\circ}\text{C}$  resulting in the formation of a homogenous red solution. This solution was allowed to stand at  $-30^{\circ}\text{C}$  for 20 min. This reaction solution was then added to stirring  $\text{Et}_2\text{O}$  that had been chilled to  $-30^{\circ}\text{C}$  (60 mL) to yield a dull yellow precipitate. The yellow solid was collected on a 30 mL fine porosity fritted disc and washed with chilled  $\text{Et}_2\text{O}$  (2 x 20 mL). The isolated yellow solid was then desiccated for 2 h yielding **2** and **3** (1.63 g, 2.24 mmol, 86% yield) in a 10:1 ratio.

CV (MeCN at  $-6^{\circ}\text{C}$ )  $E_{p,a} = +0.70$  V (NHE). IR:  $\nu(\text{BH}) = 2520$   $\text{cm}^{-1}$ ,  $\nu(\text{NO}) = 1637$   $\text{cm}^{-1}$ . **Complex 2** (major):  $^{31}\text{P}$  NMR ( $\text{CD}_3\text{CN}$ ,  $\delta$ ): -7.44 ( $J_{\text{WP}} = 274$ ).  $^1\text{H}$  NMR ( $\text{CD}_3\text{CN}$ ,  $\delta$ ,  $0^{\circ}\text{C}$ ): 8.33 (1H, d, Pz3B/5B), 8.03 (1H, d, Pz3A), 8.02 (1H, d, Pz5C), 7.97 (1H, d, Pz3C), 7.94 (1H, d, Pz3B/5B), 7.80 (1H, d, Pz5A), 6.93 (1H, broad singlet, H1), 6.54 (1H, t, Pz4C), 6.49 (1H, t, Pz4B), 6.31 (1H, t, Pz4A), 6.17 (1H, m, H4), 5.04 (1H, m, H5), 4.91 (1H, t,  $J = 7.2$ , H2), 4.24 (1H, m, H3), 4.16 (1H, d,  $J = 28.3$ , H6-*exo*), 4.00 (1H, d,  $J = 28.3$ , H6-*endo*), 1.18 (9H, d,  $J_{\text{PH}} = 9.9$ ,  $\text{PMe}_3$ ).  $^{13}\text{C}$  NMR ( $\text{CD}_3\text{CN}$ ,  $\delta$ ,  $0^{\circ}\text{C}$ ): 147.9 (Pz3A), 146.7 (Pz5C), 145.7 (C1), 143.0 (Pz3/5), 139.4 (Pz3/5), 139.3 (2C, Pz3/5), 126.1 (C4), 119.5 (C5), 109.2 (Pz4B), 108.7 (Pz4C), 107.8 (Pz4A), 95.1 (C2), 64.5 (C3), 30.7 (C6), 13.1 ( $\text{PMe}_3$ , d,  $J_{\text{PC}} = 34.2$ ). **Complex 3** (minor):  $^1\text{H}$  NMR ( $\text{CD}_3\text{CN}$ ,  $\delta$ ,  $0^{\circ}\text{C}$ ): 8.31 (1H, d, Pz3/5), 8.11 (1H, d, Pz3/5), 8.01 (1H, d, Pz3/5), 7.92 (1H, d, Pz3C), 7.81 (1H, d, Pz3/5), 6.55 (1H, buried, H4), 6.52 (1H, t, Pz4), 6.49 (1H, buried, Pz4), 6.34 (2H, overlapping, Pz4 & H3), 5.89 (1H, m, H5), 4.71 (1H, t,  $J = 7.5$ , H2), 4.65 (1H, m, H1), 4.34 (1H, d,  $J = 25.8$ , H6-*exo*), 3.36 (d,  $J = 25.8$ , 1H, H6-*endo*), 1.11 (9H, buried,  $\text{PMe}_3$ ). Attempts at elemental analysis were not successful due to the unstable nature of the complex at ambient temperatures.

#### Synthesis of $\text{WTp}(\text{NO})(\text{PMe}_3)(\eta^2\text{-1,3-cyclohexadiene})$ (**4**)

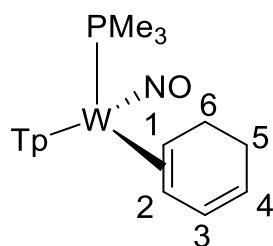


To a 4-dram vial was added 2 mL of MeCN and **1** (0.200 g, 0.344 mmol) to generate a heterogeneous yellow reaction mixture. This solution was then cooled to  $-30^{\circ}\text{C}$ . DPhAT was added to this reaction mixture and the solution was allowed to stand at  $-30^{\circ}\text{C}$ . Over 15 min a homogeneous red reaction mixture develops indicating the formation of **2** in solution. Separately a solution of 2 mL of MeOH was chilled to  $-30^{\circ}\text{C}$  and to



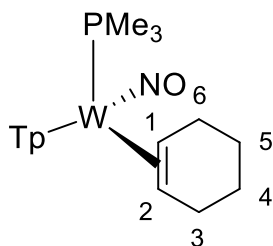
this solution  $\text{NaBH}_4$  (0.030g, 0.79 mmol) was added. The  $\text{NaBH}_4/\text{MeOH}$  solution was then added to a dewar of liquid nitrogen and the solution was frozen. The homogenous red reaction mixture of **2** was then added to this frozen solution of  $\text{MeOH}$  and  $\text{NaBH}_4$  and the reaction mixture was allowed to thaw while sitting at  $-30^\circ\text{C}$ . After one hour the reaction mixture had turned to a homogenous orange color. A 60 mL coarse fritted porosity disc was filled with  $\sim 5$  cm of neutral alumina and set in  $\text{Et}_2\text{O}$ . The homogeneous orange solution was then filtered through the neutral alumina column and a light yellow band was eluted with 100 mL of  $\text{Et}_2\text{O}$ . The solvent was removed in vacuo until a pale yellow solid remained. This was re-dissolved in 2 mL of  $\text{DCM}$  and added to a 4-dram vial that contained 15 mL of sitting hexanes. This homogeneous yellow solution was subsequently allowed to cool at  $-30^\circ\text{C}$  for 16 h. After being allowed to cool a light green crystalline product had developed on the sides of the vial. The organic layer was decanted and the product was then dried with  $\text{N}_2$  (g) and allowed to desiccate for 8 h before a mass was taken of the resultant light yellow crystalline product (0.162 g, 81%). Characterization has been reported previously (see Reference 16)..

### Synthesis of $\text{WTp}(\text{NO})(\text{PMe}_3)(\eta^2\text{-1,3-cyclohexadiene})$ (**5**)



A mixture of complexes **4** and **5** (0.298 g, 0.511 mmol) were dissolved in 2 mL of DME and allowed to cool to  $-30^\circ\text{C}$  over a period of 15 min. To this homogeneous light yellow solution was added  $\text{HOTf}$  (0.198 g, 1.311 mmol) and the reaction mixture turned to a homogeneous orange color. This reaction mixture was allowed to sit at  $-30^\circ\text{C}$  for 5 min and then subsequently added to 15 mL of standing ether at room temperature. A dark brown solid congregated on the bottom of the flask, and the organic layer was decanted before the solid was re-dissolved in 2 mL of  $\text{DCM}$  and again precipitated into 50 mL of stirring ether to generate a light yellow heterogeneous mixture. This solid was then dried under dynamic vacuum in a desiccator for 2 h and its identity as **6** was confirmed by NMR. This solid was then dissolved in  $\text{DCM}$  (2 mL) and allowed to sit at  $-30^\circ\text{C}$ . In a separate 4-dram vial was added  $\text{DBU}$  (0.582g, 3.82 mmol) along with  $\text{DCM}$  (1 mL) and this solution was also cooled to  $-30^\circ\text{C}$  over a course of 15 min. The  $\text{DBU}/\text{DCM}$  solution was then added to the  $\text{DCM}$  solution of **6** and upon addition a homogeneous pink reaction mixture develops. This reaction mixture was allowed to stand for 5 min at room temperature and then loaded onto a coarse 60 mL fritted disc that had been filled with  $\sim 3$  cm of basic alumina and set in ether. The pink band was eluted with 60 mL of ether and the solvent was then removed in vacuo. A light yellow film coats the bottom of the filter flask, this was re-dissolved in  $\text{DCM}$  (2 mL) and added to standing pentane (15 mL) and was allowed to sit at  $-30^\circ\text{C}$  for 16 hr. The next day a yellow crystalline material had formed at the sides of the vial. The organic layer was then decanted and the vial was dried under dynamic vacuum for 6 h to yield a fine yellow powder (0.102 g, 34%). Characterization has been reported previously (see Reference 16).

### Synthesis of $\text{WTp}(\text{NO})(\text{PMe}_3)(\eta^2\text{-cyclohexene})$ (**7**)



A 4-dram vial was charged with 1 mL of DME, complex **1** (0.200 g, 0.344 mmol) and cyclohexene (2.00g, 24.3 mmol) and this heterogenous yellow reaction mixture was allowed to stir. After 27 h the now homogenous purple reaction mixture was added to a 250 mL filter flask and the solvent was removed in vacuo. The resulting pink solid was re-dissolved in 2 mL of DCM and slowly added to 30 mL of stirring pentanes that had been chilled to  $-30^{\circ}\text{C}$ . Upon addition a light pink solid precipitated out of solution. This light pink solid was collected on a 30 mL fine porosity fritted disc and subsequently washed with 3 x 5 mL of chilled pentane. The collected product was then desiccated for 2 h to yield a fine light pink powder (0.083 g, 41%).

### Alternative Synthesis of $\text{WTP}(\text{NO})(\text{PMe}_3)(\eta^2\text{-cyclohexene})$ (**7**)

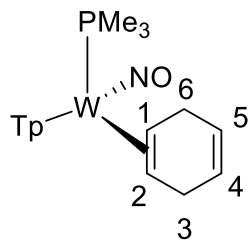
To a 4-dram vial **6** (0.107 g, 0.136 mmol) was dissolved in 1 mL of MeOH and chilled to  $-30^{\circ}\text{C}$ . To this was added  $\text{NaBH}_4$  that had been dissolved and chilled in a  $-30^{\circ}\text{C}$  MeOH solution. The solution of **6** was then added to the  $\text{NaBH}_4/\text{MeOH}$  solution and the resulting reaction mixture was allowed to sit at  $-30^{\circ}\text{C}$  for 16 h. The reaction mixture was then eluted through a silica column on a fine 15 mL fritted disc and a light yellow band was eluted with ether. The solvent was then removed in vacuo and picked up in 1 mL of DCM. This was then added to 15 mL of sitting hexanes and allowed to sit at  $-30^{\circ}\text{C}$  for 2 h during which a light yellow solid had precipitated from solution. This solid was then isolated on a fine 15 mL fritted disc, washed with 2x5 mL of hexanes to yield an off-white solid (0.058 g, 67%).

CV (MeCN)  $E_{p,a} = +0.28$  V (NHE). IR:  $\nu(\text{BH}) = 2482$   $\text{cm}^{-1}$ ,  $\nu(\text{NO}) = 1554$   $\text{cm}^{-1}$ .  $^1\text{H-NMR}$  ( $\text{CDCl}_3$ ,  $\delta$ ,  $25^{\circ}\text{C}$ ): 8.28 (1H, d, Pz3A), 8.08 (1H, d, Pz3B), 7.69 (1H, d, Pz5B), 7.64 (1H, d, Pz5C), 7.60 (1H, d, Pz5A), 7.24 (1H, d, Pz3C), 6.28 (1H, t, PzB), 6.20 (1H, t, Pz4A), 6.13 (1H, t, Pz4C), 3.00 (1H, m, H6 $_{exo}$ ) 2.92 (2H, overlap, m, H4- $endo/exo$ ), 2.71 (1H, m, H1), 2.64 (1H, m, H6- $endo$ ), 1.75 (2H, overlap, m, H6- $endo/exo$ ), 1.46 (2H, overlap, m, H5- $endo/exo$ ), 1.38 (1H, m, H2), 1.21 (9H, d,  $J_{\text{PH}} = 8.1$ ,  $\text{PMe}_3$ ).  $^{13}\text{C-NMR}$  ( $\text{CDCl}_3$ ,  $\delta$ ,  $25^{\circ}\text{C}$ ). 143.4 (Pz3B), 142.9 (Pz3A), 140.1 (Pz3C), 136.2 (Pz5), 135.6 (Pz5), 135.4 (Pz5), 106.3 (Pz4B), 105.6 (Pz4), 105.5 (Pz4), 53.8 (C2), 53.6 (C1, d,  $J_{\text{PC}} = 10.6$ ), 30.0 (C6, d,  $J_{\text{PC}} = 4.2$ ), 29.4 (C3), 24.9 (C4/5), 24.8 (C4/5), 14.0 ( $\text{PMe}_3$ , d,  $J_{\text{PC}} = 27.5$ ).  $^{31}\text{P-NMR}$  ( $\text{CDCl}_3$ ,  $\delta$ ,  $25^{\circ}\text{C}$ ): -9.1 ( $J_{\text{WP}} = 291$ ,  $\text{PMe}_3$ ). Anal. Calcd for  $20\text{C}_{18}\text{H}_{29}\text{BN}_7\text{OPW}\cdot\text{DCM}$ : C, 36.79; H, 4.98; N, 16.76. Found: C, 37.35; H, 4.58; N, 16.69.

Characterization in  $\text{MeCN-}d_3$

$^1\text{H-NMR}$  ( $\text{MeCN-}d_3$ ,  $\delta$ ,  $25^{\circ}\text{C}$ ): 8.21 (1H, d, Pz3A), 8.03 (1H, d, Pz3B), 7.85 (1H, d, Pz5B), 7.78 (1H, d, Pz5C), 7.75 (1H, d, Pz5A), 7.35 (1H, d, Pz3C), 6.36 (1H, t, Pz4B), 6.27 (1H, t, Pz4A), 6.21 (1H, t, Pz4C), 3.04 (1H, m, H6 $_{exo}$ ) 2.93 (1H, m, H3- $exo$ ), 2.86 (1H, m, H3- $endo$ ), 2.72 (1H, m, H1), 2.63 (1H, m, H6- $endo$ ), 1.69 (1H, m, H4- $endo$ ), 1.66 (1H, m, H5- $endo$ ). 1.42 (2H, overlap, m, H4/H5- $exo$ ), 1.16 (1H, m, H2), 1.10 (9H, d,  $J_{\text{PH}} = 8.2$ ,  $\text{PMe}_3$ ).  $^{13}\text{C-NMR}$  ( $\text{MeCN-}d_3$ ,  $\delta$ ,  $25^{\circ}\text{C}$ ). 144.2 (Pz3B), 143.3 (Pz3A), 141.7 (Pz3C), 137.6 (Pz5), 136.9 (2C, overlapping Pz5), 107.4 (Pz4B), 106.9 (Pz4A), 106.6 (Pz4C), 53.5 (2C, overlapping C1 and C2), 30.7 (C6), 30.2 (C3), 25.6 (2C, overlapping C4/C5), 25.4 (2C, overlapping C4/C5), 13.8 ( $\text{PMe}_3$ , d,  $J_{\text{PC}} = 27.5$ ).

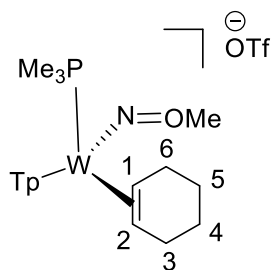
### Synthesis of $\text{WTP}(\text{NO})(\text{PMe}_3)(\eta^2\text{-1,4-cyclohexadiene})$ (**8**)



A 4-dram vial was charged with 1 mL of DME, complex **1** (0.301 g, 0.518 mmol) and 1,4-cyclohexadiene (2.00g, 24.9 mmol) and this heterogenous yellow reaction mixture was allowed to stir. After 50 h the homogenous purple reaction mixture was slowly added to 30 mL of stirring pentanes that had been chilled to  $-30^{\circ}\text{C}$ . Upon addition a light pink solid precipitated out of solution. This light pink solid was collected on a 30 mL fine porosity fritted disc and subsequently washed with 3 x 5 mL of chilled pentane. The collected product was then desiccated for 2 h to yield a fine pink powder (0.191 g, 63%).

CV (MeCN)  $E_{p,a} = +0.27$  V (NHE). IR:  $\nu(\text{BH}) = 2481$   $\text{cm}^{-1}$ ,  $\nu(\text{NO}) = 1553$   $\text{cm}^{-1}$ .  $^1\text{H-NMR}$  (acetone- $d_6$ ,  $\delta$ ,  $25^{\circ}\text{C}$ ): 8.25(1H, d, Pz3A), 8.08 (1H, d, Pz3B), 7.92 (1H, d, Pz5B), 7.88 (1H, d, Pz5C), 7.80 (1H, d, Pz5A), 7.49 (1H, d, Pz3C), 6.38 (1H, t, Pz4B), 6.28 (1H, t, Pz4A), 6.27 (1H, t, Pz4C), 5.83 (1H, m, H4) 5.78 (1H, m, H5), 3.55 (1H, m, H6-*exo*), 3.45 (2H, overlap, H3-*exo* and H3-*endo*), 3.10 (1H, d,  $J = 17.8$ , H6-*endo*), 2.83 (1H, m, H1), 1.34 (1H, m, H2), 1.21 (9H, d,  $J_{\text{PH}} = 8.2$ ,  $\text{PMe}_3$ ).  $^{13}\text{C-NMR}$  (acetone- $d_6$ ,  $\delta$ ,  $25^{\circ}\text{C}$ ): 144.0 (Pz3/5), 142.8 (Pz3/5), 141.5 (Pz3/5), 137.3 (Pz3/5), 136.7 (Pz3/5), 136.6 (Pz3/5), 127.7 (C4/5), 127.6 (C4/5), 107.1 (Pz4), 106.7 (Pz4), 106.2 (Pz4), 51.7 (C1, d,  $J_{\text{PC}} = 11.9$ ), 51.4 (C2), 30.1 (C3, buried under acetone), 29.2 (C6, buried under acetone, connected by HSQC), 13.6 ( $\text{PMe}_3$ , d,  $J_{\text{PC}} = 27.4$ ).  $^{31}\text{P-NMR}$  ( $\text{CDCl}_3$ ,  $\delta$ ,  $25^{\circ}\text{C}$ ): -8.9 ( $J_{\text{WP}} = 292$ ,  $\text{PMe}_3$ ). Anal. Calcd for  $\text{C}_{18}\text{H}_{27}\text{BN}_7\text{OPW}$ : C, 37.08; H, 4.67; N, 16.82. Found: C, 37.35; H, 4.58; N, 16.69.

### Synthesis of $\text{WTp}(\text{NOMe})(\text{PMe}_3)(\eta^2\text{-cyclohexene})(\text{OTf}^-)$ (**9**)

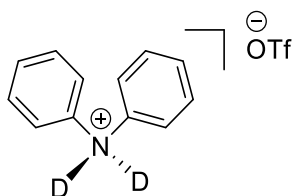


A 4-dram vial was charged with MeCN followed by **7** (0.203 g, 0.35 mmol). This heterogeneous yellow reaction mixture was cooled to  $-30^{\circ}\text{C}$ . After 20 min methyl triflate (0.252 g, 1.54 mmol) that had been cooled to  $-30^{\circ}\text{C}$  was added and the reaction mixture was allowed to warm to room temperature over a period of 5 min. During this time the reaction mixture changed to a homogeneous green solution. After the reaction mixture turned to the homogeneous solution, 12 mL of  $\text{Et}_2\text{O}$  were added and the reaction mixture was allowed to sit at  $-30^{\circ}\text{C}$  for 30 minutes. The organic layer was decanted to reveal a crystalline yellow material sticking to the bottom of the vial. This was then washed with 2 x 5 mL of  $\text{Et}_2\text{O}$  and then dried under an  $\text{N}_2$  (g) stream and subsequently desiccated over 4 h. A yellow material was collected. (0.116 g, 45%).

CV (MeCN)  $E_{p,a} = +1.2$ ,  $E_{p,c} = -1.6$  V (NHE). IR:  $\nu(\text{BH}) = 2511$   $\text{cm}^{-1}$ ,  $\nu(\text{NO}) = \text{NA}$ .  $^1\text{H-NMR}$  (MeCN- $d_3$ ,  $\delta$ ,  $25^{\circ}\text{C}$ ): 8.51(1H, d, Pz3A), 8.11 (1H, d, Pz3B), 8.02 (1H, d, Pz5B), 7.93 (2H, d, overlapping Pz5B/C), 7.47 (1H, d, Pz3C), 6.55 (1H, t, Pz4B), 6.48 (1H, t, Pz4A), 6.33 (1H, t, Pz4B), 4.03 (3H, s, NOMe), 3.97 (1H, m, H1), 3.57 (1H, m, H6-*exo*), 3.39 (1H, m, H3-*exo*), 3.14 (1H, m, H3-*endo*), 2.88 (1H, m, H6-*endo*), 2.34 (1H,

m, H2), 1.65 (1H, m, H4-*endo*), 1.60(1H, m H5-*exo*), 1.51 (1H,m, H5-*endo*), 1.48 (1H, m, H4-*exo*), 1.30 (9H, d,  $J_{PH} = 9.4$ ,  $\text{PMe}_3$ ).  $^{13}\text{C}$ -NMR ( $\text{MeCN-}d_3$ ,  $\delta$ , 25 °C). 145.6 (Pz3B), 144.8 (Pz3A), 142.8 (Pz3C), 139.7 (Pz5A/C), 138.8 (Pz5A/C), 138.5 (Pz5B), 108.9 (Pz4B), 108.3 (Pz4C), 107.9 (Pz4A), 66.5 (NOMe), 64.5 (C1,  $J_{PC} = 8.2$ ), 63.2 (C2), 31.8 (C3), 31.4 (C6), 24.6 (C4), 23.9 (C5), 13.9 ( $\text{PMe}_3$ , d,  $J_{PC} = 31.5$ ).  $^{31}\text{P}$ -NMR ( $\text{MeCN}$ ,  $\delta$ , 25 °C): -10.76 ( $J_{WP} = 268$ ,  $\text{PMe}_3$ ). Anal. Calcd for  $\text{C}_{20}\text{H}_{32}\text{BN}_7\text{O}_4\text{F}_3\text{PSW}$ : C, 32.06; H, 4.31; N, 13.09. Found: C, 32.00; H, 4.37; N, 12.92. ESI-MS : obsd (%), calcd (%): 598.1984 (83.66) 598.1985 (85.93), 599.2010 (76.17), 599.2011 (79.46), 600.2007 (100), 600.2009 (100), 601.2051 (37.70), 601.2052 (40.85), 602.2039 (83.65), 602.4041 (84.87).

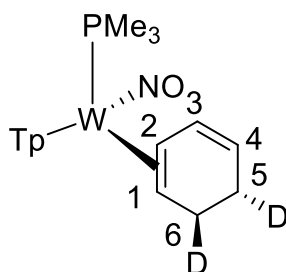
### Synthesis of Diphenylammonium- $d_2$ Triflate (DPhAT- $d_2$ )



Generation of an acidic deuterium source relied on stirring diphenyl ammonium triflate (DPhAT) (2.00 g, 6.25 mmol) in an excess of MeOD (50.0 g, 152 mmol). The mixture was allowed to stir for 16 h and the solvent was removed in vacuo to yield  $d_2$ -DPhAT. Typical yields 90%.

### Representative Synthesis for the Generation of a Tungsten-Cyclohexene Isotopologue Complex

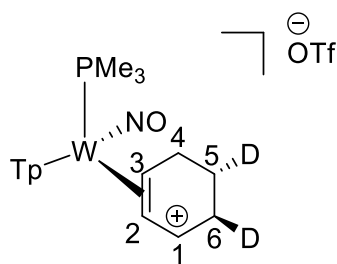
#### Synthesis of **12**



Prepared a solution of **1** (0.510 g, 0.878 mmol) in 2 mL of MeOD and 1 mL of  $\text{MeCN-}d_3$  in a 4-dram vial and chilled the reaction to  $-30^\circ\text{C}$ . Separately chilled a solution of HOTf (0.151 g, 1.00 mmol) in MeOD (5.01g, 151 mmol) in a 4-dram vial as an acidic deuterium source and separately chilled to  $-30^\circ\text{C}$  over the course of 30 minutes. In a separate, oven-dried test tube chilled in MeOD (3 mL) to  $-60^\circ\text{C}$  in a chilled toluene bath. To this test tube added  $\text{NaBD}_4$  (0.205 g, 4.90 mmol) and let this heterogeneous white reaction mixture stir over the course of 15 min. While this was stirring added the acidic solution of MeOH to the homogeneous yellow solution of **1**. Upon addition the reaction mixture turns to a homogeneous red color, indicative of the formation of **2** in solution. The solution of **2** was then allowed to sit for 15 min at  $-60^\circ\text{C}$  during which time it retained its red, homogeneous composition. After 15 min this reaction mixture was then added dropwise to the stirring test tube with  $\text{NaBD}_4$  and MeOD, upon whose addition vigorously bubbling started to commence (CAUTION! Evolution of  $\text{H}_2(\text{g})$ ). After all of **2** had been added to the test tube with the solution of  $\text{NaBD}_4$  and MeOD, the reaction mixture was allowed to stir for 1.5 h before it was determined to be completed by  $^{31}\text{P}$  NMR. The reaction mixture was then removed from the  $-60^\circ\text{C}$  bath and the cap was loosened and the reaction mixture was allowed to warm to room temperature over the course of 15 min. During this time the reaction mixture turns from a light yellow to a light lime green color and vigorous bubbling starts to occur. After the bubbling has been judged to stop, the reaction mixture was eluted through

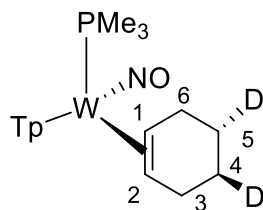
a coarse 60 mL fritted disc filled with ~3 cm of basic alumina that had been set in diethyl ether. A lime green band was then eluted with ether (100 mL) and the solvent was then removed in vacuo. Once a lime green solid film coats the bottom of the filter flask, the product was re-dissolved in a minimal amount of DCM (~ 3 mL) and added to 15 mL of standing hexanes in a 4-dram vial. This was then allowed to sit at -30°C over the course of 16 h, during which time a fine, lime green crystalline product has developed on the sides of the vial. The organic layer was then decanted and the product was dried with a N<sub>2</sub>(g) stream and allowed to desiccate for six hours before a mass was collected of the lime green crystalline solid (0.365g, 71 %).

### Synthesis of 13



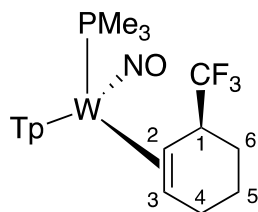
**12** (0.365 g, 0.624 mmol) was dissolved in DME (3 mL) and cooled to -30 °C to generate a homogeneous yellow mixture in a 4-dram vial. Separately HOTf (0.215 g, 1.42 mmol) was dissolved in 2 mL of DME and also allowed to cool to -30°C over a course of 15 min in a separate 4-dram vial. The acidic DME solution was then added dropwise to the standing solution of **3**. This solution was allowed to stand at room temperature for 1 min and then was added dropwise to a solution of stirring ether (250 mL). Upon addition a fine, light yellow solid precipitated from solution. The solution was allowed to triturate for 10 min before the reaction mixture was filtered through a fine 15 mL porosity frit to yield a fine, yellow powder. This solid was then washed with ether (3 x 10 mL) and allowed to desiccate for six hours under dynamic vacuum before a mass was taken (0.365g, 79 %).

### Synthesis of 14



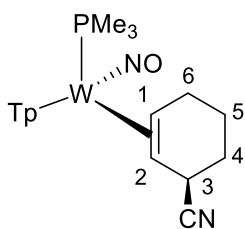
A 4-dram vial was charged with **13** (0.114 g, 0.155 mmol) and dissolved in MeOH (3 mL) to generate a homogeneous orange solution. This solution was chilled to -30°C over a course of 15 min and to this solution was added NaBH<sub>4</sub> (0.040 g, 1.06 mmol). Upon addition to the solution some bubbling occurs. This solution was allowed to stand at -30°C for one hour and turns from a homogeneous orange to a homogeneous yellow color. The solution was then allowed to stand at room temperature for 10 min before being diluted with ether (10 mL). Separately a 30 mL medium porosity frit was filled with ~ 3 cm of silica and set in ether. The reaction mixture was then loaded onto this silica column and was filtered through by elution with ~ 100 mL of ether total to elute a light yellow band. The solvent was then removed in vacuo and the product was re-dissolved in DCM (2 mL) and added to a 4-dram vial of standing pentane (15 mL). This solution was allowed to stand at -30°C for 16 h before the solvent was again stripped to dryness to yield a fine off-white solid (0.061 g, 65 %).

## Synthesis and characterization of 47



To a 4-dram vial were added  $\text{WTP}(\text{NO})(\text{PMe}_3)(\eta^2\text{-1-(trifluoromethyl)cyclohexa-1,3-diene})^{28}$  (50 mg, 0.077 mmol) followed by acetone (1.3 mL,  $-30^\circ\text{C}$ ), resulting in a heterogeneous mixture. A 1M solution of HOTf in acetonitrile (0.1 mL, 0.1 mmol,  $-30^\circ\text{C}$ ) was then added, resulting in a homogeneous yellow solution, which was allowed to stir for 19 h at room temperature. This orange solution was then cooled to  $-30^\circ\text{C}$  for 30 min. In a separate 4-dram vial,  $\text{NaBH}_4$  (10 mg, 0.26 mmol) and MeOH (0.2 mL,  $-30^\circ\text{C}$ ) were combined. The reaction solution was then added to the  $\text{NaBH}_4$  mixture with stirring, and this solution was left at  $-30^\circ\text{C}$  for 1 h. The reaction solution was allowed to warm to room temperature for 30 min, before precipitation was induced by adding  $\text{H}_2\text{O}$  (3 mL). The resulting tan solid was collected on a 15 mL fine porosity fritted disc, washed with  $\text{H}_2\text{O}$  (2 x 5 mL), and pentane (2 x 3 mL,  $-30^\circ\text{C}$ ) and desiccated, yielding **47** (40 mg, 0.061 mmol, 79% yield).  $^1\text{H}$  NMR (acetone- $d_6$ ,  $\delta$ ): 8.24 (d, 1H, PzA3), 8.15 (d, 1H, PzB3), 7.96 (d, 1H, PzB5), 7.93 (d, 1H, PzC5), 7.81 (d, 1H, PzA5), 7.50 (d, 1H, PzC3), 6.42 (t, 1H, PzB4), 6.31 (t, 1H, PzC4), 6.28 (t, 1H, PzA4), 3.49 (m, 1H, H1), 3.17 (m, 1H, H4-endo), 2.98 (m, 1H, H4-exo), 2.55 (t,  $J = 10.8$ , 1H, H2), 2.07 (buried, 1H, H6-exo), 1.76 (dm,  $J = 14.1$ , 1H, H6-endo), 1.59 (m, 1H, H5-exo), 1.57 (m, 1H, H5-endo), 1.43 (m, 1H, H3), 1.18 (d,  $J = 8.3$ , 9H,  $\text{PMe}_3$ ).  $^{13}\text{C}$  NMR (acetone- $d_6$ ,  $\delta$ ): 144.2 (PzB3), 143.0 (PzA3), 141.7 (PzC3), 137.7 (Pz5), 137.0 (Pz5), 136.8 (Pz5), 133.2 (q,  $J_{\text{CF}} = 282.3$ ,  $\text{CF}_3$ ), 107.3 (PzB4), 106.9 (PzC4), 106.3 (PzA4), 52.0 (C3), 47.9 (d,  $J_{\text{PC}} = 13.0$ , C2), 43.9 (m, C1), 29.1 (C4), 22.6 (C6), 20.9 (C5), 13.0 (d,  $J_{\text{PC}} = 27.8$ ,  $\text{PMe}_3$ ). ESI-MS: obsd (%), calcd (%): 652.1702 (84.59), 652.1702 (85.97), 653.1727 (76.24), 653.1728 (79.46), 654.1724 (100), 654.1726 (100), 655.1770 (36.53), 655.1769 (40.83), 656.1757 (80.76), 656.1758 (84.86).

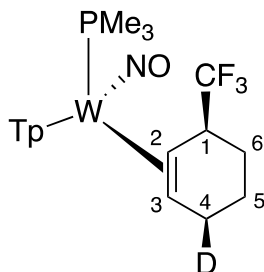
## Characterization for 48



CV (MeCN)  $E_{p,a} = 0.61$  V (NHE). IR:  $\nu(\text{BH}) = 2513$   $\text{cm}^{-1}$ ,  $\nu(\text{CN}) = 2228$   $\text{cm}^{-1}$ ,  $\nu(\text{NO}) = 1558$   $\text{cm}^{-1}$ .  $^1\text{H}$ -NMR ( $\text{CDCl}_3$ ,  $\delta$ ,  $25^\circ\text{C}$ ): 8.05 (2H, overlapping d, Pz3A and Pz3B), 7.71 (1H, d, Pz5A), 7.69 (1H, d, Pz5C), 7.64 (1H, d, Pz5B), 7.24 (1H, d, Pz3C), 6.31 (1H, t, Pz4A), 6.26 (1H, t, Pz4B), 6.19 (1H, t, Pz4C), 3.99 (1H, broad s, H3), 3.12 (1H, m, H6-endo), 2.72 (1H, m, H6-exo), 2.68 (1H, m, H1), 2.07 (1H, m, H4-endo), 1.77 (1H, m, H4-endo), 1.70 (2H, overlapping, H5-exo and H5-endo), 1.38 (1H, d,  $J = 11.1$ , H2), 1.18 (9H, d,  $J_{\text{PH}} = 8.3$ ,  $\text{PMe}_3$ ).  $^{31}\text{P}$ -NMR ( $\text{CDCl}_3$ ,  $\delta$ ,  $25^\circ\text{C}$ ): -10.55 ( $J_{\text{WP}} = 285$ )  $^{13}\text{C}$ -NMR ( $\text{CDCl}_3$ ,  $\delta$ ,  $25^\circ\text{C}$ ): 143.3 (Tp3/5), 142.4 (Tp3/5), 140.1 (Tp3/5), 136.6 (Tp3/5), 136.1 (Tp3/5), 136.1 (Tp3/5), 128.1 (CN), 106.6 (Tp4), 106.1 (Tp4), 106.0 (Tp4), 52.3 (C2), 49.7 (C1,  $J_{\text{PC}} = 11.6$ ), 31.0 (C3), 28.7 (C6, d,  $J_{\text{PC}} = 3.5$ ), 27.5 (C4), 22.0 (C5), 13.8 ( $\text{PMe}_3$ ,  $J_{\text{PC}} = 27.9$ ).

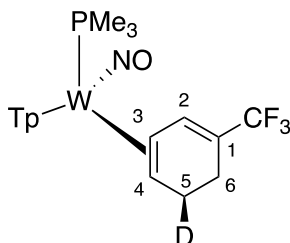
Synthesis was analogous to **48-4-*exo*,5-*endo*-*d*<sub>2</sub>** (vida infra) but utilized only the protected versions of the sodium borohydride and methanol.

### Synthesis of **52**



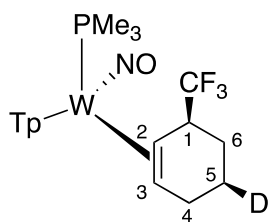
To a 4-dram vial were added  $\text{WTp}(\text{NO})(\text{PMe}_3)(\eta^2\text{-1-(trifluoromethyl)cyclohexa-1,3-diene})^{28}$  (50 mg, 0.077 mmol) followed by acetone (1.3 mL,  $-30^\circ\text{C}$ ), resulting in a heterogeneous mixture. A 1M solution of HOTf in acetonitrile (0.1 mL, 0.1 mmol,  $-30^\circ\text{C}$ ) was then added, resulting in a homogeneous yellow solution, which was allowed to stir for 19 h at room temperature. This orange solution was then cooled to  $-30^\circ\text{C}$  for 30 min. In a separate 4-dram vial,  $\text{NaBD}_4$  (11 mg, 0.26 mmol) and MeOD (0.2 mL,  $-30^\circ\text{C}$ ) were combined. The reaction solution was then added to the  $\text{NaBD}_4$  mixture with stirring, and this solution was left at  $-30^\circ\text{C}$  for 1 h. The reaction solution was allowed to warm to room temperature for 30 min, before precipitation was induced by adding  $\text{H}_2\text{O}$  (3 mL). The resulting tan solid was collected on a 15 mL fine porosity fritted disc, washed with  $\text{H}_2\text{O}$  (2 x 5 mL), and pentane (2 x 3 mL,  $-30^\circ\text{C}$ ) and desiccated, yielding **52** (48 mg, 0.073 mmol, 95% yield). 94% deuterium incorporation of C4. Deuterium incorporation determined by integration of  $^1\text{H}$  NMR signal at 2.98 ppm.

### Synthesis of $\text{WTp}(\text{NO})(\text{PMe}_3)(\eta^2\text{-1-trifluoromethyl-5-deutero-1,3-cyclohexadiene})$



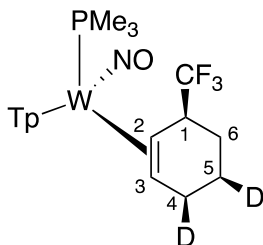
To a 4-dram vial charged with a stir pea were added  $\text{WTp}(\text{NO})(\text{PMe}_3)(\eta^2\text{-2,3-}\alpha,\alpha,\alpha\text{-trifluorotoluene})$  (200 mg, 0.308 mmol) followed by MeCN (1.8 mL,  $-30^\circ\text{C}$ ), resulting in a heterogeneous mixture. A 1M solution of HOTf in MeCN (0.32 mL, 0.32 mmol,  $-30^\circ\text{C}$ ) was immediately added with stirring, resulting in a homogeneous orange solution, which was allowed to sit for 20 min at  $-30^\circ\text{C}$ . In a separate 4-dram vial,  $\text{NaBD}_4$  (39 mg, 0.93 mmol) was dissolved in MeOH (1 mL,  $-30^\circ\text{C}$ ). This chilled hydride solution was then added to the orange reaction solution dropwise with vigorous stirring. The reaction was allowed to sit at  $-30^\circ\text{C}$  for 10 h, at which point a solid had precipitated out of solution. The reaction solution was stirred at room temperature for 5 min, before further precipitation was induced by adding  $\text{H}_2\text{O}$  (5 mL). The resulting solid was collected on a 15 mL fine porosity fritted disc, washed with  $\text{H}_2\text{O}$  (2 x 5 mL), and pentane (2 x 4 mL,  $-30^\circ\text{C}$ ) and desiccated (179 mg, 0.275 mmol, 89% yield). Greater than 95% deuterium incorporation at C5.

### Synthesis of **53**



NaBH<sub>4</sub> (14 mg, 0.37 mmol) was dissolved in d<sub>4</sub>-methanol (0.4 mL, -30°C) in a 4-dram vial charged with a stir pea. WTp(NO)(PMe<sub>3</sub>)(η<sup>2</sup>-1-(trifluoromethyl)cyclohexa-1,3-diene-5-*d*) (50 mg, 0.077 mmol) was added to another 4-dram vial charged with a stir pea. In a separate 4-dram vial, CD<sub>3</sub>CN (0.8 mL, -30°C) and a 1M solution of HOTf in MeCN (0.16 mL, 0.16 mmol, -30°C) were combined and cooled to -40°C for 20 min. The acid solution was added to the vial with tungsten complex, with stirring, resulting in a homogeneous yellow solution, which was allowed to sit for 2 min at -40°C. The yellow reaction solution was then added to the chilled hydride mixture with stirring. The pale yellow reaction was left at -40°C for 8 min then moved to the freezer at -30°C for 40 min, during which time solid precipitated out of solution. The heterogeneous reaction mixture was removed from the freezer and further precipitation was induced by adding H<sub>2</sub>O (2 mL). The pale yellow solid was collected on a 15 mL fine porosity fritted disc, washed with H<sub>2</sub>O (5 mL), and pentane (2 x 3 mL, -30°C) and desiccated, yielding **53** (35 mg, 0.054 mmol, 70% yield). 95% deuterium incorporation at C5. Deuterium incorporation determined by integration of <sup>1</sup>H NMR signal at 1.60 ppm.

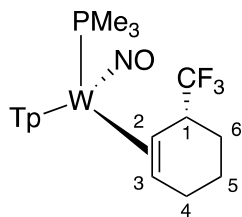
#### Synthesis of 54



NaBD<sub>4</sub> (14 mg, 0.33 mmol) was dissolved in d<sub>4</sub>-methanol (0.4 mL, -30°C) in a 4-dram vial charged with a stir pea. WTp(NO)(PMe<sub>3</sub>)(η<sup>2</sup>-1-(trifluoromethyl)cyclohexa-1,3-diene-5-*d*) (50 mg, 0.077 mmol) was added to another 4-dram vial charged with a stir pea. In a separate 4-dram vial, CD<sub>3</sub>CN (0.8 mL, -30°C) and a 1M solution of HOTf in MeCN (0.16 mL, 0.16 mmol, -30°C) were combined and cooled to -40°C. The acid solution was added to the vial with tungsten complex, with stirring, resulting in a homogeneous yellow solution, which was allowed to sit for 2 min at -40°C. The yellow reaction solution was then added to the chilled hydride mixture with stirring. The pale yellow reaction was left at -40°C for 8 min then moved to the freezer at -30°C for 40 min, during which time solid precipitated out of solution. The heterogeneous reaction mixture was removed from the freezer and further precipitation was induced by adding H<sub>2</sub>O (2 mL). The pale yellow solid was collected on a 15 mL fine porosity fritted disc, washed with H<sub>2</sub>O (5 mL), and pentane (2 x 3 mL, -30°C) and desiccated, yielding **53** (36 mg, 0.055 mmol, 71% yield). 95% deuterium incorporation at C4 and 95% deuterium incorporation at C5. Deuterium incorporation determined by integration of <sup>1</sup>H NMR signals at 2.98 and 1.60 ppm.

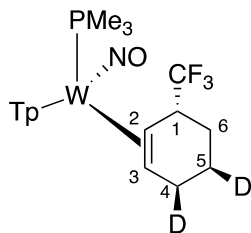
#### Synthesis of 55





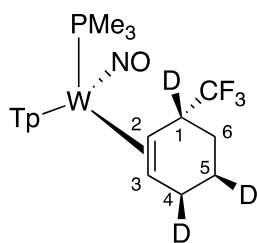
To a 4-dram vial charged with a stir pea were added WTp(NO)(PMe<sub>3</sub>)(η<sup>2</sup>-2,3-α,α,α-trifluorotoluene) (100 mg, 0.154 mmol) followed by MeCN (0.45 mL, -30°C), resulting in a heterogeneous mixture. A 1M solution of HOTf in MeCN (0.3 mL, 0.3 mmol, -30°C) was immediately added with stirring, resulting in a homogeneous orange solution, which was allowed to sit for 20 min at -30°C. In a separate 4-dram vial, NaCNBH<sub>3</sub> (29 mg, 0.46 mmol) was dissolved in MeOH (0.45 mL, -30°C). This chilled hydride solution was then added to the orange reaction solution dropwise with vigorous stirring. After addition of the hydride solution a solid precipitated out of the reaction mixture. The reaction was allowed to sit at -30°C for 1.5 h, then the pale yellow solid was collected on a 15 mL fine porosity fritted disc, washed with H<sub>2</sub>O (2 x 5 mL), and pentane (2 x 5 mL, -30°C) and desiccated, yielding **55** (81 mg, 0.12 mmol, 78% yield). *E<sub>p,a</sub>* = +0.49 V (NHE). IR: ν(BH) = 2487 cm<sup>-1</sup>, ν(NO) = 1548 cm<sup>-1</sup>. Anal. Calc'd for C<sub>19</sub>H<sub>26</sub>BF<sub>3</sub>N<sub>7</sub>OPW•2CH<sub>2</sub>Cl<sub>2</sub>: C, 30.65; H, 3.92; N, 11.91. Found: C, 31.08; H, 4.10; N, 12.21. <sup>31</sup>P NMR (acetone-*d*<sub>6</sub>, δ): -13.84 (*J*<sub>WP</sub> = 272). <sup>1</sup>H NMR (acetone-*d*<sub>6</sub>, δ): 8.18 (d, 1H, PzB3), 7.97 (d, 1H, PzB5), 7.96 (d, 1H, PzC5), 7.80 (d, 1H, PzA5), 7.73 (d, 1H, PzA3), 7.40 (d, 1H, PzC3), 6.43 (t, 1H, PzB4), 6.33 (t, 1H, PzC4), 6.28 (t, 1H, PzA4), 4.01 (m, 1H, H1), 3.18 (m, 1H, H4-*exo*), 2.96 (t, *J* = 12.1, 1H, H2), 2.17 (d of m, *J* = 14.4, 1H, H4-*endo*), 1.93 (m, 1H, H6-*endo*), 1.81 (m, 1H, H5-*endo*), 1.63 (m, 1H, H6-*exo*), 1.57 (m, 1H, H5-*exo*), 1.29 (d, *J* = 12.1, 1H, H3), 1.04 (d, *J*<sub>PH</sub> = 8.3, 9H, PMe<sub>3</sub>). <sup>13</sup>C NMR (acetone-*d*<sub>6</sub>, δ): 144.0 (PzA3), 143.1 (PzB3), 141.1 (PzC3), 137.5 (PzC5), 137.2 (PzB5), 136.7 (PzA5), 131.1 (q, *J*<sub>CF</sub> = 278.4, CF<sub>3</sub>), 107.5 (PzB4), 107.1 (PzC4), 106.6 (PzA4), 58.1 (C3), 46.7 (d, *J* = 14.6, C2), 45.0 (q, *J*<sub>CF</sub> = 24.7, C1), 25.3 (C4), 20.4 (C6), 19.8 (C5), 13.3 (d, *J*<sub>PC</sub> = 29.1, PMe<sub>3</sub>).

### Synthesis of 56



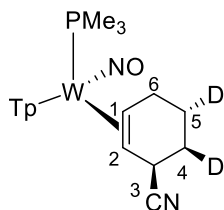
To a 4-dram vial charged with a stir pea were added WTp(NO)(PMe<sub>3</sub>)(η<sup>2</sup>-2,3-α,α,α-trifluorotoluene) (100 mg, 0.154 mmol) followed by CD<sub>3</sub>CN (0.35 mL, -30°C), resulting in a heterogeneous mixture. A 1M solution of HOTf in MeCN (0.39 mL, 0.39 mmol, -30°C) was immediately added with stirring, resulting in a homogeneous orange solution, which was allowed to sit for 20 min at -30°C. In a separate 4-dram vial, NaCNBD<sub>3</sub> (30 mg, 0.46 mmol) was dissolved in 1:1 methanol:*d*<sub>4</sub>-methanol (0.8 mL, -30°C). This chilled hydride solution was then added to the orange reaction solution dropwise with vigorous stirring. The reaction was allowed to sit at -30°C for 3 h, at which point a solid had precipitated out of solution. The pale yellow solid was collected on a 15 mL fine porosity fritted disc, washed with H<sub>2</sub>O (5 mL), and pentane (2 x 5 mL, -30°C) and desiccated, yielding **56** (75 mg, 0.11 mmol, 71% yield). 10% deuterium incorporation at C1, 81% deuterium incorporation at C5, and 60% deuterium incorporation at C4. Deuterium incorporation determined by integration of <sup>1</sup>H NMR signals at 4.01, 3.18, and 1.57 ppm.

### Synthesis of 57



To a 4-dram vial charged with a stir pea were added  $\text{WTp}(\text{NO})(\text{PMe}_3)(\eta^2\text{-}2,3\text{-}\alpha,\alpha,\alpha\text{-trifluorotoluene})$  (100 mg, 0.154 mmol) followed by  $\text{CD}_3\text{CN}$  (0.35 mL,  $-30^\circ\text{C}$ ), resulting in a heterogeneous mixture. A 1M solution of HOTf in MeCN (0.39 mL, 0.39 mmol,  $-30^\circ\text{C}$ ) was immediately added with stirring, resulting in a homogeneous orange solution, which was allowed to sit for 20 min at  $-30^\circ\text{C}$ . In a separate 4-dram vial,  $\text{NaCNBD}_3$  (30 mg, 0.46 mmol) was dissolved in  $d_4$ -methanol (0.8 mL,  $-30^\circ\text{C}$ ). This chilled hydride solution was then added to the orange reaction solution dropwise with vigorous stirring. The reaction was allowed to sit at  $-30^\circ\text{C}$  for 4 h, at which point a solid had precipitated out of solution. The pale yellow solid was collected on a 15 mL fine porosity fritted disc, washed with  $\text{H}_2\text{O}$  (2 x 5 mL), and pentane (2 x 5 mL,  $-30^\circ\text{C}$ ) and desiccated, yielding **57** (75 mg, 0.11 mmol, 71% yield). 77% deuterium incorporation at C1, 84% deuterium incorporation at C5, and 93% deuterium incorporation at C4. Deuterium incorporation determined by integration of  $^1\text{H}$  NMR signals at 4.01, 3.18, and 1.57 ppm.

### Synthesis of 58

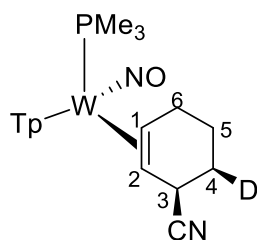


$^1\text{H}$  NMR Characterization of **58-4-exo,5-endo- $d_2$**  matches that of **48** but with an 90% loss of  $^1\text{H}$  signal intensity at 2.07 ppm and a 93% loss of  $^1\text{H}$  signal intensity at 1.77 (isotopic purity estimated by  $^1\text{H}$  NMR). There is an unintended 15% underintegration at 3.12 representing scrambling of deuterium in the H6-exo position.

A test tube was charged with NaCN (0.235 g, 4.80 mmol) and MeOD (2 mL) along with a small stir bar and was allowed to stir at room temperature for 2 h to dissolve. This reaction mixture was then transferred to a  $-60^\circ\text{C}$  toluene bath and to this solution was added HOTf (3 drops). Separately a solution of **13** (0.200 g, 0.272 mmol) was dissolved in a solution of MeOD (2 mL) and propionitrile (1mL). This homogeneous yellow reaction mixture was then transferred to the a  $-60^\circ\text{C}$  toluene bath. After sitting in the reduced temperature toluene bath for 30 min the solution of **13** was added dropwise to the stirring solution of NaCN/MeOD at  $-60^\circ$  and this light yellow solution was allowed to stir at  $-60^\circ$ . After 2 h of stirring the reaction was determined to be completed by a  $^{31}\text{P}$  NMR experiment and the reaction vessel was removed from the box and diluted with 50 mL of DCM. The reaction mixture was then added to a 100 mL solution of DI  $\text{H}_2\text{O}$  saturated with NaCl (brine solution) in a 250 mL separatory funnel and the mixture was extracted with 3 x 50 mL DCM. The organic layers were then collected and dried over anhydrous  $\text{MgSO}_4$  for 15 min. The DCM mixture was then eluted through a medium 60 mL medium porosity frit and the  $\text{MgSO}_4$  on the frit was washed with DCM (50 mL total) to dissolve any remaining product. The DCM was then removed under reduced pressure until a light brown film remained. The film was re-dissolved in 3 mL of DCM and added to 100 mL of stirring pentane. Upon addition a light pink solid precipitated from solution. This heterogeneous

solution was allowed to triturate for 10 min before the reaction mixture was filtered through a fine 15 mL frit. The isolate light pink solid was then washed with 2 x 10mL pentane and allowed to desiccate under dynamic vacuum for 3 h. A mass was taken of the fine light pink solid (0.095 g, 57 %).

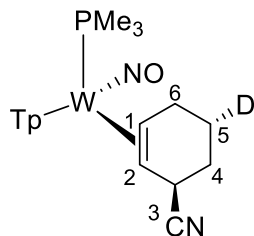
## Synthesis of 59



$^1\text{H}$  NMR Characterization of **59-4-*exo-d*<sub>1</sub>** matches that of **48** but with an 87% loss of  $^1\text{H}$  signal intensity at 1.77 ppm (isotopic purity estimated by  $^1\text{H}$  NMR).

To a 4-dram vial was added 2 mL of propionitrile and **1** (0.252 g, 0.434 mmol) to generate a heterogeneous yellow reaction mixture. This solution was then cooled to  $-30^\circ\text{C}$ . DPhAT was added to this reaction mixture and the solution was allowed to stand at  $-30^\circ\text{C}$ . Over 15 min a homogeneous red reaction mixture develops indicating the formation of **2** in solution. Separately a solution of 2 mL of MeOH was chilled to  $-60^\circ\text{C}$  in a toluene bath and to this solution  $\text{NaBD}_4$  (0.078 g, 1.86 mmol) was added. The  $\text{NaBD}_4/\text{MeOH}$  solution was then allowed to stir in a  $-60^\circ\text{C}$ . The homogenous red reaction mixture of **2** was then added to this  $-60^\circ\text{C}$  cooled solution of MeOH and  $\text{NaBD}_4$ . After seven hours the reaction mixture had turned to a homogenous orange color and was removed from the  $-60^\circ\text{C}$  toluene bath and diluted with 40 mL of  $\text{Et}_2\text{O}$  and allowed to stir for 10 min at room temperature. A 60 mL medium fritted porosity disc was filled with  $\sim 5$  cm of silica and set in  $\text{Et}_2\text{O}$ . The homogeneous orange solution was then filtered through the silica column and a light yellow band was eluted with  $\sim 100$  mL of  $\text{Et}_2\text{O}$ . The solvent was removed in vacuo until a pale yellow solid remained. This was re-dissolved in 2 mL of DCM and added to a 4-dram vial that contained 15 mL of sitting hexanes. This homogeneous yellow solution was subsequently allowed to cool at  $-30^\circ\text{C}$  for 16 h. After being allowed to cool a light green crystalline product had developed on the sides of the vial. The organic layer was decanted and the product was then dried with  $\text{N}_2$  (g) and allowed to desiccate for 16 h under static vacuum before its identity was confirmed by  $^1\text{H}$  NMR. The resulting lime green solid was subsequently dissolved in 2 mL of MeOH and cooled to  $-30^\circ\text{C}$ . Separately, a 4-dram vial was charged with  $\text{NaCN}$  (0.250 g, 5.1 mmol) along with MeOH and allowed to stir for 15 min at room temperature. This reaction mixture was then transferred to a  $-60^\circ\text{C}$  toluene bath and allowed to stir. To the  $-30^\circ\text{C}$  MeOH solution of **4-6,exo-d**<sub>1</sub> added HOTf (0.102 g, 0.680 mmol). Upon addition the reaction mixture goes from a heterogeneous green to a homogeneous yellow solution. This solution of **4-6,exo-d**<sub>1</sub> was then cooled in the  $-60^\circ\text{C}$  toluene bath over a course of 10 minutes before it was added dropwise to the stirring solution of  $\text{NaCN}/\text{MeOH}$  that had been stirring in the  $-60^\circ\text{C}$  toluene bath. This solution was allowed to stir for 5 h at  $-60^\circ\text{C}$  before it was removed from the toluene bath. The reaction mixture was diluted with  $\sim 50$  mL of  $\text{Et}_2\text{O}$  and loaded onto a 30 mL medium fritted porosity disc that was filled with  $\sim 5$  cm of silica and set in  $\text{Et}_2\text{O}$ . A lime green band was collected upon elution with 100 mL of  $\text{Et}_2\text{O}$  and the solvent was removed in vacuo to reveal a lime green solid. This solid was then dissolved in 2 mL of DCM and added to 15 mL of standing pentane in a 4-dram vial and allowed to sit at  $-30^\circ\text{C}$  for 16 hr during which time a white solid precipitated out of solution. The next day the white solid was allowed to triturate in a minimal amount of MeCN given that the desired product was marginally soluble in MeCN. The organic layer was then decanted and the reaction mixture was dried with  $\text{N}_2$ (g) and allowed to desiccate for 3 h under active vacuum before a mass was taken (0.048 g, 18% overall yield).

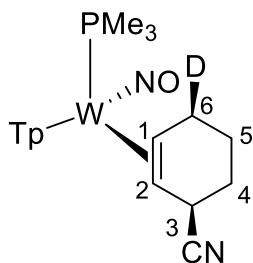
## Synthesis of 60



$^1\text{H}$  NMR Characterization of **48-5-endo- $d_1$**  matches that of **48** but with an 85% loss of  $^1\text{H}$  signal intensity at 1.70 ppm (isotopic purity estimated by  $^1\text{H}$  NMR). Although overlap is present with the H5-endo proton, the precursor compound shows suppression of the expected endo-proton.

To a 4-dram vial added **1** (0.264 g, 0.454 mmol) along with propionitrile (2 mL) and this was allowed to sit at  $-30^\circ\text{C}$ . Separately a solution of  $\text{NaBH}_4$  (0.111 g, 2.92 mmol) was added to a  $-60^\circ\text{C}$  solution of MeOD (2 mL) in a test tube. In another 4-dram vial diphenylammonium triflate (DPhAT, 0.175 g, 0.546 mmol) was dissolved in MeOD (2.78 g, 83.9 mmol) and allowed to sit at  $-30^\circ\text{C}$  for 10 min before it was added to the solution of **1** in propionitrile. This reaction mixture was then transferred to a  $-60^\circ\text{C}$  toluene bath in a 4-dram vial and allowed to cool over a period of 10 min. This reaction mixture, now a homogeneous red coloration, was then added to the  $-60^\circ\text{C}$  cooled solution of stirring  $\text{NaBH}_4/\text{MeOD}$ . Upon addition some bubbling occurs and this reaction mixture was allowed to stir for 5 h at  $-60^\circ\text{C}$ . After 5 h the reaction mixture was removed from the  $-60^\circ\text{C}$  toluene bath and diluted with 40 mL of  $\text{Et}_2\text{O}$  and allowed to stir for 10 min at room temperature. A 60 mL medium fritted porosity disc was filled with  $\sim 5$  cm of silica and set in  $\text{Et}_2\text{O}$ . The homogeneous orange solution was then filtered through the silica column and a light yellow band was eluted with  $\sim 100$  mL of  $\text{Et}_2\text{O}$ . The solvent was removed in vacuo until a pale yellow solid remained. This was re-dissolved in 2 mL of DCM and added to a 4-dram vial that contained 15 mL of sitting hexanes. This homogeneous yellow solution was subsequently allowed to cool at  $-30^\circ\text{C}$  for 16 h. After being allowed to cool a light green crystalline product had developed on the sides of the vial. The organic layer was decanted and the product was then dried with  $\text{N}_2$  (g) and allowed to desiccate for 16 h under static vacuum before its identity was confirmed by  $^1\text{H}$  NMR as **2-5-endo- $d_1$** . This solid was then combined with MeOH (2 mL) in a 4-dram vial and allowed to cool to  $-30^\circ\text{C}$  over a course of 15 min. Separately a large test tube vial was charged with MeOH (2 mL), NaCN (0.240 g, 4.90 mmol) and this heterogeneous solution was allowed to stir at room temperature for 15 min. This solution was then transferred to a  $-60^\circ\text{C}$  toluene bath and allowed to stir for 10 min. To the  $-30^\circ\text{C}$  MeOH solution of **2-5-endo- $d_1$**  added HOTf (0.102 g, 0.680 mmol) that had also been cooled to  $-30^\circ\text{C}$ . This solution, a light homogeneous yellow solution was transferred to the  $-60^\circ\text{C}$  toluene bath and allowed to stir for 5 min. This homogeneous yellow solution was then added dropwise to the  $-60^\circ\text{C}$  solution of NaCN/MeOH and allowed to stir for 5 h. This solution was allowed to stir for 5 h at  $-60^\circ\text{C}$  before it was removed from the toluene bath. The reaction mixture was diluted with  $\sim 50$  mL of  $\text{Et}_2\text{O}$  and loaded onto a 30 mL medium fritted porosity disc that was filled with  $\sim 3$  cm of silica and set in  $\text{Et}_2\text{O}$ . A lime green band was collected upon elution with 100 mL of  $\text{Et}_2\text{O}$  and the solvent was removed in vacuo to reveal a lime green solid. The next day the white solid was allowed to triturate in a minimal amount of MeCN given that the desired product was marginally soluble in MeCN. The organic layer was then decanted and the reaction mixture was dried with  $\text{N}_2$  (g) and allowed to desiccate for 3 h under active vacuum before a mass was taken (0.048 g, 17% overall yield).

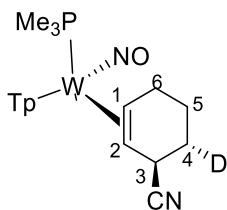
## Synthesis of 61



$^1\text{H}$  NMR Characterization of **61-6-*exo-d*<sub>1</sub>** matches that of **48** but with an 99% loss of  $^1\text{H}$  signal intensity at 3.12 ppm (isotopic purity estimated by  $^1\text{H}$  NMR, in this case proton impurity is beyond  $^1\text{H}$  NMR detection limit).

**WTp(NO)(PMe<sub>3</sub>)( $\eta^2$ -1,2-6-cyano-cyclohexadiene)** (prepared by a previously reported method)<sup>28</sup> (0.088g, 0.145 mmol) was dissolved in DME (1 mL) and allowed to cool to  $-30^\circ\text{C}$ . Separately a test tube vial was charged with MeOD (1 mL) and cooled to  $-60^\circ\text{C}$  in a toluene bath over a course of 15 min and to this solution was added NaBD<sub>4</sub> (0.050 g, 1.21 mmol) and allowed to stir at  $-60^\circ\text{C}$ . Next HOTf (0.041 g, 0.273 mmol) was then added at  $-30^\circ\text{C}$  to the solution of tungsten in DME and upon addition the reaction mixture turns to a homogeneous yellow color. This solution was allowed to cool to  $-60^\circ\text{C}$  over a course of 10 min after being transferred to the  $-60^\circ\text{C}$  toluene bath. This yellow reaction mixture was then added dropwise to the solution of NaBD<sub>4</sub>/MeOD. This solution was allowed to stir for 16 h at  $-60^\circ\text{C}$  before it was removed from the toluene bath. The reaction mixture was diluted with  $\sim 50$  mL of Et<sub>2</sub>O and loaded onto a 15 mL medium fritted porosity disc that was filled with  $\sim 2$  cm of silica and set in Et<sub>2</sub>O. The column was then eluted with 100 mL of Et<sub>2</sub>O and the solvent was removed in vacuo to reveal a white solid. This solid was then dissolved in 2 mL of DCM and added to 15 mL of standing pentane in a 4-dram vial and allowed to sit at  $-30^\circ\text{C}$  for 16 hr during which time a white solid precipitated out of solution. The next day the white solid was allowed to triturate in a minimal amount of MeCN given that the desired product was marginally soluble in MeCN. The organic layer was then decanted and the reaction mixture was dried with N<sub>2</sub> (g) and allowed to desiccate for 3 h under active vacuum before a mass was taken (0.038 g, 43% yield).

### Synthesis of 62

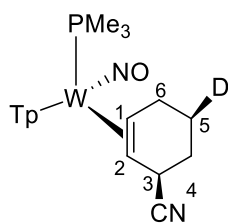


$^1\text{H}$  NMR Characterization of **62-4-*endo-d*<sub>1</sub>** matches that of **48** but with a 99% loss of  $^1\text{H}$  signal intensity at 2.07 ppm (isotopic purity estimated by  $^1\text{H}$  NMR, in this case proton impurity is beyond  $^1\text{H}$  NMR detection limit).

To a 4-dram vial added **1** (0.257 g, 0.442 mmol) along with MeCN (2 mL) and this was allowed to sit at  $-30^\circ\text{C}$ . Separately a solution of NaCN (0.197 g, 4.02 mmol) in MeOD (2 mL) was prepared in a separate 4-dram vial and allowed to stir for 15 min at room temperature before it was transferred to a toluene bath that had been chilled to  $-40^\circ\text{C}$ . In another 4-dram vial diphenylammonium triflate (DPhAT, 0.168 g, 0.525 mmol) was dissolved in MeOD (2.38 g, 71.9 mmol) to generate an in situ source of acidic deuterium and allowed to sit at  $-30^\circ\text{C}$  for 10 min. This acidic deuterium source was then added to the solution of **1** in MeCN at  $-30^\circ\text{C}$  and upon addition the reaction mixture turns from a heterogeneous yellow solution to a homogeneous red/orange solution. This reaction mixture was then allowed to sit in the  $-40^\circ\text{C}$  toluene bath for 5 min before it was added dropwise to the  $-40^\circ\text{C}$  solution of stirring NaCN/MeOD. Upon addition the

reaction mixture turns from a homogeneous red solution to a homogeneous yellow solution and this reaction mixture was allowed to stir for 16 h. After 16 h an off-white solid had precipitated out of solution. The solution was filtered through a fine 15 mL fritted porosity disc to yield an off-white solid. This solid was then washed with DI H<sub>2</sub>O (3 x 5 mL) and then pentane (3 x 5 mL) and allowed to desiccate under active vacuum for 4 h and its identity confirmed by <sup>1</sup>H NMR and a mass was taken (0.112g, 0.18 mmol). The resulting off white solid was subsequently dissolved in 2 mL of MeOH and cooled to -30 °C over the course of 10 min. Separately a test tube of MeOH was cooled in a -50°C toluene bath before NaBH<sub>4</sub> (0.117 g, 3.09 mmol) was added to the chilled solution. To the solution of **4-6,endo-d1** was added a -30°C solution of HOTf (0.061 g, 0.41 mmol) and this reaction mixture was transferred and cooled for 15 min in the - 50 °C toluene bath before the reaction mixture was added dropwise to the -50°C NaBH<sub>4</sub>/MeOH solution. This solution was allowed to stir for 16 h at -50°C before it was removed from the toluene bath. The reaction mixture was diluted with ~ 50 mL of Et<sub>2</sub>O and loaded onto a 15 mL medium fritted porosity disc that was filled with ~ 2 cm of silica and set in Et<sub>2</sub>O. A lime green band was collected upon elution with 100 mL of Et<sub>2</sub>O and the solvent was removed in vacuo to reveal a lime green solid. This solid was then dissolved in 2 mL of DCM and added to 15 mL of standing pentane in a 4-dram vial and allowed to sit at -30°C for 16 hr during which time a white solid precipitated out of solution. The next day the white solid was allowed to triturate in a minimal amount of MeCN given that the desired product was marginally soluble in MeCN. The organic layer was then decanted and the reaction mixture was dried with N<sub>2</sub>(g) and allowed to desiccate for 3 h under active vacuum before a mass was taken (0.038 g, 14% overall yield).

### Synthesis of **63**



<sup>1</sup>H NMR Characterization of **63-5-exo-d1** matches that of **48** but with an 91% loss of <sup>1</sup>H signal intensity at 1.70 ppm (isotopic purity estimated by <sup>1</sup>H NMR). Although overlap is present with the H5-endo proton, the precursor compound shows suppression of the expected exo-proton.

To a 4-dram vial added **1** (0.250 g, 0.430 mmol) along with MeCN (2 mL) and this was allowed to sit at -30°C. Separately a solution of NaCN (0.200 g, 4.08 mmol) in MeOH (2 mL) was prepared in a separate 4-dram vial and allowed to stir for 15 min at room temperature before it was transferred to a toluene bath that had been chilled to -40 °C. In another 4-dram vial diphenylammonium triflate (DPhAT, 0.150 g, 0.469 mmol) was dissolved in MeOH (1 mL) and allowed to sit at -30°C for 10 min. This acidic solution was added to the solution of **1** in MeCN at -30 °C and upon addition the reaction mixture turns from a heterogeneous yellow solution to a homogeneous red/orange solution. This reaction mixture was then allowed to sit in the -40 °C toluene bath for 5 min before it was added dropwise to the -40°C solution of stirring NaCN/MeOD. Upon addition the reaction mixture turns from a homogeneous red solution to a homogeneous yellow solution and this reaction mixture was allowed to stir for 16 h. After 16 h an off-white solid had precipitated out of solution. The solution was filtered through a fine 15 mL fritted porosity disc to yield an off-white solid. This solid was then washed with DI H<sub>2</sub>O (3 x 5 mL) and then pentane (3 x 5 mL) and allowed to desiccate under active vacuum for 4 h and its identity confirmed by <sup>1</sup>H NMR and a mass was taken (0.177g, 0.291 mmol). This solid was then added to a 4-dram vial with MeOD (3.17 g, 95.9 mmol) to generate a heterogeneous white solution and allowed to cool to -30°C. Separately a 4-dram vial was charged with HOTf (0.088g, 0.587 mmol) followed by MeOD (0.792g, 24.0 mmol) and allowed to cool to -30°C. Separately a test tube vial was charged with MeOD (1 mL) and cooled to -50 °C in a toluene bath over a

course of 15 min and to this solution was added NaBH<sub>4</sub> (0.130 g, 3.43 mmol) and allowed to stir at -50 °C. The 4-dram solution of HOTf/MeOD was then added at -30 °C to the solution of tungsten in MeOD and upon addition the reaction mixture turns to a homogeneous color. This solution was allowed to cool to -50 °C over a course of 10 min and then added dropwise to the solution of NaBH<sub>4</sub>/MeOD. This solution was allowed to stir for 16 h at -50°C before it was removed from the toluene bath. The reaction mixture was diluted with ~ 50 mL of Et<sub>2</sub>O and loaded onto a 15 mL medium fritted porosity disc that was filled with ~ 2 cm of silica and set in Et<sub>2</sub>O. A lime green band was collected upon elution with 100 mL of Et<sub>2</sub>O and the solvent was removed in vacuo to reveal a lime green solid. This solid was then dissolved in 2 mL of DCM and added to 15 mL of standing pentane in a 4-dram vial and allowed to sit at -30°C for 16 hr during which time a white solid precipitated out of solution. The next day the white solid was allowed to triturate in a minimal amount of MeCN given that the desired product was marginally soluble in MeCN. The organic layer was then decanted and the reaction mixture was dried with N<sub>2</sub> (g) and allowed to desiccate for 3 h under active vacuum before a mass was taken (0.042 g, 16% overall yield).

#### Data Availability

All data is available in the main text or the supplementary materials, including NMR spectra, experimental details, crystallographic information, DFT calculations, Rotational spectroscopy, and HRMS data. CCDC 1885723-1885725 and 1972890 contains the supplementary crystallographic data for this paper (**4**, **7**, **9** [X-ray] and **45** [neutron]). These data can be obtained free of charge from The Cambridge Crystallographic Data Centre via [www.ccdc.cam.ac.uk/structures](http://www.ccdc.cam.ac.uk/structures)

## References

1. Gant, T. G., Using Deuterium in Drug Discovery: Leaving the Label in the Drug. *J. Med. Chem.* **2014**, *57*, 3595-3611.
2. Thibblin, A.; Ahlberg, P., Reaction Branching and Extreme Kinetic Isotope Effects in the Study of Reaction Mechanisms. *Chemical Society Reviews* **1989**, *18*, 209-224.
3. Thibblin, A., Unusually Large Kinetic Deuterium Isotope Effects on Oxidation Reactions. 1. The Mechanism of Hydroxide-Catalysed Permanganate Oxidation of PhCD(CF<sub>3</sub>)OH and PhCD(CH<sub>3</sub>)OH in Water. *Journal of Physical Organic Chemistry* **1995**, *8*, 186-190.
4. Nelson, S. D.; Trager, W. F., The Use of Deuterium Isotope Effects to Probe the Active Site Properties, Mechanism, of Cytochrome P450-Catalyzed Reactions, and Mechanisms of Metabolically Dependent Toxicity. *Drug Metabolism and Disposition* **2003**, *31*, 1481-1497.
5. Dean, M.; Sung, V. W., Review of Deutetrabenazine: a Novel Treatment for Chorea Associated with Huntington's Disease. *Drug design, development and therapy* **2018**, *12*, 313-319.
6. Loh, Y. Y.; Nagao, K.; Hoover, A. J.; Hesk, D.; Rivera, N. R.; Colletti, S. L.; Davies, I. W.; MacMillan, D. W. C., Photoredox-catalyzed Deuteration and Tritiation of Pharmaceutical Compounds. *Science* **2017**, *358* (6367), 1182-1187.
7. Pony Yu, R.; Hesk, D.; Rivera, N.; Pelczer, I.; Chirik, P. J., Iron-catalysed Tritiation of Pharmaceuticals. *Nature* **2016**, *529*, 195-199.
8. Baldwin, J. E.; Kiemle, D. J.; Kostikov, A. P., Quantitative Analyses of Stereoisomeric 3,4-d<sub>2</sub>-Cyclohexenes in the Presence of 3,6-d<sub>2</sub>-Cyclohexenes. *J. Org Chem.* **2009**, *74*, 3866-3874.
9. Liebov, B. K.; Harman, W. D., Group 6 Dihapto-Coordinate Dearomatization Agents for Organic Synthesis. *Chem. Rev.* **2017**, *117*, 13721-13755.
10. Eisen, M. S.; Marks, T. J., Supported organoactinide complexes as heterogeneous catalysts. A Kinetic and Mechanistic Study of Facile Arene Hydrogenation. *J. Am. Chem. Soc.* **1992**, *114*, 10358-68.
11. Jones, R. A.; Seeberger, M. H., Synthesis of polymer-supported transition metal catalysts via phosphido linkages: heterogeneous catalysts for the hydrogenation of aromatic compounds under mild conditions. *J. Chem. Soc., Chem. Commun.* **1985**, 373-4.
12. Joannou, M. V.; Bezdek, M. J.; Chirik, P. J., Pyridine(diimine) Molybdenum-Catalyzed Hydrogenation of Arenes and Hindered Olefins: Insights into Precatalyst Activation and Deactivation Pathways. *ACS Catalysis* **2018**, *8*, 5276-5285.
13. Harman, W. D.; Taube, H., The selective hydrogenation of benzene to cyclohexene on pentaammineosmium(II). *J. Am. Chem. Soc.* **1988**, *110*, 7906-7907.
14. Welch, K. D.; Harrison, D. P.; Lis, E. C.; Liu, W.; Salomon, R. J.; Harman, W. D.; Myers, W. H., Large-Scale Syntheses of Several Synthons to the Dearomatization Agent {TpW(NO)(PMe<sub>3</sub>)} and Convenient Spectroscopic Tools for Product Analysis. *Organometallics* **2007**, *26*, 2791-2794.
15. Lankenau, A. W.; Iovan, D. A.; Pienkos, J. A.; Salomon, R. J.; Wang, S.; Harrison, D. P.; Myers, W. H.; Harman, W. D., Enantioenrichment of a Tungsten Dearomatization Agent Utilizing Chiral Acids. *J. Am. Chem. Soc.* **2015**, *137*, 10, 3649-3655.



16. Harrison, D. P.; Nichols-Nieler, A. C.; Zottig, V. E.; Strausberg, L.; Salomon, R. J.; Trindle, C. O.; Sabat, M.; Gunnoe, T. B.; Iovan, D. A.; Myers, W. H.; Harman, W. D., Hyperdistorted Tungsten Allyl Complexes and Their Stereoselective Deprotonation to Form Dihapto-Coordinated Dienes. *Organometallics* **2011**, *30*, 2587-2597.
17. Lis, E. C.; Delafuente, D. A.; Lin, Y.; Mocella, C. J.; Todd, M. A.; Liu, W.; Sabat, M.; Myers, W. H.; Harman, W. D., The Uncommon Reactivity of Dihapto-Coordinated Nitrile, Ketone, and Alkene Ligands When Bound to a Powerful  $\pi$ -Base. *Organometallics* **2006**, *25*, 5051-5058.
18. Arashiba, K.; Matsukawa, S.; Kuwata, S.; Tanabe, Y.; Iwasaki, M.; Ishii, Y., Electrophilic O-Methylation of a Terminal Nitrosyl Ligand Attained by an Early-Late Heterobimetallic Effect. *Organometallics* **2006**, *25*, 560-562.
19. Jamison, C. J. Isotope Effects on Chemical Shifts and Coupling Constants 2007, *eMagRes*. doi:[10.1002/9780470034590.emrstm0251](https://doi.org/10.1002/9780470034590.emrstm0251)
20. Pérez, C.; Lobsiger, S.; Seifert, N. A.; Zaleski, D. P.; Temelso, B.; Shields, G. C.; Kisiel, Z.; Pate, B. H., Broadband Fourier transform rotational spectroscopy for structure determination: The water heptamer. *Chemical Physics Letters* **2013**, *571*, 1-15.
21. Sharp, W. B.; Legzdins, P.; Patrick, B. O., O-Protonation of a Terminal Nitrosyl Group To Form an  $\eta^1$ -Hydroxylimido Ligand. *J. Am. Chem. Soc.* **2001**, *123*, 8143-8144.
22. Llamazares, A.; Schmalle, H. W.; Berke, H., Ligand-Assisted Heterolytic Activation of Hydrogen and Silanes Mediated by Nitrosyl Rhenium Complexes. *Organometallics* **2001**, *20*, 5277-5288.
23. Leong, V. S.; Cooper, N. J., Electrophilic activation of benzene in  $[\text{Cr}(\eta^4\text{-C}_6\text{H}_6)(\text{CO})_3]_2$ . *J. Am. Chem. Soc.* **1988**, *110*, 2644-2646.
24. Thompson, R. L.; Lee, S.; Rheingold, A. L.; Cooper, N. J., Reductive activation of the coordinated benzene in manganese complex  $[\text{Mn}(\eta^6\text{-C}_6\text{H}_6)(\text{CO})_3]^+$ : synthesis and characterization of the  $\eta^4$ -naphthalene complex  $\text{PPN}[\text{Mn}(\eta^4\text{-C}_{10}\text{H}_8)(\text{CO})_3]$ . *Organometallics* **1991**, *10*, 1657-1659.
25. Ungureanu, I.; Klotz, P.; Mann, A., Phenylaziridine as a Masked 1,3 Dipole in Reactions with Nonactivated Alkenes. **2000**, *39*, 4615-4617.
26. Sarkar, N.; Banerjee, A.; Nelson, S. G., [4 + 2] Cycloadditions of N-Alkenyl Iminium Ions: Structurally Complex Heterocycles from a Three-Component Diels-Alder Reaction Sequence. *J. Am. Chem. Soc.* **2008**, *130*, 9222-9223.
27. Shim, S. C.; Doh, C. H.; Kim, T. J.; Lee, H. K.; Kim, K. D., A new and convenient synthesis of N-substituted perhydroazepines from adipaldehyde and primary amines with tetracarbonylhydridoferrate,  $\text{HFe}(\text{CO})_4^-$ , as a selective reducing agent. *J. Heterocycl. Chem.* **1988**, *25*, 1383-5.
28. Wilson, K. B.; Myers, J. T.; Nedzbala, H. S.; Combee, L. A.; Sabat, M.; Harman, W. D., Sequential Tandem Addition to a Tungsten-Trifluorotoluene Complex: A Versatile Method for the Preparation of Highly Functionalized Trifluoromethylated Cyclohexenes. *J. Am. Chem. Soc.* **2017**, *139*, 11401-11412.
29. Murray, R. W.; Singh, M.; Williams, B. L.; Moncrieff, H. M., Diastereoselectivity in the Epoxidation of Substituted Cyclohexenes by Dimethyldioxirane<sub>1,2</sub>. *J. Org. Chem.* **1996**, *61*, 1830-1841.
30. Leiris, S.; Lucas, M.; Dupuy d'Angeac, A.; Morère, A., Synthesis and biological evaluation of cyclic nitrogen mustards based on carnitine framework. *European Journal of Medicinal Chemistry* **2010**, *45*, 4140-4148.

31. Wilson, K. B.; Smith, J. A.; Nedzbala, H. S.; Pert, E. K.; Dakermanji, S. J.; Dickie, D. A.; Harman, W. D., Highly Functionalized Cyclohexenes Derived from Benzene: Sequential Tandem Addition Reactions Promoted by Tungsten. *J. Org Chem.* **2019**, *84*, 6094-6116.

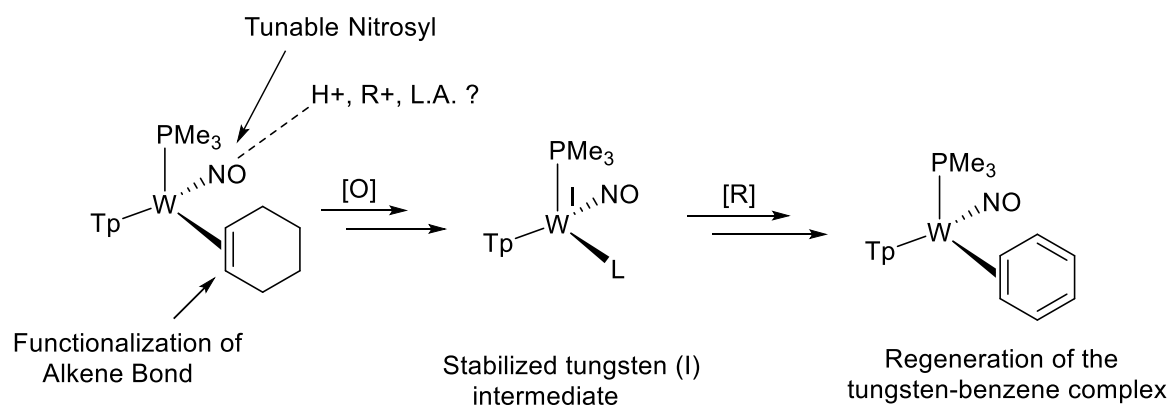
# Chapter 4

## Investigations of $\text{W Tp}(\text{NO})(\text{PMe}_3)(\eta^2\text{-cyclohexene})$

## 4.1 Introduction

Various isotopologues of  $\text{WTP}(\text{PMe}_3)(\text{NO})(\eta^2\text{-cyclohexene})$  (**1**) were synthesized from the tungsten-benzene complex as detailed in Chapter 3. The cyclohexene complex **1** could provide a model system to investigate the functionalization of the metal-bound alkene bond. The dearomatization of benzenes by the fragment  $\{\text{WTP}(\text{NO})(\text{PMe}_3)\}$  has previously resulted in the synthesis of novel cyclohexenes.<sup>1-2</sup> Further additions to the *bound*  $\pi$ -bond of the resulting cyclohexene complex to generate functionalized cyclohexanes has generally not been a synthetic target in our labs. Forays into derivatizing the remaining alkene bond in the tungsten-cyclohexene complex **1** are presented here.

In Chapter 3, the use of molecular rotational resonance (MRR) spectroscopy was crucial to establishing the identity of the resulting cyclohexene isotopomers once decomplexed from the metal.<sup>4</sup> Subjecting the isotopologue complexes of **1** to elevated temperatures enabled thermolysis of the cyclohexene ligand from the tungsten center. The population of cyclohexene isotopologues and isotopomers in the gas phase could then be evaluated by MRR techniques. More discussion is presented here regarding issues of isotopic scrambling of the cyclohexene- $d_n$  isotopologues upon heat-induced liberation from the tungsten metal.



**Scheme 4.7.** The chemical and thermal stability of **1** provides a model system to examine modulation of the nitrosyl ligand and derivatization of the metal-bound alkene functionality. Oxidation of **1** could also enable the regeneration of the tungsten-dearomatization fragment  $\{\text{WTP}(\text{NO})(\text{PMe}_3)\}$ .

Complex **1** is a thermally stable complex with an  $E_{p,a} = 0.28$  V (sweep rate at 100 mV/s) as determined by cyclic voltammetry (CV). Electrochemically, complex **1** shows a pseudo-reversible  $E_{1/2}$  as detailed in **Figure 4.1**, suggesting that **1** is transiently stable in the tungsten (I) oxidation state at 100 mV/s (the lifetime is on the order of seconds at 25 °C). In contrast, the electrochemical oxidation of tungsten-arene complexes is often an entirely chemically irreversible process. For tungsten-olefin complexes derived from dearomatized aromatic molecules, strong chemical oxidants (ceric ammonium nitrate, ferrocenium, DDQ) are needed to decomplex the functionalized organic molecule.<sup>5</sup> Herein we discuss the use of moderate acid sources as a synthetic strategy to decomplex various cyclohexene ligands from the tungsten fragment. Acid-induced liberation of a derivatized  $\pi$ -ligand could be a valuable methodology in isolating organic molecules that contain functionalities sensitive to strongly oxidizing conditions.

While the substitution half-life of the aromatic ligand for tungsten-arene complexes ranges from hours to days under pseudo-first order conditions, estimates by DFT calculations suggest the substitution half-life of the cyclohexene ligand of **1** to be on the timescale of years at 25 °C.<sup>2,6</sup> The increased oxidative and thermal stability of **1** (compared to tungsten-arene complexes) could enable investigation of the nitrosyl ligand while avoiding disassociation of the alkene  $\pi$ -ligand. Initial studies investigating nitrosyl modulation are presented.

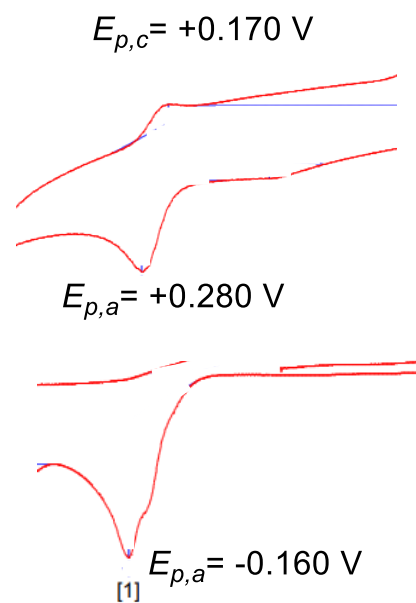
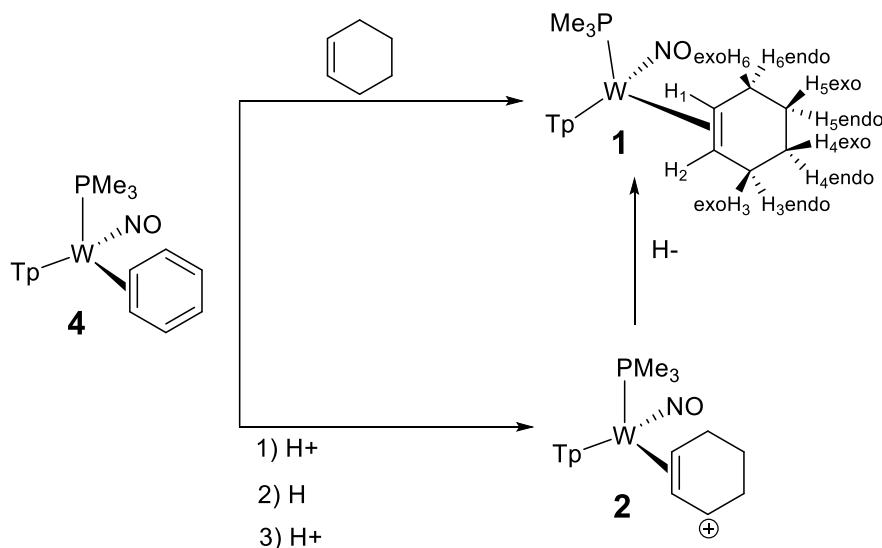


**Figure 4.1.** Illustrative differences in the CV of **1** (top) and WTp(NO)(PMe<sub>3</sub>)( $\eta^2$ -benzene) (**4**) (bottom).  $E_{p,a}$  values for each complex are aligned for easier comparison. The partial return wave ( $E_{p,c}$ ) associated with **1** implies the complex is semi-stable in the tungsten (I) oxidation state. Analogous electrochemical behavior is not observed for **4**.

Finally, osmium, rhenium and molybdenum dearomatization fragments can be recycled after  $\pi$ -ligand decomplexation with an appropriate chemical oxidant. This reactivity has not been realized for tungsten-based dearomatization.<sup>5,7</sup> The ability to stabilize the resulting tungsten (I) species after the initial oxidation process could enable the recycling of the tungsten fragment  $\{\text{WTp}(\text{NO})(\text{PMe}_3)\}$ . Preliminary data supporting the feasibility of this process are presented herein.



**Scheme 4.2.** Synthesis of **1** from **4** via ligand substitution (top) or through multiple tandem addition reactions of proton and hydride (bottom).

## 4.2 Synthesis and Conformations of $\text{WTp}(\text{PMe}_3)(\text{NO})(\eta^2\text{-cyclohexene})$

The complex  $\text{WTp}(\text{PMe}_3)(\text{NO})(\eta^2\text{-C}_6\text{H}_9)^+(\text{OTf}^-)$  (**2**) was first reported nearly a decade ago.<sup>8</sup> This complex can then be treated with a hydride to generate cyclohexene complex **1** or with a deuteride source to generate the  $d_1$ -isotopologue, the complex  $\text{WTp}(\text{PMe}_3)(\text{NO})(\eta^2\text{-cyclohexene})\text{-3-exo-}d_1$  (**3**).<sup>8</sup> Alternatively, allowing a solution of  $\text{WTp}(\text{PMe}_3)(\text{NO})(\eta^2\text{-benzene})$  **4** to stir in an excess of cyclohexene using a dried ether co-solvent (THF or DME) also yields complex **1**. Recently Dr. Katy Wilson has explored the reactivity of the tungsten-benzene complex **4** and  $\text{WTp}(\text{PMe}_3)(\text{NO})(\eta^2\text{-3,4-}\alpha,\alpha,\alpha\text{-trifluorotoluene})$  (**5**) to generate substituted cyclohexenes through elegant tandem addition reactions.<sup>1-2</sup>

Computational studies were pursued to model potential conformers of the cyclohexene ligand of **1**

using DFT calculations with the B3LYP method. The metal complex was described with a hybrid basis set, incorporating the Los Alamos pseudopotential LANL2DZ on the tungsten metal and the 6-31G(d) basis for all other atoms. These structures were originally calculated to support the assignment of diastereotopic protons through analysis of the interproton-dihedral angles and observed  $^3J_{\text{HH}}$  coupling (Karplus analysis).<sup>9-10</sup> However, more conclusive results were obtained via single crystal X-Ray (SCXRD), neutron diffraction and quantitative 1D NOESY experiments. These results are presented in the Supplemental Material associated with Chapter 3.

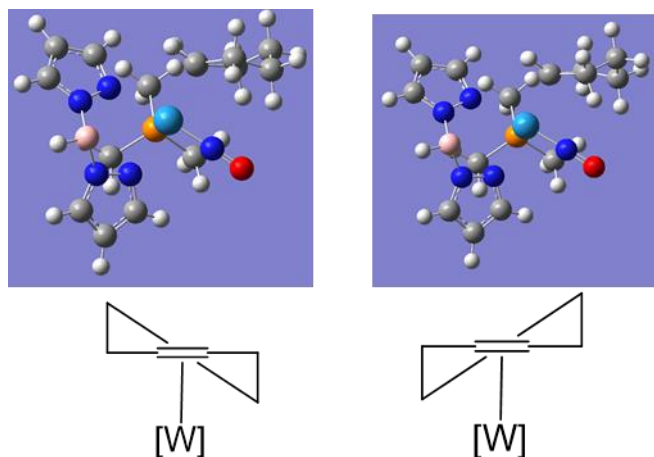


**Figure 4.2.** Figure depicting two conformations of **1** that are degenerate in electronic energy as established by DFT calculations. The TpA pyrazole ring has been removed for clarity (top). Both conformers are observed in the solid state from SCXRD. A simplified depiction of these conformers is illustrated below (ligand set not shown).

Static structures of **1** found by DFT calculations suggest that the cyclohexene ligand can exist as two different, nearly degenerate conformations as detailed in **Figure 4.2**. Complex **1** crystallizes in a 0.88:0.12 ratio of two conformational isomers as determined by SCXRD. In the  $^1\text{H}$  NMR spectra only a single diamagnetic complex is observed for **1**, suggesting that the observed  $^1\text{H}$  NMR resonances associated with **1** are most likely an average of the two conformers in solution.<sup>11</sup> While

seemingly trivial, the identification of these two conformers was crucial in accurately assigning the deuterium occupancy at the  $\text{H}_{3\text{exo}}$  and  $\text{H}_{4\text{exo}}$  position via neutron diffraction as described in Chapter 3.

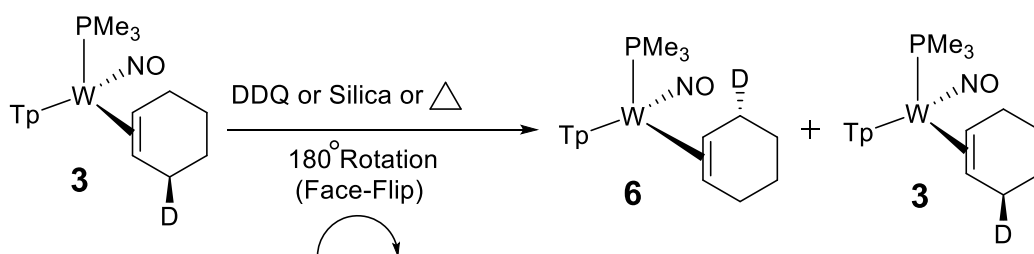
### 4.3 Evidence for Interfacial Isomerization for $\text{W Tp}(\text{PMe}_3)(\text{NO})(\eta^2\text{-cyclohexene})$

Generating the  $d_1$ -isotopologue cyclohexene complex **3** can be readily achieved by treating the tungsten-allyl complex **2** with  $\text{NaBD}_4$  as a deuteride source. This complex provides an excellent model system to evaluate the reactivity available to the cyclohexene ring. Specifically, studies of the  $d_1$ -isotopologue complex **3** reveal that an intrafacial “face-flip” isomerization pathway is accessible to the cyclohexene ligand. The net result of this isomerization pathway is a  $180^\circ$  rotation of the cyclohexene ligand

around the metal-alkene bond. After this isomerization, the metal is coordinated to the opposite face of the cyclohexene alkene bond. This type of reactivity was observed by allowing **3** to react with various chemical additives as well as exposing complex **3** to elevated temperatures.

For example, if **3** is allowed to stir with a substoichiometric amount of the oxidant DDQ for several minutes, isomerization is observed that is consistent with a “face-flip” mechanism (**Scheme 4.3**). The deuterium at the H<sub>3<sub>exo</sub></sub> position is able to exchange location with the H<sub>6<sub>endo</sub></sub> proton to generate W Tp(PMe<sub>3</sub>)(NO)(η<sup>2</sup>-cyclohexene)-6-endo-d<sub>1</sub> (**6**).<sup>12</sup> Assignment of these protons is supported with 1D and 2D NOESY NMR measurement techniques. When complex **3** is heated on a stir plate set to 150 °C in the solid state over the course of 10 minutes, the formation of **6** is observed in an approximate 1:1 ratio with **3**. These data suggest that there is a negligible thermodynamic isotope effect between complexes **3** and **6**. This result also illustrates the remarkable thermal stability of **3**, as minimal decomposition is observed during this process.

Studies investigating the ability to catalyze isomerization between alkene-bonds has been reported by Dr. Steven Dakermanji for the π-basic metal fragment {MoTp(NO)(DMAP)}.<sup>2</sup> Dr. Katy Wilson has extended this methodology to functionalized 1,3-cyclohexadienes complexes of tungsten. In these studies, a catalytic amount of oxidant promotes intramolecular ring-isomerization within a cyclohexadiene ring.<sup>2</sup>



**Scheme 4.3.** Oxidant, Lewis and/or Bronsted acid catalyzed ring isomerization at ambient temperatures observed in solution. Alternatively elevated temperatures allow analogous isomerization of the cyclohexene ring.

We speculate that similar factors may be involved in the observed isomerization of **3**. That is, through the use of the oxidant DDQ, transient oxidation of the metal center to the tungsten (I) oxidation state weakens the metal-to-ligand backbonding interaction and enables isomerization of the π-ligand. This isomerization is



accompanied by the subsequent reduction of the tungsten (I) species back to a tungsten (0) state.

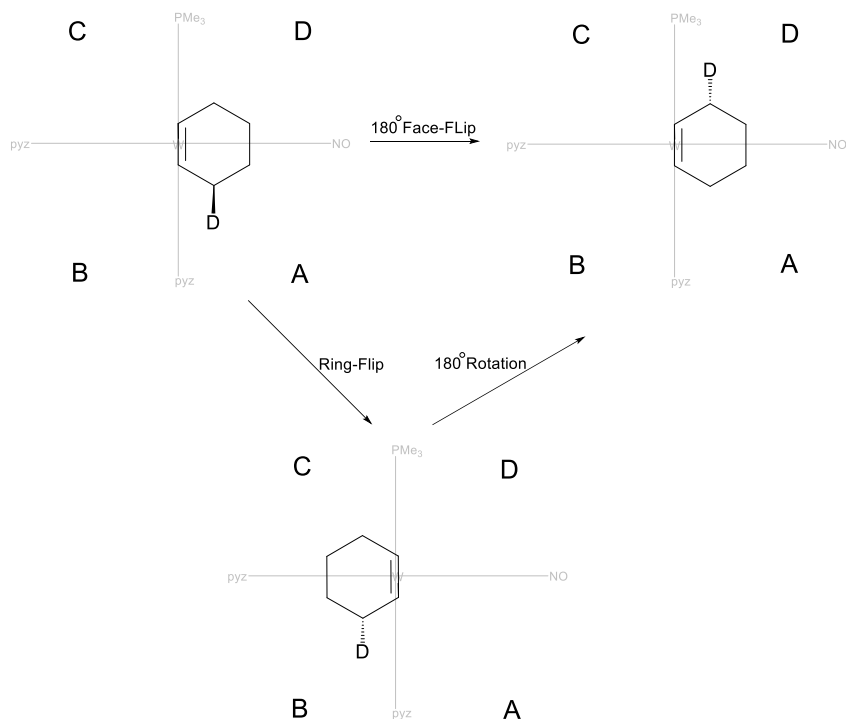


**Figure 4.3** Proposed mechanistic pathways where the ring isomerization can occur via a 180° “face-flip” about the pyr-NO axis (top). An alternative mechanism involves an initial “ring-flip” about the W-pyr axis and a subsequent 180° rotation (bottom).

Alternatively, treatment with a substoichiometric amount of DDQ may oxidize only a fraction of the *d*<sub>1</sub>-cyclohexene complex **3**.<sup>13</sup> The resulting tungsten (I) metal could be further oxidized to higher-valence tungsten metal complexes. The resulting complexes could then serve as mild oxidants that result in the transient oxidation of complex **3** and allow the ring isomerization proposed for the formation of **6**. Alternatively, these purported higher-valence tungsten complexes could serve as Lewis acids, which may be able to also catalyze the “face-flip” isomerization depicted in **Scheme 4.3**.

When complex **3** is dissolved in MeCN-*d*<sub>3</sub> and allowed to stir in the presence of silica gel, errant proton sources originating from the silica gel (i.e. silanol groups) could engage in hydrogen-bonding interactions with the nitrosyl ligand. Alternatively, these protons may transiently protonate the electron-rich metal center. In either case, a net decrease in electron density could occur at the tungsten center. This would weaken the metal-to-alkene  $\pi$ -bond and result in a reduced barrier to a “face-flip” isomerization mechanism about the NO-TpC axis (to lead directly to **6**) or about the tungsten-TpB axis to place the aliphatic portion of

the cyclohexene ring into the “B” and “C” quadrants (**Figure 4.3**). An accompanying 180° rotation to place the aliphatic portion would lead to the development of **6**.

Allowing complex **3** to stir in a solution of MeCN-*d*<sub>3</sub>/MeOD does not result in any noticeable formation of the isotopologues complex **6**. Additionally, no additional deuterium is integrated into complex **3**.

#### 4.4 Analysis by Molecular Rotational Resonance Spectroscopy (MRR)

Molecular Rotational Resonance (MRR) spectroscopy is an analytical technique that analyzes the rotational transitions of a molecule in the gas phase.<sup>12, 14</sup> These transitions are highly sensitive to the moment of inertia associated with the molecule.

The detection limits of this technique are sensitive enough to distinguish between <sup>2</sup>H and <sup>13</sup>C isotopologues of volatile, organic molecules at natural abundance levels.<sup>4</sup> This technique proved pivotal in supporting the isotopologue assignments for

the deuterated cyclohexenes presented in Chapter 3. All MRR spectroscopic measurements were performed by Reilly Sonstrom under the guidance of Professor Brooks H. Pate and Dr. Patrick Kelleher.

Isotopologues of **1** were prepared in the hope that thermally-promoted heterolytic bond cleavage (thermolysis) between metal and cyclohexene would enable facile analysis of the liberated cyclohexene ligand via MRR techniques. When the *d*<sub>1</sub>-isotopologue complex **3** was prepared and the cyclohexene ligand liberated from the metal via heating, differences in the isotopologue and isotopomer distribution determined by <sup>1</sup>H NMR spectroscopy for the cyclohexene ligand and that measured via MRR analysis were observed. That is, once decomplexed from the metal, the liberated cyclohexene ligand that originated from **3** displayed significant decreases in isotopic purity and isotopomer selectivity compared to that observed by the <sup>1</sup>H NMR analysis of complex **3**. These differences are illustrated in **Table 4.1**. It should be noted that the limit of detection in the NMR is nominally taken as ~20:1. Therefore isotopologues with abundances <5% will be

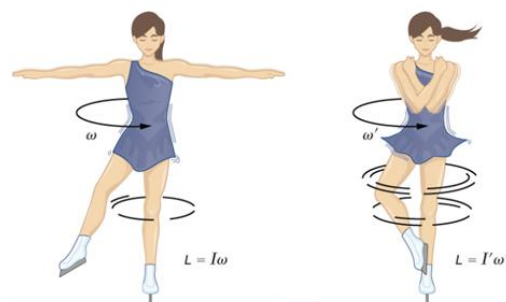


**Figure 4.4.** The different rotations of the ballerina can be exactly defined by different moments of inertia. Analogously, a molecule’s specific moment of inertia as determined by MRR analysis allows for unambiguous determination of its identity.

challenging to establish by NMR analysis.

Similar issues were observed in the preparation of the  $d_2$ -isotopologue  $\text{W}(\text{Tp})(\text{PMe}_3)(\text{NO})(\eta^2\text{-cyclohexene})\text{-4-exo,5-endo-}d_2$  (**7**), where NMR and MRR data gave conflicting results. A series of experiments with the *same* batch of the  $d_1$ -isotopologue **3** showed that significant differences in the observed isotopologue and isotopomer ratios arose depending on differences in sample preparation. These results are summarized in **Table 4.1**. Notably, samples that were pre-dissolved in DCM or samples exposed to atmosphere over extended periods of time (2 h) correlated to enhanced isotopic scrambling. A mechanism to account for this phenomenon is currently being investigated.

Interestingly, even after heating to 200 °C and exposure to atmosphere at elevated temperatures, residual mounts of **3** were recovered after MRR analysis and characterized by  $^1\text{H}$  NMR spectroscopy. Importantly, these residual samples show the development of the cyclohexene isotopologue complex **6** via  $^1\text{H}$  NMR spectroscopy that wasn't present in the original sample (**Figure 4.4**). As mentioned

Thermolysis of cyclohexene ligand under argon for MRR analysis

|  |     |      |     |    |
|--|-----|------|-----|----|
| Observed by NMR<br>(Still bound to metal)                        | 5 % | 95 % | NA  | NA |
| MRR Analysis<br>(Sample dissolved in DCM)                        | 9%  | 76%  | 7%  | 6% |
| MRR Analysis<br>(Loaded as solid, 15 min<br>atmosphere exposure) | 6%  | 84%  | 4%  | 6% |
| MRR Analysis<br>(Loaded as solid, 2 h<br>atmosphere exposure)    | 9%  | 73%  | 11% | 7% |

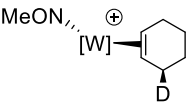
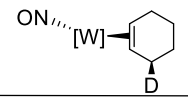
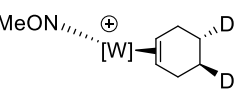
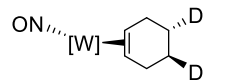
**Table 4.1.** Change in distribution of observed isotopologues depending on the conditions or pre-conditions used to liberate the free cyclohexene isotopologues.

previously, this is the product that would be expected from an interfacial “face-flip” of the cyclohexene ring on the metal.

In the case of  $\text{WTP}(\text{PMe}_3)(\text{NOMe})(\eta^2\text{-1,2-cyclohexene})^+(\text{OTf})^-$  (**8**), results were more promising in liberating the cyclohexene ligand via thermolysis. Analysis of the methylated nitrosyl complex was inspired by the more positively shifted  $E_{p,a}$  associated with complex **8** compared to its neutral analog, complex **1** (1.2 V and 0.28 V respectively). These data suggest that complex **8** is more resistant to oxidation than its neutral analog **1**, which could be a valuable property if transient oxidation of the metal promotes an isotopic scrambling process. Additionally, the metal-alkene bond of **1** has a significant  $\pi$ -backbonding component. A formal two electron oxidation of the metal (upon methylation of the nitrosyl ligand transforming **1** into **8**) would result in a metal center with less electron density. The reduction in electron density should reduce the metal-alkene bond strength due to diminished backbonding from the higher oxidation state complex **8** to the cyclohexene  $\pi$ -ligand. Ideally, this would weaken the metal-to-cyclohexene bond enabling efficient thermolysis of the cyclohexene ligand.

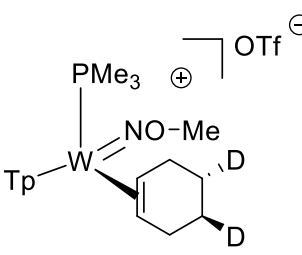
| Desired Complex | Deuterium Occupancy (NMR)<br>Deuterium Occupancy (Neutron) | Percentage of Desired Isotopologue (HRMS)<br>Percentage of Desired Isotopologue (MRR) | Percentage of Desired Stereoisomer (MRR)<br>(relative to other stereoisomers) |
|-----------------|--|---|---|
|                 | 95%  | 99% >95%  | >95%  |
|                 | 95% 92%<br>97% 91%   | NA >60%   | >66%  |
|                 | 95%<br>95%   | NA >82%   | >76%  |
|                 | 95%<br>95%<br>95%  | 96% >78%  | 100%  |
|                 | 72%<br>28%   | 76% >57%  | 100%  |

**Table 4.2.** Estimates of isotopic purity for various isotopologues of **1** by HRMS,  $^1\text{H}$  NMR and neutron diffraction data. Data is compared to estimates of isotopic purity of the free cyclohexene ligand as established by MRR measurements by Reilly Sonstrom. Discrepancies are postulated to occur as a result of isotopic scrambling upon heating and before release of the cyclohexene ligand. Investigation into this mechanism is ongoing.

| Complex   | Desired Isotopologue (%) | Desired Isotopomer (%) |
|---|--------------------------|------------------------|
|  | > 95%                    | > 95%                  |
|  | 91%                      | 82%                    |
|  | 82%                      | 76%                    |
|  | 31%                      | 66%                    |

**Table 4.3.** Differences in isotopologue distributions between neutral and cationic, nitrosyl-methylated tungsten-cyclohexene complexes.

In the case of the methylated nitrosyl cyclohexene complex **8**, thermal decomplexation of the cyclohexene ligand was observed to begin at lower temperatures (60 °C compared to 200 °C for the neutral analog **1**). The concentration of liberated cyclohexene liberated from the methylated nitrosyl complex **8** in the gas phase increased by more than one hundred-fold compared to the cyclohexene liberated from the neutral complex **1**.

| Complex   | Thermolysis Conditions  | Desired Isotopologue (%) | Desired Isotopomer (%) |
|---|---|--------------------------|------------------------|
|  | *Held at 200 °C   | 82%                      | 86%                    |
|   | Held at 140 °C (2.5 h)  | 70%                      | 80%                    |
|   | Held at 140 °C (3.25 h)   | 63%                      | 75%                    |
|   | Heated from 140 °C (3.25 h total) then heated at 200 °C (for 30 min)) | 80%                      | 86%                    |

**Table 4.4** Change in the distribution of observed isotopologues as a function of varying the temperature. Isotopologue numbers correspond to the free cyclohexene organic (desired isotopologue is  $d_2$ , desired isotopomer features deuteriums at the four and five position carbons in a mutual trans-arrangement. The \* designates a different run at 200 °C of the same sample.

When **3** was subjected to this method as a solid to release cyclohexene-3- $d_1$ , 95% of a  $d_1$ -isotopologue species was observed in the mixture of isotopologues, with 96% of the  $d_1$ -isotopologue population corresponding to the cyclohexene-3- $d_1$  isotopomer (**Table 4.2**). These results are more in agreement with the observed isotopologue distribution of **8** as determined by  $^1\text{H}$  NMR.

Overall, MRR analysis of the cyclohexene- $d_n$  isotopologues proved to be more efficient for isotopologues of the cationic tungsten-cyclohexene complex **8** than isotopologues of the neutral cyclohexene complex

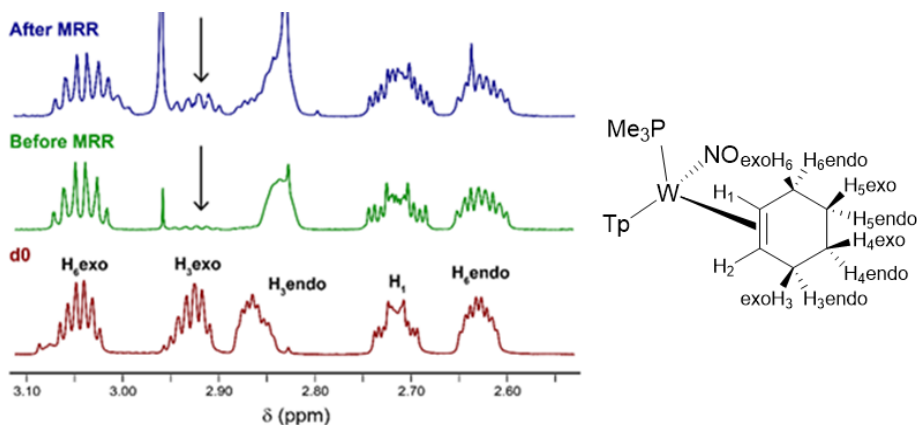


**Figure 4.5.** Generation of **6** from the heating of **3**. An increase the  $\text{H}_{3\text{exo}}$  position resonances and a corresponding decrease in the  $\text{H}_{6\text{endo}}$  proton resonance is observed after heating, consistent with the process illustrated in **Scheme 4.2**.

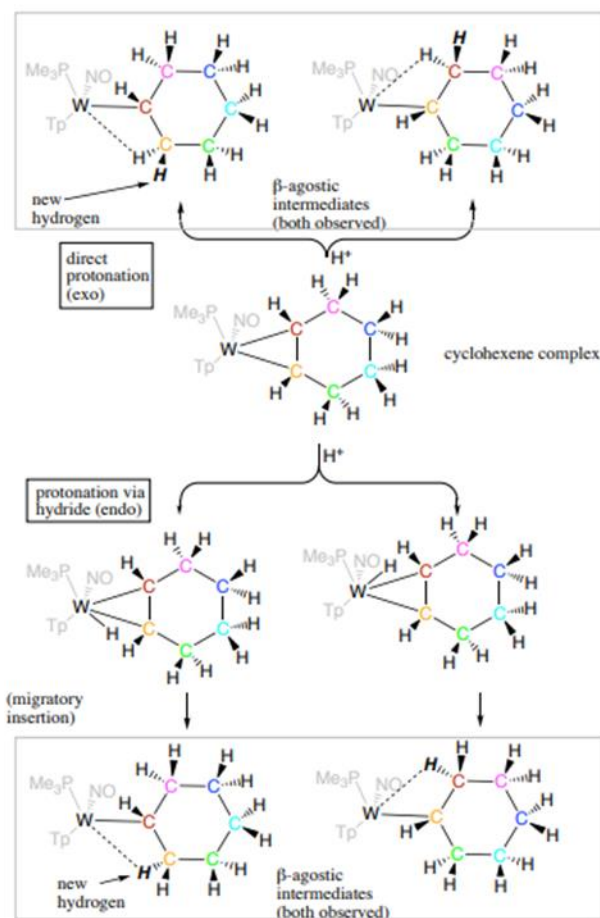
1. Even so, depending on the temperature and handling of the metal complex, different isotopologue distributions were observed in the MRR analysis *from the same sample*. For instance, a tungsten-cyclohexene complex that was assayed as having 90% + deuterium incorporation at the  $\text{H}_{3\text{exo}}$  and  $\text{H}_{4\text{exo}}$  positions (confirmed by neutron diffraction and  $^1\text{H}$  NMR) shows significant scrambling in the resulting MRR measurements of the cyclohexene ligand. In the MRR spectra of the free cyclohexene derived from this  $d_2$ -isotopologue complex, 66% of the total sample was assayed as being a  $d_2$ -isotopologue, and only 60% of that population corresponds to the major  $d_2$ -isotopomer established by  $^1\text{H}$  NMR and neutron diffraction techniques ((3R,4R)-cyclohex-1-ene-3,4- $d_2$ ). This sample was extensively exposed to atmosphere in its preparation for neutron diffraction and also for travel to and from Oak Ridge National Lab (ORNL) in Oak Ridge, Tennessee.

While an investigation into this mechanism is ongoing, an intrafacial ring rotation would account for the observed deuterium scrambling as determined by MRR analysis. Potential intermediates could include alpha or beta-agostic structures derived from protonation of the metal from an errant proteo-source as depicted in **Scheme 4.4**.<sup>15</sup> Given the correlation between atmospheric exposure and isotopic scrambling, adsorption of trace water by the tungsten compound could provide an adventitious proton source. Credit is given to Karl Westendorff for the experimental and computational pursuit of agostic complexes available to various tungsten-olefin scaffolds.

The data from MRR experiments support the stereochemical assignments for the isotopomers of the tungsten-cyclohexene complex **1**. That is, while scrambling was observed, the relative stereochemistry of isotopologues higher than cyclohexene-*d*<sub>1</sub> observed by MRR spectroscopy was consistent with the results predicted by <sup>1</sup>H NMR analysis.

For example, in the case of complex **7** the expected cyclohexene-*d*<sub>2</sub> species is expected to be that of cyclohexene-4,5-*trans-d*<sub>2</sub>. In this case, the *only other cyclohexene-d*<sub>2</sub> isotopologue observed is that of cyclohexene-3,4-*trans-d*<sub>2</sub>. The dominant isomerization pathway then is an intramolecular 60° ring rotation that effectively preserves the relative stereochemical arrangement of the deuterium atoms.

A more efficient analysis of isotopologues of cyclohexene could be enabled by efficient oxidation of the tungsten metal to liberate the cyclohexene ring. Given the high volatility of the cyclohexene ligand, the



**Scheme 4.4.** Potential mechanisms involving exogenous acid source and the sequential formation of agostic intermediates followed by beta-hydride elimination to account for observed isotopic scrambling upon thermolysis. Experimental and theoretical studies of agostic complexes of tungsten are being pursued by Karl Westendorff.

oxidation conditions would need to use an oxidant in the solid state or a low volume of a high boiling point solvent to be compatible with analysis by MRR spectroscopy.

Optimizations to cyclohexene ligand liberation from the tungsten fragment and resulting analysis by MRR measurements are ongoing. The MRR spectroscopic technique provides a definitive spectroscopic “fingerprint” once the spectrum of a molecule is recorded, enabling unambiguous assignment of the organic molecule.<sup>4</sup> This methodology could very well be applied to other organic ligands derived from dearomatization-enabled products in our lab. Given the ability to enantioenrich the tungsten chiral-at-metal center, the enantioselective synthesis of isotopomers of cyclohexene is being pursued for MMR analysis in conjunction with Reilly Sonstrom.<sup>16</sup>

#### 4.5 Decomplexation of the $\eta^2$ -Bound Alkene Bonds with Acid Sources

Complex **1** can be easily prepared and is a practical synthetic model to investigate derivatization of the metal-bound alkene carbons. A postulated synthetic scheme to the stereoselective generation of a functionalized cyclohexane is generically illustrated in **Scheme 4.5**.

Previously, our lab has reported the synthesis of the beta-agostic complex  $\text{Wtp}(\text{NO})(\text{PMe}_3)(\kappa^2\text{-cyclopentanyl})^+ \text{OTf}^-$  obtained from treating  $\text{Wtp}(\text{PMe}_3)(\text{NO})(\eta^2\text{-cyclopentene})$  with DPhAT in a THF solution.<sup>17</sup> Complex **1** was treated with DPhAT in an effort to synthesize an agostic tungsten(II) cyclohexyl complex. After the initial electrophilic addition (protonation), subsequent treatment with a nucleophile could lead to a functionalized cyclohexane molecule.

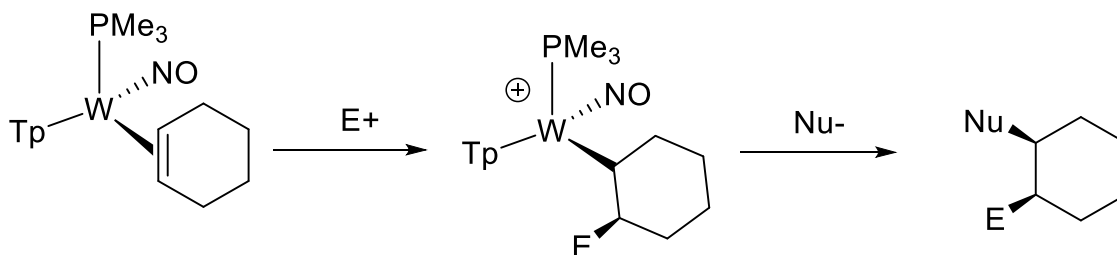
Treating the tungsten-cyclohexene complex **1** with DPhAT did not give analogous results for those observed for the tungsten-cyclopentene complex. Instead of the intended agostic complex, a new diamagnetic metal complex was observed (**1H**). Spectral features observed in the <sup>1</sup>H NMR spectra for **1H** include a proton resonance at 11.1 ppm in MeCN-*d*<sub>3</sub> with a  $J_{\text{PH}} = 119$  Hz. These results are consistent with the formation of a seven-coordinate tungsten hydride species.<sup>6</sup> The formation of this complex (**1H**) was accompanied by the concomitant release of the cyclohexene ligand. Tungsten satellites arising from proton-



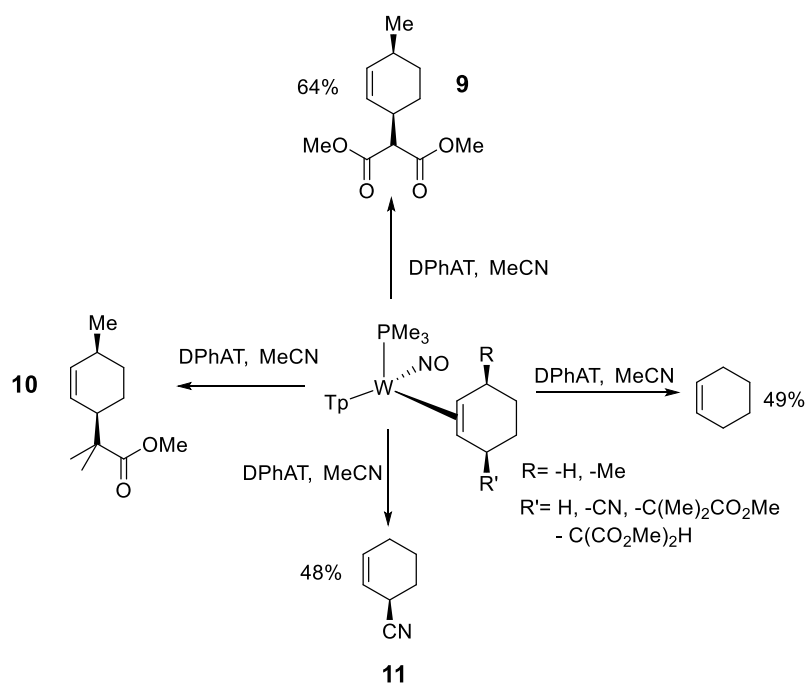
tungsten coupling interactions ( $J_{WH}$ ) for the purported tungsten-hydride resonance of **1H** are not observed; however a previous report from our lab shows loss of tungsten coupling in certain higher oxidation state tungsten complexes.<sup>18</sup> The ability to liberate the cyclohexene ligand from the metal with the moderate Bronsted acid (DPhAT pKa ~ 1) prompted further investigation.

To determine if cyclohexene ligand decomplexation could be achieved with acid, various functionalized cyclohexene complexes were subjected to acid sources (DPhAT, pyridinium triflate). Gratifyingly, liberation of the organic cyclohexene ligands methyl 2-methyl-2-((1R,4S)-4-methylcyclohex-2-en-1-yl)propanoate (**9**), dimethyl 2-((1R,4S)-4-methylcyclohex-2-en-1-yl)malonate (**10**) and cyclohex-2-ene-1-carbonitrile (**11**) was achieved by treating the corresponding tungsten-cyclohexene adduct with either DPhAT or pyridinium triflate (**Scheme 4.6**). Full credit is given to Dr. Katy B. Wilson for the synthesis of the tungsten-olefin-complexes corresponding to the cyclohexene molecules **9** and **10**.

The yield of the free organic after decomplexation with acid was moderate (~ 50% NMR yield), however this methodology could prove a productive route for ligand decomplexation at the tungsten-alkene stage in cases where the resulting organic ligand is sensitive to oxidation. The bond acidolysis is compatible with ester, cyano and alkyl groups. Acid-induced liberation was compatible with electron-deficient cyclohexene complexes. For instance, the tungsten-3-cyano-cyclohexene complex **11** has an  $E_{p,a} = 0.61$  V and the cyclohexene ligand could be readily decomplexed with acid. Decomplexation with a moderate acid source could be an alternative to using strong oxidants to liberate functionalized organics molecules derived from aromatic starting materials.



**Scheme 4.5.** Theorized tandem addition reaction on **1** with selectivity imbued by the metal. The result would be the synthesis of novel cyclohexanes.



**Scheme 4.6.** Decomplexation of various cyclohexene ligands upon exposure to a moderate Bronsted acid. When possible NMR yields are given. Decomplexations were performed on an NMR scale and utilized large excesses of acid (> 150 equivalents).

#### 4.6 Nitrosyl Modulation Studies

Methylation of the nitrosyl ligand of the neutral tungsten-cyclohexene complex **1** to generate cationic, nitrosyl-methylated adduct **8** was detailed in Chapter 3. We postulate that the nitrosyl ligand could play a role in mediating organic reactivity. Due to the enhanced thermal stability of the complex **1** (compared to the arene complex **4**), studies were pursued to determine if chemical additives could be used to manipulate electronic properties of the metal center while avoiding ligand decomplexation.

$^{31}\text{P}$  NMR spectroscopy has proven to be a valuable tool in the development of the dearomatization fragment  $\{\text{WTp}(\text{NO})(\text{PMe}_3)\}$ .<sup>6</sup> The  $^{31}\text{P}$  nucleus demonstrates coupling with the NMR active,  $I = \frac{1}{2}$  nuclei associated with the  $^{183}\text{W}$  isotope (14.4 % natural abundance). Previous studies have shown a correlation between the ligand set of the tungsten complex and the magnitude of  $J_{\text{WP}}$ .<sup>6</sup> One explanation relates the degree of s character on the tungsten metal to the magnitude of the  $J_{\text{WP}}$  coupling constant. For instance, the complex  $\text{WTp}(\text{PMe}_3)(\text{NO})(\text{CO})$  has an

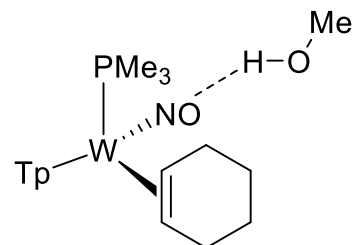


**Figure 4.6.** Theorized H-bonding interactions between the tungsten-nitrosyl ligand and an H-bond donor (here methanol).

associated  $J_{WP} = 400$  Hz. For the seven-coordinate complex  $WTP(PMe_3)(NO)(F)(Ph)$  the  $J_{WP}$  coupling approaches 212 Hz.<sup>6</sup> This can be rationalized as in the seven-coordinate form, the s orbital character associated with the tungsten atom is involved in sigma bonding interactions across seven different sigma donor ligands, resulting in a lower  $J_{WP}$  value compared to a tungsten complex with six coordinated ligands. There is less s-orbital character interaction available between the tungsten and phosphine as the number of ligand interactions increases.

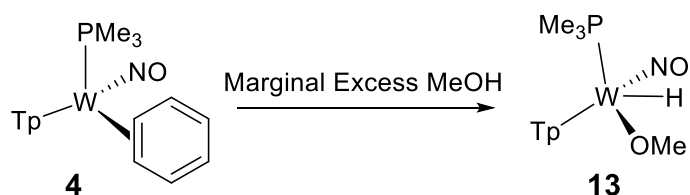
For the tungsten-benzene complex **4** the  $J_{WP}$  value lies between the thresholds of six and seven-coordinate species with a  $J_{WP} = 310$  Hz. However, upon protonation to generate the tungsten-benzenium complex (detailed in Chapter 2), the coupling decreases to a  $J_{WP}$  of 270 Hz. Presumably, this is due to an enhanced bonding interaction between the tungsten atom and resulting benzenium ligand, which in turn reduces the tungsten-phosphine bonding interaction.

With this rationale in mind, the magnitude of the tungsten-phosphorus coupling constant of complex **1** was observed in different solvent environments. In  $MeCN-d_3$  or  $CDCl_3$  the value of  $J_{WP}$  of complex **1** is 290 Hz. While the polarity differences between these solvent systems is significant, no observed reduction is seen in the  $J_{WP}$  coupling. Presumably the nature of bonding between the tungsten and its ligand set remains the same despite solvent polarity differences. When MeOH is used as a solvent however, a noticeable decrease of the  $J_{WP}$  value is observed to  $J_{WP} = 280$  Hz. A similar change in the magnitude of  $J_{WP}$  coupling is observed if a  $CDCl_3$  solution of **1** is treated with several drops of hexafluoroisopropanol (HFIP), a strong hydrogen-bond donor. Here a decrease of tungsten-phosphorous coupling to a value of  $J_{WP} = 282$  Hz is observed.

One possible explanation for the decrease in  $J_{WP}$  values is that in protic solvents (or in the presence of hydrogen-bond donors such as HFIP), hydrogen-bonding interactions can occur with the oxygen lone pairs of the nitrosyl ligand. This could make the nitrosyl ligand a stronger  $\pi$ -acceptor ligand. Accordingly, the relatively electron-rich metal center is able to  $\pi$ -backbond more efficiently into the nitrosyl ligand, enhancing

the metal-nitrosyl interaction. Consequently, the bonding interaction between tungsten and phosphine ligand would decrease. The effect would be bolstered if enhanced  $\pi$ -backdonation into the nitrosyl ligand results in decreased  $\pi$ -backdonation into the phosphine. This would result in decreased s-orbital overlap given the synergistic relationship between  $\sigma$  donation and  $\pi$ -backdonation. The coupling of the  $J_{WP}$  value should lower accordingly, and this is what is observed experimentally. In support of this, interatom distances from single-crystal X-Ray Diffraction (SC-XRD) show that the W-P bond in the methylated cyclohexene complex **8** is longer than in the neutral cyclohexene complex **1**.

When **4** is allowed to stir in MeOH over a period of several minutes, a significant decrease in coupling is also observed for the  $J_{WP}$  constant to 295 Hz. Along with the lowered  $J_{WP}$  constant, over time signals consistent with the liberation of the  $\text{PMe}_3$  ligand evolve in the  $^{31}\text{P}$  NMR spectra.



**Scheme 4.7.** Exposure of **4** to methanol and the associated O-H activation adduct.

Spectral features consistent with the tungsten (II) complex  $\text{WTp}(\text{NO})(\text{OMe})_2$  (**12**) develop in the  $^1\text{H}$  NMR over time. In this case, along with the decrease in coupling constant, the weaker benzene-W bonding interaction in **4** (compared to **1**) is more sensitive to changes in electron density at the metal center. Accordingly, a decrease in electron density at the metal via enhanced  $\pi$ -backbonding to the nitrosyl ligand would weaken the tungsten-benzene bond. This could account for the accelerated ligand substitution that is observed experimentally.

When a solution of **4** is dissolved in benzene- $d_6$  and only a few drops of MeOH are added, spectral signals consistent with activation of the methanol O-H bond to generate **13** are observed. Among these are retention of the  $\text{PMe}_3$  ligand and appearance of a highly downfield proton resonance at 12.31 ppm with a  $J_{\text{PH}} = 130.1$  Hz and tungsten satellites with a  $J_{\text{WH}} = 31.5$  Hz. Presumably the O-H activated adduct **13** is an intermediate en route to the bis-methoxide complex **12**. Allowing complex **13** to sit over time indeed results in the formation of **12**. A mechanism for this transformation has not been determined. Investigation was then

focused on the ability of Lewis Acids to induce observable spectroscopic changes. Presumably, we postulate that chemical interactions between a hydrogen-bond donor and the nitrosyl ligand would be responsible for such changes.

To further understand the reactivity of the nitrosyl ligand, various Lewis acids were surveyed to see if either chemical reactivity or spectral changes could be observed. Addition of  $\text{BH}_3\text{-THF}$  or  $\text{BF}_3\text{-etherate}$  to complex **1** led to  $J_{\text{WH}}$  values of  $\sim 285$  Hz in  $\text{CDCl}_3$ . Attempts to isolate these Lewis acid adducts from boron coordination led to the recovery of the starting material **1**. When TBDSOTf is used however,  $^1\text{H}$  NMR analysis in  $\text{MeCN-}d_3$  leads to a systematic downfield shift for every proton resonance on the cyclohexene ring. Attempts to isolate this complex led to the generation of multiple diamagnetic complexes and the concomitant release of the cyclohexene ligand. Importantly, effects from Lewis Acid coordination were only observed with relatively non-polar, aprotic solvents (benzene,  $\text{CDCl}_3$ , DCM, MeCN). Solvents such as acetone or methanol effectively “quench” the Lewis acid, at least to such an extent that differences arising from Lewis acid interactions are not observed with  $^1\text{H}$  or  $^{31}\text{P}$  NMR spectroscopy.

Legzdins et al have shown the ability of various Lewis acids to coordinate to the nitrosyl ligand of  $\text{Cp}^*\text{M}(\text{NO})(\kappa^2\text{-Ph}_2\text{PCH}_2\text{CH}_2\text{PPh}_2)$  ( $\text{M} = \text{molybdenum, tungsten}$ ).<sup>3</sup> A formal two electron oxidation occurs at the tungsten metal as the nitrosyl ligand goes from a linear to bent geometry upon coordination of a strong Lewis acid. The change in geometry results in a coordinatively unsaturated complex,

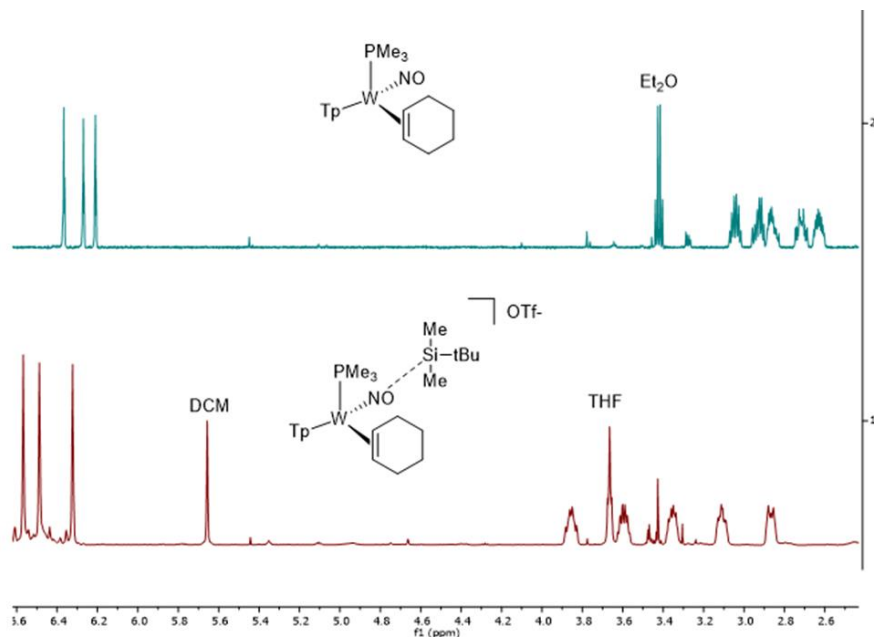
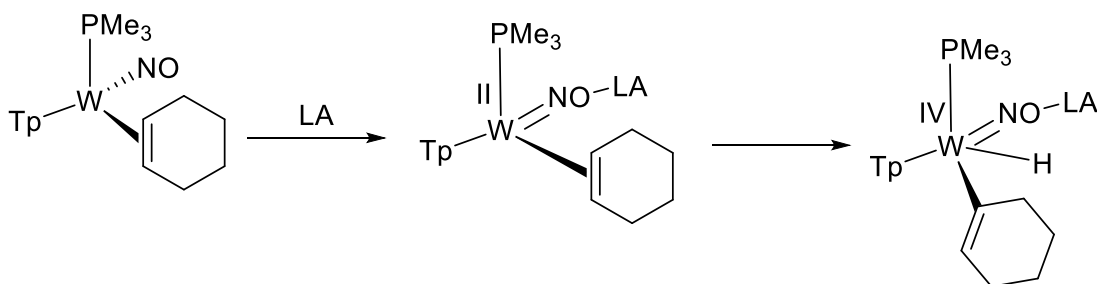


**Figure 4.7.** Proposed complexation of a Lewis Acid (TBDSOTf) to **1**. Systematic downfield shifting for proton resonances of the cyclohexene and those corresponding to the Tp4 protons is shown. A  $^1\text{H}$  NMR spectra of **1** without any chemical additive is shown at the top. The bottom is the resulting spectra after addition of TBDSOTf as a chemical additive. Both spectra are recorded in  $\text{MeCN-}d_3$ .

which is able to undergo oxidative addition to generate the metal (IV) species  $\text{Cp}^*\text{M}(\text{NO} \rightarrow \text{Sc}(\text{OTf})_3)(\text{H})(\kappa^3\text{-}(\text{C}_6\text{H}_4)\text{PhPCH}_2\text{CH}_2\text{PPh}_2)$  ( $\text{M}$  = molybdenum, tungsten).<sup>3</sup> Here oxidative addition occurs across the C-H bond of a phenyl ring. If analogous reactivity is available to the **1** or to its derivatives (**Scheme 4.8**), this could be a useful chemical transformation to activate an olefinic C-H bond.



**Scheme 4.8.** Theoretical access to a C-H activation product via modulation of the nitrosyl ligand with a Lewis Acid. This theorized reaction sequence is inspired by work reported by Legzdins and co-workers for different tungsten and molybdenum nitrosyl complexes.<sup>3</sup>

#### 4.7 Methylation of $\text{WTp}(\text{NO})(\text{PMe}_3)(\eta^2\text{-1,2-cyclohexene})$ and $\text{WTp}(\text{NO})(\text{PMe}_3)(\eta^2\text{-1,2-1,4-cyclohexadiene})$

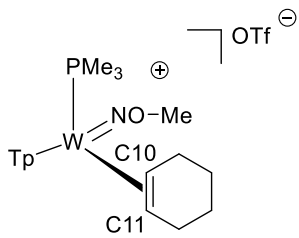
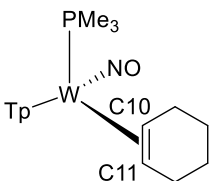
Treating **1** with methyl triflate in nitrile (MeCN, EtCN) or chlorinated solvents ( $\text{CHCl}_3$ , DCM) generates  $\text{WTp}(\text{NOMe})(\text{PMe}_3)(\eta^2\text{-1,2-cyclohexene})^+(\text{OTf}^-)$  (**8**). This complex has been effectively used to determine the location of deuterium integration as detailed in Chapter 3. Herein, the structural features and reactivity of **8** will be investigated. Additionally, the ability to methylate the nitrosyl ligand of other tungsten  $\pi$ -complexes will be examined.

Electrochemically, methylation of **1** to give **8** yields a complex with a significantly positive  $E_{p,a}$  at 1.2 V, implying that **8** is more stable to oxidation than in its neutral form **1** ( $E_{p,a} = 0.28$  V). In the FTIR spectra, loss of the nitrosyl stretching frequency is observed. This feature is consistent with previous literature reports that report alteration of the nitrosyl ligand.<sup>3, 17</sup> Tangentially we note that the phosphorous-tungsten coupling of the methylated tungsten-cyclohexene complex **8** is now  $J_{\text{WP}} = 268$  Hz, a significant decrease from the  $J_{\text{WP}} = 290$  Hz associated with the neutral cyclohexene complex **1** in MeCN.

Crystals suitable for SCXRD were grown from a chilled solution of DCM and diethyl ether.

Structurally the cyclohexene ligand on **8** shows minimal changes in the tungsten-carbon bond distances compared to **1** (Table 4.3). Additionally, no significant change is observed in the alkene bond distances associated with **1** and **8**. From the electrochemical data discussed *vide supra*, **8** is significantly more electron deficient than **1**, and therefore the tungsten metal should be a markedly weaker  $\pi$ -base. To account for the similarity in the bond lengths of the metal-coordinated alkene carbons **1** and **8**, we propose that enhanced  $\sigma$ -donation from the cyclohexene  $\pi$ -bond to the now electron deficient metal of **8** plays a more significant role in the metal-cyclohexene bonding interaction.

Compared to **1**, there is an increase in the bond order between the tungsten and the nitrogen of the nitrosyl ligand. Additionally, there is a reduction of the nitrosyl nitrogen-oxygen bond order. Accordingly, we believe this complex can be accurately represented by the resonance structure of **8** drawn in Table 4.5. This structure depicts a formal tungsten-nitrosyl double bond.

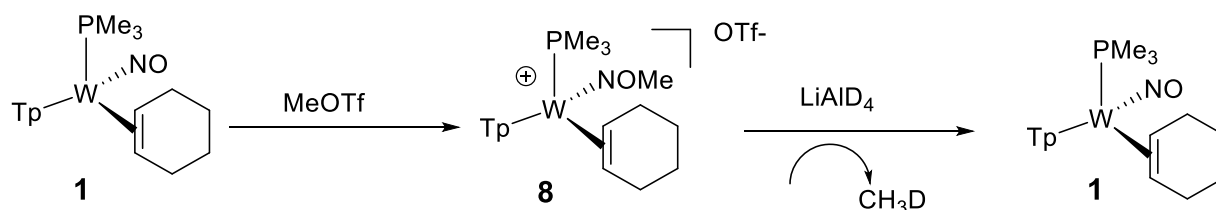
|  |        |              |  |        |              |
|--|--------|--------------|---|--------|--------------|
| atom 1   | atom 2 | Distance (Å) | atom 1  | atom 2 | Distance (Å) |
| W  | C10    | 2.23         | W   | C10    | 2.24         |
| W  | C11    | 2.21         | W   | C11    | 2.20         |
| W  | N(NO)  | 1.69         | W   | N(NO)  | 1.77         |
| N(NO)  | O      | 1.39         | N(NO)   | O      | 1.23         |
| C10  | C11    | 1.44         | C10   | C11    | 1.45         |
| W  | P      | 2.53         | W   | P      | 2.49         |

**Table 4.5.** Bond distances between **1** (right) and **8** (left) as determined from crystal structure determination. Negligible difference are observed in tungsten-cyclohexene bond distances. The shortened W-N bond distance of **8** and elongated N-O bond distance (compared to **1**) suggest that the resonance structure depicted for **8** is weighted significantly.

Treating an NMR solution of **8** in MeCN-*d*<sub>3</sub> with LiAlD<sub>4</sub> leads to vigorous bubbling and the re-generation of **1**. The evolved gas is most likely CH<sub>3</sub>D resulting from the cleavage of the methyl group by deuteride. This process is accompanied by the two electron reduction of the metal as depicted in **Scheme 4.9**.

Treating the cationic complex **8** with the strong acid HOTf in MeCN-*d*<sub>3</sub> does not result in any reactivity, but subjecting the neutral cyclohexene complex **1** to this strongly acidic solution results in the oxidative decomposition of the metal to uncharacterized paramagnetic material. This last data point serves as a case-in-point of the enhanced stability of **8** toward electrophiles compared to **1**.

MeOTf was used to routinely generate **8**, however use of trimethyl oxonium tetrafluoroborate (Meerwein's Reagent) could also be used to attain **8**. Both of these methylating agents (MeOTf and Meerwein's Reagent) were then used on the tungsten-benzene complex **4** and the tungsten-PhCF<sub>3</sub> complex **5** in the hope that methylation of the aromatic complexes would yield air stable metal complexes. Unfortunately, treatment with either methylation source led to decomplexation of the aromatic ligand and to the formation of multiple diamagnetic tungsten complexes. Analogous results were observed when WTp(NOMe)(PMe<sub>3</sub>)(η<sup>2</sup>-1,2-1,3-cyclohexadiene) was treated with either methylating agent.



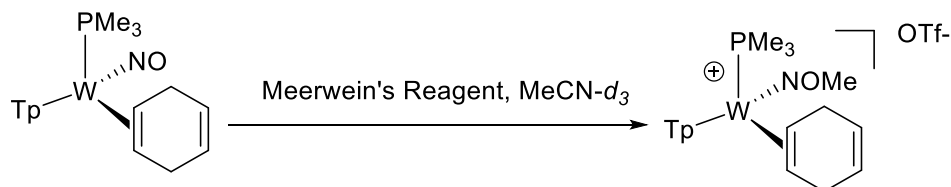
**Scheme 4.9.** Reactivity of **8** with a strong hydridic nucleophile. Cleavage of the methyl group is observed along with the regeneration of **1**.

In the case of WTp(NO)(PMe<sub>3</sub>)(η<sup>2</sup>-1,2-1,4-cyclohexadiene), exposure to MeOTf led to oxidative decomposition. Treatment of the tungsten-1,4-cyclohexadiene complex with Meerwein's reagent however gives a single diamagnetic complex that displays <sup>1</sup>H NMR spectral features consistent with the successful nitrosyl methylation of WTp(NOMe)(PMe<sub>3</sub>)(η<sup>2</sup>-1,2-1,4-cyclohexadiene) to yield WTp(NOMe)(PMe<sub>3</sub>)(η<sup>2</sup>-1,2-1,4-cyclohexadiene)<sup>+</sup> (OTf<sup>-</sup>) (**14**). Additionally, the complex WTp(NO)(PMe<sub>3</sub>)(η<sup>2</sup>-3-cyano-cyclohexene) **11**, a substituted cyclohexene, can be treated with MeOTf to generate the methylated nitrosyl adduct **15**.



Signals that support this reactivity include a purported methyl group resonating at ~4 ppm as well as significant downfield shift accompanying of all Tp and cyclohexene-ring protons. Analogous spectral features were observed in the  $^1\text{H}$  NMR spectra of **8** and are consistent with methylation of the nitrosyl ligand.

Although no synthetic value has been realized from these complexes as of yet, these complexes and the corresponding experiments with Lewis and Bronsted acids suggest that the nitrosyl ligand may be manipulated



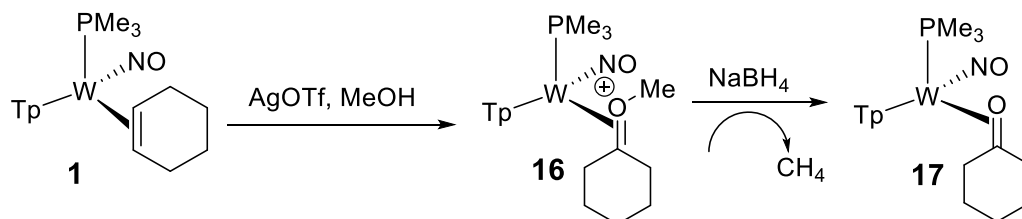
**Scheme 4.10.** Methylating the nitrosyl ligand for a tungsten-1,3-cyclohexadiene complex. Species is observed in situ. Attempts to isolate lead to various decomposition products.

with appropriate chemical reagents. This could ultimately promote reactivity of the tungsten metal center. For example, treating methylated-nitrosyl complexes with stronger electrophiles may enable modifications of the dihapto-coordinate ligand that would otherwise be pre-empted by oxidation of the metal by the electrophile.

#### 4.8 Functionalization of the Tungsten-Alkene Bond

The formation of the agostic tungsten-cyclohexyl complexes in our lab presents a potential avenue for further modification of the olefin  $\pi$ -ligand. We also pursued the ability for other electrophiles to be added to the alkene bond of **1**. Initial results using N-Bromo-succinimide (NBS) with methanol and silver triflate gave a single diamagnetic tungsten complex. Further investigation showed that NBS was not needed to engender this reaction. When **1** is treated with *only* silver triflate in methanol, the same diamagnetic complex forms in solution. This complex has ten associated proton resonances and a new methyl group. When MeOD- $d_4$  is utilized, the methyl group

associated with the resulting complex disappears but none of the ten proton resonances associated

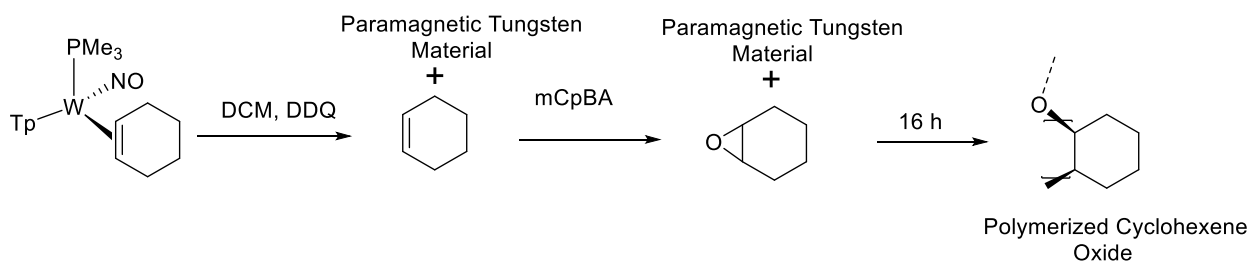


**Scheme 4.11.** The generation of a methyl cyclohexanium complex upon exposure to oxidant (AgOTf) and methanol source. The mechanism of this transformation is unknown. Demethylation occurs in the presence of a moderate deuteride source.

with the ring decrease in intensity.

Analysis by 2D NMR techniques analysis suggests that the new complex is the dihapto-coordinated ketone adduct  $\text{W Tp}(\text{NO})(\text{PMe}_3)(\eta^2\text{-CO-methylcyclohexanonium})$  **16** as detailed in **Scheme 4.11**. In support of this, when **16** is treated with  $\text{NaBH}_4$  the resulting product is identified as a single isomer of the neutral-cyclohexanone complex **17**. The identity of this complex was confirmed after allowing the tungsten-benzene complex **4** to stir in cyclohexanone to generate **17** via a ligand substitution reaction.

The yields for the transformation of **1** to **16** are low (10-20% mass recovery) and suggest that this is not a very efficient synthetic process. Additionally, the mechanism for this transformation is unknown. Even so, the potential to derivatize the alkene bond and potentially differentiate between the two alkene carbons suggests that metal-controlled alteration of the bound alkene bonds may be a viable synthetic route.



**Scheme 4.12.** Oxidation of **1** to yield free cyclohexene followed by the in situ epoxidation to generate cyclohexene oxide. Over time spectra features in the  $^1\text{H}$  and  $^{13}\text{C}$  NMR spectra consistent with the polymerization of cyclohexene oxide are observed. We propose that higher oxidation state complexes of tungsten could be responsible for this polymerization given previous reports detailing the ability of Lewis Acids to catalyze polymerization of cyclohexene oxide.

Subsequent investigation focused on the ability to functionalize the alkene bond with a wider scope of electrophiles. Experiments to epoxidize the alkene bond by exposing the tungsten-cyclohexene complex **1** to mCpBA in various solvents showed only oxidation of the metal. No formation of cyclohexene oxide (the desired product) was observed.

Efforts were then extended to metal oxidation with the chemical oxidant DDQ. The solution was treated with excess meta-chloroperoxybenzoic acid (mCpBA), a common epoxidizing reagent. Even with metal decomposition in solution, the desired cyclohexene product **18** could be formed in situ. Over several hours however, proton resonances associated with the cyclohexene oxide monomer decrease and signals consistent with the polymerization of cyclohexene oxide develop. Previous reports have documented the

ability of Lewis acids to promote polymerization of cyclohexene oxide.<sup>19-20</sup> Here it is possible that higher oxidation state tungsten complexes may serve as Lewis acids to catalyze the polymerization process. Efforts to analyze isotopologues of cyclohexene oxide by MRR analysis (through the synthesis of isotopologues of **1** and the subsequent treatment with DDQ and mCpBA) were unsuccessful.

Treatment of complex **1** with Br<sub>2(l)</sub> in CDCl<sub>3</sub> leads to the development of 1,2-trans-dibromocyclohexane (**19**) and decomposition of the metal to paramagnetic material. Interestingly, if the methylated cyclohexene complex **8** is treated

with Br<sub>2(l)</sub> in CDCl<sub>3</sub> the generation of **19** Br<sub>2(l)</sub> is observed with the concomitant formation of

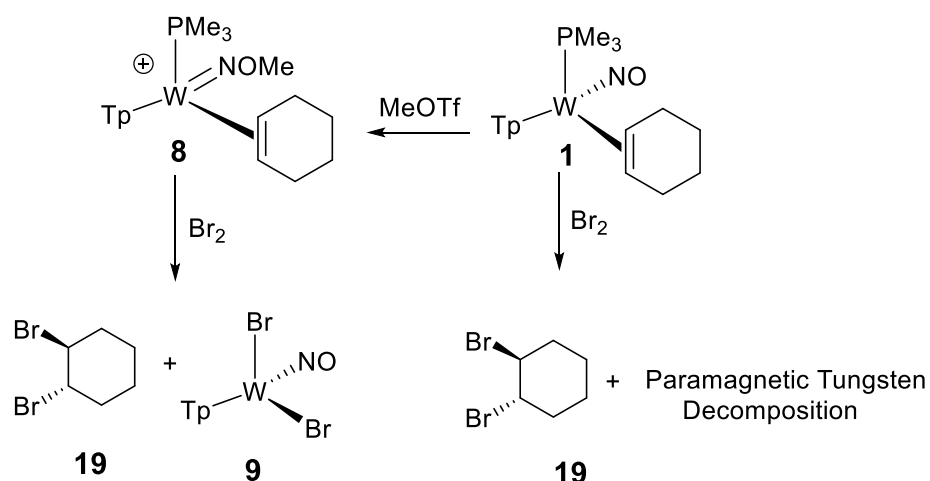
WTp(NO)(Br)<sub>2</sub> (**20**). While **20** is a precursor to complex **4**, a more practical synthetic target for

tungsten recyclability is the immediate synthon to **4**,

WTp(NO)(PMe<sub>3</sub>)(Br). This precursor can be readily reduced in the presence of an arene to generate various tungsten-arene adducts. Efforts to generating a dearomatization synthon in the form of WTp(NO)(PMe<sub>3</sub>)(X) (where X is a labile ligand upon reduction to the tungsten (0) oxidation state) are discussed *vide infra*.

#### 4.9 Efforts Toward Tungsten Recyclability

Key studies by Dr. Jeffrey Myers showed that oxidation of MoTp(NO)(DMAP)( $\pi$ -ligand) with iodine generates MoTp(NO)(DMAP)(I), the second row congener to WTp(NO)(PMe<sub>3</sub>)(Br).<sup>7</sup> Treating the tungsten-anisole complex WTp(NO)(PMe<sub>3</sub>)( $\eta^2$ -anisole) with half an equivalent of I<sub>2(s)</sub> at reduced temperatures (-30 °C) produced multiple electrochemically active species. Previous investigations have shown difficulty in recycling of the tungsten metal. The instability of the resulting tungsten (I) leads to over-oxidation to

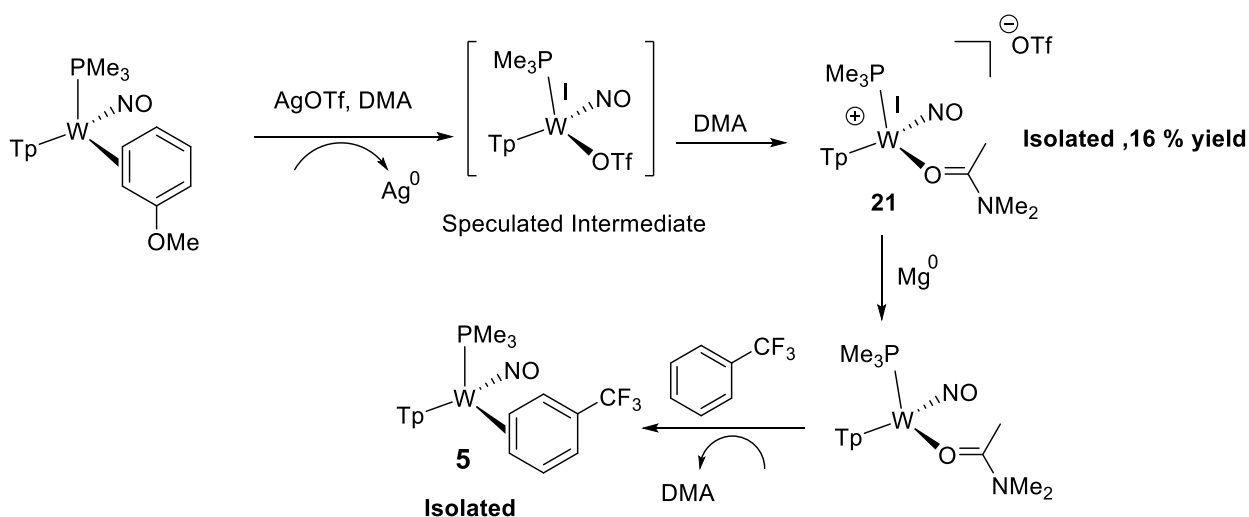


**Scheme 4.13.** Bromination of cyclohexene complexes **1** and **8** to generate trans-1,2-dibromocyclohexane adducts. Partial recovery of a tungsten (II) species is observed from **8** but no diamagnetic tungsten species is observed upon the bromination of **1**. Differences in reactivity could be attributed by the more positive oxidation potential associated with **8** (1.2 V) compared to **1** (0.28 V).

uncharacterized higher valence tungsten complexes.<sup>5</sup> Therefore, conditions that would allow an incoming ligand to stabilize the tungsten (I) oxidation state could help realize a recyclable tungsten dearomatization scaffold.

Initial attempts to oxidize the tungsten-anisole complex with a moderate, one electron oxidizing agent, AgOTf, were pursued in THF. We hoped that the putative THF complex  $\text{WTp}(\text{NO})(\text{PMe}_3)(\kappa^1\text{-O-THF})$  would be stable enough in the tungsten (I) form to be synthetically useful. Experiments at room temperature and at reduced temperatures (-30 °C) revealed similar results, where upon addition of AgOTf to the solution of  $\text{WTp}(\text{NO})(\text{PMe}_3)(\eta^2\text{-2,3-anisole})$  in THF, the originally homogeneous yellow reaction mixture first turns an emerald green before the solution turns to a deep heterogeneous black color. Tangentially, we note that many tungsten (I) halide species are green, and therefore the initial color change may be associated with the in situ formation of a highly unstable  $\text{WTp}(\text{NO})(\text{PMe}_3)(\kappa^1\text{-O-THF})^+ (\text{OTf}^-)$  complex followed by rapid decomposition.

Work by Dr. Steven Dakermanji has showed that the complexes  $\text{MoTp}(\text{NO})(\text{DMAP})(\kappa^1\text{-O-DMA})^+ (\text{OTf}^-)$ , are stable enough to be isolated and can be reduced with magnesium to generate certain  $\text{MoTp}(\text{NO})(\text{DMAP})(\eta^2\text{-arene})$  complexes.<sup>2</sup> A key feature in accessing this chemistry is the ability of the DMA ligand to stabilize molybdenum (I) and (0) oxidation states. Following this logic, when  $\text{WTp}(\text{NO})(\text{PMe}_3)(\eta^2\text{-2,3-anisole})$  is dissolved in neat DMA and treated with AgOTf at reduced temperatures (-30 °C), a CV of the reaction mixture shows a major species that is consistent with the formation of the species  $\text{WTp}(\text{NO})(\text{PMe}_3)(\kappa^1\text{-O-DMA})^+ (\text{OTf}^-)$  (**21**) with an  $E_{1/2} = -1.1$  V and  $E_{p,a} = 0.3$  V. Other electrochemically active species are observed in this reaction mixture though the identity of these complexes was not pursued.



**Mass Recovery < 10%**

**Scheme 4.14.** A low yielding proof of concept that show the ability to partially regenerate the {WTP(NO)(PMe<sub>3</sub>)} fragment and reduce a tungsten (I) precursor to the tungsten trifluorotoluene complex **5**.

Isolation of **21** can be achieved by precipitation into Et<sub>2</sub>O. A cyclic voltammogram of the isolated product shows only a single  $E_{1/2}$  and  $E_{p,a}$  that we previously speculated correspond to the tungsten-DMA complex **21**. When the isolated green solid of **21** is dried and allowed to stir in an excess of neat  $\alpha,\alpha,\alpha$ -trifluorotoluene and cleaned magnesium, over 16 hours a cyclic voltammogram of this species reveals an  $E_{p,a} = 0.05$  V, an oxidation potential consistent with the formation of the tungsten- $\alpha,\alpha,\alpha$ -trifluorotoluene complex **5**.<sup>6</sup> An aliquot of the reaction mixture was analyzed by <sup>1</sup>H NMR spectroscopy and confirms the successful synthesis of **5**. By cyclic voltammetry however, the conversion of **21** to **5** does not proceed using magnesium as a reducing agent over the course of several days.

Although the mass recovery for this process was low and the resulting <sup>1</sup>H NMR spectra shows obvious signs of impurities, this experiment demonstrates the ability of the DMA to stabilize the tungsten (I) oxidation state long enough for reduction a less pyrophoric metal (magnesium compared to sodium) to access a reduced tungsten complex capable of coordinating aromatic molecules. Optimization of either process, tungsten recyclability or reduction with magnesium, would enhance the practicality of the tungsten dearomatization agent. Gratitude is given to Dr. Steven Dakermanji for the initial investigation of magnesium-enabled reductions. Investigation of this process has been continued by Andrew Chung under the guidance of Spenser Simpson.

#### 4.10 Conclusion

The tungsten-cyclohexene complex **1** and its derivatives are robust  $\pi$ -acceptor ligands. These  $\eta^2$ -tungsten-olefin complexes are more resistant to reactivity engendered by elevated temperatures, oxidative conditions and strong electrophiles compared to dihapto-coordinated aromatic  $\pi$ -ligands. These complexes have shown that the nitrosyl ligand itself can play a role in effectively modulating the electronic environment around the tungsten metal center. While the controlled reactivity of the metal-bound alkene carbons remains a formidable synthetic challenge, the ability to access metal-mediated transformations would enable a wider array of metal-promoted complexity. This could enable access to functionalized cyclohexanes.

Oxidative decomposition of the metal of tungsten-cyclohexene complexes has been achieved with moderate Bronsted acids. This methodology could prove fruitful for the liberation of organic ligands with functionalities sensitive to strong oxidants. Additionally, treatment with  $\text{Br}_{2(l)}$  leads to the successful oxidation of the cyclohexene ligand and the development of two new stereocenters in the form of 1,2-trans-dibromocyclohexane (**19**) and the synthesis of  $\text{WTP}(\text{NO})(\text{Br})_2$  (**20**), a precursor to tungsten-enabled dearomatization. Within the context of recyclability, oxidation to a tungsten (I) species has been achieved with partial success with the moderate oxidant  $\text{AgOTf}$  in DMA. The resulting complex is a tungsten (I)-amide complex **21** where the DMA ligand is speculated to be bound  $\kappa^1$  through the oxygen to the tungsten center. Reduction of this complex with magnesium in the presence of arene successfully generates a metal-arene complex, albeit in low yields (< 10 %). Further investigation into ligands able to stabilize the tungsten adduct at the tungsten (I) oxidation states, which would still be labile upon reduction to a tungsten (0) species could enable the recycling of the tungsten scaffold. This feature has been unlocked for the dearomatization agents of osmium, rhenium and molybdenum.

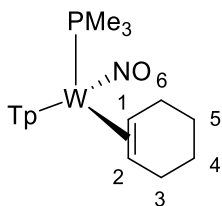
Efficient recyclability of the molybdenum dearomatization scaffold is one facet of molybdenum-based dearomatization that provides an advantage over its tungsten-analog. Development of molybdenum-enabled chemistry has been historically limited by the inability of the molybdenum fragment

{MoTp(NO)(L)} (L=sigma donor ligand) to form thermally stable  $\eta^2$ -complexes with benzene or its derivatives. An investigation into the aromatic ligand scope amenable to molybdenum-promoted dearomatization is examined in Chapter 5.

## Experimental Section

General Methods. NMR spectra were obtained on 500, 600, or 800 MHz spectrometers. Chemical shifts are referenced to tetramethylsilane (TMS) utilizing residual  $^1\text{H}$  or  $^{13}\text{C}$  signals of the deuterated solvents as internal standards. Phosphorus NMR signals are referenced to 85%  $\text{H}_3\text{PO}_4$  ( $\delta$  0.00) using a triphenyl phosphate external standard ( $\delta$  -16.58). Chemical shifts are reported in ppm, and coupling constants ( $J$ ) are reported in hertz (Hz). Infrared spectra (IR) were recorded on a spectrometer as a glaze on a diamond anvil attenuated total reflectance assembly, with peaks reported in  $\text{cm}^{-1}$ . Electrochemical experiments were performed under a nitrogen atmosphere. Most cyclic voltammetric data were recorded at ambient temperature at 100 mV/s, unless otherwise noted, with a standard three-electrode cell from +1.8 to -1.8 V with a platinum working electrode, N,N-dimethylacetamide or acetonitrile solvent, and tetrabutylammonium hexafluorophosphate electrolyte (~1.0 M). All potentials are reported versus the normal hydrogen electrode (NHE) using cobaltocenium hexafluorophosphate ( $E_{1/2} = -0.78, -1.75$  V) or ferrocene ( $E_{1/2} = 0.55$  V) as an internal standard. Peak separation of all reversible couples was less than 100 mV. All synthetic reactions were performed in a glovebox under a dry nitrogen atmosphere unless otherwise noted. All solvents were purged with nitrogen prior to use. Deuterated solvents were used as received from Cambridge isotopes. NMR assignments of all compounds were determined using 2D NMR methods including nuclear Overhauser enhancement spectroscopy, correlation spectroscopy, heteronuclear multiple bond correlation, and heteronuclear single quantum coherence. When possible, pyrazole (Tp) protons of the (trispyrazolyl)borate (Tp) ligand were uniquely assigned (e.g., “Tp3B”) using two-dimensional NMR data (see Figure S1). If unambiguous assignments were not possible, Tp protons were labeled as “Tp3/5 or Tp4”. All  $J$  values for Tp protons are 2 ( $\pm 0.4$ ) Hz. BH peaks (around 4–5 ppm) in the  $^1\text{H}$  NMR spectra are not assigned due to their quadrupole broadening; however, the confirmation of the BH group is provided by IR data (around 2500  $\text{cm}^{-1}$ ). Compound **1** was prepared according to the previous literature procedure.<sup>7</sup> High-resolution electrospray ionization mass spectrometry (ESI-MS) analyses were taken on an Agilent 6545B quadrupole time-of-flight (TOF) liquid chromatography/mass spectrometry (LC/MS) using purine and hexakis(1H,1H,3H-tetrafluoropropoxy)-phosphazine as internal standards. Samples were dissolved in MeCN and eluted with a MeCN/ $\text{H}_2\text{O}$  solution containing 0.1% formic acid.

### Synthesis of $\text{WTp}(\text{NO})(\text{PMe}_3)(\eta^2\text{-1,2-cyclohexene})$ (**1**)



A 4-dram vial was charged with 1 mL of DME, complex **1** (0.200 g, 0.344 mmol) and cyclohexene (2.00g, 24.3 mmol) and this heterogenous yellow reaction mixture was allowed to stir. After 27 h the now homogenous purple reaction mixture was added to a 250 mL filter flask and the solvent was removed in vacuo. The resulting pink solid was re-dissolved in DCM (2 mL) and slowly added to a solution of stirring pentane (30 mL) that had been chilled to  $-30^\circ\text{C}$ . Upon addition a light pink solid precipitated out of solution. This light pink solid was collected on a 30 mL fine porosity fritted disc and subsequently washed with chilled pentane (3 x 5 mL). The collected product was then desiccated for 2 h to yield a fine light pink powder (0.083 g, 41%).

### Alternative Synthesis of $\text{WTp}(\text{NO})(\text{PMe}_3)(\eta^2\text{-cyclohexene})$ (**1**)



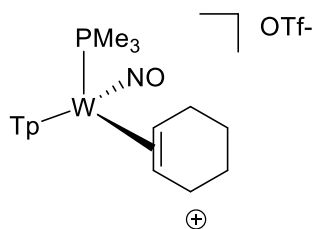
To a 4-dram vial **6** (0.107 g, 0.136 mmol) was dissolved in 1 mL of MeOH and chilled to  $-30^{\circ}\text{C}$ . To this was added  $\text{NaBH}_4$  that had been dissolved and chilled in a  $-30^{\circ}\text{C}$  MeOH solution. The solution of **6** was then added to the  $\text{NaBH}_4/\text{MeOH}$  solution and the resulting reaction mixture was allowed to sit at  $-30^{\circ}\text{C}$  for 16 h. The reaction mixture was then eluted through a silica column on a fine 15 mL fritted disc and a light yellow band was eluted with ether. The solvent was then removed in vacuo and picked up in DCM ( $\sim 1$  mL). This was then added to a solution of sitting hexanes (15 mL) and allowed to sit at  $-30^{\circ}\text{C}$  for 2 h during which a light yellow solid had precipitated from solution. This solid was then isolated on a fine 15 mL fritted disc, washed with hexanes (2 x 5 mL) to yield an off-white solid (0.058 g, 67%).

CV (MeCN)  $E_{p,a} = +0.28$  V (NHE). IR:  $\nu(\text{BH}) = 2482$   $\text{cm}^{-1}$ ,  $\nu(\text{NO}) = 1554$   $\text{cm}^{-1}$ .  $^1\text{H-NMR}$  ( $\text{CDCl}_3$ ,  $\delta$ ,  $25^{\circ}\text{C}$ ): 8.28 (1H, d, Pz3A), 8.08 (1H, d, Pz3B), 7.69 (1H, d, Pz5B), 7.64 (1H, d, Pz5C), 7.60 (1H, d, Pz5A), 7.24 (1H, d, Pz3C), 6.28 (1H, t, PzB), 6.20 (1H, t, Pz4A), 6.13 (1H, t, Pz4C), 3.00 (1H, m, H6*exo*) 2.92 (2H, overlap, m, H4-*endo/exo*), 2.71 (1H, m, H1), 2.64 (1H, m, H6-*endo*), 1.75 (2H, overlap, m, H6-*endo/exo*), 1.46 (2H, overlap, m, H5-*endo/exo*), 1.38 (1H, m, H2), 1.21 (9H, d,  $J_{\text{PH}} = 8.1$ ,  $\text{PMe}_3$ ).  $^{13}\text{C-NMR}$  ( $\text{CDCl}_3$ ,  $\delta$ ,  $25^{\circ}\text{C}$ ). 143.4 (Pz3B), 142.9 (Pz3A), 140.1 (Pz3C), 136.2 (Pz5), 135.6 (Pz5), 135.4 (Pz5), 106.3 (Pz4B), 105.6 (Pz4), 105.5 (Pz4), 53.8 (C2), 53.6 (C1, d,  $J_{\text{PC}} = 10.6$ ), 30.0 (C6, d,  $J_{\text{PC}} = 4.2$ ), 29.4 (C3), 24.9 (C4/5), 24.8 (C4/5), 14.0 ( $\text{PMe}_3$ , d,  $J_{\text{PC}} = 27.5$ ).  $^{31}\text{P-NMR}$  ( $\text{CDCl}_3$ ,  $\delta$ ,  $25^{\circ}\text{C}$ ): -9.1 ( $J_{\text{WP}} = 291$ ,  $\text{PMe}_3$ ). Anal. Calcd for  $20\text{C}_{18}\text{H}_{29}\text{BN}_7\text{OPW}\cdot\text{DCM}$ : C, 36.79; H, 4.98; N, 16.76. Found: C, 37.35; H, 4.58; N, 16.69.

Characterization in  $\text{MeCN-}d_3$

$^1\text{H-NMR}$  ( $\text{MeCN-}d_3$ ,  $\delta$ ,  $25^{\circ}\text{C}$ ): 8.21 (1H, d, Pz3A), 8.03 (1H, d, Pz3B), 7.85 (1H, d, Pz5B), 7.78 (1H, d, Pz5C), 7.75 (1H, d, Pz5A), 7.35 (1H, d, Pz3C), 6.36 (1H, t, Pz4B), 6.27 (1H, t, Pz4A), 6.21 (1H, t, Pz4C), 3.04 (1H, m, H6*exo*) 2.93 (1H, m, H3-*exo*), 2.86 (1H, m, H3-*endo*), 2.72 (1H, m, H1), 2.63 (1H, m, H6-*endo*), 1.69 (1H, m, H4-*endo*), 1.66 (1H, m, H5-*endo*). 1.42 (2H, overlap, m, H4/H5-*exo*), 1.16 (1H, m, H2), 1.10 (9H, d,  $J_{\text{PH}} = 8.2$ ,  $\text{PMe}_3$ ).  $^{13}\text{C-NMR}$  ( $\text{MeCN-}d_3$ ,  $\delta$ ,  $25^{\circ}\text{C}$ ). 144.2 (Pz3B), 143.3 (Pz3A), 141.7 (Pz3C), 137.6 (Pz5), 136.9 (2C, overlapping Pz5), 107.4 (Pz4B), 106.9 (Pz4A), 106.6 (Pz4C), 53.5 (2C, overlapping C1 and C2), 30.7 (C6), 30.2 (C3), 25.6 (2C, overlapping C4/C5), 25.4 (2C, overlapping C4/C5), 13.8 ( $\text{PMe}_3$ , d,  $J_{\text{PC}} = 27.5$ ).

### Synthesis of $\text{WTp}(\text{NO})(\text{PMe}_3)(\text{C}_6\text{H}_9)^+(\text{OTf}^-)$ (**2**)



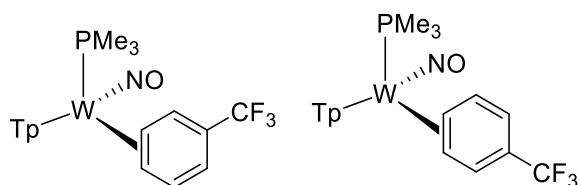
$\text{WTp}(\text{NO})(\text{PMe}_3)(\eta^2\text{-}1,3\text{-cyclohexadiene})$  (0.365 g, 0.624 mmol) was dissolved in DME (3 mL) and cooled to  $-30^{\circ}\text{C}$  to generate a homogeneous yellow mixture in a 4-dram vial. Separately HOTf (0.215 g, 1.42 mmol) was dissolved in 2 mL of DME and also allowed to cool to  $-30^{\circ}\text{C}$  over a course of 15 min in a separate 4-dram vial. The acidic DME solution was then added dropwise to the standing solution of  $\text{WTp}(\text{NO})(\text{PMe}_3)(\eta^2\text{-}1,3\text{-cyclohexadiene})$ . This solution was allowed to stand at room temperature for 1 min and then was added dropwise to a solution of stirring ether (250 mL). Upon addition a fine, light yellow solid precipitated from solution. The solution was allowed to triturate for 10 min before the reaction mixture was filtered through a fine 15 mL porosity fritted disc to yield a fine, yellow powder. This solid was then washed

with ether (3 x 10 mL) and allowed to desiccate for six hours under dynamic vacuum before a mass was taken (0.365 g, 79 %). Characterization has been reported previously.<sup>8</sup>

### Synthesis of $\text{WTp}(\text{NO})(\text{PMe}_3)(\eta^2\text{-1,2-cyclohexene-3-exo-d}_1)$ (**3**)

A 4-dram vial was charged with **13** (0.114 g, 0.155 mmol) and dissolved in MeOH (3 mL) to generate a homogeneous orange solution. This solution was chilled to  $-30^\circ\text{C}$  over a course of 15 min and to this solution was added  $\text{NaBD}_4$  (0.040 g, 1.06 mmol). Upon addition to the solution some bubbling occurs. This solution was allowed to stand at  $-30^\circ\text{C}$  for one hour and turns from a homogeneous orange to a homogeneous yellow color. The solution was then allowed to stand at room temperature for 10 min before being diluted with ether (10 mL). Separately a 30 mL medium porosity frit was filled with ~ 3 cm of silica and set in ether. The reaction mixture was then loaded onto this silica column and was filtered through by elution with ~ 100 mL of ether total to elute a light yellow band. The solvent was then removed in vacuo and the product was re-dissolved in DCM (2 mL) and added to a 4-dram vial of standing pentane (15 mL). This solution was allowed to stand at  $-30^\circ\text{C}$  for 16 h before the solvent was again stripped to dryness to yield a fine off-white solid (0.061 g, 65 %).

### Synthesis of $\text{WTp}(\text{NO})(\text{PMe}_3)(\eta^2\text{-3,4-}\alpha,\alpha,\alpha\text{-trifluorotoluene})$ (**5**)



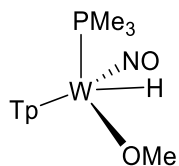
An optimized reduction of **5** has been reported previously.<sup>6</sup> The following synthesis shows the potential of recycling the tungsten metal.

A 4-dram vial was charged with **21** (0.096 g, 0.134 mmol) along with  $\alpha,\alpha,\alpha$ -trifluorotoluene (1 mL, 8.14 mmol) and to this was added magnesium (0.500 g, 20.5 mmol) that had been activated via previous exposure to iodine. The heterogeneous green reaction mixture was allowed to stir and after 24 h a cyclic voltammogram was taken of an aliquot of this solution and consistent with the formation of **5** was observed in the resulting cyclic voltammogram. An aliquot of this solution (~ 1/2 mL) was added to 3 mL of pentane and upon addition a brown-tan solid precipitates from solution. The organic layer was decanted off and the resulting solid was subjected to analysis by  $^1\text{H}$  NMR in acetone- $d_6$ . Signs consistent with the formation of **5** (previously reported) were observed indicating the successful recycling of the tungsten metal as well as reduction with magnesium. Given the prevalence of **21** observed in the cyclic voltammogram, the bulk reaction mixture was allowed to continue to stir, however no further progression in converting **21** to **5** was observed over a period of 4 days and a mass recovery was not attempted due to obvious impurities in the  $^1\text{H}$  NMR and the small scale that the reaction was performed on.

### General Procedure for the Synthesis of **9**, **10** and **11**:

A solution of the substituted cyclohexene was dissolved in  $\text{MeCN-}d_3$  (~ 1/2 mL) in an NMR tube and the solution was frozen in  $\text{N}_2(l)$ . The NMR tube solution was removed and to this thawing solution added DPhAT in excess. Over a period of 15 min the substituted cyclohexene ligand was released (dimethyl 2-((1R,4S)-4-methylcyclohex-2-en-1-yl)malonate (**9**)), dimethyl 2-((1R,4S)-4-methylcyclohex-2-en-1-yl)malonate (**10**), (R)-cyclohex-2-ene-1-carbonitrile (**11**). Characterization matches that of previously reported compounds.<sup>2</sup>

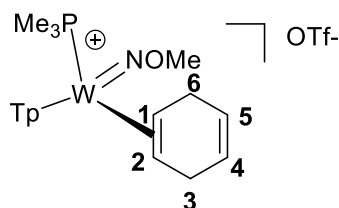
### Synthesis of WTp(NO)(OMe)(H) (13)



A solution of WTp(NO)(PMe<sub>3</sub>)(anisole) (NMR scale, approximately 20 mgs) was dissolved in benzene-*d*<sub>6</sub> (~ ½ mL) in an NMR tube and the solution was frozen in N<sub>2</sub>(l). The NMR tube solution was removed and to this thawing solution added MeOH (5 drops) in excess. The solution was then analyzed by <sup>1</sup>H NMR spectroscopy.

<sup>1</sup>H NMR (benzene-*d*<sub>6</sub>, δ, 25 °C): 11.24 (1H, m, *J*<sub>PH</sub> = 129.2, *J*<sub>WP</sub> = 11.2, W-H), 8.29 (1H, d, Tp3/5), 7.92 (1H, d, Tp3/5), 7.46 (1H, d, Tp3/5), 7.35 (1H, d, Tp3/5), 7.23 (1H, d, Tp3/5), 7.1 (1H, d, Tp3/5), 5.98 (1H, t, Tp4), 5.84 (1H, t, Tp4), 5.79 (1H, t, Tp4), 4.03 (3H, d, *J*<sub>PH</sub> = 1.7, -OMe), 1.44 (9H, d, *J*<sub>PH</sub> = 9.5, PMe<sub>3</sub>).

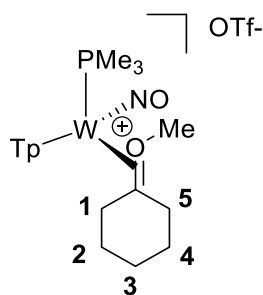
### Synthesis of WTp(NO)(PMe<sub>3</sub>)(η<sup>2</sup>-1,2-,1,4-cyclohexadiene)<sup>+</sup>(OTf<sup>-</sup>) (14)



A solution of the substituted cyclohexene was dissolved in MeCN-*d*<sub>3</sub> (~ ½ mL) in an NMR tube and the solution was frozen in N<sub>2</sub>(l). The NMR tube solution was removed and to this thawing solution added MeOTf (3 drops) in excess and the sample was analyzed by NMR spectroscopy.

<sup>1</sup>H NMR (MeCN-*d*<sub>3</sub>, δ, 25 °C): 8.47 (1H, d, Tp3/5), 8.03 (1H, d, Tp3/5), 8.00 (1H, d, Tp3/5), 7.94 (1H, d, Tp3/5), 7.93 (1H, d, Tp3/5), 7.55 (1H, d, Tp3/5), 6.53 (1H, t, Tp4), 6.48 (1H, t, Tp4), 6.37 (1H, t, Tp4), 5.80 (1H, m, H4/H5), 5.73 (1H, m, H4/H5), 4.07 (3H, s, NOME), 3.36 (1H, m, H), 3.68 (1H, m, H), 2.29 (1H, m, H), 1.30 (1H, m, H2), 1.25 (9H, d, *J*<sub>PH</sub> = 9.4, PMe<sub>3</sub>). <sup>31</sup>P NMR (CDCl<sub>3</sub>, δ, 25 °C): -9.6 (*J*<sub>WP</sub> = 268).

### Synthesis of WTp(NO)(PMe<sub>3</sub>)(η<sup>2</sup>-COMe-cyclohexanone)<sup>+</sup>(OTf<sup>-</sup>) (16)

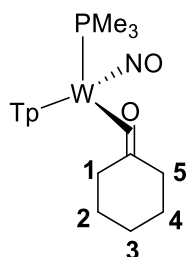


A 4-dram vial was charged with **1** (0.072 g, 0.123 mmol) followed by MeOH (0.200 g, 6.24 mmol) and to this reaction mixture added N-bromo-succinimide (0.040 g, 0.225 mmol) followed by AgOTf (0.040 g, 0.156 mmol). To this solution was added **1** and the reaction mixture was allowed to sit at room temperature for 10

min. An aliquot of the homogeneous, dark red layer was taken and added to diethyl ether (10 mL) and allowed to sit at -30 °C for 4 h. Over time a red solid develops at the bottom of the flask and this solid was dried with N<sub>2</sub>(g) before being allowed to dry in a desiccator overnight before a mass was taken of the resulting solid (mass recovery 0.048 g). Of the mass, approximately 1/4<sup>th</sup> (by mol, determined by <sup>1</sup>H NMR) of the isolated complex was the species WTp(NO)(PMe<sub>3</sub>)(C<sub>6</sub>H<sub>9</sub>)<sup>+</sup> (OTf<sup>-</sup>) (**2**). It is unknown if the formation of WTp(NO)(PMe<sub>3</sub>)(C<sub>6</sub>H<sub>9</sub>)<sup>+</sup> (OTf<sup>-</sup>) from **1** is a productive step in the generation of **16** or a side reaction unrelated to the formation of **16**.

<sup>1</sup>H NMR (CDCl<sub>3</sub>, δ, 25 °C): 8.15 (1H, d, Tp3B), 8.07 (1H, d, Tp3A), 7.88 (1H, d, Tp3C), 7.87 (1H, d, Tp5C), 7.82 (1H, d, Tp5B), 7.72 (1H, d, Tp5A), 6.49 (1H, t, Tp4C), 6.42 (1H, t, Tp4B), 6.33 (1H, t, Tp4A), 4.76 (3H, s, -OMe), 3.15 (1H, d, *J* = 15.5, H6-exo), 2.95 (1H, m, H6-endo), 2.09 (1H, d, *J* = 14.5, H5), 1.97 (1H, d, *J* = 13.3, H4), 1.84 (1H, m, H5'), 1.68 (1H, d, *J* = 13.0, H3), 1.49 (1H, m, H3'), 1.36 (9H, d, *J*<sub>PH</sub> = 9.2, PMe<sub>3</sub>), 1.29 (1H, m, H4'), 1.09 (1H, d, *J* = 15.5, H2-exo), 0.95 (1H, td, *J* = 4.1, 15.5, H2-endo). <sup>13</sup>C NMR (MeCN-*d*<sub>3</sub>, δ, 25 °C): 143.8 (Tp3/5), 143.7 (Tp3/5), 141.7 (Tp3/5), 138.0 (Tp3/5), 137.7 (Tp3/5), 137.6 (Tp3/5), 108.2 (Tp4), 108.1 (Tp4), 107.1 (Tp4), 104.9 (C=O, d, *J*<sub>PC</sub> = 5.7), 68.8 (-OMe), 34.3 (C2), 32.6 (C6), 28.0 (C5), 27.8 (C3), 25.2(C4), 12.8 (PMe<sub>3</sub>, d, *J*<sub>PC</sub> = 30.0). <sup>31</sup>P NMR (CDCl<sub>3</sub>, δ, 25 °C): -9.86 (*J*<sub>WP</sub> = 265).

### Selective Synthesis of WTp(NO)(PMe<sub>3</sub>)(η<sup>2</sup>-CO-cyclohexanone) (**17**)



#### Synthesis A

Added NaBD<sub>4</sub> to a -30 °C chilled solution of MeCN-*d*<sub>3</sub> (~ ¼ mL) and to this added a solution of **1** (NMR scale, approximately 20 mgs) in MeCN-*d*<sub>3</sub> (~ ¼ mL). Upon addition vigorous bubbling occurs and after the bubbling had succeeded the reaction mixture was filtered through a pipette silica plug and the resulting eluent was analyzed to confirm the identity of **17**.

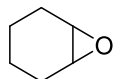
#### Synthesis B

To a 4-dram filled with WTp(NO)(PMe<sub>3</sub>)(anisole) (0.200 g, 0.327 mmol) added cyclohexanone (1 mL, 9.66 mmol) along with cobaltocenium hexafluorophosphate (III) (0.006 g, 0.017 mmol) and let the reaction mixture stir for 30 min before adding DME (1 mL). The heterogeneous yellow reaction mixture was allowed to stir over 20 h and the next day the reaction mixture was added to 20 mL of stirring hexanes. Upon addition a light pink solid precipitates from solution and this solid was isolated on a fine 15 mL porosity fritted disc and washed with hexanes (3 x 5 mL) and allowed to desiccate under dynamic vacuum for 2 h. A mass was taken of the isolated light pink solid (0.142 g, 72.1% yield). Characterization by <sup>1</sup>H NMR spectroscopy confirms the identity of the complex **17** generated in **Synthesis A**. Spectral features consistent with a second isomer of a dihapto-bound cyclohexanone ligand were observed as the major species (10:1 to **17**) but complete characterization of this second complex was not pursued.

<sup>1</sup>H NMR (MeCN-*d*<sub>3</sub>, δ, 25 °C): 8.11 (1H, d, Tp3B), 8.09 (1H, d, Tp5B), 7.77 (1H, d, Tp5C), 7.75 (1H, d, Tp5A), 7.73 (1H, d, Tp3C), 7.87 (1H, d, Tp3C), 6.35 (1H, t, Tp4B), 6.29 (1H, t, Tp4), 6.20 (1H, t, Tp4C), 2.37 (1H, td, *J* = 4.0, 13.1, H6-endo), 1.88 (1H, m, H5), 1.82 (1H, buried m, H6-anti), 1.80 (1H, buried m, H4), 1.70

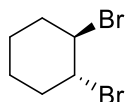
(1H, m, H5'), 1.57 (1H, m, H3), 1.51 (1H, m, H3'), 1.32 (1H, m, H4'), 1.30 (9H, d,  $J_{PH} = 9.3$ ,  $PMe_3$ ) 1.24 (1H, m, H2-exo), 0.35 (1H, d,  $J = 13.0$ , H2-endo).  $^{13}C$  NMR (MeCN- $d_3$ ,  $\delta$ , 25 °C): 144.9 (Tp3/5), 144.4 (Tp3/5), 143.7 (Tp3/5), 137.1 (Tp3/5), 137.0 (Tp3/5), 136.6 (Tp3/5), 107.3 (Tp4), 107.0 (Tp4), 106.2 (Tp4), 41.9 (C6), 36.4 (C2), 31.6 (C5), 30.9 (C3), 27.7 (C4), 11.4 ( $PMe_3$ , d,  $J_{PC} = 28.4$ ).  $^{31}P$  NMR (MeCN- $d_3$ ,  $\delta$ , 25 °C): -10.4 ( $J_{WP} = 293$ ).

### Synthesis of 7-oxabicyclo[4.1.0]heptane (**18**)



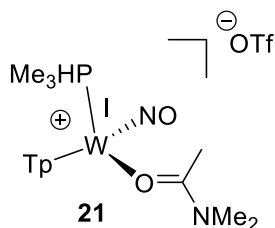
To an NMR tube added **1** (0.041 g, 0.070 mmol) along with DCM- $d_2$  (1.07 g) and added this solution to a 4-dram vial containing solid DDQ (0.045 g, 0.198 mmol). Upon addition the reaction mixture turns to a vivid red color. The vial was shaken by hand (< 1 min) and an aliquot was taken of the organic layer that had developed at the top of the vial and transferred to an NMR tube before taking a  $^1H$  NMR spectra to confirm the liberation of the cyclohexene ligand. This reaction mixture was then added to mCpBA (0.100 g, 0.579 mmol) and a  $^1H$  NMR spectra of that product showed the development of **18** which has been previously reported. Isolation of **18** was not pursued.

### Synthesis of (1R,2R)-1,2-dibromocyclohexane (**19**)



To an NMR tube added **1** (0.025 g, 0.0427 mmol) along with  $CDCl_3$  (~ 1/2 mL) and brought the resulting reaction mixture, a pale yellow, outside of the box. Proceeded to add  $Br_{2(l)}$  in excess (10 drops) and let the now red reaction mixture sit at room temperature for a period of 15 min before a  $^1H$  NMR was taken of the spectra. Development of **19** is observed in the  $^1H$  NMR and matches previous characterization reported in the literature. Isolation of this product was not pursued. Interestingly, if complex **8** is used in this analogous process, the formation of **19** is accompanied by the concomitant synthesis of  $WTp(NO)(Br)_2$  (**20**). Isolation of this complex was not pursued.

### Synthesis of $WTp(NO)(PMe_3)(\kappa^1\text{-DMA})(OTf^-)$ (**21**)



A solution of  $WTp(NO)(PMe_3)(\eta^2\text{-2,3-anisole})$  (0.500 g, 0.818 mmol) was prepared in DMA (2 mL) and chilled to -30 C over a course of 5 min. To this solution added  $AgOTf$  (0.064 g, x mmol) and upon addition the reaction mixture turns from a light homogeneous yellow color to a dark, green reaction mixture. This reaction mixture was allowed to stir at room temperature for 5 min before a CV was taken in DMA of an aliquot of the reaction mixture. CV analysis showed signs consistent with the formation of **21** ( $E_{1/2} = -1.1$  V,  $E_{p,a} = 0.4$  V).

The green reaction mixture was added to 40 mL of stirring diethyl ether to precipitate out a green solid. This solid was then isolated on a fine 15mL porosity fritted disc, washed with diethyl ether (3 x 10 mL) and allowed to dry under dynamic vacuum for 1 h before a mass was taken (0.096 g, 15.9% yield). The resulting solid shows electrochemical behavior in a CV taken in DMA that support the formation of **21**. ( $E_{1/2} = -1.1$  V,  $E_{p,a} = 0.4$  V).

## References

1. Wilson, K. B.; Myers, J. T.; Nedzbala, H. S.; Combee, L. A.; Sabat, M.; Harman, W. D., Sequential Tandem Addition to a Tungsten–Trifluorotoluene Complex: A Versatile Method for the Preparation of Highly Functionalized Trifluoromethylated Cyclohexenes. *Journal of the American Chemical Society* **2017**, *139* (33), 11401-11412.
2. Wilson, K. B.; Smith, J. A.; Nedzbala, H. S.; Pert, E. K.; Dakermanji, S. J.; Dickie, D. A.; Harman, W. D., Highly Functionalized Cyclohexenes Derived from Benzene: Sequential Tandem Addition Reactions Promoted by Tungsten. *The Journal of Organic Chemistry* **2019**, *84* (10), 6094-6116.
3. Handford, R. C.; Wakeham, R. J.; Patrick, B. O.; Legzdins, P., Cationic and Neutral Cp\*M(NO)( $\kappa^2$ -Ph<sub>2</sub>PCH<sub>2</sub>CH<sub>2</sub>PPh<sub>2</sub>) Complexes of Molybdenum and Tungsten: Lewis-Acid-Induced Intramolecular C–H Activation. *Inorganic Chemistry* **2017**, *56* (6), 3612-3622.
4. Pate, B. H., Taking the Pulse of Molecular Rotational Spectroscopy. *Science* **2011**, *333* (6045), 947.
5. Liebov, B. K.; Harman, W. D., Group 6 Dihapto-Coordinate Dearomatization Agents for Organic Synthesis. *Chemical Reviews* **2017**, *117* (22), 13721-13755.
6. Welch, K. D.; Harrison, D. P.; Lis, E. C.; Liu, W.; Salomon, R. J.; Harman, W. D.; Myers, W. H., Large-Scale Syntheses of Several Synthons to the Dearomatization Agent {TpW(NO)(PMe<sub>3</sub>)} and Convenient Spectroscopic Tools for Product Analysis. *Organometallics* **2007**, *26* (10), 2791-2794.
7. Myers, J. T.; Shivokevich, P. J.; Pienkos, J. A.; Sabat, M.; Myers, W. H.; Harman, W. D., Synthesis of 2-Substituted 1,2-Dihydronaphthalenes and 1,2-Dihydroanthracenes Using a Recyclable Molybdenum Dearomatization Agent. *Organometallics* **2015**, *34* (14), 3648-3657.
8. Harrison, D. P.; Nichols-Nielander, A. C.; Zottig, V. E.; Strausberg, L.; Salomon, R. J.; Trindle, C. O.; Sabat, M.; Gunnoe, T. B.; Iovan, D. A.; Myers, W. H.; Harman, W. D., Hyperdistorted Tungsten Allyl Complexes and Their Stereoselective Deprotonation to Form Dihapto-Coordinated Dienes. *Organometallics* **2011**, *30* (9), 2587-2597.
9. Minch, M. J., Orientational dependence of vicinal proton-proton NMR coupling constants: The Karplus relationship. *Concepts in Magnetic Resonance* **1994**, *6* (1), 41-56.
10. Karplus, M., Vicinal Proton Coupling in Nuclear Magnetic Resonance. *Journal of the American Chemical Society* **1963**, *85* (18), 2870-2871.
11. Laane, J.; Choo, J., The Barrier to Interconversion of Cyclohexene. *Journal of the American Chemical Society* **1994**, *116* (9), 3889-3891.
12. Brooks, B. C.; Meiere, S. H.; Friedman, L. A.; Carrig, E. H.; Gunnoe, T. B.; Harman, W. D., Interfacial and Intrafacial Linkage Isomerizations of Rhenium Complexes with Aromatic Molecules. *Journal of the American Chemical Society* **2001**, *123* (15), 3541-3550.
13. Connelly, N. G.; Geiger, W. E., Chemical Redox Agents for Organometallic Chemistry. *Chemical Reviews* **1996**, *96* (2), 877-910.
14. Wilson, E. B., Microwave Spectroscopy in Chemistry. *Science* **1968**, *162* (3849), 59.
15. Bau, R.; Mason, S. A.; Patrick, B. O.; Adams, C. S.; Sharp, W. B.; Legzdins, P.,  $\alpha$ -Agoctic Interactions in Cp\*W(NO)(CH<sub>2</sub>CMe<sub>3</sub>)<sub>2</sub> and Related Nitrosyl Complexes. *Organometallics* **2001**, *20* (22), 4492-4501.
16. Lanckenau, A. W.; Iovan, D. A.; Pienkos, J. A.; Salomon, R. J.; Wang, S.; Harrison, D. P.; Myers, W. H.; Harman, W. D., Enantioenrichment of a Tungsten Dearomatization Agent Utilizing Chiral Acids. *Journal of the American Chemical Society* **2015**, *137* (10), 3649-3655.
17. Lis, E. C.; Delafuente, D. A.; Lin, Y.; Mocella, C. J.; Todd, M. A.; Liu, W.; Sabat, M.; Myers, W. H.; Harman, W. D., The Uncommon Reactivity of Dihapto-Coordinated Nitrile, Ketone, and Alkene Ligands When Bound to a Powerful  $\pi$ -Base. *Organometallics* **2006**, *25* (21), 5051-5058.
18. Liu, W.; Welch, K.; Trindle, C. O.; Sabat, M.; Myers, W. H.; Harman, W. D., Facile Intermolecular Aryl–F Bond Cleavage in the Presence of Aryl C–H Bonds: Is the  $\eta^2$ -Arene Intermediate Bypassed? *Organometallics* **2007**, *26* (10), 2589-2597.

19. Plommer, H.; Reim, I.; Kerton, F. M., Ring-opening polymerization of cyclohexene oxide using aluminum amine–phenolate complexes. *Dalton Transactions* **2015**, 44 (27), 12098-12102.
20. Yahiaoui, A.; Belbachir, M.; Soutif, J. C.; Fontaine, L., Synthesis and structural analyses of poly (1, 2-cyclohexene oxide) over solid acid catalyst. *Materials Letters* **2005**, 59 (7), 759-767.



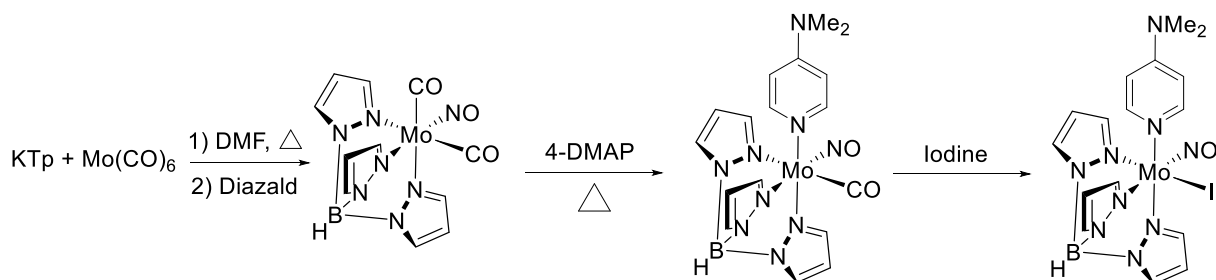
## Chapter 5

# **Molybdenum-Enabled Dearomatization of $\alpha, \alpha, \alpha$ - Trifluorotoluene and Benzene: Labile Arene Complexes for $\pi$ - Ligand Exchange**

## 5.1 Introduction

The  $\pi$ -basic fragment  $\{\text{WTp}(\text{PMe}_3)(\text{NO})\}$  is able to form thermally stable  $\eta^2$ -complexes with a wide range of aromatic molecules. Once coordinated to the metal in a dihapto-fashion, the aromatic is dearomatized and activated toward novel organic reactivity.<sup>1</sup> The tungsten fragment is able to dearomatize molecules with high resonance stabilization energies such as benzene, anisole and trifluorotoluene.<sup>1, 3-5</sup> The analogous molybdenum dearomatization agent  $\{\text{MoTp}(\text{L})(\text{NO})\}$  (L = methylimidazole, 4-dimethylaminopyridine) readily coordinates unsaturated molecules (ethylene, acetone, cyclohexene).<sup>6</sup> However, this fragment has been less effective in forming thermally stable  $\eta^2$ -bonds with aromatic molecules. The scope of aromatic molecules amenable to molybdenum-promoted dearomatization historically has been limited to five-membered rings such (furan, thiophene) or polycyclic aromatic hydrocarbons (PAHs).<sup>2, 6-10</sup> These aromatic molecules are less stabilized by aromaticity than benzene and its derivatives.<sup>11</sup> Work by Dr. Jeffrey Myers has shown that the fragment  $\{\text{MoTp}(\text{DMAP})(\text{NO})\}$  effectively promotes tandem addition reactions on PAHs.<sup>9</sup>

We postulate that the 3d orbitals of the molybdenum metal are less able to  $\pi$ -backbond into the  $\pi^*$ -orbital associated with an aromatic molecule. This is in contrast to the third row dearomatization fragments  $\{\text{Os}(\text{NH}_3)_5\}^{2+}$ ,  $\{\text{ReTp}(\text{CO})(\text{MeIm})\}$  and  $\{\text{WTp}(\text{NO})(\text{PMe}_3)\}$ . Here the HOMO of these metal complexes is localized on a 4d  $d\pi$ -orbital.<sup>12-13</sup> The higher energy associated with the 4d orbital could allow for better overlap with the LUMO of the aromatic molecule, allowing a more efficient metal-to-aromatic  $\pi$ -backbonding interaction.



**Scheme 5.1.** Optimized route to a molybdenum dearomatization synthon. The complex  $\text{MoTp}(\text{NO})(\text{DMAP})(\text{I})$  can be prepared outside an inert glovebox on a ~200 g yield.

Dr. Jeffrey Myers showed that the molybdenum dearomatization synthon MoTp(NO)(DMAP)(I) can be successfully be prepared on 200 g scale with a 70% overall yield. This synthesis can be achieved without the use of an inert glovebox atmosphere. A synthetic pathway to the molybdenum-iodo complex is given in **Scheme 5.1**. This dearomatization synthon can be prepared at approximately one fourth of the cost of its tungsten congener WTp(NO)(PMe<sub>3</sub>)(Br).<sup>2, 10</sup>

Reduction of MoTp(NO)(DMAP)(I) with sodium in the presence of an unsaturated molecule leads to complexes where the molybdenum fragment is bound to a  $\pi$ -bond of the molecule in an  $\eta^2$ -fashion.<sup>6</sup> The ability for molybdenum to dihapto-coordinate benzene or its derivatives via the direct reduction of the molybdenum-iodo precursor historically had been unsuccessful. This chapter seeks to expand the scope of aromatic molecules that can be coordinated to the molybdenum scaffold.

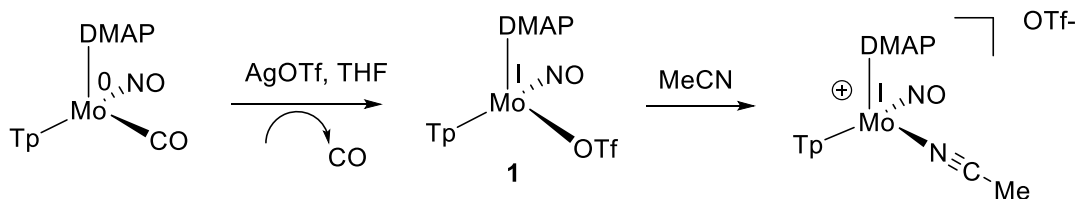
## 5.2. Synthesis of a Molybdenum-Triflate Complex

Triflate groups are often poorly coordinating ligands to transition metal complexes.<sup>13-14</sup> Therefore, metal-triflate complexes are often ideal candidates for ligand substitution reactions, as the triflate group can be readily displaced from the metal center. Synthetic efforts were focused on the synthesis of the molybdenum-triflate complex MoTp(NO)(DMAP)(OTf) (**1**). Here, substitution of the halogen with a triflate group could offer numerous synthetic advantages. The enhanced lability of the triflate group could result in reduced reaction times to generate dihapto-coordinate molybdenum complexes. Additionally, **1** could be more electron deficient than MoTp(NO)(DMAP)(I) due to weaker  $\sigma$ -donation from the triflate group (compared to the iodide ligand). Consequently, complex **1** would be more susceptible to reduction than its halogenated analogs. Ideally, this would allow for the use of relatively mild reducing agents (i.e. magnesium). The majority of molybdenum-aromatic complexes generated via direct reduction of MoTp(NO)(DMAP)(I) requires pyrophoric sodium to be used as a chemical reducing agent.

Initial synthetic routes focused on generating **1** from MoTp(NO)(DMAP)(CO) via chemical oxidation with a triflate salt. Treating MoTp(NO)(DMAP)(CO) with AgOTf or Cu(OTf)<sub>2</sub> in THF results in vigorous

bubbling and the formation of an emerald green solution (**Scheme 5.2**). A vibrant green solid can be readily precipitated from solution and purified via silica chromatography. The resulting solid is paramagnetic, consistent with the formation of molybdenum (I) adduct. A cyclic voltammogram (CV) taken in MeCN initially shows an  $E_{p,c} = -1.26$  V and an  $E_{p,a} = +0.79$  V (100 mV/s) that correspond to Complex **1**. For comparison, a CV of the complex MoTp(NO)(DMAP)(I) reveals a reversible  $E_{1/2}$  at -1.43 V and an  $E_{p,a} = +0.65$  V (100 mV/s). Additionally, whereas MoTp(NO)(DMAP)(I) has an NO stretch of  $\nu_{\text{NO}} = 1607^{-1}$ , that of **1** is blue-shifted to  $\nu_{\text{NO}} = 1618$   $\text{cm}^{-1}$ . These data suggest that the molybdenum-triflate complex **1** is more electron deficient than the MoTp(NO)(DMAP)(I) species.

If complex **1** is dissolved in a solution of MeCN, over a period of 30 minutes the original  $E_{p,c}$  at -1.26 V is replaced by another  $E_{p,c}$  at -1.40 V. We speculate that this feature is consistent with the formation of the molybdenum complex  $\{\text{MoTp}(\text{NO})(\text{DMPA})(\kappa^1\text{-N-MeCN})\}^+(\text{OTf}^-)$ . This experiment demonstrates that the triflate ligand is labile enough to undergo substitution with another sigma-donor ligand *without the need for a reducing agent* (**Scheme 5.2**).



**Scheme 5.2.** Synthesis of a molybdenum triflate complex. The triflate group can be readily displaced by a sigma-donating ligand (i.e. MeCN) without the need for a reductant.

Despite these initially promising data, using non-sodium-based reductants (Zn, Mg) in the presence of an aromatic (naphthalene, thiophene, furan) resulted in negligible signs of an  $\eta^2$ -bound product. Reduction conditions utilizing sodium as a reducing agent gave yields comparable with those obtained from the molybdenum-iodo species. These reactions required  $\sim 16$  hours to go to completion, a similar timeframe to synthesize  $\eta^2$ -products derived from MoTp(NO)(DMAP)(I). Due to the lower cost associated with its preparation and the large-scale synthesis optimized for MoTp(NO)(DMAP)(I), efforts to scale the synthesis of **1** were not pursued.<sup>10</sup>

### 5.3 Labile $\pi$ -Ligands and Molybdenum Dearomatization

The complex MoTp(NO)(DMAP)( $\eta^2$ - $\alpha$ -pinene) (**2**) is synthetically valuable due to the relative lability of the  $\alpha$ -pinene ligand and potential applications in the enantioenrichment of the molybdenum dearomatization fragment.<sup>2</sup> Complex **2** can undergo ligand exchange with a wide variety of unsaturated ligands (ketones, esters, polycyclic aromatic hydrocarbons, thiophene, furan). Complex **2** can be prepared from the direct reduction of MoTp(NO)(DMAP)(I) with sodium in the presence of  $\alpha$ -pinene and its synthesis was optimized by Dr. Jeffrey Myers and Dr. Phillip Shivokevich.<sup>2</sup>

Ligand substitution experiments were pursued with complex **2** to evaluate the lability of the  $\alpha$ -pinene ligand. All kinetic experiments investigating the ligand exchange of complex **2** were performed in triplicate and evaluated over three to four half-lives. In cases where contaminant oxidants were avoided, the substitution half-life of the alpha-pinene ligand of **2** is approximately ~15 hours at ambient temperatures. These rates are largely independent of the nature of the incoming ligand, so long as trace oxidants are avoided.<sup>2</sup> A summary of these experiments is given in **Table 5.1**. The use of chemical additives for increased rates of exchange was explored to investigate the ability of the molybdenum scaffold to engage in redox catalysis in conjunction with Dr. Steven Dakermanji.

| L  | Compound | NMR Yield | Half-life deuterated solvent (h) | $\Delta^\ddagger G^\ddagger$ (25 °C) kcal/mol |
|--|----------|-----------|----------------------------------|---|
| Acetone (neat)   | <b>3</b> | 89%       | 10.3                             | 23.9  |
| Acetone (0.1M benzene-d6)  | <b>3</b> | 88%       | 16.3                             | 24.2  |
| Acetone-d6 (10% D2O)   | <b>3</b> | 58%       | 6.8                              | --  |
| Naphthalene (0.1M benzene-d6)  | <b>4</b> | 57%       | 15.6                             | 24.1  |
| Ethyl acetate (0.1M benzene-d6)  | <b>5</b> | 49%       | 15.5                             | 24.1  |
| Acetonitrile (neat)  | <b>6</b> | 58%       | 11.5                             | 24.0  |
| DMF (neat)   | <b>7</b> | 63%       | 15.0                             | 24.1  |
| Benzaldehyde (0.1M benzene-d6)   | <b>8</b> | 70%       | 1.5                              | --  |
| Benzaldehyde (0.1M benzene-d6) with 0.5 eq of CoCp <sub>2</sub>              | <b>8</b> | 40%       | 10.3                             | --  |
| Benzaldehyde (0.1M benzene-d6) with 0.1 eq of FeCp <sub>2</sub> <sup>+</sup> | <b>8</b> | >90%      | >0.1                             | 23.9  |
| Acetone-d6 with 0.1 eq FeCp <sub>2</sub> <sup>+</sup>                        | <b>3</b> | 93%       | 0.6                              | --  |
| Acetone-d6 (10% D <sub>2</sub> O) with 0.1 eq FeCp <sub>2</sub> <sup>+</sup> | <b>3</b> | 86%       | 3.2                              | --  |
| Acetone-d6 (10% D <sub>2</sub> O) with 0.1 eq CoCp <sub>2</sub> <sup>+</sup> | <b>3</b> | 98%       | 0.9                              | --  |

**Table 5.1.** Ligand substitution rates to a variety of unsaturated ligands starting from Complex **2**. Accelerated rates are observed under conditions where trace oxidants are used or under conditions which could oxidize the molybdenum metal center.<sup>2</sup>

Catalyzed substitution was observed for a number of ligands with aldehyde and ketone functionalities through a redox-catalyzed process detailed more efficiently elsewhere.<sup>8</sup> Catalyzed reactions to aldehyde or ketone-containing ligands occurred through use of chemical oxidants (ferrocenium hexafluorophosphate, cobaltecenium hexafluorophosphate) or in the presence of trace acid impurities. In the case of acid impurities, deleterious oxidation of the molybdenum metal by the acid could generate a molybdenum species in situ capable of participating in redox catalyzed reactions. That is, the acid is speculated to generate a chemical oxidant able to engender a redox-catalyzed process.

Additionally, when water is added as a chemical additive, accelerated ligand substitution occurs where the  $\alpha$ -pinene ligand of **2** is replaced by acetone to generate the molybdenum-acetone complex **3**. Decomposition of the molybdenum species in the presence of water could generate a higher oxidation state, redox-active molybdenum complex. In support of this, the reported NMR yield is 30% lower when water is used as an additive in the exchange of **2** to the acetone complex **3**. This indicates decomposition of the molybdenum (0) complex (89% NMR in neat acetone-*d*<sub>6</sub> compared to a 58% NMR yield with 10% molar water additive in acetone-*d*<sub>6</sub>). A study on the ability to access redox catalysis in the presence of oxidants to catalyze ligand substitution has been reported by Dr. Steven Dakermanji.<sup>8</sup> Efforts to generally extend this methodology to catalyze substitution to molybdenum-arene complexes have, as of yet, proven to be unsuccessful.

While complex **2** enabled access to various  $\pi$ -ligands, substitution to benzene or its derivatives was largely accompanied by decomposition during the exchange process. No signs of a diamagnetic molybdenum-benzene complex were observed, even if **2** was allowed to sit in a solution of neat benzene-*d*<sub>6</sub> and monitored over several days.

Although sterically encumbering, the bulky  $\alpha$ -pinene ligand of **2** is substantially more stable than a proposed molybdenum-benzene complex (estimates for the BDE of these complexes are presented *vide infra*). Over the time frame of the ligand substitution, the decomposition of a molybdenum-benzene complex presumably occurs faster than the desired ligand substitution. Additionally, the relative stability of the  $\alpha$ -

pinene complex **2** compared to a theorized molybdenum-benzene adduct would require a large excess (concentration) of benzene to prevent re-coordination of the  $\alpha$ -pinene ligand.

A more practical ligand exchange precursor was developed by Dr. Jeffery Myers and Dr. Steven Dakermanji in the form of the complex

MoTp(NO)(DMAP)( $\eta^2$ -2,3-2,5-dimethylfuran) (**9**).

The steric bulk of the methyl groups decrease the thermal stability of the  $\eta^2$ -furan derivative complex, thereby increasing its substitution rate. Kinetic studies give an approximate substitution half-life of  $\sim 2$  hours at ambient temperatures under pseudo-first order conditions.

If the 2,5-dimethylfuran complex **9** is allowed to sit in an excess of  $\alpha,\alpha,\alpha$ -trifluorotoluene

(PhCF<sub>3</sub>), ligand substitution occurs to generate MoTp(NO)(DMAP)( $\eta^2$ -3,4- $\alpha,\alpha,\alpha$ -trifluorotoluene) (**10**). This synthesis was achieved by Dr. Jeffery Myers and represents the first benzene dearomatized by molybdenum. Benzene and its derivatives are a class of aromatics that had been unable to form thermally stable  $\eta^2$ -complexes with the {MoTp(NO)(DMAP)} fragment. The molybdenum promoted dearomatization of PhCF<sub>3</sub> was utilized by Dr. Jeffery Myers for the synthesis of novel trifluoromethylated cyclohexadienes and cyclohexenes.<sup>15</sup>

Complex **10** forms an approximate  $\sim 1:1$  ratio of coordination diastereomers where the molybdenum is bound across the 3,4-carbons of the PhCF<sub>3</sub> ligand in a dihapto-fashion. This is similar to the coordination mode of PhCF<sub>3</sub> upon complexation to the tungsten fragment {WTP(NO)(PMe<sub>3</sub>)}.<sup>16</sup> Unlike its tungsten congener however, the protons for each coordination diastereomer associated with **10** exist as five-broadened

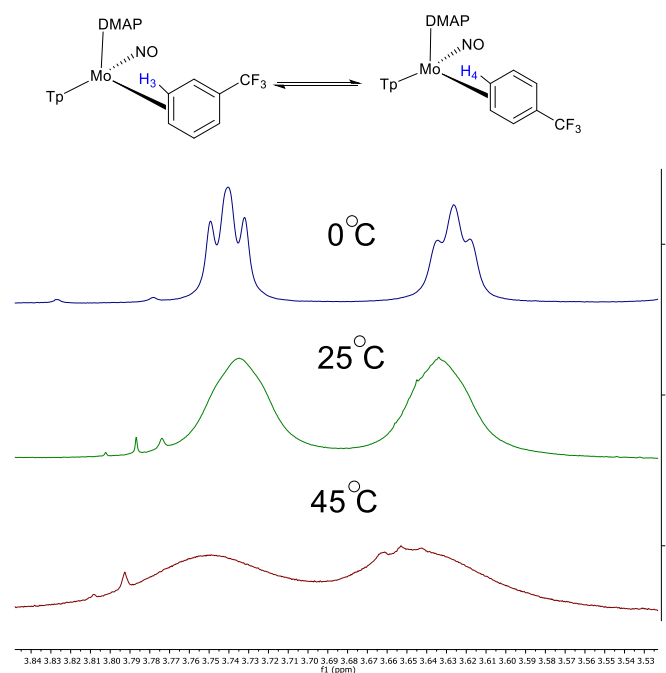


**Figure 5.1.** Fluxional behavior displayed by the two coordination diastereomers of **10** as a function of temperature. Proton resonances here correspond to the H<sub>3</sub> and H<sub>4</sub> protons as depicted at the top of the figure.

resonances at ambient temperatures in  $^1\text{H}$  NMR experiments. This fluctuational behavior is not observed at ambient temperatures for the tungsten- $\text{PhCF}_3$  congener. Cooling an acetone- $d_6$  solution of **10** to  $0^\circ\text{C}$  slows down the ring-walk isomerization and the multiplicity of the proton resonances can be observed. A series of variable temperature  $^1\text{H}$  NMR spectra are presented in **Figure 5.1** to illustrate the dynamic behavior of complex **10** in solution.

A NOESY experiment reveals that the two coordination diastereomers are able to interconvert through an

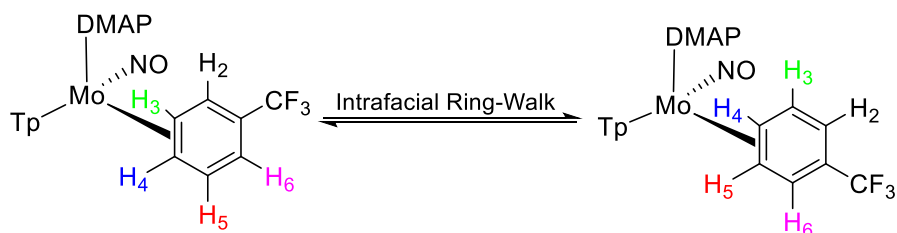


**Figure 5.2:** A purported intrafacial “ring-walk” mechanism that would account for the observed spin saturation exchanges as observed by NOESY experiments.

intrafacial “ring-walk” mechanism as depicted in **Figure 5.2**. The ring-walk mechanism proposed is consistent with spin saturation exchanges observed in the NOESY experiment. We do note, however, that a separate isomerization process cannot be ruled out (primarily that of an interfacial “ring-flip” mechanism), though data to support this mechanism are not observed on the timescale of the NMR experiment.

The optimized synthesis of **10** was achieved from the direct reduction of  $\text{MoTp}(\text{NO})(\text{DMAP})(\text{I})$ . Essential to an effective reduction process are relatively high concentrations of  $\text{MoTp}(\text{NO})(\text{DMAP})(\text{I})$  in a minimal amount of neat  $\alpha,\alpha,\alpha$ -trifluorotoluene ligand (general concentrations are 25 g of  $\text{MoTp}(\text{NO})(\text{DMAP})(\text{I})$  in 200 mL of  $\text{PhCF}_3$ ). The product **10** is marginally soluble in neat  $\text{PhCF}_3$ . We speculate that this heterogeneity helps to protect **10** from decomposition. Once in the solid state the desired product **10** would not coexist in solution with trace impurities that could decompose the molybdenum scaffold.

Additionally, the surface area of the sodium reducing agent plays an integral role in the efficiency of the reduction. At the time of its optimization, 30% weight sodium dispersion in toluene (0.1 mm mesh size) was not commercially available. As such 30% by weight sodium dispersion in paraffin needed to be dissolved in hexanes at high stir speeds ( $> 1000$  rpm) over a course of 16 hours to generate the appropriately-



sized “sodium flecks”. Optimized conditions detailed in the experimental section show that **10** can be prepared on a 17 g scale with a 70% yield as a red-orange powder. Complex **10** can be prepared as an analytically pure solid (confirmed by microanalysis) without the need for chromatography.

We hypothesize that

energetically, benzene or

substituted benzenes are

significantly stabilized by

aromaticity compared to PAHs or

heterocycle aromatics. As such,

forming a thermally stable

dihapto-bond with a benzene

ligand would be challenging for

the molybdenum complex.

Molybdenum as a second row

transition metal system is less efficacious at  $\pi$ -backbonding compared to its third row congeners (even when

the electrochemical potentials of these complexes are “matched”). The inability of molybdenum to  $\pi$ -

backbond effectively into an aromatic molecule would make the molybdenum complex more electron-rich

and prone to oxidative decomposition. In the case of  $\text{PhCF}_3$ , the electron withdrawing effects of the  $-\text{CF}_3$

substituent help to increase the strength of the  $\eta^2$ -bond by making the benzene ring a better  $\pi$ -acceptor ligand.

#### 5.4 Studies of $\text{MoTp}(\text{NO})(\text{DMAP})(\eta^2\text{-}\alpha,\alpha,\alpha\text{-trifluorotoluene})$

A comparison of substitution rates in the presence of acetone- $d_6$  indicated that the  $\text{PhCF}_3$  ligand of **10** is even more labile than the 2,5-dimethylfuran ligand of complex **9**. A table comparing the oxidative potentials and lability of the exchange synthons ( $\alpha$ -pinene, 2,5-dimethylfuran and  $\alpha,\alpha,\alpha$ -trifluorotoluene) is given in **Table 5.2**. An estimate for the bond dissociation energy extrapolated from rate data is also included.

| Complex | $E_{p,a}$<br>(relative to NHE) | Substitution Half-<br>Life at 25 °C | Metal-Arene Bond<br>Strength (kcal/mol) |
|---------|--------------------------------|-------------------------------------|---|
|         | -0.17 V                        | 15.5 hr                             | 24                                      |
|         | -0.35 V                        | 2.1 hr                              | 23                                      |
|         | -0.28 V                        | 0.65 hr                             | 22                                      |

**Table 5.2.** Comparison of electrochemical properties, substitution rates and estimated heterolytic BDE values between labile  $\pi$ -ligands for the  $\{\text{MoTp}(\text{NO})(\text{DMAP})\}$  fragment. BDE values are extrapolated from substitution half-life data at 25 °C and estimate that the value for  $\Delta G^\ddagger$  approximates that relative energy of an unobserved 5-coordinate intermediate.

Assumptions underlying this approximation will be examined *vide infra*. Substitution of molybdenum-PhCF<sub>3</sub> complex **10** to the molybdenum-acetone complex **3** was investigated given the irreversible nature of this reaction. Pseudo-first order conditions were employed (excess of acetone) and experiments were performed in triplicate at ambient temperatures. At the time of investigation, the ability for molybdenum to engage in redox catalysis with ketone-containing ligands had not been elucidated.

The kinetics of the dissociation of the PhCF<sub>3</sub> ligand of **10** were probed at various temperatures with acetone-*d*<sub>6</sub> to form **3**. Experiments performed at 25 °C determined a  $\Delta G^\ddagger = 22.3$  kcal/mol. Surveying the  $k_{\text{rate}}$  dependence on temperature over a range of 25 °C to 45 °C allowed for the generation of an Eyring Plot (included in the Experimental Section). Analysis of this data yields  $\Delta H^\ddagger = 25.5 \pm 1.4$  kcal/mol a  $\Delta S^\ddagger = 12.1 \pm 4.5$  eu for the substitution process of the molybdenum-PhCF<sub>3</sub> complex **10** to the molybdenum-acetone complex **3**. These data support a largely dissociative mechanism where the rate determining step is the dissociation of the PhCF<sub>3</sub> ligand. This interpretation is consistent with studies reported by Bengali who reported the activation parameters of a manganese-toluene complex Mn( $\eta^5$ -C<sub>5</sub>H<sub>5</sub>)(CO)<sub>2</sub>( $\eta^2$ -toluene) to be  $\Delta H^\ddagger = 14.2 \pm 0.8$  kcal/mol and  $\Delta S^\ddagger = 6.0 \pm 3$  eu.<sup>17</sup> In this study ligand substitution was speculated to be largely dissociative due to the determination of a positive  $\Delta S^\ddagger$ .

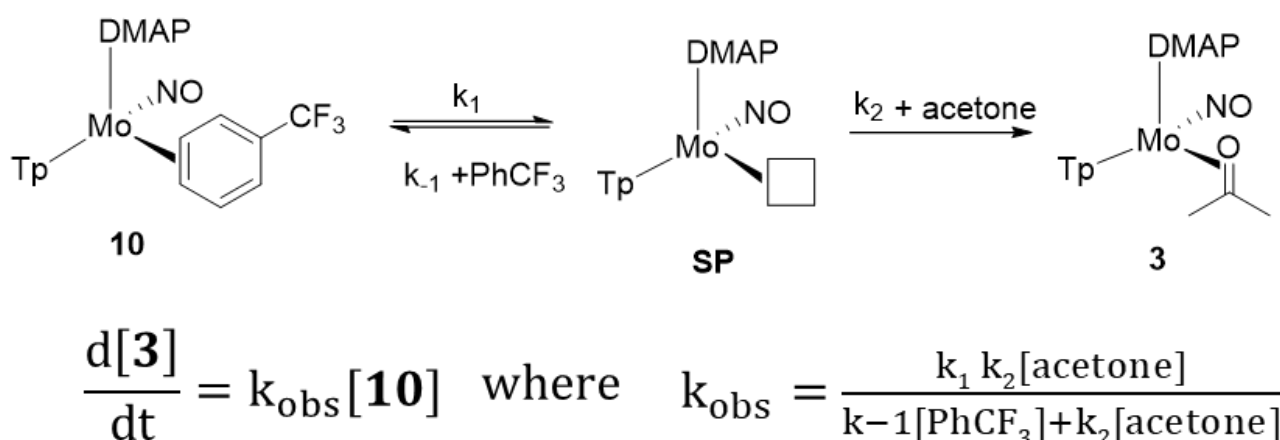


**Figure 5.3.** Proposed ligand dissociation mechanism and accompanying rate expression. The rate determining step is that of dissociation of the PhCF<sub>3</sub> ligand and the formation of the square-pyramidal intermediate.

Dissociation of the  $\text{PhCF}_3$  ligand of complex **10** would presumably result in the formation of an unobserved coordinatively unsaturated five-coordinate square pyramidal intermediate (species **SP** in **Figure 5.3**). This species is speculated to readily coordinate an incoming ligand. Such a process implies that the rate of ligand substitution should remain invariant to the identity of the incoming ligand. To support this, when **10** is allowed to exchange to the molybdenum-naphthalene complex **4**,  $\text{MoTp}(\text{NO})(\text{DMAP})(\kappa^1\text{-pyridine})$  (**11**), furan (**12**) or thiophene (**13**) under pseudo-first order conditions, the rate of dissociation does indeed remain largely invariant with a substitution half-life of  $\sim 40 \text{ min} \pm 4 \text{ minutes}$ .

The steady-state approximation relates the rate of formation of the molybdenum-acetone complex **3** with the concentration of the molybdenum- $\text{PhCF}_3$  complex **10** and the observed rate ( $k_{\text{obs}}$ ) as detailed in **Figure 5.3**. For approximations of the heterolytic BDE (BDE between the molybdenum and the  $\text{PhCF}_3$  ligand), we note a key assumption is made; the postulated unsaturated five-coordinate intermediate is speculated to be energetically close to the  $\Delta G^\ddagger$  of the rate determining step of this process. In this way, measurements of  $\Delta G^\ddagger$  of the rate-limiting step of the reaction (ligand dissociation) are invoked as approximate BDE values.

The entropic component ( $\Delta S^\ddagger$ ) of the proposed ligand substitution process is positive as determined *vide supra*. Therefore, the BDE determined from determination of the  $\Delta G^\ddagger$  established with rate data is most

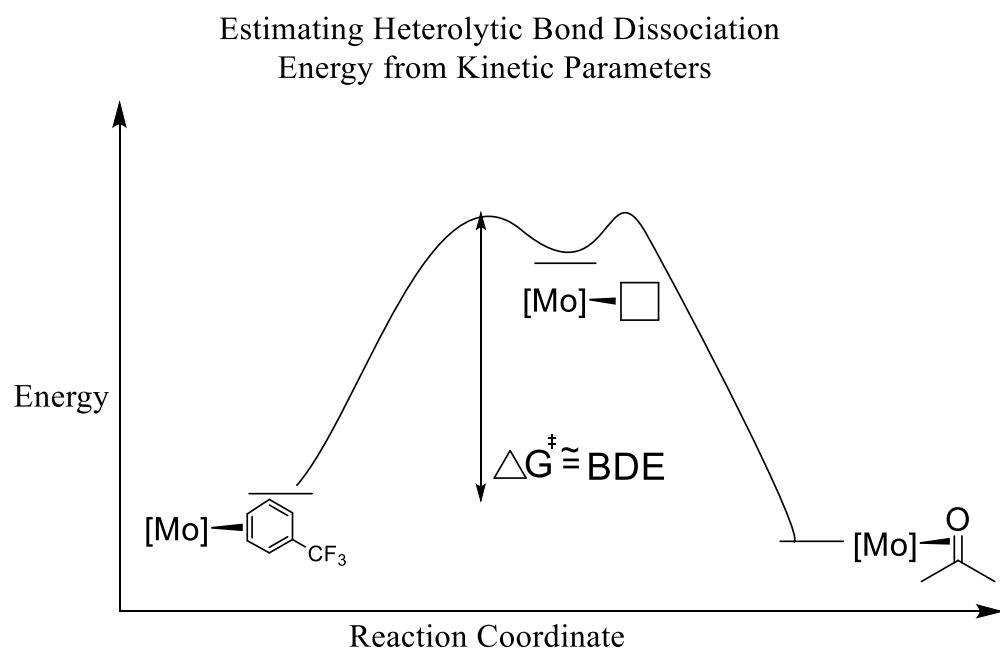
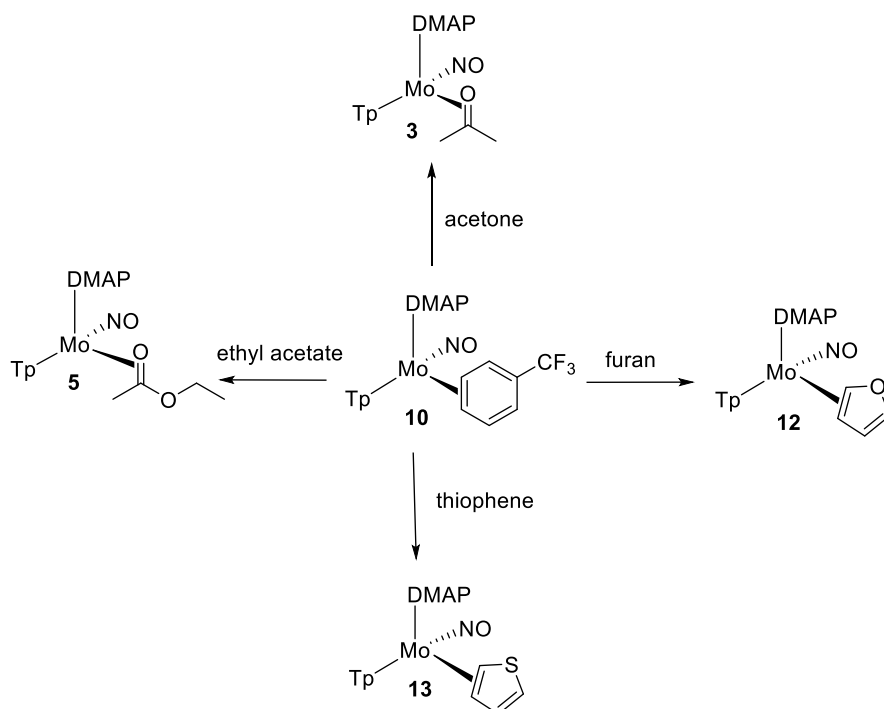


**Figure 5.4.** Pictorial representation supporting the use of the free energy of activation for an estimate of the difference heterolytic BDE between complex **10** and complex **17**.

likely an underestimate of the BDE for these molybdenum  $\pi$ -ligand complexes given the contribution of  $\Delta S^\ddagger$  and the reliance of the value of  $\Delta G^\ddagger$  on temperature ( $\Delta G^\ddagger = \Delta H^\ddagger - T\Delta S^\ddagger$ ).

A better estimate of the BDE of complex **10** there may be the  $\Delta H^\ddagger$  value. For the molybdenum-  $\text{PhCF}_3$  complex **10**,  $\Delta H^\ddagger$  is determined to be approximately 25.5 kcal/mol as extrapolated from the Eyring equation for ligand substitution by acetone to generate **3**. Calculations by Karl Westendorff have sought to better estimate BDEs through DFT methods but these methods generally lead to BDE approximations that are generally ~2-5 kcal/mol lower than BDEs approximated by substitution rate processes.<sup>8</sup>

Utilizing **10** then as a ligand exchange synthon, ligand exchanges were pursued to coordinate a variety of unsaturated molecules. Complete exchange of the  $\text{PhCF}_3$  ligand of **10** to an unsaturated ligand takes approximately two to three hours under pseudo-first order conditions. A brief survey of exchanges to unsaturated molecules is given in **Scheme 5.4**. The ability for the molybdenum fragment  $\{\text{MoTp}(\text{DMAP})(\text{NO})\}$  to stabilize an electron deficient benzene and lability of **10** begged the question: what benzenes are amenable to molybdenum-enabled dearomatization?



**Scheme 5.3.** Exchange of the arene ligand of **10** to various unsaturated molecules. Ligand exchanges were completed < 3 hours at ambient temperatures in an excess of ligand (~ 10 equivalents).

## 5.5 Synthesis of MoTp(NO)(DMAP)( $\eta^2$ -benzene)

Previous rate data for the  
 WTp(NO)(PMe<sub>3</sub>)( $\eta^2$ -benzene) complex (**14**) and

WTp(NO)(PMe<sub>3</sub>)( $\eta^2$ - $\alpha,\alpha,\alpha$ -trifluorotoluene)  
 (**15**) complexes to WTp(NO)(PMe<sub>3</sub>)( $\eta^2$ -

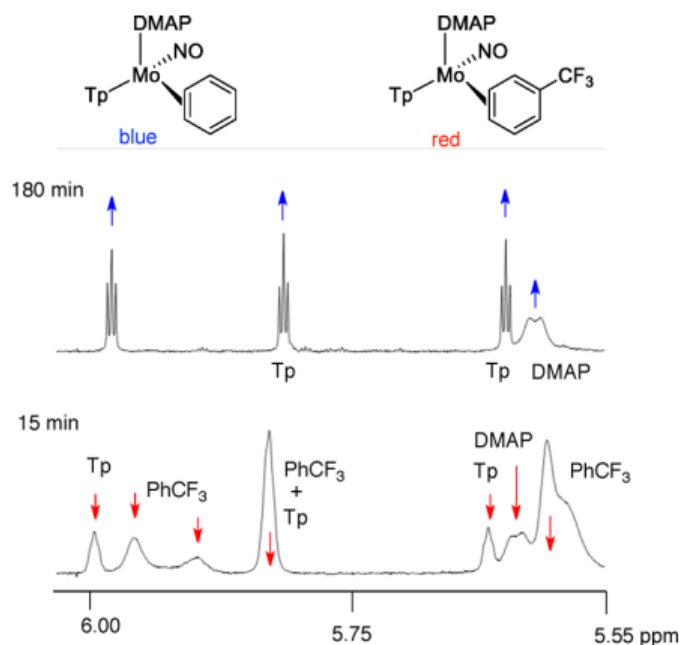
acetone) (**16**) have been previously reported.<sup>16</sup> Extrapolating of the rate data to approximate the BDE of **15** and **14** predicts complex **15** to be ~ 2.4 kcal/mol more stable than **14**. In other words, the -CF<sub>3</sub> group essentially imbues ~ 2.4 kcal/mol of stability to the metal-arene bond.

Solving the equilibrium defined in **Equation 5.1** for the analogous molybdenum-PhCF<sub>3</sub> complex **10** and a theoretical molybdenum-benzene complex suggests that to attain 90% purity, ~ 400 equivalents of incoming ligand (here benzene) would be needed to compete with the thermal stability of the **15** complex. In other words, the exchange reaction could be driven to completion so long as a high enough concentration of benzene is used to drive the reaction forward. Initial experiments dissolving **10** (~ 30 mgs, 0.050 mmol) in benzene-*d*<sub>6</sub> (~ 1 g, 10.4) mmol) show that overtime a new diamagnetic species is observed in solution.

In a separate experiment, approximately 20 mg of the trifluorotoluene complex **10** was added to a 1:1 mixture of THF (used to solubilize electrolyte) and benzene in a CV cell. The  $E_{p,a}$  associated with **10** (-0.28 V at 100 mV/s) decreased, and the concomitant growth of an  $E_{p,a} = -0.55$  V (100 mV/s) occurred over two hours, consistent with the formation of the more electron-rich benzene complex **17**. Addition of 1 mL of acetone to this solution resulted in the immediate loss of the anodic wave at

$$K_{eq} = \frac{[\text{Mo} - \text{benzene}][\text{PhCF}_3]}{[\text{Mo} - \text{PhCF}_3][\text{benzene}]} = e^{-\Delta G/RT}$$

**Equation 5.1:** Equation approximating the concentration of benzene needed to push the equilibrium to 90% + of the molybdenum-benzene complex. Here the  $\Delta G$  value is extrapolated from rate data collected from the analogous tungsten-arene complexes.

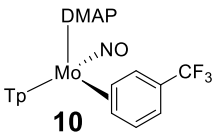
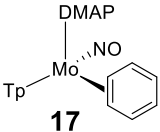


**Figure 5.5.** Development of the molybdenum-benzene-*d*<sub>6</sub> complex observed in situ over time via substitution of the PhCF<sub>3</sub> ligand of complex **10**.

-0.55 V (100 mV/s) and the growth of a new anodic wave at  $E_{p,a} = 0.08$  V (100 mV/s), consistent with the formation of the acetone complex **3**.

When 200 mgs of **10** is allowed to stir in 20 mL of dried benzene over the course of three hours, subsequent evaporation and exposure of the reaction mixture to pentane results in the isolation of a dark yellow solid. Analysis in either acetone- $d_6$  or benzene- $d_6$  shows distinct proton resonances for the Tp and DMAP ligands, however no benzene protons are observed at room temperature. An NMR taken in acetone- $d_6$  at -30 °C reveals four unambiguously broadened proton resonances at -30 °C. Raising the solution to room temperature results in the rapid formation of the molybdenum-acetone complex **3**. Dynamic NMR analysis of the protons associated with **17** kcal/mol associated with the  $\Delta G^\ddagger = 13.8$  kcal/mol to a ring-walking process at ambient temperatures.

Kinetic experiments looking at the substitution of the molybdenum-benzene adduct **17** to the molybdenum acetone complex **3** give a substitution half-life for complex **17** of ~ 20 s at ambient temperatures. Approximating these kinetic data to the heterolytic bond dissociation energy (**Figure 5.4**) gives as estimated BDE of ~ 19 kcal/mol. The approximated BDE of **10** was taken as 22 kcal/mol, indicating that the stabilizing effects of the -CF<sub>3</sub> group in the substituted benzene imbues ~ 3 kcal/mol of stability for the {MoTp(NO)(DMAP)} fragment, which agrees with our previous findings on tungsten. A comparison of the

| Ligand   | $E_{pa}$ (relative to NHE) | Substitution Half-Life at 25 °C | Metal-Arene Bond Strength (kcal/mol) | Barrier to Ring-Walk Isomerization (kcal/mol) |
|--|----------------------------|---------------------------------|--------------------------------------|---|
| <br><b>10</b> | -0.28                      | 40 min                          | 22 kcal/mol                          | 14.7 kcal/mol                                 |
| <br><b>17</b> | -0.55 V                    | 21 s                            | 19 kcal/mol                          | 13.8 kcal/mol                                 |

**Table 5.3:** The electrochemical and stabilizing effects of a -CF<sub>3</sub> group on a benzene ring within the context of dearomatization mediated by the {MoTp(NO)(DMAP)} fragment. Estimates of the barrier to ring walk were determined at 50 °C for **10** and -30 °C for **17**.

electrochemical, kinetic and approximated thermodynamic properties between the molybdenum complex **17** and the trifluoromethylated variant **10** are given in **Table 5.3**.

Complex **17** is the first isolable  $\eta^2$ -benzene complex for a molybdenum transition metal complex to the best of our knowledge.<sup>15</sup> Several months prior to its publication, observation of a molybdenum  $\eta^2$ -benzene complex observed in situ was reported by Chirik and co-workers, though this species could not be isolated.<sup>18</sup> Efforts by Dr. Jeffery Myers showed that the large-scale synthesis of **17** could be achieved utilizing a large excess of benzene and **10** and this synthesis is detailed in Chapter 8.

Although analysis was not pursued as in-depth as the molybdenum-benzene complex **17**, analogous conditions were utilized to effect the exchange from **10** to the complex MoTp(NO)(DMAP)( $\eta^2$ -2,3-anisole) complex (**18**). The anisole ligand of **18** was exceptionally labile with ligand dissociation substitution occurring on the timeframe of minutes. Partial characterization of the molybdenum-anisole complex **18** is presented in the experimental section of this chapter. This extends further proof of concept that the molybdenum-scaffold is able to bind other benzenes (even electron-rich benzenes) in a dihapto-fashion.

## 5.6 Conclusions

The ability for the fragment {MoTp(NO)(DMAP)} to dihapto-coordinate benzene serves as an important proof of concept and demonstrates the ability for molybdenum to bind aromatic molecules with high resonance stabilization energies. There are numerous advantages of molybdenum-enabled dearomatization compared to its 3<sup>rd</sup> row congeners. Among those properties are enhanced scalability, lower cost and relatively facile oxidation of molybdenum-olefin adducts.

The withdrawing nature of the -CF<sub>3</sub> functionality significantly stabilizes the molybdenum-benzene bond. This is reflected in both lowered substitution rates of PhCF<sub>3</sub> compared to PhH as well as an increased barrier to a ring-walk isomerization. With this in mind, other electron-deficient benzenes were coordinated to the molybdenum fragment {MoTp(NO)(DMAP)}. A survey of the ability of molybdenum to form thermally stable  $\eta^2$ -complexes with electron deficient aromatics is explored in Chapter 6.

## Experimental

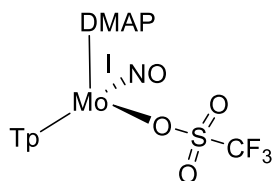
**General Methods.** NMR spectra were obtained on 500, 600 or 800 MHz spectrometers. Chemical shifts are referenced to tetramethylsilane (TMS) utilizing residual  $^1\text{H}$  signals of the deuterated solvents as internal standards. Chemical shifts are reported in ppm and coupling constants ( $J$ ) are reported in hertz (Hz). Chemical shifts for  $^{19}\text{F}$  and  $^{31}\text{P}$  spectra were reported relative to standards of hexafluorobenzene (164.9 ppm) and triphenylphosphine (-6.00 ppm). Infrared Spectra (IR) were recorded on a spectrometer as a solid with an ATR crystal accessory, and peaks are reported in  $\text{cm}^{-1}$ . Electrochemical experiments were performed under a nitrogen atmosphere. Most cyclic voltammetric data were recorded at ambient temperature at 100 mV/s, unless otherwise noted, with a standard three electrode cell from +1.8 V to -1.8 V with a platinum working electrode, acetonitrile (MeCN) solvent, and tetrabutylammonium (TBAH) electrolyte (~1.0 M). All potentials are reported versus the normal hydrogen electrode (NHE) using cobaltocenium hexafluorophosphate ( $E_{1/2} = -0.78$  V,  $-1.75$  V) or ferrocene ( $E_{1/2} = 0.55$  V) as an internal standard. Peak separation of all reversible couples was less than 100 mV. All synthetic reactions were performed in a glovebox under a dry nitrogen atmosphere unless otherwise noted. All solvents were purged with nitrogen prior to use. Deuterated solvents were used as received from Cambridge Isotopes and were purged with nitrogen under an inert atmosphere. When possible, pyrazole (Tp) protons of the (trispyrazolyl) borate (Tp) ligand were uniquely assigned (e.g., “Tp3B”) using two-dimensional NMR data (see Fig. S1). If unambiguous assignments were not possible, Tp protons were labeled as “Tp3/5 or Tp4”. All  $J$  values for Tp protons are 2 ( $\pm 0.4$ ) Hz.

### Synthesis of $\text{MoTp}(\text{CO})_2(\text{NO})$ (altered procedure)

To a 3 L round bottom flask was added DMF (1L), KTp (141.73 g, 0.560 mol) and this solution was allowed to stir while  $\text{Mo}(\text{CO})_6$  was added (132.8 g, 0.503 mol). The sides of the round bottom flask were then rinsed with 500 mL of DMF. This solution was allowed to heat to reflux (154 C) over a course of 90 minutes and the reaction mixture, a heterogeneous white-yellow solution, was refluxed over the course of one hour. The reaction mixture was then cooled to 100 C. While this was cooling a solution of  $\text{NaNO}_2$  (52.27 g, 0.757 mol) was added to a beaker of DI  $\text{H}_2\text{O}$  (300 mL) and allowed to stir. This solution was then added to the stirring solution of  $\text{DMF}/\text{MoTp}(\text{CO})_3^- \text{K}^+$ . A solution of glacial acetic acid was then added to a 150 mL addition funnel which was allowed to sit over the reaction mixture. The funnel was then opened to allow for addition of the acetic acid to the reaction mixture in a steady, dropwise manner (CAUTION! Evolution of CO!). After a course of 5-10 minutes all of the glacial acetic acid had been added and the reaction mixture had turned to a vibrant orange color. This solution was then allowed to heat at 100 C for 30 min before it was allowed to cool to room temperature. The heterogeneous orange reaction mixture was then added to 4 L of stirring DI  $\text{H}_2\text{O}$  in a 6 L Erlenmeyer flask. Upon addition an orange solid precipitates from solution. After adding all of the reaction mixture to the stirring water the reaction was filtered through a 2 L medium porosity frit to isolate a vibrant orange solid. This solid was then washed with DI  $\text{H}_2\text{O}$  (500 mL) followed by EtOH (3 x 500 mL) and  $\text{Et}_2\text{O}$  (3 x 1 L) to yield a vibrantly colored orange solid. The resulting solid was allowed to dry over the course of 24 h in a desiccator before a mass was taken (183.86 g, 92.5% yield). A  $^1\text{H}$  NMR was taken in acetone- $d_6$  and matches previously reported characterization.



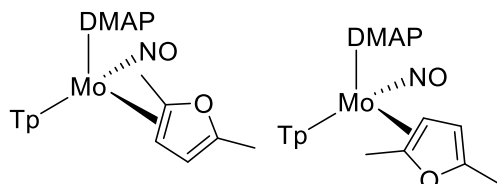
### Synthesis of TpMo(NO)(DMAP)(OTf) (1)



To a 4-dram vial with a stir pea was added THF (3 mL) followed by AgOTf (0.151 g, 0.587 mmol). To this solution was added MoTp(DMAP)(NO)(CO) (0.144 g, 0.293 mmol). Upon addition vigorous bubbling occurs ( $\text{CO}_{(g)}$  evolution) and over a period of ten minutes the reaction mixture turns to a dark emerald green solution. This solution was added to 25 mL of stirring,  $-30\text{ }^{\circ}\text{C}$  chilled pentane. Upon addition a vibrant green solid precipitates from solution. This mixture was then filtered through a medium 30 mL fritted disc and the resulting solid was washed with pentane (3 x 10 mL) to yield a dark green powder (0.272 g, 61.1%). The paramagnetic nature of the material prevented analysis by NMR spectroscopy.

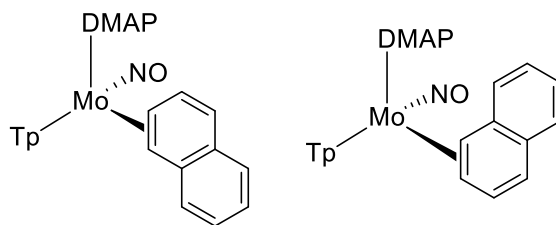
CV (DMA):  $E_{p,c} = -1.29\text{ V}$ ,  $E_{p,a} = +0.79\text{ V}$ . (NHE). IR,  $\nu_{\text{BH}} = 2492\text{ cm}^{-1}$ ,  $\nu_{\text{NO}} = 1618\text{ cm}^{-1}$ .

### Synthesis of TpMo(NO)(DMAP)( $\eta^2$ -2,3-2,5-dimethylfuran) (3)



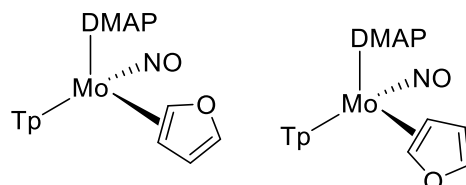
Chunks of 30-35% by mass Na dispersion in paraffin (6.59 g, 95.5 mmol) were added to a plastic weigh boat and were chopped into smaller pieces by applying pressure of a metal spatula. These smaller sodium pieces were then added to a 100 mL flask that had been pre-dried in an oven before being brought into the inert atmosphere glovebox. To this solution was added hexanes (50 mL) and the solution (a deep grey color) was allowed to stir overnight. After approximately 16 h of stirring the hexanes layer was decanted to reveal small flakes of cleaned sodium. The sodium was washed with THF ( $\sim 50\text{ mL}$ ) and allowed to stir for 5 min before the THF layer was decanted and a further 50 mL of THF was added followed by 2,5-dimethyl-furan (6.02 g, 62.6 mmol). The solution was allowed to stir and is a light yellow coloration. To this solution was added MoTp(NO)(DMAP)(I) (5.99 g, 10.2 mmol) and the initially heterogeneous green reaction mixture turns to a deep black color over the course of several minutes. After 2 h the reaction mixture, still a deep black, was evaluated by CV after an aliquot of the reaction mixture had been passed through a pipette-filled celite column and evaluated. An  $E_{p,a}$  of  $-350\text{ mV}$  was observed, indicative of the formation of a dihapto product and the bulk reaction mixture was then added to a 1 L filter flask and solvent was removed in vacuo until a dried, off-brown solid remains. To this solid was added MeOH ( $\sim 100\text{ mL}$ ) and upon addition vigorous bubbling occurs ( $\text{H}_{2(g)}$  evolution). The resulting solid was then filtered through a fine 30 mL fritted disc to yield a “goeey” yellow colored solid. This resulting solid was washed with MeOH (3 x 15 mL) followed by pentane (3 x 15 mL) before it was allowed to dry under dynamic vacuum for 2 h before a mass was taken of the yellow powder (5.69 g, 50%). Characterization has been reported previously.<sup>10</sup>

### Synthesis of TpMo(NO)(DMAP)( $\eta^2$ -naphthalene) (3)



A 4-dram vial was charged with Complex **10** (0.524 g, 0.863 mmol), THF (5 mL) and naphthalene (1.05 g, 8.25 mmol). This homogeneous brown mixture was capped and stirred at room temperature for 4 h. This reaction mixture was then slowly added to 50 mL of stirring pentane to evolve a golden yellow precipitate. The precipitate was then isolated on a 15mL fine porosity fritted disc, washed with chilled pentane (2 x 15 mL) and dried under static vacuum for 2 h to yield **3**. A golden-yellow solid was obtained (0.399 g, 78 %). Complex has been previously reported.<sup>10</sup>

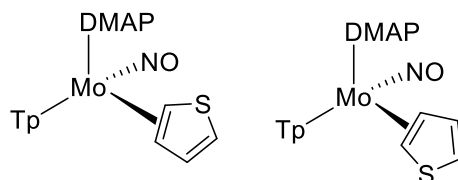
### Synthesis of TpMo(NO)(DMAP)( $\eta^2$ -2,3-furan) (**9**)



A 4-dram vial was charged with Complex **10** (0.486 g, 0.800 mmol), THF (3 mL) and furan (0.570, 8.37 mmol). This homogeneous red mixture was capped and stirred at room temperature for 3 h. This reaction mixture was then slowly added to 50 mL of stirring pentane to evolve a yellow precipitate. The precipitate was then isolated on a 15mL fine porosity fritted disc, washed with chilled pentane (2 x 15 mL) and dried under static vacuum for 2 h to yield **9**. A yellow solid was obtained (0.343 g, 81%).

Present in a 1 : 1 mix of isomers. CV:  $E_{p,a} = -0.38$  V. IR:  $\nu_{NO} = 1580$   $\text{cm}^{-1}$ ;  $\nu_{BH} = 2481$   $\text{cm}^{-1}$ .  $^1\text{H}$  NMR (acetone- $d_6$ ,  $\delta$ , 25 °C): 8.20 (d,  $J = 1.7$ , 1H, Tp 3/5), 7.92 (d,  $J = 2.1$ , 1H, Tp 3/5), 7.88 (d,  $J = 2.1$ , Tp 3/5), 7.86 (d,  $J = 2.1$ , 1H, Tp 3/5), 7.81 (bd,  $J = 5.7$ , 2H, DMAP 2/6), 7.26 (d,  $J = 1.3$ , 1H, Tp 3/5), 7.04, (d,  $J = 1.6$ , 1H, Tp 3/5), 7.64-7.59 (m, 3H, DMAP 3/5, furan H5), 6.33 (m, 1H, Tp 4), 6.25 (m, 1H, Tp 4), 6.16 (m, 2H, Tp 4, furan H4), 5.92 (t,  $J = 1.6$ , 1H, Tp 4), 5.77 (d,  $J = 4.5$ , 1H, furan H2), 3.67 (dd,  $J = 4.4, 2.8$ , 1H, furan H3), 3.07 (s, 6H, DMAP Me). (Minor isomer) 8.08 (d,  $J = 1.0$ , 1H, Tp 3/5), 7.91 (d,  $J = 1.9$ , 1H, Tp 3/5), 7.88 (d,  $J = 2.3$ , Tp 3/5), 7.86 (d,  $J = 2.1$ , 1H, Tp 3/5), 7.76 (bs, 2H, DMAP 2/6), 7.21 (d,  $J = 1.8$ , 1H, Tp 3/5), 7.03, (d,  $J = 1.5$ , 1H, Tp 3/5), 7.64-7.59 (m, 3H, DMAP 3/5, furan H5), 6.33 (m, 1H, Tp 4), 6.28 (d,  $J = 4.2$ , 1H, furan 2H), 6.25 (m, 2H, Tp 4, furan H4), 6.09 (m, 1H, Tp 4), 5.92 (t,  $J = 1.6$ , 1H, Tp 4), 3.21 (dd,  $J = 4.5, 2.8$ , 1H, furan H3), 3.07 (s, 6H, DMAP Me).  $^{13}\text{C}$ -NMR (acetone- $d_6$ ,  $\delta$ , 25 °C): (major isomer) 155.1 (DMAP-4), 151.0 (DMAP-2/6), 143.1 (Tp3/5), 142.6 (Tp3/5), 141.9 (Tp3/5), 139.2 (Tp3/5), 137.2 (Tp3/5), 136.3 (Tp3/5), 115.0 (furan H2), 108.1 (DMAP-3/5), 106.5 (Tp4), 106.3 (Tp4), 106.2 (Tp4), 677.3 (furan H3), 39.2 (NMe<sub>2</sub> methyl Cs). (Minor isomer): 155.1 (DMAP-4), 151.5 (DMAP-2/6), 143.4 (Tp3/5), 142.7 (Tp3/5), 142.0 (Tp3/5), 139.6 (Tp3/5), 137.0 (Tp3/5), 136.5 (Tp3/5), 115.6 (DMAP-3/5), 106.5 (Tp4), 106.4 (Tp4), 106.4 (Tp4), 66.3 (furan H2), 39.2 (NMe<sub>2</sub> methyl Cs).

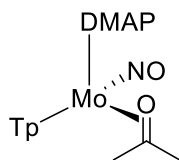
### Synthesis of MoTp(NO)(DMAP)( $\eta^2$ -2,3-thiophene) (**10**)



A 4-dram vial was charged with  $\text{TpMo(NO)(DMAP)(}\eta^2\text{-}\alpha,\alpha,\alpha\text{-trifluorotoluene)}$  (0.500 g, 0.823 mmol), THF (3 mL) and thiophene 0.690 g (8.37 mmol). This homogeneous dark red mixture was capped and stirred at room temperature for 3 h. This reaction mixture was then slowly added to 50 mL of stirring pentane to evolve a yellow precipitate. The precipitate was then isolated on a 15mL fine porosity fritted disc, washed with chilled pentane (2 x 10 mL) and dried under static vacuum for 2 h to yield **10**. A yellow solid was obtained (0.374 g, 83%).

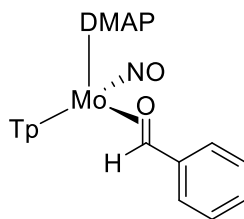
$^1\text{H-NMR}$  (acetone- $d_6$ ,  $\delta$ , 25 °C): (Mix of isomers) 8.45 (1H, d,  $J = 1.4$ , Tp 3/5), 8.09 (d,  $J = 1.9$ , 1H, Tp 3/5), 7.95 (d,  $J = 2.2$ , 2H, DMAP 2/6), 7.92 (d,  $J = 2.5$ , Tp3/5), 7.89 (d,  $J = 2.2$ , 1H, Tp 3/5), 7.85 (d,  $J = 2.3$ , 1H, Tp 3/5), 7.85 (d,  $J = 2.4$ , 1H, Tp 3/5), 7.80 (bs, 2H, DMAP 2/6), 7.45 (d,  $J = 2.3$ , 1H, Tp 3/5), 7.39 (d,  $J = 1.7$ , 1H, Tp 3/5), 7.00 (d,  $J = 2.1$ , 1H, Tp 3/5), 6.98 (d,  $J = 2.5$ , 1H, Tp 3/5), 6.71 (dd,  $J = 5.3, 2.6$ , 1H, thiophene H5), 6.65 (m, 4H, DMAP3/5), 6.46 (dd,  $J = 5.5, 2.9$ , 1H, thiophene H5), 6.33 (t,  $J = 1.6$ , 2H, Tp 4), 6.31 (t,  $J = 1.9$ , 2H, Tp 4), 6.18 (dd,  $J = 5.1, 1.5$ , 1H, thiophene H4), 6.16 (dd,  $J = 5.3, 1.3$ , 1H, thiophene H4), 6.14 (t,  $J = 2.0$ , 2H, Tp 4), 4.39 (d,  $J = 7.1$ , 1H, thiophene H2), 3.95 (dd,  $J = 7.2, 2.9$ , 1H, thiophene H3), 3.89 (dd,  $J = 6.9, 1.4$ , 1H, thiophene H3), 3.56 (dd,  $J = 6.9, 3.0$ , 1H, thiophene H3), 3.08 (s, 6H, DMAP Me), 3.08 (s, 6H, DMAP Me). CV:  $E_{p,a} = -0.38$  V. IR:  $\nu_{\text{NO}} = 1580$   $\text{cm}^{-1}$ ;  $\nu_{\text{BH}} = 2481$   $\text{cm}^{-1}$ .  $^{13}\text{C-NMR}$  ( $d^6$ -Acetone,  $\delta$ , 25 °C): (Mix of isomers): 155.2 (DMAP-4), 155.1 (DMAP-4), 150.9 (DMAP-2/6), 150.4 (DMAP-2/6), 143.6 (Tp3/5), 142.6 (Tp3/5), 142.4 (Tp3/5), 141.8 (Tp3/5), 141.8 (Tp3/5), 140.1 (Tp3/5), 135.9 (Tp3/5), 135.8 (Tp3/5), 137.3 (Tp3/5), 136.8 (Tp3/5), 136.6 (Tp3/5), 129.8 (H5), 129.4 (H5), 117.3 (H4), 117.2 (H4), 108.3 (DMAP-3/5 overlap), 106.7 (Tp4), 106.6 (Tp4), 106.4 (Tp4), 106.3 (Tp4), 106.3 (Tp4), 106.1 (Tp4), 79.6 (H2), 79.1 (H2), 77.3 (H3), 77.2 (H3), 39.1 (NMes methyl Cs overlap).

### Synthesis of $\text{TpMo(NO)(DMAP)(}\eta^2\text{-acetone)}$ (**11**)



A 4-dram vial was charged with  $\text{TpMo(NO)(DMAP)(}\eta^2\text{-}\alpha,\alpha,\alpha\text{-trifluorotoluene)}$  (0.543 g, 0.894 mmol), THF (4 mL) and acetone 0.500 g (8.61 mmol). This homogeneous dark red mixture was capped and stirred at room temperature for 3 h. This reaction mixture was then slowly added to 30 mL of stirring pentane to evolve a white precipitate. The precipitate was then isolated on a 15mL fine porosity fritted disc, washed with chilled pentane (2 x 10 mL) and dried under static vacuum for 2 h to yield **11**. A white solid was obtained (0.401 g, 86%). Complex has been previously reported.<sup>15</sup>

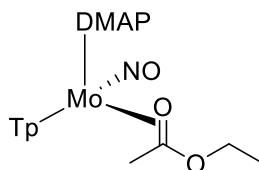
### Synthesis of $\text{TpMo(NO)(DMAP)(}\eta^2\text{-benzaldehyde)}$ (**15**)



A 4-dram vial was charged with Complex **10** (1.05 g, 1.72 mmol) and benzaldehyde 10.4 g (98.0 mmol). This homogeneous light green mixture was capped and stirred at room temperature for 10 minutes. This reaction mixture was then loaded onto a 60 mL coarse porosity fritted disc 2/3 full with silica gel. This column was washed with diethyl ether (50 mL) and the product was isolated using THF (100 mL). The green solution was evaporated *in vacuo* to 20 mL and added to chilled pentane (100 mL) yielding a white precipitate. This reaction mixture was then decanted to collect a white solid on a fine 15 mL frit. Some product had oiled out on the bottom of the filter flask, and this was re-dissolved in a minimal amount of THF (~5 mL) and then re-precipitated into ~ 50 mL of stirring pentane that had been chilled. A white precipitate was again isolated on a 15mL fine porosity fritted disc. The white product was then washed with chilled pentane (2 x 10 mL) and dried under static vacuum for 2 h to yield **15**. An off-white solid was obtained (0.518 g, 55%).

CV (THF)  $E_{p,a} = +0.40$  (NHE). IR:  $\nu(\text{BH}) = 2484 \text{ cm}^{-1}$ ,  $\nu(\text{NO}) = 1580 \text{ cm}^{-1}$ .  $^1\text{H NMR}$  (acetone- $d_6$ ,  $\delta$ , 25 °C): 7.95 (1H, d, Tp 3/5), 7.92 (1H, d, Tp3/5), 7.88 (1H, d, Tp3), 7.78 (2H, m, DMAP-2/6), 7.56 (1H, d, Tp3/5), 7.48 (1H, d, Tp3/5), 7.32 (1H, d, Tp3), 7.28 (2H, t,  $J = 7.84$ , H3 and H5), 7.19 (2H, d,  $J = 7.31$ , H2 and H6), 7.02 (1H, t of t,  $J = 7.25$ , 1.25, H4), 6.65 (2H, m, DMAP-3/5), 6.29 (1H, t, Tp4), 6.24 (1H, t, Tp4), 6.23 (1H, t, Tp4), 4.45 (1H, s, aldehyde H), 3.10 (6H, s, NMe).  $^{13}\text{C-NMR}$  (acetone- $d_6$ , 25 °C). 155.7 (DMAP-4), 151.63 (DMAP-2/6), 149.13 (C1), 143.5 (Tp3/5), 143.5 (Tp3/5), 141.9 (Tp3/5), 136.8 (Tp3/5), 136.6 (Tp3/5), 136.3 (Tp3/5), 127.7 (C3 and C5), 126.30 (C2 and C6), 125.4 (C4), 107.6 (DMAP B), 106.8 (Tp4), 106.3 (Tp4), 106.0 (Tp4), 98.1 (aldehyde carbonyl C), 39.2 (NMe methyl Cs). Calculated for  $\text{C}_{23}\text{H}_{26}\text{BMoN}_9\text{O}_2$ : C, 48.70; H, 4.62; N, 22.22. Found: C, 48.32; H, 4.63; N, 20.23. Calculated for  $4(\text{C}_{23}\text{H}_{26}\text{BMoN}_9\text{O}_2) \cdot \text{CH}_2\text{Cl}_2$ : C, 48.26; H, 4.93; N, 20.89.

### Synthesis of $\text{TpMo}(\text{NO})(\text{DMAP})(\eta^2\text{-ethyl acetate})$ (**12**)

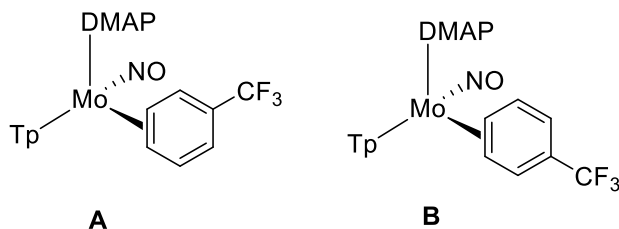


A 4-dram vial was charged with  $\text{TpMo}(\text{NO})(\text{DMAP})(\eta^2\text{-}\alpha,\alpha,\alpha\text{-trifluorotoluene})$  (0.490 g, 0.79 mmol), THF (3 mL) and ethyl acetate 0.730 g (8.29 mmol). This homogeneous dark red mixture was capped and stirred at room temperature for 3 h. This reaction mixture was then slowly added to 30 mL of stirring pentane to evolve a white precipitate. The precipitate was then isolated on a 15mL fine porosity fritted disc, washed with chilled pentane (2 x 10 mL) and dried under static vacuum for 2 h to yield **12**. An off-white solid was obtained (0.283 g, 64%).

CV(DMA):  $E_{p,a} = +0.72$  V. IR:  $\nu(\text{NO}) = 1540 \text{ cm}^{-1}$ ;  $\nu(\text{BH}) = 2487 \text{ cm}^{-1}$ .  $^1\text{H NMR}$  (acetone- $d_6$ ,  $\delta$ , 25 °C): 8.07 (1H, d, Tp 3/5), 8.02 (1H, d, Tp 3/5), 7.99 (1H, d, Tp3/5), 7.95 (1H, d, Tp 3/5), 7.62 (2H, m, DMAP 2/6), 7.61 (2H, m, DMAP 2/6), (1H, d, Tp 3/5), 7.09 (1H, d, Tp 3/5), 6.69 (2H, m, DMAP 3/5), 6.39 (1H, t, Tp 4), 6.34 6.39 (1H, t, Tp 4), 6.20 6.39 (1H, t, Tp 4), 3.84 (1H, m, EtOAc methylene), 3.77 (1H, m, EtOAc methylene),

3.00 (6H, s, DMAP NMe<sub>2</sub>), 1.20 (3H, t, *J* = 5.2, EtOAc Me), 0.78 (3H, s, EtOAc Me). <sup>13</sup>C NMR (acetone-*d*<sub>6</sub>, δ, 25 °C): 170.8 (carbonyl), 151.9 (DMAP 4), 151.6 (DMAP 2/6), 143.5 (Tp3/5), 143.2 (Tp3/5), 143.0 (Tp3/5), 137.0 (Tp3/5), 136.4 (Tp3/5), 136.1 (Tp3/5), 107.4 (DMAP 3/5), 107.0 (Tp4), 106.8 (Tp4), 106.3 (Tp4), 60.5 (ethyl group EtOAc), 39.0 (NMe methyls) 25.8 (methyl EtOAc), 16.7 (methyl EtOAc).

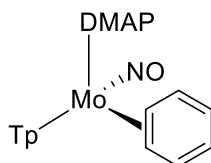
### Synthesis of MoTp(NO)(DMAP)(η<sup>2</sup>-3,4-trifluorotoluene) (12)



To an oven-dried 500 mL round bottom flask added a stir bir along with sodium dispersion (12 g, x mmol), hexanes (~ 200 mL) and let the reaction stir vigorously over a period of 3 h over which time silver flakes have formed in solution. Proceeded to decant off the grey hexanes layers then rinsed the remaining sodium with Et<sub>2</sub>O (25 mL) and decanted the clear organic layer. To the round bottom added trifluorotoluene (75 mL) along with Et<sub>2</sub>O (25 mL) before adding MoTp(NO)(DMAP)(I) (24.0 g, 40.6 mmol) and let the vivid green heterogeneous reaction mixture vigorously stir. Over a period of 6 h the reaction mixture turned from a heterogeneous green color to a heterogeneous brown/red coloration with the brown/red solid accumulating on the sides of the round bottom flask. The reaction mixture had been judged to have gone to completion by CV (*E*<sub>*p,a*</sub> develops at ~ -250 mV 100 mV/s). The reaction mixture was then poured into a 500 mL Erlenmeyer flask along with more Et<sub>2</sub>O (200 mL). Half of this heterogeneous red reaction mixture was then SLOWLY added to a stirring solution of MeOH (150 mL) in a 500 mL Erlenmeyer flask. Upon addition vigorous bubbling occurs (evolution of H<sub>2</sub>). The resulting red solid was then isolated on a fine 150 mL porosity fritted disc. The second half of the original reaction mixture in Et<sub>2</sub>O (~ 250 mL remains) was then added to a solution of stirring MeOH (150 mL) and the resulting solid from this analogous process was filtered through the same fine 150 mL porosity fritted disc to isolate a red solid. This solid was then washed with water (3 x 50 mL) followed by Et<sub>2</sub>O (5 x 100 mL) until a dried red solid is apparent on the fritted disc. This solid was allowed to dry under dynamic vacuum for 2 h before a mass was taken of the orange-red solid (17.35 g, 70.0 %).<sup>15</sup>

CV (DMAc) *E*<sub>*p,a*</sub> = -0.28 V (NHE). IR: ν<sub>BH</sub> = 2481 cm<sup>-1</sup>, ν<sub>NO</sub> = 1586 cm<sup>-1</sup>. Two coordination diastereomers A:B = 1:1 <sup>1</sup>H NMR (acetone-*d*<sub>6</sub>, δ, -30 °C): 8.17 (4H, buried broad s, DMAP-2/6 for A and B), 8.11 (2H, overlapping doublets, Tp3/5), 8.02(1H, d, Tp3/5), 8.01 (1H, d, Tp3/5), 7.95 (3H, m, Tp3/5), 7.84 (1H, d, Tp3/5), 7.58 (1H, d, Tp3/5), 7.57 (1H, d, Tp3/5), 7.46 (1H, d, *J* = 6.3, H2B), 7.12 (1H, dd, *J* = 9.1 and 6.2, H5A), 7.08 (1H, d, *J* = 5.8, H2A), 6.90 (1H, d, Tp3/5), 6.88 (1H, d, Tp3/5), 6.74 (4H, buried broad s, DMAP-3/5 for A and B), 6.70 (1H, dd, *J* = 9.1 and 6.2, H5B), 6.41 (3H, m, Tp4), 6.37 (1H, t, Tp4), 6.29 (1H, dd, *J* = 9.1 and 1.5, H6A), 6.25(1H, dd, *J* = 9.1 and 1.5, H6B), 6.15 (2H, m, Tp4), 3.71 (1H, dd, *J* = 8.5 and 6.2, H4B), 3.60 (1H, t, *J* = 7.3, H3A), 3.30 (1H, dd, *J* = 8.5 and 6.3, H4A), 3.14 (1H, t, *J* = 7.2, H3B), 3.09 (12H, s, NMe). <sup>13</sup>C NMR (acetone-*d*<sub>6</sub>, δ, -30 °C): 154.7 (DMAP-4), 150.2 (DMAP-4), 142.4(Tp3/5), 142.3 (Tp3/5), 142.0 (Tp3/5), 141.5 (2C, Tp3/5), 137.5 (2C, Tp3/5), 136.9 (Tp3/5), 136.8 (Tp3/5), 135.9 (4C, C6A & C2B, Tp3/5), 135.8 (2C, C1B & C1A), 135.2 (2C, C2A & C5B), 127.3 (q, *J* = 261.0, CF<sub>3</sub>), 125.5 (q, *J* = 261.0, CF<sub>3</sub>), 111.7 (C5A), 111.4 (C6B), 108.0 (4C, DMAP-3/5), 106.9 (3C, Tp4), 106.4 (3C, Tp4), 78.7 (C4B), 76.2 (C4A), 75.4 (C3A), 72.9 (C3B), 30.1 (NMe). <sup>19</sup>F NMR (acetone-*d*<sub>6</sub>, δ): -62.41. Calculated for C<sub>23</sub>H<sub>25</sub>BF<sub>3</sub>MoN<sub>9</sub>O: C, 45.49; H, 4.15; N, 20.76; F, 9.39. Found: C, 45.11; H, 4.34; N, 20.39; F, 9.05.

### Synthesis of TpMo(NO)(DMAP)(η<sup>2</sup>-benzene) (14)

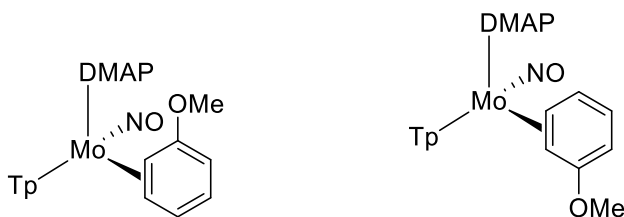


**14**

A 4-dram vial was charged with TpMo(NO)(DMAP)( $\eta^2$ - $\alpha,\alpha,\alpha$ -trifluorotoluene) (0.201 g, 0.328 mmol) and benzene that had been dried over sodium (9.98 g, 128 mmol). This mixture was capped and stirred at room temperature for 3 h. This mixture was then slowly added to a  $-60\text{ }^\circ\text{C}$  solution of pentane yielding a brown precipitate. The precipitate was then isolated on a 15mL fine porosity fritted disc, washed with pentane (3 x 10 mL) and desiccated to yield **13**. A golden-brown solid was obtained (0.072 g, 11.3 %).<sup>15</sup>

CV (THF:Benzenes 1:1, TBAH, 100 mV/s vs NHE):  $E_{p,a} = -0.55\text{ V}$ . IR,  $\nu_{\text{BH}} = 2459\text{ cm}^{-1}$ ,  $\nu_{\text{NO}} = 1563\text{ cm}^{-1}$ .  $^1\text{H}$  NMR (benzene- $d_6$ , 600 MHz,  $25\text{ }^\circ\text{C}$ ):  $\delta$  ppm 7.93 ppm (1H, d, Tp), 7.64 (1H, d, Tp), 7.55 (1H, d, Tp), 7.46 (1H, d, Tp), 7.08 (1H, d, Tp3/5), 7.07 (1H, d, Tp3/5), 6.03 (1H, t, Tp4), 5.88 (1H, t, Tp4), 5.69 (1H, t, Tp4), 2.06 (s, 6H, NMe<sub>s</sub>).

#### Synthesis of MoTp(NO)(DMAP)(5,6- $\eta^2$ -anisole) (**15**)



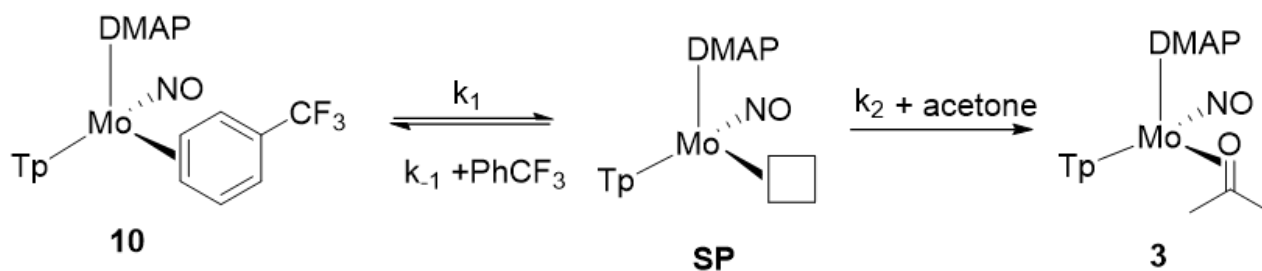
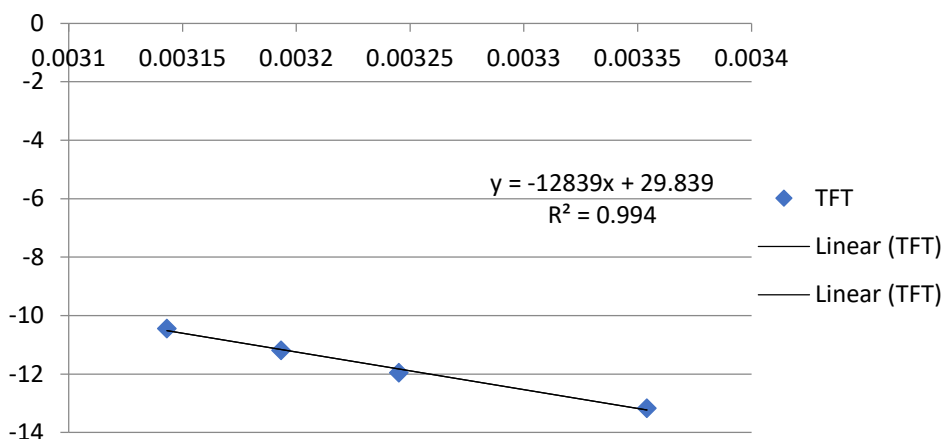
**15A**

**15B**

A 4-dram vial was charged with MoTp(NO)(DMAP)( $\eta^2$ - $\alpha,\alpha,\alpha$ -trifluorotoluene) (0.250 g, 0.410 mmol) and anisole (11.11 g, 103 mmol). This mixture was capped and stirred at room temperature for 3 h. This mixture was then slowly added to a  $-60\text{ }^\circ\text{C}$  solution of pentane yielding a yellow precipitate. The precipitate was then isolated on a 15mL fine porosity fritted disc, washed with pentane (3 x 10 mL) and desiccated to yield **14**. A yellow solid was obtained (0.032 g, 13.68 %).

CV (THF, TBAH, 100 mV/s vs NHE):  $E_{p,a} = -0.32\text{ V}$ . IR,  $\nu_{\text{BH}} = 2472\text{ cm}^{-1}$ ,  $\nu_{\text{NO}} = 1566\text{ cm}^{-1}$ . Two coordination diastereomers **A**:**B** = 2:1.  $^1\text{H}$ -NMR (acetone- $d_6$ , 600 MHz,  $-30\text{ }^\circ\text{C}$ ):  $\delta$  8.05 (2H, overlapping, Tp3/5), 8.04 (2H, overlapping doublets, Tp3/5), 7.95 (2H, overlapping, Tp3/5), 7.89 (2H, overlapping, Tp3/5), 7.52 (1H, d, Tp3/5 for **A**), 7.49 (1H, d, Tp3/5 for **B**), 6.60 (2H, broad, DMAP B for **A**), 6.50 (2H, overlapping, H4 for **A** and **B**), 6.38 (2H, overlapping, Tp4), 6.43 (1H, t, Tp4 for **A**), 6.24 (1H, t, Tp4 for **B**), 6.12 (4H, Tp4 and H3 for **A** and **B**), 5.42 (1H, d,  $J = 6.71$ , H2**B**), 5.36 (1H, d,  $J = 6.55$ , H2**A**), 3.70 (1H, m, H5**B**), 3.63 (3H, s, OMe for **B**), 3.50 (1H, d,  $J = 9.70$  H2**A**), 3.46 (3H, s, OMe**A**), 3.33 (1H, m, H5**A**), 3.20 (1H, m, H6**B**), 3.07 (6H, s, NMe**sB**), 3.06 (6H, s, NMe**sA**).

## Eyring Plot for the Substitution of MoTp(NO)(DMAP)( $\eta^2$ -trifluorotoluene) to MoTp(NO)(DMAP)( $\eta^2$ -acetone)



$$\frac{d[\mathbf{3}]}{dt} = k_{\text{obs}}[\mathbf{10}] \quad \text{where} \quad k_{\text{obs}} = \frac{k_1 k_2 [\text{acetone}]}{k_{-1}[\text{PhCF}_3] + k_2 [\text{acetone}]}$$

Surveying the  $k_{\text{rate}}$  dependence on temperature over a range of 25 °C to 45 °C allowed for the generation of an Eyring Plot (included in the Experimental Section). Analysis of this data yields  $\Delta H^\ddagger = 25.5 \pm 1.4$  kcal/mol a  $\Delta S^\ddagger = 12.1 \pm 4.5$  eu for the substitution process of the molybdenum-PhCF<sub>3</sub> complex **10** to the molybdenum-acetone complex **3**. These data support a largely dissociative mechanism where the rate determining step is the dissociation of the PhCF<sub>3</sub> ligand.

## References

1. Liebov, B. K.; Harman, W. D., Group 6 Dihapto-Coordinate Dearomatization Agents for Organic Synthesis. *Chemical Reviews* **2017**, *117* (22), 13721-13755.
2. Shivokevich, P. J.; Myers, J. T.; Smith, J. A.; Pienkos, J. A.; Dakermanji, S. J.; Pert, E. K.; Welch, K. D.; Trindle, C. O.; Harman, W. D., Enantioenriched Molybdenum Dearomatization: Dissociative Substitution with Configurational Stability. *Organometallics* **2018**, *37* (23), 4446-4456.
3. Lis, E. C.; Salomon, R. J.; Sabat, M.; Myers, W. H.; Harman, W. D., Synthesis of 1-Oxadecalins from Anisole Promoted by Tungsten. *Journal of the American Chemical Society* **2008**, *130* (37), 12472-12476.
4. Wilson, K. B.; Myers, J. T.; Nedzbala, H. S.; Combee, L. A.; Sabat, M.; Harman, W. D., Sequential Tandem Addition to a Tungsten–Trifluorotoluene Complex: A Versatile Method for the Preparation of Highly Functionalized Trifluoromethylated Cyclohexenes. *Journal of the American Chemical Society* **2017**, *139* (33), 11401-11412.
5. Wilson, K. B.; Smith, J. A.; Nedzbala, H. S.; Pert, E. K.; Dakermanji, S. J.; Dickie, D. A.; Harman, W. D., Highly Functionalized Cyclohexenes Derived from Benzene: Sequential Tandem Addition Reactions Promoted by Tungsten. *The Journal of Organic Chemistry* **2019**, *84* (10), 6094-6116.
6. Meiere, S. H.; Keane, J. M.; Gunnoe, T. B.; Sabat, M.; Harman, W. D., Binding and Activation of Aromatic Molecules by a Molybdenum  $\pi$ -Base. *Journal of the American Chemical Society* **2003**, *125* (8), 2024-2025.
7. Mocella, C. J.; Delafuente, D. A.; Keane, J. M.; Warner, G. R.; Friedman, L. A.; Sabat, M.; Harman, W. D., Coordination Chemistry and Properties of Unusually  $\pi$ -Basic Molybdenum Fragments. *Organometallics* **2004**, *23* (16), 3772-3779.
8. Dakermanji, S. J.; Smith, J. A.; Westendorff, K. S.; Pert, E. K.; Chung, A. D.; Myers, J. T.; Welch, K. D.; Dickie, D. A.; Harman, W. D., Electron-Transfer Chain Catalysis of  $\eta^2$ -Arene,  $\eta^2$ -Alkene, and  $\eta^2$ -Ketone Exchange on Molybdenum. *ACS Catalysis* **2019**, *9* (12), 11274-11287.
9. Myers, J. T.; Shivokevich, P. J.; Pienkos, J. A.; Sabat, M.; Myers, W. H.; Harman, W. D., Synthesis of 2-Substituted 1,2-Dihydronaphthalenes and 1,2-Dihydroanthracenes Using a Recyclable Molybdenum Dearomatization Agent. *Organometallics* **2015**, *34* (14), 3648-3657.
10. Myers, J. T.; Dakermanji, S. J.; Chastanet, T. R.; Shivokevich, P. J.; Strausberg, L. J.; Sabat, M.; Myers, W. H.; Harman, W. D., 4-(Dimethylamino)pyridine (DMAP) as an Acid-Modulated Donor Ligand for PAH Dearomatization. *Organometallics* **2017**, *36* (3), 543-555.
11. Wertjes, W. C.; Southgate, E. H.; Sarlah, D., Recent advances in chemical dearomatization of nonactivated arenes. *Chemical Society Reviews* **2018**, *47* (21), 7996-8017.
12. Meiere, S. H.; Brooks, B. C.; Gunnoe, T. B.; Sabat, M.; Harman, W. D., A Promising New Dearomatization Agent: Crystal Structure, Synthesis, and Exchange Reactions of the Versatile Complex  $\text{TpRe}(\text{CO})(1\text{-methylimidazole})(\eta^2\text{-benzene})$  (Tp = Hydridotris(pyrazolyl)borate). *Organometallics* **2001**, *20* (6), 1038-1040.
13. Harman, W. D.; Taube, H., Reactivity of pentaammineosmium(II) with benzene. *Journal of the American Chemical Society* **1987**, *109* (6), 1883-1885.
14. Lawrance, G. A., Coordinated trifluoromethanesulfonate and fluorosulfate. *Chemical Reviews* **1986**, *86* (1), 17-33.
15. Myers, J. T.; Smith, J. A.; Dakermanji, S. J.; Wilde, J. H.; Wilson, K. B.; Shivokevich, P. J.; Harman, W. D., Molybdenum(0) Dihapto-Coordination of Benzene and Trifluorotoluene: The Stabilizing and Chemo-Directing Influence of a  $\text{CF}_3$  Group. *Journal of the American Chemical Society* **2017**, *139* (33), 11392-11400.



16. Welch, K. D.; Harrison, D. P.; Lis, E. C.; Liu, W.; Salomon, R. J.; Harman, W. D.; Myers, W. H., Large-Scale Syntheses of Several Synthons to the Dearomatization Agent  $\{\text{TpW}(\text{NO})(\text{PMe}_3)\}$  and Convenient Spectroscopic Tools for Product Analysis. *Organometallics* **2007**, *26* (10), 2791-2794.
17. Bengali, A. A., Observation of the  $(\eta^5\text{-C}_5\text{H}_5)\text{Mn}(\text{CO})_2(\text{toluene})$  Complex by Low-Temperature IR Spectroscopy and Determination of the Manganese–Toluene Bond Strength. *Organometallics* **2000**, *19* (19), 4000-4003.
18. Margulieux, G. W.; Bezdek, M. J.; Turner, Z. R.; Chirik, P. J., Ammonia Activation, H<sub>2</sub> Evolution and Nitride Formation from a Molybdenum Complex with a Chemically and Redox Noninnocent Ligand. *Journal of the American Chemical Society* **2017**, *139* (17), 6110-6113.
19. Meiere, S. H.; Valahovic, M. T.; Harman, W. D., Strategy for the Resolution of a Chiral Dearomatization Agent:  $\{\text{TpRe}(\text{CO})(1\text{-methylimidazole})\}$  Coordination of  $\alpha$ -Pinene (Tp = Hydridotris(pyrazolyl)borate). *Journal of the American Chemical Society* **2002**, *124* (50), 15099-15103.
20. Wilde, J. H.; Smith, J. A.; Dickie, D. A.; Harman, W. D., Molybdenum-Promoted Synthesis of Isoquinuclidines with Bridgehead CF<sub>3</sub> Groups. *Journal of the American Chemical Society* **2019**, *141* (47), 18890-18899.

## **Chapter 6**

# **Dearomatization of Electron Deficient Arenes with Group 6 Dearomatization Agents**

## 6.1 Introduction

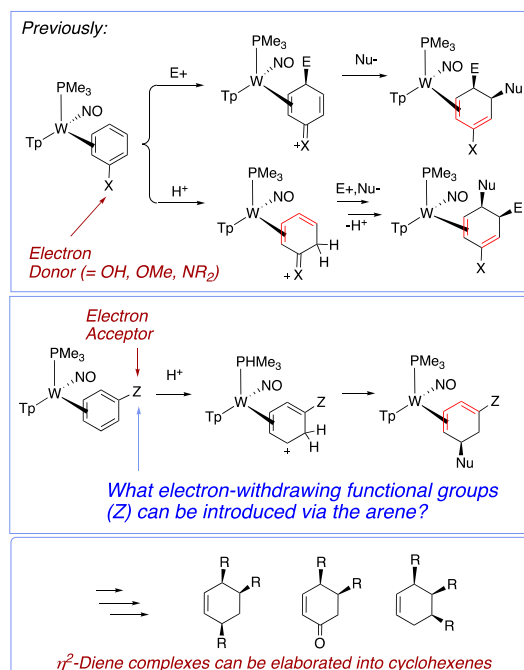
The binding of aromatic molecules to a transition-metal can enable a wide array of chemical transformations, often inaccessible by other means. Over the past several decades, our research group has endeavored to explore how transition-metal complexes can activate aromatic molecules toward new organic transformations through their coordination to just two carbons ( $\eta^2$ ).<sup>1-3</sup> Most of these studies concerning benzene have focused on anisoles,<sup>4-6</sup> phenols,<sup>7-9</sup> anilines,<sup>7, 10-11</sup> and other arenes bearing a single  $\pi$ -donor group. In this situation, the metal and heteroatom substituent act together to render the arene susceptible to protonation and electrophilic addition (**Scheme 6.1**).

Until recently, it was thought that although arenes with electron-withdrawing groups are better  $\pi$ -acids, they would be inferior as  $\eta^2$ -aromatic substrates for organic reactions since this type of substituent and the electron-

donating metal are at cross-purposes. Despite this apparent contradiction in effects, we recently showed that when bound {WTp(NO)(PMe<sub>3</sub>)},  $\alpha,\alpha,\alpha$ -trifluorotoluene was capable of being protonated by strong acid.<sup>12</sup> The electron-withdrawing

CF<sub>3</sub> group polarizes the arene in such a way that protonation occurs selectively at an ortho carbon. Nucleophiles are then selectively directed to the adjacent carbon of the corresponding  $\eta^2$ -arenium complex. The resulting diene is electronically complementary to  $\eta^2$ -diene complexes prepared from electron-rich arenes and can be elaborated

further into novel trisubstituted cyclohexenes (**Scheme 6.1**).<sup>12</sup>



**Scheme 6.1.** The incorporation of functional groups into cyclohexenes via a benzene precursor

The potential for organic transformations of  $\eta^2$ -arenes with electron-withdrawing substituents has prompted us to evaluate the scope and binding selectivity of arenes that can be coordinated by the {W Tp(NO)(PMe<sub>3</sub>)} and {Mo Tp(NO)(DMAP)} systems. Of note,  $\eta^2$ -arene complexes are still exceedingly rare; besides the trifluorotoluene complex of these systems,<sup>13</sup> the only other reported examples of  $\eta^2$ -benzene complexes in which the arene has a single EWG are pentaammineosmium(II) complexes of trifluorotoluene (TFT), benzophenone, and 2,2-dimethylpropiophenone (DMPP).<sup>14</sup>

## 6.2 Studies of $\pi$ -EWGs on Benzenes and Molybdenum and Tungsten Fragments

Various benzenes bearing a single electron-withdrawing group (Z) were surveyed for their potential coordination to either {Mo Tp(DMAP)(NO)} or {W Tp(PMe<sub>3</sub>)(NO)} fragments. The complexes Mo Tp(DMAP)(NO)(TFT) (**1**) and W Tp(PMe<sub>3</sub>)(NO)(benzene) (**2**) serve as synthons to these fragments.

In many of these cases, the EWG itself often proved to be a superior position for coordination, and DFT results (M06; hybrid LANL2DZ, 6-31G(d,p) basis set; in vacuum) supporting this notion are summarized in **Table 6.1**. For benzaldehyde, benzonitrile, methyl benzoate and even the bulky ketone 2,2-dimethylpropiophenone, these calculations indicate that binding at the substituent is heavily favored over

|   |                         |                              |
|---|-------------------------|------------------------------|
|   |                         |                              |
| <b>3A:</b> M = Mo, L = DMAP 18.1 (17.8)               | <b>3B:</b> 18.8 (17.8)  | <b>3C:</b> 38.0 (34.5)       |
| <b>4A:</b> M = W, L = PMe <sub>3</sub> , 23.7 (23.9)  | <b>4B:</b> 20.7 (22.4)  | <b>4B:</b> 46.6 (44.4)       |
|   |                         |                              |
| <b>5A:</b> M = Mo, L = DMAP 17.3 (16.5)               | <b>5B:</b> 18.1(15.3)   | <b>5C:</b> 25.8 (20.4)       |
| <b>6A:</b> M = W, L = PMe <sub>3</sub> , 23.3 (22.1)  | <b>6B:</b> 21.2 (22.1)  | <b>6C:</b> 35.0 (26.1)       |
|   |                         |                              |
| <b>7A:</b> M = Mo, L = DMAP 17.7 (16.4)               | <b>7B:</b> 18.5 (15.6)  | <b>7C:</b> 20.3 (19.8)       |
| <b>8A:</b> M = W, L = PMe <sub>3</sub> , 23.0 (22.9)  | <b>8B:</b> 22.1 (21.4)  | <b>8C:</b> 29.4 (30.3)       |
|   |                         |                              |
| <b>9A:</b> M = Mo, L = DMAP 17.5 (16.6)               | <b>9B:</b> 19.0 (17.4)  | <b>10C:</b> 17.9 (15.5)      |
| <b>10A:</b> M = W, L = PMe <sub>3</sub> , 22.6 (22.8) | <b>10B:</b> 22.2 (22.9) | <b>10C:</b> 27.2 (19.4)      |
|   |                         |                              |
| <b>11A:</b> M = Mo, L = DMAP 18.6 (18.0)              | <b>11B:</b> 19.8 (18.0) | <b>11C:</b> 30.6 (27.8) 23.4 |
| <b>12A:</b> M = W, L = PMe <sub>3</sub> , 23.4 (23.4) | <b>12B:</b> 25.8 (23.3) | <b>12C:</b> 40.7 (38.6) 33.1 |

**Table 6.1.** DFT calculations of relative binding energies for electron-deficient benzenes. (Gibbs free energies;kcal/mol)

coordination in the arene. Thus, formation of a purported  $\eta^2$ -benzene complex would need to rely on kinetic trapping of this isomer.

A case in point, while benzonitrile forms the  $\eta^2$ -nitrile complex exclusively upon addition to **1**, when PhCN is allowed to react with tungsten complex **1**, multiple isomers are formed of WTp(NO)(PMe<sub>3</sub>)( $\eta^2$ -PhCN). After elution through a silica column, *five dihapto-coordinate isomers are formed, all of which feature the tungsten bound to two of the aromatic carbons*. Of these five species, the two major species show resonances consistent with  $\eta^2$ -arene formation where the metal is bound to the 3,4-carbons. The major isomer shows five ring resonances at 7.74, 6.88, 5.67, 4.00, and 2.14 ppm which favorably compare with the known complex WTp(NO)(PMe<sub>3</sub>)( $\eta^2$ -3,4-PhCF<sub>3</sub>) (cf., 7.50, 6.87, 6.03, 3.95, and 2.30 ppm). These signals persist over several hours in solution indicating the remarkable kinetic stability of the  $\eta^2$ -arene isomers.

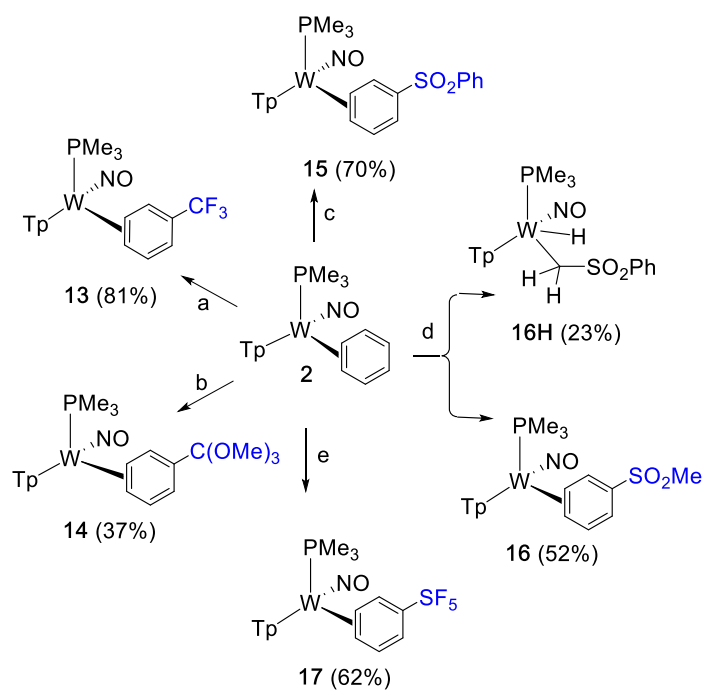
Two other isomers observed that feature isomers bound to the tungsten are those of the 2,3-carbons. A final isomer is observed where the tungsten is bound in a dihapto-fashion to the 1,2-carbons, where the -CN group is located on the carbon distal to the phosphine ligand and is directed toward the TpA and TpB ligands. Although severe spectral overlap and the low population of several isomers (notably those proposed to be where the metal is bound in 2,3-position and the single isomer where the tungsten is bound to the 1,2-positions) preclude unambiguous determination, <sup>1</sup>H and <sup>13</sup>C data are provided where clear distinctions can be made. Credit is given to Spenser Simpson for the characterization and synthesis of the tungsten-benzonitrile complex.

### 6.3 Benzenes with Sulfur-Based EWGs

Given the large energetic preferences for coordination across the bonds of the nitrile and carbonyl double bonds (**4**, **6**, **8**, **10**, **12**); 10-20 kcal/mol), (**Table 6.1**), We decided to explore benzenes, which had an EWG that did not have well-formed  $\pi$ -bonds (**Scheme 6.2**). Stirring a solution of benzene complex **2** and an excess of the target arene resulted in formation of several new dihapto-coordinate arene complexes of the form WTp(NO)(PMe<sub>3</sub>)( $\eta^2$ -arene), where arene = trimethyl o-benzoate (**14**), methyl phenyl sulfone (**16**), diphenyl

sulfone (**15**), and phenylsulfur pentafluoride (**17**). Despite the strongly electron-withdrawing substituents, these complexes were formed with minimal oxidative decomposition. In most cases the metal complex was isolated as a mixture of two coordination diastereomers in which the metal bound to the C3/C4 carbons of the aromatic.

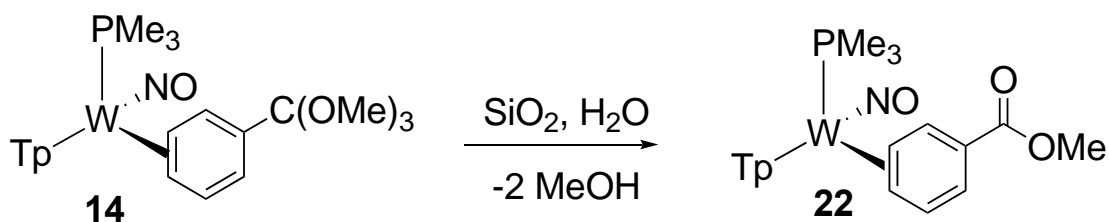
The reaction mixture resulting from methyl phenyl sulfone contained a third species, which we tentatively assign as the sulfonyl hydride **16H**. Key features in the  $^1\text{H}$  NMR spectrum include a diastereotopic methylene group at 3.14 and 1.88 ppm, and a matching hydride signal at 9.03 ppm with a large  $J_{\text{PH}} = 114.9$  Hz and tungsten-183 satellites ( $J_{\text{WH}} = 9.3$  Hz). While DFT calculations suggested that in some cases the 2,3- $\eta^2$  arene isomers were energetically competitive (**Table 6.1**), in no case were they conclusively identified. Judging from IR and electrochemical data, the sulfur analogs ( $\text{SO}_2\text{Ph}$ ; **15**,  $\text{SO}_2\text{Me}$ ; **16**,  $\text{SF}_5$ ; **17**) appear to have a stronger metal-arene backbonding interaction for **15-17**, compared to **2**, **13**, or **14**. An increase in  $E_{p,a}$  for  $\text{W}(0) \rightarrow \text{W}(\text{I})$  (100 mV/s), and an increase in NO stretch frequency in the infrared absorption spectrum further support this notion (**Table 6.2**).



**Scheme 6.2.** Dearomatization of electron-deficient arenes promoted by tungsten.

## 6.4 Accessing EWGs with $\pi$ -Bonds

During our attempts to purify the ortho-benzoate complex **14**, hydrolysis occurred on silica, and the resulting *C,C*- $\eta^2$ -benzoate ester, **22**, was recovered. This provided a rare example of a dihapto-coordinated arene with a  $\pi$ -withdrawing group (**Equation 6.1**). We note that metal coordination to the ester functionality is thermodynamically favored by roughly 8 kcal/mol, compared to dihapto-coordination of the aromatic ring. However, once the metal is bound to the aromatic, the rate of arene-to-ester isomerization is sufficiently slow that none of the carbonyl-bound complex is observed in solution, even after several hours. Said another way, the barrier to isomerization from the aromatic ring to the ester functionality is sufficiently high that no  $\eta^2$ -ester isomer is observed to develop over several hours. In most aspects, compound **22** is similar to the other monosubstituted arene complexes **13-17**, where the 3,4- $\eta^2$ - and 4,5- $\eta^2$ - isomers dominate.

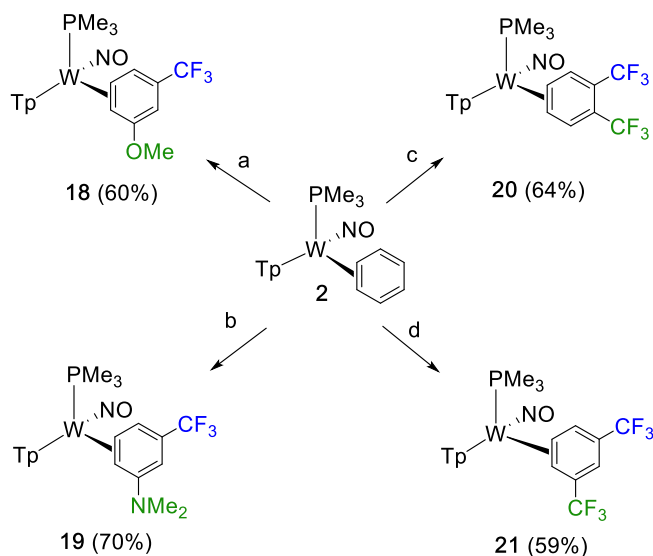


**Scheme 6.3.** The formation of an arene-bound benzoate complex (**22**).

## 6.5 Substituted Trifluoromethylated Benzenes

We next questioned how an  $\eta^2$ -complex of benzene bearing an electron withdrawing group would be influenced by an additional benzene substituent (**Scheme 6.4**). Thus, we examined a family of trifluorotoluene derivatives with a methoxy- (**18**), dimethylamino- (**19**), or trifluoromethyl -(**21**), group at the 3-position. In addition, we examined one case of a 1,2-disubstituted arene (**20**; **Figure 6.1**). For cases where the second substituent was a  $\pi$ -donor, the metal was directed to the 4,5 position, exclusively, although these complexes (**18**, **19**) were both isolated as two different coordination diastereomers. In contrast, for the case

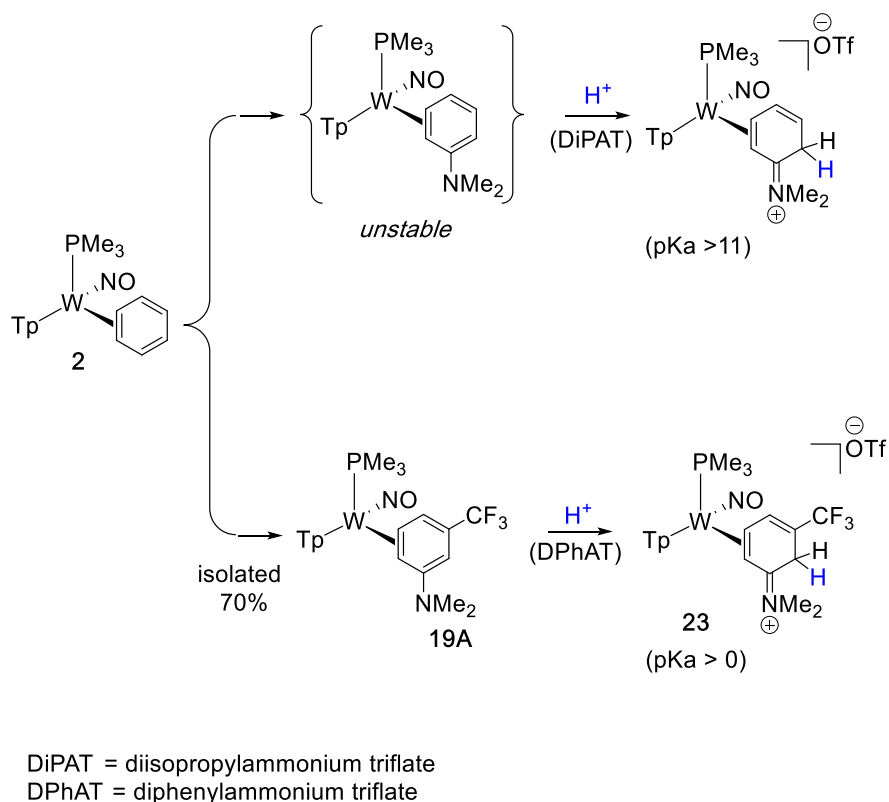
of the bis(trifluoromethyl)benzene complexes (**21**, **22**), symmetry of the arene results in isolation of a single diastereomer (as a racemic mixture).



**Scheme 6.4.** Trifluorotoluene complexes with an additional substituent.

Combining **2** and 3-(trifluoromethyl)-*N,N*-dimethylaniline, which was prepared by a modified literature procedure,<sup>18</sup> resulted in the synthesis of **19**. The stability of this compound is in contrast to that prepared from *N,N*-dimethylaniline, which is too unstable to isolate. In the latter case, the aniline ligand must be “trapped” as an  $\eta^2$ -2H-anilinium complex (**Scheme 6.5**) by the action of a weak acid.<sup>11</sup> The ability then to isolate **19** in its neutral form shows the ability of the  $-\text{CF}_3$  group to enhance the  $\pi$ -acceptor capability of a substituted arene. This complex can be subsequently protonated under moderately acidic conditions to yield **23** as a single isomer. This compound has spectroscopic features similar to those of the previously observed complex  $[\text{W}(\text{PMe}_3)(\text{NO})(\eta^2\text{-N,N-dimethyl-2H-anilinium})]\text{OTf}$  (**Scheme 6.5**).<sup>11</sup>





**Scheme 6.5.** Preparation of 3-(trifluoromethyl)-N,N-dimethylaniline complex **19** and its protonation to give the tungsten-anilinium **23** as a single coordination diastereomer.

## 6.6. Properties of Electron Deficient Benzenes on {W Tp(NO)(PMe<sub>3</sub>)}

When **2** was dissolved in a DME solution of nitrobenzene, oxidation of the metal occurs rapidly, resulting in the free aromatic and uncharacterized paramagnetic materials. Cationic benzene derivatives such as trimethylanilinium iodide, triethylanilinium iodide or trityl triflate, when combined with **2** resulted in reaction mixtures that showed encouraging signs of dihapto-coordination. <sup>1</sup>H NMR spectroscopy supported the formation of small amounts of dihapto-coordinate products but

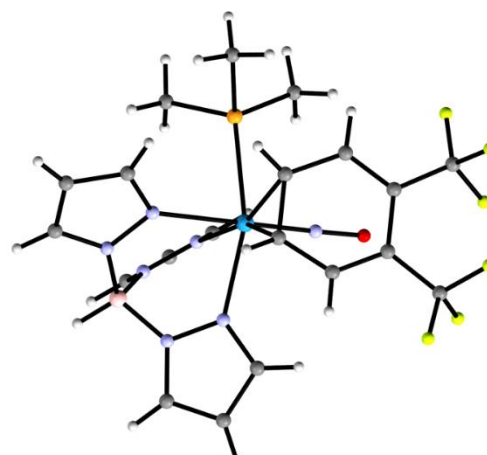
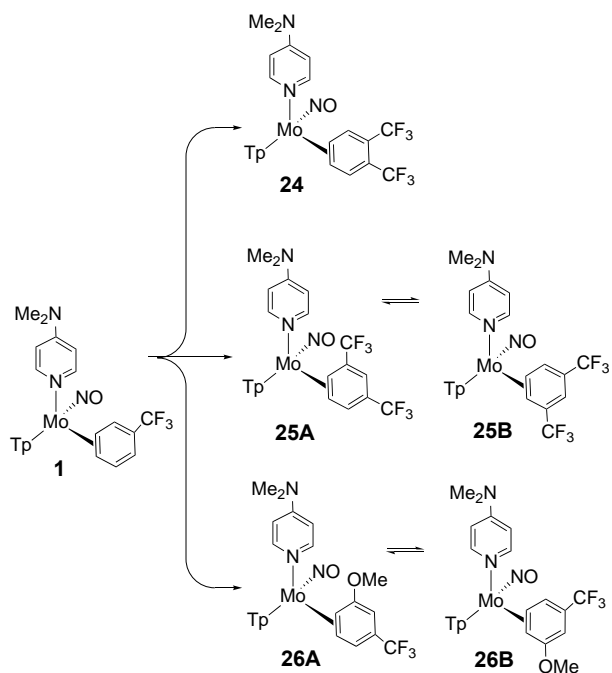


**Figure 6.1.** SC-XRD molecular structure determination for the 1,2-bis(trifluoromethyl)benzene complex **20**.

difficulties in purification and low yields of the desired products dissuaded us from pursuing of these

complexes further. Other arenes bearing a single electron-withdrawing group that did not give satisfactory results included PhOCF<sub>3</sub>, PhCCl<sub>3</sub>, and PhSCF<sub>3</sub>. A summary of all new η<sup>2</sup>-arene complexes for the WTp(NO)(PMe<sub>3</sub>) system appears in **Table 6.2**.

Turning our attention to the weaker π-base {MoTp(NO)(DMAP)}, the complex MoTp(NO)(DMAP)(η<sup>2</sup>-α,α,α,-trifluorotoluene) (**10**) can be prepared from the precursor



**Scheme 6.6.** Preparation of several derivatives of a molybdenum trifluorotoluene complex.

without the need for chromatography as an analytically pure red powder.<sup>13</sup> We found this complex to be an efficient precursor to several trifluoromethylated aromatic ligands (**Scheme 6.6; Figure 6.2**).

## 6.7 Dihapto-Coordination of Aryl Halides.

The ability of the tungsten complex {WTp(NO)(PMe<sub>3</sub>)} to form complexes with aryl halides has been largely unsuccessful. Reactions with iodobenzene, bromobenzene, and chlorobenzene all result in intractable mixtures of paramagnetic materials. Only in the case of fluorinated arenes have well-defined reactions been observed. For fluorobenzene itself, a clean oxidative addition product, WTp(NO)(PMe<sub>3</sub>)(F)(Ph), was observed in a matter of minutes at ambient temperature.<sup>19</sup> In contrast, stable arene complexes were realized for 1-fluoronaphthalene, as well as WTp(NO)(PMe<sub>3</sub>)(C<sub>6</sub>F<sub>6</sub>).<sup>19</sup> We questioned if the molybdenum fragment, {MoTp(NO)(DMAP)}, which is more tempered in its π-basicity than its tungsten analog, might allow for a stable dihapto-coordinated arene complex. Additionally, we hoped that additional fluorines would lower the energy of the π\* orbitals of the arene and strengthen the Mo-arene backbonding interaction.

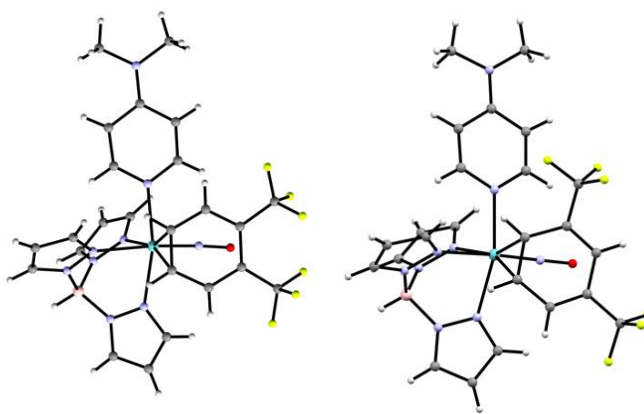
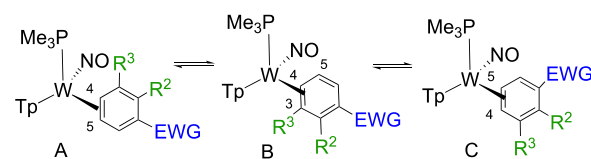


**Figure 6.2.** SC-XRD molecular structure determination for the bis(trifluoromethyl)benzene complexes **24** and **25A**.

Gratifyingly, while {WTP(NO)(PMe<sub>3</sub>)} undergoes oxidative addition of most fluorobenzenes, the {MoTp(DMAP)(NO)} fragment successfully binds fluorobenzene, o-, m-, and p- difluorobenzene, and various tetrafluorotoluenes in a dihapto fashion (**Scheme 6.7**).<sup>20</sup> These compounds constitute rare examples of dihapto-coordinated fluorobenzenes, where the arene is not exhaustively fluorinated, in which C-H or C-F insertion does not pre-empt formation of stable  $\eta^2$ -arene complexes.<sup>21-26</sup> In no case were there any spectroscopic indications of either aryl hydride or aryl fluoride formation in the analysis of complexes **27-29**. Yields and synthetic procedures were analogous to those employed for the tungsten fragment, and details are provided in the experimental section.

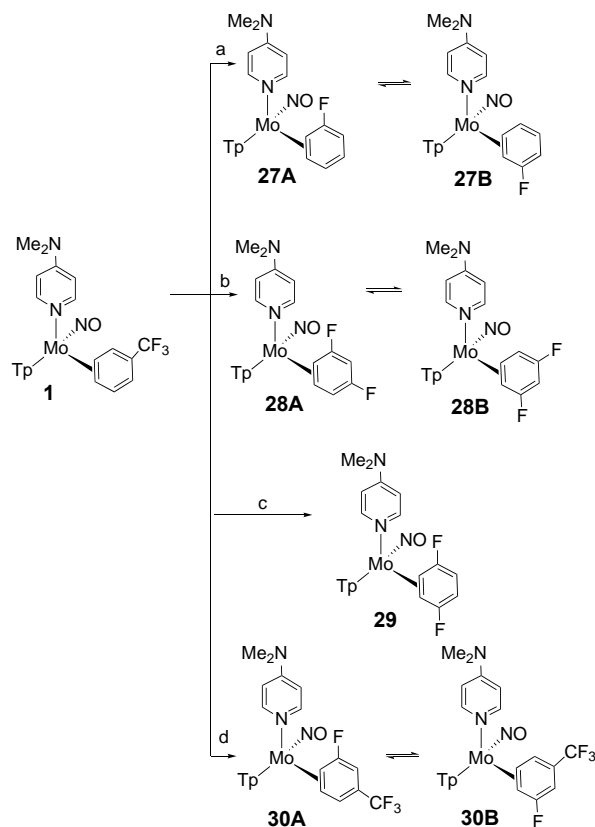
Fluorobenzene reacts with the TFT complex **1** to provide two isomers of the fluorobenzene complex, **27A** and **27B** in a 1:1 ratio, and this compound can be isolated by precipitation into cold pentane (-60 °C). Electrochemical ( $E_{p,a} = -0.36$  V), IR( $\nu_{\text{NO}} = 1573$  cm<sup>-1</sup>), and NMR data (<sup>13</sup>C, <sup>1</sup>H, <sup>19</sup>F) support the presence of dihapto-coordinated arene complexes.<sup>27</sup> Well resolved resonances for the arene protons



| Cpd | EWG                 | R <sup>2</sup>  | R <sup>3</sup>   | cdr<br>A:B:C | IR ( $\nu_{\text{NO}}$ )<br>(cm <sup>-1</sup> ) | CV ( $E_{p,a}$ )<br>(V, NHE) |
|-----|---------------------|-----------------|------------------|--------------|---|------------------------------|
| 2   | H                   | H               | H                | NA : NA : NA | 1564  | -0.13                        |
| 13  | CF <sub>3</sub>     | H               | H                | NA : 5 : 4   | 1575  | 0.06                         |
| 14  | C(OMe) <sub>3</sub> | H               | H                | NA : 4 : 3   | 1580  | -0.08                        |
| 15  | SO <sub>2</sub> Ph  | H               | H                | NA : 3 : 2   | 1564  | 0.07                         |
| 16  | SO <sub>2</sub> Me  | H               | H                | NA : 11 : 10 | 1568  | 0.07                         |
| 17  | SF <sub>5</sub>     | H               | H                | NA : 4 : 3   | 1573  | 0.14                         |
| 18  | CF <sub>3</sub>     | H               | OMe              | 10 : NA : 1  | 1573  | 0.07                         |
| 19  | CF <sub>3</sub>     | H               | NMe <sub>2</sub> | 1 : NA : 20  | 1570  | -0.16                        |
| 20  | CF <sub>3</sub>     | CF <sub>3</sub> | H                | 20 : 1 : 1   | 1592  | 0.45                         |
| 21  | CF <sub>3</sub>     | H               | CF <sub>3</sub>  | 1 : NA : 7   | 1582  | 0.42                         |
| 22  | CO <sub>2</sub> Me  | H               | H                | NA : 5 : 4   | 1568  | -0.03                        |

**Table 6.2.** Coordination diastereomer ratios, infrared and electrochemical data for **2-22**.

include a signal near 5.7 ppm for each isomer, corresponding to the unbound ortho-proton (H6). Despite its proximity to the fluorine,  $\pi$  donation from both the halogen and the molybdenum cause this proton to be relatively shielded (cf. H4,  $\sim$  6.7 ppm). In acetone solution at 25 °C, this complex has a substitution half-life of only 8 min, just slightly longer than the parent benzene complex (cf. **33** 25 seconds at 25 °C).



**Scheme 6.7.** Preparation of several molybdenum fluorobenzene, difluorobenzene, and tetrafluorotoluene complexes.

A DFT study was carried out for the fluorobenzene complex (**27**). These calculations support the experimental observation that the metal favors binding across C2 and C3, similar to that predicted for ReCp(CO)<sub>2</sub>,<sup>23</sup> and experimentally determined for anisole complexes of W, Re, and Os. Coordination diastereomers (**27A**, **27B**) of the 2,3-η<sup>2</sup> form (8.4, 8.5 kcal/mol) were roughly four kcal/mol more stable than **27C** and **27D**, the corresponding 3,4-η<sup>2</sup> isomers (10.4, 10.7 kcal/mol). Remarkably, DFT calculations indicate that these ring-bound isomers are not as stable as the aryl fluoride isomers **27G** and **27H** (0, 6.7 kcal/mol;

**Table 6.3).** This suggests that the lack of observed C-F activation in the reaction of molybdenum with fluorobenzene is a result of a large *kinetic* barrier for this pathway, which is preempted by arene dissociation followed by decomposition. Even if the arene complex (**27**) is allowed to stand in neat fluorobenzene for longer reaction times (48 h) or elevated temperatures (50 °C), results in an intractable mixture of paramagnetic materials. Similar conclusions were reached by Caulton, Eisenstein, and Perutz whose DFT calculations predicted high kinetic barriers of C-F addition for osmium and rhodium systems.<sup>21</sup>

As anticipated, the integration of -F or -CF<sub>3</sub> as substituents of the benzene ring stabilizes the complex toward dissociation and oxidation. Calculated BDEs, approximate half-lives, and anodic peak potentials are given in **Table 6.4** along with the observed diastereomer ratios. The addition of two fluorine atoms increases the BDE by roughly 4 kcal/mol and renders the arene over 300 mV more resistant to oxidation. Meanwhile, substitution half-lives in acetone increase from seconds to hours. In **Table 6.4**, the effects of CF<sub>3</sub> substituents are also highlighted, where again this substituent acts to raise both the BDE and anodic peak potential ( $E_{p,a}$ , V NHE, 100 mV/s).

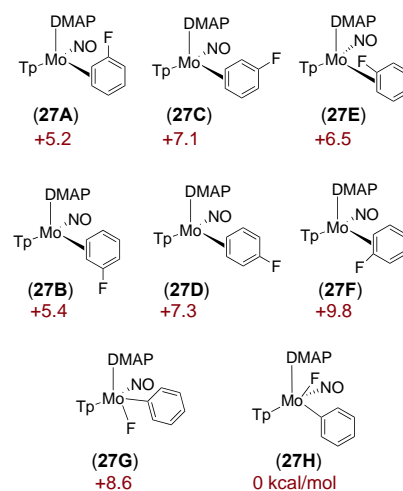


**Table 6.3.** DFT calculations for relative stabilities (Gibbs free energies, vacuum) for various isomers of MoTp(NO)(DMAP)(fluorobenzene).

From the observed coordination diastereomers in Table 4, we recognize several trends regarding the ability of -CF<sub>3</sub> and -F groups to direct the location of metal coordination. As observed for tungsten, trifluoromethyl groups direct the metal to the 3,4- $\eta^2$  position, whereas a fluorine substituent directs the metal to the 2,3-position. We speculate that, as with the methoxy group of anisole,<sup>4, 28</sup> it is the  $\pi$ -donor ability of the fluorine whose interaction with the uncoordinated portion of the arene  $\pi$ -system (C1-C4; linear conjugation) is maximized with the metal blocking C5 and C6. These trends are consistent for all fluorinated arene complexes shown in **Table 6.4**.

## 6.8 Dynamic Behavior of Electron Deficient Benzenes on Tungsten and Molybdenum

Finally, we briefly explored the solution dynamics for the molybdenum and tungsten complexes of trifluorotoluene, **1** and **13** respectively, along with the molybdenum fluorobenzene complex **27** (Scheme 6.8). Interestingly, both of the molybdenum complexes show spin saturation exchange, even at reduced temperatures (0 °C), that is consistent with an *intramolecular* ring-walk isomerization **Figure 6.1** and **Figure 6.2**).

In contrast, an NOESY experiment for the tungsten analog **13** at 50 °C in MeCN-*d*<sub>3</sub> reveals an exchange process that passes through an aryl hydride intermediate. While this tungsten-hydride species exists as only a minor isomer (~4 % of population) and full characterization is thwarted by the low concentration of tungsten hydride in solution, exchange-correlations clearly demonstrate that isomerization occurs through the C-H activation of the arene ring at the meta and para

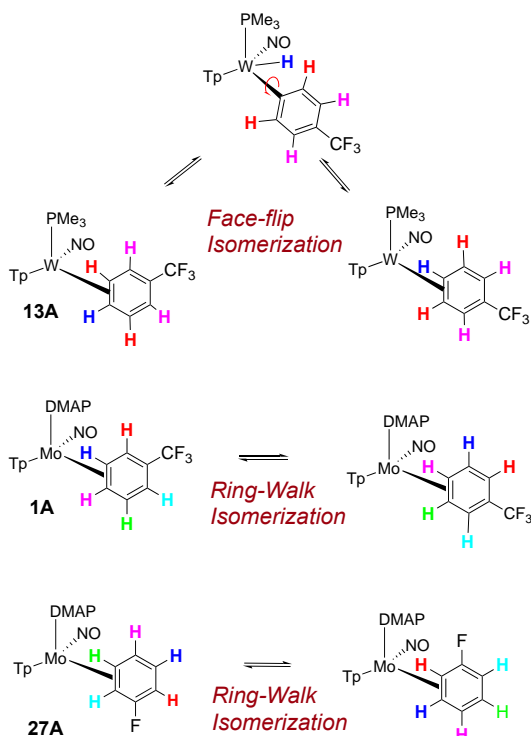
positions corresponding to the positions where the tungsten is bound in an  $\eta^2$ -fashion (Scheme 6.8). This behavior is not observed at ambient temperatures on the timescale of the NOESY NMR experiment (25 °C).

| Complex | (#)  | BDE (kcal/mol) | t <sub>1/2</sub> (min) | E <sub>p,a</sub> (V) |
|---------|------|----------------|------------------------|----------------------|
|         | (32) | 14             | 0.4                    | -0.55                |
|         | (27) | 16.4           | 8                      | -0.36                |
|         | (28) | 17.1           | 80                     | -0.35                |
|         | (1)  | 16.0           | 40                     | -0.28                |
|         | (29) | 18.9           | 280                    | -0.21                |
|         | (30) | 18.9           | 1390                   | -0.05                |
|         | (24) | 20.9           | 2880                   | -0.06                |
|         | (25) | 21.0           | 3040                   | -0.10                |

**Table 6.4.** Compilation of DFT (Gibbs free energies, 298 K, kcal/mol) and electrochemical data for fluorinated molybdenum benzene complexes.

## 6.9 Conclusions

We have prepared a series of tungsten and molybdenum complexes of dihapto-coordinated benzenes bearing electron-deficient substituents. In general, arenes with electron-withdrawing groups that contain  $\pi$  bonds tend to form mixtures or exclusive  $\eta^2$ -adducts with the substituent itself, as forming such complexes retain the arene's aromatic stabilization. A notable exception to this is complexation of an ortho-benzoate ( $\text{PhC}(\text{OMe})_3$ ) by tungsten and subsequent hydrolysis to provide an benzoate ester bound through the arene. In addition, compounds of  $\text{PhCF}_3$ ,  $\text{PhSF}_5$ , and  $\text{Ph}_2\text{SO}_2\text{R}$  were realized. An investigation to the organic chemistry available to these systems is currently underway.



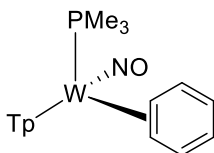
**Scheme 6.8.** Comparison of isomerization pathways for **1**, **13**, and **27**.

Additionally, we have explored the ability of the  $\{\text{MoTp}(\text{NO})(\text{DMAP})\}$  system to form stable dihapto-coordinate complexes with fluorinated benzenes, systems that have not been realized for tungsten, owing to C-F or C-H insertion. The isomerization dynamics of trifluorotoluene complexes were examined for both molybdenum and tungsten, and there appears to be mechanistic divergence for these Group 6 metals. Notably, isomerization of the tungsten trifluorotoluene complex appears to involve a C-H activated adduct while the analogous complex of molybdenum, along with the fluorobenzene analog, undergo an intrafacial ring-walk mechanism. A comparison of C-F activated and dihapto-coordinate molybdenum-fluorobenzene isomers have been evaluated by DFT calculations and we conclude that lack of an observed C-F activated product is the result of a high kinetic barrier for C-F addition as opposed to any fundamental thermodynamic argument.

## Experimental Section.

**General Methods.** NMR spectra were obtained on 500, 600 or 800 MHz spectrometers. Chemical shifts are referenced to tetramethylsilane (TMS) utilizing residual  $^1\text{H}$  signals of the deuterated solvents as internal standards. Chemical shifts are reported in ppm and coupling constants ( $J$ ) are reported in hertz (Hz). Chemical shifts for  $^{19}\text{F}$  and  $^{31}\text{P}$  spectra were reported relative to standards of hexafluorobenzene (164.9 ppm) and triphenylphosphine (-6.00 ppm). Infrared Spectra (IR) were recorded on a spectrometer as a solid with an ATR crystal accessory, and peaks are reported in  $\text{cm}^{-1}$ . Electrochemical experiments were performed under a nitrogen atmosphere. Most cyclic voltammetric data were recorded at ambient temperature at 100 mV/s, unless otherwise noted, with a standard three electrode cell from +1.8 V to -1.8 V with a platinum working electrode, acetonitrile (MeCN) or dimethylacetamide (DMA) solvent, and tetrabutylammonium (TBAH) electrolyte (~1.0 M). All potentials are reported versus the normal hydrogen electrode (NHE) using cobaltocenium hexafluorophosphate ( $E_{1/2} = -0.78$  V, -1.75 V) or ferrocene ( $E_{1/2} = 0.55$  V) as an internal standard. Peak separation of all reversible couples was less than 100 mV. All synthetic reactions were performed in a glovebox under a dry nitrogen atmosphere unless otherwise noted. All solvents were purged with nitrogen prior to use. Deuterated solvents were used as received from Cambridge Isotopes and were purged with nitrogen under an inert atmosphere. When possible, pyrazole (Tp) protons of the (trispyrazolyl) borate (Tp) ligand were uniquely assigned (e.g., “Tp3B”) using two-dimensional NMR data (see Fig. S1). If unambiguous assignments were not possible, Tp protons were labeled as “Tp3/5 or Tp4”. All  $J$  values for Tp protons are 2 ( $\pm 0.4$ ) Hz.

### WTp(NO)(PMe<sub>3</sub>)( $\eta^2$ -benzene) (2) Alternative Procedure

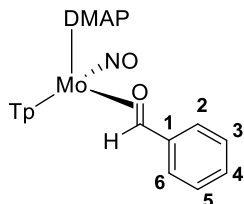


A 1 L round bottom flask was dried in a 150 °C oven along with a 350 mL coarse porosity fritted disc which was  $\frac{3}{4}$  filled with silica. After 4 h the glassware was removed from the oven and brought into an inert atmosphere glovebox. The 1L round bottom flask was then charged with anhydrous benzene (~800 mL) followed by WTp(NO)(PMe<sub>3</sub>)(Br) (12.3 g, 21.1 mmol) followed by an excess of 30-35% by weight sodium dispersion in toluene solution (14.41 g, ~ 207 mmol). The sides of the round bottom flask were rinsed with another wash of benzene (200 mL) and the resulting heterogeneous green reaction mixture was allowed to rapidly stir over a course of 16 h. The next day the reaction mixture had turned to a dark brown/black color and the solution was first filtered through a 150 mL medium porosity fritted disc that was filled with Celite (~ 5 cm) and set in benzene. The resulting eluent was then loaded onto a 350 mL coarse porosity fritted disc which was filled with silica (~ 6 cm) and set in benzene. The eluent was then loaded onto the column and allowed to filter. A green band develops on the solid phase followed closely by a vibrant orange band. When all of the reaction mixture had been loaded the column was rinsed with a 3:1 solution of benzene: diethyl ether (~ 3 x 300 mL). At this point vacuum was cautiously applied to the column until the majority of the green band had eluted through the column. The resulting green filtrate was then discarded and the resulting orange band was allowed to continue to filter. The initial filtrate, a lime green colored eluent, was discarded again and the column was then rinsed with diethyl ether (2 L total) while the filter flask was under vacuum to elute all of the orange colored band which turns to a yellow colored fraction upon elution. This fraction appears as a homogeneous yellow colored solution once eluted into the filter flask. The solvent of this solution was then removed in vacuo until ~ 300 mL of solution remained. At this point a vibrant yellow solid had begun to precipitate from solution. Next hexanes (1 L) was added to induce further precipitation and generate a golden yellow suspension. This heterogeneous yellow solution was then eluted through a 150 mL fine porosity fritted disc to isolate a vibrant



yellow solid. The solid was washed with hexanes (2 x 50 mL) and to desiccated over a period of 6 h before a mass was taken of the vibrant yellow solid (5.31 g, 43.4%). Characterization of **2** has been reported previously.<sup>22</sup>

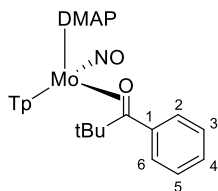
### MoTp(NO)(DMAP)(C,O- $\eta^2$ -benzaldehyde) (**3C**)



A 4-dram vial was charged with **1** (1.05 g, 1.72 mmol) and benzaldehyde 10.4 g (98.0 mmol). This homogeneous light green mixture was capped and stirred at room temperature for 10 minutes. This substitution reaction is believed to be catalyzed by the presence of trace acid that forms from benzaldehyde over time; and this phenomenon has been reported elsewhere.<sup>37</sup> This reaction mixture was then loaded onto a 60 mL coarse porosity fritted disc 2/3 full with silica gel. This column was washed with diethyl ether (50 mL) and the product was isolated using THF (100 mL). The green solution was evaporated *in vacuo* to an approximate volume of 20 mL and added to chilled pentane (100 mL) yielding a white precipitate. This reaction mixture was then decanted to collect a white solid on a fine 15 mL fritted disc. Some product had oiled out on the bottom of the filter flask, and this was re-dissolved in a minimal amount of DCM (~3 mL) and then re-precipitated into stirring pentane (50 mL) that had been chilled to -30 °C. A white precipitate was again isolated on a 15mL fine porosity fritted disc. The white products obtained but both precipitation steps were combined and then washed with chilled pentane (2 x 10 mL) and dried under static vacuum for 2 h to yield **3C**. An off-white solid was obtained (0.518 g, 55.0 %).

CV (DMA)  $E_{p,a} = + 0.40$  V (NHE). IR:  $\nu(\text{BH}) = 2484$   $\text{cm}^{-1}$ ,  $\nu(\text{NO}) = 1580$   $\text{cm}^{-1}$ .  $^1\text{H-NMR}$  (acetone- $d_6$ ,  $\delta$ , 25 °C): 7.95 (1H, d, Tp3/5), 7.92 (1H, d, Tp3/5), 7.88 (1H, d, Tp3), 7.78 (2H, m, DMAP-2/6), 7.56 (1H, d, Tp3/5), 7.48 (1H, d, Tp3/5), 7.32 (1H, d, Tp3), 7.28 (2H, t,  $J = 7.84$ , H3 and H5), 7.19 (2H, d,  $J = 7.31$ , H2 and H6), 7.02 (1H, t of t,  $J = 7.25$ , 1.25, H4), 6.65 (2H, m, DMAP-3/5), 6.29 (1H, t, Tp4), 6.24 (1H, t, Tp4), 6.23 (1H, t, Tp4), 4.45 (1H, s, aldehyde H), 3.10 (6H, s, NMe<sub>2</sub>).  $^{13}\text{C}$  { $^1\text{H}$ } NMR (acetone- $d_6$ ,  $\delta$ , 25 °C). 155.7 (DMAP-C4), 151.63 (DMAP-C2/C6), 149.13 (C1), 143.5 (Tp3/5), 143.5 (Tp3/5), 141.9 (Tp3/5), 136.8 (Tp3/5), 136.6 (Tp3/5), 136.3 (Tp3/5), 127.7 (C3 and C5), 126.30 (C2 and C6), 125.4 (C4), 107.6 (DMAP-C3/C5), 106.8 (Tp4), 106.3 (Tp4), 106.0 (Tp4), 98.1 (aldehyde carbonyl C), 39.2 (NMe<sub>2</sub> Cs). This compound is a simple derivative of the complex WTp(NO)(PMe<sub>3</sub>)(C,O- $\eta^2$ -acetaldehyde) with closely matching spectra and its characterization was not further pursued.<sup>38</sup>

### MoTp(NO)(DMAP)(C,O- $\eta^2$ -2,2,2-trimethyl-acetophenone) (**5C**)

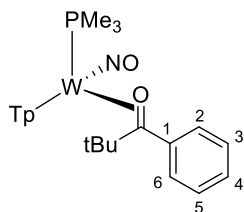


An oven-dried 4-dram vial was charged with **1** (0.198 g, 0.326 mmol), 2,2,2-trimethylacetophenone (0.440 g, 2.71 mmol) and DME (2 mL) and the heterogeneous orange mixture was allowed to stir. After 5 h the reaction mixture had turned to a light homogenous brown solution and the reaction mixture was added to a solution of

stirring pentane (30 mL). Upon addition to the pentane solution, an off-white precipitate forms in the solution. The solid was then filtered through a 15 mL fine porosity fritted disc and washed with pentane (3 x 10 mL). The off-white powder was allowed to desiccate under dynamic vacuum for 8 h before a mass was taken of the off-white solid (0.109 g, 53.7 % yield).

CV (DMA):  $E_{p,a} = +0.32$  V (NHE). IR:  $\nu(\text{BH}) = 2481$   $\text{cm}^{-1}$ ,  $\nu(\text{NO}) = 1574$   $\text{cm}^{-1}$ .  $^1\text{H}$  NMR (acetone- $d_6$ ,  $\delta$ , 25  $^\circ\text{C}$ ): 8.49 (1H, d, Tp3/5C), 7.83 (1H, d, Tp3/5), 7.71 (1H, d, Tp3/5), 7.57 (2H, m, DMAP-2/6), 7.43 (2H, d, overlapping Tp3/5), 7.21 (1H, d, Tp3/5), 7.13 (1H, d,  $J = 7.84$ , H3/5), 6.70 (1H, t,  $J = 7.53$ , H2/H4), 6.58 (2H, m, DMAP-3/5), 6.51 (1H, t,  $J = 7.84$ , H3/H5), 6.42 (1H, t, Tp4), 6.39 (1H, t,  $J = 7.53$ , H2/H4), 6.22 (1H, d,  $J = 7.53$ , H4/H5), 6.15 (1H, t, Tp4), 5.79 (1H, t, Tp4), 3.09 (6H, s,  $\text{NMe}_2$ ), 1.29 (9H, s, -tBu).  $^{13}\text{C}$   $\{^1\text{H}\}$  NMR (acetone- $d_6$ ,  $\delta$ , 25  $^\circ\text{C}$ ): 155.6 (DMAP-C4), 151.8 (DMAP-C2/6), 147.1 (Tp3/5), 144.7 (Tp3/5), 142.6 (Tp3/5), 138.0 (Tp3/5), 135.4 (Tp3/5), 135.2 (Tp3/5), 130.0 (C1/C5), 127.5 (C1/6), 126.3 (C2/4), 125.3 (C2/4), 124.3 (C3), 112.1 (C=O), 107.2 (DMAP-3/5), 106.3 (Tp4), 106.5 (Tp4), 104.9 (Tp4), 39.2 (DMAP-NMe $_2$ ), 31.8 (-tBu). This compound is a simple derivative of the complex  $\text{MoTp}(\text{NO})(\text{DMAP})(\text{C},\text{O}-\eta^2\text{-acetone})$  with closely matching spectra and its characterization was not further pursued.<sup>13</sup>

### WTp(NO)(PMe $_3$ )(C,O- $\eta^2$ -2,2,2-trimethyl-acetophenone) (6C)



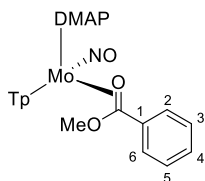
An oven-dried 4-dram vial was charged with **2** (0.201 g, 0.346 mmol) and trimethylacetophenone (0.505 g, 3.11 mmol) and DME (1 mL) and the heterogeneous orange mixture was allowed to stir. After 24 h, the reaction mixture had turned to a light homogenous brown solution and the reaction mixture was added to a solution of stirring pentane (30 mL). Upon addition to the stirring pentane solution, a light pink precipitate forms in the solution. The solid was then filtered through a 15 mL fine porosity fritted disc and washed with pentane (3 x 10 mL) before the yellow powder was allowed to desiccate under dynamic vacuum for 3 h and a mass was taken of the light pink solid (0.162 g, 70.0 % yield). The ratio of the major isomer (**6C**) to minor (**6C'**) is approximately 9:1.

CV (DMA):  $E_{p,a} = +0.55$  V (NHE). Characterization of **6C**  $^1\text{H}$  NMR (acetone- $d_6$ ,  $\delta$ , 25  $^\circ\text{C}$ ): 8.57 (1H, d, Tp3/5C), 8.17 (1H, d, Tp3/5), 7.89 (1H, d, Tp3/5), 7.76 (1H, d, Tp3/5), 7.74 (1H, d, Tp3/5), 7.73 (1H, d, Tp3/5), 7.47 (1H, d, Tp3/5), 7.29 (1H, dt,  $J = 1.39$ , 7.89, H2), 6.80 (1H, td,  $J = 1.39$ , 7.45, H3), 6.51 (1H, tt,  $J = 1.27$ , 7.33, H4), 6.42 (1H, td,  $J = 1.27$ , 8.01, H5), 6.35 (1H, roofing m, H6), 6.38 (1H, t, Tp4), 6.28 (1H, t, Tp4), 5.91 (1H, t, Tp4), 1.37 (9H, d,  $J_{\text{PH}} = 9.32$ ,  $\text{PMe}_3$ ), 1.16 (9H, s, -tBu).  $^{13}\text{C}$   $\{^1\text{H}\}$  NMR (acetone- $d_6$ ,  $\delta$ , 25  $^\circ\text{C}$ ): 149.7 (C1), 147.0 (Tp3/5), 145.5 (Tp3/5), 143.7 (Tp3/5), 136.3 (Tp3/5), 135.9 (Tp3/5), 130.8 (C2), 128.1 (C6), 126.2 (C3), 125.2 (C5), 124.1 (C4), 106.6 (Tp4), 106.5 (Tp4), 105.1 (Tp4), 95.3 (C=O), 31.7 (-tBu), 10.7 (d,  $J_{\text{PC}} = 27.2$ ,  $\text{PMe}_3$ ).  $^{31}\text{P}$   $\{^1\text{H}\}$  NMR (acetone- $d_6$ ,  $\delta$ , 25  $^\circ\text{C}$ ): -14.46 ( $J_{\text{WP}} = 278$ ). This compound is a simple derivative of the complex  $\text{WTp}(\text{NO})(\text{PMe}_3)(\text{C},\text{O}-\eta^2\text{-acetone})$  with closely matching spectra and its characterization was not further pursued.<sup>38</sup>

Characterization of **6C'**  $^1\text{H}$  NMR (acetone- $d_6$ ,  $\delta$ , 25  $^\circ\text{C}$ ): 8.65 (1H, d, Tp3/5), 8.07 (1H, d, Tp3/5), 8.05 (1H, d, Tp3/5), 7.93 (1H, d, Tp3/5), 7.92 (1H, d, Tp3/5), 7.85 (1H, d, Tp3/5), 7.72 (1H, buried, -Ph ring), 7.50 (1H, tt,  $J = 1.40$ , 7.38, -Ph ring), 7.31 (1H, dt,  $J = 1.49$ , 7.76, -Ph ring), 7.17 (1H, buried, Ph-ring), 6.85 (1H, m, -Ph

ring), 6.38 (1H, buried, Tp4), 6.35 (1H, t, Tp4), 6.28 (1H, buried, Tp4), 1.26 (9H, d,  $J_{\text{PH}} = 9.16$ ,  $\text{PMe}_3$ ), 0.61 (9H, s, -tBu).

### MoTp(NO)(DMAP)(C,O- $\eta^2$ -(methyl benzoate) (7)

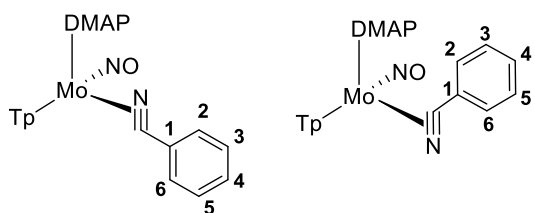


An oven-dried 4-dram vial was charged with **1** (0.200 g, 0.330 mmol) and methyl benzoate (1 mL, ~7.34 mmol) and DME (1 mL). The heterogeneous orange mixture was allowed to stir. After 20 h the reaction mixture had turned to a dark homogenous brown solution and to the reaction vessel was added pentane (10 mL) to induce precipitation. The resulting heterogeneous brown reaction mixture was then allowed to sit at reduced temperature (-30 °C) to further induce precipitation over the course of an hour. The organic layer of the reaction mixture was subsequently discarded and the solid contents were dissolved in a minimal amount of THF (~2 mL) before it was added to a solution of stirring pentane (15 mL) to induce precipitation of an off-white solid. The solid was then isolated on a fine porosity 15 mL fritted disc and washed with pentane (3 x 10 mL). The off-white powder was allowed to desiccate under dynamic vacuum for 8 h before a mass was taken of the off-white solid (0.148 g, 75.5 % yield). The isolated product shows a 2.5:1 ratio of **7C** to **7C'**

CV (DMA):  $E_{p,a} = +0.26$  V (NHE). IR:  $\nu(\text{BH}) = 2483$   $\text{cm}^{-1}$ ,  $\nu(\text{NO}) = 1599$   $\text{cm}^{-1}$ . Characterization of **7C**  $^1\text{H}$  NMR (acetone- $d_6$ ,  $\delta$ , 25 °C): 7.91 (1H, d, Tp3/5), 7.83 (1H, d, Tp3/5), 7.82 (1H, d, Tp3/5), 7.75 (2H, m, DMAP-2/6), 7.51 (1H, d, Tp3/5), 7.50 (1H, d, Tp3/5), 7.45 (1H, d, Tp3/5), 7.42 (2H, m, H2/6), 7.37 (2H, m, H3/H5), 7.12 (1H, tt,  $J = 1.22$ , 7.24, H4), 6.68 (2H, m, DMAP-3/5), 6.27 (1H, t, Tp4), 6.20 (1H, t, Tp4), 6.19 (1H, t, Tp4), 3.12 (6H, s,  $\text{NMe}_2$ ), 2.92 (3H, s, -OMe).  $^{13}\text{C}$   $\{^1\text{H}\}$  NMR (acetone- $d_6$ ,  $\delta$ , 25 °C) of **7C**: 155.7 (DMAP-C4), 151.6 (DMAP-C2/6), 143.6 (Tp3/5), 143.2 (Tp3/5), 142.4 (Tp3/5), 136.6 (Tp3/5), 135.9 (Tp3/5), 135.7 (Tp3/5), 128.0 (Ph-ring), 127.8 (Ph-ring), 126.1 (Ph-ring), 107.5 (DMAP-C3/5), 106.7 (Tp4), 105.6 (Tp4), 105.3 (Tp4), 54.4 (OMe), 39.2 (- $\text{NMe}_2$ ). This compound is a simple derivative of the complex MoTp(NO)(DMAP)(C,O- $\eta^2$ -ethyl acetate) with closely matching spectra and its characterization was not further pursued.<sup>13</sup>

Characterization of **7C'**  $^1\text{H}$  NMR (acetone- $d_6$ ,  $\delta$ , 25 °C): 8.05 (1H, d, Tp3/5), 8.00 (1H, d, Tp3/5), 7.93 (1H, d, Tp3/5), 7.90 (1H, d, Tp3/5), 7.87 (1H, d, Tp3/5), 7.56 (2H, m, DMAP-2/6), 7.29 (2H, m, H3/5), 7.21 (2H, m, H2/H6), 6.91 (2H, overlapping, H4 and Tp3/5), 6.53 (2H, m, DMAP-3/5), 6.41 (1H, t, Tp4), 6.25 (1H, t, Tp4), 6.18 (1H, t, Tp4), , 3.30 (3H, s, -OMe), 3.07 (6H, s,  $\text{NMe}_2$ ).  $^{13}\text{C}$   $\{^1\text{H}\}$  NMR (acetone- $d_6$ ,  $\delta$ , 25 °C) of **7C'**: 155.2 (DMAP-C4), 151.1 (DMAP-C2/6), 144.1 (Tp3/5), 143.4 (Tp3/5), 142.1 (Tp3/5), 136.7 (Tp3/5), 136.4 (Tp3/5), 136.2 (Tp3/5), 127.7 (Ph-ring), 127.6 (Ph-ring), 126.3 (Ph-ring), 107.7 (DMAP-C3/5), 106.6 (Tp4), 106.5 (Tp4), 105.7 (Tp4), 55.2 (-OMe), 39.2 (overlapping with **7C**, - $\text{NMe}_2$ ).

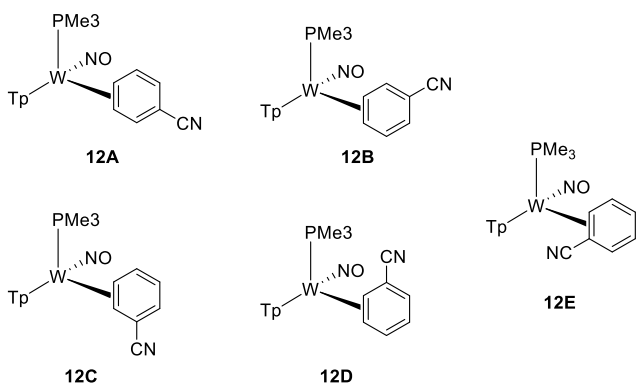
### MoTp(NO)(DMAP)( $\eta^2$ -CN-benzonitrile) (11C and 11C')



An oven-dried 4-dram vial was charged with **1** (0.201 g, 0.331 mmol), benzonitrile (0.750 g, 7.28 mmol), and DME (1.5 mL). The heterogeneous red mixture was allowed to stir overnight. After 20 h, the reaction mixture had turned to a dark homogenous brown solution and to the reaction vessel was added pentane (12 mL) to induce precipitation. Upon addition of pentane the reaction mixture becomes a gummy, oily substance. The organic layer was decanted and the resulting brown film was dissolved in THF (2 mL) and added to a solution of stirring pentane (15 mL) in a 4-dram vial. Upon addition, a pink solid precipitates from solution. This solid was isolated on a fine 15 mL porosity fritted disc. Washed with pentane (2x 10 mL) and the resulting solid was dried under dynamic vacuum for 3 h before a mass was taken of the light pink solid (0.117 g, 62.3 %). A second isomer, **11C'**, was observed in solution in an approximate 1:4 ratio with the major species **11** but overlapping resonances precluded unambiguous characterization. <sup>1</sup>H NMR data show uncoordinated phenyl rings for both isomers so the compound characterization was not further pursued. We note that based on the acetonitrile derivative, MoTp(NO)(DMAP)( $\eta^2$ -NCMe) we suspect the nitrile is dihapto-coordinated.<sup>13</sup>

<sup>1</sup>H NMR (acetone-*d*<sub>6</sub>,  $\delta$ , 25° C) : 7.92 (1H, d, Tp3/5), 7.89 (1H, d, Tp3/5), 7.88 (1H, d, Tp3/5), 7.85 (2H, m, DMAP-2/6), 7.47 (2H, overlapping resonances), 7.31 (1H, broad s), 7.18 (3H, overlapping resonances), 6.62 (2H, m, DMAP-3/5), 6.28 (1H, t, Tp4), 6.15 (1H, t, Tp4), 6.13 (1H, t, Tp4), 3.09 (6H, s, NMe<sub>2</sub>).

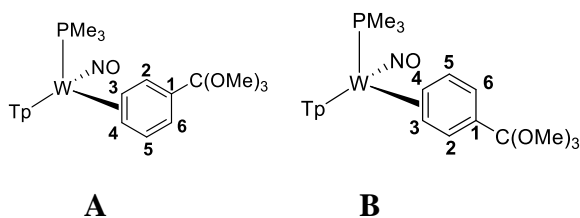
#### WTp(NO)(PMe<sub>3</sub>)( $\eta^2$ -benzonitrile) (**12A-E**)



A 4-dram vial was charged with WTp(NO)(PMe<sub>3</sub>)( $\eta^2$ -2,3-anisole) complex (1.00 g, 1.64 mmol) and a stir pea. To this vial was added benzonitrile (7.00 mL, 67.9 mmol).<sup>22</sup> This yellow heterogeneous solution was allowed to stir at room temperature. After 48 h, the reaction had turned to a black homogenous mixture. A 60 mL course porosity fritted disc was filled 2/3 full of silica and set in diethyl ether. The reaction mixture was added to the column and hexanes (200 mL) were eluted through the column. An orange band could be seen beginning eluting down the column. Next diethyl ether (500 mL) was used to elute the orange band. The resulting orange filtrate was evaporated to dryness under vacuum, pick up in a minimal amount of DCM, and added to a solution of stirring pentane (50 mL). An orange solid was isolated on a 15 mL fine porosity fritted disc. The resulting solid was desiccated overnight yielding **12** (0.271 g, 27.0 % yield).

CV (DMA)  $E_{p,a} = +0.09$ , IR:  $\nu(\text{BH}) = 2493 \text{ cm}^{-1}$ ,  $\nu(\text{CN}) = 2189 \text{ cm}^{-1}$ ,  $\nu(\text{NO}) = 1550 \text{ cm}^{-1}$ .  $^1\text{H}$  NMR (MeCN- $d_3$ ,  $\delta$ , 25 °C): 8.20 (1H, Tp3/5E), 8.11 (1H, Tp3/5B), 8.10 (1H, Tp3/5C), 8.06 (1H, Tp/5A), 8.05 (1H, Tp3/5D), 7.93 (6H, Tp3/5A 2B 2D E), 7.91 (7H, Tp3/5 2A B 2C 2E), 7.89 (1H, Tp3/5E), 7.87 (3H, Tp3/5 2C D), 7.84 (1H, Tp3/5D), 7.82 (1H, Tp3/5B), 7.81 (1H, Tp3/5A), 7.74 (1H, d,  $J = 6.26$ , H2A), 7.62 (1H, d,  $J = 5.73$ , H2B), 7.55 (1H, Tp3/5E), 7.38 (1H, dd  $J = 8.57$ , 6.34, H4D), 7.33 (1H, Tp3/5A), 7.29 (1H, Tp3/5B), 7.25 (1H, Tp3/5C), 7.23 (1H, Tp3/5D), 7.19 (1H, dd,  $J = 9.04$ , 5.64, H4C), 7.01 (1H, dd,  $J = 9.17$ , 6.03, H5B), 6.88 (1H, dd,  $J = 8.08$ , 5.40, H5A), 6.84 (1H, dd,  $J = 9.28$ , 5.57, H3E), 6.55 (1H, d,  $J = 9.12$ , H6E), 6.54 (1H, d  $J = 7.40$ , H6D), 6.45 (1H, d,  $J = 6.34$ , H6C), 6.33 (15H, Tp3A B C D E), 5.77 (2H, m, H5C H5E), 5.74 (1H, dd,  $J = 8.41$ , 6.38, H5D), 5.69 (1H, dd,  $J = 9.04$ , 6.05, H4E), 5.67 (1H, dd,  $J = 9.19$ , 1.38, H6A), 5.60 (1H, dd,  $J = 9.17$ , 1.21, H6B), 4.16 (1H, dd,  $J = 13.26$ , 9.89, H2D), 3.85 (2H, m, H4A H2E), 3.82 (1H, dd,  $J = 8.79$ , 5.42, H3C), 3.75 (1H, m, H3B), 2.17 (2H, m, H4B H2C), 2.14 (1H, m, H3A), 2.06 (1H, ddd,  $J = 9.96$ , 6.25, 1.55, H3D), 1.29 (9H, d,  $J = 8.70$ , PMe<sub>3</sub>C), 1.23 (18H, d,  $J = 8.69$ , PMe<sub>3</sub>B E), 1.22 (18H, d,  $J = 8.70$ , PMe<sub>3</sub>A D).  $^{13}\text{C}$  { $^1\text{H}$ } NMR (MeCN- $d_3$ ,  $\delta$ , 25 °C): 150.7 (1C, C2A), 147.6 (1C, d,  $J_{\text{PC}} = 3.71$ , C2B), 145.5 (1C, Tp3/5A), 145.2 (2C, Tp3/5B E), 143.3 (1C, Tp3/5A), 143.2 (1C, Tp3/5E), 142.2 (1C, Tp3/5B), 142.0 (1C, Tp3/5A), 142.0 (1C, Tp3/5B), 141.9 (1C, Tp3/5E), 138.2 (2C, Tp3/5A E), 138.1 (1C, Tp3/5B), 137.6 (1C, Tp3/5E), 137.6 (1C, Tp3/5A), 137.5 (1C, Tp3/5B), 137.4 (1C, Tp3/5E), 137.1 (1C, Tp3/5A), 137.1 (1C, Tp3/5B), 136.5 (1C, C4B), 134.6 (1C, d,  $J_{\text{PC}} = 3.17$ , C4A), 133.6 (1C, d,  $J_{\text{PC}} = 3.48$ , C3E), 128.4 (1C, C6E), 126.0 (1C, CNE), 121.8 (1C, CNA), 121.7 (1C, CNB), 117.3 (1C, C4E), 116.9 (1C, C5E), 114.8 (1C, C6A), 113.1 (1C, C6B), 107.7 (1C, Tp4E), 107.6 (1C, Tp4A), 107.6 (1C, Tp4B), 107.3 (2C, Tp4A B), 107.3 (1C, Tp4E), 107.1 (1C, Tp4A), 107.1 (1C, Tp4E), 106.8 (1C, Tp4B), 100.3 (1C, C1B), 98.4 (1C, C1A), 67.0 (1C, d,  $J_{\text{PC}} = 10.13$ , C2E), 64.9 (1C, d,  $J_{\text{PC}} = 9.05$ , C4A), 63.5 (1C, d,  $J_{\text{PC}} = 7.53$ , C3B), 63.1 (1C, C4B), 61.9 (1C, C3A), 13.2 (3C, d,  $J_{\text{PC}} = 28.3$ , PMe<sub>3</sub>B), 13.2 (3C, d,  $J_{\text{PC}} = 29.15$ , PMe<sub>3</sub>A), 13.0 (3C, d,  $J_{\text{PC}} = 30.1$ , PMe<sub>3</sub>E). Anal. Calcd for C<sub>19</sub>H<sub>24</sub>BN<sub>8</sub>OPW · 1/2 (DCM): C, 36.11; H, 3.89; N, 17.28. Found: C, 36.44; H, 3.90; N, 17.19.

#### WTp(NO)(PMe<sub>3</sub>)(3,4- $\eta^2$ -(trimethylortho)benzoate) (14)



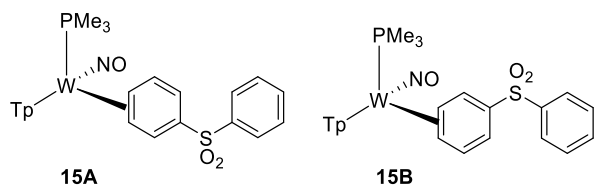
An oven-dried 4-dram vial was charged with **2** (0.092 g, 0.158 mmol) and trimethyl orthobenzoate (1.00 g, 5.49 mmol). The heterogeneous yellow reaction mixture was allowed to stir with a small stir bar. Over time the reaction mixture turns to a homogeneous brown reaction mixture and after 16 h the reaction mixture was added to 15 mL of stirring pentane that had been chilled to -30 °C. Upon addition, a light-yellow solid precipitates from solution. The solid was then filtered through a 15 mL medium porosity fritted disc and washed with pentane (2 x 5 mL) before the light tan powder was allowed to desiccate under active vacuum for 2 h and a mass taken (0.040 g, 37.0 % yield).

CV (DMA):  $E_{p,a} = -0.08 \text{ V}$  (NHE). IR:  $\nu(\text{BH}) = 2496 \text{ cm}^{-1}$ ,  $\nu(\text{NO}) = 1580 \text{ cm}^{-1}$ . Characterization of **14A**  $^1\text{H}$  NMR (acetone- $d_6$ ,  $\delta$ , 0° C): 8.35 (1H, d, Tp3A), 8.00 (1H, d, Tp3/5), 7.95 (1H, d, Tp3B), 7.87 (1H, d, Tp5), 7.49 (1H, d, Tp3C), 7.31 (1H, d,  $J = 5.94$ , H2), 7.05 (1H, dd,  $J = 5.60$ , 9.09, H5), 6.36 (2H, t, overlapping Tp4), 6.35 (1H, t, Tp4A), 6.32 (2H, t, overlapping Tp4), 6.31 (1H, t, Tp4C), 5.74 (1H, d,  $J = 9.22$ , H6), 3.90 (1H, m, H3), 3.14 (9H, overlapping s, (OMe)), 2.28 (1H, m, H4), 1.37 (9H, d,  $J_{\text{PH}} = 8.22$ , PMe<sub>3</sub>).  $^{31}\text{P}$  NMR (acetone- $d_6$ ,  $\delta$ , 25 °C): -12.15 ( $J_{\text{WP}} = 310.3$ ).  $^{13}\text{C}$  { $^1\text{H}$ } NMR (acetone- $d_6$ ,  $\delta$ , 25 °C): 137.7/136.3 (C1 for **A** or **B**), 136.4 (C2), 134.9 (C5), 114.9 (C6), 115.8 (overlapping with **A**, ipso C-(OR)<sub>3</sub>), 63.5 (C3, d,  $J_{\text{PC}} = 7.00$ ), 62.3 (C4),

49.7/49.6 (OMe groups for **A** or **B**), 13.6 (PMe<sub>3</sub>, d,  $J_{PC} = 28.3$ ). <sup>13</sup>C {<sup>1</sup>H} NMR (acetone-*d*<sub>6</sub>, δ, 25 °C): Tp resonances for **A** and **B**. 145.0 (Tp3/5), 144.4 (Tp3/5), 142.4 (Tp3/5), 142.4 (Tp3/5), 141.8 (Tp3/5), 141.5 (Tp3/5), 137.7 (Tp3/5), 137.7 (Tp3/5), 137.6 (Tp3/5), 136.8 (Tp3/5), 136.7 (Tp3/5), 136.5 (Tp3/5), 136.3 (Tp3/5), 107.0 (Tp4), 106.9 (Tp4), 106.8 (Tp4), 106.7 (Tp4), 106.5 (Tp4), 106.4 (Tp4).

Characterization of **14B** <sup>1</sup>H NMR (acetone-*d*<sub>6</sub>, δ, 0° C): 8.25 (1H, d, Tp3A), 8.01 (1H, d, Tp5C), 7.93 (1H, d, Tp3B), 7.89 (1H, d, Tp3/5), 7.40 (1H, d, Tp3C), 7.39 (1H, buried, H2), 6.84 (1H, dd,  $J = 4.91, 9.40$ , H5), 6.36 (1H, t, overlapping Tp4), 6.35 (1H, t, Tp4A), 6.32 (2H, t, overlapping Tp4), 6.31 (1H, t, Tp4C), 5.84 (1H, d,  $J = 9.74$ , H6), 4.13 (1H, m, H4), 3.14 (9H, overlapping s, (OMe)), 2.17 (1H, t,  $J = 7.89$ , H3), 1.37 (9H, d,  $J_{PH} = 8.22$ , PMe<sub>3</sub>). <sup>31</sup>P NMR (acetone-*d*<sub>6</sub>, δ, 25° C): -12.79 ( $J_{WP} = 310$ ). 137.7/136.3 (C1 for **A** or **B**), 137.5 (C2), 133.4 (C5), 116.4 (C6), 115.8 (overlapping with **A**, ipso C-(OR)<sub>3</sub>), 63.9 (C4, d,  $J_{PC} = 7.68$ ), 62.3 (C3), 49.7/49.6 (OMe groups for **A** or **B**), 12.9 (PMe<sub>3</sub>, d,  $J_{PC} = 27.7$ ). Attempts to purify **14** for elemental analysis by chromatography led to the generation of **22**.

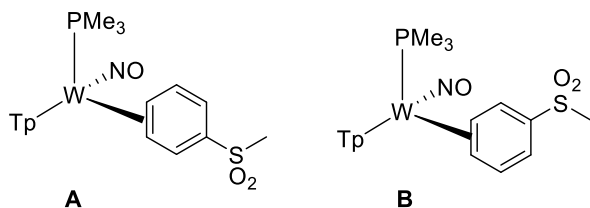
### WTp(NO)(PMe<sub>3</sub>)(3,4-η<sup>2</sup>-diphenyl sulfone) (**15**)



A 4-dram bottle was charged with WTp(NO)(PMe<sub>3</sub>)(η<sup>2</sup>-2,3-anisole) complex (5.00 g, 8.18 mmol), diphenyl sulfone (5.35 g, 24.5 mmol), and a stir pea.<sup>22</sup> To this vial was added 1,2-dimethoxyethane (20 mL) along with a stir bar. The yellow heterogeneous mixture was stirred for 48 hours, until the reaction became a bright orange heterogeneous mixture. The orange precipitate was collected on a 30 mL fine porosity fritted disc. The product was washed with diethyl ether (2 x 20 mL) then hexanes (4 x 20 mL). The product was desiccated overnight, yielding **15A** and **B** (4.13 g, 5.73 mmol, 70.0 % yield).

CV (DMA)  $E_{p,a} = +0.07$ , (NHE). IR:  $\nu(\text{BH}) = 2482$ ,  $\nu(\text{NO}) = 1564 \text{ cm}^{-1}$ ,  $\nu(\text{SO}) = 14074 \text{ cm}^{-1}$ . <sup>1</sup>H NMR (MeCN-*d*<sub>3</sub>, δ, 25 °C): 8.13 (1H, d, Tp3/5**B**), 8.00 (1H, dd  $J = 6.54, 1.41$ , H2**A**), 7.95 (4H, m, H8/12**A B**), 7.90 (6H, m, 3Tp3/5**A**, H2**B**, 2Tp3/5**B**), 7.85 (1H, d, Tp3/5**B**), 7.82 (2H, d, 2Tp3/5**A**), 7.80 (1H, d, Tp3/5**B**), 7.56 (1H, m, H10**B**), 7.52 (3H, m, H10**A**, H11/9**B**), 7.48 (2H, m, H11/9**A**), 7.30 (1H, d, Tp3/5**B**), 7.27 (1H, d, Tp3/5**A**), 7.07 (1H, dd,  $J = 9.46, 5.90$ , H5**B**), 6.91 (1H, dd,  $J = 9.32, 5.20$ , H5**A**), 6.36 (1H, t, Tp4**A**), 6.33 (2H, t, Tp4**A B**), 6.29 (1H, t, Tp4**B**), 6.28 (2H, t, Tp4**A B**), 5.93 (1H, dd,  $J = 9.55, 1.78$ , H6**A**), 5.82 (1H, dd,  $J = 9.28, 1.55$ , H6**B**), 3.85 (1H, m, H4**A**), 3.70 (1H, m, H3**B**), 2.10 (2H, m, H3**A**, H4**B**), 1.27 (9H, d,  $J_{PH} = 8.37$ , PMe<sub>3</sub>**B**), 1.20 (9H, d  $J_{PH} = 8.45$ , PMe<sub>3</sub>**A**). <sup>13</sup>C {<sup>1</sup>H} NMR (MeCN-*d*<sub>3</sub>, δ, 25 °C): 147.3 (1C, C2**A**), 145.3 (1C, Tp3/5**B**), 144.8 (1C, C7**A**), 144.6 (1C, C7**B**), 143.7 (1C, d,  $J_{PC} = 3.19$ , C2**B**), 143.2 (2C, Tp3/5**B**), 142.4 (1C, Tp3/5**B**), 142.1 (1C, Tp3/5**B**), 141.9 (1C, Tp3/5**A**), 138.2 (1C, Tp3/5**B**), 138.1 (1C, Tp3/5**A**), 137.6 (1C, Tp3/5**A**), 137.4 (1C, Tp3/5**B**), 137.4 (1C, Tp3/5**A**), 137.1 (1C, C5**B**), 137.0 (1C, Tp3/5**B**), 135.2 (1C, d,  $J_{PC} = 3.93$ , C5**A**), 133.4 (1C, C10**B**), 133.2 (1C, C10**A**), 129.9 (1C, C1**B**), 129.8 (4C, C11/9**A B**), 128.3 (1C, C1**A**), 128.2 (4C, C12/8**A B**), 111.9 (1C, C6**A**), 110.2 (1C, C6**B**), 107.6 (1C, Tp4**A**), 107.5 (1C, Tp4**B**), 107.3 (1C, Tp4**A**), 107.2 (1C, Tp4**B**), 107.2 (1C, Tp4**A**), 106.9 (1C, Tp4**B**), 65.4 (1C, d,  $J_{PC} = 9.06$ , H4**A**), 63.4 (1C, C4**B**), 63.1 (1C, d,  $J_{PC} = 7.52$ , H3**B**), 61.6 (1C, C3**A**), 13.4 (3C, d,  $J_{PC} = 29.04$ , PMe<sub>3</sub>**B**), 13.2 (3C, d,  $J_{PC} = 28.84$ , PMe<sub>3</sub>**A**) Anal. Calcd for C<sub>24</sub>H<sub>29</sub>BN<sub>7</sub>O<sub>3</sub>PSW: C, 39.97; H, 4.05; N, 13.59. Found: C, 40.13; H, 4.03; N, 13.42.

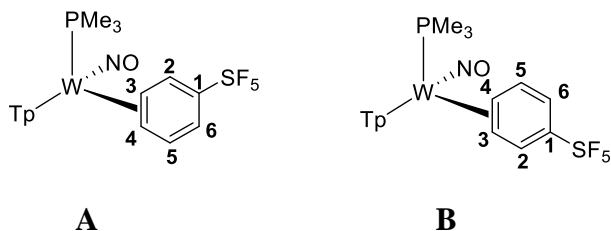
### WTp(NO)(PMe<sub>3</sub>)(3,4-η<sup>2</sup>-methyl phenyl sulfone) (**16**)



A 4-dram vial was charged with **2** (5.00 g, 8.60 mmol) and methyl phenyl sulfone (2.42 g, 15.5 mmol) along with THF (8 mL). This heterogeneous mixture was stirred at room temperature for 16 h. During this time, an orange solid precipitates out of solution. The orange product was collected on a 30 mL fine porosity fritted disc, washed with diethyl ether (4 x 20 ml) and desiccated under static vacuum overnight to yield **16** (2.95 g, 52.0% yield).

CV (DMA):  $E_{p,a} = +0.07$  V (NHE). IR:  $\nu(\text{BH}) = 2487$   $\text{cm}^{-1}$ ,  $\nu(\text{NO}) = 1568$   $\text{cm}^{-1}$ ,  $\nu(\text{SO}) = 1407$   $\text{cm}^{-1}$ .  $^1\text{H-NMR}$  (acetone- $d_6$ ,  $\delta$ , 25 °C): 8.23 (1H, d, Tp3A, **B**), 8.10 (1H, d, Tp3A, **A**), 8.03 (4H, overlapping d, Tp3/5, **A B**), 7.99 (1H, d, Tp3B, **B**), 7.96 (1H, d, Tp3B, **A**), 7.92 (1H, d,  $J = 6.22$ , H2, **A**), 7.90 (1H, d, Tp5, **A**), 7.89 (1H, d, Tp5, **B**), 7.77 (1H, d,  $J = 5.53$ , H2, **B**), 7.53 (1H, d, Tp3C, **A**), 7.51 (1H, d, Tp3C, **B**), 7.13 (1H, dd,  $J = 9.47$ , 5.89, H5, **B**), 6.98 (1H, dd,  $J = 9.27, 5.32$ , H5, **A**), 6.39 (3H, overlapping t, Tp4A **A**, Tp4B **B**, Tp4B), 6.35 (3H, overlapping t, Tp4B **A**, Tp4C **A**, Tp4B), 6.01 (1H, dd,  $J = 9.17, 1.62$ , H6, **A**), 5.95 (1H, dd,  $J = 9.15, 1.61$ , H6, **B**), 4.00 (1H, m, H4, **A**), 3.83 (1H, m, H3, **B**), 2.97 (3H, s, S-CH3, **A**), 2.93 (3H, s, S-CH3, **B**), 2.26 (1H, m, H4, **B**), 2.17 (1H, m, H3, **A**), 1.36 (9H, d,  $J = 8.42$ , **B**), 1.33 (9H, d,  $J_{\text{PH}} = 8.45$ ,  $\text{PMe}_3$ , **A**).  $^{13}\text{C}$  { $^1\text{H}$ } NMR (acetone- $d_6$ ,  $\delta$ , 25 °C): 145.4 (Tp 3/5), 145.4 (Tp 3/5), 145.0 (C2 **A**), 143.1 (Tp 3/5), 142.3 (C2, **B**), 142.1 (Tp 3/5), 142.0 (Tp 3/5), 138.2 (Tp 3/5), 137.6 (Tp 3/5), 137.5 (Tp 3/5), 137.2 (Tp 3/5), 137.1 (Tp 3/5), 137.0 (C5, **B**), 135.0 (C5, **A**), 135.0 (Tp 3/5), 129.5 (C1, **B**), 129.3 (Tp 3/5), 127.3 (C1, **A**), 110.3 (C6, **B**), 112.0 (C6, **A**), 107.6 (Tp 4), 107.6 (Tp 4), 107.3 (Tp 4), 107.3 (Tp 4), 107.2 (Tp 4), 106.9 (Tp 4), 63.6 (C4, **B**), 65.4 (C4, **A**), 62.3 (C5, **B**), 60.5 (C3, **A**), 46.7 (S-Me, **B**), 46.6 (S-Me, **A**), 13.3 (d,  $J_{\text{PC}} = 29.0$ ,  $\text{PMe}_3$ ).  $^{31}\text{P}$  { $^1\text{H}$ } NMR (MeCN- $d_3$ ,  $\delta$ , 25 °C): -13.2 ( $J_{\text{WP}} = 308$ ,  $\text{PMe}_3$ , **A**), -13.9 ( $J_{\text{WP}} = 302$ ,  $\text{PMe}_3$ , **B**). Anal. Calcd for  $\text{C}_{19}\text{H}_{27}\text{BN}_7\text{O}_3\text{PSW}\cdot\text{THF}$ : C, 37.78; H, 4.82; N, 13.41. Found: C, 37.70; H, 4.62; N, 13.60. A SC-XRD study confirms the identity of this compound (SI). Approximately 23% of the total mass recovery corresponds to the C-H activation of the methyl group (**16H**), though full characterization of this complex was not pursued.

### WTp(NO)(PMe<sub>3</sub>)(3,4- $\eta^2$ -pentafluorosulfanyl benzene) (**17**)



An oven-dried 4-dram vial was charged with **2** (0.411 g, 0.707 mmol), pentafluorosulfanyl benzene (2.21 g, 10.8 mmol), and the heterogeneous yellow reaction mixture was allowed to stir. Over time, the reaction mixture turns to a homogeneous red solution and after 24 h the reaction mixture was added to stirring pentane (50 mL) and upon addition a light tan solid precipitates from solution. The solid was then filtered through a fine porosity 15 mL fritted disc and washed with pentane (3 x 10 mL) before the light tan powder was allowed to desiccate under active vacuum for 3 h and a mass was taken (0.311 g, 62.2 %). The filtrate was collected and the pentane

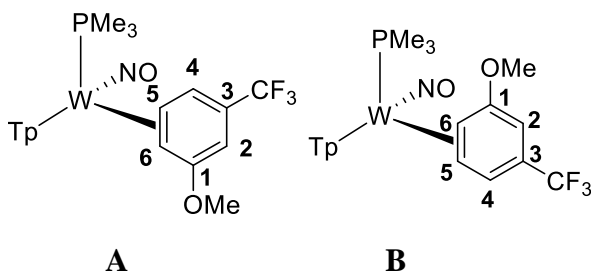
was distilled to re-collect the excess pentafluorosulfanyl benzene. The recovered aromatic ligand was used in similar reaction procedures without noticeable inhibition of yield.

Characterization of **17A**: CV (DMA):  $E_{p,a} = +0.14$  V (NHE). IR:  $\nu(\text{BH}) = 2496$   $\text{cm}^{-1}$ ,  $\nu(\text{NO}) = 1573$   $\text{cm}^{-1}$ .  $^1\text{H}$  NMR (acetone- $d_6$ ,  $\delta$ , 25 °C): 8.22 (1H, d, Tp3A), 8.08 (1H, d, Tp3/5), 7.98 (1H, d, Tp3/5), 7.87 (1H, d, Tp3/5), 7.51 (1H, d,  $J = 5.9$ , H2), 7.02 (1H, m, H5), 6.48 (1H, t, Tp4), 6.37 (2H, t, overlapping Tp4), 6.34 (2H, t, overlapping Tp4), 5.89 (1H, dd,  $J = 2.2, 9.6$ , H6), 3.83 (1H, m, H3), 2.15 (1H, t,  $J = 7.78$ , H4), 1.34 (9H, d,  $J_{\text{PH}} = 8.56$ ,  $\text{PMe}_3$ ).  $^{19}\text{F}$  NMR (acetone- $d_6$ ,  $\delta$ , 25 °C): 91.53 (- $\text{SF}_5$  (1F), overlapping diastereomers q,  $J_{\text{FF}} = 148.6$ ), 64.12 ( $\text{SF}_5$  (4F),  $J_{\text{FF}} = 148.6$ ).  $^{31}\text{P}$  NMR { $^1\text{H}$ } (acetone- $d_6$ ,  $\delta$ , 25 °C): -13.54 (buried  $J_{\text{WP}}$ ). Characterization of **17B**:  $^1\text{H}$  NMR (acetone- $d_6$ ,  $\delta$ , 25 °C): 8.21 (1H, d, Tp3A), 8.08 (1H, d, Tp3/5), 7.98 (1H, d, Tp3/5), 7.96 (1H, d, Tp3/5), 7.89 (1H, d, Tp3/5), 7.60 (1H, d,  $J = 6.90$ , H2), 7.47 (1H, t, Tp3A), 6.86 (1H, m, H5), 6.48 (2H, t, overlapping Tp4), 6.37 (1H, t, Tp4), 6.34 (2H, t, overlapping Tp4), 5.96 (1H, dd,  $J = 2.21, 5.89$ , H6), 3.93 (1H, m, H4), 2.11 (1H, buried, H4), 1.32 (9H, d,  $J_{\text{PH}} = 8.20$ ,  $\text{PMe}_3$ ).  $^{19}\text{F}$  NMR (acetone- $d_6$ ,  $\delta$ , 25 °C): 85.10 (- $\text{SF}_5$  (1F), overlapping diastereomers q,  $J_{\text{FF}} = 147.3$ ), 64.52 (- $\text{SF}_5$  (4F),  $J_{\text{FF}} = 147.3$ ).  $^{31}\text{P}$  { $^1\text{H}$ } NMR (acetone- $d_6$ ,  $\delta$ , 25 °C): -12.88 (buried  $J_{\text{WP}}$ ).

Combined  $^{13}\text{C}$  { $^1\text{H}$ } data for Diastereomers **A** and **B**. When possible, distinction between the isomers is made.

$^{13}\text{C}$  NMR (acetone- $d_6$ ,  $\delta$ , 25 °C): 146.0 (C-SF5, identified by HMBC interactions, **A**), 145.2 (overlapping 2C, Tp3/5s), 146.0 (C-SF5, identified by HMBC interactions, **B**), 142.6 (Tp3/5), 142.2 (Tp3/5), 142.6 (Tp3/5), 141.9 (Tp3/5), 141.8 (Tp3/5), 139.1 (C2 for **B**), 137.9 (Tp3/5), 137.9 (Tp3/5), 137.8 (Tp3/5), 137.2 (Tp3/5), 137.1 (Tp3/5), 136.8 (C2 for **A**), 136.7 (Tp3/5), 136.6 (Tp3/5), 135.9 (C2 for **A**), 134.0 (C5 for **B**), 113.3 (C6 for **B**), 111.6 (C6 for **A**), 107.3 (Tp4), 107.2 (2C, overlapping Tp4s), 107.1 (Tp4), 106.8 (Tp4), 106.5 (Tp4), 63.5 (C4 for **B**, d,  $J_{\text{PC}} = 9.5$ ), 62.0 (C4 for **A**), 61.2 (C3 for **A**, d,  $J_{\text{PC}} = 8.5$ ), 59.8 (C3 for **B**), 13.4 ( $\text{PMe}_3$  for **A**, d,  $J_{\text{PC}} = 28.0$ ), 13.3 ( $\text{PMe}_3$  for **B**, d,  $J_{\text{PC}} = 28.5$ ).

### WTp(NO)(PMe<sub>3</sub>)(5,6- $\eta^2$ -(3-trifluoromethylanisole)) (**18**)



A 4-dram vial was charged with WTp(NO)(PMe<sub>3</sub>)( $\eta^2$ -2,3-anisole) (0.519 g, 0.404 mmol), 3-(trifluoromethyl)anisole (2.15 g, 23.8 mmol), DME (2 mL) and a stir pea.<sup>22</sup> This yellow, heterogeneous mixture was stirred over 48 hours. Over this period, the mixture became dark brown and homogenous. Next a medium 30 mL fritted disc was filled with silica (~ 3 cm) and set in diethyl ether. The reaction mixture was loaded onto the column and subsequently eluted with diethyl ether. Upon elution a golden yellow band developed and was eluted with diethyl ether (100 mL). The resulting homogeneous, yellow solution was evaporated in vacuo until product began to precipitate from solution. Next pentane (50 mL) was added to induce further precipitation. The resulting gold precipitate was collected on a fine porosity 15 mL fritted disc (0.154 g, 59.5%).

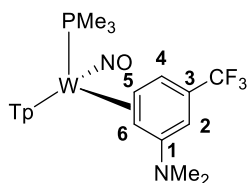
CV (DMA):  $E_{p,a} = +0.07$ , IR:  $\nu(\text{NO}) = 1573$   $\text{cm}^{-1}$ . Characterization of **18A**:  $^1\text{H}$  NMR (MeCN- $d_3$ ,  $\delta$ , 0 °C): 7.98 (1H, d, Tp3/5), 7.91 (1H, d, Tp3/5), 7.90 (1H, d, Tp3/5), 7.86 (1H, d, Tp3/5), 7.80 (1H, d, Tp3/5), 7.26 (1H, d, Tp3/5), 7.09 (1H, d,  $J = 5.57$ , H4), 6.34 (1H, t, Tp4), 6.30 (1H, t, Tp4), 6.27 (1H, t, 1H), 5.18 (1H, s, H2),



3.88 (1H, dd,  $J = 13.7, 12.8$ , H5), 3.75 (3H, s, -OMe), 2.05 (1H, m, H6), 1.20 (9H, d,  $J_{\text{PH}} = 8.73$ ,  $\text{PMe}_3$ ).  $^{13}\text{C}$  { $^1\text{H}$ } NMR ( $\text{MeCN-}d_3$ ,  $\delta$ , 25 °C): 165.9 (C2), 145.0 (Tp3/5), 142.4 (Tp3/5), 141.7 (Tp3/5), 137.9 (Tp3/5), 137.3 (Tp3/5), 137.0 (Tp3/5), 129.2 (d,  $J_{\text{PC}} = 6.03$ , C4), 126.1 (q,  $J_{\text{CF}} = 270$ , C8), 118.2 (buried, C3), 107.5 (Tp4), 107.0 (Tp4), 106.8 (Tp4), 85.6 (C2), 60.7 (C6), 58.7 (d,  $J_{\text{PC}} = 10.3$ , C5), 54.9 (-OMe), 13.6 (d,  $J_{\text{PC}} = 29.7$ ,  $\text{PMe}_3$ ).  $^{31}\text{P}$  NMR ( $\text{MeCN-}d_3$ ,  $\delta$ , 25 °C): -1.51 ( $J_{\text{WP}} = 304$ ,  $\text{PMe}_3$ ).  $^{19}\text{F}$  { $^1\text{H}$ } NMR ( $\text{MeCN-}d_3$ ,  $\delta$ , 25 °C): -64.58 ( $\text{CF}_3$ ). A SC-XRD study confirms the identify of this compound (SI).

Although a minor isomer (**B**) with features of the isomer below were observed along with a C-H activated adduct unambiguous assignment of the carbon resonances was precluded by the low intensity of signals (~10% of major isomer) and significant overlap with Tp resonances of **18A**. Partial Characterization of **18B**  $^1\text{H}$ -NMR ( $\text{MeCN-}d_3$ ,  $\delta$ , 0 °C): 6.86 (1H, broad d, H4), 4.94 (1H, broad s, H2), 4.03 (1H, dd,  $J = 10.8, 12.8$ , H6), 3.66 (3H, s, -OMe), 2.16 (1H, dd,  $J = 5.9, 10.8$ ), 1.21 (9H, buried,  $\text{PMe}_3$ ).

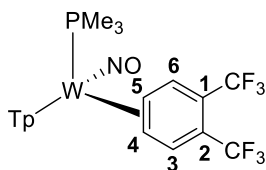
### WTp(NO)(PMe<sub>3</sub>)( $\eta^2$ -5,6-(3-trifluoromethyl-N,N-dimethylaniline)) (19)



An oven-dried 4-dram vial was charged with **2** (0.817 g, 1.41 mmol) and 3-trifluoromethyl-N,N-dimethylaniline (3.89 g, 20.6 mmol), and the heterogeneous yellow reaction mixture was allowed to stir. After 16 h the reaction mixture had retained its heterogeneous golden-colored consistency but analysis by  $^{31}\text{P}$  NMR confirmed the absence of **1** and the generation of a new species. The heterogeneous yellow reaction mixture was added to a solution of stirring pentane (50 mL) to precipitate out a light yellow solid. The solid was then filtered through a 30 mL fine porosity fritted disc and washed with pentane (3 x 20 mL) before the light tan powder was allowed to desiccate under active vacuum and a mass taken of the vibrant yellow solid (0.680 g, 70.0 %). The filtrate was collected and the pentane was distilled to re-collect the excess 3-trifluoromethyl-N,N-dimethylaniline and the recovered aromatic ligand was used in similar reaction procedures without noticeable inhibition of yield.

CV (DMA):  $E_{p,a} = -0.16$  V (NHE). IR:  $\nu(\text{BH}) = 2483$   $\text{cm}^{-1}$ ,  $\nu(\text{NO}) = 1570$   $\text{cm}^{-1}$ .  $^1\text{H}$  NMR ( $\text{acetone-}d_6$ ,  $\delta$ , 25 °C): 8.03 (1H, d, Tp5C), 7.96 (1H, d, Tp3/5), 7.92 (1H, d, Tp3B), 7.90 (1H, d, Tp3A), 7.88 (1H, d, Tp3/5), 7.48 (1H, d, Tp3C), 6.50 (1H, d,  $J = 5.22$ , H4), 6.38 (1H, t, Tp4C), 6.33 (1H, t, Tp4), 6.23 (1H, t, Tp4), 4.54 (1H, s, H2), 4.07 (1H, m, H5), 2.47 (6H, broad s,  $\text{NMe}_2$ ), 2.23 (1H, d,  $J = 10.94$ , H6), 1.33 (9H, d,  $J_{\text{PH}} = 8.18$ ,  $\text{PMe}_3$ ).  $^{13}\text{C}$  { $^1\text{H}$ } NMR ( $\text{acetone-}d_6$ ,  $\delta$ , 25 °C): 157.8 (C1), 144.5 (Tp3/5), 142.4 (Tp3/5), 142.1 (Tp3/5), 140.8 (Tp3/5), 136.7 (Tp3/5), 136.5 (Tp3/5), 126.5 (- $\text{CF}_3$ , q,  $J_{\text{CF}} = 270.6$ ), 121.5 (C3, q,  $J_{\text{CF}} = 28.9$ ), 118.2 (C4), 105.8 (overlap 2Cs, Tp4), 105.3 (Tp4), 82.6 (C2), 61.0 (C5, d,  $J_{\text{PC}} = 8.51$ ), 56.3 (C6), 39.1 ( $\text{NMe}_2$ ), 13.2 (d,  $J_{\text{CP}} = 28.7$ ,  $\text{PMe}_3$ ).  $^{19}\text{F}$  { $^1\text{H}$ } NMR ( $\text{acetone-}d_6$ ,  $\delta$ , 25 °C): -61.68 (s, - $\text{CF}_3$ ).  $^{31}\text{P}$  { $^1\text{H}$ } NMR ( $\text{acetone-}d_6$ ,  $\delta$ , 25 °C): -12.43 ( $J_{\text{WP}} = 308$ ). HRMS ESI-MS ( $m/z$ , calculated (rel. intensity, %), observed (rel. intensity, %), ppm, (M + H)<sup>+</sup>: 691.1812 (84.71), 691.1819 (87.15), 692.1837 (80.03), 692.1844 (83.95), 693.1835 (100), 693.1845 (100), 694.1877 (42.5), 694.1880 (46.17), 695.1868 (84.18), 695.1875 (87.58).

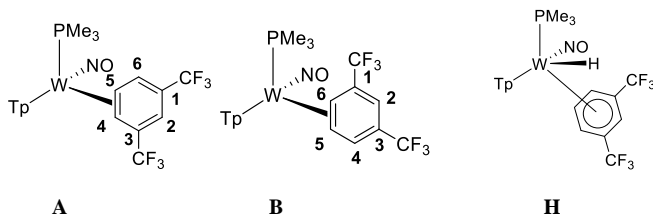
### WTp(NO)(PMe<sub>3</sub>)(4,5- $\eta^2$ -(1,2-bistrifluoromethylbenzene)) (20)



An oven-dried 4-dram vial was charged with **2** (0.608 g, 1.05 mmol) and 1,2-bis-trifluoromethylbenzene (3.02 g, 14.1 mmol), and the heterogeneous yellow reaction mixture was allowed to stir. After 16 h the reaction mixture had retained its heterogeneous golden-colored consistency but analysis by  $^{31}\text{P}$  NMR confirmed the absence of **1** and the generation of a new species. The heterogeneous yellow reaction mixture was added to 50 mL of stirring pentane to precipitate out a vibrant yellow solid. The solid was then filtered through a 30 mL fine porosity fritted disc and washed with pentane (3 x 20 mL) before the yellow powder was allowed to desiccate under active vacuum and a mass taken of the vibrant yellow solid (0.477 g, 64.0 % yield).

CV (DMA):  $E_{p,a} = +0.45$  V (NHE). IR:  $\nu(\text{BH}) = 2482$   $\text{cm}^{-1}$ ,  $\nu(\text{NO}) = 1592$   $\text{cm}^{-1}$ .  $^1\text{H}$  NMR (acetone- $d_6$ ,  $\delta$ , 25  $^\circ\text{C}$ ): 8.04 (3H, d, overlapping Tp3/5), 8.00 (1H, d, Tp3/5), 7.90 (1H, d, Tp3/5), 7.68 (1H, d,  $J = 6.87$ , H3), 7.55 (1H, d,  $J = 5.50$ , H6), 7.53 (1H, d, Tp3C), 6.40 (1H, t, Tp4A), 6.38 (1H, t, Tp4B), 6.37 (1H, t, Tp4C), 3.80 (1H, m, H5), 2.15 (1H, t,  $J = 7.60$ , H4), 1.71 (9H, d,  $J_{\text{PC}} = 8.48$ ,  $\text{PMe}_3$ ).  $^{31}\text{P}$   $\{^1\text{H}\}$  NMR (acetone- $d_6$ ,  $\delta$ , 25 $^\circ\text{C}$ ): -13.57 ( $J_{\text{WP}} = 302$ ).  $^{19}\text{F}$   $\{^1\text{H}\}$  NMR (acetone- $d_6$ ,  $\delta$ , 25 $^\circ\text{C}$ ): -56.6 (3F, q,  $^5J_{\text{FF}} = 12.5$ ,  $\text{CF}_3$ ), -56.7 (3F, q,  $^5J_{\text{FF}} = 12.5$ ,  $\text{CF}_3$ ).  $^{13}\text{C}$   $\{^1\text{H}\}$  NMR (acetone- $d_6$ ,  $\delta$ , 25  $^\circ\text{C}$ ): 144.5 (Tp3/5), 141.7 (Tp3/5), 141.3 (C3), 141.0 (Tp3/5), 138.5 (C6), 137.2 (Tp3/5), 136.5 (Tp3/5), 136.0 (Tp3/5), 124.1 (overlapping  $\text{CF}_3$ , q,  $J_{\text{CF}} = 273.4$ ), 113.3 (C1/C2, q,  $J_{\text{CF}} = 30.1$ ), 111.0 (C1/C2, q,  $J_{\text{CF}} = 31.2$ ), 106.5 (Tp4), 106.4 (Tp4), 106.0 (Tp4), 60.7 (C5, d,  $J_{\text{PC}} = 9.5$ ), 58.2 (C4), 13.6 ( $\text{PMe}_3$ , d,  $J_{\text{PC}} = 28.7$ ). A SC-XRD study confirms the identify of this compound (SI).

### WTp(NO)(PMe<sub>3</sub>)(4,5- $\eta^2$ -(1,3-bistrifluoromethylbenzene)) (**21**)



A 4-dram vial was charged with **2** (0.097 g, 0.167 mmol) and neat 1,3-bis(trifluoromethyl)benzene (3.17 g, 14.8 mmol) and the initially heterogeneous yellow reaction mixture was allowed to stir. After 18 h the reaction mixture was still a heterogeneous yellow but no starting material was detected by cyclic voltammetry. This mixture was then slowly added a solution of stirring hexanes (20 mL) that had been cooled to -30  $^\circ\text{C}$  to generate a yellow precipitate. The precipitate was then isolated on a 15mL fine porosity fritted disc, washed with hexanes (3x 10 mL) and desiccated to yield **5**. A yellow solid was obtained (0.041 g, 34%). The filtrate was collected and the pentane was distilled to re-collect the excess aromatic ligand which was used in similar reaction procedures without noticeable inhibition of yield. This complex is isolated in an approximate 7:1 ratio of A:B.

CV (DMA):  $E_{p,a} = +0.42$  V (NHE). IR:  $\nu(\text{BH}) = 2493$   $\text{cm}^{-1}$ ,  $\nu(\text{NO}) = 1582$   $\text{cm}^{-1}$ . Characterization for **21A**  $^1\text{H}$  NMR (acetone- $d_6$ ,  $\delta$ , 25  $^\circ\text{C}$ ): 8.06 (1H, d, Tp5C), 8.00 (1H, d, Tp5B), 7.95 (1H, d, Tp3B), 7.88 (1H, d, Tp3/5A), 7.71 (1H, d, Tp3/5A), 7.57 (1H, d,  $J = 4.96$ , H6), 7.50 (1H, d, Tp3C), 6.39 (1H, t, Tp4C), 6.36 (1H, t, Tp4B), 6.27 (1H, t, Tp4A), 6.25 (1H, broad s, H2), 3.91 (1H, m, H5), 2.30 (1H, d,  $J = 9.32$ , H4), 1.36 (9H, d,  $J = 8.44$ ,

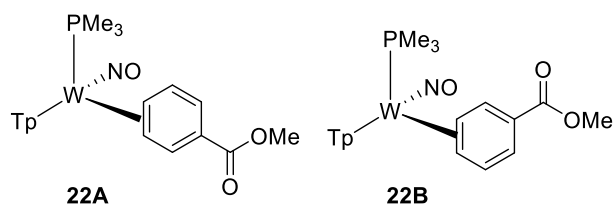
PMe<sub>3</sub>). <sup>13</sup>C {<sup>1</sup>H} NMR (acetone-*d*<sub>6</sub>, δ, 25 °C): 145.3 (Tp3/5A), 142.5 (Tp3/5A), 141.7 (Tp3C), 138.5 (C6), 138.0 (Tp3/5), 137.5 (Tp5B), 137.2 (Tp3/5), 128.8 (C1/C3, q, *J*<sub>CF</sub> = 31.5), 126.3 (CF<sub>3</sub>, q, *J*<sub>CF</sub> = 272.1), 125.7 (CF<sub>3</sub>, q, *J*<sub>CF</sub> = 272.7), 116.8 (C1/C3, q, *J*<sub>CF</sub> = 32.1), 107.5 (Tp4), 107.3 (Tp4), 106.2 (Tp4), 106.5 (H2), 62.1 (H5), 60.7 (H4, *J* = 25.0), 12.95 (d, *J*<sub>PC</sub> = 28.7, PMe<sub>3</sub>). <sup>31</sup>P {<sup>1</sup>H} NMR (acetone-*d*<sub>6</sub>, δ, 25 °C): -14.46 (*J*<sub>WP</sub> = 289).

Partial characterization for **21B** 7.70 (1H, buried, H4), 6.49 (1H, broad s, H2), 4.33 (1H, dd, *J* = 9.3, 12.4, H4), 2.19 (1H, broad t, *J* = 9.3, H5), 1.14 (9H, d, *J*<sub>PH</sub> = 8.50, PMe<sub>3</sub>). <sup>31</sup>P NMR (acetone-*d*<sub>6</sub>, δ, 25 °C): -12.17.

Partial characterization for **21H**: <sup>1</sup>H NMR (acetone-*d*<sub>6</sub>, δ, 25 °C): 9.23 (1H, m, *J*<sub>PH</sub> = 102.1 *J*<sub>WH</sub> = 30.8, W-H resonance), 6.01 (1H, t, Tp4). <sup>31</sup>P {<sup>1</sup>H} NMR (acetone-*d*<sub>6</sub>, δ, 25 °C): -2.84 (*J*<sub>WP</sub> = 172).

<sup>19</sup>F {<sup>1</sup>H} NMR resonances for all isomers (acetone-*d*<sub>6</sub>, δ, 25 °C): -56.9, -59.7 for **21A**, -60.0 for **21A**, -60.8, -61.8, -62.4. Elemental Analysis for C<sub>20</sub>H<sub>23</sub>BF<sub>6</sub>N<sub>7</sub>OPW: Calculated: C, 33.50; H, 3.23; N, 13.67. Found: C, 33.50; H, 3.09; N, 13.54.

### WTp(NO)(PMe<sub>3</sub>)(η<sup>2</sup>-1,2-methyl benzoate) (**22**)

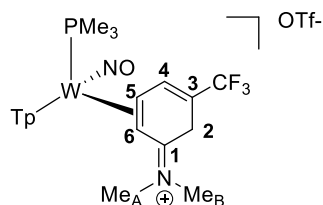


A 4-dram vial was charged with **2** (1.00 g, 1.72 mmol) and trimethyl orthobenzoate (0.94 g, 5.16 mmol) followed by THF (3 mL). This homogenous mixture was stirred at room temperature for 16 h. The resulting solution had turned black over the course of the reaction. A 150 mL coarse porosity fritted disc was filled 2/3 full with silica and set in diethyl ether. The reaction solution was then loaded onto this silica column. Upon eluting with diethyl ether a green band develops on the column followed by a yellow colored band. Upon continued elution with diethyl ether (~ 700 mL total) the initial green filtrate was discarded and with continued elution the original yellow-colored band undergoes a color change to an orange colored band while on the silica column. This orange band was collected in a filter flask and all of the solvent was removed in vacuo. The resulting orange film was picked up in a minimal amount of DCM (~ 3 mL) and added to a solution of stirring pentane (100 mL). Upon addition of the reaction mixture to the pentane solution an orange solid precipitates from solution. The resulting orange precipitant was collected on a 30 mL fine porosity fritted disc and washed with hexanes (4 x 15mL). The resulting solid was desiccated overnight, yielding **22** (0.495 g, 45% yield).

CV (DMA) *E*<sub>p,a</sub> = -0.03 (NHE). IR: ν(BH) = 2480 cm<sup>-1</sup>, ν(CO) = 1688 cm<sup>-1</sup>, ν(NO) = 1568 cm<sup>-1</sup>. <sup>1</sup>H NMR (MeCN-*d*<sub>3</sub>, δ, 25 °C): 8.18 (1H, d, Tp5A, **B**), 8.13 (1H, d, *J* = 6.3, H3, **A**), 8.06 (1H, d, Tp5A, **A**), 7.99 (1H, d, *J* = 5.5, H6, **B**), 7.92 (1H, d, Tp5B, **A**), 7.91 (2H, overlapping d, Tp5C for **A** and Tp5B for **B**), 7.90 (1H, d, Tp5C, **B**), 7.87 (1H, d, Tp3B, **A**), 7.86 (1H, d, Tp3B, **B**), 7.82 (2H, overlapping d, TpA3 for **A** and TpA3 for **B**), 7.35 (1H, d, TpC3, **A**), 7.34 (1H, d, TpC3, **B**), 6.96 (1H, dd, *J* = 9.8, 5.9, H3, **B**), 6.82 (1H, dd, *J* = 9.6, 4.97, H6, **A**), 6.35 (1H, t, Tp4A, **A**), 6.34 (1H, t, Tp4B, **A**), 6.33 (1H, t, Tp4A, **B**), 6.31 (1H, t, Tp4B, **B**), 6.29 (1H, t, Tp4C, **A**), 6.28 (1H, t, Tp4C, **B**), 6.14 (1H, dd, *J* = 9.6, 1.5, H5, **A**), 6.07 (1H, dd, *J* = 9.3, 1.3, H4, **B**), 4.02 (1H, m, H1, **A**), 3.87 (1H, m, H1, **B**), 3.76 (3H, s, -OMe, **A**), 3.75 (3H, s, -OMe, **B**), 2.29 (1H, m, H2, **B**), 2.23 (1H, m, H2, **A**), 1.26 (9H, d, *J*<sub>PH</sub> = 8.53, PMe<sub>3</sub>, **B**), 1.24 (9H, d, *J*<sub>PH</sub> = 8.51, PMe<sub>3</sub>, **A**). <sup>13</sup>C {<sup>1</sup>H} NMR (MeCN-*d*<sub>3</sub>, δ, 25 °C): 167.9 (C7B), 167.7 (C7A), 147.7 (2C, overlapping, Tp3/5A, **B**), 145.4 (Tp3/5A), 145.2 (Tp3/5B), 144.4 (d, *J*<sub>PC</sub> = 2.76, C6B), 143.3 (2C, overlapping Tp3/5A, **B**), 142.1 (Tp3/5A), 142.1 (Tp3/5B), 142.0 (C3A), 138.1 (Tp3/5A), 137.4 (Tp3/5B), 137.0 (Tp3/5A), 136.9 (Tp3/5B), 134.4 (C3B), 132.9 (d, *J*<sub>PC</sub>

= 2.62, C6A), 129.3 (C4A), 129.2 (C5B), 115.5 (C5A), 113.9 (C4B), 107.5 (Tp4A), 107.4 (Tp4B), 107.3 (Tp4A), 107.2 (Tp4B), 107.0 (Tp4A), 106.7 (Tp4B), 66.3 (d,  $J_{PC} = 8.54$ , C1A), 64.6 (C2B), 64.0 (d,  $J_{PC} = 7.03$ , C1B), 62.4 (C2A), 51.5 (-OMeB), 51.5 (-OMeA), 13.4 (3C, d,  $J_{PC} = 28.89$ , PMe<sub>3</sub>B), 13.32 (3C, d,  $J_{PC} = 28.71$ , PMe<sub>3</sub>B).

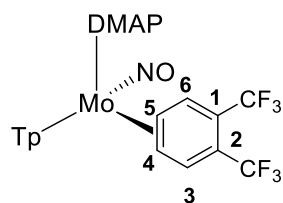
### WTp(NO)(PMe<sub>3</sub>)(5,6-η<sup>2</sup>-(3-trifluoromethyl-N,N-dimethyl-anilinium)]OTf (23)



To an oven dried 4-dram vials added **19** (0.096 g, 0.139 mmol) and along with MeOH (~ 2 mL) to generate a heterogeneous yellow reaction mixture. This solution was allowed to cool in a -30 °C freezer over a course of 30 min before DPhAT (0.072 g, 0.225 mmol) was added to the reaction mixture at reduced temperature. After 1.5 h the reaction mixture was added to a stirring solution of diethyl ether (30 mL) to precipitate out a yellow solid and the isolated solid was washed with pentane (3 x 10 mL) after isolation on a fine 15 mL fritted disc and allowed to desiccate for 3 h (0.096 g, 82.1%).

CV (DMA):  $E_{p,a} = +1.34$  V (NHE),  $E_{p,c} = -1.54$  V (NHE). IR:  $\nu(\text{BH}) = 2519$  cm<sup>-1</sup>,  $\nu(\text{NO}) = 1602$  cm<sup>-1</sup>,  $\nu(\text{CN iminium}) = 1581$  cm<sup>-1</sup>. <sup>1</sup>H NMR (acetone-*d*<sub>6</sub>,  $\delta$ , 25 °C):  $\delta$  ppm 8.22 (1H, d, Tp3/5C), 8.16 (1H, d, Tp5B), 8.07 (2H overlapping, d, Tp5A and Tp3/5), 8.03 (1H, d, Tp3C), 7.49 (1H, d, Tp3A), 7.27 (1H, broad s, Tp3/5C), 6.55 (1H, t, Tp4C), 6.49 (1H, t, Tp4B), 6.47 (1H, t, Tp4A), 4.00 (1H, m, H5), 3.80 (3H, s, NMe<sub>A</sub>), 3.74 (1H, d,  $J = 22.4$ , H2), 3.47 (1H, d,  $J = 22.4$ , H2'), 2.67 (1H, m, H6), 2.58 (3H, s, NMe<sub>B</sub>), 1.41 (9H, d,  $J_{PH} = 9.20$ , PMe<sub>3</sub>). <sup>13</sup>C NMR (acetone-*d*<sub>6</sub>,  $\delta$ , 25 °C): 181.7 (C1), 145.9 (Tp3/5C), 143.1 (Tp3/5), 142.7 (Tp3/5), 142.6 (Tp3C), 139.2 (Tp5B), 138.8 (Tp3/5), 133.6 (C4), 122.3 (CF<sub>3</sub>, q,  $J_{CF} = 322.2$ ), 113.0 (C3, q,  $J_{CF} = 31.6$ ), 108.4 (Tp4), 108.3 (Tp4), 107.8 (Tp4), 61.2 (C5,  $J_{PC} = 12.3$ ), 55.3 (C6), 28.6 (C2), 43.1 (NMe<sub>A</sub>), 41.8 (NMe<sub>B</sub>) 28.5 (C3, buried) 13.5 (PMe<sub>3</sub>, d,  $J_{CP} = 31.7$ ). <sup>19</sup>F NMR (acetone-*d*<sub>6</sub>,  $\delta$ , 25 °C): -78.28 (s, CF<sub>3</sub>). <sup>31</sup>P NMR (acetone-*d*<sub>6</sub>,  $\delta$ , 25 °C): -11.16 ( $J_{WP} = 281$ ).

### MoTp(NO)(DMAP)(4,5-η<sup>2</sup>-(1,2-bis(trifluoromethyl)benzene)) (24)

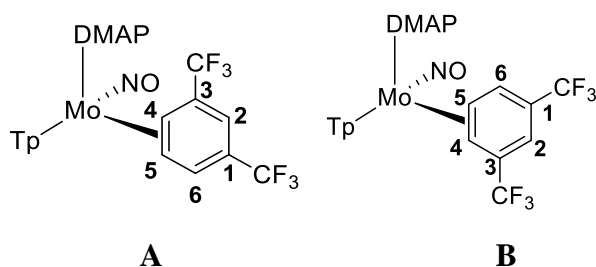


An oven-dried 4-dram vial was charged with complex **1** (0.230 g, 0.379 mmol) followed by 1,2-bis-trifluoromethylbenzene (1.95 g, 1.07 mmol) and DME (4 mL). This initially heterogeneous orange reaction mixture was capped and stirred at room temperature for 3 h. This mixture was then slowly added to a -60 °C solution of stirring pentane (50 mL) yielding an orange precipitate. The precipitate was then isolated on a 15mL fine porosity fritted disc, washed with pentane (3 x 10mL) and desiccated to yield **24**. A vibrant orange-red solid was obtained (0.074 g, 28.9%).

CV (DMA)  $E_{p,a} = -0.06$  V (NHE). IR:  $\nu_{\text{BH}} = 2478$  cm<sup>-1</sup>,  $\nu_{\text{NO}} = 1597$  cm<sup>-1</sup>. <sup>1</sup>H NMR (acetone-*d*<sub>6</sub>,  $\delta$ , 25 °C): 8.07 (1H, d, Tp5C), 7.97 (1H, d, Tp3/5), 7.90 (1H, d, Tp3/5), 7.84 (1H, d, Tp3/5), 7.80 (broad, 2H, DMAP-2/6),

7.66 (1H, d,  $J = 6.50$ , H3), 7.58 (1H, d, Tp3C), 7.29 (1H, d,  $J = 6.39$ , H6), 6.97 (1H, d, Tp3/5), 6.72 (2H, d,  $J = 5.97$ , DMAP-3/5), 6.41 (1H, t, Tp4C), 6.40 (t, 1H, Tp4), 6.14 (1H, t, Tp4), 3.68 (1H, t,  $J = 7.10$ , H5), 3.19 (1H, t,  $J = 7.23$ , H4), 3.11 (s, 6H, NMe<sub>2</sub>). <sup>13</sup>C {<sup>1</sup>H} NMR (acetone-*d*<sub>6</sub>,  $\delta$ , 25 °C): 155.4 (DMAP-4), 150.6 (DMAP-2/6), 142.8 (Tp3/5), 142.7 (Tp3/5), 141.8 (Tp3C), 140.8 (C3), 140.3 (C6), 137.9 (Tp5C), 137.2 (Tp3/5), 136.2 (Tp3/5), 125.6 (-CF<sub>3</sub>, q,  $J_{CF} = 272.0$ ), 125.5 (-CF<sub>3</sub>, q,  $J_{CF} = 271.2$ ), 113.5 (2C, overlapping m, C1/C2) 108.6 (DMAP-3/5), 107.2 (Tp4), 106.7 (Tp4), 106.6 (Tp4), 75.5 (C5), 73.2 (C4), 39.2 (NMe<sub>2</sub>). <sup>19</sup>F {<sup>1</sup>H} NMR (acetone-*d*<sub>6</sub>, 25 °C):  $\delta$  ppm -58.03 (6F, s, overlapping, CF<sub>3</sub>s). Calculated for C<sub>24</sub>H<sub>24</sub>BF<sub>6</sub>MoN<sub>9</sub>O: Calculated: C, 42.69; H, 3.58; N, 18.67. Found: C, 42.90; H, 3.56; N, 18.93. A SC-XRD study confirms the identify of this compound (SI).

### MoTp(NO)(DMAP)(4,5- $\eta^2$ -(1,3-bis(trifluoromethyl)benzene)) (25)

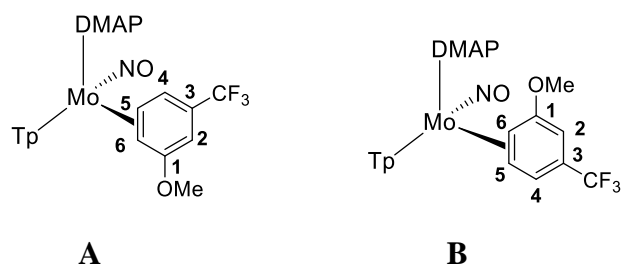


A 4-dram vial was charged with complex **1** (0.500 g, 0.820 mmol) 1,3-bis-trifluoromethylbenzene (2.00 g, 9.34 mmol) and DME (5 mL). This mixture was capped and stirred at room temperature for 3 h. This mixture was then slowly added to a -60 °C solution of stirring pentane (50 mL) yielding an orange precipitate. The precipitate was then isolated on a 15mL fine porosity fritted disc, washed with pentane (3 x 10 mL) and desiccated to yield **25**. An orange solid was obtained (0.240 g, 43.2%). The complex is isolated in an approximate 3:1 ratio of A:B.

CV (DMA):  $E_{p,a} = -0.10$  V (NHE). IR:  $\nu_{BH} = 2488$  cm<sup>-1</sup>,  $\nu_{NO} = 1585$  cm<sup>-1</sup>. Characterization of **25A** <sup>1</sup>H NMR (acetone-*d*<sub>6</sub>,  $\delta$ , 3 °C): 8.10 (1 H, d, Tp3/5), 7.99 (1H, d, Tp3/5), 7.88 (1H, d, Tp3/5), 7.86 (1H, d, Tp3/5), 7.71 (1H, d, Tp3C), 7.70 (1H, d,  $J = 6.34$ , H6), 6.96 (1H, d, Tp3/5), 6.76 (2H, broad, DMAP-3/5), 6.65 (1H, s, H2), 6.45 (1H, buried, Tp4), 6.41 (1H, t, Tp4), 6.11 (1H, buried, H4), 3.89 (1H, d,  $J = 8.48$ , H4), 3.19 (1H, t,  $J = 7.70$ , H5), 3.07 (6H, s, NMe<sub>2</sub>). <sup>13</sup>C {<sup>1</sup>H} NMR (acetone-*d*<sub>6</sub>,  $\delta$ , 3 °C): 155.1 (DMAP-4), 150.6 (DMAP-2/6), 142.8 (Tp3/5), 142.4 (Tp3/5), 141.8 (Tp3/5), 141.2 (C6), 137.9 (Tp3/5), 137.2 (Tp3/5), 136.2 (Tp3/5), 126.0 (-CF<sub>3</sub>, q,  $J_{CF} = 269.0$ ), 125.5 (-CF<sub>3</sub>, q,  $J_{CF} = 274.0$ ), 116.4 (2C, overlapping, C1/C3), 112.2 (C2), 108.6 (DMAP-3/5), 108.4 (Tp4), 106.4 (Tp4), 106.2 (Tp4), 75.9 (C5), 73.1 (C4), 39.1 (NMe<sub>2</sub>). <sup>19</sup>F {<sup>1</sup>H} NMR (acetone-*d*<sub>6</sub>,  $\delta$ , 25 °C): -61.52 ppm (-CF<sub>3</sub>), -62.66 ppm (CF<sub>3</sub>) –overlapping for both diastereomers.

Characterization of **25B** <sup>1</sup>H NMR (acetone-*d*<sub>6</sub>,  $\delta$ , 3 °C): 8.10 (1 H, buried, Tp3/5), 7.97 (1H, d, Tp3/5), 7.59 (1H, d, Tp3/5), 7.55 (1H, d, Tp3/5), 7.32 (1H, d,  $J = 5.20$ , H6), 6.93 (1H, d, Tp3/5), 6.71 (1H, s, H2), 6.46 (1H, buried, Tp4), 6.30 (1H, t, Tp4), 6.11 (1H, buried, Tp4), 3.72 (1H, t,  $J = 6.56$ , H5), 3.36 (1H, d,  $J = 8.20$ , H4), 3.11 (6H, s, -NMe<sub>2</sub>). <sup>13</sup>C {<sup>1</sup>H} NMR (acetone-*d*<sub>6</sub>,  $\delta$ , 25 °C): 155.1 (DMAP-4), 150.6 (DMAP-2/6), 142.5 (Tp3/5), 141.3 (Tp3/5), 140.1 (C6), 140.1 (Tp3/5), 137.4 (Tp3/5), 136.0 (Tp3/5), 135.7 (Tp3/5), 135.5 (Tp3/5), 126.0 (-CF<sub>3</sub>, q,  $J_{CF} = 269.0$ ), 125.5 (-CF<sub>3</sub>, q,  $J_{CF} = 274.0$ ), 112.1 (C2), 108.6 (DMAP-3/5), 108.4 (Tp4), 106.4 (Tp4), 106.2 (Tp4), 75.9 (C5), 73.1 (C4), 39.1 (NMe<sub>2</sub>). A SC-XRD study confirms the identify of this compound (SI).

## MoTp(NO)(DMAP)(5,6- $\eta^2$ -(3-methoxytrifluorotoluene)) (26)

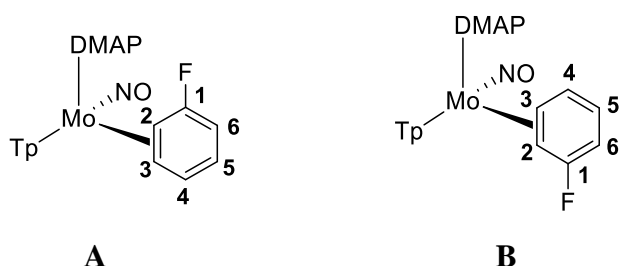


A 4-dram vial was charged with complex **1** (0.217 g, 0.357 mmol) along with 3-(Trifluoromethyl)anisole (1 mL, 6.91 mmol) and DME (1 mL). This mixture was capped and stirred at room temperature for 4 h. This mixture was then loaded onto a medium 30 mL fritted disc filled with silica (~ 2 cm) that had been set in diethyl ether. The column was then eluted with diethyl ether (~ 100 mL) to elute a vibrant yellow band. The eluent was collected in a filter flask and the solvent was removed in vacuo until a minimal amount of solvent remained (< 10 mL). To this solution was added pentane (50 mL) to induce precipitation. Upon addition of pentane a vibrant yellow solid precipitates from solution. The precipitate was then isolated on a 15mL fine porosity fritted disc, washed with pentane (3 x 10 mL) and desiccated under dynamic vacuum for 3 h to yield **26**. A yellow solid was obtained (0.106 g, 46.7%). The complex is isolated as an approximate 2.5:1 ratio of A:B.

CV (DMA):  $E_{p,a} = -0.260$  V. IR:  $\nu_{\text{BH}} = 2458$   $\text{cm}^{-1}$ ,  $\nu_{\text{NO}} = 1575$   $\text{cm}^{-1}$ . Characterization of **26A**  $^1\text{H}$  NMR (acetone- $d_6$ ,  $\delta$ , 25 °C):  $\delta$  ppm 8.02 (1 H, d, Tp3/5), 7.94 (1H, d, Tp3/5), 7.93 (1H, d, Tp3/5), 7.85 (1H, d, Tp3/5), 7.80 (2H, broad, DMAP-2/6), 7.52 (1H, d, Tp3/5), 7.01 (1H, d,  $J = 6.1$ , H4), 6.93 (1H, d, Tp3/5), 6.63 (2H, broad d,  $J = 6.3$  DMAP-3/5), 6.38 (1H, t overlapping with minor isomer, Tp4), 6.36 (1H, t, Tp4), 6.11 (1H, t overlapping with minor isomer, Tp4), 5.43 (1H, s, H2), 3.56 (3H, s, -OMe), 3.52 (1H, d,  $J = 9.1$ , H6), 3.19 (1H, m, H5), 3.08 (6H, s, NMe<sub>2</sub>).  $^{13}\text{C}$   $\{^1\text{H}\}$  NMR (acetone- $d_6$ , 0 °C): 166.9 (C1), 155.0 (DMAP-C4), 150.6 (DMAP-C2/6), 142.5 (Tp3/5), 142.4 (Tp3/5), 141.6 (Tp3/5), 137.5 (Tp3/5), 136.9 (Tp3/5), 135.9 (Tp3/5), 126.4 (-CF<sub>3</sub>, q,  $J_{\text{CF}} = 269.6$ ), 126.1 (C4, overlapping m), 119.4 (C3, q,  $J_{\text{CF}} = 30.1$ ), 108.3 (DMAP-3/5), 107.0 (Tp4), 106.4 (Tp4), 106.3 (Tp4), 85.8 (C2), 73.7 (C6), 72.8 (C5), 54.2 (-OMe), 39.1 (NMe<sub>2</sub>).  $^{19}\text{F}$   $\{^1\text{H}\}$  NMR (acetone- $d_6$ ,  $\delta$ , 25 °C): -60.5 (-CF<sub>3</sub>).

Characterization of **26B**  $^1\text{H}$  NMR (acetone- $d_6$ ,  $\delta$ , 25 °C): 8.02 (1 H, d, Tp3/5), 7.87 (1H, d, Tp3/5), 7.84 (1H, d, Tp3/5), 7.81 (1H, d, Tp3/5), 7.80 (2H, broad overlapping with major isomer, DMAP-2/6), 7.55 (1H, buried, H4), 6.95 (1H, d, Tp3/5), 6.68 (2H, broad d,  $J = 6.21$ , DMAP-3/5), 6.38 (1H, t overlapping with major isomer, Tp4), 6.25 (1H, t, Tp4), 6.11 (1H, t overlapping with minor isomer, Tp4), 5.50 (1H, s, H2), 3.63 (1H, m, H5), 3.45 (3H, s, -OMe), 3.19 (1H, buried, H6), 3.09 (6H, s, NMe<sub>2</sub>).  $^{13}\text{C}$   $\{^1\text{H}\}$  NMR (acetone- $d_6$ ,  $\delta$ , 0 °C): 167.3 (C1), 154.9 (DMAP-C4), 150.6 (overlapping DMAP-C2/C6), 144.2 (Tp3/5), 142.5 (Tp3/5), 142.4 (Tp3/5), 141.5 (Tp3/5), 136.8 (Tp3/5), 135.8 (Tp3/5), 126.3 (-CF<sub>3</sub>, q,  $J_{\text{CF}} = 269.6$ ), 126.1 (C4, overlapping m with major isomer), 119.1 (C3, q,  $J_{\text{CF}} = 29.5$ ), 108.3 (2C, overlapping with major isomer, DMAP-3/5), 112.2 (C2), 107.0 (Tp4), 106.3 (Tp4), 105.5 (Tp4), 86.3 (C2), 75.6 (C5), 71.0 (C6), 54.5 (-OMe), 39.1 (NMe<sub>2</sub>).  $^{19}\text{F}$   $\{^1\text{H}\}$  NMR (acetone- $d_6$ ,  $\delta$ , 25 °C): -61.7. A SC-XRD study confirms the identify of this compound (SI).

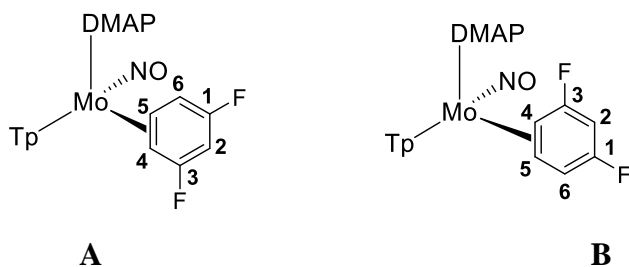
### MoTp(NO)(DMAP)(2,3- $\eta^2$ -(fluorobenzene)) (27)



A 4-dram vial was charged with **1** (0.500 g, 0.820 mmol) and fluorobenzene (8.03 g, 83.6 mmol). This mixture was capped and stirred at room temperature for 3 h. This mixture was then slowly added to a  $-60\text{ }^\circ\text{C}$  solution of pentane yielding a yellow precipitate. The precipitate was then isolated on a 15mL fine porosity fritted disc, washed with pentane (3x10mLs) and desiccated to yield **27**. A yellow solid was obtained (0.233 g, 50.8%). The complex is isolated as an approximate 1:1 ratio of A:B.

CV (DMA):  $E_{p,a} = -0.36\text{ V}$  (NHE). IR:  $\nu_{\text{BH}} = 2481\text{ cm}^{-1}$ ,  $\nu_{\text{NO}} = 1573\text{ cm}^{-1}$ . Two coordination diastereomers **A** : **B** = 1:1.  $^1\text{H}$  NMR (acetone- $d_6$ ,  $\delta$ ,  $-20\text{ }^\circ\text{C}$ ): 6.70 (1H, m, H4**B**), 6.68 (1H, m, H4**A**), 6.39 (2H, overlapping triplets, Tp **A** and **B**), 6.34 (1H, t, Tp**A/B**), 6.30 (1H, t, Tp**A/B**), 6.13 (2H, overlapping triplets, Tp **A** and **B**), 6.09 (1H, m, H3**A**), 6.06 (1H, m, H3**B**), 5.74 (1H, m, H2**B**), 5.70 (1H, m, H2**A**), 3.80 (1H, m, H5**B**), 3.64 (1H, t,  $J = 9.84$ , H6**A**), 3.35 (1H, m, H5**A**), 3.23 (1H, t,  $J = 9.90$ , H6**B**), 3.08 (12H, overlapping singlets, NMe for **A** and **B**).  $^{19}\text{F}$   $\{^1\text{H}\}$  NMR (acetone- $d_6$ ,  $25\text{ }^\circ\text{C}$ ):  $-97.6$  (1F, m, FA/**B**),  $-100.0$  (1F, m, FA/**B**). Attempts at elemental analysis were thwarted by the thermal instability of this complex and its sensitivity to oxidation.

### MoTp(NO)(DMAP)(4,5- $\eta^2$ -(1,3-difluorobenzene)) (28)

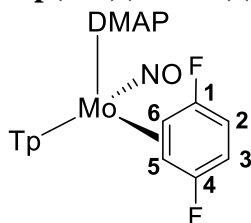


A 4-dram vial was charged with **1** (0.500 g, 0.82 mmol), 1,3-difluorobenzene (1.00g, 8.76 mmol), and 3 mLs of DME. The mixture was capped and stirred at room temperature for 3 h. This mixture was then slowly added to 30 mL solution of stirring pentane at  $-60\text{ }^\circ\text{C}$  to generate a yellow precipitate. The precipitate was then isolated on a 15mL fine porosity fritted disc, washed with pentane (3x10mLs), and desiccated to yield **5**. A yellow solid was obtained (0.330 g, 70%).

CV (DMA):  $E_{p,a} = -0.35\text{ V}$  (NHE). IR:  $\nu_{\text{BH}} = 2472\text{ cm}^{-1}$ ,  $\nu_{\text{NO}} = 1580\text{ cm}^{-1}$ .  $^1\text{H}$  NMR (acetone- $d_6$ ,  $\delta$ ,  $25\text{ }^\circ\text{C}$ ): Two coordination diastereomers **A** : **B** = 1:1. 8.03 (2H, overlapping doublets, Tp **A** and **B**), 7.97 (2H, overlapping doublets, Tp**A/B**), 7.94 (1H, d, Tp**A/B**), 7.92 (1H, d, Tp**A/B**), 7.90 (1H, d, Tp**A/B**), 7.86 (1H, d, Tp**A/B**), 7.82 (4H, broad, DMAPs **A** for **A** and **B**) 7.55 (1H, d, Tp**A**), 7.53 (1H, d, Tp**B**), 6.97 (2H, overlapping doublets, Tp **A** and **B**), 6.70 (2H, broad, DMAP **B** **A/B**), 6.64 (2H, broad, DMAP **B** **A/B**), 6.40 (2H, overlapping triplets, Tp **A** and **B**), 6.38 (1H, t, Tp**A/B**), 6.31 (1H, t, Tp**A/B**), 6.25 (1H, m, H4**A**), 6.13 (2H, overlapping triplets, Tp **A** and **B**), 5.83 (1H, dd,  $J_{\text{HF}} = 11.43$ ,  $J = 5.79$ , H4**B**), 5.79 (1H, t,  $J = 10.10$ , H2**A/B**), 5.74 (1H, t,  $J = 9.80$ ,

H2A/B), 3.68 (1H, m, H5B), 3.53 (1H, t,  $J=9.44$ , H6A), 3.18 (1H, m H5A), 3.09 (1H, buried, H6B), 3.07 (12H, overlapping singlets, NMe<sub>2</sub>). <sup>19</sup>F {<sup>1</sup>H} NMR (acetone-*d*<sub>6</sub>,  $\delta$ , 25 °C): -94.9 (1F, m), -97.3 (1F, m), -125.8 (1F, 1m), -126.2 (1F, m). Attempts at elemental analysis were thwarted by the thermal instability of this complex and its sensitivity to oxidation.

### MoTp(NO)(DMAP)(5,6- $\eta^2$ -(1,4-difluorobenzene)) (29)

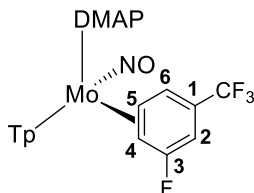


29

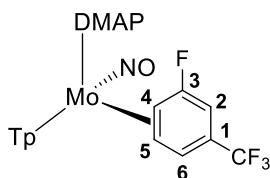
A 4-dram vial was charged with **1** (0.500 g, 0.82 mmol), 1,4-difluorobenzene (1.00g, 8.76 mmol) and 3 mLs of DME. The heterogeneous red reaction mixture was capped and stirred at room temperature for 3 h during which time it turns to a homogeneous brown/black coloration. This mixture was then slowly added to 50 mL of pentane that had been cooled to -60 °C and upon addition, a yellow precipitate forms. The yellow solid was then isolated on a 15mL fine porosity fritted disc, washed with pentane (3 x 10 mL), and desiccated under static vacuum for 16 h to yield **15**. (0.416 g, 87.8%).

CV (DMA)  $E_{p,a} = -0.21$  V (NHE). IR:  $\nu_{\text{BH}} = 2472$  cm<sup>-1</sup>,  $\nu_{\text{NO}} = 1581$  cm<sup>-1</sup>. <sup>1</sup>H NMR (acetone-*d*<sub>6</sub>,  $\delta$ , 15 °C): 8.04 (1H, d, Tp5C), 7.93 (1H, d, Tp3A), 7.91 (1H, d, Tp3/5B), 7.90 (2H, broad, DMAP-2/6), 7.87 (1H, d, Tp), 7.57 (1H, d, Tp3C), 6.99 (1H, d, Tp3/5A), 6.63 (2H, broad, DMAP B), 6.40 (1H, t, Tp4C), 6.29 (1H, t, Tp4A), 6.13 (1H, t, Tp4B), 5.59 (1H, m, H3), 5.54 (1H, m, H2), 3.74 (1H, m, H6), 3.27 (1H, m, H5), 3.07 (6H, s, NMe<sub>2</sub>). <sup>13</sup>C {<sup>1</sup>H} NMR (acetone-*d*<sub>6</sub>,  $\delta$ , 15 °C): 165.0 (C1/C4, d,  $J_{\text{CF}} = 248.6$ ), 164.9 (C1/C4, d,  $J_{\text{CF}} = 246.8$ ), 155.1 (DMAP-C), 150.5 (DMAP-2/6), 142.5 (Tp3/5), 141.6 (Tp3/5), 137.7 (Tp3/5), 137.0 (Tp3/5), 135.9 (Tp3/5), 107.4 (DMAP-3/5), 107.1 (Tp4C), 106.4 (Tp4B), 106.1 (Tp4A), 95.1 (C3, dd,  $J_{\text{CF}} = 9.9, 26.0$ ), 94.7 (C2, dd,  $J_{\text{CF}} = 9.7, 24.6$ ), 71.0 (C6, dd,  $J_{\text{CF}} = 8.5, 30.1$ ), 68.4 (C5, dd,  $J_{\text{CF}} = 8.4, 29.6$ ), 39.1 (NMe<sub>2</sub>). <sup>19</sup>F {<sup>1</sup>H} NMR (acetone-*d*<sub>6</sub>,  $\delta$ , 25 °C): -107.3 (1F, m), -109.5 (1F, m). Attempts at elemental analysis were thwarted by the thermal instability of this complex and its sensitivity to oxidation.

### MoTp(NO)(DMAP)(4,5- $\eta^2$ -(3-fluorobenzotrifluoride)) (30)



30A



30B

A 4-dram vial was charged with MoTp(NO)(DMAP)( $\eta^2$ -2,5-dimethylfuran) (0.250 g, 0.410 mmol) and 3-fluorobenzotrifluoride (1.50 g, 9.14 mmol).<sup>35</sup> This mixture was capped and stirred at room temperature for 5 days. This mixture was then isolated on a 15 mL fine porosity fritted disc. The precipitate was washed with pentane (3 x 10mL) and desiccated to yield **30**. An orange solid was obtained (0.135 g, 48.0%). Initially the ratio of **30A** : **30B** is approximately 9:1 due to what we believe is selective precipitation that results in a high



population of **30A** in the solid state under the precipitation conditions described. Over time (6 h) a 1:1 equilibrium is established between the two coordination diastereomers.

CV (DMA):  $E_{p,a} = -0.05$  V (NHE). IR:  $\nu_{\text{BH}} = 2490$   $\text{cm}^{-1}$ ,  $\nu_{\text{NO}} = 1590$   $\text{cm}^{-1}$ . Two coordination diastereomers A : B = 1:1 after 6 hours in solution. Characterization for **30A**  $^1\text{H}$  NMR (acetone- $d_6$ ,  $\delta$ , 25 °C): A (initial major): 8.05 (1H, d, Tp5C), 7.96 (1H, d, Tp5A), 7.88 (1H, d, Tp5B), 7.85 (1H, d, Tp3A), 7.80 (2H, broad, DMAP-2/6), 7.58 (1H, d, Tp3C), 7.19 (1H, d,  $J = 6.25$ , H6), 6.96 (1H, d, Tp3B), 6.65 (2H, d,  $J = 6.53$ , DMAP-3/5), 6.40 (1H, t, Tp4C), 6.38 (1H, t, Tp4A), 6.13 (1H, t, Tp4B), 5.79 (1H, dt,  $J = 11.71$ , 1.26, H2), 3.65 (1H, t,  $J = 9.66$ , H4), 3.24 (1H, m, H5), 3.08 (6H, s, NMe $_2$ ).  $^{13}\text{C}$  { $^1\text{H}$ } NMR (acetone- $d_6$ ,  $\delta$ , 25 °C): 169.4 (C3), 155.3 (DMAP 4), 142.7 (Tp3B), 142.6 (Tp3A), 141.7 (Tp3C), 137.7 (Tp5C), 137.2 (Tp5A), 136.1 (Tp5B), 131.1 (H6), 108.4 (DMAP-3/5), 107.2 (Tp4C), 106.6 (Tp4), 106.5 (Tp4), 91.6 (H2), 74.1 (H5), 70.4 (H4), 39.1 (NMe $_2$ ).  $^{19}\text{F}$  NMR { $^1\text{H}$ } (acetone- $d_6$ ,  $\delta$ , 25 °C):  $\delta$  -62.18 (3F, -CF $_3$ ), -99.54 (1F, F).

Characterization for **30B**  $^1\text{H}$  NMR (acetone- $d_6$ ,  $\delta$ , 25 °C): B (initial minor): 8.07 (1H, d, Tp3/5), 8.05 (1H, d, Tp3/5), 7.97 (1H, d, Tp3/5), 7.84 (1H, d, Tp3/5), 7.86 (2H, broad, DMAP-2/6), 7.56 (1H, d, Tp3/5), 7.34 (1H, d, Tp3/5), 6.82 (1H, d,  $J = 5.76$ , H6), 6.71 (2H, d,  $J = 6.48$ , DMAP-3/5), 6.40 (1H, t, Tp4), 6.31 (1H, t, Tp4), 6.14 (1H, t, Tp4), 5.84 (1H, dt,  $J = 11.67$ , 1.17, H2), 3.74 (1H, m, H5), 3.19 (1H, t,  $J = 8.49$ , H4), 3.10 (6H, s, NMe $s$ ).  $^{19}\text{F}$  { $^1\text{H}$ } NMR (acetone- $d_6$ ,  $\delta$ , 25 °C): -62.2 (3F, -CF $_3$ ), -97.05 (-F). Calculated for C $_{23}$ H $_{24}$ BF $_4$ MoN $_9$ O: Calculated: C, 44.18; H, 3.87; N, 20.16. Found: C, 43.94; H, 4.11; N, 20.41.

## References.

1. Liebov, B. K.; Harman, W. D., Group 6 Dihapto-Coordinate Dearomatization Agents for Organic Synthesis. *Chemical Reviews* **2017**, *117* (22), 13721-13755.
2. Keane, J. M.; Harman, W. D., A New Generation of  $\pi$ -Basic Dearomatization Agents. *Organometallics* **2005**, *24* (8), 1786-1798.
3. Harman, W. D., The Activation of Aromatic Molecules with Pentaammineosmium(II). *Chem. Rev.* **1997**, *97*, 1953-1978.
4. Lis, E. C.; Salomon, R. J.; Sabat, M.; Myers, W. H.; Harman, W. D., Synthesis of 1-Oxadecalins from Anisole Promoted by Tungsten. *Journal of the American Chemical Society* **2008**, *130* (37), 12472-12476.
5. Kolis, S. P.; Kopach, M. E.; Liu, R.; Harman, W. D., Osmium-Promoted Electrophilic Substitution of Anisoles: A Versatile New Method for the Incorporation of Carbon Substituents. *J. Org. Chem.* **1997**, *62* (1), 130.
6. Kopach, M. E.; Harman, W. D., The Osmium-Promoted [4+2] Cycloaddition Reaction of Anisole and Characterization of the  $h^2$ -4H-Anisolum Intermediate. *J. Org. Chem.* **1994**, *59*, 6506-6507.
7. Kopach, M. E.; Gonzalez, J.; Harman, W. D., Electrophilic substitutions on  $\eta^2$ -coordinated arenes: an unprecedented Michael addition for phenol and aniline. *Journal of the American Chemical Society* **1991**, *113* (23), 8972-8973.
8. Todd, M. A.; Grachan, M. L.; Sabat, M.; Myers, W. H.; Harman, W. D., Common Electrophilic Addition Reactions at the Phenol Ring: The Chemistry of  $TpW(NO)(PMe_3)(\eta^2\text{-phenol})$ . *Organometallics* **2006**, *25* (16), 3948-3954.
9. Todd, M. A.; Sabat, M.; Myers, W. H.; Smith, T. M.; Harman, W. D., Stereoselective Umpolung Tandem Addition of Heteroatoms to Phenol. *Journal of the American Chemical Society* **2008**, *130* (22), 6906-6907.
10. Gonzalez, J.; Sabat, M.; Harman, W. D., A Novel Dearomatization of Anilines via Complexation to Pentaammineosmium(II): Synthesis of Highly Functionalized 3-Aminocyclohexenes from Anilines. *J. Am. Chem. Soc.* **1993**, *115*, 8857.
11. Salomon, R. J.; Todd, M. A.; Sabat, M.; Myers, W. H.; Harman, W. D., Single and Double Electrophilic Addition Reactions to the Aniline Ring Promoted by a Tungsten  $\pi$ -Base. *Organometallics* **2010**, *29* (4), 707-709.
12. Wilson, K. B.; Myers, J. T.; Nedzbala, H. S.; Combee, L. A.; Sabat, M.; Harman, W. D., Sequential Tandem Addition to a Tungsten–Trifluorotoluene Complex: A Versatile Method for the Preparation of Highly Functionalized Trifluoromethylated Cyclohexenes. *Journal of the American Chemical Society* **2017**, *139* (33), 11401-11412.
13. Myers, J. T.; Smith, J. A.; Dakermanji, S. J.; Wilde, J. H.; Wilson, K. B.; Shivokevich, P. J.; Harman, W. D., Molybdenum(0) Dihapto-Coordination of Benzene and Trifluorotoluene: The Stabilizing and Chemo-Directing Influence of a  $CF_3$  Group. *Journal of the American Chemical Society* **2017**, *139* (33), 11392-11400.
14. Harman, W. D.; Sekine, M.; Taube, H., Substituent Effects on  $h^2$ -Coordinated Arene Complexes of Pentaammineosmium(II). *J. Am. Chem. Soc.* **1988**, *110*, 5725.
15. Lis, E. C.; Delafuente, D. A.; Lin, Y.; Mocella, C. J.; Todd, M. A.; Liu, W.; Sabat, M.; Myers, W. H.; Harman, W. D., The Uncommon Reactivity of Dihapto-Coordinated Nitrile, Ketone, and Alkene Ligands When Bound to a Powerful  $\pi$ -Base. *Organometallics* **2006**, *25* (21), 5051-5058.
16. Graham, P. M.; Meiere, S. H.; Sabat, M.; Harman, W. D., Dearomatization of Benzene, Deamidization of N,N-Dimethylformamide, and a Versatile New Tungsten  $\pi$  Base. *Organometallics* **2003**, *22* (22), 4364-4366.
17. Graham, P. M.; Mocella, C. J.; Sabat, M.; Harman, W. D., Dihapto-Coordinated Amide, Ester, and Aldehyde Complexes and Their Role in Decarbonylation. *Organometallics* **2005**, *24* (5), 911-919.

18. Sheppard, W. A., m-TRIFLUOROMETHYL-N,N-DIMETHYLANILINE. *Organic syntheses* **1969**, 49, 111-113.
19. Liu, W.; Welch, K.; Trindle, C. O.; Sabat, M.; Myers, W. H.; Harman, W. D., Facile Intermolecular Aryl-F Bond Cleavage in the Presence of Aryl C-H Bonds: Is the  $\eta$ -2-Arene Intermediate Bypassed? *Organometallics* **2007**, 26 (10), 2589-2597.
20. Liu, W.; Welch, K.; Trindle, C. O.; Sabat, M.; Myers, W. H.; Harman, W. D., Facile Intermolecular Aryl-F Bond Cleavage in the Presence of Aryl C-H Bonds: Is the  $\eta$ -2-Arene Intermediate Bypassed? *Organometallics* **2007**, 26 (10), 2589-2597.
21. Bosque, R.; Clot, E.; Fantacci, S.; Maseras, F.; Eisenstein, O.; Perutz, R. N.; Renkema, K. B.; Caulton, K. G., Inertness of the Aryl-F Bond toward Oxidative Addition to Osmium and Rhodium Complexes: Thermodynamic or Kinetic Origin? *Journal of the American Chemical Society* **1998**, 120 (48), 12634-12640.
22. Reinhold, M.; McGrady, J. E.; Perutz, R. N., A Comparison of C-F and C-H Bond Activation by Zerovalent Ni and Pt: A Density Functional Study. *Journal of the American Chemical Society* **2004**, 126 (16), 5268-5276.
23. Clot, E.; Oelckers, B.; Klahn, A. H.; Eisenstein, O.; Perutz, R. N., cis-trans Isomerisation of CpRe(CO)<sub>2</sub>(H)(ArF) (ArF = C<sub>6</sub>F<sub>n</sub>H<sub>5-n</sub>; n = 0-5) is the rate determining step in C-H activation of fluoroarenes: a DFT study. *Dalton Transactions* **2003**, (21), 4065-4074.
24. Clot, E.; Eisenstein, O.; Jasim, N.; Macgregor, S. A.; McGrady, J. E.; Perutz, R. N., C-F and C-H Bond Activation of Fluorobenzenes and Fluoropyridines at Transition Metal Centers: How Fluorine Tips the Scales. *Accounts of Chemical Research* **2011**, 44 (5), 333-348.
25. Johnson, S. A.; Mroz, N. M.; Valdizon, R.; Murray, S., Characterization of intermediates in the C-F activation of tetrafluorobenzenes using a reactive Ni(PET<sub>3</sub>)<sub>2</sub> synthon: combined computational and experimental investigation. *Organometallics* **2011**, 30 (3), 441-457.
26. Ladogana, S.; Dobson, G. R.; Smit, J. P., Bonding of halogenated arenes in photogenerated (arene)M(CO)<sub>5</sub> complexes (M = Cr, Mo, W). *Inorg. Chim. Acta* **1998**, 278 (2), 202-208.
27. Myers, J. T.; Dakermanji, S. J.; Chastanet, T. R.; Shivokevich, P. J.; Strausberg, L. J.; Sabat, M.; Harman, W. D., 4-(Dimethylamino)pyridine (DMAP) as an Acid-Modulated Donor Ligand for PAH Dearomatization. *Organometallics* **2017**, 36 (3), 543-555.
28. Harman, W. D.; Sekine, M.; Taube, H., Redox-promoted linkage isomerizations of aldehydes and ketones on pentaammineosmium. *Journal of the American Chemical Society* **1988**, 110 (8), 2439-2445.

# Chapter 7

## The Double Protonation of WTP(NO)(PMe<sub>3</sub>)( $\eta^2$ -2,3-anisole) and its Versatility in Carbon-Carbon Bond Forming Reactions

## 7.1 Introduction

The selective formation of carbon-carbon bonds is a valuable synthetic tool that allows for the rapid generation of complicated chemical architectures. Carbon-carbon bond formation is central to industrial processes, medicinal chemistry, catalysis and integral to other chemical transformations.<sup>1-3</sup> Friedel-Crafts reactions allow for the alkylation and acetylation of aromatic rings. Carbon-carbon formation reactions that promote “cross-coupling” with a palladium catalyst include the Heck, Negishi, Suzuki, Sonogashira and Buchwald-Hartwig named reactions.<sup>4-5</sup> Recently Fletcher and co-workers have recently shown rhodium-promoted asymmetric catalysis in Suzuki-Miyaura coupling reactions that prepare enantioenriched organic frameworks using halogenated cyclohexenes.<sup>6</sup>

Previous reports in our lab showed that N,N-dimethylaniline, indoline along with 2-amino pyridine and pyrimidines can undergo double electrophilic additions once

coordinated to the

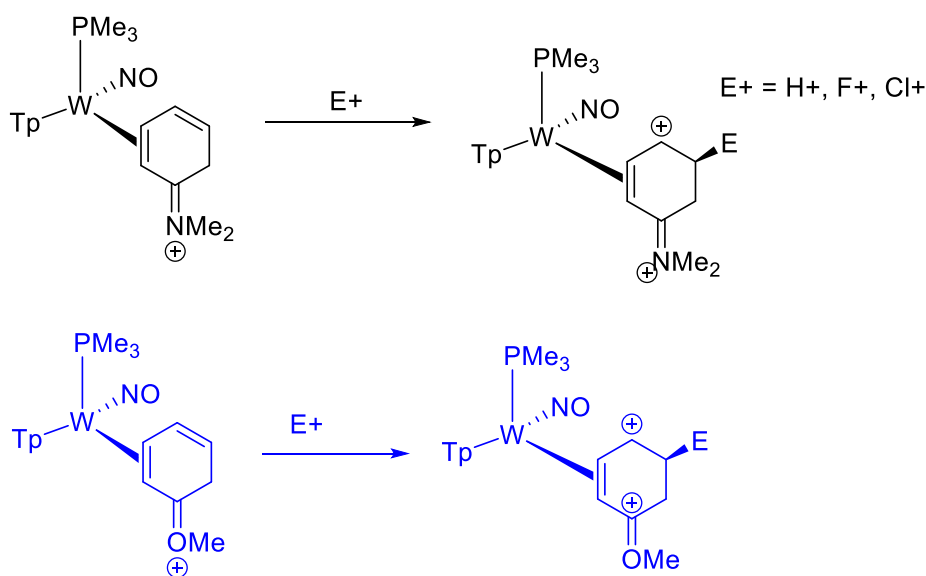
{WTp(NO)(PMe<sub>3</sub>)} fragment.<sup>7-9</sup> The resulting dicationic species can serve

as moderate electrophiles,

undergoing Friedel-Crafts-like

reactivity with an array of electron

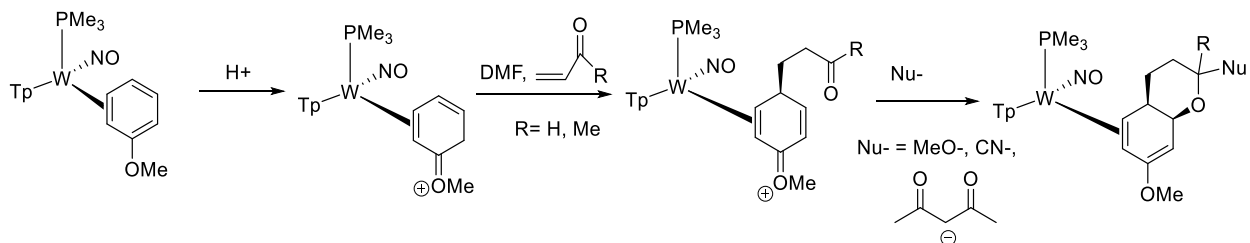
rich aromatic nucleophiles. Carbon-carbon coupling reactions have also been realized for tungsten complexes of naphthalene and phenol as well, though in these cases only a single electrophilic addition to the bound aromatic was needed in order to engender Friedel-Crafts-like reactivity.<sup>10</sup>



**Scheme 7.1.** Previous work showing the ability of a tungsten-anilinium complex to undergo a second electrophilic addition (top). The resulting dicationic species readily reacts with various nucleophiles. A proposal to doubly protonate the tungsten-anisole system is investigated here (bottom, blue).

A more reactive electrophilic species may be accessible from the double protonation of  $\text{WTp}(\text{NO})(\text{PMe}_3)(\eta^2\text{-2,3-anisole})$  (**1**). We speculate that a dicationic species derived from the tungsten anisole complex **1** would be even more reactive than those derived from the reported pnictogen-containing aromatics.<sup>7-9</sup> The protonation of the neutral tungsten-anisole complex **1** occurs readily with diphenylammonium triflate (DPhAT,  $\text{pK}_a \sim 1$ ) to generate  $\text{WTp}(\text{NO})(\text{PMe}_3)(\eta^2\text{-5,6-2-H-anisolum})(\text{OTf}^-)$  (**2**).<sup>11</sup>

Previous reports have shown that **1** can be used as a precursor to novel chroman cores.<sup>12</sup> This methodology was inspired by the ability of the complex  $\{\text{Os}(\text{NH}_3)_5(\eta^2\text{-2,3-anisole})\}$  to undergo protonation to generate a 4-H-anisolum complex.<sup>13</sup> Although attempts to directly access a 4-H anisolum from **1** were unsuccessful, treating a DMF solution of **2** with acrolein or methyl vinyl ketone results in alkylation at the four position. Subsequent treatment with a nucleophile yields a novel oxadecalin structure as detailed in **Scheme 7.2**. This chapter discusses the synthesis of electron-deficient  $\pi$ -ligands derived from the double electrophilic addition of the tungsten-anisole complex **1**; and the resulting reactivity with aromatic nucleophiles.



**Scheme 7.2.** Previous work showing the ability of the complex (**1**) to generate novel chroman cores.

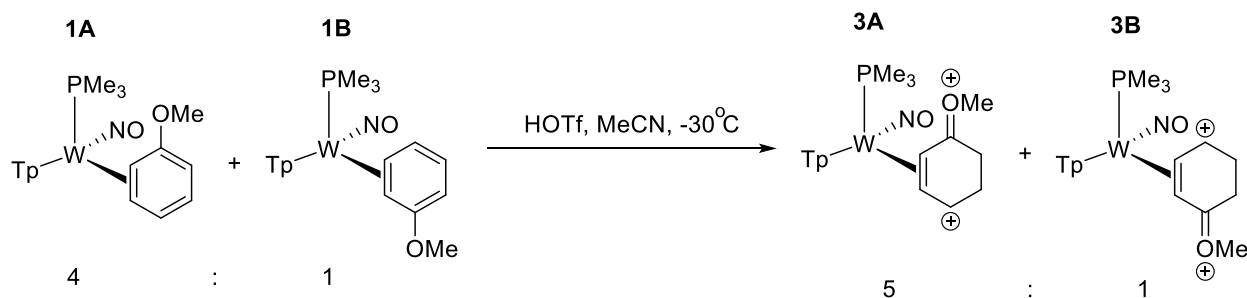
## 7.2 The Double Protonation of Anisole and DFT Calculations

The complex  $\text{WTp}(\text{NO})(\text{PMe}_3)(\eta^2\text{-2,3-anisole})$  **1** can be prepared in  $> 50\%$  yield on an eight gram scale as an analytically pure yellow powder following the one electron reduction of  $\text{WTp}(\text{NO})(\text{PMe}_3)(\text{Br})$  in an excess of anisole. The tungsten-anisole complex **1** exists in solution as a 4:1 ratio of two coordination diastereomers. The major species (**1A**) has the methoxy group bound to the carbon position proximal to the

phosphine ligand. The minor coordination diastereomer (**1B**) orients the methoxy group on the carbon position distal to the phosphine.

Previous reports have utilized **1** as a precursor to 1-oxadecalins via initial protonation in the presence of a Michael Acceptor after the formation of  $\text{W Tp}(\text{NO})(\text{PMe}_3)(\eta^2\text{-5,6-2-H-anisolum})(\text{OTf}^-)$  (**2**).<sup>12</sup> A single isomer of **2** can be isolated in nearly quantitative yields by treating a solution of **1A** and **1B** with DPhAT in DME at reduced temperatures. Allowing the reaction mixture to react at room temperature results in single 2H-anisolum complex **2**. Here, the resulting oxonium-functionality is on the carbon distal to the phosphine ligand. The tungsten metal's ability to localize cationic charges on the carbon distal to the phosphine ligand has been previously documented.<sup>14</sup> The diastereomeric resolution associated with **2** relies on the use of thermodynamic conditions.<sup>11</sup>

Treating an acetonitrile solution of **1A** and **1B** at reduced temperatures ( $-30\text{ }^\circ\text{C}$ ) with triflic acid (HOTf) results in the formation of two dicationic species, **3A** and **3B**. The ratio of coordination diastereomers of **3A** and **3B** ( $\sim 5:1$ ) roughly matches the 4:1 ratio of **1A** and **1B** in solution. Attempts to utilize differences in the ratio of **1A** and **1B** based on differences in solid state "packing" to prefer one coordination diastereomer of **3** over the other, through the solid-state induced control of kinetically unstable stereoisomers (SICKUS), resulted in lower selectivity between **3A** and **3B**.<sup>15</sup> These results imply that as a solid, the ratio of **1A** and **1B** exists closer to a 1:1 mixture than the equilibrium mixture observed in solution.



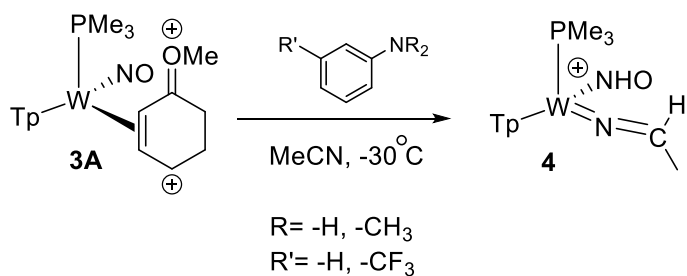
**Scheme 7.3.** Double protonation of the tungsten-anisole complex to generate two dicationic  $\pi$ -ligands. The ratio of the resulting coordination diastereomers roughly matches the ratio of the anisole diastereomers **1A** and **1B**.

The major dicationic species formed from the double protonation of the neutral tungsten-anisole complex **1**, **3A**, is moderately stable at room temperature in acetonitrile ( $t_{1/2(\text{decomposition})} \sim 10$  minutes). Attempts to isolate **3A** via precipitation into diethyl ether resulted in its deprotonation and the isolation of the mono-protonated adduct **2**. Spectral features in the resulting  $^{31}\text{P}$  NMR of **3A** reveal a  $J_{\text{WP}} = 248$  Hz resonating at 0.76 ppm. For comparison, **2** has a  $J_{\text{WP}} = 280$  Hz and that of **1A** and **1B** have  $J_{\text{WP}} = 310$  Hz. These data are all consistent with a more electron-deficient species, where a larger amount of the tungsten  $s$ -character is involved in the bonding with the dicationic anisolum ligand.<sup>16</sup> Additionally, carbon resonances in the  $^{13}\text{C}$  NMR spectra at 217 ppm and 150 ppm correspond to the oxonium-carbon and the carbon distal to the phosphine ligand respectively. Taken together, these data support the generation of a strongly electrophilic  $\pi$ -ligand derived from the double protonation of anisole.

### 7.3 Investigation of Electrophilic Aromatic Substitution Reactions

Original efforts focused on adding aromatic nucleophiles to nitrile solutions of **3A**. Initial attempts to engage in formal electrophilic aromatic substitution (EAS) reactions with benzene, naphthalene, fluorobenzene, toluene or any of the xylenes series were unsuccessful. No reactivity was observed at reduced temperatures ( $-30$  °C) and raising the temperature of the reaction to room temperature led to the formation of multiple decomposition products over the course of several hours. It was not determined if any of the new species (observed via  $^{31}\text{P}$  NMR) corresponded to the desired addition product.

Attempts to add aniline and derivatives such as *N,N*-dimethylaniline or 3-trifluoromethylaniline led to the formation of the  $\kappa^1$ -acetonitrilium complex **4**.<sup>17</sup> The mechanism for this transformation is unknown. Presumably the amino-functionality of the aniline is basic enough to deprotonate **3A**.



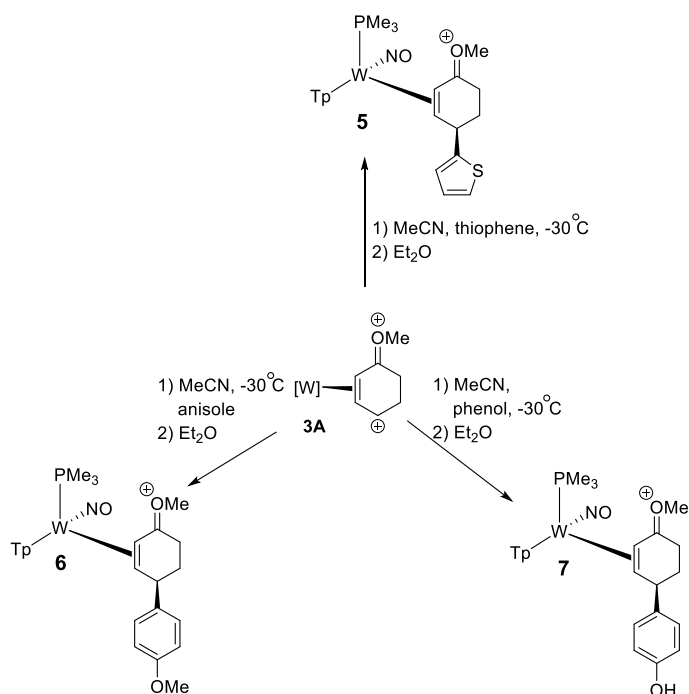
**Scheme 7.4** Attempts to add aniline and aniline derivatives to **3A** led to the development of a  $\kappa^1$ -acetonitrilium complex.



Under the reaction conditions, the resulting species is able to engage in a mechanism that must involve dissociation of the anisole-derived ligand. This is followed by the coordination and subsequent protonation of acetonitrile once it is bound in a  $\kappa^1$ -fashion to the tungsten fragment. Other conditions that have led to the unintentional generation of **4** from the unsuccessful protonation of the tungsten-benzene complex have been documented in Chapter 2.

Attempts to add cyclohexene, 1,3-cyclohexadiene or pyrrole as nucleophiles to acidic solutions of **3A** at  $-30\text{ }^\circ\text{C}$  were thwarted by the purported acid-induced polymerization of the desired nucleophiles under the strongly acidic conditions. Attempts to add these nucleophiles to a thawing solution of **3A** in HOTf and propionitrile (the freezing point of propionitrile is  $-92\text{ }^\circ\text{C}$ ) were also accompanied by what is most likely acid-induced polymerization.<sup>18</sup> Signs of polymerization include the generation of an insoluble, sticky “goo-like” substance that proved difficult to work with. While the addition may have been successful, isolation of the desired product away from the polymer phase was not pursued.

In contrast to the reactivity of pyrrole, when thiophene was added to an acidic nitrile solution of **3A**, the conversion to two new products in acetonitrile was achieved in under 30 min at  $-30\text{ }^\circ\text{C}$ . Addition of the reaction mixture to a solution of stirring  $\text{Et}_2\text{O}$  led to the precipitation of a yellow solid. Analysis of this solid in acetone- $d_6$  showed features consistent with the successful addition of thiophene to **3A**, with addition occurring at the  $\alpha$ -position on the thiophene ring (complex **5**). Addition reactions



**Scheme 7.5.** Successful additions of aromatic nucleophiles to **3A**. Depicted products place the oxonium functionality on the carbon proximal to the phosphine ligand. [W] = {WTP(NO)(PMe<sub>3</sub>)}

using anisole (**6**) and phenol (**7**) as nucleophiles were also successful. In these cases, a formal electrophilic aromatic substitution occurs at the para-position of the substituted benzene ring.

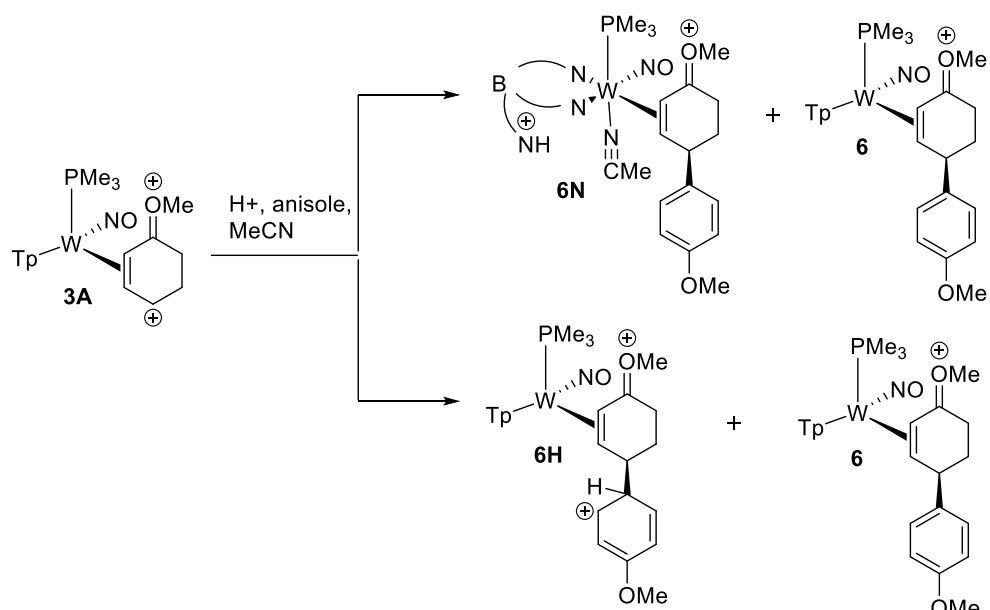
Interestingly, if the isolated solid from *any* of these products (**5** – **7**) is analyzed by  $^1\text{H}$  NMR spectroscopy in a solution of  $\text{MeCN-}d_3$ , *two complexes are observed which both feature incorporation of the aromatic nucleophile into the final product*. When the same analysis is performed of any of these complexes in acetone- $d_6$ , only a single diamagnetic complex is observed.

In the case of the anisole addition complex **6**, a 2D NMR spectra of **6** in  $\text{MeCN-}d_3$  reveals two species in a 3:1 ratio, one of which is not present in spectra recorded in acetone- $d_6$ .

Analysis of the 2D NMR data suggest that not only did the anisole add to the electrophilic fragment **3A**, but that the regio-

and stereochemistry of the site of addition of the anisole is the same in each product. Additionally, while the spectra is complicated due to two diamagnetic complexes, the  $\text{PMe}_3$ , pyrazole ligands and the cyclohexene ring portions are all intact. While the identity of the “second complex” is unknown, speculation is included as to its identity *vide infra*.

Under the strongly acidic conditions it may be possible to protonate one of the pyrazole ring. Protonation of the chelating nitrogen heterocycle would prevent coordination to the tungsten center. This



**Scheme 7.6.** Proposed species which could account for the existence of two complexes as observed in the NMR spectra. Both complexes feature the addition of anisole at the indicated position. NMR analysis of the same sample in acetone- $d_6$  reveals only a single complex consistent with the formation of complex **6**.

could then be followed by coordination of a nitrile solvent which could act as a sufficient sigma-donor to stabilize the tungsten- $\pi$  complex, generating the proposed **6N** complex.

Alternatively, given the strongly acidic conditions the product observed via  $^{31}\text{P}$  NMR of the analysis of the reaction mixture of **3A**, HOTf and anisole may in fact be the intermediate product **6H**. The nitrile solvent may not be sufficiently basic to complete the formal EAS process which would require deprotonation of the initial addition product. Upon precipitation into  $\text{Et}_2\text{O}$ , it may be possible that only a fraction of the purported **6H** is able to deprotonate before its precipitation from solution.

Once the solid is re-dissolved in  $\text{MeCN-}d_3$  for analysis by NMR, the acetonitrile solvent may not be basic enough to deprotonate the **6H** intermediate. Alternatively, if it is the case that one of the pyrazole ligands has become dislodged from coordination to the metal center, the nitrile solvent may not be basic enough to appreciably deprotonate the proposed, protonated pyrazole ring. When the solid of **6** is analyzed in acetone- $d_6$  however, acetone may itself be basic enough to deprotonate either the uncoordinated pyrazole ring associated with the proposed **6N** species or the hypothetical **6H** intermediate. Alternatively, trace water in the acetone solvent (via the aldol condensation of acetone) may be sufficiently basic to lead to the exclusive formation of **6**. To summarize, when a  $^1\text{H}$  NMR spectra of an isolated solid of **6** is performed in  $\text{MeCN-}d_3$ , two complexes are observed in an approximate 3:1 ratio with the features described *vide supra*. If the NMR analysis is performed in acetone- $d_6$  however, only a single complex was observed. Further investigation of this phenomenon was not pursued.

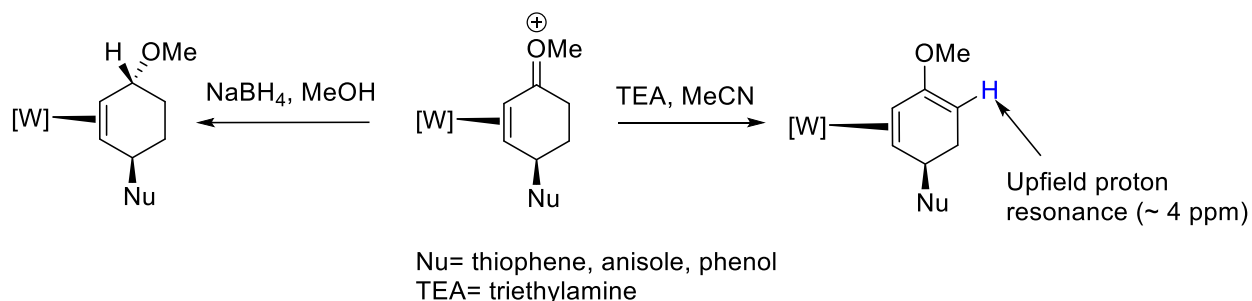
The  $\{\text{WTP}(\text{NO})(\text{PMe}_3)\}$  fragment had previously not been able to generate  $\pi$ -ligands that were sufficiently electrophilic to engage in EAS reactions with anisole or phenol. Phenolic moieties are often common components of natural products, bioactive molecules developed by the body and are often components of man-made drugs. The reactivity of phenolic-containing structures will be examined *vide infra*.

## 7.4 Hydride Reduction and Allyl-Formation and Subsequent Reactivity

Deprotonation of the thiophene addition complex **5** and phenol addition **7** can be readily achieved with an excess of triethylamine in acetonitrile to generate the corresponding methoxy-diene complexes **8** and **9** respectively (**Scheme 7.7**). Notably, these complexes feature a significantly upfield proton resonances at ~ 4 ppm. This upfield shift is attributed to electron donation both from the methoxy substituent as well as from electron donation from the tungsten metal via a  $\pi$ -backbonding interaction. We speculate that this site could be amenable to electrophilic additions with carbon or heteroatom electrophiles, though synthetic efforts in treating these methoxy-diene complexes with electrophilic reagents were not systematically pursued.

Instead, reduction of the oxonium-functionality of **5** was examined with a series of reducing agents ( $\text{LiAlH}_4$ , 9-BBN lithium hydride,  $\text{NaBH}_4$ ). Optimized conditions utilized  $\text{NaBH}_4$  as a reducing agent in methanol. This methodology was applied to the thiophene addition complex **5** and analysis confirms the reduction of the oxonium functionality. Treating the anisole (**6**) and phenol (**7**) addition products gave similar results by  $^1\text{H}$  NMR, though full characterization of these complexes were not pursued.

When the tungsten-thiophene addition complex **5** is allowed to sit in MeOH at reduced temperatures ( $-30\text{ }^\circ\text{C}$ ) and treated with  $\text{NaBH}_4$ , vigorous bubbling occurs as the originally homogeneous yellow solution turns to an off white solution. Addition of this reaction mixture to a solution of stirring DI  $\text{H}_2\text{O}$  leads to the precipitation of an off-grey solid. The resulting product features a proton resonance at 5.18 ppm in the  $^1\text{H}$

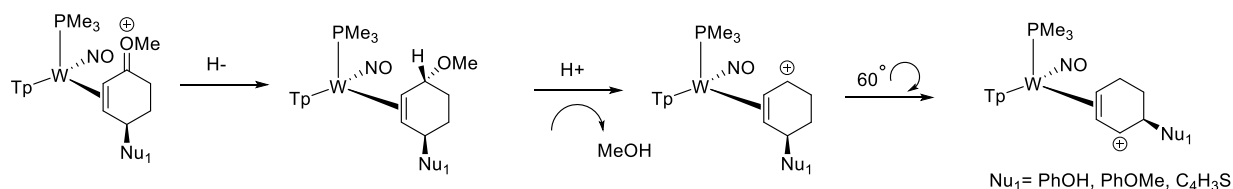


**Scheme 7.7.** Generation of methoxy-diene complexes via deprotonation (right). The resultant complex features significantly upfield shifted  $^1\text{H}$  resonance indicating a significant build-up of electron density at the unbound alkene carbon ortho to the methoxy group. Alternatively, treating with sodium borohydride leads to exclusive reduction of the oxonium carbon to generate a substituted cyclohexene complex (left).

NMR spectra recorded in acetone- $d_6$  which corresponds to the methine position of the nucleophilic addition. Performing the same reaction with the deuteride source NaBD<sub>4</sub> leads to near total suppression of the methine resonance (> 95 % deuterium incorporation). Features of deuterium incorporation with the remaining protected resonances display upfield shifts and changes in multiplicity consistent with those reported in Chapter 3.

Treating the resulting methoxy-cyclohexene complexes derived from **5**, **6** and **7** with HOTf leveled in DME at reduced temperatures generates the corresponding tungsten-allyl complexes **11** (thiophene), **12** (anisole) and **13** (phenol) respectively. Here we speculate that protonation of the methoxy group first occurs. Subsequent loss of methanol leads to the tungsten-allyl adduct. This complex is heavily stabilized by  $\pi$ -backbonding from metal to the now cationic  $\pi$ -ligand. As has been detailed previously, the tungsten-fragment preferentially localizes positive charge on carbon-based  $\pi$ -ligands on the carbon that is distal to the phosphine ligand. As such, the removal of the methoxy group is accompanied by a counterclockwise (ccw) 60° rotation to place the resulting positive charge on the carbon distal to the phosphine ligand.

A comparison of these tungsten-allyl species derived from the initial additions of thiophene (**11**), anisole (**12**) and phenol (**13**) is presented in **Scheme 7.8**. These species are stable as isolated solids over the course of several weeks at room temperature. Experiments were next pursued to examine the nucleophile scope available to these tungsten-allyl systems.



**Scheme 7.8.** Schematic sequence showing the hydride addition and ability to generate tungsten-allyl species derived from the addition of aromatic nucleophiles.

When **11** is treated with H-, MTDA or CN- mixtures of two products are observed. One is speculated to be the elimination product corresponding to **14**. Treating a solution of the allyl derived from the thiophene

addition complex **11** with TEA leads exclusively to the tungsten-cyclohexadiene complex **14**. Features of the cyclohexadiene complex **14** correspond to one of the products observed upon the attempted nucleophilic addition as detailed above. Key features of the elimination include a set of alkene resonances at 6.56 ppm in the case of **14** and that at 4.95 ppm. Similar features are observed when the anisole complex **16** or that of phenol **17** are treated with various nucleophiles. Elimination by the nucleophile was competitive with addition even at reduced temperatures (-60 °C).

In an attempt to better mechanistically understand the mechanism of deprotonation, the initial thiophene addition product complex **5** was treated with NaBD<sub>4</sub> instead of NaBH<sub>4</sub>. In this way, the deuterium could essentially be “tracked” throughout the reaction sequence to give insight into the mechanism of deprotonation. The results of this experiment and treating the resulting isotopologue product **10-d<sub>1</sub>** with a proton source to generate **11-d<sub>1</sub>** and then deprotonation to yield **14-d<sub>1</sub>** are summarized in **Scheme 7.9**. These experiments support that the site of deprotonation actually arises from the deprotonation of a minor tungsten-

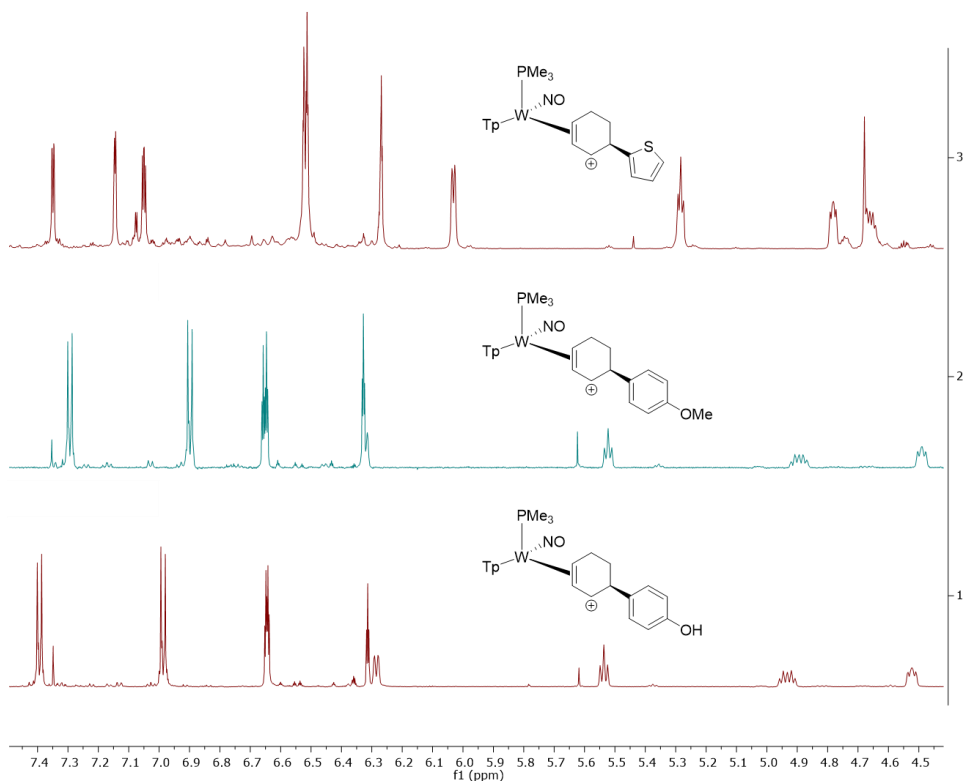
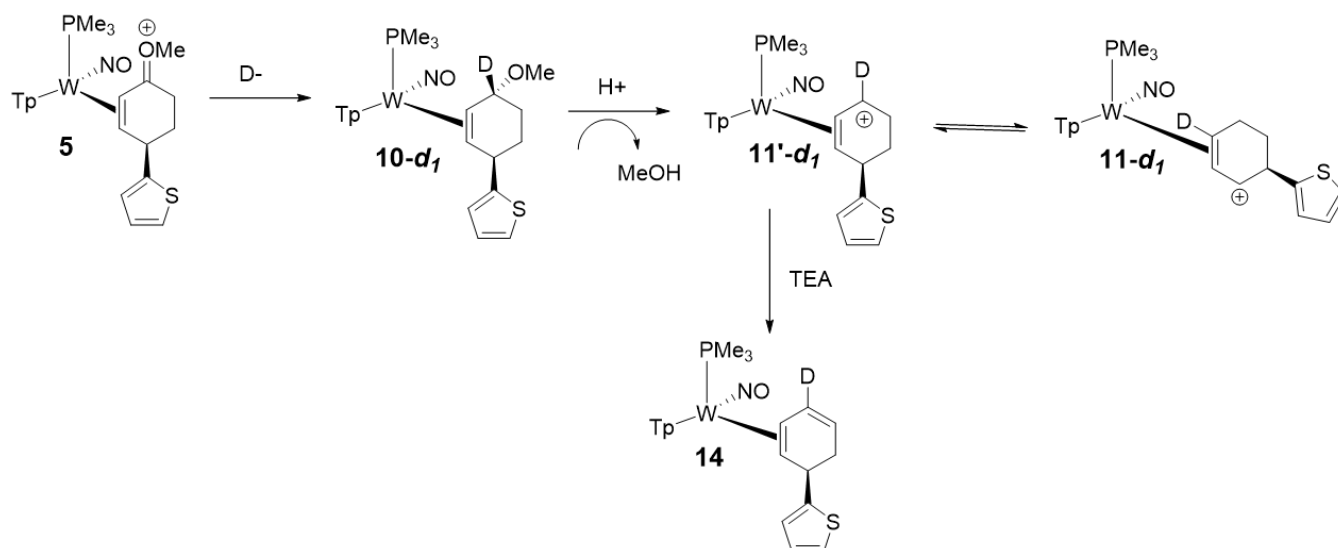


**Figure 7.1.** Comparison of various tungsten-allyl complexes derived from the addition of aromatic nucleophiles. The spectra at the top (complex **11**) is recorded at 0 °C in MeCN-*d*<sub>3</sub>. The middle (complex **12**) and bottom spectra (complex **13**) are recorded in acetone-*d*<sub>6</sub> at 25 °C.

allyl (**11'-d<sub>1</sub>**) conformational isomer whose population is not high enough to be observed by NMR spectroscopy.

Even at lowered temperatures (-60 °C) mixtures of addition and elimination products were observed. Previously we have noted the remarkable ability of lowered temperatures to lead to better chemoselectivity, with addition reactions pre-empting deprotonation. In the case where an addition product would lead to a 1,2-substituted cyclohexene however, we speculate that the steric bulk of the initial aromatic nucleophile may make addition at the tungsten-allyl supported carbocation untenable. This would presumably be exacerbated with increasing the size of the initial aromatic nucleophile. While optimized conditions in certain instances may enable exclusive addition over deprotonation products to generate 1,2-substituted cyclohexene products, efforts were extended to analyzing the reactivity of **3B**. Tungsten-allyl products derived from this species would presumably be less sterically demanding for the final nucleophilic addition, as the resulting product would be a 1,4-substituted cyclohexene. Here, the site of the final nucleophilic addition would occur at a site relatively distant from the initial, bulky aromatic nucleophile.

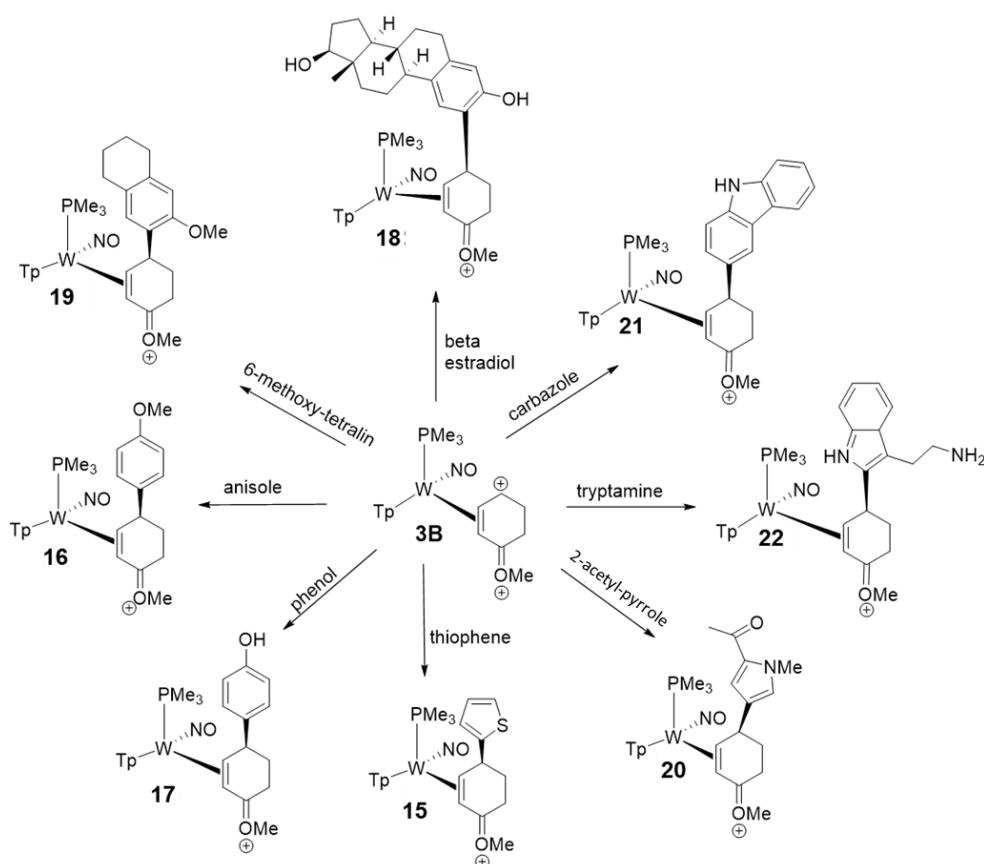


**Scheme 7.9.** Proposed mechanism that results in the deprotonation of the species **11-d<sub>1</sub>**. Use of a deuterium atom allows one to track intramolecular rotations and elucidate a proposed mechanism.

## 7.5 Double Protonation of Another Coordination Diastereomer of a Tungsten-Anisole Complex

Complex **2**, the tungsten 2-H anisolum species, can be prepared in nearly quantitative yields in a >20:1 ratio diastereomeric ratio. Treating **2** with an acetonitrile and triflic acid solution leads to the formation of **3B** with similar diastereomeric selectivity.

Treating this complex in situ with a range of nucleophiles such as N-methylpyrrole or aniline in acetonitrile gave the previously reported  $\kappa^1$ -acetonitrilium complex (**4**) through an unknown mechanism. Additionally, aromatics such as benzene, naphthalene, toluene and m-xylenes were attempted and these attempts led to either no reaction with **3B** or decomposition to unidentifiable paramagnetic material. In this methodology, either aromatics that are not “activated” enough to engage in an EAS mechanism, or were sufficiently basic to yield **4**. These results suggest that the nucleophile scope available to **3A** and **3B** is similar in size.



**Scheme 7.10.** Range of compatible nucleophiles able to effectively undergo electrophilic aromatic substitution reactions with **3B** acting as the electrophile.



Gratifyingly however, we found that treating **3B** with a range of weak, non-basic aromatic nucleophiles such as thiophene (**15**), anisole (**16**) and phenol (**17**) among others lead to selective C-C bond formation. In the case of phenol and anisole, electrophilic aromatic substitution by **3B** occurs exclusively at the para-position of the aromatic ring. The addition of beta-estradiol to **3B** generates the ortho-addition product **18**. Analogous reactivity was observed in the addition of 6-methoxy-tetralin to **3B** (**19**). Effectively “blocking” the para-position of a phenol or anisole containing molecule with an alkyl group leads to a formal EAS at the ortho phenolic/anisolic ring. Further considerations regarding the beta-estradiol addition will be discussed *vide infra*.

Electron rich pyrroles (pyrrole, N-Me-pyrrole) led to the development of the  $\kappa^1$ -acetonitrilium complex **4**. In contrast however, a more electron-deficient pyrrole, 2-acetyl-N-Me-pyrrole could be added to **3B** to generate **20**. Interestingly, in this case addition occurs at the three-position of the pyrrole-derivative ring. This is in contrast to that of thiophene where addition occurred at the two-position of the thiophene ring.

Efforts to add more biologically relevant molecules were also pursued given the success of the beta-estradiol addition to generate complex **18**. Of the molecules surveyed, the indole-derived molecules carbazole (**21**) and tryptamine (**22**) successfully added and have been fully characterized. Bioactive molecules that did not yield conclusive results include dopamine hydrochloride, serotonin hydrochloride, tryptophan, duloxetine hydrochloride among others.

Addition of the antibiotic tetracycline was also pursued and initially gave promising results in being able to engage in an EAS reaction with **3B**. However, this synthesis was not easily repeatable and subsequent addition reactions were accompanied by large amounts of decomposition. An HRMS of this complex reveals a parent *m/z* peak of 1038.3071. This peak could correspond to a process of protonation and subsequent dehydration within the tetracycline ring addition product.

Additionally, tetracycline is sensitive to strong oxidants and acids, and decomposition is observed upon extended exposure to light. The ability to add tetracycline would represent an important class of compounds that could be derivatized by the tungsten fragment. However, the chemical instability of the ligand and difficulty in spectroscopic analysis precluded further investigation. The chirality associated of the tetracycline molecule made analysis by  $^1\text{H}$  NMR difficult, as the addition of this chiral molecule to racemic tungsten-complex would lead to the generation of at least two diastereomers. Attempts to make enantioenriched forms of the tungsten metal to generate a resolved anisolum complex analogous to that used for beta-estradiol was attempted. In these cases however, no sign of successful addition was observed. It may very well be the case that lingering metal-based impurities may preclude the successful addition of tetracycline.

The successful addition of beta-estradiol to **3B** was confirmed via  $^1\text{H}$  NMR spectroscopy as well as measurements by HRMS. In the bottom spectra depicted in **Figure 7.3**, two sets of resonances associated with the Tp4 positions are observed in the  $^1\text{H}$  NMR spectra of **18**. These pyrazole signals correspond to a set of diastereomers that arise due to the stereocenters of the chiral beta-estradiol molecule. That is,

upon addition of the chiral molecule beta-estradiol to the unresolved chiral-at-metal tungsten complex, the  $W_R$  and  $W_S$  metal centers now each form a C-C with the added beta-estradiol nucleophile. Accordingly, the

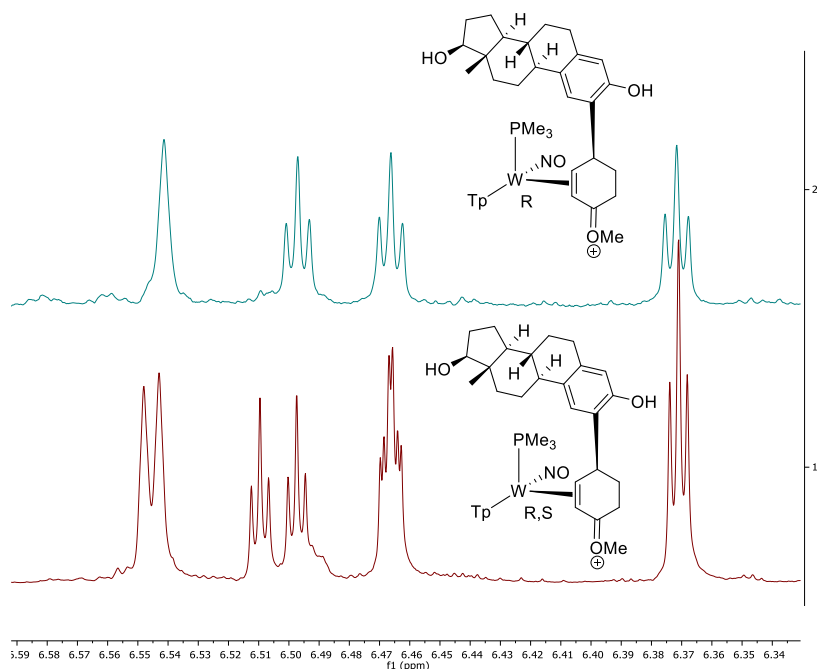


**Figure 7.2.** Illustrative  $^1\text{H}$  NMR spectra depicting the Tp4 resonances and a beta-estradiol resonance of the phenolic core (the proton ortho to the hydroxy group). Addition of the chiral beta-estradiol nucleophile to an unresolved form of **3B** leads to a mixture of diastereomers (top). Chiral resolution of the metal center leads to a single diastereomer upon addition of beta estradiol bottom, the tungsten center is resolved to be predominantly the  $W_R$  designated hand).

tungsten complexes are now diastereomers of one another given the chirality associated with the beta-estradiol nucleophile.

Resolution of the two hands of the tungsten fragment has been achieved by protonating the complex  $\text{WTP}(\text{NO})(\text{PMe}_3)(\eta^2\text{-5,6-1,3-dimethoxybenzene})$  with the chiral acid dibenzoyl tartaric acid.<sup>19</sup> The resulting diastereomeric salts can then be separated from run another due to solubility differences. Exposing either salt to basic alumina regenerates the neutral tungsten-dimethoxybenzene complex. The tungsten-coordinated dimethoxybenzene ligand can then undergo a ligand substitution reaction with another aromatic ligand (in this case anisole).<sup>16</sup>

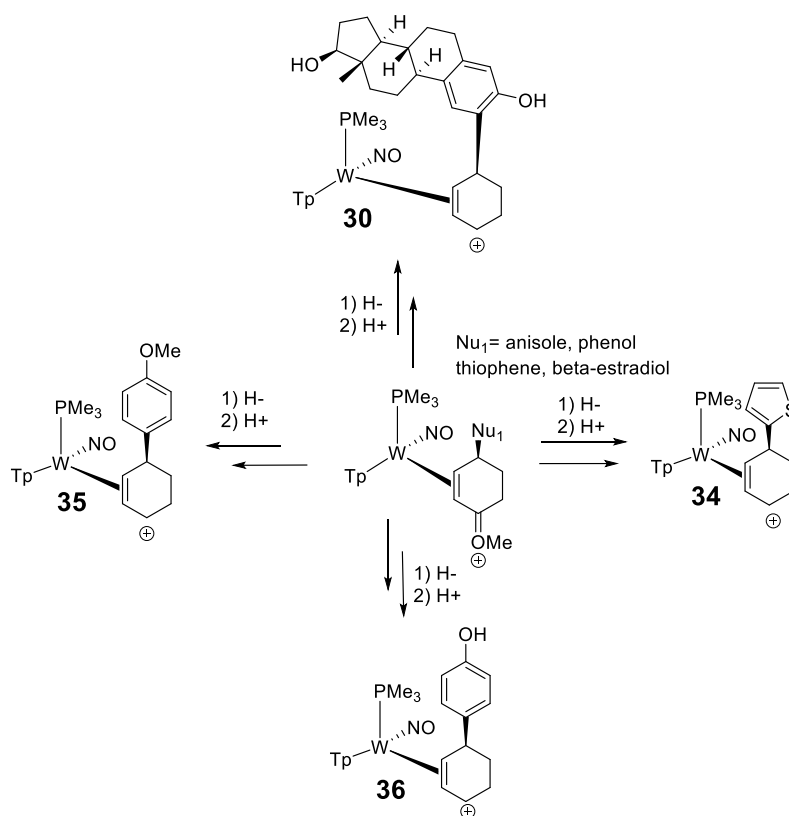
Recently Dr. Katy Wilson has applied this methodology to the asymmetric synthesis of novel cyclohexenes achieved by the tungsten-promoted dearomatization of benzene and  $\alpha,\alpha,\alpha$ -trifluorotoluene with ee values ranging from 86 to 99.<sup>20-21</sup> In the case of beta-estradiol, the chiral resolution of the tungsten center proved to be particularly useful in the resulting spectroscopic analysis of the addition of a chiral nucleophile. This strategy could be employed for easing the spectroscopic analysis of other chiral reagents that are integrated into tungsten-supported  $\pi$ -ligands.

## 7.6 Hydride Addition, Resulting Allyls and Successful 2<sup>nd</sup> Nucleophilic Additions

A series of successful nucleophilic addition derived from **3B** were then evaluated on the basis of the oxonium functionality's ability to be derivatized. Work by Justin Weatherford-Pratt has shown that the oxonium moiety can be treated with anionic carbon nucleophiles (Grignard, organolithiums, anionic  $-\text{CF}_3$  sources) and masked enolates (MTDA) to engage in versatile carbon-carbon bond formation reactions. The exceptional scope of compatible nucleophiles speaks to the remarkable reactivity of the oxonium functionality. A detailed account of this work is beyond the scope of this chapter.

Initial pursuits were focused at pursuing the hydride addition products which resulted in the generation of novel methoxy-cyclohexene complexes upon reduction of the oxonium functionality. The resulting complexes could then be treated with acid in a reaction sequence analogous to **Scheme 7.8** to generate substituted tungsten-allyl species. A schematic of this reaction strategy is detailed in **Scheme 7.11**. Notably, the initial beta-estradiol addition **28** can be treated with a hydride to generate **23**. Subsequent treatment with an acid gives the corresponding tungsten-allyl complex **34**. A similar sequence can be elucidated by adding a hydride source from NaBH<sub>4</sub> to the thiophene addition adduct **15**, that of anisole (**16**) and phenol (**17**) to give the corresponding hydride addition adducts **25**, **26** and **27** respectively. Treating with an acid source yield tungsten-allyl complexes which incorporate functionalities derived from thiophene (**28**), anisole (**29**) and phenol (**30**).

Treating these complexes with hydride or deuteride sources, MTDA or NaCN gave successful addition products with minimal elimination (> 20:1) by <sup>1</sup>H NMR. Here the first aromatic nucleophile is oriented well-away from localized carbocation of the electron-deficient allyl system. Signs of successful addition to the phenol allyl complex **30** with piperidine (**31**) was supported by <sup>1</sup>H NMR spectra of the reaction mixture. Reactivity of **30** with hard nucleophiles such as NaCN and NaBD<sub>4</sub> gave more conclusive addition adducts (**32** and **33** respectively). Full credit is given to Karl Westendorff for the synthesis of **33**.



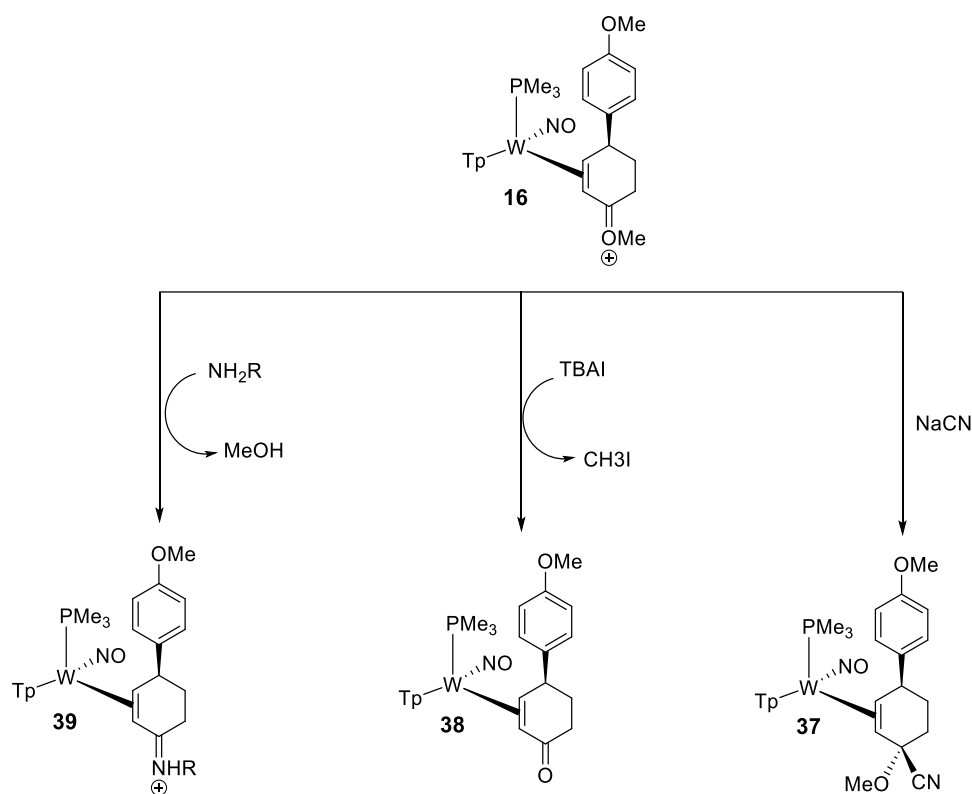
**Scheme 7.11.** Generation of various tungsten allyl complexes obtained by treating the oxo-carbenium species with a hydride followed by a strong acid to cleave off the resulting methoxy-group.

For the thiophene allyl adduct **28** initial treatment with  $\text{PPh}_3$  and MTDA gave signs of success (**34** and **35** respectively) by  $^1\text{H}$  NMR. Treating the anisole allyl complex **35** with NaCN led to the addition complex **36**. Work by Justin Weatherford-Pratt has shown that the final tungsten-allyl species are amenable to anionic carbon-based nucleophiles (Grignards, organolithiums) suggesting that a wide expanse of nucleophiles is available to this system as well.

### 7.7 Additional Reactivity of the Oxonium Functionality

Apart from the reduction of the oxonium functionality with a hydride source, treating Complex **20** with NaCN at reduced temperatures led to the formation of a product we that speculate corresponds to the successful cyanide addition to yield complex **37**. When tetrabutyl ammonium iodide (TBAI) was added as a nucleophilic source of iodide in acetone- $d_6$  to **20**, no reactivity is observed initially. Over a period of several days however,  $^1\text{H}$  spectroscopic signals consistent with the oxonium complex **20** decrease in intensity and are replaced with  $^1\text{H}$  spectroscopic features consistent with a new diamagnetic species.

A  $^{13}\text{C}$  NMR taken of the reaction mixture suggests that the resulting species is the enone product **38**. Key features are the development of a carbonyl resonance in the  $^{13}\text{C}$  NMR spectra at 208.1 ppm and the concomitant formation of methyl iodide which has a distinct carbon resonance at -23.6 ppm in the  $^{13}\text{C}$  NMR spectra. Attempts to cleanly isolate **38** away from TBAI with chromatography were unsuccessful, though using excess TBAI as an internal standard suggests that this conversion occurs in a quantitative manner.



**Scheme 7.12.** Derivatization of the oxonium moiety with non-hydride reagents to yield iminium and enone complexes as well as cyanide addition adducts.

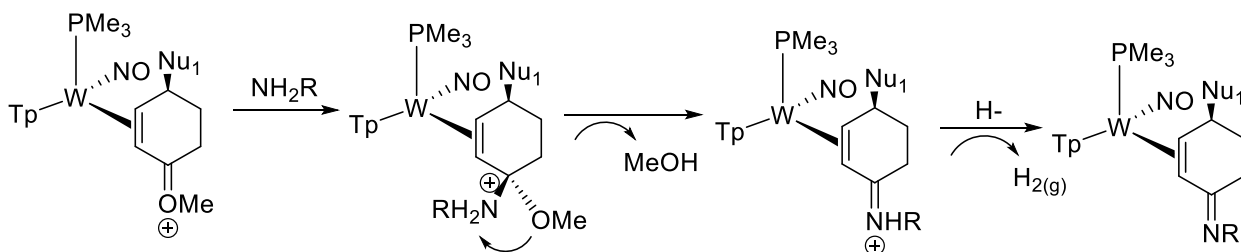
Treating **16** with a methanol/ammonia solution at room temperature yields a new diamagnetic complex as observed with  $^{31}\text{P}$  NMR spectroscopy. Isolation of this product by precipitation in  $\text{Et}_2\text{O}$  and analysis by  $^1\text{H}$  NMR shows signs of consistent with the loss of the oxonium functionality and the substitution to the iminium-product **39**. A speculated mechanism for this process is given in **Scheme 7.14**. Features that support the formations of this product include proposed iminium N-H resonances in  $\text{CDCl}_3$  which are severely broadened when  $^1\text{H}$  NMR analysis is done  $\text{MeCN-}d_3$ . The methyl group associated with the oxonium functionality is also not apparent in the resulting  $^1\text{H}$  NMR of **39**.

A crystal suitable for X-Ray diffraction was grown, and the solved structure confirms the formations of the iminium-functionality. Additionally, the regio- and stereochemistry of the initial anisole addition

adduct is confirmed from this crystal structure. Treating the thiophene incorporated oxonium product **15** with 4-bromobenzylamine led to the generation of a substituted iminium scaffold **40**.

Attempts were extended to generating iminium scaffolds by treating the oxonium-containing products with secondary amines or anilines, though these attempts led to elimination products to yield methoxy-cyclohexadiene complexes.

The iminium complexes **39** and **40** were treated with a variety of hydride sources, though in these cases deprotonation of the iminium pre-empts reduction of the carbon and these experiments result in a proposed imine product. We speculate that enhanced kinetic basicity of the iminium N-H carbons makes precluding addition over elimination synthetically challenging. Synthetic efforts were not pursued further, though the imine or iminium functionalities could provide a scaffold upon which to generate oxaziridine or oxaziridinium functionalities.



**Scheme 7.13.** Proposed mechanism for iminium formation. Subsequent treatment with a hydride leads to the formation of an imine complex.

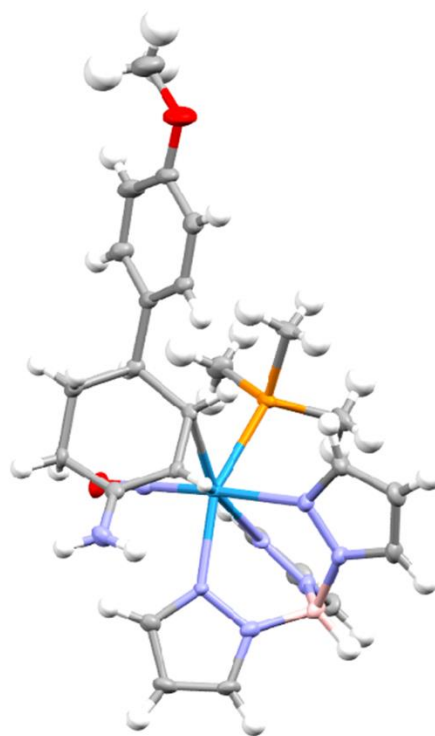


**Figure 7.3.** Crystal structure determination (Ellipsoid plot) of COMPLEX X confirming the proposed product. Regio- and stereochemistry of the anisole addition is confirmed as well. The triflate anion and an equivalent of co-crystallized methanol have been removed for clarity.

## 7.8 Electrochemical Behavior of Tungsten-Oxonium Complexes

The thiophene addition complexes **19** displays a pseudo-reversible  $E_{1/2} = -1.15$  V followed by an  $E_{1/2} = -1.73$  V as determined by cyclic voltammetry (CV). The two electron reduction process suggests that a reactive, anionic species may be formed in the CV cell as a result of the two electron reduction of **19**.

When a DMA solution of **19** is reduced electrochemically in the presence of excess MeOH, no reactivity is observed. When the strong hydrogen bond donor HFIP is added to this CV solution however, the original  $E_{1/2}$  waves are replaced by an  $E_{p,c} = -1.26$  V and an irreversible  $E_{p,c} = -1.66$  V when the negative scan is extended past the second  $E_{p,c}$  value. This is accompanied by the formation of an  $E_{p,a} = 0.48$  V which is not present in the initial voltammogram. When the negative scan is stopped after the first reduction, the initial  $E_{p,c}$  regenerates the associated  $E_{1/2}$  feature, indicating that the generated species is chemically reversible so long as a second electrochemical reduction does not occur. Additionally, in this experiment, no  $E_{p,a}$  at 0.48 V is observed.

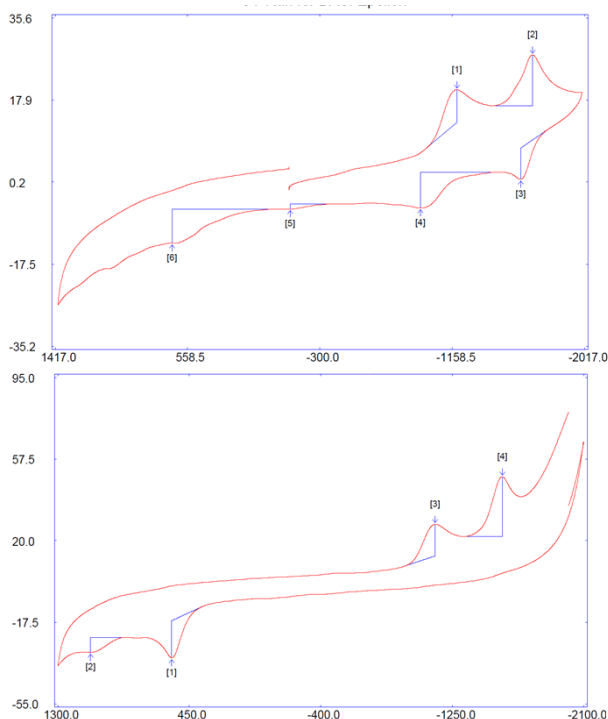
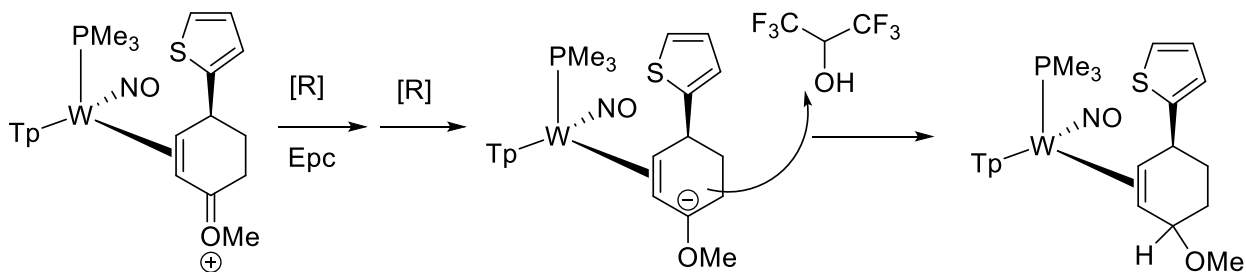


**Figure 7.4.** Negative scans (different starting potentials) of **19** in DMA (top scan) and in a solution of DMA/MeOH/HFIP (bottom). Development of the  $E_{p,a} = 0.48$  V after addition of the HFIP-hydrogen bond donor is speculated to be due to the formation of a tungsten-methoxy-cyclohexene adduct whose mechanism is speculated on in **Scheme 7.14**.



**Scheme 7.14.** Proposed chemical reaction that is electrochemically induced in the presence of a strong H-bond donor. The net result is protonation upon the two electron reduction of the oxo-carbenium species.



Thus, a two electron reduction must take place before a presumably reaction with the H-bond donor HFIP. The observed chemical reactivity is consistent with the formation of a highly reactive anionic species following the two electron reduction of **19**; which is then able to react with mild electrophiles detailed in **Scheme 7.14** (in this case a proton from HFIP). This proof of concept further extends insights into potential reactivity associated with the oxonium-functionality and could be potentially applied to other cationic  $\pi$ -ligands.

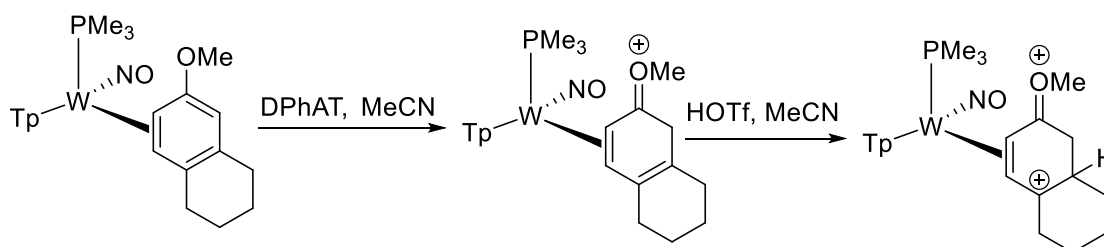
### 7.9. Double Protonation of a Tungsten-6-Methoxy-Tetralin Complex

Finally, attempts were made to investigate the reactivity of 6-methoxy-tetralin once bound to the  $\pi$ -basic tungsten fragment. Difficulties were encountered in exchanging the tungsten benzene complex in an excess of 6-methoxy-tetralin to generate the complex  $\text{WTP}(\text{NO})(\text{PMe}_3)(\eta^2\text{-6-methoxy-tetralin})$  (**41**). Here it appears that the tungsten-benzene complex is significantly more stable and energetically resistant to a substitution process that would result in the formation of **41**. Only partial substitution to **41** was achieved even in an excess of 6-methoxy-tetralin (45 equivalents).

Characterization of **41** shows only a single coordination diastereomer. Protonation with DPhAT yields the 2-H anisolum complex **42**. When a solution of **42** is immediately treated with HOTf in MeCN at  $-30\text{ }^\circ\text{C}$  and monitored by  $^1\text{H}$  NMR at  $0\text{ }^\circ\text{C}$ , two initial diamagnetic complexes are observed. Over time (10 min at  $25\text{ }^\circ\text{C}$ ) a single diamagnetic complex is observed which is postulated to be the complex **43**, a species consistent with the successful double protonation of the 6-methoxy-tetralin tungsten complex **41**. While we believe the second protonation leads to the development of a stereocenter (via protonation of a bridgehead carbon), confirmation of the resulting stereochemistry was not possible.

Attempts were then focused on treating **43** with nucleophiles that had been compatible with the double protonation of anisole. Treating this solution with thiophene, analogous to the successful conditions employed for the thiophene addition to **3** did not result in any reactivity and decomposition of **43** was

observed over time. When a solution of **43** is treated with an excess of  $\text{ZnEt}_2$  and analyzed via HRMS, a  $m/z$  isotopic pattern with a parent ion peak at 696.1682  $m/z$  is observed. These data are consistent with the successful addition of an ethyl group to **43** though the identity of this complex was not exclusively determined. It is likely the stronger nucleophiles would be needed to engender the desired addition adducts from **43** as the addition product would result in a quaternary carbon.



**Scheme 7.15.** Proposed synthetic pathway to a double-protonated 6-methoxy tetralin complex of tungsten.

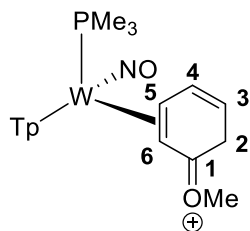
## 7.10 Conclusion

The double-protonation of a tungsten anisole complex has been achieved and can act as a versatile electrophile for a large number of weakly activated aromatic substrates. The resulting complexes can then be treated with a wide number of reagents to generate substituted enones, cyclohexadienes, allyl-methoxy ethers or iminium complexes that can be readily deprotonated to generate Schiff bases. The most immediate route to derivatization leads though the reduction of the oxo-carbenium with a hydride source and the resulting acidolysis of the methoxy group to generate a versatile tungsten-allyl complex. This class of complexes can be subsequently treated with a wide range of moderate to strong nucleophiles to generate 1,4-substituted cyclohexenes. The range of the first aromatic nucleophile can be extended to complicated chemical architectures with multiple functionalities that form selective C-C formed adducts. The ability to optically resolve the tungsten-system allows for the selective formation of well-characterized metal complexes, an

important feature when the initial aromatic is a chiral molecule itself. A pursuit into the available reactivity for this new class of interesting compounds is ongoing.

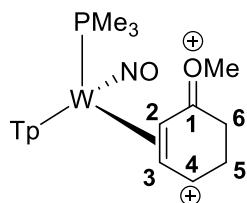


## Synthesis of WTp(NO)(PMe<sub>3</sub>)( $\eta^2$ -5,6-2H-anisolium) (2)



An oven-dried 4-dram vial was charged with **1** (0.858 g, 1.40 mmol) and dimethoxyethane (DME, 6 mL) and the heterogeneous yellow reaction mixture was allowed to sit at  $-30\text{ }^{\circ}\text{C}$  for 15 min. To this heterogeneous yellow reaction mixture diphenylammonium triflate (DPhAT, 0.511 g, 1.59 mmol) was added and upon addition the reaction mixture turns to a homogeneous red solution and was allowed to sit at  $-30\text{ }^{\circ}\text{C}$  for 10 min. This homogeneous red reaction mixture was then added to 100 mL of standing ether to precipitate out an orange/red solid and this solid was then collected on a 30 mL medium porosity fritted disc and washed with diethyl ether (2 x 20 mL) to yield a red solid. This was allowed to desiccate under active vacuum for 4 h before a mass was taken of the dark orange/red solid (1.02 g, 95.3 % yield). Characterization has been reported previously.<sup>11</sup>

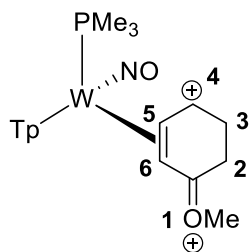
## Synthesis of WTp(NO)(PMe<sub>3</sub>)( $\eta^2$ -2,3-5,6-dihydro-anisolium)) (3A)



The synthesis of **3A** occurred in situ and was not isolated before treatment with nucleophiles. Observation and characterization of **3A** was possible by low temperature protonation of **1** (0.030 g, 0.049 mmol) and an excess of triflic acid ( $\sim 5$  drops) at  $-30\text{ }^{\circ}\text{C}$ . This NMR tube was then frozen in a dewar of  $\text{N}_2$  (l) and the solution was thawed before 2D NMR characterization was pursued at  $0\text{ }^{\circ}\text{C}$ . **3A** is the major observed coordination diastereomer and exists in solution as a 5:1 mixture with **3B** which reflects the ratio of the original coordination diastereomers of **1**.

$^1\text{H}$  NMR ( $\text{MeCN-}d_3$ ,  $\delta$ ,  $0\text{ }^{\circ}\text{C}$ ): 8.36 (1H, d, Tp3/5), 8.15 (1H, d, Tp5C), 8.10 (1H, d, Tp3C), 8.05 (1H, d, Tp3/5B), 7.92 (1H, d, Tp3A), 7.90 (1H, d, Tp5A), 6.84 (1H, m, H4), 6.66 (1H, t, Tp4C), 6.58 (1H, t, Tp4B), 6.36 (1H, t, Tp4A), 5.75 (1H, t,  $J = 6.98$ , H3), 5.37 (1H, dd,  $J = 4.91, 5.47$ , H2), 4.64 (3H, s, -OMe), 3.75 (1H, buried, H5-anti), 3.54 (1H, dd,  $J = 10.03, 21.76$ , H5-syn), 3.42 (1H, dd,  $J = 10.03, 22.50$ , H6), 3.02 (1H, m, H6 $^{\ominus}$ ), 1.13 (9H, d,  $J_{\text{PH}} = 10.55$ ,  $\text{PMe}_3$ ).  $^{31}\text{P}$  NMR ( $\text{MeCN-}d_3$ ,  $\delta$ ,  $0\text{ }^{\circ}\text{C}$ ): 0.76 ( $J_{\text{WP}} = 248.0$ ).  $^{13}\text{C}$  NMR ( $\text{MeCN-}d_3$ ,  $\delta$ ,  $0\text{ }^{\circ}\text{C}$ ): 217.4 (C1), 149.5 (C4), 148.5 (Tp3/5), 146.0 (Tp3/5), 144.2 (Tp3/5), 140.8 (2C, overlapping Tp3/5), 140.5 (Tp3/5), 110.3 (Tp4, d,  $J_{\text{PC}} = 4.0$ ), 109.8 (Tp4), 108.6 (Tp4, d,  $J_{\text{PC}} = 7.0$ ), 98.7 (C3), 64.9 (2C, overlap, -OMe and C2), 27.1 (C6), 24.5 (C5), 12.6 ( $\text{PMe}_3$ , d,  $J_{\text{PC}} = 34.4$ ).

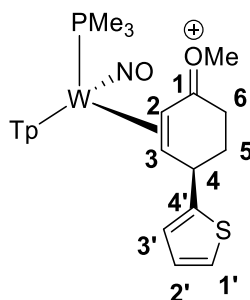
## Synthesis of WTp(NO)(PMe<sub>3</sub>)( $\eta^2$ -5,6-2,3-dihydro-anisolium) (3B)



The synthesis of **3B** occurs in situ and is not isolated before treatment of a nucleophile. Attempts to isolate with pentane were unsuccessfully and isolation using Et<sub>2</sub>O led to the regeneration of **2**. Observation and characterization of **3B** was possible by low temperature protonation of **2** (0.030 g, 0.039 mmol) and an excess of triflic acid (~ 5 drops) at -30 °C. This NMR tube was then frozen in a dewar of N<sub>2(l)</sub> and the solution was thawed before NMR characterization was pursued at 0 °C. In this case, preparation of **3B** from the direct protonation of **2** gives much higher degrees of diastereomeric resolution compared to the double protonation of **1**.

<sup>1</sup>H NMR (MeCN-*d*<sub>3</sub>, δ, 0 °C): 8.23 (2H, overlapping d, Tp3/5), 8.20 (1H, d, Tp5C), 8.08 (1H, d, Tp3/5), 8.06 (1H, d, Tp3/5), 7.23 (1H, d, Tp3/5), 7.07 (1H, m, H4), 6.68 (Tp4), 6.58 (1H, t, Tp4), 6.44 (1H, t, Tp4), 6.13 (1H, broad m, H5), 4.36 (1H, d, *J* = 5.70, H6), 3.77 (1H, m, H3), 3.31 (1H, buried, H3'), 3.18 (1H, m, H2), 2.72 (3H, s, -OMe), 2.68 (1H, buried, H2'), 1.21 (9H, d, *J*<sub>PH</sub> = 10.3, PMe<sub>3</sub>). <sup>31</sup>P NMR (MeCN-*d*<sub>3</sub>, δ, 25 °C): -0.20 (*J*<sub>WP</sub> = 240.0). <sup>13</sup>C NMR (MeCN-*d*<sub>3</sub>, δ, 0 °C): 212.2 (C1), 145.5 (2C, overlapping Tp3/5), 142.9 (Tp3/5), 141.5 (Tp3/5), 141.3 (Tp3/5), 141.2 (Tp3/5), 136.5 (C4), 110.3 (2C, overlapping, Tp4), 110.0 (Tp4), 92.8 (C5), 64.1 (C6), 53.0 (OMe), 26.6 (C2), 23.9 (C3), 12.3 (PMe<sub>3</sub>, d, *J*<sub>PC</sub> = 34.2).

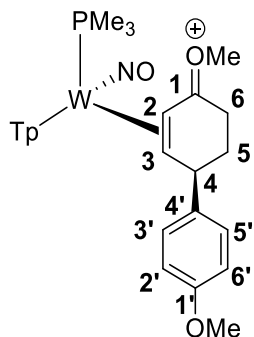
#### Synthesis of WTp(NO)(PMe<sub>3</sub>)(η<sup>2</sup>-2,3-methyl(4-(thiophen-2-yl)cyclohex-2-en-1-ylidene)oxonium) (**5**)



An oven-dried 4-dram vial was charged with complex **1** (0.294 g, 0.481 mmol) and MeCN (~ 1.5 mL) and the resulting homogeneous red reaction mixture was cooled to -30 °C for 15 min. To this heterogeneous yellow reactions mixture a -30 °C solution of triflic acid (HOTf, 0.332 g, 2.19 mmol) was added and upon addition the reaction turns to a homogeneous red solution. To this still homogeneous red solution room temperature thiophene (3 mL, ~ 37.4 mmol) was added and the reaction mixture was allowed to sit at room temperature for 30 min before being allowed to sit at -30 °C for an additional 30 min. The reaction mixture was then added to 75 mL of stirring Et<sub>2</sub>O and upon addition a yellow precipitate initially forms but upon further trituration a red solid “oils” out and sticks to the sides of the Erlenmeyer flask. This solid was dissolved in DCM (5 mL) and added to another 75 mL solution of stirring Et<sub>2</sub>O. Upon addition a vibrant yellow solid precipitates from solution. The yellow solid was then collected on a fine porosity 30 mL fritted disk and washed with Et<sub>2</sub>O (3 x 10 mL) and allowed to desiccate under active vacuum for 2 h before a mass was taken of the yellow solid (0.352 g, 86.5 % yield).

CV (MeCN):  $E_{p,c} = -1.26$ ,  $E_{1/2} = -1.58$  V (NHE).  $^1\text{H}$  NMR (acetone- $d_6$ ,  $\delta$ , 25 °C): 8.32 (1H, d, Tp3B), 8.19 (2H, overlapping d, Tp3C and Tp5C), 8.17 (1H, d, Tp5B), 7.98 (1H, d, Tp3/5A), 7.91 (1H, d, Tp3/5A), 7.27 (1H, dd,  $J = 1.15$ , 5.15, thiophene-H1'), 7.01 (1H, m, thiophene-H3'), 6.94 (1H, dd,  $J = 3.43$ , 5.15, thiophene-H2'), 6.58 (1H, t, Tp4B), 6.55 (1H, t, Tp4C), 6.40 (1H, t, Tp4A), 4.96 (1H, t,  $J = 9.22$ , H2), 4.54 (3H, s, -OMe), 4.07 (1H, broad s, H4), 3.09 (1H, m, H6-exo), 2.78 (1H, d,  $J = 9.2$ , H3), 2.61 (1H, m, H5), 2.19 (1H, m, H5'), 1.24 (9H, d,  $J_{\text{PH}} = 9.65$ ,  $\text{PMe}_3$ ).  $^{31}\text{P}$  NMR (acetone- $d_6$ ,  $\delta$ , 25 °C): -6.2 ( $J_{\text{WP}} = 266$ ).

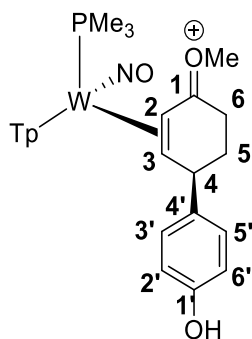
**Synthesis of WTp(NO)(PMe<sub>3</sub>)( $\eta^2$ -2,3-(4'-methoxy-2,3-dihydro-[1,1'-biphenyl]-4(1H)-ylidene)(methyl)oxonium) (6)**



An oven-dried 4-dram vial was charged with complex **1** (0.308 g, 0.504 mmol) and MeCN (~ 1.5 mL) and the resulting homogeneous red reaction mixture was cooled to -30 °C for 15 min. To this heterogeneous yellow reactions mixture a -30 °C solution of triflic acid (HOTf, 0.321 g, 2.13 mmol) was added and upon addition the reaction turns to a homogeneous red solution. To this still homogeneous red solution room temperature anisole (4 mL, ~ 36.9 mmol) was added and the reaction mixture was allowed to sit at room temperature for 2.5 h before being allowed to sit at -30 °C for an additional 15 min. Half of the reaction mixture was then added to 75 mL of stirring diethyl ether. Upon addition a vibrant yellow solid precipitates from solution. The yellow solid was then collected on a fine porosity 15 mL fritted disk. The second half of the reaction mixture was worked-up in a similar manner (addition of reaction mixture to 75 mL of stirring Et<sub>2</sub>O) and the resulting yellow solid was isolated on the same fine porosity 15 mL frit as the first isolated product. The combined solid was then washed with Et<sub>2</sub>O (2 x 10 mL) and allowed to desiccate under active vacuum for 1h before a mass was taken of the yellow solid (0.378 g, 86.3 % yield).

$^1\text{H}$  NMR (acetone- $d_6$ ,  $\delta$ , 25 °C): 8.32 (1H, d, Tp3/5), 8.18 (2H, overlapping d, Tp3/5s), 8.17 (1H, d, Tp3/5), 7.98 (1H, d, Tp3/5), 7.96 (1H, d, Tp3/5), 7.33 (2H, m, anisole-H3'/5'), 6.83 (1H, m, anisole-H2'/6'), 6.58 (1H, t, Tp4), 6.54 (1H, t, Tp4), 6.39 (1H, t, Tp4), 5.06 (1H, t,  $J = 9.73$ , H2), 4.54 (3H, s, oxonium-OMe), 3.89 (1H, broad s, H4), 3.74 (3H, s, anisole-OMe), 3.08 (1H, roofing m, H6), 2.98 (1H, roofing dd,  $J = 7.10$ , 20.6, H6'), 2.65 (1H, d,  $J = 8.9$ , H3), 2.58 (1H, m, H5), 2.09 (1H, m, H5'), 1.24 (9H, d,  $J_{\text{PH}} = 9.26$ ,  $\text{PMe}_3$ ).  $^{31}\text{P}$  NMR (MeCN- $d_3$ ,  $\delta$ , 25 °C): -6.0 ( $J_{\text{WP}} = 265$ ).  $^{13}\text{C}$  NMR (acetone- $d_6$ ,  $\delta$ , 25 °C): 206.4 (C1-buried), 159.1 (anisole-C1), 144.1 (Tp3/5), 143.3 (Tp3/5), 143.1 (Tp3/5), 142.1 (anisole-C4'), 139.2 (Tp3/5), 138.8 (Tp3/5), 138.2 (Tp3/5), 129.3 (anisole C3/5), 114.5 (anisole-C2/6), 108.7 (Tp4), 108.4 (Tp4), 107.6 (Tp4), 74.8 (C3), 63.2 (C2), 60.0 (oxonium-OMe), 55.5 (anisole-OMe), 39.0 (C4), 28.4 (C5-buried), 27.4 (C6-buried), 11.8 (d,  $J_{\text{CP}} = 31.0$ ,  $\text{PMe}_3$ ).

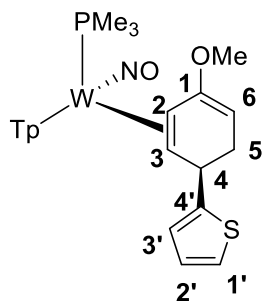
**Synthesis of WTp(NO)(PMe<sub>3</sub>)( $\eta^2$ -2,3-(4'-methoxy-2,3-dihydro-[1,1'-biphenyl]-4(1H)-ylidene)(methyl)oxonium) (7)**



An oven-dried 4-dram vial was charged with complex **1** (0.195 g, 0.319 mmol) and MeCN (~ 1 mL) and the resulting homogeneous red reaction mixture was cooled to  $-30\text{ }^{\circ}\text{C}$  for 5 min. To this heterogeneous yellow reactions mixture a  $-30\text{ }^{\circ}\text{C}$  solution of triflic acid (HOTf, 0.120 g, 0.795 mmol) was added and upon addition the reaction turns to a homogeneous red solution. To this still homogeneous red solution room temperature phenol (1.98 g, ~ 21.0 mmol) was added and the reaction mixture was allowed to sit at room temperature for 2.5 h before being allowed to sit at  $-30\text{ }^{\circ}\text{C}$  for an additional 2 h. The reaction mixture then added to 75 mL of stirring Et<sub>2</sub>O) and the resulting yellow solid was isolated on a medium porosity 30 mL fritted disc. The yellow solid was then washed with Et<sub>2</sub>O (4 x 20 mL) and allowed to desiccate under static vacuum for 16 h before a mass was taken of the vibrant yellow solid (0.210 g, 76.9 % yield).

<sup>1</sup>H NMR (acetone-*d*<sub>6</sub>,  $\delta$ , 25  $^{\circ}\text{C}$ ): 8.31 (1H, d, Tp3/5), 8.17 (3H, overlapping d, Tp3/5s), 7.96 (1H, d, Tp3/5), 7.93 (1H, d, Tp3/5), 7.22 (2H, m, phenol-H3/5), 6.74 (1H, m, phenol-H2/6), 6.57 (1H, t, Tp4), 6.52 (1H, t, Tp4), 6.38 (1H, t, Tp4), 5.04 (1H, t,  $J = 9.1$ , H2), 4.53 (3H, s, oxonium-OMe), 3.83 (1H, broad s, H4), 3.07 (3H, m, H6), 2.96 (1H, m, H6'), 2.63 (1H, d,  $J = 8.32$ , H3), 2.57 (1H, m, H5), 2.06 (1H, m, H5'), 1.23 (9H, d,  $J_{\text{PH}} = 9.10$ , PMe<sub>3</sub>).

### Synthesis of WTp(NO)(PMe<sub>3</sub>)( $\eta^2$ -2,3-(-2-(4-methoxycyclohexa-2,4-dien-1-yl)thiophene) (**8**)



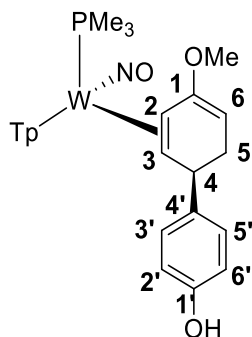
A solution of **5** (0.100 g, 0.118 mmol) was dissolved in MeOH (1 mL) and cooled to  $-30\text{ }^{\circ}\text{C}$  over a period of 10 min. To this solution was added triethyl amine (TEA, 0.119 g, 1.18 mmol) in excess. Upon addition the originally homogeneous red reaction mixture turns to a homogeneous turquoise. This reaction mixture was then added to a solution of stirring DI H<sub>2</sub>O (20 mL) and upon addition a turquoise solid precipitates from solution. This solid was then isolated on a fine 15 mL porosity fritted disc and dried under static vacuum for 16 h before a mass was taken of the light turquoise solid (0.033 g, 40.2 %).

<sup>1</sup>H NMR (acetone-*d*<sub>6</sub>,  $\delta$ , 25  $^{\circ}\text{C}$ ): 8.13 (1H, d, Tp3B), 8.06 (1H, d, Tp3A), 7.94 (1H, d, Tp5B), 7.92 (1H, d, Tp5C), 7.81 (1H, d, Tp5A), 7.49 (1H, d, Tp3C), 7.03 (1H, dd,  $J = 1.20, 5.04$ , thiophene-H1'), 6.84 (1H, d,  $J = 3.18$ , thiophene-H3'), 6.77 (1H, dd,  $J = 3.18, 5.04$ , thiophene-H2'), 6.39 (1H, t, Tp4B), 6.32 (1H, t, Tp4A), 6.29 (1H, t, Tp4C), 4.13 (1H, d,  $J = 5.6$ , H4), 3.98 (1H, d,  $J = 7.12$ , H6), 3.58 (3H, s, -OMe), 3.07 (1H, t,  $J = 12.06$ , H2), 3.04 (1H, dd,  $J = 5.67, 15.0$ , H5), 2.09 (1H, m, H5), 1.37 (1H, m, H3), 1.31 (9H, d,  $J_{\text{PH}} = 8.87$ , PMe<sub>3</sub>). <sup>31</sup>P NMR (MeOH,  $\delta$ , 25  $^{\circ}\text{C}$ ): -12.3 ( $J_{\text{WP}} = 276$ ). <sup>13</sup>C NMR (acetone-*d*<sub>6</sub>,  $\delta$ , 25  $^{\circ}\text{C}$ ): 161.5 (C1), 158.4



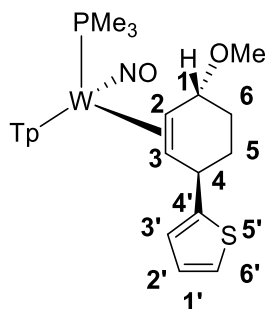
(thiophene-C4'), 144.6 (Tp3/5), 142.5 (Tp3/5), 141.7 (Tp3/5), 137.5 (Tp3/5), 137.1 (Tp3/5), 136.7 (Tp3/5), 126.1 (thiophene), 122.9 (thiophene), 122.8 (thiophene), 107.0 (Tp4), 106.8 (Tp4), 106.6 (Tp4), 83.5 (C6), 53.6 (-OMe), 48.0 (C2, d,  $J_{PC} = 10.6$ ), 66.5 (C6), 47.1 (C3), 39.0 (C4), 29.7 (buried-C5), 13.7 (d,  $J_{CP} = 27.9$ ,  $\text{PMe}_3$ ).

### Synthesis of $\text{WTp}(\text{NO})(\text{PMe}_3)(\eta^2\text{-2,3-(-1'-methoxy-1',2'-dihydro-[1,1'-biphenyl]-4-ol)})$ (**9**)



$^1\text{H}$  NMR (acetone- $d_6$ ,  $\delta$ , 25 °C): 8.13 (1H, d, Tp3/5), 8.12 (1H, d, Tp3/5), 7.91 (1H, d, Tp3/5), 7.89 (1H, d, Tp3/5), 7.79 (1H, d, Tp3/5), 7.51 (1H, d, Tp3/5), 7.30 (2H, m, Anisole-H3/H5), 6.64 (2H, m, Anisole-H2'/H6'), 6.37 (1H, t, Tp4), 6.30 (1H, t, Tp4), 6.27 (1H, t, Tp4), 3.92 (1H, d,  $J = 6.92$ ., H4/H6), 3.82 (1H, d,  $J = 7.00$ , H4/H6), 3.54 (3H, s, -OMe), 3.17 (1H, t,  $J = 11.7$ , H2), 3.03 (1H, m, H5), 1.95 (1H, ddt,  $J = 1.41, 7.40, 15.5$ , H5'), 1.30 (10H, overlapping d for  $\text{PMe}_2$  and H3,  $J_{\text{PH}} = 8.87$ , H3 and  $\text{PMe}_3$ ).  $^{31}\text{P}$  NMR (acetone- $d_6$ ,  $\delta$ , 25 °C): -6.2 ( $J_{\text{WP}} = 280$ ).

### Synthesis of $\text{WTp}(\text{NO})(\text{PMe}_3)(\eta^2\text{-2,3-(2-(4-methoxycyclohex-2-en-1-yl)thiophene)})$ (**10**)

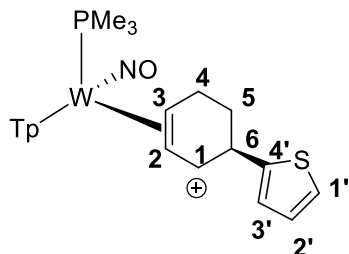


An oven-dried 4-dram vial was charged with **5** (0.300 g, 0.355 mmol) and MeOH (2 mL) and the resulting yellow mixture was cooled to -30 °C for 30 min. To this homogeneous yellow reaction mixture a -30 °C solution an excess of  $\text{NaBH}_4$  (0.150 g, 3.97 mmol) was added. Upon addition to the methanol solution vigorous bubbling occurs (evolution of  $\text{H}_{2(\text{g})}$ ) and the solution was allowed to sit at -30 °C over a course of 16 h. The next day the methanol solution was added to a solution of DI  $\text{H}_2\text{O}$  (30 mL). Upon addition an off-grey solid precipitates from solution. This solid was then collected on a medium porosity 30 mL fritted disk and washed with pentane (2 x 15 mL) and allowed to desiccate under active vacuum for 6 h before a mass was taken of the resulting off-white solid (0.084 g, 34.0%).

CV (MeCN):  $E_{p,a} = 0.42$  V (NHE).  $^1\text{H}$  NMR (acetone- $d_6$ ,  $\delta$ , 25 °C): 8.20 (1H, d, Tp3/5), 8.11 (1H, d, Tp3/5), 7.92 (1H, d, Tp3/5), 7.89 (1H, d, Tp3/5), 7.72 (1H, d, Tp3/5), 7.51 (1H, d, Tp3/5), 7.03 (1H, dd,  $J = 1.68, 4.77$ , thiophene-H1'), 6.77 (2H, overlapping resonances, thiophene-H3' and H2'), 6.40 (1H, t, Tp4), 6.29 (1H, t, Tp4A), 6.08 (1H, t, Tp4), 5.17 (1H, d,  $J = 6.76$ , H1), 4.59 (1H, m, H4), 3.38 (3H, s, -OMe), 3.15 (1H, m, H2),

2.12 (1H, m H5), 1.97 (1H, m, H6), 1.79 (1H, m, H6'), 1.56 (1H, dq,  $J = 2.11, 11.4$ , H3), 1.50 (1H, m, H5'), 1.07 (9H, broad s,  $\text{PMe}_3$ ).  $^{31}\text{P}$  NMR (acetone- $d_6$ ,  $\delta$ , 25 °C): -12.14 ( $J_{\text{WP}} = 285$ ).  $^{13}\text{C}$  NMR (acetone- $d_6$ ,  $\delta$ , 25 °C): 158.8 (thiophene-C4'), 143.4 (Tp3/5), 142.9 (Tp3/5), 141.2 (Tp3/5), 137.5 (Tp3/5), 137.0 (Tp3/5), 136.8 (Tp3/5), 126.9 (thiophene), 123.0 (thiophene), 122.6 (thiophene), 107.3 (Tp4), 106.8 (Tp4), 105.8 (Tp4), 85.8 (C1), 61.5 (C3), 59.4 (-OMe), 57.6 (C2), 42.4 (C4), 36.7 (C5), 29.2 (buried-C6), 14.1 (d,  $J_{\text{CP}} = 29.0$ ,  $\text{PMe}_3$ ).

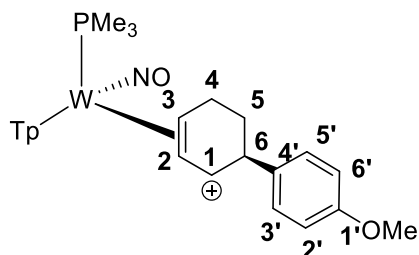
### Synthesis of $\text{WTp}(\text{NO})(\text{PMe}_3)(\eta^2\text{-2,3-(-6-(thiophen-2-yl)cyclohex-2-en-1-yl)ium})$ (**11**)



A solution of **10** (0.216 g, 0.310 mmol) in MeOH (1 mL) was prepared and cooled to -30 °C over a course of 10 min. To this solution was added an excess of HOTf (0.116 g, 0.768 mmol) that had been pre-chilled to -30 °C. The resulting homogeneous red solution was then added to a solution of standing diethyl ether (~ 8 mL) in a 4-dram vial. Upon addition a solid red film-like substance accumulates on the side of the vial. The organic layer was decanted and the resulting oily, red substance was dissolved in a minimal amount of DCM (1 mL) and added to a separate solution of stirring Et<sub>2</sub>O (30 mL). Upon addition a light yellow solid precipitates from solution. This yellow solid was then isolated on a fine 15 mL porosity fritted disc and the resulting yellow solid was washed with diethyl ether (2 x 15 mL) and the solid was allowed to dry for 2 h before a mass was taken of the yellow solid (0.040 g, 15.8 %).

$^1\text{H}$  NMR (MeCN- $d_3$ ,  $\delta$ , 0 °C): 8.41 (1H, d, Tp3/5), 7.99 (1H, d, Tp3/5), 7.96 (1H, d, Tp3/5), 7.95 (1H, d, Tp3/5), 7.92 (1H, d, Tp3/5), 7.78 (1H, d, Tp3/5), 7.35 (1H, dd,  $J = 0.84, 5.11$ , thiophene-H1'), 7.14 (1H, d,  $J = 3.38$ , thiophene-H3'), 7.05 (1H, dd,  $J = 3.38, 5.11$ , thiophene-H2'), 6.52 (1H, t, Tp4), 6.51 (1H, t, Tp4), 6.27 (1H, t, Tp4), 6.03 (1H, d,  $J = 7.28$ , H1), 5.32 (1H, t,  $J = 7.28$ , H2), 4.78 (1H, m, H6), 4.66 (1H, m, H3), 3.26 (1H, m, H4), 2.54 (1H, m, H4'), 1.98 (1H, buried, H5), 1.21 (1H, m, H5'), 1.18 (9H, d,  $J_{\text{PH}} = 9.80$ ,  $\text{PMe}_3$ ).

### Synthesis of $\text{WTp}(\text{NO})(\text{PMe}_3)(\eta^2\text{-2,3-(-4'-methoxy-1,2,5,6-tetrahydro-[1,1'-biphenyl]-2-yl)ium})$ (**12**)

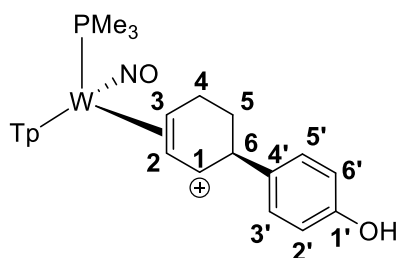


An oven-dried 4-dram vial was charged with **6** (0.205 g, 0.236 mmol) and MeOH (2 mL) and the resulting homogeneous red reaction mixture was cooled to -30 °C for 5 min. To this homogeneous red reaction mixture was added NaBH<sub>4</sub> (0.040 g, 1.06 mmol). Upon addition vigorous bubbling occurs (evolution of H<sub>2(g)</sub>) and this reaction mixture was allowed to sit at -30 °C for 5 min and then allowed to warm to room temperature for an additional 5 min. The reaction mixture was then eluted through a coarse 15 mL fritted disc ½ filled with basic alumina that had been set in diethyl ether. The reaction mixture was then eluted with 70 mL of diethyl ether and the solvent was evaporated in vacuo. A separate 4-dram vial was charged with MeOH (1 mL) and an excess

of HOTf (10 drops) and this acidic methanol solution was allowed to sit at  $-30\text{ }^{\circ}\text{C}$  over a course of 15 min. Next, when  $<10\text{ mL}$  of the solvent corresponding to the reaction mixture remained the acidic methanol solution was added. Upon addition the reaction mixture turns to a homogeneous yellow colored solution. To this yellow solution diethyl ether was added (40 mL) to induce precipitation as a yellow solid precipitates from solution. The solvent was removed in vacuo again, and when 10 mL of solution remained the heterogeneous yellow reaction mixture was transferred to an oven-dried 4-dram vial which was allowed to sit at  $-30\text{ }^{\circ}\text{C}$  overnight. The next day ( $\sim 16\text{ h}$  later) the reaction mixture was filtered through a fine 15 mL fritted disc and desiccated for 2 h under dynamic vacuum before a mass was taken. (0.172 g, 86.7%).

$^1\text{H}$  NMR (acetone- $d_6$ ,  $\delta$ ,  $25\text{ }^{\circ}\text{C}$ ): 8.63 (1H, d, Tp3/5), 8.34 (1H, d, Tp3/5), 8.20 (1H, d, Tp3/5), 8.17 (1H, d, Tp3/5), 8.01 (1H, d, Tp3/5), 7.94 (1H, d, Tp3/5), 7.39 (2H, m, Anisole-H3'/H5'), 6.99 (2H, m, Anisole-H2'/H6'), 6.65 (2H, overlapping t, Tp4s), 6.31 (1H, t, Tp4), 6.29 (1H, d,  $J = 7.56$ , H1), 5.54 (1H, t,  $J = 7.56$ , H2), 4.93 (1H, m, H3), 4.52 (1H, m, H6), 3.81 (3H, s, -OMe), 3.34 (1H, buried, H4), 2.65 (1H, m, H4'), 1.86 (1H, m, H5), 1.38 (9H, d,  $J_{\text{PH}} = 9.73$ ,  $\text{PMe}_3$ ), 1.30 (1H, buried, H5').  $^{31}\text{P}$  NMR (acetone- $d_6$ ,  $\delta$ ,  $25\text{ }^{\circ}\text{C}$ ): -8.29 ( $J_{\text{WP}} = 272$ ).

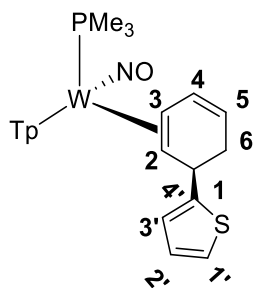
### Synthesis of $\text{WTP}(\text{NO})(\text{PMe}_3)(\eta^2\text{-}2,3\text{-}(\text{S})\text{-}1'\text{-hydroxy-}1,2,5,6\text{-tetrahydro-}[6,4'\text{-biphenyl}]\text{-}2\text{-ylium})$ (13)



To a 4-dram vial was added a solution of **7** (0.300 g, 0.350 mmol) along with MeOH (2 mL) and the resulting yellow mixture was cooled to  $-30\text{ }^{\circ}\text{C}$  for 30 min. To this homogeneous yellow reaction mixture a  $-30\text{ }^{\circ}\text{C}$  solution an excess of  $\text{NaBH}_4$  (0.160 g, 4.23 mmol) was added. Upon addition to the methanol solution vigorous bubbling occurs (evolution of  $\text{H}_{2(\text{g})}$ ) and the solution was allowed to sit at  $-30\text{ }^{\circ}\text{C}$  over a course of 16 h. The next day the methanol solution was added to a solution of DI  $\text{H}_2\text{O}$  (30 mL). Upon addition an off-grey solid precipitates from solution. This solid was then collected on a medium porosity 30 mL fritted disk and washed with pentane (2 x 15 mL) and allowed to desiccate under active vacuum for 6 h before a mass was taken of the resulting off-white solid (0.143 g, 57.7%). Some of this off-white solid (0.060 g, 0.0848 mmol) was then dissolved in MeCN (1 mL) and cooled to  $-30\text{ }^{\circ}\text{C}$  over a course of 10 min. To this solution was added an excess of HOTf (5 drops) and upon addition the off-white solution turns to a homogeneous orange colored solution. This reaction mixture was then added to 10 mL of diethyl ether that had been prepared in a separate 4-dram vial and the resulting red-orange reaction mixture was allowed to sit at  $-30\text{ }^{\circ}\text{C}$  over  $\frac{1}{2}$  an hour to induce precipitation of an orange-red solid. This solid was then isolated on a 30 mL fine porosity fritted disc and washed with diethyl ether (2 x 5 mL) and allowed to desiccate under static vacuum for 16 h before a mass was taken of the light red solid (0.068 g, 97.1%).

CV (MeCN):  $E_{p,c} = -1.75\text{ V}$  (NHE).  $^1\text{H}$  NMR (acetone- $d_6$ ,  $\delta$ ,  $25\text{ }^{\circ}\text{C}$ ): 8.64 (1H, d, Tp3/5), 8.34 (1H, d, Tp3/5), 8.21 (1H, d, Tp3/5), 8.17 (1H, d, Tp3/5), 8.02 (1H, d, Tp3/5), 7.94 (1H, d, Tp3/5), 7.30 (2H, m, Phenol-H3'/H5'), 6.90 (2H, m, Phenol-H2'/H6'), 6.66 (1H, t, Tp4), 6.65 (1H, t, Tp4), 6.33 (1H, t, Tp4), 6.32 (1H, buried, H1), 5.52 (1H, t,  $J = 7.24$ , H2), 4.89 (1H, m, H3), 4.49 (1H, m, H6), 3.33 (1H, m, H4), 2.65 (1H, m, H4'), 1.85 (1H, m, H5), 1.39 (9H, d,  $J_{\text{PH}} = 9.86$ ,  $\text{PMe}_3$ ), 1.36 (1H, buried, H5').  $^{31}\text{P}$  NMR (MeCN- $d_3$ ,  $\delta$ ,  $25\text{ }^{\circ}\text{C}$ ) = -7.96 ppm.

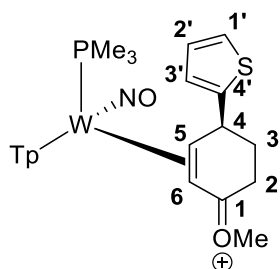
### Synthesis of $\text{WTP}(\text{NO})(\text{PMe}_3)(\eta^2\text{-}2,3\text{-}(2\text{-}(\text{cyclohexa-}2,4\text{-dien-}1\text{-yl})\text{thiophene}))$ (14)



Dissolved a solution of **15** (0.050 g, 0.0613 mmol) in MeCN (1/2 mL) and to this solution added an excess of TEA (5 drops) that had been pre-chilled to  $-30\text{ }^{\circ}\text{C}$ . Upon addition of the amine base the reaction mixture turns from a homogeneous red color to a homogeneous yellow colored solution. This yellow solution was added to a solution of 5 mL of standing DI H<sub>2</sub>O on a fine 15 mL porosity fritted disc. Upon addition of the reaction mixture to the water solution a white solid precipitates from solution. The solution was allowed to drip filter before vacuum was applied and the resulting white solid was washed with pentane (2 x 5 mL) and allowed to dry under dynamic vacuum for 2 h before a mass was taken of the sample (0.012 g, 29.3%).

<sup>1</sup>H NMR (MeCN-*d*<sub>3</sub>,  $\delta$ , 25  $^{\circ}\text{C}$ ): 8.09 (1H, d, Tp3/5), 8.06 (1H, d, Tp3/5), 7.87 (1H, d, Tp3/5), 7.84 (1H, d, Tp3/5), 7.79 (1H, d, Tp3/5), 7.45 (1H, d, Tp3/5), 7.06 (1H, dd,  $J = 1.29, 5.08$ , thiophene-H1'), 6.87 (1H, m, thiophene-H3'), 6.83 (1H, dd,  $J = 3.51, 5.08$ , thiophene-H2'), 6.56 (1H, m, H4), 6.38 (1H, t, Tp4), 6.33 (1H, t, Tp4), 6.26 (1H, t, Tp4), 4.95 (1H, m, H5), 4.21 (1H, d,  $J = 7.20$ , H1), 3.01 (2H, overlapping signals m, H3 and H6), 2.16 (1H, buried, H6'), 1.30 (10H, overlapping H2 and PMe<sub>3</sub>, d for PMe<sub>3</sub>,  $J_{\text{PH}} = 8.51$ , PMe<sub>3</sub>).

#### WTp(NO)(PMe<sub>3</sub>)( $\eta^2$ -5,6-methyl(4-(thiophen-2-yl)cyclohex-2-en-1-ylidene)oxonium) (**15**)

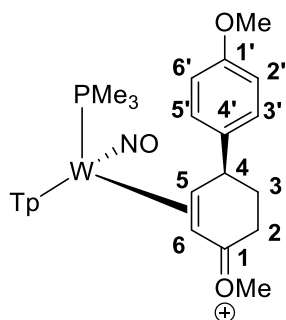


An oven-dried 4-dram vial was charged with Complex **2** (0.101 g, 0.132 mmol) and MeCN (1/2 mL) and the resulting homogeneous red reaction mixture was cooled to  $-30\text{ }^{\circ}\text{C}$  for 15 min. To this homogeneous red reaction mixture a  $-30\text{ }^{\circ}\text{C}$  solution of triflic acid (HOTf, 0.061 g, 0.404 mmol) was added and upon addition the reaction was allowed to sit at  $-30\text{ }^{\circ}\text{C}$  for 5 min. To this still homogeneous red solution room temperature thiophene (1.31 g, 15.6 mmol) was added and the reaction mixture was allowed to sit at  $-30\text{ }^{\circ}\text{C}$ . After 2 h the reaction mixture was added to 40 mL of stirring diethyl ether and upon addition a yellow precipitate forms as a suspension. After allowing to triturate  $\sim 5$  min a red solid had congealed on the sides of the Erlenmeyer flask and the organic layer was decanted. The solid that had collected on the sides was re-dissolved in DCM (2 mL) and added to 20 mL of stirring diethyl ether to generate a yellow precipitate. The yellow solid was then collected on a fine porosity 15 mL fritted disk and washed with diethyl ether (3 x 5 mL) and allowed to desiccate under active vacuum for 4 h before a mass was taken of the yellow solid (0.102 g, 91.1 % yield).

CV (MeCN):  $E_{\text{p,c}} = -1.37\text{ V}$  (NHE). IR,  $\nu(\text{BH}) = 2521\text{ cm}^{-1}$ ,  $\nu(\text{NO}) = 1612\text{ cm}^{-1}$ . <sup>1</sup>H NMR (acetone-*d*<sub>6</sub>,  $\delta$ , 25  $^{\circ}\text{C}$ ): 8.37 (1H, d, Tp3B), 8.23 (1H, d, Tp5C), 8.22 (1H, d, Tp3C), 8.14 (1H, d, Tp5B), 8.11 (1H, d, Tp5A), 7.63 (1H, d, Tp3A), 7.37 (1H, dd,  $J = 1.12, 5.10$ , thiophene-H1), 7.20 (1H, d,  $J = 3.55$ , thiophene-H3), 7.04 (1H, dd,  $J = 3.55, 5.10$ , thiophene-H2), 6.60 (1H, t, Tp4C), 6.57 (1H, t, Tp4B), 6.48 (1H, t, Tp4A), 4.59 (1H, td,  $J = 2.23, 6.30$ , H4), 4.34 (1H, m, H5), 3.58 (1H, d,  $J = 8.16$ , H6), 3.40 (3H, s, -OMe), 3.00 (1H, m, H2-syn),

2.54 (1H, m, H3-syn), 1.96 (1H, m, H3-anti), 2.91 (1H, m, H2-anti), 1.35 (9H, d,  $J_{\text{PH}} = 9.65$ ,  $\text{PMe}_3$ ).  $^{31}\text{P}$  NMR (acetone- $d_3$ ,  $\delta$ , 25 °C): -9.2 ( $J_{\text{WP}} = 280$ ).  $^{13}\text{C}$  NMR (acetone- $d_6$ ,  $\delta$ , 25 °C): 198.2 (C1), 146.0 (Tp3/5), 144.6 (Tp3/5), 143.1 (Tp3/5), 139.8 (Tp3/5), 139.5 (2C, overlapping Tp3/5s), 127.8 (thiophene-C2), 126.1 (thiophene-C4), 125.2 (thiophene-C3), 124.5 (thiophene-C1), 108.9 (Tp4), 108.7 (Tp4), 108.5 (Tp4), 76.9 (C5, d,  $J_{\text{PC}} = 16.6$ ), 66.1 (C1), 64.8 (C6), 58.7 (OMe), 39.9 (C4), 31.7 (C3), 28.7 (C2), 13.6 (d,  $J_{\text{CP}} = 32.5$ ,  $\text{PMe}_3$ ). ESI-MS (m/z, calculated (rel intens, %), **observed (rel intens, %)**, (M +): 694.1655 (80.28), **694.1659 (79.39)**, 695.1680 (78.29), **695.1685 (77.17)**, 696.1677 (100), **696.1682 (100)**, 697.1714 (46.13), **697.1720 (41.58)**, 698.1708 (84.86), **698.1713 (82.66)**.

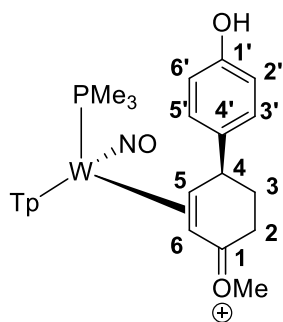
**WTP(NO)(PMe<sub>3</sub>)( $\eta^2$ -5,6-(E)-(4'-methoxy-2,3-dihydro-[1,1'-biphenyl]-4(1H)-ylidene)(methyl)oxonium) (16)**



An oven-dried 4-dram vial was charged with **2** (0.944 g, 1.24 mmol) and MeCN (3 mL) and the resulting homogeneous red reaction mixture was cooled to -30 °C for 15 min. To this homogeneous red reaction mixture a -30 °C solution of triflic acid (HOTf, 0.700 g, 4.64 mmol) was added and upon addition the reaction was allowed to sit at -30 °C for 1 min. To this still homogeneous red solution room temperature anisole (5 mL, ~46.2 mmol) was added and the reaction mixture was allowed to sit at -30 °C. After 16 h the reaction mixture was added to 500 mL of stirring Et<sub>2</sub>O and upon addition a yellow precipitate forms as a suspension. After allowing to triturate ~5 min a red solid had congealed on the sides of the Erlenmeyer flask and the organic layer was decanted. The solid that had collected on the sides was re-dissolved in DCM (10 mL) and added to 100 mL of stirring diethyl ether to generate a yellow precipitate. The yellow solid was then collected on a fine porosity 60 mL fritted disk and washed with diethyl ether (3 x 20 mL) and allowed to desiccate under active vacuum for 4 h before a mass was taken of the yellow solid (0.707 g, 65 % yield).

CV (MeCN):  $E_{\text{p,c}} = -1.26$  V (NHE). IR,  $\nu(\text{BH}) = 2518$   $\text{cm}^{-1}$ ,  $\nu(\text{NO}) = 1600$   $\text{cm}^{-1}$ .  $^1\text{H}$  NMR (acetone- $d_6$ ,  $\delta$ , 25 °C): 8.37 (1H, d, Tp3B), 8.21 (1H, d, Tp5C), 8.16 (1H, d, Tp3C), 8.13 (1H, d, Tp5), 8.11 (1H, d, Tp5), 7.61 (1H, d, Tp3A), 7.49 (2H, m, anisole-H3/5), 6.97 (1H, m, anisole-H2/6), 6.58 (1H, t, Tp4), 6.57 (1H, t, Tp4B), 6.48 (1H, t, Tp4), 4.35 (2H, overlapping m, H4 and H5), 3.81 (3H, s, anisole-OMe), 3.61 (1H, d,  $J = 8.10$ , H6), 3.26 (3H, s, oxonium-OMe), 3.13 (1H, m, H2-syn), 2.85 (1H, m, H2-anti), 2.26 (1H, m, H3-syn), 1.81 (1H, m, H3-anti), 1.21 (9H, d,  $J_{\text{PH}} = 9.60$ ,  $\text{PMe}_3$ ).  $^{31}\text{P}$  NMR (MeCN- $d_3$ ,  $\delta$ , 25 °C): -9.43 ( $J_{\text{WP}} = 284$ ).  $^{13}\text{C}$  NMR (acetone- $d_6$ ,  $\delta$ , 25 °C): 196.2 (C1), 159.4 (anisole-C1), 144.8 (Tp3/5), 143.0 (Tp3/5), 139.9 (Tp3/5), 139.5 (Tp3/5), 139.3 (Tp3/5), 129.4 (anisole 3/5), 115.1 (anisole-C2/6), 109.0 (Tp4), 108.7 (Tp4), 108.5 (Tp4), 76.0 (C5, d,  $J_{\text{PC}} = 15.1$ ), 66.5 (C6), 58.2 (oxonium-OMe), 55.5 (anisole-OMe), 44.3 (C4), 35.3 (C3), 29.7 (C2), 13.9 (d,  $J_{\text{CP}} = 31.4$ ,  $\text{PMe}_3$ ). ESI-MS (m/z, calculated (rel intens, %), **observed (rel intens, %)**, (M +): 718.2197 (81.87), **718.2201 (81.05)**, 719.2223 (80.79), **719.2227 (79.60)**, 720.2222 (100), **720.2227 (100)**, 721.2262 (46.01), **721.2265 (43.71)**, 722.2254 (83.08), **722.2256 (83.13)**.

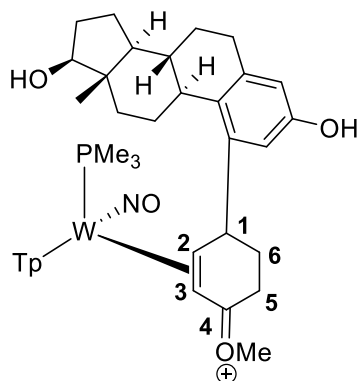
**Synthesis of WTP(NO)(PMe<sub>3</sub>)( $\eta^2$ -5,6-(E)-(4'-hydroxy-2,3-dihydro-[1,1'-biphenyl]-4(1H)-ylidene)(methyl)oxonium) (17)**



An oven-dried 4-dram vial was charged with Complex **2** (0.672 g, 0.882 mmol) and MeCN (4 mL) and the resulting homogeneous red reaction mixture was cooled to  $-30\text{ }^{\circ}\text{C}$  for 15 min. To this homogeneous red reaction mixture a  $-30\text{ }^{\circ}\text{C}$  solution of triflic acid (0.944 g, 6.25 mmol) was added and upon addition the reaction was allowed to sit at  $-30\text{ }^{\circ}\text{C}$  for 1 min. To this still homogeneous red solution room temperature phenol (3.65 g, 38.7 mmol) was added and the reaction mixture was allowed to sit at  $-30\text{ }^{\circ}\text{C}$ . After 16 h the reaction mixture was added dropwise to 500 mL of stirring diethyl ether and upon addition a yellow precipitate forms as a suspension.. The yellow solid was then collected on a fine porosity 30 mL fritted disk and washed with diethyl ether (3 x 20 mL) and allowed to desiccate under active vacuum for 4 h before a mass was taken of the resulting yellow powder (0.530 g, 70.2 % yield).

CV (MeCN):  $E_{p,c} = -1.24\text{ V}$  (NHE). IR,  $\nu(\text{BH}) = 2531\text{ cm}^{-1}$ ,  $\nu(\text{NO}) = 1616\text{ cm}^{-1}$ .  $^1\text{H NMR}$  (acetone- $d_6$ ,  $\delta$ ,  $25\text{ }^{\circ}\text{C}$ ): 8.36 (1H, d, Tp3B), 8.20 (1H, d, Tp5C), 8.16 (1H, d, Tp3C), 8.13 (1H, d, Tp5B), 8.11 (1H, d, Tp5A), 7.60 (1H, d, Tp3A), 7.37 (2H, m, anisole-H3/5), 6.89 (1H, m, anisole-H2/6), 6.58 (1H, t, Tp4C), 6.56 (1H, t, Tp4B), 6.48 (1H, t, Tp4A), 4.33 (2H, overlapping m, H4 and H5), 3.59 (1H, d,  $J = 8.10$ , H6), 3.24 (3H, s, -OMe), 3.12 (1H, m, H2-syn), 2.83 (1H, m, H2-anti), 2.23 (1H, m, H3-syn), 1.79 (1H, m, H3-anti), 1.21 (9H, d,  $J_{\text{PH}} = 9.62$ ,  $\text{PMe}_3$ ).  $^{31}\text{P NMR}$  (MeCN- $d_3$ ,  $\delta$ ,  $25\text{ }^{\circ}\text{C}$ ):  $-9.34$  ( $J_{\text{WP}} = 285$ ).  $^{13}\text{C NMR}$  (acetone- $d_6$ ,  $\delta$ ,  $25\text{ }^{\circ}\text{C}$ ): 196.2 (C1), 157.0 (phenol-C1), 144.8 (Tp3/5), 143.0 (Tp3/5), 140.9 (phenol-C4), 139.9 (Tp3/5), 139.5 (Tp3/5), 139.3 (Tp3/5), 129.3 (anisole 3/5), 116.4 (anisole-C2/6), 109.0 (Tp4), 108.7 (Tp4), 108.5 (Tp4), 76.2 (C5, d,  $J_{\text{PC}} = 16.1$ ), 66.6 (C6), 58.2 (OMe), 44.3 (C4), 35.4 (C3), 29.9 (C2), 13.9 (d,  $J_{\text{CP}} = 31.3$ ,  $\text{PMe}_3$ ). ESI-MS ( $m/z$ , calculated (rel intens, %), **observed (rel intens, %)**, (M +): 704.2041 (82.41), **704.2045 (81.37)**, 705.2066 (80.6), **705.2070 (80.29)**, 706.2065 (100), **706.2070 (100)**, 707.2106 (45.32), **707.2107 (44.17)**, 708.2097 (83.33), **708.2101 (82.89)**.

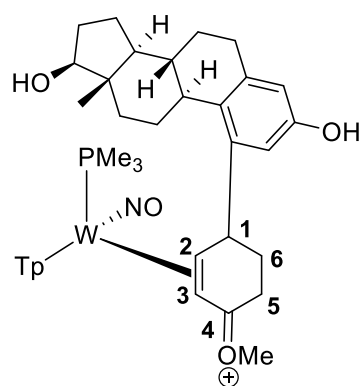
**Synthesis of WTp(NO)(PMe<sub>3</sub>)( $\eta^2$ -2,3-(E)-(4-((8R,9S,13S,14S,17S)-3,17-dihydroxy-13-methyl-7,8,9,11,12,13,14,15,16,17-decahydro-6H-cyclopenta[a]phenanthren-2-yl)cyclohex-2-en-1-ylidene)(methyl)oxonium) (18)**



An oven-dried 4-dram vial was charged with Complex **2** (0.200 g, 0.262 mmol) and MeCN (1 mL) and the resulting homogeneous red reaction mixture was cooled to  $-30\text{ }^{\circ}\text{C}$  for 15 min. To this homogeneous red reaction mixture a  $-30\text{ }^{\circ}\text{C}$  solution of triflic acid (HOTf, 0.333 g, 2.21mmol) was added and upon addition the reaction was allowed to sit at  $-30\text{ }^{\circ}\text{C}$  for 5 min. To this still homogeneous red solution room temperature beta-estradiol (0.200 g, 0.734 mmol) was added and the reaction mixture was allowed to sit at  $-30\text{ }^{\circ}\text{C}$  over a course of 16 h. The next day the reaction mixture was added to 100 mL of stirring diethyl ether and upon addition a yellow precipitate forms as a suspension. The yellow solid was then collected on a fine porosity 15 mL fritted disk and washed with diethyl ether (3 x 10 mL) and allowed to desiccate under active vacuum for 6 h before a mass was taken of the yellow solid (0.142 g, 52.4% yield).

Due to difficulties in spectral overlap between the two diastereomers, characterization is included for only a single hand of the tungsten complex. The resolved form of the tungsten-anisole complex was generated by using an adapted procedure previously reported to generate an optically resolved tungsten-benzene complex.<sup>20</sup>

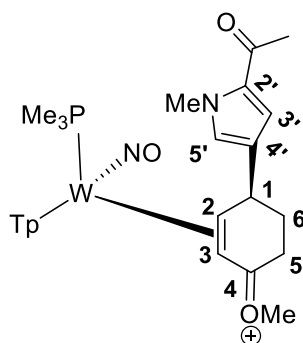
#### W<sub>R</sub>-Hand Characterization Only



CV (DMA):  $E_{p,c} = -1.76\text{ V}$  (NHE). IR,  $\nu(\text{BH}) = 2515\text{ cm}^{-1}$ ,  $\nu(\text{NO}) = 1614\text{ cm}^{-1}$ .  $^1\text{H NMR}$  (acetonitrile- $d_3$ ,  $\delta$ ,  $25\text{ }^{\circ}\text{C}$ ): 8.18 (1H, d, Tp3/5), 8.02 (1H, d, Tp3/5), 7.94 (1H, d, Tp3/5), 7.92 (1H, d, Tp3/5), 7.82 (1H, d, Tp3/5), 7.50 (1H, d, Tp3/5), 7.39 (1H, s, beta-estradiol-phenolic), 6.54 (1H, s, beta-estradiol-phenolic), 6.50 (1H, t, Tp4), 6.47 (1H, t, Tp4), 6.37 (1H, t, Tp4), 4.76 (1H, m, H4), 4.08 (1H, ddd,  $J = 8.14, 7.05, 2.30$ , H5), 3.64 (1H, t,  $J = 8.60$ , beta-estradiol), 3.34 (1H, d,  $J = 8.14$ , H6), 3.06 (4H, overlapping, -OMe and H2), 2.79 (1H, m, beta-estradiol), 2.72 (1H, m, H2'), 2.48 (1H, m, beta-estradiol), 2.20 (1H, m, beta-estradiol), 2.10 (2H, buried, beta-estradiol and H3), 1.90 (2H, buried, beta-estradiol), 1.69 (1H, buried, H3'), 1.42 to 1.30 (9H, overlapping, beta-estradiol resonance), 1.07 (9H, d,  $J_{\text{PC}} = 9.63$ ,  $\text{PMe}_3$ ), 0.75 (3H, s, beta-estradiol methyl).

$^{13}\text{C NMR}$  (MeCN- $d_3$ ,  $\delta$ ,  $25\text{ }^{\circ}\text{C}$ ):  $\delta$  ppm 196.2 (C1), 151.9 (beta-estradiol), 145.9 (Tp3/5), 144.8 (Tp3/5), 142.9 (Tp3/5), 139.9 (Tp3/5), 139.6 (Tp3/5), 139.3 (Tp3/5), 133.7 (2C, beta-estradiol), 126.3 (beta-estradiol), 109.0 (2C, Tp4s), 108.6 (Tp4), 82.0 (beta-estradiol), 76.5 (C5, d,  $J_{\text{PC}} = 15.4$ ), 66.3 (C6), 58.4 (-OMe), 51.0 (beta-estradiol), 45.2 (beta-estradiol), 44.1 (beta-estradiol), 37.9 (beta-estradiol), 30.2 (C3), 33.9 (C2), 37.8 (C4), 13.9 (d,  $J_{\text{CP}} = 31.4$ ,  $\text{PMe}_3$ ), 11.7 (beta-estradiol).  $^{31}\text{P NMR}$  (acetone- $d_6$ ,  $\delta$ ,  $25\text{ }^{\circ}\text{C}$ ):  $-5.83$  ( $J_{\text{WP}} = 286.5$ ). ESI-MS ( $m/z$ , calculated (rel intens, %), **observed** (rel intens, %), ppmc, (M + H)<sup>+</sup>: 882.3399 (75.96), **882.3392 (73.35)**, 883.3424 (82.24), **883.3418 (81.98)**, 884.3427 (100), **884.3420 (100)**, 885.3462 (53.27), **885.3454 (50.44)**, 886.3458 (81.00), **886.3450 (79.57)**.

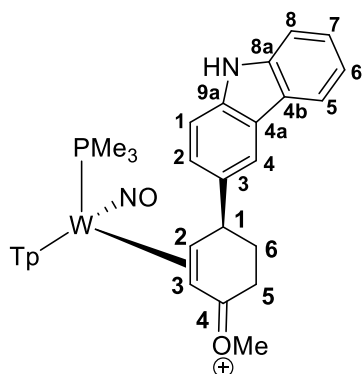
**Synthesis of WTp(NO)(PMe<sub>3</sub>)( $\eta^2$ -2,3-((E)-(4-(5-acetyl-1-methyl-1H-pyrrol-3-yl)cyclohex-2-en-1-ylidene)(methyl)oxonium) (20)**



An oven-dried 4-dram vial was charged with Complex **2** (0.110 g, 0.145 mmol) and MeCN (1 mL) and the resulting homogeneous red reaction mixture was cooled to  $-30\text{ }^{\circ}\text{C}$  for 10 min. To this homogeneous red reaction mixture a  $-30\text{ }^{\circ}\text{C}$  solution of triflic acid in excess (HOTf, 10 drops) was added. To this acidic solution added 2-acetyl-N-Me-pyrrole (0.603 g, 4.90 mmol) and upon addition the reaction was allowed to sit at  $-30\text{ }^{\circ}\text{C}$  for 16 h. The next day this homogeneous red reaction mixture was added to 50 mL of stirring diethyl ether and upon addition a yellow precipitate forms as a suspension transiently before the solid became the consistency of a thick, viscous red oil that sticks to the sides of the Erlenmeyer flask. The organic layer from this solution was decanted and the red, oil-like film was re-dissolved in a minimal amount of DCM (5 mL). This red reaction mixture was then added to a stirring solution of Et<sub>2</sub>O to generate an orange solid. This solid was then collected on a medium porosity 15 mL fritted disk and washed with diethyl ether (2 x 10 mL) and allowed to desiccate under active vacuum for 2 h before a mass was taken of the yellow solid (0.063 g, 49.2% yield).

<sup>1</sup>H NMR (acetone-*d*<sub>6</sub>,  $\delta$ , 25  $^{\circ}\text{C}$ ): 8.17 (1H, d, Tp3/5), 8.06 (1H, d, Tp3/5), 7.99 (1H, d, Tp3/5), 7.96 (1H, d, Tp3/5), 7.93 (1H, d, Tp3/5), 7.79 (1H, s, 2-acetyl-N-Me-pyrrole-resonance), 7.67 (1H, s, 2-acetyl-N-Me-pyrrole-resonance), 7.49 (1H, d, Tp3/5), 6.54 (2H, t, Tp4), 6.47 (1H, t, Tp4), 6.37 (1H, t, Tp4), 4.06 (1H, broad t,  $J = 5.24$ , H1), 4.02 (1H, dd,  $J = 8.37, 13.6$ , H2), 3.97 (3H, s, -N-Me), 3.26 (3H, s, -OMe), 2.73 (3H, s, -acetyl-Me), 3.31 (1H, d,  $J = 9.00$ , H), 2.82 (1H, dt,  $J = 5.91, 19.88$ ), 2.40 (1H, m, H), 1.84 (1H, m, H), 1.21 (9H, d,  $J_{\text{PH}} = 9.46$ , PMe<sub>3</sub>).

### Synthesis of WTp(NO)(PMe<sub>3</sub>)( $\eta^2$ -2,3-((S,E)-(4-(9H-carbazol-3-yl)cyclohex-2-en-1-ylidene)(methyl)oxonium)) (21)

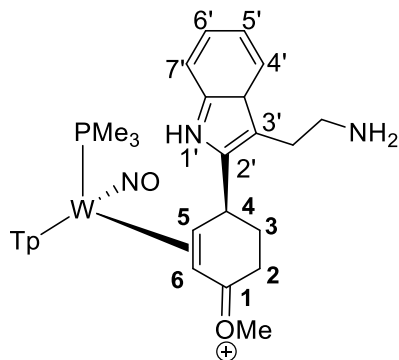


CV (DMA):  $E_{\text{p,c}} = -1.20\text{ V}$ ,  $E_{\text{p,a}} = 1.64\text{ V}$  (NHE). IR,  $\nu(\text{BH}) = 2501\text{ cm}^{-1}$ ,  $\nu(\text{NO}) = 1602\text{ cm}^{-1}$ . <sup>1</sup>H NMR (MeCN-*d*<sub>3</sub>,  $\delta$ , 16  $^{\circ}\text{C}$ ): 9.45 (1H, s, N-H), 8.23 (1H, s, carbazole-3H), 8.20 (1H, d, Tp3/5), 8.15 (1H, buried, carbazole-H5), 8.03 (1H, d, Tp5C), 7.95 (1H, d, Tp3/5), 7.94 (1H, d, Tp3/5), 7.87 (1H, d, Tp3C), 7.52 to 7.55 (4H, overlapping Tp3/5 and carbazole-H1,H2 and H8), 7.43 (1H, td,  $J = 1.12, 5.22$ , carbazole-H7), 7.23 (1H, td,  $J = 0.82, 7.33$ , carbazole-H6), 6.49 (1H, t, Tp4), 6.48 (1H, t, Tp4), 6.39 (1H, t, Tp4C), 4.50 (1H, td,  $J = 2.19, 8.21$ , H1), 4.30 (1H, m, H2), 3.43 (1H, buried, H3), 3.11 (4H, overlapping -OMe and H5), 2.79 (1H, m, H5'),



2.29 (1H, m, H6), 1.89 (1H, m, H6'), 1.03 (9H, d,  $J_{\text{PH}} = 9.60$ ,  $\text{PMe}_3$ ).  $^{13}\text{C}$  NMR ( $\text{MeCN-}d_3$ ,  $\delta$ , 16 °C): 196.5 (C1), 145.9 (Tp3/5), 144.8 (Tp3/5), 142.2 (Tp3/5), 141.3 (Tp3/5), 141.0 (Tp3/5), 139.9 (carbazole-8a/9a), 139.7 (carbazole-8a/9a), 139.3, 129.3, 126.8 (carbazole-C7), 126.5, 124.2 (carbazole-4a/4b), 123.7 (carbazole-4a/4b), 121.2 (carbazole-C5), 119.9 (carbazole-C6), 119.8 (carbazole), 112.2 (carbazole), 112.0 (carbazole-C8), 109.0 (Tp4), 108.6 (overlapping Tp4), 76.7 (C2, d,  $J_{\text{PC}} = 15.0$ ), 66.6 (C3), 58.5 (-OMe), 45.2 (C1, d,  $J_{\text{PC}} = 3.1$ ) 36.2 (C6), 30.1 (C5), 13.9 ( $\text{PMe}_3$ , d,  $J_{\text{PC}} = 32.00$ ).

### Synthesis of $\text{W}(\text{NO})(\text{PMe}_3)(\eta^2\text{-5,6-(E)-((4S)\text{-4-(3-(2-aminoethyl)-3aH-114-indol-2-yl)cyclohex-2-en-1-ylidene)(methyl)oxonium})$ (22)



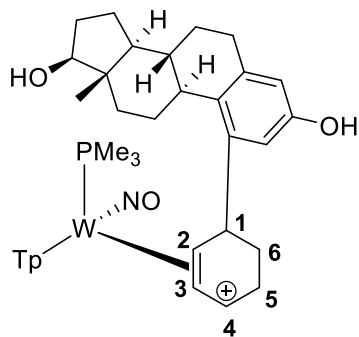
To a 4-dram vial added tryptamine (0.100 g, 0.624 mmol) and MeCN (3 mL) and let the heterogeneous white solution cool to -40 °C. To a separate vial added Complex **2** (0.250 g, 0.328 mmol) along with MeCN (2 mL) and let the homogeneous red reaction mixture cool to -40 °C over a period of ten minutes. Proceeded to added 5 drops of a -40 °C chilled solution of HOTf to the solution of tryptamine and also to the solution of **2** in acetonitrile and let both reaction mixtures continue to chill at -40 °C. Proceeded to added the acidic tryptamine solution to the solution of **2** in MeCN and let the reaction mixture stir at -40 °C. After 17 h at -40 °C a room temperature solution of MeOH (1 mL) was added to the reaction mixture and the reaction mixture was then added dropwise into a solution of stirring Et<sub>2</sub>O (~ 100 mL). Upon trituration for 5 min a red, oily substance had accumulated on the sides of the flask. This was re-dissolved in a 1:1 MeOH/DCM mixture (~ 10 mL total) and this was again added to 200 mL of stirring Et<sub>2</sub>O. Upon trituration ~ 10 min an oily red substance accumulated on the sides of the flask again. The red oil was then dissolved in ~ 5 mL of THF and added to 100 mL of stirring Et<sub>2</sub>O and upon addition a dull yellow solid develops in the solution. This yellow solid was then isolated on a fine 60 mL fritted disc and washed with Et<sub>2</sub>O (3 x 10 mL) and allowed to dry under active vacuum in a desiccator for 3 h before a mass was taken (0.192 g, 63.4 %).

CV (DMA):  $E_{p,c} = -1.27$  V,  $E_{p,a} = 1.31$  V (NHE). IR,  $\nu(\text{BH}) = 2516$  cm<sup>-1</sup>,  $\nu(\text{NO}) = 1617$  cm<sup>-1</sup>.  $^1\text{H}$  NMR (acetonitrile-*d*<sub>3</sub>,  $\delta$ , 25 °C): 9.86 (1H, s, N-H), 8.20 (1H, d, Tp3B), 8.04 (1H, d, Tp5C), 7.97 (1H, d, Tp5A), 7.95 (1H, d, Tp5B), 7.89 (1H, d, Tp3C), 7.59 (1H, d,  $J = 8.11$ , tryptamine), 7.53 (1H, d, Tp3A), 7.49 (1H, dt,  $J = 8.11, 0.86$ , tryptamine), 7.17 (1H, td,  $J = 7.1, 0.86$ , tryptamine), 7.10 (1H, dt,  $J = 7.54, 0.86$ , tryptamine), 6.51 (1H, t, Tp4), 6.48 (1H, t, Tp4), 6.39 (1H, t, Tp4), 4.62 (1H, m, H4), 4.21 (1H, ddd,  $J = 8.0, 6.9, 2.1$ , H5), 3.45 (1H, d,  $J = 8.4$ , H6), 3.28 (2H, buried, tryptamine-ethyl), 3.13 (3H, s, -OMe), 3.12 (3H, buried, ethyl-tryptamine and H2), 2.81 (1H, m, H2'), 2.26 (1H, m, H6), 1.97 (1H, m, H6'), 1.04 (9H, d,  $J_{\text{PC}} = 9.51$ ,  $\text{PMe}_3$ ).  $^{13}\text{C}$  NMR (acetonitrile-*d*<sub>3</sub>,  $\delta$ , 25 °C):  $\delta$  ppm 196.5 (C1), 146.0 (tryptamine), 144.9 (Tp3/5), 143.3 (tryptamine), 142.9 (Tp3/5), 140.1 (Tp3/5), 139.8 (Tp3/5), 139.4 (Tp3/5), 137.3 (Tp3/5), 128.7 (tryptamine), 122.7 (tryptamine), 120.4 (tryptamine), 119.0 (tryptamine), 112.4 (tryptamine), 109.0 (Tp4), 108.8 (Tp4), 108.7 (Tp4), 105.6 (tryptamine), 73.1 (C5, d,  $J_{\text{PC}} = 15.9$ ), 66.5 (C6), 58.7 (-OMe), 41.6 (tryptamine-ethyl), 35.9 (C4, d,  $J_{\text{PC}} = 3.00$ ), 33.3 (C3), 22.9 (C2), 23.3 (tryptamine-ethyl), 13.8 (d,  $J_{\text{CP}} = 32.0$ ,  $\text{PMe}_3$ ).  $^{31}\text{P}$  NMR (acetonitrile-*d*<sub>3</sub>,  $\delta$ , 25

$^{\circ}\text{C}$ ): -8.44 ( $J_{\text{WP}} = 282$ ). ESI-MS ( $m/z$ , calculated (rel intens, %), **observed** (rel intens, %), ppm, (M + H) $^{+}$ ): 770.2623 (80.07), **770.2617 (74.44)**, 771.2648 (81.51), **771.2647 (79.10)**, 772.2648 (100), **772.2648 (100)**, 773.2686 (48.38), **773.2690 (50.15)**, 774.2680 (82.21), **774.2679 (79.91)**.

**Synthesis of WTp(NO)(PMe<sub>3</sub>)( $\eta^2$ -2,3-4-((8R,9S,13S,14S,17S)-3,17-dihydroxy-13-methyl-7,8,9,11,12,13,14,15,16,17-decahydro-6H-cyclopenta[a]phenanthren-2-yl)cyclohex-2-en-1-ylum) (30)**

**Ws-Hand-Only**

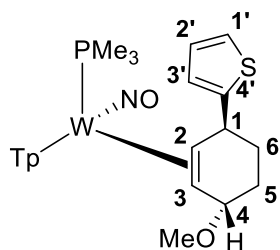


The Ws-dimethoxybenzenium complex was resolved in a similar manner as has been previously reported.<sup>20-21</sup> This complex was then allowed to undergo a ligand exchange with anisole and an analogous procedure as detailed to the complex **18** was pursued. A hydride addition in methanol at reduced temperature was achieved under adapted conditions to **25** described *vide infra*. This intermediate was characterized by  $^1\text{H}$  NMR but full characterization was not pursued. To generate **17**, the hydride addition complex WTp(NO)(PMe<sub>3</sub>)( $\eta$ -(4-(cyclohex-2-en-1-yl)-13-methyl-7,8,9,11,12,13,14,15,16,17-decahydro-6H-cyclopenta[a]phenanthrene-3,17-diol)) (0.040 g, 0.0468 mmol) was dissolved in a solution of MeCN (1 mL) and cooled to  $-40\text{ }^{\circ}\text{C}$ . To this chilled solution was added an excess of HOTf (5 drops) and the resulting homogeneous red solution was added to a solution of standing diethyl ether (10 mL) and allowed to sit at reduced temperature ( $-30\text{ }^{\circ}\text{C}$ ) to induce precipitation. The organic layer was decanted and the resulting off-yellow solid was dried with a stream of  $\text{N}_2(\text{g})$  before a mass was taken (0.027g, 42.6 %). and characterization was pursued. Characterization for the IR and electrochemical potentials were derived from a racemic sample prepared under analogous conditions.

CV (DMA):  $E_{p,c} = -1.03\text{ V}$  (NHE). IR,  $\nu(\text{BH}) = 2515\text{ cm}^{-1}$ ,  $\nu(\text{NO}) = 1632\text{ cm}^{-1}$ .  $^1\text{H}$  NMR (acetonitrile- $d_3$ ,  $\delta$ ,  $25\text{ }^{\circ}\text{C}$ ): 8.42 (1H, d, Tp3/5), 8.17 (1H, d, Tp3/5), 8.00 (1H, d, Tp3/5), 7.95 (1H, d, Tp3/5), 7.87 (1H, d, Tp3/5), 7.82 (1H, d, Tp3/5), 7.28 (1H, s, beta-estradiol-phenolic), 6.53 (1H, s, beta-estradiol-phenolic), 6.52 (2H, overlapping t, Tp4s), 6.49 (1H, broad t,  $J = 6.40$  (H1)), 6.35 (1H, t, Tp4), 5.36 (1H, t,  $J = 7.35$ , H2), 4.32 (1H, dd,  $J = 7.35$ , 15.7, H3), 4.25 (1H, dd,  $J = 6.26$ , 10.76, H4), 3.66 (1H, t,  $J = 8.54$ , beta-estradiol), 3.51 (1H, m, H6), 3.31 (1H, dt,  $J = 6.35$ , 20.0, H6'), 2.78 (2H, overlapping, beta-estradiol), 2.45 (1H, m, beta-estradiol), 2.17 (1H, td,  $J = 3.96$ , 11.64, beta-estradiol), 2.01 (1H, m, beta-estradiol), 1.92 (1H, buried, beta-estradiol), 1.87 (1H, buried, beta-estradiol), 1.68 (1H, m, H5), 1.58 to 1.19 (9H, overlapping, beta-estradiol resonances), 1.04 (9H, d,  $J_{\text{PC}} = 9.91$ , PMe<sub>3</sub>), 0.79 (3H, s, beta-estradiol methyl). The signal intensity in the resulting  $^{13}\text{C}$  NMR were not sufficient (low concentration) to provide unambiguous characterization.

ESI-MS ( $m/z$ , calculated (rel intens, %), **observed** (rel intens, %), ppm, (M + H) $^{+}$ ): 852.3294 (76.61), **852.3296 (69.33)**, 853.3319 (82.23), **853.3325 (84.42)**, 854.3321 (100), **854.3330 (100)**, 855.3357 (52.54), **855.3363 (61.75)**, 856.3352 (81.09), **856.3360 (78.27)**.

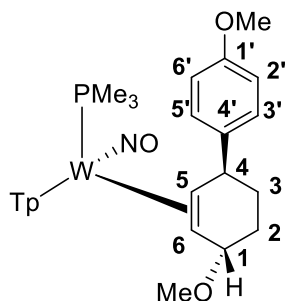
**Synthesis of WTp(NO)(PMe<sub>3</sub>)( $\eta^2$ -2,3-2-((1R,4R)-4-methoxycyclohex-2-en-1-yl)thiophene) (25)**



A solution of **15** (0.287 g, 0.339 mmol) was added to a 4-dram vial along with MeOH (~1.5 mL). The reaction mixture was allowed to cool to -30 °C over the course of 20 min. To this chilled solution NaBH<sub>4</sub> (0.084 g, 2.22 mmol) was added. Upon addition of the hydride source to the methanol solution bubbling is observed to occur (CAUTION! Evolution of H<sub>2(g)</sub>). The reaction mixture was allowed to sit at -30 °C for 30 min before the reaction mixture was allowed to stir at room temperature for an additional 30 min. The reaction mixture is initially a homogeneous brown solution. After 30 min of stirring at ambient temperatures the solution To the reaction mixture was added to a stirring solution of DI water (20 mL) solution of DI water. Upon addition of water to the reaction mixture, a light grey solid precipitates from solution. This reaction mixture was then filtered through a fine 15 mL porosity fritted disc and washed with DI water (1 x 10 mL) and vacuum was applied to marginally dry the resulting off-grey solid. Next the solid was washed with pentane (3 x 10 mL) and allowed to desiccate under dynamic vacuum over a course of 4 h before a mass was taken of the resulting off-white solid (0.232 g, 58.5 %).

<sup>1</sup>H NMR (acetone-*d*<sub>6</sub>, δ, 25 °C): 8.85 (1H, d, Tp3A), 8.16 (1H, d, Tp3B), 7.94 (1H, d, Tp5C), 7.91 (1H, d, Tp5B), 7.69 (1H, d, Tp5A), 7.47 (1H, d, Tp3C), 7.27 (1H, dd, *J* = 1.21, 5.12, thiophene-H1'), 7.08 (1H, dd, *J* = 1.21, 3.46, thiophene-H3'), 6.98 (1H, dd, *J* = 3.46, 5.12, thiophene-H2'), 6.39 (1H, t, Tp4B), 6.34 (1H, t, Tp4C), 6.13 (1H, t, Tp4A), 5.34 (1H, m, H4), 4.39 (1H, t, *J* = 7.20, H1), 3.07 (1H, m, H2), 3.03 (3H, s, -OMe), 2.16 (1H, buried, H6-syn), 2.01 (1H, m, H5-syn), 1.85 (1H, dd, *J* = 5.03, 12.2, H3), 1.78 (1H, m, H5-anti), 1.60 (1H, m, H6-anti), 0.96 (9H, d, *J*<sub>PC</sub> = 8.41, PMe<sub>3</sub>). <sup>13</sup>C NMR (acetone-*d*<sub>6</sub>, δ, 25 °C): δ ppm 159.4 (thiophene-C4'), 149.7 (Tp3A), 143.7 (Tp3B), 141.3 (Tp3C), 137.5 (Tp3/5), 136.8 (Tp3/5), 136.4 (Tp5A), 127.4 (thiophene), 123.9 (thiophene), 123.4 (thiophene), 107.3 (Tp4B), 106.9 (Tp4C), 105.3 (Tp4A), 86.2 (C4), 59.9 (C2, d, *J*<sub>PC</sub> = 11.1), 55.6 (C3), 55.4 (-OMe), 41.3 (C1, d, *J*<sub>PC</sub> = 4.1), 36.3 (C6), 28.2 (buried-solvent-C5), 13.4 (d, *J*<sub>CP</sub> = 28.0, PMe<sub>3</sub>).

### Synthesis of WTp(NO)(PMe<sub>3</sub>)(η<sup>2</sup>-5,6-(1R,4R)-4,4'-dimethoxy-1,2,3,4-tetrahydro-1,1'-biphenyl) (**26**)

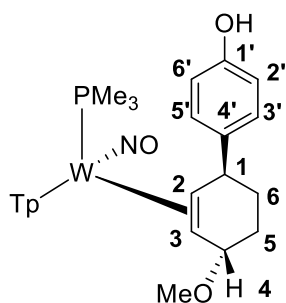


A solution of **16** (0.707 g, 0.812 mmol) was added to a 4-dram vial along with MeOH (5 mL). The reaction mixture was allowed to cool to -30 °C over the course of 20 min. To this chilled solution NaBH<sub>4</sub> (0.163 g, 4.31 mmol) was added. Upon addition bubbling is observed to occur (CAUTION! Evolution of H<sub>2(g)</sub>). The reaction mixture was allowed to sit at -30 °C for 5 min before the reaction mixture was allowed to sit at room temperature for 10 min. The reaction mixture was then added dropwise to a 40 mL solution of DI water in an Erlenmeyer flask. Upon addition a beige-white solid precipitates from solution. This reaction mixture was then filtered through a fine 15 mL porosity fritted disc and washed with DI water (1 x 10 mL) and vacuum was

applied to marginally dry the resulting off-white solid. Next the solid was washed with pentane (3 x 10 mL) and allowed to desiccate under dynamic vacuum over a course of 4 h before a mass was taken of the resulting off-white solid (0.374 g, 63.8 %).

CV (DMA):  $E_{p,a} = +0.36$  V (NHE). IR,  $\nu(\text{BH}) = 2483$   $\text{cm}^{-1}$ ,  $\nu(\text{NO}) = 1546$   $\text{cm}^{-1}$ .  $^1\text{H}$  NMR (acetone- $d_6$ ,  $\delta$ , 25  $^\circ\text{C}$ ): 8.85 (1H, d, Tp3A), 8.13 (1H, d, Tp3B), 7.93 (1H, d, Tp5C), 7.89 (1H, d, Tp5B), 7.68 (1H, d, Tp5A), 7.45 (2H, m, Anisole-3'/5'), 7.43 (1H, d, Tp3C), 6.93 (2H, m, Anisole-2'/6'), 6.38 (1H, t, Tp4B), 6.31 (1H, t, Tp4C), 6.12 (1H, t, Tp4A), 5.35 (1H, s, H4), 4.15 (1H, m, H1), 3.79 (3H, s, Anisole-OMe), 3.04 (1H, m, H2), 3.01 (3H, s, -OMe), 2.07 (1H, buried, H5-syn), 2.00 (1H, m, H6-syn), 1.90 (1H, dd,  $J = 5.2, 11.7$ , H3), 1.72 (1H, m, H5-anti), 1.38 (1H, m, H6-anti), 0.86 (9H, d,  $J_{\text{PC}} = 8.20$ ,  $\text{PMe}_3$ ).  $^{13}\text{C}$  NMR (acetone- $d_6$ ,  $\delta$ , 25  $^\circ\text{C}$ ):  $\delta$  ppm 158.5 (Anisole-C1'), 149.8 (Tp3A), 146.3 (Anisole-C4'), 143.6 (Tp3B), 141.3 (Tp3C), 137.5 (Tp5C), 136.7 (Tp5B), 136.4 (Tp5A), 129.7 (Anisole-3'/5'), 114.6 (Anisole-2'/6'), 107.2 (Tp4B), 106.8 (Tp4C), 105.2 (Tp4A), 87.4 (C1), 59.1 (C2, d,  $J_{\text{PC}} = 12.3$ ), 56.6 (C3), 55.4 (-OMe), 55.3 (-OMe), 45.2 (C1, d,  $J_{\text{PC}} = 4.10$ ), 37.9 (C6), 29.7 (C5), 13.6 (d,  $J_{\text{CP}} = 27.5$ ,  $\text{PMe}_3$ ).

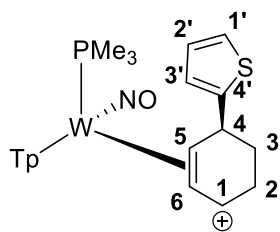
### Synthesis of $\text{WTP}(\text{NO})(\text{PMe}_3)(\eta^2\text{-2,3-(1'R,4'R)-4'-methoxy-1',2',3',4'-tetrahydro-[1,1'-biphenyl]-4-ol})$ (27)



A solution of **17** (0.450 g, 0.812 mmol) was added to a 4-dram vial along with MeOH (5 mL). The reaction mixture was allowed to cool to -30  $^\circ\text{C}$  over the course of 20 min. To this chilled solution  $\text{NaBH}_4$  (0.069 g, 1.82 mmol) was added. Upon addition bubbling is observed to occur (CAUTION! Evolution of  $\text{H}_{2(\text{g})}$ ). The reaction mixture was allowed to sit at -30  $^\circ\text{C}$  for 3.5 h before the reaction mixture was allowed to sit at room temperature for 3 min. To the reaction mixture 20 mL solution of DI water was added. Upon addition of water to the reaction mixture, a beige-white solid precipitates from solution. This reaction mixture was then filtered through a fine 15 mL porosity fritted disc and washed with DI water (1 x 10 mL) and vacuum was applied to marginally dry the resulting off-white solid. Next the solid was washed with pentane (2 x 20 mL) and allowed to desiccate under dynamic vacuum over a course of 4 h before a mass was taken of the resulting off-white solid (0.232 g, 62.4 %).

CV (DMA):  $E_{p,a} = +0.38$  V (NHE). IR,  $\nu(\text{BH}) = 2485$   $\text{cm}^{-1}$ ,  $\nu(\text{NO}) = 1547$   $\text{cm}^{-1}$ .  $^1\text{H}$  NMR (acetone- $d_6$ ,  $\delta$ , 25  $^\circ\text{C}$ ): 8.85 (1H, d, Tp3A), 8.13 (1H, d, Tp3B), 7.93 (1H, d, Tp5C), 7.89 (1H, d, Tp5B), 7.68 (1H, d, Tp5A), 7.43 (1H, d, Tp3C), 7.35 (2H, m, Phenol-3'/5'), 6.84 (2H, m, Anisole-2'/6'), 6.37 (1H, t, Tp4B), 6.31 (1H, t, Tp4C), 6.12 (1H, t, Tp4A), 5.35 (1H, s, H4), 4.13 (1H, m, H1), 3.05 (1H, m, H2), 3.02 (3H, s, -OMe), 2.06 (1H, buried, H5-syn), 1.98 (1H, m, H6-syn), 1.90 (1H, dd,  $J = 4.8, 11.7$ , H3), 1.72 (1H, m, H5-anti), 1.38 (1H, m, H6-anti), 0.86 (9H, d,  $J_{\text{PC}} = 8.40$ ,  $\text{PMe}_3$ ).  $^{13}\text{C}$  NMR (acetone- $d_6$ ,  $\delta$ , 25  $^\circ\text{C}$ ):  $\delta$  ppm 155.9 (Phenol-C1'), 149.8 (Tp3A), 145.1 (Phenol-C4'), 143.6 (Tp3B), 141.3 (Tp3C), 137.5 (Tp5C), 136.7 (Tp5B), 136.4 (Tp5A), 129.7 (Phenol-3'/5'), 116.0 (Phenol-2'/6'), 107.2 (Tp4B), 106.8 (Tp4C), 105.2 (Tp4A), 87.5 (C4), 59.2 (C2, d,  $J_{\text{PC}} = 11.8$ ), 56.7 (C3), 55.3 (-OMe), 45.2 (C1, d,  $J_{\text{PC}} = 4.2$ ), 38.1 (C6), 28.9 (buried-solvent-C5), 13.6 (d,  $J_{\text{CP}} = 27.2$ ,  $\text{PMe}_3$ ).

### Synthesis of $\text{WTP}(\text{NO})(\text{PMe}_3)(\eta^2\text{-5,6-(-4-(thiophen-2-yl)cyclohex-2-en-1-yl)ium})$ (28)

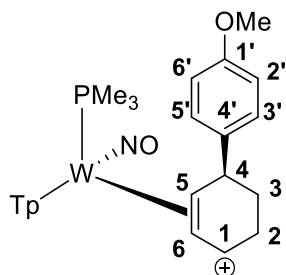


To an oven dried 4-dram vial added **25** (0.202 g, 0.290 mmol) along with MeCN (~ 1 mL). This solution was allowed to cooled to -30 °C before a -30 °C solution of pre-chilled HOTf (0.152 g, 1.01 mmol) was added to the reaction mixture. Upon addition the initially off-white reaction mixture turns to a homogeneous red solution. This solution was allowed to sit at ambient temperatures for 2 min before room temperature Et<sub>2</sub>O (15 mL) was added to the 4-dram vial to induce precipitation. The reaction mixture was then stored at -30 °C over the course of 3 days and during this time a yellow crystalline material had developed on the sides of the 4-dram vial. The organic layers was decanted, the vial was dried with an N<sub>2(g)</sub> stream before a mass was taken of the light yellow solid (0.195 g, 82.6%).

CV (DMA):  $E_{p,c} = -1.05$  V (NHE). <sup>1</sup>H NMR (MeCN-*d*<sub>3</sub>, δ, 25 °C): 8.41 (1H, d, Tp3/5), 8.13 (1H, d, Tp3/5), 8.01 (1H, d, Tp3/5), 7.96 (1H, d, Tp3/5), 7.94 (1H, d, Tp3/5), 7.82 (1H, d, Tp3/5), 7.34 (1H, dd,  $J = 1.1, 5.2$ , thiophene-H1'), 7.10 (1H, m, thiophene 3), 7.04 (1H, dd,  $J = 1.1, 5.04$ , thiophene-H2'), 6.64 (1H, broad t,  $J = 6.41$ , H1), 6.53 (1H, t, Tp4), 6.51 (1H, t, Tp4), 6.34 (1H, t, Tp4), 5.37 (1H, t,  $J = 7.43$ , H6), 4.36 (1H, dd,  $J = 1.74, 7.43$ , H5), 4.10 (1H, m, H4), 3.44 (1H, buried, H2), 3.31 (1H, m H2'), 1.91 (1H, m, H3), 1.42 (1H, m, H3'), 1.09 (9H, d,  $J_{PH} = 9.8$ , PMe<sub>3</sub>).

<sup>1</sup>H NMR (acetone-*d*<sub>6</sub>, δ, 25 °C): 8.62 (1H, d, Tp3/5), 8.37 (1H, d, Tp3/5), 8.36 (1H, d, Tp3/5), 8.22 (1H, d, Tp3/5), 8.17 (1H, d, Tp3/5), 7.99 (1H, d, Tp3/5), 7.41 (1H, dd,  $J = 1.1, 5.2$ , thiophene-H1'), 7.21 (1H, m, thiophene 3), 7.06 (1H, dd,  $J = 1.1, 5.04$ , thiophene-H2'), 6.86 (1H, broad t,  $J = 6.41$ , H1), 6.65 (1H, t, Tp4), 6.62 (1H, t, Tp4), 6.43 (1H, t, Tp4), 5.55 (1H, t,  $J = 7.43$ , H6), 4.64 (1H, dd,  $J = 1.74, 7.43$ , H5), 4.21 (1H, m, H4), 3.56 (1H, m, H2), 3.42 (1H, m H2'), 1.98 (1H, m, H3), 1.48 (1H, m, H3'), 1.26 (9H, d,  $J_{PH} = 9.90$ , PMe<sub>3</sub>). <sup>13</sup>C NMR (acetone-*d*<sub>6</sub>, δ, 25 °C): 153.6 (thiophene-C4'), 149.4 (Tp3/5), 146.4 (Tp3/5), 143.7 (Tp3/5), 139.7 (C4), 139.6 (Tp3/5), 139.5 (Tp3/5), 136.7 (C1), 127.9 (thiophene-C2'), 125.1 (thiophene-C3'), 124.9 (thiophene-C1'), 109.6 (Tp4), 109.1 (Tp4), 108.2 (Tp4), 103.7 (C6, d,  $J_{PC} = 3.5$ ), 74.5 (C5, d,  $J_{PC} = 12.9$ ), 40.0 (C4, d,  $J_{PC} = 4.0$ ), 32.0 (C2), 25.9 (C3), 13.6 (d,  $J_{CP} = 32.6$ , PMe<sub>3</sub>). 158.2 (thiophene-C4'), 144.4 (Tp3/5), 142.9 (Tp3/5), 141.7 (Tp3/5), 138.1 (Tp3/5), 137.8 (Tp3/5), 137.6 (Tp3/5), 128.1 (-CN), 127.7 (thiophene-C2'), 124.8 (thiophene-C3'), 124.0 (thiophene-C1'),

#### Synthesis of WTp(NO)(PMe<sub>3</sub>)(η<sup>2</sup>-5,6-(-4'-methoxy-1,2,3,4-tetrahydro-[1,1'-biphenyl]-4-ylum) (**29**)



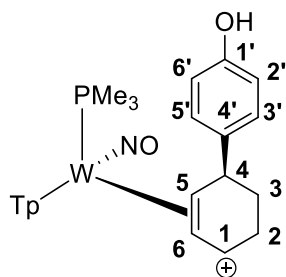
To an oven dried 4-dram vial added **26** (0.350 g, 0.485 mmol) along with anhydrous DME (~ 2 mL). This heterogeneous white solution was cooled to -30 °C over the course of 10 min. To this solution was added a solution of -30 °C chilled HOTf (0.130 g, 0.867 mmol). Upon addition the reaction mixture turns to a homogeneous red color within 1 minute of addition of HOTf. After shaking by hand to insure homogeneity,

the homogeneous red reaction mixture was added to a solution of standing Et<sub>2</sub>O (~ 10mL). Upon addition a red solid “gums” up and sticks to the side of the vial. The organic layer was decanted and the red film layer was redissolved in a minimal amount of DCM (2 mL) and this homogeneous red solution was added to another 20 mL of standing Et<sub>2</sub>O to generate a light yellow solid. The resulting heterogeneous reaction mixture was filtered through a fine 15 mL fritted disc and the resulting pale yellow solid was washed with Et<sub>2</sub>O (3 x 10 mL) and allowed to desiccate under static vacuum for 16 h before a mass was taken of the resulting solid the next day of the pale yellow solid (0.304 g, 74.5%).

CV (DMA):  $E_{p,c} = -0.93$  V (NHE). IR,  $\nu(\text{BH}) = 2519$  cm<sup>-1</sup>,  $\nu(\text{NO}) = 1635$  cm<sup>-1</sup>. <sup>1</sup>H NMR (MeCN-*d*<sub>3</sub>,  $\delta$ , 25 °C): 8.42 (1H, d, Tp3B), 8.15 (1H, d, Tp3A), 8.00 (1H, d, Tp5C), 7.95 (1H, d, Tp5B), 7.92 (1H, d, Tp3C), 7.82 (1H, d, Tp5A), 7.35 (2H, m, Anisole-H3'/H5'), 6.97 (2H, m, Anisole-H2'/H6'), 6.54 (1H, t,  $J = 6.73$ , H1), 6.52 (1H, t, Tp4B), 6.50 (1H, t, Tp4C), 6.35 (1H, t, Tp4A), 5.39 (1H, t,  $J = 7.40$ , H6), 4.36 (1H, dd,  $J = 7.40$ , 16.1, H5), 3.80 (3H, s, anisole-OMe), 3.72 (1H, dd,  $J = 6.31$ , 10.94, H4), 3.50 (1H, m H2-syn), 3.31 (1H, m, H2-anti), 1.77 (1H, m, H3-syn), 1.22 (1H, m, H3-anti), 1.01 (9H, d,  $J_{\text{PH}} = 10.0$ , PMe<sub>3</sub>). <sup>13</sup>C NMR (acetone-*d*<sub>3</sub>,  $\delta$ , 25 °C): 159.6 (Anisole-C1), 149.2 (Tp3A), 146.2 (Tp3/5), 143.4 (Tp3/5), 141.6 (C4), 139.6 (Tp3/5), 139.5 (Tp3/5), 134.4 (Anisole-C1), 129.5 (Anisole-C3/C5), 115.2 (Anisole-C2/C6), 109.6 (Tp4), 108.9 (Tp4), 108.1 (Tp4), 105.5 (C6, d,  $J_{\text{PC}} = 4.2$ ), 75.4 (C5, d,  $J_{\text{PC}} = 12.2$ ), 56.0 (Anisole-OMe), 44.5 (C4, d,  $J_{\text{PC}} = 4.0$ ), 32.2 (C2), 26.2 (C3), 13.8 (d,  $J_{\text{CP}} = 32.9$ , PMe<sub>3</sub>).

### Synthesis of WTp(NO)(PMe<sub>3</sub>)( $\eta^2$ -5,6-*4'*-hydroxy-1,2,3,4-tetrahydro-[1,1'-biphenyl]-4-ylium) (30)

#### 13-JAS-77

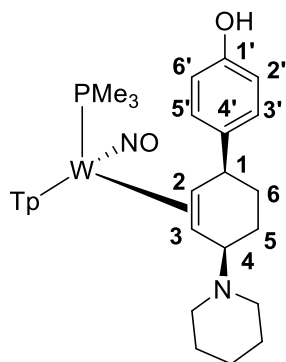


To an oven dried 4-dram vial added **27** (0.188 g, 0.266 mmol) along with anhydrous DME (~ 1 mL). This heterogeneous white solution was cooled to -30 °C over the course of 10 min. To this solution was added a solution of -30 °C chilled HOTf in excess (10 drops). Upon addition the reaction mixture turns to a homogeneous red color within 1 minute of addition of HOTf. The resulting acidic solution was allowed to stand at -30 °C over the course of 10 min. This solution was then added to a solution of standing Et<sub>2</sub>O (10 mL). Upon addition a light yellow solid precipitates from solution. This heterogeneous, light yellow solution was allowed to sit at -30 °C for approximately 20 min to induce further precipitation. The resulting heterogeneous yellow reaction mixture was then filtered through a fine 15 mL porosity fritted disc and washed with Et<sub>2</sub>O (2 x 10 mL) before the resulting pale yellow solid was allowed to desiccate for 16 h under static vacuum before a mass was taken of the light yellow solid (0.161 g, 73.2 %).

<sup>1</sup>H NMR (MeCN-*d*<sub>3</sub>,  $\delta$ , 25 °C): 8.41 (1H, d, Tp3B), 8.15 (1H, d, Tp3A), 8.00 (1H, d, Tp5C), 7.95 (1H, d, Tp5B), 7.92 (1H, d, Tp3C), 7.82 (1H, d, Tp5A), 7.25 (2H, m, Phenol-H3'/H5'), 6.85 (2H, m, Anisole-H2'/H6'), 6.53 (1H, buried, H1), 6.52 (1H, t, Tp4B), 6.50 (1H, t, Tp4C), 6.35 (1H, t, Tp4A), 5.37 (1H, t,  $J = 7.16$ , H6), 4.35 (1H, dd,  $J = 7.40$ , 16.1, H5), 3.69 (1H, dd,  $J = 6.24$ , 10.95, H4), 3.49 (1H, m, H2-syn), 3.30 (1H, dt,  $J = 6.23$ , 19.53, H2-anti), 1.76 (1H, m, H3-syn), 1.21 (1H, m, H3-anti), 1.00 (9H, d,  $J_{\text{PH}} = 9.85$ , PMe<sub>3</sub>). <sup>13</sup>C NMR (MeCN-*d*<sub>3</sub>,  $\delta$ , 25 °C): 156.7 (Phenol-C1), 149.3 (Tp3A), 146.2 (Tp3B), 143.4 (Tp3/5), 140.7 (Tp3/5), 139.6 to 139.5 (3C, 2 overlapping Tp3/5 and Phenol-C4), 134.4 (C1), 129.5 (Phenol-C3/C5), 116.5 (Phenol-C2/C6), 109.5 (Tp4), 108.9 (Tp4), 108.1 (Tp4), 105.5 (C6), 75.6 (C5, d,  $J_{\text{PC}} = 12.2$ ), 44.6 (C4, d,  $J_{\text{PC}} = 3.9$ ),

32.2 (C2), 26.2 (C3), 13.8 (d,  $J_{CP} = 33.0$ ,  $\text{PMe}_3$ ). ESI-MS ( $m/z$ , calculated (rel intens, %), **observed** (rel intens, %), ppm,  $(M + H)^+$ : 674.1935 (83.10), **674.1936 (82.40)**, 675.1960 (80.48), **675.1960 (80.95)**, 676.1959 (100), **676.1962 (100)**, 677.2000 (44.49), **677.2002 (44.03)**, 678.1992 (83.53), **678.1993 (83.14)**.

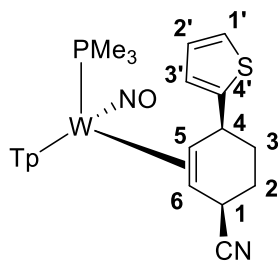
### Synthesis of $\text{WTp}(\text{NO})(\text{PMe}_3)(\eta^2\text{-2,3-(1'S,4'R)-4'-(piperidin-1-yl)-1',2',3',4'-tetrahydro-[1,1'-biphenyl]-4-ol})$ (**31**)



Cooled a solution of **28** (NMR scale, ~ 20 mgs) in  $\text{MeCN-}d_3$  (~1/2 mL) to  $-30\text{ }^\circ\text{C}$  over a period of 10 min in an NMR tube. To this solution added an excess of piperidine (0.117 g, x mmol) that had been frozen. This reaction mixture was allowed to sit at  $-30\text{ }^\circ\text{C}$  for 16 h. The next day this solution was analyzed by  $^1\text{H}$  NMR and partial characterization is included below.

$^1\text{H}$  NMR ( $\text{MeCN-}d_3$ ,  $\delta$ ,  $25\text{ }^\circ\text{C}$ ): 8.54 (1H, d, Tp3/5), 8.14 (1H, d, Tp3/5), 7.90 (1H, d, Tp3/5), 7.84 (1H, d, Tp3/5), 7.76 (1H, d, Tp3/5), 7.42 (2H, m, Anisole- $\text{H3}'/\text{H5}'$ ), 7.36 (1H, d, Tp3/5), 6.74 (2H, m, anisole  $2\text{H}'/6\text{H}'$ ), 6.42 (1H, t, Tp4), 6.25 (1H, t, Tp4), 6.22 (1H, t, Tp4), 4.43 (1H, broad m, cyclohexene H), 4.04 (1H, d,  $J = 3.8$ , cyclohexene-H), 2.25 (1H, m, cyclohexene-H), 1.01 (9H, d,  $J_{\text{PH}} = 8.12$ ,  $\text{PMe}_3$ ).

### Synthesis of $\text{WTp}(\text{NO})(\text{PMe}_3)(\eta^2\text{-2,3(1R,4S)-4-(thiophen-2-yl)cyclohex-2-ene-1-carbonitrilecarbonitrile})$ (**32**)

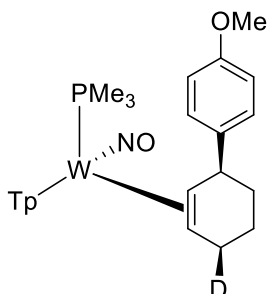


Cooled a solution of **28** (NMR scale, ~ 20 mgs) in  $\text{MeCN-}d_3$  to  $-30\text{ }^\circ\text{C}$  over a period of 10 min in an NMR tube. To this solution added an excess of NaCN (0.030 g, x mmol) that had been pre-chilled to  $-30\text{ }^\circ\text{C}$  and let the reaction mixture sit at  $-30\text{ }^\circ\text{C}$  for 18 h. The next day this solution was analyzed by 2D NMR spectroscopy and characterization is provided below.

$^1\text{H}$  NMR ( $\text{MeCN-}d_3$ ,  $\delta$ ,  $25\text{ }^\circ\text{C}$ ): 8.09 (1H, d, Tp3A), 8.05 (1H, d, Tp3B), 7.88 (1H, d, Tp5B), 7.85 (1H, d, Tp5C), 7.83 (1H, d, Tp5A), 7.32 (1H, d, Tp3C), 7.29 (1H, dd,  $J = 1.10, 5.12$ , thiophene- $\text{H2}'$ ), 7.16 (1H, dm, thiophene- $\text{H3}'$ ), 7.04 (1H, dd,  $J = 3.52, 5.10$ , thiophene- $\text{H2}'$ ), 6.39 (1H, t, Tp4B), 6.34 (1H, t, Tp4A), 6.26 (1H, t, Tp4C), 4.42 (1H, t,  $J = 5.9$ , H1), 4.08 (1H, broad s, H4), 2.78 (1H, t,  $J = 12.3$ , H2), 2.09 (1H, buried, H6-endo), 1.95 (1H, buried m, H5-endo), 1.79 (1H, m, H5-exo), 1.67 (1H, m, H6-exo), 1.30 (1H, m, H3), 1.01 (9H, d,  $J_{\text{PH}} = 8.58$ ,  $\text{PMe}_3$ ).  $^{31}\text{P}$  NMR ( $\text{MeCN-}d_3$ ,  $\delta$ ,  $25\text{ }^\circ\text{C}$ ):  $J_{\text{WP}} = 286$ .  $^{13}\text{C}$  NMR ( $\text{MeCN-}d_3$ ,  $\delta$ ,  $25\text{ }^\circ\text{C}$ ): 158.2

(thiophene-C4'), 144.4 (Tp3/5), 142.9 (Tp3/5), 141.7 (Tp3/5), 138.1 (Tp3/5), 137.8 (Tp3/5), 137.6 (Tp3/5), 128.1 (-CN), 127.7 (thiophene-C2'), 124.8 (thiophene-C3'), 124.0 (thiophene-C1'), 107.8 (Tp4), 107.4 (Tp4), 107.0 (Tp4), 55.9 (C2, d,  $J_{PC} = 11.1$ ), 52.3 (C3), 41.1 (C1, d,  $J_{PC} = 4.7$ ), 33.1 (C6), 31.5 (C4), 25.0 (C5), 13.6 (d,  $J_{CP} = 28.7$ ,  $\text{PMe}_3$ ).

### Synthesis of $\text{W}(\text{NO})(\text{PMe}_3)(\eta^2\text{-2,3-1',2',3',4'-tetrahydro-[1,1'-biphenyl]-4'-d-4-ol})$ (**39**)

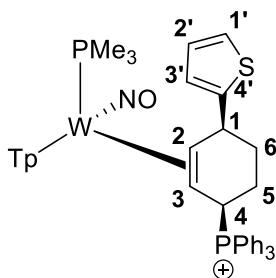


Dissolved a solution of **29** (0.194 g, 0.0281 mmol) in MeOH (1 mL) and cooled this solution to  $-50\text{ }^\circ\text{C}$  in a large test tube with a stir pea. To this solution was added  $\text{NaBD}_4$  (0.064 g, 1.54 mmol) and this reaction mixture was allowed to stir for 5 min at  $-50\text{ }^\circ\text{C}$ . This solution was then added to a solution of stirring DI water (7 mL) and upon addition an off-white solid precipitates from solution. This solid was collected on a fine 15 mL fritted disc and vacuum was applied to remove residual water. The resulting off-grey solid was then washed with pentane (3 x 10 mL) and allowed to dry before a mass was taken of the off-white solid (0.054 g, 28.0%).

$^1\text{H}$  NMR ( $\text{MeCN-}d_3$ ,  $\delta$ ,  $25\text{ }^\circ\text{C}$ ): 8.22 (1H, d, Tp3/5), 8.05 (1H, d, Tp3/5), 7.85 (1H, d, Tp3/5), 7.80 (1H, d, Tp3/5), 7.78 (1H, d, Tp3/5), 7.52 (2H, m, Anisole-H3'/H5'), 7.27 (1H, d, Tp3/5), 6.93 (2H, m, anisole 2H'/6H'), 6.38 (1H, t, Tp4), 6.29 (1H, t, Tp4), 6.19 (1H, t, Tp4), 4.07 (1H, broad t,  $J = 6.00$ , H1), 3.79 (Anisole-OMe), 2.99 (1H, broad s, H4-endo), 2.76 (1H, t,  $J = 12.02$ , H2), 2.02 (1H, m, H6), 1.52 (1H, m, H5), 1.45 (2H, overlapping, H3 and H5'), 1.32 (1H, m, H6'), 0.96 (9H, d,  $J_{PH} = 8.23$ ,  $\text{PMe}_3$ ).  $^{13}\text{C}$  NMR ( $\text{MeCN-}d_3$ ,  $\delta$ ,  $25\text{ }^\circ\text{C}$ ): 157.5 (Anisole-C1'), 145.7 (Anisole-C4'), 143.1 (Tp3/5), 142.2 (Tp3/5), 140.6 (Tp3/5), 136.7 (Tp3/5), 136.2 (Tp3/5), 136.0 (Tp3/5), 129.3 (Anisole-C3'/C5'), 113.4 (Anisole-C2'/C6'), 106.5 (Tp4), 105.9 (Tp4), 105.6 (Tp4), 57.7 (C2, d,  $J_{PC} = 9.7$ ), 54.8 (Anisole-OMe), 52.6 (C3), 45.2 (C1), 34.5 (C6), 29.9 (C4,  $J_{CD} = 19.1$ ), 20.3 (C5), 12.9 (d,  $J_{CP} = 28.1$ ,  $\text{PMe}_3$ ).

### Synthesis of $\text{W}(\text{NO})(\text{PMe}_3)(\eta^2\text{-2,3-(S)-4-(thiophen-2-yl)-1-(triphenyl-14-phosphaneyl)cyclohex-2-en-1-ylum})$ (**34**)

To a solution of **28** (NMR scale,  $\sim 20$  mgs) in  $\text{MeCN-}d_3$  added an excess of  $\text{PPh}_3$  and over the course of an hour let homogeneous red reaction mixture sit at room temperature in an inert atmosphere glovebox. The resulting mixture was evaluated by  $^1\text{H}$  and  $^{31}\text{P}$  NMR and partial characterization with these techniques is provided. No mass recovery was attempted.



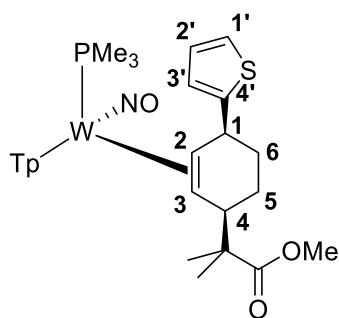
$^1\text{H}$  NMR ( $\text{MeCN-}d_3$ ,  $\delta$ ,  $25\text{ }^\circ\text{C}$ ): 8.15 (1H, d, Tp3/5), 8.05 (1H, d, Tp3/5), 8.01 (1H, d, Tp3/5), 7.88 (1H, d, Tp3/5), 7.79 (1H, d, Tp3/5), 7.65 (3H, t,  $J = 7.4$ ,  $\text{PPh}_3$ ), 7.43 to 7.50 (12H, overlapping m,  $\text{PPh}_3$ ), 7.13 (1H, d,



Tp3/5), 7.18 (1H, buried m, thiophene), 6.92 (1H, dd,  $J = 1.42, 3.65$ , thiophene), 6.80 (1H, d,  $J = 3.65$ , thiophene), 6.45 (1H, t, Tp4), 6.36 (1H, t, Tp4), 6.06 (1H, t, Tp4), 4.87 (1H, m, cyclohexyl-H), 4.31 (1H, m, cyclohexyl-H), 3.01 (1H, m, cyclohexyl-H), 2.34 (2H, overlapping m, cyclohexyl-Hs), 1.57 (1H, m, cyclohexyl-H), 1.07 (1H, dd,  $J = 10.9, 19.8$ , cyclohexyl-H), 0.97 (9H, d,  $J_{\text{PH}} = 8.92$ ,  $\text{PMe}_3$ ), 0.74 (1H, dq,  $J = 3.1, 13.4$ , cyclohexyl-H).  $^{31}\text{P}$  NMR ( $\text{MeCN-}d_3$ ,  $\delta$ , 25 °C): -12.7 ( $\text{PMe}_3$ ),

### Synthesis of $\text{WTP}(\text{NO})(\text{PMe}_3)(\eta^2\text{-2,3-methyl 2-methyl-2-}((1\text{R},4\text{S})\text{-4-(thiophen-2-yl)cyclohex-2-en-1-yl)propanoate)$ (35)

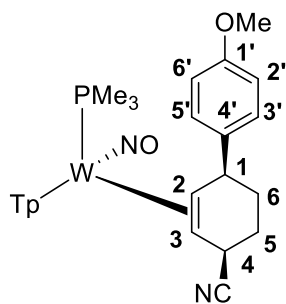
Cooled a solution of **28** (NMR scale, ~ 20 mgs) in  $\text{MeCN-}d_3$  to -30 °C over a period of 10 min in an NMR tube. To this solution added an excess of MTDA (5 drops) that had been pre-chilled to -30 °C and let the reaction mixture sit at -30 °C for 18 h. The next day this solution was analyzed by 1H NMR and partial characterization is included below.



$^1\text{H}$  NMR ( $\text{MeCN-}d_3$ ,  $\delta$ , 0 °C): 8.25 (1H, d, Tp3/5), 8.05 (3H, overlapping d, Tp3/5), 7.96 (1H, d, Tp3/5), 7.55 (1H, d, Tp3/5), 7.34 (1H, dd,  $J = 1.13, 5.1$ , thiophene), 7.23 (1H, broad m, thiophene), 7.08 (1H, dd,  $J = 3.46, 5.10$ , thiophene), 6.50 (2H, overlapping t, Tp4s), 6.42 (1H, t, Tp4), 4.49 (1H, broad s, cyclohexyl-H), 4.17 (1H, t,  $J = 14.2$ , cyclohexyl-H), 3.65 (1H, broad m, cyclohexyl-H), 3.43 (3H, s, -OMe), 2.00 (1H, m, cyclohexyl-H), 1.89 (1H, d,  $J = 11.8$ , cyclohexyl-H), 1.67 (1H, m, cyclohexyl-H), 1.17 (9H, d,  $J_{\text{PH}} = 9.12$ ,  $\text{PMe}_3$ ), 0.98 (3H, s, -Me), 0.85 (3H, s, -Me)

### Synthesis of $\text{WTP}(\text{NO})(\text{PMe}_3)(\eta^2\text{-2,3-(4'-methoxy-1,2,3,4-tetrahydro-[1,1'-biphenyl]-4-carbonitrile)}$ (36)

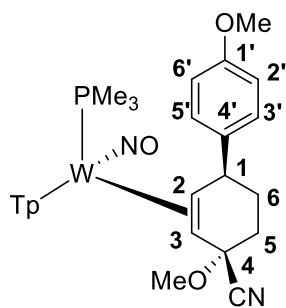
Cooled a solution of NaCN (~ 0.030 g) in  $\text{MeCN-}d_3$  to -30 °C over a period of 10 min in a 4 dram vial. To this solution added **29** (~ 0.020 g) and let the reaction mixture sit at -30 °C for 16 h. The next day an aliquot of this solution (a turquoise color) was analyzed by NMR spectroscopy.



$^1\text{H}$  NMR (MeCN- $d_3$ ,  $\delta$ , 25 °C): 8.07 (1H, d, Tp3A), 8.05 (1H, d, Tp3B), 7.87 (1H, d, Tp5B), 7.85 (1H, d, Tp5C), 7.83 (1H, d, Tp5A), 7.53 (2H, m, Anisole-H3'/H5'), 7.30 (1H, d, Tp3C), 6.97 (2H, m, anisole 2H'/6H'), 6.39 (1H, t, Tp4B), 6.34 (1H, t, Tp4A), 6.25 (1H, t, Tp4C), 4.11 (1H, t,  $J = 6.15$ , H1), 4.04 (1H, m, H4), 3.80 (Anisole-OMe), 2.72 (1H, t,  $J = 12.4$ , H2), 2.00 (1H, m, H6-endo), 1.92 (1H, m, H5-endo), 1.70 (1H, m, H5-exo), 1.50 (1H, m, H6-exo), 1.36 (1H, dt,  $J = 2.3, 11.4$ , H3), 0.96 (9H, d,  $J_{\text{PH}} = 8.5$ ,  $\text{PMe}_3$ ).  $^{13}\text{C}$  NMR (MeCN- $d_3$ ,  $\delta$ , 25 °C): 158.8 (Anisole-C1'), 145.5 (Tp3/5), 144.3 (Tp3/5), 143.0 (anisole-C4), 141.7 (Tp3/5), 138.1 (Tp3/5), 137.8 (Tp3/5), 137.5 (Tp3/5), 130.2 (Anisole-C3'/C5'), 128.2 (-CN), 114.6 (Anisole-C2'/C6'), 107.7 (Tp4), 107.3 (Tp4), 107.0 (Tp4), 55.9 (Anisole-OMe), 55.4 (C2, d,  $J_{\text{PC}} = 11.2$ ), 53.3 (C3), 44.9 (C1), 32.7 (C6), 31.6 (C4), 24.6 (C5), 13.7 (d,  $J_{\text{CP}} = 29.3$ ,  $\text{PMe}_3$ ).

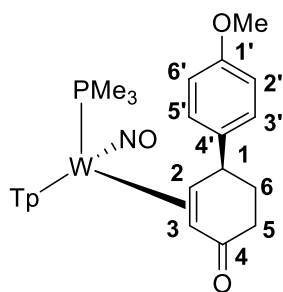
### Synthesis of $\text{WTP}(\text{NO})(\text{PMe}_3)(\eta^2\text{-5,6-(1S,4S)-4,4'-dimethoxy-1,2,3,4-tetrahydro-[1,1'-biphenyl]-4-carbonitrile})$ (37)

To a 4-dram vial added **29** (0.020 g, x mmol) along with acetone- $d_6$  (1/2 mL) and the reaction mixture sit at -30 °C. To another 4-dram vial added NaCN (0.057 g, x mmol), 15-crown-5 ether (0.088 g, x mmol) and acetone- $d_6$  and let this reaction stir at room temperature for 30 min before allowing to cool to -30 °C over a course of 10 min. Proceed to add the acetone- $d_6$  solution of **29** to the NaCN/crown-ether acetone- $d_6$  solution and let the reaction mixture sit at -30 °C over a course of 24 h before analyzing the reaction mixture by  $^1\text{H}$  and  $^{13}\text{C}$  NMR.



$^1\text{H}$  NMR (acetone- $d_6$ ,  $\delta$ , 25 °C): 8.38 (1H, d, Tp3/5), 8.07 (1H, d, Tp3/5), 8.00 (1H, d, Tp3/5), 7.93 (1H, d, Tp3/5), 7.78 (1H, d, Tp3/5), 7.46 (2H, m, Anisole-H3'/H5'), 7.42 (1H, d, Tp3/5), 6.95 (2H, m, anisole 2H'/6H'), 6.41 (1H, t, Tp4), 6.38 (1H, t, Tp4), 6.21 (1H, t, Tp4), 4.07 (1H, broad t,  $J = 8.61$ , H1), 3.79 (Anisole-OMe), 3.09 (1H, m, -cyclohexyl), 2.96 (3H, s, -OMe), 2.34 (1H, m, -cyclohexyl), 2.00 (1H, m, -cyclohexyl), 1.88 (1H, m, -cyclohexyl), 1.85 (1H, d,  $J = 11.8$ , -cyclohexyl), 1.77 (1H, m, -cyclohexyl), 1.25 (1H, m, -cyclohexyl), 0.86 (9H, d,  $J_{\text{PH}} = 8.71$ ,  $\text{PMe}_3$ ).

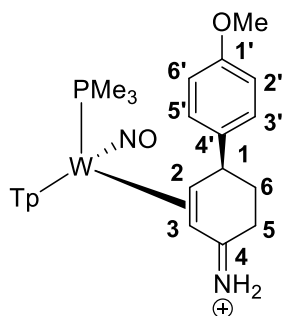
### Synthesis of $\text{WTP}(\text{NO})(\text{PMe}_3)(\eta^2\text{-2,3-(S)-4'-methoxy-2,3-dihydro-[1,1'-biphenyl]-4(1H)-one})$ (38)



Complex **16** (0.048, 0.0552 mmol) was dissolved in acetone- $d_6$  ( $\sim 1/2$  mL) and to this solution was added an excess of tetra-butyl ammonium iodide (0.100 g, 0.271 mmol). The reaction mixture was monitored over a period of 5 days until complete conversion to **38** was observed. Attempts to purify the resulting complex with chromatography (separation of the complex and the excess iodide salt) were unsuccessful. Using one of the tetrabutyl ammonium peaks as an internal standard showed that conversion from **16** to **38** occurred quantitatively (quantitative NMR yield).

$^1\text{H}$  NMR (acetone- $d_6$ ,  $\delta$ , 25 °C): 8.27 (1H, d, Tp3/5), 8.02 (1H, d, Tp3/5), 7.98 (1H, d, Tp3/5), 7.93 (1H, d, Tp3/5), 7.77 (1H, d, Tp3/5), 7.61 (1H, d, Tp3/5), 7.51 (2H, m, Anisole-H3'/H5'), 6.94 (2H, m, anisole 2H'/6H'), 6.48 (1H, t, Tp4), 6.33 (1H, t, Tp4), 6.18 (1H, t, Tp4), 4.10 (1H, broad t,  $J = 6.65$ , H1), 3.80 (Anisole-OMe), 3.26 (1H, dt,  $J = 2.30, 10.98$ , H2), 2.53 (1H, m, H5-syn), 2.40 (1H, m, H6-syn), 2.10 (1H, d,  $J = 9.91$ , H3), 2.08 (1H, buried, H5-anti), 1.72 (1H, m, H6-anti), 1.11 (9H, d,  $J_{\text{PH}} = 8.71$ ,  $\text{PMe}_3$ ).  $^{13}\text{C}$  NMR (acetone- $d_6$ ,  $\delta$ , 25 °C): 208.1 (C=O overlap with solvent, C4), 158.9 (Anisole-C1'), 144.6 (Tp3/5), 144.5 (Anisole-C4'), 144.2 (Tp3/5), 141.9 (Tp3/5), 138.1 (Tp3/5), 137.6 (Tp3/5), 136.8 (Tp3/5), 129.6 (Anisole-C3'/C5'), 114.6 (Anisole-C2'/C6'), 107.8 (Tp4), 107.2 (Tp4), 106.0 (Tp4), 67.8 (C2, d,  $J_{\text{PC}} = 13.7$ ), 59.4 (C3, d,  $J_{\text{PC}} = 3.6$ ), 55.5 (Anisole-OMe), 35.5 (C5), 34.9 (C6), 13.6 (d,  $J_{\text{CP}} = 29.5$ ,  $\text{PMe}_3$ ).

### Synthesis of $\text{WTp}(\text{NO})(\text{PMe}_3)(\eta^2\text{-5,6-4'-methoxy-2,3-dihydro-[1,1'-biphenyl]-4(1\text{H})\text{-iminium})$ (**39**)

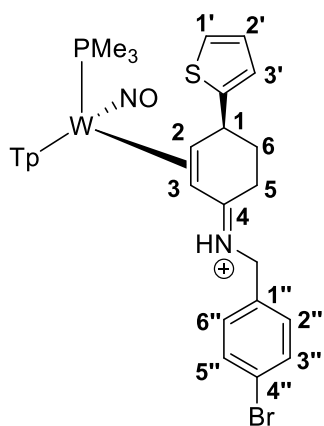


A solution of **16** (0.105 g, 0.121 mmol) in MeOH (2 mL) was chilled to -30 °C over the course of 20 min in a 4-dram vial. To this solution was added 2 mL of a 7 N solution of  $\text{NH}_3/\text{MeOH}$  (approximately 14.0 mmol) and the reaction mixture was allowed to sit at -30 °C over the course of 30 min. The reaction mixture was then allowed to sit at ambient temperature for another 30 min before the solution was added to 200 mL of stirring  $\text{Et}_2\text{O}$ . The resulting reaction mixture was allowed to sit at -30 °C to induce precipitation over a period of 16 hr. The next day a fine yellow-white crystalline solid had developed in solution and this was filtered through a fine 15 mL porosity fritted disc. The resulting light yellow solid was then washed with  $\text{Et}_2\text{O}$  (2 x 10 mL) and allowed to dry over a period of 24 hours under static vacuum in a desiccator before a mass was taken (0.072g, 70.0 %). Crystals suitable for X-Ray diffraction were grown by allowing the resulting filtrate to sit at reduced temperatures.

CV (DMA): pseudo $E_{1,2} = -1.76$  V,  $E_{\text{p,a}} = +1.19$  V (NHE). IR,  $\nu(\text{BH}) = 2490$   $\text{cm}^{-1}$ ,  $\nu(\text{NO}) = 1578$   $\text{cm}^{-1}$ ,  $\nu(\text{iminium}) = 1543$   $\text{cm}^{-1}$ .  $^1\text{H}$  NMR ( $\text{MeCN-}d_3$ ,  $\delta$ , 25 °C): 8.13 (1H, d, Tp3/5), 8.07 (1H, broad s, NH proton),

7.97 (1H, d, Tp3/5), 7.94 (1H, d, Tp3/5), 7.87 (1H, d, Tp3/5), 7.62 (1H, broad s, NH proton), 7.61 (1H, d, Tp3/5), 7.44 (2H, m, Anisole-H3'/H5'), 7.43 (1H, d, Tp3/5), 6.96 (2H, m, anisole 2H'/6H'), 6.45 (1H, t, Tp4), 6.40 (1H, t, Tp4), 6.32 (1H, t, Tp4), 4.19 (1H, m, H1), 3.80 (3H, s, Anisole-OMe), 3.66 (1H, m, H2), 2.82 (1H, m, H5), 2.57 (1H, dt,  $J = 4.80, 17.16$ , H5'), 2.50 (1H, d,  $J = 8.73$ , H3), 2.19 (1H, m, H6), 1.69 (1H, m, H6'), 1.00 (9H, d,  $J_{PH} = 8.96$ , PMe<sub>3</sub>). <sup>13</sup>C NMR (MeCN-*d*<sub>3</sub>δ, 25 °C): 192.8 (iminium, C4), 159.3 (Anisole-C1'), 145.4 (Tp3/5), 143.7 (Tp3/5), 142.7 (Anisole-C4'), 142.2 (Tp3/5), 139.0 (Tp3/5), 138.7 (Tp3/5), 138.5 (Tp3/5), 129.7 (Anisole-C3'/C5'), 115.1 (Anisole-C2'/C6'), 108.5 (Tp4), 108.0 (Tp4), 107.8 (Tp4), 72.3 (C2, d,  $J_{PC} = 14.0$ ), 56.6 (C3 or Anisole-OMe), 55.9 (C3 or Anisole-OMe), 36.0 (C5), 29.1 (C6), 13.9 (d,  $J_{CP} = 30.6$ , PMe<sub>3</sub>). <sup>31</sup>P NMR (MeCN-*d*<sub>3</sub>, δ, 25 °C): **-12.43** ( $J_{WP} = 285$ ). ESI-MS (m/z, calculated (rel intens, %), **observed** (rel intens, %), ppm, (M + H)<sup>+</sup>: 703.2200 (82.37), **703.2199 (80.73)**, 704.2225 (80.75), **704.2225 (79.97)**, 705.2224 (100), **705.2224 (100)**, 706.2264 (45.44), **706.2264 (45.00)**, 707.2256 (83.19), **707.2256 (82.24)**.

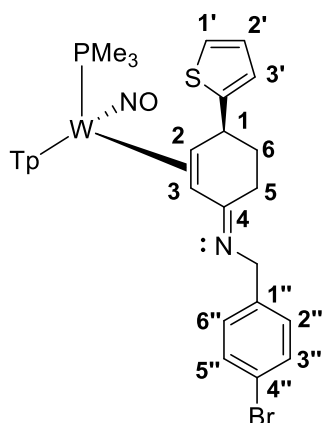
### Synthesis of WTp(NO)(PMe<sub>3</sub>)(η<sup>2</sup>-2,3-(S,Z)-1-(4-bromophenyl)-N-(4-(thiophen-2-yl)cyclohex-2-en-1-ylidene)methanaminium) (40)



Complex (0.198 g, 0.234 mmol) was added to a solution of propionitrile (4 mL) in an oven-dried 4-dram vial. This solution was then cooled to -60 °C over the course of 15 min. In a separate 4-dram vial, a solution of 4-bromobenzylamine (0.771 g, 4.14 mmol in propionitrile (2 mL) was prepared and this solution was also allowed to cool to -60 °C over the course of 15 min. The tungsten-complex solution in propionitrile was then added to the solution of 4-bromobenzylamine and the reaction mixture was then transferred to a -30 °C freezer and allowed to sit over a course of 75 min. The reaction mixture was then added to a solution of stirring Et<sub>2</sub>O (125 mL) and upon addition a light tan solid precipitates from solution. This solid was then isolated on a fine 15 mL fritted disc and washed with Et<sub>2</sub>O (2 x 15mL) and allowed to dry over the course of 3 h under dynamic vacuum before a mass was taken of the light tan solid (0.082 g, 35.0%). The low mass recovery is believed to be due to the relative solubility of this complex in Et<sub>2</sub>O.

CV (DMA): pseudo- $E_{1,2} = -1.71$  V,  $E_{p,a} = +1.32$  V (NHE).  $\nu(\text{NO}) = 1585$  cm<sup>-1</sup>. <sup>1</sup>H NMR (MeCN-*d*<sub>3</sub>, δ, 25 °C): 8.12 (1H, d, Tp3/5), 8.00 (1H, d, Tp3/5), 7.94 (1H, d, Tp3/5), 7.93 (1H, d, Tp3/5), 7.58 (1H, d, Tp3/5), 7.55 (1H, d, Tp3/5), 7.46 (2H, m, benzylamine-H3''/H5''), 7.30 (1H, dd,  $J = 1.5, 4.7$ , thiophene), 7.01 (2H, overlapping, thiophene), 6.89 (2H, m, benzylamine-H2''/H6''), 6.45 (1H, t, Tp4), 6.43 (1H, t, Tp4), 6.38 (1H, t, Tp4), 4.51 (1H, m, H1), 3.73 (1H, dd,  $J = 2.67, 8.90$ , H2), 3.59 (1H, d,  $J = 15.4$ , benzylamine0-methylene), 3.30 (1H, d,  $J = 15.4$ , methylene-benzylamine), 2.84 (1H, m, H5), 2.70 (1H, m, H5'), 2.40 (1H, m, H6), 2.35 (1H, d,  $J = 8.7$ , H3), 1.85 (1H, m, H6), 1.13 (9H, d,  $J_{PH} = 9.30$ , PMe<sub>3</sub>). ESI-MS (m/z, calculated (rel intens, %), **observed** (rel intens, %), ppm, (M + H)<sup>+</sup>: 848.1256 (52.46), **848.1256 (52.25)**, 849.1238 (96.91), **849.1247 (98.03)**, 850.1259 (70.65), **850.1266 (69.77)**, 851.1266 (100), **851.1269 (100)**, 852.1268 (42.51), **852.1288 (42.80)**, 853.1270 (49.38), **853.1272 (48.21)**.

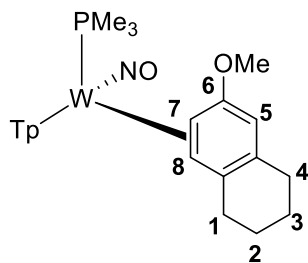
## Synthesis of $\text{W}(\text{NO})(\text{PMe}_3)(\eta^2\text{-2,3-(S,Z)-N-(4-bromobenzyl)-4-(thiophen-2-yl)cyclohex-2-en-1-imine})$ (**41**)



To a 4-dram vial was added **40** (0.050 g, 0.05 mmol) along with MeOH (1 mL) and this solution was allowed to cool to  $-30\text{ }^\circ\text{C}$  over the course of 30 minutes. To this chilled solution as added  $\text{NaBH}_4$  (0.030g, 0.793 mmol). The reaction mixture turns to a homogeneous orange colored solution over the course of sitting at  $-30\text{ }^\circ\text{C}$  for 10 minutes. The reaction mixture was then allowed to sit at ambient temperatures for 15 min before the solvent was removed in vacuo. The resulting orange film was then dissolved in a minimal amount of DCM ( $\sim 1\text{ mL}$ ) and reprecipitated into a solution of standing pentane (10 mL). The resulting mixture was allowed to sit under reduced temperatures ( $-30\text{ }^\circ\text{C}$ ) over the course of an hour to induce precipitation. At the end of the hour at reduced temperatures a white solid had precipitated from solution. The organic layer was then decanted and the resulting solid was dried with a stream of  $\text{N}_{2(g)}$  and desiccated under dynamic vacuum for 90 min before the resulting solid was dissolved in  $\text{MeCN-}d_3$  and analyzed. A mass was not taken of the resulting solid though analysis by NMR spectroscopy and cyclic voltammetry was achieved.

CV (DMA):  $E_{p,a} = +0.73\text{ V}$  (NHE).  $^1\text{H NMR}$  ( $\text{MeCN-}d_3$ ,  $\delta$ ,  $25\text{ }^\circ\text{C}$ ): 8.07 (1H, d, Tp3/5), 7.89 (1H, d, Tp3/5), 7.87 (1H, d, Tp3/5), 7.74 (1H, d, Tp3/5), 7.56 (1H, d, Tp3/5), 7.37 (1H, d, Tp3/5), 7.36 (2H, m, benzylamine- $\text{H}_{3''}/\text{H}_{5''}$ ), 7.27 (1H, dd,  $J = 1.6, 5.2$ , thiophene), 7.10 (1H, dd,  $J = 1.3, 3.5$ , thiophene), 7.03 (2H, m, benzylamine- $\text{H}_{2''}/\text{H}_{6''}$ ), 7.00 (1H, dd,  $J = 3.5, 5.2$ , thiophene), 6.39 (1H, t, Tp4), 6.31 (1H, t, Tp4), 6.07 (1H, t, Tp4), 4.56 (1H, m, H1), 3.70 (1H, d,  $J = 17.0$ , methylene-benzylamine), 3.36 (1H, m, H2), 3.08 (1H, d,  $J = 17.0$ , methylene-benzylamine), 2.74 (1H, m, H5), 2.28 (1H, dt,  $J = 4.78, 14.44$ ,  $\text{H}_{5'}$ ), 2.17 (1H, m, H6), 1.98 (1H, d,  $J = 10.45$ , H3), 1.75 (1H, m,  $\text{H}_{6'}$ ), 1.04 (9H, d,  $J_{\text{PH}} = 8.71$ ,  $\text{PMe}_3$ ).

## Synthesis of $\text{W}(\text{NO})(\text{PMe}_3)(\eta^2\text{-7,8-6-methoxy-tetralin})$ (**41**)



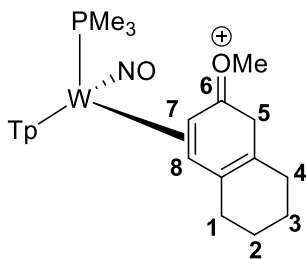
A 4-dram vial was charged with tungsten-benzene (0.200 g, 0.344 mmol) along with 6-methoxy tetralin (1.5 mL, 12.3 mmol) and this homogeneous orange reaction mixture was allowed to stir at room temperature in an inert atmosphere glovebox for 16 h. The next day the now homogeneous reaction mixture was filtered through

a medium 15 mL fritted disc that was ½ full of silica and set in diethyl ether. A light yellow band was eluted after elution of the diethyl ether (100 mL) and the solvent was removed in vacuo until < 10 mL of diethyl ether remained and pentane was added (50 mL) to induce precipitation of a vibrant yellow solid. The solid was then isolated on a fine 15 mL porosity fritted disc and washed with pentane (2 x 10 mL) and dried for 2 h under dynamic vacuum before a mass was taken (0.132 g). Obvious impurities of the tungsten-benzene complex were observed indicating that the reaction did not go to completion and precluded unambiguous analysis by <sup>13</sup>C NMR.

CV (DMA):  $E_{p,a} = -0.25$  V (NHE). <sup>1</sup>H NMR (MeCN-*d*<sub>3</sub>, δ, 0 °C): 7.89 (1H, d, Tp3/5), 7.84 (1H, d, Tp3/5), 7.82 (1H, d, Tp3/5), 7.79 (1H, d, Tp3/5), 7.69 (1H, d, Tp3/5), 7.19 (1H, d, Tp3/5), 6.28 (1H, t, Tp4), 6.27 (1H, t, Tp4), 6.22 (1H, t, Tp4), 4.95 (1H, s, H5), 4.30 (1H, dd,  $J = 10.5, 6.10$ , H2), 3.67 (3H, s, -OMe), 2.74 (1H, m, H4), 2.42 (1H, dt,  $J = 5.1, 16.3$ , H4'), 1.88 (1H, d,  $J = 10.5$ , H8), 1.79, 1.74, 1.64, 1.61, 1.53 overlapping aliphatic resonances (6H, overlapping, C1, C2, C3 methylene protons), 1.21 (9H, d,  $J_{PH} = 8.60$ , PMe<sub>3</sub>). <sup>31</sup>P NMR (MeCN-*d*<sub>3</sub>, δ, 25 °C): -12.45 ( $J_{WP} = 304.5$ ).

### Synthesis of WTp(NO)(PMe<sub>3</sub>)(η<sup>2</sup>-7,8-6-methoxy-5H-tetralinium) (42)

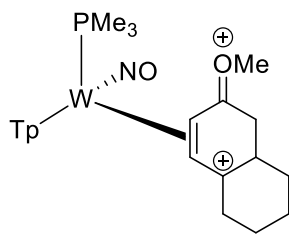
A solution of **41** (NMR scale) was chilled to -30 °C and to this solution was added an excess of DPhAT (NMR scale). This solution was analyzed by 2D NMR characterization is presented below.



<sup>1</sup>H NMR (MeCN-*d*<sub>3</sub>, δ, 0 °C): 8.06 (1H, d, Tp3/5), 7.96 (1H, d, Tp3/5), 7.94 (1H, d, Tp3/5), 7.87 (1H, d, Tp3/5), 7.77 (1H, d, Tp3/5), 7.53 (1H, d, Tp3/5), 6.49 (1H, t, Tp4), 6.42 (1H, t, Tp4), 6.28 (1H, t, Tp4), 4.62 (1H, m, H7), 4.33 (3H, s, -OMe), 3.89 (1H, d,  $J = 27.7$ , H5-exo), 3.69 (1H, d,  $J = 27.2$ , H5-endo), 2.80 (1H, m, H1/H2/H3/H4), 2.44 (1H, d,  $J = 7.7$ , H8), 2.34 (1H, m, H1/H2/H3/H4), 1.88 (1H, d,  $J = 10.5$ , H8), 1.71 (1H, m, H1/H2/H3/H4), 1.61 (1H, m, H1/H2/H3/H4), 1.54 (1H, m, H1/H2/H3/H4), 1.50 (1H, m, H1/H2/H3/H4), 1.46 (1H, m, H1/H2/H3/H4), 1.31 (1H, m, H1/H2/H3/H4), 1.07 (9H, d,  $J_{PH} = 9.3$ , PMe<sub>3</sub>).

### Synthesis of WTp(NO)(PMe<sub>3</sub>)(η<sup>2</sup>-(E)-(4a,5,6,7,8,8a-hexahydronaphthalen-2(1H)-ylidene)(methyl)oxonium) (43)

A solution of **41** (NMR scale) was chilled to -30 °C and to this solution was added an excess of DPhAT (NMR scale). This solution was allowed to stand at -30 °C over a course of 5 min and this solution was then treated with an excess of HOTf (10 drops) that had been pre-chilled to -30 °C. This reaction mixture was allowed to sit at room temperature for 15 min before the solution was frozen and analyzed by <sup>1</sup>H NMR.



$^1\text{H}$  NMR ( $\text{MeCN-}d_3$ ,  $\delta$ ,  $0^\circ\text{C}$ ): 8.16 (1H, d, Tp3/5), 8.14 (1H, d, Tp3/5), 8.11 (1H, d, Tp3/5), 8.00 (2H, overlapping d, Tp3/5), 7.70 (1H, d, Tp3/5), 6.93 (1H, m, H), 6.68 (1H, t, Tp4), 6.50 (1H, t, Tp4), 6.40 (1H, t, Tp4), 5.44 (1H, m, H), 5.04 (1H, m, H), 4.61 (3H, s, -OMe), 3.46 (1H, dd,  $J = 9.53, 22.2$ , H), 3.24 (1H, broad m, H), 3.18 (1H, d, 22.2, H), 1.23 to 2.14 (8J, multiple proton resonances), 1.13 (9H, d,  $J_{\text{PH}} = 9.84$ ,  $\text{PMe}_3$ ).

## References

1. Yin; Liebscher, J., Carbon–Carbon Coupling Reactions Catalyzed by Heterogeneous Palladium Catalysts. *Chemical Reviews* **2007**, *107* (1), 133-173.
2. Molnár, Á., Efficient, Selective, and Recyclable Palladium Catalysts in Carbon–Carbon Coupling Reactions. *Chemical Reviews* **2011**, *111* (3), 2251-2320.
3. Jana, R.; Pathak, T. P.; Sigman, M. S., Advances in Transition Metal (Pd,Ni,Fe)-Catalyzed Cross-Coupling Reactions Using Alkyl-organometallics as Reaction Partners. *Chemical Reviews* **2011**, *111* (3), 1417-1492.
4. Biffis, A.; Centomo, P.; Del Zotto, A.; Zecca, M., Pd Metal Catalysts for Cross-Couplings and Related Reactions in the 21st Century: A Critical Review. *Chemical Reviews* **2018**, *118* (4), 2249-2295.
5. Beletskaya, I. P.; Cheprakov, A. V., The Heck Reaction as a Sharpening Stone of Palladium Catalysis. *Chemical Reviews* **2000**, *100* (8), 3009-3066.
6. Goetzke, F. W.; Mortimore, M.; Fletcher, S. P., Enantio- and Diastereoselective Suzuki–Miyaura Coupling with Racemic Bicycles. *Angewandte Chemie International Edition* **2019**, *58* (35), 12128-12132.
7. MacLeod, B. L.; Pienkos, J. A.; Myers, J. T.; Sabat, M.; Myers, W. H.; Harman, W. D., Stereoselective Synthesis of trans-Tetrahydroindolines Promoted by a Tungsten  $\pi$  Base. *Organometallics* **2014**, *33* (22), 6286-6289.
8. MacLeod, B. L.; Pienkos, J. A.; Wilson, K. B.; Sabat, M.; Myers, W. H.; Harman, W. D., Synthesis of Novel Hexahydroindoles from the Dearomatization of Indoline. *Organometallics* **2016**, *35* (3), 370-387.
9. Pienkos, J. A.; Knisely, A. T.; MacLeod, B. L.; Myers, J. T.; Shivokevich, P. J.; Teran, V.; Sabat, M.; Myers, W. H.; Harman, W. D., Double Protonation of Amino-Substituted Pyridine and Pyrimidine Tungsten Complexes: Friedel–Crafts-like Coupling to Aromatic Heterocycles. *Organometallics* **2014**, *33* (19), 5464-5469.
10. Pienkos, J. A.; Zottig, V. E.; Iovan, D. A.; Li, M.; Harrison, D. P.; Sabat, M.; Salomon, R. J.; Strausberg, L.; Teran, V. A.; Myers, W. H.; Harman, W. D., Friedel–Crafts Ring-Coupling Reactions Promoted by Tungsten Dearomatization Agent. *Organometallics* **2013**, *32* (2), 691-703.
11. Keane, J. M.; Chordia, M. D.; Mocella, C. J.; Sabat, M.; Trindle, C. O.; Harman, W. D., Transition Metal-Stabilized Arenium Cations: Protonation of Arenes Dihapto-Coordinated to  $\pi$ -Basic Metal Fragments. *Journal of the American Chemical Society* **2004**, *126* (21), 6806-6815.
12. Lis, E. C.; Salomon, R. J.; Sabat, M.; Myers, W. H.; Harman, W. D., Synthesis of 1-Oxadecalins from Anisole Promoted by Tungsten. *Journal of the American Chemical Society* **2008**, *130* (37), 12472-12476.
13. Kopach, M. E.; Harman, W. D., The Osmium(II)-Promoted [4 + 2] Cycloaddition Reaction of Anisole and N-Methylmaleimide and Characterization of the  $\eta^2$ -4H-Anisolum Intermediate. *The Journal of Organic Chemistry* **1994**, *59* (22), 6506-6507.
14. Harrison, D. P.; Nichols-Nieler, A. C.; Zottig, V. E.; Strausberg, L.; Salomon, R. J.; Trindle, C. O.; Sabat, M.; Gunnoe, T. B.; Iovan, D. A.; Myers, W. H.; Harman, W. D., Hyperdistorted Tungsten Allyl Complexes and Their Stereoselective Deprotonation to Form Dihapto-Coordinated Dienes. *Organometallics* **2011**, *30* (9), 2587-2597.
15. Keane, J. M.; Ding, F.; Sabat, M.; Harman, W. D., Solid-State Induced Control of Kinetically Unstable Stereoisomers. *Journal of the American Chemical Society* **2004**, *126* (3), 785-789.
16. Welch, K. D.; Harrison, D. P.; Lis, E. C.; Liu, W.; Salomon, R. J.; Harman, W. D.; Myers, W. H., Large-Scale Syntheses of Several Synthons to the Dearomatization Agent {TpW(NO)(PMe<sub>3</sub>)} and Convenient Spectroscopic Tools for Product Analysis. *Organometallics* **2007**, *26* (10), 2791-2794.
17. Lis, E. C.; Delafuente, D. A.; Lin, Y.; Mocella, C. J.; Todd, M. A.; Liu, W.; Sabat, M.; Myers, W. H.; Harman, W. D., The Uncommon Reactivity of Dihapto-Coordinated Nitrile, Ketone, and Alkene Ligands When Bound to a Powerful  $\pi$ -Base. *Organometallics* **2006**, *25* (21), 5051-5058.



18. Smith, G. F., The Acid-Catalyzed Polymerization of Pyrroles and Indoles. In *Advances in Heterocyclic Chemistry*, Katritzky, A. R., Ed. Academic Press: 1963; Vol. 2, pp 287-309.
19. Lankenau, A. W.; Iovan, D. A.; Pienkos, J. A.; Salomon, R. J.; Wang, S.; Harrison, D. P.; Myers, W. H.; Harman, W. D., Enantioenrichment of a Tungsten Dearomatization Agent Utilizing Chiral Acids. *Journal of the American Chemical Society* **2015**, *137* (10), 3649-3655.
20. Wilson, K. B.; Smith, J. A.; Nedzbala, H. S.; Pert, E. K.; Dakermanji, S. J.; Dickie, D. A.; Harman, W. D., Highly Functionalized Cyclohexenes Derived from Benzene: Sequential Tandem Addition Reactions Promoted by Tungsten. *The Journal of Organic Chemistry* **2019**, *84* (10), 6094-6116.
21. Wilson, K. B.; Myers, J. T.; Nedzbala, H. S.; Combee, L. A.; Sabat, M.; Harman, W. D., Sequential Tandem Addition to a Tungsten–Trifluorotoluene Complex: A Versatile Method for the Preparation of Highly Functionalized Trifluoromethylated Cyclohexenes. *Journal of the American Chemical Society* **2017**, *139* (33), 11401-11412.

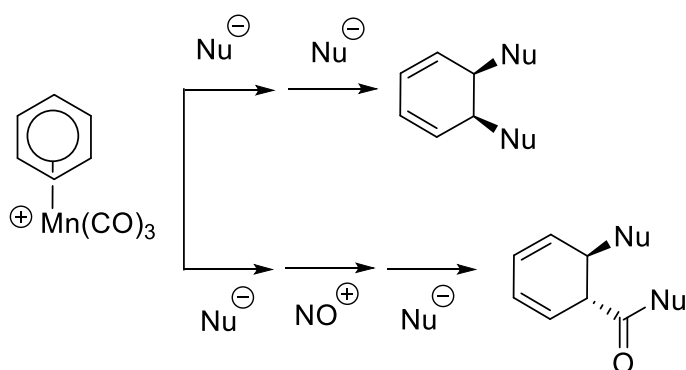
## **Chapter 8**

# **The Double Protonation of Benzene Enabled by Group 6 Dearomatization Agents**

## 8.1 Introduction

The transition-metal-enabled reactivity of benzene has proven to be a powerful synthetic methodology in accessing substituted benzenes and dearomatized products.<sup>1</sup> Several methodologies rely on binding aromatic ligands to electrophilic metal fragments such as  $\{\text{Cr}(\text{CO})_3\}$ ,  $\{\text{Mn}(\text{CO})_3\}^+$  or  $\{\text{FeCp}\}^+$  in an  $\eta^6$ -fashion.<sup>1</sup> After complexation, the bound aromatic is promoted toward reactivity with nucleophiles and can result in substitution or addition products.

In the case of  $\{\text{Mn}(\text{CO})_3\}^+$  promoted reactions, two nucleophiles can sequentially be added to the aromatic ring to generate novel cyclohexadiene products. These nucleophiles are often hard, anionic carbon nucleophiles or strong hydride donors such as  $\text{LiAlH}_4$ . An alternative strategy involves an initial nucleophilic addition to the arene, resulting in a manganese-cyclohexadienyl adduct. Ligand substitution of a carbonyl ligand by a nitrosyl ligand on the manganese core can prime the bound  $\pi$ -ligand to react with another nucleophilic reagent (**Scheme 8.1**). In some cases, the second nucleophile initially adds to a carbonyl ligand. Subsequent reductive elimination results in the substituted cyclohexadiene-5-one product (**Scheme 8.1**).

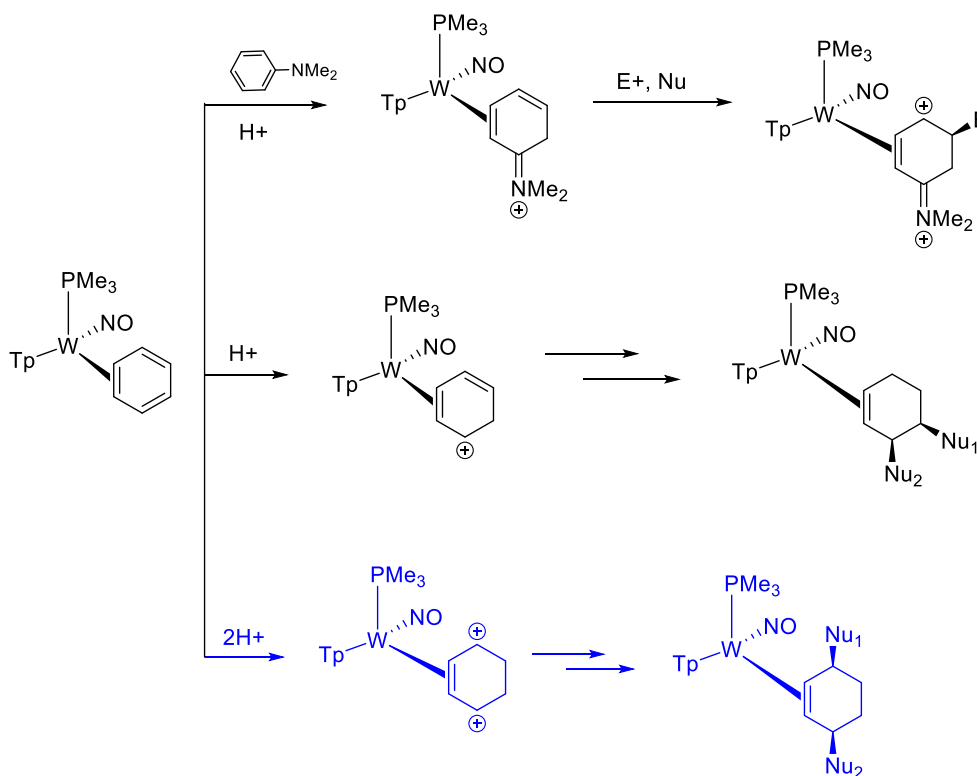


**Scheme 8.1.** Double nucleophilic additions to benzene promoted by an electron deficient manganese complex.

A complementary dearomatization methodology developed in our lab shows the ability of the  $\pi$ -basic metal fragments  $\{\text{MTP}(\text{NO})(\text{L})\}$  ( $\text{M} = \text{Mo}$  or  $\text{W}$ ,  $\text{L} = 4$ -dimethylamino pyridine or  $\text{PMe}_3$  respectively) to coordinate aromatic molecules in an  $\eta^2$ -motif across a single double-bond on an aromatic ring.<sup>2-3</sup> This dihapto-coordinate bond is achieved through a strong metal-to-ligand  $\pi$ -backbonding interaction, and the aromatic is subsequently dearomatized. After metal complexation, the unbound alkene bonds behave analogously to an electron-rich diene. These aromatic  $\pi$ -ligands are subsequently able to react with an array of electrophilic reagents.

Recently we reported the ability of **1**  $\text{WTp}(\text{NO})(\text{PMe}_3)(\eta^2\text{-benzene})$  to undergo protonation followed by nucleophilic addition to selectively generate a series of tungsten cyclohexadiene complexes.<sup>4</sup> These complexes could then be treated with an analogous sequence (protonation followed by nucleophile) to synthesize a series of novel 1,2-substituted cyclohexenes. The cyclohexene ligand can be isolated as a free organic upon oxidation of the tungsten metal. This synthetic sequence was enabled by the ability of the tungsten fragment to promote the protonation of benzene with diphenylammonium triflate (DPhAT), resulting in the clean formation of  $\text{WTp}(\text{NO})(\text{PMe}_3)(\eta^2\text{-benzenium})$  (**2**) as detailed in Chapter 2.

In this previous study, the tungsten-benzenium complex **2** underwent reactivity with various nucleophiles including enolates, cyanides, phosphines, amines and hydrides.<sup>4</sup> While the cationic complex **2** was moderately electrophilic, it was not sufficiently electrophilic to undergo Friedel-Crafts reaction with weak aromatic nucleophiles such as those examined in Chapter 7 (anisole, phenol, thiophene). The  $\text{pK}_a$  of **2** is estimated to be  $\sim 1$ , and this complex can be isolated as a solid in good yield ( $\sim 90\%$ ) upon precipitation into chilled diethyl ether. The generation of an even more electrophilic species then would enable a wider scope of available reactions. To achieve this, we hoped to perform two sequential protonations on **1** in the hopes of yielding a highly reactive electrophilic species.



**Scheme 8.2.** The double protonation of *N,N*-dimethylaniline (top), chemistry demonstrated via the single protonation of benzene demonstrated by Dr. Katy Wilson (middle) and the proposed double protonation of benzene (bottom).

## 8.2 The Double Protonation of Benzene

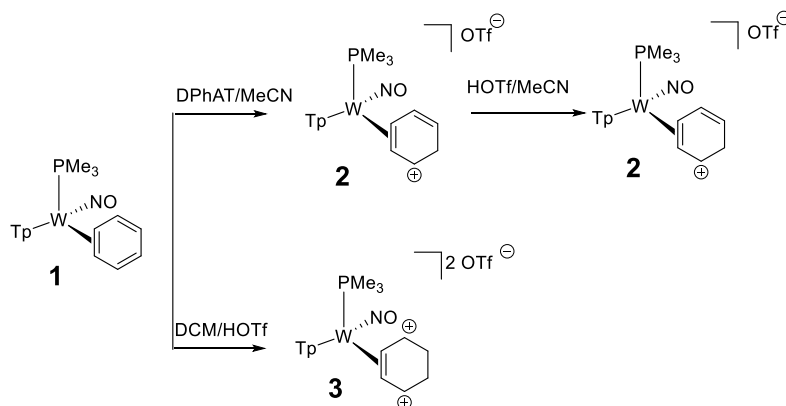
Treating **1** with diphenylammonium triflate (DPhAT) at reduced temperatures in various organic solvents (acetone, DCM, acetonitrile) results in the clean formation of  $\text{Wtp}(\text{NO})(\text{PMe}_3)(\eta^2\text{-benzenium})(\text{OTf}^-)$  (**2**).

However, no further reactivity is observed when a solution of **2** in  $\text{MeCN-}d_3$  is treated with HOTf. We postulate that triflic acid

leveled in the nitrile solvent is insufficiently acidic to deliver a second proton to **2**.

Gratifyingly, when **2** is formed in situ at  $-60\text{ }^\circ\text{C}$  with DPhAT in a solution of  $\text{DCM-}d_2$  and treated with an excess of HOTf, a new complex is observed.  $^1\text{H}$  NMR analysis taken at reduced temperatures ( $0\text{ }^\circ\text{C}$ ). Spectral features are consistent with a complex that we assign to the double protonation of benzene and assign as the tungsten (II) species  $\text{Wtp}(\text{NO})(\text{PMe}_3)(\eta^4\text{-cyclohexadiene})(2\text{ OTf}^-)$  (**3**). Analysis of the  $^1\text{H}$  NMR spectra reveals 8 proton resonances ranging from 3.11 to 7.13 ppm (full details in Experimental Section). We note that treating a cold DCM solution of the neutral tungsten-benzene complex **1** with HOTf leads to the efficient conversion to **3** without pre-treating the solution with DPhAT.

DFT calculations (B3LYP method with the LANL2Z basis set for the tungsten atom, 6-31(g) for all other atoms) were used to further evaluate complex **3**. The optimized structures shows double-bond character between two sets of carbon atoms, suggesting that the resulting dicationic  $\pi$ -ligand is bound in an  $\eta^4$ -fashion to the tungsten center. As such, this complex can be thought of as either a tungsten (0) complex supporting a dicationic  $\pi$ -ligand, or as a formal tungsten (II) fragment bound  $\eta^4$ -to a cyclohexadiene ligand (**Figure 8.1**). Attempts to isolate this proposed dicationic complex **3** resulted in oxidative decomposition to uncharacterized paramagnetic material.



**Scheme 8.3.** The reactivity of the tungsten-benzene complex **1** under various acidic conditions. The double protonation of benzene is possible in an HOTf solution of DCM.

### 8.3 Nucleophilic Additions to a Double Protonated Benzene Complex

When **3** is prepared in the presence of various aromatics with electron donor substituents (i.e. phenol, anisole, 6-methoxy-tetralin) and allowed to react at reduced temperatures over an hour, a new chemical entity is observed by  $^{31}\text{P}$  NMR.

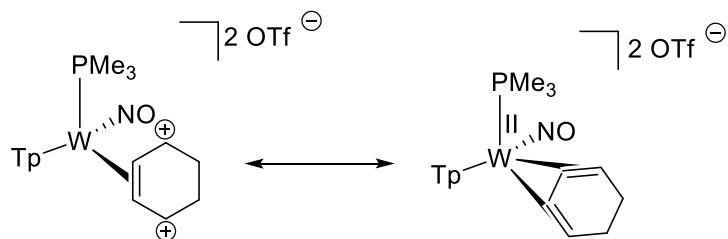
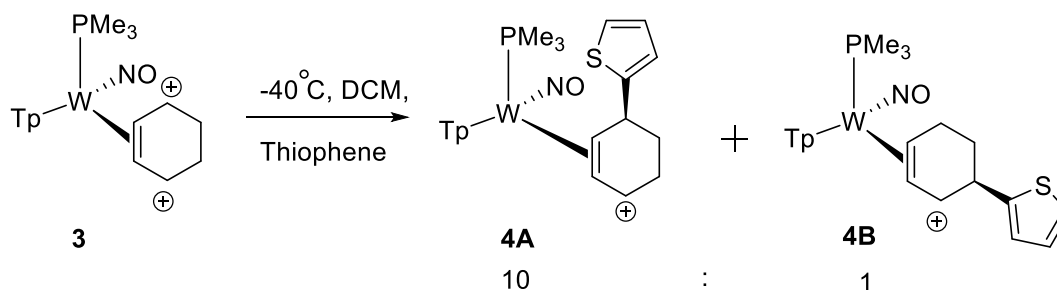


**Figure 8.1.** Resonance structures that described the system as either a double protonated benzene complex on a tungsten (0) metal or of a tungsten (II)  $\eta^4$ -cyclohexadiene complex.

Exposing **3** at reduced temperatures with thiophene, for example, allows for the isolation of a fine yellow powder via precipitation into diethyl ether. Resulting spectroscopic features observed with  $^1\text{H}$  NMR spectroscopy are consistent with the addition of thiophene to complex **3** (**4A**). This complex corresponds to an electrophilic aromatic substitution reaction occurring at the alpha-position of the thiophene ring. A minor complex ( $\sim 6:1$ ) is also observed (**4B**). Attempts to improve the regioselectivity of this addition by lowering the temperature ( $-30\text{ }^\circ\text{C}$  to  $-60\text{ }^\circ\text{C}$ ) did not appreciably improve the observed isomer ratio.

Following these results, **3** was synthesized in situ and treated with anisole (**5**), 6-methoxytetralin (**6**) and phenol (**7**) and isolated under analogous conditions as **4** to yield the corresponding adducts (**Scheme 8.5**). With regard to anisole and 6-methoxy-tetralin, excellent degrees of regio- and stereoselectivity in the resulting carbon-carbon bond formations is observed ( $> 20:1$ ), with the aromatic ring adding anti to the metal.



**Scheme 8.4.** Addition of thiophene to **3** and the resulting regio-selectivity.

## 8.4 Deuterium Studies

In a recent report involving deuterium studies we determined that the initial protonation of **1** to form **2** occurs through a mechanism that delivers the proton-*endo* relative to the metal. We sought to investigate if the metal would be able to selectively control the integration of protons into the benzene ring to enable the formation of **3**. To simplify the resulting spectral analysis, we first synthesized the isotopologue of **1** in the form of  $\text{W}(\text{NO})(\text{PMe}_3)(\eta^2\text{-benzene-}d_6)$  (**1- $d_6$** ) before treating the resulting complex with HOTf in a DCM solution (**Scheme 8.6**).

Treatment of **1- $d_6$**  with acid in the presence of anisole led to the formation of the isotopologue (**5- $d_6$** ) (**Scheme 8.6**). Analysis of the sites of protonation on **5- $d_6$**  show proton resonances at the 4-*exo* and 5-*endo* positions.

Assignment of the diastereotopic protons was determined by evaluating NOE interactions between resonances associated with the anisolic ring

and evaluating NOE interactions

between the H5-*endo* proton and

the Tp3A pyrazole ring. Although

we are unable to distinguish

which proton was introduced first,

these results are consistent with

the initial protonation occurring

*endo* relative to the metal. The

second protonation is observed to

occur *exo* relative to the metal.

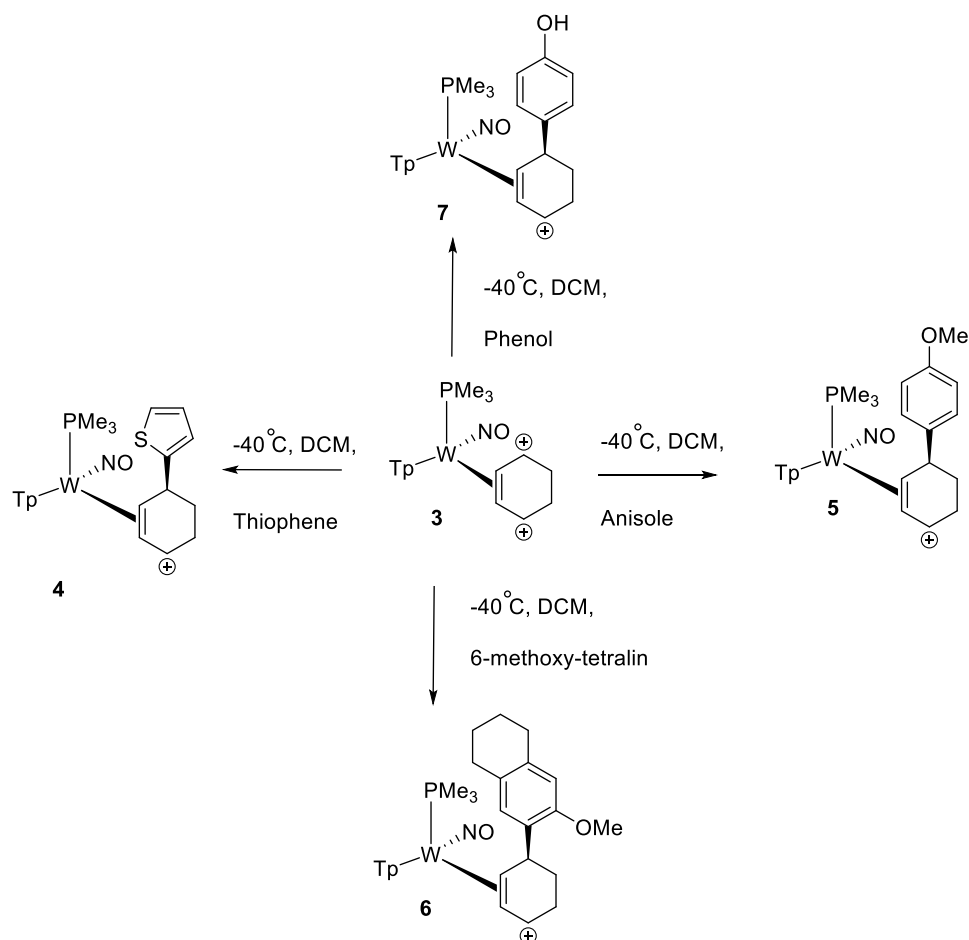
The introduced proton resonances

integrate to 95% + relative to a

non-deuterated pyrazole ring

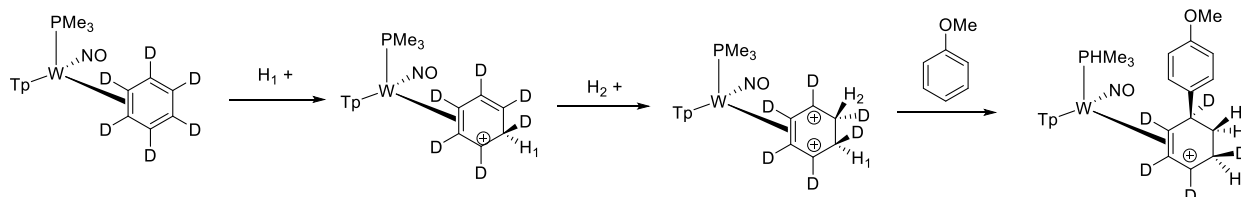
proton. These results suggest

minimal scrambling of the



**Scheme 8.5.** Electrophilic aromatic substitution on various aromatic rings by the electrophilic species **3**. Products shown are the major isomer observed in solution with selectivity levels at a minimum of 6:1 relative to a minor isomer.

introduced proteo-resonances, showing that the metal retains excellent levels of control in directing the site of proton addition.

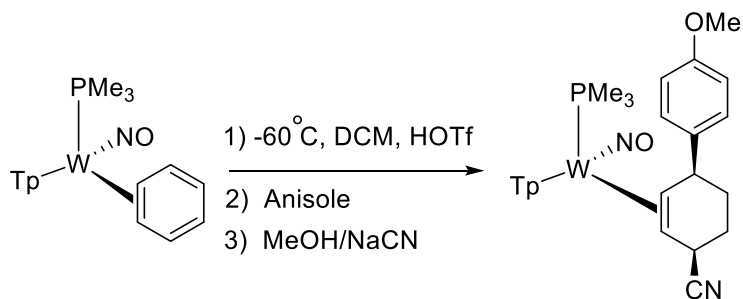


**Scheme 8.6.** Generation of a benzene- $d_6$  tungsten complex and the resulting selectivity of the double-protonation and nucleophilic addition with anisole.

Interestingly, when a solution of **1** in DCM is treated with thiophene and then DOTf at reduced temperatures ( $-40$  °C), no appreciable deuterium is detected as being integrated in the product. This result suggests that an exceptionally high KIE ( $\sim 100$ ) may be at play, given that the isotopic purity of commercially available DOTf is  $> 99\%$ . Similar behavior has been observed previously and is detailed in Chapter 3, where treating  $\text{W}(\text{Tp})(\text{NO})(\text{PMe}_3)(\eta^2\text{-1,3-cyclohexadiene})$  with an acidic deuterium source leads to only partial deuteration ( $\sim 70\%$ ). Investigation into enhanced KIE effects and their dependence on acid strength are ongoing. This deuterium labeling experiment was performed by Mary Shindler.

### 8.5 Double Protonation of Benzene on Molybdenum and Nucleophilic Additions

In another example of synthetic utility, complex **5** was prepared in situ from tungsten and molybdenum respectively. Treating these complexes with a cold solution of NaCN/MeOH led to the development of a substituted cis-1,4-substituted cyclohexene product (**9**) (**Scheme 8.7**). This shows



**Scheme 8.7.** One pot synthesis of a 1,4-substituted cyclohexadiene complex derived from the double protonation of benzene.

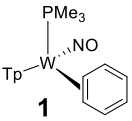
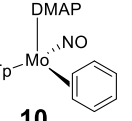
the ability to generate a substituted 1,4-substituted cyclohexene ring from the dearomatization of benzene *in a one pot reaction*.

The ability of tungsten to support the formation of a dicationic electrophile via the dearomatization of benzene prompted us to question whether its molybdenum congener  $\text{Mo}(\text{Tp})(\text{NO})(4\text{-DMAP})(\eta^2\text{-benzene})$  (**10**) could enable similar reactivity.<sup>5</sup> In contrast to **1**, the molybdenum analog is exceptionally labile in solution ( $t_{1/2} \sim 20$ s at ambient



temperatures) and a previous report detailed its isolation on a small scale (~ 70 mgs).<sup>5</sup> The low thermal stability of the molybdenum benzene complex, relative to previously reported 3<sup>rd</sup> row congeners is attributed to the limited  $\pi$ -backbonding ability of the molybdenum scaffold.

Despite this, molybdenum-promoted dearomatization features a large number of advantages compared to dearomatization by its 3<sup>rd</sup> row predecessors. Advantages include enhanced scalability and a most cost effective dearomatization agent.<sup>1,5-6</sup> Additionally, the molybdenum metal is more easily oxidized than its third row congener. Therefore, the use of relatively mild oxidants can be used on molybdenum-olefin complexes which yields to increased yields of the free organic (in contrast to tungsten-olefin complexes where stronger oxidants sometimes have to be utilized). Finally, oxidation with iodine allows for the molybdenum dearomatization agent to be recycled.<sup>6</sup> Expanding the ability of molybdenum-based dearomatization then could enable a more practical dearomatization synthon. A comparison between the tungsten and molybdenum benzene complexes (**1** and **10**) is given in **Table 8.1**.

| Complex  | $E_{p,a}$<br>(relative to NHE) | Substitution Half-<br>Life at 25 °C | Metal-Arene Bond<br>Strength (kcal/mol) | Barrier to ring-walk<br>isomerization (kcal/mol) |
|--|--------------------------------|-------------------------------------|---|--|
| <br><b>1</b>  | -0.13 V                        | 1.1 h                               | 23                                      | 15.1   |
| <br><b>10</b> | -0.55 V                        | 20 s                                | 21                                      | 13.8   |

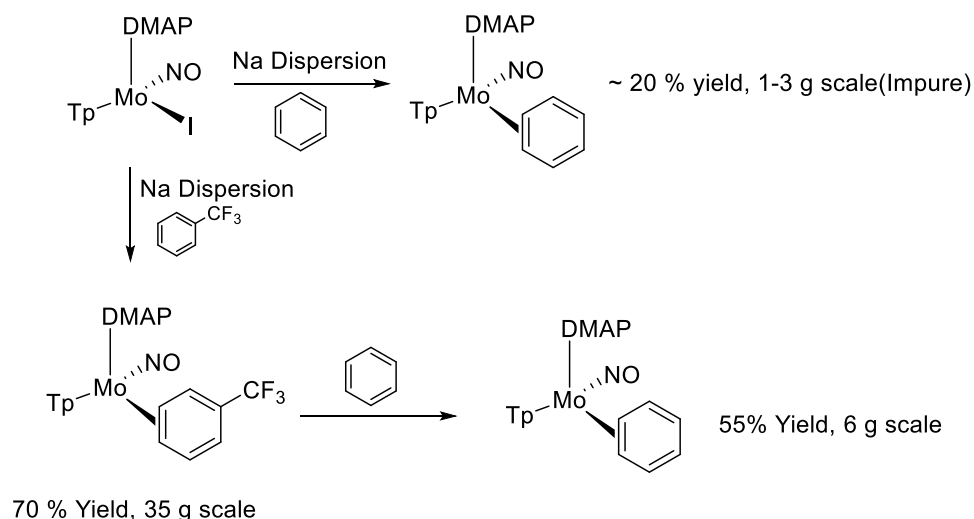
**Table 8.1.** Comparison between benzene complexes of molybdenum and tungsten. Metal-arene bond strength is extrapolated from substitution half-life data. The assumptions implicit in this analysis are explained in Chapter 5. Barrier to ring-walk isomerization was determined via line-broadening techniques and variable temperature <sup>1</sup>H NMR spectroscopy.

Initial investigative efforts sought to increase the scale associated with the synthesis of **10**. Optimized conditions utilize the MoTp(NO)(4-DMAP)( $\eta^2$ -3,4- $\alpha,\alpha,\alpha$ -trifluorotoluene) (**11**) complex as a precursor which can be prepared on a 37 g scale.<sup>5</sup> Ligand exchange to **10** can be affected using a large excess of benzene (details in Experimental Section)

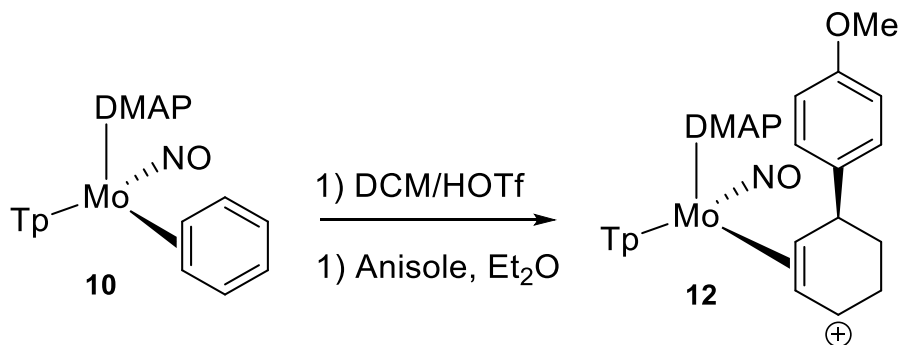
on a six gram scale. Notably, this complex is stable for more than a year at reduced temperatures (-30 °C) under an inert N<sub>2(g)</sub> glovebox atmosphere.

While treatment of **10** with DCM, anisole and triflic acid at -60 °C results in the oxidative decomposition of the

molybdenum scaffold. However, adding a cold solution of HOTf to a frozen solution of **10**, DCM (m.p. -96.7 °C) and anisole and allowing the frozen solution to thaw at -60 °C over the course of an hour results in the generation of a molybdenum-allyl complex where the major product features incorporation of the anisole ring on the carbon proximal to the phosphine ligand (**12**). This product is consistent with the double protonation of benzene followed by an electrophilic aromatic substitution reaction at the para-position of the anisole ring. Presumably, this occurs by the in situ generated electrophilic molybdenum-fragment. The formation of **12** occurs in greatly reduced yield (<10 %) compared to its tungsten analog, and large amounts of protonated DMAP are observed, indicating competitive decomposition of the metal center. The resulting metal complexes are paramagnetic and their characterization was not pursued further.



**Scheme 8.8.** Large-scale optimization of the molybdenum-benzene complex **10**.



**Scheme 8.9.** Addition of a weak aromatic nucleophile enabled by the molybdenum-promoted dearomatization of benzene.

## 8.6 Conclusions

We have identified conditions that lead to the successful double protonation of benzene supported by exceptionally  $\pi$ -basic transition metals. The resulting dicationic systems can serve as potent electrophiles with an array of weakly nucleophilic aromatic ligands.

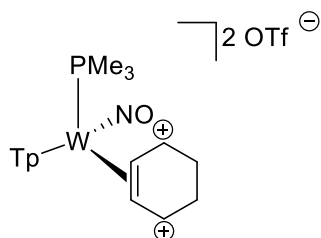
Given the ability of nucleophiles that have been shown to react with tungsten-stabilized allyls, one can imagine a wide array of nucleophiles that could be added to generate elaborate 1,4-substituted cyclohexene products. In the case of molybdenum, despite the lability of the molybdenum-benzene complex in solution at ambient temperatures, the bound benzene is primed to undergo analogous reactivity; though current conditions result in the concomitant decomposition of the metal. Even so, this serves as an important proof of concept and suggests that molybdenum-enabled dearomatization may be more activating than previously thought. Investigations are undergoing to investigate the double protonation of substituted benzenes supported by Group 6 metal architectures. Additionally, we are seeking to expand the range of nucleophiles that can be engaged in selective carbon-carbon bond formations with these dicationic scaffolds.

This chemistry was accessible due to the electron-rich nature of the  $\pi$ -basic tungsten fragment  $\{\text{WTP}(\text{NO})(\text{PMe}_3)\}$ . The ligand set of this fragment has been carefully engineered to generate an electron rich metal center with ligands that are relatively sterically innocuous. Even so, the phosphine ligand  $\text{PMe}_3$  is relatively expensive. Unpublished work in our lab has sought to replace the  $\text{PMe}_3$  ligand with more practical alternatives (i.e.  $\text{P}(\text{OMe})_3$ ) led to fragments that were either unable to coordinate any aromatic molecules or that were unable to bind highly aromatic systems such as benzene.<sup>7</sup> With these studies in mind, efforts were focused on examining whether tri-*n*-butyl phosphine ( $\text{P}(\text{n-Bu})_3$ ) would be able to sustain  $\eta^2$ -coordination of aromatic molecules. This ligand is cheaper by a factor of ten compared to the  $\text{PMe}_3$  ligand. The results of this study are explored in Chapter 9.

## Experimental

**General Methods.** NMR spectra were obtained on 500, 600 or 800 MHz spectrometers. Chemical shifts are referenced to tetramethylsilane (TMS) utilizing residual  $^1\text{H}$  signals of the deuterated solvents as internal standards. Chemical shifts are reported in ppm and coupling constants ( $J$ ) are reported in hertz (Hz). Chemical shifts for  $^{19}\text{F}$  and  $^{31}\text{P}$  spectra were reported relative to standards of hexafluorobenzene (164.9 ppm) and triphenylphosphine (-6.00 ppm). Infrared Spectra (IR) were recorded on a spectrometer as a solid with an ATR crystal accessory, and peaks are reported in  $\text{cm}^{-1}$ . Electrochemical experiments were performed under a nitrogen atmosphere. Most cyclic voltammetric data were recorded at ambient temperature at 100 mV/s, unless otherwise noted, with a standard three electrode cell from +1.8 V to -1.8 V with a platinum working electrode, acetonitrile (MeCN) solvent, and tetrabutylammonium (TBAH) electrolyte (~1.0 M). All potentials are reported versus the normal hydrogen electrode (NHE) using cobaltocenium hexafluorophosphate ( $E_{1/2} = -0.78$  V, -1.75 V) or ferrocene ( $E_{1/2} = 0.55$  V) as an internal standard. Peak separation of all reversible couples was less than 100 mV. All synthetic reactions were performed in a glovebox under a dry nitrogen atmosphere unless otherwise noted. All solvents were purged with nitrogen prior to use. Deuterated solvents were used as received from Cambridge Isotopes and were purged with nitrogen under an inert atmosphere. When possible, pyrazole (Pz) protons of the (trispyrazolyl) borate (Tp) ligand were uniquely assigned (e.g., “Tp3B”) using two-dimensional NMR data (see Fig. S1). If unambiguous assignments were not possible, Tp protons were labeled as “Tp3/5 or Tp4”. All  $J$  values for Tp protons are 2 ( $\pm 0.4$ ) Hz.

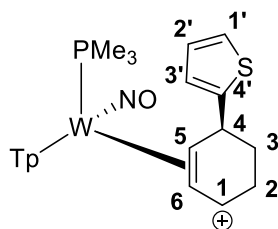
### Synthesis of $\text{MoTp}(\text{NO})(\text{DMAP})(\eta^2\text{-benzene})$ (3)



To an NMR tube was added **1** along with  $\text{DCM-}d_2$  and this homogeneous yellow reaction mixture was allowed to cool to  $-60$  °C in a cold toluene bath. To this homogeneous reaction mixture was added recently thawed HOTF (8 drops) and the NMR tube was then removed from a glovebox and placed in a small dewar filled with  $\text{N}_{2(l)}$  that froze the contents of the NMR tube solution. The reaction mixture was allowed to thaw to reveal a homogeneous red reaction mixture. The resulting NMR solution was analyzed at 0 °C in  $\text{DCM-}d_2$ .

$^1\text{H-NMR}$  ( $\text{DCM-}d_2$ ,  $\delta$ , 0 °C): 8.25 (1H, d, Tp3/5), 8.20 (1H, d, Tp3/5), 8.07 (1H, d, Tp3/5), 7.94 (1H, d, Tp3/5), 7.64 (1H, d, Tp3/5), 7.13 (1H, broad s, benzenium), 6.86 (1H, broad s, benzenium), 6.82 (1H, t, Tp4), 6.71 (1H, t, Tp4), 6.48 (1H, t, Tp4), 6.14 (1H, broad s, benzenium), 5.88 (1H, broad s, benzenium), 3.80 (1H, broad s, benzenium), 3.65 (1H, broad s, benzenium), 3.14 (1H, broad s, benzenium), 3.11 (1H, broad s, benzenium), 1.24 (9H, d,  $J_{\text{PH}} = 10.6$ ,  $\text{PMe}_3$ ).  $^{13}\text{C-NMR}$  ( $\text{DCM-}d_2$ ,  $\delta$ , 0 °C): 146.4 (Tp3/5), 145.2 (Tp3/5), 144.0 (Tp3/5), 141.7 (Tp3/5), 141.4 (Tp3/5), 141.2 (Tp3/5), 111.1 (3C, overlapping Tp4s and benzenium), 110.7 (benzenium), 109.4 (Tp4), 96.3 (benzenium), 87.1 (benzenium), 23.0 (benzenium), 22.6 (benzenium), 12.7 (d,  $J_{\text{PC}} = 33.9$ ,  $\text{PMe}_3$ ).

## Synthesis of $\text{W}(\text{NO})(\text{PMe}_3)(\eta^2\text{-5,6-(-4-(thiophen-2-yl)cyclohex-2-en-1-yl)ium})$ (**4A**)

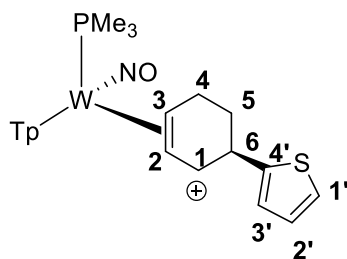


A solution of **1** (0.213 g, 0.344 mmol) was dissolved in DCM (1 mL) and this solution was cooled to  $-60\text{ }^\circ\text{C}$  over a course of 10 min. To this solution was added thiophene ( $\sim 1/2$  mL, 5.94 mmol) After allowing this reaction mixture to stir for 5 min at  $-60\text{ }^\circ\text{C}$  an excess of recently thawed HOTf (0.1 mL, 1.13 mmol) was added to the reaction mixture. The reaction mixture was allowed to stir for 30 min before the reaction mixture was treated with DME (1 mL) that had been cooled to  $-60\text{ }^\circ\text{C}$ . This solution as then added to a solution of stirring diethyl ether (50 mL) and upon addition an orange solid precipitates form solution. This solid was then isolated on a fine 60 mL porosity fritted disc, washed with diethyl ether (3 x 10 mL) and allowed to desiccate under static vacuum for 16 h before a mass was taken of the resulting burnt orange solid (0.191 g, 63.9 %). The resulting solid shows an approximate ratio of **4A**:**4B** of approximately 6:1.

CV (DMA):  $E_{p,c} = -1.05$  V (NHE).  $^1\text{H}$  NMR (MeCN- $d_3$ ,  $\delta$ ,  $25\text{ }^\circ\text{C}$ ): 8.41 (1H, d, Tp3/5), 8.13 (1H, d, Tp3/5), 8.01 (1H, d, Tp3/5), 7.96 (1H, d, Tp3/5), 7.94 (1H, d, Tp3/5), 7.82 (1H, d, Tp3/5), 7.34 (1H, dd,  $J = 1.1, 5.2$ , thiophene-H1'), 7.10 (1H, m, thiophene 3), 7.04 (1H, dd,  $J = 1.1, 5.04$ , thiophene-H2'), 6.64 (1H, broad t,  $J = 6.41$ , H1), 6.53 (1H, t, Tp4), 6.51 (1H, t, Tp4), 6.34 (1H, t, Tp4), 5.37 (1H, t,  $J = 7.43$ , H6), 4.36 (1H, dd,  $J = 1.74, 7.43$ , H5), 4.10 (1H, m, H4), 3.44 (1H, buried, H2), 3.31 (1H, m H2'), 1.91 (1H, m, H3), 1.42 (1H, m, H3'), 1.09 (9H, d,  $J_{\text{PH}} = 9.8$ ,  $\text{PMe}_3$ ).

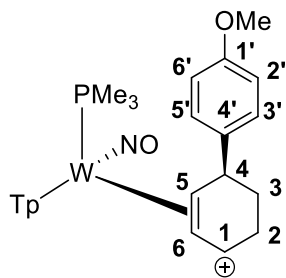
$^1\text{H}$  NMR (acetone- $d_6$ ,  $\delta$ ,  $25\text{ }^\circ\text{C}$ ): 8.62 (1H, d, Tp3/5), 8.37 (1H, d, Tp3/5), 8.36 (1H, d, Tp3/5), 8.22 (1H, d, Tp3/5), 8.17 (1H, d, Tp3/5), 7.99 (1H, d, Tp3/5), 7.41 (1H, dd,  $J = 1.1, 5.2$ , thiophene-H1'), 7.21 (1H, m, thiophene 3), 7.06 (1H, dd,  $J = 1.1, 5.04$ , thiophene-H2'), 6.86 (1H, broad t,  $J = 6.41$ , H1), 6.65 (1H, t, Tp4), 6.62 (1H, t, Tp4), 6.43 (1H, t, Tp4), 5.55 (1H, t,  $J = 7.43$ , H6), 4.64 (1H, dd,  $J = 1.74, 7.43$ , H5), 4.21 (1H, m, H4), 3.56 (1H, m, H2), 3.42 (1H, m H2'), 1.98 (1H, m, H3), 1.48 (1H, m, H3'), 1.26 (9H, d,  $J_{\text{PH}} = 9.90$ ,  $\text{PMe}_3$ ).  $^{13}\text{C}$  NMR (acetone- $d_6$ ,  $\delta$ ,  $25\text{ }^\circ\text{C}$ ): 153.6 (thiophene-C4'), 149.4 (Tp3/5), 146.4 (Tp3/5), 143.7 (Tp3/5), 139.7 (C4), 139.6 (Tp3/5), 139.5 (Tp3/5), 136.7 (C1), 127.9 (thiophene-C2'), 125.1 (thiophene-C3'), 124.9 (thiophene-C1'), 109.6 (Tp4), 109.1 (Tp4), 108.2 (Tp4), 103.7 (C6, d,  $J_{\text{PC}} = 3.5$ ), 74.5 (C5, d,  $J_{\text{PC}} = 12.9$ ), 40.0 (C4, d,  $J_{\text{PC}} = 4.0$ ), 32.0 (C2), 25.9 (C3), 13.6 (d,  $J_{\text{CP}} = 32.6$ ,  $\text{PMe}_3$ ), 158.2 (thiophene-C4'), 144.4 (Tp3/5), 142.9 (Tp3/5), 141.7 (Tp3/5), 138.1 (Tp3/5), 137.8 (Tp3/5), 137.6 (Tp3/5), 128.1 (-CN), 127.7 (thiophene-C2'), 124.8 (thiophene-C3'), 124.0 (thiophene-C1'),

## Characterization of $\text{W}(\text{NO})(\text{PMe}_3)(\eta^2\text{-2,3-(-6-(thiophen-2-yl)cyclohex-2-en-1-yl)ium})$ (**4B**)



$^1\text{H}$  NMR (MeCN- $d_3$ ,  $\delta$ , 0 °C): 8.41 (1H, d, Tp3/5), 7.99 (1H, d, Tp3/5), 7.96 (1H, d, Tp3/5), 7.95 (1H, d, Tp3/5), 7.92 (1H, d, Tp3/5), 7.78 (1H, d, Tp3/5), 7.35 (1H, dd,  $J = 0.84$ , 5.11, thiophene-H1'), 7.14 (1H, d,  $J = 3.38$ , thiophene-H3'), 7.05 (1H, dd,  $J = 3.38$ , 5.11, thiophene-H2'), 6.52 (1H, t, Tp4), 6.51 (1H, t, Tp4), 6.27 (1H, t, Tp4), 6.03 (1H, d,  $J = 7.28$ , H1), 5.32 (1H, t,  $J = 7.28$ , H2), 4.78 (1H, m, H6), 4.66 (1H, m, H3), 3.26 (1H, m, H4), 2.54 (1H, m, H4'), 1.98 (1H, buried, H5), 1.21 (1H, m, H5'), 1.18 (9H, d,  $J_{\text{PH}} = 9.80$ , PMe $_3$ ).

### Synthesis of WTp(NO)(PMe $_3$ )( $\eta^2$ -5,6-(-4'-methoxy-1,2,3,4-tetrahydro-[1,1'-biphenyl]-4-yl)ium) (5)

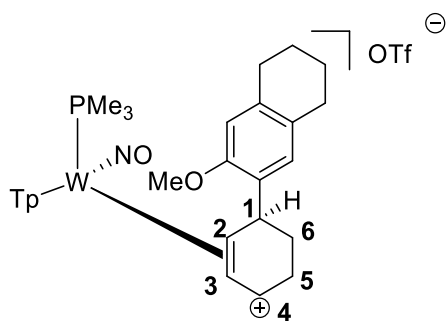


A solution of **1** (0.200 g, 0.344 mmol) was dissolved in DCM (1 mL) and this solution was cooled to -30 °C over a course of 10 min. To this solution was added DPhAT (0.125 g, 0.390 mmol) and upon addition the initially homogeneous yellow reaction mixture turns to a homogeneous red colored solution. After allowing this reaction mixture to stir for 5 min at -30 °C an excess of -30 °C chilled HOTf (10 drops) was added to the reaction mixture to generate **3** in situ. The reaction mixture is still a homogeneous red colored solution. Separately a solution of anisole (1 mL, ~ 9.25 mmol) was dissolved in DCM (2 mL) and this reaction mixture was also cooled to -30°C in a large test tube over a period of 5 min. Next, the solution of **3** was added to the anisole/DCM solution and the reaction mixture was allowed to stir for 1 h. The reaction mixture was then added to a solution of stirring diethyl ether (100 mL). Upon addition a vibrant yellow solid precipitates from solution but after 5 min of trituration in the diethyl ether mixture a red, sticky film develops on the side of the Erlenmeyer flask. The solid was redissolved in a minimal amount of DCM (2 mL) and again precipitated into a new solution of diethyl ether (50 mL). The reaction mixture oiled out again. The resulting red film was re-dissolved in a 1:1 by volume solution solution of MeCN:MeOH (4 mL total) and added to a new solution of diethyl ether (100 mL). Upon addition a dull yellow solid precipitates form solution. This solid was then isolated on a fine 15 mL porosity fritted disc, washed with diethyl ether (3 x 10 mL) and allowed to desiccate under static vacuum for 4 h before a mass was taken of the yellow solid (0.072 g, 24.9 %).

CV (DMA):  $E_{\text{p,c}} = -0.93$  V (NHE). IR,  $\nu(\text{BH}) = 2519$   $\text{cm}^{-1}$ ,  $\nu(\text{NO}) = 1635$   $\text{cm}^{-1}$ .  $^1\text{H}$  NMR (MeCN- $d_3$ ,  $\delta$ , 25 °C): 8.42 (1H, d, Tp3B), 8.15 (1H, d, Tp3A), 8.00 (1H, d, Tp5C), 7.95 (1H, d, Tp5B), 7.92 (1H, d, Tp3C), 7.82 (1H, d, Tp5A), 7.35 (2H, m, Anisole-H3'/H5'), 6.97 (2H, m, Anisole-H2'/H6'), 6.54 (1H, t,  $J = 6.73$ , H1), 6.52 (1H, t, Tp4B), 6.50 (1H, t, Tp4C), 6.35 (1H, t, Tp4A), 5.39 (1H, t,  $J = 7.40$ , H6), 4.36 (1H, dd,  $J = 7.40$ , 16.1, H5), 3.80 (3H, s, anisole-OMe), 3.72 (1H, dd,  $J = 6.31$ , 10.94, H4), 3.50 (1H, m H2-syn), 3.31 (1H, m, H2-anti), 1.77 (1H, m, H3-syn), 1.22 (1H, m, H3-anti), 1.01 (9H, d,  $J_{\text{PH}} = 10.0$ , PMe $_3$ ).  $^{13}\text{C}$  NMR (acetone- $d_3$ ,  $\delta$ , 25 °C): 159.6 (Anisole-C1), 149.2 (Tp3A), 146.2 (Tp3/5), 143.4 (Tp3/5), 141.6 (C4), 139.6 (Tp3/5), 139.5 (Tp3/5), 134.4 (Anisole-C1), 129.5 (Anisole-C3/C5), 115.2 (Anisole-C2/C6), 109.6 (Tp4), 108.9 (Tp4), 108.1 (Tp4), 105.5 (C6, d,  $J_{\text{PC}} = 4.2$ ), 75.4 (C5, d,  $J_{\text{PC}} = 12.2$ ), 56.0 (Anisole-OMe), 44.5 (C4, d,  $J_{\text{PC}} = 4.0$ ), 32.2 (C2), 26.2 (C3), 13.8 (d,  $J_{\text{CP}} = 32.9$ , PMe $_3$ ).

### Synthesis of WTp(NO)(PMe $_3$ )( $\eta^2$ -2,3,4-(3-methoxy-5,6,7,8-tetrahydronaphthalen-2-yl)cyclohex-2-en-1-yl)ium) (6)

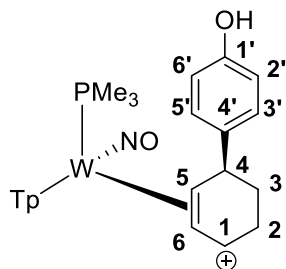
(6)



A solution of **1** (0.070 g, 0.120 mmol) was dissolved in DCM (2 mL) and this solution was cooled to  $-30\text{ }^{\circ}\text{C}$  over a course of 10 min. After allowing this reaction mixture to cool to  $-30\text{ }^{\circ}\text{C}$  an excess of 6-methoxy-teralin (0.460 g, 2.84 mmol) was added and the reaction mixture was allowed to stir at  $-30\text{ }^{\circ}\text{C}$  for 10 min. To this solution was added  $-30\text{ }^{\circ}\text{C}$  chilled HOTf (8 drops) was added to the reaction mixture to generate **3** in situ. The reaction mixture turns to a homogeneous red colored solution from a homogeneous yellow solution after addition of the acid. This reaction mixture was allowed to stir for 16 h at  $-30\text{ }^{\circ}\text{C}$ . The next day the reaction mixture was then added to a solution of stirring diethyl ether (100 mL). Upon addition a vibrant yellow solid precipitates from solution. This solid was then isolated on a fine 15 mL porosity fritted disc, washed with diethyl ether (2 x 10 mL) and allowed to desiccate under static vacuum for 4 h before a mass was taken of the yellow solid (0.057 g, 53.8 %).

CV (DMA)  $E_{p,c} = -1.12\text{ V}$  (NHE). IR:  $\nu(\text{BH}) = 2534\text{ cm}^{-1}$ ,  $\nu(\text{NO}) = 1641\text{ cm}^{-1}$ .  $^1\text{H-NMR}$  (MeCN- $d_3$ ,  $\delta$ ,  $25\text{ }^{\circ}\text{C}$ ): 8.42 (1H, d, Tp3/5), 8.16 (1H, d, Tp3/5), 8.00 (1H, d, Tp3/5), 7.95 (1H, d, Tp3/5), 7.93 (1H, d, Tp3/5), 7.81 (1H, d, Tp3/5), 7.17 (1H, s, 6-methoxy-teralin), 6.68 (1H, s, 6-methoxy-teralin), 6.52 (1H, t, Tp4), 6.51 (2H, overlapping, Tp4 and H4), 6.35 (1H, t, Tp4), 5.35 (1H, t,  $J = 7.5$ , H3), 4.32 (1H, dd,  $J = 7.5, 15.6$ , H2), 4.27 (1H, dd,  $J = 6.2, 5.1$ , H1), 3.77 (3H, s, -OMe), 3.50 (1H, m, H5), 3.31 (1H, dt,  $J = 6.0, 19.8$ , H5'), 2.77 (4H, broad overlapping, 6-methoxy-teralin), 1.79 (4H, broad overlapping, 6-methoxy-teralin), 1.68 (1H, m, H6), 1.18 (1H, m, H6'), 1.02 (9H, d,  $J_{\text{PH}} = 9.9$ ,  $\text{PMe}_3$ ).  $^{31}\text{P-NMR}$  (MeCN- $d_3$ ,  $\delta$ ,  $25\text{ }^{\circ}\text{C}$ ): ( $J_{\text{WP}} = 270$ ).  $^{13}\text{C-NMR}$  (MeCN- $d_3$ ,  $\delta$ ,  $25\text{ }^{\circ}\text{C}$ ): 154.7 (6-methoxy-teralin), 149.3 (Tp3/5), 146.2 (Tp3/5), 143.3 (Tp3/5), 139.5 (3C, overlapping, 2x Tp3/5 and 6-methoxy-teralin), 137.4 (6-methoxy-teralin), 134.6 (Tp3/5), 133.7 (C4), 130.6 (6-methoxy-teralin), 129.6 (6-methoxy-teralin), 112.0 (6-methoxy-teralin), 109.5 (Tp4), 108.9 (Tp4), 108.1 (Tp4), 105.4 (C3, d,  $J_{\text{PC}} = 3.9$ ), 76.4 (C2, d,  $J_{\text{PC}} = 12.6$ ), 56.1 (-OMe), 36.1 (C1), 30.5 (C5), 30.0 (6-methoxy-teralin), 29.3 (6-methoxy-teralin), 26.2 (C6), 24.3 (6-methoxy-teralin), 24.0 (6-methoxy-teralin), 13.6 (d,  $J_{\text{PC}} = 32.6$ ,  $\text{PMe}_3$ ).

#### Synthesis of WTP(NO)(PMe<sub>3</sub>)( $\eta^2$ -5,6-\*4'-hydroxy-1,2,3,4-tetrahydro-[1,1'-biphenyl]-4-ylum) (**7**)

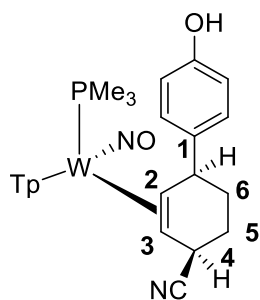


A solution of **1** (0.090 g, 0.155 mmol) was dissolved in DCM (1 mL) and this solution was cooled to  $-30\text{ }^{\circ}\text{C}$  over a course of 10 min. To this solution was added DPhAT (0.054 g, 0.169 mmol) and upon addition the initially homogeneous yellow reaction mixture turns to a homogeneous red colored solution. After allowing this reaction mixture to stir for 5 min at  $-30\text{ }^{\circ}\text{C}$  an excess of  $-30\text{ }^{\circ}\text{C}$  chilled HOTf (5 drops) was added to the reaction mixture to generate **3** in situ. The reaction mixture is still a homogeneous red colored solution. Separately a solution of phenol (0.496 g, 5.27 mmol) was dissolved

in DCM (2 mL) and this reaction mixture was also cooled to  $-30^{\circ}\text{C}$  in a large test tube over a period of 5 min. Next, the solution of **3** was added to the phenol/DCM solution and the reaction mixture was allowed to stir for 2 h. After confirming the formation of a new species by  $^{31}\text{P}$  NMR spectroscopy of an aliquot of the reaction mixture at room temperature, the reaction mixture was then added to a solution of stirring diethyl ether (100 mL). Upon addition a vibrant yellow solid precipitates from solution. This solid was then isolated on a fine 15 mL porosity fritted disc, washed with diethyl ether (3 x 10 mL) and allowed to desiccate under static vacuum for 4 h before a mass was taken of the yellow solid (0.072 g, 56.3 %).

$^1\text{H}$  NMR ( $\text{MeCN-}d_3$ ,  $\delta$ ,  $25^{\circ}\text{C}$ ): 8.41 (1H, d, Tp3B), 8.15 (1H, d, Tp3A), 8.00 (1H, d, Tp5C), 7.95 (1H, d, Tp5B), 7.92 (1H, d, Tp3C), 7.82 (1H, d, Tp5A), 7.25 (2H, m, Phenol- $\text{H3}'/\text{H5}'$ ), 6.85 (2H, m, Anisole- $\text{H2}'/\text{H6}'$ ), 6.53 (1H, buried, H1), 6.52 (1H, t, Tp4B), 6.50 (1H, t, Tp4C), 6.35 (1H, t, Tp4A), 5.37 (1H, t,  $J = 7.16$ , H6), 4.35 (1H, dd,  $J = 7.40$ , 16.1, H5), 3.69 (1H, dd,  $J = 6.24$ , 10.95, H4), 3.49 (1H, m, H2-syn), 3.30 (1H, dt,  $J = 6.23$ , 19.53, H2-anti), 1.76 (1H, m, H3-syn), 1.21 (1H, m, H3-anti), 1.00 (9H, d,  $J_{\text{PH}} = 9.85$ ,  $\text{PMe}_3$ ).  $^{13}\text{C}$  NMR ( $\text{MeCN-}d_3$ ,  $\delta$ ,  $25^{\circ}\text{C}$ ): 156.7 (Phenol-C1), 149.3 (Tp3A), 146.2 (Tp3B), 143.4 (Tp3/5), 140.7 (Tp3/5), 139.6 to 139.5 (3C, 2 overlapping Tp3/5 and Phenol-C4), 134.4 (C1), 129.5 (Phenol-C3/C5), 116.5 (Phenol-C2/C6), 109.5 (Tp4), 108.9 (Tp4), 108.1 (Tp4), 105.5 (C6), 75.6 (C5, d,  $J_{\text{PC}} = 12.2$ ), 44.6 (C4, d,  $J_{\text{PC}} = 3.9$ ), 32.2 (C2), 26.2 (C3), 13.8 (d,  $J_{\text{CP}} = 33.0$ ,  $\text{PMe}_3$ ).  $^{31}\text{P}$  NMR ( $d^6$ -acetone,  $\delta$ ,  $25^{\circ}\text{C}$ ): -12.43. ESI-MS ( $m/z$ , calculated (rel intens, %), **observed** (rel intens, %), ppm,  $(\text{M} + \text{H})^+$ ): 674.1935 (83.10), **674.1936 (82.40)**, 675.1960 (80.48), **675.1960 (80.95)**, 676.1959 (100), **676.1962 (100)**, 677.2000 (44.49), **677.2002 (44.03)**, 678.1992 (83.53), **678.1993 (83.14)**.

#### Synthesis of $\text{W}(\text{NO})(\text{PMe}_3)(\eta^2\text{-2,3-(1S,4R)-4'-hydroxy-1,2,3,4-tetrahydro-[1,1'-biphenyl]-4-carbonitrile})$ (**9**)

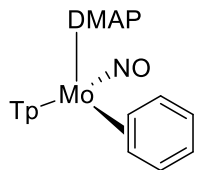


To a large test tube added DCM (1 mL) and allowed the reaction mixture to sit at  $-60^{\circ}\text{C}$  over the course of 5 min. To this added complex **1** (0.040 g, 0.069 mmol) and allowed the reaction mixture to stir for 10 min before adding an excess of HOTf (10 drops to the solution) to in situ generate **3**. Upon addition the reaction mixture turns to a homogeneous blood red solution. Separately phenol (0.283 g, 3.01 mmol) was dissolved in DCM (2 mL) and this mixture was also cooled to  $-60^{\circ}\text{C}$  over a course of 10 min. The dissolved phenol solution was then added to the acidic solution of **3** and allowed to stir for 4 h at  $-60^{\circ}\text{C}$ . After 4 h an excess of NaCN (0.200 g, 4.08 mmol) was added and the reaction mixture, now a homogeneous yellow colored reaction mixture, was allowed to further stir over 20 h at  $-60^{\circ}\text{C}$ . The next day the reaction mixture was extracted from a water/brine solution ( $\sim 100$  mL) with DCM (3 x 50 mL). The DCM fraction was dried over magnesium sulfate and the solvent was removed in vacuo. The resulting yellow film was redissolved in a minimal amount of DCE (2 mL) and added to a solution of stirring pentane (15 mL). The reaction mixture was then allowed to sit at  $-8^{\circ}\text{C}$  over a course of 72 hours to induce precipitation. After this time the organic layer was decanted to reveal a yellow film that was analyzed by  $^1\text{H}$  NMR. No mass was taken given the low mass recovery of this product.



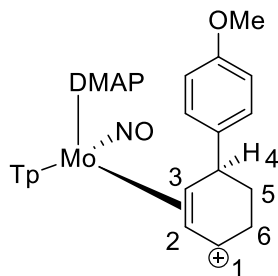
$^1\text{H}$  NMR ( $\text{MeCN-}d_3$ ,  $\delta$ , 25 °C): 8.12 (1H, d, Tp3/5), 8.11 (1H, d, Tp3/5), 7.96 (1H, d, Tp3/5), 7.94 (1H, d, Tp3/5), 7.87 (1H, d, Tp3/5), 7.44 (2H, m, phenol H3/H5), 7.43 (1H, d, Tp3/5), 6.89 (2H, m, phenol-H2'/H6'), 6.41 (1H, t, Tp4), 6.36 (1H, t, Tp4), 6.31 (1H, t, Tp4), 4.12 (1H, t,  $J = 6.6$ , H1), 4.07 (1H, m, H4), 3.80 (3H, s, -OMe), 2.85 (1H, tdc,  $J = 1.6$ , 12.5), 2.02 (1H, m, H6), 1.98 (1H, m, H5), 1.75 (1H, m, H5'), 1.55 (1H, m, H6'), 1.4cc3 (1H, dt,  $J = 2.3$ , 11.5, H3), 1.03c (9H, d,  $J_{\text{PH}} = 8.4$ ,  $\text{PMe}_3$ ).

### Large Scale Synthesis of $\text{MoTp}(\text{NO})(\text{DMAP})(\eta^2\text{-benzene})$ (**10**)



To a 1000 mL oven dried round Erlenmeyer flask was added  $\text{MoTp}(\text{NO})(\text{DMAP})(\eta^2\text{-3,4-}\alpha,\alpha\text{-trifluorotoluene})$  (8.28 g, 0.0165 mmol) followed by anhydrous benzene (1 L, 11.2 mol) and the homogeneous red reaction mixture was allowed to stir over a period of 2.5 h. This reaction mixture was then added to 1 L of stirring hexanes in a 2 L filter flask and the resulting mixture was filtered through a fine 350 mL fine porosity fritted disc. The filtrate from this reaction was then concentrated in vacuo to ~ 1700 mL and a vibrant orange solid was isolated on a new 350 mL fine porosity fritted disc and washed with hexanes (2 x 100 mL). The solvent of the resulting filtrate was then removed in vacuo until ~ 1200 mL of solvent remained upon removal of solvent and cooling more orange solid precipitates from solution. The resulting heterogeneous orange solution was filtered through another fine 350 mL fritted disc to isolate an orange solid and this solid was washed with hexanes (2 x 100 mL) before it too was allowed to desiccate. After several hours of desiccation under dynamic vacuum the orange solids were combined and the  $^1\text{H}$  NMR signals were consistent with those previously reported for **2** (4.94 g, 55%).<sup>5</sup>

### Synthesis of $\text{MoTp}(\text{NO})(\text{DMAP})(\eta^2\text{-2,3-4'-methoxy-1,2,3,4-tetrahydro-[1,1'-biphenyl]-4-ylum}))$ (**12**)



To a solution of DCM (1 mL) complex **10** (0.122 g, 0.220 mmol) was added and this solution was frozen in  $\text{N}_{2(l)}$ . To this solution as added a recently thawed solution of HOTf (10 drops) and the reaction mixture was allowed to thaw at -40 °C over the course of 15 min. This reaction mixture was then added to a standing solution of diethyl ether (15 mL) and this solution as allowed to sit at -40 °C over a period of 16 hours to induce precipitation. The next day a yellow solid had developed form solution. The organic layer was decanted and the solid was dried under active vacuum for 1 h

before the solid was analyzed by  $^1\text{H}$  NMR spectroscopy. Given the obvious signs of decomposition a mass was not taken of the isolated solid.

$^1\text{H}$  NMR (acetone- $d_6$ ,  $\delta$ , 25 °C): 8.29 (3H, overlapping resonances, Tp3/5 and DMAP-H3'/H5'), 8.18 (2H, overlapping d, Tp3/5s), 8.07 (1H, d, Tp3/5), 7.92 (1H, d, Tp3/5), 7.51 (1H, d, Tp3/5), 7.22 (2H, m, anisole-H3/H5), 7.11 (2H, m, DMAP-2/6), 6.85 (2H, m, anisole-H2'/H6'), 6.60 (1H, t, Tp4), 6.48 (1H, t, Tp4), 6.46 (1H, broad t, H1), 6.28 (1H, t, Tp4), 6.16 (1H, t,  $J = 7.25$ , H2), 4.88 (1H, dc,  $J = 7.00$ , H3), 4.03 (1H, dd,  $J = 4.00$ , 6.02, H4), 3.76 (3H, s, -OMe), 3.50 (1H, m, H6), 3.34 (6H, s, -NMe $_2$ ), 3.16 (1H, m, H6'), 2.03 (1H, m, H5), 1.56 (1H, m, H5').

## References

1. Kündig, E. P.; Pape, A., Dearomatization via  $\eta^6$ -Arene Complexes. In *Transition Metal Arene  $\pi$ -Complexes in Organic Synthesis and Catalysis*, Kündig, E. P., Ed. Springer Berlin Heidelberg: Berlin, Heidelberg, 2004; pp 71-94.
2. Liebov, B. K.; Harman, W. D., Group 6 Dihapto-Coordinate Dearomatization Agents for Organic Synthesis. *Chemical Reviews* **2017**, *117* (22), 13721-13755.
3. Meiere, S. H.; Keane, J. M.; Gunnoe, T. B.; Sabat, M.; Harman, W. D., Binding and Activation of Aromatic Molecules by a Molybdenum  $\pi$ -Base. *Journal of the American Chemical Society* **2003**, *125* (8), 2024-2025.
4. Wilson, K. B.; Smith, J. A.; Nedzbala, H. S.; Pert, E. K.; Dakermanji, S. J.; Dickie, D. A.; Harman, W. D., Highly Functionalized Cyclohexenes Derived from Benzene: Sequential Tandem Addition Reactions Promoted by Tungsten. *The Journal of Organic Chemistry* **2019**, *84* (10), 6094-6116.
5. Myers, J. T.; Smith, J. A.; Dakermanji, S. J.; Wilde, J. H.; Wilson, K. B.; Shivokevich, P. J.; Harman, W. D., Molybdenum(0) Dihapto-Coordination of Benzene and Trifluorotoluene: The Stabilizing and Chemo-Directing Influence of a CF $_3$  Group. *Journal of the American Chemical Society* **2017**, *139* (33), 11392-11400.
6. Myers, J. T.; Shivokevich, P. J.; Pienkos, J. A.; Sabat, M.; Myers, W. H.; Harman, W. D., Synthesis of 2-Substituted 1,2-Dihydronaphthalenes and 1,2-Dihydroanthracenes Using a Recyclable Molybdenum Dearomatization Agent. *Organometallics* **2015**, *34* (14), 3648-3657.
7. Graham, Peter, PhD Dissertation, UVA, **2005**

## Chapter 9

# Experiments and Direct Dynamics Simulations Reveal Network of Reaction Pathways for $\text{WTp}(\text{NO})(\text{PR}_3)(\eta^2\text{-arene})$ to Aryl Hydride Equilibrium

## 9.1. Introduction

Transition-metal mediated activation of arene C-H bonds has become an extremely useful organometallic transformation.<sup>1-7</sup> For oxidative addition, the reaction mechanism is typically viewed as the linear sequence of dihapto  $\pi$  coordination followed by C-H  $\sigma$  bond cleavage to generate an aryl hydride (**Scheme 9.1a**). For  $\eta^2$ -arene complexes, coordination ranges from relatively weak acid-base adducts<sup>8</sup> to metal-arene bonding fortified through significant  $\pi$  interactions. Depending on the metal, supporting ligands, and arene substrate, experiments either observe the  $\eta^2$ -arene complex, the aryl hydride, or in rare circumstances an equilibrium of both.<sup>9-13</sup>

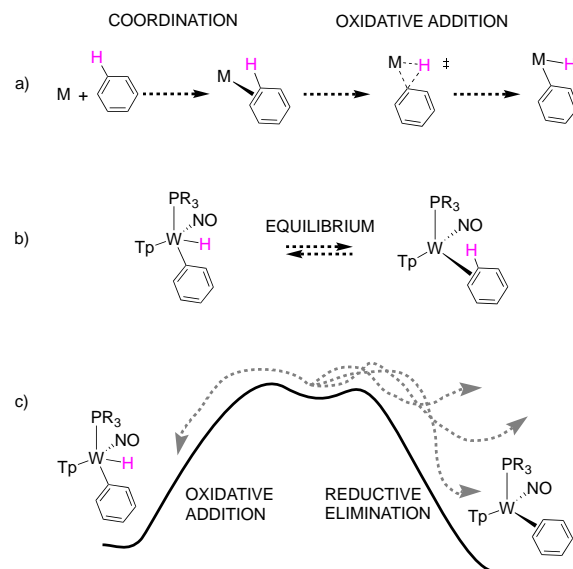
For example, Jones showed that at 60 °C,  $\text{RhCp}^*(\text{PMe}_3)(\eta^2\text{-naphthalene})$  exists in a 1:2 equilibrium ratio with  $\text{RhCp}^*(\text{PMe}_3)(\text{naphthyl})(\text{H})$ .<sup>14-15</sup> This ratio can be altered by adjusting auxiliary ligands or temperature.<sup>15</sup> However, for benzene, only the phenyl hydride was observed. In contrast, electron-rich octahedral  $d^6$  complexes  $[\text{Os}(\text{NH}_3)_5]^{2+}$ ,<sup>16</sup>  $\{\text{ReTp}(\text{CO})(\text{L})\}$ ,<sup>17</sup> and  $\{\text{WTp}(\text{NO})(\text{PMe}_3)\}$ <sup>10</sup> resist the formation of a seven-coordinate phenyl hydride. Therefore,  $\eta^2$ -benzene complexes are not only generally observed but are sufficiently stable that organic reactions can be carried out on the bound arene.<sup>10, 16-17</sup> In the case of the tungsten system  $\text{WTp}(\text{NO})(\text{PMe}_3)(\eta^2\text{-benzene})$  a second set of signals (~1:10 in acetone at 0 °C) in the <sup>1</sup>H NMR spectrum was observed that included a hydride signal at 9.32 ppm ( $J_{\text{PH}} = 101$  Hz suggesting that this was a rare case of an  $\eta^2$ -benzene/phenyl hydride equilibrium.<sup>18</sup>

The oxidative addition reaction sequence of  $\eta^2$ -arene coordination followed by C-H bond cleavage is supported by the corresponding equilibrium observations. Experimental kinetic isotope effects (KIEs) have also been measured as evidence supporting the connection of intermediates prior to aryl hydride structures generated from oxidative addition.<sup>19-20</sup> However, in many circumstances it is not known whether the intermediate is exclusively an  $\eta^2$ -arene complex or in combination with a  $\sigma$ -type complex. Importantly, Bergman, Field, and others have demonstrated that dihapto  $\pi$ -coordination is not always a necessary precondition to C-H oxidative addition, at least for ethylene.<sup>21</sup>

Herein, we report that for the system  $\text{WTp}(\text{NO})(\text{PMe}_3)(\eta^2\text{-benzene})$ , the replacement of  $\text{PMe}_3$  by  $\text{P}(\text{n-Bu})_3$  shifts the benzene/phenyl hydride equilibrium to a 1:1 ratio ( $0^\circ\text{C}$ ), making it an ideal candidate for a more in-depth study of this process. Hence, below we examine the details of this equilibrium using  $^1\text{H}$  NMR NOESY experiments and thermodynamic data for benzene and substituted benzenes (**Scheme 9.1b**). Significantly, the hydride resonance corresponding to  $\text{WTp}(\text{NO})(\text{P}(\text{n-Bu})_3)(\text{Ph})(\text{H})$  is observed to undergo spin saturation exchange with all six proton resonances of the dihapto-coordinate isomer. Additionally, there is rapid ring-walking around the benzene  $\pi$  framework with no observable KIE or equilibrium isotope effect (EIE). Examination of several electron-rich and electron-poor arene substrates also reveal intrafacial and interfacial (face-flip)  $\eta^2$ -ring walking.

Density functional theory (DFT) calculations are used to outline the energy landscape for  $\text{WTp}(\text{NO})(\text{PMe}_3)(\text{C},\text{C}\text{-}\eta^2\text{-$

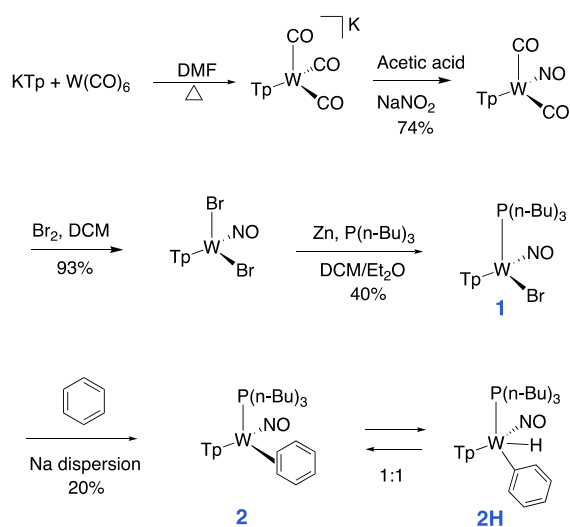
benzene) to  $\text{WTp}(\text{NO})(\text{PMe}_3)(\text{Ph})(\text{H})$  isomerization. These calculations further show that on the intrinsic reaction coordinate (IRC),<sup>22</sup> the  $\sigma$ -complex intervenes between the phenyl hydride and  $\text{C},\text{C}\text{-}\eta^2$  form. Additionally, these static DFT calculations identify a direct C-H coordination transition state as well as a long-range noncovalent W-benzene complex. Significantly, the energy surface for  $\eta^2$ -benzene to phenyl hydride isomerization is relatively flat and contains several weakly coordinating benzene intermediates. Therefore, we used DFT quasiclassical dynamics simulations to examine transition state connections. This revealed a network of isomerization pathways with non-IRC connections and nonstatistical intermediates (**Scheme 9.1c**).



**Scheme 9.1.** a) Typically proposed linear sequence for oxidative addition of benzene. b) Here we report experimental details for the  $\text{WTp}(\text{NO})(\text{PR}_3)(\eta^2\text{-arene})/\text{WTp}(\text{NO})(\text{PR}_3)(\text{H})(\text{Ar})$  equilibrium and c) static DFT landscape and quasiclassical dynamics simulations that reveal a network of isomerization pathways with non-IRC connections and nonstatistical intermediates.

## 9.2 Synthesis and equilibrium studies.

Using a modified version of a literature procedure,<sup>23</sup> WTp(NO)Br<sub>2</sub> was prepared from W(CO)<sub>6</sub> (**Scheme 9.2**). Combining WTp(NO)(Br)<sub>2</sub> and P(n-Bu)<sub>3</sub> with zinc dust in a DCM/ether solvent mixture resulted in formation of WTp(P(n-Bu)<sub>3</sub>)(NO)(Br) (**1**). If WTp(NO)(Br)<sub>2</sub> and P(n-Bu)<sub>3</sub> are combined in DCM with no reducing agent, **1** is still detected (< 10%) and this observation suggests a possible disproportionation reaction. Crystals suitable for X-ray diffraction were grown of this paramagnetic complex via vapor diffusion of ether into a DCM solution of **1**, and details are included in the supplementary material. We also characterized this complex by cyclic voltammetry and IR spectroscopy. There is a chemically reversible couple with  $E_{1/2} = -1.36$  V (W<sup>I</sup>/W<sup>0</sup>) as well as an anodic peak of similar size, with  $E_{p,a} = 0.44$  V (W<sup>I</sup> → W<sup>II</sup>). An infrared spectrum shows a nitrosyl stretch absorption of 1578 cm<sup>-1</sup>, and this feature along with the electrochemical data are similar to those reported previously for WTp(PMe<sub>3</sub>)(NO)(Br).<sup>23</sup>



**Scheme 9.2.** Synthesis of benzene complex (**2**) and its phenyl hydride isomer (**2H**).

Treatment of **1** with sodium dispersed in benzene yields complex **2** isolated in 20% yield after chromatography. The greater solubility of P(n-Bu)<sub>3</sub> compared to PMe<sub>3</sub> led to more rapid conversion of **1** to **2/2H** (4 h), even with lower amounts of sodium,<sup>23</sup> compared to the PMe<sub>3</sub> analog. Complex **2** features an anodic wave in a cyclic voltammogram at  $E_{p,a} = -0.16$  V, which is consistent with the  $\eta^2$ -bound benzene complex WTp(NO)(PMe<sub>3</sub>)(benzene).<sup>23</sup> NMR analysis confirmed the identity of **2** as WTp(NO)(P(n-Bu)<sub>3</sub>)( $\eta^2$ -benzene). A second set of NMR signals in the solution of **2** indicates the presence of the phenyl hydride isomer WTp(NO)(P(n-Bu)<sub>3</sub>)(H)(C<sub>6</sub>H<sub>5</sub>) (**2H**). The phenyl hydride features a doublet at 9.62 ppm ( $J_{PH} = 97.3$  Hz) that is accompanied by <sup>183</sup>W satellites ( $J_{WH} = 32.1$  Hz). At 25 °C, **2** has a substitution half-life ( $t_{1/2} = 4$  min) that is significantly less than its PMe<sub>3</sub> complex (cf.  $t_{1/2} = 66$  min).<sup>23</sup> A weak IR absorption observed at 1989 cm<sup>-1</sup> (cf. DFT prediction

1988  $\text{cm}^{-1}$ ) of an isolated solid of **2/2H** is tentatively assigned to a W-H vibrational mode. Even as a solid stored at  $-30\text{ }^\circ\text{C}$ , **2/2H** material decomposes to uncharacterized paramagnetic materials after several weeks.

The equilibrium ratio of **2:2H** in benzene- $d_6$  is 1:1, which contrasts with the  $\sim 10:1$  ratio found for the  $\text{PMe}_3$  analog.<sup>18</sup> When the isolated solid of **2/2H** obtained from an ether/pentane precipitation is added to a cold solution ( $\sim 10\text{ }^\circ\text{C}$ ) of benzene- $d_6$  and monitored we observed an initial ratio of **2:2H** of 1:3. Over time the equilibrium 1:1 ratio is restored. These observations suggest that this solid was enriched in the hydride isomer, possibly to the exclusion of the dihapto-coordinated arene.

Unfortunately, attempts to grow crystals of **2H** suitable for X-ray diffraction were unsuccessful.

To understand the structures and equilibrium of **2/2H**, we carried out  $^1\text{H}$  NMR NOESY experiments in acetone- $d_6$  solution (**Figure 9.1**). The  $\eta^2$ -benzene complex at  $0\text{ }^\circ\text{C}$  shows spin-saturation transfer between this arene complex and the phenyl hydride, indicating that these two species are in a dynamic equilibrium. Specifically, the tungsten-hydride proton undergoes chemical exchange with every benzene ring proton of the dihapto-coordinated isomer, and this observation demonstrates that interconversion of **2** and **2H** occurs on the seconds timescale at  $0\text{ }^\circ\text{C}$ . An exchange process was also detected between hydrogens of the  $\eta^2$ -benzene ligand in **2**. A similar ring-walk was observed for the  $\text{PMe}_3$  analog.

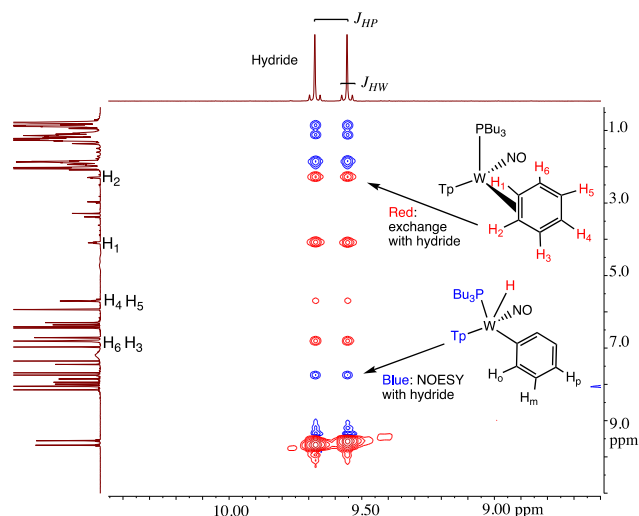
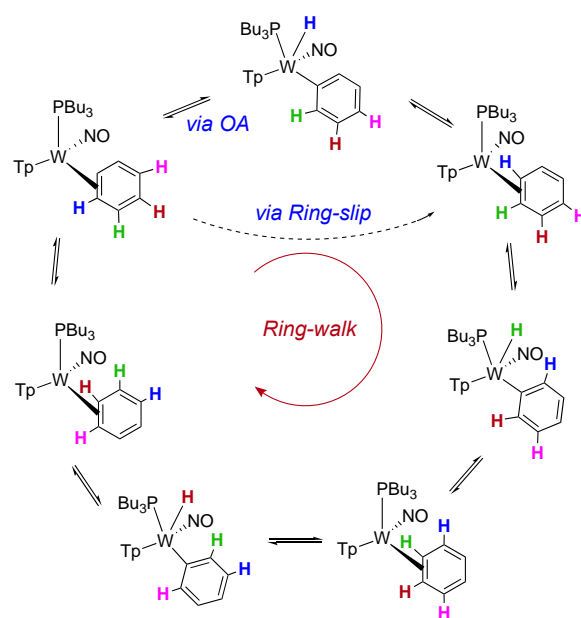


**Figure 9.1.**  $^1\text{H}$  NMR spectrum of the hydride region and its NOESY correlations of **2/2H**.

Using the H<sub>1</sub> proton for **2** and line-broadening techniques, the Gibbs free energy of activation barrier for hydrogen exchange in **2** was determined to be 16 ± 2 kcal/mol. Similar correlation intensities in the NOESY data for both the benzene ring walk (e.g., H<sub>1</sub> of **2** ⇌ H<sub>6</sub> of **2**) and phenyl hydride (e.g., W-H of **2H** ⇌ H<sub>1</sub> of **2**) exchanges suggest that these rates are similar, and may be the same. Using Tp4 protons that distinguish **2** from **2H**, a free energy of activation ( $\Delta G^\ddagger$ ) for the oxidative cleavage from **2** to **2H** was determined to be 15 ± 2 kcal/mol at 44 °C. Although this value is statistically identical to that determined for the ring walk of **2**, these data do not rule out an alternative mechanism in which the tungsten moves from 1,2- $\eta^2$  to 2,3- $\eta^2$  *without* oxidative cleavage of the benzene C-H bond. The ring-walk mechanism via oxidative cleavage followed by reductive coupling, and the resulting hydrogen exchange, is outlined in **Scheme 9.3**. This scheme also illustrates a potential direct exchange pathway without oxidative cleavage and reductive coupling, which is termed ring-slip (i.e., intrafacial isomerization). We note that NOESY data recorded for the deuterated analog W Tp(NO)(P(n-Bu)<sub>3</sub>)( $\eta^2$ -benzene-*d*<sub>6</sub>) (**2-d**<sub>6</sub>) show correlation intensities resulting from exchange for the Tp ring protons that appear practically identical to what was observed for **2**. This observation suggests that there is a negligible kinetic or thermodynamic isotope effect for the ring-walk.



**Scheme 9.3.** Isomerization and spin-saturation-exchange (represented by blue, green, red, and pink colored hydrogens) for the phenyl hydride complex (**2H**) and its benzene isomer (**2**).

### 9.3 Static DFT landscape for $\eta^2$ -benzene and phenyl hydride equilibrium

NOESY experiments established the dynamic equilibrium of the  $\eta^2$ -benzene (**2**) and phenyl hydride (**2H**) complexes. Because the measured barriers for hydrogen exchange for the  $\eta^2$ -benzene and the phenyl hydride complex are similar, this measurement was not able to determine if the ring walking mechanism occurs only via oxidative cleavage and reductive coupling or if there is also a ring slip mechanism. Additionally, the time



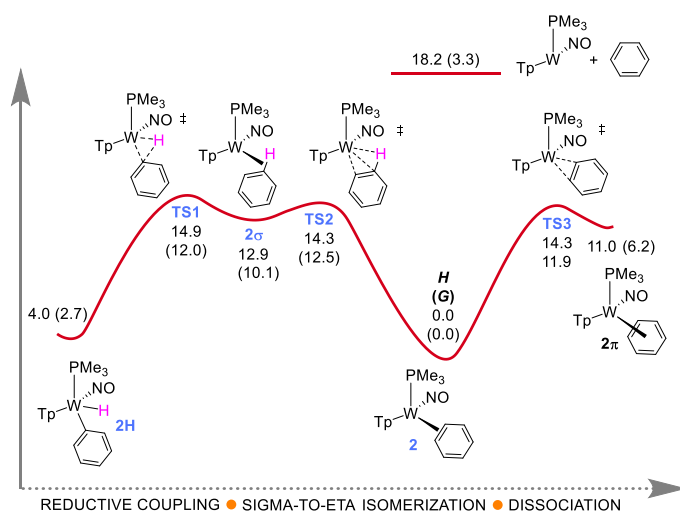
scale of the NMR experiments is too long to capture key intermediates that may be only briefly sampled during the exchange process. Therefore, we used DFT calculations for the  $\text{PMe}_3$  analog to explore intermediate and transition-state structures that connect the  $\eta^2$ -benzene and phenyl hydride complexes.

All stationary points were optimized with M06/6-31G\*\*[LANL2DZ for W] in Gaussian 16. Energies reported are M06/Def2-TZVPD// M06/6-31G\*\*[LANL2DZ]. Structures were confirmed as minima or transition states by vibrational frequency analysis. All transition-state structures have a single negative vibrational frequency. Rigid-rotor-harmonic-oscillator thermochemical corrections at 298 K and 1 atm were added using the default implementation in Gaussian 16. Optimizations and single point calculations were performed using the SMD continuum solvent model for acetone, which provided an estimate of  $\Delta G_{\text{solv}}$  that was added to gas-phase enthalpy and Gibbs free energy values. All calculations were pursued by Anna Schouten under the guidance of Professor Dan Ess at BYU.

The static M06 enthalpy landscape for  $\text{WTp}(\text{NO})(\text{PMe}_3)(\eta^2\text{-benzene})$  (model for **2**) in equilibrium with  $\text{WTp}(\text{NO})(\text{PMe}_3)(\text{H})(\text{Ph})$  (model for **2H**) is displayed in **Scheme 9.4**. We modeled the  $\text{PBU}_3$  as  $\text{PMe}_3$  because we later report extremely time intensive direct dynamics simulations. However, as noted above, previous experiments we reported for this  $\text{PMe}_3$  complex. Similar to previous computational studies, we located a reductive coupling transition state **TS1** with an enthalpy barrier of 9.3 kcal/mol and Gibbs barrier of 10.9 kcal/mol relative to **2H**. From **2**, this oxidative cleavage transition state **TS1** has an enthalpy barrier of 14.9 kcal/mol, which is very close to the experimental NMR barrier estimate (15.1 kcal/mol at 317 K). As expected, this reductive coupling/oxidative cleavage transition state features a partial W-Ph bond along with simultaneous rearrangement of W-H and C-H bonding (**Figure 9.2**). IRC calculations indicate that **TS1** connects **2H** to a  $C,H\text{-}\eta^2$  complex ( $\sigma$ -complex, **2 $\sigma$** ). Importantly, the energy surface surrounding this  $\sigma$ -complex is extremely flat. While we located a  $C,H\text{-}\eta^2$  to  $C,C\text{-}\eta^2$  isomerization transition **TS2**, and IRC calculations suggest that it connects **2 $\sigma$**  with the  $\eta^2$ -benzene complex **2**, the transition-state reaction coordinate motion vibrational frequency is only -70  $\nu$ . Overall, while this section of the energy landscape suggests that there is an

intervening  $\sigma$ -complex connecting the phenyl hydride and  $\eta^2$ -benzene complexes the flat energy surface profile suggests it might have a very short lifetime or have nonstatistical population. We also located the transition state for the W-Ph bond rotation of **2H**. The enthalpy barrier for this process from **2H** is only 12.4 kcal/mol, which indicates rapid W-Ph rotation compared to reductive coupling through **TS1**. Hence, this sequence provides a mechanism for *interfacial* isomerization (face-flip).

In addition to locating the stationary points connecting **2H** and **2**, we also searched for structures that could potentially describe direct benzene coordination/dissociation to/from WTp(NO)(PMe<sub>3</sub>). We located coordination transition state **TS3** (Scheme 9.4 and Figure 9.2). Relative to **2**, the enthalpy barrier for **TS3** is 14.3 kcal/mol, which is a similar barrier height to **TS2**. As with **TS2**, the energy surface region surrounding **TS3** is very flat. This is confirmed with the transition-state reaction coordinate motion having a negative vibrational frequency of only -106  $\nu$ . While IRC calculations tentatively suggest that in one direction **TS3** connects to  $\eta^2$ -benzene **2**, the opposite direction was significantly less clear. It is unlikely that **TS3** connects to separated benzene and WTp(NO)(PMe<sub>3</sub>) because these species are ~7 kcal/mol higher in enthalpy than **TS3**. However, on the Gibbs surface separated species are lower in energy than **TS3**, but this is likely due to an overestimate of translational entropy. Therefore, we searched for another possible WTp(NO)(PMe<sub>3</sub>)-benzene complex. This led to the location of the weak coordination complex **2 $\pi$** . In this complex, the W-C interaction distances are on average 3.3 Å (Figure 9.3a), the C-C bond lengths within the aromatic ring are all roughly equal to the free aromatic 1.39 Å), and the C-C axis of the bound carbons is now parallel to the W-NO axis. In contrast, for **2** the C-C axis is parallel to the W-P axis in order for there to be a backbonding interaction with the  $d_{\pi}$  orbital that does not interact with the nitrosyl ligand. These features suggested to us that the  $\eta^2$ -benzene complex **2** is a tight charge-transfer (orbital) interaction complex with bonding and backbonding interactions while **2 $\pi$**  is likely held together through dispersion interactions.



**Scheme 9.4.** DFT enthalpy and Gibbs landscape for isomerization of phenyl hydride to  $\eta^2$ -benzene complex. The  $\text{PBU}_3$  groups of **2** and **2H** were modeled as  $\text{PMe}_3$ . Enthalpies reported in kcal/mol.

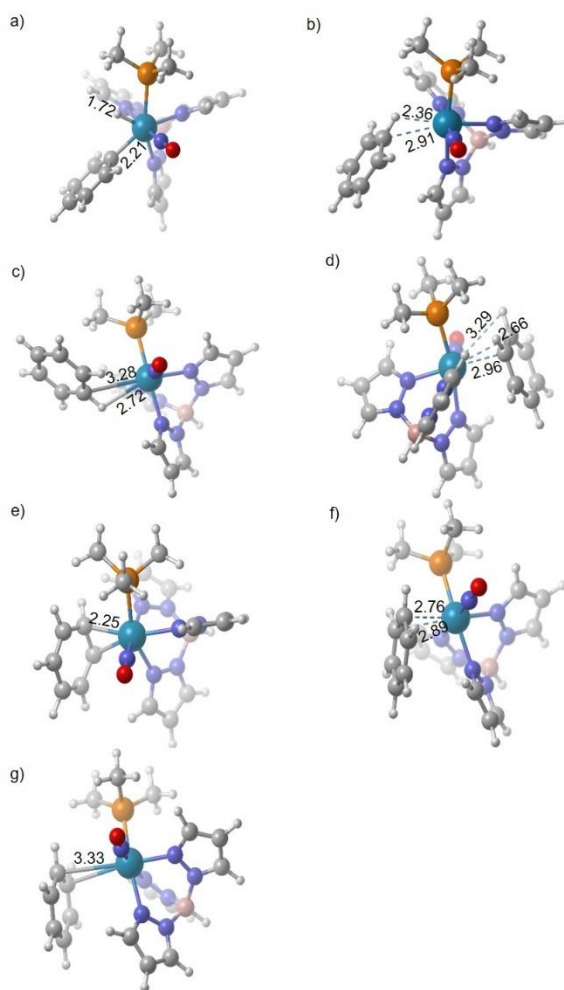


**Figure 9.2.** M06 ground state, intermediate, and transition-state structures for  $\text{WTp}(\text{NO})(\text{PMe}_3)(\eta^2\text{-benzene})$  equilibrium with  $\text{WTp}(\text{NO})(\text{PMe}_3)(\text{H})(\text{Ph})$ . a) **2H** b) **TS1** c) **2σ** d) **TS2** e) **2** f) **TS3** g) **2π**. The  $\text{PBU}_3$  groups of **2** and **2H** were modeled as  $\text{PMe}_3$ . Distances reported in Å.

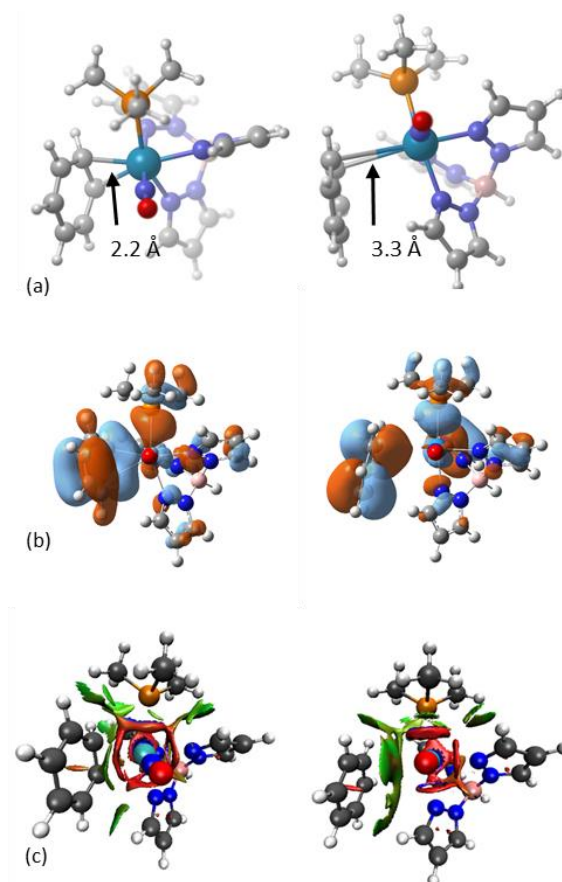


**Figure 9.3.** a) Structure, b) molecular orbitals, and c) noncovalent interaction plot comparisons of  $\text{WTp}(\text{NO})(\text{PMe}_3)(\eta^2\text{-benzene})$  (**2**) with the elongated  $\text{WTp}(\text{NO})(\text{PMe}_3)\text{-benzene}$  complex ( $2\pi$ ).

Indeed, Figure 3b shows that only in the  $\eta^2$  complex is there significant frontier orbital overlap between benzene and the W metal center. **Figure 9.3c** compares the noncovalent interaction plots (using NCIPLOT) between these two complexes. This shows that the noncovalent interaction significantly increases as the W-benzene distance increases. An energy decomposition analysis using the absolutely localized molecular orbital method in Q-Chem confirmed that 2/3 of the W-benzene interaction in  $2\pi$  is due to dispersion. In contrast, in **2** charge transfer orbital interactions dominate the interaction stabilization (see Chapter 9 Appendix for values).

Although the calculations were performed on the  $\text{PMe}_3$  system (vide supra), calculations were also performed using  $\text{PBU}_3$  for **2** and **2H**, and  $\Delta G$  between these two species improved from 2.7 to 1.3 kcal/mol at 298 K. The latter value is close to experimental observation ( $\Delta G \sim 0$  at 273 K).<sup>24</sup> We also examined other functionals for Gibbs energy difference between **2** and **2H**. Interestingly, another DFT method that is typically

accurate for transition-metal complexes,  $\omega$ B97X-D, showed a lower energy for **2H** over **2** by slightly more than 1 kcal/mol.

#### 9.4 Quasiclassical direct dynamics simulations

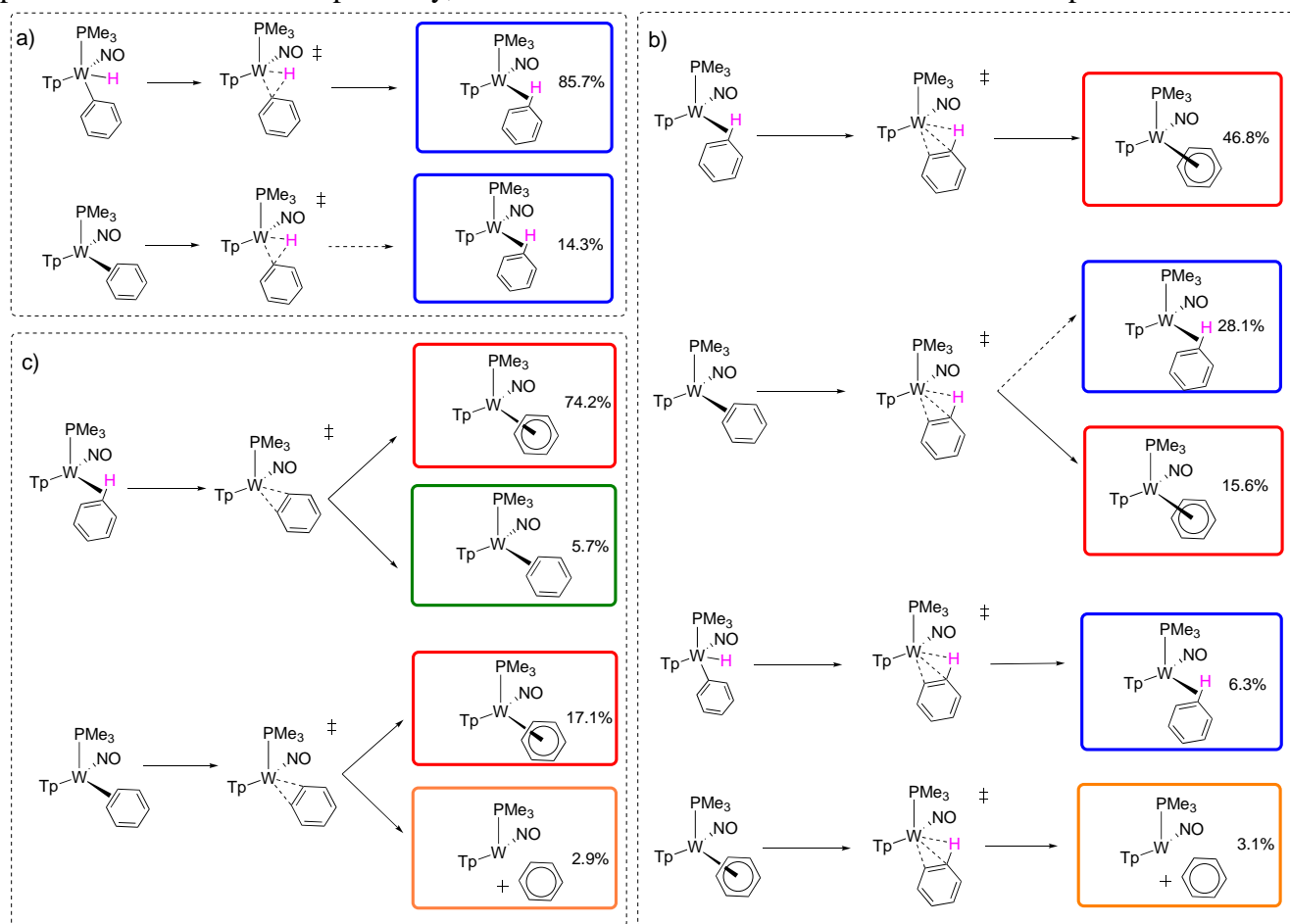
While the energy landscape connecting the phenyl hydride **2H** with the  $\eta^2$ -benzene **2** indicates that there is an intervening  $\sigma$ -complex intermediate and a  $C,H-\eta^2$  to  $C,C-\eta^2$  isomerization transition state, the very flat shape of this surface suggests that there might be non-IRC motion and nonstatistical sampling of these structures. Also, IRC calculations were not definitive about the connection from **2** going through **TS3**. Therefore, we carried out quasiclassical trajectory calculations with M06/6-31G\*\*[LANL2DZ]. Trajectories were initialized and propagated in forward and reverse directions from all transition states using local mode and thermal sampling that included zero-point energy at 273 K. Trajectories were propagated in mass-weighted Cartesian velocities with an approximate time step of 1 femtosecond (fs). For **TS2** and **TS3**, >50 trajectories were propagated in both forward and reverse directions to ensure reactive connection. For **TS1** >10 trajectories were run.

This trajectory analysis revealed several unexpected non-IRC connections where a transition state can lead to multiple products in each direction. The SI gives details about all trajectories. **Scheme 9.5** outlines all the unique reaction trajectories that proceeded through **TS1**, **TS2**, and **TS3**. **Scheme 9.5** also gives the relative percentage of each pathway that utilizes each of these transition states.

On the static energy surface shown in **Scheme 9.4**, IRC calculations indicate that **TS1** only connects the phenyl hydride with **2 $\sigma$** . In accord with this IRC perspective, all trajectories connect **TS1** with **2 $\sigma$** . 86% of all trajectories showed **2H** $\rightarrow$ **TS1** $\rightarrow$ **2 $\sigma$**  connection. For the direction of **TS1** to **2H**, we did not generally observe W-Ph bond rotation and therefore this rotation is not coupled with the reductive coupling process. Unanticipated, approximately 14% of trajectories showed **TS1** connecting the  $\sigma$ -complex and the  $C,C-\eta^2$ -benzene complex. This demonstrates that the weak  $\sigma$ -complex, or the energy surface surrounding it, provides a pathway branching point for reductive coupling/oxidative cleavage and  $\pi$  coordination. This also suggests

that during the isomerization mechanism after **TS1** there will be formation of both **2 $\sigma$**  and **2** and only the  $C,C$ - $\eta^2$ -complex is likely to be observed on the NMR time scale.

The static DFT surface indicates that **TS2** is slightly lower in energy than **TS1**. Therefore, during the isomerization process **2 $\sigma$**  will not only return to **TS1** but will also achieve **TS2**. While on the static surface the IRC suggests that **TS2** connects **2 $\sigma$**  with **2**, the energy surface surrounding **TS2** is flat and dynamical effects are likely to impact pathways leading to and from **TS2**. Indeed, our trajectories revealed five unique reaction pathway connections that involve **TS2** (**Scheme 9.5b**). In addition to these five connected reaction pathways, nearly half of all trajectories propagated showed recrossing, which is perhaps not unexpected for a very flat energy surface. Recrossing trajectories were not considered in the relative percentages of reaction pathways reported in **Scheme 9.5**. Importantly, the five connections shown in **Scheme 9.5b** represent the first major



**Scheme 9.5.** Outline of trajectory connections to and emanating from a) **TS1**, b) **TS2**, and c) **TS3**. Percentages are the relative amount of each pathway that utilize these transition states. Solid lines represent reaction pathways identified in the forward direction and dotted arrows represent connections identified in the reverse direction.

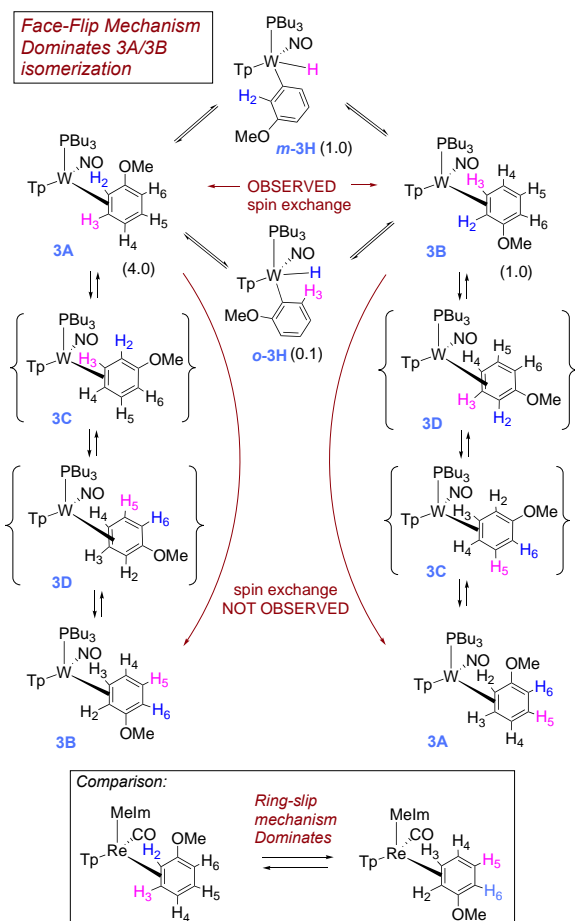
connection for **TS2**. Many of the structures sampled from **TS2** evolved further. For example, some trajectories rotated between **2 $\sigma$**  and **2 $\pi$**  while other trajectories showed rotation of **2 $\sigma$**  and **2 $\pi$**  where multiple carbon and hydrogen atoms encounter the W metal center.

Unexpectedly, the major reaction pathway that accounts for ~50% of the trajectories involves conversion of **2 $\sigma$**  to **TS2** and then to **2 $\pi$** . However, because this pathway leads to benzene that is loosely bound to the W metal center it is unclear if this pathway would be as significant if modeled with explicit solvent. The next significant trajectory pathway accounts for >25% of trajectories and is the IRC-identified  $\sigma$ -to-C,C- $\eta^2$  pathway. We note that *this pathway along with the microscopic reverse provides a mechanism for intrafacial isomerization (ring-slip) that does not require C-H cleavage*. Roughly similar in magnitude, ~15% of the trajectories connected **2**→**TS2**→**2 $\pi$** . This connection with **2** is perhaps not surprising since the W- $\pi$  interaction in **2** is significantly stronger than W- $\sigma$  interaction in **2 $\sigma$** . Two other pathways account for ~10% of the trajectory connections. These include **2H**→**TS2**→**2 $\sigma$**  and **2 $\pi$** →**TS2**→[WTp(NO)(PMe<sub>3</sub>) + benzene]. This later reaction pathway leading to benzene dissociation was unexpected and, similar to connections to **2 $\pi$** , might be significantly influenced by explicit solvation spheres. We note that the experimental rate of benzene ring-walking (seconds timescale) is much faster than for benzene displacement by either benzene-*d*<sub>6</sub> or acetone-*d*<sub>6</sub> (hours timescale).

The static DFT surface indicates that when the  $\eta^2$ -benzene complex is formed there is a nearly equal barrier for going towards **TS2** as there is to achieve **TS3**. This suggests that during the isomerization process **TS3** will also be sampled. Similar to trajectories for **TS2**, trajectories for **TS3** showed ~1/3 recrossing. Perhaps unexpected, for the fully connected reactive trajectories, the major pathway shown in Scheme 5c is **2 $\sigma$** →**TS3**→**2 $\pi$** , which accounts for nearly 75% of all connections. Only 17% of the trajectories connect the  $\eta^2$ -benzene complex **2** with **2 $\pi$**  through **TS3**. This indicates that **TS3** should not be interpreted as a direct  $\pi$  coordination transition state, but rather a general coordination transition state where collision can lead to either

$\sigma$  or  $\pi$  type coordination. Also important, similar to trajectories for **TS2**, trajectories from **TS3** moved through other intermediates after arriving at either **2 $\sigma$**  or **2 $\pi$**  and occasionally continued on to **2** or **2H**.

Overall, the static DFT calculations suggest that during the isomerization process there is access to **TS1**, **TS2**, and **TS3**. The dynamics trajectories further revealed all of these transition states provide a complex



**Scheme 9.6.** The interconversion of **3A** and **3B** occurs through C-H insertion for anisole complex **3**. Blue and pink colored hydrogens indicate observed or expected spin saturation exchange for each mechanism.

network for interconversion of **2H** with **2 $\sigma$** , **2**, and **2 $\pi$** . While these calculations indicate pathways for ring-slip that do not require C-H oxidative addition, the same is not true for face-flipping, which appears to require C-H scission followed by rotation of the phenyl-W bond.

## 9.5 Equilibrium Dynamics of Anisole

We also examined substituent effects on the  $\eta^2$ -benzene to phenyl hydride equilibrium. Reduction of **1** with sodium dispersion in neat anisole led to the formation of WTp(NO)(P(n-Bu)<sub>3</sub>)( $\eta^2$ -2,3-anisole) (**3**) isolated as a 4:1 mixture of two dihapto-bound coordination diastereomers **3A**(4) and **3B** (1) along with two aryl hydride species ***o*-3H** (0.1) and ***m*-3H** (1) (**Scheme 9.6**). Spin saturation exchange processes observable in NOESY data showed an equilibrium between all four isomers of the anisole complex **3** in solution.

In particular, NOESY data suggests that diastereomers **3A** and **3B**, which are both coordinated 2,3- $\eta^2$ , interconvert with both C2 (***o*-3H**) and C3 (***m*-3H**) aryl-hydride isomers (**Scheme 9.6**). Significantly, there is no exchange between the *ortho* proton H<sub>2</sub> in **3A** with the *ortho* proton H<sub>6</sub> in either **3A** or **3B**. Likewise, the only exchange observed between meta protons is H<sub>3</sub> of **3A** with H<sub>3</sub> of **3B**. Taken together, this indicates that for the



$\eta^2$ -anisole complex **3**, the interconversion of diastereomers **3A** and **3B** occurs via a face-flip (interfacial) isomerization, which is significantly faster than a purported ring-slip (intrafacial) isomerization.

For an isomerization pathway from **3A** to **3B** involving ring-walk (Scheme 9.6), the system would have to pass through the 3,4- $\eta^2$  intermediates, **3C** and **3D**, but DFT calculations indicate that these isomers are both 3.4 kcal/mol less stable (enthalpy) as a result of the methoxy group's enhanced  $\pi$ -interaction with the uncoordinated portion of the arene.<sup>25</sup> All DFT energies presented for anisole were calculated with M06/6-31G\*\*[LANL2DZ].

In contrast to that observed for **3**, the complex ReTp(CO)(MeIm)( $\eta^2$ -anisole) undergoes intrafacial isomerization (ring-slip) roughly four times faster than interfacial isomerization (face-flip).<sup>26</sup> Perutz et al. showed similar concurrent ring-slip and C-H insertion processes for the RhCp(PMe<sub>3</sub>)(naphthalene) system, where two  $\eta^2$ -naphthalene complex diastereomers were related by a ring-walk as well as being equilibrated with their aryl hydride forms.<sup>27</sup> In this system, the free energy barrier to C-H insertion (cf. 19.9 kcal/mol; 50 °C; RhCp\*PMe<sub>3</sub>)<sup>15</sup> is likely to be greater than that of the ring-walk (17.6 kcal/mol; 300 °C, RhCpPMe<sub>3</sub>)<sup>27</sup> and therefore, like the rhenium system, the aryl-hydride is unlikely to be involved in the ring-walk mechanism (We note that in the RhCp(PMe<sub>3</sub>)(naphthalene) system, a purported face-flip process is undetectable because the {RhCp(PMe<sub>3</sub>)} moiety has a plane of symmetry). As is the case for the anisole system **3**, in order to ring-walk from one side of the naphthalene ring to the other (i.e., 1,2- $\eta^2$  to 3,4- $\eta^2$ ), the metal must pass through a less stable dihapto-coordinate intermediate (i.e., 2,3- $\eta^2$ ). Similar ring-walking mechanisms for naphthalene were determined for nickel,<sup>28</sup> ruthenium,<sup>11</sup> rhenium,<sup>26</sup> and osmium,<sup>29</sup> but none of these were shown to be directly related to C-H activation.

In the case of the face-flip, starting from the 2,3- $\eta^2$  isomer **3A**, oxidative addition followed by rotation of the W-aryl bond and reductive elimination would return isomer **3B**. Consistent with NOESY experiments, the W-Ar group rotation barriers for *m*-**3H** and *p*-**3H** are 15.7 and 16.1 kcal/mol, which are lower than the C-H

oxidative cleavage transition state. however, the W-Ar bond rotation for *o*-**3H** is 23.3 kcal/mol, and this would not be competitive with C-H reductive elimination. Thus, a face-flip isomerization could only take place via the *m*-**3H** intermediate.

Given that the rates of C-H activation and ring-walk are similar for the benzene complex **2**, and the fact that for the anisole complex **3**, a purported ring-walk is significantly slower than the face-flip

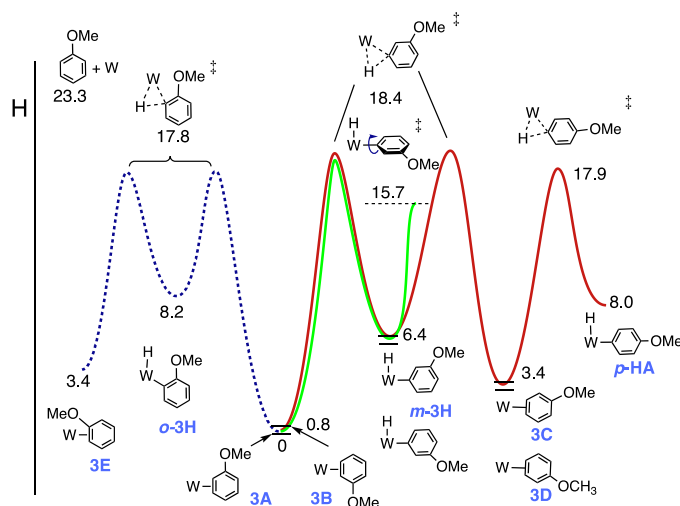


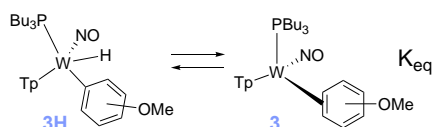
**Figure 9.4.** Reaction coordinate diagram for an interfacial (face-flip; green) and intrafacial (ring walk; red) isomerization for the anisole complex from **3A** to **3B**.

mechanism, it is likely that the ring-walk also operates through an sigma complex (i.e., C,H- $\eta^2$ ) or aryl hydride intermediate. DFT calculations also helped explain whether the lack of experimentally observed para aryl hydride isomer, *p*-**3H**, is the result of a higher kinetic pathway for oxidative cleavage or unfavorable thermodynamics. For anisole, the *ortho*, *meta*, and *para* C-H oxidative cleavage transition enthalpy barriers are 17.8, 18.4, and 17.9 kcal/mol, relative to the  $\eta^2$  complex **3A** that was found to be the lowest energy isomer (**Figure 9.4**). Thus, a purported para aryl hydride intermediate, *p*-**3H**, should be kinetically accessible. These transition states are all about 3 kcal/mol higher than for benzene, owing to the increased stabilization of the ground state from the methoxy  $\pi$  interaction (vide supra). The aryl hydride complexes of anisole are 8.2 (*o*-**3H**), 6.4 (*m*-**3H**), and 8.0 (*p*-**3H**) kcal/mol higher in enthalpy than **3A**. Given that the calculated Gibbs free energies for the PBU<sub>3</sub> analogs are expected to be several kcal/mol lower energy than these values (vide supra), the species *p*-**3H** is predicted to be in equilibrium with the observed species (*o*-**3H**, *m*-**3H**, **3A**, **3B**) but barely out of range for detection by <sup>1</sup>H NMR.

## 9.6 Solvent Dependence on Equilibrium and O-H Activation

Interestingly, we found in the case of the anisole complex **3** that the ratio of **3** to **3H** can be modulated by choice of solvent. Table 1 summarizes these results, where we find that the use of MeOH enhances the amount of dihapto-coordinate arene at equilibrium. We speculate that hydrogen bonding interactions with the NO ligand could result in an overall decrease in electron density of the metal, and this could disfavor the formation of the oxidative addition process.

To further test the hypothesis that H-bonding interactions support the  $\eta^2$ -arene isomer, we combined the strong hydrogen-bond donor hexafluoroisopropanol (HFIP)<sup>30</sup> in benzene along with the anisole complex **3**. Unexpectedly, a new species (**11**) is formed in solution with the concomitant loss of the aromatic ligand (**Scheme 9.7**).



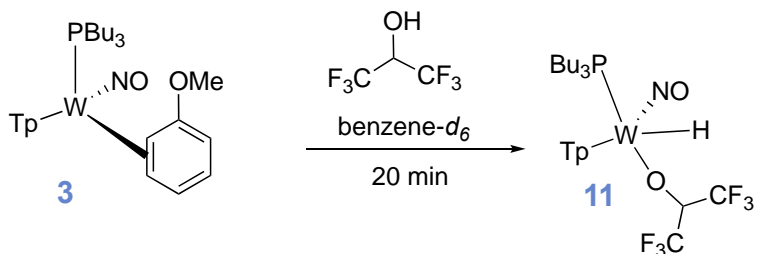
| Solvent        | $K_{\text{eq}}$ (298 K) | $\Delta G^\circ$ (kcal/mol) |
|----------------|-------------------------|-----------------------------|
| benzene- $d_6$ | 4.3                     | -0.87                       |
| acetone- $d_6$ | 3.7                     | -0.77                       |
| MeOD- $d_4$    | 23.2                    | -1.86                       |

**Table 9.1.** Solvent dependence on the arene/aryl hydride equilibrium.

Notable features of this new complex include a tungsten hydride signal at 12.7 ppm ( $J_{\text{HP}} = 128$  Hz) along with a septet at 5.59 ppm ( $J_{\text{HF}} = 6$  Hz). Utilizing HFIP-*OD*, the purported hydride resonance at 12.7 ppm disappears. We speculate that this complex is the result of accelerated ligand substitution and subsequent oxidative addition of HFIP (**Scheme 9.7**), though further characterization of this complex was not pursued.

Treatment of the previously reported  $\text{WTp}(\text{NO})(\text{PMe}_3)(\eta^2\text{-2,3-anisole})$  complex<sup>23</sup> with HFIP did not produce similar results: While a minor product develops with a similar tungsten-hydride resonance and splitting ( $\delta$  11.35 ppm in benzene- $d_6$ ,  $J_{\text{PH}}=129$  Hz), over time decomposition to uncharacterized paramagnetic material is observed.

Parenthetically, the anisole complex **3** can be prepared on a 15 g scale at 50% yield, a value comparable to that of the {WTP(NO)(PMe<sub>3</sub>)} analog.<sup>23</sup> This complex is stable for months while stored as a solid at low temperatures (-30 °C). The substitution half-life of **3** at 25 °C is ~ 20 minutes, making it a suitable synthon for {WTP(NO)(PBu<sub>3</sub>)}, especially in cases where a potential ligand is incompatible with sodium.

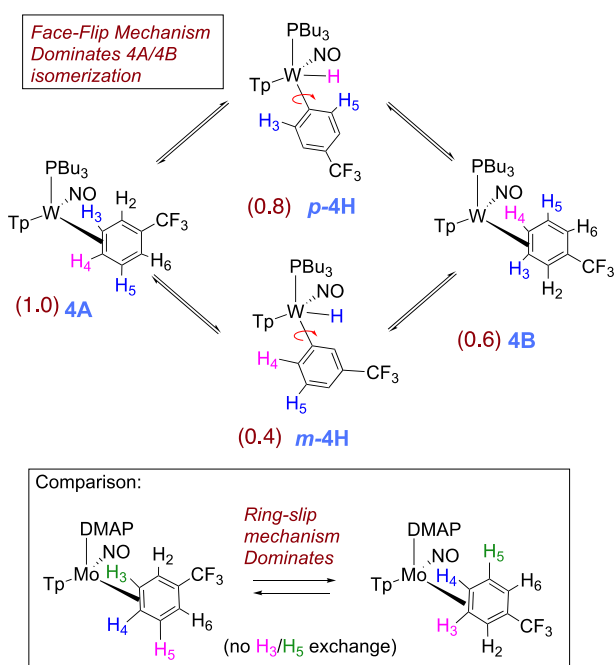


**Scheme 9.7.** Oxidative addition of HFIP to {WTP(NO)(PMe<sub>3</sub>)}.

### 9.7. Electron Deficient Benzenes on {WTP(NO)(P(n-Bu)<sub>3</sub>)}

To study the effects of an electron-withdrawing substituent, we performed an exchange reaction using anisole complex **3** in neat  $\alpha,\alpha,\alpha$ -trifluorotoluene. Although the reaction mixture is initially a homogeneous orange solution, over time a yellow solid spontaneously precipitates (**4**). <sup>1</sup>H NMR analysis of this powder (**4**) reveals the presence of two  $\eta^2$ -arene complexes (**4A** and **4B**) along with two C-H activated products (*m*-**4H** and *p*-**4H**). The 1: 0.6 ratio of coordination diastereomers of WTP(NO)(P(n-Bu)<sub>3</sub>)( $\eta^2$ -3,4-trifluorotoluene) (**4A** and **4B**) is comparable to that of the PMe<sub>3</sub> analog.<sup>23</sup> Interestingly, while exchanges on the timescale of the NOE experiment were observed between the dihapto- and C-H activated adducts for **2** and **3**, no such exchange was observed for **4** at 25 °C. But at 50 °C, exchange was observed between the para proton (H<sub>4</sub>) of **4A** and **4B** and the hydride for *p*-**4H**. Also, spin saturation exchange was observed between the two meta protons (H<sub>3</sub> and H<sub>5</sub>) of **4A** and **4B** and the hydride of *m*-**4H** (**Scheme 9.8**). Given that the equilibrium constants are close to unity for the three arene complexes **2** - **4** and their aryl hydride isomers, the better  $\pi$ -acceptor abilities of the electron-deficient arene *must slow both the rate of oxidative addition and that of reductive elimination*.

The spin transfer exchange observed from NOESY data of the trifluorotoluene system **4** is also consistent with an interfacial isomerization (“face-flip”) mechanism operative through a C-H activated intermediate. In contrast, the previously reported MoTp(DMAP)(NO)( $\eta^2$ -3,4-trifluorotoluene) complex is able to interconvert between the analogous coordination diastereomers predominantly through an intrafacial mechanism (ring-slip)



**Scheme 9.8.** Divergent mechanism across group 6 complexes of molybdenum and tungsten.

that is operative at ambient temperatures.<sup>31</sup> We speculate that this difference in the predominant isomerization mechanism between the Group 6 congeners is due to the more  $\pi$ -basic nature of the tungsten fragment. The further stabilization of the ground state for the tungsten system raises the barrier to the purported  $C,H-\eta^2$  transition state that is likely on the path to either ring walk or C-H insertion (see **Scheme 9.8**). For both the molybdenum and rhenium systems mentioned above, any purported C-H insertion would likely result in a face-flip isomerization via aryl rotation (*vide supra*). Thus, insertion must be significantly slower than the ring-walk for the Mo and Re

complexes, since the necessary spin exchange correlations are not observed in their NOESY data.<sup>26,31</sup>

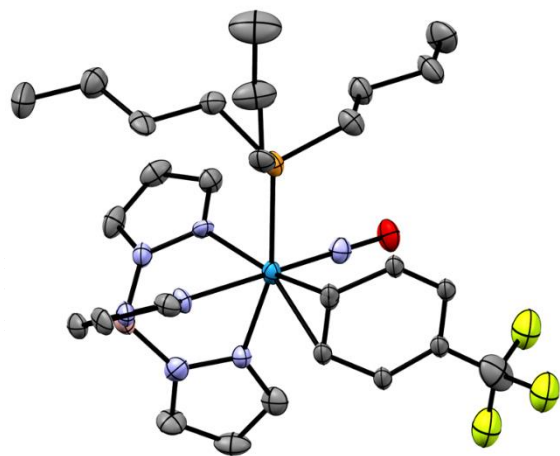


**Figure 9.5.** Molecular structure of the trifluorotoluene complex, isomer **4B**. Co-crystallized solvent and H atoms removed for clarity.<sup>8</sup>

Crystals of the trifluorotoluene complex suitable for X-ray diffraction were prepared by allowing a DCM/hexanes (1:10) solution of **4** to stand at reduced temperature (-30 °C). A molecular structure determination reveals that the crystal contains an internal disorder in which *both* **4A** and **4B** are present. An ORTEP diagram of the higher population species (81:19) of the crystal is shown in **Figure 9.5**.

The temperature dependence of the C-H insertion process was determined for a sample of **4** in acetonitrile-*d*<sub>3</sub> solution over a temperature range of 20 – 55 °C. A Van't Hoff plot (**Figure**

**9.6**) shows that the reductive elimination (**4H** → **4**) is exothermic, with a  $\Delta H^\circ = -2.8 \pm 0.2$  kcal/mol and  $\Delta S^\circ$

=  $-9.0 \pm 0.6$  eu. These values are in good agreement with those obtained for the naphthyl hydride to naphthalene conversion on  $\{\text{RhCp}^*(\text{PMe}_3)\}$  (cf.  $-4.1$  kcal/mol,  $-12$  eu).<sup>15</sup>

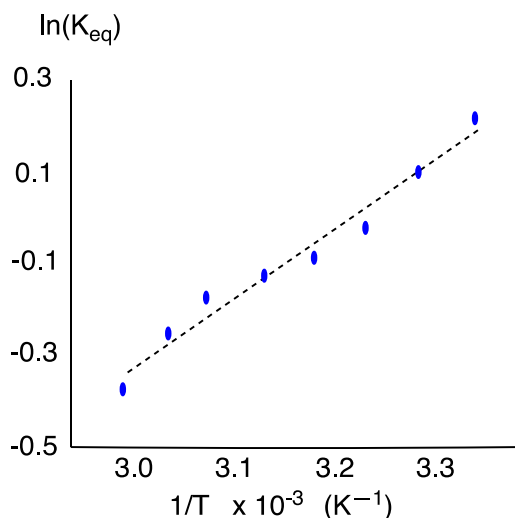


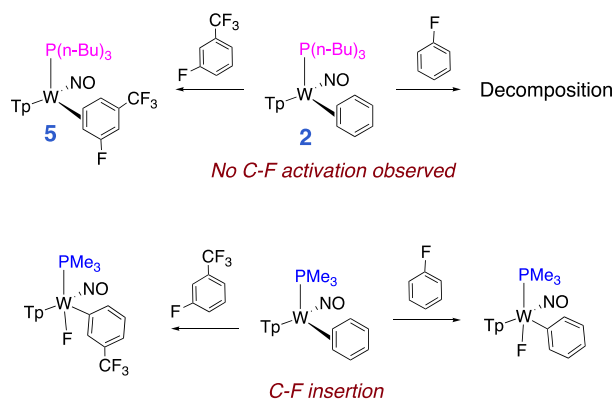
**Figure 9.6.** Van't Hoff plot for the equilibrium:  $4\mathbf{H} = \Delta H^\circ = -2.8 \pm 0.2$  kcal/mol  $\Delta S^\circ = -9.0 \pm 0.6$  eu.

The complex  $\text{WTp}(\text{NO})(\text{PMe}_3)(\text{benzene})$  readily reacts with fluorobenzene to give  $\text{WTp}(\text{NO})(\text{PMe}_3)(\text{Ph})(\text{F})$ .<sup>18</sup> However, when **2** was dissolved in fluorobenzene and the solution allowed to stand, no appreciable  $\eta^2$ -arene, aryl-hydride, or aryl fluoride  $\eta$  complex was observed; rather, a slow degradation to paramagnetic products was observed. We next screened 1-fluoro-3-(trifluoromethyl)benzene for binding, a compound also known to undergo facile C-F activation with the tungsten  $\text{PMe}_3$  system (**Scheme 9.8**).<sup>18</sup> In contrast to expectation, when a sample of **2** was allowed to react with a solution of 1-fluoro-3-(trifluoromethyl)benzene, two  $\eta^2$ -coordinated arene complexes and one aryl hydride were formed. Features of this mixture include  $^{31}\text{P}$  NMR resonances at  $-5.1$  and  $-5.6$  ppm with  $J_{\text{WP}} = 288$  Hz and  $286$  Hz respectively, consistent with the two dihapto-coordinated arenes,<sup>23</sup> and a major resonance at  $+15.7$  ppm with a  $J_{\text{WP}} = 171$  Hz, which is attributed to the C-H activated isomer. Overlapping signals in the  $^1\text{H}$  NMR spectrum prevent complete assignments, but support the notion that C-H oxidative addition occurs at C5, and the two dihapto-coordinated isomers showing coordination across the C4 and C5 carbons. The lack of identifiable phosphorous-

to-fluorine coupling in either  $^{31}\text{P}$  or  $^{19}\text{F}$  NMR experiments suggest that the purported diamagnetic C-F activated product is not formed in appreciable amounts. However, allowing the reaction solution to stand over 16 hours led to the evolution of free  $\text{P}(\text{n-Bu})_3$  ligand and decomposition of **5** to uncharacterized paramagnetic materials. DFT calculations estimate that the C-F activated adduct of **5** is predicted to be 20.4 kcal/mol more stable ( $\Delta G^\circ$ ; 298 K) than either the  $\eta^2$ - or aryl-hydride isomers. Given the reduced time needed for ligand dissociation for **2** (4 minutes cf. 1 h for  $\text{WTp}(\text{NO})(\text{PMe}_3)(\text{benzene})$ ), we speculate that  $\eta^2$ -arene and aryl-hydride isomers analogous to those seen for **5** were likely formed transiently for the  $\text{PMe}_3$  analog as well, but went undetected owing to the longer time needed for benzene dissociation. This rapid rate of benzene dissociation for **2** provides a potential advantage over the  $\text{PMe}_3$  system in that unstable intermediates such as **5** have an increased chance of being observed.

## 9.8 Coordination of Aromatic and Unsaturated Ligands

In their landmark studies, Jones and Perutz showed how the  $\eta^2$ -arene/aryl hydride equilibrium was affected by the extent of aromaticity.<sup>1</sup> We briefly explored different classes of aromatic molecules to determine to what extent the  $\eta^2$ -aromatic/aryl-hydride differed as a function of aromatic character of the ligand. Beyond the complexes of benzene (**2**), anisole (**3**), trifluorotoluene (**4**) and 1-fluoro-3-



**Scheme 9.9.** Comparison of C-F oxidative addition for  $\text{PMe}_3$  and  $\text{P}(\text{n-Bu})_3$  variants of  $\{\text{WTp}(\text{NO})(\text{PR}_3)\}$  system.

(trifluoromethyl)benzene (**5**) already discussed, we surveyed 1,2-bis(trifluoromethyl)benzene (**6**), pyridine-borane (**7**), naphthalene (**8**), thiophene (**9**) and cyclohexene (**10**). For **8-10**, no C-H activated isomer is observed over time. For the bis-trifluoromethylated benzene complex **6**, however, while initially no C-H activated product was observed, over five days in benzene- $d_6$  a new complex is formed in a 1:20 ratio that has resonances consistent with C-H activation (notably a new set of  $\text{Tp4}$  protons at 5.76, 5.70 and 5.31 ppm) along with a resonance at 9.30 ppm with  $J_{\text{PH}} = 98$  Hz and  $J_{\text{WP}} = 31$  Hz) grows in over time. Analogous to **4**, the C-H and  $\eta^2$ -

coordinate forms of **6** do not appear to undergo spin saturation exchange at ambient temperature and no fluxional behavior was observed even when heating the reaction mixture to 50 °C. For the  $\eta^2$ -bound pyridine-borane complex **7** a mixture of 3,4- $\eta^2$  and 4,5- $\eta^2$  isomers<sup>32</sup> was found to be in equilibrium with roughly 10% of a C-H activated isomer (**7H**). Meanwhile, naphthalene and thiophene complexes were formed exclusively as their  $\eta^2$ -bound isomers, with proton NMR data very similar to their  $\text{PMe}_3$  analogs,<sup>23, 33-34</sup> and characterization was not pursued further.

A comparison of  $\eta^2$ - and C-H activated isomers as observed in benzene- $d_6$  is provided in **Table 9.2**. As has been noted by Jones and co-workers for the rhodium-based systems  $\text{RhCp(L)}$  and  $\text{RhCp}^*(\text{L})$  ( $\text{L} = \text{PMe}_3, \text{P(OMe)}_3$ ), the equilibrium between  $\eta^2$ -arene and C-H activated adducts depends on the extent of disruption to the  $\pi$ -system when dihapto-coordination occurs. Hence just as for  $\text{RhCp}^*(\text{PMe}_3)$ , the  $\eta^2$ - $(\text{R}_2\text{C}=\text{CHR}) / (\text{R}_2\text{C}=\text{CR})(\text{H})$  equilibrium constant increases as the ligand is adjusted from alkene to naphthalene to benzene. This trend is followed for the  $\text{Wtp(NO)}(\text{P}(\text{n-Bu})_3)$  system, except with  $K_{\text{eq}}$  is shifted more toward the  $\eta^2$ - $(\text{R}_2\text{C}=\text{CHR})$  form. With regard to substituent effects, an interesting difference arises in these two systems. For  $\text{RhCp}^*(\text{PMe}_3)$ , the addition of a methoxy substituent shifts the  $\eta^2$ -naphthalene/naphthyl hydride equilibrium to heavily favor the  $\eta^2$ -arene isomer.<sup>14</sup> In a similar manner, the addition of two  $\text{CF}_3$  groups (*para*-hexafluoroxylylene) shifts the benzene/phenyl hydride equilibrium to favor the  $\eta^2$ -arene.<sup>35</sup> In contrast, the introduction of either a OMe or

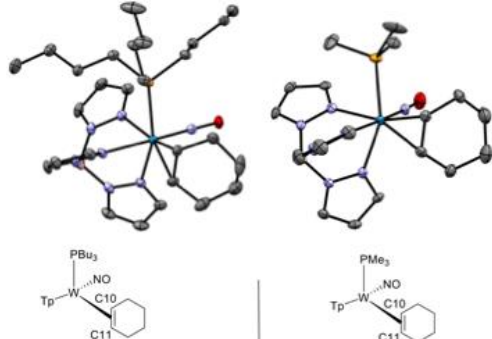
| Dihapto-Coordinated |                    | C-H Activated |                   |
|---------------------|--------------------|---------------|-------------------|
|                     | 46% ( <b>2</b> )   |               | 54% (equilibrium) |
|                     | 82% ( <b>3</b> )   |               | 18% (equilibrium) |
|                     | 62% ( <b>4</b> )   |               | 38% (equilibrium) |
|                     | 63% ( <b>5</b> )   |               | 37%               |
|                     | 95% ( <b>6</b> )   |               | 5%                |
|                     | 90% ( <b>7</b> )   |               | 10% (equilibrium) |
|                     | >99% ( <b>8</b> )  |               | <1%               |
|                     | >99% ( <b>9</b> )  |               | <1%               |
|                     | >99% ( <b>10</b> ) |               | <1%               |

**Table 9.2.** Percentages of dihapto-coordinated aromatic complexes and their C-H activated isomers at 25 °C. All values recorded in benzene- $d_6$  except for 5 and 7, both recorded in acetone- $d_6$ , and 10 in  $\text{CDCl}_3$ . Where equilibrium has been conclusively verified, this is noted.



CF<sub>3</sub> group to WTp(NO)(PMe<sub>3</sub>)(benzene) leaves the equilibrium constant practically unchanged, despite clearly stabilizing the complex with respect to ligand dissociation in both cases (**Table 9.2**).

As noted for the rhodium system and expected for oxidative addition in general,<sup>36</sup> the more electron-rich the metal, the more favorable oxidative addition is expected to be. It's tempting to attribute the increased amount of aryl hydride in equilibrium for **2** compared to its PMe<sub>3</sub> analog, to an increase in electron-donation from the P(n-Bu)<sub>3</sub> ligand (cf. PMe<sub>3</sub>). However, structural comparisons show negligible differences in metal-alkene bond lengths between **10** and the previously reported WTp(NO)(PMe<sub>3</sub>)(η<sup>2</sup>-cyclohexene) (**Table 9.3**). And, data collected from NMR and electrochemical experiments of



| atom 1 | atom 2 | Distance (Å) | atom 1 | atom 2 | Distance (Å) |
|--------|--------|--------------|--------|--------|--------------|
| W      | P      | 2.5366(7)    | W      | P      | 2.4961(13)   |
| W      | C10    | 2.247(3)     | W      | C10    | 2.226(4)     |
| W      | C11    | 2.210(3)     | W      | C11    | 2.193(5)     |
| W      | N(NO)  | 1.773(2)     | W      | N(NO)  | 1.768(4)     |
| C10    | C11    | 1.439(4)     | C10    | C11    | 1.437(7)     |

**Table 9.3.** Molecular structure comparisons for cyclohexene complexes WTp(NO)(PMe<sub>3</sub>)(cyclohexene) and WTp(NO)(P(n-Bu)<sub>3</sub>)(cyclohexene).

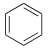
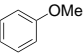
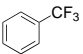
the cyclohexene complex **10** closely resemble those of the analogous PMe<sub>3</sub> system.<sup>37</sup> Similarly, electrochemical and infrared data presented in Table 4 indicate that the electronic differences between the PMe<sub>3</sub> and the P(n-Bu)<sub>3</sub> systems are negligible for η<sup>2</sup>-arene complexes. Hence, the large shift in the arene/aryl hydride equilibrium constant resulting when PMe<sub>3</sub> is replaced by P(n-Bu)<sub>3</sub> is either a result of steric interactions or entropy arising from the butyl groups. The methyl/butyl switch also causes the half-life to acetone substitution to be reduced from an hour to four minutes (acetone solvolysis) at 25 °C. At 298 K, solution equilibrium data indicate ΔΔG is 1.6 kcal/mol. Further, from the half-life data for the displacement of benzene by acetone, for **2** and its PMe<sub>3</sub> analog at 298 K, ΔΔG\* can be estimated as ~1.5 kcal/mol, approximating ΔS\* as 13 eu (the corresponding value experimentally determined for molybdenum).<sup>31</sup> A destabilization of the dihapto-coordinated form, without the same steric penalty for the aryl hydride would explain the shift in equilibrium constant from 15 to 1 and increase in rate of substitution for **2** but DFT

calculations show a slight *increase* in  $\Delta H$  for **2** to **2H** when methyl groups are replaced by butyl groups. Yet these calculations show a reduction in Gibbs free energy for this process, a direct result of the increased  $\Delta S$  for the butyl system. In other words, the calculations suggest that both the enhanced amount of aryl hydride and the more rapid substitution rate for **2** compared to its methylated analog is a direct result of greater entropy experienced by the butyl chains upon either oxidative addition or arene decomplexation.

### 9.9 Synthetic implications.

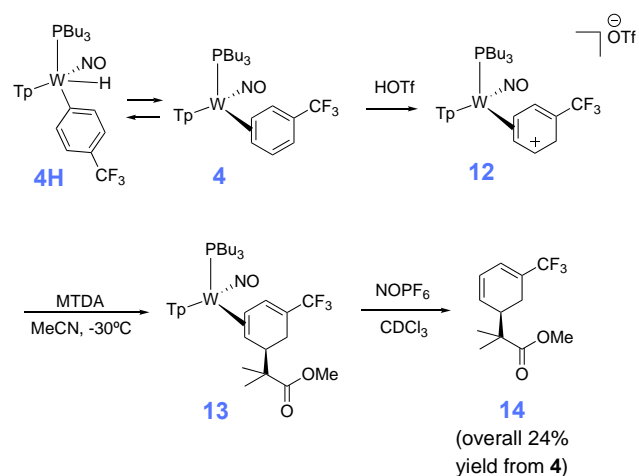
Although roughly 40% of the trifluorotoluene complex **4** is in the form of an aryl hydride, we found that upon treatment with strong acid (HOTf in MeCN) a single allylic species (**12**) is formed. Features of this complex in MeCN-*d*<sub>3</sub> at 0 °C include tungsten-allyl resonances in the <sup>1</sup>H NMR spectrum at 7.04, 5.06 and 4.27 ppm, corresponding to the allylic protons.<sup>38</sup> Additionally, “roofing” signals at 4.15 and 4.01 ppm corresponding to a methylene group is present, all features consistent with a distorted  $\eta^2$ -arenium intermediate.<sup>37</sup> Subsequent

treatment with the masked enolate MTDA yields the  $\eta^2$ -diene **13** prepared in situ (Scheme 9). This reactivity is fully consistent with that observed for the PMe<sub>3</sub> analog.<sup>38</sup> This complex (**13**) was subjected to oxidative decomplexation to provide the free organic methyl 2-methyl-2-(5-(trifluoromethyl)cyclohexa-2,4-dien-1-yl)propanoate (**14**) in 24% overall yield (The full characterization of this compound has been previously reported).<sup>38</sup> For comparison, the same series of transformations using the PMe<sub>3</sub> variant was accomplished with

| WTp(NO)(L)(arene)   |                  | $E_{pa}$<br>(V, NHE) <sup>a</sup> | Substitution<br>Half-Life<br>(h, 25 °C) | Bond<br>Strength<br>(kcal/mol) <sup>b</sup> | NO Stretch<br>(cm <sup>-1</sup> ) | $K_{eq}$ <sup>c</sup> |
|---|------------------|-----------------------------------|---|---|-----------------------------------|-----------------------|
| arene   | L                |                                   |   |   |                                   |                       |
|  | PMe <sub>3</sub> | -0.13                             | 1.2                                     | 26  | 1564                              | 15                    |
|   | PBu <sub>3</sub> | -0.16                             | 0.066                                   | 23  | 1564                              | 0.85                  |
|  | PMe <sub>3</sub> | -0.15                             | 4.0                                     | 27  | 1568                              | >99                   |
|   | PBu <sub>3</sub> | -0.18                             | 0.33                                    | 24  | 1559                              | 4.3                   |
|  | PMe <sub>3</sub> | +0.05                             | 192                                     | 30  | 1575                              | 20                    |
|   | PBu <sub>3</sub> | +0.10                             | 17                                      | 28  | 1567                              | 1.6                   |

a 100 mV/s). b. estimation from substitution rate. c. equilibrium recorded in benzene (25 °C) as the ratio of [sum of all arene species] / [sum of all aryl hydride species].

**Table 9.4.** Comparison of  $\eta^2$ -arene complexes as a function of phosphine.  $K_{eq}$  determined in acetone at 25 °C; substitution half-lives determined at 25 °C.



**Scheme 9.10.** Conversion of the trifluorotoluene complexes **4** and **4H** to a functionalized cyclohexadiene (**14**).

an overall yield of 32%. Compound **14** is a rare example of a diene with a CF<sub>3</sub> substituent. Such compounds are of interest in Diels-Alder reactions<sup>42,43</sup> and should be good candidates to participate in the inverse-electron-demand variant. As a practical note, in consideration of yields for all reactions starting from W(CO)<sub>6</sub>, we estimate the cost to synthesize **14** starting from the anisole complex **3** is roughly 1/4<sup>th</sup> the cost in comparison to the published route that uses PMe<sub>3</sub>.<sup>38</sup>

## 9.10 Conclusions

The complex WTp(NO)(P(n-Bu)<sub>3</sub>)(benzene) provides a rare example of a facile equilibrium between an η<sup>2</sup>-benzene complex and its phenyl hydride isomer with an equilibrium constant close to unity at ambient temperatures. We have explored how temperature, solvent, and substituents affect this equilibrium, and have carried out detailed DFT calculations that map out the pathways connecting these two ground states. We have also explored how these reaction pathways enable both interfacial (face-flip) and intrafacial (ring slip) linkage isomerizations for the arene complex. Highlights of the study include:

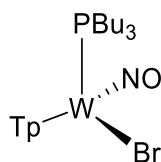
1. Replacement of PMe<sub>3</sub> by P(n-Bu)<sub>3</sub> creates an entropy penalty of roughly 1.6 kcal/mol at 298 K for the dihapto-coordinated isomer. This results in a significantly shortened substitution half-life, and a significant increase in the proportion of phenyl hydride at equilibrium.
2. The bulkier phosphine does not appear to significantly increase the electron-density at the metal, as gauged by electrochemical potential, IR absorptions, and solid-state structural data.
3. The η<sup>2</sup>-benzene and phenyl hydride isomers are connected through an intermediate best described as C,H-η<sup>2</sup> (C-H sigma bond) complex. Two transition states (**TS1** and **TS2**) are closely associated with this intermediate and the energy surface for all three is remarkably flat. A third transition state (**TS3**) connects the η<sup>2</sup>-benzene isomer to another benzene complex, still bound η<sup>2</sup>, but held together primarily by dispersion forces.

4. In contrast to our previous findings with molybdenum, rhenium, and osmium  $\eta^2$ -benzene complexes, the tungsten system undergoes both a face-flip that seems to depend directly on C-H insertion as the rate limiting step, and a ring-walk that involves a  $C,H-\eta^2$  intermediate.
5. The addition of an electron-donating (OMe) *or* an electron-withdrawing substituent (CF<sub>3</sub>) to the benzene ring increases the stability of *both* the  $\eta^2$ -arene and the aryl hydride isomers (with little change in the equilibrium constant). This is especially notable for the CF<sub>3</sub> analog, which for the dihapto-coordinate form has a substitution half-life over 250 times longer and a calculated bond strength that is five kcal/mol more stable than its benzene analog.
6. Both the anisole and trifluorotoluene systems undergo coordination diastereomer isomerization through a face-flip mechanism involving C-H insertion. This is in contrast to earlier studies with molybdenum, rhenium, or osmium, where ring-walking was more facile.
7. Despite the presence of a considerable amount of aryl hydride, the novel organic chemistry of the  $\eta^2$ -trifluorotoluene ligand, initially reported for {WTP(NO)(PMe<sub>3</sub>)}, is not compromised by replacement of PMe<sub>3</sub> with the bulkier phosphine, and the latter system is considerably more economical.

## Experimental Section.

**General Methods.** NMR spectra were obtained on 500, 600 or 800 MHz spectrometers. Chemical shifts are referenced to tetramethylsilane (TMS) utilizing residual  $^1\text{H}$  signals of the deuterated solvents as internal standards. Chemical shifts are reported in ppm and coupling constants ( $J$ ) are reported in hertz (Hz). Chemical shifts for  $^{19}\text{F}$  and  $^{31}\text{P}$  spectra were reported relative to standards of hexafluorobenzene (164.9 ppm) and triphenylphosphine (-6.00 ppm). Infrared Spectra (IR) were recorded on a spectrometer as a solid with an ATR crystal accessory, and peaks are reported in  $\text{cm}^{-1}$ . Electrochemical experiments were performed under a nitrogen atmosphere. Most cyclic voltammetric data were recorded at ambient temperature at 100 mV/s, unless otherwise noted, with a standard three electrode cell from +1.8 V to -1.8 V with a platinum working electrode, acetonitrile (MeCN) solvent, and tetrabutylammonium (TBAH) electrolyte (~1.0 M). All potentials are reported versus the normal hydrogen electrode (NHE) using cobaltocenium hexafluorophosphate ( $E_{1/2} = -0.78$  V, -1.75 V) or ferrocene ( $E_{1/2} = 0.55$  V) as an internal standard. Peak separation of all reversible couples was less than 100 mV. All synthetic reactions were performed in a glovebox under a dry nitrogen atmosphere unless otherwise noted. All solvents were purged with nitrogen prior to use. Deuterated solvents were used as received from Cambridge Isotopes and were purged with nitrogen under an inert atmosphere. When possible, pyrazole (Pz) protons of the (trispyrazolyl) borate (Tp) ligand were uniquely assigned (e.g., “Tp3B”) using two-dimensional NMR data (see Fig. S1). If unambiguous assignments were not possible, Tp protons were labeled as “Tp3/5 or Tp4”. All  $J$  values for Tp protons are 2 ( $\pm 0.4$ ) Hz.

### Synthesis of $\text{WTp}(\text{NO})(\text{P}(\text{n-Bu})_3)(\text{Br})$ (**1**)

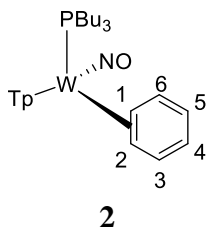


To a 100 mL round bottom flask added  $\text{WTp}(\text{Br})_2(\text{NO})$  (18.48 g, 31.6 mmol) along with 80 mL of DCM that had been purged with  $\text{N}_{2(\text{g})}$  for 15 min beforehand and the heterogeneous yellow reaction mixture was allowed to vigorously stir. To this stirring solution Zn dust (7.05 g, 100.8 mmol) was added followed *immediately* by the addition of tri-*n*-butyl-phosphine (10.03 g, 49.6 mmol). Initially the reaction mixture turns to a lime green color. The solution was allowed to sit for 40 min at which point the reaction mixture had turned to a deep green color. The reaction mixture was then loaded onto a medium 150 mL fritted disc that had been filled with two inches of neutral alumina and saturated in DCM. The green reaction mixture was then eluted through the neutral alumina column and a vibrant dark green band was eluted with DCM (200 mL) into a 500 mL filter flask. The DCM solvent was then removed *in vacuo* until ~ 100 mL solvent remained. To this homogeneous green solution added 200 mL hexanes and the solvent was again removed *in vacuo* until ~ 100 mL of the solvent mixture remained. To this solution was added 200 mL of pentane and the solvent was again removed *in vacuo* until a green precipitate was observed to form in solution. Filtering the now heterogeneous green reaction mixture through a fine 60 mL fritted disk allowed for the recovery of a deep green crystalline solid. This solid was then washed 3 x 20 mL pentane and allowed to dry under dynamic vacuum in a desiccator for six hours before a mass was taken (9.16 g, 42%). The paramagnetic nature of the compound prevented use of NMR spectroscopy, but crystals of **1** of suitable quality for X-ray diffraction were grown utilizing vapor diffusion by dissolving in DCM and allowing ether to diffuse into the mixture over several days.

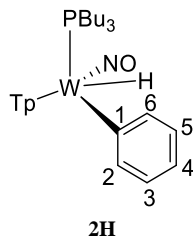
CV (MeCN)  $E_{1/2} = -1.36$  V,  $E_{p,a} = 0.44$  V (NHE). IR:  $\nu(\text{BH}) = 2521$   $\text{cm}^{-1}$ ,  $\nu(\text{NO}) = 1580$   $\text{cm}^{-1}$ .  
 Anal. Calcd for  $\text{C}_{21}\text{H}_{37}\text{BBrN}_7\text{OPW}$ : C, 35.57; H, 5.26; N, 13.87. Found: C, 35.67; H, 5.26; N, 13.99.

### Synthesis of $\text{WTp}(\text{NO})(\text{P}(\text{n-Bu})_3)(\eta^2\text{-benzene})$ (**2**) and $\text{WTp}(\text{NO})(\text{P}(\text{n-Bu})_3)(\text{H})(\text{C}_6\text{H}_5)$ (**2H**)

To a 250 mL oven dried round bottom flask was added **1** (6.02 g, 8.50 mmol) followed by benzene (200mL) and the homogeneous green reaction mixture was allowed to stir. To this solution was added 30-33% by weight sodium dispersion in paraffin (7.04 g, 54.0 mmol). After 4 h of stirring the reaction mixture had turned to a golden yellow color and the reaction was confirmed to be completed by cyclic voltammetry (no indication of **1**) after a ~2 mL aliquot of this reaction mixture had been filtered through a pipette-column filled with Celite. The golden-brown reaction mixture was then filtered through a coarse 60 mL fritted disc that had been filled with one inch of celite and set in pentane. The Celite was then washed with 100 mL of ether to collect a brown band that developed on the Celite. This reaction mixture was then loaded on a coarse 150 mL fritted disc that had been filled with two inches of silica and saturated with pentane. The reaction mixture was eluted through and once the original solvent mixture had been eluted through the column the filtrate was discarded. A yellow-orange band had developed on the column and this was washed with 100 mL of pentane and this yellow band was then then eluted with a 10:1 ether:benzene mixture (300 mL total) to collect a yellow band. The solvent was then removed in vacuo until 50 mL of ether remained and to this solution was added 200 mL of pentane. The volume was reduced by half *in vacuo* until a yellow solid precipitated from solution. The mixture was then filtered through a fine 30 mL fritted disc to isolate a vibrant yellow solid. This solid was then washed with chilled pentane (3 x 10 mL) and allowed to desiccate for six hours to yield a bright yellow powder (1.21 g, 20%).



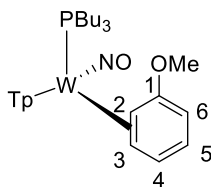
CV (MeCN)  $E_{p,a} = -0.16$  V (NHE). IR:  $\nu(\text{BH}) = 2504$   $\text{cm}^{-1}$ ,  $\nu(\text{NO}) = 1564$   $\text{cm}^{-1}$ .  $^1\text{H-NMR}$  (acetone- $d_6$ ,  $\delta$ , 0 °C): 8.00 (1H, d, Tp5), 7.99 (1H, d, Tp5), 7.94 (1H, d, Tp3), 7.85 (1H, d, Tp5), 7.45 (1H, d, Tp3C), 6.97 (1H, d, Tp3A), 6.81 (1H, buried, H6), 6.80 (1H, buried, H3), 6.36 (1H, t, Tp4), 6.30 (2H, overlapping t, Tp4), 5.70 (2H, overlapping m, H4 and H5), 4.11 (1H, m, H1), 2.30 (1H, m, H2), 1.26 (6H, m,  $\text{PBu}_3$ ), 1.14 (6H, overlapping with **2H**,  $\text{PBu}_3$ ), 0.89 (6H, overlapping with **2H**,  $\text{PBu}_3$ ), 0.76 (9H, t,  $J = 7.3$ ,  $\text{PBu}_3$ ).  $^{31}\text{P-NMR}$  (benzene- $d_6$ ,  $\delta$ , 25°C): -2.74 ( $J_{\text{WP}} = 308$ ).  $^{13}\text{C-NMR}$  (acetone- $d_6$ ,  $\delta$ , 0°C): 141.9 (Tp3/5), 141.3 (Tp3/5), 137.4 (Tp3/5), 136.6 (Tp3/5), 136.1 (Tp3/5), 134.4 (Tp3/5), 133.2 (C6), 128.9 (C3), 117.4 (C4/C5), 116.6 (C4/C5), 107.0 (Tp4), 106.9 (Tp4), 106.1 (Tp4), 63.9 (C2), 62.9 (C1,  $J_{\text{PC}} = 8.6$ ), 26.6, 26.0, 25.5, 25.1, 24.9, 22.6, 14.4 14.1 (overlapping  $\text{PBu}_3$  signals for **2** and **2H** isomer).



IR:  $\nu(\text{WH}) = 1989 \text{ cm}^{-1}$ .  $^1\text{H-NMR}$  (acetone- $d_6$ ,  $\delta$ ,  $0^\circ\text{C}$ ): 9.62 (1H, m,  $J_{\text{WP}} = 97.3$ ,  $J_{\text{WH}} = 31.1$ , W-H), 8.15 (1H, d, Tp3/5), 8.06 (1H, d, Tp3/5), 8.04 (1H, d, Tp3/5), 7.75 (1H, d, Tp3/5), 7.68 (1H, d, Tp3/5), 7.20 (2H, broad, H2 and H6), 6.97 (1H, d, Tp3/5), 7.20 (2H, broad, H3/H5), 6.81 (2H, t,  $J = 7.2$ , H2/6), 6.71 (1H, t,  $J = 7.2$ , H4), 6.45 (1H, t, Tp4), 6.41 (1H, t, Tp4), 5.94 (1H, t, Tp4), 1.26, 1.14, 0.89 (overlapping  $\text{PBU}_3$  resonances for **2** and **2H isomers**), 0.79 (9H, t,  $J = 7.3$ ,  $\text{PBU}_3$ ).  $^{31}\text{P-NMR}$  (benzene- $d_6$ ,  $\delta$ ,  $25^\circ\text{C}$ ): +16.3 ( $J_{\text{WP}} = 173$ ).  $^{13}\text{C-NMR}$  (acetone- $d_6$ ,  $\delta$ ,  $0^\circ\text{C}$ ): 178.5 (C1,  $J_{\text{PC}} = 6.0$ ), 145.9 (Tp3/5), 145.7 (Tp3/5), 145.2 (Tp3/5), 138.3 (Tp3/5), 137.4 (Tp3/5), 137.3 (Tp3/5), 135.4 (C2/C6), 127.6 (C3/C5), 107.3 (Tp4), 107.0 (Tp4), 105.7 (Tp4), 26.6, 26.0, 25.5, 25.1, 24.9, 22.6, 14.4 14.1 (overlapping  $\text{PBU}_3$  signals for **2** and **2H isomers**).

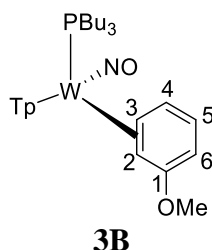
### Synthesis of $\text{WTp}(\text{NO})(\text{P}(\text{n-Bu})_3)(\eta^2\text{-2,3-anisole})$ (**3A** and **3B**) and $\text{WTp}(\text{NO})(\text{P}(\text{n-Bu})_3)(\text{H})(\text{C}_6\text{H}_4\text{OMe})$ (**3HA** and **3HB**)

An oven-dried 250 mL round bottom flask was charged with a stir bar and 200 mL of anisole, followed by complex **1** (11.35g, 16.0 mmol) and allowed to vigorously stir to generate a homogeneous green reaction mixture. Next 30-33% by weight sodium dispersion in paraffin (6.13 g, 88.8 mmol) was added. After 2.5 h, the reaction mixture had turned to a golden yellow color and the reaction was confirmed to be completed by cyclic voltammetry after a ~2 mL aliquot of this reaction mixture had been filtered through a pipette-column filled with Celite. The bulk golden-brown reaction mixture was then filtered through a coarse 150 mL fritted disc that had been filled with two inches of Celite and saturated with anisole. Vacuum was applied to elute the colored filtrate and the Celite plug was washed with 100 mL of addition anisole to collect the brown solution into a 500 mL filter flask. The filtrate was then loaded onto a 10 cm silica column on a coarse 150 mL fritted disc that had been set in pentane. After the entire filtrate had been loaded the column was washed with 250 mL pentane total to wash away free anisole. The column was then rinsed with ~200 mL of ether to elute a vibrant orange band. Once the orange band was near the bottom of the column, the clear filtrate was discarded and elution with ether continued so as to collect the desired product. The orange band on the column was eluted with a total of 700 mL and collected in a 1000 mL filter flask. In the filter flask the initially orange band now appears as a homogeneous yellow solution. The solvent was removed in vacuo until the volume had been reduced to < 100 mL of ether. To this solution was added 500 mL of pentane to generate a heterogeneous yellow mixture. The volume was reduced by half in vacuo and the resulting yellow solid was filtered through a fine 60 mL fritted disc and wash with 3 x 30 mL pentane to yield a vibrant yellow solid (5.79g, 49 %). Single-crystals suitable for X-ray diffraction were grown from a DCM/pentane mixture that was allowed to sit at  $-30^\circ\text{C}$  over several hours to grow **3A** and support the elemental composition of the complex.

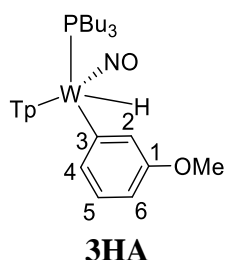


### 3A

CV (MeCN)  $E_{p,a} = -0.17$  V (NHE). IR:  $\nu(\text{BH}) = 2488$   $\text{cm}^{-1}$ ,  $\nu(\text{NO}) = 1559$   $\text{cm}^{-1}$ .  $^1\text{H-NMR}$  (acetone- $d_6$ ,  $\delta$ , 0  $^\circ\text{C}$ ): 8.13 (1H, d, Tp3A), 8.00 (1H, d, Tp3/5), 7.97 (1H, d, Tp3/5B), 7.95 (1H, d, Tp5C), 7.84 (1H, d, Tp5A), 7.41 (1H, d, Tp3C), 6.41 (1H, overlap, H4), 6.35 (1H, t, Tp4B), 6.31 (1H, t, Tp4C), 6.27 (1H, t, Tp4A), 5.70 (1H, dd,  $J = 6.9, 1.7$ , H5), 5.08 (1H, d,  $J = 6.9$ , H6) 4.01 (1H, t,  $J = 10.7$ , H2), 3.68 (3H, s, OMe), 2.30 (1H, m, H3), 2.20, 2.03, 1.93, 1.86, 1.75, 1.27, 1.14, 1.00, 0.88, 0.78 (overlapping PBU<sub>3</sub> resonances for **3A**, **3B**, **3HA**).  $^{31}\text{P-NMR}$  (DME,  $\delta$ , 25 $^\circ\text{C}$ ): -3.34 ( $J_{\text{WP}} = 303$ ).  $^{13}\text{C-NMR}$  (acetone- $d_6$ ,  $\delta$ , 0  $^\circ\text{C}$ ): 165.1 (C1), 145.7 (Tp3/5), 141.9 (Tp3/5), 141.5 (Tp3/5), 137.3 (Tp3/5), 136.7 (Tp3/5), 136.2 (Tp3/5), 124.8 (C4), 117.2 (C5), 107.0 (Tp4), 106.8 (Tp4), 105.9 (Tp4), 91.6 (C6), 64.5 (C3), 58.4 (C2, d,  $J_{\text{PC}} = 10.9$ ), 54.0 (OMe), 26.5, 26.0, 25.4, 25.1, 24.9, 22.9, 22.6, 14.0 (overlapping PBU<sub>3</sub> resonances for **3A**, **3B**, **3HA**).



$^1\text{H-NMR}$  (acetone- $d_6$ ,  $\delta$ , 0  $^\circ\text{C}$ ): 8.13 (1H, d, Tp3A), 8.05 (1H, d, Tp3B/C), 7.99 (1H, d, Tp3/5), (1H, d, Tp3/5), 7.45 (1H, d, Tp3/5), 7.05 (1H, d, Tp3/5), 7.46 (1H, d, Tp3C), 6.34 (1H, t, Tp4C), 6.30 (2H, overlapping resonances for **3A**, **3B**, **3HA**, Tp4A/B and H4), 5.60 (1H, dd,  $J = 6.5, 2.1$ , H5), 4.89 (1H, d,  $J = 6.5$ , H6), 4.18 (1H, m, H3), 2.30 (1H, m, H2), 2.20, 2.03, 1.93, 1.86, 1.75, 1.27, 1.14, 1.00, 0.88, 0.78 (overlapping PBU<sub>3</sub> resonances for **3A**, **3B**, **3HA**).  $^{31}\text{P-NMR}$  (DME,  $\delta$ , 25 $^\circ\text{C}$ ): -2.98 ( $J_{\text{WP}} = 299$ ).  $^{13}\text{C-NMR}$  (acetone- $d_6$ ,  $\delta$ , 0  $^\circ\text{C}$ ): 159.7 (C1), 135.0-147.0 overlapping Tp3/5 resonances for **3A**, **3B**, **3HA**, 141.8 (Tp3/5), 145.8 (Tp3/5), 107.6 (Tp4), 106.5 (Tp4), 105.0 (Tp4), 125.0 (C4), 117.2 (C5 overlap with **3A**), 88.8 (C6), 63.1 (C3, d,  $J_{\text{PC}} = 11.1$ ), 60.6 (C2), 53.9 (OMe), 26.5, 26.0, 25.4, 25.1, 24.9, 22.9, 22.6, 14.0 (overlapping PBU<sub>3</sub> resonances for **3A**, **3B**, **3HA**).

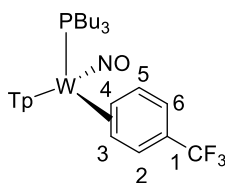


$^1\text{H-NMR}$  (acetone- $d_6$ ,  $\delta$ , 0  $^\circ\text{C}$ ): 9.57 (1H, m,  $J_{\text{PH}} = 97.2$ ,  $J_{\text{WH}} = 31.2$ , W-H), 8.03 (1H, d, Tp3/5), 7.85 (1H, d, Tp3/5), 7.77 (1H, d, Tp3/5), 7.45 (1H, d, Tp3/5), 7.68 (1H, d, Tp3/5), 7.28 (1H, t,  $J = 8.05$ , H5), 7.05 (1H, d, Tp3/5), 6.92 (1H, s, H4), 6.76 (1H, broad, H6), 6.44 (1H, t, Tp4), 6.30 (2H, buried, H2 and Tp4), 5.95 (1H, t, Tp4), 3.51 (3H, broad s, OMe). 2.20, 2.03, 1.93, 1.86, 1.75, 1.27, 1.14, 1.00, 0.88, 0.78 (overlapping PBU<sub>3</sub> resonances for **3A**, **3B**, **3HA**).  $^{31}\text{P-NMR}$  (DME,  $\delta$ , 25 $^\circ\text{C}$ ): 15.55 ( $J_{\text{WP}} = 176$ ).  $^{13}\text{C-NMR}$  (acetone- $d_6$ ,  $\delta$ , 0  $^\circ\text{C}$ ): 180.1 (C3), 159.7 (C1), 144.3 (Tp3/5), 142.9 (Tp3/5), 136.5 (Tp3/5), 135.2 (Tp3/5), 134.5 (Tp3/5), 130.9 (C4), 127.7 (C6), 125.0 (C2), 121.0 (C4), 107.3 (Tp4), 105.7 (Tp4), 106.4 (Tp4), 53.9 (OMe), 26.5, 26.0, 25.4, 25.1, 24.9, 22.9, 22.6, 14.0 (overlapping PBU<sub>3</sub> resonances for **3A**, **3B**, **3HA**).



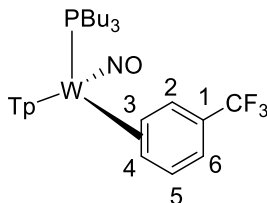
## Synthesis of WTp(NO)(P(n-Bu)<sub>3</sub>)( $\eta^2$ -3,4-a,a,a-trifluorotoluene) (**4A** and **4B**) and WTp(NO)(P(n-Bu)<sub>3</sub>)(H)(C<sub>6</sub>H<sub>5</sub>CF<sub>3</sub>) (**4HA** and **4HB**)

A 4-dram vial was charged with a stir pea, trifluorotoluene (2 mL, 16.2 mmol) and **2** (1.00 g, 1.35 mmol) and the initially homogeneous yellow reaction mixture was allowed to stir. Over time the reaction mixture turns from a homogeneous yellow to a heterogeneous yellow and at the end of 6 h this reaction mixture was added to 10 mL of pentane and allowed to sit at -30 °C for 30 min. The heterogeneous yellow mixture was then filtered through a fine 15 mL fritted disc to yield a vibrant yellow-gold powder. This powder was washed with 3 x 10 mL of pentane that had been chilled to -30 °C and allowed to dry under active vacuum in a desiccator for 4 h and then static vacuum in a desiccator overnight. A mass was then taken the next day of the product, a vibrant yellow solid (0.716 g, 68 %).



**4B**

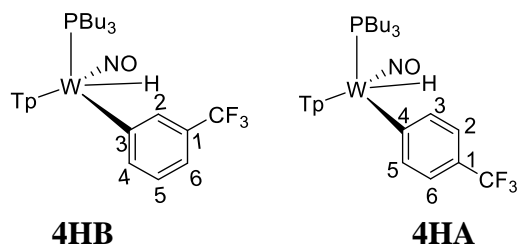
CV (MeCN)  $E_{p,a} = +0.10$  V (NHE). IR:  $\nu(\text{BH}) = 2519$   $\text{cm}^{-1}$ ,  $\nu(\text{NO}) = 1567$   $\text{cm}^{-1}$ .  $^1\text{H-NMR}$  (MeCN- $d_3$ ,  $\delta$ , 0 °C): 7.93 (1H, d, Tp3/5), 7.88-7.90 (4H, overlapping Tpd resonances with **4A**, **4B**, **4HA** and **4HB**), 7.80 (2H, overlapping d, Tp3/5), 7.33 (1H, d,  $J = 5.9$ , H2), 6.97 (2H, overlapping, H5), 6.33 (1H, t, overlapping resonances with **4A**, **4B**, **4HA** and **4HB**, Tp4), 6.31 (1H, t, Tp4), 6.25 (1H, t overlapping resonances with **4A**, **4B**, **4HA** and **4HB**, Tp4), 5.76 (1H, overlapping d, H6), 3.89 (1H, m, H4), 2.08 (1H, m, H3), 1.83 (6H, overlapping resonances with **4A**, **4B**, **4HA** and **4HB**, PBU<sub>3</sub>), 1.24 (6H, overlapping resonances with **4A**, **4B**, **4HA** and **4HB**, PBU<sub>3</sub>), 1.08 (6H, overlapping resonances with **4A**, **4B**, **4HA** and **4HB**, PBU<sub>3</sub>), 0.80 (9H, overlapping resonances with **4A**, **4B**, **4HA** and **4HB**, PBU<sub>3</sub>).  $^{31}\text{P-NMR}$  (MeCN- $d_3$ ,  $\delta$ , 25 °C): -4.77 ( $J_{\text{WP}} = 294$ ).  $^{19}\text{F-NMR}$  (MeCN- $d_3$ ,  $\delta$ , 25 °C): -62.88 (CF<sub>3</sub>, s).  $^{13}\text{C-NMR}$  (MeCN- $d_3$ ,  $\delta$ , 0 °C): 146.0 (3C, overlapping resonances with **4A**, **4B**, **4HA** and **4HB**, Tp3/5), (3C, 141.9, overlapping resonances with **4A**, **4B**, **4HA** and **4HB**, Tp3/5), 111.1 (C1 of **4B**), 106.2 to 107.7 (Tp4, overlapping resonances with **4A**, **4B**, **4HA** and **4HB**), 126.0 or 125.3 (CF<sub>3</sub>, q,  $J_{\text{CF}} = 269.0$  or 267.0), 63.2 (C4, d,  $J_{\text{PC}} = 9.2$ ), 63.5 (C3), 25.3 (overlapping PBU<sub>3</sub> resonances), 25.0 (overlapping PBU<sub>3</sub> resonances with **4A**, **4B**, **4HA** and **4HB**), 22.8 (overlapping PBU<sub>3</sub> resonances for isomers **4A**, **4B**, **4HA** and **4HB**), 13.9 (overlapping PBU<sub>3</sub> resonances with **4A**, **4B**, **4HA** and **4HB**). Anal. Calcd for C<sub>28</sub>H<sub>42</sub>BF<sub>3</sub>N<sub>7</sub>OPW: C, 43.38; H, 5.46; N, 12.65. Found: C, 43.08; H, 5.52; N, 12.39.



**4A**

$^1\text{H-NMR}$  (MeCN- $d_3$ ,  $\delta$ , 0 °C): 8.07 (1H, d, Tp3A), 7.90 (3H, overlapping d, Tp3/5), 7.79 (1H, d, Tp5A), 7.38 (1H, d, 5.13, H2), 7.29 (1H, d, Tp3C), 6.97 (1H, overlapping, H5), 6.33 (1H, t, Tp4B), 6.29 (1H, t, Tp4A),

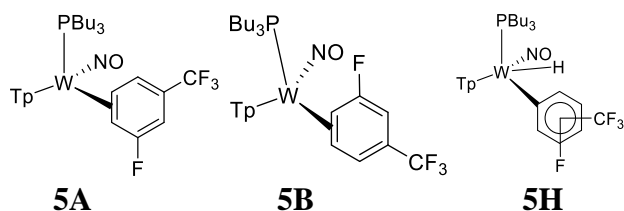
6.25 (1H, t, Tp4C), 5.76 (1H, overlapping, H6), 3.76 (1H, m, H3), 2.17 (1H, m, H4), 1.83 (6H, overlapping with other isomers **4A**, **4B**, **4HA** and **4HB**, PBU<sub>3</sub>), 1.24 (6H, overlapping with other isomers **4A**, **4B**, **4HA** and **4HB**, PBU<sub>3</sub>), 1.08 (6H, overlapping with other isomers **4A**, **4B**, **4HA** and **4HB**, PBU<sub>3</sub>). <sup>31</sup>P-NMR (MeCN-*d*<sub>3</sub>, δ, 25°C): -5.09 (*J*<sub>WP</sub> = 294). <sup>19</sup>F-NMR (MeCN-*d*<sub>3</sub>, δ, 25°C): -62.13 (CF<sub>3</sub>, s). <sup>13</sup>C-NMR (MeCN-*d*<sub>3</sub>, δ, 0 °C): 146.0 (3C, overlapping with other isomers Tp3/5), (3C, 141.9 overlapping with other isomers), 135.7 (overlapping C2 and C5), 110.3 (C6), 126.0 or 125.3 (CF<sub>3</sub>, q, *J*<sub>CF</sub> = 269 or 267), 106.2 to 107.7 (overlapping Tp4 resonances for isomers **4A**, **4B**, **4HA** and **4HB**), 63.6 (C4), 60.3 (C3, d, *J*<sub>PC</sub> = 7.9), 25.3 (overlapping PBU<sub>3</sub> resonances for isomers **4A**, **4B**, **4HA** and **4HB**), 25.0 (overlapping PBU<sub>3</sub> resonances for isomers **4A**, **4B**, **4HA** and **4HB**), 22.8 (overlapping PBU<sub>3</sub> resonances for isomers **4A**, **4B**, **4HA** and **4HB**), 13.9 (overlapping PBU<sub>3</sub> resonances for isomers **4A**, **4B**, **4HA** and **4HB**).



#### Select resonances for **4HA** and **4HB**

<sup>1</sup>H-NMR (MeCN-*d*<sub>3</sub>, δ, 0 °C): 9.59 (1H, m, *J*<sub>PH</sub> = 98, *J*<sub>WP</sub> = 30, W-H for **4HA**), 9.56 (1H, m, *J*<sub>PH</sub> = 95, *J*<sub>WP</sub> = 30, W-H for **4HB**), 7.64 (1H, d, overlapping Tpd for either **4HA** or **4HB**), 7.11 (1H, d, *J* = 7.19, Ph-Ring proton for **4HA** or **4HB**), 7.06 (1H, d, *J* = 7.44, Ph-Ring proton for **4HA** or **4HB**), 6.91 (3H, buried, overlapping Tpd for either **4HA** or **4HB** and H3/5 for **4HA**), 5.95 (1H, t, Tp4 for **4HB**), 5.94 (1H, t, Tp4 for **4HA**). <sup>31</sup>P-NMR (MeCN-*d*<sub>3</sub>, δ, 25°C): 15.80 and 15.53, (*J*<sub>WP</sub> = 176 for 15.53 resonance, *J*<sub>WP</sub> = 174 for 15.80 resonance, **4HA** and **4HB**). <sup>13</sup>C-NMR (MeCN-*d*<sub>3</sub>, δ, 0 °C): 180.2 (overlapping C4 and C3 for **4HA** and **4HB**), 146.1 (Ph-ring carbon for **4HA**), 145.0 (Ph-ring-carbon for **4HB**), 136.3 (Ph-ring carbon for **4HA**), 130.5 (Ph-ring carbon for **4HA**).

#### Synthesis of WTp(NO)(P(*n*-Bu)<sub>3</sub>)(η<sup>2</sup>-4,5,-3-fluoro-trifluoromethyl-benzene) (**6**)

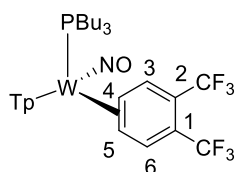


To a 4-dram vial was added complex **2** (0.550 g, 0.778 mmol) along with 3-fluoro-trifluoromethylbenzene (2 g, 12.2 mmol) and this reaction mixture was allowed to stir for 30 min. After that time the reaction mixture was added to a solution of stirring pentane (20 mL) and this solution was allowed to cool to -30 °C for 15 min to aid in inducing precipitation of a red solid. The solid was then isolated on a fine 15 mL porosity fritted disc and was washed with pentane (1x 5 mL). The solid was dried overnight under static vacuum before a mass

was taken of the red-orange solid (0.080 g, x 13%). Partial characterization of either  $\eta^2$ -complex is provided below along with some spectroscopic features of the **5H** complex (site of C-H activation undetermined).

$^1\text{H-NMR}$  (acetone- $d_6$ ,  $\delta$ , 0 °C): 9.41 (1H, m,  $J_{\text{PH}} = 102.9$ , **5H**), 6.12 to 6.43 (multiple overlapping Tpt resonances for all isomers), 5.49 (1H, d,  $J_{\text{HF}} = 14.1$ , H2 for **5A/5B**), 5.36 (1H, d,  $J_{\text{HF}} = 12.9$ , H2 for **5A/5B**), 3.98 (2H, overlapping for both dihapto-bound isomers broad m, **5A** and **5B**), 2.01 (2H, overlapping for both dihapto-bound isomers broad m, **5A** and **5B**), 0.8 to 1.90 (overlapping  $\text{PBu}_3$  resonances).  $^{31}\text{P-NMR}$  (acetone- $d_6$ ,  $\delta$ , 25°C): -5.1 and -5.6, ( $J_{\text{WP}} = 288$  for -5.1 resonance,  $J_{\text{WP}} = 268$  for -5.6 resonance, **5A** and **5B**), +15.7 ( $J_{\text{WP}} = 171$  for **5H**).  $^{13}\text{C-NMR}$  (acetone- $d_6$ ,  $\delta$ , 0 °C): 60.9, 56.3, 88.5 (d,  $J_{\text{CF}} = 24.3$ , C2), 91.0 (d,  $J_{\text{CF}} = 27.4$ , C2).

### Synthesis of $\text{WTP}(\text{NO})(\text{P}(\text{n-Bu})_3)(\eta^2\text{-4,5-bis-trifluoromethyl-benzene})$ (**6**)



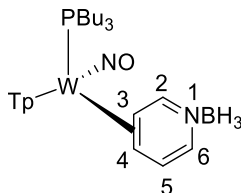
A 4-dram vial was charged with a stir bar, 1,2-bis(trifluoromethyl)benzene (2.00 g, 9.34 mmol) and **3** (0.103 g, 0.140 mmol) and the initially homogeneous yellow reaction mixture was allowed to stir for 24 h. Over time the reaction mixture turns from a homogeneous yellow to a light brown color and at the end of 6 h this reaction mixture was added to 10 mL of pentane and allowed to sit at -30 °C for 16 h. Over time crystals suitable for x-ray diffraction developed and the light tan solid was then isolated on a fine 15 mL fritted disc. This solid was then washed with 3 x 10 mL of pentane that had been chilled to -30 °C and allowed to dry under static vacuum for 16 h. A mass was then taken the next day of the product, a light tan solid (0.053 g, 45 %). Atomic composition consistent with crystal structure.

CV (MeCN)  $E_{p,a} = +0.47$  V (NHE). IR:  $\nu(\text{BH}) = 2490$   $\text{cm}^{-1}$ ,  $\nu(\text{NO}) = 1587$   $\text{cm}^{-1}$ .  $^1\text{H-NMR}$  (benzene- $d_6$ ,  $\delta$ , 25 °C): 8.18 (1H, d, Tp3/5), 7.80 (1H, d,  $J = 6.50$ , H6), 7.79 (1H, d, Tp3/5), 7.71 (1H, d,  $J = 5.9$ , H3), 7.30 (1H, d, Tp3/5), 7.28 (1H, d, Tp3/5), 7.26 (1H, d, Tp3/5), 6.71 (1H, d, Tp3/5), 5.75 (2H, overlapping t, Tp4), 5.69 (1H, t, Tp4), 3.42 (1H, m, H4), 2.12 (1H, m, H5), 1.71 (3H, m,  $\text{PBu}_3$ ), 1.59 (3H, m,  $\text{PBu}_3$ ), 1.15 (3H, m,  $\text{PBu}_3$ ), 1.10 (3H, m,  $\text{PBu}_3$ ), 0.91 (3H, m,  $\text{PBu}_3$ ), 0.78 (9H, t,  $J = 7.36$ ,  $\text{PBu}_3$ ),  $^{31}\text{P-NMR}$  (benzene- $d_6$ ,  $\delta$ , 25°C): -3.96 ( $J_{\text{WP}} = 292$ ).  $^{19}\text{F-NMR}$  (benzene- $d_6$ ,  $\delta$ , 25°C): -57.6 (3F, q,  $J_{\text{FF}} = 12.6$ ,  $\text{CF}_3$ ), -57.9 (3F, q,  $J_{\text{FF}} = 12.6$ ,  $\text{CF}_3$ ).  $^{13}\text{C-NMR}$  (benzene- $d_6$ ,  $\delta$ , 25 °C): 145.6 (Tp3/5), 142.3 (Tp3/5), 140.7 (Tp3/5), 140.4 (C6, q,  $J_{\text{CF}} = 7.2$ ), 139.3 (broad, C3), 136.4 (Tp3/5), 135.8 (Tp3/5), 135.5 (Tp3/5), 125.1 (overlapping  $\text{CF}_3$  resonances,  $J_{\text{CF}} = 270.0$ ), 115.1 (q,  $J_{\text{CF}} = 31.1$ , C1/C2), 113.2 (q,  $J_{\text{CF}} = 31.1$ , C1/C2), 106.6 (Tp4), 106.5 (Tp4), 106.4 (Tp4), 60.1 (C5), 60.0 (C4,  $J_{\text{PC}} = 9.3$ ), 25.1 (d,  $J_{\text{PC}} = 3.1$ ,  $\text{PBu}_3$ ), 24.7 (d,  $J_{\text{PC}} = 12.4$ ,  $\text{PBu}_3$ ), 22.8 (d,  $J_{\text{PC}} = 23.1$ ,  $\text{PBu}_3$ ), 13.8 ( $\text{PBu}_3$ ).

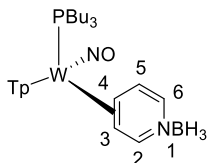
### Synthesis of $\text{WTP}(\text{NO})(\text{P}(\text{n-Bu})_3)(\eta^2\text{-3,4-pyridineborane})$ (**7**)

A solid of **3** (500 mg, 0.678 mmol) was added to a 4-dram vial containing stirring neat pyridine-borane (3.00 g, 32.3 mmol). After stirring for 2 h, the reaction mixture was diluted with 6 mL THF, followed by 25 mL  $\text{Et}_2\text{O}$  and then 90 mL of hexanes. The solution was allowed to settle for 15 min, while a Celite column (1 cm tall) was prepared in a 15 mL medium porosity fritted disk. The solution was decanted through the Celite, leaving

a green oil. The oil was again diluted with 6 mL THF, followed by 25 mL Et<sub>2</sub>O and then 90 mL of hexanes. The solution was decanted through the Celite, leaving a clumpy material in the vial. The material captured by the Celite was dissolved in 6 mL THF and returned to the vial. Upon complete dissolution of all solids, the solution was diluted with 25 mL followed by 150 mL hexanes. The precipitate was collected on the Celite column, and then redissolved with 20 mL THF. The resulting solution was diluted with 35 mL Et<sub>2</sub>O and 150 mL hexanes, forming a bright yellow precipitate. The precipitate was collected on a 15 mL medium porosity fritted funnel, rinsed with 2 x 5 mL hexanes, transferred wet to a vial, and placed under dynamic vacuum (0.185 g, 38%).

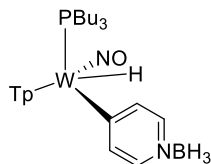


CV (DMA)  $E_{p,a} = +0.59$  V (NHE). IR:  $\nu(\text{BH}) = 2519$   $\text{cm}^{-1}$ ,  $\nu(\text{BH}_3) = 2348, 2288, 2256$   $\text{cm}^{-1}$ ,  $\nu(\text{NO}) = 1587$   $\text{cm}^{-1}$ . <sup>1</sup>H-NMR (acetone-*d*<sub>6</sub>,  $\delta$ , 15 °C): 8.62 (1H, d,  $J = 4.21$ , H2), 8.14 (1H, d, Tp3/5), 8.09 (1H, Tp3/5), 8.04 (1H, d, Tp3/5), 7.92 (2H, d overlapping, Tp3/5), 7.62 (1H, d, Tp3/5), 6.77 (1H, t,  $J = 6.34$ , H5), 6.44 (1H, t, Tp4), 6.37 (1H, t, Tp4), 6.34 (1H, t, Tp4), 6.18 (1H, d,  $J = 7.03$ , H6), 3.65 (1H, m, H3), 2.17 (1H, t,  $J = 7.54$ , H4), 1.92 (6H, m overlapping with minor, PBu<sub>3</sub>), 1.20 (12H, overlapping resonances and overlapping with minor, PBu<sub>3</sub>), 0.79 (9H, t,  $J = 7.51$ , PBu<sub>3</sub>). <sup>31</sup>P-NMR (acetone-*d*<sub>6</sub>,  $\delta$ , 25 °C): -3.6 (PMe<sub>3</sub>,  $J_{\text{WP}} = 284$ ). <sup>13</sup>C-NMR (acetone-*d*<sub>6</sub>,  $\delta$ , 0 °C): 167.7 (C2), 146.0 (Tp3/5), 142.3 (Tp3/5), 141.7 (Tp3/5), 138.2 (Tp3/5), 137.4 (Tp3/5), 136.7 (Tp3/5), 127.2 (C5/6), 125.3 (C5/6), 107.6 (Tp4 overlapping with minor), 107.4 (Tp4), 106.7 (Tp4), 61.1 (C4), 59.3 (C3, d,  $J_{\text{PC}} = 7.1$ ), 25.5 (PBu<sub>3</sub> overlap with minor isomer), 25.0 (PBu<sub>3</sub>, overlap with minor isomer **7B**), 23.4 (PBu<sub>3</sub>, d,  $J_{\text{PC}} = 24.6$ ), 14.0 (PBu<sub>3</sub> overlap with minor isomer **7A**). Anal. Calcd for C<sub>26</sub>H<sub>45</sub>B<sub>2</sub>N<sub>8</sub>OPW: C, 43.24; H, 6.28; N, 15.52. Found: C, 42.94; H, 6.31; N, 15.37.



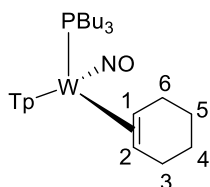
<sup>1</sup>H-NMR (acetone-*d*<sub>6</sub>,  $\delta$ , 15 °C): 8.50 (1H, d,  $J = 4.50$ , H2), 8.10 (1H, d, Tp3/5), 8.09 (2H, d overlapping, Tp3/5), 8.01 (1H, d, Tp3/5), 7.92 (1H, d overlapping with major, Tp3/5), 7.59 (1H, d, Tp3/5), 6.74 (1H, t,  $J = 6.62$ , H5), 6.43 (1H, t, Tp4), 6.41 (1H, t, Tp4), 6.39 (1H, t, Tp4), 6.24 (1H, d,  $J = 6.62$ , H6), 3.92 (1H, m, H4), 2.07 (1H, buried, H3), 1.91 (6H, m overlapping with major, PBu<sub>3</sub>), 1.20 (12H, overlapping resonances and overlapping with major, PBu<sub>3</sub>), 0.77 (9H, t,  $J = 7.41$ , PBu<sub>3</sub>). <sup>31</sup>P-NMR (acetone-*d*<sub>6</sub>,  $\delta$ , 25 °C): -3.9 ( $J_{\text{WP}} = 291$ ). <sup>13</sup>C-NMR (acetone-*d*<sub>6</sub>,  $\delta$ , 0 °C): 169.9 (C2), 146.4 (Tp3/5), 144.1 (Tp3/5), 142.3 (Tp3/5), 138.1 (Tp3/5), 137.6 (Tp3/5), 136.7 (Tp3/5), 127.6 (C5/6), 126.7 (C5/6), 107.6 (Tp4 overlapping with minor), 107.5 (Tp4), 107.1 (Tp4), 61.4 (C4, d,  $J_{\text{PC}} = 9.86$ ), 58.8 (C3), 25.5 (PBu<sub>3</sub> overlap with major isomer), 25.0 (PBu<sub>3</sub>, overlap with major isomer), 22.8 (PBu<sub>3</sub>, d,  $J_{\text{PC}} = 24.2$ ), 14.0 (PBu<sub>3</sub> overlap with major isomer).

## Partial Characterization of 4H



$^1\text{H-NMR}$  (acetone- $d_6$ ,  $\delta$ , 25 °C): 9.40 (1H, m,  $J_{\text{PH}} = 92.5$ ,  $J_{\text{WH}} = 26.3$ , W-H), 8.20 (1H, d, Tp3/5), 8.08 (1H, Tp3/5), 7.80 (1H, d, Tp3/5), 7.79 (1H, d, Tp3/5), 7.14 (1H, d, Tp3/5), 6.53 (1H, t, Tp4), 6.14 (1H, t, Tp4).

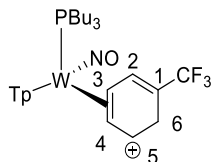
## Synthesis of $\text{WTp}(\text{NO})(\text{P}(\text{n-Bu})_3)(\eta^2\text{-1,2-cyclohexene})$ (10)



To a 4-dram vial was added **3** (0.492 g, 0.67 mmol) along with cyclohexene (1 mL, 9.9 mmol). The initially heterogeneous yellow reaction mix was allowed to stir over 4 h, during which time the solution turned to a light homogeneous brown color. The reaction mixture was then added to 15 mL of pentane that had been chilled to -30 °C to precipitate out a light pink solid. This solid was then collected on a fine 15 mL fritted disc. The solid was then washed with 3 x 5 mL pentane and the filtrate was evaporated in vacuo and subsequently picked up in a minimal amount of DCM (1 mL) and added to 15 mL of standing pentane in a 4-dram vial. This solution was allowed to sit at -30 °C overnight during which time a light yellow solid precipitates from solution. Combining the masses of the two isolated fractions gave a final yield (0.235 g, 49 % yield). Atomic composition of complex consistent with crystal structure.

CV (DMA)  $E_{p,a} = +0.30$  V (NHE). IR:  $\nu(\text{BH}) = 2483$   $\text{cm}^{-1}$ ,  $\nu(\text{NO}) = 1535$   $\text{cm}^{-1}$ .  $^1\text{H-NMR}$  ( $\text{CDCl}_3$ ,  $\delta$ , 20 °C): 8.19 (1H, d, Tp3/5), 8.08 (1H, d, Tp3/5), 7.67 (1H, d, Tp3/5), 7.64 (1H, d, Tp3/5), 7.58 (1H, d, Tp3/5), 7.27 (1H, d, Tp3/5), 6.27 (1H, t, Tp4), 6.17 (1H, t, Tp4), 6.12 (1H, t, Tp4), 2.74 (2H, overlapping m, H3 and H6), 2.64 (2H, overlapping m, H1 and H3), 2.48 (1H, m, H6), 1.87 (3H, m,  $\text{PBu}_3$ ), 1.73 (3H, m,  $\text{PBu}_3$ ), 1.79 (1H, m, H4/5), 1.76 (1H, m, H4/H5), 1.44 (2H, overlapping m, H4/H5), 1.35 (1H, m, H2), 1.21 (3H, m,  $\text{PBu}_3$ ), 1.16 (3H, m,  $\text{PBu}_3$ ), 0.96 (3H, m,  $\text{PBu}_3$ ), 0.87 (3H, m,  $\text{PBu}_3$ ), 0.78 (9H, t,  $J = 7.22$ ,  $\text{PBu}_3$ ).  $^{31}\text{P-NMR}$  ( $\text{CDCl}_3$ ,  $\delta$ , 20 °C): -1.83 ( $J_{\text{WP}} = 276$ ).  $^{13}\text{C-NMR}$  ( $\text{CDCl}_3$ ,  $\delta$ , 25 °C): 145.0 (Tp3/5), 142.6 (Tp3/5), 140.6 (Tp3/5), 136.1 (Tp3/5), 135.4 (Tp3/5), 135.0 (Tp3/5), 136.1 (Tp3/5), 135.4 (Tp3/5), 135.0 (Tp3/5), 106.3 (Tp4), 195.6 (Tp4), 105.4 (Tp4), 53.8 (C2, m,  $J_{\text{WC}} = 29.9$ ), 52.4 (C1, m,  $J_{\text{PC}} = 11.0$ ,  $J_{\text{WC}} = 24.5$ ), 29.6 (C6), 27.6 (C3), 25.1 (C4/5), 25.0 ( $\text{PBu}_3$ ), 24.9 ( $\text{PBu}_3$ ,  $J_{\text{PC}} = 15.1$ ), 24.7 ( $\text{PBu}_3$ ,  $J_{\text{PC}} = 11.8$ ), 22.9 ( $\text{PBu}_3$ ,  $J_{\text{PC}} = 23.4$ ), 22.5 (C4/5), 13.88 ( $\text{PBu}_3$ ).

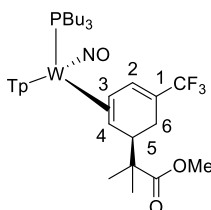
## Synthesis of $\text{WTp}(\text{NO})(\text{P}(\text{n-Bu})_3)(\eta^2\text{-3,4-trifluoromethyl-benzenium})$ (11)



An in situ sample of **12** was prepared by chilling an NMR scale solution with MeCN-*d*<sub>3</sub> (~1/2 mL) of **4** (~ 30 mgs) to -30 °C over a period of 15 min. To this initially heterogeneous yellow solution was added 5 drops of HOTf that had also been chilled to -30 °C. Upon addition the reaction mixture turns to a homogeneous red solution and this sample was frozen in N<sub>2</sub>(l) and a <sup>1</sup>H NMR spectra was taken of this sample upon thawing at reduced temperatures.

. <sup>1</sup>H-NMR (MeCN-*d*<sub>3</sub>, δ, 0 °C): 8.32 (1H, d, Tp3/5), 8.04 (1H, d, Tp3/5), 8.03 (1H, d, Tp3/5), 7.95 (1H, d, Tp3/5), 7.93 (1H, d, Tp3/5), 7.77 (1H, d, Tp3/5), 7.04 (2H, overlapping broad d, H2 and H5), 6.54 (1H, t, Tp4), 6.48 (1H, t, Tp4), 6.29 (1H, t, Tp4), 5.06 (1H, t, *J* = 6.75, H4), 4.26 (1H, buried, H3), 4.15 (1H, roofing d, *J* = 27.3, H6 syn/anti), 4.01 (1H, roofing d, *J* = 27.3, H6 syn/anti), 1.92 (3H, broad, PBU<sub>3</sub>), 1.48 (3H, broad, PBU<sub>3</sub>), 1.22 (3H, m, PBU<sub>3</sub>), 1.16 (3H, m, PBU<sub>3</sub>), 0.98 (3H, broad, PBU<sub>3</sub>), 0.77 (9H, t, *J* = 7.60, PBU<sub>3</sub>), 0.61 (3H, broad, PBU<sub>3</sub>).

#### Synthesis of WTP(NO)(P(*n*-Bu)<sub>3</sub>)(η<sup>2</sup>-3,4-(methyl-2-methyl-2-(5-(trifluoromethyl)cyclohexa-2,4-dien-1-yl)-propanoate)) (**12**)



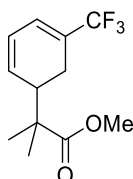
First **3** (0.802 g, 1.03 mmol) was dissolved in 3 mL of MeCN and chilled to -30 °C over a period of 15 min. After 15 min HOTf (0.241 g, 1.59 mmol) was added and upon addition the reaction mixture, initially a heterogeneous yellow solution turns to a homogeneous red reaction mixture. This solution was allowed to sit at -30 °C for 15 min and then methyl trimethylsilyl dimethylketene acetal (MTDA, 1.70 g, 9.77 mmol) was added to the reaction mixture and this was allowed to sit for 22 h at -30 °C. The next day a -30 °C solution of triethylamine (1.00 g, 9.88 mmol) was added to the reaction mixture. The reaction mixture was then filtered through a medium 30 mL fritted disc that had been filled with ~ 3cm of silica and set in diethyl ether. The reaction mixture was eluted with diethyl ether until a lime green band began to elute through the column. Before collection the clear eluent was discarded and the lime green band was washed with ~60 mL of diethyl ether. The solvent was then removed in vacuo until a light green solid developed on the bottom of the flask and NMR analysis was performed in acetone-*d*<sub>6</sub> before the reaction was carried on to the synthesis of **15**. Crystals suitable for X-ray diffraction were grown in a mixture of acetone:chloroform at reduced temperatures and support the elemental composition of the complex.

<sup>1</sup>H-NMR (acetone-*d*<sub>6</sub>, δ, 25 °C): 8.09 (1H, d, Tp3/5), 7.98 (1H, d, Tp3A), 7.95 (1H, d, Tp5C), 7.93 (1H, d, Tp3/5B), 7.84 (1H, d, Tp5A), 7.68 (1H, d, Tp3C), 7.17 (1H, broad s, H2), 6.39 (1H, t, Tp4B), 6.33 (2H, overlapping t, Tp4A/C), 3.42 (1H, d, *J* = 9.06, H5-syn), 3.17 (3H, OMe, s), 2.95 (1H, m, H3), 2.85 (1H, m, H6-syn), 2.02 (1H, d, *J* = 17.44, H6-anti), 1.92 (3H, m, PBU<sub>3</sub>), 1.82 (3H, m, PBU<sub>3</sub>), 1.25 (3H, m, PBU<sub>3</sub>), 1.27 (3H,



m, PBU<sub>3</sub>), 1.09 (3H, m, PBU<sub>3</sub>), 0.81 (3H, broad m, PBU<sub>3</sub>), 0.77 (9H, t,  $J = 7.15$ , PBU<sub>3</sub>), 1.23 (3H, s, Me), 1.16 (3H, s, Me). <sup>31</sup>P-NMR (acetone-*d*<sub>6</sub>,  $\delta$ , 25 °C): -3.40 ( $J_{WP} = 269$ ). <sup>19</sup>F-NMR (acetone-*d*<sub>6</sub>,  $\delta$ , 25 °C): -66.36 (CF<sub>3</sub>). <sup>13</sup>C-NMR (acetone-*d*<sub>6</sub>,  $\delta$ , 25 °C): 178.7 (CO<sub>2</sub>Me), 145.1 (Tp3/5), 142.2 (Tp3/5), 141.8 (Tp3/5), 137.9 (C2), 137.6 (Tp3/5), 137.2 (Tp3/5), 136.9 (Tp3/5), 126.6 (CF<sub>3</sub>, q,  $J_{CF} = 271$ ), 116.7 (C1, q,  $J_{CF} = 29.5$ ), 107.3 (Tp4), 107.1 (Tp4), 106.3 (Tp4), 55.1 (C4), 52.2 (C-Me<sub>2</sub>), 51.1 (OMe), 47.3 (C3, d,  $J_{CP} = 10.4$ ), 42.3 (C5), 25.8 (PBU<sub>3</sub>), 25.0 (PBU<sub>3</sub>, d,  $J_{PC} = 12.84$ ), 23.8 (PBU<sub>3</sub>, d,  $J_{PC} = 24.0$ ), 23.5 (PBU<sub>3</sub>), 22.3 (Me), 21.4 (Me), 13.9 (PBU<sub>3</sub>).

### Synthesis of methyl-2-methyl-2-(5-(trifluoromethyl)cyclohexa-2,4-dien-1-yl)-propanoate (**13**)



A solution of **13** in acetone-*d*<sub>6</sub> had its solvent removed in vacuo and was subsequently dissolved in 3 mL of CDCl<sub>3</sub>. This solution was then added to a 1 mL solution of NOPF<sub>6</sub> (0.250g, 1.42 mmol) in CDCl<sub>3</sub> and upon addition of the solution of **13** the reaction mixture turned from a lime green color to a brown and finally to a yellow colored solution. This solution was then checked by <sup>1</sup>H NMR and upon observation that some of **13** still remained, the solution was then allowed to stir in a 4-dram vial and to this more NOPF<sub>6</sub> (0.330 g, 1.89 mmol) was added. Upon checking the reaction mixture by <sup>1</sup>H NMR again the absence of **13** was insured and the reaction mixture was purified with chromatography as has been previously reported.<sup>38</sup> Characterization matches the previously reported free organic and was isolated in 24% total yield (0.061 g, 0.246 mmol) starting from **4** (0.802 g, 1.03 mmol).<sup>31,38</sup>

### References

1. Jones, W. D., On the Nature of Carbon–Hydrogen Bond Activation at Rhodium and Related Reactions. *Inorganic Chemistry* **2005**, *44* (13), 4475-4484.
2. Balcells, D.; Clot, E.; Eisenstein, O., C–H Bond Activation in Transition Metal Species from a Computational Perspective. *Chemical Reviews* **2010**, *110* (2), 749-823.
3. Eisenstein, O.; Milani, J.; Perutz, R. N., Selectivity of C–H Activation and Competition between C–H and C–F Bond Activation at Fluorocarbons. *Chemical Reviews* **2017**, *117* (13), 8710-8753.
4. Gandeepan, P.; Müller, T.; Zell, D.; Cera, G.; Warratz, S.; Ackermann, L., 3d Transition Metals for C–H Activation. *Chemical Reviews* **2019**, *119* (4), 2192-2452.
5. Lersch, M.; Tilset, M., Mechanistic Aspects of C–H Activation by Pt Complexes. *Chemical Reviews* **2005**, *105* (6), 2471-2526.
6. Shilov, A. E.; Shul'pin, G. B., Activation of C–H Bonds by Metal Complexes. *Chemical Reviews* **1997**, *97* (8), 2879-2932.
7. Xue, X.-S.; Ji, P.; Zhou, B.; Cheng, J.-P., The Essential Role of Bond Energetics in C–H Activation/Functionalization. *Chemical Reviews* **2017**, *117* (13), 8622-8648.
8. Solomon, R. G.; Kochi, J. K., Cationic Benzene and Olefin Complexes of Copper(I) Trifluoromethanesulphonate. *J. Chem. Soc., Comm.* **1972**, 559.

9. Norris, C. M.; Reinartz, S.; White, P. S.; Templeton, J. L., Barriers for Arene C–H Bond Activation in Platinum(II)  $\eta^2$ -Arene Intermediates. *Organometallics* **2002**, *21* (25), 5649-5656.
10. Liebov, B. K.; Harman, W. D., Group 6 Dihapto–Coordinate Dearomatization Agents for Organic Synthesis. *Chemical Reviews* **2017**, *117* (22), 13721-13755.
11. Tagge, C. D.; Bergman, R. G., Synthesis, X-ray Structure Determination, and Reactions of (Pentamethylcyclopentadienyl)(nitrosyl)ruthenium  $\eta^2$ -Arene Complexes. *Journal of the American Chemical Society* **1996**, *118* (29), 6908-6915.
12. Driver, T. G.; Williams, T. J.; Labinger, J. A.; Bercaw, J. E., C–H Bond Activation by Dicationic Platinum(II) Complexes. *Organometallics* **2007**, *26* (2), 294-301.
13. Sweet, J. R.; Graham, W. A. G., Cationic  $\eta^2$ -arene complexes of rhenium in carbon-hydrogen bond activation. *Journal of the American Chemical Society* **1983**, *105* (2), 305-306.
14. Jones, W. D.; Dong, L., Direct observation of  $\eta^2$ -arene complexes of [(C5Me5)Rh(PMe3)]. *Journal of the American Chemical Society* **1989**, *111* (23), 8722-8723.
15. Chin, R. M.; Dong, L.; Duckett, S. B.; Partridge, M. G.; Jones, W. D.; Perutz, R. N., Control of  $\eta^2$ -coordination vs. carbon-hydrogen bond activation by rhodium: the role of aromatic resonance energies. *Journal of the American Chemical Society* **1993**, *115* (17), 7685-7695.
16. Harman, W. D., The Activation of Aromatic Molecules with Pentaammineosmium(II). *Chem. Rev.* **1997**, *97*, 1953-1978.
17. Keane, J. M.; Harman, W. D., A New Generation of Pi-Basic Dearomatization Agents. *Organomet.* **2005**, *24*, 1786-1798.
18. Liu, W.; Welch, K.; Trindle, C. O.; Sabat, M.; Myers, W. H.; Harman, W. D., Facile Intermolecular Aryl–F Bond Cleavage in the Presence of Aryl C–H Bonds: Is the  $\eta^2$ -Arene Intermediate Bypassed? *Organometallics* **2007**, *26* (10), 2589-2597.
19. Jones, W. D., Isotope effects in C–H bond activation reactions by transition metals. *Accounts of chemical research* **2003**, *36* (2), 140-146.
20. Churchill, D. G.; Janak, K. E.; Wittenberg, J. S.; Parkin, G., Normal and Inverse Primary Kinetic Deuterium Isotope Effects for C–H Bond Reductive Elimination and Oxidative Addition Reactions of Molybdenocene and Tungstenocene Complexes: Evidence for Benzene  $\sigma$ -Complex Intermediates. *Journal of the American Chemical Society* **2003**, *125* (5), 1403-1420.
21. Stoutland, P. O.; Bergman, R. G., Insertion of iridium into the carbon-hydrogen bonds of alkenes: the  $\pi$ -complex cannot be an intermediate. *Journal of the American Chemical Society* **1985**, *107* (15), 4581-4582.
22. Fukui, K., The path of chemical reactions - the IRC approach. *Accounts of Chemical Research* **1981**, *14* (12), 363-368.
23. Welch, K. D.; Harrison, D. P.; Lis, E. C.; Liu, W.; Salomon, R. J.; Harman, W. D.; Myers, W. H., Large-Scale Syntheses of Several Synthons to the Dearomatization Agent {TpW(NO)(PMe3)} and Convenient Spectroscopic Tools for Product Analysis. *Organometallics* **2007**, *26* (10), 2791-2794.
24.  $\Delta H^\ddagger$  was also calculated for  $2\sigma$  (12.9),  $2\pi$  (17.1), and separated (21.6) for the PBu3 system. The corresponding Gibbs values at 298 K are:  $2\sigma$  (9.6),  $2\pi$  (13.6), and separated (5.5) kcal/mol.
25. Harman, W. D.; Sekine, M.; Taube, H., Substituent effects on  $\eta^2$ -coordinated arene complexes of pentaammineosmium(II). *Journal of the American Chemical Society* **1988**, *110* (17), 5725-5731.
26. Brooks, B. C.; Meiere, S. H.; Friedman, L. A.; Carrig, E. H.; Gunnoe, T. B.; Harman, W. D., Interfacial and Intrafacial Linkage Isomerizations of Rhenium Complexes with Aromatic Molecules. *Journal of the American Chemical Society* **2001**, *123* (15), 3541-3550.
27. Cronin, L.; Higgitt, C. L.; Perutz, R. N., Structure and Dynamic Exchange in Rhodium  $\eta^2$ -Naphthalene and Rhodium  $\eta^2$ -Phenanthrene Complexes: Quantitative NOESY and EXSY Studies. *Organometallics* **2000**, *19* (4), 672-683.
28. Benn, R.; Mynott, R.; Topalovic, I.; Scott, F., Fluxionality of ( $\eta^2$ -naphthalene)(iso-Pr2P(CH2) $n$ -iso-Pr2P)Ni0 ( $n = 2,3$ ) in the solid state and solution as studied by CP/MAS and 2D carbon-13 NMR spectroscopy. *Organometallics* **1989**, *8* (10), 2299-2305.



29. Winemiller, M. D.; Kelsch, B. A.; Sabat, M.; Harman, W. D., The Characterization and Isomerization of  $h^2$ -Naphthalene and  $h^2$ -Phenanthrene Complexes of Pentaammineosmium(II). *Organometallics* **1997**, *16*, 3672.
30. Colomer, I.; Batchelor-McAuley, C.; Odell, B.; Donohoe, T. J.; Compton, R. G., Hydrogen Bonding to Hexafluoroisopropanol Controls the Oxidative Strength of Hypervalent Iodine Reagents. *Journal of the American Chemical Society* **2016**, *138* (28), 8855-8861.
31. Myers, J. T.; Smith, J. A.; Dakermanji, S. J.; Wilde, J. H.; Wilson, K. B.; Shivokevich, P. J.; Harman, W. D., Molybdenum(0) Dihapto-Coordination of Benzene and Trifluorotoluene: The Stabilizing and Chemo-Directing Influence of a CF<sub>3</sub> Group. *Journal of the American Chemical Society* **2017**, *139* (33), 11392-11400.
32. Harrison, D. P.; Welch, K. D.; Nichols-Nielander, A. C.; Sabat, M.; Myers, W. H.; Harman, W. D., Efficient Synthesis of an  $\eta^2$ -Pyridine Complex and a Preliminary Investigation of the Bound Heterocycle's Reactivity. *Journal of the American Chemical Society* **2008**, *130* (50), 16844-16845.
33. Strausberg, L.; Li, M.; Harrison, D. P.; Myers, W. H.; Sabat, M.; Harman, W. D., Exploiting the o-Quinodimethane Nature of Naphthalene: Cycloaddition Reactions with  $\eta^2$ -Coordinated Tungsten–Naphthalene Complexes. *Organometallics* **2013**, *32* (3), 915-925.
34. Delafuente, D. A.; Myers, W. H.; Sabat, M.; Harman, W. D., Tungsten(0) - $\eta^2$ -Thiophene Complexes: Dearomatization of Thiophene and Its Facile Oxidation, Protonation, and Hydrogenation. *Organometallics* **2005**, *23*, 3772-3779.
35. Belt, S. T.; Dong, L.; Duckett, S. B.; Jones, W. D.; Partridge, M. G.; Perutz, R. N., Control of  $\eta^2$ -arene coordination and C–H bond activation by cyclopentadienyl complexes of rhodium. *Journal of the Chemical Society, Chemical Communications* **1991**, (4), 266-269.
36. Crabtree, R. H., *The organometallic chemistry of the transition metals*. John Wiley: New York, 2001.
37. Harrison, D. P.; Nichols-Nielander, A. C.; Zottig, V. E.; Strausberg, L.; Salomon, R. J.; Trindle, C. O.; Sabat, M.; Gunnoe, T. B.; Iovan, D. A.; Myers, W. H.; Harman, W. D., Hyperdistorted Tungsten Allyl Complexes and Their Stereoselective Deprotonation to Form Dihapto-Coordinated Dienes. *Organometallics* **2011**, *30* (9), 2587-2597.
38. Wilson, K. B.; Myers, J. T.; Nedzbala, H. S.; Combee, L. A.; Sabat, M.; Harman, W. D., Sequential Tandem Addition to a Tungsten–Trifluorotoluene Complex: A Versatile Method for the Preparation of Highly Functionalized Trifluoromethylated Cyclohexenes. *Journal of the American Chemical Society* **2017**, *139* (33), 11401-11412.

## Concluding Remarks

The heart of this thesis relies on the fact that novel reactivity can be achieved from existing transition metal scaffolds by appropriate manipulation of conditions. For example, while the tungsten-benzene complex was first reported in 2003 (nearly 17 years ago at the time of this writing), efficient access to mono- and double-protonated adducts of benzene was not accessible until use of an appropriate acid source (inherently tied to solvent conditions) was realized. The large number of variables for any given reaction including time, temperatures, solvent, co-solvent, chemical additives and appropriate choice of chemical reagent likely means that many synthetic “dead ends” were merely synthetic endeavors pursued under the “wrong” reaction conditions. The ability to *in situ* protonate fluorobenzene on tungsten (and thereby prevent oxidative addition across the aryl C-F bond) for instance could still well be possible despite my long-standing failure toward that synthetic aim. Tangentially, it was the attempt to “acid-trap” fluorobenzene that led to the protonation of benzene, and ultimately to the generation of the cyclohexene isotopologues, a project that ended up teaching me more than I ever could have hoped.

The fluorobenzene example (C-F activation) serves as a segue into a potentially contentious topic, namely, *how important is  $\eta^2$ -coordination?* More specifically, how important is the ability to see a dihapto-coordinate adduct at the aromatic stage to achieve  $\eta^2$ -coordination in subsequent synthetic steps? Consider, for instance, the minor tungsten-hydride complexes (corresponding to the oxidative addition of tungsten into an aryl C-H bond) sporadically observed as side products for aromatics such as benzene or trifluorotoluene once bound to the tungsten fragment. Treat either system with the appropriate acid source, and the only observed diamagnetic species observed is that of a tungsten-supported arenium in excellent yields. Further consider that NOESY experiments show that for each of these aromatic systems, the tungsten-hydride and dihapto-coordinate arene forms are in equilibrium with one another (the tungsten-hydride is not a kinetically

trapped product). Work with the  $\text{PBU}_3$  system is even more telling, as enhanced tungsten-hydride formation does not prohibit treatment with acid and the efficient formation of dihapto-arenium products. From these results it seems possible that if the oxidative addition product is enhanced, so long as there is even a mild equilibrium (say a 100:1 tungsten-hydride to dihapto-coordinate isomer) operative to a reductively eliminated intermediate, efficient protonation could essentially “trap” the isomer as to enable efficient avenue into  $\eta^2$ -like reactivity. One way to enhance the oxidative addition arene product would be to switch to extremely donating ancillary ligands for the tungsten-scaffold. The result would be a metal (II) species that could be stable to oxidation in the 7-coordinate form but that would transiently reductively eliminate, donate electron density into the dihapto-coordinate aromatic and thereby enable its protonation. Analogous considerations could be made in an effort to synthesize cycloadducts utilizing weak dienophiles.

Imagine then a metal so electron rich that the only observed adduct is a C-H activated benzene product in a tungsten (II) oxidation state. Such a compound could be resistant to oxidation and stored as a solid outside of an inert glovebox atmosphere. Adding this solid to a cold, acidic solution, outside the box could enable “trapping” of the dihapto-coordinate form as an arenium species. Subsequent exposure to an appropriate nucleophile could lead to a novel cyclohexadiene product *without the need for an inert atmosphere*.

Now imagine a much more electron-deficient chiral-at-metal  $\pi$ -base. It may not be able to effectively coordinate aromatic ligands, but it would be much more resistant to a wide array of reaction conditions. Perhaps replace the Tp ligand with a Tz ligand to help with water solubility and to guard against oxidation of the metal via protonation (shown by Shivokevich and Heyer) and you now have a chiral reagent potentially capable of dihapto-coordination to a wide array of unsaturated functionalities. Enhanced water solubility would make it amenable to more directly biological applications.

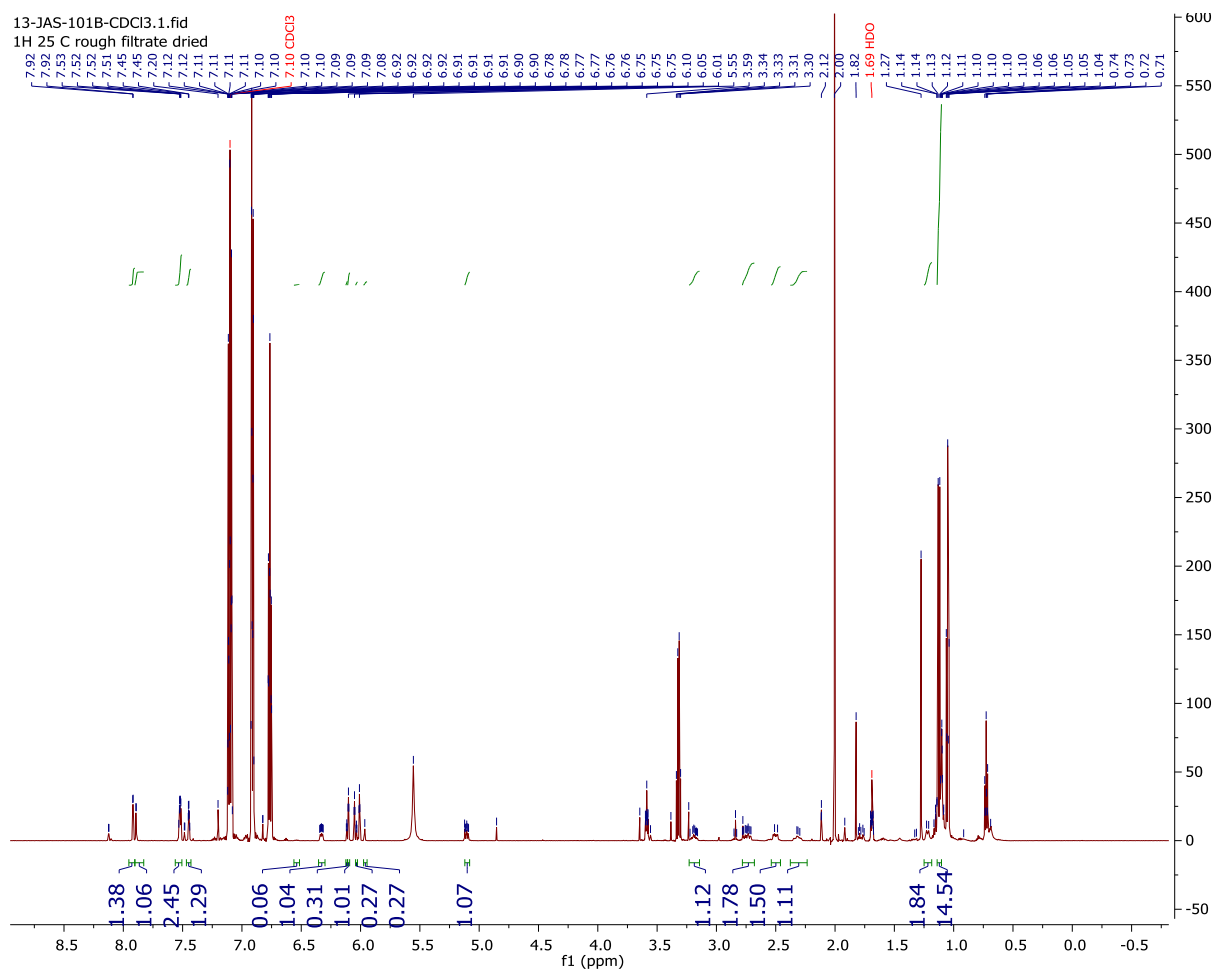
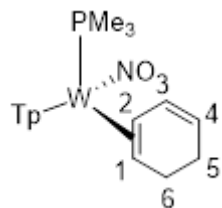
The power of dearomatization promoted by electron-rich metal systems is a potent synthetic strategy. However, I would argue that the knowledge and engineering of metal complexes, across third and second row metals, could extend into useful chemical tools for a broad range of applications. The ability to design a wide array of chiral-at-metal centers, with varying degrees of “electron-richness”, many of which readily coordinate unsaturated bounds is a powerful technology that could be used in a myriad of chemical applications (chemical sensing, spin transfer, chiral recognition, elucidating mechanisms in catalysis, generation of multi-metallic systems). Importantly, the various metal systems in our lab generate a holistic comparison in being able to relate the abilities of disparate metal centers (Os, Re, W and Mo) to attain similar types of reactivity. The ability for these metals to promote novel organic reactivity on aromatic molecules is a powerful technology. However, it is the accumulated knowledge (more than 30 years) regarding the electrochemistry, steric parameters and measurements of  $\pi$ -basicity (determined by structural elucidation and spectroscopic techniques) that have enabled the state-of-the-art dearomatization technology pioneered by Dean Harman. It is possible that enough holistic knowledge has been accumulated to generate metal-systems on a case-by-case basis (being able to readily alter ancillary ligand or even the metal itself), with their engineering fine-tuned for other chemical applications.

## **Appendix**

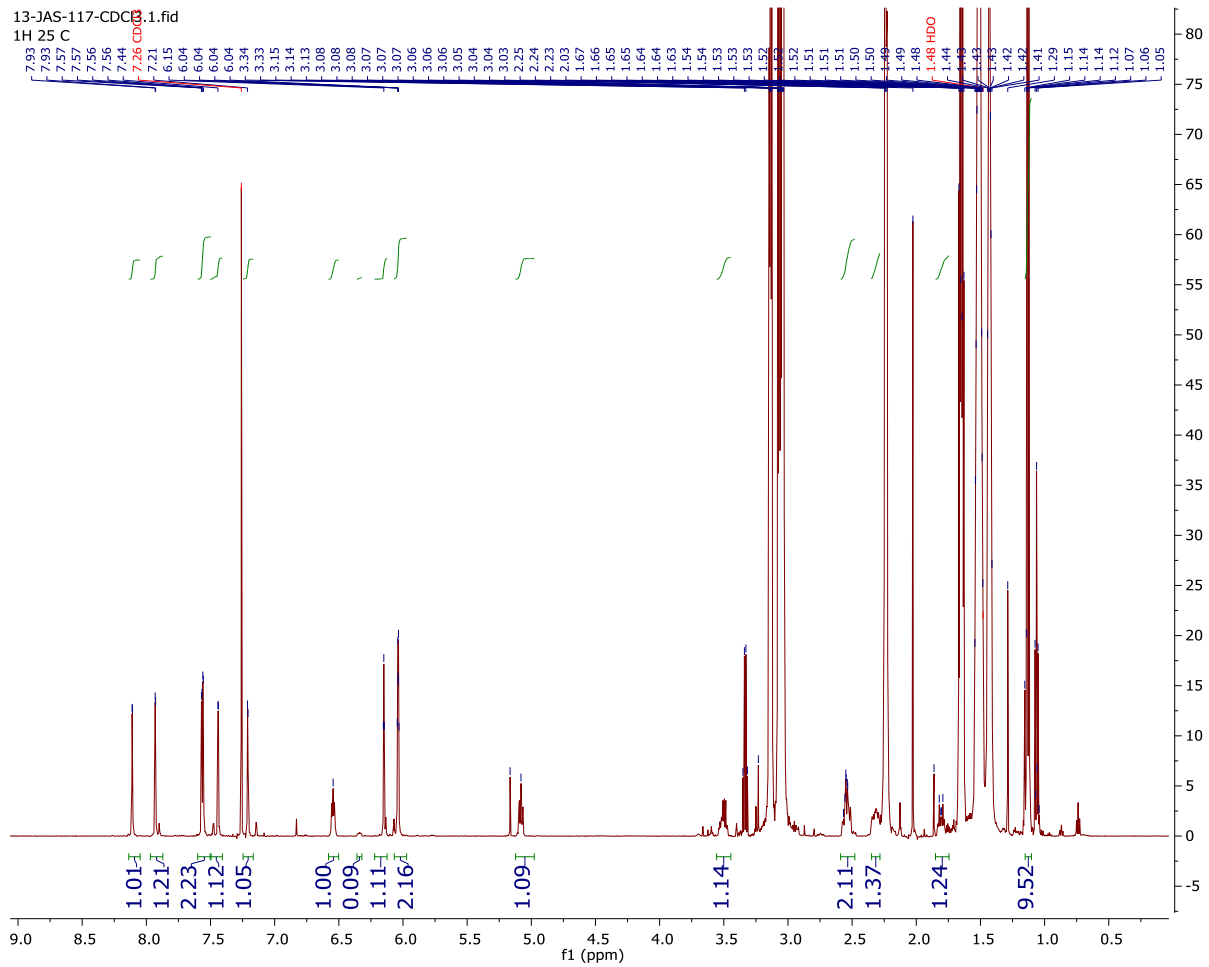
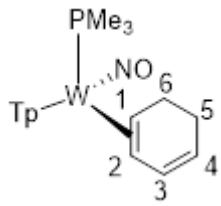
Includes supporting spectroscopic data, crystal data, MRR data and analysis and other characterization details for molecules discussed throughout this work. The organization goes by presenting data on a per-chapter basis.

# Supporting Information for Chapter 2

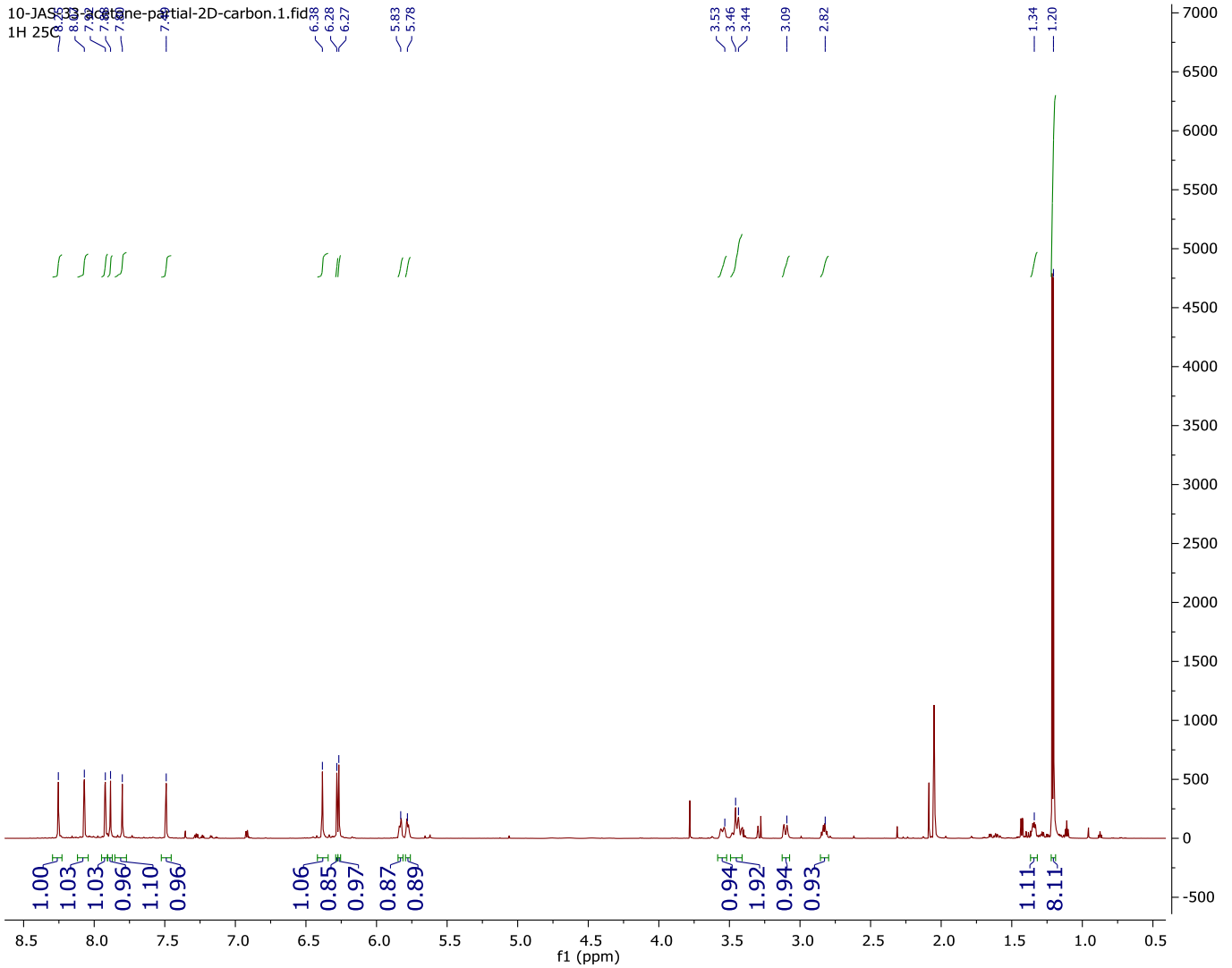
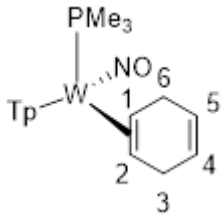
## <sup>1</sup>H NMR Spectrum of 3P



# <sup>1</sup>H NMR Spectrum of 3D

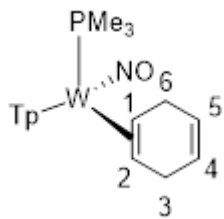


# <sup>1</sup>H NMR Spectrum of 4

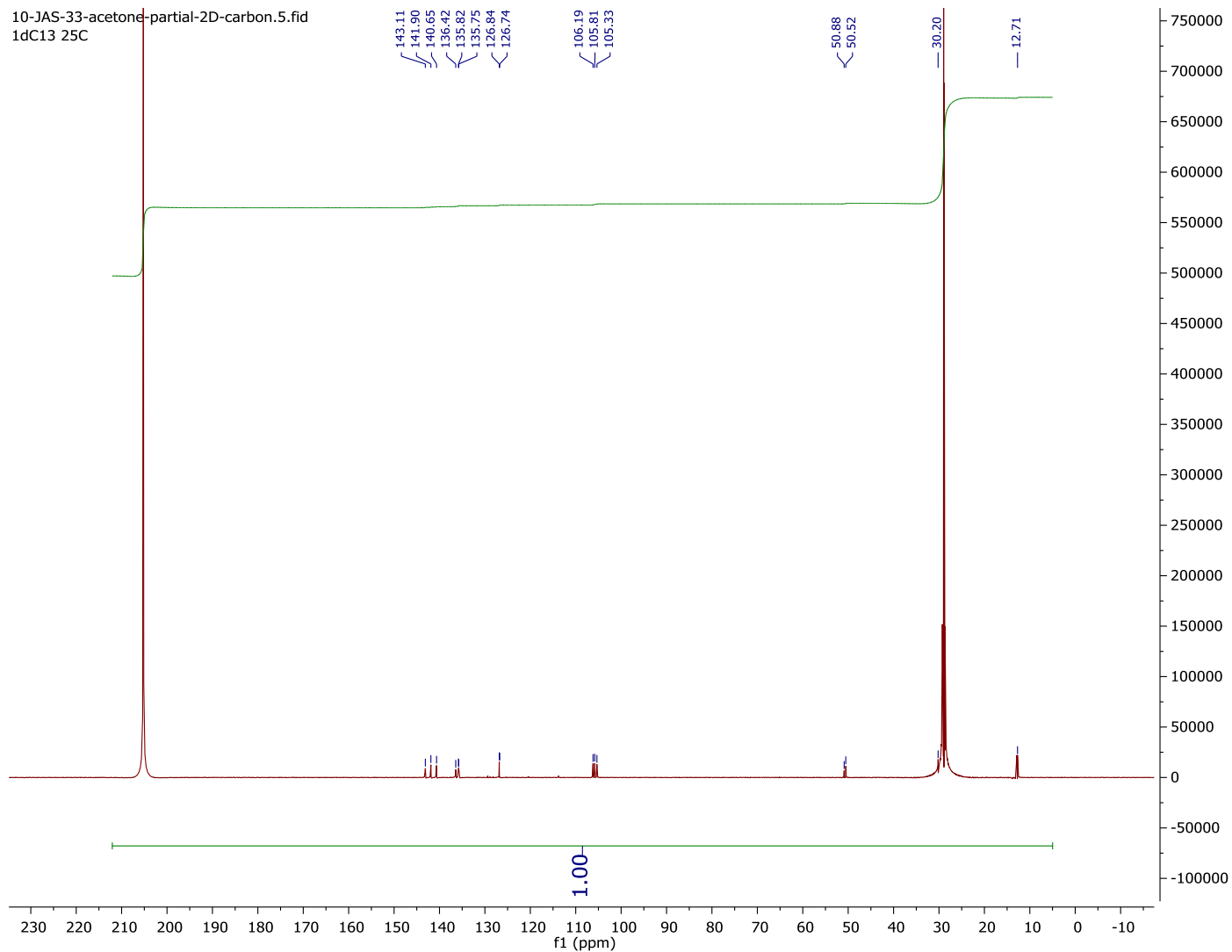




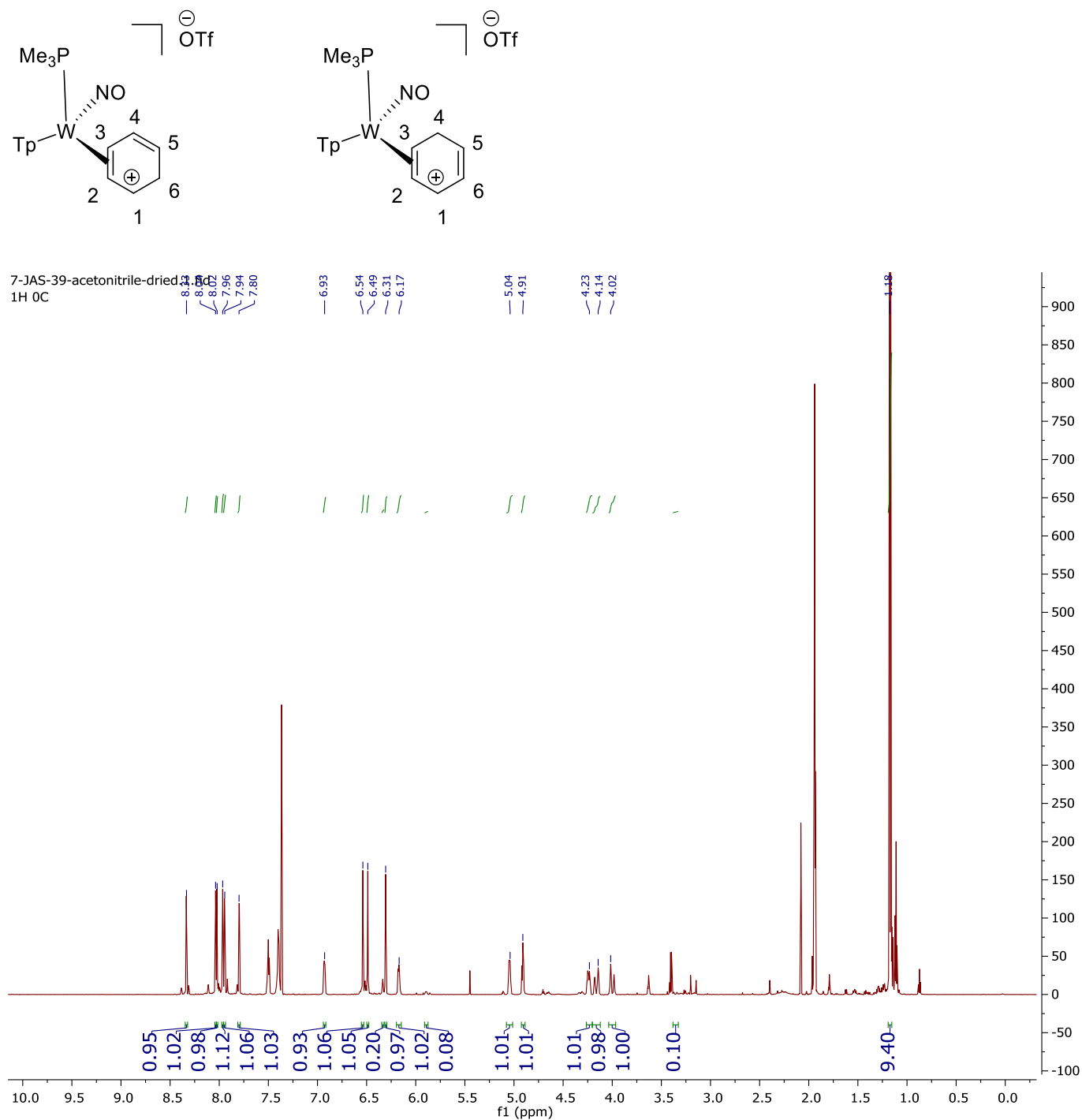
# <sup>13</sup>C{<sup>1</sup>H} NMR Spectrum of 4



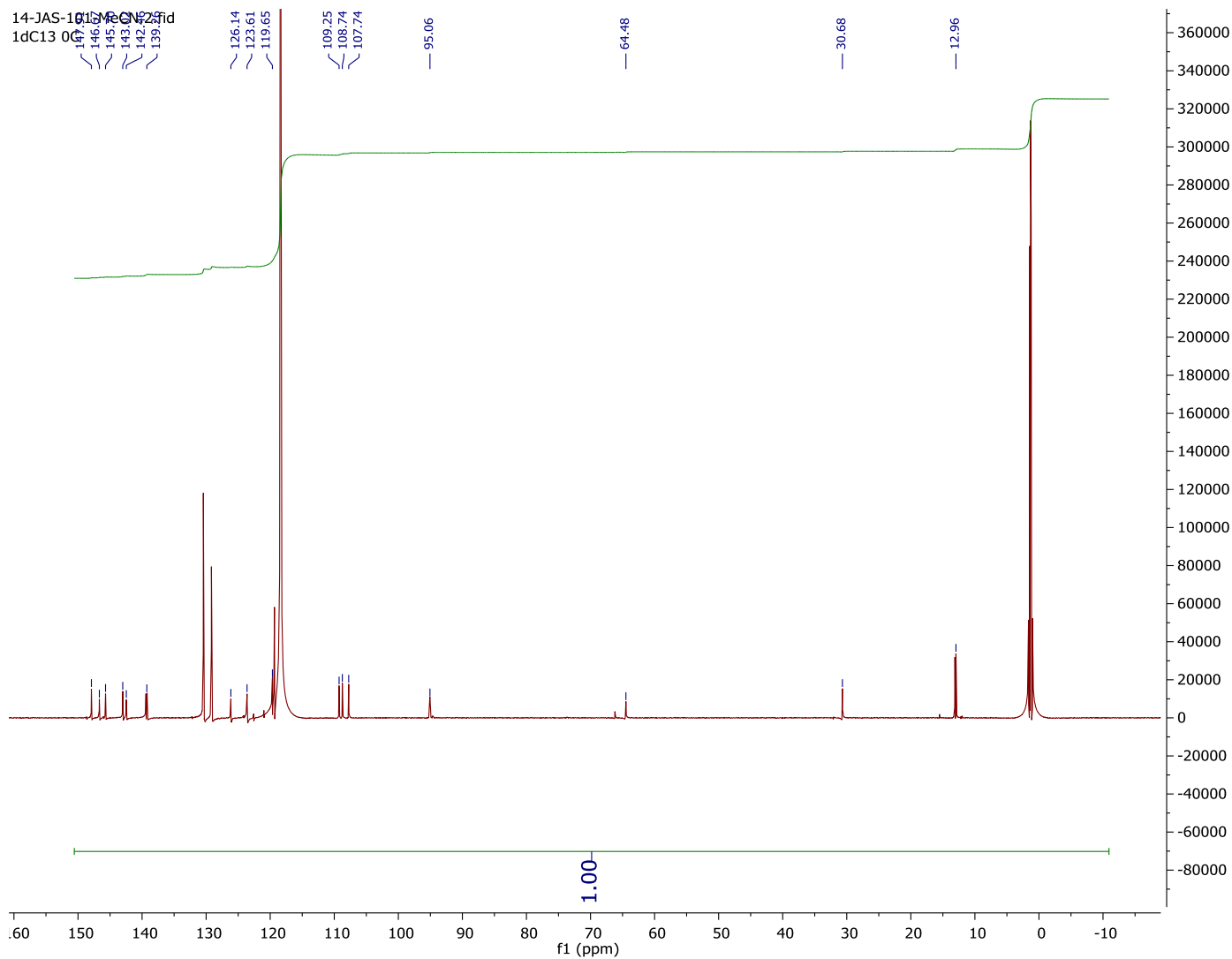
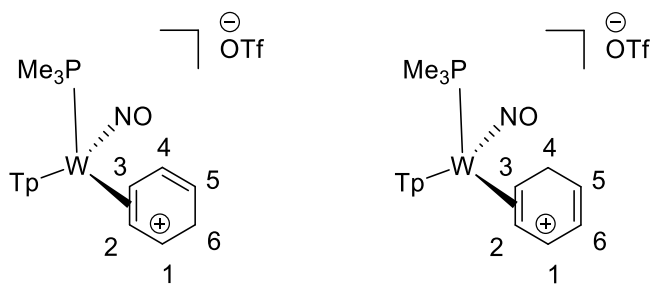
10-JAS-33-acetone-partial-2D-carbon.5.fid  
1dC13 25C



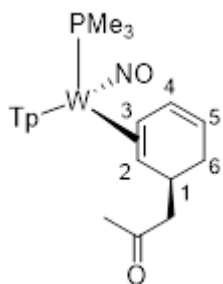
# <sup>1</sup>H NMR Spectrum of 5A and 5B



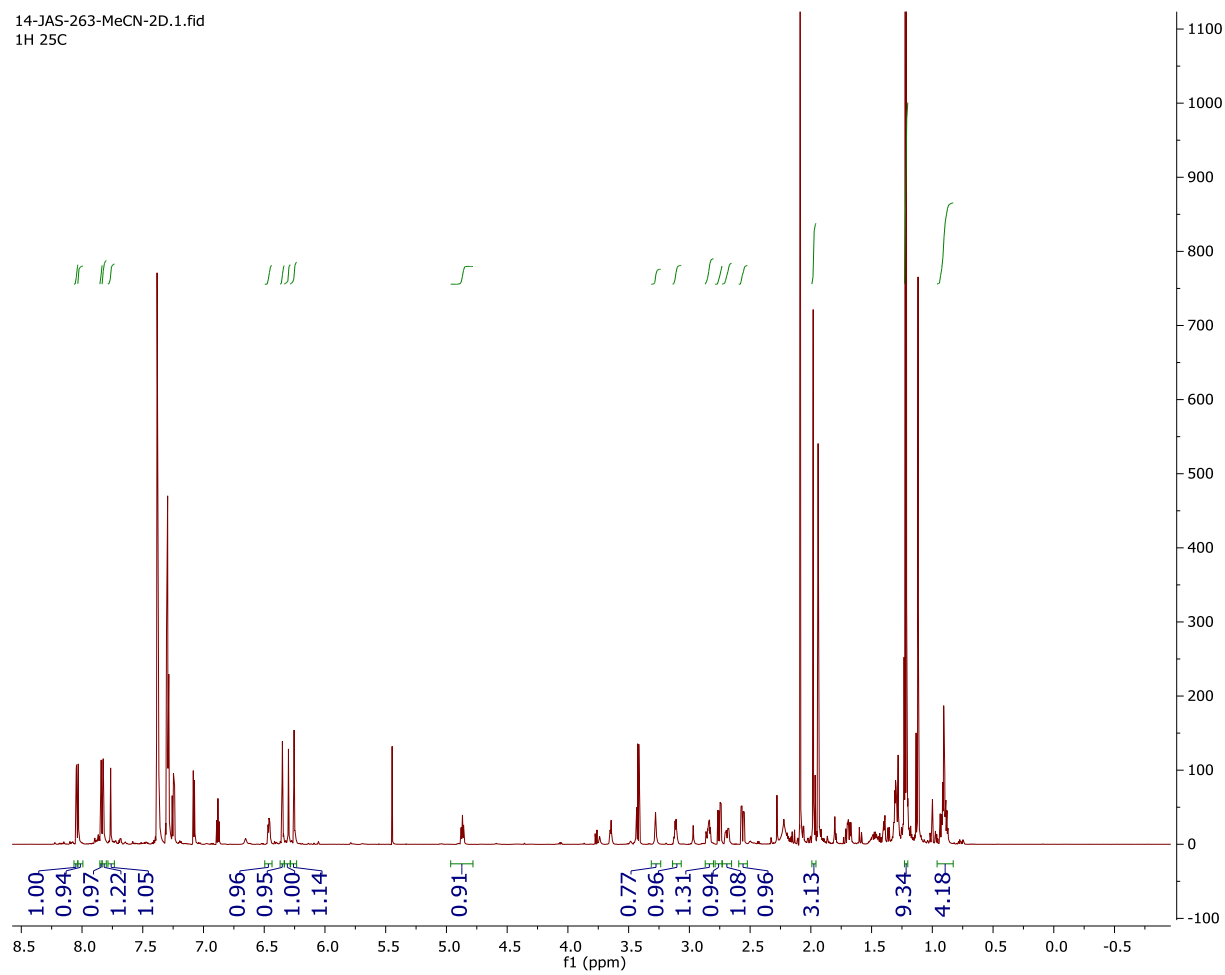
# <sup>13</sup>C{<sup>1</sup>H} NMR Spectrum of 5A and 5B



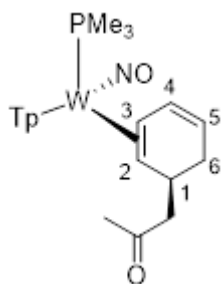
# <sup>1</sup>H NMR Spectrum of 6



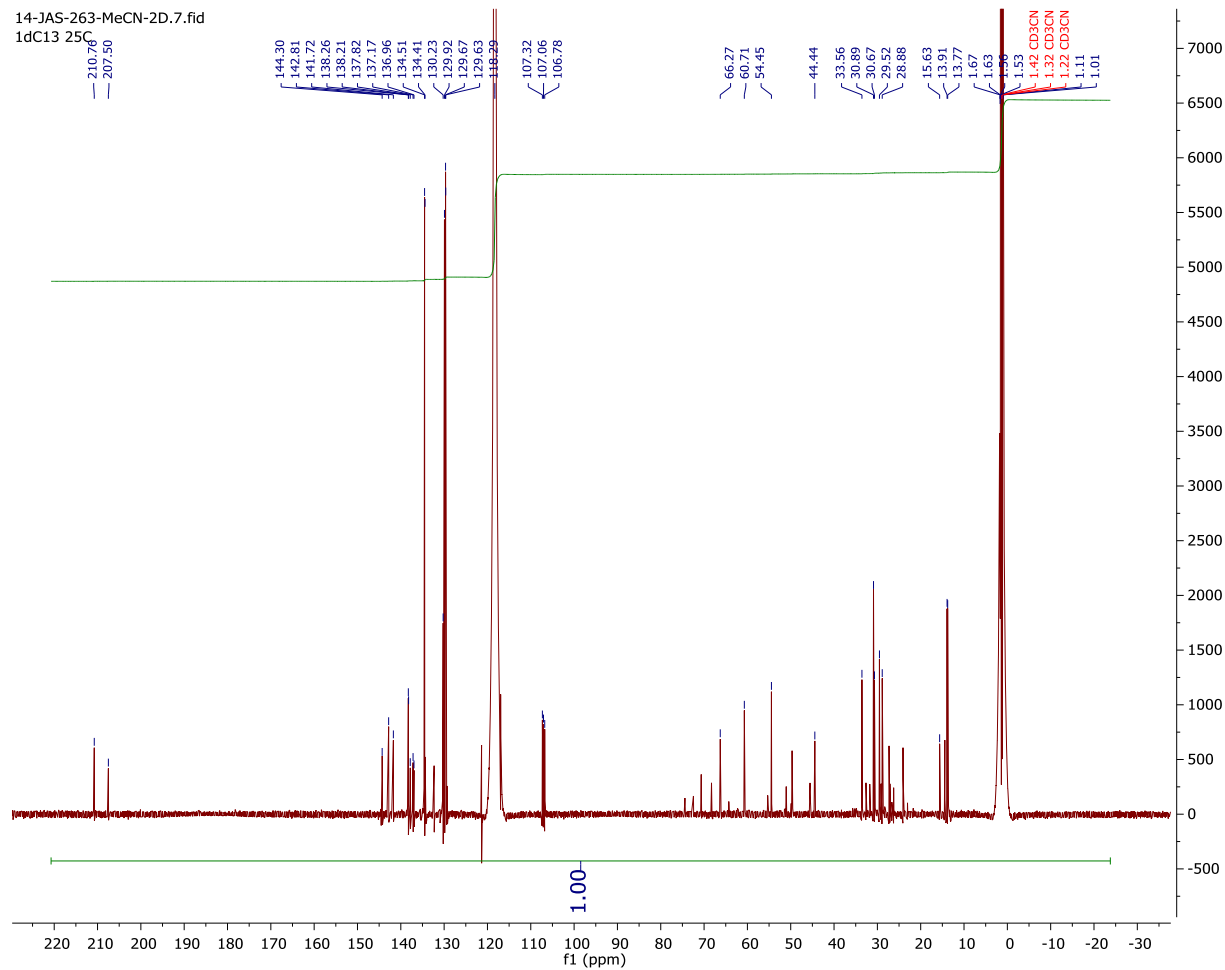
14-JAS-263-MeCN-2D.1.fid  
1H 25C



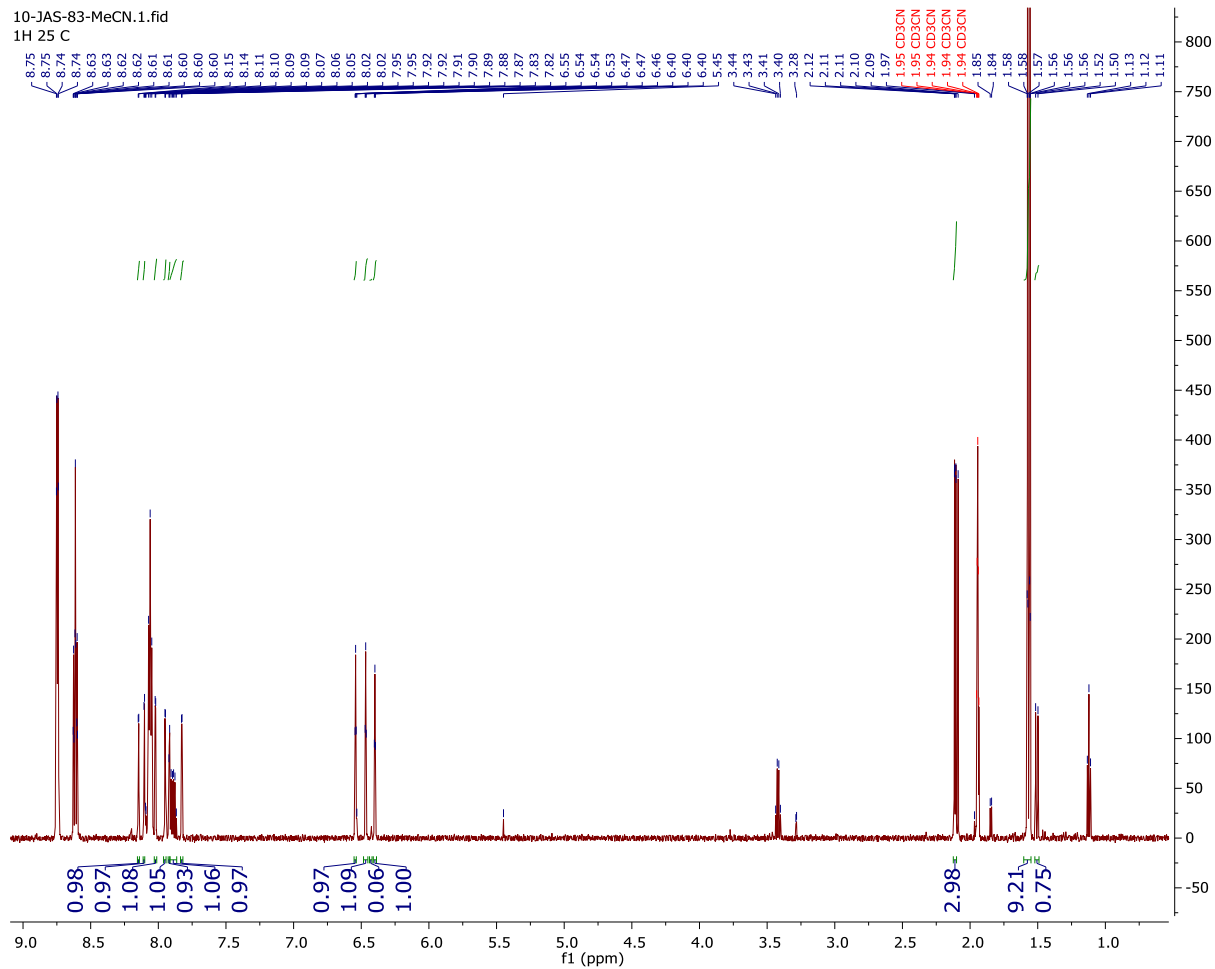
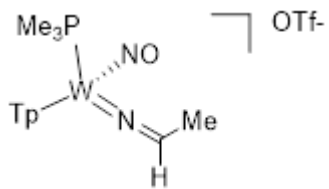
# <sup>13</sup>C{<sup>1</sup>H} NMR Spectrum of 6



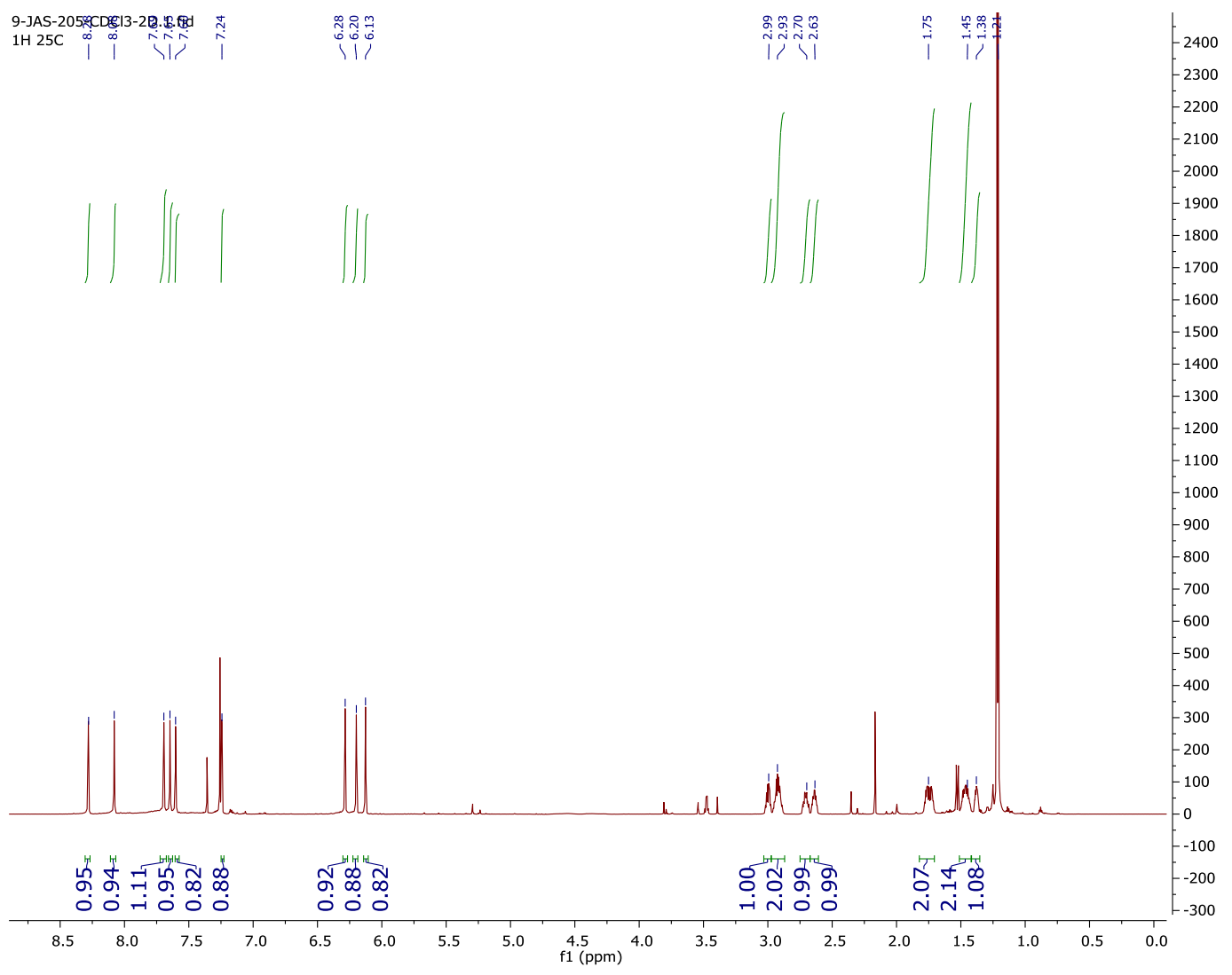
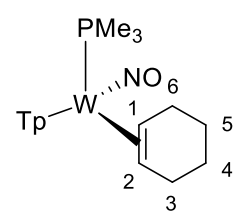
14-JAS-263-MeCN-2D.7.fid  
1dC13 25C



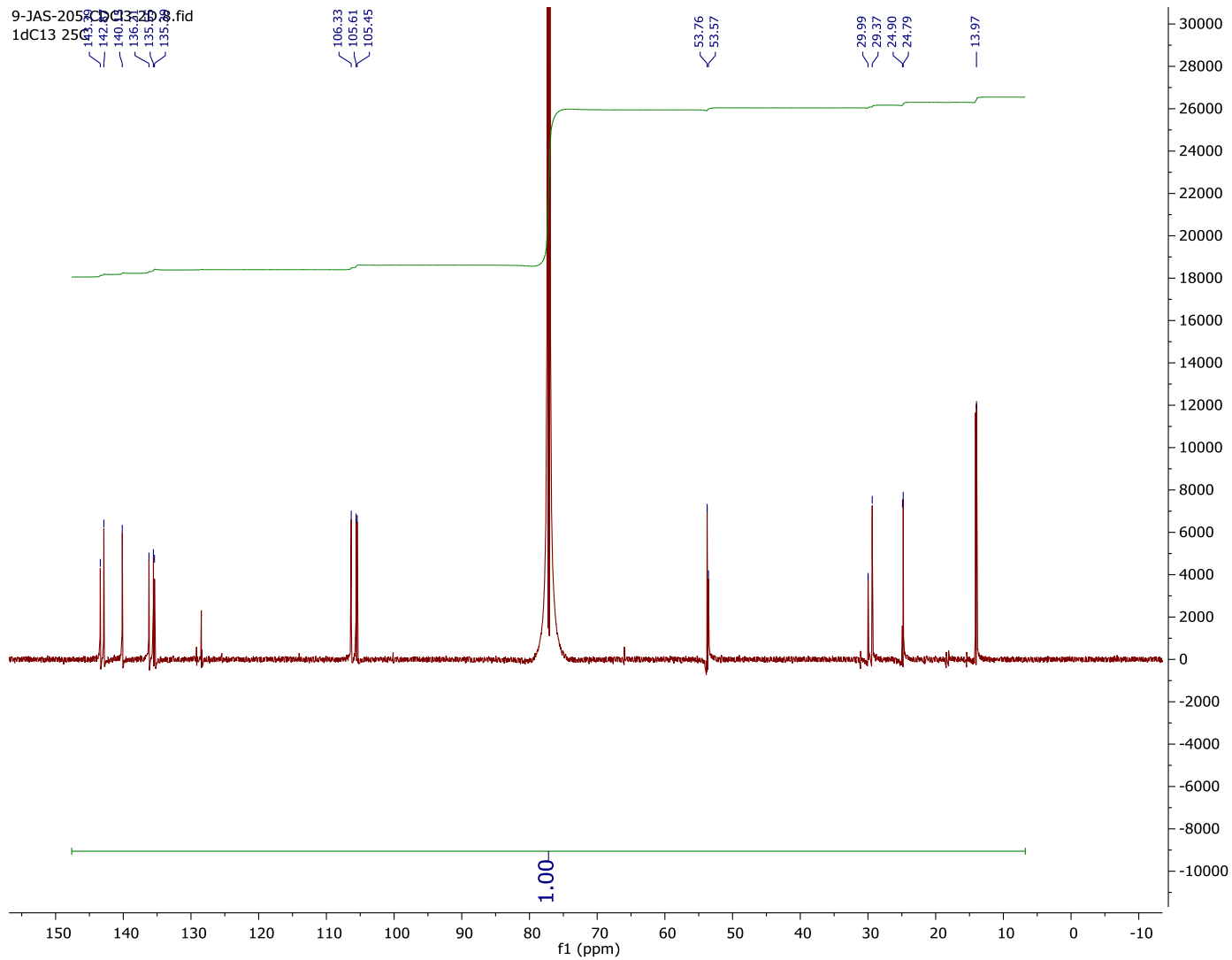
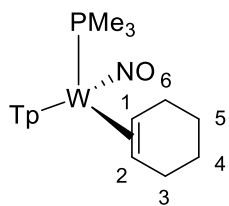
# <sup>1</sup>H NMR Spectrum of 7



# <sup>1</sup>H NMR Spectrum of 10 in CDCl<sub>3</sub>



# <sup>13</sup>C{<sup>1</sup>H} NMR Spectrum of 10 in CDCl<sub>3</sub>





# Supporting Information for Chapter 3

## A. Figures

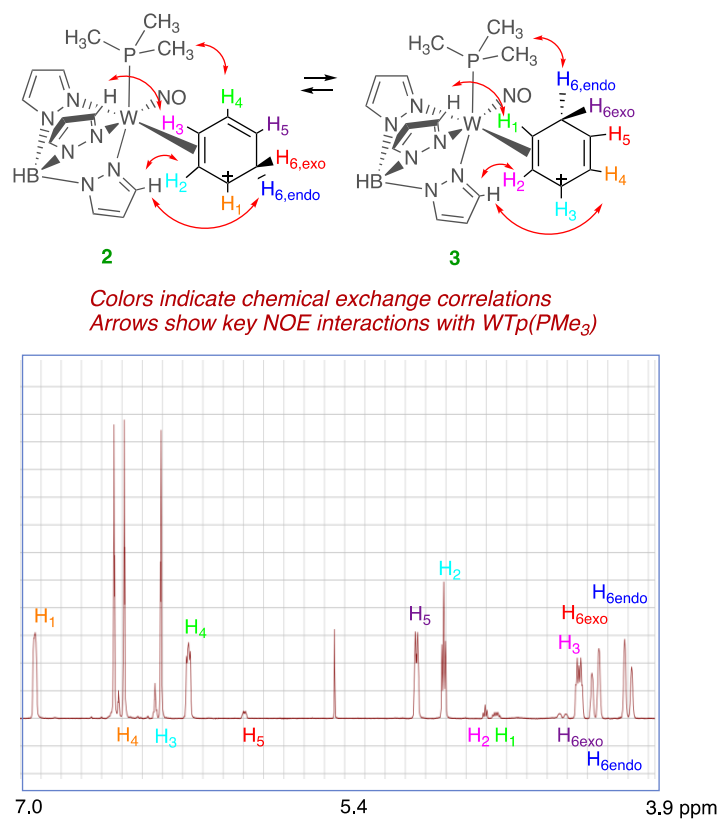


**Fig. S1.**  $^1\text{H}$ NMR spectrum (0 °C) of the tungsten  $\eta^2$ -benzenium complex **2**, and NOE (red arrows) and chemical exchange correlations (colored protons) for  $\eta^2$ -benzenium complex **2** and **3**.

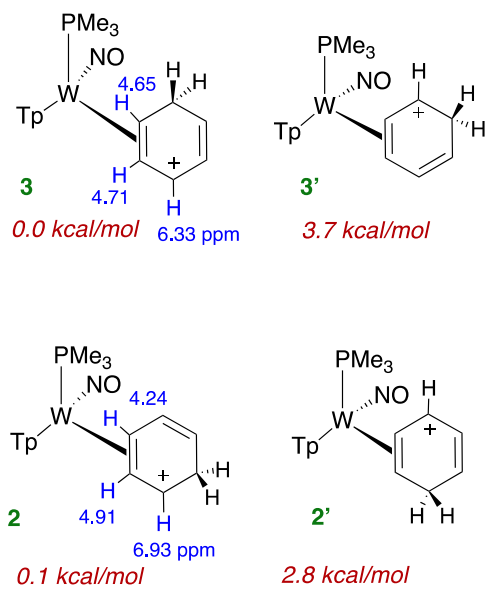


**Fig. S2.** Relative energies (calculated) of  $\eta^2$ -benzenium isomers.

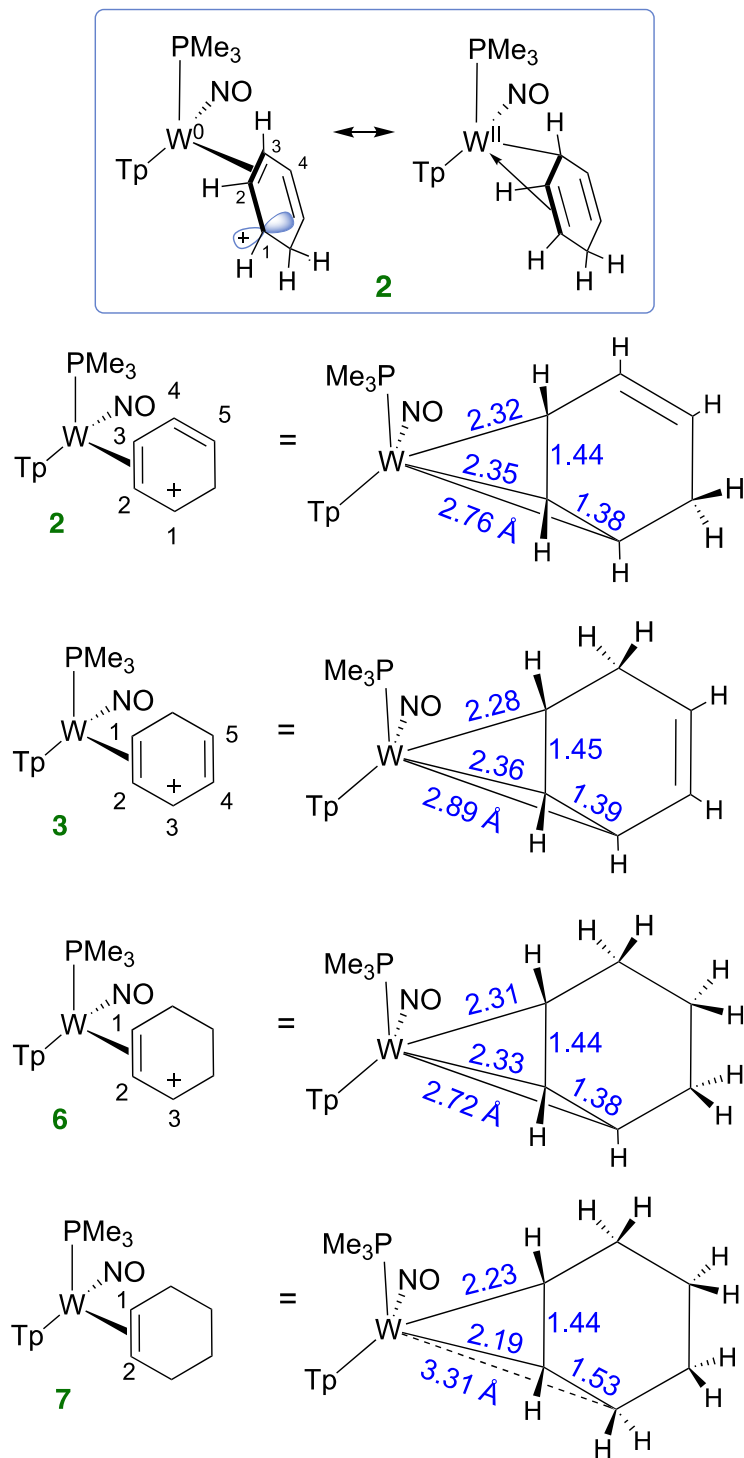


**Fig. S3.** DFT calculations for  $\eta^2$ -benzenium complexes **2** and **3** and a comparison to the  $\pi$ -allyl (**6**) and cyclohexene (**7**) analogs (all distances reported in Å). Note in **2** the shortened C1-C2 bond (1.38Å) (cf.

cyclohexene **7**, 1.53 Å) indicating a significant  $\pi$  interaction. A  $W^II$  resonance contributor is shown for comparison.

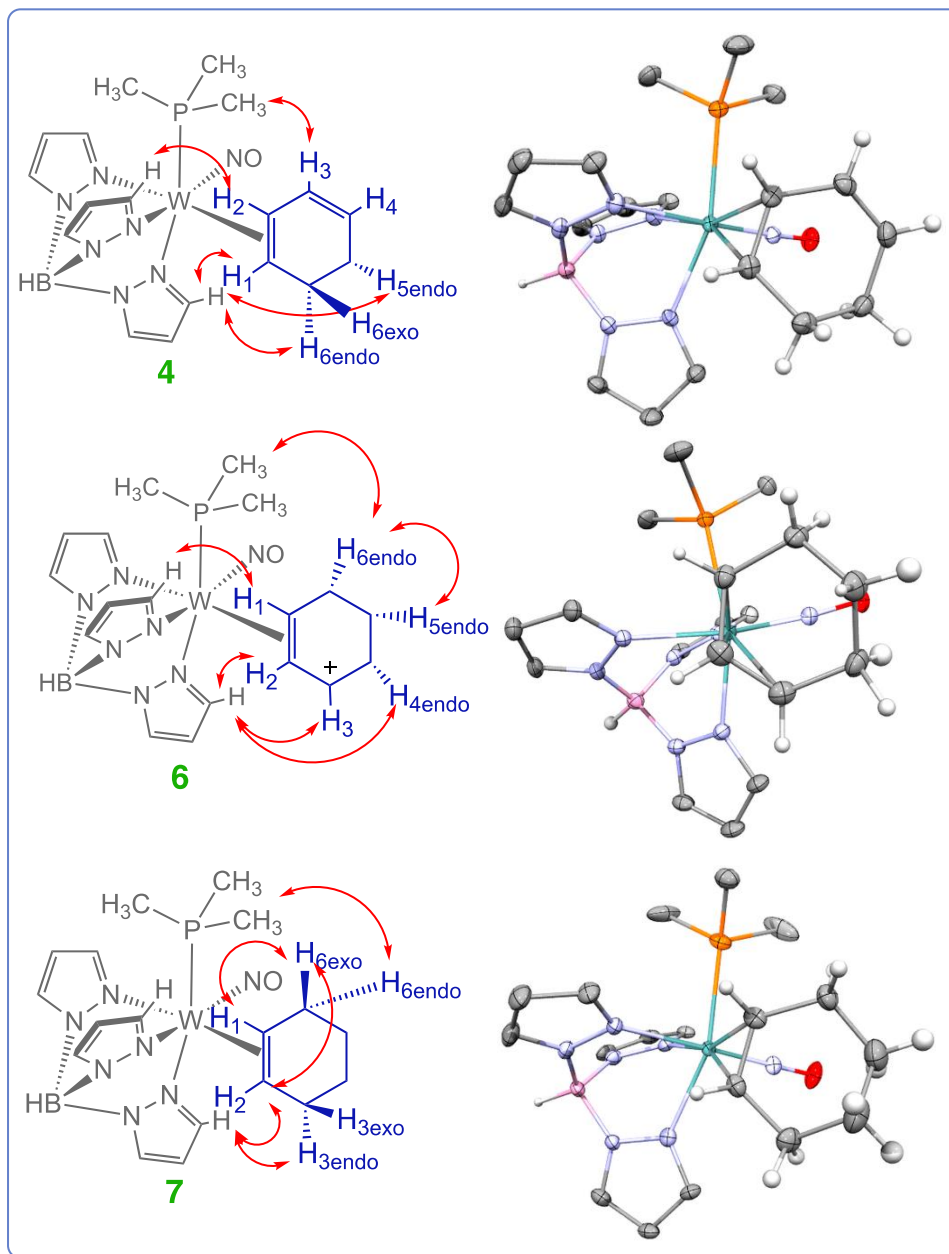


**Fig. S4.** Molecular structure determinations and relevant NOE interactions for **4**, **6**, and **7**.

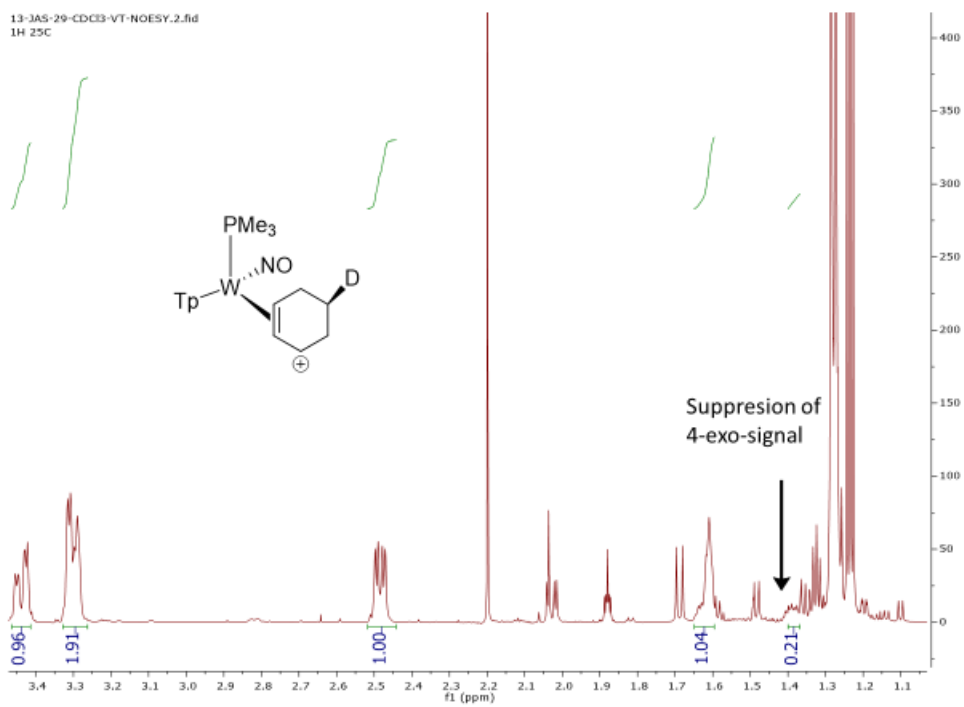
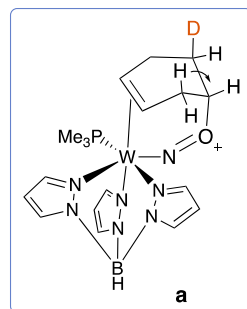
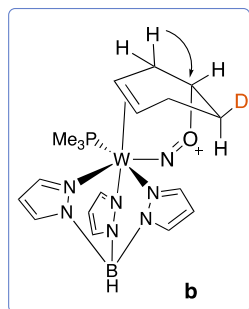
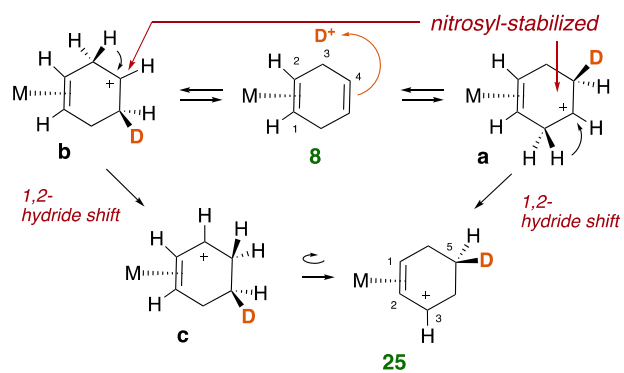
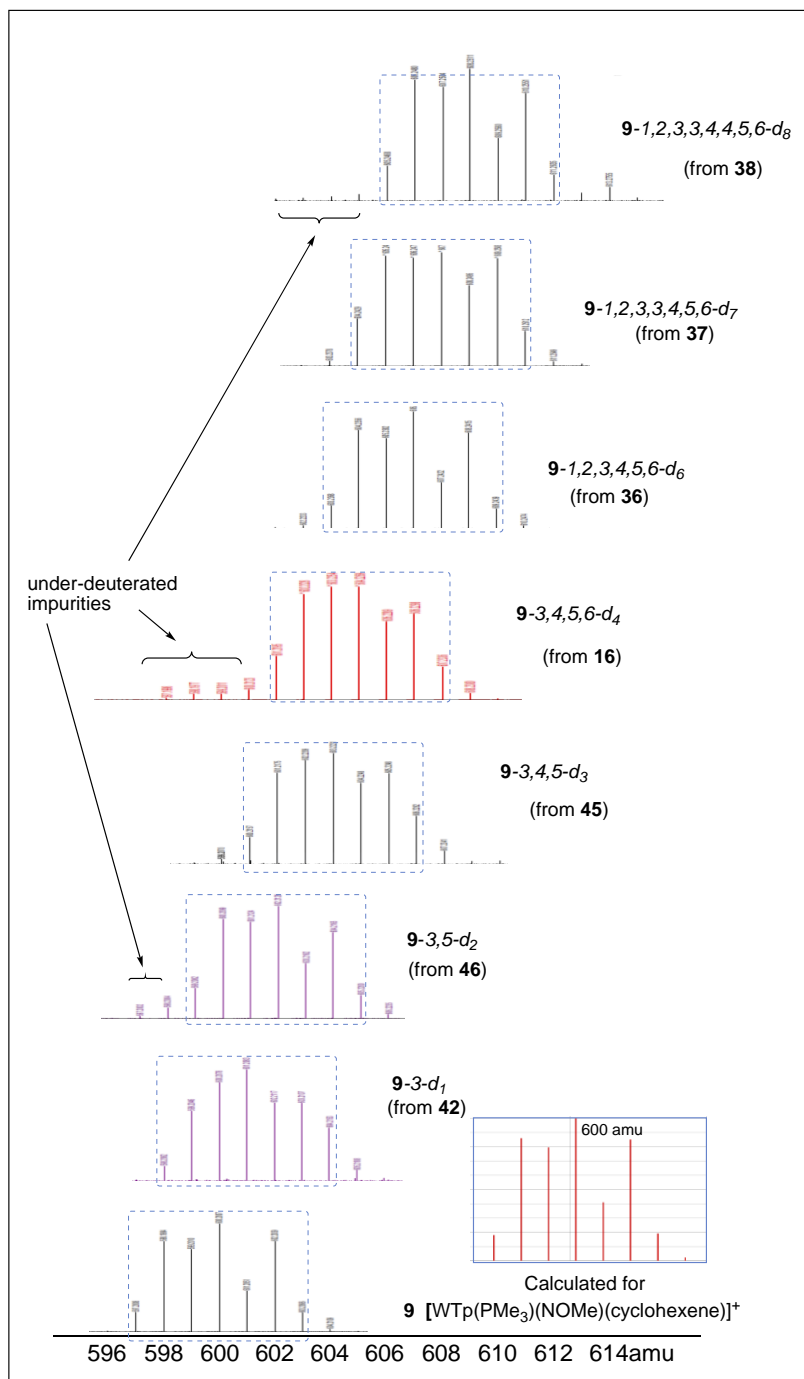


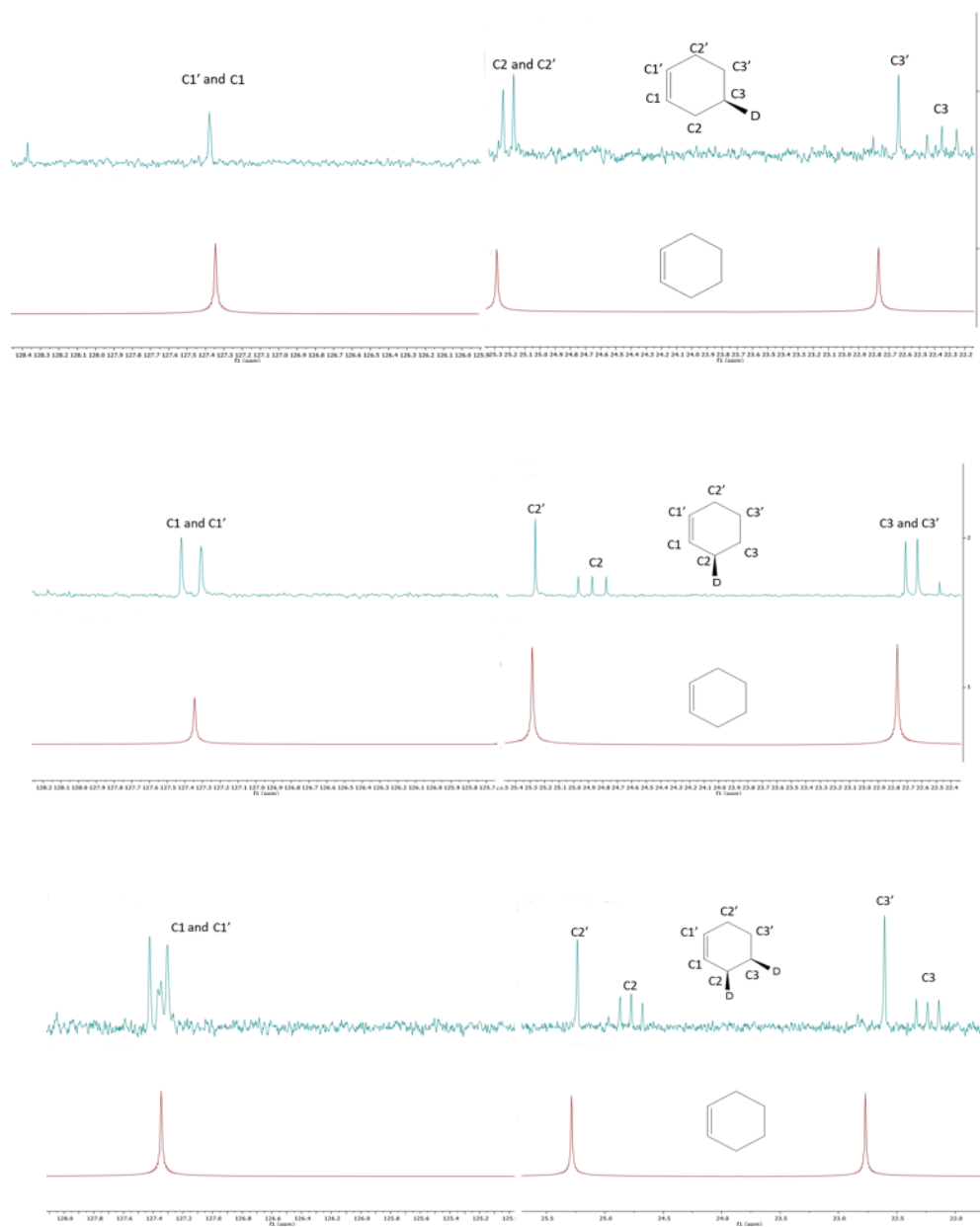
Fig. S5. Direct protonation of 1,4-diene complex (**8**) with purported nitrosyl assist and  $^1\text{H}$ NMR spectrum of **25**.



W isotopes:  $^{184}\text{W}$ : 183.95 (100.0%),  $^{186}\text{W}$ : 185.95 (92.8%),  $^{182}\text{W}$ : 181.95 (86.5%),  $^{183}\text{W}$ : 182.95 (46.7%)

B isotopes:  $^{11}\text{B}$ : 11.01 (100.0%),  $^{10}\text{B}$ : 10.01 (24.8%)

Figure S6. Composite of HRMS data showing parent ion envelope of complexes **9-d<sub>n</sub>**





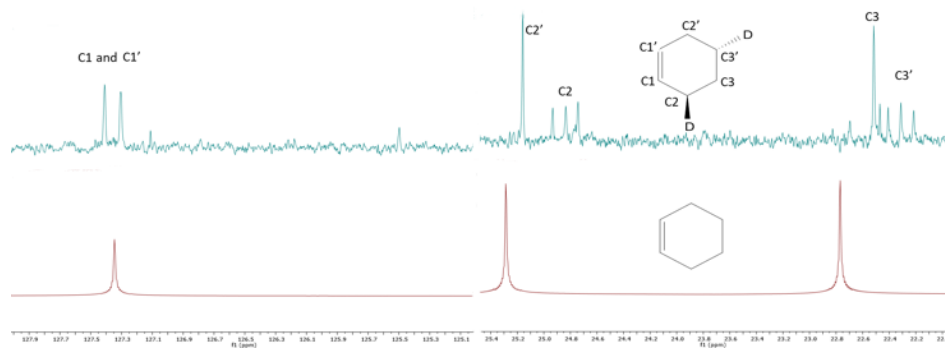


**Figure S7.**  $^{13}\text{C}$  NMRs of Cyclohexene- $d_1$  (derived from Complexes **42** and **32**) and  $d_2$  (derived from Complexes **45** and **46**) Isotopologues Compared to  $d_0$ -Cyclohexene

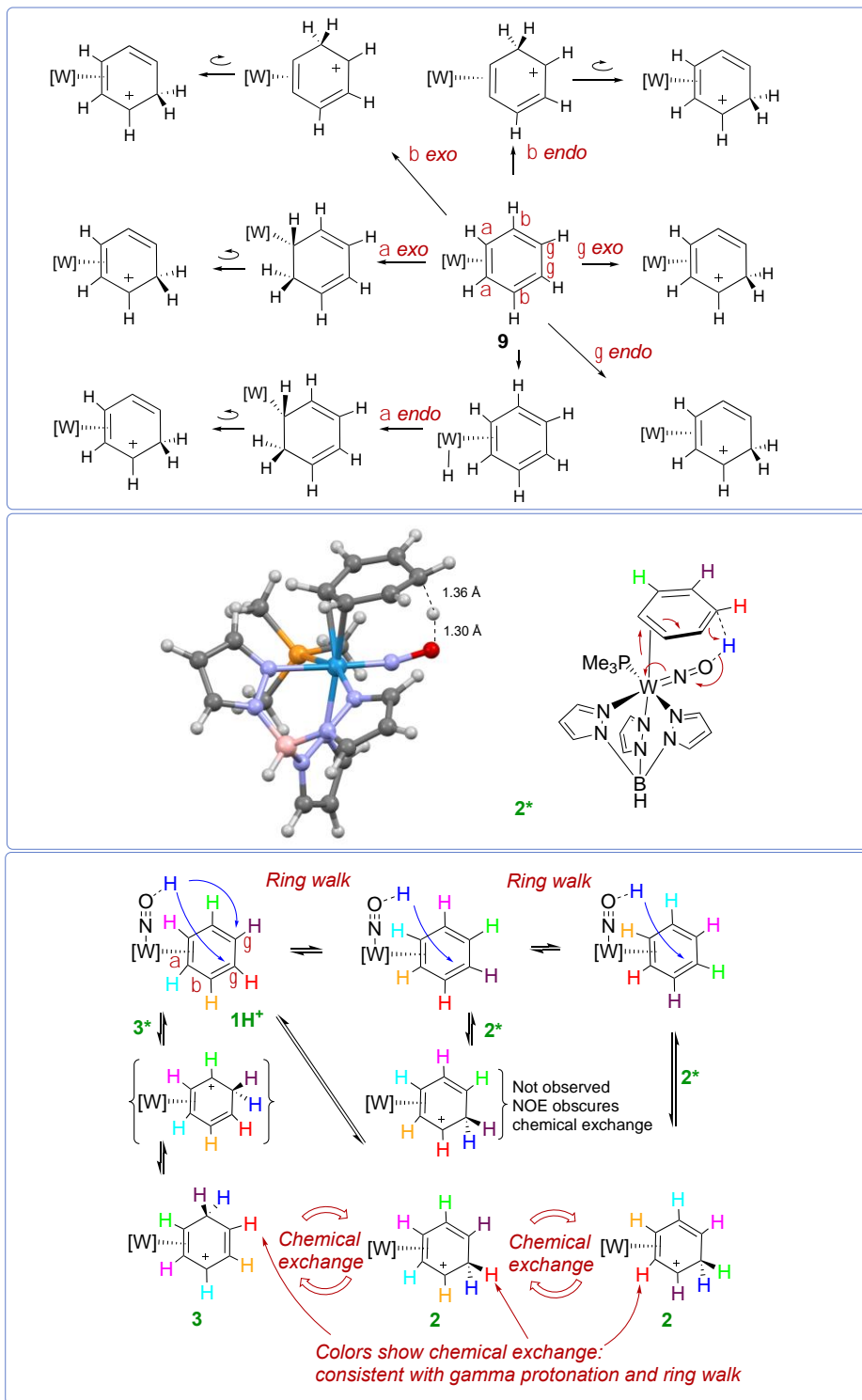


**Fig. S8.** Several mechanisms which could result in the formation of **2**, proposed nitrosyl-assisted transition state, and observed chemical exchange.

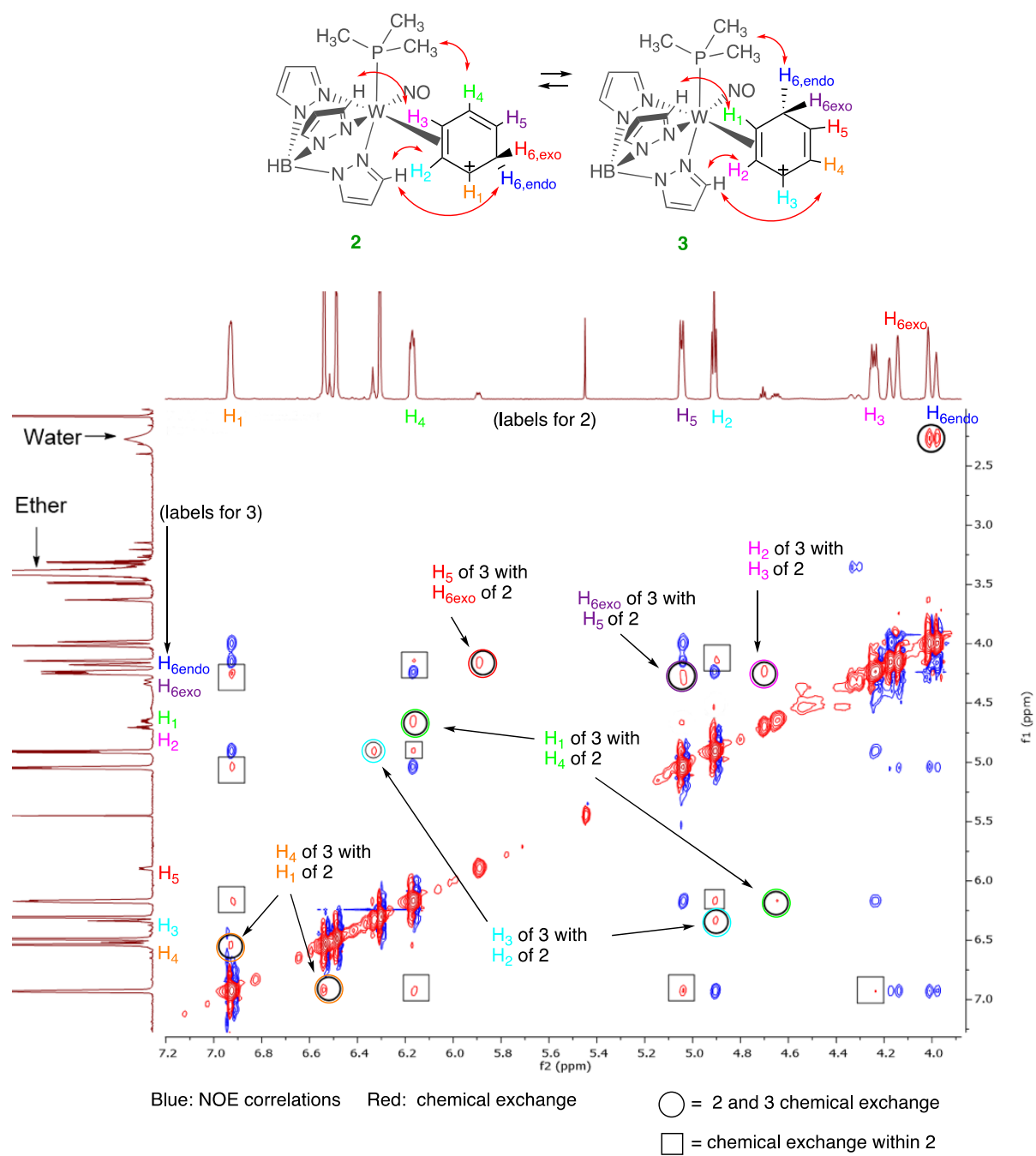


**Figure S9.** Chemical exchange between **2** and **3** along with chemical exchange due to ring isomerization in **2**.

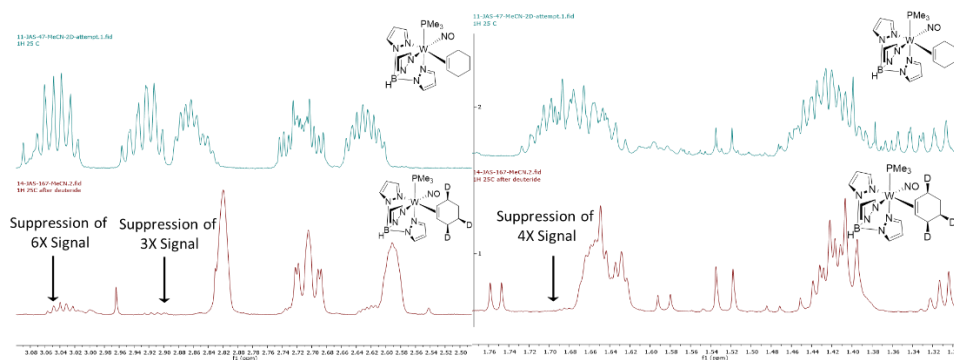


**Figure S10.** Illustrative  $^1\text{H}$  NMR comparison between **7** and **7-3,4,6-*exo*- $d_3$**  (**49**;  $6X = \text{H}_{6,\text{exo}}$ ;  $3X = \text{H}_{3,\text{exo}}$ ;  $4X = \text{H}_{4,\text{exo}}$ )

Common features include a simplification in splitting pattern of remaining  $^1\text{H}$  signals along with isotopic shifts.

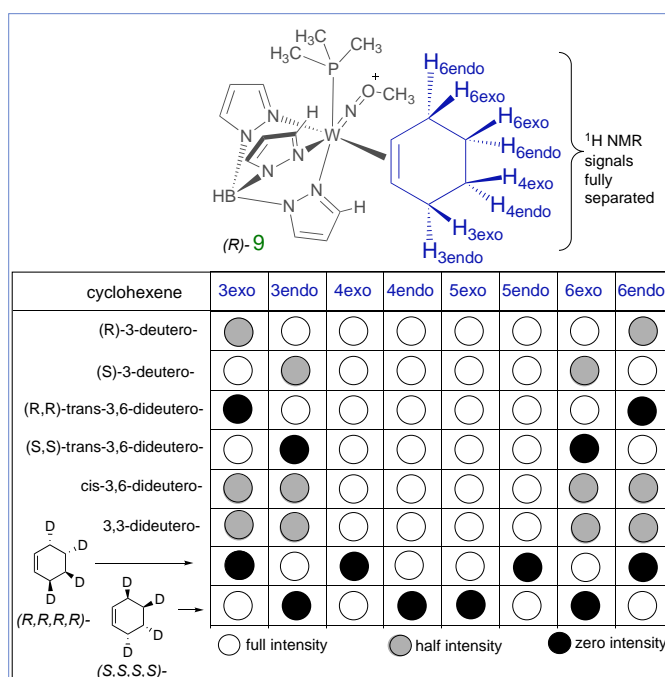


**Fig. S11.** The potential of  $(R)$ - $\text{WtP}(\text{NO})(\text{PMe}_3)$  to determine absolute configurations of enantiomers.

The figure above (S11) illustrates the ability of a resolved form of  $\{\text{WTP}(\text{NO})(\text{PMe}_3)(\text{benzene})\}$  to differentiate between various cyclohexene isotopologues. For example, when the benzene complex (*R*)-**1** is combined with (*R*)-3-deuterocyclohexene, two isotopomers of the resulting cyclohexene complex will be formed (This is a result of the tungsten complex's inability to chemically differentiate between the two faces of the 3-deuterocyclohexene). A  $^1\text{H}$  NMR spectrum will show the 3-exo and the 6-endo positions each at half intensity. In contrast, if *S*-3-deuterocyclohexene is complexed, then only the 3-endo and 6-exo signals will be diminished. The ee of the 3-deuterocyclohexene can easily be determined from the relative ratios of the 3-endo and 3-exo signals. In a similar manner (*R,R*)-trans-3,6-dideuterocyclohexene and its enantiomer can be easily differentiated, both from each other and from the cis isomer. Finally, the (*R,R,R,R*)-3,4,5,6-tetradeuterocyclohexene stereoisomer shown above can be differentiated from its enantiomer and from the all-cis diastereomers. We note that there is virtually no other practical method to differentiate these cyclohexene stereoisotopomers.

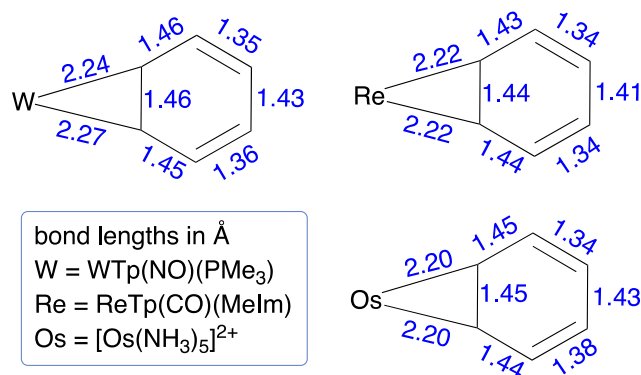


**Fig. S12.** Distortions in the benzene ring as a result of dihapto-coordination.

**Note on DFT Calculations.** Optimized geometries and intermediates were calculated using B3LYP and the associated basis functions for tungsten and the 6-31G(d) basis for all other atoms. This combination has proved to be reliable for Os, Mo, Re, and W systems for relative (binding) energies, charge transfer, and preferred structures, especially in similar systems. Transition state modeling utilized unrestricted B3LYP and the SDD basis set.

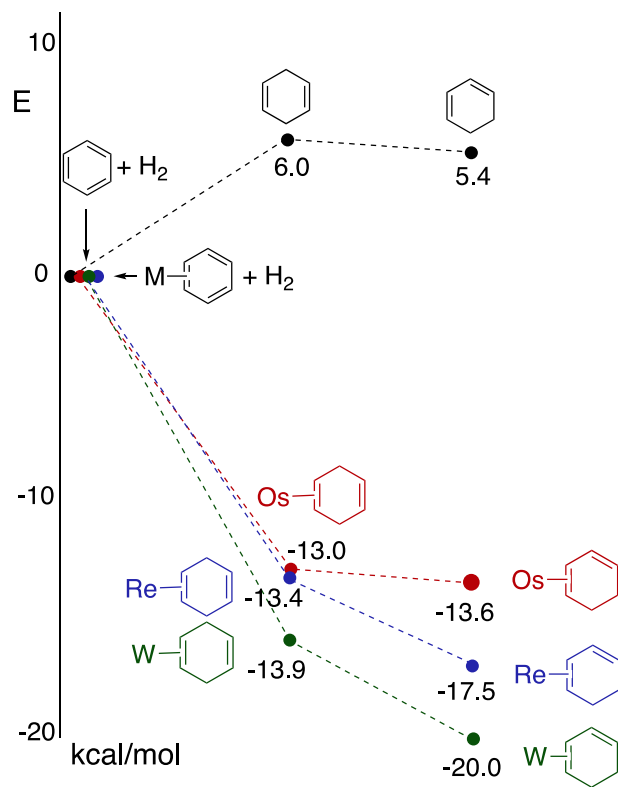


**Fig. S13.** DFT calculations show enhanced stabilization of conjugated  $\eta^2$ -diene complexes relative to  $\eta^2$ -arene and unconjugated  $\eta^2$ -diene counterparts.

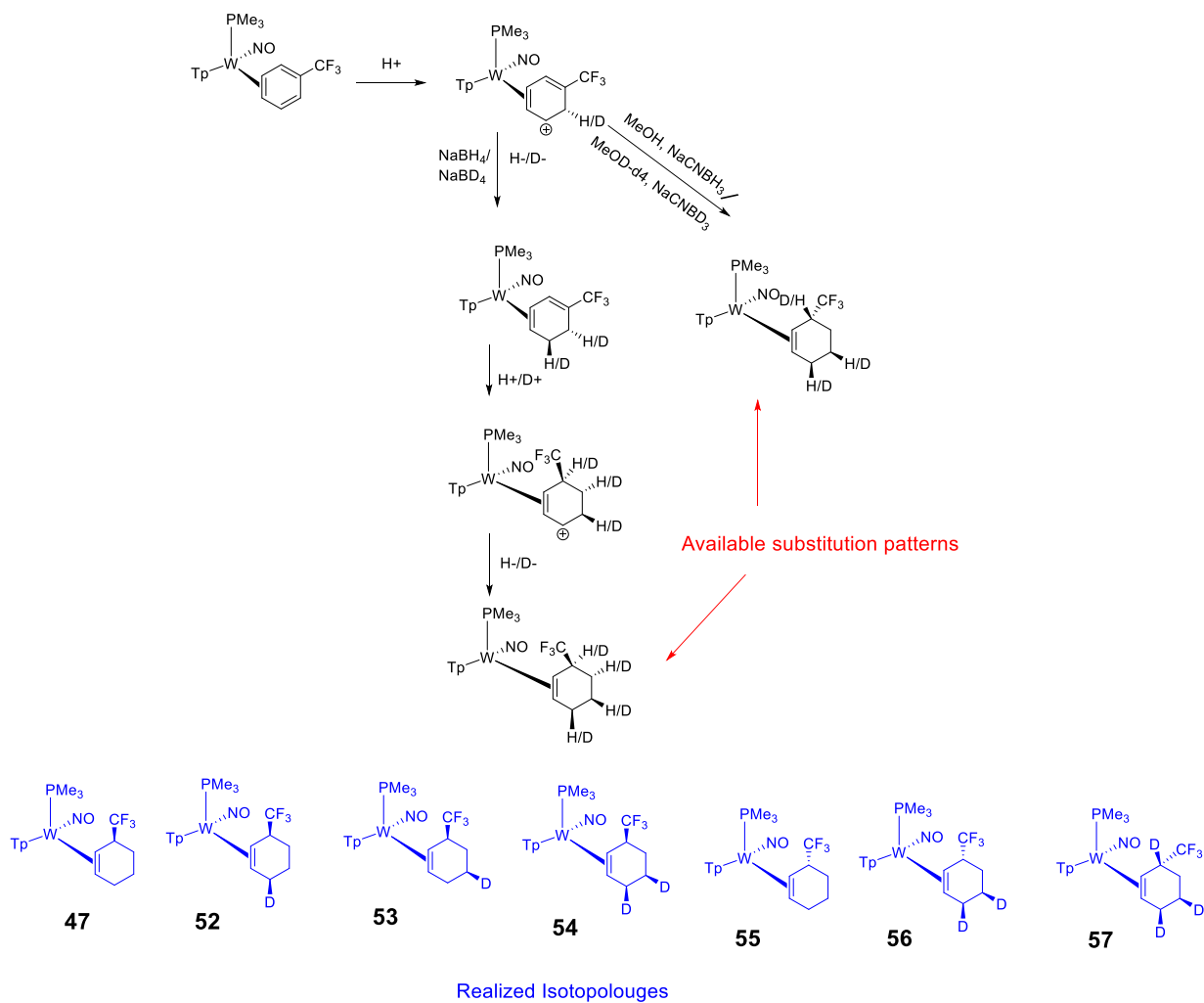
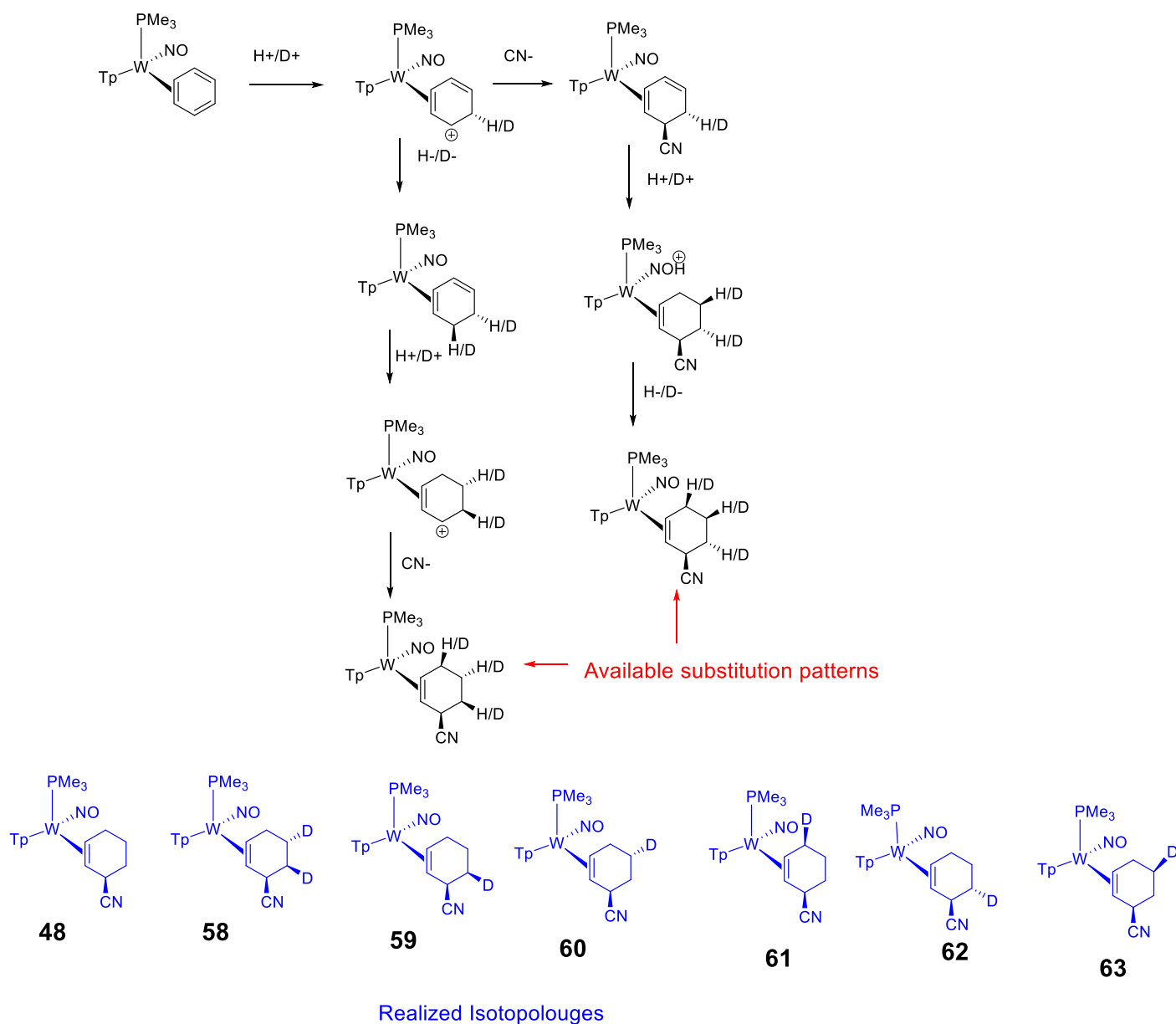


**Fig. S14.** Synthetic Pathways to isotopologues of a 3-(trifluoromethyl)cyclohex-1-ene tungsten complex

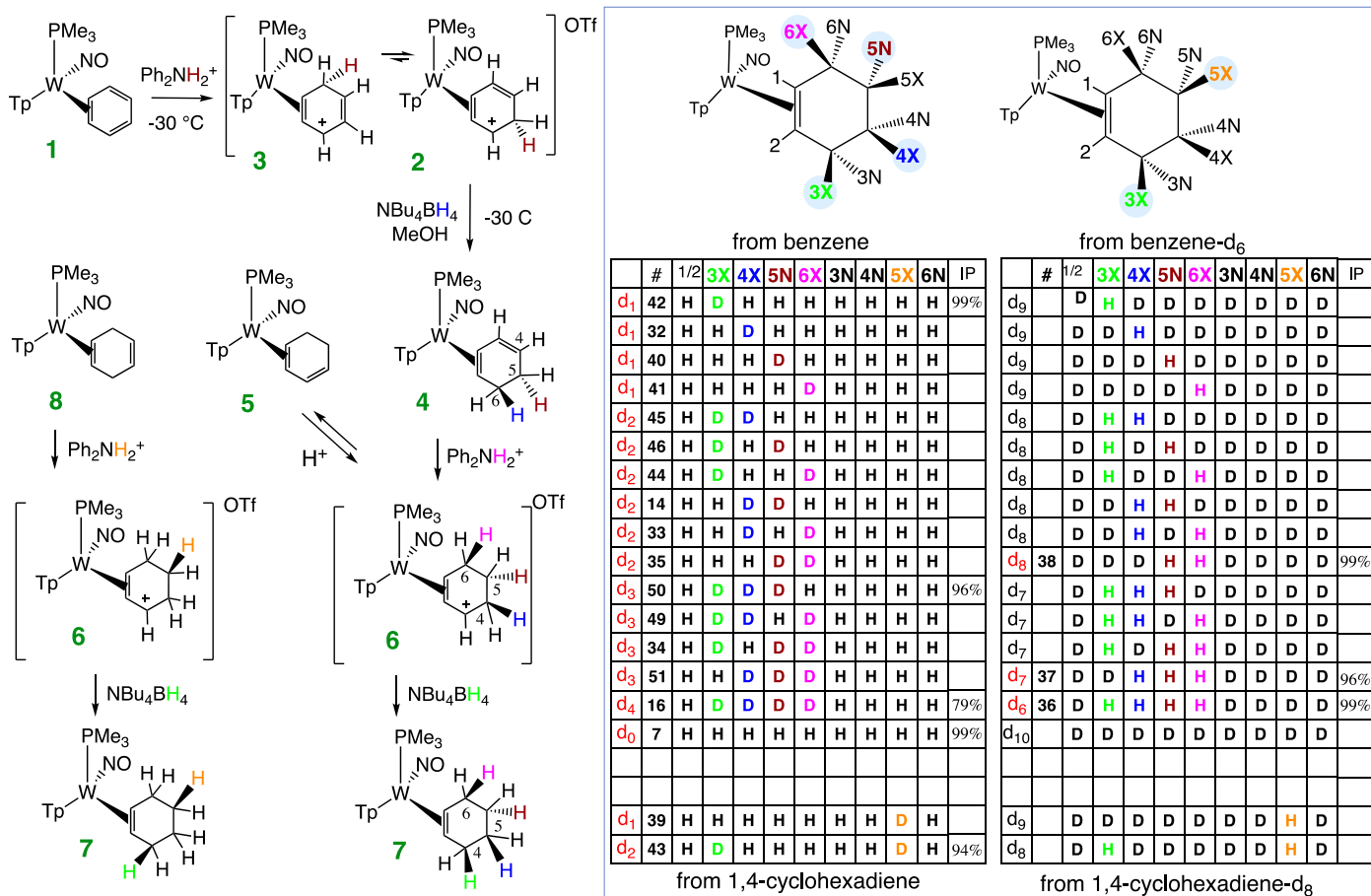
**Fig. S15.** Synthetic pathways to isotopologues of a 3-cyanocyclohex-1-ene tungsten complex.





## B. Tables.

**Table S1.** The sequential reduction of benzene to cyclohexene bound to tungsten: Possible isotopomers.



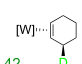
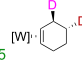
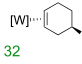
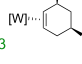
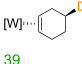
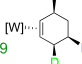
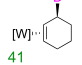
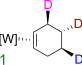
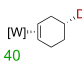
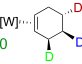
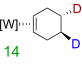
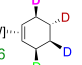
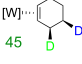
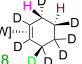
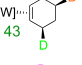
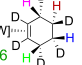
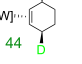
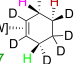
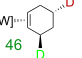
Red indicates prepared complex. IP = isotopic purity as determined by HRMS

**Table S2.** Isotopologues and isotopomers of cyclohexene complex **7** and cyclohexene.

| Isotopologue         | Complex 7-d <sub>n</sub> | Cyclohexene-d <sub>n</sub> | Cyclohexene-d <sub>n</sub> |
|----------------------|--------------------------|----------------------------|----------------------------|
|                      | # of Isotopomers         | # of Isotopomers           | Isotopomers possible       |
| <b>d<sub>0</sub></b> | 2                        | 1                          | 1                          |
| <b>d<sub>1</sub></b> | 10                       | 4                          | 5                          |
| <b>d<sub>2</sub></b> | 14                       | 11                         | 25                         |
| <b>d<sub>3</sub></b> | 8                        | 8                          | 60                         |

|                       |           |           |            |
|-----------------------|-----------|-----------|------------|
| <b>d<sub>4</sub></b>  | 2         | 2         | 110        |
| <b>d<sub>5</sub></b>  | 0         | 0         | 126        |
| <b>d<sub>6</sub></b>  | 2         | 2         | 110        |
| <b>d<sub>7</sub></b>  | 8         | 8         | 60         |
| <b>d<sub>8</sub></b>  | 14        | 11        | 25         |
| <b>d<sub>9</sub></b>  | 10        | 4         | 5          |
| <b>d<sub>10</sub></b> | 2         | 1         | 1          |
| <b>Total:</b>         | <b>72</b> | <b>52</b> | <b>528</b> |

**Table S3.** Table of select cyclohexene isotopologue complexes with isolated yields and estimates of purity and selectivity (determination by <sup>1</sup>H NMR).

|   | Percent Yield | Selectivity estimated by <sup>1</sup> H NMR | Purity estimated by <sup>1</sup> H NMR |  | Percent Yield | Selectivity estimated by <sup>1</sup> H NMR | Purity estimated by <sup>1</sup> H NMR |
|---|---------------|---|--|--|---------------|---|--|
| <br>42   | 63%           | 99%   | 95%                                    | <br>35  | 37%           | 90%   | 77%                                    |
| <br>32   | 70%           | 99%   | 85%                                    | <br>33  | 52%           | 90%   | 95%                                    |
| <br>39   | 59%           | 93 %  | 92 %                                   | <br>49  | 56%           | 91%   | 87%                                    |
| <br>41   | 50%           | 92%   | 75%                                    | <br>51  | 53%           | 93%   | 92%                                    |
| <br>40   | 55%           | 99%   | 92%                                    | <br>50  | 36%           | 93%   | 98%                                    |
| <br>14   | 66%           | 91%   | 95%                                    | <br>16  | 39%           | 94%   | 73%                                    |
| <br>45   | 59%           | 95%   | 93%                                    | <br>38  | 52%           | 78%   | 99%                                    |
| <br>43   | 39%           | 95%   | 80%                                    | <br>36  | 27%           | 85%   | 99%                                    |
| <br>44  | 44%           | 95%   | 82%                                    | <br>37 | 63%           | 67%   | 90%                                    |
| <br>46 | 48%           | 90%   | 91%                                    |  |               |   |  |

**Table S4.** Determination of enhanced KIE in deuteration of complex **4**

| Theoretical <sup>1</sup> H Impurity | Observed <sup>1</sup> H Impurity | KIE Determination |
|-------------------------------------|----------------------------------|-------------------|
| 3%                                  | 49%                              | 31                |
| 5%                                  | 57%                              | 40                |
| 10%                                 | 82%                              | 41                |

(see section K for detailed explanation)

**C. Synthetic methods.** NMR spectra were obtained on 500, 600 or 800 MHz spectrometers. Chemical shifts are referenced to tetramethylsilane (TMS) utilizing residual <sup>1</sup>H signals of the deuterated solvents as internal standards. Chemical shifts are reported in ppm and coupling constants (*J*) are reported in hertz (Hz). Infrared Spectra (IR) were recorded on a spectrometer as a glaze on a Horizontal Attenuated Total Reflectance (HATR) accessory, with peaks reported in cm<sup>-1</sup>. Electrochemical experiments were performed under a nitrogen atmosphere. Most cyclic voltammetric data were recorded at ambient temperature at 100 mV/s, unless otherwise noted, with a standard three electrode cell from +1.8 V to -1.8 V with a platinum working electrode, acetonitrile (MeCN) solvent, and tetrabutylammonium (TBAH) electrolyte (~1.0 M). All potentials are reported versus the normal hydrogen electrode (NHE) using cobaltocenium hexafluorophosphate ( $E_{1/2} = -0.78$  V,  $-1.75$  V) or ferrocene ( $E_{1/2} = 0.55$  V) as an internal standard. Peak separation of all reversible couples was less than 100 mV. All synthetic reactions were performed in a glovebox under a dry nitrogen atmosphere unless otherwise noted. All solvents were purged with nitrogen prior to use. Deuterated solvents were used as received from Cambridge Isotopes. When possible, pyrazole (Pz) protons of the (trispyrazolyl) borate (Tp) ligand were uniquely assigned (e.g., "Pz3B") using two-dimensional NMR data (see Fig. S1). If unambiguous assignments were not possible, Tp protons were labeled as "Pz3/5 or Pz4". All *J* values for Pz protons are 2 (±0.4) Hz.

## D. Synthesis of compounds

## E) HRMS determinations

Theoretical values were calculated from <https://www.envipat.eawag.ch/index.php>

### HRMS Spectra for 9- $d_n$ Complexes

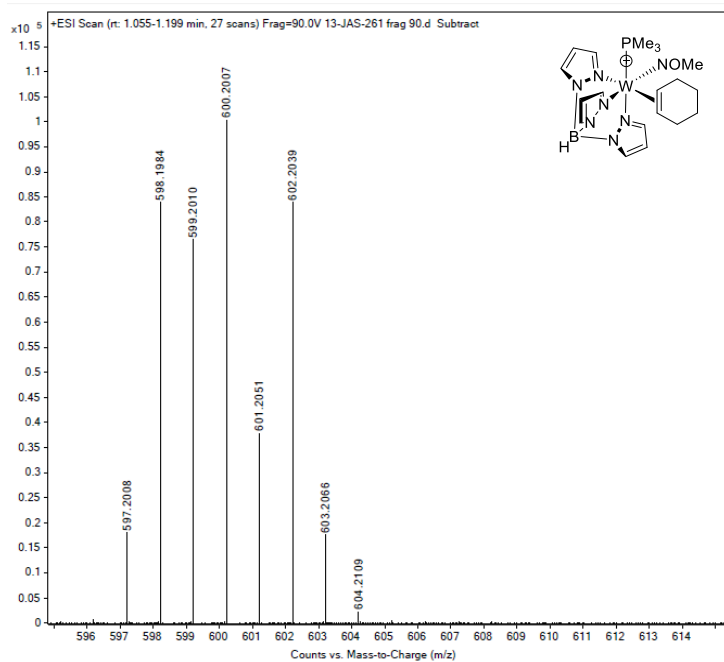
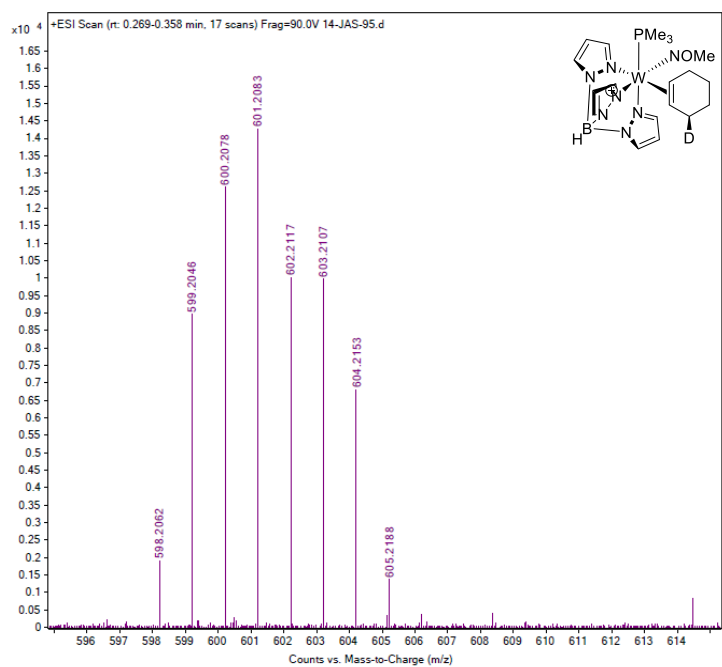


Figure SE1. HRMS data for Compound 9- $d_0$

ESI-MS : obsd (%), calcd (%),

598.1984 (83.66), 598.1985 (85.93), 599.2010 (76.17), 599.2011 (79.46), 600.2007 (100), 600.2009 (100), 601.2051 (37.70), 601.2052 (40.85), 602.2039 (83.65), 602.4041 (84.87).



**Figure SE2.** HRMS data for Compound **9-3-d<sub>1</sub>**

ESI-MS : obsd (%), calcd (%),

599.2045 (62.97), 599.2048 (85.94), 600.2078 (88.55), 600.2074 (79.46), 601.2083 (100), 601.2071 (100), 602.2117 (70.63), 602.2115 (40.85), 603.2106 (70.21), 603.2104 (84.88).

**99% deuterium incorporation.**

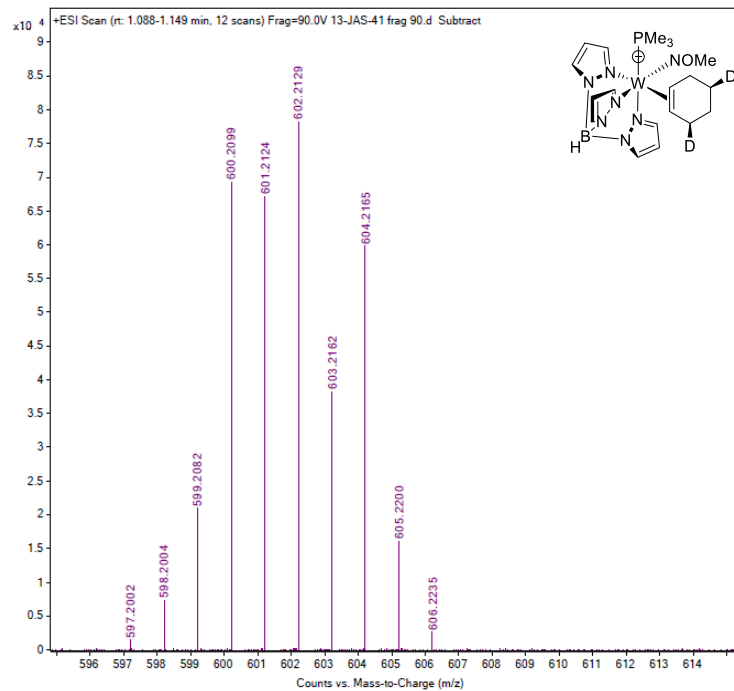


**Figure SE3.** HRMS data for Compound **9-3,5-*d*<sub>2</sub>**

ESI-MS : obsd (%), calcd (%),

600.2099 (88.06) 600.2111 (85.94), 601.2124 (85.46), 601.2136 (79.46), 602.2129 (100), 602.2134 (100),  
603.2162 (48.65), 603.2178 (40.84), 604.2165 (76.72) 604.2167 (84.88).

**86% deuterium incorporation for 7-3*exo*,5*exo*-*d*<sub>2</sub>**

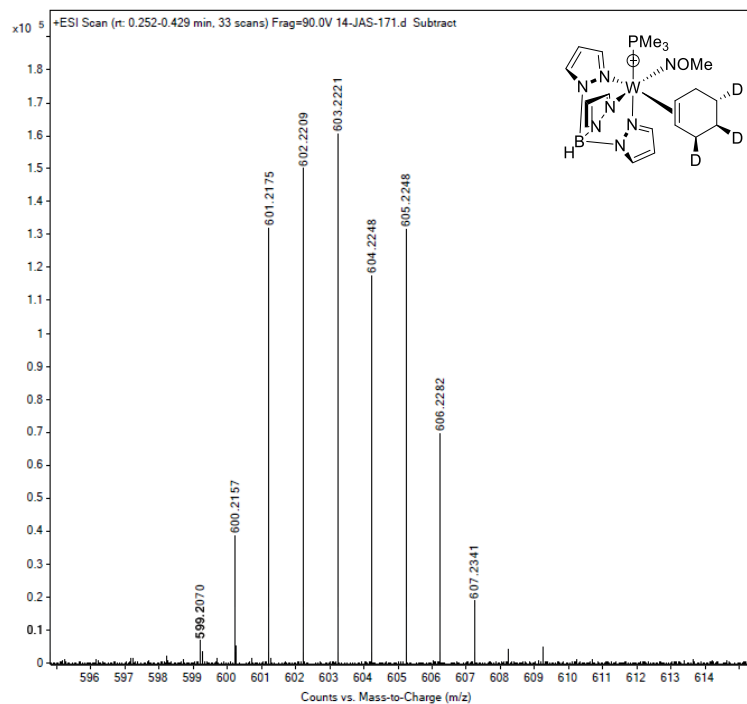


**Figure SE4.** HRMS data for Compound **9-3,4,5- $d_3$**

ESI-MS : obsd (%), calcd (%)

601.2175 (82.27), 601.2173 (85.95), 602.2209 (93.57), 602.2199 (79.46), 603.2221 (100), 603.2197 (100),  
604.2248 (73.32), 604.2240 (40.84), 605.2248 (81.91), 605.2229 (84.88).

**96% deuterium incorporation for 9-3 $exo$ ,4 $exo$ ,5 $endo$ - $d_3$**



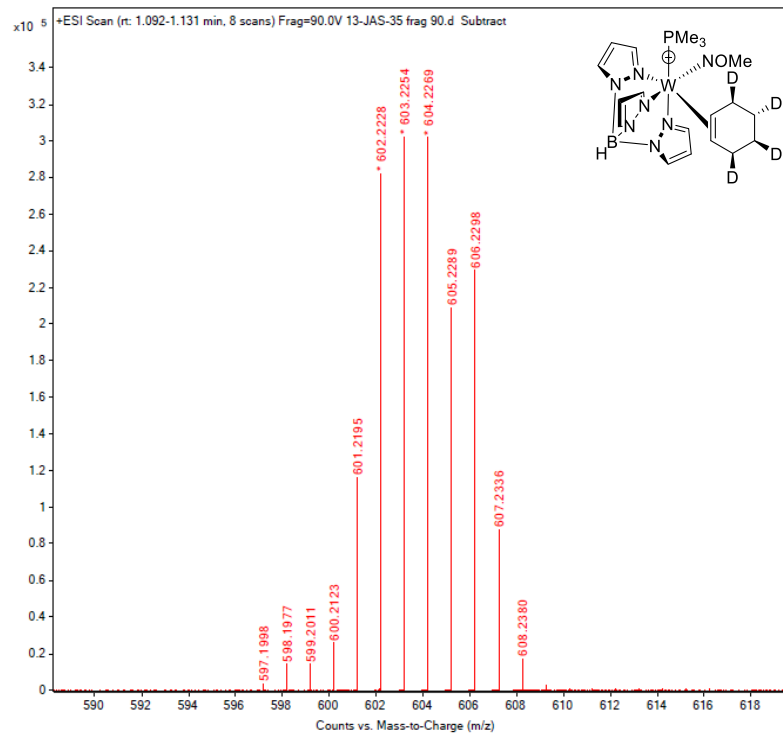


**Figure SE5.** HRMS data for Compound **9-3,4,5,6- $d_4$**

ESI-MS : obsd (%), calcd (%)

602.2228 (93.37), 602.2242 (85.95), 603.2254 (100), 603.2267 (79.45), 604.2269 (100), 604.2265 (100),  
605.2289 (69.22), 605.2309 (40.82), 606.2298 (75.93), 606.2298 (84.88).

**79% deuterium incorporation for 9-3 $exo$ ,4 $exo$ ,5 $endo$ ,6 $exo$ - $d_4$**

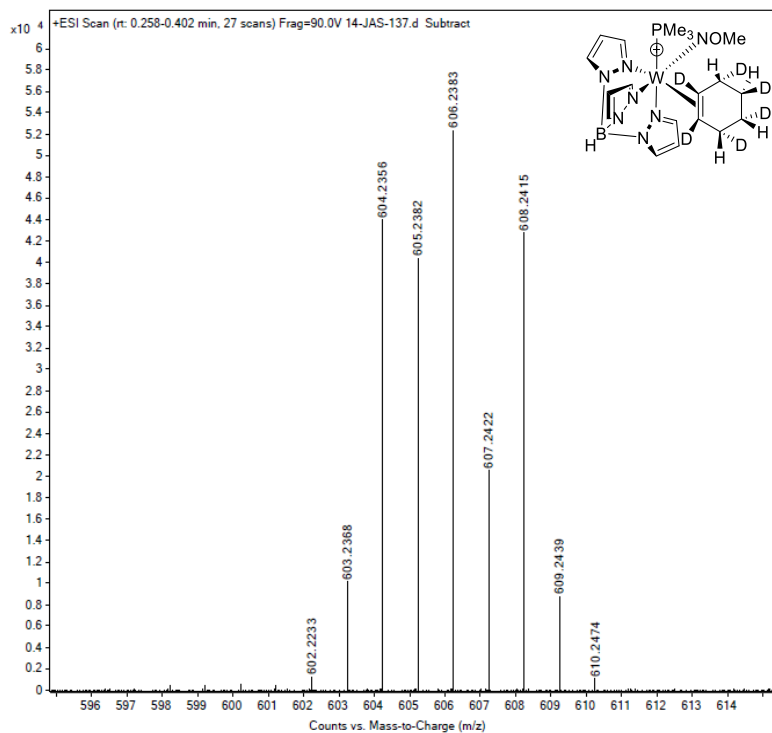


**Figure SE6.** HRMS data for Compound **9-1,2,3,4,5,6-d<sub>6</sub>**

ESI-MS : obsd (%), calcd (%),

604.2356 (84.02), 604.2362 (85.94), 605.2382 (77.11), 605.2387 (79.46), 606.2383 (100), 606.2385 (100), 607.2422 (39.32), 607.2429 (40.81), 608.2415 (81.77), 608.2418 (84.89).

**98% deuterium incorporation for 9-1,2,3endo,4endo,5exo,6endo-d<sub>6</sub>**

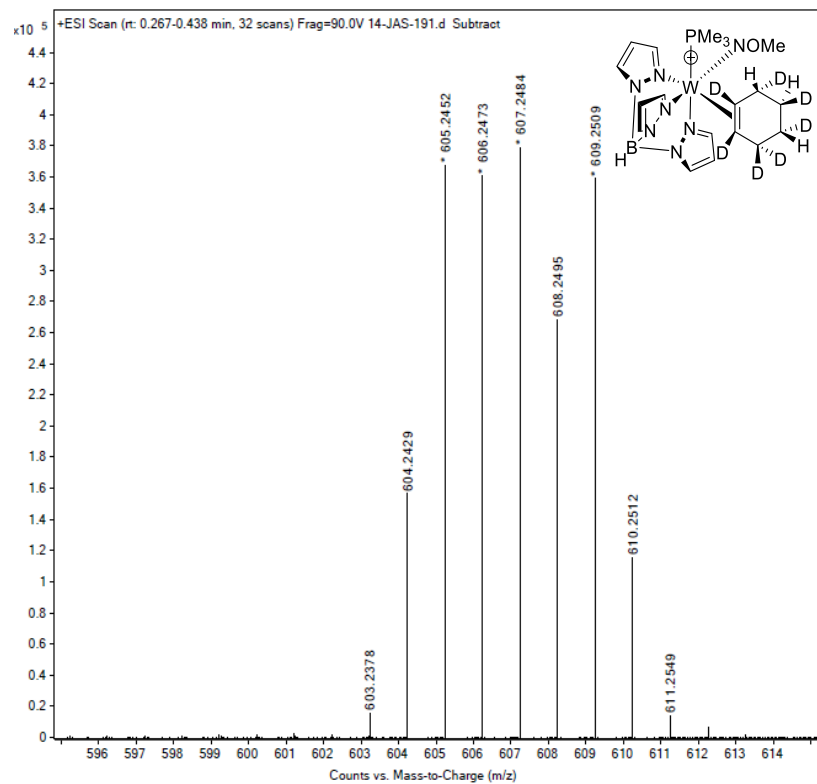


**Figure SE7.** HRMS data for Compound **9-1,2,3,3,4,5,6-d<sub>7</sub>**

ESI-MS : obsd (%), calcd (%)

605.2452 (96.99), 605.2424 (85.97), 606.2473 (95.24), 606.2450 (79.44), 607.2484 (100), 607.2448 (100),  
608.2495 (48.65), 608.2495 (70.86), 609.2509 (94.74), 609.2481 (84.89).

**96% deuterium incorporation for 9-1,2,3,3,4endo,5exo,6endo-d<sub>7</sub>**

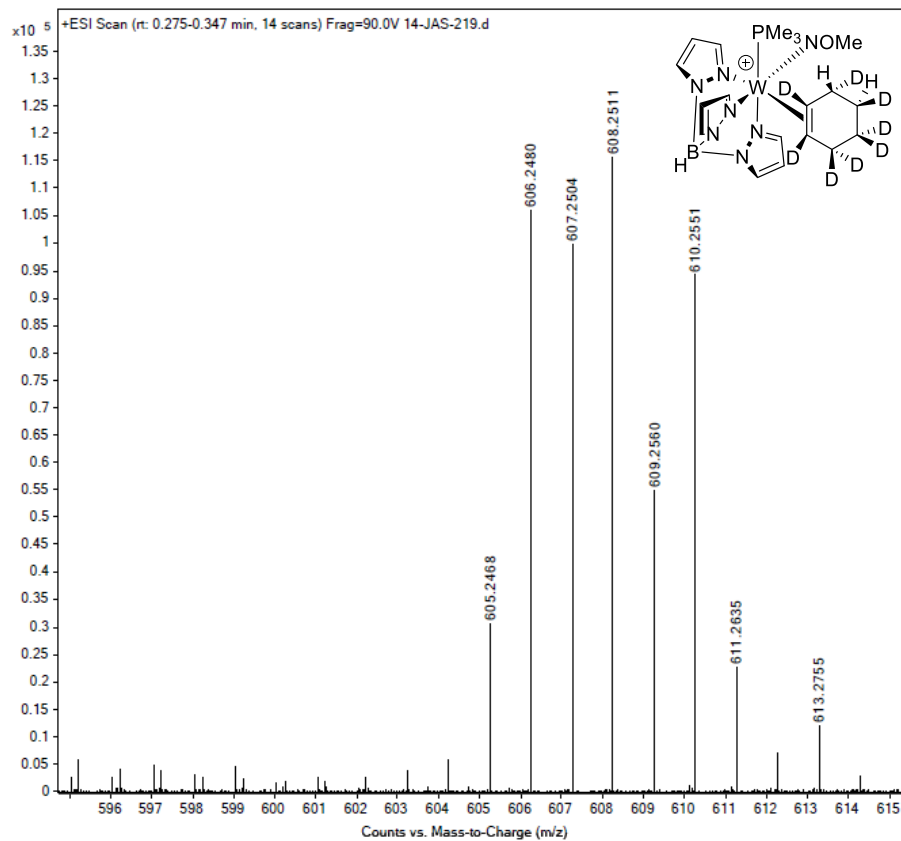


**Figure SE8.** HRMS data for Compound **9-1,2,3,3,4,4,5,6-*d*<sub>8</sub>**

ESI-MS : obsd (%), calcd (%),

606.2480 (91.56), 606.2487 (85.97), 607.2504 (86.25), 607.2513 (79.44), 608.2511 (100), 608.2511 (100),  
609.2560 (47.46), 609.2554 (40.79), 610.2551 (81.53), 610.2543 (84.89).

**99% deuterium incorporation for 9-1,2,3,3,4,4,5<sub>exo</sub>,6<sub>endo</sub>-*d*<sub>8</sub>**

F)  $^1\text{H}$  and  $^{13}\text{C}$  { $1\text{H}$ } Spectra of compounds.

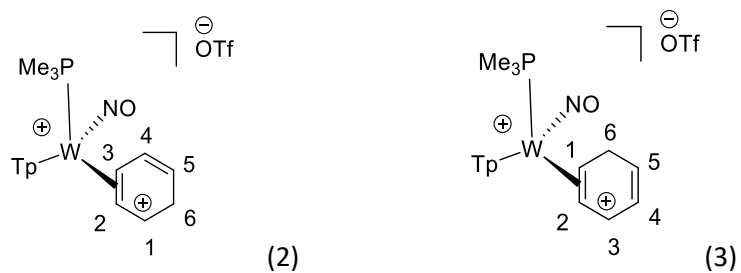
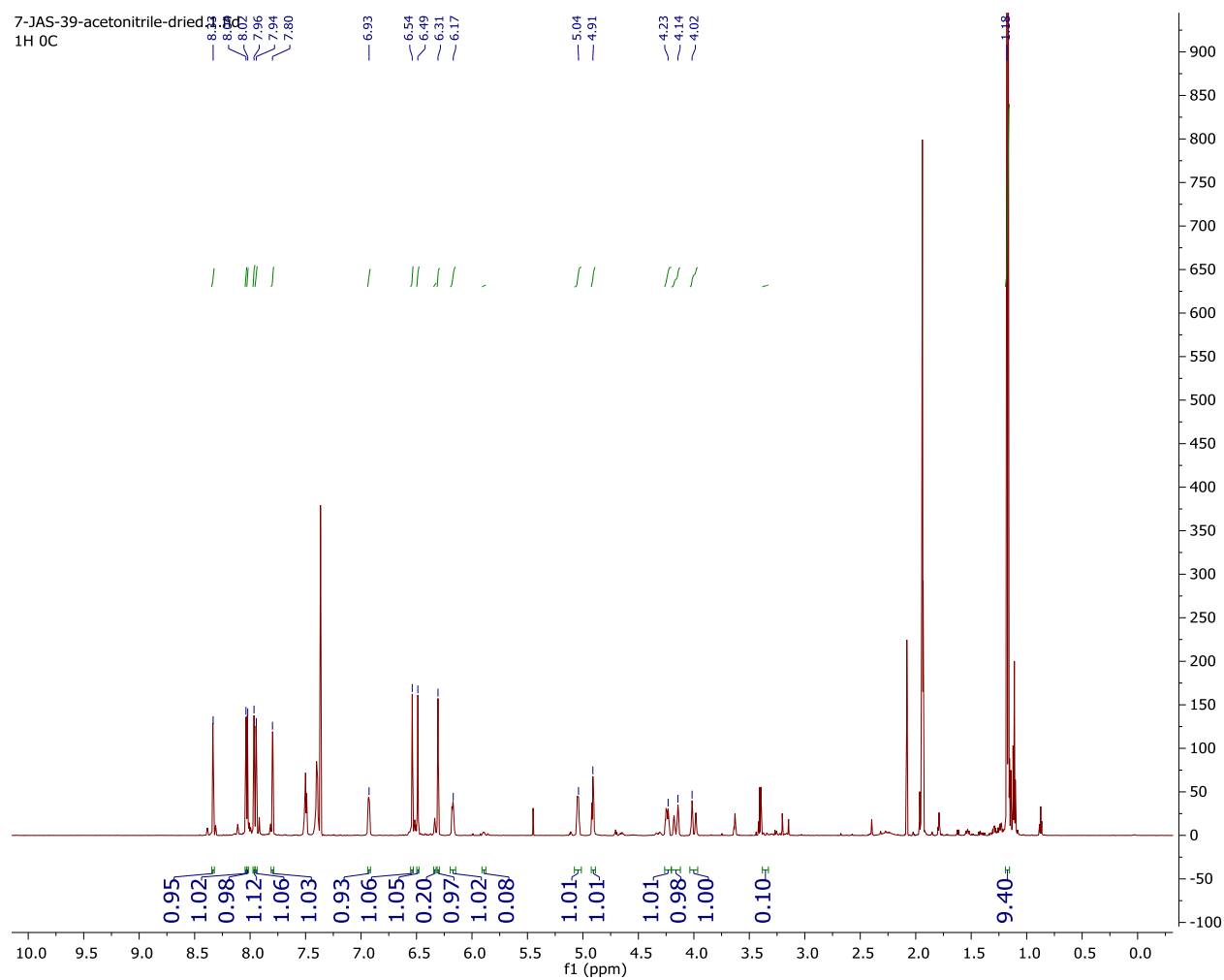


Figure SF1.  $^1\text{H}$  NMR Spectrum of 2 and 3





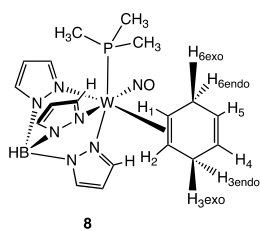
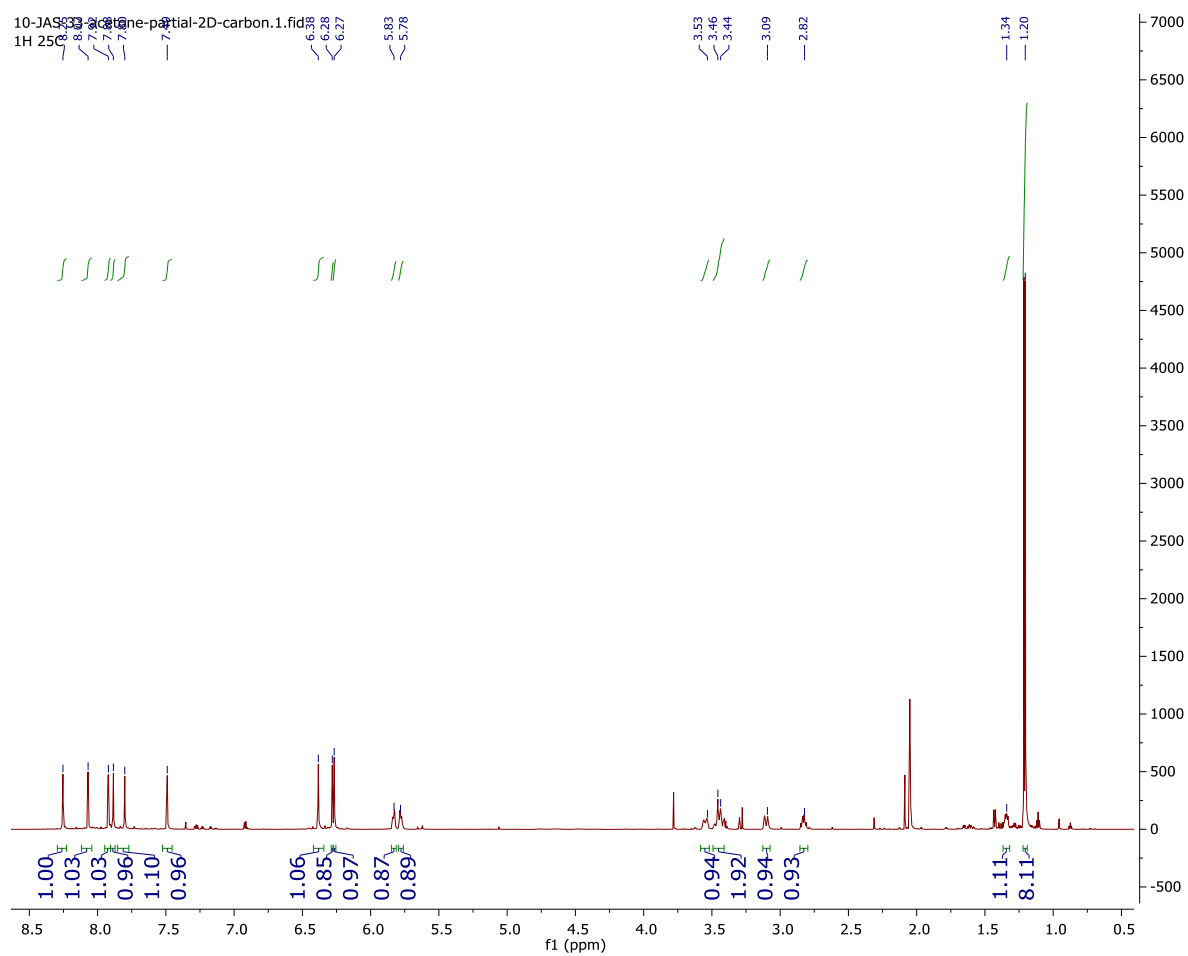


Figure SF3. <sup>1</sup>H NMR Spectrum of 8



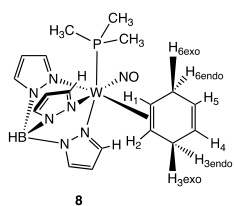
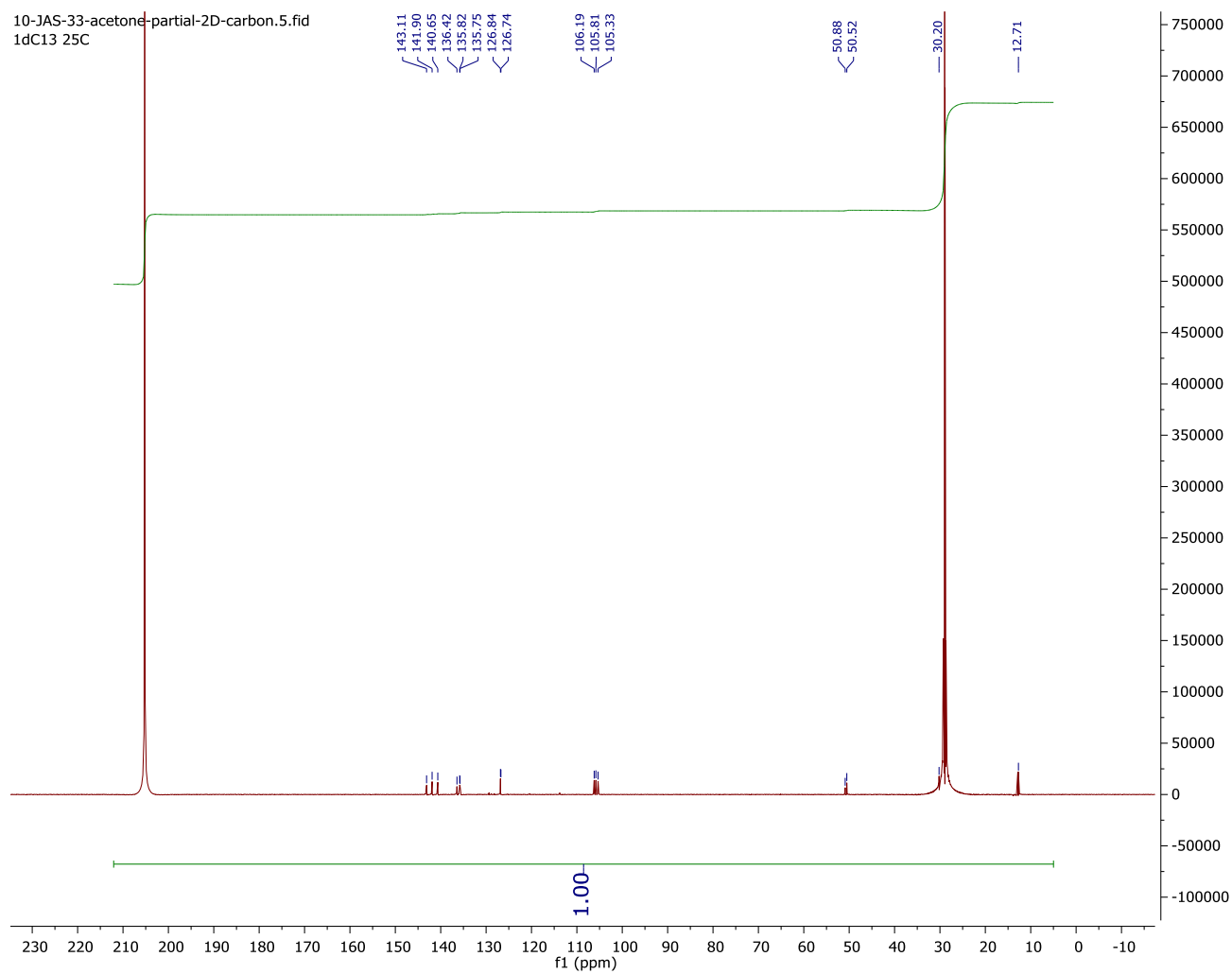


Figure SF4. <sup>13</sup>C{<sup>1</sup>H} NMR Spectrum of 8





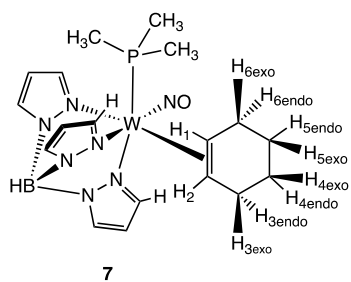
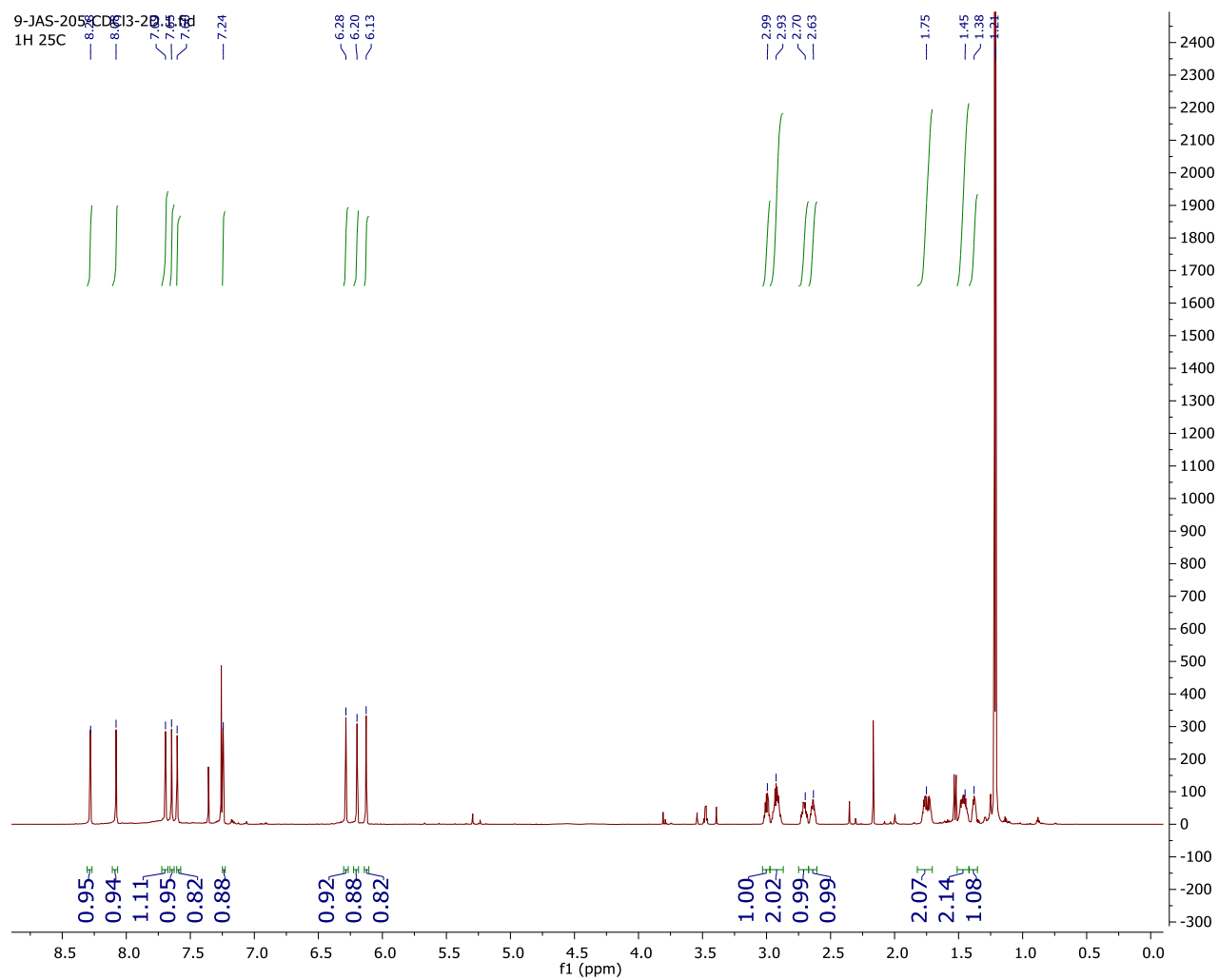


Figure SF5. <sup>1</sup>H NMR Spectrum of 7



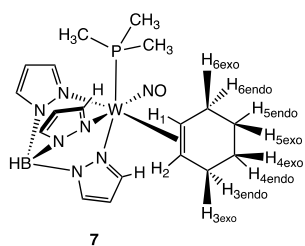
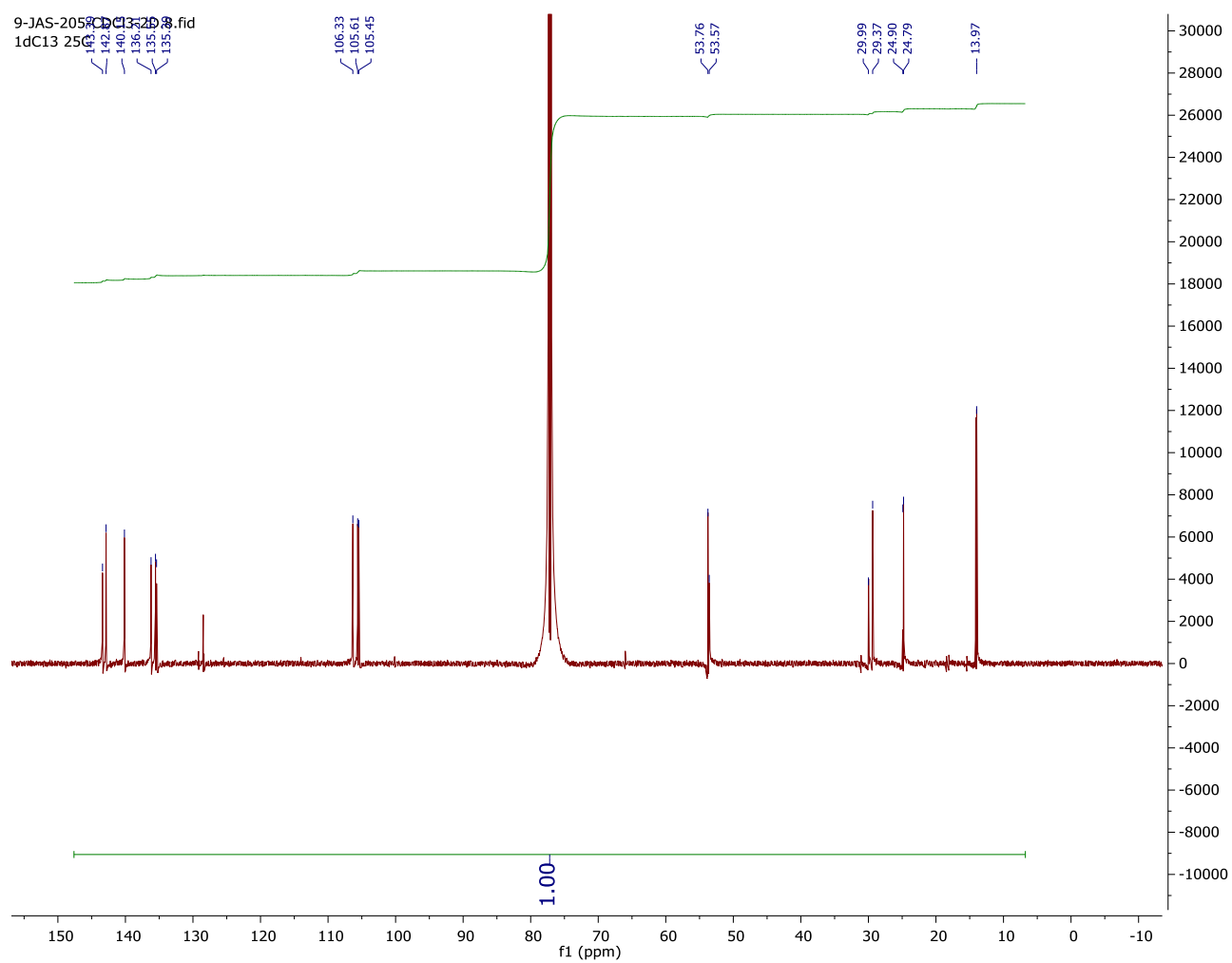


Figure SF6.  $^{13}\text{C}\{^1\text{H}\}$  NMR Spectrum of 7



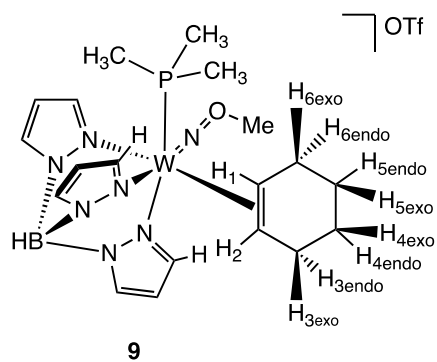
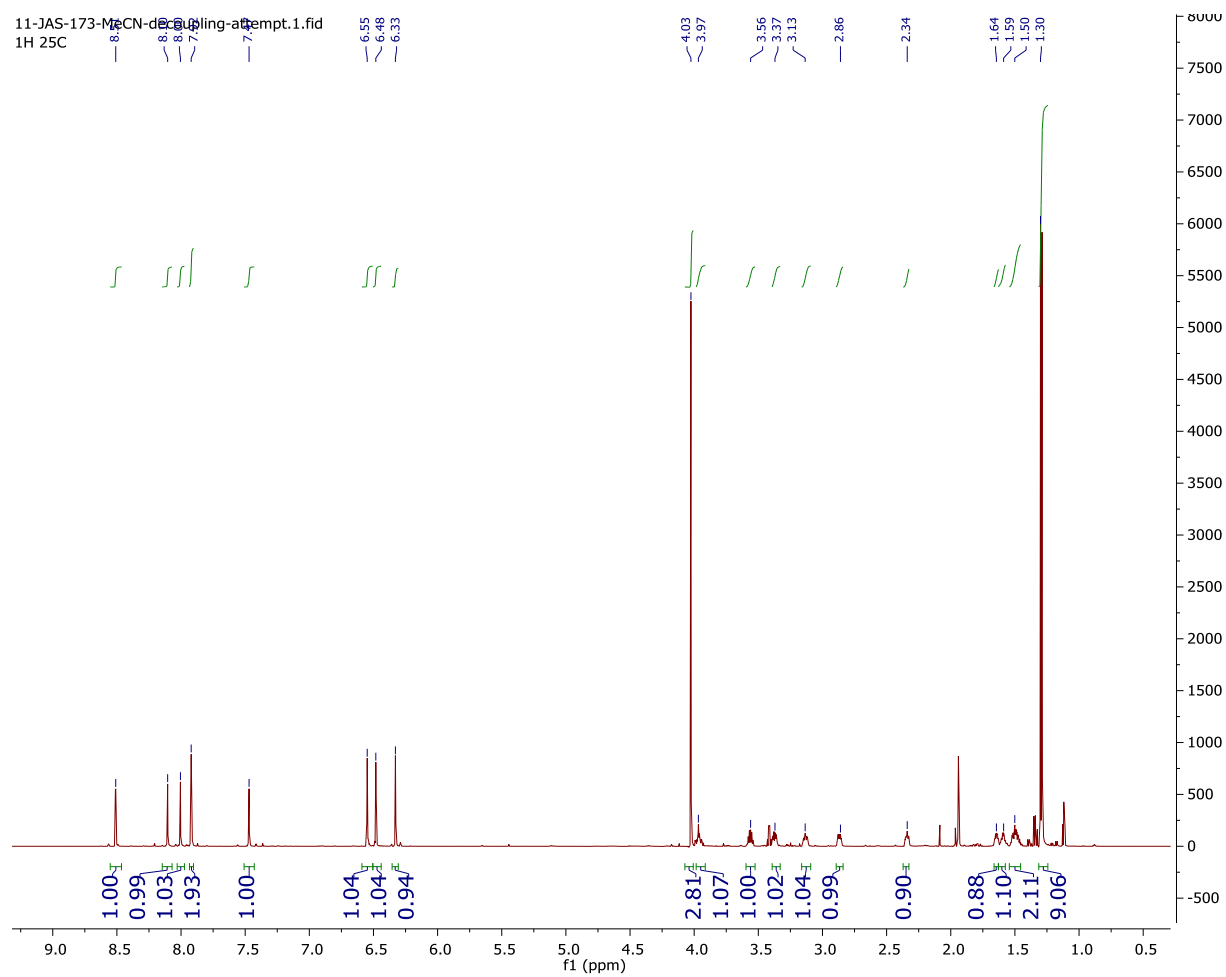


Figure SF7. <sup>1</sup>H NMR Spectrum of 9



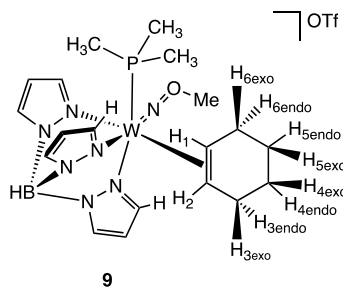
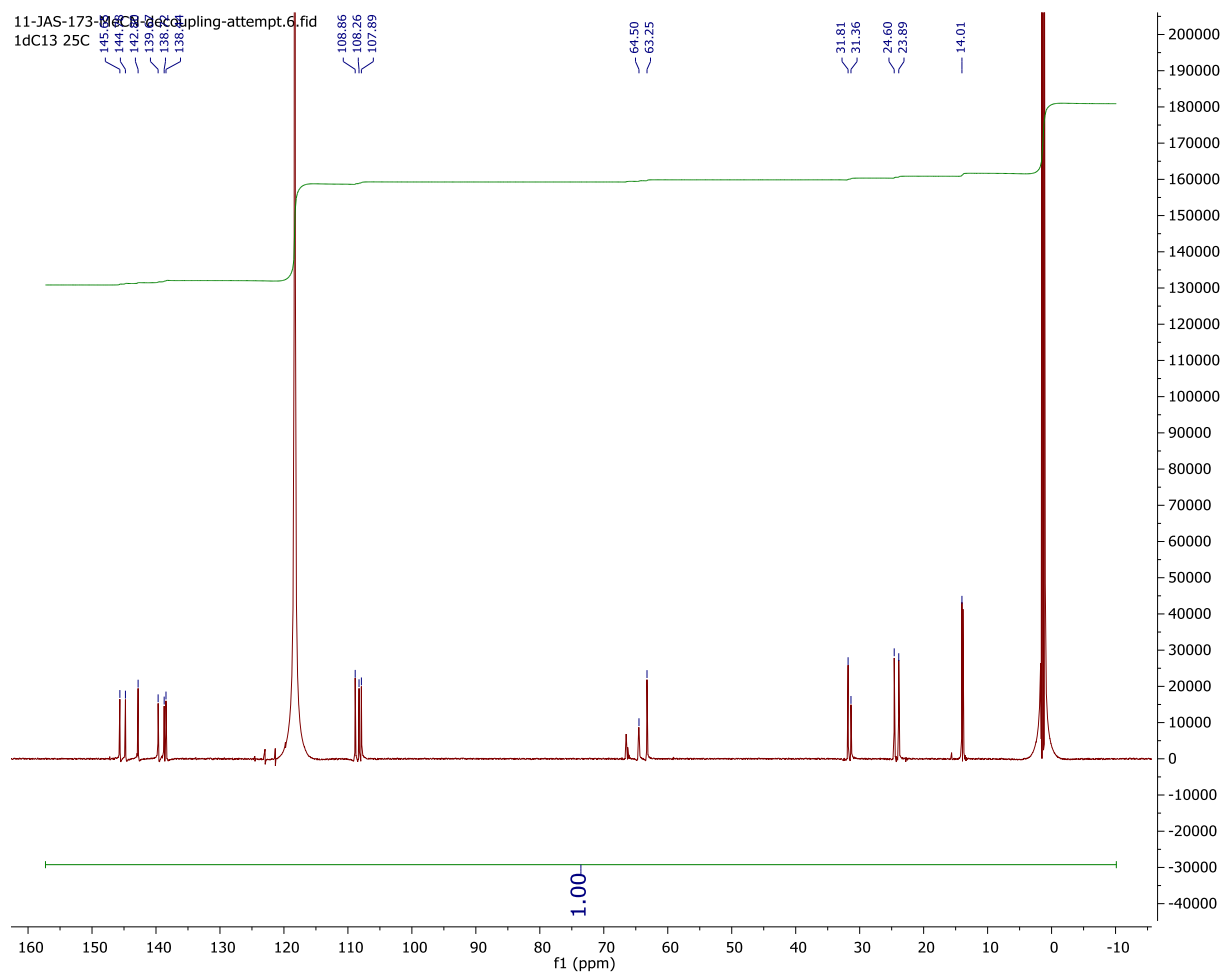


Figure SF8.  $^{13}\text{C}$   $\{^1\text{H}\}$  NMR Spectrum of 9



## Supporting Data for Isotopologues:

### $d_1$ -Isotopologues

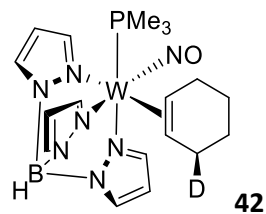
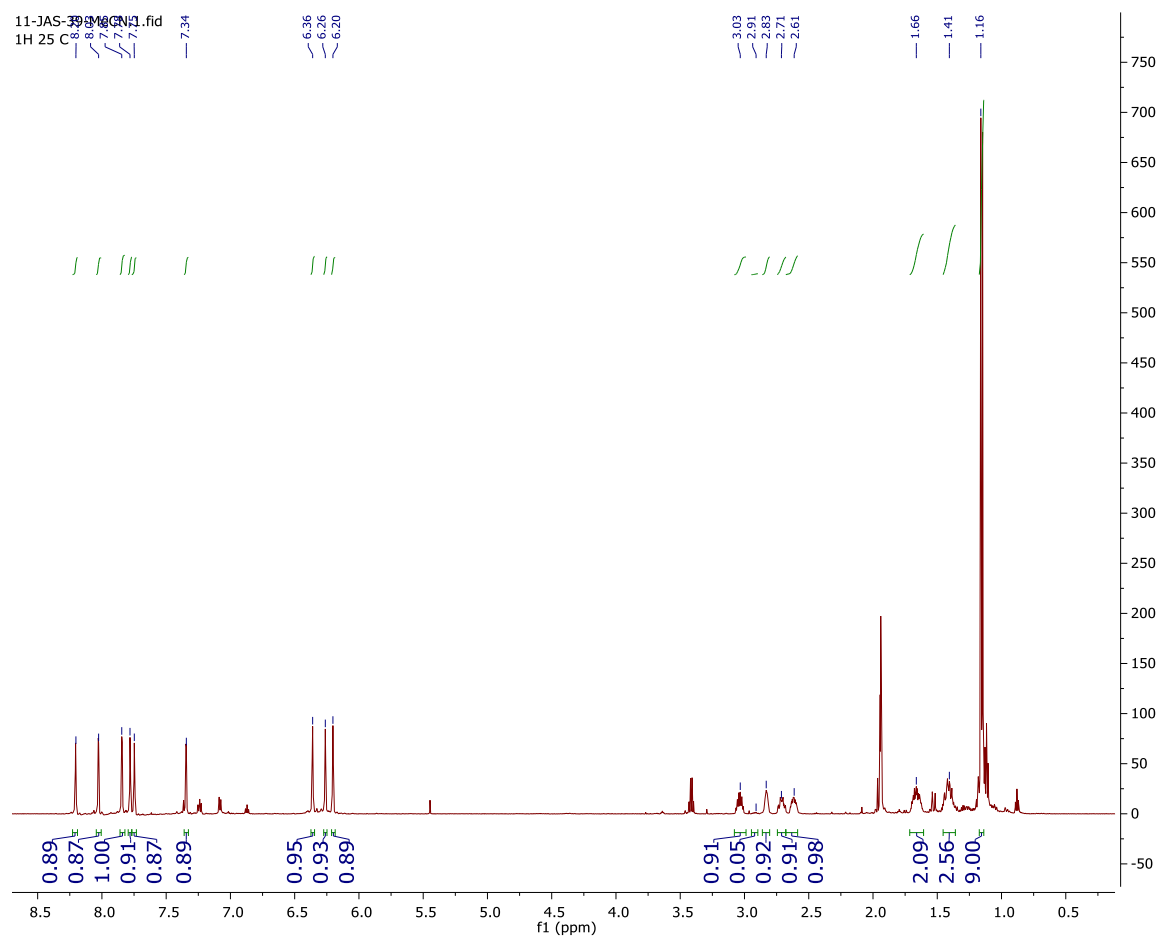


Figure SF9. <sup>1</sup>H NMR Spectrum of 42



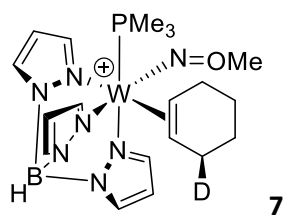
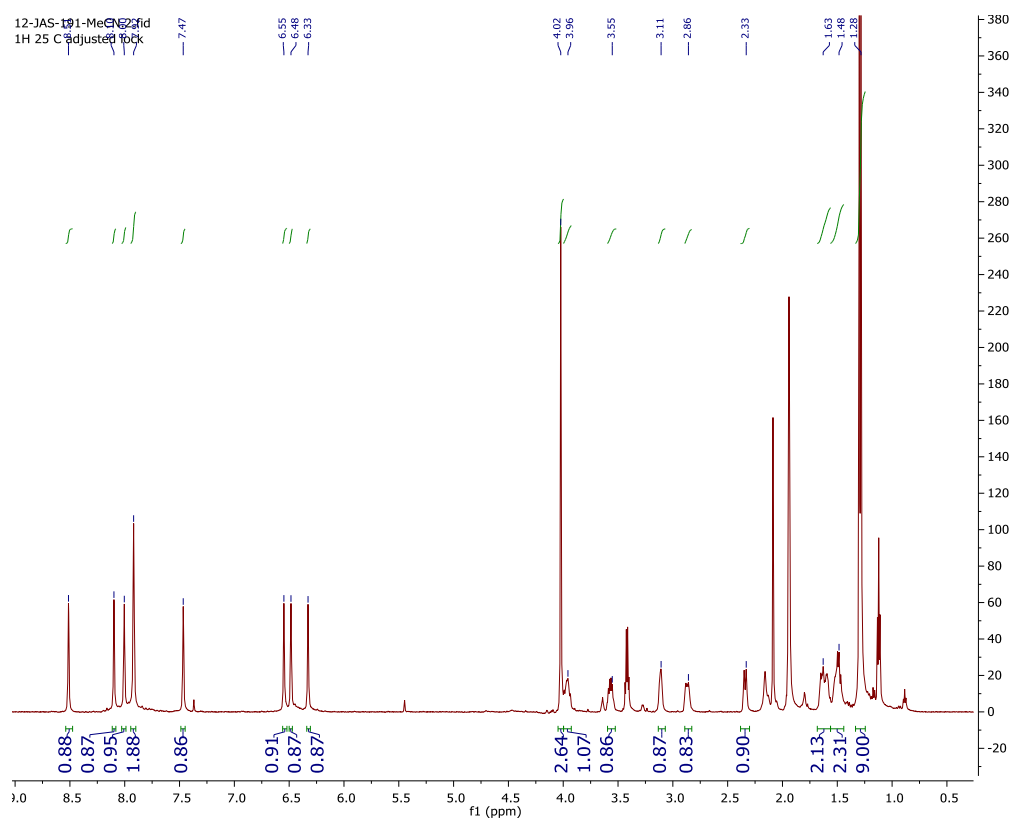
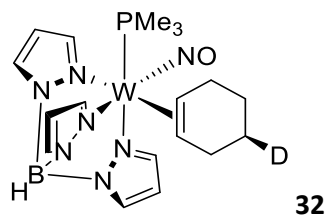
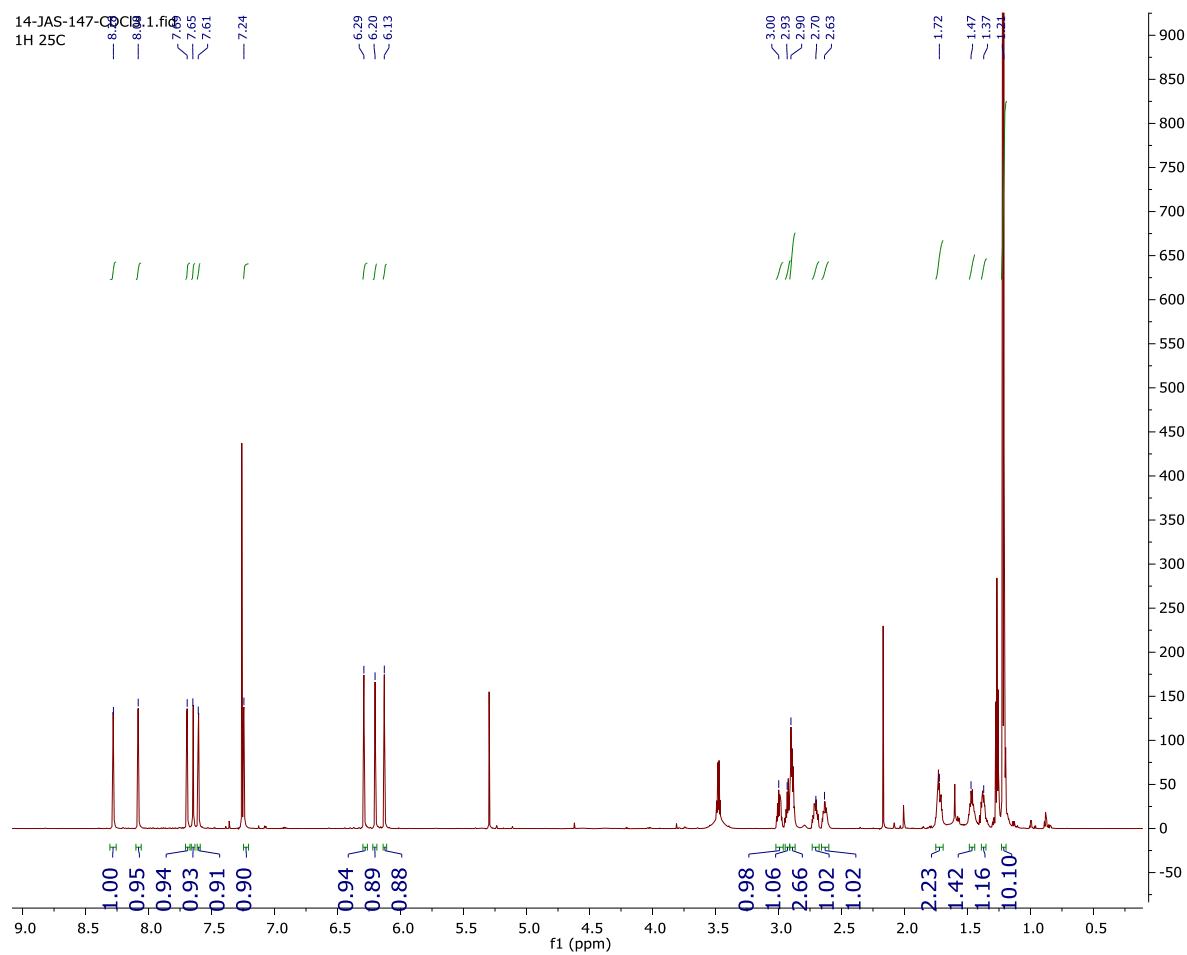


Figure SF10. <sup>1</sup>H NMR Spectrum of 7





**Figure SF11. <sup>1</sup>H NMR Spectrum of 32**



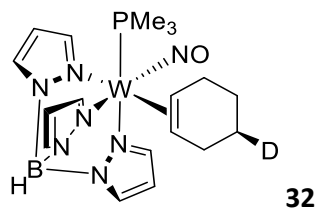
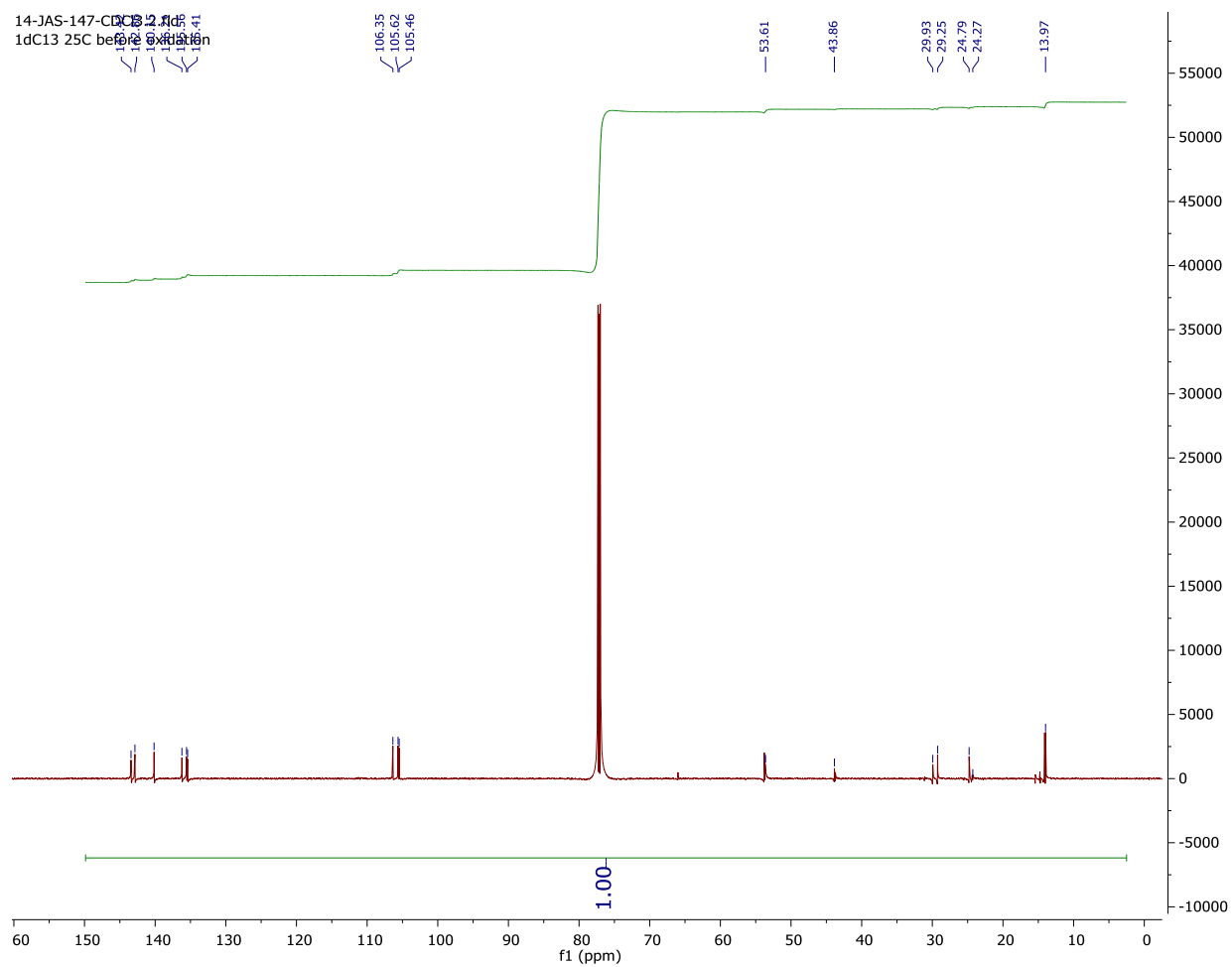


**Figure SF12.  $^{13}\text{C}\{^1\text{H}\}$  NMR Spectrum of 32**





**d<sub>2</sub>-Isotopologues:**

**Figure SF13. <sup>1</sup>H NMR Spectrum of 45**

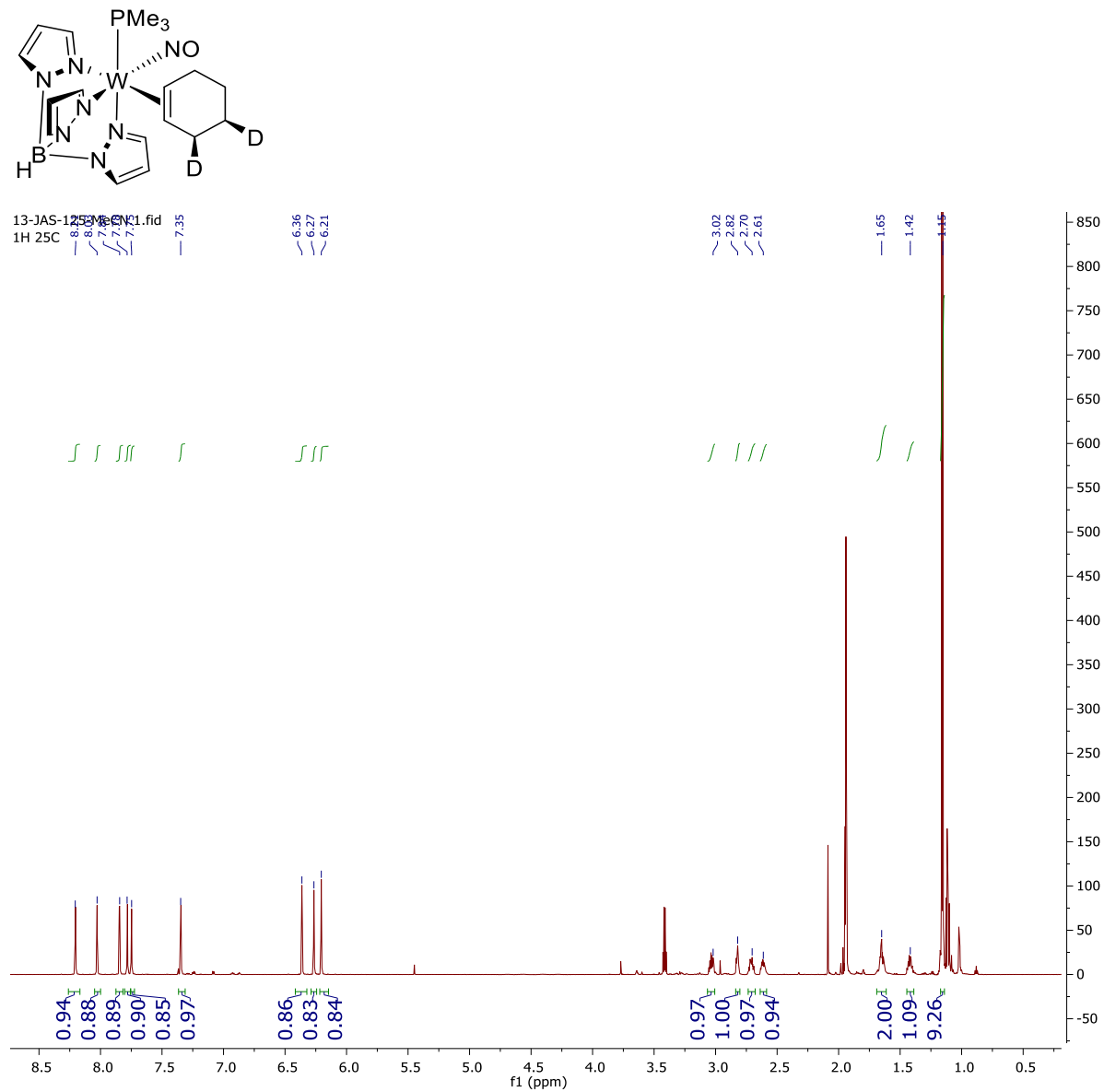


Figure SF14. <sup>1</sup>H NMR Spectrum of 43

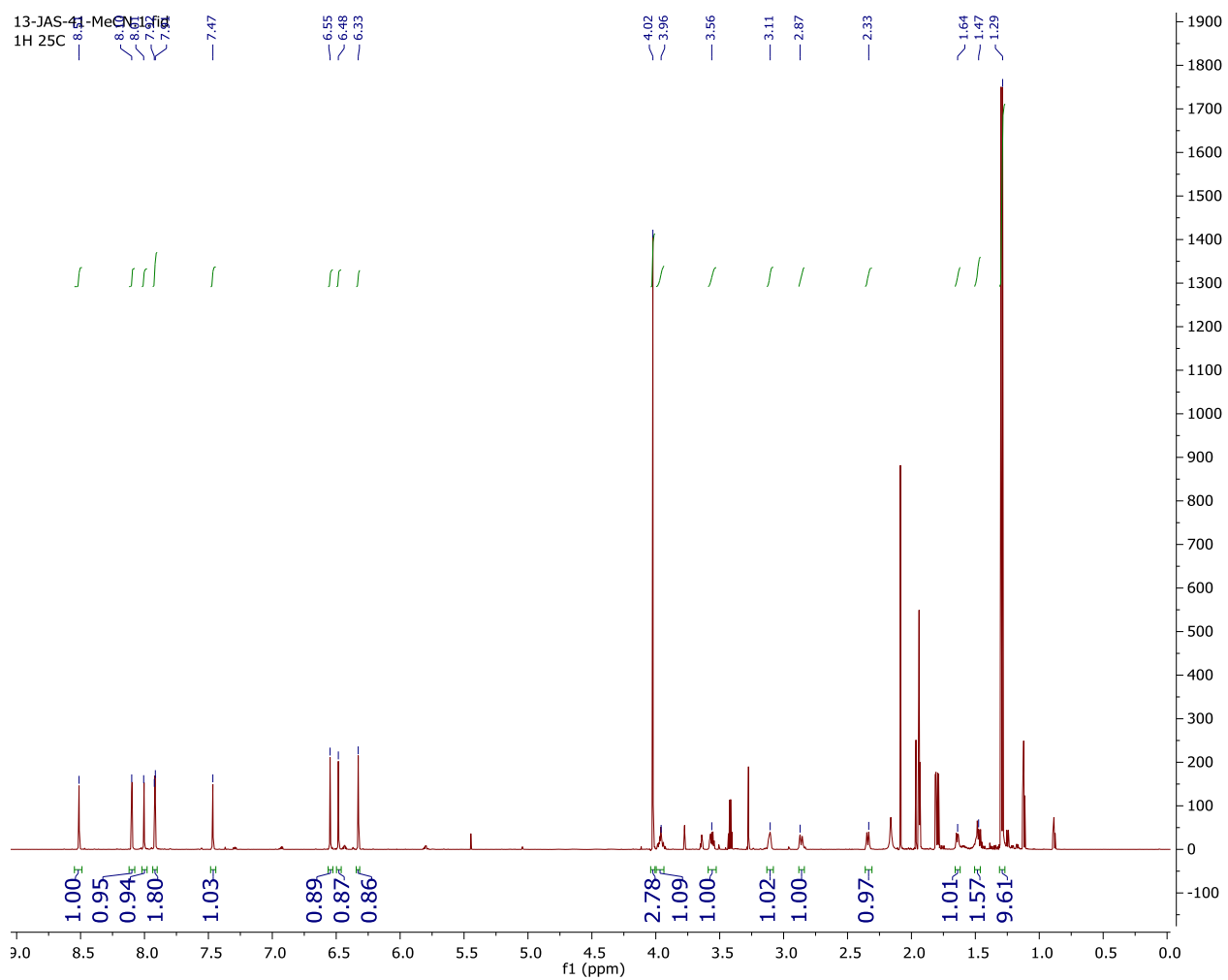
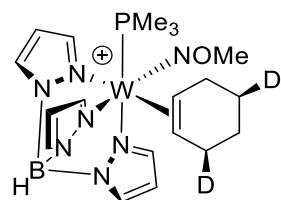
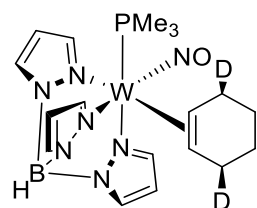


Figure SF15. <sup>1</sup>H NMR Spectrum of 44



13-JAS-127-M80-360-1-NaBD4-5sec-delay  
Std proton

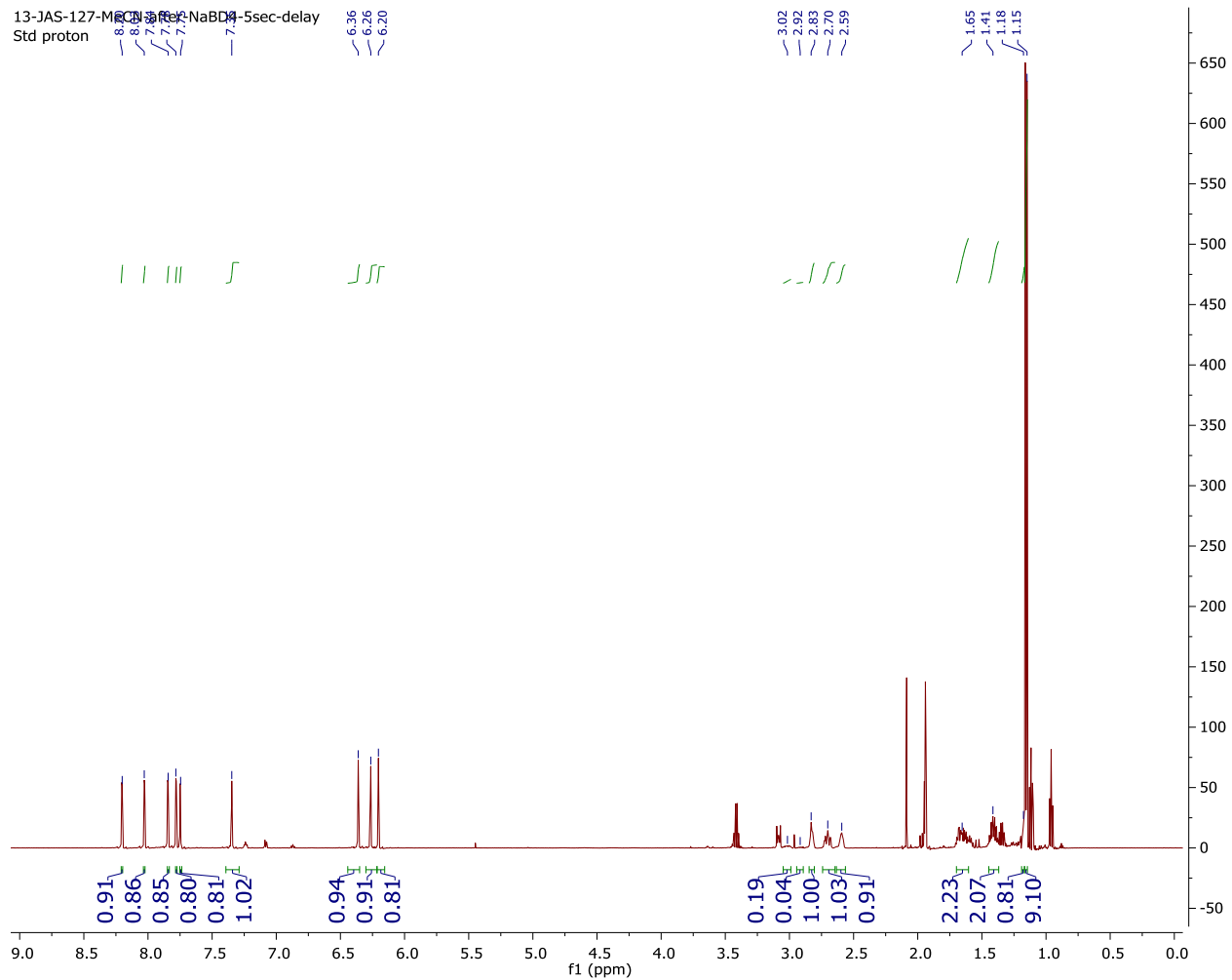


Figure SF16. <sup>1</sup>H NMR Spectrum of 14

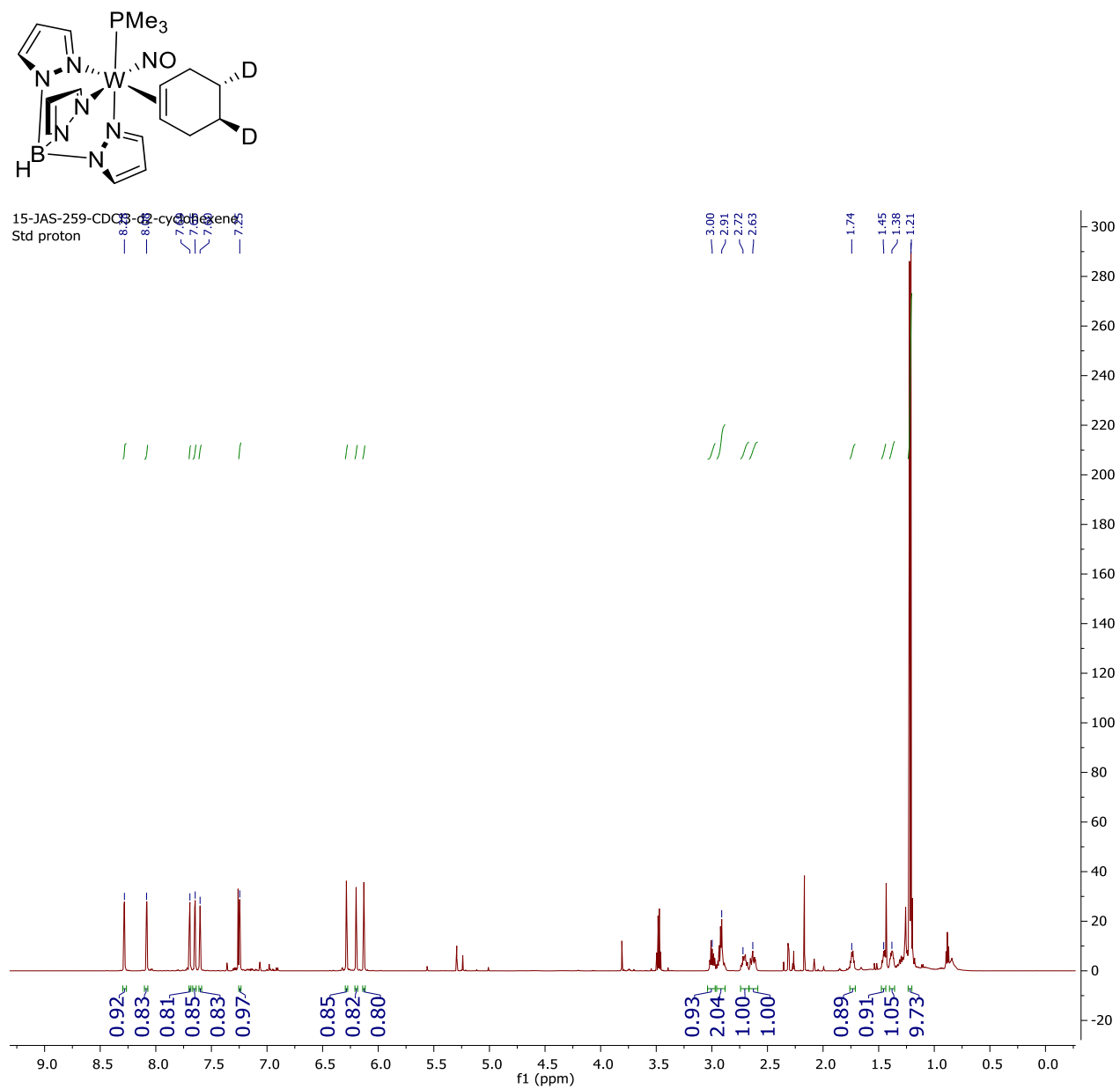




Figure SF18. <sup>1</sup>H NMR Spectrum of Compound 46

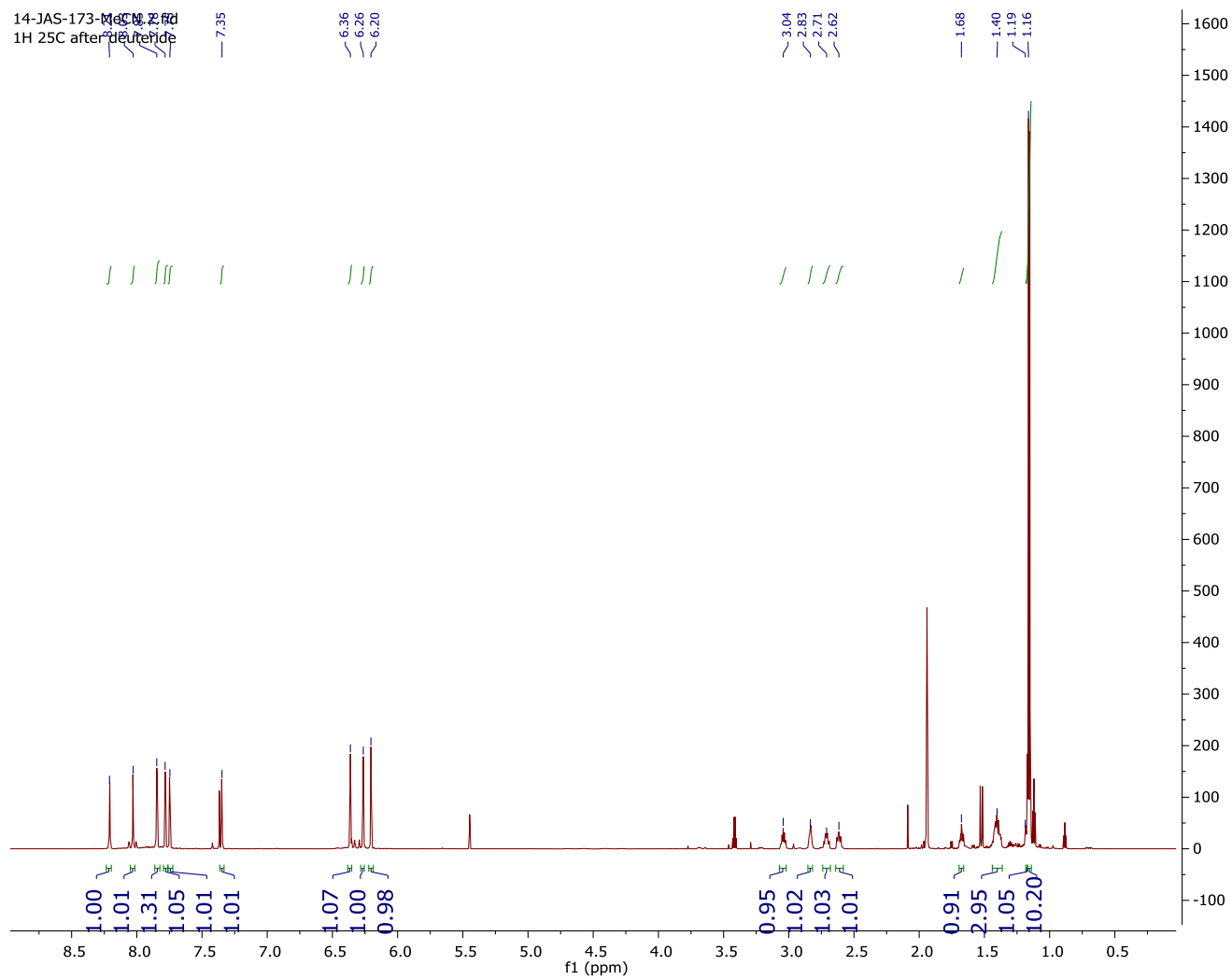
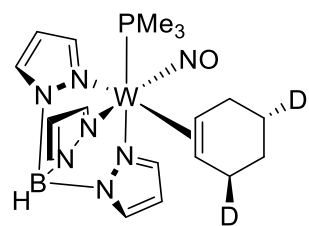
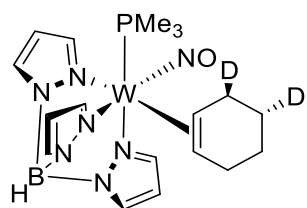


Figure SF19. <sup>1</sup>H NMR Spectrum of Compound 35



14-JAS-1774-MCN-2.fid  
<sup>1</sup>H 25C after NaBH<sub>4</sub> and eluted through basic alumina

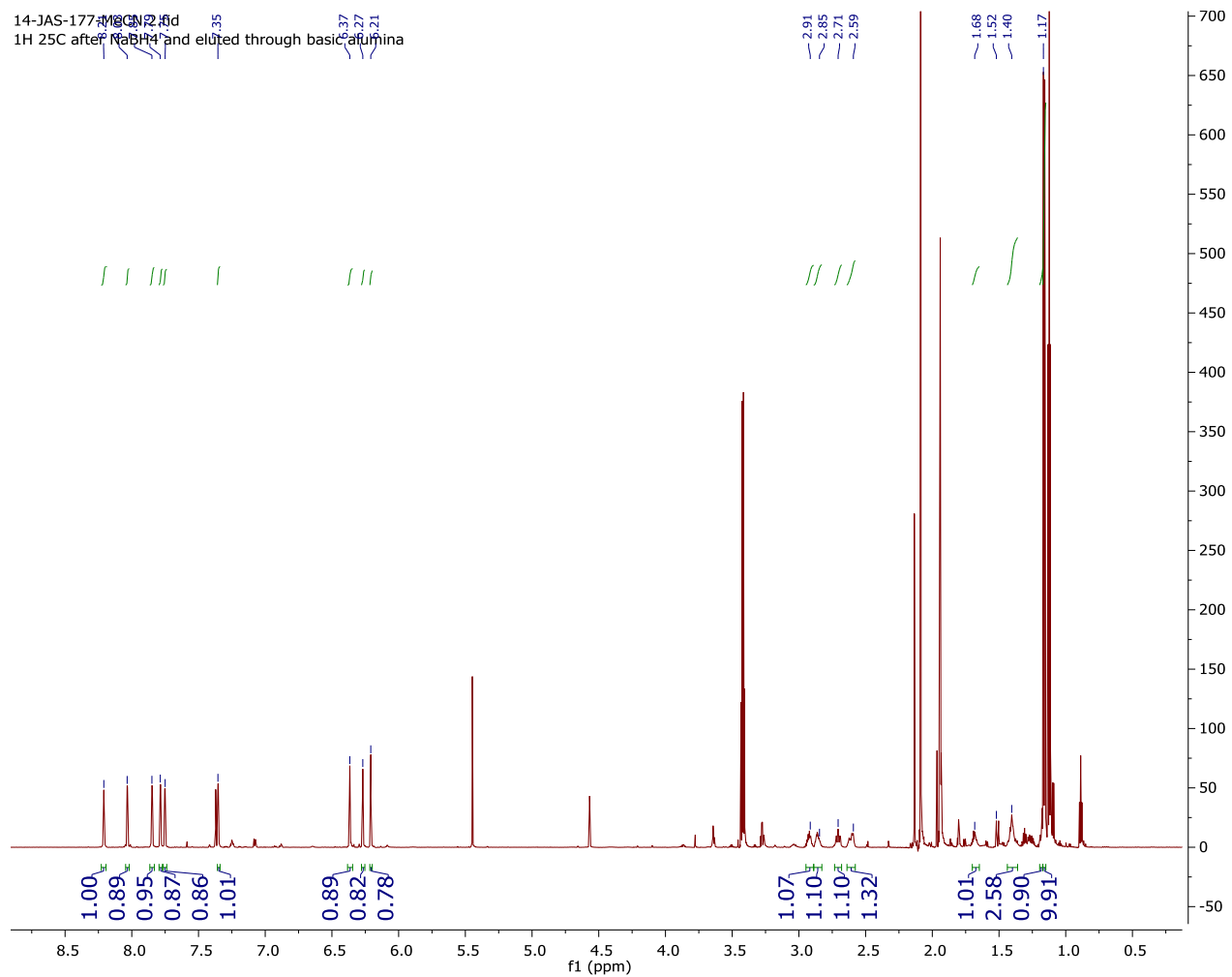
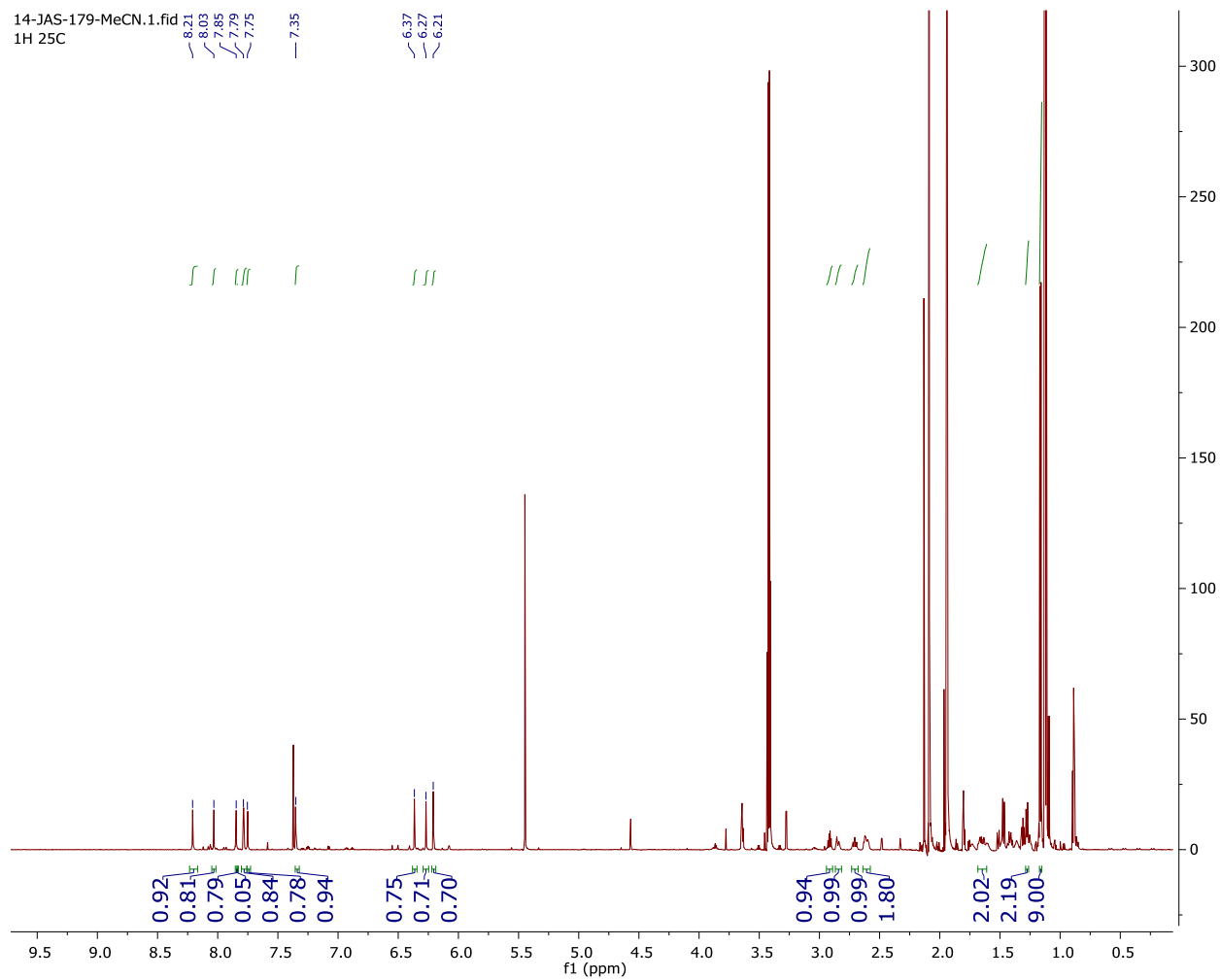
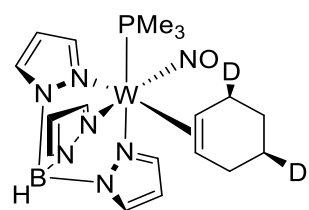


Figure SF20. <sup>1</sup>H NMR Spectrum of Compound 33





## D3-Isotopologues

Figure SF21. <sup>1</sup>H NMR Spectrum of Compound 50

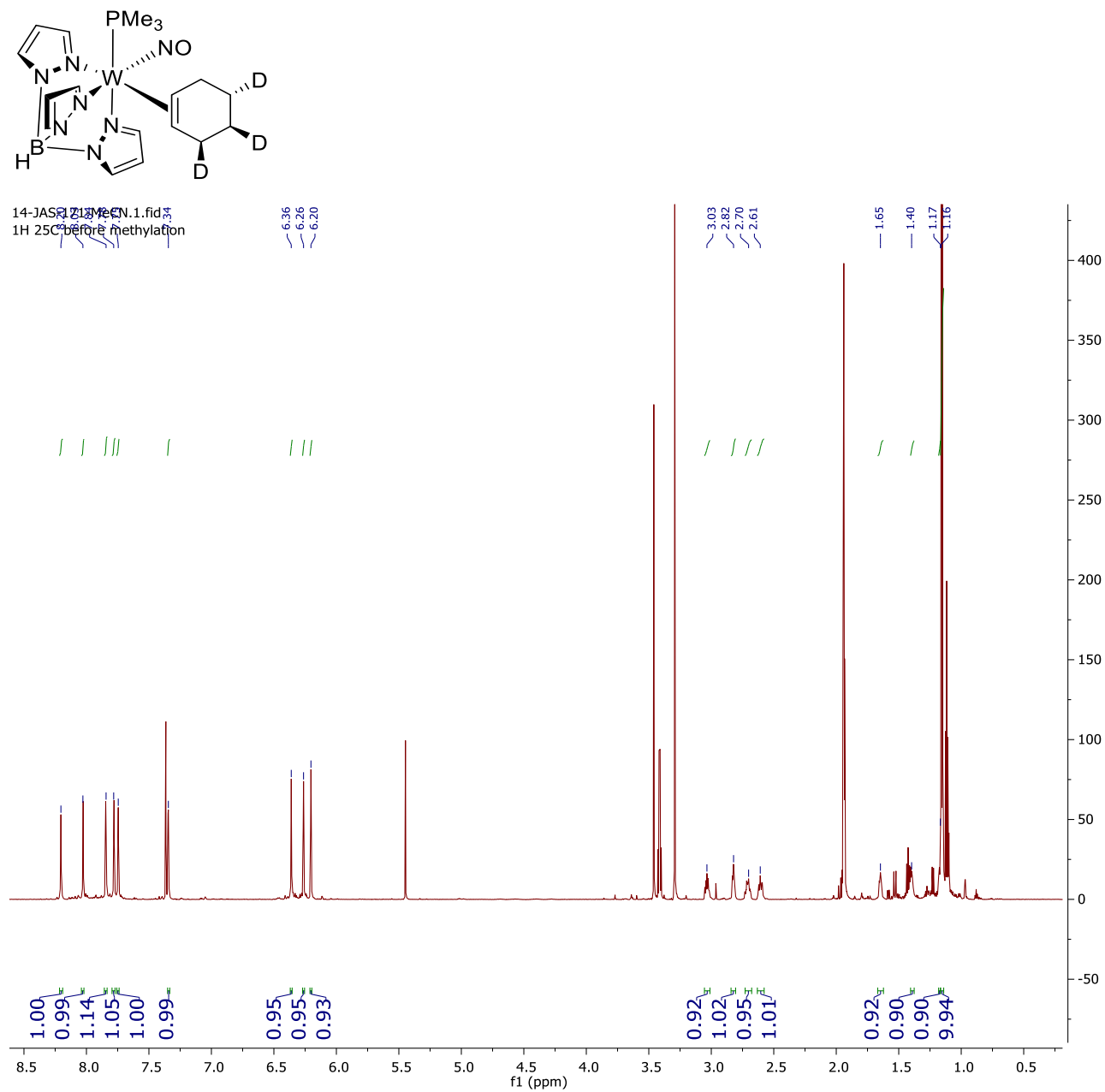
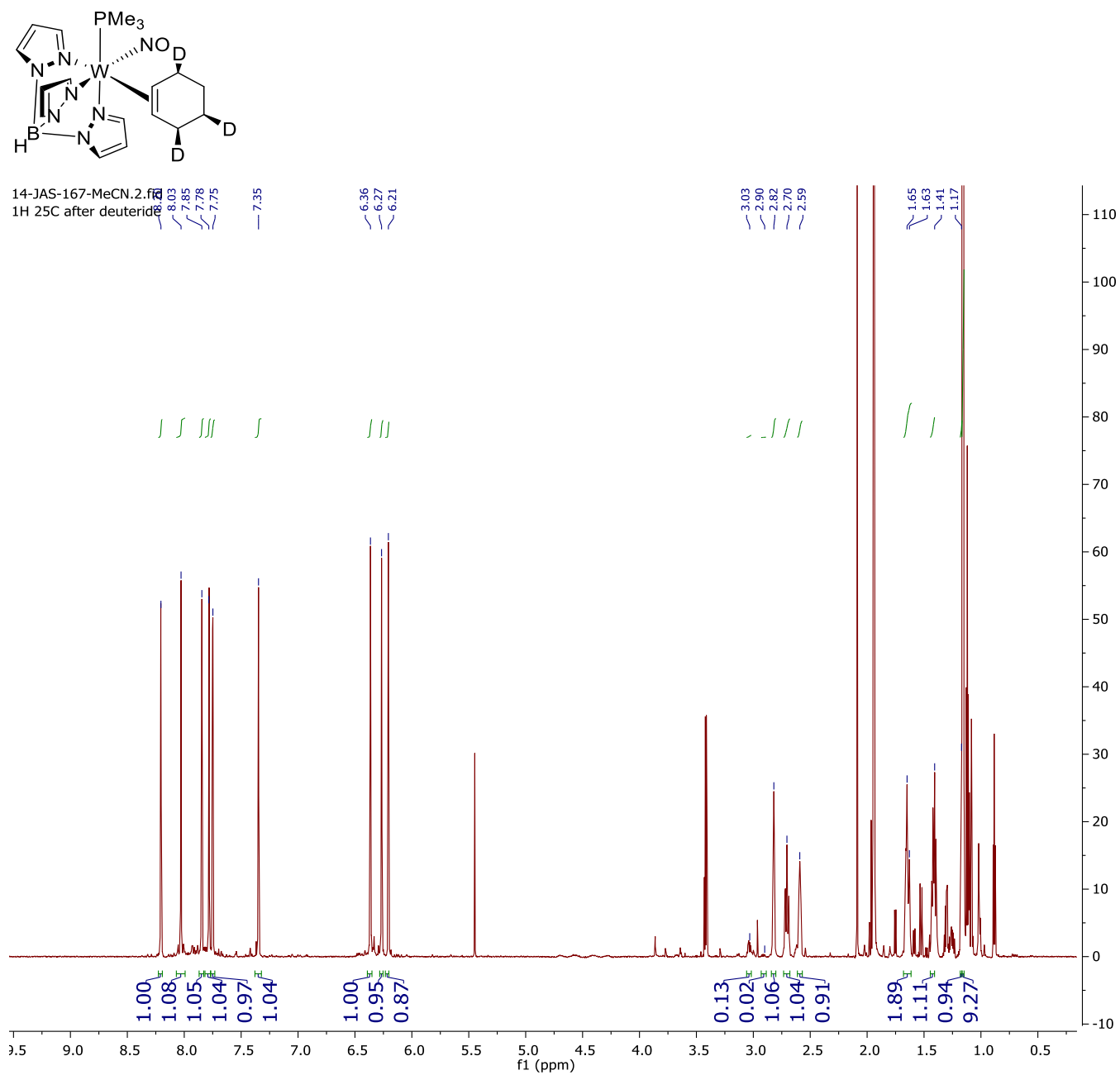
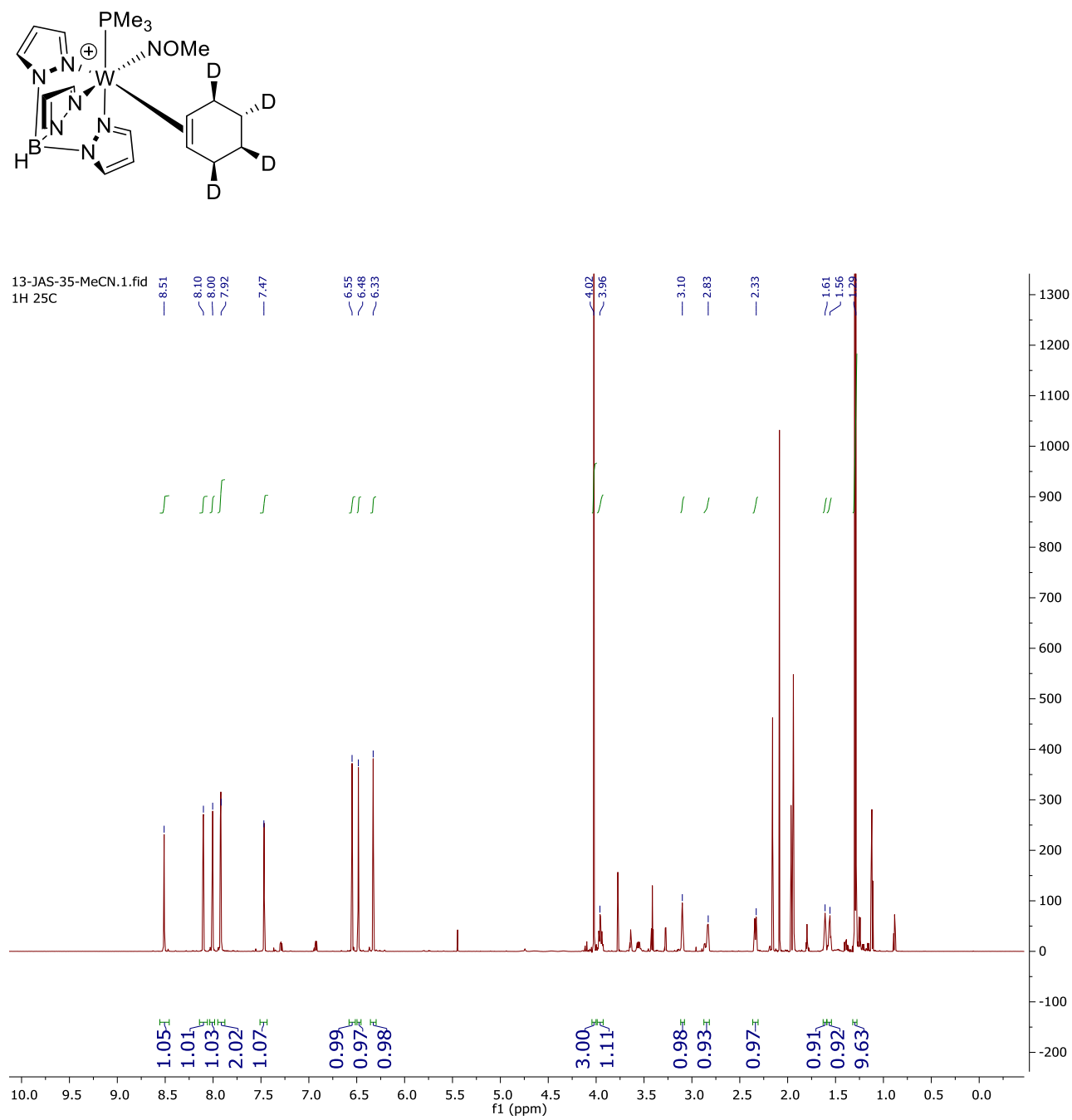


Figure SF22. <sup>1</sup>H NMR Spectrum of Compound 49



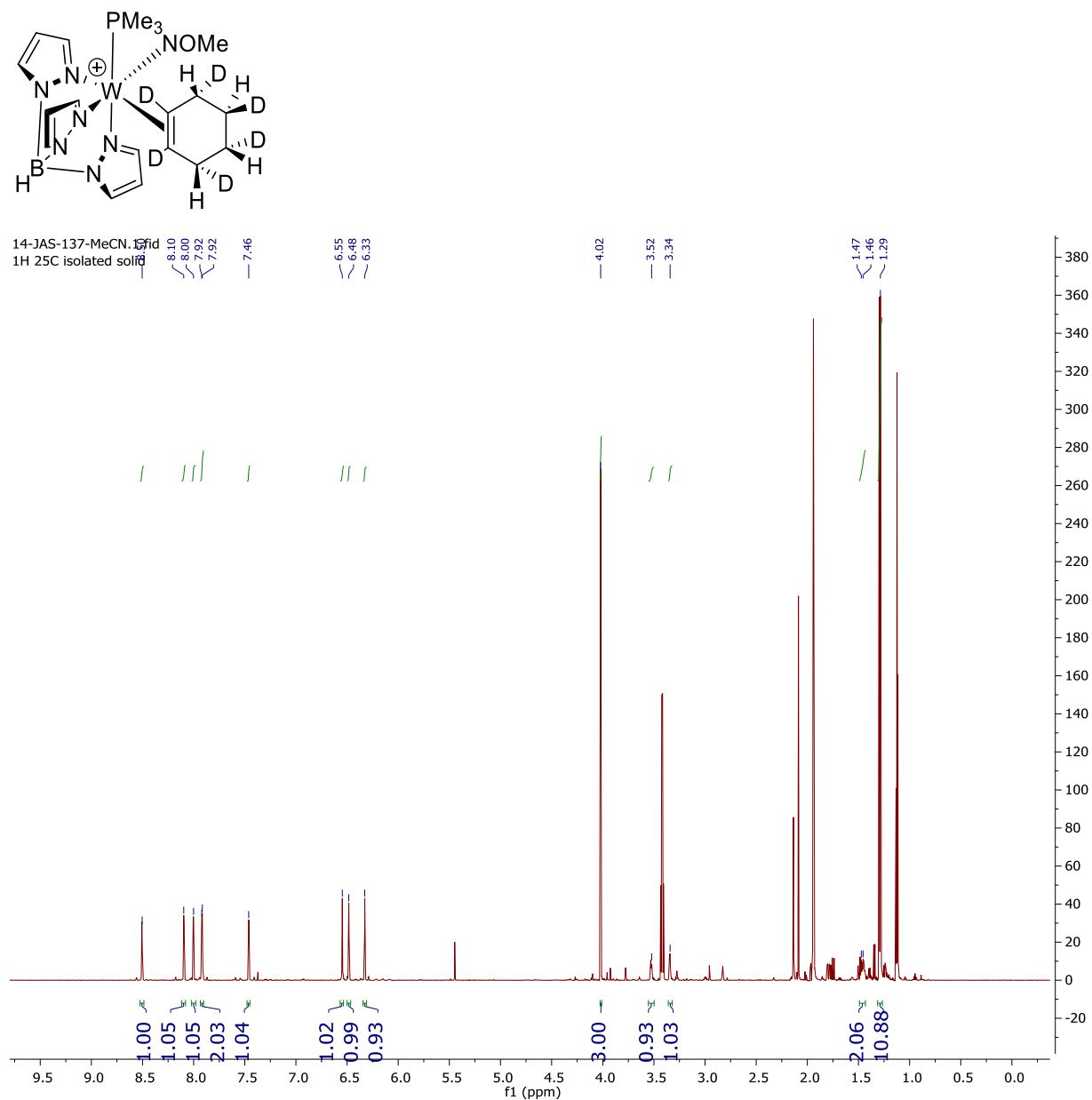
## D4-Isotopologues

Figure SF23. <sup>1</sup>H NMR Spectrum of Compound 16



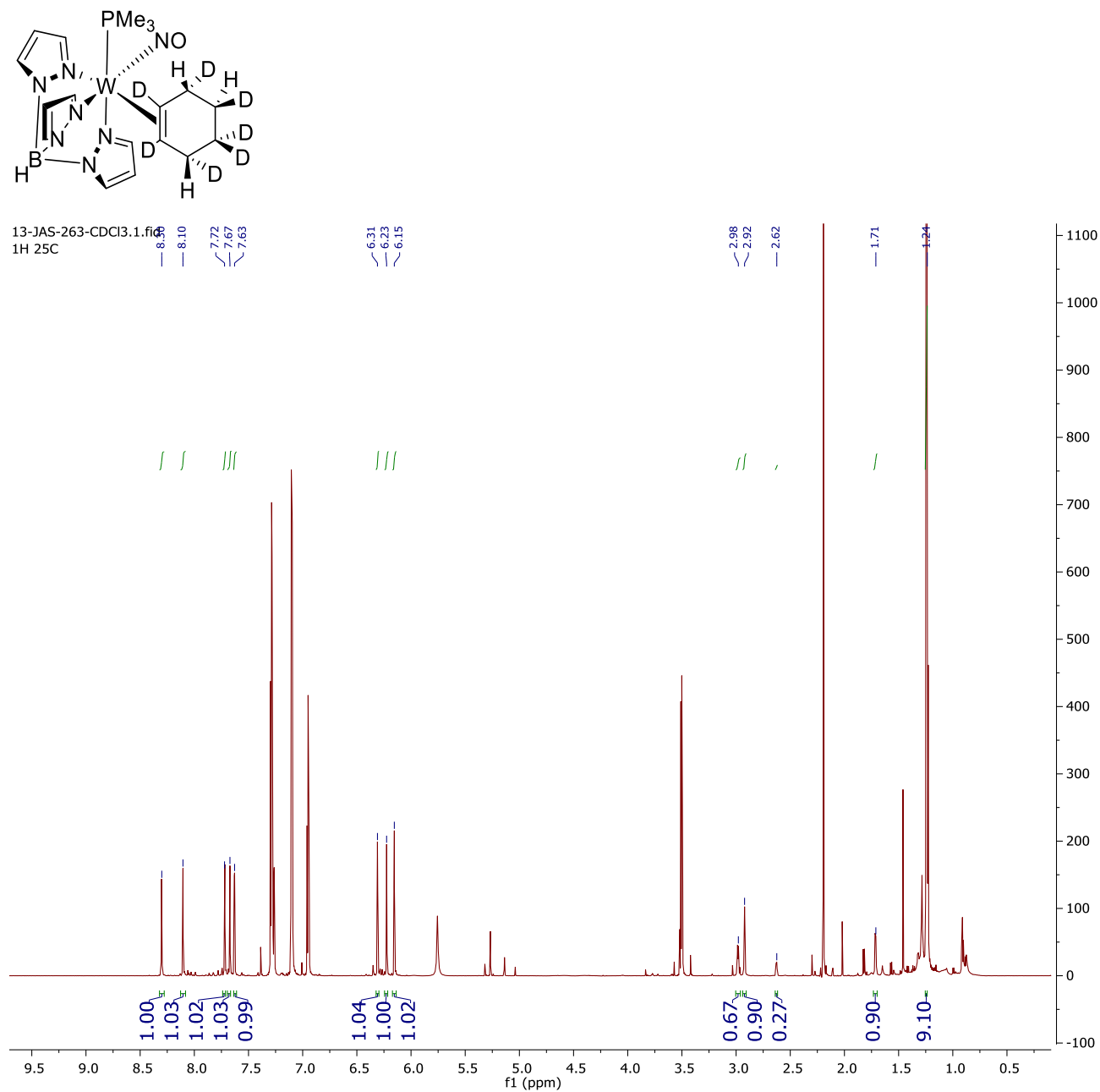
## D6-Isotopologues

Figure SF24. <sup>1</sup>H NMR Spectrum of Compound 37



## D7-Isotopologues

Figure SF25. <sup>1</sup>H NMR Spectrum of Compound 37



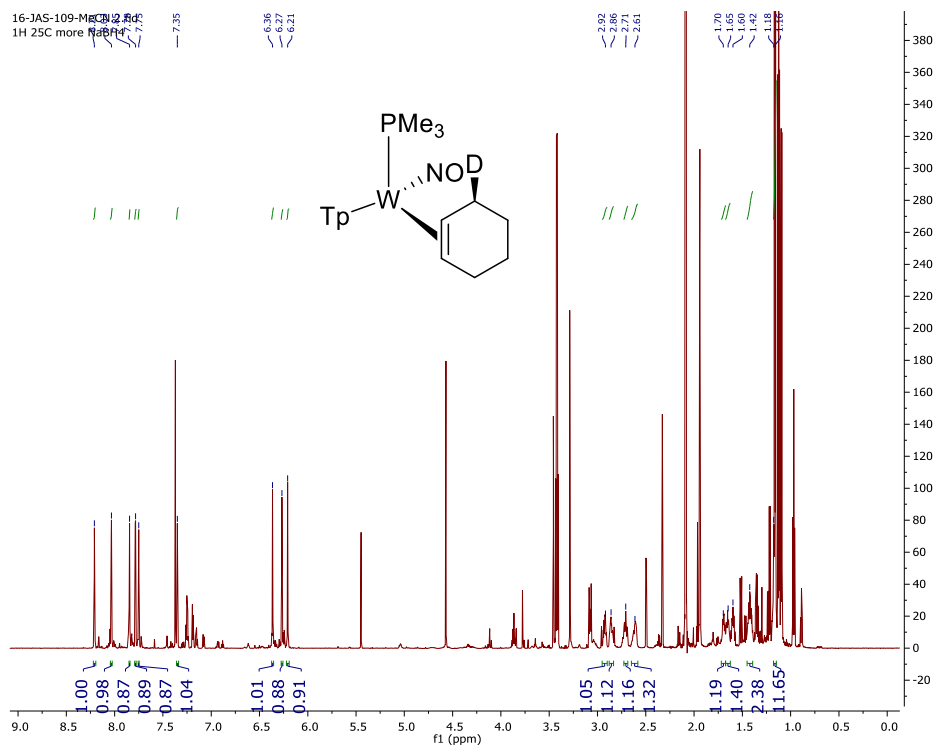
Note: Resonances from 7.00 to 7.30 are those of free diphenylammonium triflate salt. The resonances at 2.64 and 3.10 show the loss in stereofidelity at carbon position C6.

## D8-Isotopologues





41



50

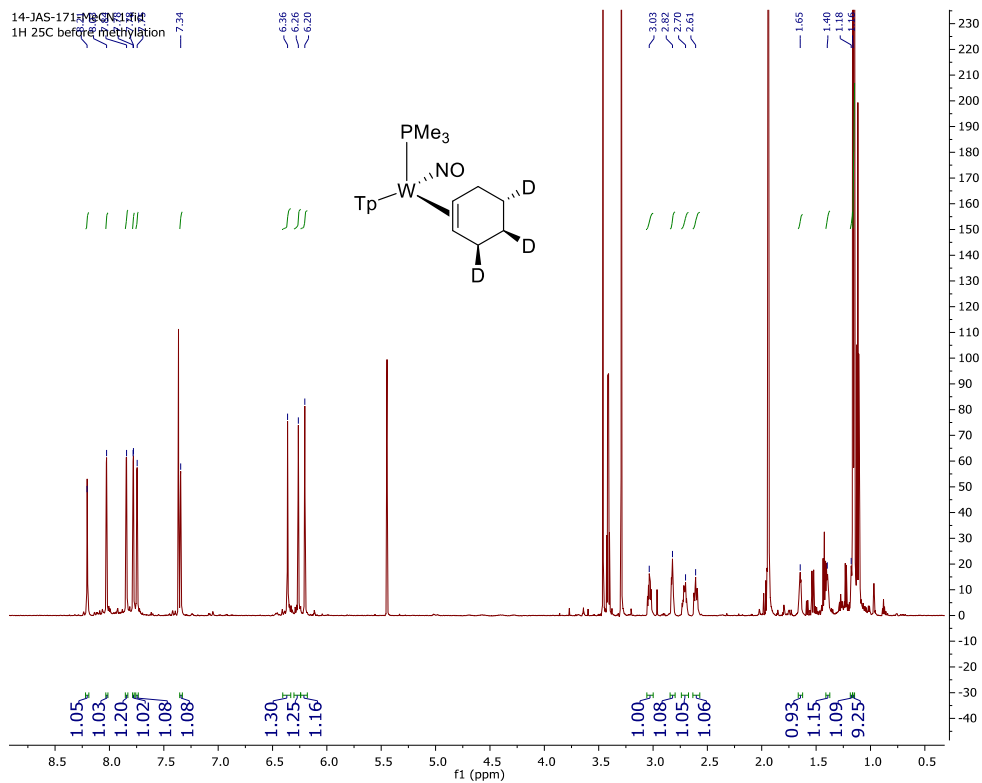
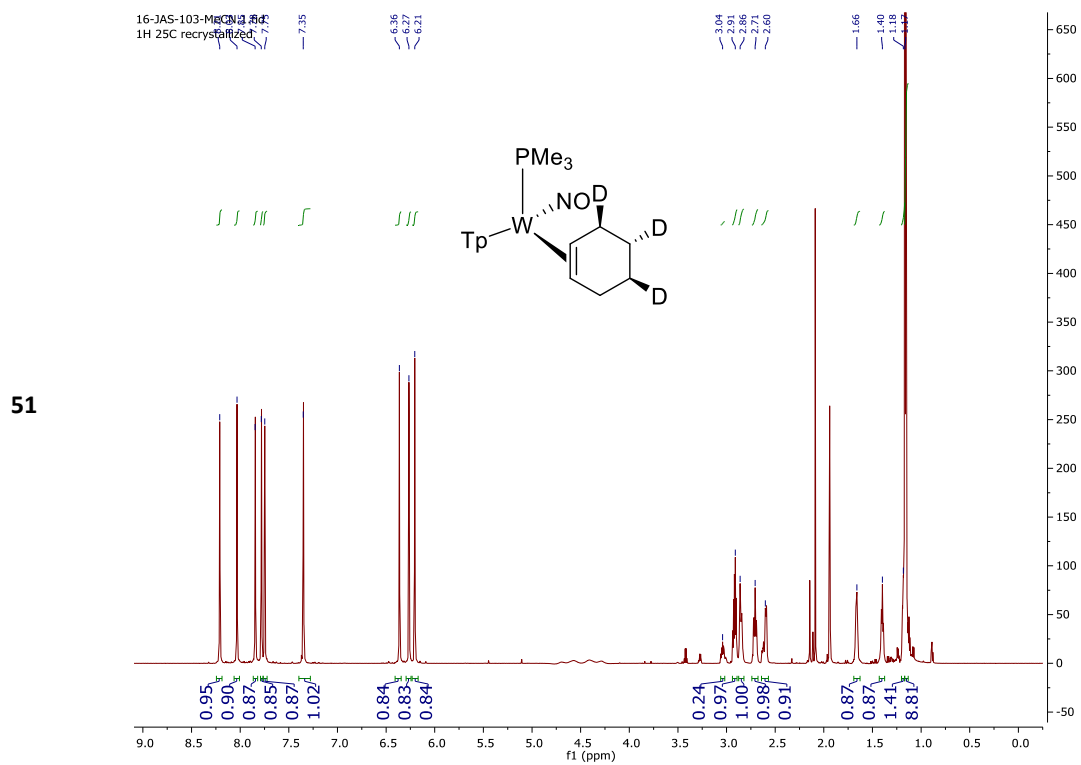
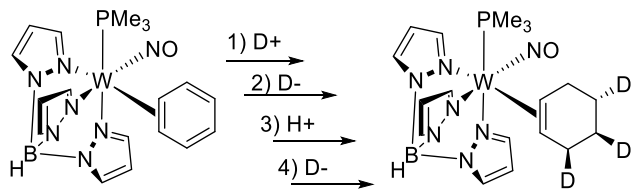




Figure SF29. <sup>1</sup>H NMR Spectrum of Compound 51



NMR Spectra for Representative Intermediates in converting 1 to 11 to 12 to 13 to 50.



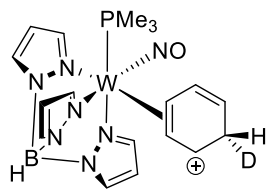
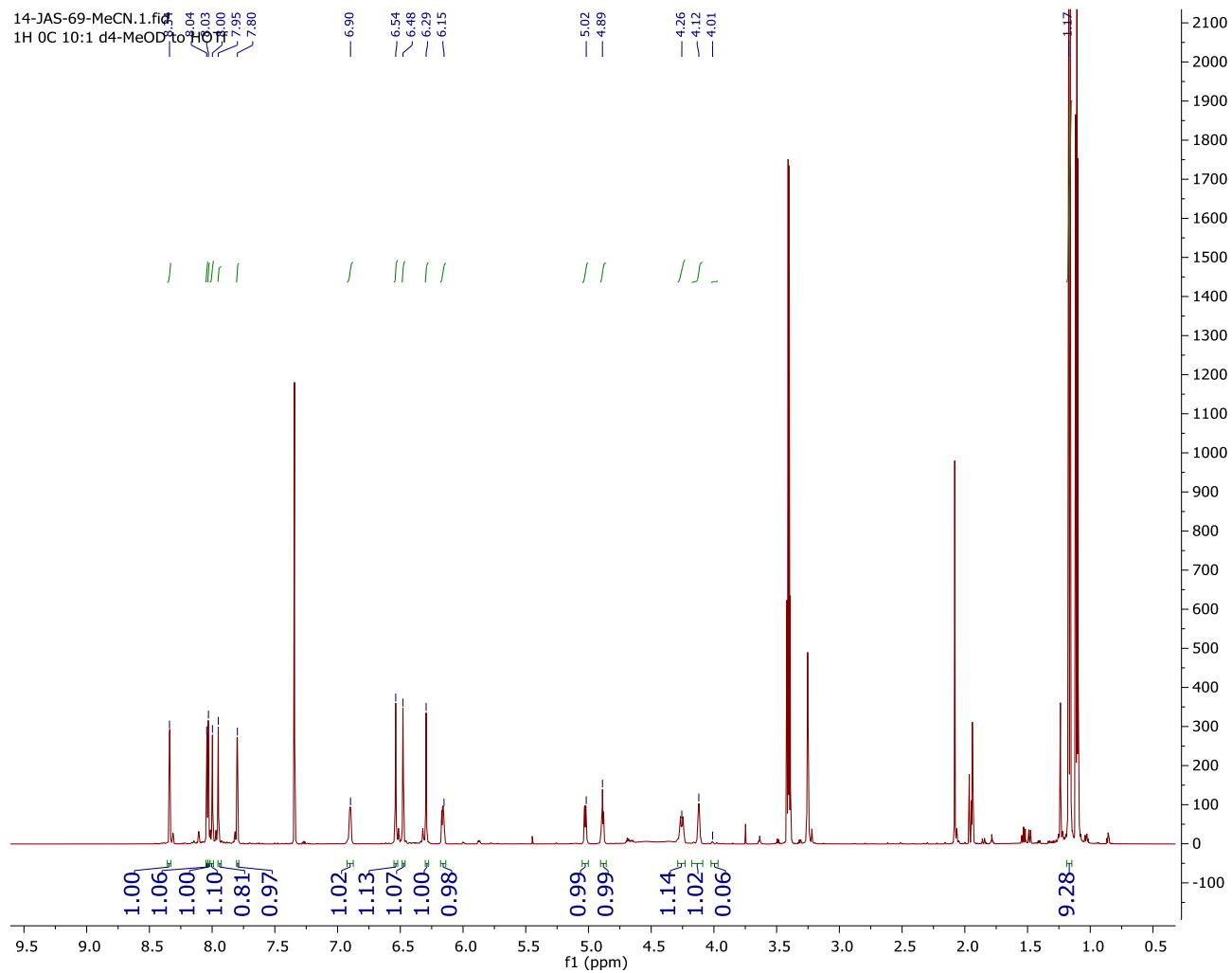


Figure SF30. <sup>1</sup>H NMR Spectrum of (11)



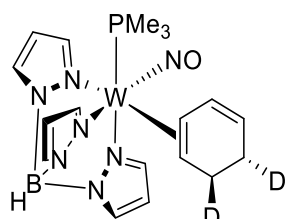
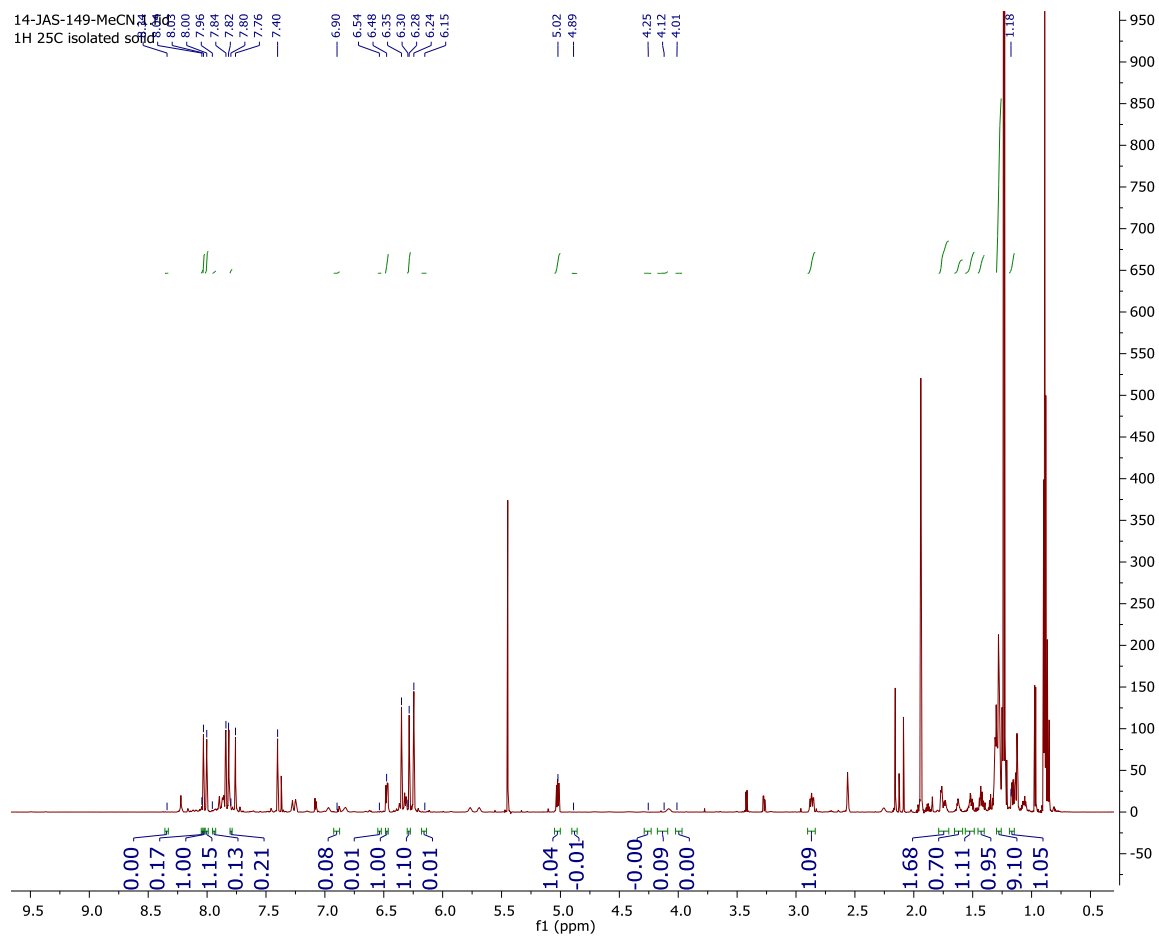


Figure SF31. <sup>1</sup>H NMR Spectrum of (12)



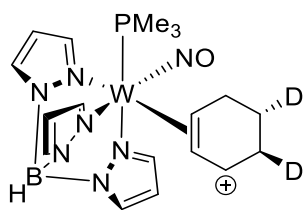
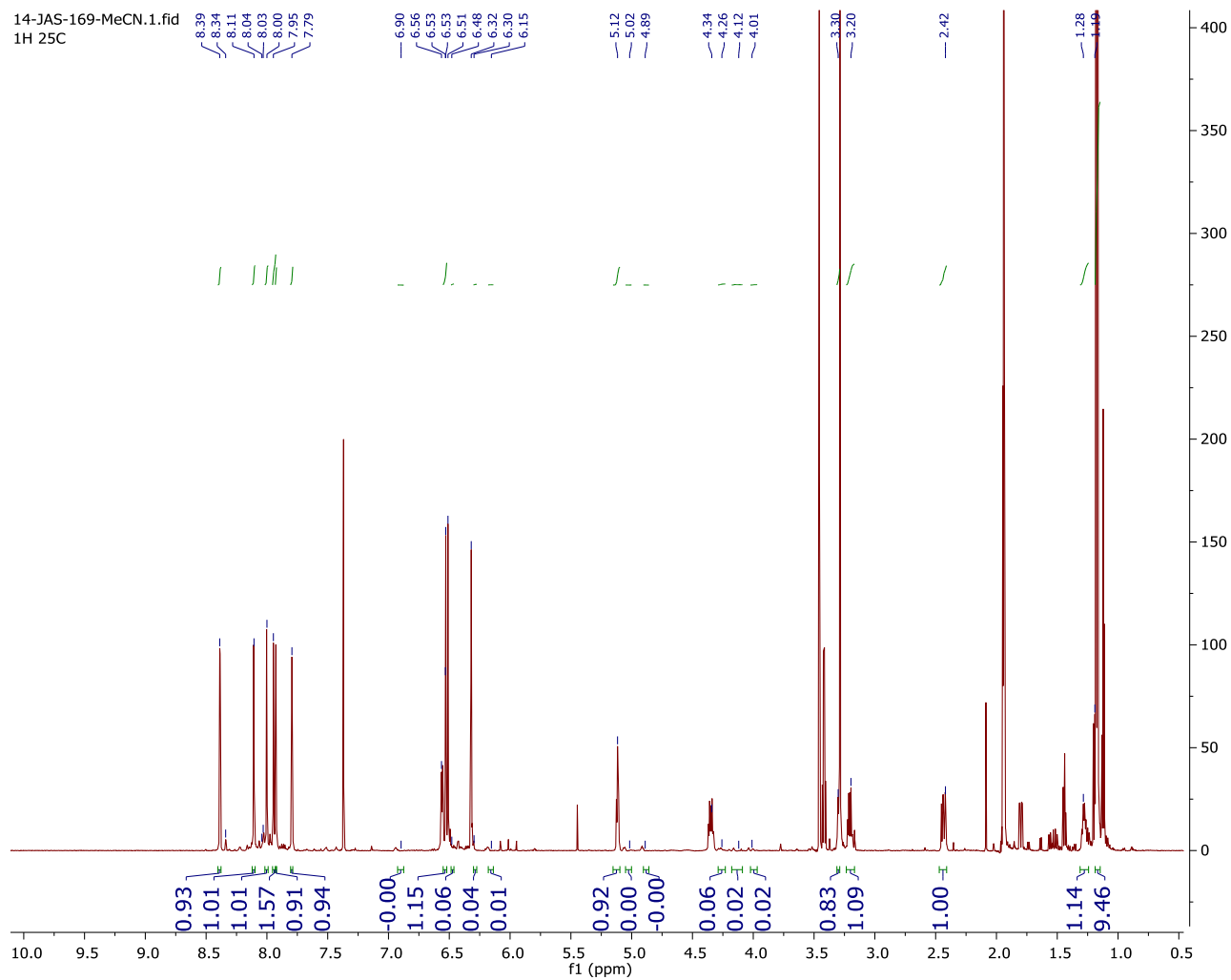


Figure SF32.  $^1\text{H}$  NMR Spectrum of (13)



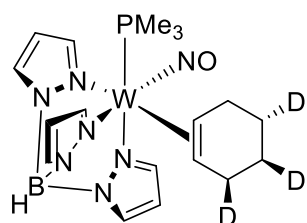
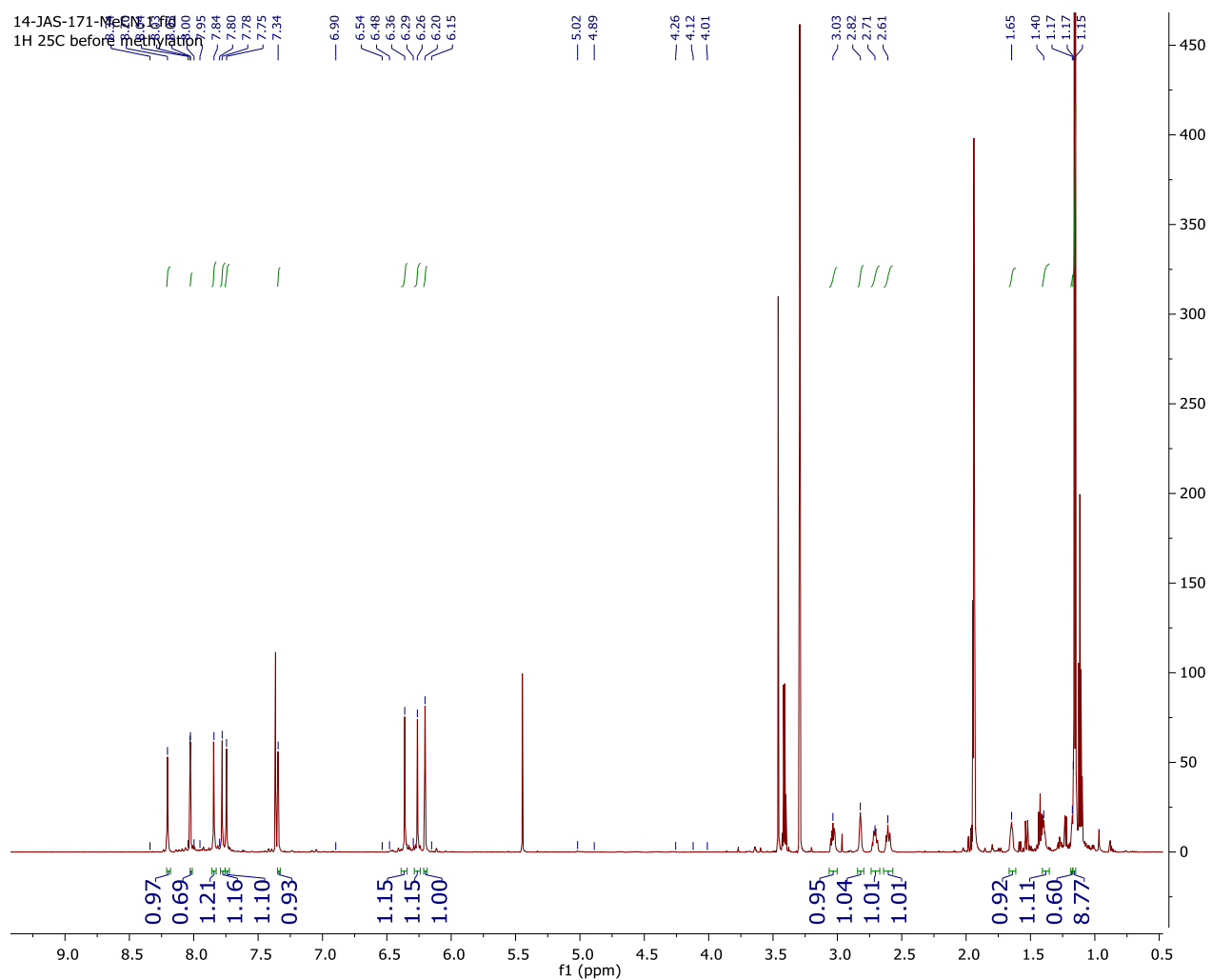


Figure SF33. <sup>1</sup>H NMR Spectrum of (50)



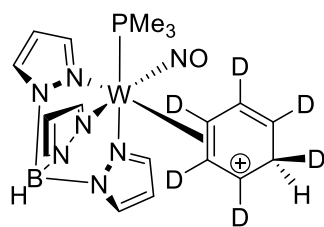


Figure SF34. <sup>1</sup>H NMR Spectrum of 18

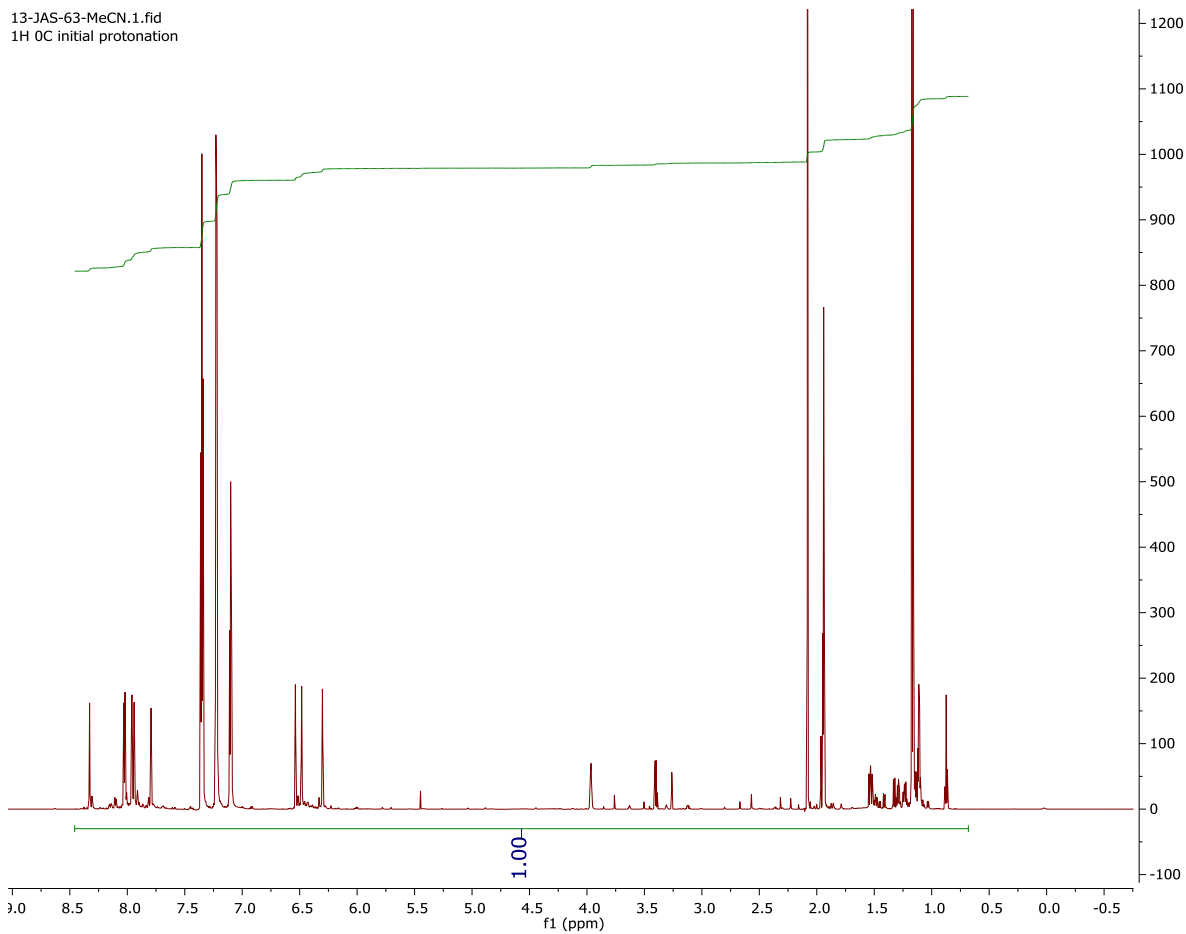
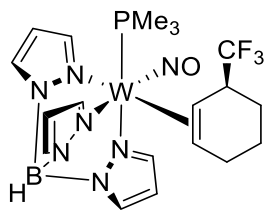
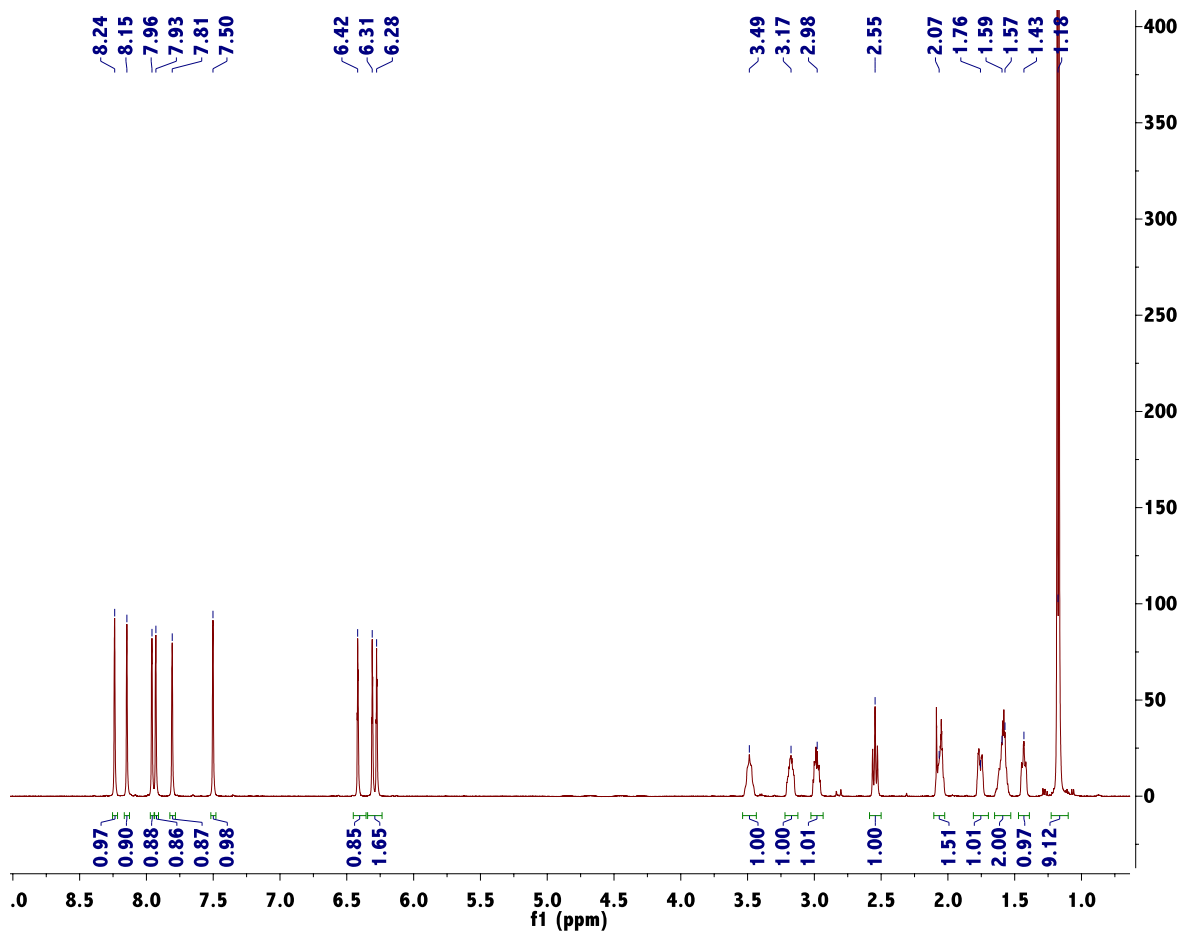


Figure SF35. <sup>1</sup>H NMR Spectrum of Compound 47



<sup>1</sup>H NMR Spectrum



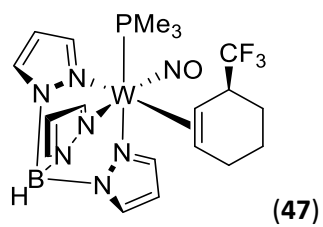
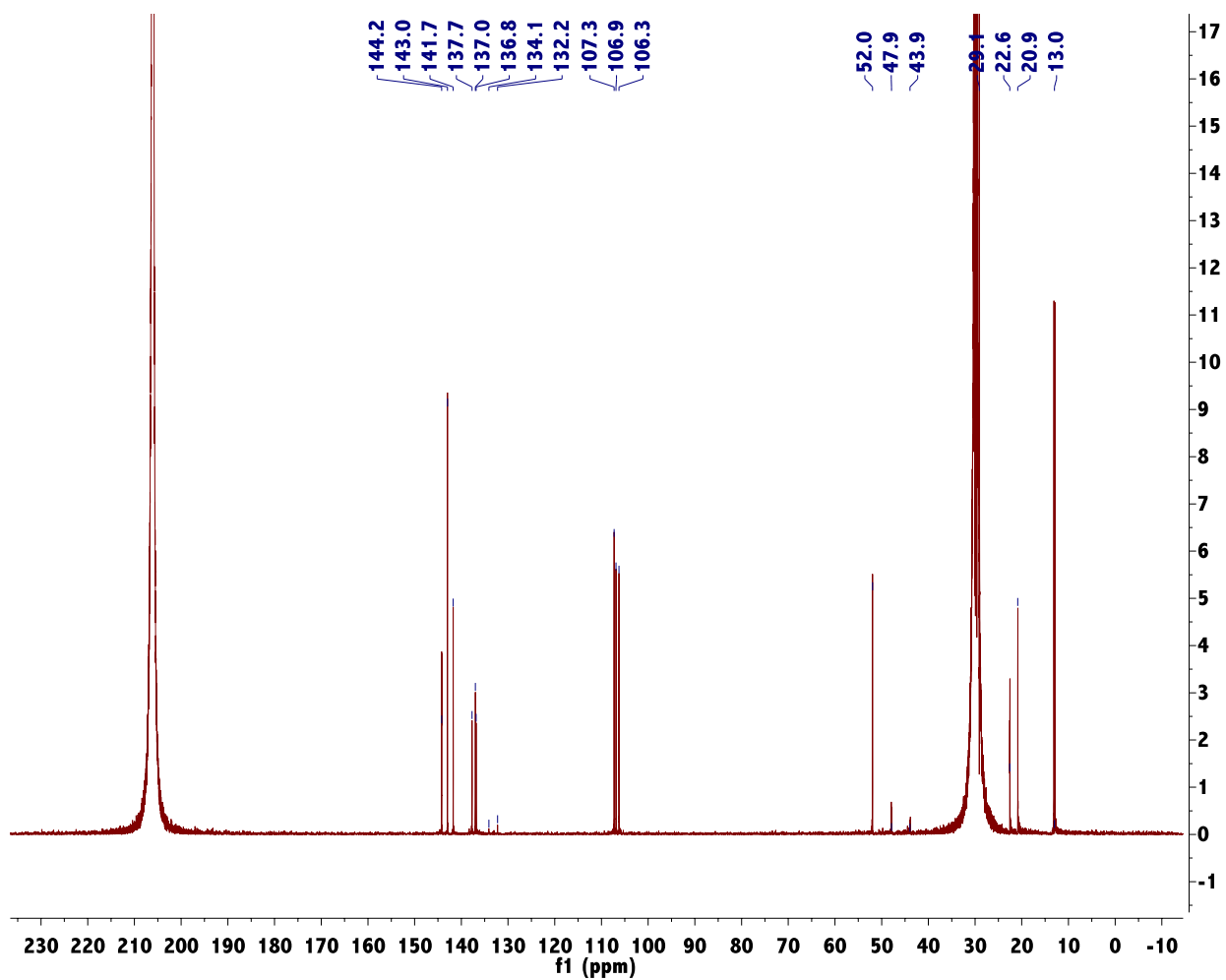


Figure SF36.  $^{13}\text{C}$  { $^1\text{H}$ } NMR Spectrum





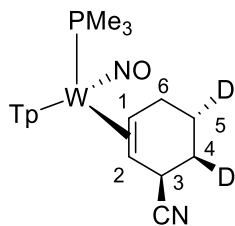
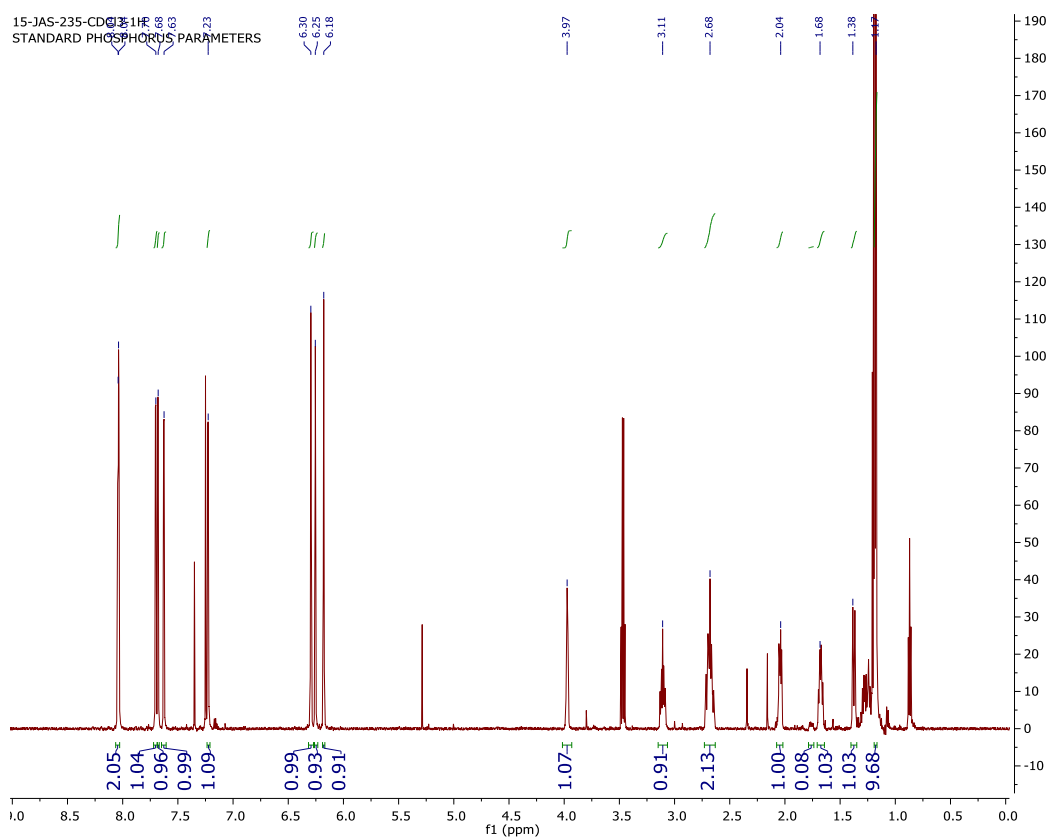


Figure SF37.  $^1\text{H}$  NMR Data of Compound **58**





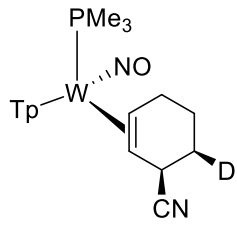
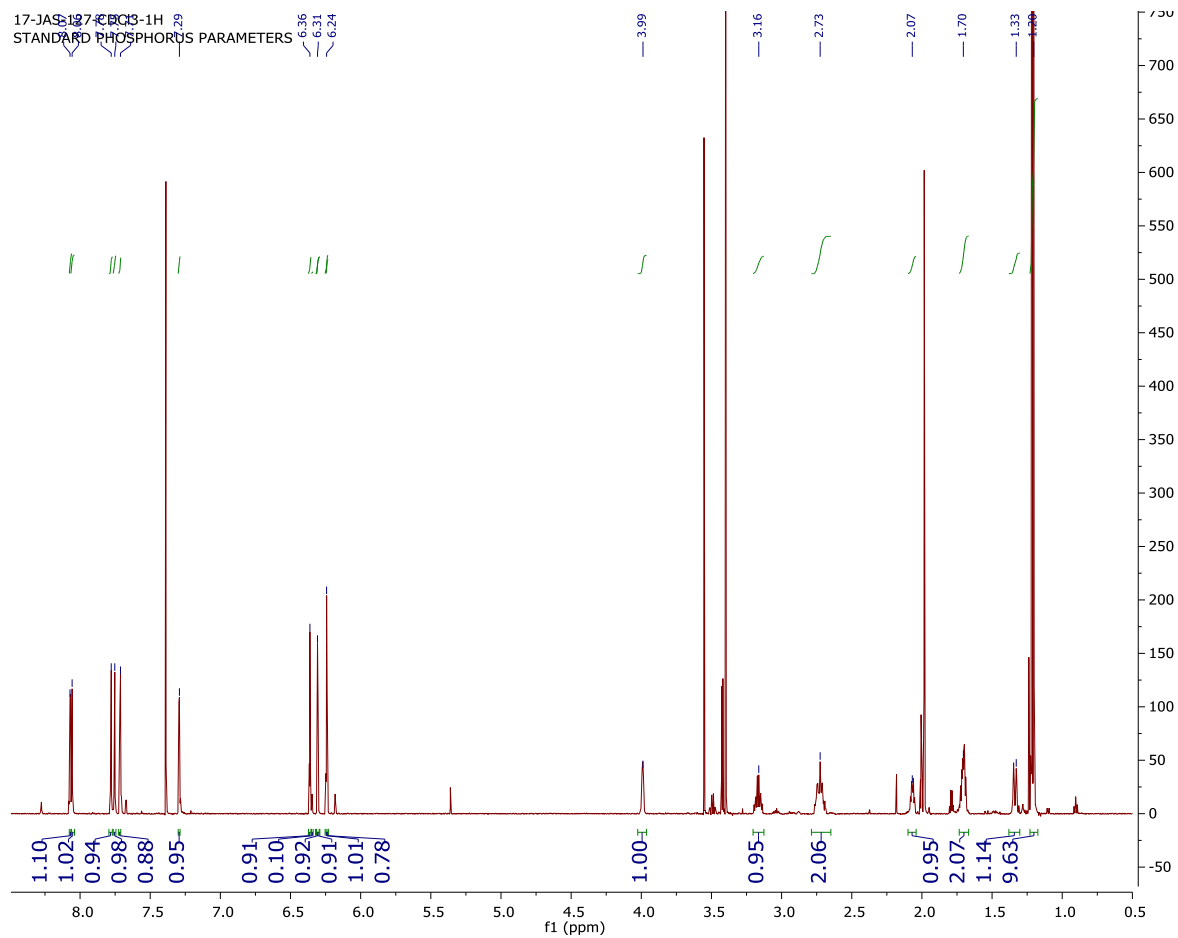


Figure SF39.  $^1\text{H}$  NMR Data of Compound 59



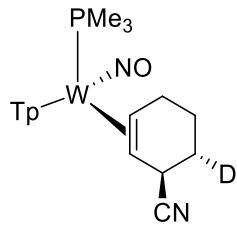
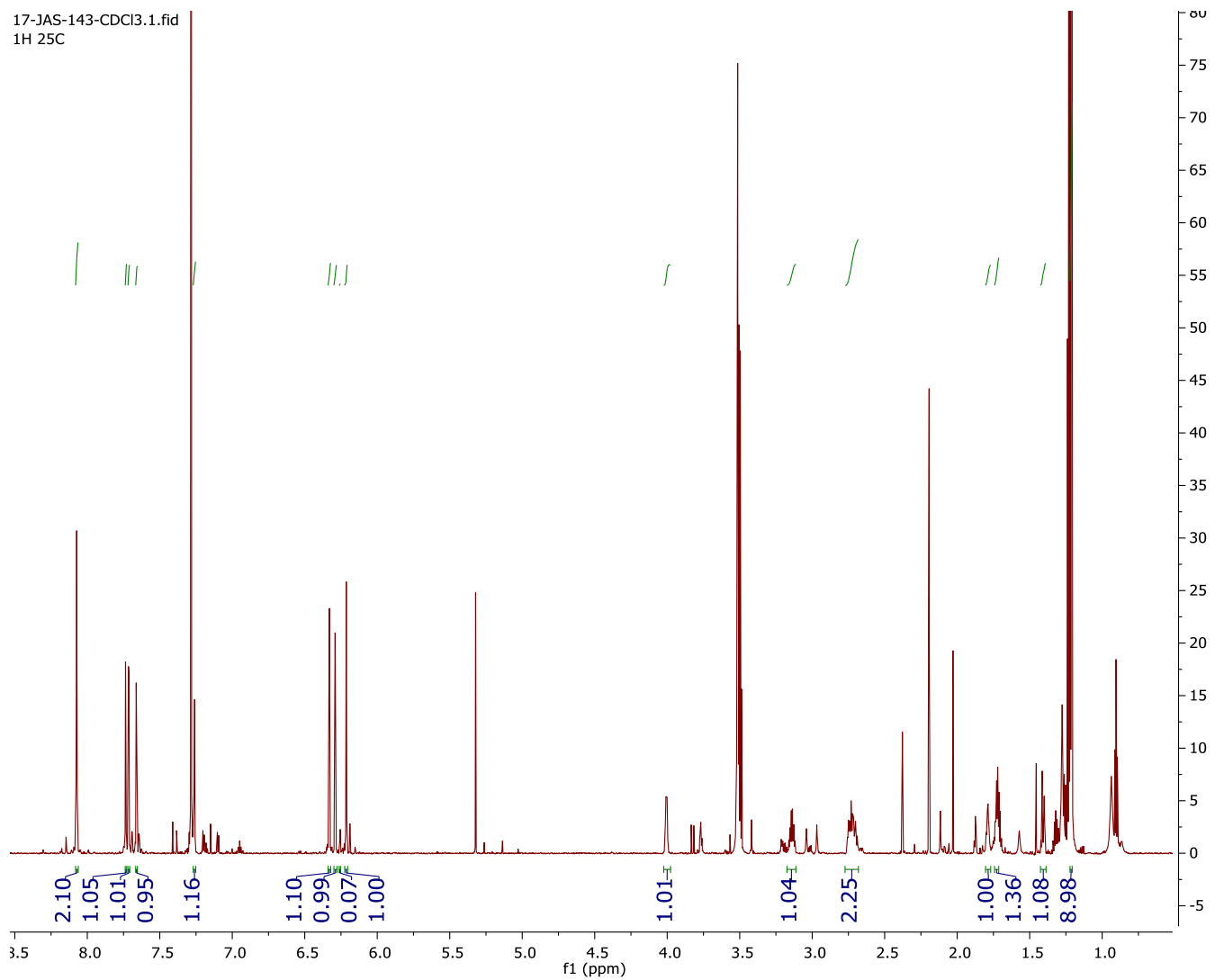


Figure SF40. <sup>1</sup>H NMR Data of Compound 62



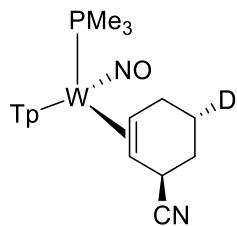
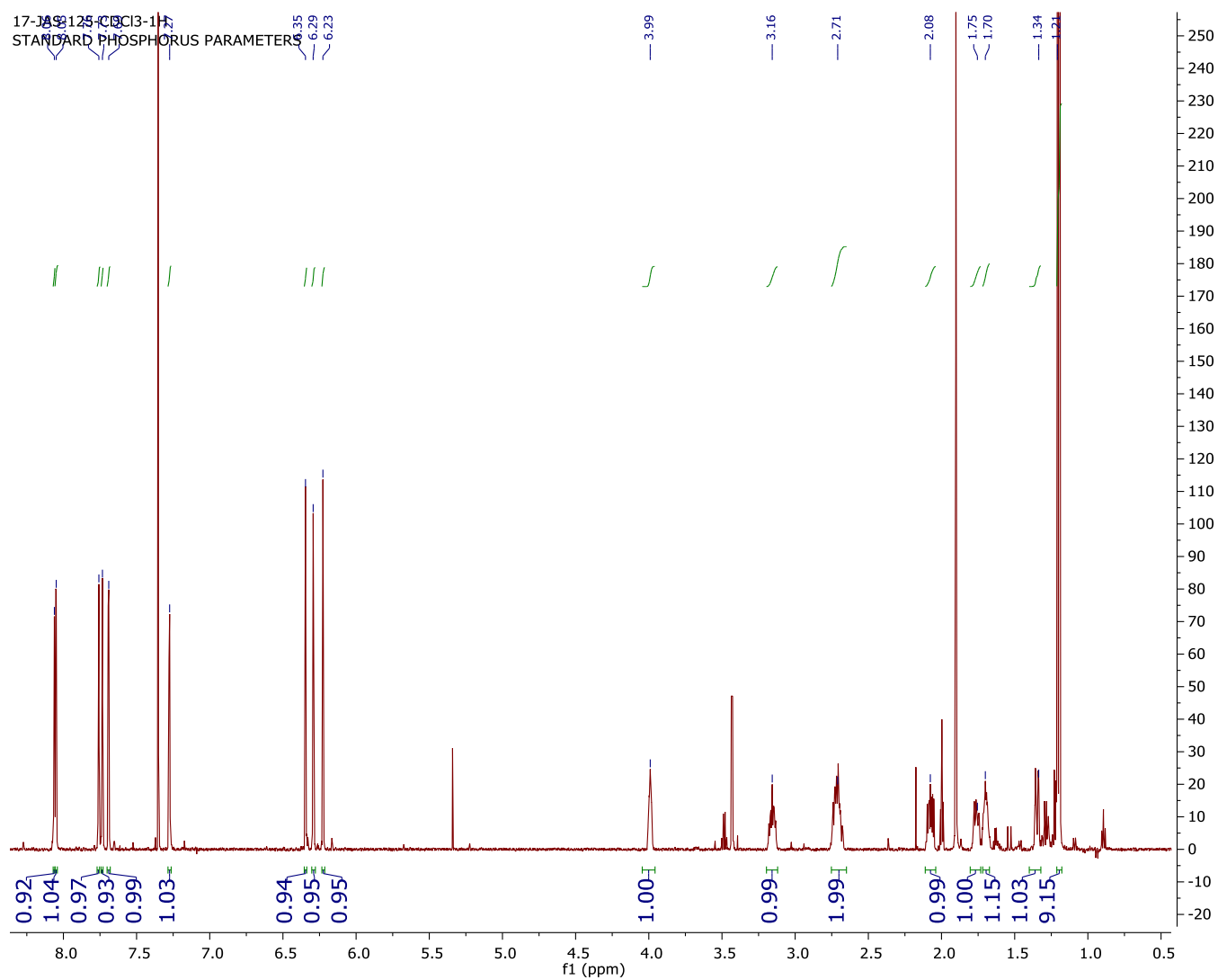


Figure SF41. <sup>1</sup>H NMR Data of Compound 60



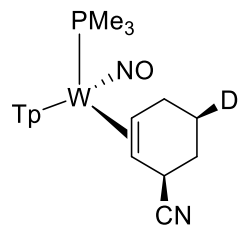
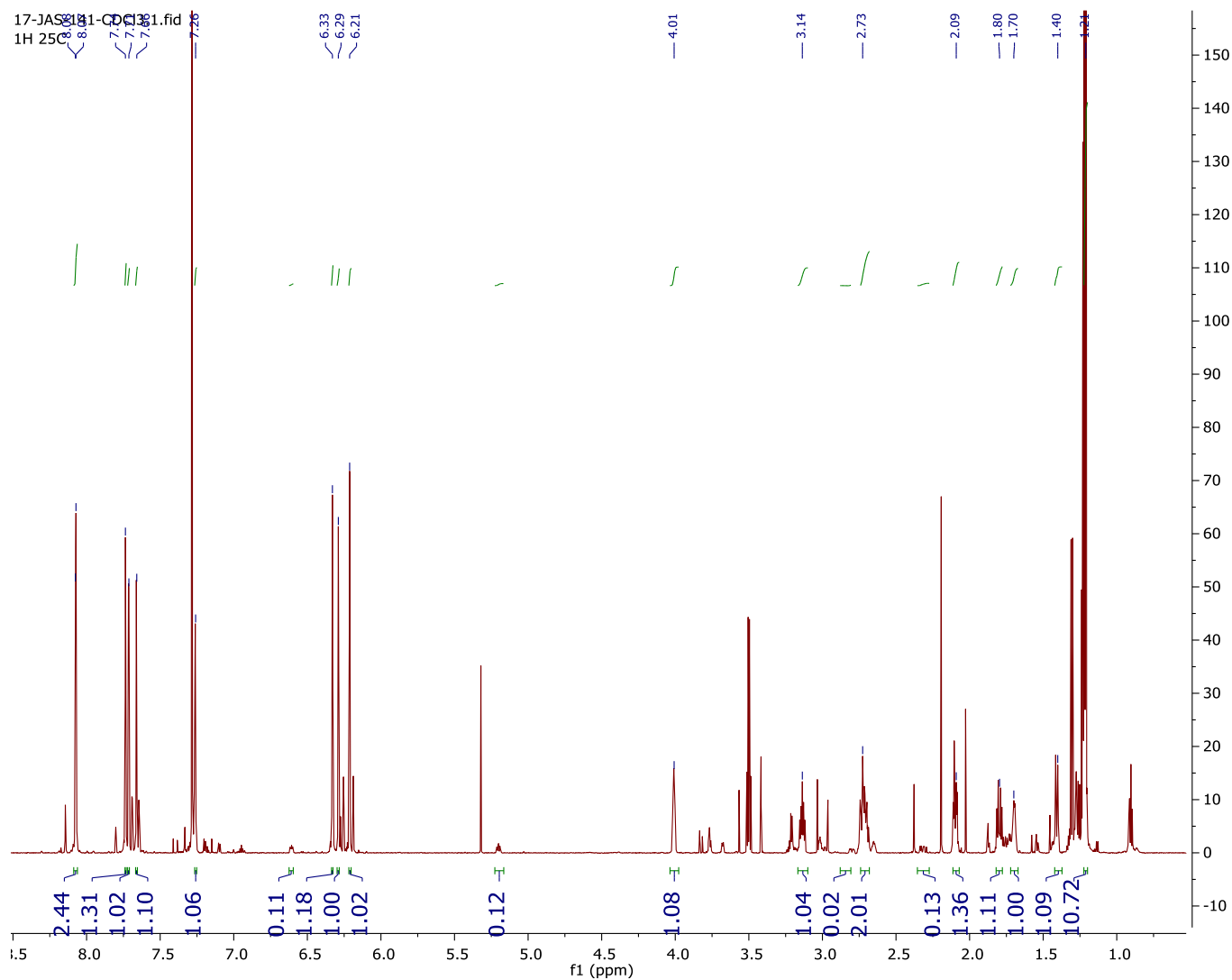
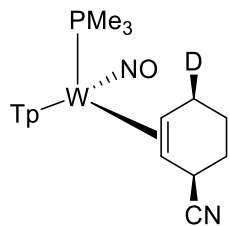


Figure SF42. <sup>1</sup>H NMR Data of Compound 63





**Figure SF43.** <sup>1</sup>H NMR Data of Compound 61

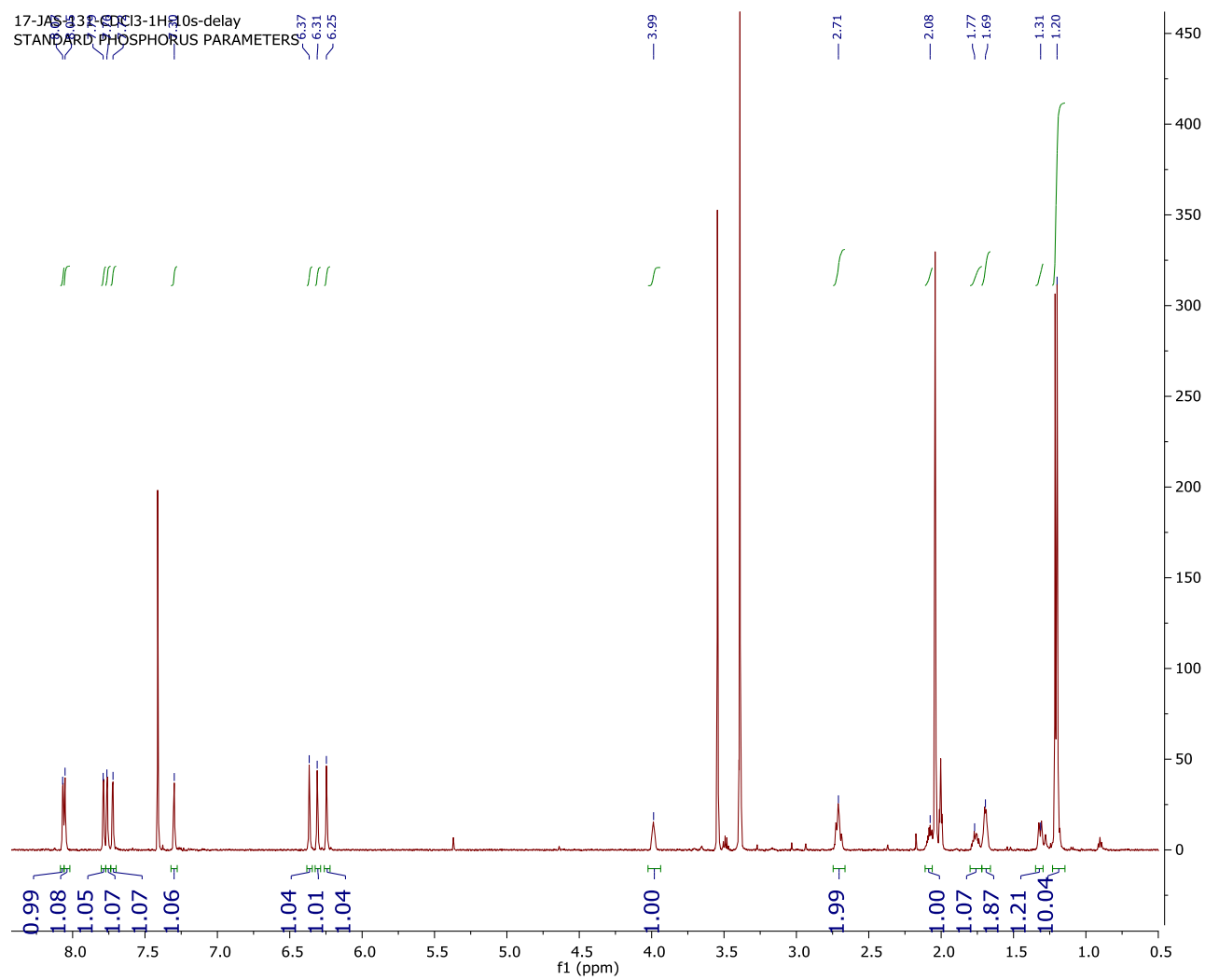


Figure SF44. Comparison of 1H NMR Spectra for 48 and 58

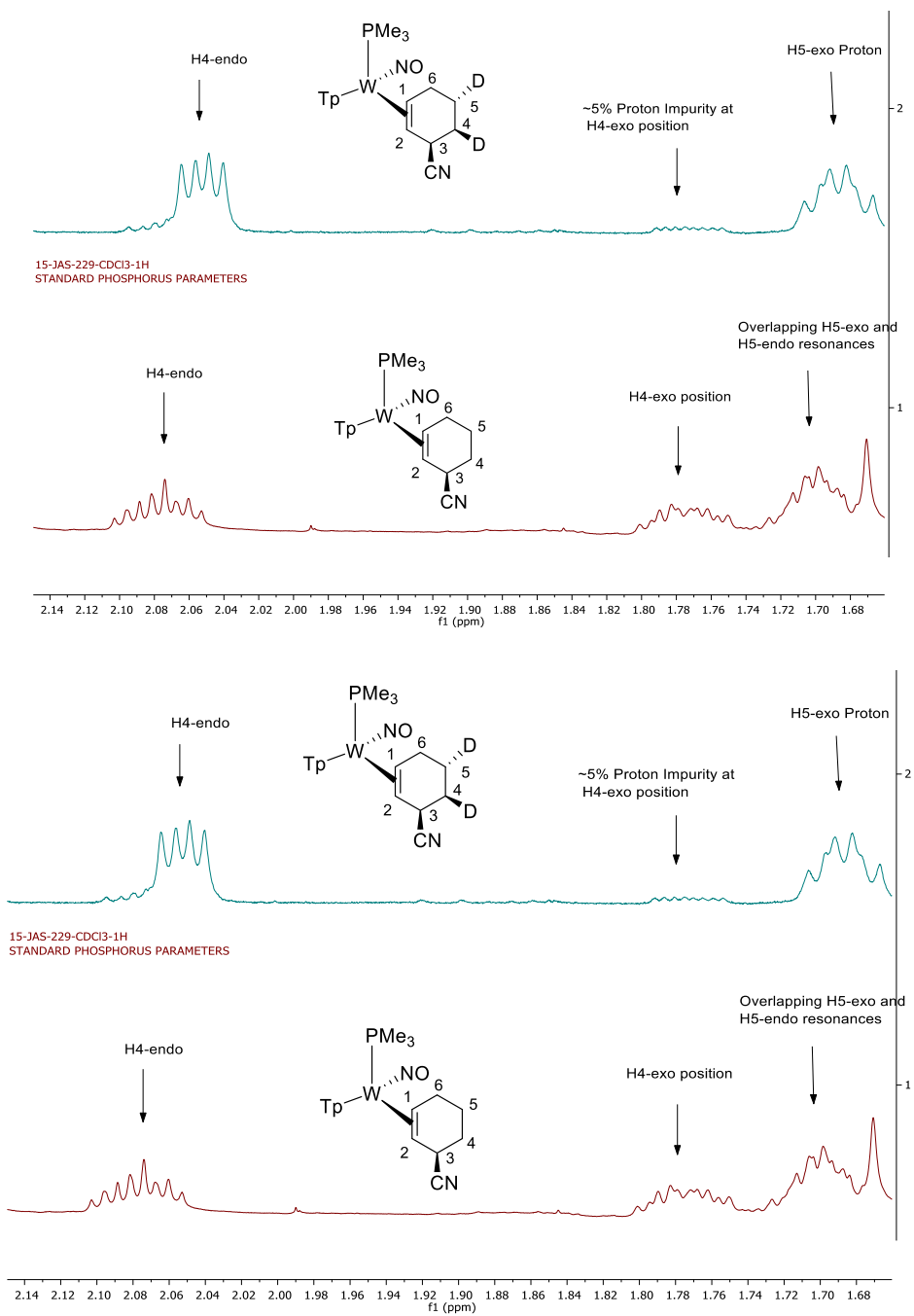
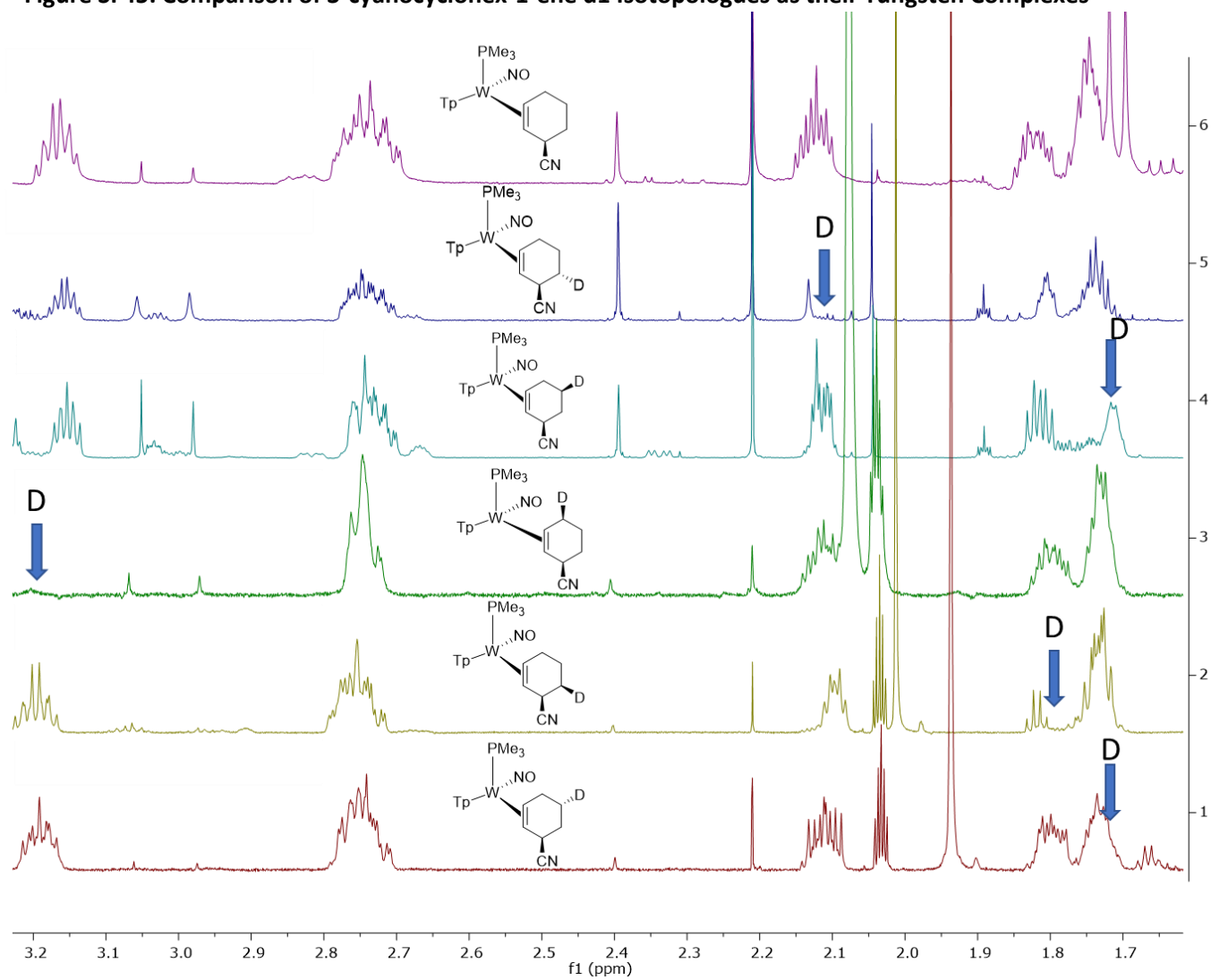




Figure SF45. Comparison of 3-cyanocyclohex-1-ene d1 Isotopologues as their Tungsten Complexes



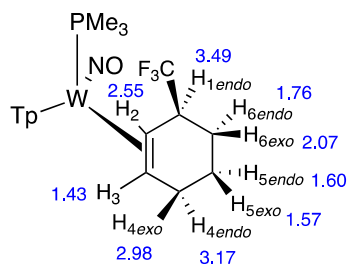
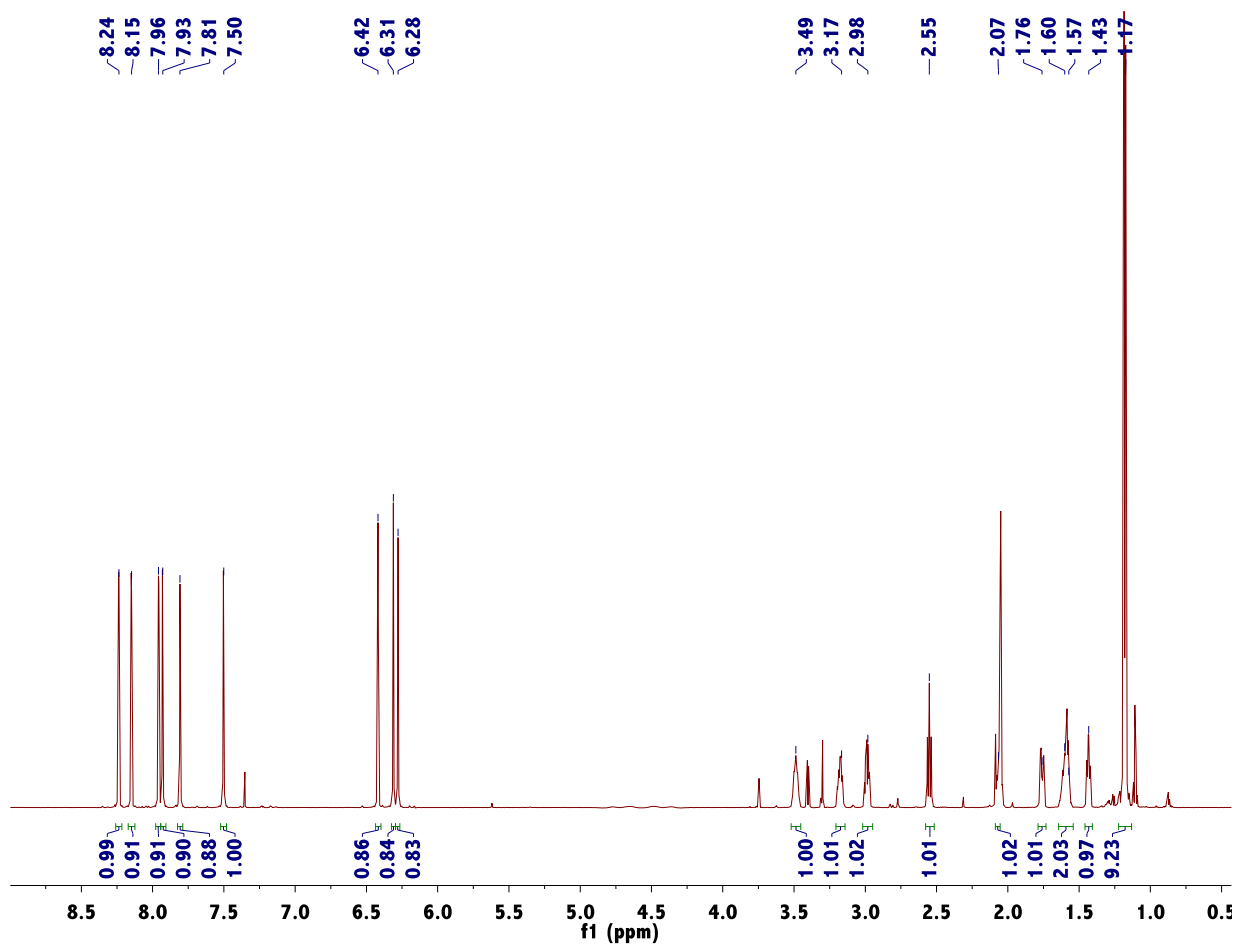


Figure SF46. Compound 47  $^1\text{H}$  NMR



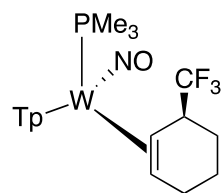
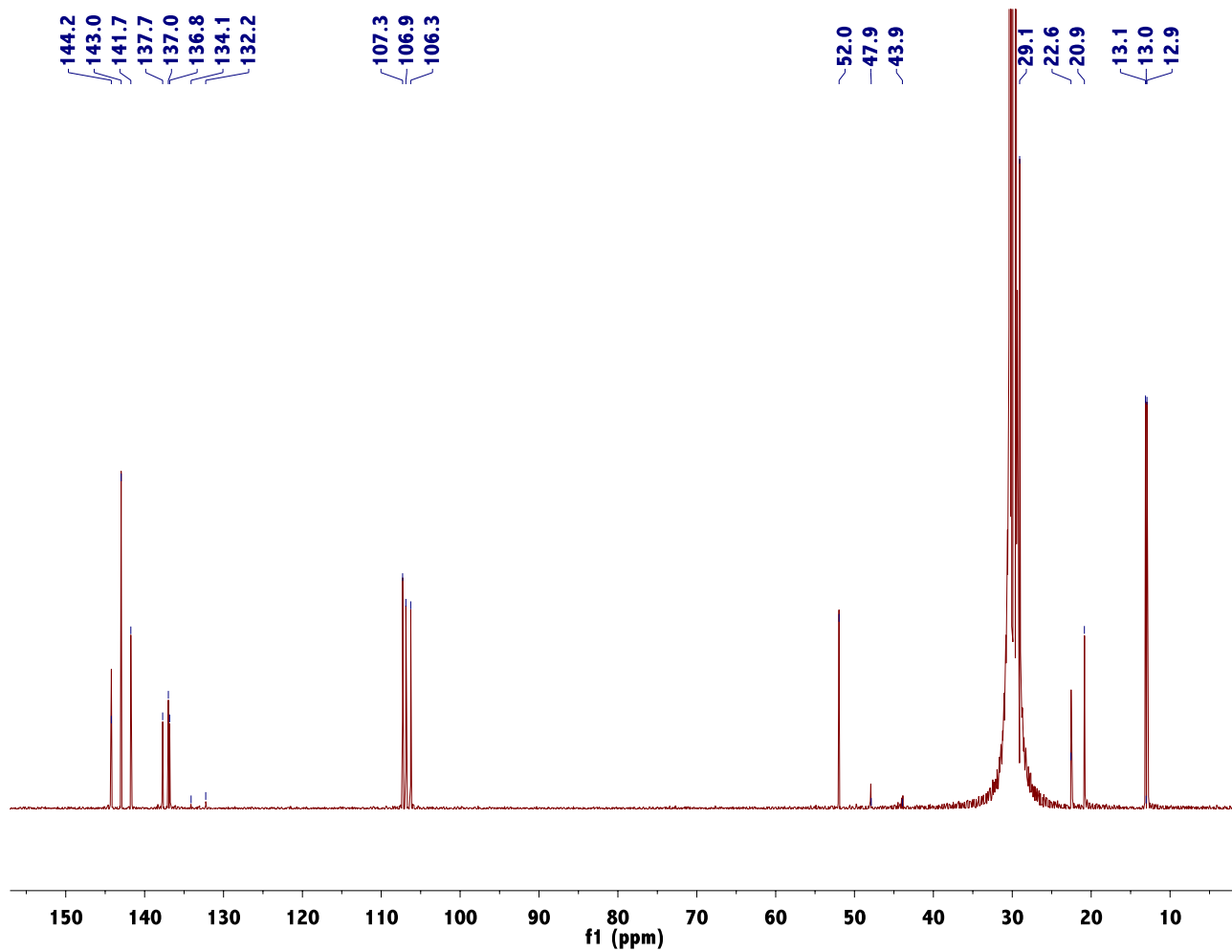


Figure SF47. Compound 47 <sup>13</sup>C {1H}



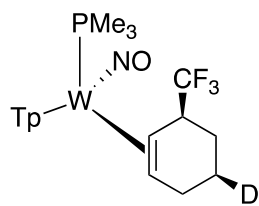
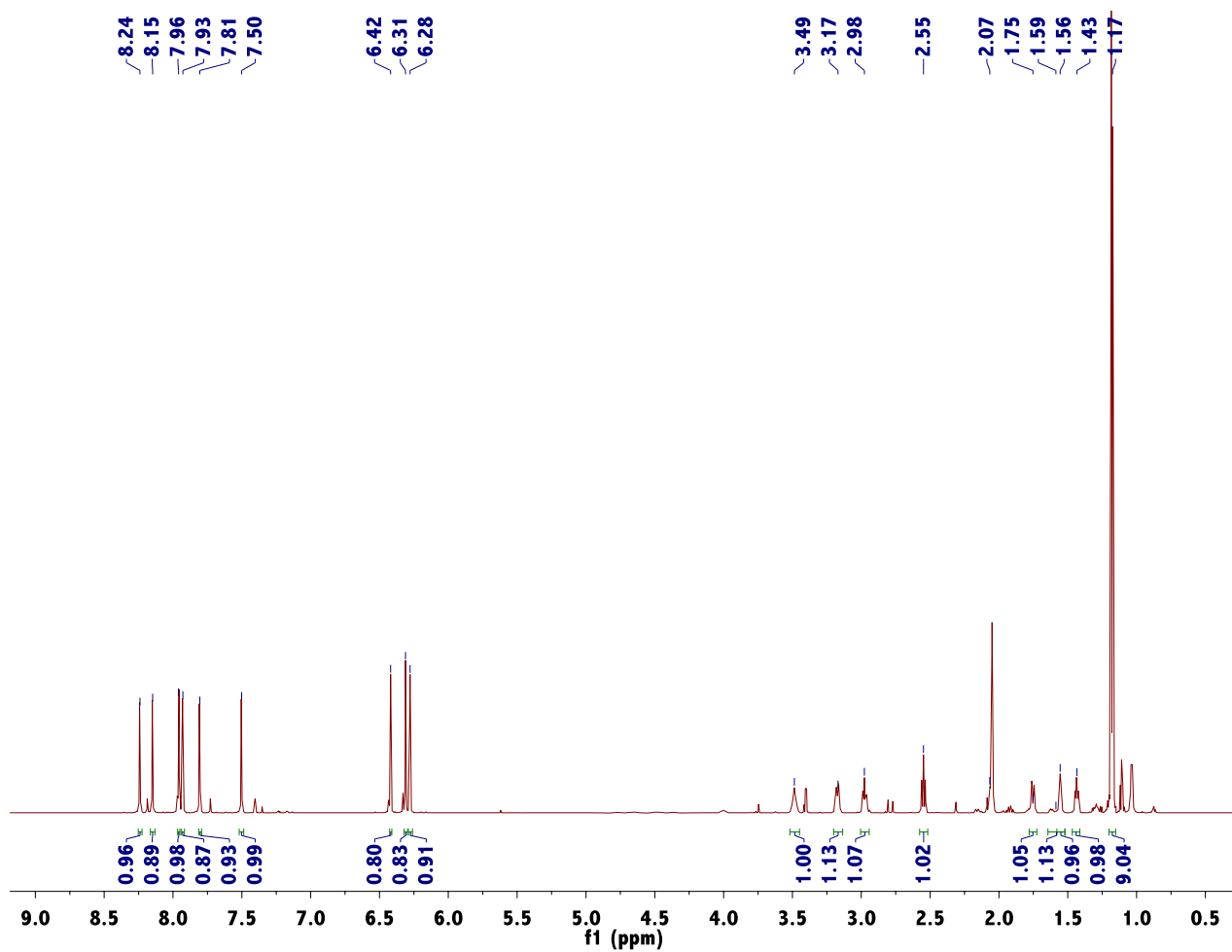


Figure SF48. Compound 53  $^1\text{H}$  NMR



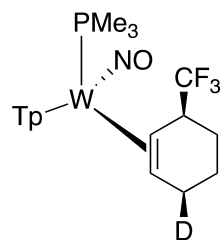


Figure SF49. Compound 52  $^1\text{H}$  NMR

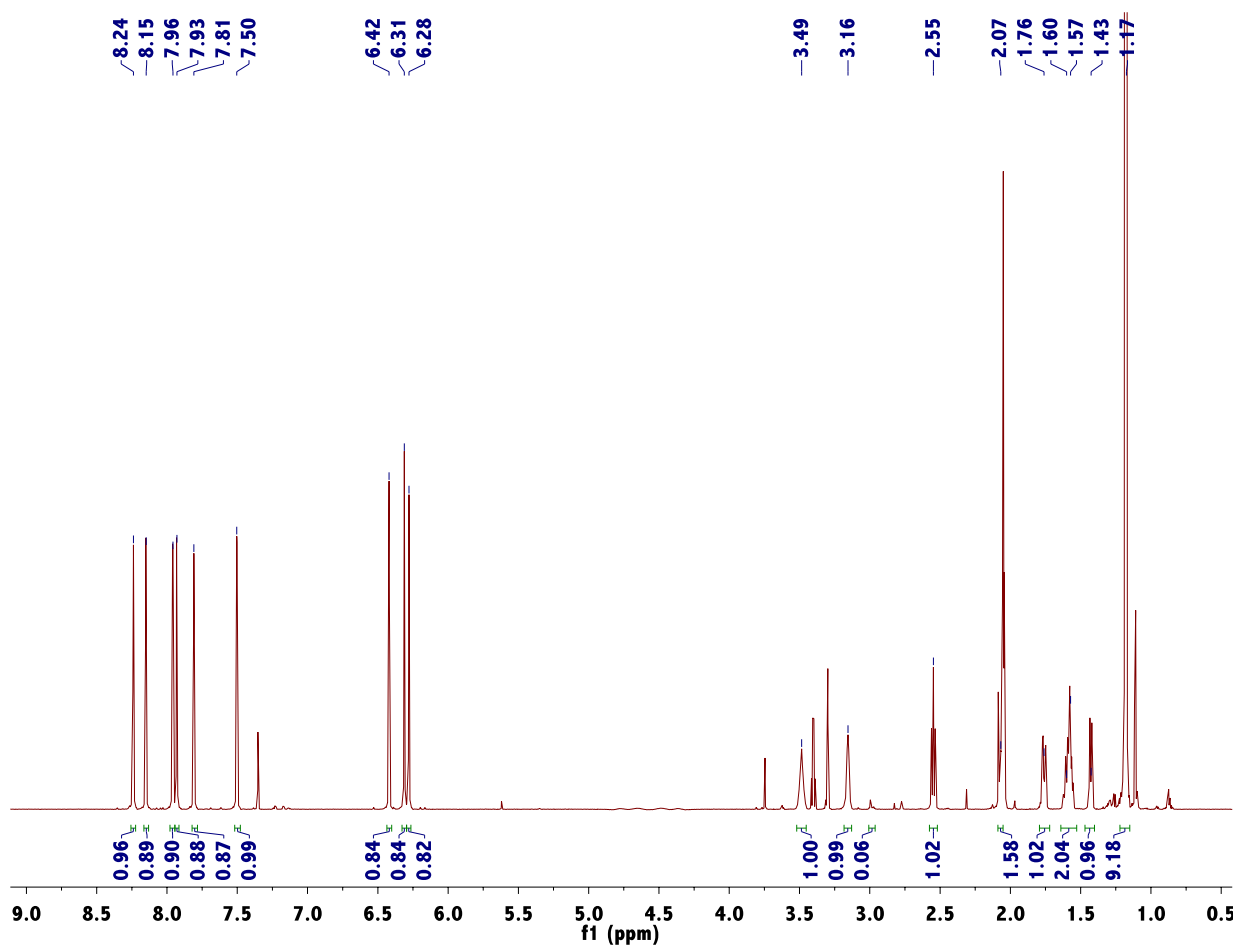
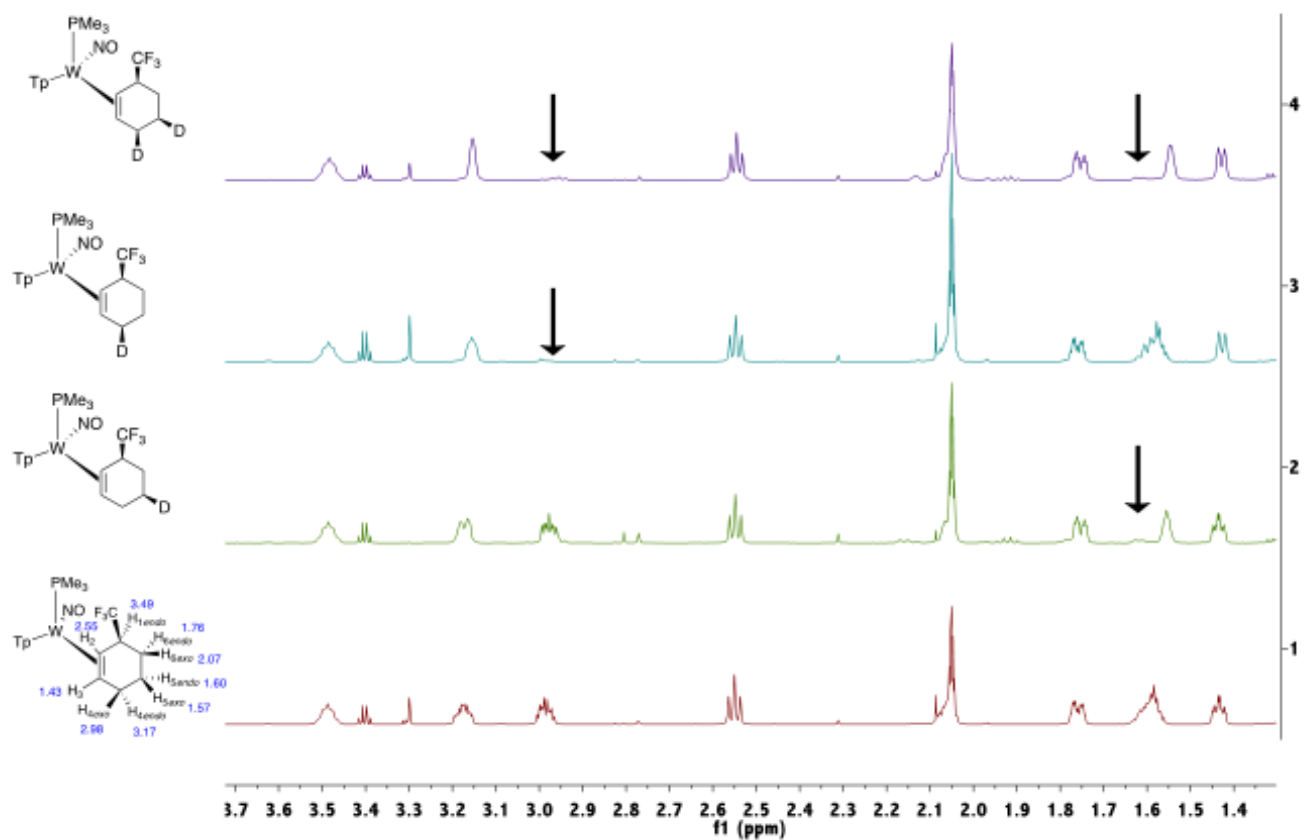




Figure SF51. Comparison of *exo*-3-(trifluoromethyl)cyclohexene isotopologues as their tungsten complexes (47, 52-54)



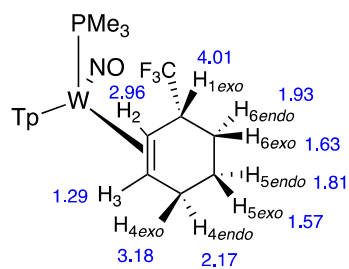
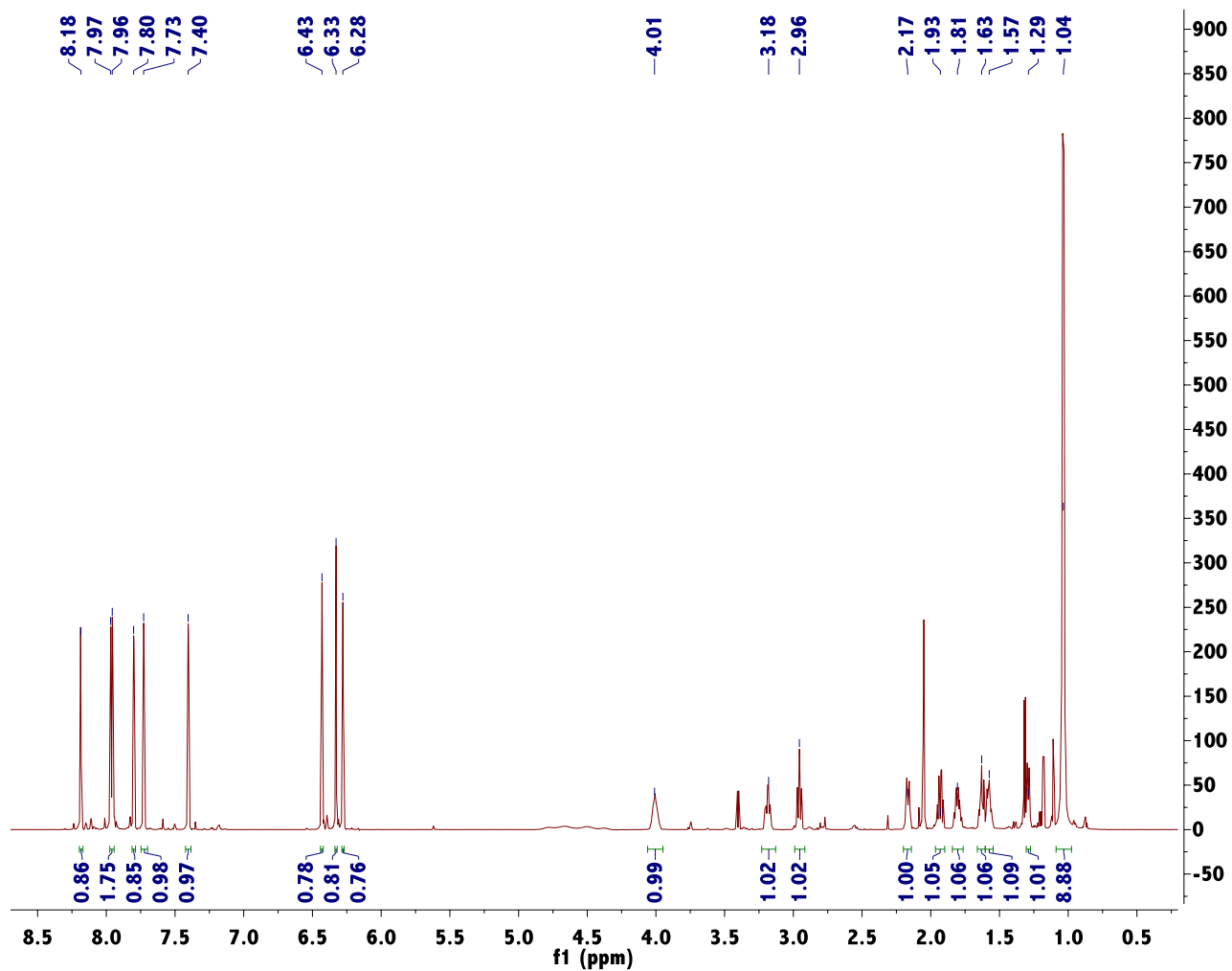


Figure SF52. Compound 55  $^1\text{H}$  NMR





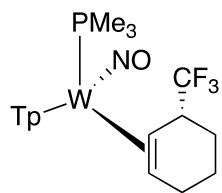
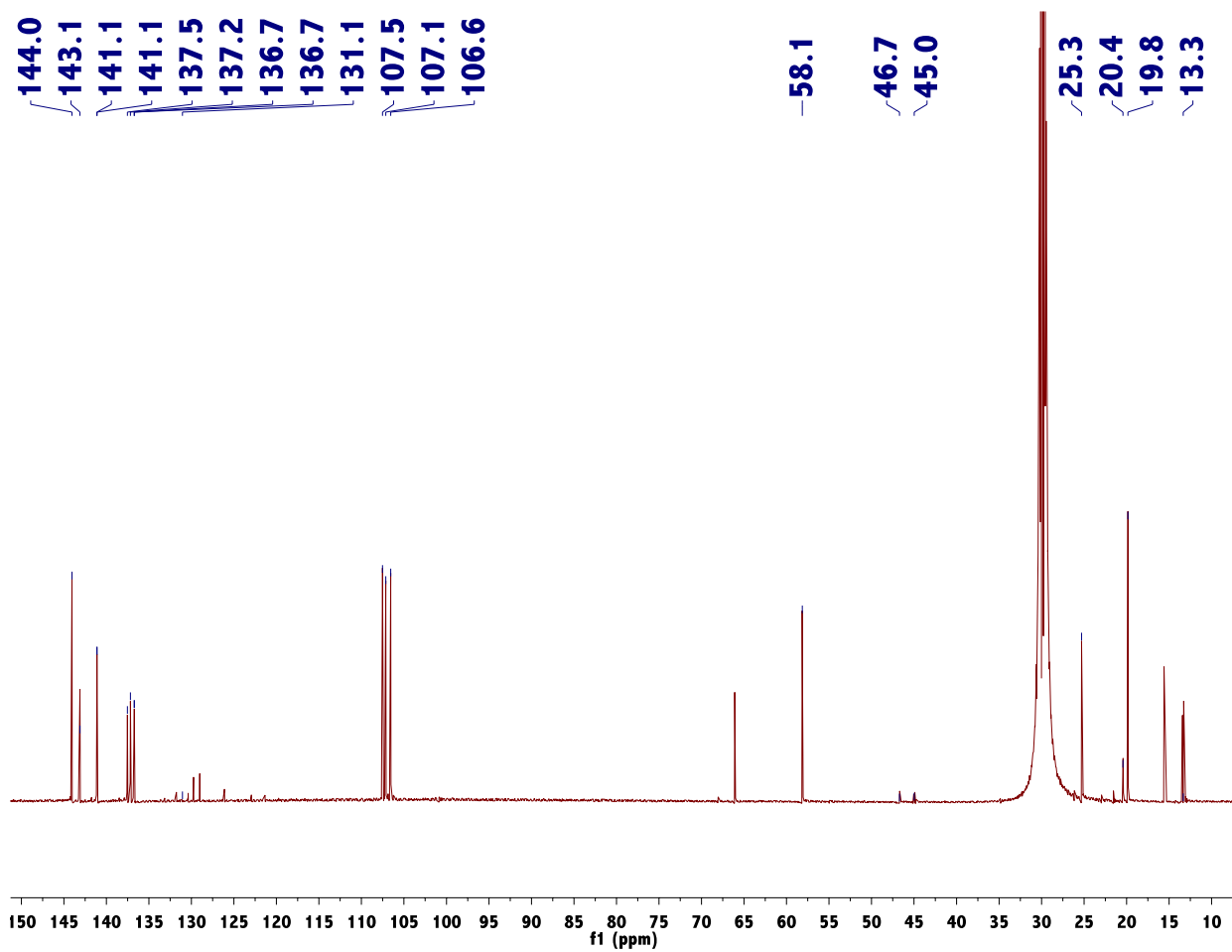


Figure SF53. Compound 55  $^{13}\text{C}$  { $^1\text{H}$ } NMR



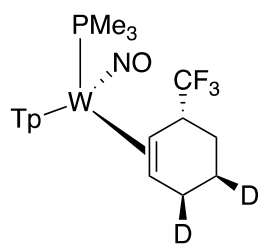
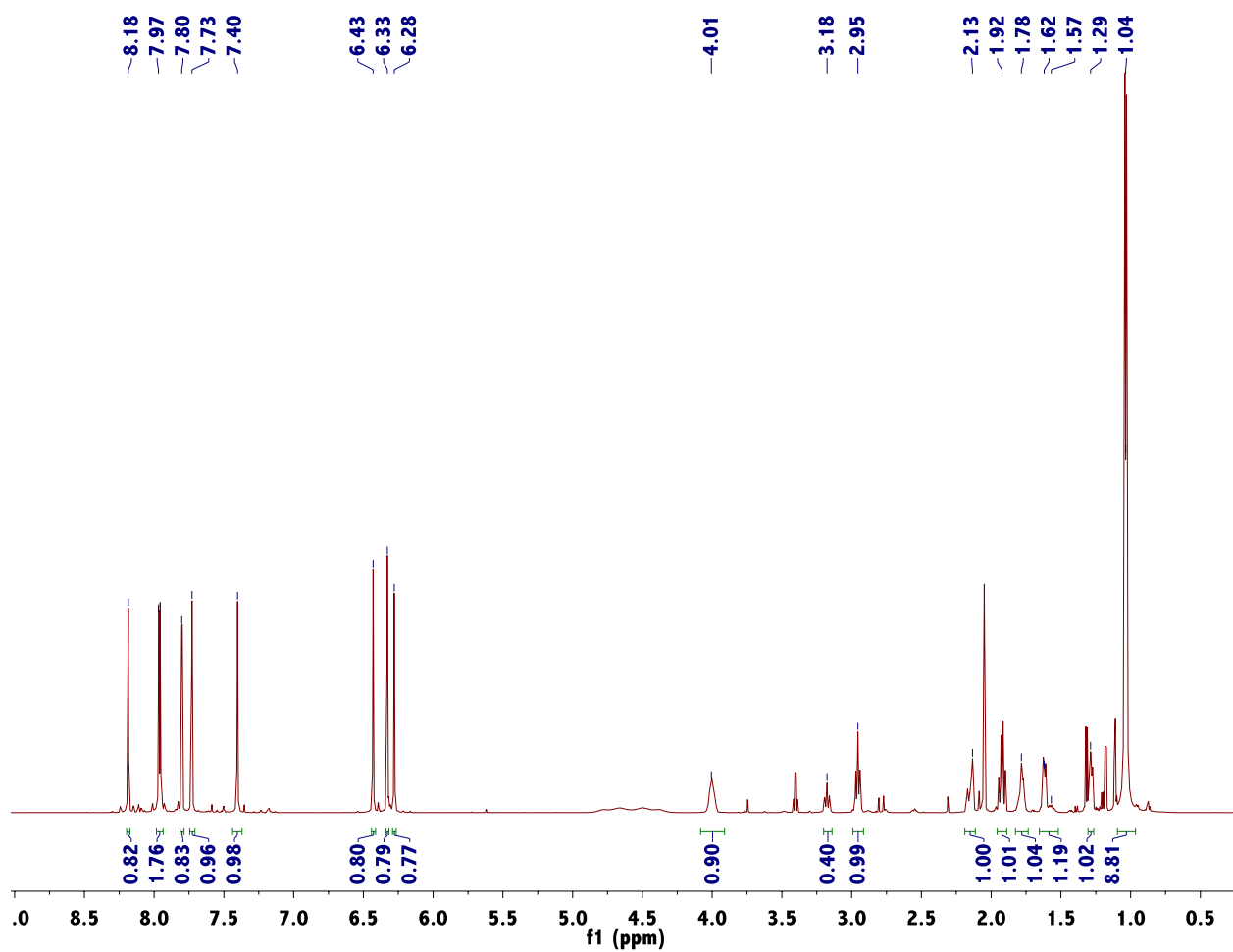


Figure SF54. Compound 56  $^1\text{H}$  NMR



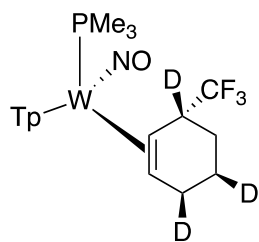


Figure SF55. Compound 57  $^1\text{H}$  NMR

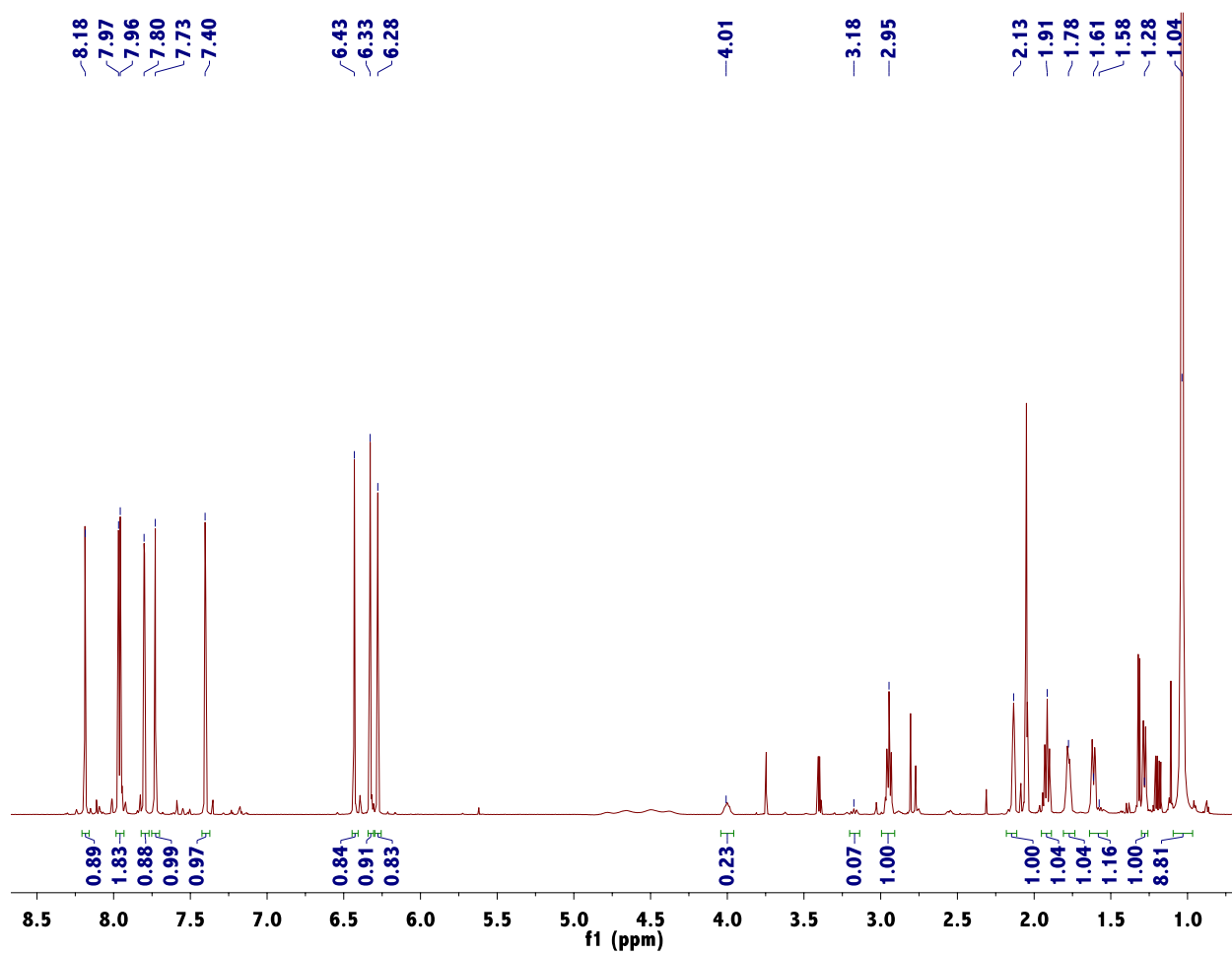
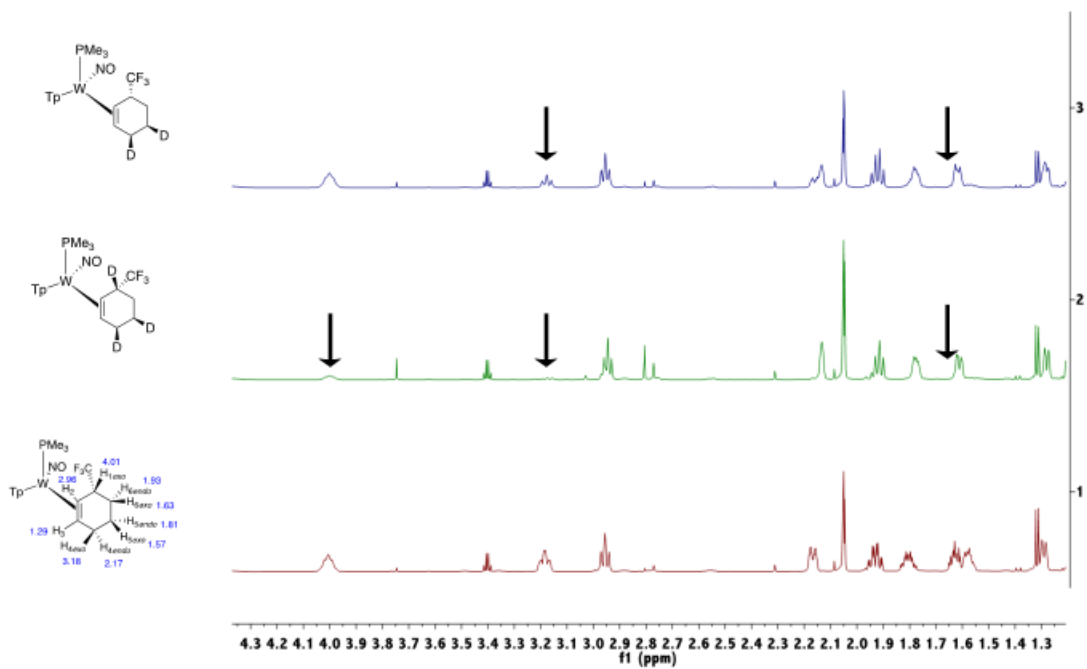
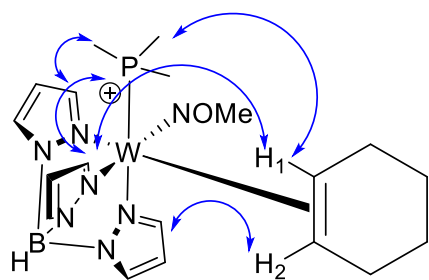
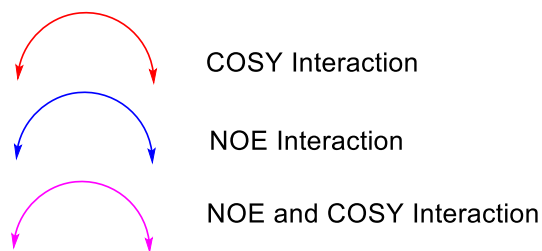


Figure SF56. Comparison of endo-3-(trifluoromethyl)cyclohexene isotopologues as their tungsten complexes (55-57)



## G. Stereochemical Determination of Complexes 6, 7, and 9 via 2D NMR Data

### 1. Description of data supporting the regiochemical assignments of protons for cyclohexene ligand of Complex 9



#### a. Assignment of H<sub>1</sub> and H<sub>2</sub>:

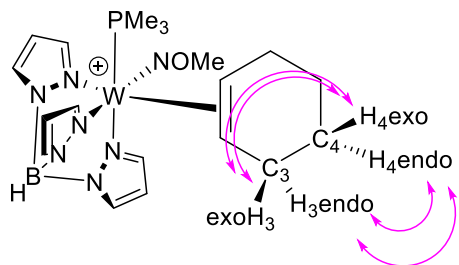
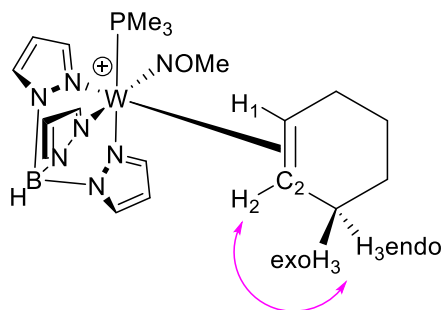
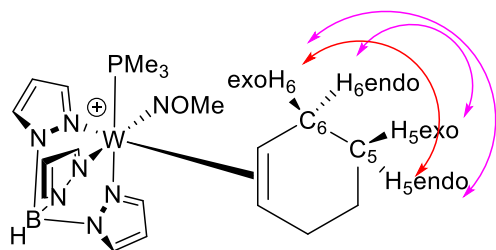
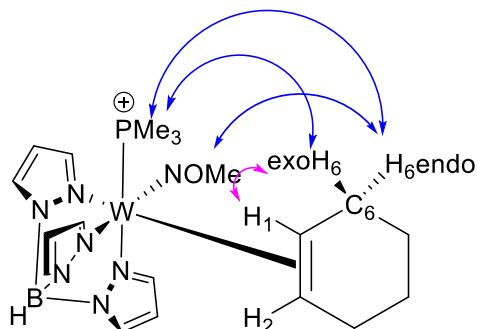
PMe<sub>3</sub> resonance at 1.29 ppm shows NOE correlations to Pz<sub>3B</sub> resonance at 8.11 and Pz<sub>3C</sub> resonance at 7.47. Additionally, the PMe<sub>3</sub> ligand shows an NOE interaction to a signal at 3.96 ppm. A <sup>1</sup>H {<sup>31</sup>P} NMR spectrum results in a simplification of multiplicity of H<sub>1</sub> due to large splitting with the <sup>31</sup>P nucleus ( $I = 1/2$ ;  $J_{HP}$  is typically 10-12 Hz for Wtp(NO)(PMe<sub>3</sub>)(alkene) complexes). The Pz<sub>3C</sub> resonance at 7.47 ppm shows a strong NOE correlation with H<sub>1</sub> resonance at 3.96 ppm and Pz<sub>3A</sub> shows an NOE interaction with H<sub>2</sub> that resonates at 2.34 ppm.

#### c. Assignment of H<sub>6exo</sub> and H<sub>6endo</sub>:

These protons resonating at 3.56 and 2.87 show an HSQC correlation with C<sub>6</sub> (31.3 ppm), implying that they are a diastereotopic methylene group. The resonance at 3.96 ppm (H<sub>1</sub>) shows a strong COSY interaction with a signal at 3.56 ppm. Further, C<sub>1</sub> (64.2 ppm) shows HMBC interactions to proton resonances at 3.56 (H<sub>6exo</sub>) and 2.87 (H<sub>6endo</sub>) ppm. These H<sub>6</sub> resonances show NOE interactions with the PMe<sub>3</sub> ligand with the 2.87 ppm (H<sub>6endo</sub>) showing a more intense NOE interaction. The 2.87 resonance also shows an NOE interaction with the methyl group on the nitrosyl, supporting its assignment as the "endo" proton. An NOE resonance between the methyl group and the resonance at 3.56 is not observed.

#### b. Assignment of C<sub>1</sub> and C<sub>2</sub>:

The H<sub>1</sub> resonance at 3.96 and shows a strong HSQC correlation 64.2 ppm, assigned as C<sub>1</sub>. Additionally this signal is split by the <sup>31</sup>P nucleus with a  $J_{PC} = 8.2$  Hz. The H<sub>2</sub> signal (2.34 ppm) shows an HSQC interaction with the 63.2 ppm resonance assigned as C<sub>2</sub>.



d. Assignment of H<sub>5</sub> protons:

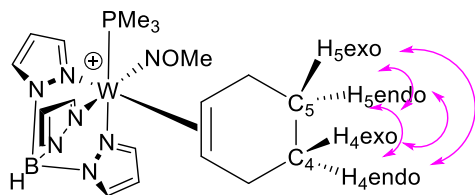
These resonances show an HSQC interaction to the same carbon at 23.8 ppm implying that they are a diastereotopic methylene group. The H<sub>6</sub> protons both display COSY interactions with resonances at 1.59 and 1.51 ppm.

e. Assignment of the H<sub>3</sub> protons

The resonance for the H<sub>2</sub> proton at 2.34 ppm shows a strong COSY and NOESY interaction with a resonance at 3.38 ppm, assigned as H<sub>3</sub>. This H<sub>3</sub> resonance, along with a second at 3.13 ppm show HSQC correlations with a carbon at 31.8 ppm. Therefore, these resonances are a diastereotopic methylene group.

f. Assignment of the H<sub>4</sub> protons:

The 1.48 and 1.64 protons show HSQC interactions with a carbon resonance at 24.6 ppm implying that they are part of a diastereotopic methylene group. H<sub>3</sub> resonances at 3.13 and 3.38 ppm show strong COSY and NOESY Interactions to proton resonances at 1.48 and 1.64 ppm which are assigned as the H<sub>4</sub> protons.



g. internal check: Although the similarity in resonances precludes unambiguous determination of interacting protons, there are COSY and NOSY interactions between all of the H<sub>5</sub> and H<sub>4</sub> protons the there is an HMBC interaction from C<sub>4</sub> (24.6 ppm) to the H<sub>5</sub> resonances and likewise HMBC interactions from C<sub>5</sub> (23.8) to the H<sub>4</sub> resonances. Note: There is no stereochemistry implied for H<sub>4</sub> or H<sub>5</sub> pairs. This is only an assignment of regiochemistry.

The analysis described above for **9** was used to assign the regiochemical positions for other fully proteated complexes (namely complex **6** and **7**) and elucidation of the stereochemical assignments for complex **6**, **7**, and **9** is highlighted below.

2. Assignments for [Wtp(PMe<sub>3</sub>)(NO)(η<sup>2</sup>-cyclohexadienium)](OTf) (6)

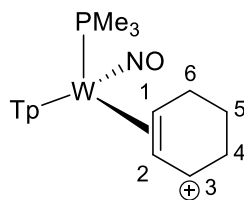


Figure SG1. Tp Doublets for 6

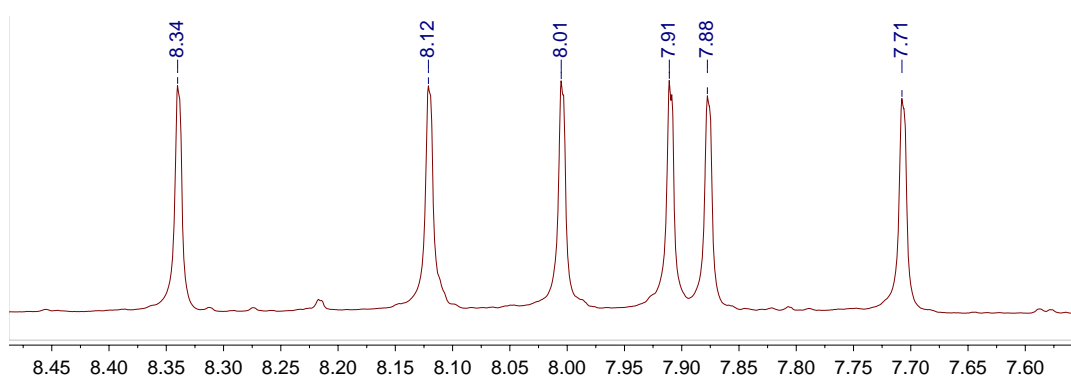
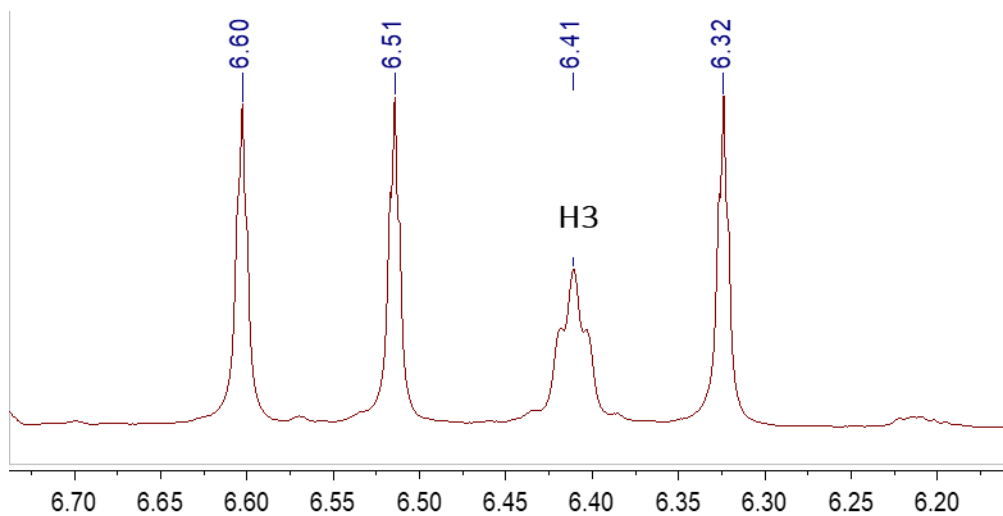
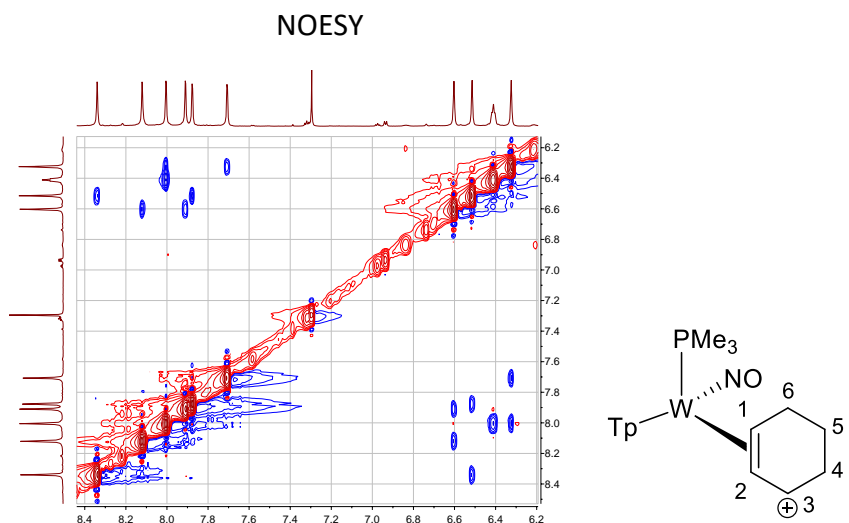


Figure SG2. Tp Triplets (and H<sub>3</sub>) for 6





a. Tp Assignments for Compound 6:



From NOESY data:

The signal at 6.32 ppm correlates to 8.01 & 7.71 ppm *Tp group 1*

The signal at 6.51 ppm correlates to 8.34 & 7.88 ppm *Tp group 2*

The signal at 6.60 ppm correlates to 8.12 & 7.91 ppm *Tp group 3*

Also from NOESY data:

The signal at **8.01** correlates to 3.45 (cyclohexene) & 6.45 (cyclohexene) *Tp group 1* → **PzA**

The signal at **8.12** correlates to 1.26 ppm (PMe<sub>3</sub>), 4.62 (cyclohexene), 5.19 (cyclohexene)

*Tp group 3* → **PzC**

The signal at **8.34** correlates to 1.26 ppm signal (PMe<sub>3</sub>)

*Tp group 2* → **PzB**

|     | TpH <sub>3</sub> (ppm) | TpH <sub>4</sub> (ppm) | TpH <sub>5</sub> (ppm) |
|-----|------------------------|------------------------|------------------------|
| PzA | 8.01                   | 6.32                   | 7.71                   |
| PzB | 8.34                   | 6.51                   | 7.88                   |

PzC

8.12

6.60

7.91

Summary: Both TpH<sub>5</sub> and TpH<sub>3</sub> protons (doublets) interact with TpH<sub>4</sub> (NOESY), but TpH<sub>3</sub> protons have interactions with other ligands whereas TpH<sub>5</sub> protons do not.)

b. Cyclohexadienium ligand Assignments (Compound 6)

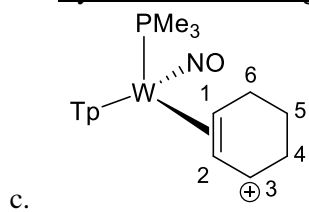


**Figure SG3.**  $^1\text{H}$  NMR of 3.1-5.3 ppm range (ligand protons)

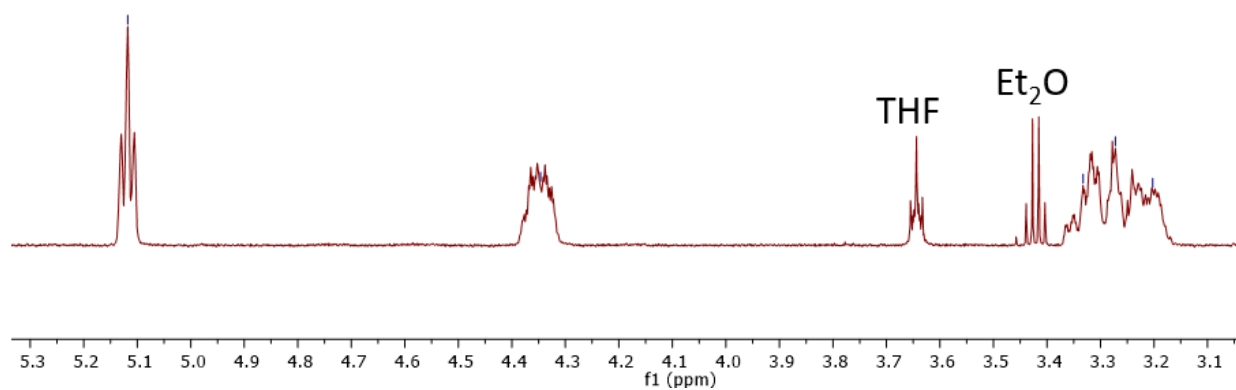
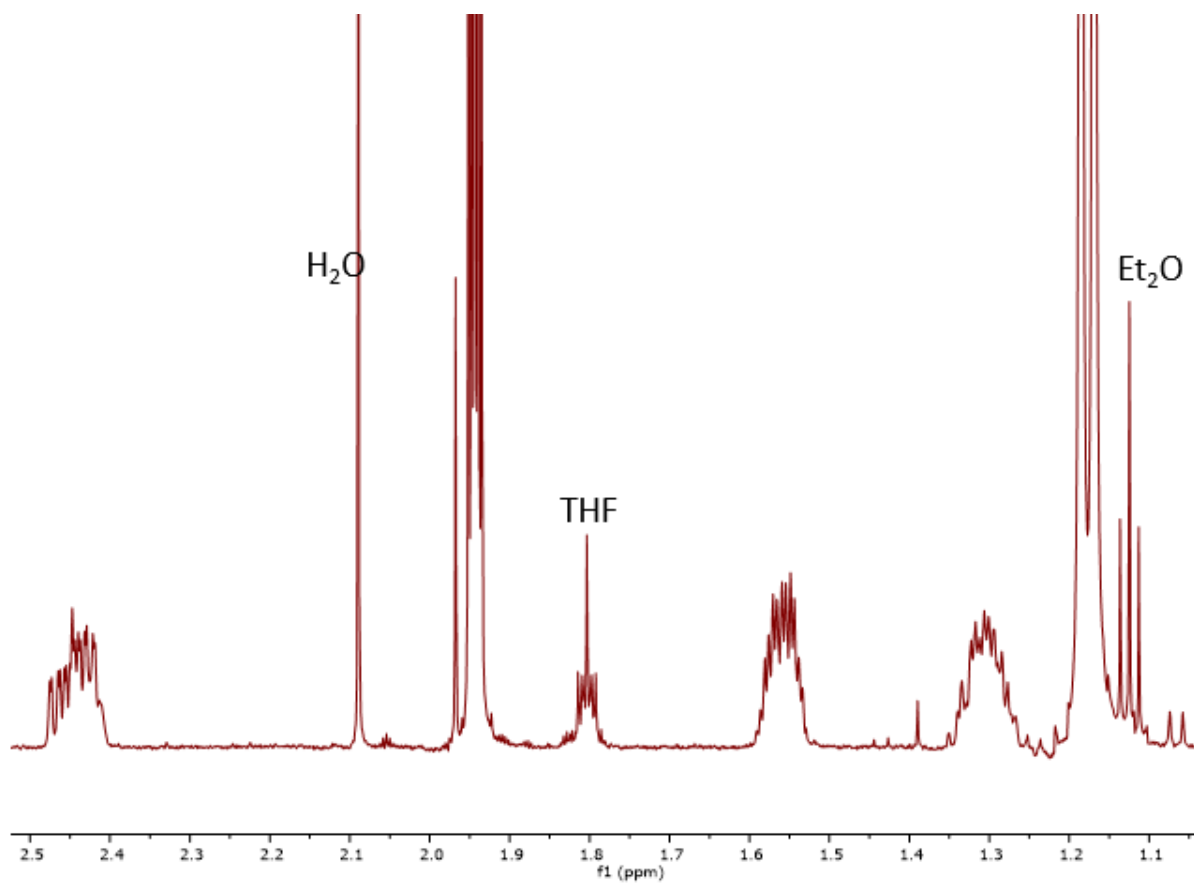
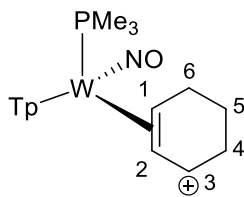


**Figure SG4.**  $^1\text{H}$  NMR of 1.0-2.5 ppm range (ligand protons)

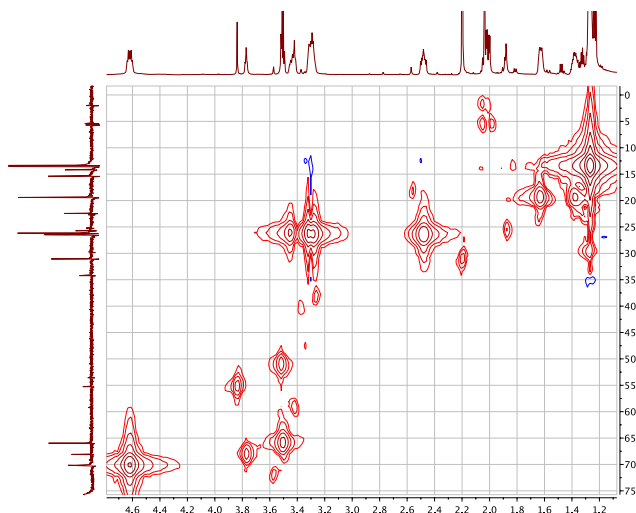


Identification of diastereotopic methylene groups and bound protons (carbon shifts in



parenteses) by HSQC data:

HSQC



Allyl Protons ( $H_1$ ,  $H_2$ , &  $H_3$ )

4.62 (**70.5**), 5.18 (**105.2**), 6.41 (**134.2**)

Diastereotopic methylene groups:

Pair A: 1.38 & 1.63 (**19.5**)

Pair B: \*\*

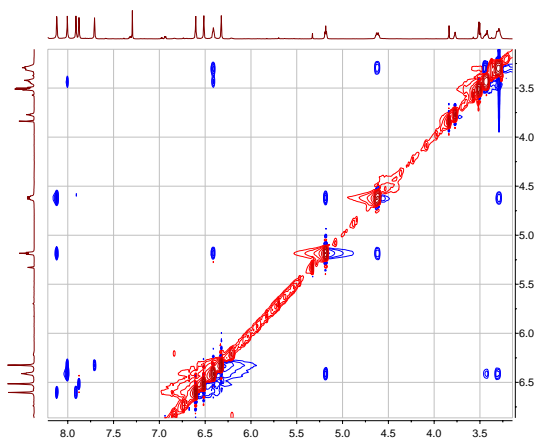
Pair C: \*\*

\*\* Four protons at 2.48, 3.30 (2), and 3.43 ppm correlate to two carbons at **26.3** & **26.4** ppm. Cannot be distinguished by HSQC.

**Figure SG5:** NOESY: 4.62 ppm correlates to 1.26 ( $\text{PMe}_3$ ) and 5.18 (allyl) ppm. 5.18 ppm correlates to 4.62 (allyl) and 6.41 (allyl) ppm. 6.41 ppm correlates to 5.18 (allyl) and 8.01 ppm ( $\text{PzA } H_3$ ).

*These data support 4.62 ppm as  $H_1$ , 5.18 ppm as  $H_2$ , and 6.41 ppm as  $H_3$*

d. Diastereotopic methylene group assignments (Compound **6** continued)  
NOESY (detail)



Both 3.43 ppm and 3.30 ppm correlate to 6.41 ppm (allyl peak,  $H_3$ ).

*This suggests these signals correspond to  $H_4$  protons.*

Both 3.30 ppm (the right side of the 3.30 peak) and 2.48 ppm (not shown) correlate to 4.62 ( $H_1$ ).

*This suggests these signals correspond to  $H_6$  protons.*

*By elimination, pair A (1.38 & 1.63 ppm) is assigned to correspond to  $H_5$ .*

**Figure SG6.** Endo/Exo assignments by NOESY (Compound **6** continued)

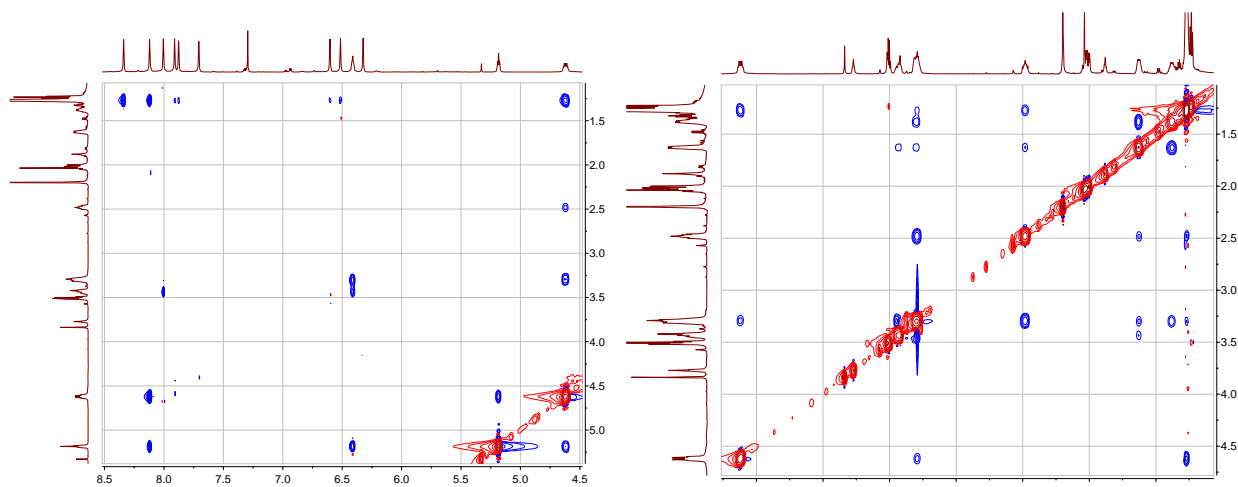


**Figure SG7.** NOESY Correlations: The signal at 2.48 (H<sub>6</sub>) correlates to: 1.27 (PMe<sub>3</sub>), 1.63 (H<sub>5</sub>), 3.30 (H<sub>6</sub>/H<sub>4</sub> strong), 3.44 (H<sub>4</sub> weak), 4.63 (H<sub>1</sub> weak)

*These NOE correlations suggest that 2.48 ppm corresponds to H<sub>6</sub> endo.*

The signal at 3.30 (H<sub>6</sub>) correlates to: 1.27 (PMe<sub>3</sub> weak), 4.63 ppm (H<sub>1</sub>)

*These NOE correlations further support that 2.48 ppm corresponds to H<sub>6</sub> exo.*

The signal at 3.30 (H<sub>4</sub>) correlates to: 6.42 ppm (H<sub>3</sub>)

*Note that NOESY correlations between 3.30 ppm protons and peaks between 1.3 and 3.5 ppm cannot be assigned definitively to one of the two protons. Definitively assigned peaks are the only ones listed.*

The signal at 3.43 (H<sub>4</sub>) correlates to: 1.63 (H<sub>5</sub>), 2.48 (H<sub>6</sub> weak), 6.42 (H<sub>3</sub> weak), 8.02 (PzA H<sub>3</sub>)

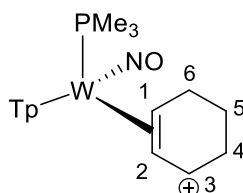
*These NOE correlations suggest that 3.43 ppm is H<sub>4</sub> endo.*

The signal at 1.38 (H<sub>5</sub>) correlates to: 1.63 (H<sub>5</sub> strong), 2.48 (H<sub>6</sub> very weak), 3.30 (H<sub>4</sub>/H<sub>6</sub> strong)

The signal at 1.63 (H<sub>5</sub>) correlates to: 1.38 (H<sub>5</sub> strong), 2.48 (H<sub>6</sub>), 3.30 (H<sub>4</sub>/H<sub>6</sub>), 3.44 (H<sub>4</sub>)

*These NOE correlations suggest that the proton corresponding to 1.63 ppm is on same side of the cyclohexene ring as that for 2.48 ppm. Therefore, the proton represented by 1.63 ppm is H<sub>5</sub> endo.*

### Final <sup>1</sup>H NMR Assignments for Complex 6



### Cyclohexadienium Ligand

| H <sub>1</sub> (ppm) | H <sub>2</sub> (ppm) | H <sub>3</sub> (ppm) |      | H <sub>4</sub> (ppm) | H <sub>5</sub> (ppm) | H <sub>6</sub> (ppm) |
|----------------------|----------------------|----------------------|------|----------------------|----------------------|----------------------|
| 4.62                 | 5.18                 | 6.41                 | exo  | 3.43                 | 1.63                 | 2.48                 |
|                      |                      |                      | endo | 3.30                 | 1.38                 | 3.30                 |

### Tp Ligand

|     | H <sub>3</sub> (ppm) | H <sub>4</sub> (ppm) | H <sub>5</sub> (ppm) |
|-----|----------------------|----------------------|----------------------|
| PzA | 8.01                 | 6.32                 | 7.71                 |
| PzB | 8.34                 | 6.51                 | 7.88                 |
| PzC | 8.12                 | 6.60                 | 7.91                 |

**PMe<sub>3</sub>: 1.27 ppm**

### 3. Assignments for $\text{WTp}(\text{PMe}_3)(\text{NO})(\eta^2\text{-cyclohexene})$ (7)

Figure SG8.  $^1\text{H}$  NMR of **Tp Doublets (compound 7)**

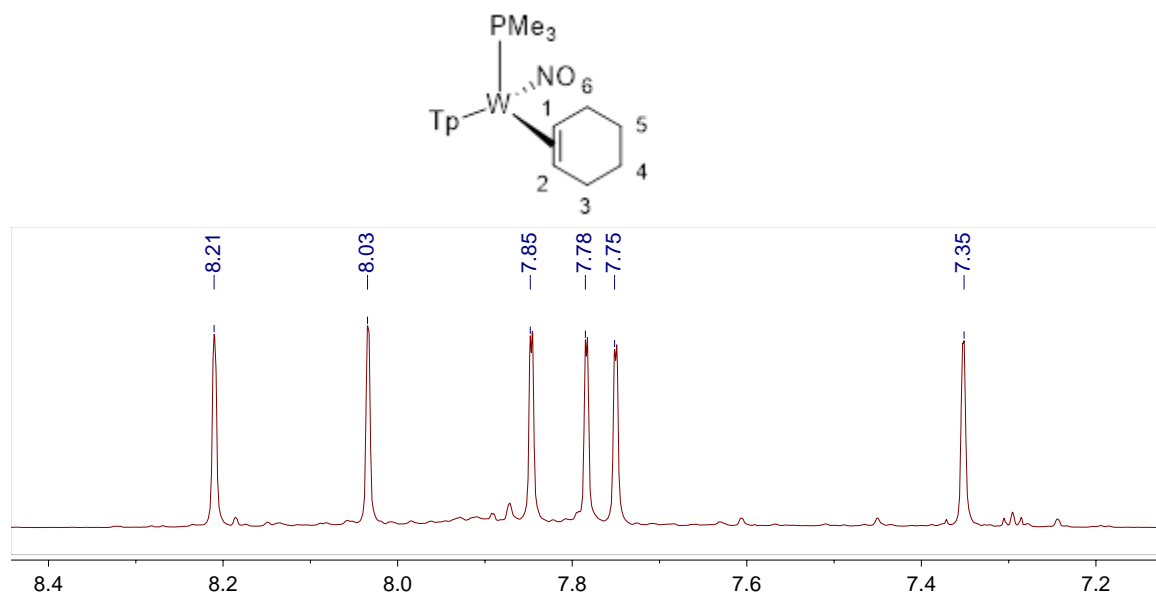
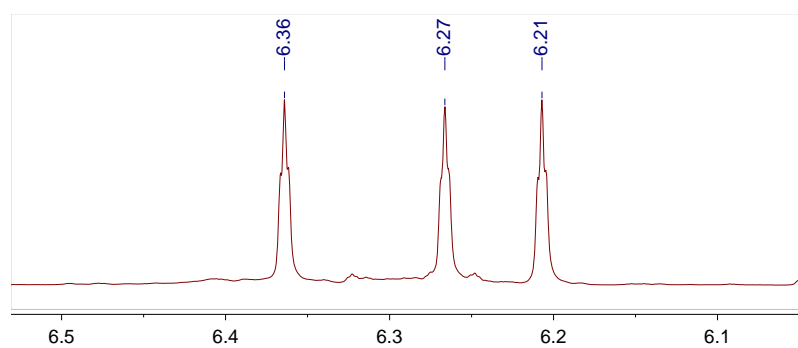


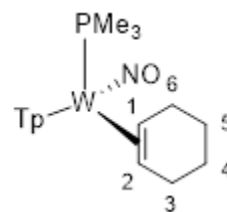
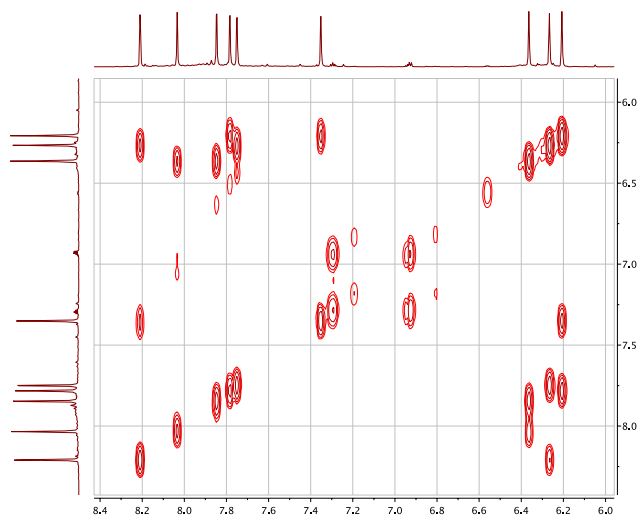
Figure SG9.  $^1\text{H}$  NMR of **Tp Triplets (compound 7)**



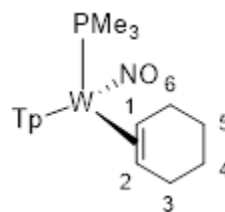
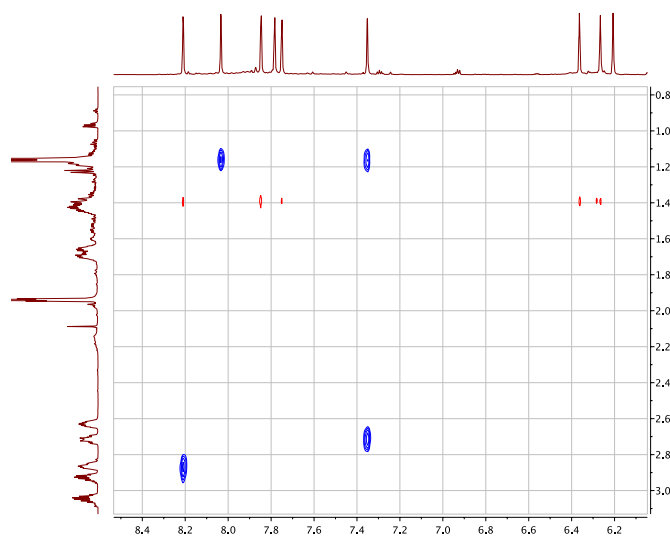
a. Tp Assignments (compound 7)

Figure SG10. COSY (compound 7)





**Figure SG11.** NOESY (compound 7)



*From COSY data:*

The signal at 6.21 ppm correlates to 7.35 & 7.78 ppm

*Tp group 1*

The signal at 6.27 ppm correlates to 7.75 & 8.21 ppm

*Tp group 2*

The signal at 6.36 ppm correlates to 7.85 & 8.03 ppm

*Tp group 3*

*From NOESY data:*

The signal at 7.35 ppm correlates to 1.16 (PMe<sub>3</sub>) & 2.72 ppm (cyclohexene) *Tp group 1* →  
**PzC**

The signal at 8.03 ppm correlates to 1.16 ppm (PMe<sub>3</sub>) *Tp group 3* →  
**PzB**

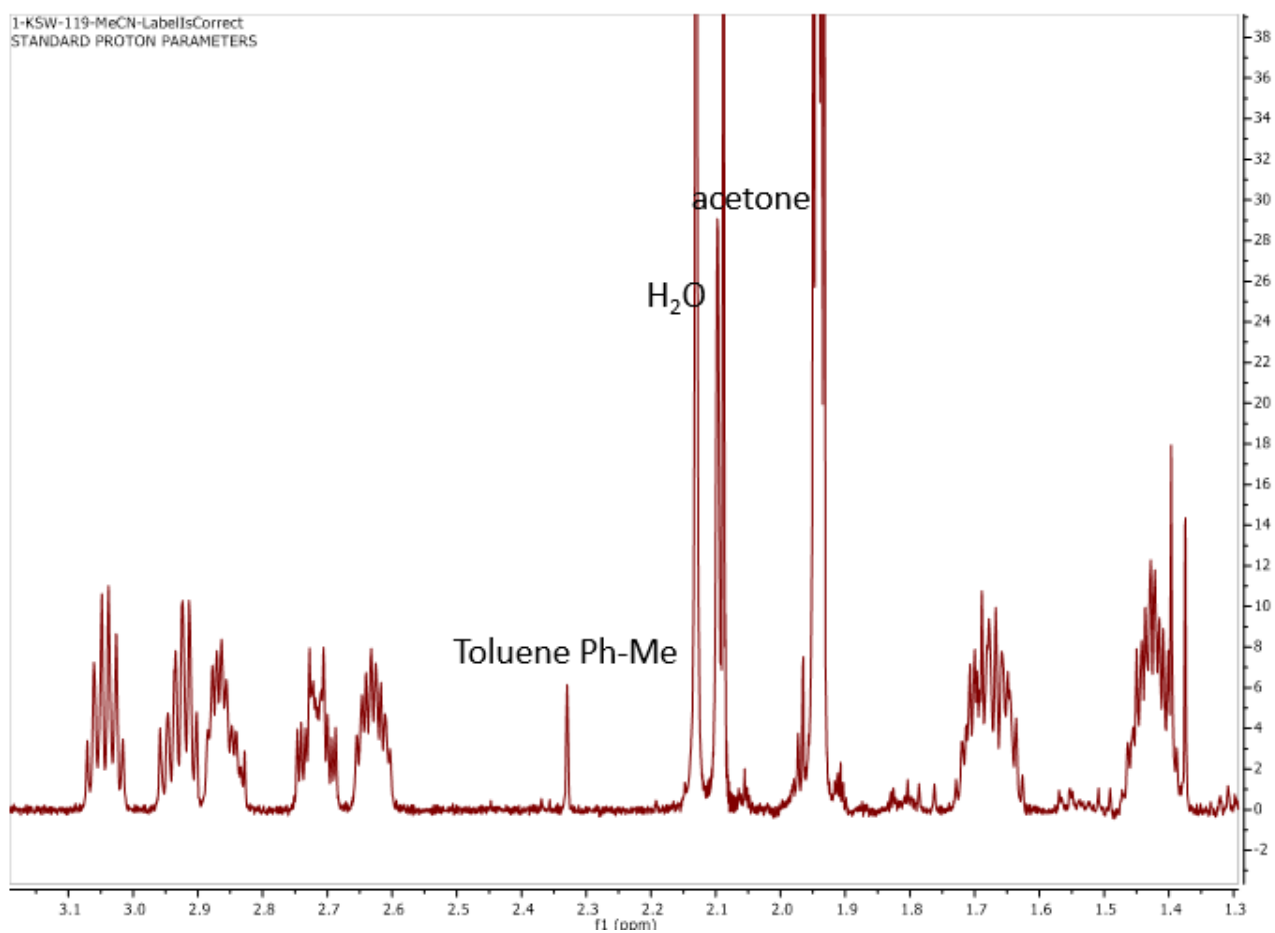
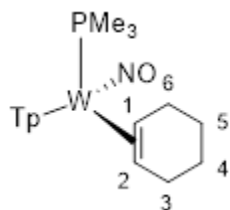
The signal at 8.21 ppm correlates to 2.86 ppm (cyclohexene) *Tp group 2* →  
**PzA**

|            | H <sub>3</sub> (ppm) | H <sub>4</sub> (ppm) | H <sub>5</sub> (ppm) |
|------------|----------------------|----------------------|----------------------|
| <b>PzA</b> | 8.21                 | 6.27                 | 7.75                 |
| <b>PzB</b> | 8.03                 | 6.36                 | 7.85                 |
| <b>PzC</b> | 7.35                 | 6.21                 | 7.78                 |

Summary: Both TpH<sub>5</sub> and TpH<sub>3</sub> protons (doublets) interact with TpH<sub>4</sub> (NOESY, COSY), but TpH<sub>3</sub> protons have interactions with other ligands whereas TpH<sub>5</sub> protons do not.).

(Continued Analysis of Complex 7)

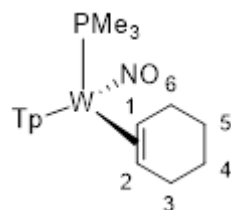
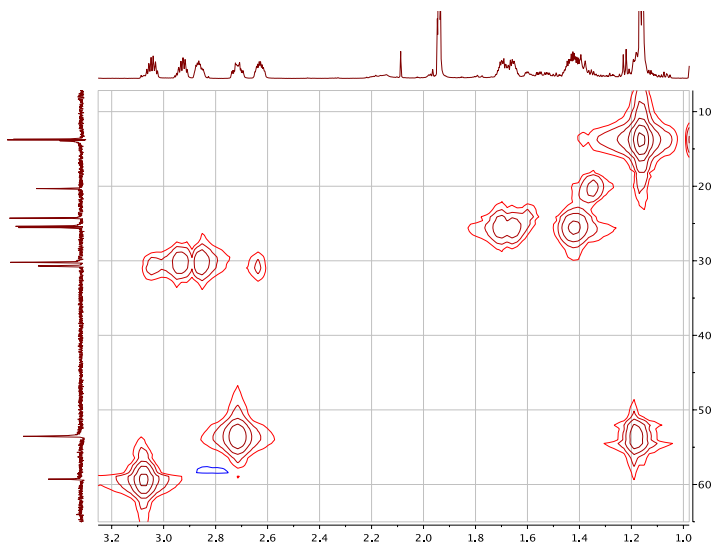
Figure SG12. 1.3-3.15 ppm Range (Cyclohexene protons)



Cyclohexene Ligand Assignments

Identification of diastereotopic methylene groups and bound protons (carbon shifts in parentheses) by HSQC data

Figure SG13. HSQC data for compound 7



Tungsten-bound methane groups:

H<sub>1</sub>: 2.72 ppm (**53.6 ppm**)

H<sub>2</sub>: 1.18 ppm (**53.6 ppm**)

Diastereotopic methylene groups

Pair A: \*\* (**25.4 ppm**)

Pair B: \*\* (**25.5 ppm**)

Pair C: 2.63 & 3.04 ppm (**30.7 ppm**)

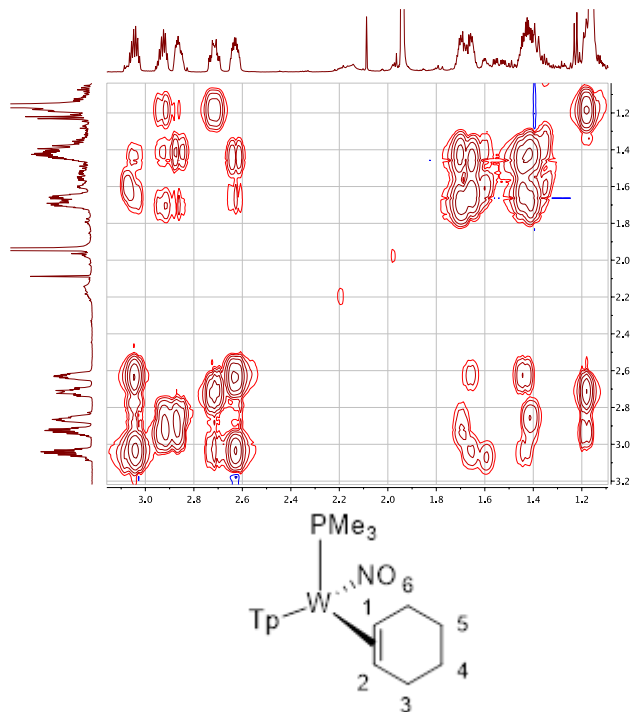
Pair D: 2.86 & 2.93 ppm (**30.2 ppm**)

\*\* Two protons at 1.41 ppm and protons resonating at 1.66 and 1.70 ppm could not be specifically assigned due to close proximity of the carbon signals.

## Continued Analysis of Complex 7

b. Pair assignment by COSY data.

**Figure SG14.** COSY data for complex 7



2.72 ppm (H<sub>1</sub>) correlates to 1.18 ppm (H<sub>2</sub>) and 3.04 ppm, which is part of CH<sub>2</sub> "Pair C"

"Pair C" → H<sub>6</sub> protons

1.18 ppm signal (H<sub>2</sub>) correlates to 2.72 ppm (H<sub>1</sub>) and 2.93 ppm, which is part of CH<sub>2</sub> "Pair D"

"Pair D" → H<sub>3</sub> protons

2.63 ppm and 3.05 ppm ("Pair C") both correlate with 1.66 ppm and 1.41 ppm signals

1.66, 1.41 ppm → H<sub>5</sub> protons

2.93 ppm (part of "Pair D") correlates with 1.70 ppm signal.

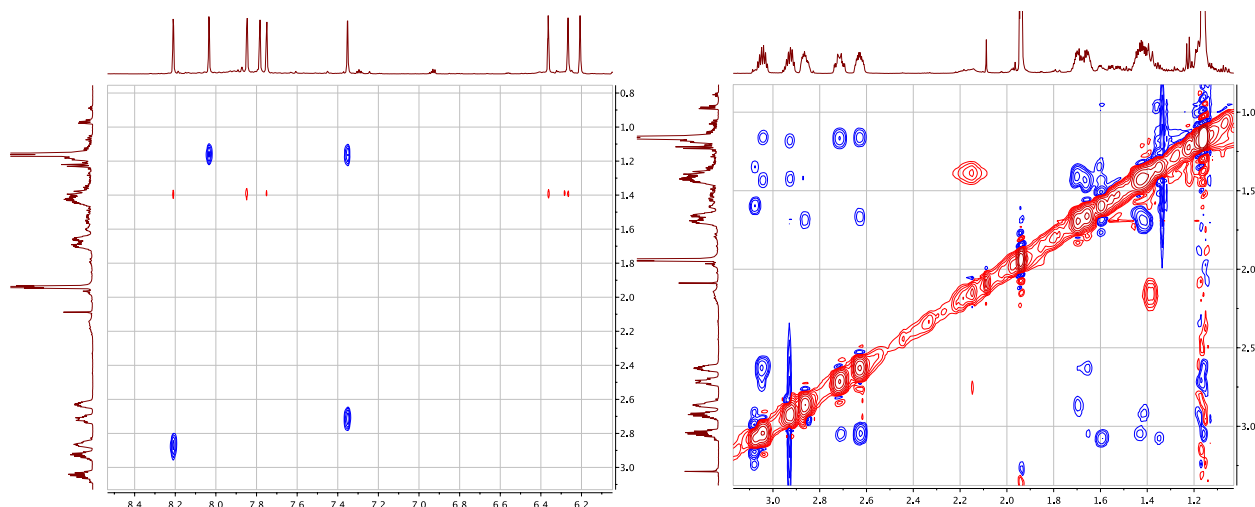
1.70 ppm → H<sub>4</sub> proton

2.03 (part of "Pair D") correlates with 1.41 ppm

1.41 ppm → H<sub>4</sub> proton

c. endo/exo assignments by NOESY

**Figure SG15.** NOESY (complex 7)



The peak at 2.72 ppm ( $H_1$ ) correlates with one at 1.16 ppm (either  $PMe_3$  or  $H_2$ ), 3.04 ppm ( $H_6$ )

This indicates that the proton resonating at 3.04 ppm is  $H_{6exo}$  and therefore 2.63 ppm is  $H_{6endo}$

The peak at 1.18 ppm ( $H_2$ ) correlates with one at 2.86 ppm (weak,  $H_3$ ), 2.93 ppm ( $H_3$ )

This indicates that the proton resonating at 2.93 ppm is  $H_{3exo}$  since 2.86 ppm is much weaker, so the resonance at 2.86 ppm corresponds to  $H_{3endo}$ .

The peak at 2.86 ( $H_3$ ) correlates with 1.18 (weak,  $H_2$ ), 1.41– (weak,  $H_4$ ), 1.70 (strong,  $H_4$ ), 8.21 (PzA  $H_3$ )

This indicates that 2.86 ppm is  $H_{3endo}$ , due to Tp NOE interaction; this suggests that 1.70 ppm is  $H_{4endo}$  and the signal at 1.41 ppm is  $H_{4exo}$ .

The peak at 2.93 ( $H_3$ ) correlates with 1.18 ( $H_2$ ), 1.41– (strong,  $H_4$ ), 1.70 (weak,  $H_4$ )

This further supports that 1.41 ppm is  $H_{4exo}$  and 1.70 ppm is  $H_{4endo}$

The peak at 2.63 ( $H_6$ ) correlates with peaks at 1.16 ppm ( $PMe_3$ ), 1.66 ppm ( $H_5$ ), 3.04 ppm ( $H_6$ )

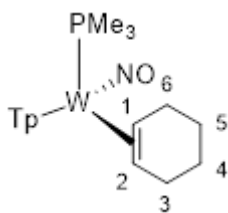
This supports that 2.63 ppm is  $H_{6endo}$ , due to the  $PMe_3$  NOE interaction

This suggests that 1.66 ppm is  $H_{5endo}$  and 1.41 ppm is  $H_{5exo}$

The peak at 3.04 ppm ( $H_6$ ) correlates with peaks at 1.16 ppm ( $PMe_3$ ), 1.41 ppm ( $H_5$ ), 2.63 ppm ( $H_6$ ), and 2.72 ppm ( $H_1$ ); This confirms that 1.41 ppm is  $H_{5exo}$  and 1.66 ppm is  $H_{5endo}$

d. Final  $^1\text{H}$  NMR Assignments for Complex 7

**Cyclohexene Ligand**



| $H_1$ (ppm) | $H_2$ (ppm) |      | $H_3$ (ppm) | $H_4$ (ppm) | $H_5$ (ppm) | $H_6$ (ppm) |
|-------------|-------------|------|-------------|-------------|-------------|-------------|
| 2.72        | 1.18        | endo | 2.86        | 1.70        | 1.66        | 2.63        |
|             |             | exo  | 2.93        | 1.41        | 1.41        | 3.04        |

**Tp Ligand**

|     | $H_3$ (ppm) | $H_4$ (ppm) | $H_5$ (ppm) |
|-----|-------------|-------------|-------------|
| PzA | 8.21        | 6.27        | 7.75        |
| PzB | 8.03        | 6.36        | 7.85        |
| PzC | 7.35        | 6.21        | 7.78        |

**PMe<sub>3</sub>: 1.16 ppm**

#### 4. Stereochemical Assignments for $\text{Wtp}(\text{PMe}_3)(\text{NOMe})(\eta^2\text{-cyclohexene}) [\text{OTf}]^-$ (**9**)

Figure SG16. Tp Doublets

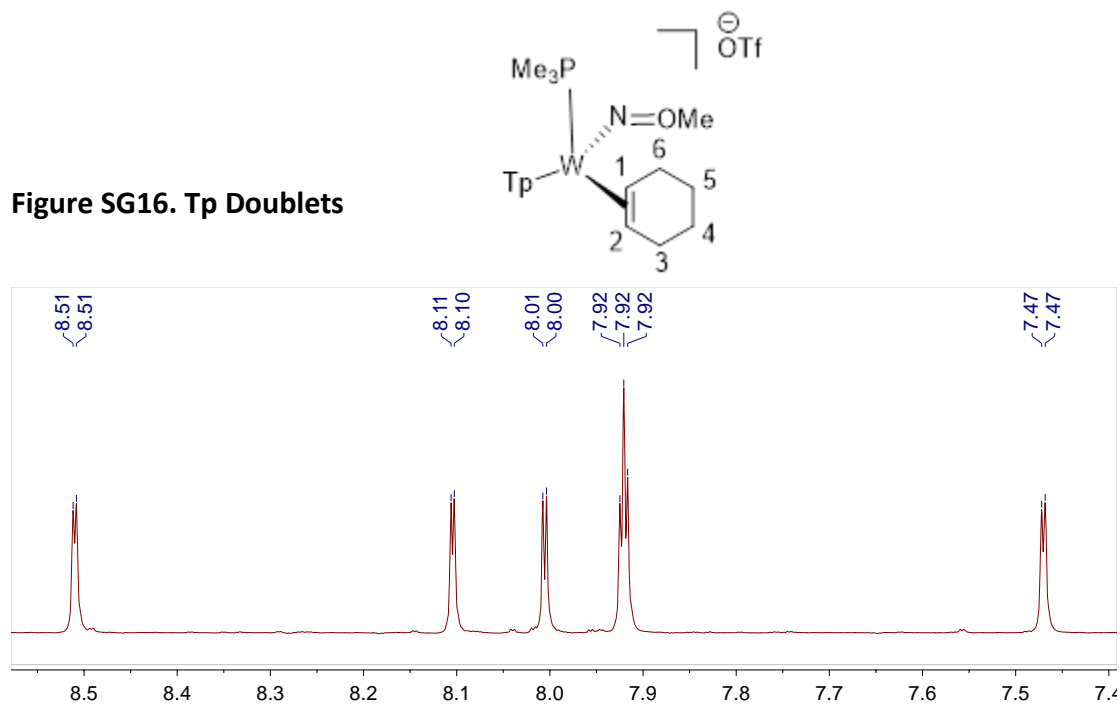
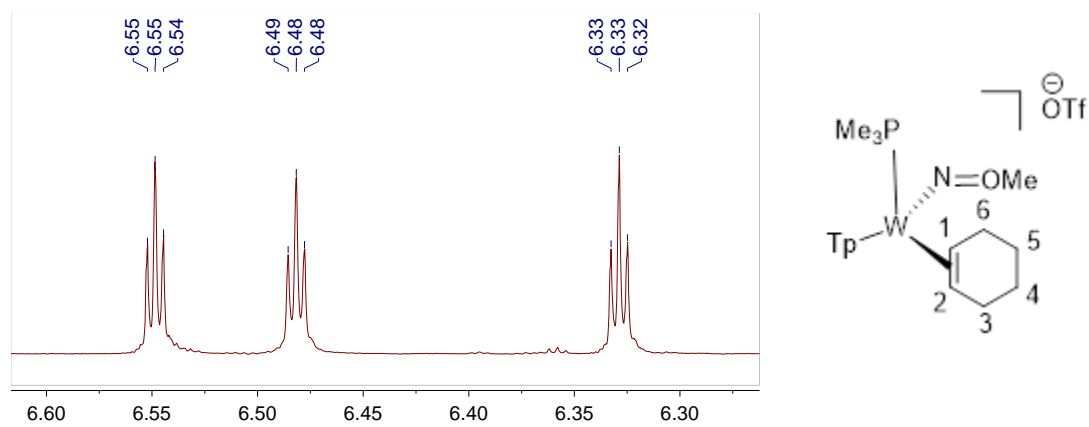


Figure SG17. Tp Triplets





a. Tp Assignments Analysis of Complex 9

Figure SG18. COSY data of Complex 9

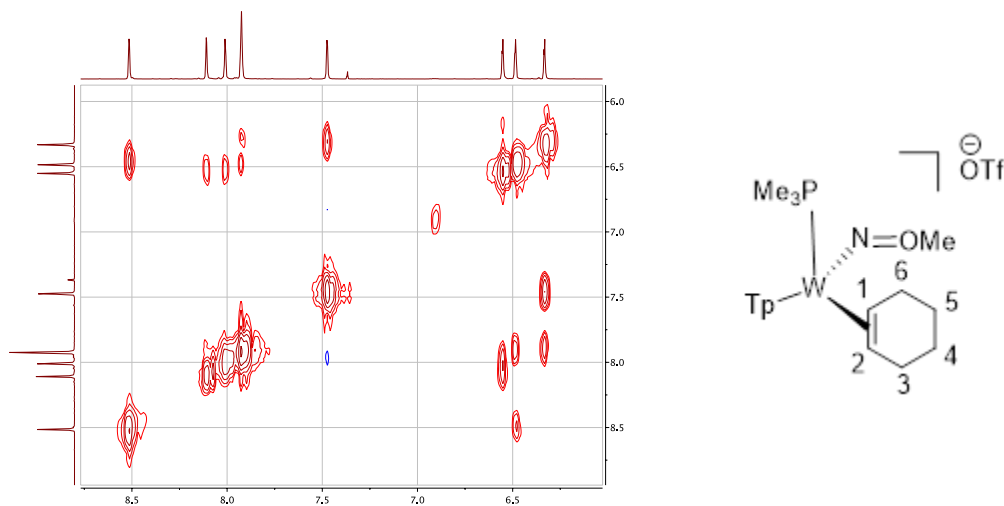
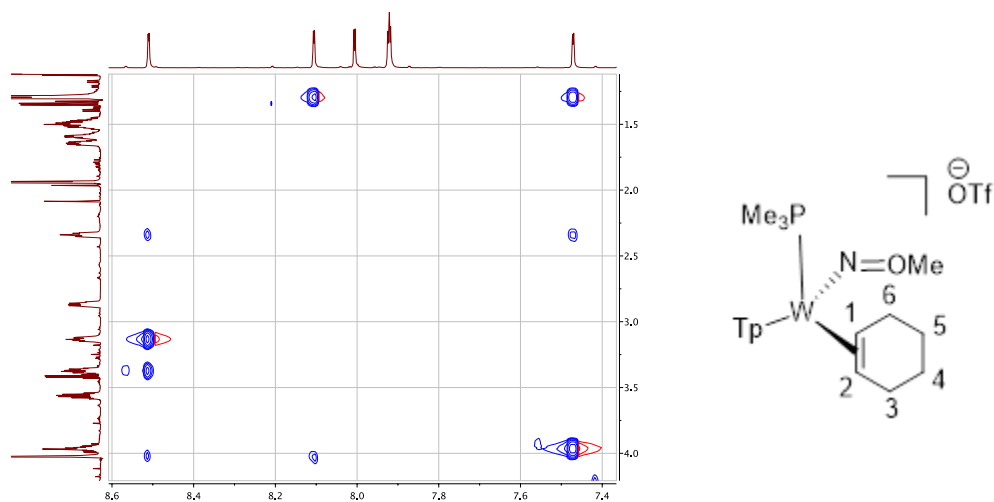


Figure SG19. NOESY data of Complex 9



From COSY data:

The peak at 6.33ppm correlates to 7.47 & 7.92ppm

*Tp group 1*

The peak at 6.48ppm correlates to 7.92 & 8.51ppm

*Tp group 2*

The peak at 6.55ppm correlates to 8.01 & 8.11ppm

*Tp group 3*

From NOESY:

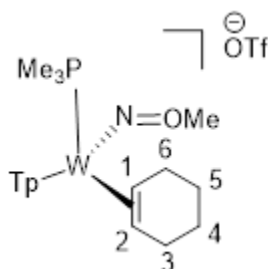
The peak at 7.47 ppm correlates to 1.29 (PMe<sub>3</sub>) & 3.97ppm (cyclohexene) *Tp group 1* → **PzC**

The peak at 8.11 ppm correlates to 1.29 (PMe<sub>3</sub>) & 4.03 ppm (NOMe) *Tp group 3* → **PzB**

The peak at 8.51 ppm correlates to 2.34, 3.13, 3.38 (cyclohexene) & 4.03ppm (NOMe) *Tp group 2* → **PzA**

|     | H <sub>3</sub> (ppm) | H <sub>4</sub> (ppm) | H <sub>5</sub> (ppm) |
|-----|----------------------|----------------------|----------------------|
| PzA | 8.51                 | 6.48                 | 7.92                 |
| PzB | 8.11                 | 6.55                 | 8.01                 |
| PzC | 7.47                 | 6.33                 | 7.92                 |

Summary: Both TpH<sub>5</sub> and TpH<sub>3</sub> protons (doublets) interact with TpH<sub>4</sub> (NOESY, COSY), but TpH<sub>3</sub> protons have interactions with other ligands, whereas TpH<sub>5</sub> protons do not.



(Continued Analysis of Complex 9)

Figure SG20. 2.7-4.1 ppm Complex 9

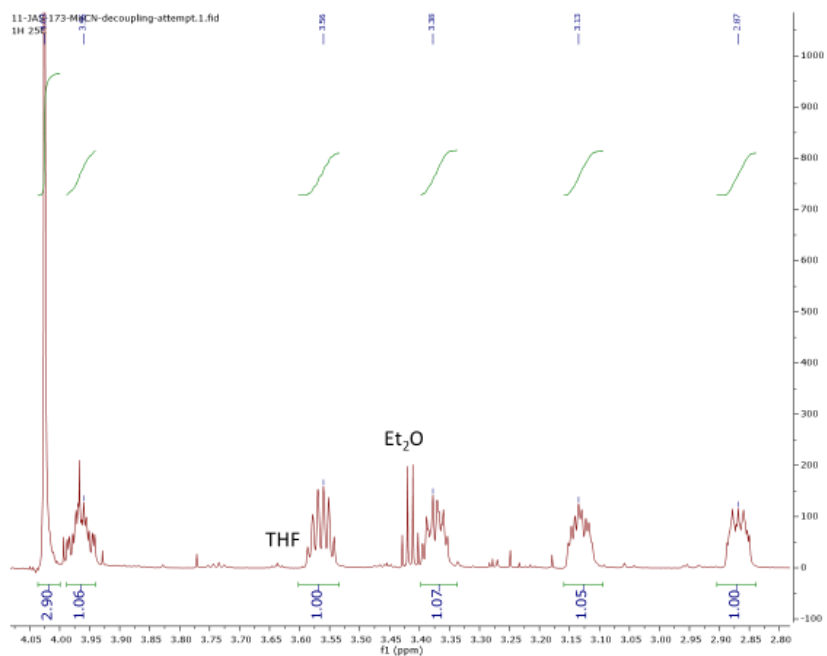
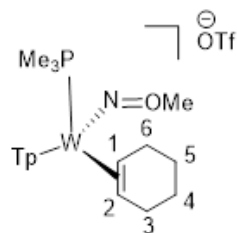
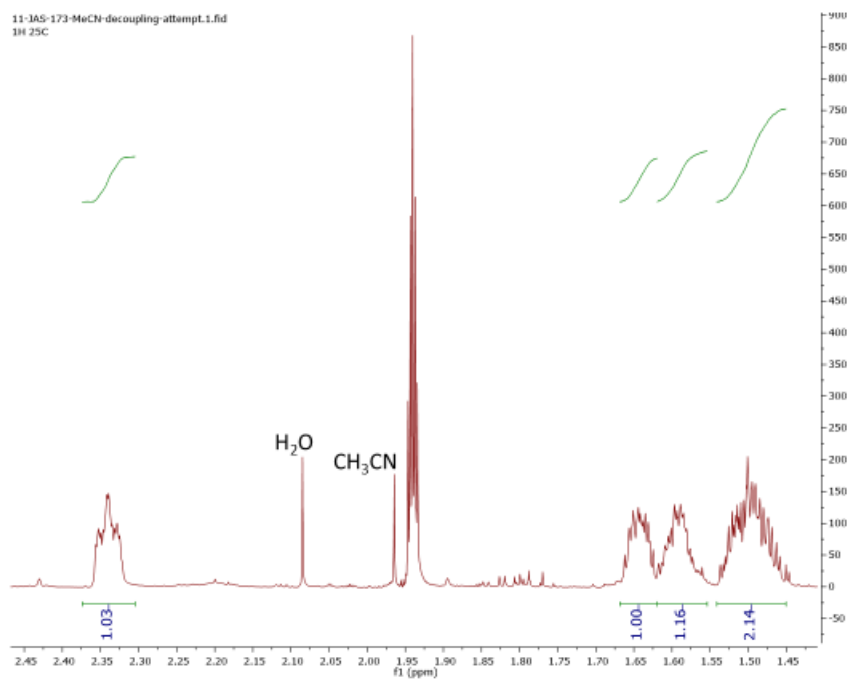


Figure SG21. 1.3-2.5 ppm Complex 9



b. Cyclohexene Ligand Assignments

Identification of diastereotopic methylene groups and tungsten-bound methine groups (carbon shifts in parentheses) by HSQC data

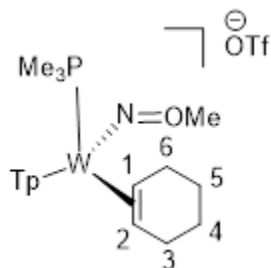
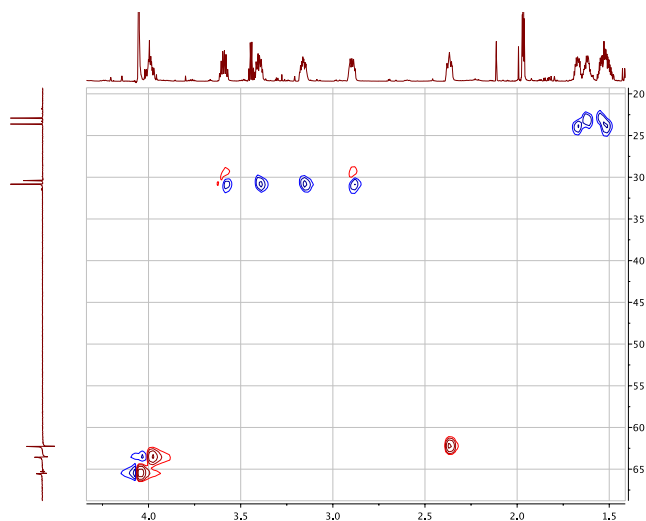


Figure SG22. Complex 9 HSQC



Bound methine protons:

H<sub>1</sub> 3.97 ppm (**63.6 ppm**)

H<sub>2</sub> 2.34 ppm (**62.3 ppm**)

Diastereotopic methylene groups:

Pair A: 1.59 & 1.50 ppm (**22.9 ppm**)

Pair B: 1.64 & 1.50 ppm (**23.7 ppm**)

Pair C: \*\*

Pair D: \*\*

\*\* data suggests that 3.13 & 3.38 (**30.7**) and 3.56 & 2.87 (**30.4**) are pairs, but difficult to confirm from HSQC data alone.

(Continued Analysis of Complex 9)

c. Methylene assignments by COSY data

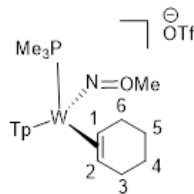
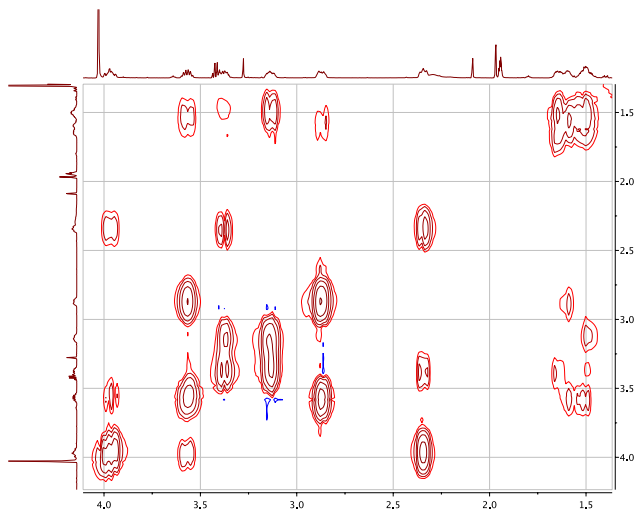


Figure SG23. Complex 9 COSY



COSY correlations are present between:

2.87 & 3.56 ppm (Pair C)

3.13 & 3.38 ppm (Pair D)

*Pairs confirmed*

H<sub>1</sub> (3.97) correlates to 2.34 ppm (H<sub>2</sub>) and 3.56 ppm (pair C): "Pair C" → H<sub>6</sub> protons

H<sub>2</sub> (2.34 ppm) correlates to 3.97 (H<sub>1</sub>) and 3.38 ppm (pair D): "Pair D" → H<sub>3</sub> protons

1.59 (Pair A) correlates with 2.87 & 3.56 (Pair C)

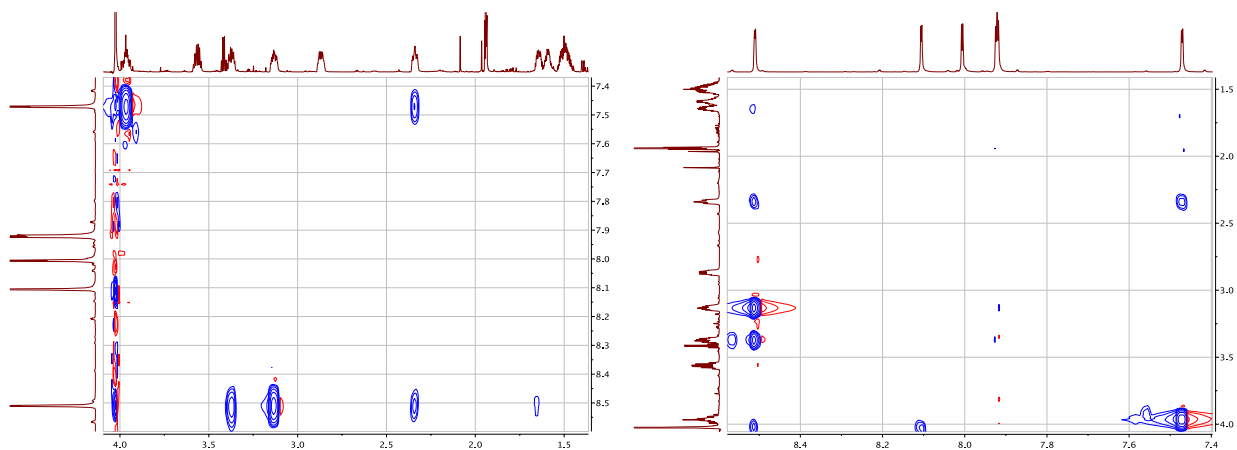
"Pair A" → H<sub>5</sub> protons

1.64 (Pair B) correlates with 3.38 (Pair D)

"Pair B" → H<sub>4</sub> protons

Endo/Exo assignments by NOESY

Figure SG24. Complex 9. NOESY



Signals present in both quadrants:

Peaks at 3.13 & 3.38 ppm ( $H_3$  protons) correlate with 8.51 ppm (PzA  $H_3$ )

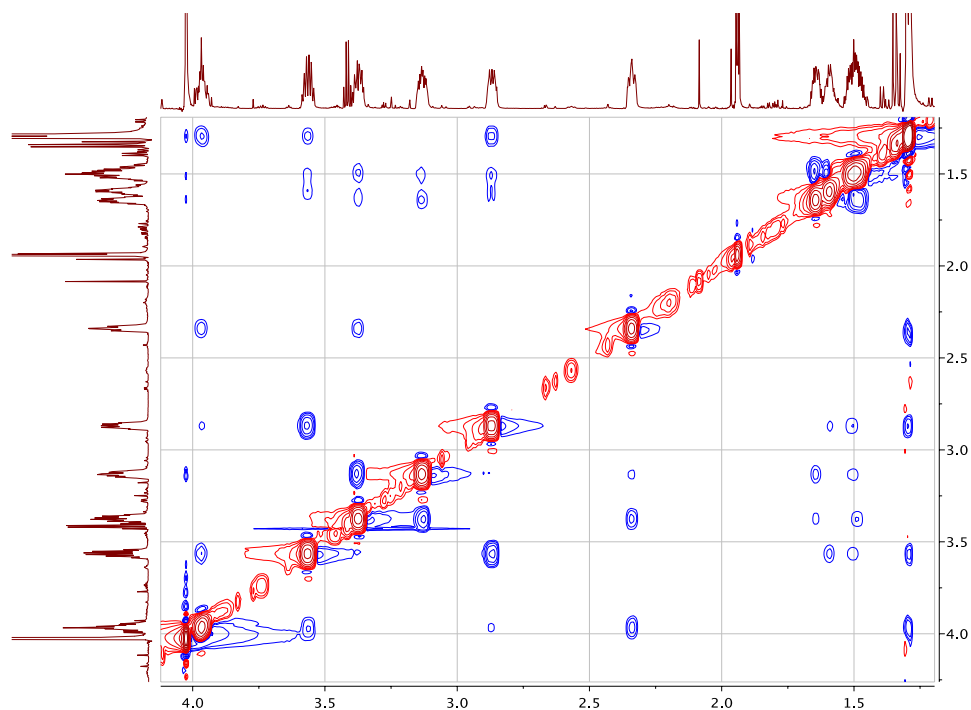
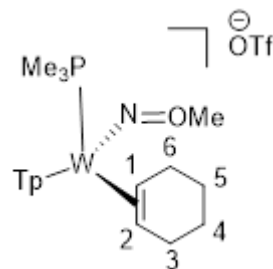
*3.13ppm has a stronger signal: this indicates that 3.13ppm is  $H_{3endo}$  and 3.38 is  $H_{3exo}$*

Peak at 1.64 ( $H_4$ ) correlates weakly with 8.51ppm (PzA  $H_3$ )

*This suggests that 1.64ppm signal is  $H_{4endo}$*

(Continued Analysis of Complex 9)

Figure SG25. Complex 9 NOESY (upper right quadrant)



The H<sub>1</sub> signal (3.97 ppm) correlates with: 3.56 (strong, H<sub>6</sub>), 2.87 (weak, H<sub>6</sub>), 2.34 ppm (strong, H<sub>2</sub>)

→ This indicates 3.56 ppm is H<sub>6exo</sub>, and 2.87 ppm is H<sub>6endo</sub>

The H<sub>2</sub> signal (2.34 ppm) correlates with: 3.97 (strong, H<sub>1</sub>), 3.38 (strong, H<sub>3</sub>), 3.13 (weak H<sub>3</sub>)

→ This indicates that 3.38 ppm is H<sub>3exo</sub>, and 3.13 ppm is H<sub>3endo</sub>

Note: this assignment also agrees with Tp NOE interaction data

Correlations of H<sub>6</sub> protons

H<sub>6exo</sub> (3.56 ppm) correlates with 3.97, 2.87, and 1.59 ppm (strong, H<sub>5</sub>), 1.50 ppm (weak, H<sub>5</sub>)



H<sub>6endo</sub> (2.87ppm) correlates with 3.97, 3.56, and 1.59 ppm (weak, H<sub>5</sub>), 1.50ppm (strong, H<sub>5</sub>)

*This suggests that hydrogens corresponding to 3.56, 1.59ppm are on same side of the cyclohexene ring (exo), and that hydrogens corresponding to 2.87, 1.50ppm are on the same side of this ring (endo).*

#### Correlations of H3 protons

H<sub>3exo</sub> (3.38ppm) correlates with signals at 3.13, 2.34, and 1.64 ppm (weak, H<sub>4</sub>), 1.50 (strong, H<sub>4</sub>)

H<sub>3endo</sub> (3.13ppm) correlates with signals at 3.38, 2.34, and 1.64 ppm (strong, H<sub>4</sub>), 1.50 (weak, H<sub>4</sub>)

*This suggests that protons corresponding to 3.38, 1.50ppm are on same side of the ring (exo) and that protons corresponding to 3.13, 1.64 ppm are on same side (endo)*

#### Correlations of PMe<sub>3</sub>

The signal for PMe<sub>3</sub> (1.29 ppm) correlates with those at 3.97 ppm (strong, H<sub>1</sub>), 3.56 (weak, H<sub>6</sub>), and 2.87 (strong, H<sub>6</sub>).

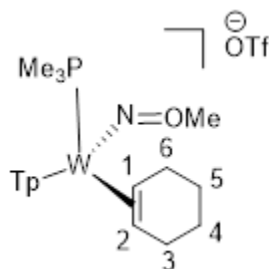
*These data indicate that the signal at 2.87ppm corresponds to H<sub>6endo</sub>*

#### Correlations of NOME

NOME (4.03 ppm) correlates with 3.13 (H<sub>3</sub>), 1.64 (H<sub>4</sub>), 1.50 (H<sub>5</sub>), 1.29 ppm (PMe<sub>3</sub>)

*These data indicate that the three ring protons 3.13 (H<sub>3</sub>), 1.64 (H<sub>4</sub>), and 1.50 ppm (H<sub>5</sub>) are endo*

#### d. Final <sup>1</sup>H NMR Assignments for Complex 9



#### Cyclohexene Ligand

H<sub>1</sub> (ppm)      H<sub>2</sub> (ppm)                      H<sub>3</sub> (ppm)      H<sub>4</sub> (ppm)      H<sub>5</sub> (ppm)      H<sub>6</sub> (ppm)

|      |      |      |      |      |      |      |
|------|------|------|------|------|------|------|
| 3.97 | 2.34 | endo | 3.13 | 1.64 | 1.50 | 2.87 |
|      |      | exo  | 3.38 | 1.50 | 1.59 | 3.56 |

### **Tp Ligand**

|     | H <sub>3</sub> (ppm) | H <sub>4</sub> (ppm) | H <sub>5</sub> (ppm) |
|-----|----------------------|----------------------|----------------------|
| PzA | 8.51                 | 6.48                 | 7.92                 |
| PzB | 8.11                 | 6.55                 | 8.01                 |
| PzC | 7.47                 | 6.33                 | 7.92                 |

**PMe<sub>3</sub>**: 1.29 ppm

**NOMe**: 4.03 ppm

Stereochemical assignments are further corroborated by quantitative NOE data, XRD and neutron diffraction crystal structure data (see below).

## 5. 1D NOESY Spectra analysis of Complex 9

Technical: Data were collected on a 600 MHz Varian NMR and experiments were conducted in CDCl<sub>3</sub>. Each spectral run utilized a 500 ms mixing time. The irradiated resonance integration was set to 1000. Inverted spectral signals indicated through space NOE interactions between the irradiated peak and protons at the indicated positions. Larger integrations for the inverted proton signals indicated stronger NOE interactions (and therefore closer H-H distances).

**Figure SG26.** Irradiation of Tp<sub>3A</sub> Resonance

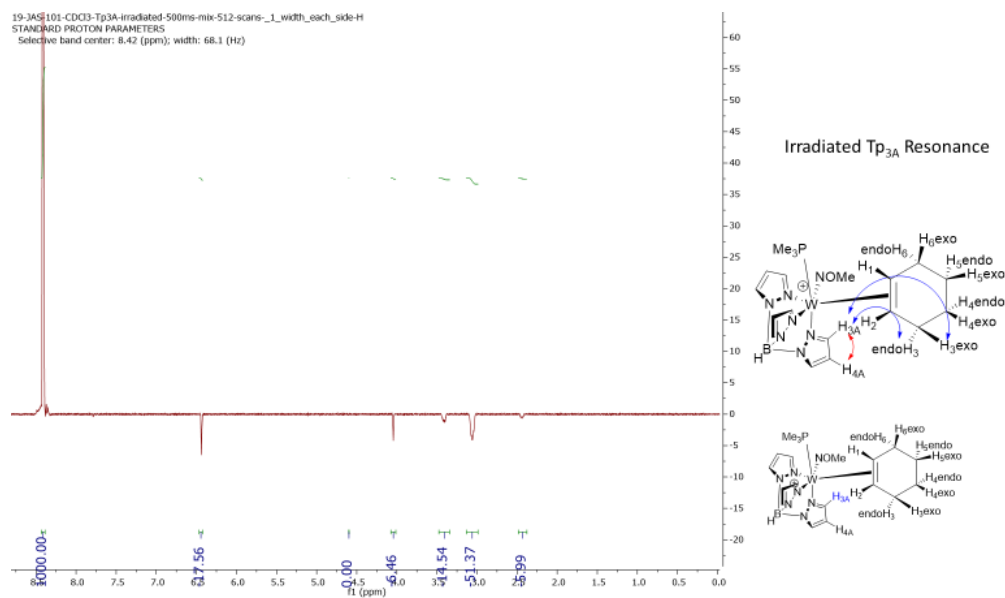


**Figure SG27.** Spectra of Protons that Display NOE Interactions with the Tp<sub>3A</sub> Resonance

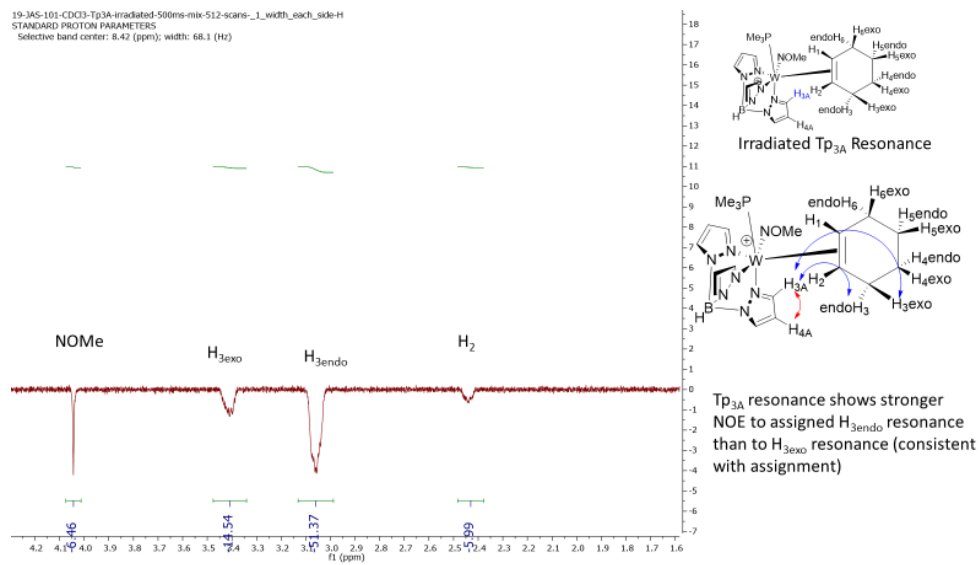


**Figure SG28.** Irradiation of H<sub>6endo</sub> Resonance

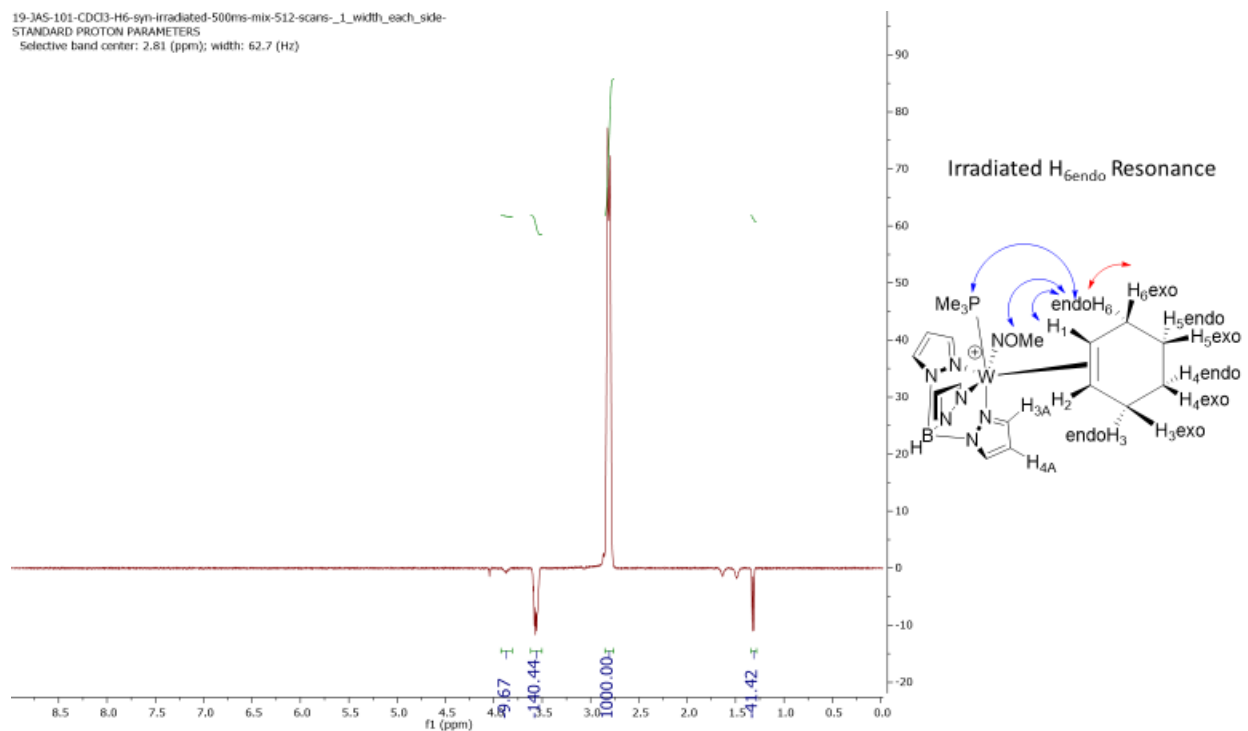


**Figure SG29.** Spectra of Protons that Display NOE Interactions with the H<sub>6endo</sub> Resonance

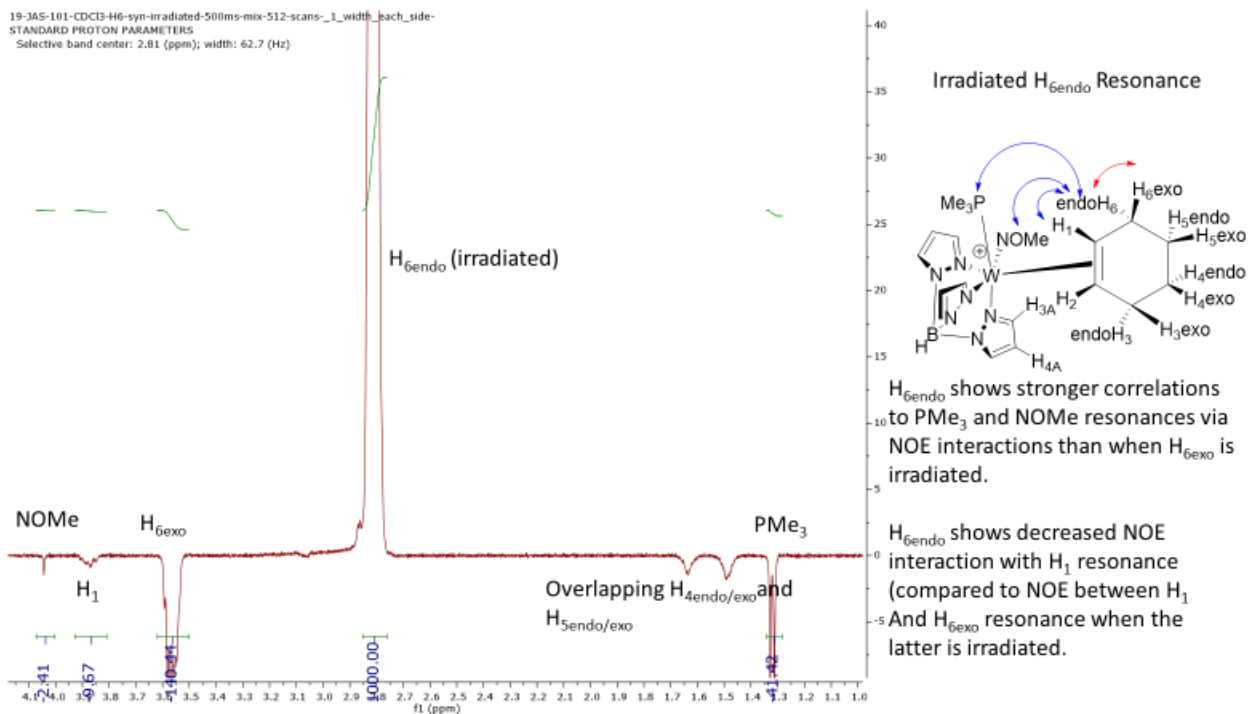


**Figure SG30. Irradiation of H<sub>6exo</sub> Resonance**

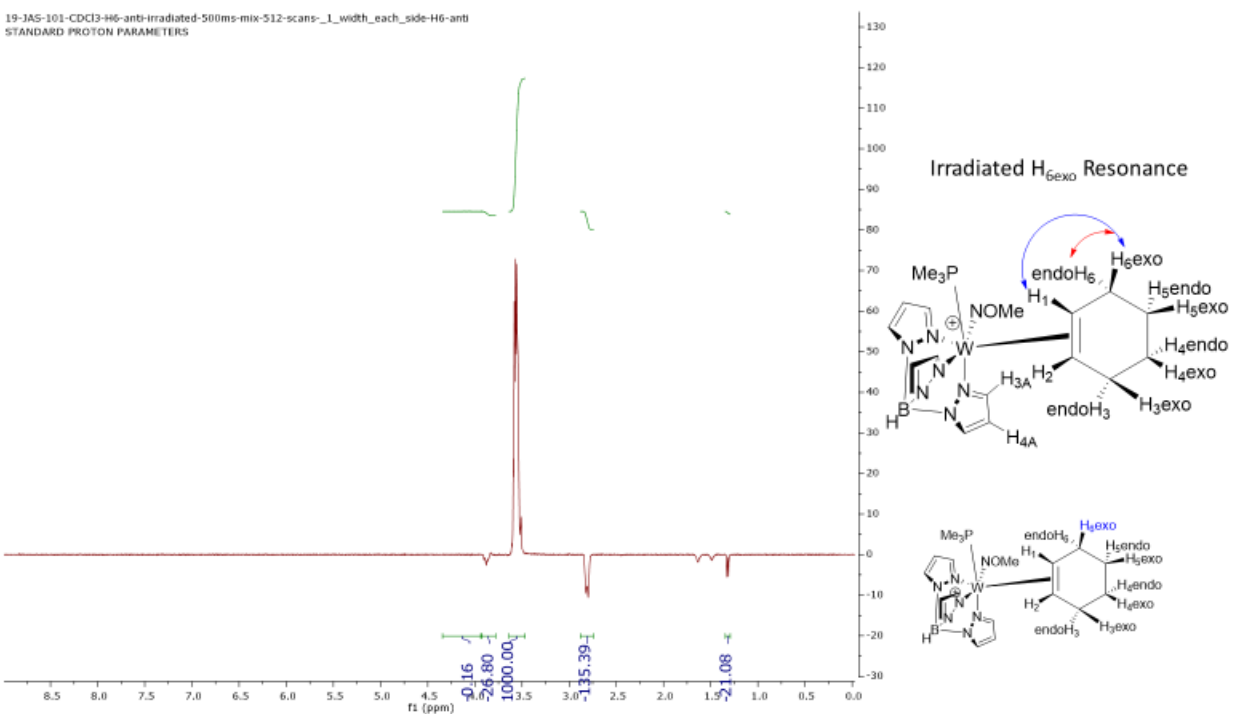


**Figure SG31.** Spectra of Protons that Display NOE Interactions with the H<sub>6exo</sub> Resonance

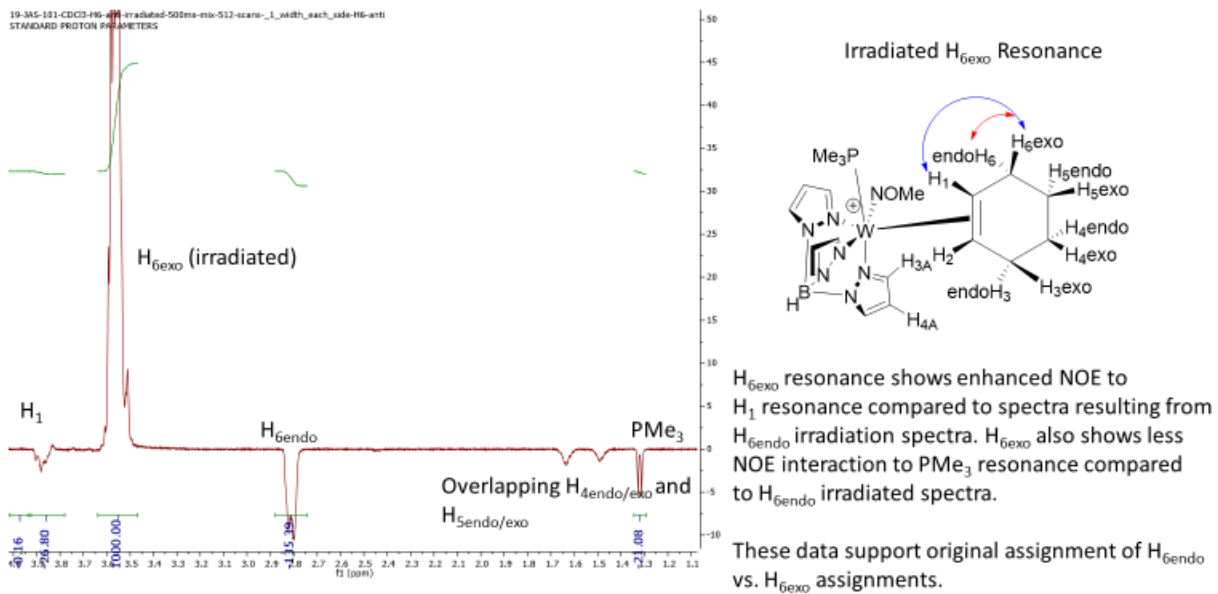


**Figure SG32.** Irradiation of H<sub>3exo</sub> Resonance

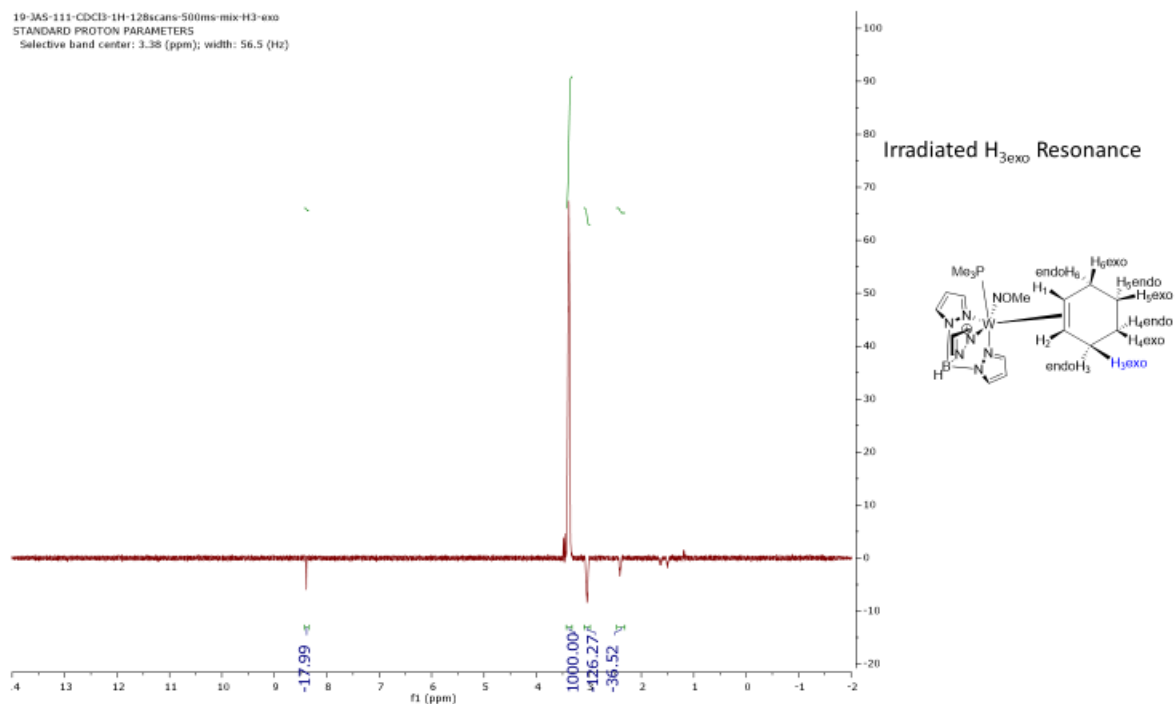


**Figure SG33.** Spectra of Protons that Display NOE Interactions with the H<sub>3<sub>exo</sub></sub> Resonance

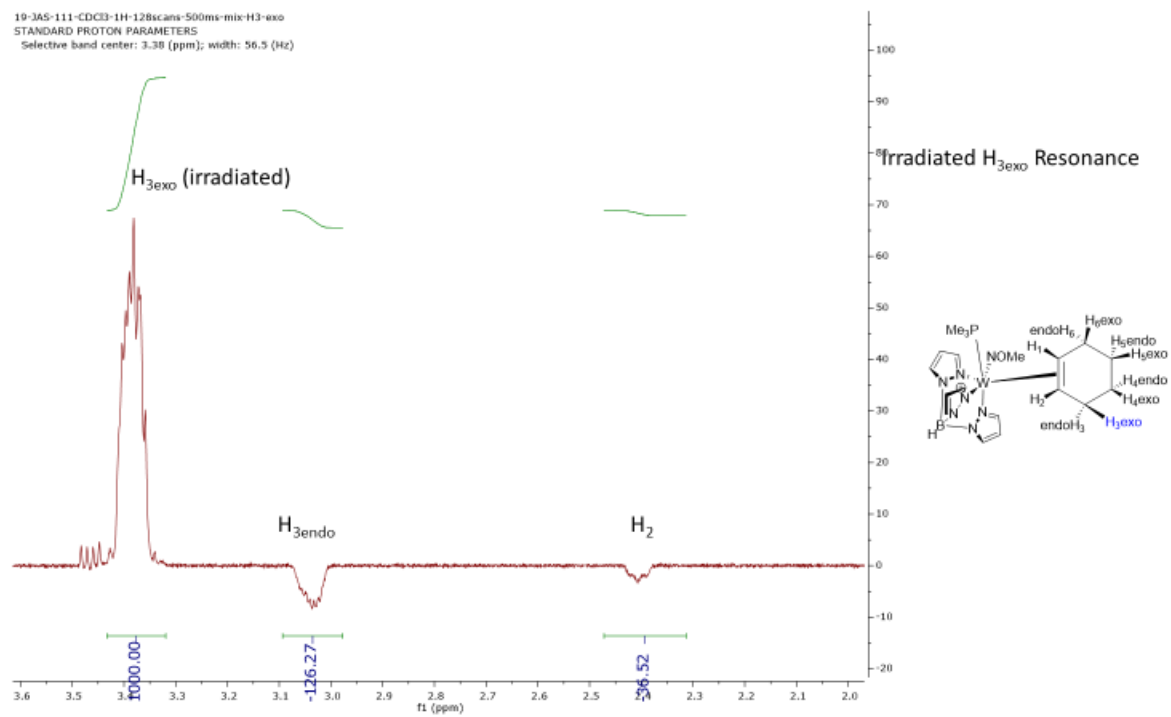


**Figure SG34.** Irradiation of H<sub>3<sub>endo</sub></sub> Resonance

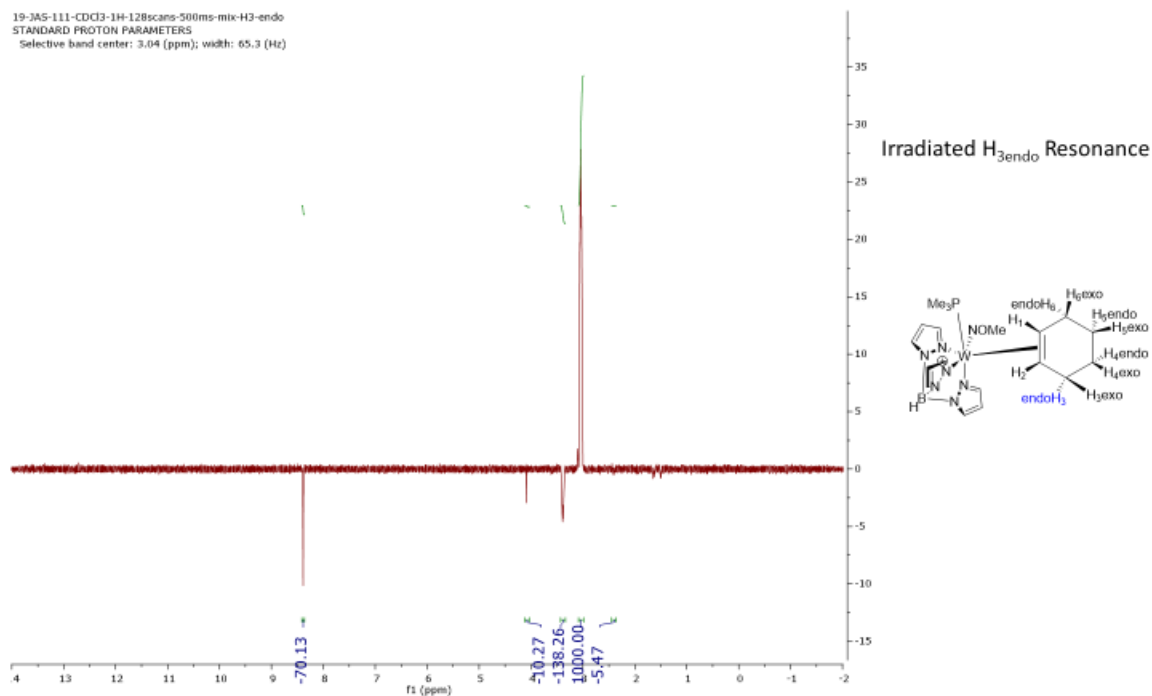


Figure SG35. Spectra of Protons that Display NOE Interactions with the H<sub>3endo</sub> Resonance

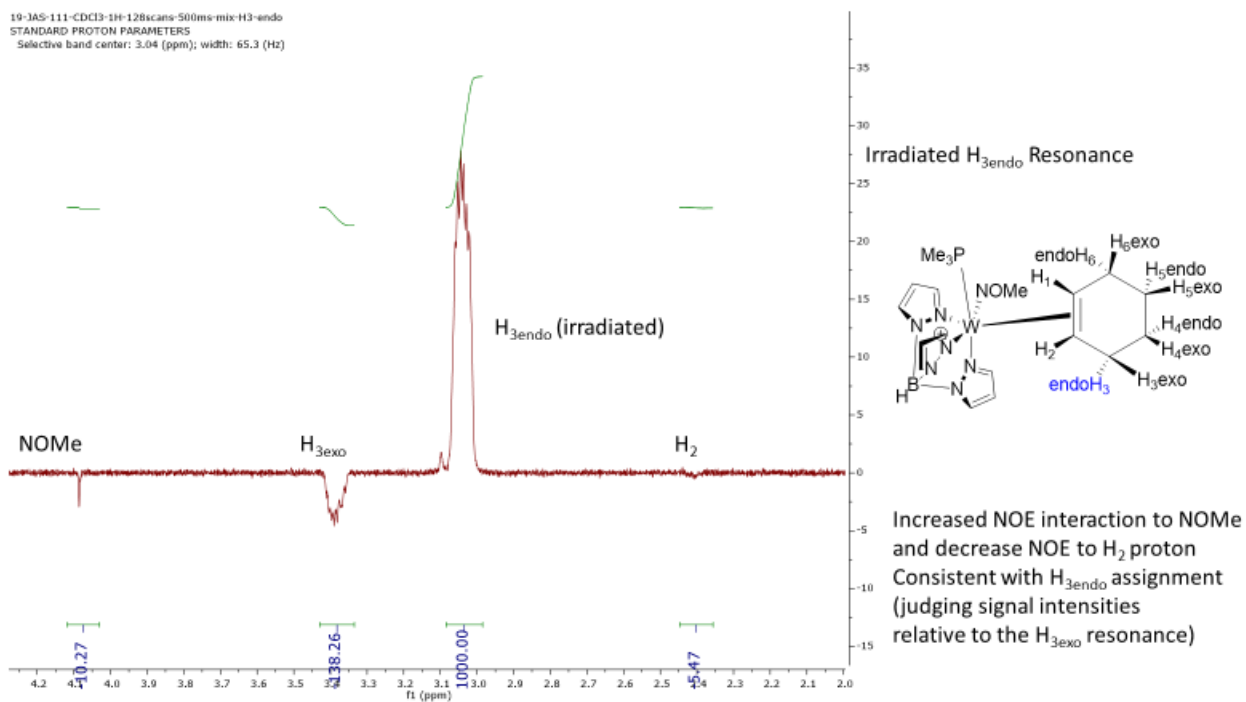


Figure SG36. Irradiation of H<sub>1</sub> Resonance



19-JAS-111-CDCl3-1H-128scans-500ms-mix-H1  
STANDARD PROTON PARAMETERS  
Selective band center: 3.87 (ppm); width: 62.0 (Hz)

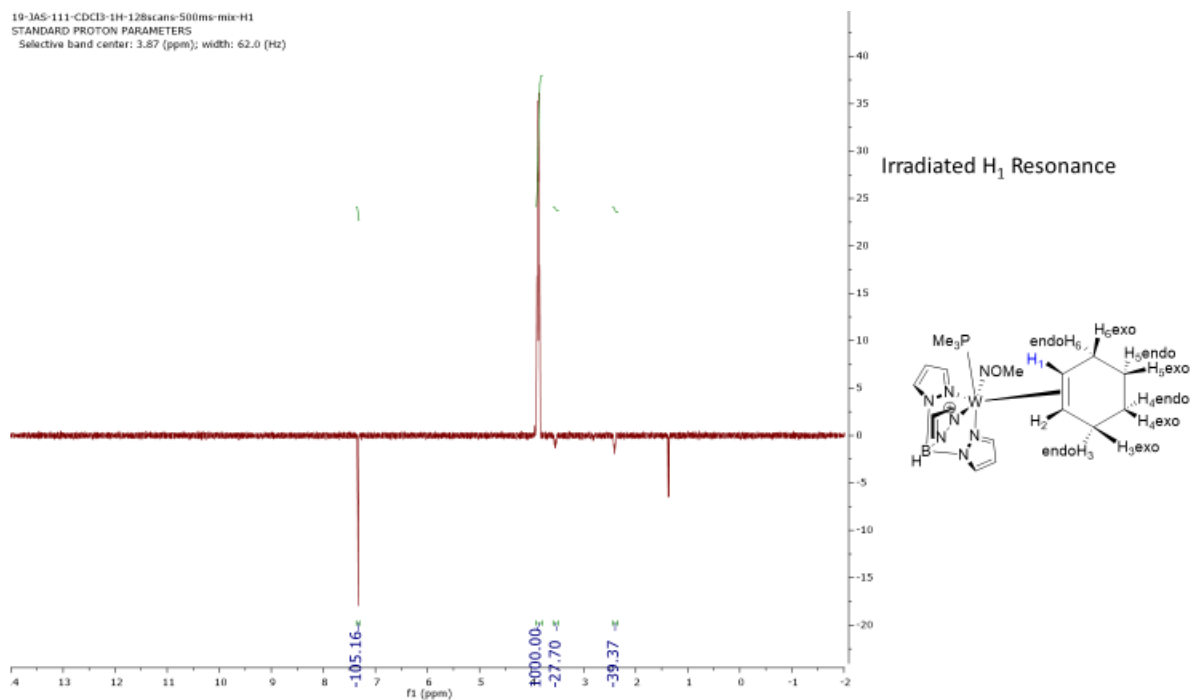
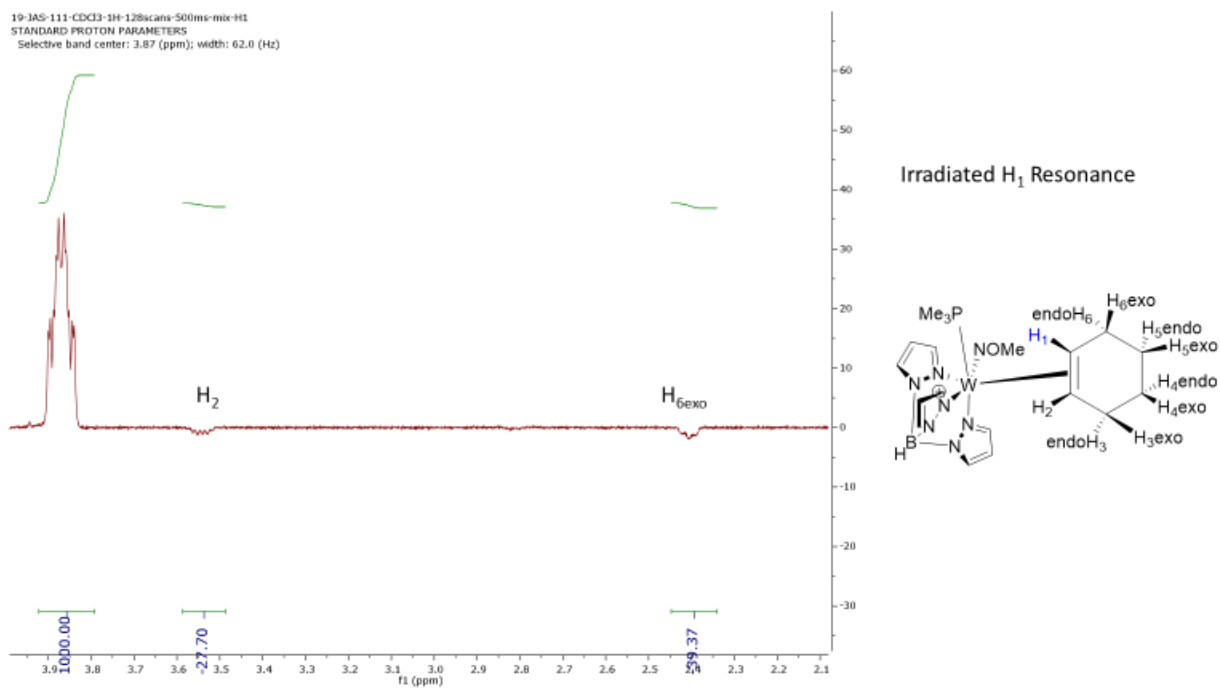


Figure SG37. Spectra of Protons that Display NOE Interactions with the H<sub>1</sub> Resonance

19-JAS-111-CDCl3-1H-128scans-500ms-mix-H1  
STANDARD PROTON PARAMETERS  
Selective band center: 3.87 (ppm); width: 62.0 (Hz)



## H. Confirmation of Stereochemical Assignment of Complex 9 from One-Dimensional NOE Data

### Quantitative NOE determinations for compound 9

Estimates for the interproton distances for the cyclohexene ligand of **9**, [Wtp(NOMe)(PMe<sub>3</sub>)( $\eta^2$ -1,2-cyclohexene)](OTf), were estimated via quantitative NOE experiments so as to confirm the assigned resonances of protons on the cyclohexene ligand (i.e. protons on sp<sup>3</sup> carbons that are exo or endo, relative to the metal). Quantitative NOE data was combined with bond lengths experimentally determined from single crystal X-ray diffraction data for **9**, using the dominant conformation of the cyclohexene ring. Mixing time was set at 500 ms.

Only H<sub>1</sub>, H<sub>2</sub>, H<sub>3exo</sub>, H<sub>3endo</sub> and H<sub>6exo</sub>, H<sub>6endo</sub> gave isolated resonances in CDCl<sub>3</sub> (no overlap with signals).

See the following reference:

“Interproton distance determinations by NOE – surprising accuracy and precision in a rigid organic molecule,” Craig P. Butts,\* Catharine R. Jones, Emma C. Towers, Jennifer L. Flynn, Lara Appleby, and Nicholas J. Barron. *Org. Biomol. Chem.*, 2011, 9, 177-184.

Experimental proton-proton distances from crystallographic data are compared with estimated distances derived from 1D NOE data in the table below. This comparison provides additional evidence supporting the proton NMR assignments for the ligand of **9**. Error in the distance determination ranged from 0-19%, with most values being under 10%, in strong support of the original assignments. **Average error: 8.7%** (conformation A; major conformer)

For comparison, we also did this analysis using *contra-indicated* assignments of stereochemistry (reversing endo and exo assignments) to determine the significance of the error analysis. Here, errors ranged from 11-44%, with 7 out of 9 values being 20% or greater. **Average error: 28.3%** (conformation A; major conformer)

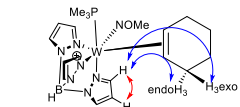
**Note on conformational disorder:**

The crystal structure determination of **9** by X-ray diffraction shows significant disorder around the C<sub>4</sub>, C<sub>5</sub> and C<sub>6</sub> carbons indicating that the cyclohexene ligand exists as two different conformers in the crystal. DFT calculations suggest a minimal energy difference between the two conformers. Therefore, the solution NMR spectra may reflect an average of more than one conformer in solution.

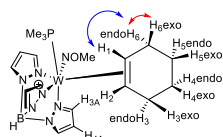
Proton distances estimated by the 1D NOESY experiments are in closer agreement with the distances obtained from the major conformer in the X-ray structure than they are from those of the minor conformer, and the former are the values reported in the table below. We note that minor conformers of small organic compounds have been demonstrated to significantly alter calculated interproton distances. We propose that the existence of a minor conformation is partly responsible for the errors observed between calculated and observed proton distances. See reference below for the impact of minor amounts of conformational isomers on the estimation of interproton distances:

“High precision NOEs as a probe for low level conformers—a second conformation of strychnine,” Craig P. Butts,\* Catharine R. Jones, Jeremy N. Harvey, *Chemical Communications* 2011, 47, 1193-1195.

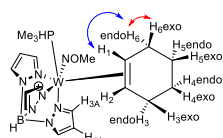
## For Conformer A



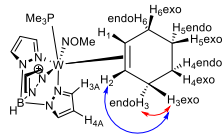
| atom 1 | atom 2             | Crystal Structure Distance (Å) | NOE Predicted Distance (Å) | % Error |
|--------|--------------------|--------------------------------|----------------------------|---------|
| Tp3A   | Tp4A               | 2.52                           | NA                         | NA      |
| Tp3A   | H <sub>3exo</sub>  | 3.20                           | 2.60                       | 10%     |
| Tp3A   | H <sub>3endo</sub> | 1.91                           | 2.11                       | 19%     |



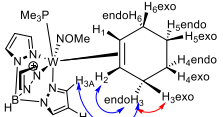
| atom 1            | atom 2             | Crystal Structure Distance (Å) | NOE Predicted Distance (Å) | % Error |
|-------------------|--------------------|--------------------------------|----------------------------|---------|
| H <sub>6exo</sub> | H <sub>6endo</sub> | 1.60                           | NA                         | NA      |
| H <sub>1</sub>    | H <sub>6endo</sub> | 2.79                           | 2.49                       | 11%     |



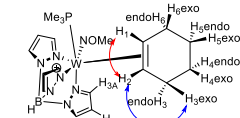
| atom 1            | atom 2             | Crystal Structure Distance (Å) | NOE Predicted Distance (Å) | % Error |
|-------------------|--------------------|--------------------------------|----------------------------|---------|
| H <sub>6exo</sub> | H <sub>6endo</sub> | 1.60                           | NA                         | NA      |
| H <sub>1</sub>    | H <sub>6exo</sub>  | 2.25                           | 2.11                       | 6%      |



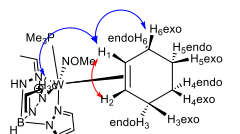
| atom 1            | atom 2             | Crystal Structure Distance (Å) | NOE Predicted Distance (Å) | % Error |
|-------------------|--------------------|--------------------------------|----------------------------|---------|
| H <sub>3exo</sub> | H <sub>3endo</sub> | 1.60                           | NA                         | NA      |
| H <sub>3exo</sub> | H <sub>2</sub>     | 2.21                           | 1.97                       | 11%     |





| atom 1             | atom 2             | Crystal Structure Distance (Å) | NOE Predicted Distance (Å) | % Error |
|--------------------|--------------------|--------------------------------|----------------------------|---------|
| H <sub>3exo</sub>  | H <sub>3endo</sub> | 1.60                           | NA                         | NA      |
| H <sub>3endo</sub> | H <sub>2</sub>     | 2.61                           | 2.74                       | 5%      |
| H <sub>3endo</sub> | Tp3A               | 1.91                           | 1.79                       | 6%      |



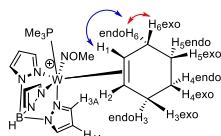
| atom 1            | atom 2         | Crystal Structure Distance (Å) | NOE Predicted Distance (Å) | % Error |
|-------------------|----------------|--------------------------------|----------------------------|---------|
| H <sub>2</sub>    | H <sub>1</sub> | 2.20                           | NA                         | NA      |
| H <sub>3exo</sub> | H <sub>2</sub> | 2.21                           | 2.21                       | 0%      |



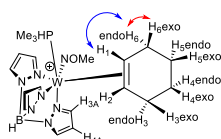
| atom 1            | atom 2         | Crystal Structure Distance (Å) | NOE Predicted Distance (Å) | % Error |
|-------------------|----------------|--------------------------------|----------------------------|---------|
| H <sub>2</sub>    | H <sub>1</sub> | 2.20                           | NA                         | NA      |
| H <sub>6exo</sub> | H <sub>1</sub> | 2.25                           | 2.33                       | 4%      |
| Tp3C              | H <sub>1</sub> | 2.2                            | 1.87                       | 15%     |

 NOE Interaction Used to Standardize Observed NOE Resonance Strength Between Protons (Standardized to Distance from Crystal Structure)  
 Estimated Distance by Quantifying NOE Interaction

## For Conformer B



| atom 1            | atom 2             | Crystal Structure Distance (Å) | NOE Predicted Distance (Å) | % Error |
|-------------------|--------------------|--------------------------------|----------------------------|---------|
| H <sub>6exo</sub> | H <sub>6endo</sub> | 1.59                           | NA                         | NA      |
| H <sub>1</sub>    | H <sub>6endo</sub> | 2.56                           | 2.47                       | 3%      |



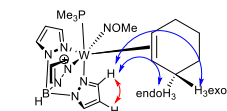
| atom 1            | atom 2             | Crystal Structure Distance (Å) | NOE Predicted Distance (Å) | % Error |
|-------------------|--------------------|--------------------------------|----------------------------|---------|
| H <sub>6exo</sub> | H <sub>6endo</sub> | 1.59                           | NA                         | NA      |
| H <sub>1</sub>    | H <sub>6exo</sub>  | 2.27                           | 2.09                       | 8%      |

### Contra-indicated Assignments for Complex 9: analysis using quantitative NOE data

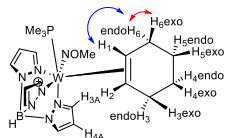
**NOTE:** The data summarized below represent INVERTED stereochemical assignments, used for comparison with what we believe to be the correct assignments (see previous page). HSQC data confirms the carbon associations (vide infra) of all ring protons for **9**, but exo/endo assignments rely on NOE data. If the assignment of endo/exo protons for the diastereotopic methylene protons on a given carbon of the cyclohexene ring is inverted, there is an increase in the observed % error between each predicted proton-proton distance and its agreement with crystal structure data.

The only value that stays the same between both the Correct and Inverted Assignment Distances is the distance approximated between H<sub>6exo</sub> and H1 (both measurements give ~11% error between observed proton-proton distance in the crystal structure).

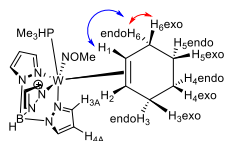
## For Conformer A (Inverted Assignments)



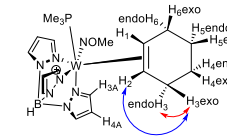
| atom 1 | atom 2             | Crystal Structure Distance (Å) | NOE Predicted Distance (Å) | % Error |
|--------|--------------------|--------------------------------|----------------------------|---------|
| Tp3A   | Tp4A               | 2.52                           | NA                         | NA      |
| Tp3A   | H <sub>3exo</sub>  | 3.20                           | 2.60                       | 36%     |
| Tp3A   | H <sub>3endo</sub> | 1.91                           | 2.11                       | 34%     |



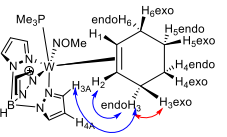
| atom 1            | atom 2             | Crystal Structure Distance (Å) | NOE Predicted Distance (Å) | % Error |
|-------------------|--------------------|--------------------------------|----------------------------|---------|
| H <sub>6exo</sub> | H <sub>6endo</sub> | 1.60                           | NA                         | NA      |
| H <sub>1</sub>    | H <sub>6endo</sub> | 2.79                           | 2.49                       | 11%     |



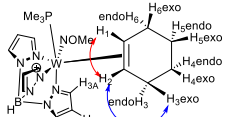
| atom 1            | atom 2             | Crystal Structure Distance (Å) | NOE Predicted Distance (Å) | % Error |
|-------------------|--------------------|--------------------------------|----------------------------|---------|
| H <sub>6exo</sub> | H <sub>6endo</sub> | 1.60                           | NA                         | NA      |
| H <sub>1</sub>    | H <sub>6exo</sub>  | 2.25                           | 2.11                       | 25%     |



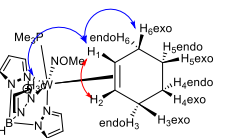
| atom 1            | atom 2             | Crystal Structure Distance (Å) | NOE Predicted Distance (Å) | % Error |
|-------------------|--------------------|--------------------------------|----------------------------|---------|
| H <sub>3exo</sub> | H <sub>3endo</sub> | 1.60                           | NA                         | NA      |
| H <sub>3exo</sub> | H <sub>2</sub>     | 2.61                           | 1.97                       | 25%     |



| atom 1             | atom 2             | Crystal Structure Distance (Å) | NOE Predicted Distance (Å) | % Error |
|--------------------|--------------------|--------------------------------|----------------------------|---------|
| H <sub>3exo</sub>  | H <sub>3endo</sub> | 1.60                           | NA                         | NA      |
| H <sub>3endo</sub> | H <sub>2</sub>     | 2.61                           | 2.74                       | 24%     |
| H <sub>3endo</sub> | Tp3A               | 1.91                           | 1.79                       | 44%     |





| atom 1            | atom 2         | Crystal Structure Distance (Å) | NOE Predicted Distance (Å) | % Error |
|-------------------|----------------|--------------------------------|----------------------------|---------|
| H <sub>2</sub>    | H <sub>1</sub> | 2.20                           | NA                         | NA      |
| H <sub>3exo</sub> | H <sub>2</sub> | 2.61                           | 2.21                       | 40%     |



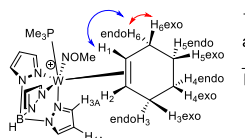
| atom 1            | atom 2         | Crystal Structure Distance (Å) | NOE Predicted Distance (Å) | % Error |
|-------------------|----------------|--------------------------------|----------------------------|---------|
| H <sub>2</sub>    | H <sub>1</sub> | 2.20                           | NA                         | NA      |
| H <sub>6exo</sub> | H <sub>1</sub> | 2.25                           | 2.33                       | 16%     |

For Conformer A

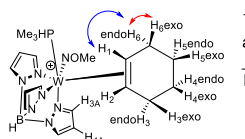
 NOE Interaction Used to Standardize Observed NOE Resonance Strength Between Protons (Standardized to Distance from Crystal Structure)

 Estimated Distance by Quantifying NOE Interaction

## For Conformer B (Inverted Assignments)



| atom 1            | atom 2             | Crystal Structure Distance (Å) | NOE Predicted Distance (Å) | % Error |
|-------------------|--------------------|--------------------------------|----------------------------|---------|
| H <sub>6exo</sub> | H <sub>6endo</sub> | 1.59                           | NA                         | NA      |
| H <sub>1</sub>    | H <sub>6endo</sub> | 2.27                           | 2.47                       | 9%      |



| atom 1            | atom 2             | Crystal Structure Distance (Å) | NOE Predicted Distance (Å) | % Error |
|-------------------|--------------------|--------------------------------|----------------------------|---------|
| H <sub>6exo</sub> | H <sub>6endo</sub> | 1.59                           | NA                         | NA      |
| H <sub>1</sub>    | H <sub>6exo</sub>  | 2.56                           | 2.09                       | 18%     |

## I. Structural Determination by Single Crystal X-Ray and Neutron Diffraction

### Single crystal X-ray diffraction

Single crystals of **4**, **7** and **9** were coated with Paratone oil and mounted on a MiTeGen MicroLoop. The X-ray intensity data were measured on a Bruker Kappa APEXII Duo system. A graphite monochromator and a Mo K $\alpha$  fine-focus sealed tube ( $\lambda = 0.71073 \text{ \AA}$ ) were used for **4** and **7**. An Incoatec Microfocus I $\mu$ S (Cu K $\alpha$ ,  $\lambda = 1.54178 \text{ \AA}$ ) and a multilayer mirror monochromator were used for **9**. The frames were integrated with the Bruker SAINT software package<sup>1</sup> using a narrow-frame algorithm. Data were corrected for absorption effects using the Multi-Scan method (SADABS).<sup>1</sup> The structures were solved and refined using the Bruker SHELXTL Software Package<sup>2</sup> within APEX3<sup>1</sup> and OLEX2.<sup>3</sup> Non-hydrogen atoms were refined anisotropically. The B-H hydrogen atom in **4** and **7** were located in the diffraction map and refined isotropically. All other hydrogen atoms were placed in geometrically calculated positions with  $U_{iso} = 1.2U_{equiv}$  of the parent atom ( $U_{iso} = 1.5 U_{equiv}$  for methyl). In **7**, the cyclohexene ring was disordered over two positions. The relative occupancy of the disordered atoms was freely refined. Constraints were used on the anisotropic displacement parameters of the disordered atoms, and restraints were used on the disordered bonds. In **9**, one carbon atom in the ring was found to be disordered over two positions. The relative occupancies were freely refined and constraints were used on the anisotropic displacement parameters of the disordered atoms. Disorder modeling of the triflate CF<sub>3</sub> group was attempted, but nothing was found to improve it significantly so it was left as is.

### Report on the disorder in the molecular structure determination of Complex 9

A yellow rod-like specimen of C<sub>20</sub>H<sub>32</sub>BF<sub>3</sub>N<sub>7</sub>O<sub>4</sub>PSW, approximate dimensions 0.082 mm x 0.092 mm x 0.135 mm, was coated with Paratone oil and mounted on a MiTeGen MicroLoop. The X-ray intensity data were measured on a Bruker Kappa APEXII Duo system equipped with a Incoatec Microfocus I $\mu$ S (Cu K $\alpha$ ,  $\lambda = 1.54178 \text{ \AA}$ ) and a multilayer mirror monochromator.

The total exposure time was 17.66 hours. The frames were integrated with the Bruker SAINT software package (Bruker (2012). *Saint*; *SADABS*; *APEX3*. Bruker AXS Inc.) using a narrow-frame algorithm. The integration of the data using a triclinic unit cell yielded a total of 13453 reflections to a maximum  $\theta$  angle of 68.85° (0.83 Å resolution), of which 5018 were independent (average redundancy 2.681, completeness = 97.4%,  $R_{int} = 9.76\%$ ,  $R_{sig} = 10.23\%$ ) and 3778 (75.29%) were greater than  $2\sigma(F^2)$ . The final cell constants of  $\underline{a} = 10.2029(10) \text{ \AA}$ ,  $\underline{b} = 11.9605(15) \text{ \AA}$ ,  $\underline{c} = 13.3686(14) \text{ \AA}$ ,  $\alpha = 65.417(9)^\circ$ ,  $\beta = 82.701(8)^\circ$ ,  $\gamma = 69.064(8)^\circ$ , volume = 1385.1(3) Å<sup>3</sup>, are based upon the refinement of the XYZ-centroids of 6197 reflections above  $20 \sigma(I)$  with  $7.271^\circ < 2\theta < 136.1^\circ$ . Data were corrected for absorption effects using the numerical method (SADABS).<sup>1</sup> The ratio of minimum to maximum apparent transmission was 0.589. The

<sup>1</sup> Bruker (2012). *Saint*; *SADABS*; *APEX3*. Bruker AXS Inc., Madison, Wisconsin, USA.

<sup>2</sup> Sheldrick, G. M. Crystal structure refinement with SHELXL. *Acta Crystallographica Section C-Structural Chemistry* **71**, 3-8, doi:10.1107/S2053229614024218 (2015).

<sup>3</sup> Dolomanov, O. V.; Bourhis, L. J.; Gildea, R. J.; Howard, J. A. K.; Puschmann, H. *J. Appl. Cryst.* (2009). **42**, 339-341.

calculated minimum and maximum transmission coefficients (based on crystal size) are 0.4666 and 0.7921.

The structure was solved and refined using the Bruker SHELXTL Software Package within APEX3 and OLEX2, using the space group P -1, with Z = 2 for the formula unit, C<sub>20</sub>H<sub>32</sub>BF<sub>3</sub>N<sub>7</sub>O<sub>4</sub>PSW. Non-hydrogen atoms were refined anisotropically. Hydrogen atoms were placed in geometrically calculated positions with  $U_{iso} = 1.2U_{equiv}$  of the parent atom ( $U_{iso} = 1.5U_{equiv}$  for methyl). One carbon atom in the ring was found to be disordered over two positions. The relative occupancies were freely refined and constraints were used on the anisotropic displacement parameters of the disordered atoms. Disorder modeling of the triflate CF<sub>3</sub> group was attempted, but nothing was found to improve it significantly so it was left as is. The final anisotropic full-matrix least-squares refinement on F<sup>2</sup> with 351 variables converged at R1 = 7.36%, for the observed data and wR2 = 21.70% for all data. The goodness-of-fit was 1.077. The largest peak in the final difference electron density synthesis was 2.100 e<sup>-</sup>/Å<sup>3</sup> and the largest hole was -2.904 e<sup>-</sup>/Å<sup>3</sup> with an RMS deviation of 0.223 e<sup>-</sup>/Å<sup>3</sup>. On the basis of the final model, the calculated density was 1.796 g/cm<sup>3</sup> and F(000), 740 e<sup>-</sup>.

#### Single crystal neutron diffraction.

Neutron diffraction data for W(Tp)(NO)(PMe<sub>3</sub>)( $\eta^2$ -*cis*-3,4-dideutero-cyclohexene), **45-d<sub>2</sub>**, were measured on the TOPAZ single-crystal time-of-flight Laue diffractometer at the Spallation Neutron Source (SNS), Oak Ridge National Laboratory.<sup>4</sup> A block-shaped crystal of **45-d<sub>2</sub>**, with dimensions of 0.30 × 0.35 × 0.50 mm was mounted on the tip of a MiTeGen loop using fluorinated grease and transferred to the TOPAZ goniometer for data collection at 100 K. To ensure good coverage and redundancy, data were collected using crystal orientations optimized with CrystalPlan<sup>5</sup> software for optimal coverage of symmetry-equivalent reflections of the monoclinic cell. The integrated raw Bragg intensities were obtained using the 3-D ellipsoidal Q-space integration in accordance with previously reported methods.<sup>3</sup> Data reduction, including neutron TOF spectrum, Lorentz, and detector efficiency corrections, was carried out with the ANVRED3 program.<sup>6</sup> Spherical absorption correction was applied with  $\mu = 0.14332 + 0.18050\lambda$ .

---

<sup>4</sup> Jogl, G. *et al.* High-resolution neutron crystallographic studies of the hydration of the coenzyme cob(II)alamin. *Acta Crystallographica Section D-Biological Crystallography* **67**, 584-591, doi:10.1107/S090744491101496X (2011).

<sup>5</sup> Zikovsky, J., Peterson, P., Wang, X., Frost, M. & Hoffmann, C. CrystalPlan: an experiment-planning tool for crystallography. *J. Appl. Crystallogr.* **44**, 418-423, doi:10.1107/S0021889811007102 (2011).

<sup>6</sup> Schultz, A. *et al.* Integration of neutron time-of-flight single-crystal Bragg peaks in reciprocal space. *J. Appl. Crystallogr.* **47**, 915-921, doi:10.1107/S1600576714006372 (2014).



mm<sup>-1</sup>. The reduced data were saved as SHELX HKLF2 format, in which the wavelength is recorded separately for each reflection, and data were not merged. Starting with the X-ray structure at 100 K as an input model, the neutron crystal structure was refined using the SHELXL-2018/3 program.<sup>2</sup>

**Table SI.1** Crystal Data for the X-ray diffraction structures **4**, **7** and **9**, and the neutron diffraction structure **45**.

|                          | <b>4</b>  | <b>7</b>  | <b>9</b>  | <b>45</b>  |
|--------------------------|---|---|---|--|
| <b>CCDC</b>              | 1885723   | 1885724   | 1885725   | 1972890  |
| <b>Chemical formula</b>  | C <sub>21</sub> H <sub>33</sub> BN <sub>7</sub> O <sub>2</sub> PW | C <sub>18</sub> H <sub>29</sub> BN <sub>7</sub> OPW | C <sub>20</sub> H <sub>32</sub> BF <sub>3</sub> N <sub>7</sub> O <sub>4</sub> PSW | C <sub>18</sub> H <sub>27.16</sub> BD <sub>1.84</sub> N <sub>7</sub> OPW |
| <b>FW (g/mol)</b>        | 641.17  | 585.11  | 749.21  | 586.96   |
| <b>T (K)</b>             | 150(2)  | 100(2)  | 100(2)  | 100(2)   |
|                          | 0.71073   | 0.71073   | 1.54178   | 0.40 – 3.46  |
| <b>Crystal size (mm)</b> | 0.242 x 0.268 x 0.528   | 0.185 x 0.211 x 0.220                               | 0.082 x 0.092 x 0.135   | 0.30 x 0.35 x 0.50   |
| <b>Crystal habit</b>     | yellow block  | yellow block  | yellow rod  | yellow block   |
| <b>Crystal system</b>    | monoclinic  | monoclinic  | triclinic   | monoclinic   |
| <b>Space group</b>       | P 2 <sub>1</sub> /c   | P 2 <sub>1</sub> /n                                 | P -1  | P 2 <sub>1</sub> /n  |
| <b>a (Å)</b>             | 11.5210(7)  | 8.6369(10)  | 10.2029(10)   | 8.6247(6)  |
| <b>b (Å)</b>             | 15.1962(10)   | 15.2743(17)   | 11.9605(15)   | 15.2535(10)  |
| <b>c (Å)</b>             | 15.1514(10)   | 17.0360(19)   | 13.3686(14)   | 17.0072(12)  |
| <b>α (°)</b>             | 90  | 90  | 65.417(9)   | 90   |
| <b>β (°)</b>             | 103.9590(10)  | 97.190(2)   | 82.701(8)   | 97.164(7)  |
| <b>γ (°)</b>             | 90  | 90  | 69.064(8)   | 90   |
| <b>V (Å<sup>3</sup>)</b> | 2574.3(3)   | 2229.8(4)   | 1385.1(3)   | 2219.9(3)  |
| <b>Z</b>                 | 4   | 4   | 2   | 4  |

|   |                        |                         |                        |                                  |
|---|------------------------|-------------------------|------------------------|----------------------------------|
| $\rho_{\text{calc}}$ (g/cm <sup>3</sup> ) | 1.654                  | 1.743                   | 1.796                  | 1.756                            |
| $\mu$ (mm <sup>-1</sup> )                 | 4.581                  | 5.276                   | 9.520                  | $0.1433 + 0.1805 \times \lambda$ |
| $\theta$ range (°)                        | 1.93 to 29.59          | 1.80 to 36.34           | 3.64 to 68.85          | 7.687 to 78.007                  |
|   | $-16 \leq h \leq 15$   | $-14 \leq h \leq 14$    | $-12 \leq h \leq 12$   | $-12 \leq h \leq 12$             |
| Index ranges                              | $-21 \leq k \leq 17$   | $-25 \leq k \leq 25$    | $-12 \leq k \leq 14$   | $-21 \leq k \leq 21$             |
|   | $-20 \leq h \leq 21$   | $-28 \leq h \leq 28$    | $-16 \leq h \leq 16$   | $-23 \leq h \leq 24$             |
| Reflns coll.                              | 30092                  | 75222                   | 13453                  | 12475                            |
| Ind. reflns                               | 7224 [R(int) = 0.0254] | 10831 [R(int) = 0.0255] | 5018 [R(int) = 0.0976] | 3653 [R(int) = 0.1099]           |
| Data / restraints / parameters            | 7224 / 0 / 307         | 10831 / 3 / 276         | 5018 / 0 / 351         | 3653 / 17 / 518                  |
| Goodness-of-fit on F <sup>2</sup>         | 1.047                  | 1.054                   | 1.077                  | 1.290                            |
| R <sub>1</sub> [I > 2 $\sigma$ (I)]       | 0.0171                 | 0.0153                  | 0.0736                 | 0.0959                           |
| wR <sub>2</sub> [all data]                | 0.0392                 | 0.0344                  | 0.2170                 | 0.1330                           |

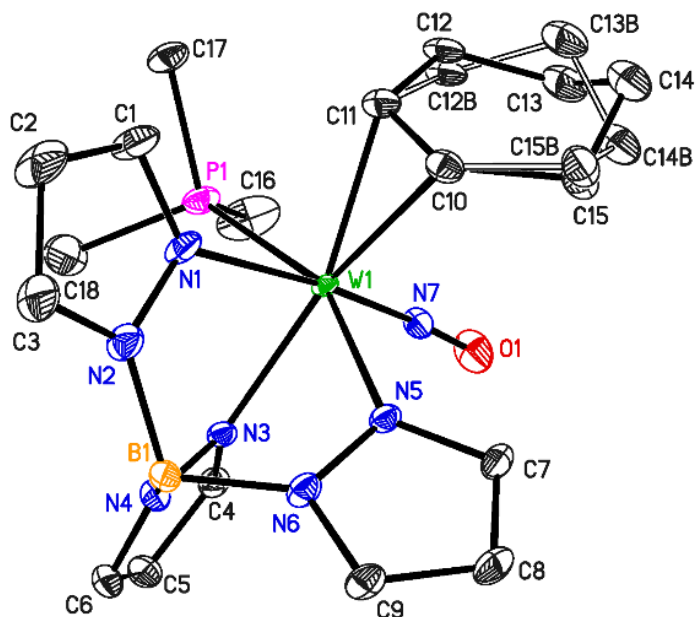


**Figure SI1.** ORTEP drawing of the molecule of **45-d<sub>2</sub>**. Carbon atoms C12, C13, C14, C15 / C12B, C13B, C14B, C15B of the cyclohexene ring with attached hydrogen/deuterium atoms are disordered over two

positions; the site occupancy factors refined to 0.885 (2) and 0.115 (2) for the disordered carbon atoms on the two conformers. Atom displacement ellipsoids are drawn at the 50% probability level. Hydrogen atoms are omitted for clarity.

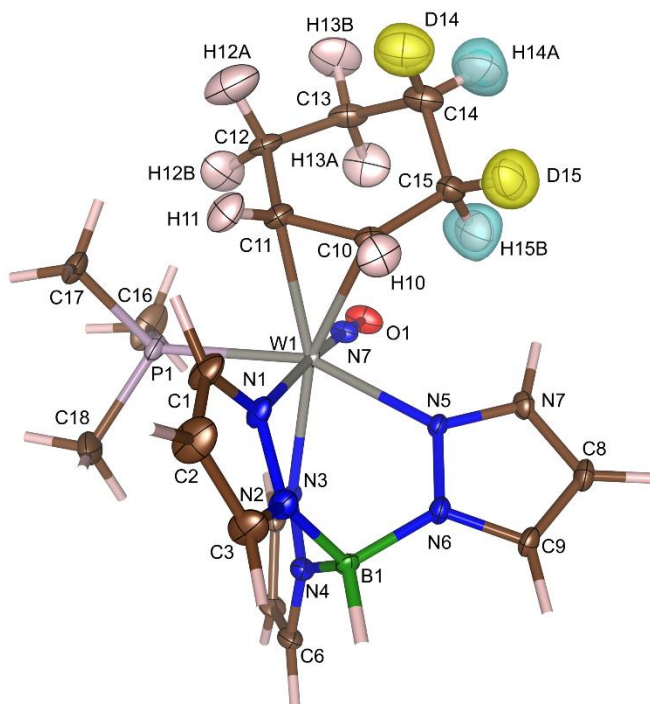


**Figure S12.** Omit map showing the nuclear scattering density of the missing deuterium D14, D15 (positive: yellow) and H14A, H15B hydrogen (negative: cyan) atoms in *cis* configuration of the neutron structure of **45-d<sub>2</sub>**. Site occupancies from neutron diffraction: {0.812(3) / 0.073(3)} for {D14 / H14B} on C14, {0.817(3) / 0.068(3)} for {D15 / H15A} on C15 in the major component of the cyclohexene-*d*<sub>2</sub> ring. Atom displacement ellipsoids are drawn at the 50% probability level. Hydrogen atoms except those on the cyclohexene-*d*<sub>2</sub> group are shown as sticks for clarity.

**Conclusion: deuterium positions are consistent with initial assignments determined from NMR data.**

## J. Estimates of Isotopic Purity Using Various Techniques

Detailed estimates of deuterium integration utilizing high resolution mass spectrometry (HRMS) are provided in **Figure S6**. Deuterium occupancy at stereospecific sites on the cyclohexene ring is determined primarily from <sup>1</sup>HNMR data (relying on the suppression of proton resonances that have been substituted for a deuterium in complex **9**; **Table S3**). As a confirmation of the stereochemical analysis in **S3**, several isotopomers of **9** (derived from complexes **42**, **45**, **14**, **50** and **16**), were also analyzed by Molecular Rotation Resonance (MRR) spectroscopy through the analysis of their deuterated cyclohexene ligand. Compounds of the form **9-d<sub>n</sub>** were heated at 200 °C, which caused a portion of the cyclohexene ligand to be liberated. The free cyclohexene was then analyzed by MRR spectroscopy. Details on the MRR technique and analysis are described in a separate document (**MRR Supporting**

**Materials).** It's important to note that while the major observed cyclohexene species in all MRR measurements corresponds to the stereoisotopomer predicted by NMR data, some isotopic scrambling was observed during the heating process used to liberate the cyclohexene ligand. The major mechanisms that accounts for the rearrangement appears to be a shift of the alkene bond. The amount of scrambling was affected by the temperature used to release the cyclohexene ligand, the amount of oxygen exposure of the metal complex before MRR analysis, and potentially to solvent impurities. Thus, % composition presented in Table SJ1 should be considered a lower limit for the anticipated stereoisotopomer.

In the case of the sample **45-d<sub>2</sub>**, crystals were grown which were subjected to neutron diffraction. The same material used in the diffraction study was then dissolved and treated with methyl triflate to give the methylated nitrosyl complex isotopologue (**9**). While neutron diffraction and <sup>1</sup>H NMR spectroscopy give >90% deuterium occupancy at the H<sub>3<sub>exo</sub></sub> and H<sub>4<sub>exo</sub></sub> positions, MRR analysis shows significant loss of isotopic purity, again due to the thermal decomplexation process used in MRR analysis. Studies regarding the efficient liberation of the cyclohexene organic using oxidants and subsequent analysis by MRR spectroscopy are forthcoming. Table SJ1 provides a composite of the findings for all three analytical methods (HNMR, neutron diffraction, and MRR). All MRR percentages below represent lower limits (owing to the scrambling process that accompanies thermal decomplexation (200 °C) of the cyclohexene.

**Table SJ1.** Deuterium occupancy and percentage composition of various isotopomers and isotopologues.

| Desired Complex | Deuterium Occupancy (NMR)<br>Deuterium Occupancy (Neutron) | Percentage of Desired Isotopologue (HRMS)<br>Percentage of Desired Isotopologue (MRR) | Percentage of Desired Stereoisotopomer (MRR)<br>(relative to other stereoisotopomers) |
|-----------------|--|---|---|
| 42<br>          | 95%  | 99% >95%  | >95%  |
| 45<br>          | 95% 92%<br>97% 91%   | NA >60%   | >66%  |
| 14<br>          | 95%<br>95%   | NA >82%   | >76%  |
| 50<br>          | 95%<br>95%<br>95%  | 96% >78%  | 100%  |
| 16<br>          | 72%<br>28%   | 76% >57%  | 100%  |

- Notes:
- \* Difficulty in achieving > 90% deuteration of 4. In this case, estimates of the entire isotopologue distribution are presented instead of occupancy.
  - Samples for HRMS were prepared analogously to those of other methods but these values were prepared from different samples of the same isotopomers.
  - NMR and MRR experiments (and when possible, neutron diffraction) were performed on the same metal-cyclohexene isotopomer samples.
  - ">" Designation implies that the observed free cyclohexene isotopomer by MRR analysis should be regarded as a lower limit of the isotopomer when bound to the metal. For example, in the case of 45, NMR and Neutron Diffraction both give estimates of deuterium occupancy > 90% at the indicated positions. The analysis by MRR, due to the conditions under which the cyclohexene was decomplexed, shows significant scrambling and loss of isotopic purity. Thus the observed species by MRR is a lower limit of the cyclohexene isotopomer observed on the metal BEFORE the scrambling observed in the MRR analysis.

## K. Determination of KIE for protonation of **4**.

Solutions of HOTf/MeOD were prepared after drying glass pipette and three 4-dram vials in a 150 °C oven overnight. This glassware was then brought into an inert atmosphere (N<sub>2(g)</sub>) glovebox. Each of these vials was rinsed with ~ ½ mL of MeOD, dried with a stream of N<sub>2(g)</sub> and then 3%, 5% and 10 % (mole percent) solutions of HOTf in MeOD were prepared by mass. The goal was to generate known quantities of protio-impurities at various known concentrations to gauge the KIE associated with deuteration after observing difficulty in fully deuterating either **4** or **5** with an acidic deuterium source. Protonation experiments were conducted at -30 °C on **4**, the same temperature that protonation was performed at in the synthesis of these complexes. The results were then incorporated into the following equation and solved for the KIE value:

### Equation SK1

$$\left(\frac{\text{Theoretical Proton Suppression}}{\text{Theoretical Proton Impurity}}\right) = \left(\frac{\text{Observed Suppression}}{\text{Observed Proton Impurity}}\right) * \text{KIE}$$

This equation seeks to determine the KIE by extrapolating the k<sub>H</sub>/k<sub>D</sub> ratio as a result of observed products distributions in the resulting <sup>1</sup>H NMR. Further discussion on the determination of KIE values can be found in the reference below.

“On the Interpretation of Deuterium Kinetic Isotope Effects in C-H Bond Functionalizations by Transition-Metal Complexes”; Eric M. Simmons, John F. Hartwig, *Angewandte Essays* 2012, 51, 13, 3066-3072.

| Theoretical <sup>1</sup> H Impurity | Observed <sup>1</sup> H Impurity | KIE Determination |
|-------------------------------------|----------------------------------|-------------------|
| 3%                                  | 49%                              | 31                |
| 5%                                  | 57%                              | 40                |
| 10%                                 | 82%                              | 41                |

These results give an average KIE ~ 37.

Analogous experiments with treating **1** with varying amounts of H+ impurity in MeOD led to the expected suppression of the protio-signal (i.e., there was not a significant kinetic isotope effect).

#### Experiment A: 3% Proton Impurity

To a 4-dram vial that had been rinsed with MeOD- $d_4$  (~ ½ mL) and subsequently dried with N<sub>2(g)</sub> was added HOTf (0.131 g, 0.873 mmol) along with MeOD- $d_4$  (0.997 g, 27.6 mmol) to generate a solution with an estimated 3.1% proton impurity given the ratios of HOTf and MeOD- $d_4$  in solution. At ambient temperatures the rate of protonation of methanol by triflic acid is estimated as being diffusion controlled. Next complex **4** (0.101 g, 0.173 mmol) was added to MeCN- $d_3$  (1/2 mL) and cooled to -30 °C. Separately the 3.1 % protio-impurity solution of HOTf/ MeOD- $d_4$  was also cooled to -30 °C. This acidic solution was then added in excess (1/2 mL) to the chilled solution of **4** in MeCN- $d_3$ . Upon addition the reaction mixture turns to a homogeneous yellow color, and this solution was then added to 15 mL of ether and allowed to cool at -30 °C. Over a period of 1 h a yellow crystalline material develops on the side of the vial. The organic layer was decanted, the resulting solid dried with N<sub>2(g)</sub> stream and analyzed via <sup>1</sup>H NMR in MeCN- $d_3$  to give the observed 49% proton impurity.

Once isolated, the product, **26**, displays no isotopic scrambling is observed when the complex is re-dissolved in MeCN- $d_3$  over a week.

#### Experiment B: 5% Proton Integration

To a 4-dram vial that had been rinsed with MeOD- $d_4$  (~ ½ mL) and subsequently dried with N<sub>2(g)</sub> was added HOTf (0.224 g, 1.49 mmol) along with MeOD- $d_4$  (1.03 g, 28.6 mmol) to generate a solution with an estimated 5.0% proton impurity given the ratios of HOTf and MeOD-  $d_4$  in solution. At ambient temperatures the rate of protonation of methanol by triflic acid is estimated as being diffusion controlled. Next complex **4** (0.100 g, 0.172 mmol) was added to MeCN- $d_3$  (1/2 mL) and cooled to -30 °C. Separately the 5.0 % protio-impurity solution of HOTf/MeOD-  $d_4$  was also cooled to -30 °C. This acidic solution was then added in excess (1/2 mL) to the chilled solution of **4** in MeCN-  $d_3$ . Upon addition the reaction mixture turns to a homogeneous yellow color, and this solution was then added to 15 mL of ether and allowed to cool at -30 °C. Over a period of 1 h a yellow crystalline material develops on the side of the vial. The organic layer was decanted, the resulting solid dried with N<sub>2(g)</sub> stream and analyzed via <sup>1</sup>H NMR in MeCN- $d_3$  to give the observed 57% proton impurity at the site of protonation/deuteration.

#### Experiment C: 10% Proton Integration

To a 4-dram vial that had been rinsed with MeOD- $d_4$  ( $\sim 1/2$  mL) and subsequently dried with  $N_{2(g)}$  was added HOTf (0.465 g, 3.10 mmol) along with MeOD- $d_4$  (0.998 g, 27.7 mmol) to generate a solution with an estimated 10.1% proton impurity given the ratios of HOTf and MeOD in solution. At ambient temperatures the rate of protonation of methanol by triflic acid is estimated as being diffusion controlled. Next complex **4** (0.100 g, 0.172 mmol) was added to MeCN- $d_3$  (1/2 mL) and cooled to  $-30$  °C. Separately the 10.1 % protio-impurity solution of HOTf/ MeOD- $d_4$  was also cooled to  $-30$  °C. This acidic solution was then added in excess (1/2 mL) to the chilled solution of **4** in MeCN- $d_3$ . Upon addition the reaction mixture turns to a homogeneous yellow color, and this solution was then added to 15 mL of ether and allowed to cool at  $-30$  °C. Over a period of 1 h a yellow crystalline material develops on the side of the vial. The organic layer was decanted, the resulting solid dried with  $N_{2(g)}$  stream and analyzed via  $^1H$  NMR in MeCN- $d_3$  to give the observed 82% proton impurity protonation/deuteration.

#### Experiment D: Nominal 1% Impurity

When approximately a 1% H<sup>+</sup> solution is prepared DPhAT- $d_2$  (0.147 g, 0.456 mmol) with 99% MeOD (2.30 g, 69.6 mmol) in excess is allowed to react with complex **12** (0.221 g, 0.378 mmol) followed by a deuteride source, NaBD<sub>4</sub> (0.075 g, 1.81 mmol), at reduced temperatures ( $-40$  C), complex **16** is generated. The site of initial protonation, now the H5-*endo* resonance, shows  $\sim 95\%$  proton suppression, implying a mild KIE for the initial protonation. Full determination is obfuscated by overlapping signals.

However, at the H6-*exo* position, the proton resonance is expected to be suppressed from the second deuteration with an acidic deuterium source, a 28% proton signal remains.

Solving **Equation SK1**, using 1% for the expected proton resonance and 28% for the observed impurity, yields an approximated KIE of  $\sim 38.5$ , similar to the averaged KIE from previous experiments. A separate sample of **16** prepared by an analogous route and subjected to HRMS shows  $\sim 24\%$ , % proton impurity, consistent with what is observed by NMR (and indicating difficulty in attaining  $> 90\%$  levels of deuteration at the H6-*exo* site)

(Figure SK1).



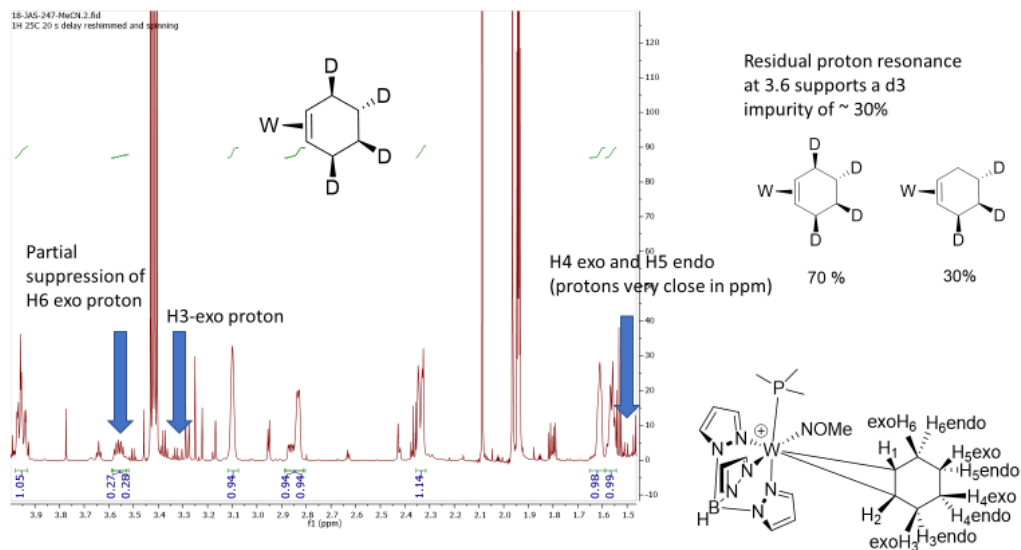


**Figure SK1.** HNMR spectrum of compound **16** showing incomplete deuterium incorporation at H6exo.

Integration of the proton resonance at 3.55 (the H<sub>6exo</sub> resonance) was used to determine the KIE of the 1% proton solution (99% D). This is the expected site of deuteration arising from the treatment of the diene complex **4** with DPhAT-*d*<sub>2</sub>/MeOD.

The proton resonances at 1.60 (H<sub>4endo</sub>) and 1.55 (H<sub>5exo</sub>) are shifted upfield due to secondary isotopic shifts. Residual protons signals from (H<sub>4exo</sub>) and (H<sub>5endo</sub>) resonances that would arise from incomplete deuteration at those sites are estimated to be < 10%.

#### L. Summary of MRR spectroscopic analysis for samples 9-d<sub>n</sub>

as derived **42**, **45**, **14**, **50** and **16**

#### Introduction

Molecular rotational resonance spectroscopy is used to identify and quantitate the relative abundance of the deuterated isomers of cyclohexene. The exceptionally high spectral resolution of spectrometers for rotational spectroscopy make it possible to analyze complex sample mixtures without the need for chemical separation. The spectrum is measured for a gas phase sample produced by pulsed-jet expansion of a dilute mixture of the analyte in an inert gas (neon is used in these measurements). As a result, there are no matrix effects on the transition frequencies and once the signature of a deuterated isotopomer is known, it can be identified to extremely high confidence in other samples by transition frequency. All

isotopomers are detected against zero-background and the measurement dynamic range exceeds 100:1 for the samples in this study.

### *Measurement Principles*

The deuterium isomer composition of cyclohexene is analyzed using molecular rotational resonance (MRR) spectroscopy after cyclohexene is removed from the metal by thermal decomposition. The MRR spectrum signature is a sensitive function of the mass distribution relative to the center-of-mass. The spectrum depends on the principal moments-of-inertia, which are inversely proportional to the rotational constants of the rigid-rotor Hamiltonian operator for rotational kinetic energy, and the dipole moment vector in the principal axis system. In the spectrum, the geometry (from which the principal moments-of-inertia can be calculated) determines the quantized energies and the dipole moment determines the transition intensities for allowed rotational transitions.<sup>1</sup> A specific isotopomer of cyclohexene is identified by the comparison between measured rotational constants obtained from a fit using the experimental MRR transition frequencies and the rotational constants calculated from a theoretical structure.

Under the Born-Oppenheimer approximation, all isotopomers have the same equilibrium geometry. The rotational kinetic energies depend on a molecular structure that includes zero-point vibrational energy effects, however, the differences between the equilibrium and zero-point geometries is small. In practice, quantum chemistry is used to provide the initial geometry from the equilibrium structure and this geometry is slightly modified to match the experimental constants. The refined geometry has good accuracy for predicting the rotational constants of the different isotopologues and isotopomers. Transition intensities are needed to convert measured signal strengths into relative populations of the isomers. The dipole moment is calculated from quantum chemistry and is assumed to be the same for all isotopologues. Deuterium substitution does change the bond dipole of the substituted C-H bond, but these changes has been shown to be small and these effects are neglected in the present analysis.<sup>2</sup>

### *Rotational Spectroscopy of Deuterated Isomers of Cyclohexene*

Cyclohexene has 10 hydrogens and, therefore, there are 1024 different ways to distribute deuterium using a fixed geometry as the reference as seen in **Figure SL1**. However, not all of these isomers give unique rotational spectra due to the  $C_2$  symmetry axis. Of the 1024 possible isomers, 992 of the geometries are pairs or rotationally equivalent geometries producing only 496 isomers with distinguishable rotational spectra. Using the atom labeling in **Figure SL1**, the geometries that are equivalent under  $C_2$ -rotation are obtained by the following label changes: H1 $\leftrightarrow$ H7, H2 $\leftrightarrow$ H6, H3 $\leftrightarrow$ H8, H4 $\leftrightarrow$ H9, and H5 $\leftrightarrow$ H10. There are 32 species that yield identical structure for  $C_2$ -rotation. Therefore, there are 528 different deuterium isomers that have distinguishable rotational spectra (see Table S2 in Supporting Information).

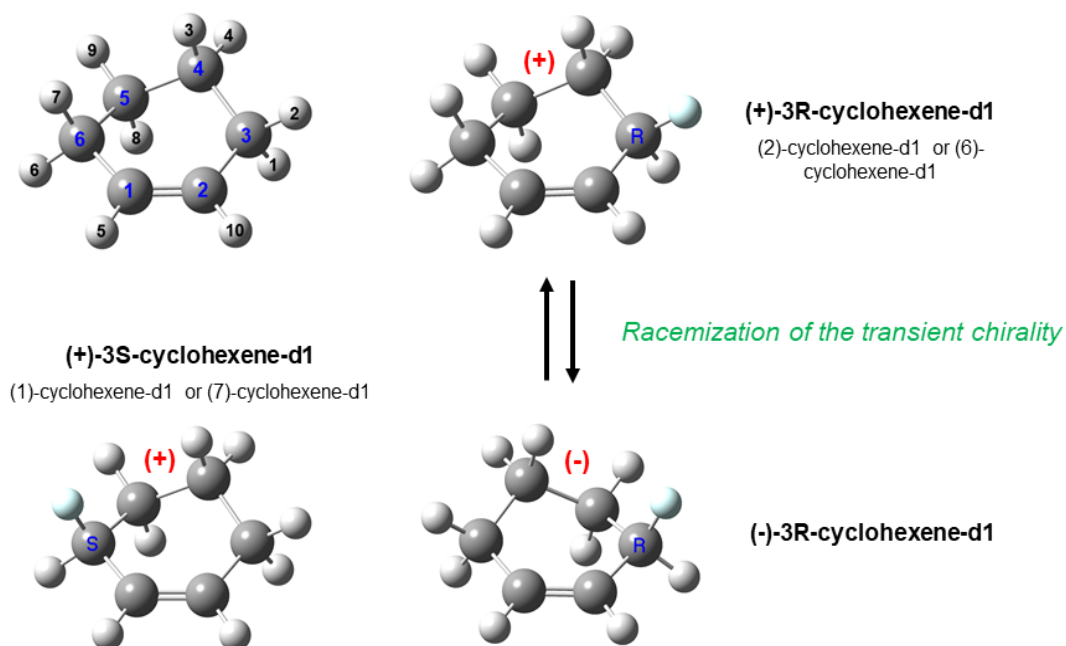


**Figure SL1.** Geometry and labeling for cyclohexene conformations.

Labeling convention of cyclohexene used in this document is shown at the top left. For rotationally distinct isotopomers, the positions the deuterium atoms are listed using the H-atom positions 1-10. When chemically distinct isotopomers are described, the carbon atom position (1-6) where the deuteration occurs is given. In most cases, each chemically distinct isotopomer occurs in two rotationally distinct forms due to the transient chirality associated with the ring pucker. The structure of (3)-cyclohexene-d1 is shown at the top right. In this representation, the chirality of the asymmetric carbon is denoted with its Cahn-Ingold-Prelog notation. The chiral element of the ring pucker is denoted by the (+) notation which gives the slope of the C-C bond where the ring pucker transient chirality occurs. Due to its low interconversion barrier, racemization of the ring pucker chirality will occur so that the sample will have equal amounts of the two diastereomers. In most cases, these diastereomers are rotationally distinct. To determine the H-atom labeling for the diastereomer in the reference configuration, the mirror image of the racemized diastereomer is considered (enantiomers have identical rotational spectra). The mirror image structure is rotationally indistinct from the structure obtained by  $C_2$ -rotation. As a result, the (2)-cyclohexene-d1 rotationally distinct isotopomer has a ring pucker diastereomer that is (1)-cyclohexene-d1.

Cyclohexene has a ring pucker geometry that adds an element of transient chirality. After cyclohexene is liberated from the transition metal, rapid equilibration between the ring pucker isomers occurs. As a result, for a specific deuterium isotopomer produced in the synthesis, there is the possibility that two rotationally distinct isomers will be present in the gas sample when analyzed by MRR spectroscopy. The identity of the second ring-pucker isomer can be determined examining the mirror image of the ring pucker isomer. **Figure SL1** shows the ring pucker isomers that occur from the incorporation of deuterium

in the carbon-3 position. The ring pucker of (+)-3R-cyclohexene-d1 ((2)-d1 or (6)-d1) is (-)-3R-cyclohexene-d1. The enantiomer of this ring pucker is (+)-3S-cyclohexene-d1 ((1)-d1 or (7)-d1)). This means that for deuterium incorporation at the 3C position, the two ring pucker isomers that will be observed using MRR are (2)-d1 and (1)-d1. This approach for determining the observed ring puckers also applies to cyclohexene with deuterium incorporated at more than one position. In terms of the reference geometry, the ring-pucker isomerization converts the following H-atom positions: H1 $\leftrightarrow$ H2, H3 $\leftrightarrow$ H4, H6 $\leftrightarrow$ H7, H8 $\leftrightarrow$ H9, with H5 and H10 unchanged. Finally, most of the possible deuterium isomers of cyclohexene are chiral. However, MRR spectroscopy cannot distinguish enantiomers in a direct measurement. Furthermore, the transition metal complexes used in this study are racemic so no enantiomeric excess is expected.

### *Sample Preparation and MRR Spectroscopy Measurements*

The design of the chirped-pulse Fourier transform microwave spectrometer and the experimental principles have been described in detail previously.<sup>3-4</sup> The technique is briefly summarized here, with emphasis on the sample preparation and MRR measurements unique to the cyclohexene complex that is the subject of this study.

Approximately 30 mg of the cyclohexene transition metal complex per measurement were loaded directly into three stainless steel reservoir nozzles as a solid (~10 mg/reservoir). The samples were stored under inert conditions prior to loading. Loading the sample required exposure to ambient conditions for several minutes before the reservoirs could be reinstalled in the spectrometer and flushed with neon gas. The reservoirs were heated to 60°C, and neon carrier gas was flowed over the reservoirs at 15 psig. Each nozzle was pulsed at 3 Hz and the presence of residual solvents (acetone, water) were monitored by their signatures in the MRR spectrum. The temperature was gradually ramped up to 100°C and pulsing continued until the sample was determined to be sufficiently free of solvent.

To liberate the cyclohexene from the metal complex, the reservoirs were heated to 200°C. The nozzles were not pulsed during this time to allow cyclohexene to accumulate and mix with the Neon carrier gas above the sample, the pressure of which was increased to 45 psig. After 20-30 minutes of heating, the reservoirs were cooled to 140°C, the maximum operating temperature for optimal performance of the pulsed nozzles. Each heating cycle liberated enough cyclohexene gas for ~100 valve pulses. During each injection of gas through the nozzle, the supersonic expansion was excited by a microwave pulse with a 4  $\mu$ s frequency sweep and 8 free induction decay (FID) emissions were collected and coherently averaged in the time domain. Two different microwave pulses were employed in this study. A 6-18 GHz excitation provided broad spectral coverage to observe six rotational transitions for each cyclohexene isotopologue/isotopomer present in the sample. These six rotational transitions are sufficient to produce an accurate determination of the rotational constants of the isotopomer using nonlinear least squares fitting. The spectra used in the composition analysis were obtained by coadding 200-1000 FID averages in the time domain.

In addition to cyclohexene, other species originating from the metal complex ligands were identified in the MRR spectrum after heating. These thermal decomposition products include trimethyl phosphine and pyrazole (produced through thermal decomposition of the Tp-ligand).

The measurement uncertainty for percentage sample composition determination by MRR spectroscopy has been estimated in two ways: 1) Uncertainty in the percentage of  $^{13}\text{C}$ -isotopomers in the commercial cyclohexene sample using the same number of FID averages as a typical analysis in this work ( $^{13}\text{C}$  is expected at 2% abundance due to the  $\text{C}_2$ -rotation symmetry), and 2) the difference in transition intensity for the ring pucker isomer pairs of the observed, chemically distinct isotopomers (where racemization is expected to produce equal populations of the ring pucker isomers). From these experimental observations, the measurement uncertainty for percentage composition is estimated to be 10% of the reported value.

#### *The Refined Reference Geometry for Isotopomer Analysis of Cyclohexene*

The rotational constants of the parent species were first reported in 1968,<sup>5</sup> but have been refit here using updated analysis programs.<sup>6-8</sup> The rotational spectra of the singly-substituted  $^{13}\text{C}$ , doubly-substituted  $^{13}\text{C}$ , and singly-substituted D isotopomers were assigned in a measurement using a commercial cyclohexene sample. The spectra of each cyclohexene isotopomer were identified with high confidence by comparing the experimentally determined rotational constants from this broadband spectrum to those obtained from a quantum chemistry molecular structure (B3LYP D3BJ 6-311++G(d,p) using Gaussian 09<sup>9</sup>). Summaries of the experimental fits for these carbon isotopomers are presented in **Table SL1**. The fit results for the singly-substituted deuterium isotopologues are listed in **Table SL2** (where the rotational constants for all deuterium isotopomers identified in this study are summarized). The assigned transition frequencies for each species are given in **Tables SL11-50**.

A single cyclohexene geometry is used to predict the rotational spectroscopy for all possible deuterium isomers. This geometry is refined from the quantum chemistry equilibrium geometry through a nonlinear least squares fit of the atom coordinates in the principal axis system to the rotational constants for all isotopomers identified in the initial measurement using a commercial sample of cyclohexene. The positions of the nuclei in the principal axis system of the normal species are given in **Table SL3** for the reference geometry.

**Table SL1.** Spectroscopic constants determined for the carbon isotopologues of cyclohexene. Spectral assignments were done by fitting experimental transition to the rigid-rotor Hamiltonian using Pickett's SPCAT/SPFIT analysis program.<sup>6</sup> All species were observed in natural abundance in a commercial sample.

| Isomer                             | A (MHz)       | B (MHz)       | C (MHz)       | N <sup>a</sup> | $\sigma$ (kHz) |
|------------------------------------|---------------|---------------|---------------|----------------|----------------|
| Parent                             | 4739.1511(26) | 4544.4159(33) | 2562.3985(17) | 22             | 14.6           |
| <sup>13</sup> C3=6                 | 4738.774(25)  | 4455.3936(33) | 2534.0678(15) | 11             | 14.7           |
| <sup>13</sup> C4=5                 | 4679.2185(27) | 4513.7430(39) | 2537.7829(18) | 10             | 15.2           |
| <sup>13</sup> C1=2                 | 4676.8357(26) | 4518.3805(35) | 2535.9716(16) | 11             | 14.9           |
| <sup>13</sup> C3- <sup>13</sup> C4 | 4675.3239(36) | 4429.882(12)  | 2510.3068(22) | 6              | 7.4            |
| <sup>13</sup> C4- <sup>13</sup> C6 | 4676.544(14)  | 4427.011(46)  | 2509.6874(85) | 6              | 5.8            |
| <sup>13</sup> C2- <sup>13</sup> C3 | 4673.3790(94) | 4434.119(31)  | 2508.5169(57) | 6              | 19.1           |
| <sup>13</sup> C1- <sup>13</sup> C3 | 4673.1670(31) | 4432.393(10)  | 2507.9307(18) | 6              | 6.3            |
| <sup>13</sup> C1- <sup>13</sup> C2 | 4601.208(32)  | 4508.40(12)   | 2510.378(24)  | 6              | 58.2           |
| <sup>13</sup> C3- <sup>13</sup> C6 | 4738.3999(66) | 4367.752(19)  | 2505.6794(39) | 6              | 13.4           |
| <sup>13</sup> C4- <sup>13</sup> C5 | 4606.8606(87) | 4497.374(32)  | 2513.9581(54) | 6              | 17.6           |
| <sup>13</sup> C1- <sup>13</sup> C4 | 4637.9591(47) | 4467.863(16)  | 2511.2782(29) | 6              | 9.5            |
| <sup>13</sup> C2- <sup>13</sup> C4 | 4600.8(15)    | 4503.5(58)    | 2511.56(99)   | 6              | 85.6           |

<sup>a</sup>number of experimental transitions in the fit

**Table SL2.** Spectroscopic constants determined for the deuterium isotopologues of cyclohexene. Spectral assignments were done by fitting experimental transition to the rigid-rotor Hamiltonian using Pickett's SPCAT/SPFIT analysis program.<sup>6</sup>

| Isomer | A (MHz)       | B (MHz)       | C (MHz)       | N <sup>a</sup> | $\sigma$ (kHz) |
|--------|---------------|---------------|---------------|----------------|----------------|
| d0     | 4739.1511(26) | 4544.4159(33) | 2562.3985(17) | 22             | 15.6           |
| (1)-d1 | 4684.2226(71) | 4358.123(22)  | 2517.5716(42) | 6              | 16.0           |
| (2)-d1 | 4728.0271(47) | 4314.894(14)  | 2490.7470(28) | 6              | 9.8            |
| (3)-d1 | 4598.9903(53) | 4448.224(19)  | 2540.1285(33) | 6              | 13.6           |
| (4)-d1 | 4618.9129(69) | 4402.508(19)  | 2482.7260(34) | 9              | 16.5           |
| (5)-d1 | 4628.0530(62) | 4407.556(17)  | 2486.8528(31) | 9              | 15.0           |

|              |               |               |               |   |      |
|--------------|---------------|---------------|---------------|---|------|
| (4,9)-d2     | 4421.811(12)  | 4375.1906(29) | 2416.4423(19) | 6 | 6.0  |
| (3,8)-d2     | 4456.8531(68) | 4360.890(25)  | 2519.1458(43) | 6 | 13.9 |
| (4,8)-d2     | 4480.8460(37) | 4330.5911(38) | 2466.4428(34) | 6 | 6.8  |
| (2,4)-d2     | 4562.8274(31) | 4239.7120(99) | 2419.9967(18) | 6 | 5.7  |
| (1,3)-d2     | 4543.0663(71) | 4269.946(23)  | 2496.8638(43) | 6 | 14.5 |
| (2,3)-d2     | 4584.6894(38) | 4233.998(11)  | 2469.8934(23) | 6 | 7.9  |
| (1,4)-d2     | 4547.2620(60) | 4258.508(16)  | 2445.4059(34) | 8 | 13.9 |
| (1,6)-d2     | 4671.9466(19) | 4143.1205(23) | 2447.6730(10) | 8 | 7.0  |
| (2,9)-d2     | 4581.0458(22) | 4219.0130(92) | 2418.3460(15) | 7 | 7.8  |
| (1,8)-d2     | 4543.0236(66) | 4274.228(21)  | 2496.1954(40) | 6 | 13.5 |
| (1,9)-d2     | 4535.320(15)  | 4265.422(20)  | 2444.0443(44) | 5 | 8.9  |
| (2,8)-d2     | 4587.8261(63) | 4226.954(19)  | 2468.9146(37) | 6 | 12.9 |
| (1,5)-d2     | 4536.705(19)  | 4251.294(25)  | 2439.7907(56) | 5 | 11.2 |
| (2,5)-d2     | 4549.7472(16) | 4234.144(16)  | 2414.7016(16) | 5 | 4.7  |
| (1,10)-d2    | 4519.399(46)  | 4270.658(47)  | 2441.122(19)  | 4 | 19.4 |
| (2,10)-d2    | 4563.434(31)  | 4226.355(31)  | 2416.498(13)  | 4 | 13.0 |
| (2,3,8)-d3   | 4448.6526(83) | 4148.764(26)  | 2449.2613(50) | 6 | 17.0 |
| (1,4,9)-d3   | 4328.3962(65) | 4245.123(27)  | 2376.7715(48) | 5 | 11.9 |
| (1,3,8)-d3   | 4405.5468(69) | 4189.116(25)  | 2476.7582(48) | 5 | 12.6 |
| (2,4,9)-d3   | 4366.5701(84) | 4202.971(29)  | 2352.3619(51) | 6 | 17.0 |
| (2,3,7,8)-d4 | 4396.2294(58) | 3989.815(16)  | 2408.5446(34) | 6 | 11.9 |
| (2,4,7,9)-d4 | 4318.2255(35) | 4040.268(11)  | 2314.1446(21) | 6 | 7.2  |

<sup>a</sup>number of experimental transitions in the fit

**Table S13.** Refined atomic coordinates (Å) of cyclohexene in the principal axis system. The refinements were done using the experimental constants for the normal species, <sup>13</sup>C, <sup>13</sup>C-<sup>13</sup>C, and D isotopologues observed in natural abundance using a commercial sample of cyclohexene.

|    | <i>a</i> | <i>b</i> | <i>c</i> |
|----|----------|----------|----------|
| C1 | 0.66475  | 1.26747  | 0.08957  |

|     |          |          |          |
|-----|----------|----------|----------|
| C2  | -0.66475 | 1.26747  | -0.08957 |
| C3  | -1.48960 | 0.00604  | -0.17879 |
| C4  | -0.70417 | -1.22101 | 0.30042  |
| C5  | 0.70417  | -1.22101 | -0.30042 |
| C6  | 1.48960  | 0.00604  | 0.17879  |
| H1  | -1.81547 | -0.13878 | -1.21812 |
| H2  | -2.40256 | 0.12761  | 0.41504  |
| H3  | -0.61912 | -1.19277 | 1.39509  |
| H4  | -1.18480 | -2.21303 | 0.18833  |
| H5  | 1.24005  | 2.13513  | 0.05683  |
| H6  | 2.40256  | 0.12761  | -0.41504 |
| H7  | 1.81547  | -0.13878 | 1.21812  |
| H8  | 0.61912  | -1.19277 | -1.39509 |
| H9  | 1.18480  | -2.21303 | -0.18833 |
| H10 | -1.24005 | 2.13513  | 0.05683  |

---

### *Example Spectrum Analysis*

The spectrum analysis methodology is illustrated using the reaction product from the synthesis targeting *trans*-4,5-cyclohexene-d<sub>2</sub>, compound **14** in the paper. For this analysis, the region near the lowest frequency transition ( $1_{11}-0_{00}$  using the usual asymmetric top notation of the rotational kinetic energy levels,  $J_{KaKc}^1$ ) is shown in **Figure S12**. This region offers the highest measurement sensitivity. The spectrum is acquired over the 6-18 GHz frequency range but the higher frequency regions are not shown here. Candidate cyclohexene isotopomers in this frequency range are identified by an automated analysis routine. The routine checks each measured transition frequency for a match to the predicted transition frequency of all 528 rotationally distinct isotopomers of cyclohexene calculated using the reference geometry. If an experimental transition frequency is within 500 kHz of a predicted frequency, then the transition frequency for the ring pucker isomer of the candidate match is identified for the list of predicted frequencies. If there is an experimental transition frequency within 500 kHz of the predicted ring pucker transition pair, then these isotopomer are flagged as likely components of the mixture. The presence of a rotationally distinct isotopomer is verified by examining the full measured spectrum region to see that the other rotational transition expected for the isotopomer are present with the correct intensity and that the spectrum can be fit to high accuracy.



For the *trans*-4,5-cyclohexene-d<sub>2</sub> reaction sample, 26 rotationally distinct isotopomers were identified, corresponding to 15 chemically distinct isotopomers. The relative abundance of the rotationally distinct species are determined from the transition intensities using the calculated intensity of the transition in the low frequency region (this calculation includes effects of rotation of the principal axis system upon deuteration). The results for the relative abundance of the rotationally distinct deuterated isomers of cyclohexene in this sample are reported in **Table SL6** where the relative abundances of the chemically distinct isotopomers and the isotopologues are also given.

The accuracy of the refined structure makes it straightforward to identify the cyclohexene isotopomer from its spectrum even without the availability of synthesized reference samples. The performance of the reference structure for the rotationally distinct isotopomers observed over all experimental samples is summarized in **Table SL4**. This table lists the predicted rotational constants for all identified isotopomers. The experimental rotational constants are listed next where the percentage error for each constant is given. As a metric for isotopomer identification, we use the root-mean-squared (RMS) percent error for the three rotational constants of each species. The confidence in the isotopomer identification is assessed by comparing the RMS percent error of the matched geometry to the RMS percent errors of the two next closest geometry matches (the last column of the **Table SL4**). In all cases, the error for the matched geometry is at least a factor of 10 smaller than the next best geometry match.

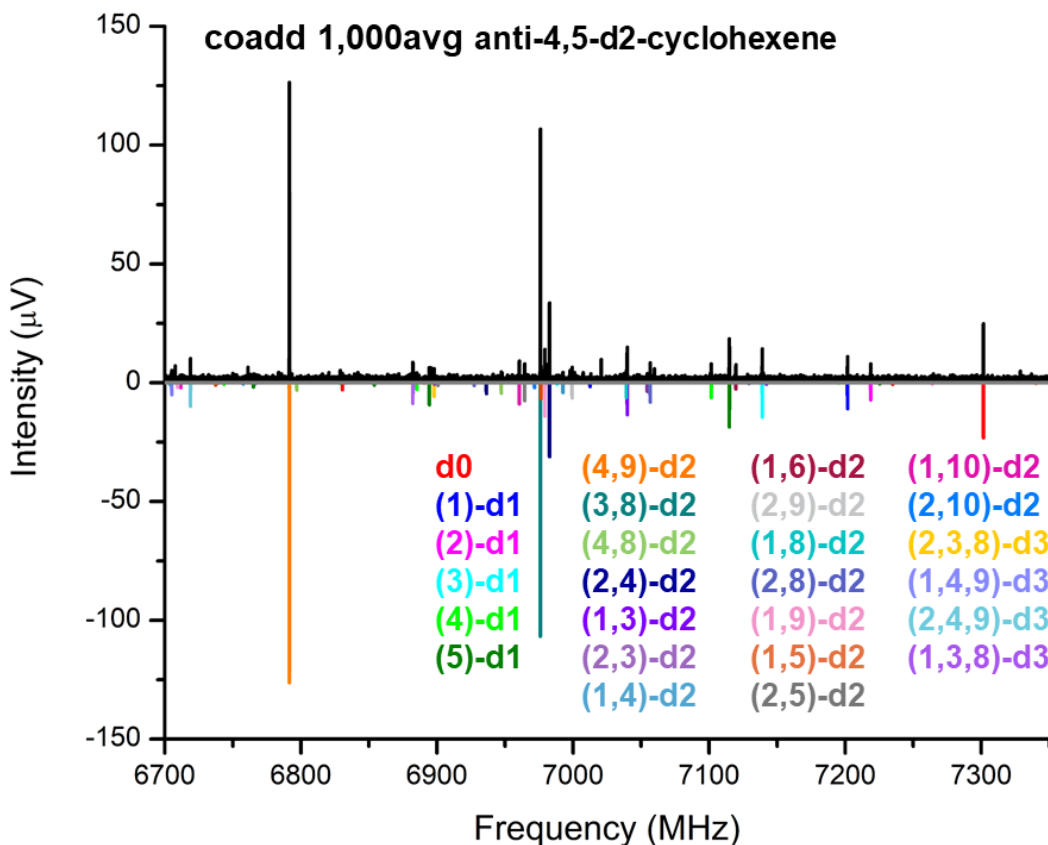


**Figure SL2.** MRR spectrum of *trans*-4,5-d<sub>2</sub>-cyclohexene. Twenty-six rotationally distinct isotopomers of cyclohexene, corresponding to 15 chemically distinct species, were identified in the sample and are illustrated by the colored traces below. The simulated spectra were generated using Pickett's SPCAT/SPFIT software.<sup>6</sup>

## Results

A summary of all deuterium isotopomers of cyclohexene identified in the samples for this study is given in **Table SL4**. The table gives the rotational constants for each isotopomer predicted from the reference geometry and the experimentally determined rotational constants. The assigned transitions for each deuterium isotopomer are given in **Tables SL24-50**. The percent error for each rotational constant determination is also listed in **Table SL4**. An assessment of the confidence of each isotopomer identification by MRR spectroscopy is provided by giving the rms error for the three rotational constants for each isotopomer and the rms error to the next closest set of rotational constants from all 528 rotationally distinct deuterated isomers. In all cases, there is a significant increase in the rms error for the next closest possible isotopomer.

The relative abundance of all known isotopomers in each synthetic sample is summarized in **Tables SL5-10**. The abundance analysis first gives the composition for all rotationally distinct isotopomers. The relative abundance for each chemically distinct deuterated isomer is also given. This value is the sum of the two ring-pucker isomers for each isomer where these give rotationally distinguishable structures. Finally, the relative abundance of the isotopologues, cyclohexene isomers with the same total number of deuterium atoms, is also given in **Tables SL5-10**.

## Discussion

### 1) Isotopic Scrambling by Internal Rotation of Cyclohexene on the Metal

There were some discrepancies in the relative abundance of the isotopomers in the samples determined by NMR and MRR believed to be caused by isotopic scrambling. This scrambling appears to occur early in the sample processing while the cyclohexene is still attached to the metal. The mechanism of this scrambling is believed to be due to a beta hydride elimination which results in shifting of the deuterium to a new carbon, and in some cases the replacement with a hydrogen.<sup>10</sup> Evidence of the isotopic scrambling by internal rotation is illustrated in **Figure SL3**. <sup>1</sup>H NMR spectra of a 3-cyclohexene-d1 sample was taken prior to and directly following an MRR measurement (**Figure SL3, Panel A**). Prior to MRR, the amount of the H<sub>3</sub>-endo proton impurity in the sample was ~5%, while after MRR it was ~30%. The MRR spectrum of the same sample is shown in **Figure SL3, Panel B** and the relative amount of 3-cyclohexene-d1 in this sample was 76% (10% d0 impurity, **Table SL5**). These spectra were acquired using a sample that was bound to a different metal complex than reported on in this study; it did not have the methyl on the nitrosyl group. This metal complex variant is known to be more reactive with oxygen and also binds to the cyclohexene more tightly.

In order to minimize the extent of scrambling, the metal complex that is reported in the body of this paper was used, which is known to be less reactive than the other complex. **Figure SL3, Panel C** shows the

spectrum of a 3-d1-cyclohexene sample using the methylated complex where the relative amount of 3-d1 was determined to be ~90% (Table SL6). In this sample, the relative impurity of cyclohexene d0 was ~5%, while the other 5% of the sample was made up of the 1-d1 and 4-d1 isotopomers. Migration of the metal complex on the ring explains the presence of these isotopomers. The observed scrambling does not change the identity of the most abundant species. The MRR spectrum can therefore be used to confirm the assignment of the dominant isotopomer in a sample, though the values determined by MRR represent a lower limit for the purity of a sample.

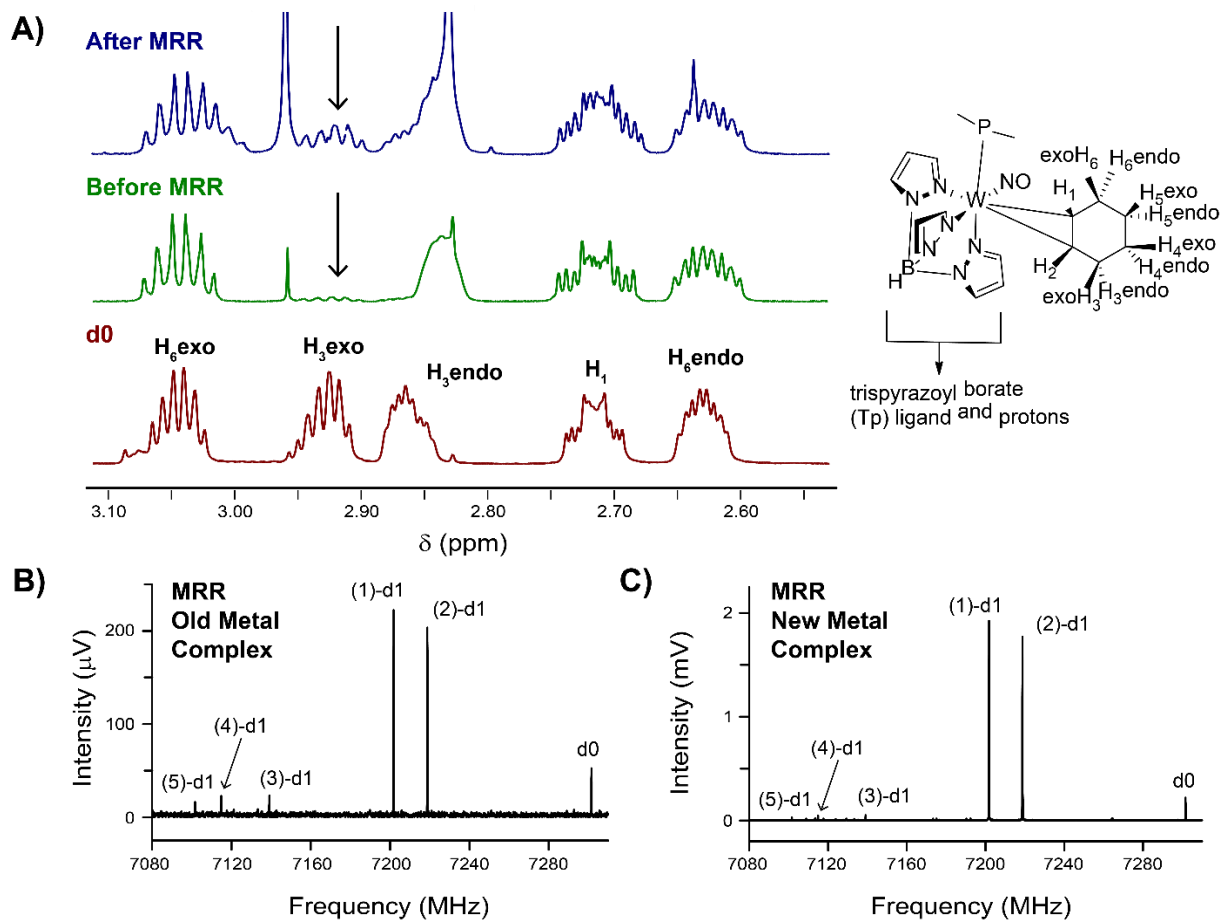


**Figure SL3.** Isotopic scrambling of cyclohexene on the metal complex. **Panel A** shows  $^1\text{H}$  NMR spectra of a 3-cyclohexene-d1 sample taken before and after MRR. The amount of  $\text{H}_3\text{exo}$  protio impurity before and after MRR was ~5% and ~30% respectively. A spectrum of fully protonated cyclohexene is shown for reference. The MRR spectrum of the sample used for the NMR study is shown in **Panel B**. Analysis of this spectrum by MRR gave a relative amount of the desired product was 76% 3-d1. **Panel C** shows the MRR spectrum of a different 3-cyclohexene-d1 sample that was made using a different metal complex. The relative composition of the desired product in this sample was 90% 3-d1.

### Stereoselectivity in the Synthesis

In this work, MRR spectroscopy is used to analyze isotopologues and isotopomer purity of the synthetic targets. The analysis is performed on the cyclohexene that is thermally dissociated from the metal by heating. As described above, there is evidence for internal rotation of the cyclohexene on the metal prior to thermal dissociation to produce isotopomer impurities estimated at the 5-10% level. As a result, the stereoisomer purities are lower limits to the values produced directly in the synthesis of the transition metal complex. The main conclusions from MRR analysis are presented below.

#### Isotopologue Purity of 3-d1-cyclohexene

The isotopomer analysis of 3-d1-cyclohexene is presented in **Table SL6** for the preferred methylated nitroso complex. The isotopologue purity is 95%. No overdeuteration of the cyclohexene is detected placing d2-isotopomer impurities below 1%. NMR analysis of the cyclohexene transition metal complex prior to sample preparation for MRR spectroscopy indicated that the target cyclohexene isotopomer is synthesized is very high purity, possibly higher than 99%. The MRR measurement detects the other two monodeuterated d1-isotopomers at about 2% each.

In addition, MRR measures about 5% of the d0-parent cyclohexene. These results are consistent with isomerization by internal rotation of cyclohexene on the metal prior to dissociation possibly through the agnostic metal complex geometry.<sup>10</sup> This mechanism can also result in reduction of total deuterium content if the sample is in a proton rich environment (possibly from the residual solvents in the samples). In general, MRR analysis indicates lower total deuterium content of the cyclohexene than indicated in the NMR measurements of the synthesized metal complex.

#### Cis - Trans Selectivity in d2-isotopomers

Two d2-isotopomers of cyclohexene were analyzed by MRR spectroscopy. The synthesis targets the preparation of *trans*-4,5-cyclohexene-d2 (**Table SL7**) and *cis*-3,4-cyclohexene-d2 (**Table SL8**). In both cases, the target compound is the dominant isotopomer. Also, in both cases evidence for internal rotation of the cyclohexene on the ring is evident through the detection of other d-2 isotopologues that would be produced through this mechanism. Reduction in total deuterium content relative to expectations from NMR spectroscopy is also indicated by the high relative abundance of the d1-isotopologue. It is noted that the relative abundance of the d1-isotopologue is much higher in *cis*-3,4-cyclohexene-d2 (30%) than *trans*-4,5-cyclohexene-d2 (10%). The *cis*-3,4-cyclohexene-d2 sample provided for MRR analysis had much higher amounts of initial solvent impurities than the other samples analyzed in this project. As a result, it required longer times at solvent removal step where the sample is heated using a temperature ramp from 60°C to 100°C. The prolonged solvent removal step might be expected to increase the isotope scrambling through the agnostic complex intermediate.

The main result that MRR provides for these samples is the stereoselectivity of *cis* vs. *trans* isotopomers. For the cyclohexene that is detected with the target deuterium substitution patterns, the stereoselectivity for *trans*-4,5-cyclohexene-d2 relative to *cis*-4,5-cyclohexene-d2 is 22:1 and the selectivity for the target *cis*-3,4-cyclohexene-d2 relative to *trans*-3,4-cyclohexene-d2 is 39:1.

For *trans*-4,5-cyclohexene-d<sub>2</sub>, MRR detects about 8% overdeuteration through the presence of two d<sub>3</sub>-isotopomers. This result is consistent with NMR analysis of the transition metal complex prior to MRR sample preparation. No overdeuteration is detected in the synthesis of *cis*-3,4-cyclohexene-d<sub>2</sub>.

#### Selectivity in *cis,trans*-3,4,5-d<sub>3</sub>-cyclohexene Synthesis

MRR measures about 20% underdeuteration of this compound entirely from d<sub>2</sub>-isotopologue impurities as shown in Table 9. Underdeuteration relative to expectations from NMR is a common feature of this analysis and, as mentioned before, could be caused by the proposed mechanism for internal rotation of the cyclohexene on the metal prior to thermal decomposition. No overdeuteration is observed.

In this case, only a single isotopomer, the target *cis,trans*-3,4,5-d<sub>3</sub>-cyclohexene, is observed and makes up about 80% of the sample composition. The measurement sensitivity was lower for this compound compared to the d<sub>1</sub>- and d<sub>2</sub>-isotopologues. We estimate that all other isotopomer impurities are below 2% giving a stereoselectivity of the synthesis of 40:1 or higher.

### Selectivity in the *cis,trans,trans*-3,4,5,6-d<sub>4</sub>-cyclohexene Synthesis

MRR analysis of this sample gives a high level of underdeuteration with about 40% of total d<sub>3</sub>-isotopologue. This high abundance of d<sub>3</sub>-isotopologues was also inferred from the NMR analysis. The origin of this isotopomer impurity through slow reaction at the exo-H<sub>6</sub> position is described in the main paper.

For d-4 isotopologues, only a single isotopomer is detected – the target *cis,trans,trans*-3,4,5,6-d<sub>4</sub>-cyclohexene. This species makes up 55% of the sample composition. No other d<sub>4</sub>-isotopomers are detected in a spectrum where the detection limit is 1%. The stereoselectivity in this synthesis is 55:1 or higher.

### *Summary*

MRR provides a simple method to quantitatively analyze the isotopomer content of cyclohexene. The measurement is performed by transfer the reaction product to the MRR spectrometer and then removing the cyclohexene ligand with heat. This sample preparation process is found to cause about 10% scrambling of the isotopomers possibly through internal rotation on the metal complex via an agnostic geometry. As a result, MRR composition analysis provides a lower limit to the isotopomer purity of the prepared transition metal complex. MRR analysis shows that overdeuteration of the samples is low – only being detected in one sample at less than 10% composition. MRR also demonstrates that the synthesis has high stereoselectivity. Undesired *cis/trans* isomers were typically a factor of 40 or more lower in abundance than the described isomer.

**Table SL4.** Comparison between calculated and experimental rotational constants of deuterium isotopologues of cyclohexene. The theoretical rotational constants are scaled using the refined structure determined from the isotopologues observed in natural abundance. Experimental fits were done using Pickett's SPCAT/SPFIT analysis program.<sup>6</sup>

|          | Theoretical Rotational Constants |           |           | Experimental Rotational Constants |                      |                        | RMS error (%) | RMS next closest (%) |
|----------|----------------------------------|-----------|-----------|-----------------------------------|----------------------|------------------------|---------------|----------------------|
|          | A (MHz)                          | B (MHz)   | C (MHz)   | A (MHz)                           | B (MHz)              | C (MHz)                |               |                      |
| (1)-d1   | 4684.219                         | 4358.111  | 2517.572  | 4684.2226 (0.00008%)              | 4358.123 (0.0003%)   | 2517.5716 (-0.000016%) | 0.0004        | 0.9989, 1.1854       |
| (2)-d1   | 4728.048                         | 4314.878  | 2490.756  | 4728.0271 (-0.0004%)              | 4314.894 (0.0004%)   | 2490.7470 (-0.0004%)   | 0.0004        | 1.0037, 1.7424       |
| (3)-d1   | 4598.989                         | 4448.217  | 2540.135  | 4598.9903 (0.00003%)              | 4448.224 (0.00016%)  | 2540.1285 (-0.0003%)   | 0.0005        | 1.3708, 1.4541       |
| (4)-d1   | 4618.901                         | 4402.491  | 2482.75   | 4618.9129 (0.0003%)               | 4402.508 (0.0004%)   | 2482.7260 (-0.0010%)   | 0.0011        | 0.163, 1.2893        |
| (5)-d1   | 4628.066                         | 4407.568  | 2486.842  | 4628.0530 (-0.0003%)              | 4407.556 (-0.0003%)  | 2486.8528 (0.0004%)    | 0.0004        | 0.1626, 1.1914       |
| (4,9)-d2 | 4421.288                         | 4375.256  | 2416.333  | 4421.811 (0.012%)                 | 4375.1906 (-0.0015%) | 2416.4423 (0.005%)     | 0.0076        | 0.3695, 0.485        |
| (3,8)-d2 | 4456.721                         | 4360.738  | 2519.087  | 4456.8531 (0.003%)                | 4360.890 (0.003%)    | 2519.1458 (0.002%)     | 0.003         | 1.312, 1.4409        |
| (4,8)-d2 | 4480.6184                        | 4330.3479 | 2466.3685 | 4480.8460 (0.005%)                | 4330.5911 (0.006%)   | 2466.4428 (0.003%)     | 0.0047        | 0.2001, 0.9340       |
| (2,4)-d2 | 4562.684                         | 4239.535  | 2419.902  | 4562.8274 (0.003%)                | 4239.7120 (0.004%)   | 2419.9967 (0.004%)     | 0.004         | 0.1973, 0.2273       |
| (1,3)-d2 | 4542.793                         | 4269.867  | 2496.803  | 4543.0663 (0.006%)                | 4269.946 (0.0019%)   | 2496.8638 (0.002%)     | 0.0043        | 0.0562, 0.7313       |
| (2,3)-d2 | 4584.407                         | 4233.947  | 2469.753  | 4584.6894 (0.006%)                | 4233.998 (0.0012%)   | 2469.8934 (0.006%)     | 0.0047        | 0.1083, 0.8206       |
| (1,4)-d2 | 4546.732                         | 4258.462  | 2445.308  | 4547.2620 (0.012%)                | 4258.508 (0.0011%)   | 2445.4059 (0.004%)     | 0.0095        | 0.1763, 0.2178       |
| (1,6)-d2 | 4671.5817                        | 4143.0032 | 2447.6479 | 4671.9466 (0.008%)                | 4143.1205 (0.003%)   | 2447.6730 (0.0010%)    | 0.0048        | 0.1188, 0.9342       |
| (2,9)-d2 | 4581.0412                        | 4218.6573 | 2418.2439 | 4581.0458 (0.00010%)              | 4219.0130 (0.008%)   | 2418.3460 (0.004%)     | 0.0054        | 0.2548, 0.0042       |
| (1,8)-d2 | 4542.8417                        | 4273.9475 | 2496.0786 | 4543.0236 (0.004%)                | 4274.228 (0.007%)    | 2496.1954 (0.005%)     | 0.0052        | 0.0606, 0.7041       |
| (1,9)-d2 | 4535.321                         | 4265.041  | 2443.964  | 4535.320 (-0.00002%)              | 4265.422 (0.009%)    | 2444.0443 (0.003%)     | 0.0055        | 0.1757, 0.2145       |
| (2,8)-d2 | 4587.667                         | 4226.731  | 2468.865  | 4587.8261 (0.003%)                | 4226.954 (0.005%)    | 2468.9146 (0.002%)     | 0.0038        | 0.1066, 0.8276       |

|              |           |           |           |                    |                     |                     |        |                |
|--------------|-----------|-----------|-----------|--------------------|---------------------|---------------------|--------|----------------|
| (1,5)-d2     | 4536.012  | 4251.504  | 2439.721  | 4536.705 (0.015%)  | 4251.294 (-0.005%)  | 2439.7907 (0.003%)  | 0.0094 | 0.2069, 0.2119 |
| (2,5)-d2     | 4549.062  | 4234.304  | 2414.656  | 4549.7472 (0.015%) | 4234.144(-0.004%)   | 2414.7016 (0.0019%) | 0.0090 | 0.2005, 0.2187 |
| (1,10)-d2    | 4519.2719 | 4270.5929 | 2441.0246 | 4519.399 (0.003%)  | 4270.658 (-0.0015%) | 2441.122 (0.004%)   | 0.003  | 0.2273,0.3364  |
| (2,10)-d2    | 4563.1005 | 4226.7668 | 2416.2462 | 4563.434 (0.007%)  | 4226.355 (-0.010%)  | 2416.498 (0.010%)   | 0.0093 | 0.1978, 0.2163 |
| (2,3,8)-d3   | 4448.28   | 4148.446  | 2449.104  | 4448.655 (0.008%)  | 4148.763 (0.008%)   | 2449.763 (0.03%)    | 0.0162 | 0.5691, 0.6681 |
| (1,4,9)-d3   | 4328.111  | 4244.478  | 2376.592  | 4328.3962 (0.007%) | 4245.123 (0.015%)   | 2376.7715 (0.008%)  | 0.0108 | 0.3581, 0.3627 |
| (2,4,9)-d3   | 4405.188  | 4188.755  | 2476.620  | 4405.5468 (0.008%) | 4189.116 (0.009%)   | 2476.7582 (0.006%)  | 0.0076 | 0.7374, 0.8750 |
| (1,3,8)-d3   | 4366.493  | 4202.289  | 2352.164  | 4366.570 (0.0018%) | 4202.971 (0.016%)   | 2352.3619 (0.008%)  | 0.0106 | 0.3785, 0.3787 |
| (2,3,7,8)-d4 | 4395.524  | 3989.456  | 2408.355  | 4396.2300 (0.016%) | 3989.815 (0.009%)   | 2408.5446 (0.008%)  | 0.0116 | 0.1099, 0.8497 |
| (2,4,7,9)-d4 | 4317.699  | 4039.583  | 2313.929  | 4318.2255 (0.012%) | 4040.268 (0.017%)   | 2314.1446 (0.009%)  | 0.0135 | 0.1087, 0.2349 |

---



**Table SL5.** Composition of 3-d1-cyclohexene sample determined by MRR (**Figure L2B**). Sample was on metal that did not have a methyl group on the nitrosyl group.

| Rotational Isomer | Percent | Chemically Distinct | Percent | Isotopologue | Percent |
|-------------------|---------|---------------------|---------|--------------|---------|
| Parent            | 9.4     | d0                  | 9.4     | d0           | 9.4     |
| (1)-d1            | 39.6    | 3-d1                | 75.9    | d1           | 90.6    |
| (2)-d1            | 36.3    |                     |         |              |         |
| (3)-d1            | 3.8     | 4-d1                | 7.8     | d1           | 90.6    |
| (4)-d1            | 4.0     |                     |         |              |         |
| (5)-d1            | 6.8     | 1-d1                | 6.8     |              |         |

**Table SL6.** Composition of 3-d1-cyclohexene sample determined by MRR. (**Figure L2C**)

| Rotational Isomer | Percent | Chemically Distinct | Percent | Isotopologue | Percent |
|-------------------|---------|---------------------|---------|--------------|---------|
| Parent            | 5.4     | d0                  | 5.4     | d0           | 5.4     |
| (1)-d1            | 47.0    | 3-d1                | 90.3    | d1           | 94.6    |
| (2)-d1            | 43.3    |                     |         |              |         |
| (3)-d1            | 1.3     | 4-d1                | 3.2     | d1           | 94.6    |
| (4)-d1            | 1.9     |                     |         |              |         |
| (5)-d1            | 1.1     | 1-d1                | 1.1     |              |         |

**Table SL7.** Composition of trans-4,5-d2-cyclohexene determined by MRR.

| Rotational Isomer | Percent | Chemically Distinct | Percent | Isotopologue | Percent |
|-------------------|---------|---------------------|---------|--------------|---------|
| Parent            | 3.9     | d0                  | 3.9     | d0           | 3.9     |
| (1)-d1            | 1.5     | 3-d1                | 2.7     | d1           | 10.0    |
| (2)-d1            | 1.2     |                     |         |              |         |
| (3)-d1            | 3.0     | 4-d1                | 6.1     |              |         |

|            |      |                              |      |    |      |
|------------|------|------------------------------|------|----|------|
| (4)-d1     | 3.1  |                              |      |    |      |
| (5)-d1     | 1.3  | 1-d1                         | 1.3  |    |      |
| (4,9)-d2   | 27.8 | <i>trans</i> -4,5-d2         | 52.6 |    |      |
| (3,8)-d2   | 24.8 |                              |      |    |      |
| (4,8)-d2   | 2.4  | <i>cis</i> -4,5-d2           | 2.4  |    |      |
| (2,4)-d2   | 3.6  | <i>trans</i> -3,4-d2         | 7.0  |    |      |
| (1,3)-d2   | 3.4  |                              |      |    |      |
| (2,3)-d2   | 1.0  | <i>cis</i> -3,4-d2           | 2.2  |    |      |
| (1,4)-d2   | 1.2  |                              |      |    |      |
| (1,6)-d2   | 0.8  | <i>cis</i> -3,6-d2           | 0.8  | d2 | 78.3 |
| (2,9)-d2   | 1.2  | <i>cis</i> -3,5-d2           | 2.6  |    |      |
| (1,8)-d2   | 1.4  |                              |      |    |      |
| (1,9)-d2   | 1.8  | <i>trans</i> -3,5-d2         | 3.8  |    |      |
| (2,8)-d2   | 2.0  |                              |      |    |      |
| (1,5)-d2   | 2.1  | 1,3-d2                       | 3.8  |    |      |
| (2,5)-d2   | 1.7  |                              |      |    |      |
| (1,10)-d2  | 1.3  | 2,3-d2                       | 3.0  |    |      |
| (2,10)-d2  | 1.7  |                              |      |    |      |
| (2,3,8)-d3 | 1.2  | <i>cis,trans</i> -3,4,5-d3   | 2.3  |    |      |
| (1,4,9)-d3 | 1.1  |                              |      | d3 | 7.9  |
| (1,3,8)-d3 | 1.8  | <i>trans,trans</i> -3,4,5-d3 | 5.6  |    |      |
| (2,4,9)-d3 | 3.8  |                              |      |    |      |

**Table SL8.** Composition of *cis*-3,4-d2-cyclohexene determined by MRR.

| Rotational Isomer | Percent | Chemically Distinct | Percent | Isotopologue | Percent |
|-------------------|---------|---------------------|---------|--------------|---------|
| Parent            | 9.4     | d0                  | 9.4     | d0           | 9.4     |
| (1)-d1            | 8.4     | 3-d1                | 18.1    | d1           | 30.1    |

|           |      |                      |      |    |      |
|-----------|------|----------------------|------|----|------|
| (2)-d1    | 9.7  |                      |      |    |      |
| (3)-d1    | 5.1  |                      |      |    |      |
| (4)-d1    | 4.7  | 4-d1                 | 9.8  |    |      |
| (5)-d1    | 2.2  | 1-d1                 | 2.2  |    |      |
| (4,8)-d2  | 12.9 | <i>cis</i> -4,5-d2   | 12.9 |    |      |
| (2,4)-d2  | 0.6  | <i>trans</i> -3,4-d2 | 1.0  |    |      |
| (1,3)-d2  | 0.4  |                      |      |    |      |
| (2,3)-d2  | 16.4 | <i>cis</i> -3,4-d2   | 38.8 |    |      |
| (1,4)-d2  | 22.4 |                      |      |    |      |
| (1,6)-d2  | 1.7  | <i>cis</i> -3,6-d2   | 1.7  | d2 | 60.6 |
| (1,5)-d2  | 0.6  | 1,3-d2               | 1.2  |    |      |
| (2,5)-d2  | 0.6  |                      |      |    |      |
| (1,10)-d2 | 2.6  | 2,3-d2               | 4.7  |    |      |
| (2,10)-d2 | 2.1  |                      |      |    |      |

**Table SL9.** Composition of *cis,trans*-3,4,5-d3-cyclohexene determined by MRR.

| Rotational Isomer | Percent | Chemically Distinct        | Percent | Isotopologue | Percent |
|-------------------|---------|----------------------------|---------|--------------|---------|
| (4,9)-d2          | 6.1     |                            |         |              |         |
| (3,8)-d2          | 4.0     | <i>trans</i> -4,5-d2       | 10.1    |              |         |
| (2,4)-d2          | 2.2     | <i>trans</i> -3,4-d2       | 4.3     |              |         |
| (1,3)-d2          | 2.1     |                            |         | d2           | 21.9    |
| (2,3)-d2          | 1.8     | <i>cis</i> -3,4-d2         | 4.4     |              |         |
| (1,4)-d2          | 2.6     |                            |         |              |         |
| (1,10)-d2         | 1.3     | 2,3-d2                     | 3.1     |              |         |
| (2,10)-d2         | 1.8     |                            |         |              |         |
| (2,3,8)-d3        | 46.1    | <i>cis,trans</i> -3,4,5-d3 | 78.1    | d3           | 78.1    |
| (1,4,9)-d3        | 32.0    |                            |         |              |         |

**Table SL10.** Composition of *cis,trans,trans*-3,4,5,6-d<sub>4</sub>-cyclohexene determined by MRR.

| Rotational Isomer        | Percent | Chemically Distinct                            | Percent | Isotopologue   | Percent |
|--------------------------|---------|--|---------|----------------|---------|
| (4,9)-d <sub>2</sub>     | 1.2     | <i>trans</i> -4,5-d <sub>2</sub>               | 1.2     | d <sub>2</sub> | 3.4     |
| (3,8)-d <sub>2</sub>     | 0.0     |  |         |                |         |
| (2,3)-d <sub>2</sub>     | 1.1     | <i>cis</i> -3,4-d <sub>2</sub>                 | 2.2     |                |         |
| (1,4)-d <sub>2</sub>     | 1.1     |  |         |                |         |
| (2,3,8)-d <sub>3</sub>   | 21.2    | <i>cis,trans</i> -3,4,5-d <sub>3</sub>         | 37.7    | d <sub>3</sub> | 41.0    |
| (1,4,9)-d <sub>3</sub>   | 16.5    |  |         |                |         |
| (1,3,8)-d <sub>3</sub>   | 2.1     | <i>trans,trans</i> -3,4,5-d <sub>3</sub>       | 3.3     |                |         |
| (2,4,9)-d <sub>3</sub>   | 1.2     |  |         |                |         |
| (2,3,7,8)-d <sub>4</sub> | 35.6    | <i>cis,trans,trans</i> -3,4,5,6-d <sub>4</sub> | 55.5    | d <sub>4</sub> | 55.5    |
| (2,4,7,9)-d <sub>4</sub> | 19.9    |  |         |                |         |

**Table SL11.** Measured rotational transitions ( $\nu_{\text{obs}}$ , MHz) of the parent and residuals ( $\nu_{\text{obs}}-\nu_{\text{calc}}$ , MHz).

| $J'$ | $K_a'$ | $K_b'$ | $\leftarrow$ | $J''$ | $K_a''$ | $K_b''$ | $\nu_{\text{obs}} / \text{MHz}$ | $\nu_{\text{obs}}-\nu_{\text{calc}} / \text{MHz}$ |
|------|--------|--------|--------------|-------|---------|---------|---------------------------------|---|
| 2    | 2      | 1      | $\leftarrow$ | 2     | 1       | 2       | 6530.228                        | -0.006  |
| 3    | 3      | 1      | $\leftarrow$ | 3     | 2       | 2       | 6830.559                        | -0.0002   |
| 4    | 4      | 1      | $\leftarrow$ | 4     | 3       | 2       | 7234.95                         | 0.0049  |
| 1    | 1      | 1      | $\leftarrow$ | 0     | 0       | 0       | 7301.565                        | 0.015   |
| 5    | 5      | 1      | $\leftarrow$ | 5     | 4       | 2       | 7745.158                        | 0.003   |
| 4    | 2      | 2      | $\leftarrow$ | 4     | 1       | 3       | 10244.94                        | -0.0075   |
| 3    | 1      | 2      | $\leftarrow$ | 3     | 0       | 3       | 10337.86                        | -0.0039   |
| 3    | 2      | 2      | $\leftarrow$ | 3     | 1       | 3       | 10405.1                         | -0.0097   |
| 4    | 3      | 2      | $\leftarrow$ | 4     | 2       | 3       | 10441.27                        | -0.0198   |
| 5    | 4      | 2      | $\leftarrow$ | 5     | 3       | 3       | 10512.48                        | -0.0305   |
| 2    | 0      | 2      | $\leftarrow$ | 1     | 1       | 1       | 12217.98                        | 0.0131  |
| 2    | 1      | 2      | $\leftarrow$ | 1     | 0       | 1       | 12426.38                        | 0.0174  |
| 6    | 3      | 3      | $\leftarrow$ | 6     | 2       | 4       | 14459.67                        | 0.014   |
| 5    | 2      | 3      | $\leftarrow$ | 5     | 1       | 4       | 14505.09                        | -0.009  |
| 5    | 3      | 3      | $\leftarrow$ | 5     | 2       | 4       | 14521.58                        | -0.0042   |
| 2    | 2      | 1      | $\leftarrow$ | 1     | 1       | 0       | 16779.85                        | 0.0114  |
| 3    | 0      | 3      | $\leftarrow$ | 2     | 1       | 2       | 17444.95                        | -0.0129   |
| 3    | 1      | 3      | $\leftarrow$ | 2     | 0       | 2       | 17459.21                        | -0.0201   |
| 6    | 4      | 3      | $\leftarrow$ | 6     | 3       | 4       | 14508.23                        | -0.0111   |
| 4    | 1      | 3      | $\leftarrow$ | 4     | 0       | 4       | 14528.16                        | 0.0249  |
| 4    | 2      | 3      | $\leftarrow$ | 4     | 1       | 4       | 14532.33                        | 0.0248  |
| 5    | 3      | 2      | $\leftarrow$ | 5     | 2       | 3       | 10073.87                        | 0.0052  |

**Table SL12.** Measured rotational transitions ( $\nu_{\text{obs}}$ , MHz) of the  $^{13}\text{C}1=2$  isotopologue and residuals ( $\nu_{\text{obs}}-\nu_{\text{calc}}$ , MHz).

| $J'$ | $K_a'$ | $K_b'$ | $\leftarrow$ | $J''$ | $K_a''$ | $K_b''$ | $\nu_{\text{obs}} / \text{MHz}$ | $\nu_{\text{obs}}-\nu_{\text{calc}} / \text{MHz}$ |
|------|--------|--------|--------------|-------|---------|---------|---------------------------------|---|
|------|--------|--------|--------------|-------|---------|---------|---------------------------------|---|

|   |   |   |   |   |   |   |          |         |
|---|---|---|---|---|---|---|----------|---------|
| 3 | 2 | 2 | ← | 3 | 1 | 3 | 10313.64 | -0.0223 |
| 3 | 0 | 3 | ← | 2 | 1 | 2 | 17271.62 | -0.0191 |
| 2 | 1 | 2 | ← | 1 | 0 | 1 | 12284.78 | 0.0186  |
| 3 | 1 | 3 | ← | 2 | 0 | 2 | 17281.08 | -0.017  |
| 1 | 1 | 1 | ← | 0 | 0 | 0 | 7212.823 | 0.015   |
| 2 | 0 | 2 | ← | 1 | 1 | 1 | 12117.2  | 0.0148  |
| 4 | 1 | 3 | ← | 4 | 0 | 4 | 14413.26 | 0.0132  |
| 2 | 2 | 1 | ← | 1 | 1 | 0 | 16566.48 | 0.0132  |
| 2 | 2 | 1 | ← | 2 | 1 | 2 | 6422.557 | -0.0119 |
| 3 | 3 | 1 | ← | 3 | 2 | 2 | 6665.764 | -0.0016 |
| 3 | 2 | 2 | ← | 3 | 1 | 3 | 10313.64 | -0.0223 |

**Table SL13.** Measured rotational transitions ( $v_{\text{obs}}$ , MHz) of the  $^{13}\text{C}_3=6$  isotopologue and residuals ( $v_{\text{obs}}-v_{\text{calc}}$ , MHz).

| $J'$ | $K_a'$ | $K_b'$ | ← | $J''$ | $K_a''$ | $K_b''$ | $v_{\text{obs}} / \text{MHz}$ | $v_{\text{obs}}-v_{\text{calc}} / \text{MHz}$ |
|------|--------|--------|---|-------|---------|---------|-------------------------------|---|
| 1    | 1      | 1      | ← | 0     | 0       | 0       | 7272.856                      | 0.0141  |
| 2    | 0      | 2      | ← | 1     | 1       | 1       | 12028.53                      | 0.0127  |
| 2    | 1      | 2      | ← | 1     | 0       | 1       | 12341.01                      | 0.0199  |
| 2    | 2      | 1      | ← | 1     | 1       | 0       | 16750.39                      | 0.0135  |
| 3    | 0      | 3      | ← | 2     | 1       | 2       | 17248.24                      | -0.0165                                       |
| 3    | 1      | 3      | ← | 2     | 0       | 2       | 17279.21                      | -0.019  |
| 3    | 1      | 2      | ← | 3     | 0       | 3       | 10190.72                      | -0.0109                                       |
| 4    | 1      | 3      | ← | 4     | 0       | 4       | 14380.37                      | 0.0176  |
| 3    | 2      | 2      | ← | 3     | 1       | 3       | 10332.33                      | -0.0175                                       |
| 2    | 2      | 1      | ← | 2     | 1       | 2       | 6614.089                      | -0.0039                                       |
| 3    | 3      | 1      | ← | 3     | 2       | 2       | 7056.459                      | -0.0071                                       |

**Table SL14.** Measured rotational transitions ( $\nu_{\text{obs}}$ , MHz) of the  $^{13}\text{C}_4=5$  isotopologue and residuals ( $\nu_{\text{obs}}-\nu_{\text{calc}}$ , MHz).

| $J'$ | $K_a'$ | $K_b'$ | $\leftarrow$ | $J''$ | $K_a''$ | $K_b''$ | $\nu_{\text{obs}} / \text{MHz}$ | $\nu_{\text{obs}}-\nu_{\text{calc}} / \text{MHz}$ |
|------|--------|--------|--------------|-------|---------|---------|---------------------------------|---|
| 1    | 1      | 1      | $\leftarrow$ | 0     | 0       | 0       | 7217.016                        | 0.0136  |
| 3    | 3      | 1      | $\leftarrow$ | 3     | 2       | 2       | 6678.509                        | -0.0045   |
| 2    | 2      | 1      | $\leftarrow$ | 2     | 1       | 2       | 6424.276                        | -0.0076   |
| 3    | 1      | 2      | $\leftarrow$ | 3     | 0       | 3       | 10250.25                        | -0.0067   |
| 3    | 2      | 2      | $\leftarrow$ | 3     | 1       | 3       | 10299.44                        | -0.0259   |
| 2    | 1      | 2      | $\leftarrow$ | 1     | 0       | 1       | 12292.6                         | 0.0181  |
| 4    | 1      | 3      | $\leftarrow$ | 4     | 0       | 4       | 14390.98                        | 0.0232  |
| 2    | 2      | 1      | $\leftarrow$ | 1     | 1       | 0       | 16575.44                        | 0.0094  |
| 3    | 1      | 3      | $\leftarrow$ | 2     | 0       | 2       | 17289.34                        | -0.019  |
| 3    | 0      | 3      | $\leftarrow$ | 2     | 1       | 2       | 17279.01                        | -0.0038   |

**Table SL15.** Measured rotational transitions ( $\nu_{\text{obs}}$ , MHz) of the  $^{13}\text{C}_1\text{-}^{13}\text{C}_2$  isotopologue and residuals ( $\nu_{\text{obs}}-\nu_{\text{calc}}$ , MHz).

| $J'$ | $K_a'$ | $K_b'$ | $\leftarrow$ | $J''$ | $K_a''$ | $K_b''$ | $\nu_{\text{obs}} / \text{MHz}$ | $\nu_{\text{obs}}-\nu_{\text{calc}} / \text{MHz}$ |
|------|--------|--------|--------------|-------|---------|---------|---------------------------------|---|
| 1    | 1      | 1      | $\leftarrow$ | 0     | 0       | 0       | 7111.4627                       | -0.1313   |
| 2    | 0      | 2      | $\leftarrow$ | 1     | 1       | 1       | 12036.3678                      | -0.0175   |
| 2    | 1      | 2      | $\leftarrow$ | 1     | 0       | 1       | 12132.3530                      | -0.0298   |
| 2    | 2      | 1      | $\leftarrow$ | 1     | 1       | 0       | 16314.0378                      | 0.0443  |
| 3    | 0      | 3      | $\leftarrow$ | 2     | 1       | 2       | 17104.7015                      | -0.0416   |
| 3    | 1      | 3      | $\leftarrow$ | 2     | 0       | 2       | 17108.0584                      | 0.0874  |

**Table SL16.** Measured rotational transitions ( $\nu_{\text{obs}}$ , MHz) of the  $^{13}\text{C}_1\text{-}^{13}\text{C}_3$  isotopologue and residuals ( $\nu_{\text{obs}}-\nu_{\text{calc}}$ , MHz).

| $J'$ | $K_a'$ | $K_b'$ | $\leftarrow$ | $J''$ | $K_a''$ | $K_b''$ | $\nu_{\text{obs}} / \text{MHz}$ | $\nu_{\text{obs}}-\nu_{\text{calc}} / \text{MHz}$ |
|------|--------|--------|--------------|-------|---------|---------|---------------------------------|---|
|------|--------|--------|--------------|-------|---------|---------|---------------------------------|---|

|   |   |   |   |   |   |   |            |         |
|---|---|---|---|---|---|---|------------|---------|
| 1 | 1 | 1 | ← | 0 | 0 | 0 | 7181.1065  | 0.0087  |
| 2 | 0 | 2 | ← | 1 | 1 | 1 | 11934.9819 | 0.0039  |
| 2 | 1 | 2 | ← | 1 | 0 | 1 | 12196.9647 | 0.0056  |
| 2 | 2 | 1 | ← | 1 | 1 | 0 | 16527.4280 | -0.0038 |
| 3 | 0 | 3 | ← | 2 | 1 | 2 | 17078.5335 | -0.0094 |
| 3 | 1 | 3 | ← | 2 | 0 | 2 | 17100.9264 | 0.0027  |

**Table SL17.** Measured rotational transitions ( $\nu_{\text{obs}}$ , MHz) of the  $^{13}\text{C}_2\text{-}^{13}\text{C}_3$  isotopologue and residuals ( $\nu_{\text{obs}} - \nu_{\text{calc}}$ , MHz).

| $J'$ | $K_a'$ | $K_b'$ | ← | $J''$ | $K_a''$ | $K_b''$ | $\nu_{\text{obs}} / \text{MHz}$ | $\nu_{\text{obs}} - \nu_{\text{calc}} / \text{MHz}$ |
|------|--------|--------|---|-------|---------|---------|---------------------------------|---|
| 1    | 1      | 1      | ← | 0     | 0       | 0       | 7181.9110                       | 0.0150  |
| 2    | 0      | 2      | ← | 1     | 1       | 1       | 11938.7447                      | 0.0136  |
| 2    | 1      | 2      | ← | 1     | 0       | 1       | 12198.939                       | 0.0343  |
| 2    | 2      | 1      | ← | 1     | 1       | 0       | 16528.6427                      | -0.0112   |
| 3    | 0      | 3      | ← | 2     | 1       | 2       | 17082.6048                      | -0.0184   |
| 3    | 1      | 3      | ← | 2     | 0       | 2       | 17104.7015                      | -0.0110   |

**Table SL18.** Measured rotational transitions ( $\nu_{\text{obs}}$ , MHz) of the  $^{13}\text{C}_4\text{-}^{13}\text{C}_6$  isotopologue and residuals ( $\nu_{\text{obs}} - \nu_{\text{calc}}$ , MHz).

| $J'$ | $K_a'$ | $K_b'$ | ← | $J''$ | $K_a''$ | $K_b''$ | $\nu_{\text{obs}} / \text{MHz}$ | $\nu_{\text{obs}} - \nu_{\text{calc}} / \text{MHz}$ |
|------|--------|--------|---|-------|---------|---------|---------------------------------|---|
| 1    | 1      | 1      | ← | 0     | 0       | 0       | 7186.2421                       | 0.0099  |
| 2    | 0      | 2      | ← | 1     | 1       | 1       | 11933.2710                      | 0.0029  |
| 2    | 1      | 2      | ← | 1     | 0       | 1       | 1205.6139                       | 0.0069  |
| 2    | 2      | 1      | ← | 1     | 1       | 0       | 16539.3174                      | -0.0042   |
| 3    | 0      | 3      | ← | 2     | 1       | 2       | 17085.2474                      | -0.0024   |
| 3    | 1      | 3      | ← | 2     | 0       | 2       | 17109.3597                      | -0.0045   |



**Table SL19.** Measured rotational transitions ( $\nu_{\text{obs}}$ , MHz) of the  $^{13}\text{C}_3\text{-}^{13}\text{C}_4$  isotopologue and residuals ( $\nu_{\text{obs}} - \nu_{\text{calc}}$ , MHz).

| $J'$ | $K_a'$ | $K_b'$ | $\leftarrow$ | $J''$ | $K_a''$ | $K_b''$ | $\nu_{\text{obs}} / \text{MHz}$ | $\nu_{\text{obs}} - \nu_{\text{calc}} / \text{MHz}$ |
|------|--------|--------|--------------|-------|---------|---------|---------------------------------|---|
| 1    | 1      | 1      | $\leftarrow$ | 0     | 0       | 0       | 7185.6385                       | 0.0078  |
| 2    | 0      | 2      | $\leftarrow$ | 1     | 1       | 1       | 11938.7447                      | 0.0053  |
| 2    | 1      | 2      | $\leftarrow$ | 1     | 0       | 1       | 12206.2557                      | 0.0115  |
| 2    | 2      | 1      | $\leftarrow$ | 1     | 1       | 0       | 16536.2737                      | -0.0046   |
| 3    | 0      | 3      | $\leftarrow$ | 2     | 1       | 2       | 17089.6622                      | -0.0088   |
| 3    | 1      | 3      | $\leftarrow$ | 2     | 0       | 2       | 17112.9780                      | -0.0018   |

**Table SL20.** Measured rotational transitions ( $\nu_{\text{obs}}$ , MHz) of the  $^{13}\text{C}_2\text{-}^{13}\text{C}_4$  isotopologue and residuals ( $\nu_{\text{obs}} - \nu_{\text{calc}}$ , MHz).

| $J'$ | $K_a'$ | $K_b'$ | $\leftarrow$ | $J''$ | $K_a''$ | $K_b''$ | $\nu_{\text{obs}} / \text{MHz}$ | $\nu_{\text{obs}} - \nu_{\text{calc}} / \text{MHz}$ |
|------|--------|--------|--------------|-------|---------|---------|---------------------------------|---|
| 1    | 1      | 1      | $\leftarrow$ | 0     | 0       | 0       | 7112.3747                       | -0.0242   |
| 2    | 0      | 2      | $\leftarrow$ | 1     | 1       | 1       | 12034.8535                      | 0.1829  |
| 2    | 1      | 2      | $\leftarrow$ | 1     | 0       | 1       | 12135.4391                      | -0.0816   |
| 2    | 2      | 1      | $\leftarrow$ | 1     | 1       | 0       | 16314.0378                      | -0.0371   |
| 3    | 0      | 3      | $\leftarrow$ | 2     | 1       | 2       | 17107.7335                      | -0.0082   |
| 3    | 1      | 3      | $\leftarrow$ | 2     | 0       | 2       | 17111.2749                      | -0.0276   |

**Table SL21.** Measured rotational transitions ( $\nu_{\text{obs}}$ , MHz) of the  $^{13}\text{C}_1\text{-}^{13}\text{C}_4$  isotopologue and residuals ( $\nu_{\text{obs}} - \nu_{\text{calc}}$ , MHz).

| $J'$ | $K_a'$ | $K_b'$ | $\leftarrow$ | $J''$ | $K_a''$ | $K_b''$ | $\nu_{\text{obs}} / \text{MHz}$ | $\nu_{\text{obs}} - \nu_{\text{calc}} / \text{MHz}$ |
|------|--------|--------|--------------|-------|---------|---------|---------------------------------|---|
| 1    | 1      | 1      | $\leftarrow$ | 0     | 0       | 0       | 7149.2501                       | 0.0128  |
| 2    | 0      | 2      | $\leftarrow$ | 1     | 1       | 1       | 11991.0813                      | -0.0012   |
| 2    | 1      | 2      | $\leftarrow$ | 1     | 0       | 1       | 12171.7931                      | -0.0004   |

|   |   |   |   |   |   |   |            |         |
|---|---|---|---|---|---|---|------------|---------|
| 2 | 2 | 1 | ← | 1 | 1 | 0 | 16425.1520 | -0.0034 |
| 3 | 0 | 3 | ← | 2 | 1 | 2 | 17102.4608 | 0.0131  |
| 3 | 1 | 3 | ← | 2 | 0 | 2 | 17113.4635 | -0.0139 |

---

**Table SL22.** Measured rotational transitions ( $\nu_{\text{obs}}$ , MHz) of the  $^{13}\text{C4-}^{13}\text{C5}$  isotopologue and residuals ( $\nu_{\text{obs}} - \nu_{\text{calc}}$ , MHz).

| $J'$ | $K_a'$ | $K_b'$ | $\leftarrow$ | $J''$ | $K_a''$ | $K_b''$ | $\nu_{\text{obs}} / \text{MHz}$ | $\nu_{\text{obs}} - \nu_{\text{calc}} / \text{MHz}$ |
|------|--------|--------|--------------|-------|---------|---------|---------------------------------|---|
| 1    | 1      | 1      | $\leftarrow$ | 0     | 0       | 0       | 7120.8353                       | 0.0165  |
| 2    | 0      | 2      | $\leftarrow$ | 1     | 1       | 1       | 12034.8531                      | 0.0128  |
| 2    | 1      | 2      | $\leftarrow$ | 1     | 0       | 1       | 12148.7618                      | 0.0268  |
| 2    | 2      | 1      | $\leftarrow$ | 1     | 1       | 0       | 16334.5295                      | -0.0103   |
| 3    | 0      | 3      | $\leftarrow$ | 2     | 1       | 2       | 17119.0710                      | -0.0241   |
| 3    | 1      | 3      | $\leftarrow$ | 2     | 0       | 2       | 17123.6139                      | -0.0009   |

**Table SL23.** Measured rotational transitions ( $\nu_{\text{obs}}$ , MHz) of the  $^{13}\text{C2-}^{13}\text{C5}$  isotopologue and residuals ( $\nu_{\text{obs}} - \nu_{\text{calc}}$ , MHz).

| $J'$ | $K_a'$ | $K_b'$ | $\leftarrow$ | $J''$ | $K_a''$ | $K_b''$ | $\nu_{\text{obs}} / \text{MHz}$ | $\nu_{\text{obs}} - \nu_{\text{calc}} / \text{MHz}$ |
|------|--------|--------|--------------|-------|---------|---------|---------------------------------|---|
| 1    | 1      | 1      | $\leftarrow$ | 0     | 0       | 0       | 7244.0910                       | 0.0117  |
| 2    | 0      | 2      | $\leftarrow$ | 1     | 1       | 1       | 11834.7816                      | 0.0101  |
| 2    | 1      | 2      | $\leftarrow$ | 1     | 0       | 1       | 12255.4600                      | 0.0218  |
| 2    | 2      | 1      | $\leftarrow$ | 1     | 1       | 0       | 16720.8712                      | -0.0079   |
| 3    | 0      | 3      | $\leftarrow$ | 2     | 1       | 2       | 17047.7867                      | -0.0171   |
| 3    | 1      | 3      | $\leftarrow$ | 2     | 0       | 2       | 17102.0857                      | -0.0028   |

**Table SL24.** Measured rotational transitions ( $\nu_{\text{obs}}$ , MHz) of the (1)-d1 isotopologue and residuals ( $\nu_{\text{obs}} - \nu_{\text{calc}}$ , MHz).

| $J'$ | $K_a'$ | $K_b'$ | $\leftarrow$ | $J''$ | $K_a''$ | $K_b''$ | $\nu_{\text{obs}} / \text{MHz}$ | $\nu_{\text{obs}} - \nu_{\text{calc}} / \text{MHz}$ |
|------|--------|--------|--------------|-------|---------|---------|---------------------------------|---|
| 1    | 1      | 1      | $\leftarrow$ | 0     | 0       | 0       | 7201.807                        | 0.0128  |
| 2    | 0      | 2      | $\leftarrow$ | 1     | 1       | 1       | 11871.22                        | -0.0053   |
| 2    | 1      | 2      | $\leftarrow$ | 1     | 0       | 1       | 12236.94                        | 0.0018  |
| 2    | 2      | 1      | $\leftarrow$ | 1     | 1       | 0       | 16570.24                        | -0.0033   |
| 3    | 0      | 3      | $\leftarrow$ | 2     | 1       | 2       | 17082.6                         | 0.0232  |

|   |   |   |   |   |   |   |         |         |
|---|---|---|---|---|---|---|---------|---------|
| 3 | 1 | 3 | ← | 2 | 0 | 2 | 17125.2 | -0.0229 |
|---|---|---|---|---|---|---|---------|---------|

**Table SL25.** Measured rotational transitions ( $\nu_{\text{obs}}$ , MHz) of the (2)-d1 isotopologue and residuals ( $\nu_{\text{obs}}-\nu_{\text{calc}}$ , MHz).

| $J'$ | $K_a'$ | $K_b'$ | ← | $J''$ | $K_a''$ | $K_b''$ | $\nu_{\text{obs}} / \text{MHz}$ | $\nu_{\text{obs}}-\nu_{\text{calc}} / \text{MHz}$ |
|------|--------|--------|---|-------|---------|---------|---------------------------------|---|
| 1    | 1      | 1      | ← | 0     | 0       | 0       | 7218.795                        | 0.0207  |
| 2    | 0      | 2      | ← | 1     | 1       | 1       | 11724.58                        | 0.0038  |
| 2    | 1      | 2      | ← | 1     | 0       | 1       | 12200.27                        | 0.0000  |
| 2    | 2      | 1      | ← | 1     | 1       | 0       | 16674.82                        | -0.0064   |
| 3    | 0      | 3      | ← | 2     | 1       | 2       | 16932.66                        | -0.0086   |
| 3    | 1      | 3      | ← | 2     | 0       | 2       | 17001.23                        | 0.0035  |

**Table SL26.** Measured rotational transitions ( $\nu_{\text{obs}}$ , MHz) of the (3)-d1 isotopologue and residuals ( $\nu_{\text{obs}}-\nu_{\text{calc}}$ , MHz).

| $J'$ | $K_a'$ | $K_b'$ | ← | $J''$ | $K_a''$ | $K_b''$ | $\nu_{\text{obs}} / \text{MHz}$ | $\nu_{\text{obs}}-\nu_{\text{calc}} / \text{MHz}$ |
|------|--------|--------|---|-------|---------|---------|---------------------------------|---|
| 1    | 1      | 1      | ← | 0     | 0       | 0       | 7139.141                        | 0.0219  |
| 2    | 0      | 2      | ← | 1     | 1       | 1       | 12060.02                        | -0.0011   |
| 2    | 1      | 2      | ← | 1     | 0       | 1       | 12219.36                        | -0.0113   |
| 2    | 2      | 1      | ← | 1     | 1       | 0       | 16337.1                         | -0.0044   |
| 3    | 0      | 3      | ← | 2     | 1       | 2       | 17218.72                        | -0.0039   |
| 3    | 1      | 3      | ← | 2     | 0       | 2       | 17227.62                        | 0.008   |

**Table SL27.** Measured rotational transitions ( $\nu_{\text{obs}}$ , MHz) of the (4)-d1 isotopologue and residuals ( $\nu_{\text{obs}}-\nu_{\text{calc}}$ , MHz).

| $J'$ | $K_a'$ | $K_b'$ | ← | $J''$ | $K_a''$ | $K_b''$ | $\nu_{\text{obs}} / \text{MHz}$ | $\nu_{\text{obs}}-\nu_{\text{calc}} / \text{MHz}$ |
|------|--------|--------|---|-------|---------|---------|---------------------------------|---|
| 1    | 1      | 1      | ← | 0     | 0       | 0       | 7114.911                        | 0.0053  |
| 2    | 0      | 2      | ← | 1     | 1       | 1       | 11850.18                        | -0.0243   |
| 2    | 1      | 2      | ← | 1     | 1       | 1       | 11868.15                        | 0.0321  |

|   |   |   |   |   |   |   |          |         |
|---|---|---|---|---|---|---|----------|---------|
| 2 | 1 | 2 | ← | 1 | 0 | 1 | 12088.62 | 0.0056  |
| 2 | 2 | 1 | ← | 1 | 1 | 0 | 16371.01 | -0.0033 |
| 3 | 0 | 3 | ← | 2 | 1 | 2 | 16940.39 | 0.0116  |
| 3 | 1 | 3 | ← | 2 | 1 | 2 | 16941.28 | -0.0122 |
| 3 | 0 | 3 | ← | 2 | 0 | 2 | 16958.29 | -0.0032 |
| 3 | 1 | 3 | ← | 2 | 0 | 2 | 16959.2  | -0.0046 |

**Table SL28.** Measured rotational transitions ( $\nu_{\text{obs}}$ , MHz) of the (5)-d1 isotopologue and residuals ( $\nu_{\text{obs}}-\nu_{\text{calc}}$ , MHz).

| $J'$ | $K_a'$ | $K_b'$ | ← | $J''$ | $K_a''$ | $K_b''$ | $\nu_{\text{obs}} / \text{MHz}$ | $\nu_{\text{obs}}-\nu_{\text{calc}} / \text{MHz}$ |
|------|--------|--------|---|-------|---------|---------|---------------------------------|---|
| 1    | 1      | 1      | ← | 0     | 0       | 0       | 7101.647                        | 0.0083  |
| 2    | 0      | 2      | ← | 1     | 1       | 1       | 11833.4                         | -0.0049   |
| 2    | 1      | 2      | ← | 1     | 1       | 1       | 11850.68                        | -0.0059   |
| 2    | 1      | 2      | ← | 1     | 0       | 1       | 12067.08                        | -0.0082   |
| 2    | 2      | 1      | ← | 1     | 1       | 0       | 16339.47                        | 0.0002  |
| 3    | 0      | 3      | ← | 2     | 1       | 2       | 16913.08                        | 0.0085  |
| 3    | 1      | 3      | ← | 2     | 1       | 2       | 16913.98                        | 0.0382  |
| 3    | 0      | 3      | ← | 2     | 0       | 2       | 16930.33                        | -0.0221   |
| 3    | 1      | 3      | ← | 2     | 0       | 2       | 16931.21                        | -0.0147   |

**Table SL29.** Measured rotational transitions ( $\nu_{\text{obs}}$ , MHz) of the (4,9)-d2 isotopomer and residuals ( $\nu_{\text{obs}}-\nu_{\text{calc}}$ , MHz).

| $J'$ | $K_a'$ | $K_b'$ | ← | $J''$ | $K_a''$ | $K_b''$ | $\nu_{\text{obs}} / \text{MHz}$ | $\nu_{\text{obs}}-\nu_{\text{calc}} / \text{MHz}$ |
|------|--------|--------|---|-------|---------|---------|---------------------------------|---|
| 1    | 0      | 1      | ← | 0     | 0       | 0       | 6791.637                        | 0.0044  |
| 2    | 1      | 2      | ← | 1     | 1       | 1       | 11624.51                        | -0.0116   |
| 2    | 0      | 2      | ← | 1     | 0       | 1       | 11670.31                        | -0.0042   |
| 2    | 1      | 1      | ← | 1     | 1       | 0       | 15542.02                        | 0.001   |

|   |   |   |   |   |   |   |          |        |
|---|---|---|---|---|---|---|----------|--------|
| 3 | 1 | 3 | ← | 2 | 1 | 2 | 16480.21 | 0.0063 |
| 3 | 0 | 3 | ← | 2 | 0 | 2 | 16481.02 | 0.0021 |

**Table SL30.** Measured rotational transitions ( $\nu_{\text{obs}}$ , MHz) of the (3,8)-d2 isotopomer and residuals ( $\nu_{\text{obs}}-\nu_{\text{calc}}$ , MHz).

| $J'$ | $K_a'$ | $K_b'$ | ← | $J''$ | $K_a''$ | $K_b''$ | $\nu_{\text{obs}} / \text{MHz}$ | $\nu_{\text{obs}}-\nu_{\text{calc}} / \text{MHz}$ |
|------|--------|--------|---|-------|---------|---------|---------------------------------|---|
| 1    | 1      | 1      | ← | 0     | 0       | 0       | 6975.987                        | -0.0123   |
| 2    | 0      | 2      | ← | 1     | 1       | 1       | 11914.68                        | 0.009   |
| 2    | 1      | 2      | ← | 1     | 0       | 1       | 12014.32                        | 0.0271  |
| 2    | 2      | 1      | ← | 1     | 1       | 0       | 15889.70                        | -0.0015   |
| 3    | 0      | 3      | ← | 2     | 1       | 2       | 17002.26                        | -0.0095   |
| 3    | 1      | 3      | ← | 2     | 0       | 2       | 17006.00                        | -0.0094   |

**Table SL31.** Measured rotational transitions ( $\nu_{\text{obs}}$ , MHz) of the (4,8)-d2 isotopomer and residuals ( $\nu_{\text{obs}}-\nu_{\text{calc}}$ , MHz).

| $J'$ | $K_a'$ | $K_b'$ | ← | $J''$ | $K_a''$ | $K_b''$ | $\nu_{\text{obs}} / \text{MHz}$ | $\nu_{\text{obs}}-\nu_{\text{calc}} / \text{MHz}$ |
|------|--------|--------|---|-------|---------|---------|---------------------------------|---|
| 1    | 1      | 1      | ← | 0     | 0       | 0       | 6947.28                         | -0.0088   |
| 1    | 0      | 1      | ← | 0     | 0       | 0       | 6797.043                        | 0.0088  |
| 2    | 2      | 1      | ← | 2     | 0       | 2       | 6051.937                        | 0.0054  |
| 2    | 2      | 1      | ← | 2     | 1       | 2       | 6043.207                        | -0.0028   |
| 2    | 1      | 1      | ← | 2     | 0       | 2       | 5601.171                        | 0.0048  |
| 2    | 1      | 1      | ← | 2     | 1       | 2       | 5592.438                        | -0.0074   |

**Table SL32.** Measured rotational transitions ( $\nu_{\text{obs}}$ , MHz) of the (2,4)-d2 isotopomer and residuals ( $\nu_{\text{obs}}-\nu_{\text{calc}}$ , MHz).

| $J'$ | $K_a'$ | $K_b'$ | ← | $J''$ | $K_a''$ | $K_b''$ | $\nu_{\text{obs}} / \text{MHz}$ | $\nu_{\text{obs}}-\nu_{\text{calc}} / \text{MHz}$ |
|------|--------|--------|---|-------|---------|---------|---------------------------------|---|
| 1    | 1      | 1      | ← | 0     | 0       | 0       | 6982.827                        | 0.0027  |

|   |   |   |   |   |   |   |          |         |
|---|---|---|---|---|---|---|----------|---------|
| 2 | 0 | 2 | ← | 1 | 1 | 1 | 11460.38 | 0.0025  |
| 2 | 1 | 2 | ← | 1 | 0 | 1 | 11822.83 | 0.011   |
| 2 | 2 | 1 | ← | 1 | 1 | 0 | 16108.48 | -0.0028 |
| 3 | 0 | 3 | ← | 2 | 1 | 2 | 16474.99 | -0.0007 |
| 3 | 1 | 3 | ← | 2 | 0 | 2 | 16517.33 | -0.0073 |

**Table SL33.** Measured rotational transitions ( $v_{\text{obs}}$ , MHz) of the (1,3)-d2 isotopomer and residuals ( $v_{\text{obs}}-v_{\text{calc}}$ , MHz).

| $J'$ | $K_a'$ | $K_b'$ | ← | $J''$ | $K_a''$ | $K_b''$ | $v_{\text{obs}} / \text{MHz}$ | $v_{\text{obs}}-v_{\text{calc}} / \text{MHz}$ |
|------|--------|--------|---|-------|---------|---------|-------------------------------|---|
| 1    | 1      | 1      | ← | 0     | 0       | 0       | 7039.932                      | 0.002   |
| 2    | 0      | 2      | ← | 1     | 1       | 1       | 11731.36                      | 0.0108  |
| 2    | 1      | 2      | ← | 1     | 0       | 1       | 12033.69                      | 0.0279  |
| 2    | 2      | 1      | ← | 1     | 1       | 0       | 16126.06                      | -0.0061                                       |
| 3    | 0      | 3      | ← | 2     | 1       | 2       | 16871.49                      | -0.0168                                       |
| 3    | 1      | 3      | ← | 2     | 0       | 2       | 16902.65                      | -0.0056                                       |

**Table SL34.** Measured rotational transitions ( $v_{\text{obs}}$ , MHz) of the (2,3)-d2 isotopomer and residuals ( $v_{\text{obs}}-v_{\text{calc}}$ , MHz).

| $J'$ | $K_a'$ | $K_b'$ | ← | $J''$ | $K_a''$ | $K_b''$ | $v_{\text{obs}} / \text{MHz}$ | $v_{\text{obs}}-v_{\text{calc}} / \text{MHz}$ |
|------|--------|--------|---|-------|---------|---------|-------------------------------|---|
| 1    | 1      | 1      | ← | 0     | 0       | 0       | 7054.597                      | 0.0142  |
| 2    | 0      | 2      | ← | 1     | 1       | 1       | 11596.4                       | -0.003  |
| 2    | 1      | 2      | ← | 1     | 0       | 1       | 11994.36                      | -0.0115                                       |
| 2    | 2      | 1      | ← | 1     | 1       | 0       | 16223.96                      | -0.002  |
| 3    | 0      | 3      | ← | 2     | 1       | 2       | 16727                         | 0.0046  |
| 3    | 1      | 3      | ← | 2     | 0       | 2       | 16778.29                      | 0.0016  |

**Table SL35.** Measured rotational transitions ( $\nu_{\text{obs}}$ , MHz) of the (1,4)-d2 isotopomer and residuals ( $\nu_{\text{obs}}-\nu_{\text{calc}}$ , MHz).

| $J'$ | $K_a'$ | $K_b'$ | $\leftarrow$ | $J''$ | $K_a''$ | $K_b''$ | $\nu_{\text{obs}} / \text{MHz}$ | $\nu_{\text{obs}}-\nu_{\text{calc}} / \text{MHz}$ |
|------|--------|--------|--------------|-------|---------|---------|---------------------------------|---|
| 1    | 1      | 1      | $\leftarrow$ | 0     | 0       | 0       | 6992.662                        | -0.006  |
| 2    | 0      | 2      | $\leftarrow$ | 1     | 1       | 1       | 11562.9                         | -0.0113   |
| 2    | 1      | 2      | $\leftarrow$ | 1     | 1       | 1       | 11594.75                        | 0.0245  |
| 2    | 0      | 2      | $\leftarrow$ | 1     | 0       | 1       | 11851.67                        | 0.0043  |
| 2    | 1      | 2      | $\leftarrow$ | 1     | 0       | 1       | 11883.5                         | 0.0222  |
| 2    | 2      | 1      | $\leftarrow$ | 1     | 1       | 0       | 16087.19                        | -0.0039   |
| 3    | 0      | 3      | $\leftarrow$ | 2     | 1       | 2       | 16608.8                         | -0.011  |
| 3    | 1      | 3      | $\leftarrow$ | 2     | 0       | 2       | 16642.82                        | -0.0109   |

**Table SL36.** Measured rotational transitions ( $\nu_{\text{obs}}$ , MHz) of the (1,6)-d2 isotopomer and residuals ( $\nu_{\text{obs}}-\nu_{\text{calc}}$ , MHz).

| $J'$ | $K_a'$ | $K_b'$ | $\leftarrow$ | $J''$ | $K_a''$ | $K_b''$ | $\nu_{\text{obs}} / \text{MHz}$ | $\nu_{\text{obs}}-\nu_{\text{calc}} / \text{MHz}$ |
|------|--------|--------|--------------|-------|---------|---------|---------------------------------|---|
| 1    | 1      | 1      | $\leftarrow$ | 0     | 0       | 0       | 7119.61                         | -0.0076   |
| 2    | 2      | 1      | $\leftarrow$ | 2     | 1       | 2       | 6672.827                        | 0.0052  |
| 4    | 4      | 0      | $\leftarrow$ | 4     | 3       | 1       | 5649.124                        | 0.01  |
| 2    | 0      | 2      | $\leftarrow$ | 1     | 1       | 1       | 11380.55                        | 0.0115  |
| 2    | 1      | 2      | $\leftarrow$ | 1     | 0       | 1       | 12014.98                        | 0.0131  |
| 2    | 2      | 1      | $\leftarrow$ | 1     | 1       | 0       | 16463.5                         | -0.006  |
| 3    | 0      | 3      | $\leftarrow$ | 2     | 1       | 2       | 16571.87                        | 0.0012  |
| 3    | 1      | 3      | $\leftarrow$ | 2     | 0       | 2       | 16690.97                        | 0.0052  |
| 1    | 1      | 1      | $\leftarrow$ | 0     | 0       | 0       | 7119.61                         | -0.0076   |
| 2    | 2      | 1      | $\leftarrow$ | 2     | 1       | 2       | 6672.827                        | 0.0052  |

**Table SL37.** Measured rotational transitions ( $\nu_{\text{obs}}$ , MHz) of the (2,9)-d2 isotopomer and residuals ( $\nu_{\text{obs}}-\nu_{\text{calc}}$ , MHz).



| $J'$ | $K_a'$ | $K_b'$ | $\leftarrow$ | $J''$ | $K_a''$ | $K_b''$ | $\nu_{\text{obs}} / \text{MHz}$ | $\nu_{\text{obs}} - \nu_{\text{calc}} / \text{MHz}$ |
|------|--------|--------|--------------|-------|---------|---------|---------------------------------|---|
| 1    | 1      | 1      | $\leftarrow$ | 0     | 0       | 0       | 6999.398                        | 0.0056  |
| 2    | 0      | 2      | $\leftarrow$ | 1     | 1       | 1       | 11424.75                        | 0.0002  |
| 2    | 1      | 2      | $\leftarrow$ | 1     | 0       | 1       | 11836.09                        | 0.0088  |
| 2    | 2      | 1      | $\leftarrow$ | 1     | 1       | 0       | 16161.48                        | -0.0004   |
| 3    | 0      | 3      | $\leftarrow$ | 2     | 1       | 2       | 16458.56                        | 0.0079  |
| 3    | 1      | 3      | $\leftarrow$ | 2     | 0       | 2       | 16512.08                        | -0.0156   |
| 2    | 2      | 1      | $\leftarrow$ | 2     | 1       | 2       | 6488.097                        | -0.002  |

**Table SL38.** Measured rotational transitions ( $\nu_{\text{obs}}$ , MHz) of the (1,8)-d2 isotopomer and residuals ( $\nu_{\text{obs}} - \nu_{\text{calc}}$ , MHz).

| $J'$ | $K_a'$ | $K_b'$ | $\leftarrow$ | $J''$ | $K_a''$ | $K_b''$ | $\nu_{\text{obs}} / \text{MHz}$ | $\nu_{\text{obs}} - \nu_{\text{calc}} / \text{MHz}$ |
|------|--------|--------|--------------|-------|---------|---------|---------------------------------|---|
| 1    | 1      | 1      | $\leftarrow$ | 0     | 0       | 0       | 7039.215                        | -0.0039   |
| 2    | 0      | 2      | $\leftarrow$ | 1     | 1       | 1       | 11734.59                        | 0.0079  |
| 2    | 1      | 2      | $\leftarrow$ | 1     | 0       | 1       | 12031.64                        | 0.0279  |
| 2    | 2      | 1      | $\leftarrow$ | 1     | 1       | 0       | 16125.26                        | -0.004  |
| 3    | 0      | 3      | $\leftarrow$ | 2     | 1       | 2       | 16870.93                        | -0.0063   |
| 3    | 1      | 3      | $\leftarrow$ | 2     | 0       | 2       | 16901.01                        | -0.0135   |

**Table SL39.** Measured rotational transitions ( $\nu_{\text{obs}}$ , MHz) of the (1,9)-d2 isotopomer and residuals ( $\nu_{\text{obs}} - \nu_{\text{calc}}$ , MHz).

| $J'$ | $K_a'$ | $K_b'$ | $\leftarrow$ | $J''$ | $K_a''$ | $K_b''$ | $\nu_{\text{obs}} / \text{MHz}$ | $\nu_{\text{obs}} - \nu_{\text{calc}} / \text{MHz}$ |
|------|--------|--------|--------------|-------|---------|---------|---------------------------------|---|
| 1    | 1      | 1      | $\leftarrow$ | 0     | 0       | 0       | 6979.3558                       | -0.0080   |
| 2    | 0      | 2      | $\leftarrow$ | 1     | 1       | 1       | 11569.7327                      | 0.0052  |
| 2    | 1      | 2      | $\leftarrow$ | 1     | 0       | 1       | 11867.4637                      | 0.0111  |
| 3    | 0      | 3      | $\leftarrow$ | 2     | 1       | 2       | 16602.1963                      | -0.0125   |
| 3    | 1      | 3      | $\leftarrow$ | 2     | 0       | 2       | 16631.8455                      | 0.0043  |

**Table SL40.** Measured rotational transitions ( $\nu_{\text{obs}}$ , MHz) of the (2,8)-d2 isotopomer and residuals ( $\nu_{\text{obs}}-\nu_{\text{calc}}$ , MHz).

| $J'$ | $K_a'$ | $K_b'$ | $\leftarrow$ | $J''$ | $K_a''$ | $K_b''$ | $\nu_{\text{obs}} / \text{MHz}$ | $\nu_{\text{obs}}-\nu_{\text{calc}} / \text{MHz}$ |
|------|--------|--------|--------------|-------|---------|---------|---------------------------------|---|
| 1    | 1      | 1      | $\leftarrow$ | 0     | 0       | 0       | 7056.7581                       | 0.0173  |
| 2    | 0      | 2      | $\leftarrow$ | 1     | 1       | 1       | 11583.6441                      | 0.0093  |
| 2    | 1      | 2      | $\leftarrow$ | 1     | 0       | 1       | 11994.5828                      | 0.0127  |
| 2    | 2      | 1      | $\leftarrow$ | 1     | 1       | 0       | 16232.2730                      | -0.0080   |
| 3    | 0      | 3      | $\leftarrow$ | 2     | 1       | 2       | 16718.1684                      | -0.0190   |
| 3    | 1      | 3      | $\leftarrow$ | 2     | 0       | 2       | 16772.6454                      | -0.0039   |

**Table SL41.** Measured rotational transitions ( $\nu_{\text{obs}}$ , MHz) of the (1,5)-d2 isotopomer and residuals ( $\nu_{\text{obs}}-\nu_{\text{calc}}$ , MHz).

| $J'$ | $K_a'$ | $K_b'$ | $\leftarrow$ | $J''$ | $K_a''$ | $K_b''$ | $\nu_{\text{obs}} / \text{MHz}$ | $\nu_{\text{obs}}-\nu_{\text{calc}} / \text{MHz}$ |
|------|--------|--------|--------------|-------|---------|---------|---------------------------------|---|
| 1    | 1      | 1      | $\leftarrow$ | 0     | 0       | 0       | 6976.4853                       | -0.0099   |
| 2    | 0      | 2      | $\leftarrow$ | 1     | 1       | 1       | 11539.5296                      | 0.0022  |
| 2    | 1      | 2      | $\leftarrow$ | 1     | 0       | 1       | 11856.0937                      | 0.0171  |
| 3    | 0      | 3      | $\leftarrow$ | 2     | 1       | 2       | 16572.3148                      | 0.0047  |
| 3    | 1      | 3      | $\leftarrow$ | 2     | 0       | 2       | 16605.5733                      | -0.0143   |

**Table SL42.** Measured rotational transitions ( $\nu_{\text{obs}}$ , MHz) of the (2,5)-d2 isotopomer and residuals ( $\nu_{\text{obs}}-\nu_{\text{calc}}$ , MHz).

| $J'$ | $K_a'$ | $K_b'$ | $\leftarrow$ | $J''$ | $K_a''$ | $K_b''$ | $\nu_{\text{obs}} / \text{MHz}$ | $\nu_{\text{obs}}-\nu_{\text{calc}} / \text{MHz}$ |
|------|--------|--------|--------------|-------|---------|---------|---------------------------------|---|
| 1    | 1      | 1      | $\leftarrow$ | 0     | 0       | 0       | 6964.4579                       | 0.0091  |
| 2    | 1      | 2      | $\leftarrow$ | 1     | 0       | 1       | 11793.8472                      | -0.0048   |
| 2    | 2      | 1      | $\leftarrow$ | 1     | 1       | 0       | 16063.9435                      | 0.0002  |

|   |   |   |   |   |   |   |            |         |
|---|---|---|---|---|---|---|------------|---------|
| 3 | 0 | 3 | ← | 2 | 1 | 2 | 16440.3788 | 0.0000  |
| 2 | 2 | 1 | ← | 2 | 1 | 2 | 6405.1353  | -0.0016 |

**Table SL43.** Measured rotational transitions ( $\nu_{\text{obs}}$ , MHz) of the (1,10)-d2 isotopomer and residuals ( $\nu_{\text{obs}} - \nu_{\text{calc}}$ , MHz).

| $J'$ | $K_a'$ | $K_b'$ | ← | $J''$ | $K_a''$ | $K_b''$ | $\nu_{\text{obs}} / \text{MHz}$ | $\nu_{\text{obs}} - \nu_{\text{calc}} / \text{MHz}$ |
|------|--------|--------|---|-------|---------|---------|---------------------------------|---|
| 1    | 1      | 1      | ← | 0     | 0       | 0       | 6960.5413                       | 0.0208  |
| 2    | 0      | 2      | ← | 1     | 1       | 1       | 11570.3628                      | 0.0177  |
| 2    | 1      | 2      | ← | 1     | 1       | 1       | 11842.7463                      | -0.0175   |
| 1    | 0      | 1      | ← | 0     | 0       | 0       | 6711.7580                       | -0.0212   |

**Table SL44.** Measured rotational transitions ( $\nu_{\text{obs}}$ , MHz) of the (2,10)-d2 isotopomer and residuals ( $\nu_{\text{obs}} - \nu_{\text{calc}}$ , MHz).

| $J'$ | $K_a'$ | $K_b'$ | ← | $J''$ | $K_a''$ | $K_b''$ | $\nu_{\text{obs}} / \text{MHz}$ | $\nu_{\text{obs}} - \nu_{\text{calc}} / \text{MHz}$ |
|------|--------|--------|---|-------|---------|---------|---------------------------------|---|
| 1    | 1      | 1      | ← | 0     | 0       | 0       | 6979.9469                       | 0.0141  |
| 2    | 0      | 2      | ← | 1     | 1       | 1       | 11433.0191                      | 0.0115  |
| 2    | 1      | 2      | ← | 1     | 1       | 1       | 11812.9179                      | -0.0113   |
| 1    | 0      | 1      | ← | 0     | 0       | 0       | 6642.8384                       | -0.0145   |

**Table SL45.** Measured rotational transitions ( $\nu_{\text{obs}}$ , MHz) of the (2,3,8)-d3 isotopomer and residuals ( $\nu_{\text{obs}} - \nu_{\text{calc}}$ , MHz).

| $J'$ | $K_a'$ | $K_b'$ | ← | $J''$ | $K_a''$ | $K_b''$ | $\nu_{\text{obs}} / \text{MHz}$ | $\nu_{\text{obs}} - \nu_{\text{calc}} / \text{MHz}$ |
|------|--------|--------|---|-------|---------|---------|---------------------------------|---|
| 1    | 1      | 1      | ← | 0     | 0       | 0       | 6897.888                        | -0.0258   |
| 2    | 0      | 2      | ← | 1     | 1       | 1       | 11460.26                        | 0.0081  |
| 2    | 1      | 2      | ← | 1     | 0       | 1       | 11796.46                        | 0.0284  |
| 2    | 2      | 1      | ← | 1     | 1       | 0       | 15795.22                        | 0.0021  |

|   |   |   |   |   |   |   |          |         |
|---|---|---|---|---|---|---|----------|---------|
| 3 | 0 | 3 | ← | 2 | 1 | 2 | 16520.78 | -0.0122 |
| 3 | 1 | 3 | ← | 2 | 0 | 2 | 16559.84 | -0.005  |

**Table SL46.** Measured rotational transitions ( $\nu_{\text{obs}}$ , MHz) of the (1,4,9)-d3 isotopomer and residuals ( $\nu_{\text{obs}} - \nu_{\text{calc}}$ , MHz).

| $J'$ | $K_a'$ | $K_b'$ | ← | $J''$ | $K_a''$ | $K_b''$ | $\nu_{\text{obs}} / \text{MHz}$ | $\nu_{\text{obs}} - \nu_{\text{calc}} / \text{MHz}$ |
|------|--------|--------|---|-------|---------|---------|---------------------------------|---|
| 1    | 1      | 1      | ← | 0     | 0       | 0       | 6705.143                        | -0.0246   |
| 2    | 0      | 2      | ← | 1     | 1       | 1       | 11372.71                        | -0.002  |
| 2    | 2      | 1      | ← | 1     | 1       | 0       | 15361.97                        | 0.0073  |
| 3    | 0      | 3      | ← | 2     | 1       | 2       | 16168.89                        | -0.0015   |
| 3    | 1      | 3      | ← | 2     | 0       | 2       | 16171.67                        | 0.0062  |

**Table SL47.** Measured rotational transitions ( $\nu_{\text{obs}}$ , MHz) of the (1,3,8)-d3 isotopomer and residuals ( $\nu_{\text{obs}} - \nu_{\text{calc}}$ , MHz).

| $J'$ | $K_a'$ | $K_b'$ | ← | $J''$ | $K_a''$ | $K_b''$ | $\nu_{\text{obs}} / \text{MHz}$ | $\nu_{\text{obs}} - \nu_{\text{calc}} / \text{MHz}$ |
|------|--------|--------|---|-------|---------|---------|---------------------------------|---|
| 1    | 1      | 1      | ← | 0     | 0       | 0       | 6882.2833                       | -0.0216   |
| 2    | 0      | 2      | ← | 1     | 1       | 1       | 11600.1449                      | 0.0009  |
| 2    | 2      | 1      | ← | 1     | 1       | 0       | 15693.4047                      | 0.0061  |
| 3    | 0      | 3      | ← | 2     | 1       | 2       | 16668.4997                      | -0.0106   |
| 3    | 1      | 3      | ← | 2     | 0       | 2       | 16688.8445                      | 0.0131  |

**Table SL48.** Measured rotational transitions ( $\nu_{\text{obs}}$ , MHz) of the (2,4,9)-d3 isotopomer and residuals ( $\nu_{\text{obs}} - \nu_{\text{calc}}$ , MHz).

| $J'$ | $K_a'$ | $K_b'$ | ← | $J''$ | $K_a''$ | $K_b''$ | $\nu_{\text{obs}} / \text{MHz}$ | $\nu_{\text{obs}} - \nu_{\text{calc}} / \text{MHz}$ |
|------|--------|--------|---|-------|---------|---------|---------------------------------|---|
| 1    | 1      | 1      | ← | 0     | 0       | 0       | 6718.8997                       | -0.0323   |
| 2    | 0      | 2      | ← | 1     | 1       | 1       | 11249.6884                      | 0.0057  |

|   |   |   |   |   |   |   |            |         |
|---|---|---|---|---|---|---|------------|---------|
| 2 | 1 | 2 | ← | 1 | 0 | 1 | 11423.6757 | 0.0198  |
| 2 | 2 | 1 | ← | 1 | 1 | 0 | 15452.0779 | 0.0055  |
| 3 | 0 | 3 | ← | 2 | 1 | 2 | 16039.8632 | -0.0145 |
| 3 | 1 | 3 | ← | 2 | 0 | 2 | 16050.6683 | 0.0045  |

**Table SL49.** Measured rotational transitions ( $\nu_{\text{obs}}$ , MHz) of the (2,3,7,8)-d4 isotopomer and residuals ( $\nu_{\text{obs}} - \nu_{\text{calc}}$ , MHz).

| $J'$ | $K_a'$ | $K_b'$ | ← | $J''$ | $K_a''$ | $K_b''$ | $\nu_{\text{obs}} / \text{MHz}$ | $\nu_{\text{obs}} - \nu_{\text{calc}} / \text{MHz}$ |
|------|--------|--------|---|-------|---------|---------|---------------------------------|---|
| 1    | 1      | 1      | ← | 0     | 0       | 0       | 6804.767                        | -0.0069   |
| 2    | 0      | 2      | ← | 1     | 1       | 1       | 11146.7                         | 0.008   |
| 2    | 1      | 2      | ← | 1     | 0       | 1       | 11621.89                        | 0.0236  |
| 2    | 2      | 1      | ← | 1     | 1       | 0       | 15597.23                        | -0.0025   |
| 3    | 0      | 3      | ← | 2     | 1       | 2       | 16188.47                        | -0.012  |
| 3    | 1      | 3      | ← | 2     | 0       | 2       | 16264.63                        | -0.005  |

**Table SL50.** Measured rotational transitions ( $\nu_{\text{obs}}$ , MHz) of the (2,4,7,9)-d4 isotopomer and residuals ( $\nu_{\text{obs}} - \nu_{\text{calc}}$ , MHz).

| $J'$ | $K_a'$ | $K_b'$ | ← | $J''$ | $K_a''$ | $K_b''$ | $\nu_{\text{obs}} / \text{MHz}$ | $\nu_{\text{obs}} - \nu_{\text{calc}} / \text{MHz}$ |
|------|--------|--------|---|-------|---------|---------|---------------------------------|---|
| 1    | 1      | 1      | ← | 0     | 0       | 0       | 6632.364                        | -0.0064   |
| 2    | 0      | 2      | ← | 1     | 1       | 1       | 10951.76                        | -0.0037   |
| 2    | 1      | 2      | ← | 1     | 0       | 1       | 11260.65                        | -0.0127   |
| 2    | 2      | 1      | ← | 1     | 1       | 0       | 15268.83                        | 0.0042  |
| 3    | 0      | 3      | ← | 2     | 1       | 2       | 15729.43                        | 0.0019  |
| 3    | 1      | 3      | ← | 2     | 0       | 2       | 15762.55                        | 0.0084  |

1. Gordy, W. C., R.L., *Microwave Molecular Spectra*. 2nd ed.; John Wiley & Sons, Inc.: New York, 1984.
2. Dommen, J.; Brubacher, T.; Grassi, G.; Bauder, A., Microwave spectra of isotopic species and substitution structure of cyclohexane. *Journal of the American Chemical Society* **1990**, *112* (3), 953-957.

3. Brown, G. G.; Dian, B. C.; Douglass, K. O.; Geyer, S. M.; Shipman, S. T.; Pate, B. H., A broadband Fourier transform microwave spectrometer based on chirped pulse excitation. *Rev Sci Instrum* **2008**, *79* (5), 053103.
4. Pérez, C.; Lobsiger, S.; Seifert, N. A.; Zaleski, D. P.; Temelso, B.; Shields, G. C.; Kisiel, Z.; Pate, B. H., Broadband Fourier transform rotational spectroscopy for structure determination: The water heptamer. *Chemical Physics Letters* **2013**, *571*, 1-15.
5. Scharpen, L. H.; Wollrab, J. E.; Ames, D. P., Microwave Spectrum, Structure, and Dipole Moment of Cyclohexene. *The Journal of Chemical Physics* **1968**, *49* (5), 2368-2372.
6. Pickett, H. M., The fitting and prediction of vibration-rotation spectra with spin interactions. *J. Mol. Spectrosc.* **1991**, *148* (2), 371-377.
7. Kisiel, Z. PROSPE - Programs for ROTational SPEctroscopy. <http://info.ifpan.edu.pl/~kisiel/prospe.htm>.
8. Kisiel, Z. P., L.; Medvedev, I.R.; Winnewisser, M.; De Lucia, F.C.; Herbst, E. , Rotational spectrum of trans-trans diethyl ether in the ground and three excited vibrational states. *J. Mol. Spectrosc.* **2005**, *233*, 231-243.
9. Frisch, M. J. T., G. W.; Schlegel, H. B.; Scuseria, G. E.; Robb, M. A.; Cheeseman, J. R.; Scalmani, G.; Barone, V.; Mennucci, B.; Petersson, G. A.; Nakatsuji, H.; Caricato, M.; Li, X.; Hratchian, H. P.; Izmaylov, A. F.; Bloino, J.; Zheng, G.; Sonnenberg, J. L.; Hada, M.; Ehara, M.; Toyota, K.; Fukuda, R.; Hasegawa, J.; Ishida, M.; Nakajima, T.; Honda, Y.; Kitao, O.; Nakai, H.; Vreven, T.; Montgomery, J. A., Jr.; Peralta, J. E.; Ogliaro, F.; Bearpark, M.; Heyd, J. J.; Brothers, E.; Kudin, K. N.; Staroverov, V. N.; Kobayashi, R.; Normand, J.; Raghavachari, K.; Rendell, A.; Burant, J. C.; Iyengar, S. S.; Tomasi, J.; Cossi, M.; Rega, N.; Millam, J. M.; Klene, M.; Knox, J. E.; Cross, J. B.; Bakken, V.; Adamo, C.; Jaramillo, J.; Gomperts, R.; Stratmann, R. E.; Yazyev, O.; Austin, A. J.; Cammi, R.; Pomelli, C.; Ochterski, J. W.; Martin, R. L.; Morokuma, K.; Zakrzewski, V. G.; Voth, G. A.; Salvador, P.; Dannenberg, J. J.; Dapprich, S.; Daniels, A. D.; Farkas, Ö.; Foresman, J. B.; Ortiz, J. V.; Cioslowski, J.; Fox, D. J. , *Gaussian 09, Revision E.01*. Gaussian, Inc.: Wallingford, CT, 2016.
10. Lis, E. C.; Delafuente, D. A.; Lin, Y.; Mocella, C. J.; Todd, M. A.; Liu, W.; Sabat, M.; Myers, W. H.; Harman, W. D., The Uncommon Reactivity of Dihapto-Coordinated Nitrile, Ketone, and Alkene Ligands When Bound to a Powerful  $\pi$ -Base. *Organometallics* **2006**, *25* (21), 5051-5058.

## M. Mechanistic Considerations.

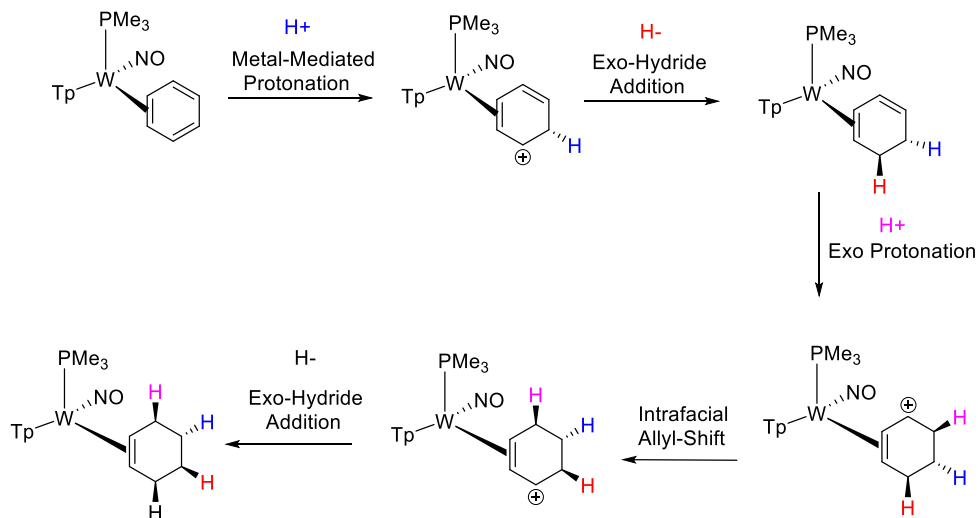


**Figure SM.1.** Sequence of proton and hydride addition reactions to tungsten-benzene complex.

In principle, protonation of the  $\eta^2$ -benzene ligand of **1** could occur at any one of the six carbons. Several mechanisms that would give rise to **2** are shown in supplementary materials (Fig. S8), which include direct protonation of the benzene endo or exo to the metal, as well as indirect protonation via a metal hydride. The reaction of **1** with  $D^+$  to form **11** results in deuterium incorporation exclusively endo to the metal, but this does not definitively show which carbon is initially protonated. Given that the endo proton of the benzene ligand in **1** completely preempts protonation from an exogenous acid (exo), we propose that the protonation must be concerted-- that *C-H bond formation is intramolecular and simultaneous with electronic changes at the metal*, which could lower the activation barrier for this process (relative to protonation by an external acid). Such a mechanism could occur via a hydride intermediate, but this seems sterically untenable. Rather, we propose a mechanism (Fig. S14) in which the nitrosyl ligand first is protonated to form a hydroxylimido ligand analogous to that reported by Legzdins et al.<sup>21</sup> This would be followed by a concerted proton transfer in which a gamma carbon of the benzene is protonated simultaneously with release of electron density back into the tungsten through the NO group. Such action would stabilize the emerging benzenium ligand (Fig. S14; **2\***). An analogous protonation at the other gamma carbon would lead to the minor isomer **3**, via **3\***. DFT calculations indicate that the  $\eta^2$ -benzenium complex **2** is only 2.4 kcal/mol lower in energy than the protonated nitrosyl (**1H<sup>+</sup>**), and the activation barrier for this process (transition state shown in Fig. S14) is only ~12 kcal/mol. The role of nitrosyl ligands in intramolecular proton transfer has been previously documented.<sup>22</sup>

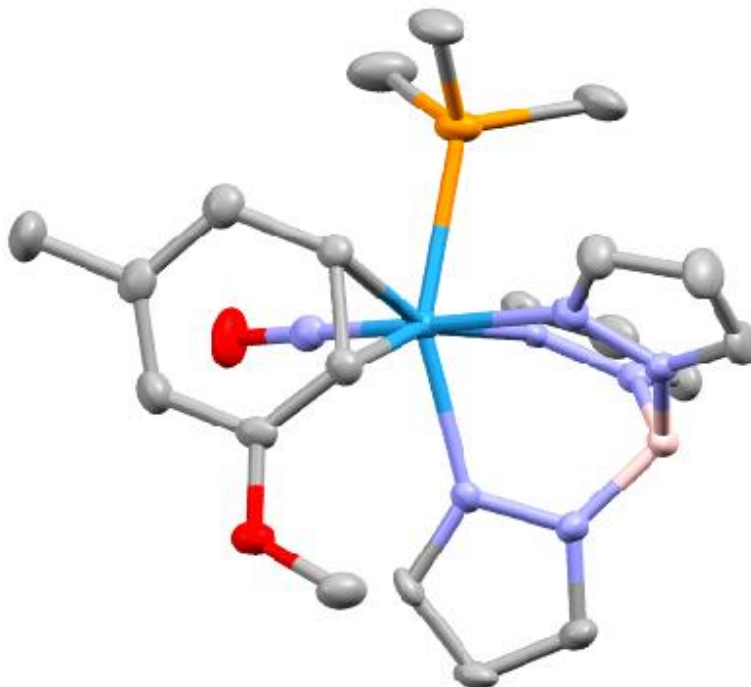
NOESY data for a sample of **1** in acidic solution (S9) include chemical exchange correlations (Fig. S9; circled correlations) that indicate the interconversion of **2** and **3** (Fig. S14). The chemical exchange between seven pairs of protons from the two isomers (each pair indicated by a different color) reveal that an *intermolecular spin transfer occurs between 2 to 3 with a concomitant 60° ccw rotation of the benzene ring* (looking from benzene to tungsten). Further, an *intramolecular spin transfer is indicated for 2 that involves a 120° cw rotation* (Fig S9; boxed correlations). We propose that these exchanges occur via the

intermediate species **1H**<sup>+</sup> (Figure S14), where a reversible nitrosyl proton transfer can involve either gamma carbon. Note that isomerization of **2/3** occurs at a rate similar to, but not significantly slower than the purported benzene ring-walk, because the latter isomerization does not completely scramble the benzene proton spin density. The chemical exchange data rules out the direct isomerization of **2** and **3**, as well as  $\alpha$  or  $\beta$  protonation as the dominant isomerization mechanism, since these pathways would result in different exchange patterns (Fig. S14).

Regarding the stereochemistry and kinetics of  $\eta^2$ -diene protonation, the reaction of complexes **4** and **5** with a deuterated acid indicates that at -30 °C, the hydrogen is delivered exogenously, exo to the tungsten (Fig 1). The allyl complex **26** was prepared from the 1,3-cyclohexadiene species **4**, while treatment of the stereoisomer **5** reacts to form the isotopomer **24**. In contrast to the  $\eta^2$ -benzene complex **1**, a metal- or nitrosyl-assisted mechanism does not appear to be involved at this temperature. We speculate that while endo protonation may still be accessible for these 1,3-cyclohexadiene complexes, the less-delocalized diene ligand is more basic than its  $\eta^2$ -benzene predecessor, and its direct exo protonation apparently preempts the endo mechanism at -30 °C.



## Crystallographic Data for Chapter 3



### Crystal Structure Report for **Complex 7** in Chapter 3

A colorless block-like specimen of  $C_{18}H_{29}BN_7OPW$ , approximate dimensions 0.098 mm x 0.099 mm x 0.119 mm, was coated with Paratone oil and mounted on a MiTeGen MicroLoop. The X-ray intensity data were measured on a Bruker Kappa APEXII Duo system equipped with a fine-focus sealed tube (Mo  $K_{\alpha}$ ,  $\lambda = 0.71073 \text{ \AA}$ ) and a graphite monochromator.

The total exposure time was 1.41 hours. The frames were integrated with the Bruker SAINT software package<sup>7</sup> using a narrow-frame algorithm. The integration of the data using a monoclinic unit cell yielded a total of 21812 reflections to a maximum  $\theta$  angle of  $27.91^{\circ}$  ( $0.76 \text{ \AA}$  resolution), of which 5285 were independent (average redundancy 4.127, completeness = 99.5%,  $R_{int} = 4.51\%$ ,  $R_{sig} = 3.93\%$ ) and 4355 (82.40%) were greater than  $2\sigma(F^2)$ . The final cell constants of  $a = 8.6285(4) \text{ \AA}$ ,  $b = 15.2499(8) \text{ \AA}$ ,  $c = 17.0041(7) \text{ \AA}$ ,  $\beta = 97.248(2)^{\circ}$ , volume =  $2219.58(18) \text{ \AA}^3$ , are based upon the refinement of the XYZ-centroids of 6396 reflections above  $20 \sigma(I)$  with  $5.057^{\circ} < 2\theta < 55.57^{\circ}$ . Data were corrected for absorption effects using the Multi-Scan method (SADABS).<sup>1</sup> The ratio of minimum to maximum apparent transmission was 0.852. The calculated minimum and maximum transmission coefficients (based on crystal size) are 0.5710 and 0.6250.

<sup>7</sup> Bruker (2012). *Saint*; *SADABS*; *APEX3*. Bruker AXS Inc., Madison, Wisconsin, USA.

The structure was solved and refined using the Bruker SHELXTL Software Package<sup>8</sup> within APEX3<sup>1</sup> and OLEX2,<sup>9</sup> using the space group  $P 2_1/n$ , with  $Z = 4$  for the formula unit,  $C_{18}H_{29}BN_7OPW$ . Non-hydrogen atoms were refined anisotropically. Hydrogen atoms were placed in geometrically calculated positions with  $U_{iso} = 1.2U_{equiv}$  of the parent atom ( $U_{iso} = 1.5 U_{equiv}$  for methyl), except for the B-H hydrogen atom, which was located in the diffraction map. The final anisotropic full-matrix least-squares refinement on  $F^2$  with 269 variables converged at  $R1 = 3.00\%$ , for the observed data and  $wR2 = 7.15\%$  for all data. The goodness-of-fit was 1.038. The largest peak in the final difference electron density synthesis was 1.694  $e^-/\text{\AA}^3$  and the largest hole was -1.103  $e^-/\text{\AA}^3$  with an RMS deviation of 0.155  $e^-/\text{\AA}^3$ . On the basis of the final model, the calculated density was 1.751  $\text{g}/\text{cm}^3$  and  $F(000)$ , 1152  $e^-$ .

**Table 1. Sample and crystal data for Harman\_10JAS\_159.**

|                               |                              |                           |
|-------------------------------|------------------------------|---------------------------|
| <b>Identification code</b>    | Harman_10JAS_159             |                           |
| <b>Chemical formula</b>       | $C_{18}H_{29}BN_7OPW$        |                           |
| <b>Formula weight</b>         | 585.11 $\text{g}/\text{mol}$ |                           |
| <b>Temperature</b>            | 100(2) K                     |                           |
| <b>Wavelength</b>             | 0.71073 $\text{\AA}$         |                           |
| <b>Crystal size</b>           | 0.098 x 0.099 x 0.119 mm     |                           |
| <b>Crystal habit</b>          | colorless block              |                           |
| <b>Crystal system</b>         | monoclinic                   |                           |
| <b>Space group</b>            | $P 1 2_1/n 1$                |                           |
| <b>Unit cell dimensions</b>   | $a = 8.6285(4) \text{\AA}$   | $\alpha = 90^\circ$       |
|                               | $b = 15.2499(8) \text{\AA}$  | $\beta = 97.248(2)^\circ$ |
|                               | $c = 17.0041(7) \text{\AA}$  | $\gamma = 90^\circ$       |
| <b>Volume</b>                 | 2219.58(18) $\text{\AA}^3$   |                           |
| <b>Z</b>                      | 4                            |                           |
| <b>Density (calculated)</b>   | 1.751 $\text{g}/\text{cm}^3$ |                           |
| <b>Absorption coefficient</b> | 5.300 $\text{mm}^{-1}$       |                           |
| <b>F(000)</b>                 | 1152                         |                           |

<sup>8</sup> Sheldrick, G. M. (2015). *Acta Cryst. A* **71**, 3-8.

<sup>9</sup> Dolomanov, O. V.; Bourhis, L. J.; Gildea, R. J.; Howard, J. A. K.; Puschmann, H. *J. Appl. Cryst.* (2009). **42**, 339-341.

**Table 2. Data collection and structure refinement for Harman\_10JAS\_159.**

|  |  |                           |
|--|--|---------------------------|
| <b>Diffractometer</b>                      | Bruker Kappa APEXII Duo Bruker Kappa APEXII Duo                |                           |
| <b>Radiation source</b>                    | fine-focus sealed tube (Mo K $\alpha$ , $\lambda$ = 0.71073 Å) |                           |
| <b>Theta range for data collection</b>     | 1.80 to 27.91°   |                           |
| <b>Index ranges</b>                        | -11 ≤ h ≤ 10, -20 ≤ k ≤ 17, -19 ≤ l ≤ 22                       |                           |
| <b>Reflections collected</b>               | 21812  |                           |
| <b>Independent reflections</b>             | 5285 [R(int) = 0.0451]   |                           |
| <b>Coverage of independent reflections</b> | 99.5%  |                           |
| <b>Absorption correction</b>               | Multi-Scan   |                           |
| <b>Max. and min. transmission</b>          | 0.6250 and 0.5710  |                           |
| <b>Structure solution technique</b>        | direct methods   |                           |
| <b>Structure solution program</b>          | SHELXT 2014/5 (Sheldrick, 2014)                                |                           |
| <b>Refinement method</b>                   | Full-matrix least-squares on F <sup>2</sup>                    |                           |
| <b>Refinement program</b>                  | SHELXL-2017/1 (Sheldrick, 2017)                                |                           |
| <b>Function minimized</b>                  | $\sum w(F_o^2 - F_c^2)^2$                                      |                           |
| <b>Data / restraints / parameters</b>      | 5285 / 0 / 269   |                           |
| <b>Goodness-of-fit on F<sup>2</sup></b>    | 1.038  |                           |
| <b><math>\Delta/\sigma_{\max}</math></b>   | 0.001  |                           |
| <b>Final R indices</b>                     | 4355 data; $I > 2\sigma(I)$                                    | R1 = 0.0300, wR2 = 0.0673 |
|  | all data   | R1 = 0.0428, wR2 = 0.0715 |

|                                    |   |
|------------------------------------|---|
| <b>Weighting scheme</b>            | $w=1/[\sigma^2(F_o^2)+(0.0284P)^2+8.2269P]$<br>where $P=(F_o^2+2F_c^2)/3$ |
| <b>Largest diff. peak and hole</b> | 1.694 and -1.103 eÅ <sup>-3</sup>   |
| <b>R.M.S. deviation from mean</b>  | 0.155 eÅ <sup>-3</sup>  |

**Table 3. Atomic coordinates and equivalent isotropic atomic displacement parameters (Å<sup>2</sup>) for Harman\_10JAS\_159.**

U(eq) is defined as one third of the trace of the orthogonalized U<sub>ij</sub> tensor.

|    | <b>x/a</b>  | <b>y/b</b> | <b>z/c</b> | <b>U(eq)</b> |
|----|-------------|------------|------------|--------------|
| W1 | 0.80769(2)  | 0.33119(2) | 0.16833(2) | 0.01176(6)   |
| P1 | 0.56433(15) | 0.25020(9) | 0.18834(8) | 0.0202(3)    |
| O1 | 0.6657(4)   | 0.5047(2)  | 0.2001(2)  | 0.0291(8)    |
| N1 | 0.9017(5)   | 0.2018(3)  | 0.1297(2)  | 0.0164(8)    |
| N2 | 0.9420(5)   | 0.1922(3)  | 0.0545(2)  | 0.0191(8)    |
| N3 | 0.6935(4)   | 0.3383(3)  | 0.0448(2)  | 0.0158(8)    |
| N4 | 0.7555(5)   | 0.3018(3)  | 0.9828(2)  | 0.0171(8)    |
| N5 | 0.9956(4)   | 0.3829(3)  | 0.1025(2)  | 0.0151(8)    |
| N6 | 0.0252(4)   | 0.3460(3)  | 0.0326(2)  | 0.0148(8)    |
| N7 | 0.7277(4)   | 0.4340(3)  | 0.1897(2)  | 0.0157(8)    |
| C1 | 0.9427(6)   | 0.1261(3)  | 0.1672(3)  | 0.0230(11)   |
| C2 | 0.0101(7)   | 0.0689(3)  | 0.1179(3)  | 0.0296(12)   |
| C3 | 0.0064(7)   | 0.1123(3)  | 0.0477(3)  | 0.0282(12)   |
| C4 | 0.5610(5)   | 0.3780(3)  | 0.0149(3)  | 0.0165(9)    |
| C5 | 0.5355(6)   | 0.3678(3)  | 0.9335(3)  | 0.0222(10)   |

|     | <b>x/a</b> | <b>y/b</b> | <b>z/c</b> | <b>U(eq)</b> |
|-----|------------|------------|------------|--------------|
| C6  | 0.6612(6)  | 0.3197(3)  | 0.9151(3)  | 0.0232(11)   |
| C7  | 0.0873(5)  | 0.4539(3)  | 0.1133(3)  | 0.0172(9)    |
| C8  | 0.1775(6)  | 0.4621(3)  | 0.0516(3)  | 0.0201(10)   |
| C9  | 0.1347(5)  | 0.3931(3)  | 0.0018(3)  | 0.0188(10)   |
| C10 | 0.9969(5)  | 0.3304(3)  | 0.2674(3)  | 0.0182(9)    |
| C11 | 0.8624(6)  | 0.2903(3)  | 0.2945(3)  | 0.0183(10)   |
| C12 | 0.7874(6)  | 0.3297(4)  | 0.3630(3)  | 0.0243(10)   |
| C13 | 0.8513(8)  | 0.4197(4)  | 0.3905(4)  | 0.0396(15)   |
| C14 | 0.0260(8)  | 0.4247(4)  | 0.3913(3)  | 0.0396(15)   |
| C15 | 0.0690(6)  | 0.4132(4)  | 0.3082(3)  | 0.0266(11)   |
| C16 | 0.4074(7)  | 0.3215(5)  | 0.2097(4)  | 0.0486(19)   |
| C17 | 0.5611(6)  | 0.1667(4)  | 0.2645(3)  | 0.0261(11)   |
| C18 | 0.4765(8)  | 0.1883(4)  | 0.1023(3)  | 0.0434(17)   |
| B1  | 0.9260(7)  | 0.2691(4)  | 0.9954(3)  | 0.0175(10)   |

**Table 4. Bond lengths (Å) for Harman\_10JAS\_159.**

|        |            |        |          |
|--------|------------|--------|----------|
| W1-N7  | 1.768(4)   | W1-C10 | 2.193(5) |
| W1-N3  | 2.208(4)   | W1-C11 | 2.226(4) |
| W1-N5  | 2.228(4)   | W1-N1  | 2.262(4) |
| W1-P1  | 2.4961(13) | P1-C16 | 1.809(6) |
| P1-C17 | 1.820(5)   | P1-C18 | 1.824(6) |
| O1-N7  | 1.226(5)   | N1-C1  | 1.345(6) |
| N1-N2  | 1.375(5)   | N2-C3  | 1.350(6) |
| N2-B1  | 1.540(7)   | N3-C4  | 1.336(6) |

|          |          |          |          |
|----------|----------|----------|----------|
| N3-N4    | 1.360(5) | N4-C6    | 1.351(6) |
| N4-B1    | 1.542(7) | N5-C7    | 1.340(6) |
| N5-N6    | 1.368(5) | N6-C9    | 1.344(6) |
| N6-B1    | 1.540(7) | C1-C2    | 1.387(7) |
| C1-H1    | 0.95     | C2-C3    | 1.363(8) |
| C2-H2    | 0.95     | C3-H3    | 0.95     |
| C4-C5    | 1.382(7) | C4-H4    | 0.95     |
| C5-C6    | 1.377(8) | C5-H5    | 0.95     |
| C6-H6    | 0.95     | C7-C8    | 1.388(7) |
| C7-H7    | 0.95     | C8-C9    | 1.373(7) |
| C8-H8    | 0.95     | C9-H9    | 0.95     |
| C10-C11  | 1.437(7) | C10-C15  | 1.534(7) |
| C10-H10  | 1.0      | C11-C12  | 1.526(7) |
| C11-H11  | 1.0      | C12-C13  | 1.530(8) |
| C12-H12A | 0.99     | C12-H12B | 0.99     |
| C13-C14  | 1.507(9) | C13-H13A | 0.99     |
| C13-H13B | 0.99     | C14-C15  | 1.516(8) |
| C14-H14A | 0.99     | C14-H14B | 0.99     |
| C15-H15A | 0.99     | C15-H15B | 0.99     |
| C16-H16A | 0.98     | C16-H16B | 0.98     |
| C16-H16C | 0.98     | C17-H17A | 0.98     |
| C17-H17B | 0.98     | C17-H17C | 0.98     |
| C18-H18A | 0.98     | C18-H18B | 0.98     |
| C18-H18C | 0.98     | B1-H1A   | 1.08(5)  |

**Table 5. Bond angles (°) for Harman\_10JAS\_159.**

|            |            |            |            |
|------------|------------|------------|------------|
| N7-W1-C10  | 96.83(18)  | N7-W1-N3   | 90.73(16)  |
| C10-W1-N3  | 158.60(16) | N7-W1-C11  | 95.23(18)  |
| C10-W1-C11 | 37.95(17)  | N3-W1-C11  | 160.99(16) |
| N7-W1-N5   | 96.71(16)  | C10-W1-N5  | 82.52(15)  |
| N3-W1-N5   | 76.71(14)  | C11-W1-N5  | 120.27(16) |
| N7-W1-N1   | 174.95(15) | C10-W1-N1  | 87.65(16)  |
| N3-W1-N1   | 84.26(14)  | C11-W1-N1  | 89.73(16)  |
| N5-W1-N1   | 81.54(14)  | N7-W1-P1   | 93.09(13)  |
| C10-W1-P1  | 116.74(13) | N3-W1-P1   | 82.63(10)  |
| C11-W1-P1  | 79.04(13)  | N5-W1-P1   | 157.19(10) |
| N1-W1-P1   | 86.93(10)  | C16-P1-C17 | 101.4(3)   |
| C16-P1-C18 | 103.1(4)   | C17-P1-C18 | 99.6(3)    |
| C16-P1-W1  | 113.2(2)   | C17-P1-W1  | 122.15(18) |
| C18-P1-W1  | 114.7(2)   | C1-N1-N2   | 105.5(4)   |
| C1-N1-W1   | 134.0(3)   | N2-N1-W1   | 120.3(3)   |
| C3-N2-N1   | 109.4(4)   | C3-N2-B1   | 129.4(4)   |
| N1-N2-B1   | 120.9(4)   | C4-N3-N4   | 107.0(4)   |
| C4-N3-W1   | 130.0(3)   | N4-N3-W1   | 123.0(3)   |
| C6-N4-N3   | 108.9(4)   | C6-N4-B1   | 130.2(4)   |
| N3-N4-B1   | 119.1(4)   | C7-N5-N6   | 106.2(4)   |
| C7-N5-W1   | 132.2(3)   | N6-N5-W1   | 121.2(3)   |
| C9-N6-N5   | 109.7(4)   | C9-N6-B1   | 128.9(4)   |
| N5-N6-B1   | 121.0(4)   | O1-N7-W1   | 175.9(3)   |
| N1-C1-C2   | 111.0(4)   | N1-C1-H1   | 124.5      |

|               |          |              |          |
|---------------|----------|--------------|----------|
| C2-C1-H1      | 124.5    | C3-C2-C1     | 105.0(5) |
| C3-C2-H2      | 127.5    | C1-C2-H2     | 127.5    |
| N2-C3-C2      | 109.1(5) | N2-C3-H3     | 125.5    |
| C2-C3-H3      | 125.5    | N3-C4-C5     | 110.5(4) |
| N3-C4-H4      | 124.7    | C5-C4-H4     | 124.7    |
| C6-C5-C4      | 104.9(4) | C6-C5-H5     | 127.6    |
| C4-C5-H5      | 127.6    | N4-C6-C5     | 108.7(4) |
| N4-C6-H6      | 125.6    | C5-C6-H6     | 125.6    |
| N5-C7-C8      | 110.3(4) | N5-C7-H7     | 124.8    |
| C8-C7-H7      | 124.8    | C9-C8-C7     | 105.3(4) |
| C9-C8-H8      | 127.3    | C7-C8-H8     | 127.3    |
| N6-C9-C8      | 108.5(4) | N6-C9-H9     | 125.8    |
| C8-C9-H9      | 125.8    | C11-C10-C15  | 120.2(4) |
| C11-C10-W1    | 72.3(3)  | C15-C10-W1   | 124.3(3) |
| C11-C10-H10   | 111.5    | C15-C10-H10  | 111.5    |
| W1-C10-H10    | 111.5    | C10-C11-C12  | 121.0(5) |
| C10-C11-W1    | 69.8(2)  | C12-C11-W1   | 124.6(3) |
| C10-C11-H11   | 111.8    | C12-C11-H11  | 111.8    |
| W1-C11-H11    | 111.8    | C11-C12-C13  | 114.5(4) |
| C11-C12-H12A  | 108.6    | C13-C12-H12A | 108.6    |
| C11-C12-H12B  | 108.6    | C13-C12-H12B | 108.6    |
| H12A-C12-H12B | 107.6    | C14-C13-C12  | 111.7(5) |
| C14-C13-H13A  | 109.3    | C12-C13-H13A | 109.3    |
| C14-C13-H13B  | 109.3    | C12-C13-H13B | 109.3    |
| H13A-C13-H13B | 107.9    | C13-C14-C15  | 110.3(5) |



|               |          |               |          |
|---------------|----------|---------------|----------|
| C13-C14-H14A  | 109.6    | C15-C14-H14A  | 109.6    |
| C13-C14-H14B  | 109.6    | C15-C14-H14B  | 109.6    |
| H14A-C14-H14B | 108.1    | C14-C15-C10   | 112.5(5) |
| C14-C15-H15A  | 109.1    | C10-C15-H15A  | 109.1    |
| C14-C15-H15B  | 109.1    | C10-C15-H15B  | 109.1    |
| H15A-C15-H15B | 107.8    | P1-C16-H16A   | 109.5    |
| P1-C16-H16B   | 109.5    | H16A-C16-H16B | 109.5    |
| P1-C16-H16C   | 109.5    | H16A-C16-H16C | 109.5    |
| H16B-C16-H16C | 109.5    | P1-C17-H17A   | 109.5    |
| P1-C17-H17B   | 109.5    | H17A-C17-H17B | 109.5    |
| P1-C17-H17C   | 109.5    | H17A-C17-H17C | 109.5    |
| H17B-C17-H17C | 109.5    | P1-C18-H18A   | 109.5    |
| P1-C18-H18B   | 109.5    | H18A-C18-H18B | 109.5    |
| P1-C18-H18C   | 109.5    | H18A-C18-H18C | 109.5    |
| H18B-C18-H18C | 109.5    | N6-B1-N2      | 108.2(4) |
| N6-B1-N4      | 106.4(4) | N2-B1-N4      | 110.0(4) |
| N6-B1-H1A     | 109.(3)  | N2-B1-H1A     | 111.(3)  |
| N4-B1-H1A     | 111.(3)  |               |          |

**Table 6. Torsion angles (°) for Harman\_10JAS\_159.**

|             |           |             |           |
|-------------|-----------|-------------|-----------|
| C1-N1-N2-C3 | -0.2(5)   | W1-N1-N2-C3 | 175.0(3)  |
| C1-N1-N2-B1 | -174.6(4) | W1-N1-N2-B1 | 0.7(6)    |
| C4-N3-N4-C6 | 0.3(5)    | W1-N3-N4-C6 | -178.1(3) |
| C4-N3-N4-B1 | 166.5(4)  | W1-N3-N4-B1 | -11.9(5)  |
| C7-N5-N6-C9 | 0.7(5)    | W1-N5-N6-C9 | 175.2(3)  |

|                 |           |                 |           |
|-----------------|-----------|-----------------|-----------|
| C7-N5-N6-B1     | -172.3(4) | W1-N5-N6-B1     | 2.1(5)    |
| N2-N1-C1-C2     | 0.8(6)    | W1-N1-C1-C2     | -173.6(4) |
| N1-C1-C2-C3     | -1.0(7)   | N1-N2-C3-C2     | -0.4(6)   |
| B1-N2-C3-C2     | 173.3(5)  | C1-C2-C3-N2     | 0.8(7)    |
| N4-N3-C4-C5     | 0.0(5)    | W1-N3-C4-C5     | 178.2(3)  |
| N3-C4-C5-C6     | -0.3(6)   | N3-N4-C6-C5     | -0.5(5)   |
| B1-N4-C6-C5     | -164.7(5) | C4-C5-C6-N4     | 0.5(6)    |
| N6-N5-C7-C8     | -0.9(5)   | W1-N5-C7-C8     | -174.5(3) |
| N5-C7-C8-C9     | 0.8(5)    | N5-N6-C9-C8     | -0.2(5)   |
| B1-N6-C9-C8     | 172.1(4)  | C7-C8-C9-N6     | -0.3(5)   |
| C15-C10-C11-C12 | 0.9(7)    | W1-C10-C11-C12  | -119.0(4) |
| C15-C10-C11-W1  | 119.9(4)  | C10-C11-C12-C13 | 8.6(7)    |
| W1-C11-C12-C13  | -77.1(6)  | C11-C12-C13-C14 | -40.2(7)  |
| C12-C13-C14-C15 | 63.0(7)   | C13-C14-C15-C10 | -52.5(7)  |
| C11-C10-C15-C14 | 21.1(7)   | W1-C10-C15-C14  | 109.4(5)  |
| C9-N6-B1-N2     | 128.1(5)  | N5-N6-B1-N2     | -60.3(5)  |
| C9-N6-B1-N4     | -113.7(5) | N5-N6-B1-N4     | 57.9(5)   |
| C3-N2-B1-N6     | -115.0(5) | N1-N2-B1-N6     | 58.1(5)   |
| C3-N2-B1-N4     | 129.1(5)  | N1-N2-B1-N4     | -57.8(6)  |
| C6-N4-B1-N6     | 110.7(5)  | N3-N4-B1-N6     | -52.2(5)  |
| C6-N4-B1-N2     | -132.3(5) | N3-N4-B1-N2     | 64.8(5)   |

**Table 7. Anisotropic atomic displacement parameters ( $\text{\AA}^2$ ) for Harman\_10JAS\_159.**

The anisotropic atomic displacement factor exponent takes the form: -  
 $2\pi^2 [ h^2 a^{*2} U_{11} + \dots + 2 h k a^* b^* U_{12} ]$

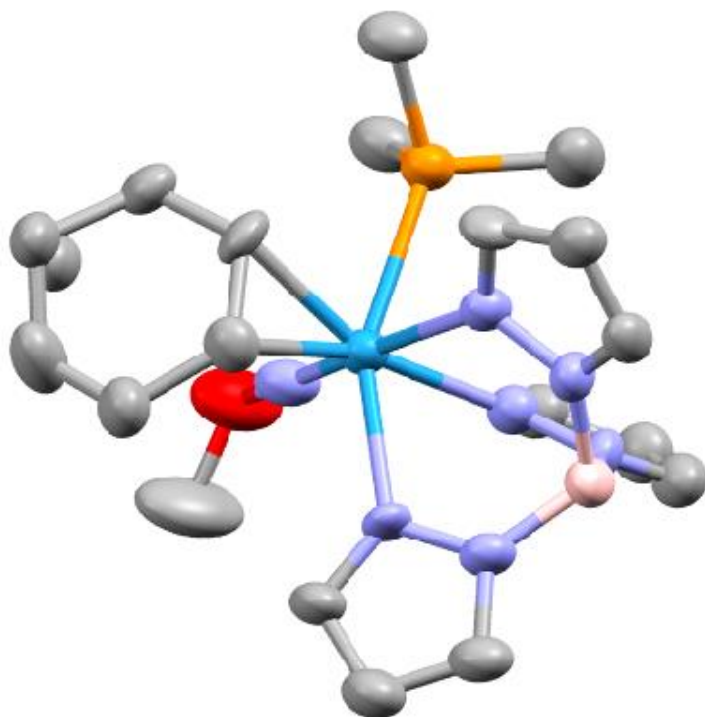
|    | <b>U<sub>11</sub></b> | <b>U<sub>22</sub></b> | <b>U<sub>33</sub></b> | <b>U<sub>23</sub></b>   | <b>U<sub>13</sub></b>   | <b>U<sub>12</sub></b>   |
|----|-----------------------|-----------------------|-----------------------|-------------------------|-------------------------|-------------------------|
| W1 | 0.01265(9)            | 0.01083(9)            | 0.01210(9)            | 0.00152(7)              | 0.00272(6)              | 0.00158(8)              |
| P1 | 0.0168(6)             | 0.0226(7)             | 0.0220(6)             | 0.0065(5)               | 0.0048(5)               | -0.0015(5)              |
| O1 | 0.037(2)              | 0.0180(18)            | 0.0301(19)            | <sup>-</sup> 0.0064(15) | <sup>-</sup> 0.0034(16) | 0.0125(17)              |
| N1 | 0.020(2)              | 0.0120(18)            | 0.019(2)              | <sup>-</sup> 0.0011(15) | 0.0067(16)              | 0.0002(16)              |
| N2 | 0.025(2)              | 0.013(2)              | 0.020(2)              | <sup>-</sup> 0.0019(15) | 0.0074(17)              | <sup>-</sup> 0.0001(16) |
| N3 | 0.0177(18)            | 0.0114(18)            | 0.0185(19)            | 0.0001(15)              | 0.0028(15)              | <sup>-</sup> 0.0020(16) |
| N4 | 0.020(2)              | 0.0177(19)            | 0.0135(19)            | <sup>-</sup> 0.0013(15) | 0.0016(15)              | <sup>-</sup> 0.0050(16) |
| N5 | 0.0168(19)            | 0.0149(19)            | 0.0130(18)            | 0.0011(14)              | <sup>-</sup> 0.0001(15) | 0.0028(15)              |
| N6 | 0.0153(18)            | 0.015(2)              | 0.0150(18)            | <sup>-</sup> 0.0001(14) | 0.0046(15)              | 0.0004(15)              |
| N7 | 0.0173(19)            | 0.016(2)              | 0.0136(18)            | 0.0008(14)              | 0.0013(15)              | 0.0030(16)              |
| C1 | 0.030(3)              | 0.014(2)              | 0.025(3)              | 0.0056(19)              | 0.006(2)                | 0.003(2)                |
| C2 | 0.040(3)              | 0.014(2)              | 0.037(3)              | 0.003(2)                | 0.011(3)                | 0.005(2)                |
| C3 | 0.039(3)              | 0.016(3)              | 0.031(3)              | -0.006(2)               | 0.009(2)                | 0.003(2)                |
| C4 | 0.014(2)              | 0.017(2)              | 0.018(2)              | 0.0051(17)              | 0.0022(18)              | <sup>-</sup> 0.0028(18) |
| C5 | 0.020(2)              | 0.024(3)              | 0.021(2)              | 0.003(2)                | <sup>-</sup> 0.0046(19) | -0.007(2)               |
| C6 | 0.029(3)              | 0.023(3)              | 0.016(2)              | <sup>-</sup> 0.0038(19) | <sup>-</sup> 0.0029(19) | -0.010(2)               |
| C7 | 0.015(2)              | 0.014(2)              | 0.021(2)              | 0.0023(18)              | <sup>-</sup> 0.0028(18) | <sup>-</sup> 0.0027(18) |

|     | <b>U<sub>11</sub></b> | <b>U<sub>22</sub></b> | <b>U<sub>33</sub></b> | <b>U<sub>23</sub></b> | <b>U<sub>13</sub></b> | <b>U<sub>12</sub></b> |
|-----|-----------------------|-----------------------|-----------------------|-----------------------|-----------------------|-----------------------|
| C8  | 0.015(2)              | 0.018(2)              | 0.027(3)              | 0.0052(19)            | 0.0031(19)            | 0.0021(19)            |
| C9  | 0.014(2)              | 0.025(3)              | 0.018(2)              | 0.0048(19)            | 0.0036(18)            | 0.0017(19)            |
| C10 | 0.018(2)              | 0.019(2)              | 0.017(2)              | 0.0032(19)            | 0.0028(17)            | 0.006(2)              |
| C11 | 0.019(2)              | 0.021(2)              | 0.015(2)              | 0.0062(18)            | 0.0003(18)            | 0.0031(19)            |
| C12 | 0.028(3)              | 0.027(3)              | 0.018(2)              | 0.002(2)              | 0.0049(19)            | 0.004(2)              |
| C13 | 0.048(4)              | 0.044(4)              | 0.028(3)              | -0.007(3)             | 0.010(3)              | 0.000(3)              |
| C14 | 0.052(4)              | 0.032(3)              | 0.033(3)              | -0.010(3)             | 0.000(3)              | 0.002(3)              |
| C15 | 0.026(3)              | 0.032(3)              | 0.020(3)              | -0.001(2)             | -0.003(2)             | -0.003(2)             |
| C16 | 0.023(3)              | 0.056(5)              | 0.072(5)              | 0.032(4)              | 0.023(3)              | 0.018(3)              |
| C17 | 0.028(3)              | 0.024(3)              | 0.027(3)              | 0.007(2)              | 0.007(2)              | 0.000(2)              |
| C18 | 0.053(4)              | 0.048(4)              | 0.027(3)              | 0.007(3)              | -0.003(3)             | -0.035(3)             |
| B1  | 0.020(3)              | 0.016(3)              | 0.017(3)              | -0.001(2)             | 0.009(2)              | 0.000(2)              |

**Table 8. Hydrogen atomic coordinates and isotropic atomic displacement parameters ( $\text{\AA}^2$ ) for Harman\_10JAS\_159.**

|    | <b>x/a</b> | <b>y/b</b> | <b>z/c</b> | <b>U(eq)</b> |
|----|------------|------------|------------|--------------|
| H1 | 0.9276     | 0.1134     | 0.2204     | 0.028        |
| H2 | 1.0502     | 0.0119     | 0.1304     | 0.036        |
| H3 | 1.0432     | 0.0899     | 0.0013     | 0.034        |
| H4 | 0.4937     | 0.4089     | 0.0453     | 0.02         |
| H5 | 0.4500     | 0.3892     | -0.1020    | 0.027        |
| H6 | 0.6786     | 0.3020     | -0.1367    | 0.028        |

|      | <b>x/a</b> | <b>y/b</b> | <b>z/c</b> | <b>U(eq)</b> |
|------|------------|------------|------------|--------------|
| H7   | 1.0903     | 0.4930     | 0.1569     | 0.021        |
| H8   | 1.2528     | 0.5062     | 0.0453     | 0.024        |
| H9   | 1.1755     | 0.3807     | -0.0463    | 0.023        |
| H10  | 1.0786     | 0.2860     | 0.2594     | 0.022        |
| H11  | 0.8745     | 0.2253     | 0.2997     | 0.022        |
| H12A | 0.8030     | 0.2887     | 0.4085     | 0.029        |
| H12B | 0.6735     | 0.3349     | 0.3467     | 0.029        |
| H13A | 0.8010     | 0.4654     | 0.3546     | 0.048        |
| H13B | 0.8247     | 0.4315     | 0.4445     | 0.048        |
| H14A | 1.0767     | 0.3783     | 0.4263     | 0.048        |
| H14B | 1.0642     | 0.4822     | 0.4127     | 0.048        |
| H15A | 1.1841     | 0.4100     | 0.3108     | 0.032        |
| H15B | 1.0330     | 0.4651     | 0.2760     | 0.032        |
| H16A | 0.4362     | 0.3499     | 0.2612     | 0.073        |
| H16B | 0.3121     | 0.2869     | 0.2113     | 0.073        |
| H16C | 0.3888     | 0.3663     | 0.1683     | 0.073        |
| H17A | 0.6379     | 0.1210     | 0.2571     | 0.039        |
| H17B | 0.4567     | 0.1405     | 0.2606     | 0.039        |
| H17C | 0.5870     | 0.1934     | 0.3169     | 0.039        |
| H18A | 0.4511     | 0.2282     | 0.0574     | 0.065        |
| H18B | 0.3809     | 0.1597     | 0.1148     | 0.065        |
| H18C | 0.5504     | 0.1437     | 0.0886     | 0.065        |
| H1A  | 0.966(6)   | 0.251(3)   | -0.060(3)  | 0.011(12)    |



### Crystal Structure Report for **Complex 9**

A **yellow rod-like** specimen of  $C_{20}H_{32}BF_3N_7O_4PSW$ , approximate dimensions **0.082 mm** x **0.092 mm** x **0.135 mm**, was coated with Paratone oil and mounted on a MiTeGen MicroLoop. The X-ray intensity data were measured on a Bruker Kappa APEXII Duo system equipped with a Incoatec Microfocus I $\mu$ S (Cu  $K_{\alpha}$ ,  $\lambda = 1.54178 \text{ \AA}$ ) and a multilayer mirror monochromator.

The total exposure time was 17.66 hours. The frames were integrated with the Bruker SAINT software package<sup>10</sup> using a narrow-frame algorithm. The integration of the data using a **triclinic** unit cell yielded a total of **13453** reflections to a maximum  $\theta$  angle of **68.85°** (**0.83 Å** resolution), of which **5018** were independent (average redundancy **2.681**, completeness = **97.4%**,  $R_{int} = 9.76\%$ ,  $R_{sig} = 10.23\%$ ) and **3778** (**75.29%**) were greater than  $2\sigma(F^2)$ . The final cell constants of  $\underline{a} = 10.2029(10) \text{ \AA}$ ,  $\underline{b} = 11.9605(15) \text{ \AA}$ ,  $\underline{c} = 13.3686(14) \text{ \AA}$ ,  $\alpha = 65.417(9)^\circ$ ,  $\beta = 82.701(8)^\circ$ ,  $\gamma = 69.064(8)^\circ$ , volume = **1385.1(3) Å<sup>3</sup>**, are based upon the refinement of the XYZ-centroids of **6197** reflections above  $20 \sigma(I)$  with  $7.271^\circ < 2\theta < 136.1^\circ$ . Data were corrected for absorption effects using the numerical method (SADABS).<sup>1</sup> The ratio of minimum to maximum apparent transmission was **0.589**. The calculated minimum and maximum transmission coefficients (based on crystal size) are **0.4666** and **0.7921**.

<sup>10</sup> Bruker (2012). *Saint*; *SADABS*; *APEX3*. Bruker AXS Inc., Madison, Wisconsin, USA.

The structure was solved and refined using the Bruker SHELXTL Software Package<sup>11</sup> within APEX3<sup>1</sup> and OLEX2,<sup>12</sup> using the space group **P -1**, with **Z = 2** for the formula unit, **C<sub>20</sub>H<sub>32</sub>BF<sub>3</sub>N<sub>7</sub>O<sub>4</sub>PSW**. Non-hydrogen atoms were refined anisotropically. Hydrogen atoms were placed in geometrically calculated positions with  $U_{iso} = 1.2U_{equiv}$  of the parent atom ( $U_{iso} = 1.5U_{equiv}$  for methyl). One carbon atom in the ring was found to be disordered over two positions. The relative occupancies were freely refined and constraints were used on the anisotropic displacement parameters of the disordered atoms. Disorder modeling of the triflate CF<sub>3</sub> group was attempted, but nothing was found to improve it significantly so it was left as is. The final anisotropic full-matrix least-squares refinement on F<sup>2</sup> with **351** variables converged at **R1 = 7.36%**, for the observed data and **wR2 = 21.70%** for all data. The goodness-of-fit was **1.077**. The largest peak in the final difference electron density synthesis was **2.100 e<sup>-</sup>/Å<sup>3</sup>** and the largest hole was **-2.904 e<sup>-</sup>/Å<sup>3</sup>** with an RMS deviation of **0.223 e<sup>-</sup>/Å<sup>3</sup>**. On the basis of the final model, the calculated density was **1.796 g/cm<sup>3</sup>** and F(000), **740 e<sup>-</sup>**.

**Table 1. Sample and crystal data for Harman\_11JAS\_173.**

|                             |   |                |
|-----------------------------|---|----------------|
| <b>Identification code</b>  | Harman_11JAS_173  |                |
| <b>Chemical formula</b>     | C <sub>20</sub> H <sub>32</sub> BF <sub>3</sub> N <sub>7</sub> O <sub>4</sub> PSW |                |
| <b>Formula weight</b>       | 749.21 g/mol  |                |
| <b>Temperature</b>          | 100(2) K  |                |
| <b>Wavelength</b>           | 1.54178 Å   |                |
| <b>Crystal size</b>         | 0.082 x 0.092 x 0.135 mm  |                |
| <b>Crystal habit</b>        | yellow rod  |                |
| <b>Crystal system</b>       | triclinic   |                |
| <b>Space group</b>          | P -1  |                |
| <b>Unit cell dimensions</b> | a = 10.2029(10) Å   | α = 65.417(9)° |
|                             | b = 11.9605(15) Å   | β = 82.701(8)° |
|                             | c = 13.3686(14) Å   | γ = 69.064(8)° |
| <b>Volume</b>               | 1385.1(3) Å <sup>3</sup>  |                |
| <b>Z</b>                    | 2   |                |
| <b>Density (calculated)</b> | 1.796 g/cm <sup>3</sup>   |                |

<sup>11</sup> Sheldrick, G. M. (2015). *Acta Cryst.* **A71**, 3-8.

<sup>12</sup> Dolomanov, O. V.; Bourhis, L. J.; Gildea, R. J.; Howard, J. A. K.; Puschmann, H. *J. Appl. Cryst.* (2009). **42**, 339-341.

|                               |                        |
|-------------------------------|------------------------|
| <b>Absorption coefficient</b> | 9.520 mm <sup>-1</sup> |
| <b>F(000)</b>                 | 740                    |

**Table 2. Data collection and structure refinement for Harman\_11JAS\_173.**

|  |   |                              |
|--|---|------------------------------|
| <b>Diffractometer</b>                      | Bruker Kappa APEXII Duo   |                              |
| <b>Radiation source</b>                    | Incoatec Microfocus I $\mu$ S (Cu K $\alpha$ , $\lambda$ = 1.54178 Å) |                              |
| <b>Theta range for data collection</b>     | 3.64 to 68.85°  |                              |
| <b>Index ranges</b>                        | -12 ≤ h ≤ 12, -12 ≤ k ≤ 14, -16 ≤ l ≤ 16                              |                              |
| <b>Reflections collected</b>               | 13453   |                              |
| <b>Independent reflections</b>             | 5018 [R(int) = 0.0976]  |                              |
| <b>Coverage of independent reflections</b> | 97.4%   |                              |
| <b>Absorption correction</b>               | numerical   |                              |
| <b>Max. and min. transmission</b>          | 0.7921 and 0.4666   |                              |
| <b>Structure solution technique</b>        | direct methods  |                              |
| <b>Structure solution program</b>          | SHELXT 2014/5 (Sheldrick, 2014)                                       |                              |
| <b>Refinement method</b>                   | Full-matrix least-squares on F <sup>2</sup>                           |                              |
| <b>Refinement program</b>                  | SHELXL-2017/1 (Sheldrick, 2017)                                       |                              |
| <b>Function minimized</b>                  | $\Sigma w(F_o^2 - F_c^2)^2$   |                              |
| <b>Data / restraints / parameters</b>      | 5018 / 0 / 351  |                              |
| <b>Goodness-of-fit on F<sup>2</sup></b>    | 1.077   |                              |
| <b>Final R indices</b>                     | 3778 data;<br>I > 2 $\sigma$ (I)                                      | R1 = 0.0736, wR2 =<br>0.1903 |
|  | all data  | R1 = 0.0964, wR2 =<br>0.2170 |



|                                    |   |
|------------------------------------|---|
| <b>Weighting scheme</b>            | $w=1/[\sigma^2(F_o^2)+(0.1325P)^2]$<br>where $P=(F_o^2+2F_c^2)/3$ |
| <b>Largest diff. peak and hole</b> | 2.100 and -2.904 eÅ <sup>-3</sup>                                 |
| <b>R.M.S. deviation from mean</b>  | 0.223 eÅ <sup>-3</sup>  |

**Table 3. Atomic coordinates and equivalent isotropic atomic displacement parameters (Å<sup>2</sup>) for Harman\_11JAS\_173.**

U(eq) is defined as one third of the trace of the orthogonalized U<sub>ij</sub> tensor.

|    | <b>x/a</b> | <b>y/b</b> | <b>z/c</b> | <b>U(eq)</b> |
|----|------------|------------|------------|--------------|
| W1 | 0.37145(5) | 0.70150(6) | 0.14154(4) | 0.0423(2)    |
| P1 | 0.2018(3)  | 0.6973(3)  | 0.2974(2)  | 0.0462(7)    |
| O1 | 0.2381(13) | 0.9988(11) | 0.0231(11) | 0.092(4)     |
| N1 | 0.4920(10) | 0.7395(11) | 0.2432(8)  | 0.046(2)     |
| N2 | 0.6196(10) | 0.6534(11) | 0.2907(8)  | 0.048(2)     |
| N3 | 0.5852(9)  | 0.6636(11) | 0.0670(7)  | 0.044(2)     |
| N4 | 0.6985(10) | 0.5925(11) | 0.1325(8)  | 0.047(2)     |
| N5 | 0.4711(9)  | 0.4905(10) | 0.2576(7)  | 0.040(2)     |
| N6 | 0.6059(10) | 0.4468(11) | 0.2945(8)  | 0.048(2)     |
| N7 | 0.3007(11) | 0.8637(11) | 0.0683(9)  | 0.050(2)     |
| C1 | 0.4639(14) | 0.8404(15) | 0.2708(11) | 0.054(3)     |
| C2 | 0.5689(15) | 0.8207(15) | 0.3387(11) | 0.058(3)     |
| C3 | 0.6649(15) | 0.7032(16) | 0.3483(11) | 0.059(3)     |
| C4 | 0.6244(13) | 0.7011(15) | 0.9645(10) | 0.053(3)     |
| C5 | 0.7699(16) | 0.6530(17) | 0.9612(11) | 0.065(4)     |

|      | <b>x/a</b> | <b>y/b</b> | <b>z/c</b> | <b>U(eq)</b> |
|------|------------|------------|------------|--------------|
| C6   | 0.8126(14) | 0.5862(14) | 0.0693(11) | 0.054(3)     |
| C7   | 0.4263(13) | 0.3893(11) | 0.2986(9)  | 0.044(3)     |
| C8   | 0.5315(13) | 0.2781(14) | 0.3616(10) | 0.051(3)     |
| C9   | 0.6436(11) | 0.3191(12) | 0.3553(9)  | 0.046(3)     |
| C10  | 0.3286(13) | 0.6301(13) | 0.0250(10) | 0.049(3)     |
| C11  | 0.2099(11) | 0.6457(13) | 0.0945(11) | 0.050(3)     |
| C12  | 0.0683(12) | 0.7481(15) | 0.0447(11) | 0.053(3)     |
| C13  | 0.056(2)   | 0.780(3)   | 0.9196(16) | 0.062(6)     |
| C13A | 0.062(5)   | 0.850(7)   | 0.930(4)   | 0.062(6)     |
| C14  | 0.1767(19) | 0.803(2)   | 0.8609(12) | 0.084(5)     |
| C15  | 0.3129(15) | 0.7069(17) | 0.9014(11) | 0.065(4)     |
| C16  | 0.2915(15) | 0.6307(17) | 0.4276(11) | 0.068(4)     |
| C17  | 0.0886(16) | 0.8586(16) | 0.2823(12) | 0.064(4)     |
| C18  | 0.0796(15) | 0.6089(14) | 0.3319(12) | 0.056(3)     |
| C19  | 0.307(3)   | 0.060(2)   | 0.928(2)   | 0.123(10)    |
| B1   | 0.6919(15) | 0.5387(15) | 0.2580(11) | 0.051(3)     |
| S1   | 0.8948(3)  | 0.7507(4)  | 0.5983(3)  | 0.0558(8)    |
| F1   | 0.6504(13) | 0.9113(18) | 0.609(2)   | 0.223(13)    |
| F2   | 0.819(2)   | 0.947(2)   | 0.654(3)   | 0.231(14)    |
| F3   | 0.7872(19) | 0.9980(15) | 0.484(2)   | 0.201(12)    |
| O2   | 0.0277(11) | 0.7694(12) | 0.5693(9)  | 0.077(3)     |
| O3   | 0.8797(13) | 0.6667(14) | 0.7113(9)  | 0.083(4)     |
| O4   | 0.8334(14) | 0.7296(13) | 0.5207(9)  | 0.083(3)     |
| C20  | 0.7814(19) | 0.908(3)   | 0.588(3)   | 0.133(12)    |

**Table 4. Bond lengths (Å) for Harman\_11JAS\_173.**

|          |           |         |           |
|----------|-----------|---------|-----------|
| W1-N7    | 1.686(11) | W1-C10  | 2.212(12) |
| W1-N1    | 2.215(10) | W1-C11  | 2.226(11) |
| W1-N3    | 2.252(8)  | W1-N5   | 2.262(10) |
| W1-P1    | 2.529(3)  | P1-C16  | 1.798(14) |
| P1-C17   | 1.801(16) | P1-C18  | 1.810(13) |
| O1-N7    | 1.390(15) | O1-C19  | 1.42(2)   |
| N1-C1    | 1.331(17) | N1-N2   | 1.366(14) |
| N2-C3    | 1.354(17) | N2-B1   | 1.52(2)   |
| N3-C4    | 1.311(14) | N3-N4   | 1.327(13) |
| N4-C6    | 1.347(15) | N4-B1   | 1.529(16) |
| N5-C7    | 1.325(14) | N5-N6   | 1.361(13) |
| N6-C9    | 1.329(16) | N6-B1   | 1.533(17) |
| C1-C2    | 1.385(19) | C1-H1   | 0.95      |
| C2-C3    | 1.36(2)   | C2-H2   | 0.95      |
| C3-H3    | 0.95      | C4-C5   | 1.390(19) |
| C4-H4    | 0.95      | C5-C6   | 1.37(2)   |
| C5-H5    | 0.95      | C6-H6   | 0.95      |
| C7-C8    | 1.381(18) | C7-H7   | 0.95      |
| C8-C9    | 1.377(17) | C8-H8   | 0.95      |
| C9-H9    | 0.95      | C10-C11 | 1.436(17) |
| C10-C15  | 1.516(17) | C10-H10 | 1.0       |
| C11-C12  | 1.527(17) | C11-H11 | 1.0       |
| C12-C13A | 1.50(5)   | C12-C13 | 1.56(2)   |

|           |           |           |           |
|-----------|-----------|-----------|-----------|
| C12-H12A  | 0.99      | C12-H12B  | 0.99      |
| C12-H12C  | 0.99      | C12-H12D  | 0.99      |
| C13-C14   | 1.42(3)   | C13-H13A  | 0.99      |
| C13-H13B  | 0.99      | C13A-C14  | 1.49(6)   |
| C13A-H13C | 0.99      | C13A-H13D | 0.99      |
| C14-C15   | 1.44(2)   | C14-H14A  | 0.99      |
| C14-H14B  | 0.99      | C14-H14C  | 0.99      |
| C14-H14D  | 0.99      | C15-H15A  | 0.99      |
| C15-H15B  | 0.99      | C16-H16A  | 0.98      |
| C16-H16B  | 0.98      | C16-H16C  | 0.98      |
| C17-H17A  | 0.98      | C17-H17B  | 0.98      |
| C17-H17C  | 0.98      | C18-H18A  | 0.98      |
| C18-H18B  | 0.98      | C18-H18C  | 0.98      |
| C19-H19A  | 0.98      | C19-H19B  | 0.98      |
| C19-H19C  | 0.98      | B1-H1A    | 1.0       |
| S1-O4     | 1.424(11) | S1-O2     | 1.432(11) |
| S1-O3     | 1.450(11) | S1-C20    | 1.78(2)   |
| F1-C20    | 1.32(2)   | F2-C20    | 1.30(4)   |
| F3-C20    | 1.37(4)   |           |           |

**Table 5. Bond angles (°) for Harman\_11JAS\_173.**

|            |          |           |          |
|------------|----------|-----------|----------|
| N7-W1-C10  | 99.4(5)  | N7-W1-N1  | 89.5(5)  |
| C10-W1-N1  | 159.4(4) | N7-W1-C11 | 96.6(5)  |
| C10-W1-C11 | 37.8(5)  | N1-W1-C11 | 159.7(4) |
| N7-W1-N3   | 99.8(4)  | C10-W1-N3 | 82.4(4)  |

|            |           |            |           |
|------------|-----------|------------|-----------|
| N1-W1-N3   | 77.8(4)   | C11-W1-N3  | 119.8(4)  |
| N7-W1-N5   | 172.6(4)  | C10-W1-N5  | 88.0(4)   |
| N1-W1-N5   | 83.7(4)   | C11-W1-N5  | 88.9(4)   |
| N3-W1-N5   | 81.7(3)   | N7-W1-P1   | 94.7(3)   |
| C10-W1-P1  | 115.3(3)  | N1-W1-P1   | 82.1(2)   |
| C11-W1-P1  | 78.1(3)   | N3-W1-P1   | 155.0(3)  |
| N5-W1-P1   | 81.4(2)   | C16-P1-C17 | 104.3(8)  |
| C16-P1-C18 | 101.1(7)  | C17-P1-C18 | 102.3(7)  |
| C16-P1-W1  | 111.9(5)  | C17-P1-W1  | 112.3(5)  |
| C18-P1-W1  | 123.0(5)  | N7-O1-C19  | 112.2(13) |
| C1-N1-N2   | 106.5(10) | C1-N1-W1   | 131.2(9)  |
| N2-N1-W1   | 122.3(8)  | C3-N2-N1   | 108.1(12) |
| C3-N2-B1   | 132.3(11) | N1-N2-B1   | 118.8(10) |
| C4-N3-N4   | 108.9(9)  | C4-N3-W1   | 131.7(8)  |
| N4-N3-W1   | 119.4(7)  | N3-N4-C6   | 108.3(10) |
| N3-N4-B1   | 123.0(9)  | C6-N4-B1   | 128.6(11) |
| C7-N5-N6   | 107.2(10) | C7-N5-W1   | 132.9(8)  |
| N6-N5-W1   | 119.8(7)  | C9-N6-N5   | 108.8(10) |
| C9-N6-B1   | 130.3(10) | N5-N6-B1   | 120.8(10) |
| O1-N7-W1   | 171.3(10) | N1-C1-C2   | 111.2(13) |
| N1-C1-H1   | 124.4     | C2-C1-H1   | 124.4     |
| C3-C2-C1   | 104.2(13) | C3-C2-H2   | 127.9     |
| C1-C2-H2   | 127.9     | N2-C3-C2   | 109.8(13) |
| N2-C3-H3   | 125.1     | C2-C3-H3   | 125.1     |
| N3-C4-C5   | 109.6(12) | N3-C4-H4   | 125.2     |

|               |           |               |           |
|---------------|-----------|---------------|-----------|
| C5-C4-H4      | 125.2     | C6-C5-C4      | 104.2(11) |
| C6-C5-H5      | 127.9     | C4-C5-H5      | 127.9     |
| N4-C6-C5      | 108.9(12) | N4-C6-H6      | 125.6     |
| C5-C6-H6      | 125.6     | N5-C7-C8      | 110.2(11) |
| N5-C7-H7      | 124.9     | C8-C7-H7      | 124.9     |
| C9-C8-C7      | 104.6(12) | C9-C8-H8      | 127.7     |
| C7-C8-H8      | 127.7     | N6-C9-C8      | 109.1(11) |
| N6-C9-H9      | 125.4     | C8-C9-H9      | 125.4     |
| C11-C10-C15   | 120.8(11) | C11-C10-W1    | 71.7(7)   |
| C15-C10-W1    | 124.1(10) | C11-C10-H10   | 111.5     |
| C15-C10-H10   | 111.5     | W1-C10-H10    | 111.5     |
| C10-C11-C12   | 119.7(11) | C10-C11-W1    | 70.6(7)   |
| C12-C11-W1    | 120.5(9)  | C10-C11-H11   | 113.2     |
| C12-C11-H11   | 113.2     | W1-C11-H11    | 113.2     |
| C13A-C12-C11  | 119.(2)   | C11-C12-C13   | 111.5(12) |
| C11-C12-H12A  | 109.3     | C13-C12-H12A  | 109.3     |
| C11-C12-H12B  | 109.3     | C13-C12-H12B  | 109.3     |
| H12A-C12-H12B | 108.0     | C13A-C12-H12C | 107.5     |
| C11-C12-H12C  | 107.5     | C13A-C12-H12D | 107.5     |
| C11-C12-H12D  | 107.5     | H12C-C12-H12D | 107.0     |
| C14-C13-C12   | 112.5(16) | C14-C13-H13A  | 109.1     |
| C12-C13-H13A  | 109.1     | C14-C13-H13B  | 109.1     |
| C12-C13-H13B  | 109.1     | H13A-C13-H13B | 107.8     |
| C14-C13A-C12  | 112.(4)   | C14-C13A-H13C | 109.2     |
| C12-C13A-H13C | 109.2     | C14-C13A-H13D | 109.2     |

|               |           |                |           |
|---------------|-----------|----------------|-----------|
| C12-C13A-H13D | 109.2     | H13C-C13A-H13D | 107.9     |
| C13-C14-C15   | 119.0(17) | C15-C14-C13A   | 125.(2)   |
| C13-C14-H14A  | 107.6     | C15-C14-H14A   | 107.6     |
| C13-C14-H14B  | 107.6     | C15-C14-H14B   | 107.6     |
| H14A-C14-H14B | 107.0     | C15-C14-H14C   | 106.0     |
| C13A-C14-H14C | 106.0     | C15-C14-H14D   | 106.0     |
| C13A-C14-H14D | 106.0     | H14C-C14-H14D  | 106.3     |
| C14-C15-C10   | 116.0(12) | C14-C15-H15A   | 108.3     |
| C10-C15-H15A  | 108.3     | C14-C15-H15B   | 108.3     |
| C10-C15-H15B  | 108.3     | H15A-C15-H15B  | 107.4     |
| P1-C16-H16A   | 109.5     | P1-C16-H16B    | 109.5     |
| H16A-C16-H16B | 109.5     | P1-C16-H16C    | 109.5     |
| H16A-C16-H16C | 109.5     | H16B-C16-H16C  | 109.5     |
| P1-C17-H17A   | 109.5     | P1-C17-H17B    | 109.5     |
| H17A-C17-H17B | 109.5     | P1-C17-H17C    | 109.5     |
| H17A-C17-H17C | 109.5     | H17B-C17-H17C  | 109.5     |
| P1-C18-H18A   | 109.5     | P1-C18-H18B    | 109.5     |
| H18A-C18-H18B | 109.5     | P1-C18-H18C    | 109.5     |
| H18A-C18-H18C | 109.5     | H18B-C18-H18C  | 109.5     |
| O1-C19-H19A   | 109.5     | O1-C19-H19B    | 109.5     |
| H19A-C19-H19B | 109.5     | O1-C19-H19C    | 109.5     |
| H19A-C19-H19C | 109.5     | H19B-C19-H19C  | 109.5     |
| N2-B1-N4      | 107.9(10) | N2-B1-N6       | 110.2(10) |
| N4-B1-N6      | 108.0(11) | N2-B1-H1A      | 110.2     |
| N4-B1-H1A     | 110.2     | N6-B1-H1A      | 110.2     |

|           |           |           |           |
|-----------|-----------|-----------|-----------|
| O4-S1-O2  | 115.6(8)  | O4-S1-O3  | 112.9(7)  |
| O2-S1-O3  | 117.1(7)  | O4-S1-C20 | 102.6(12) |
| O2-S1-C20 | 102.7(9)  | O3-S1-C20 | 103.1(14) |
| F2-C20-F1 | 108.(3)   | F2-C20-F3 | 105.(2)   |
| F1-C20-F3 | 109.(3)   | F2-C20-S1 | 113.(2)   |
| F1-C20-S1 | 111.9(17) | F3-C20-S1 | 109.(2)   |

**Table 6. Torsion angles (°) for Harman\_11JAS\_173.**

|                 |            |                  |           |
|-----------------|------------|------------------|-----------|
| C1-N1-N2-C3     | 1.3(13)    | W1-N1-N2-C3      | -179.1(8) |
| C1-N1-N2-B1     | -169.6(10) | W1-N1-N2-B1      | 10.1(13)  |
| C4-N3-N4-C6     | 0.6(15)    | W1-N3-N4-C6      | -178.6(8) |
| C4-N3-N4-B1     | 176.7(12)  | W1-N3-N4-B1      | -2.6(16)  |
| C7-N5-N6-C9     | 1.5(13)    | W1-N5-N6-C9      | -176.0(7) |
| C7-N5-N6-B1     | 177.3(11)  | W1-N5-N6-B1      | -0.3(14)  |
| N2-N1-C1-C2     | -1.8(14)   | W1-N1-C1-C2      | 178.5(9)  |
| N1-C1-C2-C3     | 1.7(16)    | N1-N2-C3-C2      | -0.2(15)  |
| B1-N2-C3-C2     | 168.9(12)  | C1-C2-C3-N2      | -0.8(16)  |
| N4-N3-C4-C5     | 0.2(17)    | W1-N3-C4-C5      | 179.2(10) |
| N3-C4-C5-C6     | -0.9(18)   | N3-N4-C6-C5      | -1.2(16)  |
| B1-N4-C6-C5     | -176.9(14) | C4-C5-C6-N4      | 1.2(17)   |
| N6-N5-C7-C8     | -0.7(13)   | W1-N5-C7-C8      | 176.4(8)  |
| N5-C7-C8-C9     | -0.3(14)   | N5-N6-C9-C8      | -1.7(13)  |
| B1-N6-C9-C8     | -177.0(13) | C7-C8-C9-N6      | 1.3(14)   |
| C15-C10-C11-C12 | -5.(2)     | W1-C10-C11-C12   | 114.7(12) |
| C15-C10-C11-W1  | -119.4(13) | C10-C11-C12-C13A | -13.(4)   |



|                  |            |                 |            |
|------------------|------------|-----------------|------------|
| W1-C11-C12-C13A  | 71.(4)     | C10-C11-C12-C13 | 25.(2)     |
| W1-C11-C12-C13   | 108.6(15)  | C11-C12-C13-C14 | -47.(3)    |
| C11-C12-C13A-C14 | 28.(6)     | C12-C13-C14-C15 | 52.(3)     |
| C12-C13A-C14-C15 | -29.(7)    | C13-C14-C15-C10 | -30.(3)    |
| C13A-C14-C15-C10 | 13.(5)     | C11-C10-C15-C14 | 5.(2)      |
| W1-C10-C15-C14   | -82.6(18)  | C3-N2-B1-N4     | -115.7(14) |
| N1-N2-B1-N4      | 52.6(13)   | C3-N2-B1-N6     | 126.6(13)  |
| N1-N2-B1-N6      | -65.1(13)  | N3-N4-B1-N2     | -57.9(15)  |
| C6-N4-B1-N2      | 117.3(14)  | N3-N4-B1-N6     | 61.2(16)   |
| C6-N4-B1-N6      | -123.6(14) | C9-N6-B1-N2     | -126.0(13) |
| N5-N6-B1-N2      | 59.2(14)   | C9-N6-B1-N4     | 116.3(13)  |
| N5-N6-B1-N4      | -58.5(15)  | O4-S1-C20-F2    | 180.(2)    |
| O2-S1-C20-F2     | -60.(3)    | O3-S1-C20-F2    | 62.(2)     |
| O4-S1-C20-F1     | 58.(3)     | O2-S1-C20-F1    | 178.(3)    |
| O3-S1-C20-F1     | -60.(3)    | O4-S1-C20-F3    | -63.3(17)  |
| O2-S1-C20-F3     | 57.0(19)   | O3-S1-C20-F3    | 179.2(16)  |

**Table 7. Anisotropic atomic displacement parameters ( $\text{\AA}^2$ ) for Harman\_11JAS\_173.**

The anisotropic atomic displacement factor exponent takes the form: -  
 $2\pi^2 [ h^2 a^{*2} U_{11} + \dots + 2 h k a^* b^* U_{12} ]$

|    | $U_{11}$   | $U_{22}$   | $U_{33}$   | $U_{23}$   | $U_{13}$    | $U_{12}$   |
|----|------------|------------|------------|------------|-------------|------------|
| W1 | 0.0344(3)  | 0.0520(4)  | 0.0389(3)  | -0.0165(2) | 0.00408(19) | -0.0158(2) |
| P1 | 0.0378(14) | 0.0539(18) | 0.0441(14) | 0.0185(13) | 0.0060(11)  | 0.0155(13) |
| O1 | 0.079(8)   | 0.050(6)   | 0.103(9)   | -0.004(6)  | 0.026(7)    | -0.012(5)  |

|      | <b>U<sub>11</sub></b> | <b>U<sub>22</sub></b> | <b>U<sub>33</sub></b> | <b>U<sub>23</sub></b> | <b>U<sub>13</sub></b> | <b>U<sub>12</sub></b> |
|------|-----------------------|-----------------------|-----------------------|-----------------------|-----------------------|-----------------------|
| N1   | 0.039(5)              | 0.059(6)              | 0.042(5)              | -0.021(4)             | 0.004(4)              | -0.017(5)             |
| N2   | 0.034(5)              | 0.066(7)              | 0.042(5)              | -0.015(5)             | -0.008(4)             | -0.018(5)             |
| N3   | 0.019(4)              | 0.066(6)              | 0.040(5)              | -0.018(4)             | 0.007(3)              | -0.012(4)             |
| N4   | 0.032(5)              | 0.059(6)              | 0.048(5)              | -0.022(5)             | 0.010(4)              | -0.017(4)             |
| N5   | 0.031(4)              | 0.045(5)              | 0.042(5)              | -0.017(4)             | 0.006(4)              | -0.012(4)             |
| N6   | 0.034(5)              | 0.057(6)              | 0.039(5)              | -0.006(4)             | -0.006(4)             | -0.013(4)             |
| N7   | 0.048(6)              | 0.052(6)              | 0.056(6)              | -0.026(5)             | 0.019(5)              | -0.024(5)             |
| C1   | 0.049(7)              | 0.069(9)              | 0.057(7)              | -0.034(6)             | 0.008(5)              | -0.025(6)             |
| C2   | 0.057(8)              | 0.065(9)              | 0.058(7)              | -0.034(7)             | 0.004(6)              | -0.020(7)             |
| C3   | 0.054(7)              | 0.083(10)             | 0.049(7)              | -0.026(7)             | 0.002(6)              | -0.033(7)             |
| C4   | 0.043(6)              | 0.077(9)              | 0.041(6)              | -0.020(6)             | 0.012(5)              | -0.030(6)             |
| C5   | 0.059(8)              | 0.087(11)             | 0.052(7)              | -0.022(7)             | 0.016(6)              | -0.039(8)             |
| C6   | 0.046(7)              | 0.062(8)              | 0.061(7)              | -0.028(6)             | 0.016(6)              | -0.028(6)             |
| C7   | 0.047(6)              | 0.031(6)              | 0.050(6)              | -0.009(5)             | 0.011(5)              | -0.020(5)             |
| C8   | 0.041(6)              | 0.061(8)              | 0.052(6)              | -0.026(6)             | 0.007(5)              | -0.017(6)             |
| C9   | 0.032(5)              | 0.048(7)              | 0.040(5)              | -0.010(5)             | 0.000(4)              | -0.003(5)             |
| C10  | 0.048(7)              | 0.054(7)              | 0.047(6)              | -0.026(5)             | 0.004(5)              | -0.012(6)             |
| C11  | 0.028(5)              | 0.059(8)              | 0.064(7)              | -0.022(6)             | -0.011(5)             | -0.016(5)             |
| C12  | 0.033(6)              | 0.072(9)              | 0.061(7)              | -0.030(7)             | 0.001(5)              | -0.021(6)             |
| C13  | 0.044(8)              | 0.081(17)             | 0.047(8)              | -0.012(10)            | -0.007(7)             | -0.020(10)            |
| C13A | 0.044(8)              | 0.081(17)             | 0.047(8)              | -0.012(10)            | -0.007(7)             | -0.020(10)            |
| C14  | 0.068(10)             | 0.104(14)             | 0.047(7)              | -0.016(8)             | -0.004(7)             | -0.005(9)             |
| C15  | 0.056(8)              | 0.091(11)             | 0.048(7)              | -0.025(7)             | -0.003(6)             | -0.026(8)             |
| C16  | 0.047(7)              | 0.086(11)             | 0.058(8)              | -0.025(7)             | 0.002(6)              | -0.013(7)             |

|     | <b>U<sub>11</sub></b> | <b>U<sub>22</sub></b> | <b>U<sub>33</sub></b> | <b>U<sub>23</sub></b> | <b>U<sub>13</sub></b> | <b>U<sub>12</sub></b> |
|-----|-----------------------|-----------------------|-----------------------|-----------------------|-----------------------|-----------------------|
| C17 | 0.066(9)              | 0.071(10)             | 0.058(8)              | -0.026(7)             | 0.017(7)              | -0.032(8)             |
| C18 | 0.056(7)              | 0.050(7)              | 0.064(8)              | -0.022(6)             | 0.016(6)              | -0.025(6)             |
| C19 | 0.112(17)             | 0.078(13)             | 0.135(19)             | -0.004(13)            | 0.052(15)             | -0.045(12)            |
| B1  | 0.042(7)              | 0.052(8)              | 0.042(7)              | -0.002(6)             | -0.004(5)             | -0.017(6)             |
| S1  | 0.0413(15)            | 0.064(2)              | 0.0578(17)            | 0.0255(15)            | 0.0054(13)            | 0.0138(14)            |
| F1  | 0.050(7)              | 0.158(15)             | 0.52(4)               | -0.21(2)              | 0.064(13)             | -0.030(8)             |
| F2  | 0.132(14)             | 0.24(2)               | 0.49(4)               | -0.31(3)              | 0.10(2)               | -0.089(15)            |
| F3  | 0.114(13)             | 0.063(8)              | 0.35(3)               | -0.009(14)            | -0.055(16)            | -0.017(8)             |
| O2  | 0.048(5)              | 0.087(8)              | 0.075(7)              | -0.016(6)             | 0.007(5)              | -0.020(5)             |
| O3  | 0.088(8)              | 0.125(11)             | 0.056(6)              | -0.040(6)             | 0.031(5)              | -0.064(8)             |
| O4  | 0.108(9)              | 0.087(8)              | 0.065(6)              | -0.026(6)             | -0.022(6)             | -0.040(7)             |
| C20 | 0.036(8)              | 0.12(2)               | 0.29(4)               | -0.14(3)              | 0.025(14)             | -0.026(11)            |

**Table 8. Hydrogen atomic coordinates and isotropic atomic displacement parameters ( $\text{\AA}^2$ ) for Harman\_11JAS\_173.**

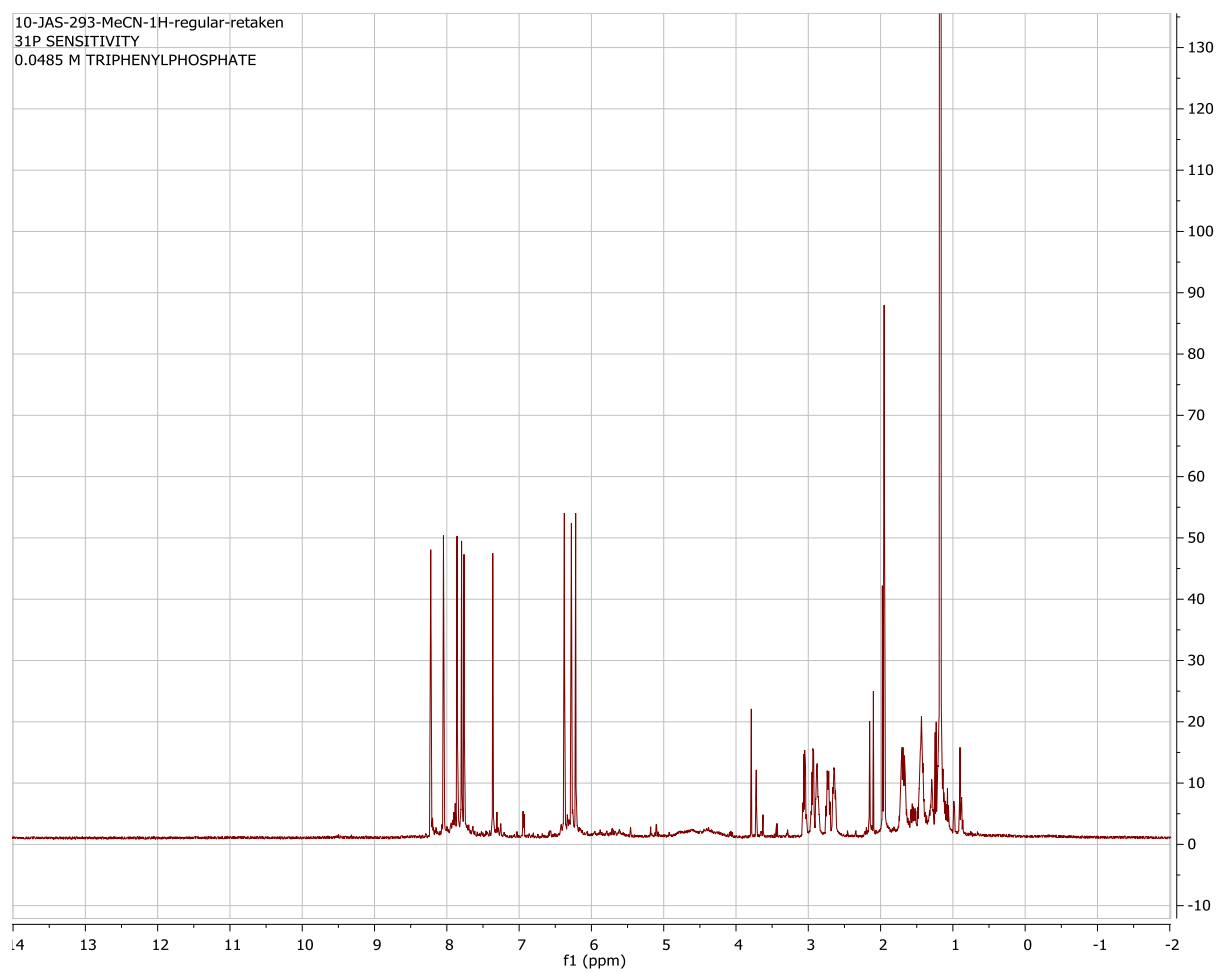
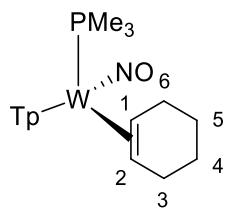
|    | <b>x/a</b> | <b>y/b</b> | <b>z/c</b> | <b>U(eq)</b> |
|----|------------|------------|------------|--------------|
| H1 | 0.3823     | 0.9161     | 0.2470     | 0.065        |
| H2 | 0.5730     | 0.8766     | 0.3712     | 0.069        |
| H3 | 0.7509     | 0.6621     | 0.3894     | 0.071        |
| H4 | 0.5628     | 0.7533     | -0.0980    | 0.064        |
| H5 | 0.8268     | 0.6640     | -0.1019    | 0.078        |
| H6 | 0.9073     | 0.5426     | 0.0957     | 0.064        |
| H7 | 0.3350     | 0.3926     | 0.2865     | 0.053        |

|      | <b>x/a</b> | <b>y/b</b> | <b>z/c</b> | <b>U(eq)</b> |
|------|------------|------------|------------|--------------|
| H8   | 0.5275     | 0.1925     | 0.4005     | 0.061        |
| H9   | 0.7335     | 0.2648     | 0.3890     | 0.055        |
| H10  | 0.3851     | 0.5359     | 0.0446     | 0.059        |
| H11  | 0.2021     | 0.5608     | 0.1495     | 0.06         |
| H12A | 0.0570     | 0.8289     | 0.0540     | 0.064        |
| H12B | -0.0080    | 0.7154     | 0.0844     | 0.064        |
| H12C | 0.0050     | 0.7011     | 0.0463     | 0.064        |
| H12D | 0.0287     | 0.7944     | 0.0940     | 0.064        |
| H13A | 0.0412     | 0.7067     | -0.0884    | 0.074        |
| H13B | -0.0277    | 0.8589     | -0.1132    | 0.074        |
| H13C | -0.0297    | 0.8751     | -0.1054    | 0.074        |
| H13D | 0.0692     | 0.9287     | -0.0669    | 0.074        |
| H14A | 0.1776     | 0.8869     | -0.1433    | 0.101        |
| H14B | 0.1648     | 0.8134     | -0.2153    | 0.101        |
| H14C | 0.1363     | 0.7686     | -0.1793    | 0.101        |
| H14D | 0.1943     | 0.8813     | -0.1952    | 0.101        |
| H15A | 0.3831     | 0.7520     | -0.1222    | 0.078        |
| H15B | 0.3359     | 0.6443     | -0.1340    | 0.078        |
| H16A | 0.3409     | 0.5368     | 0.4494     | 0.102        |
| H16B | 0.2230     | 0.6448     | 0.4834     | 0.102        |
| H16C | 0.3593     | 0.6742     | 0.4210     | 0.102        |
| H17A | 0.1457     | 0.9129     | 0.2731     | 0.096        |
| H17B | 0.0321     | 0.8531     | 0.3481     | 0.096        |
| H17C | 0.0265     | 0.8977     | 0.2176     | 0.096        |

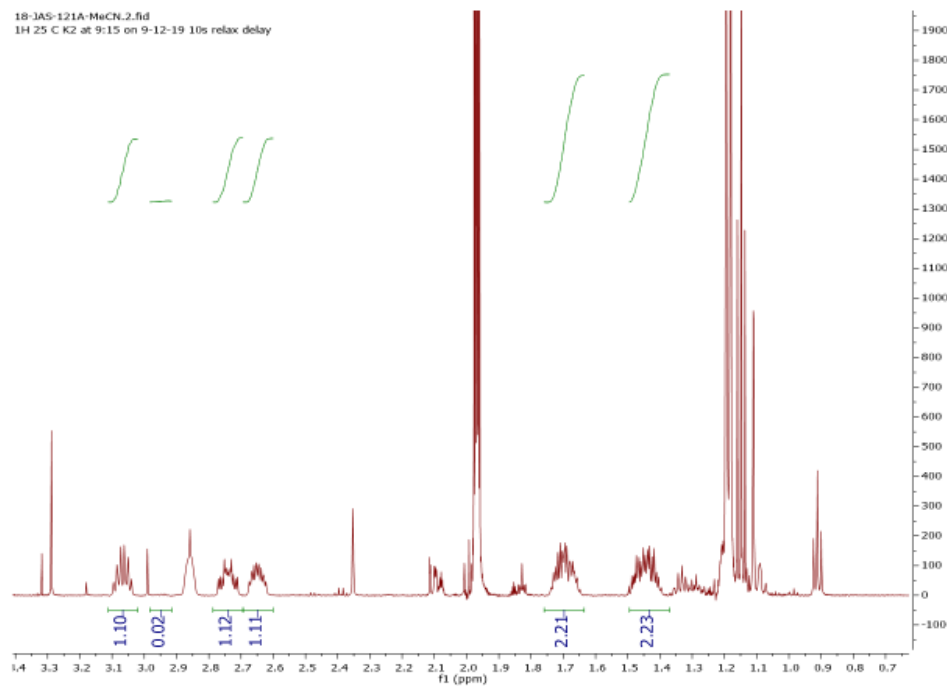
|      | <b>x/a</b> | <b>y/b</b> | <b>z/c</b> | <b>U(eq)</b> |
|------|------------|------------|------------|--------------|
| H18A | 0.0234     | 0.6361     | 0.2663     | 0.084        |
| H18B | 0.0175     | 0.6277     | 0.3894     | 0.084        |
| H18C | 0.1317     | 0.5149     | 0.3588     | 0.084        |
| H19A | 0.2907     | 1.0384     | -0.1323    | 0.184        |
| H19B | 0.4079     | 1.0276     | -0.0565    | 0.184        |
| H19C | 0.2696     | 1.1544     | -0.0947    | 0.184        |
| H1A  | 0.7887     | 0.4904     | 0.2916     | 0.061        |

# Supporting Information for Chapter 4

## $^1\text{H}$ NMR Spectrum of **1**

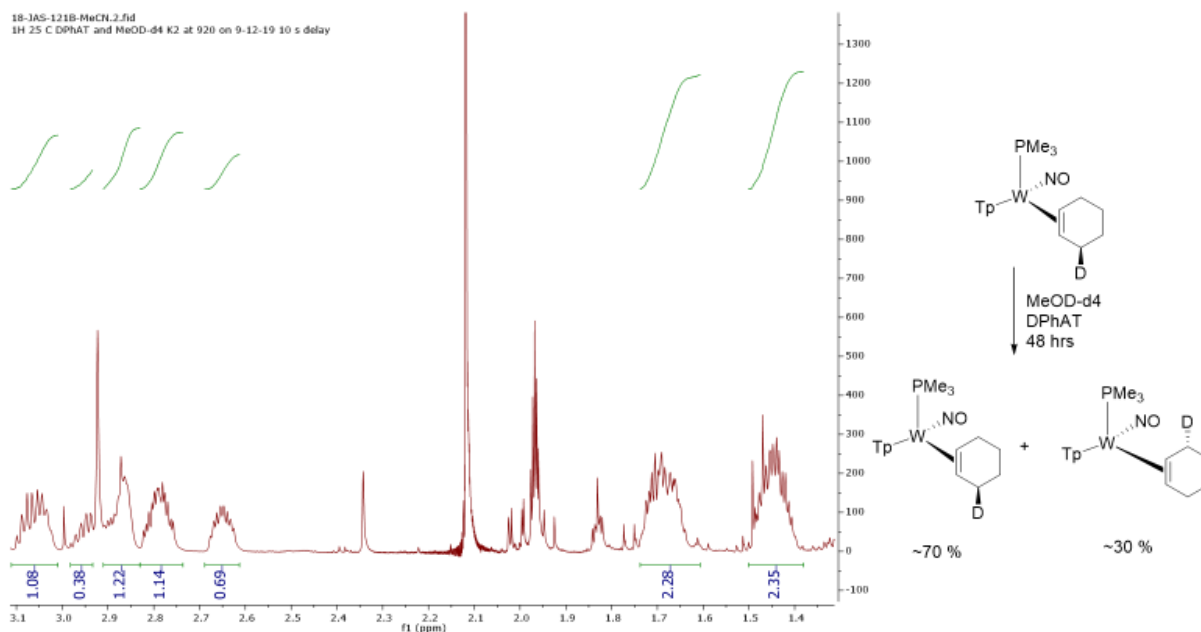


18-JAS-121A-MeCN.2.fid  
1H 25 C K2 at 9:15 on 9-12-19 10s relax delay

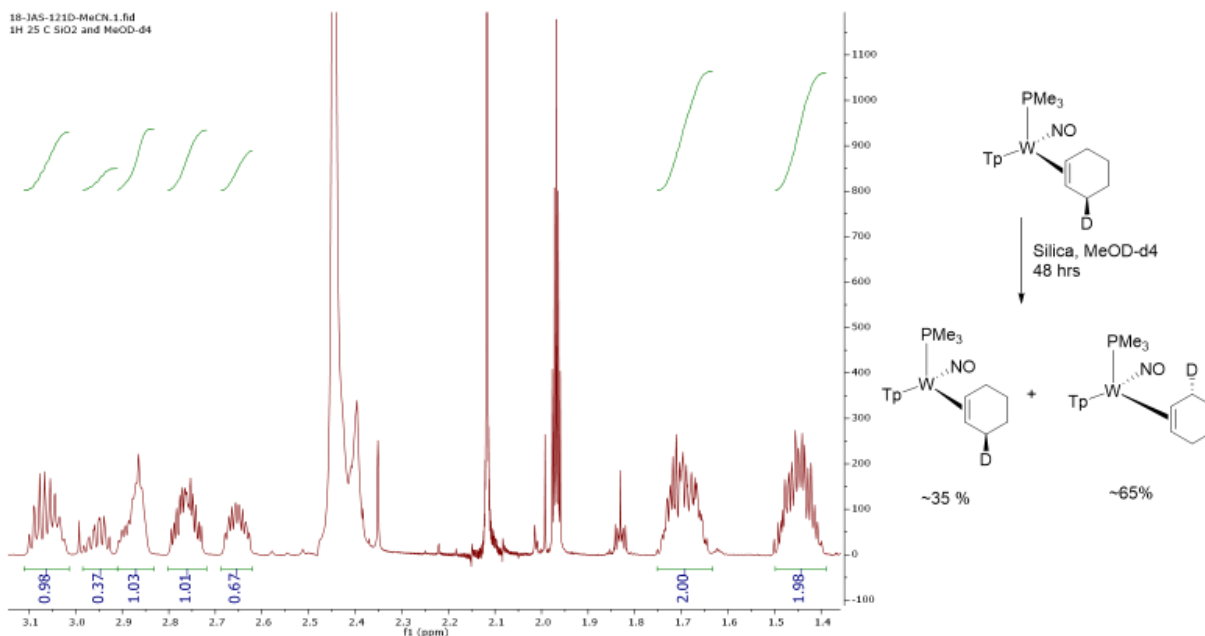


### 1H NMR Characterization of 3 and Acid/Heat Induced Face Flips

18-JAS-121B-MeCN.2.fid  
1H 25 C DPhAT and MeOD-d4 K2 at 920 on 9-12-19 10 s delay

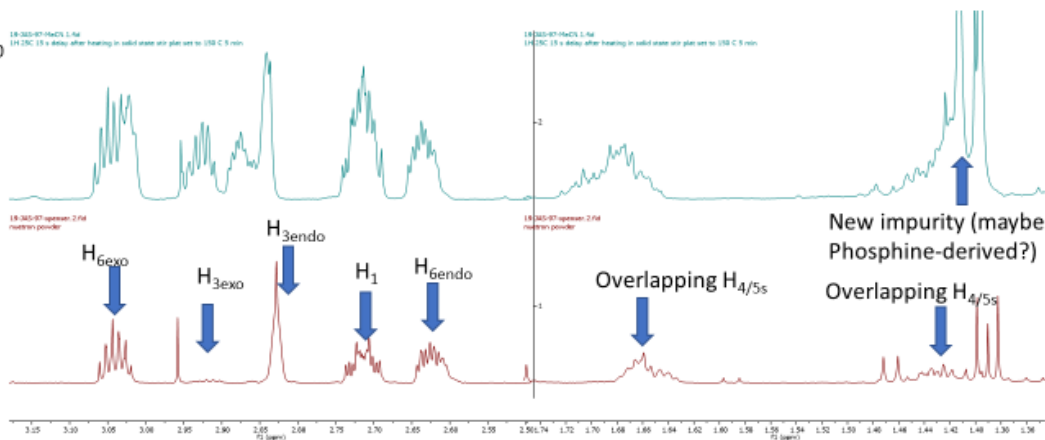


18-JAS-121D-MeCN.1.fid  
1H 25 C SiO2 and MeOD-d4

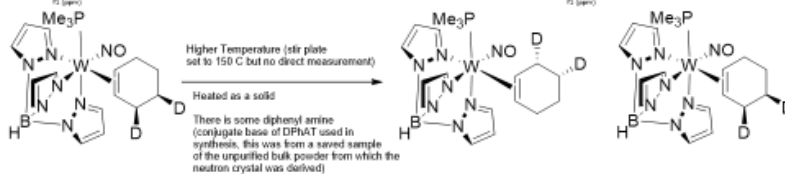


## Heating Induced Face-Flip of W-Cyclohexene Complex

Sample after heating in inert glovebox, stir plate set to 150 C, complex allowed to stand on stir plate as solid for ~ 5 min



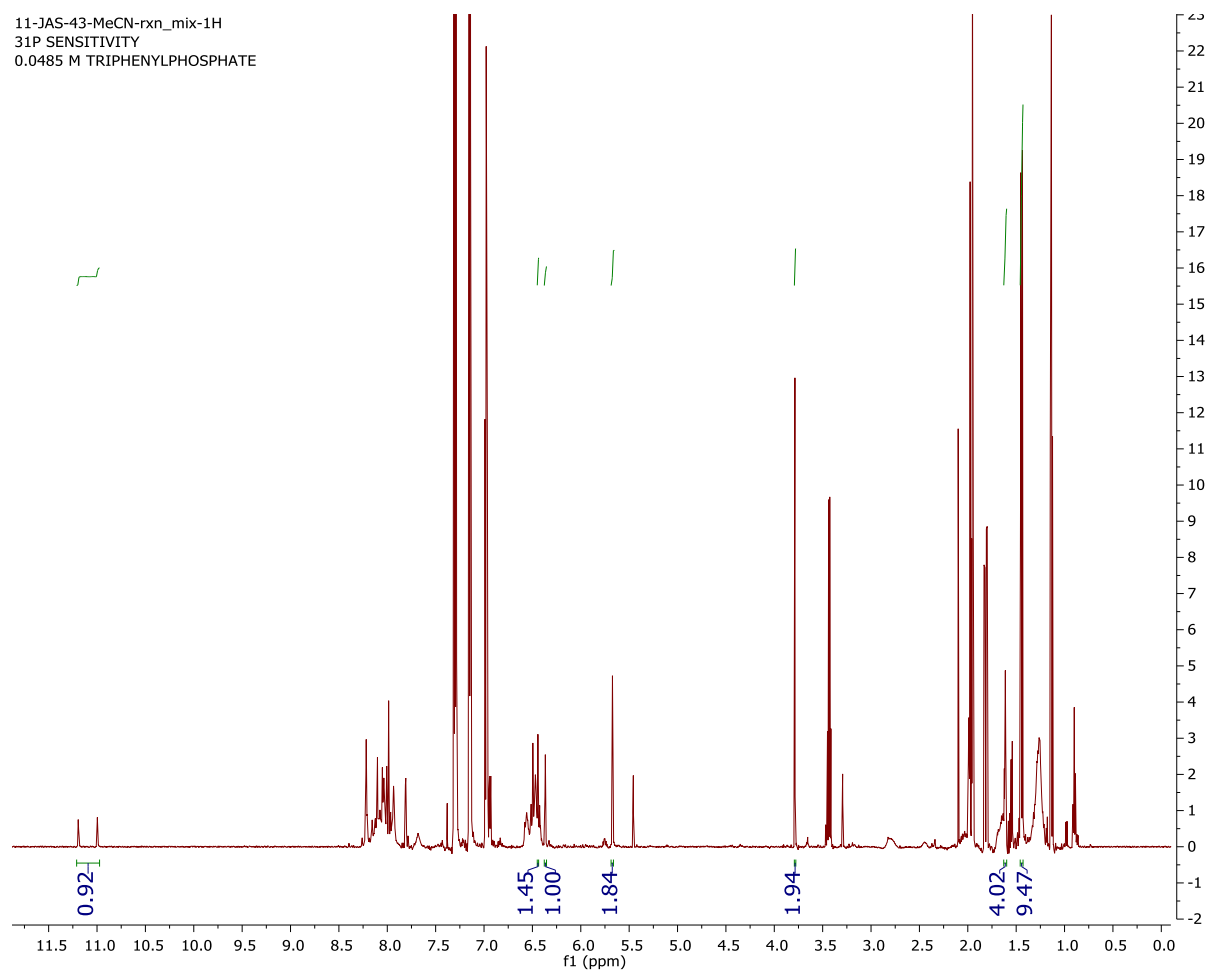
Original sample (bulk powder from which crystals were derived for neutron diffraction)



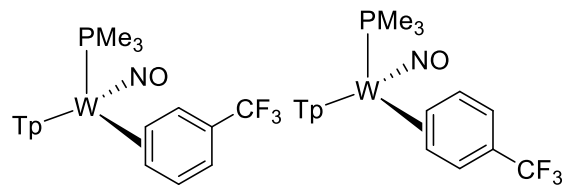


# <sup>1</sup>H NMR Spectrum of 1H (unknown structure)

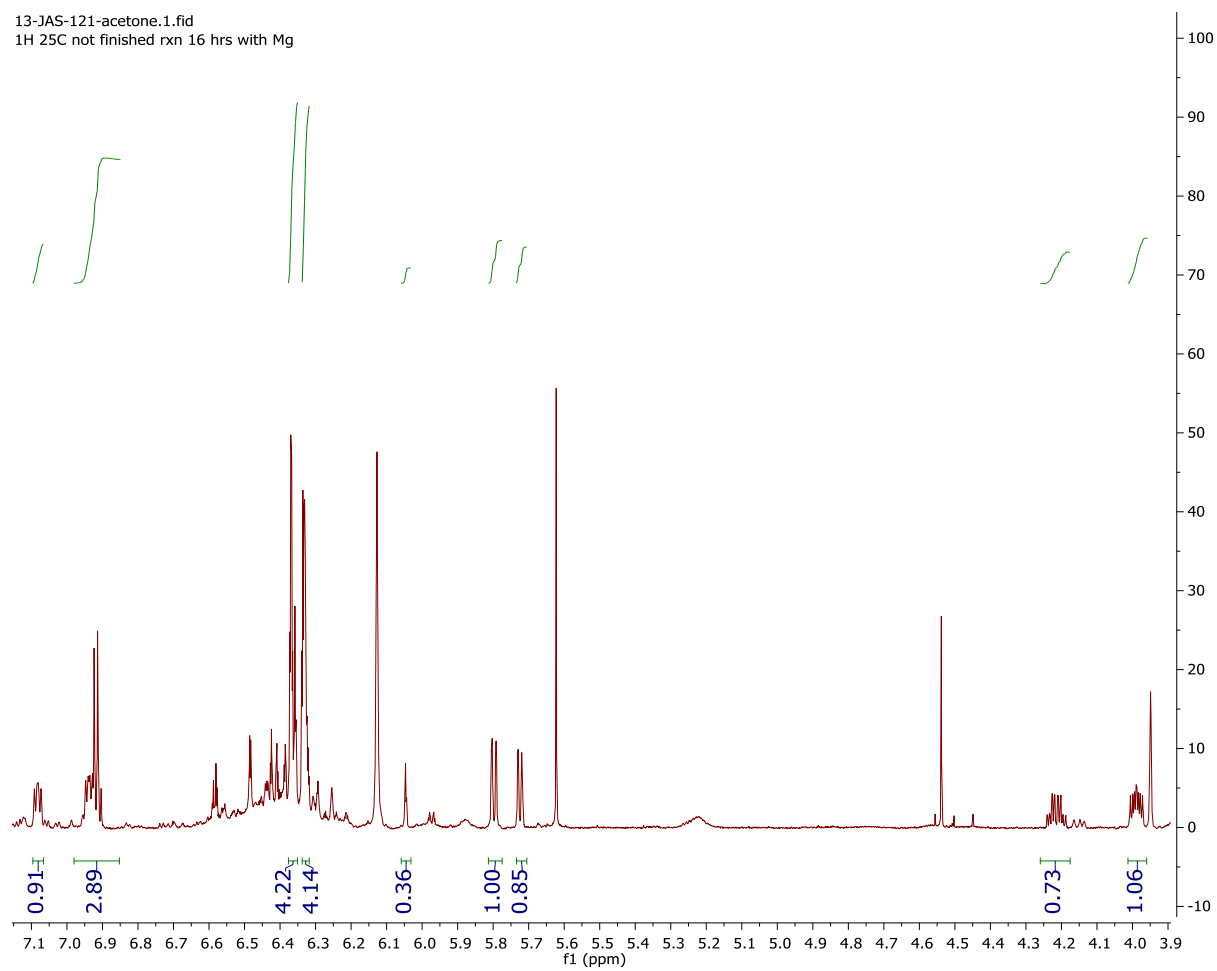
11-JAS-43-MeCN-rxn\_mix-1H  
31P SENSITIVITY  
0.0485 M TRIPHENYLPHOSPHATE



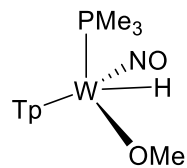
# <sup>1</sup>H NMR Spectrum of 5



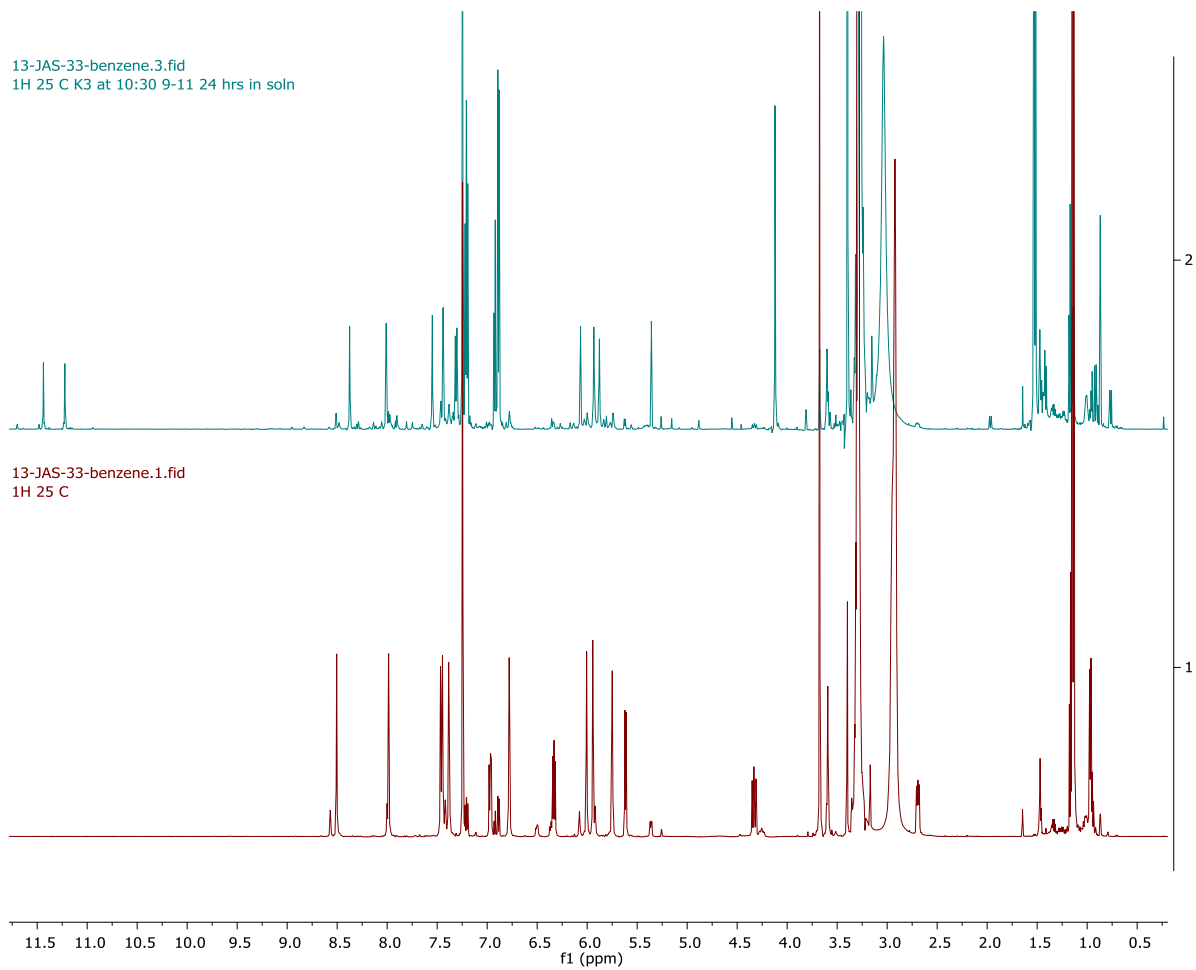
13-JAS-121-acetone.1.fid  
1H 25C not finished rxn 16 hrs with Mg



# $^1\text{H}$ NMR Spectrum of 13

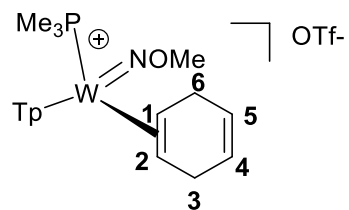


13-JAS-33-benzene.3.fid  
1H 25 C K3 at 10:30 9-11 24 hrs in soln

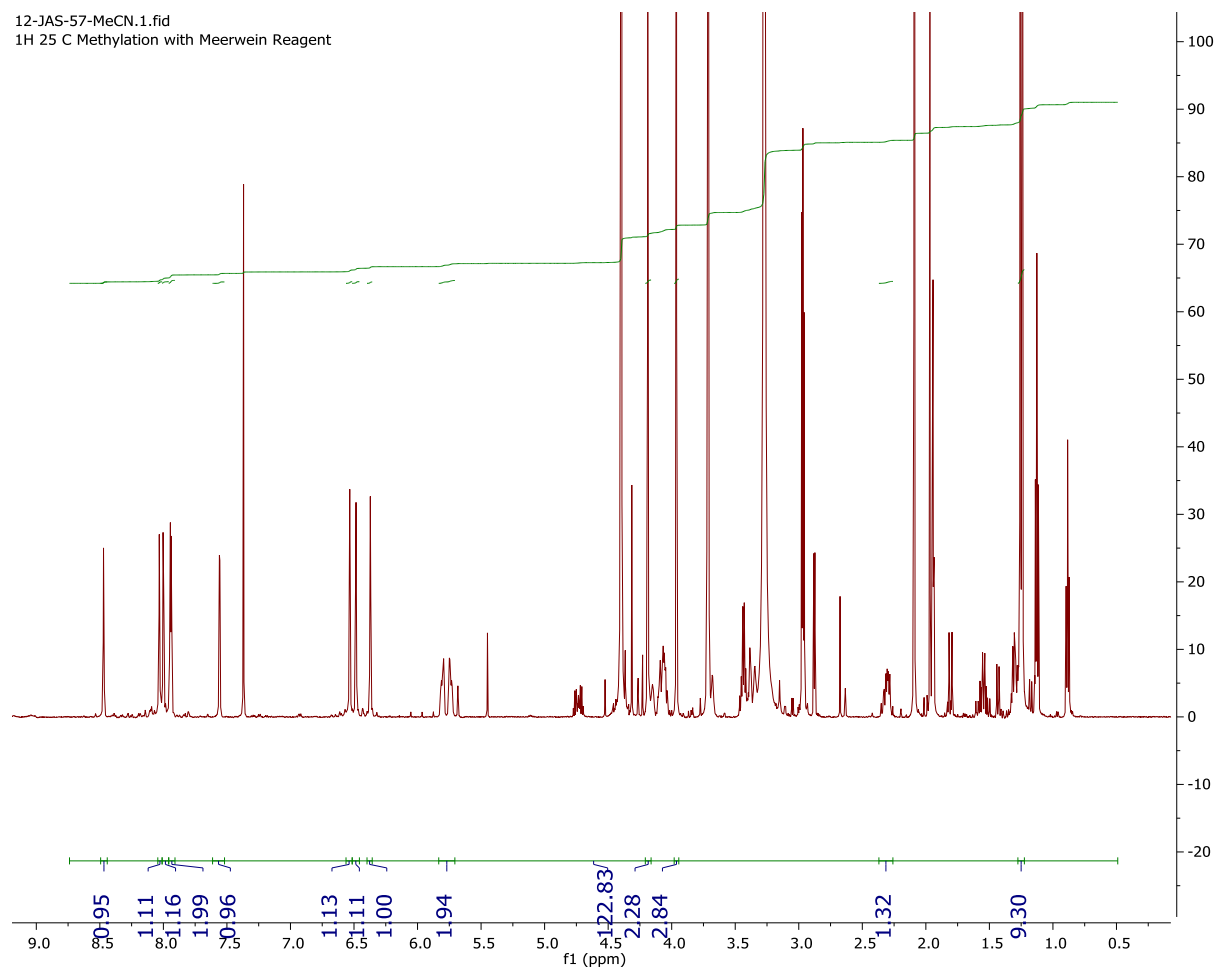


Starting point on bottom, top spectra show the development of 13

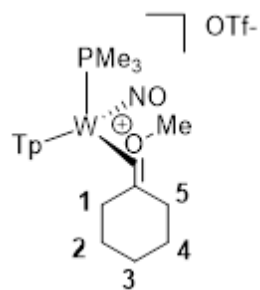
# <sup>1</sup>H NMR Spectrum of 14



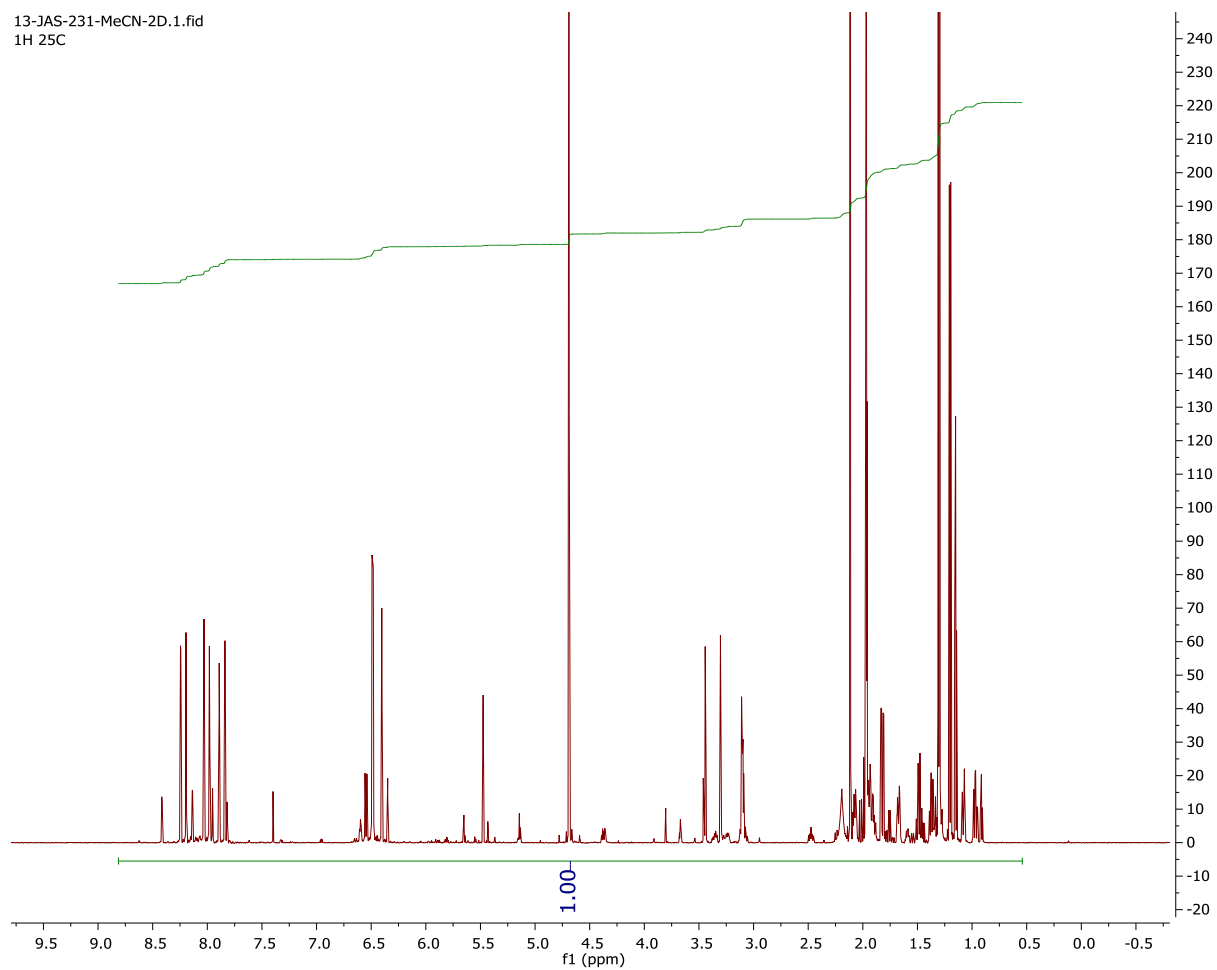
12-JAS-57-MeCN.1.fid  
1H 25 C Methylation with Meerwein Reagent



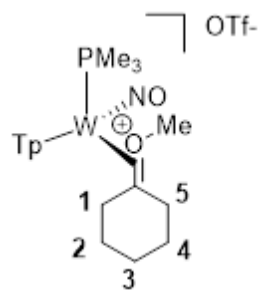
# <sup>1</sup>H NMR Spectrum of 16



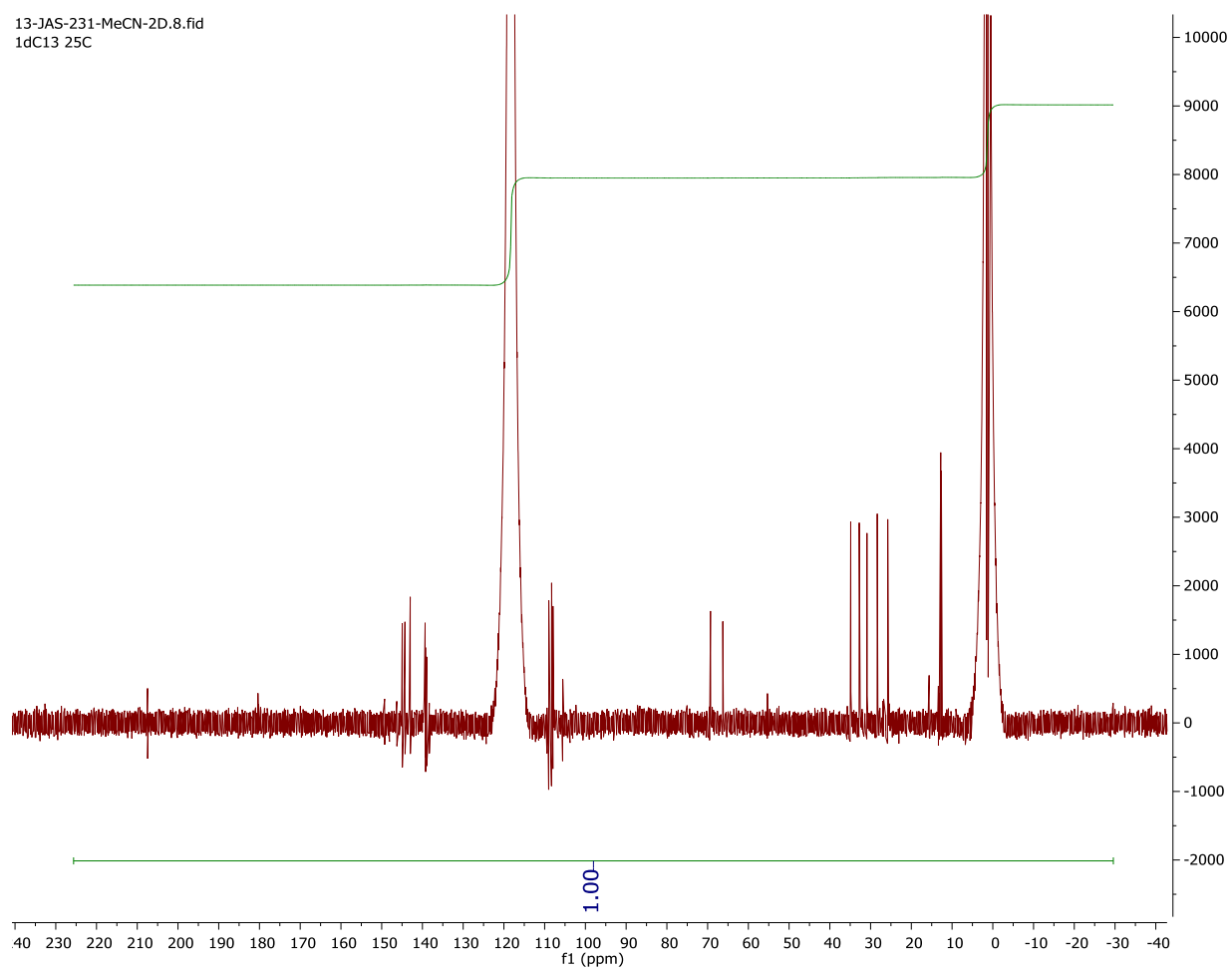
13-JAS-231-MeCN-2D.1.fid  
1H 25C



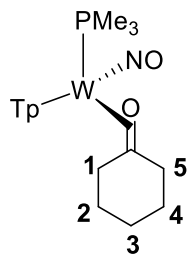
# $^{13}\text{C}$ { $^1\text{H}$ } NMR Spectrum of 16



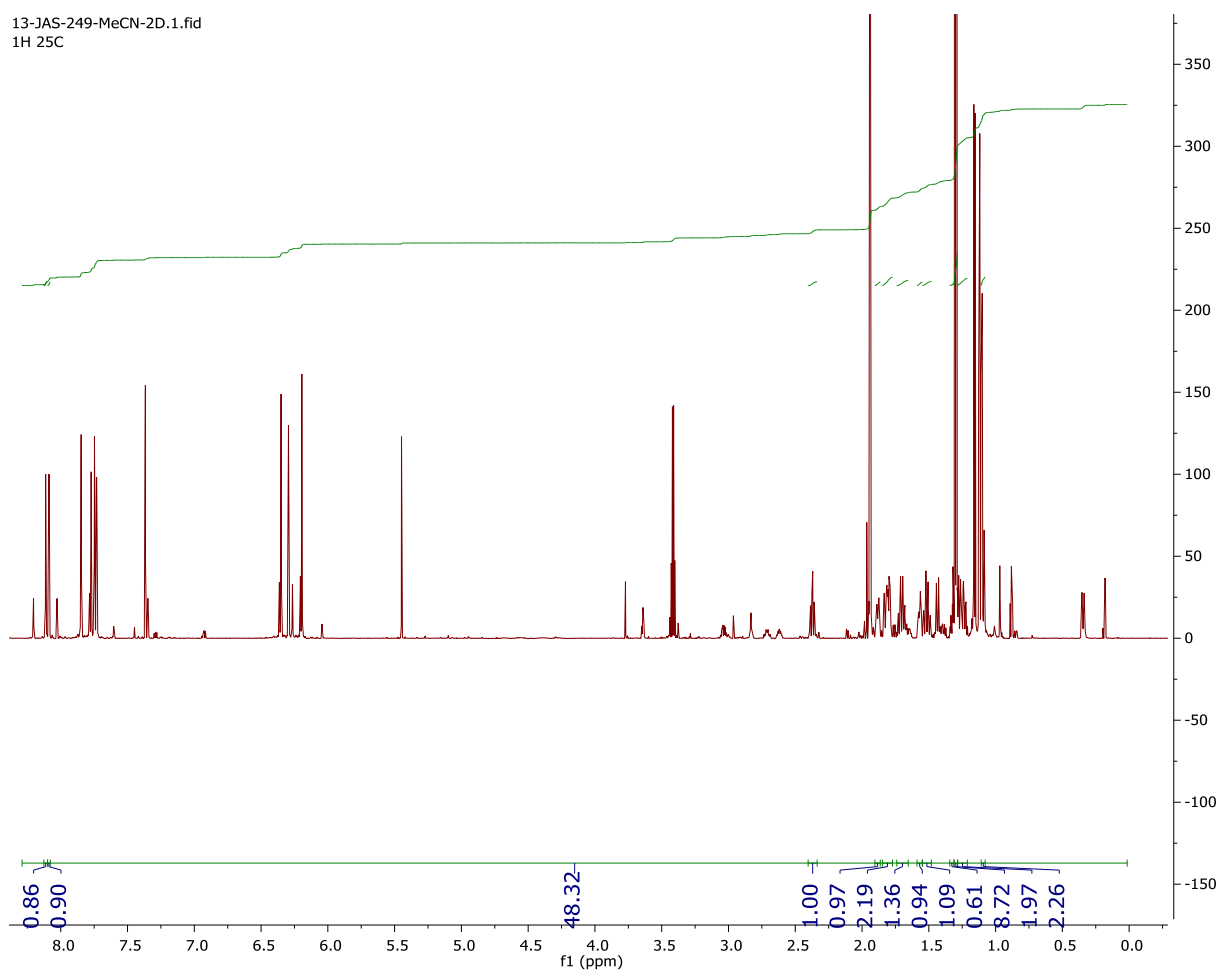
13-JAS-231-MeCN-2D.8.fid  
1dC13 25C



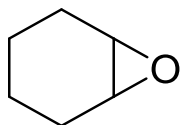
# <sup>1</sup>H NMR Spectrum of 17



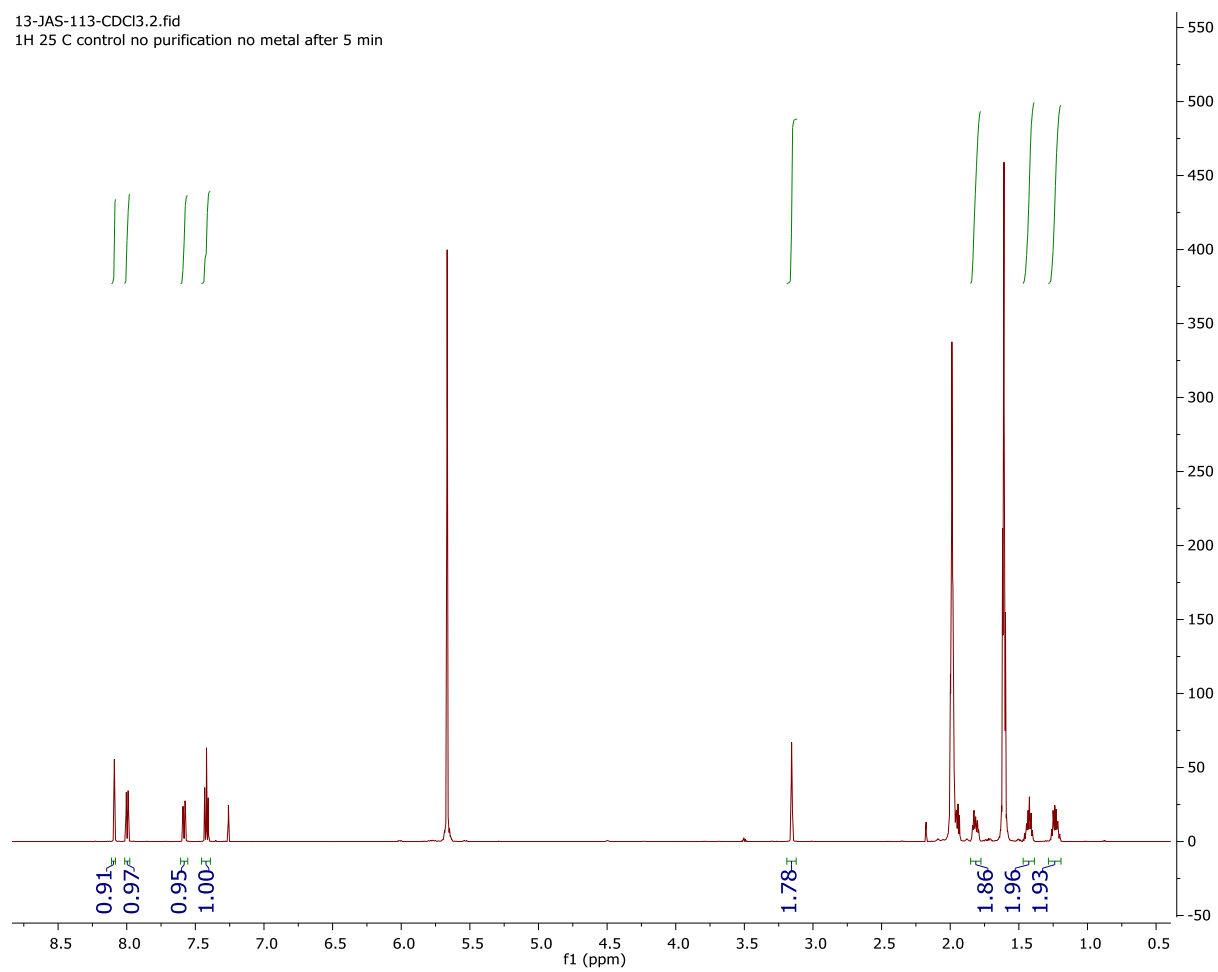
13-JAS-249-MeCN-2D.1.fid  
1H 25C



# <sup>1</sup>H NMR Spectrum of 18

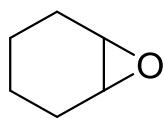


13-JAS-113-CDCl3.2.fid  
1H 25 C control no purification no metal after 5 min

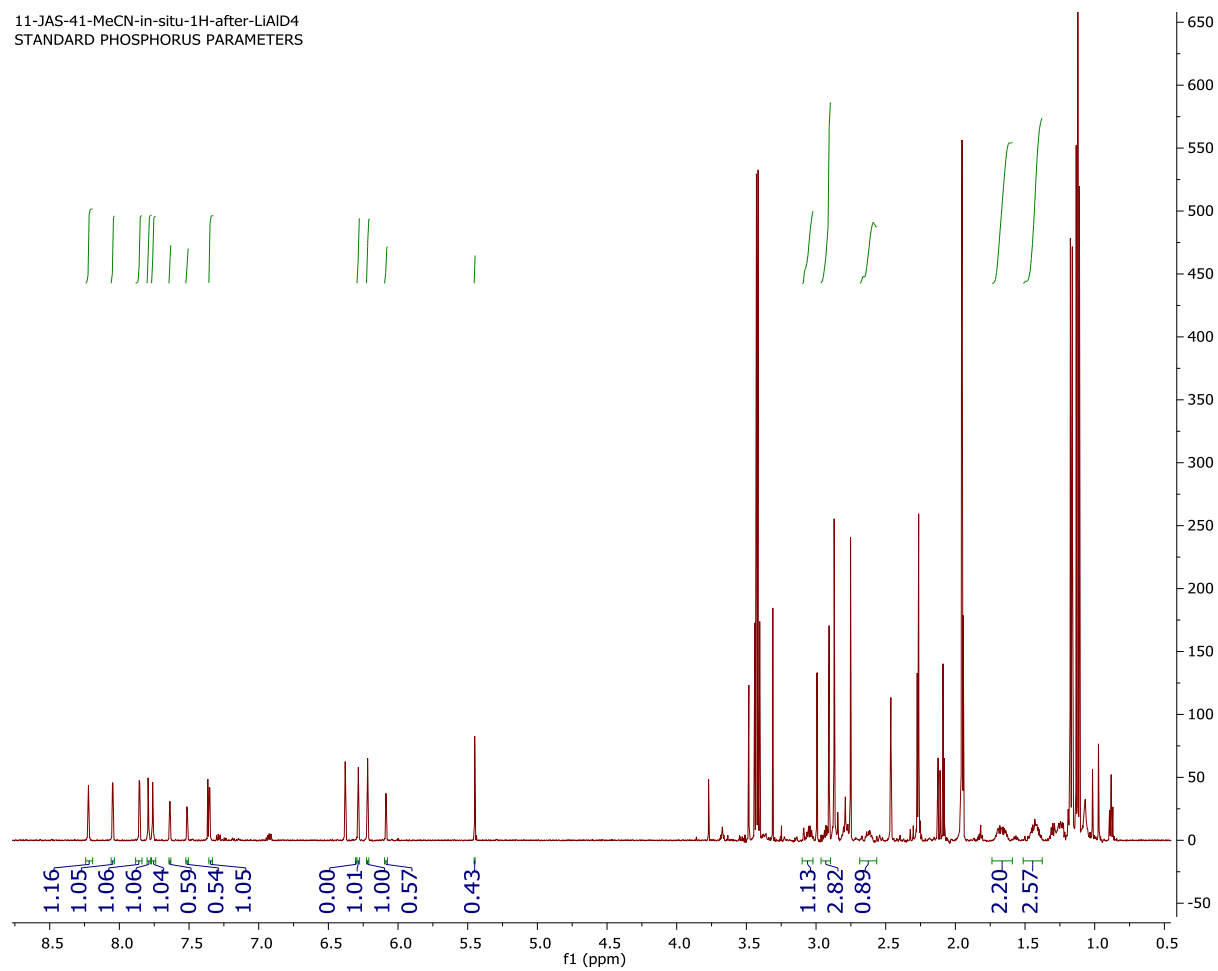




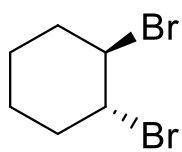
# <sup>1</sup>H NMR Spectrum of 18



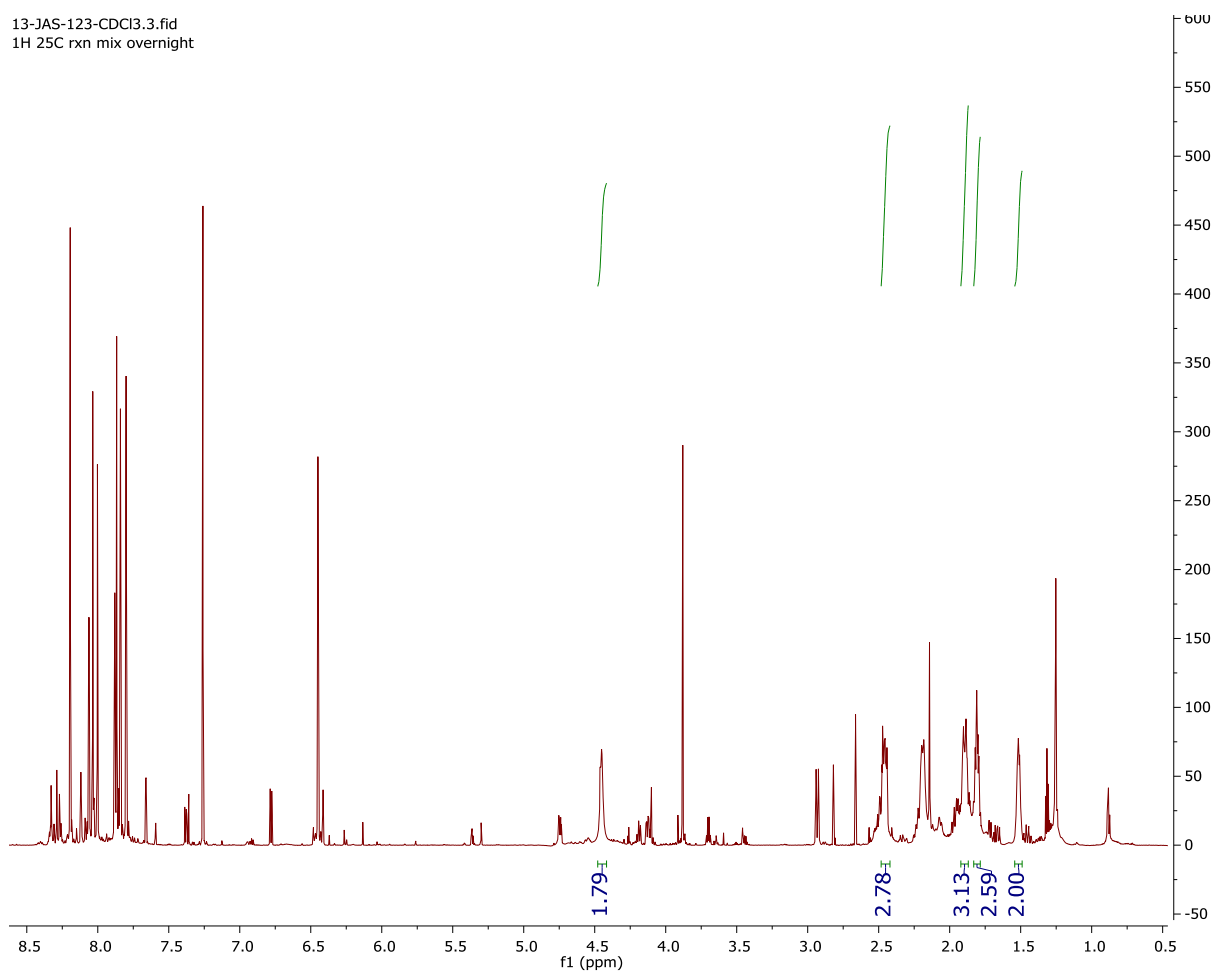
11-JAS-41-MeCN-in-situ-1H-after-LIAD4  
STANDARD PHOSPHORUS PARAMETERS



# <sup>1</sup>H NMR Spectrum of 19

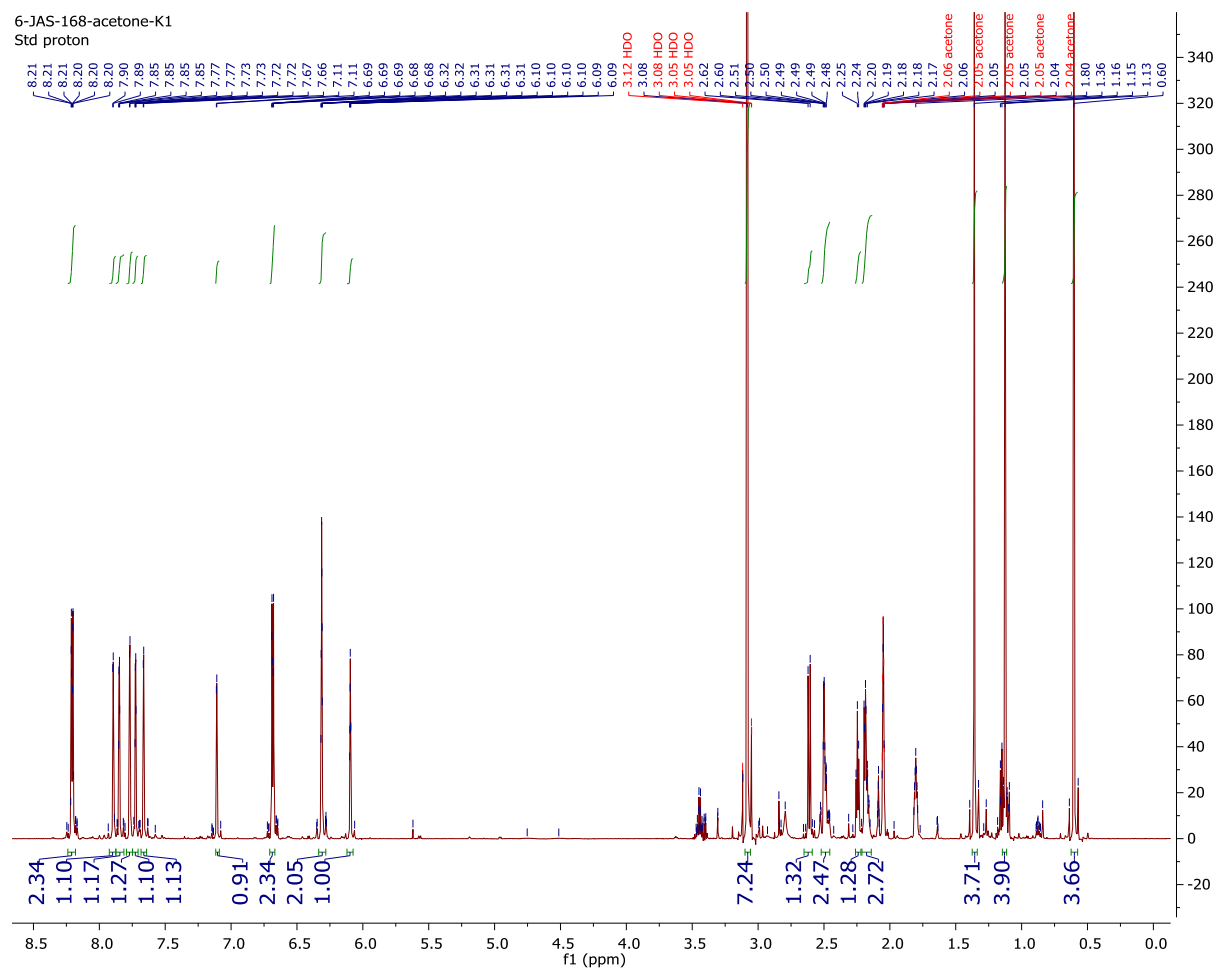
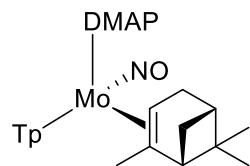


13-JAS-123-CDCl3.3.fid  
1H 25C rxn mix overnight

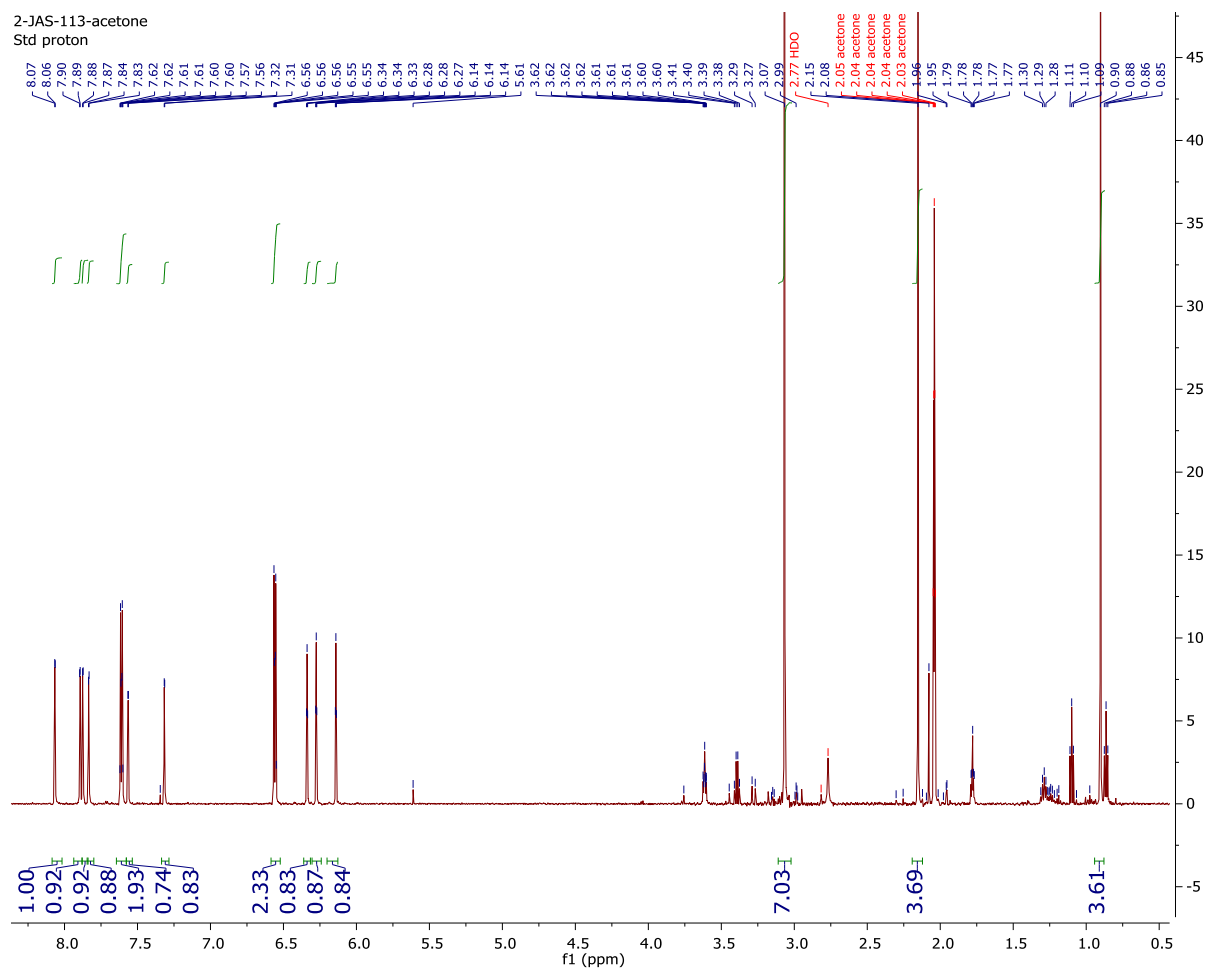
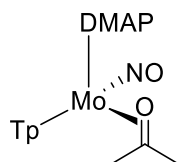


# Supporting Information for Chapter 5

## <sup>1</sup>H NMR Spectrum of 2

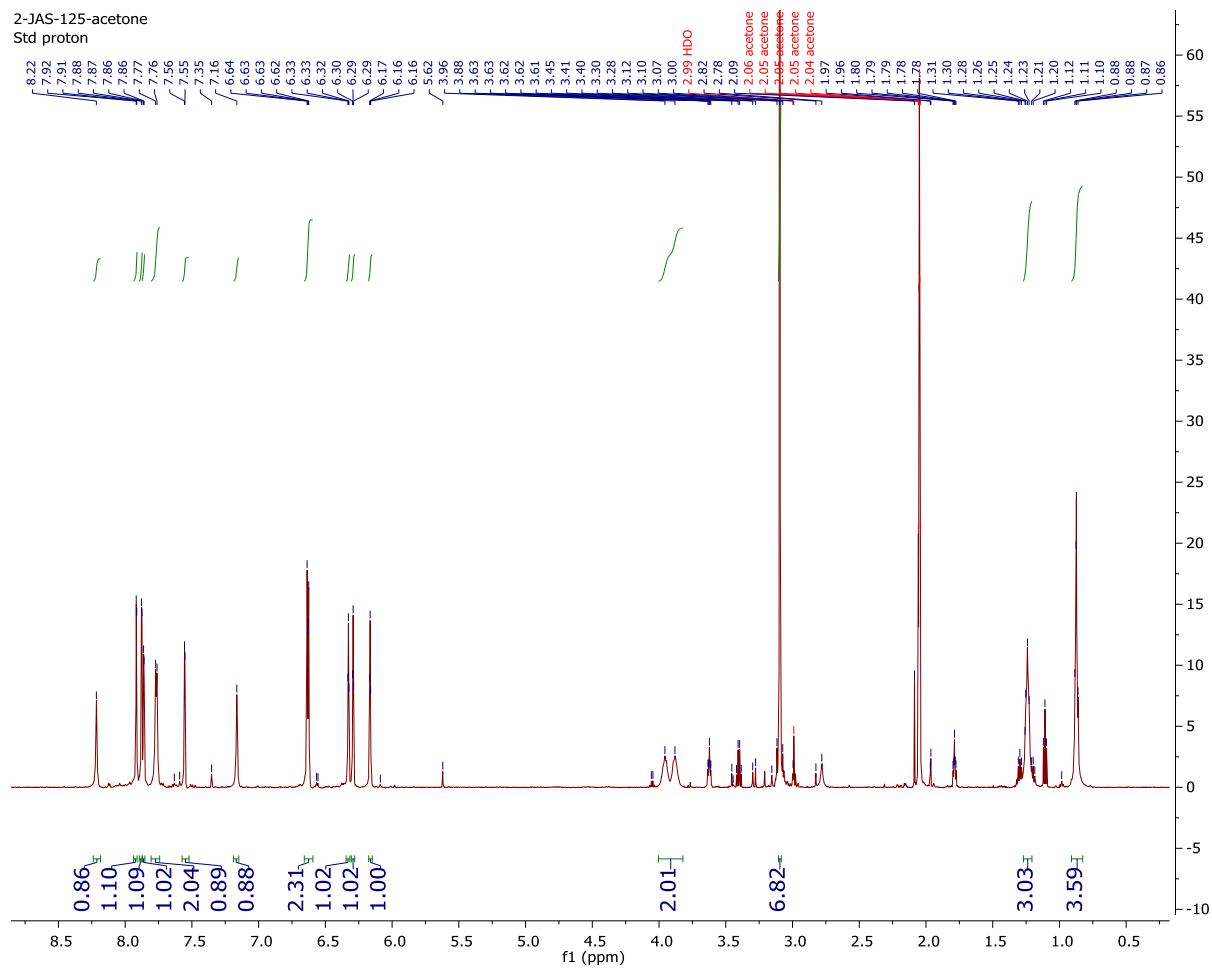
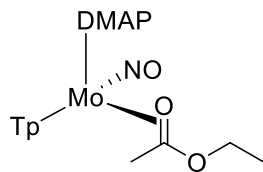


# <sup>1</sup>H NMR Spectrum of 3 Acetone

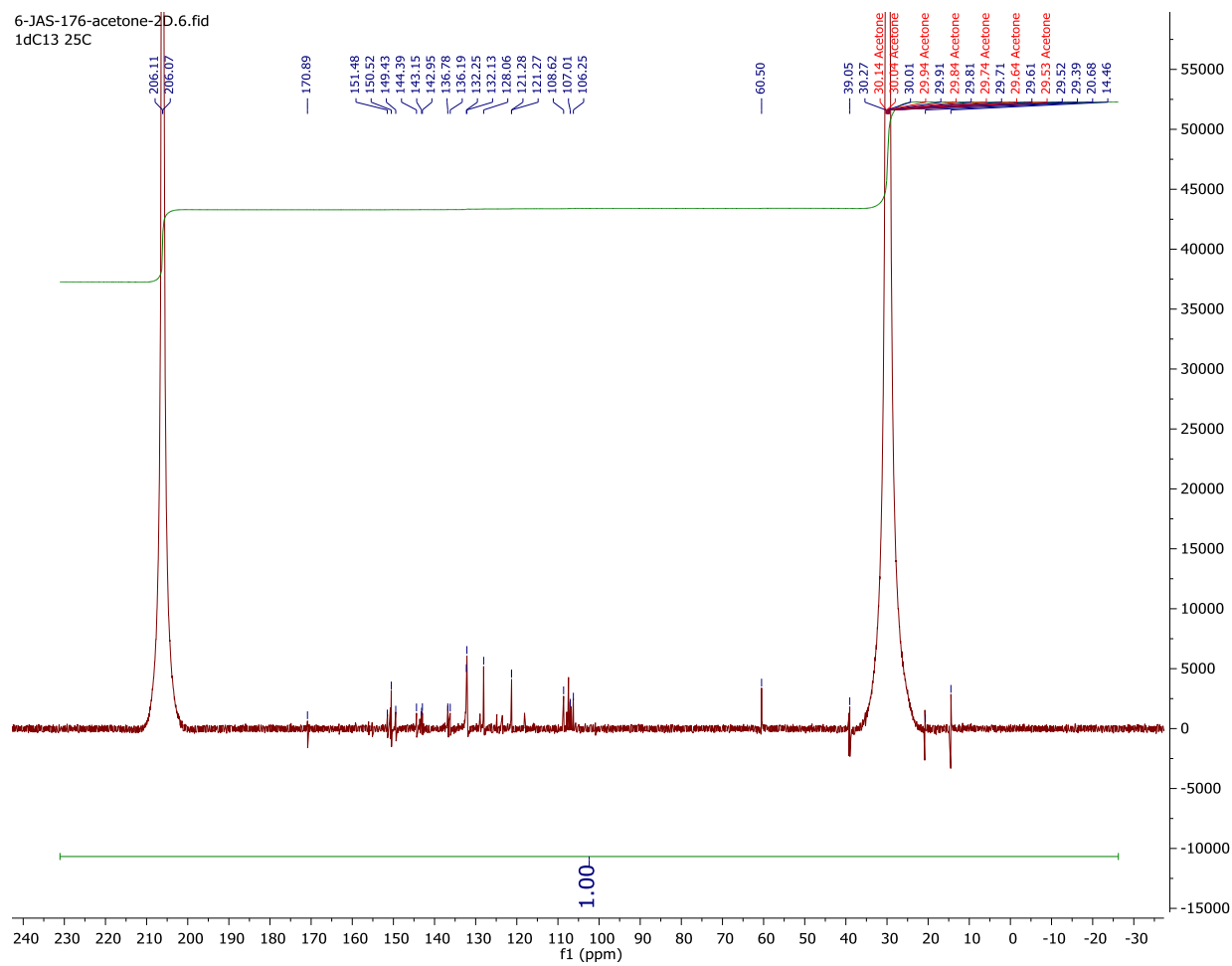
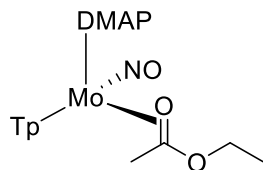




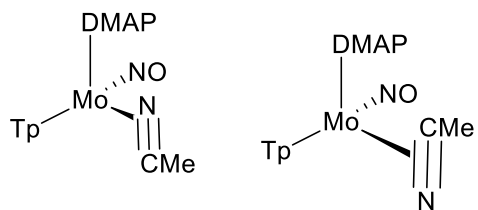
# <sup>1</sup>H NMR Spectrum of 5



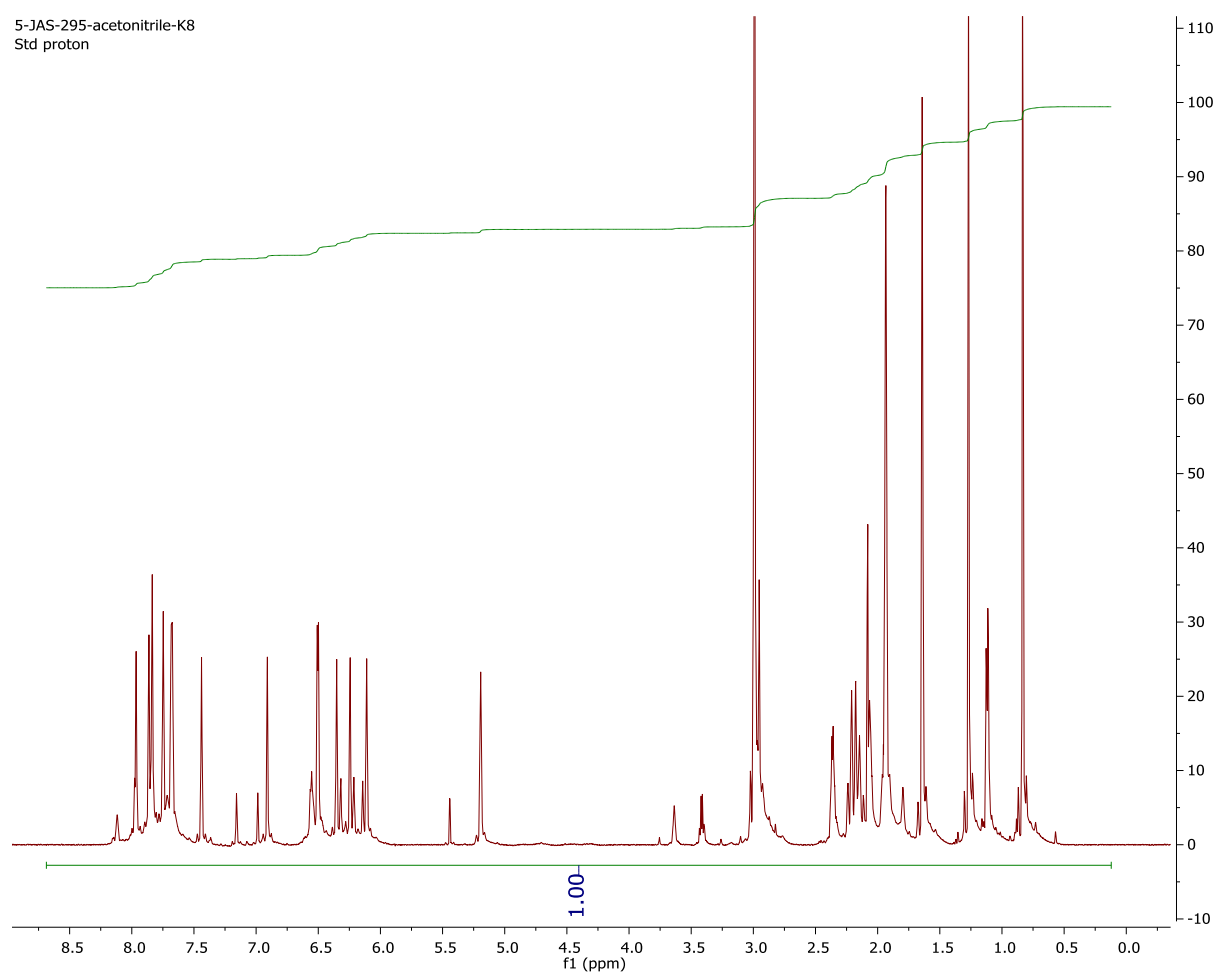
# $^{13}\text{C}\{^1\text{H}\}$ NMR Spectrum of 5



# <sup>1</sup>H NMR Spectrum of 6

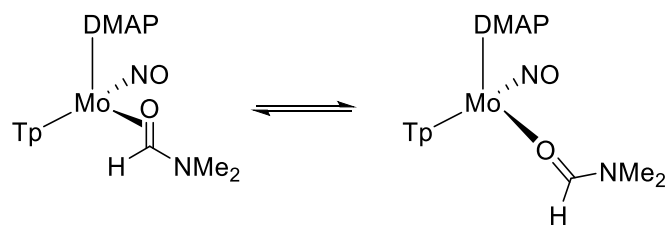


5-JAS-295-acetonitrile-K8  
Std proton

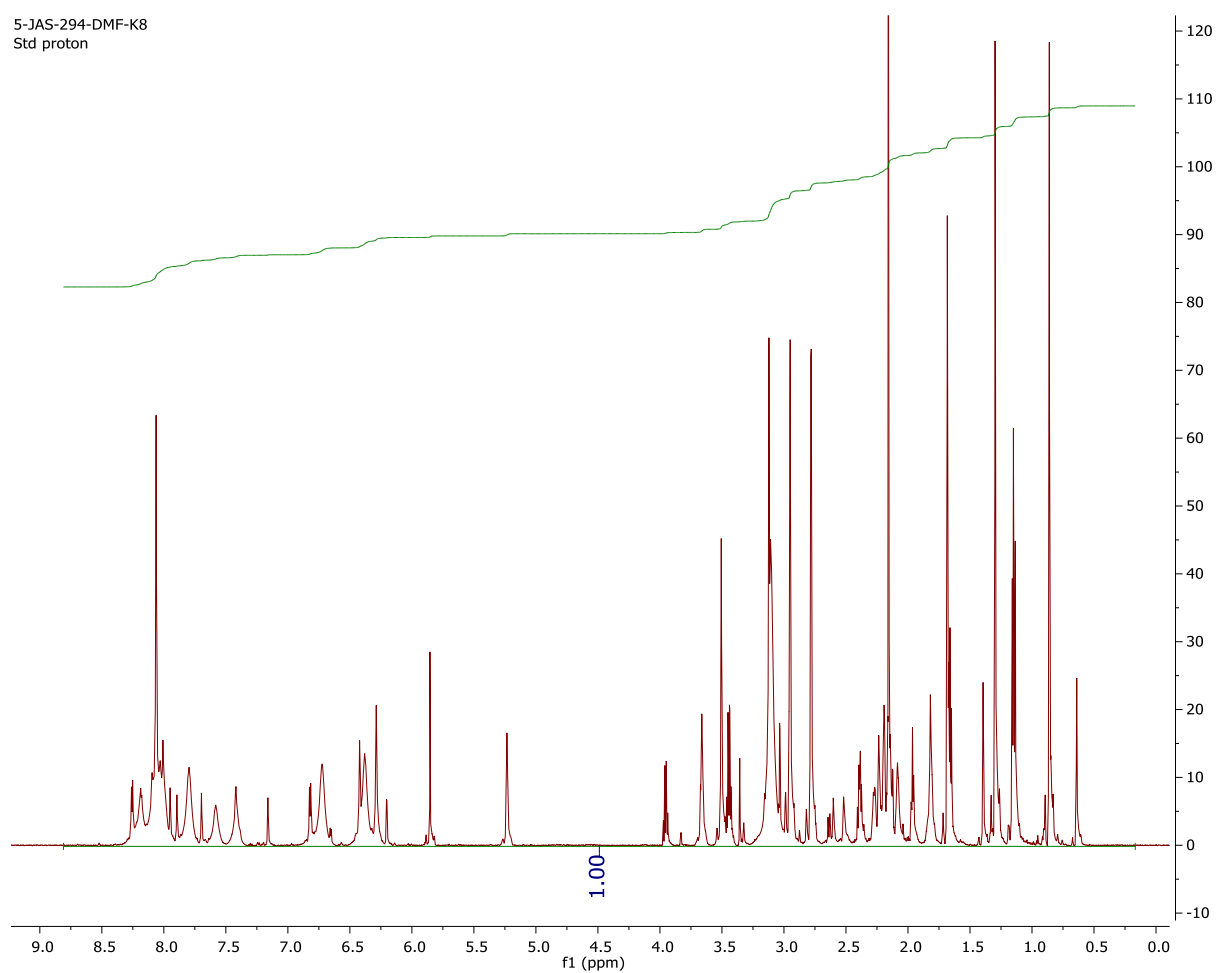




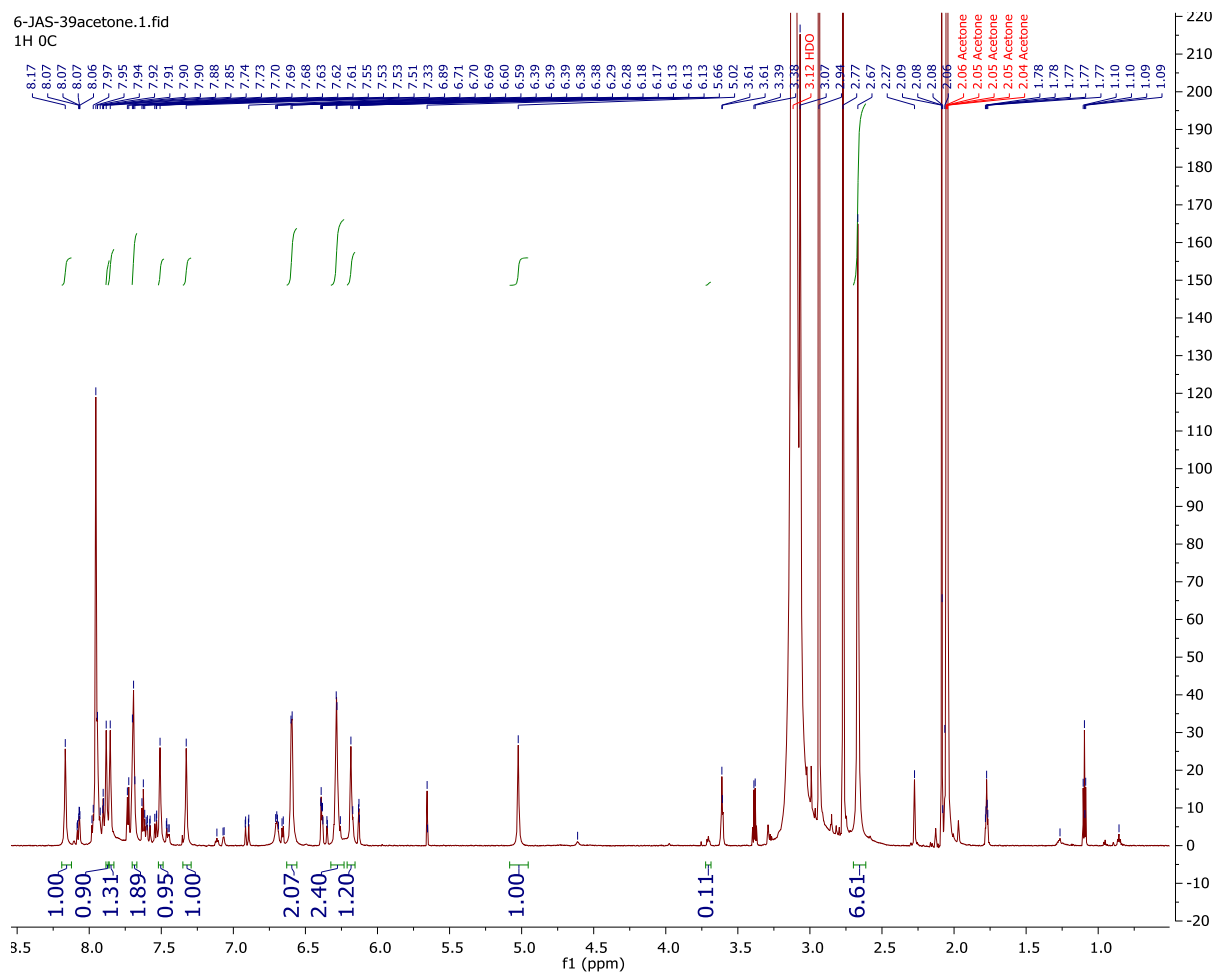
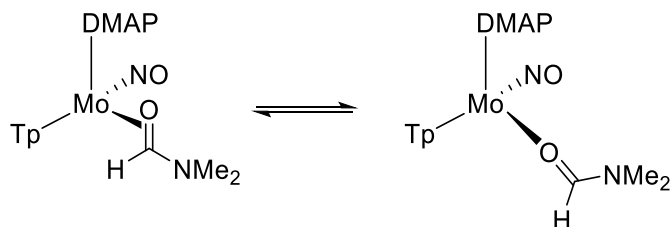
# <sup>1</sup>H NMR Spectrum of 7 in DMF-d7



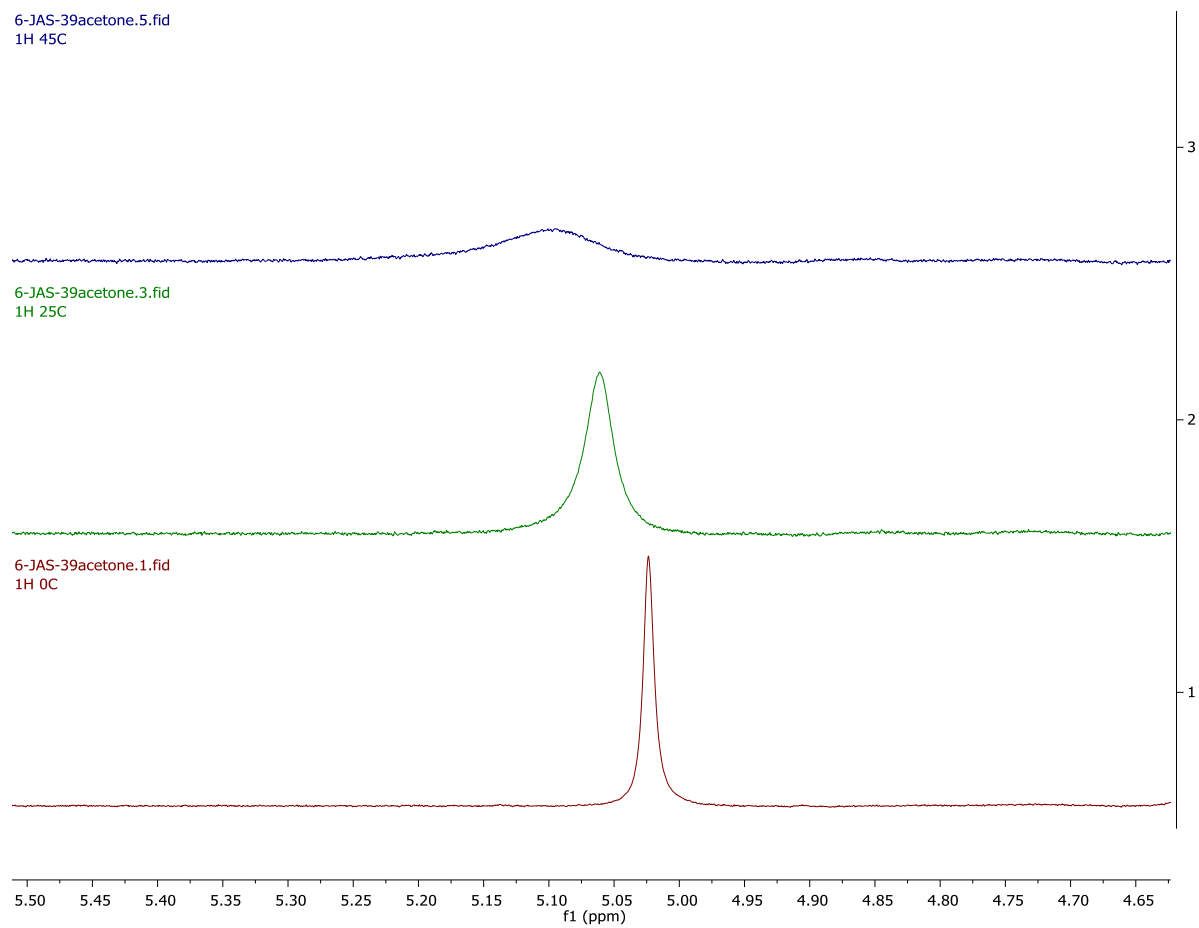
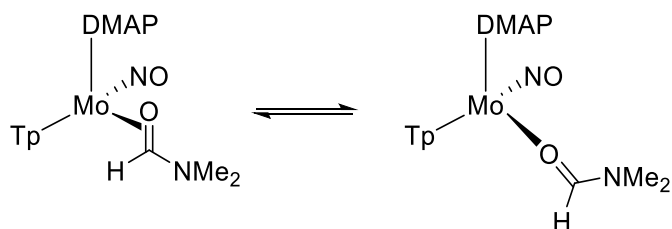
5-JAS-294-DMF-K8  
Std proton



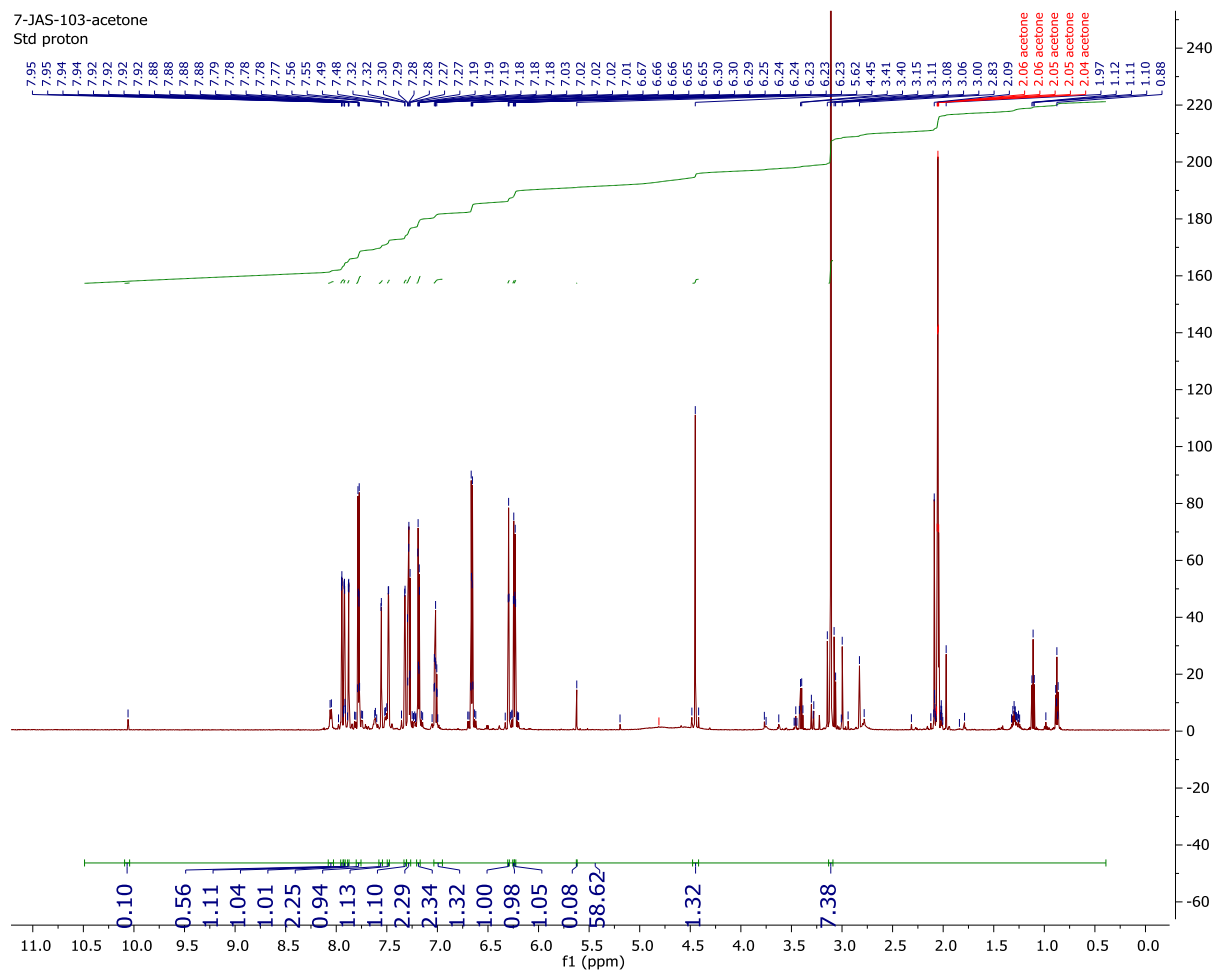
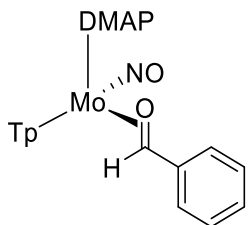
# <sup>1</sup>H NMR Spectrum of 7 in acetone-d6



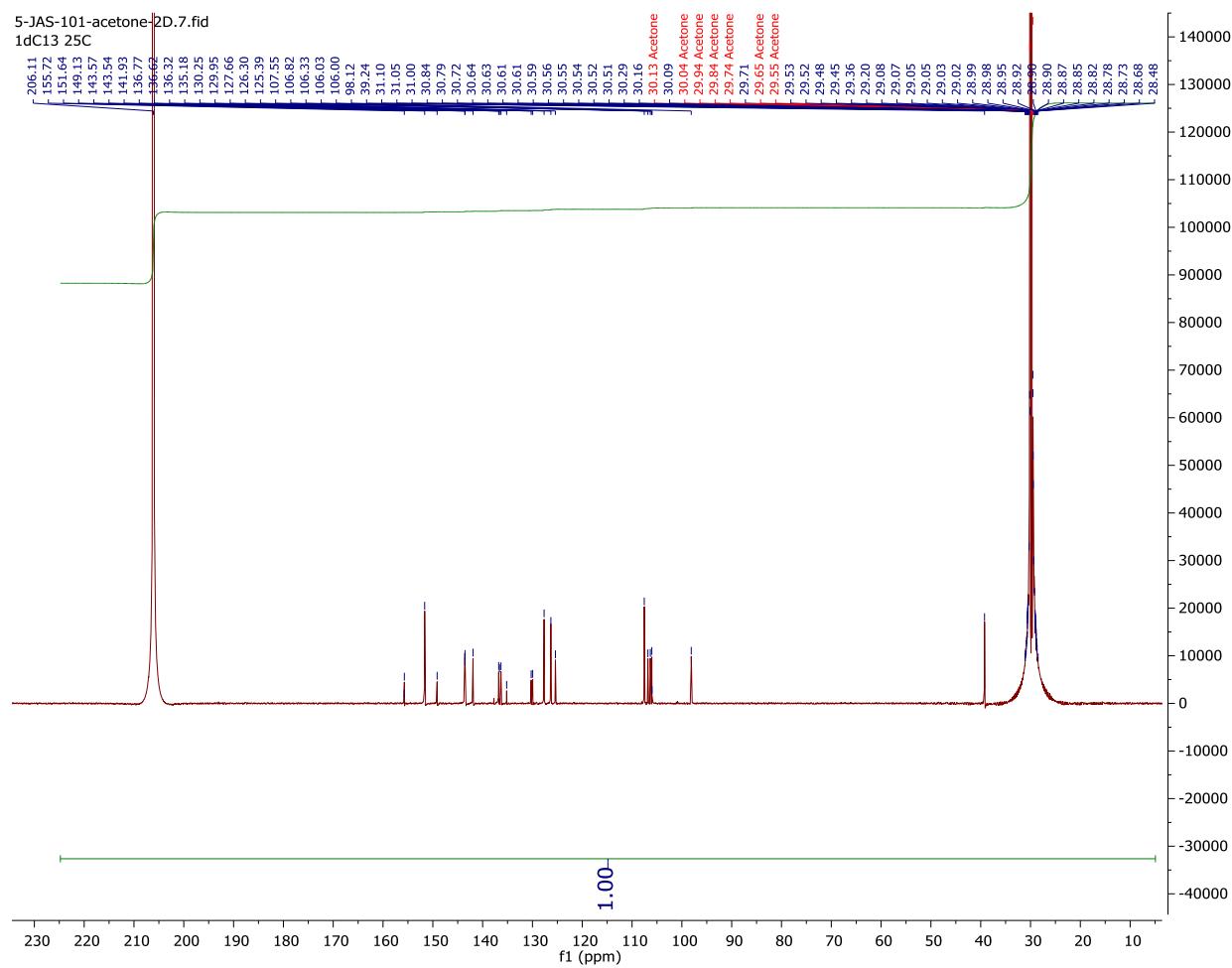
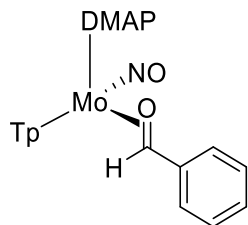
Variable Temperature Experiments of **7** in acetone-d<sub>6</sub>, Illustrations of DMF aldehyde proton fluctuonality



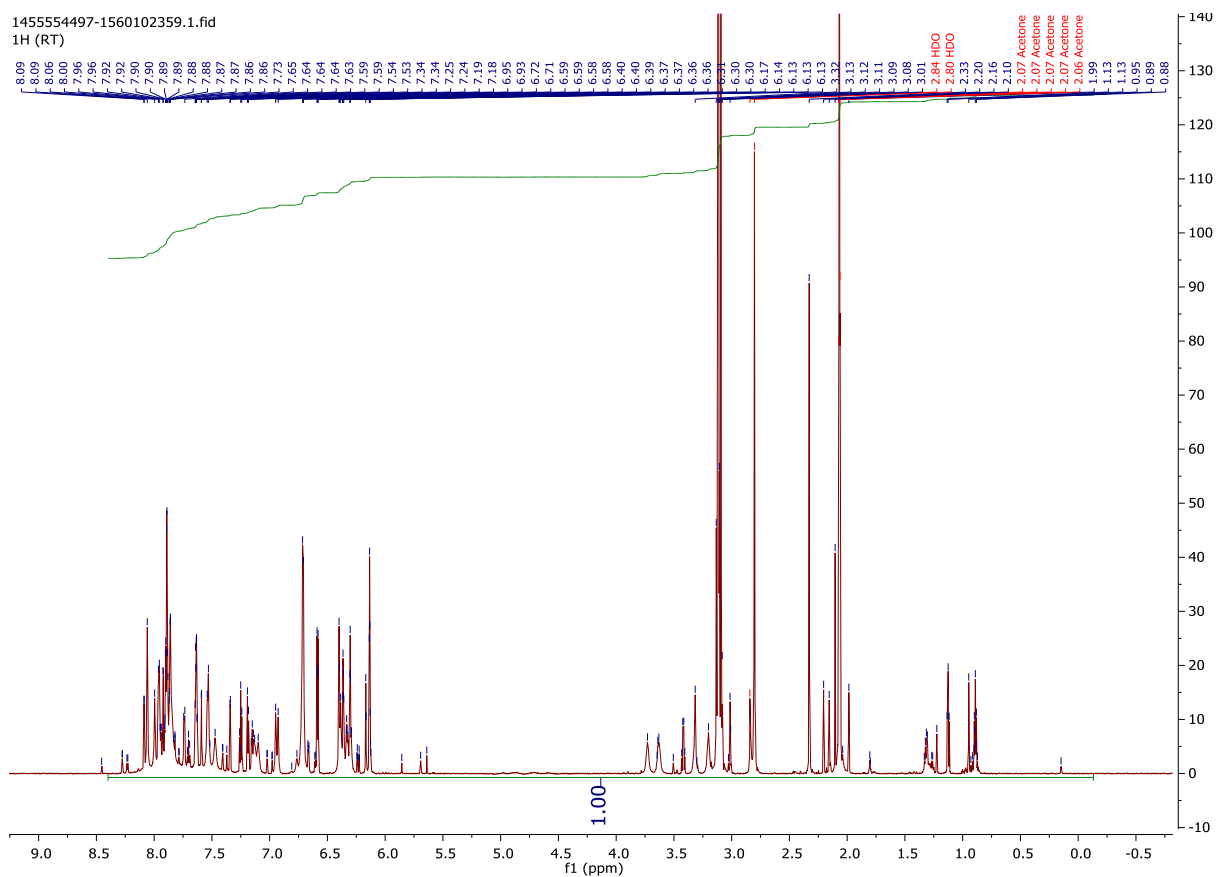
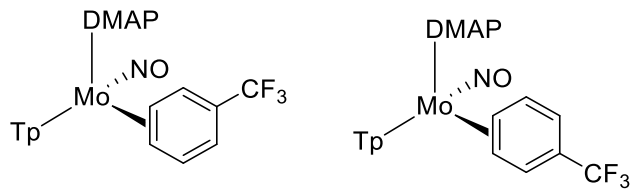
# <sup>1</sup>H NMR Spectrum of 8



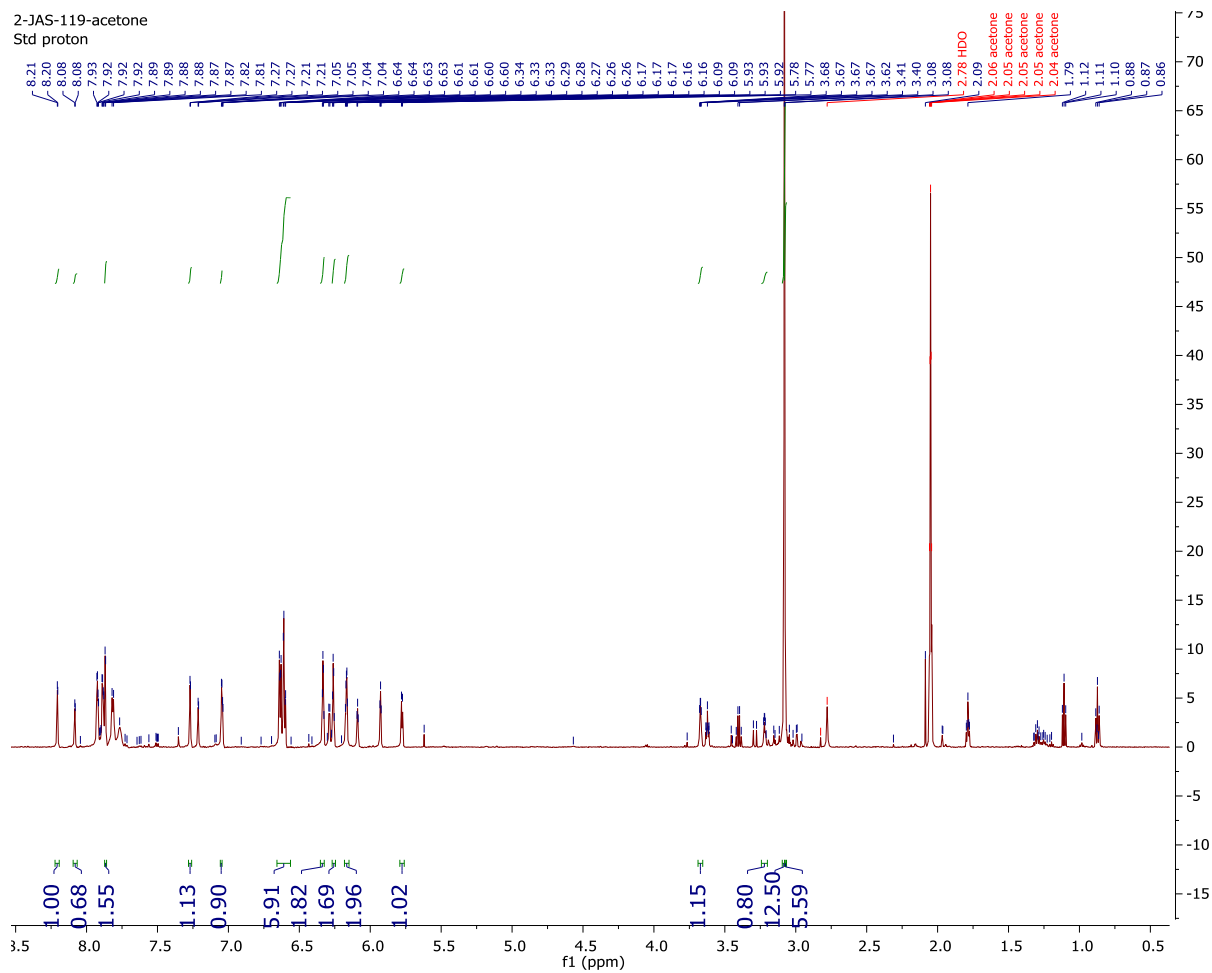
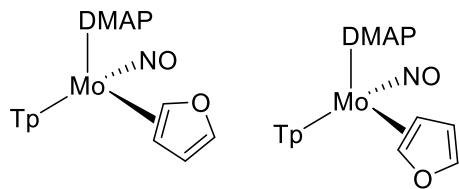
# $^{13}\text{C}\{^1\text{H}\}$ NMR Spectrum of 8



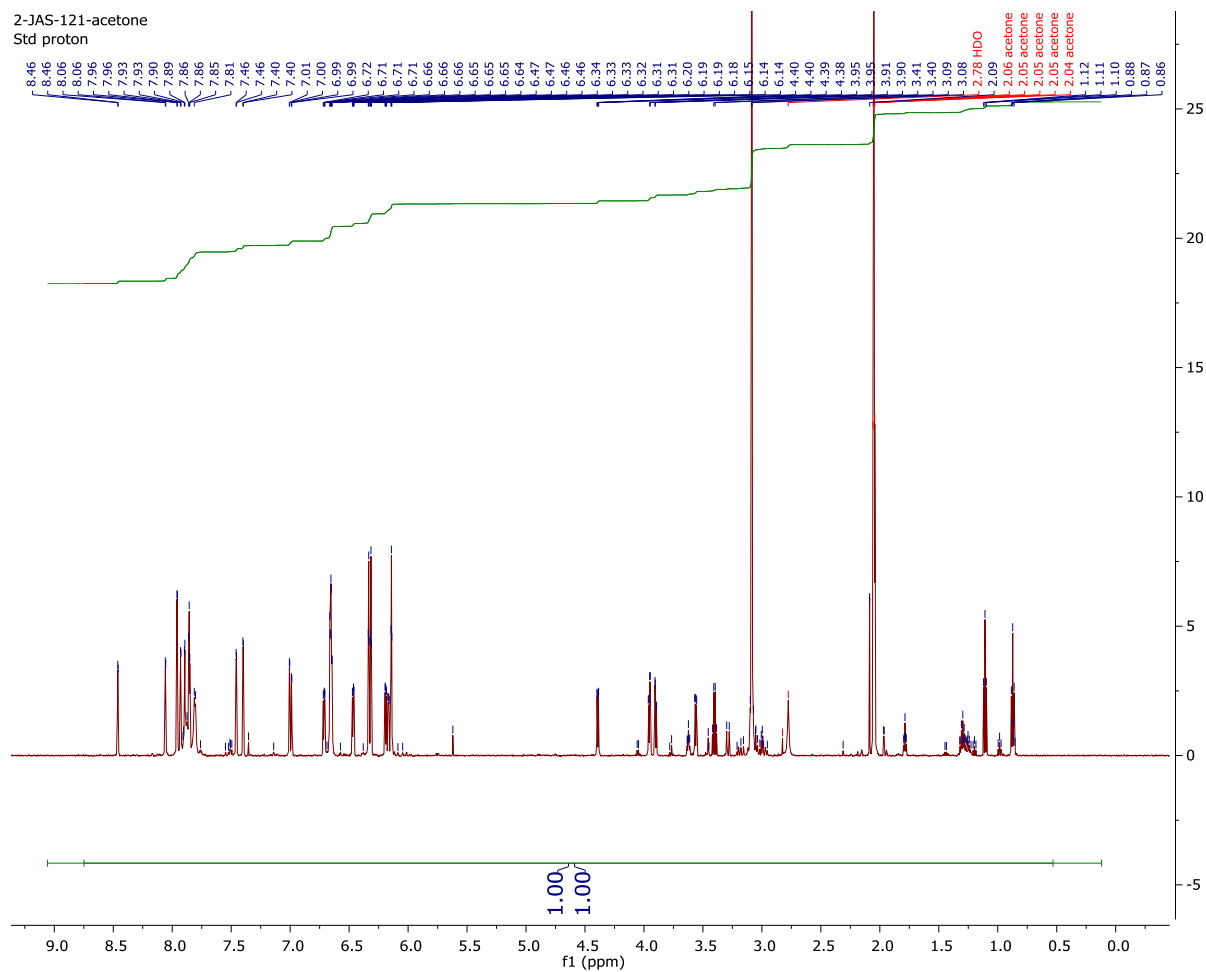
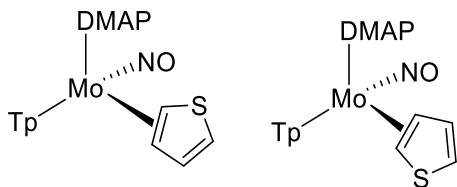
# <sup>1</sup>H NMR Spectrum of 10



# <sup>1</sup>H NMR Spectrum of 12

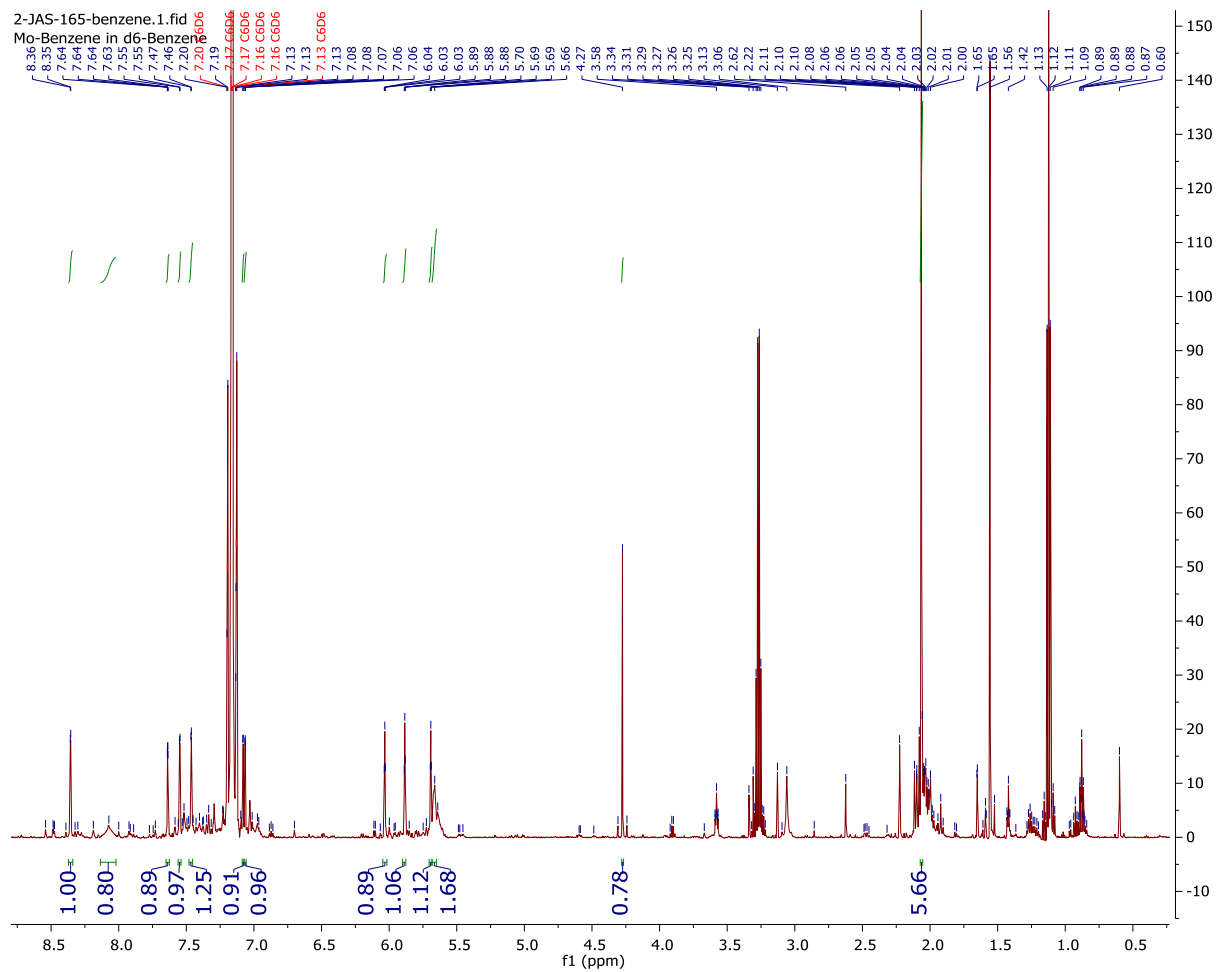
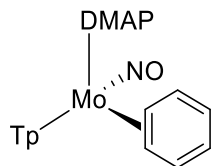


# <sup>1</sup>H NMR Spectrum of 10 thiophene

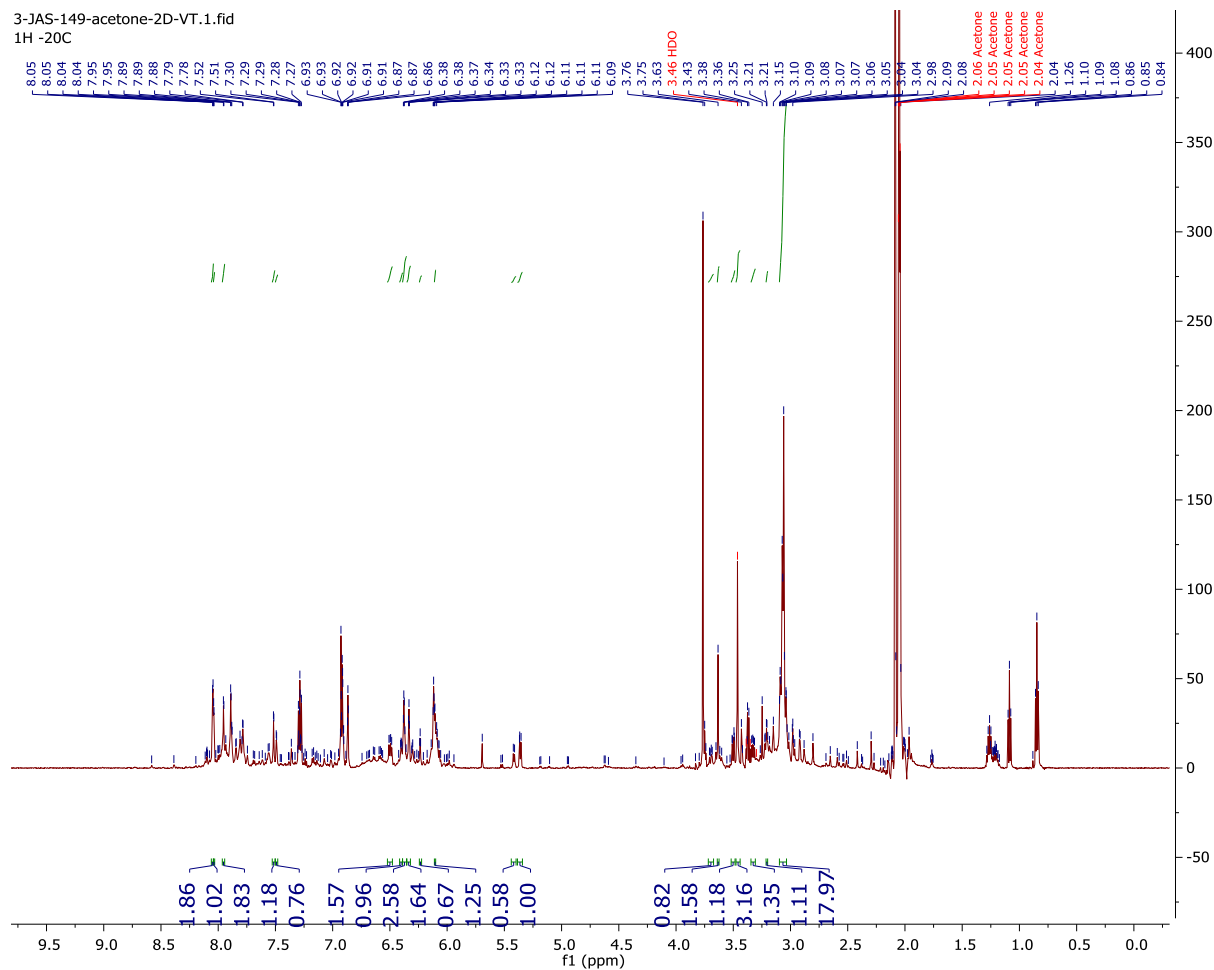
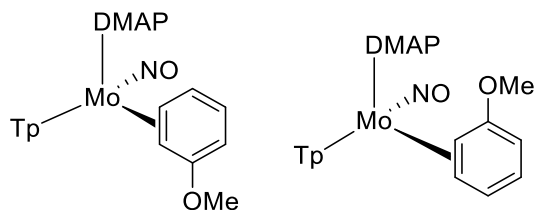




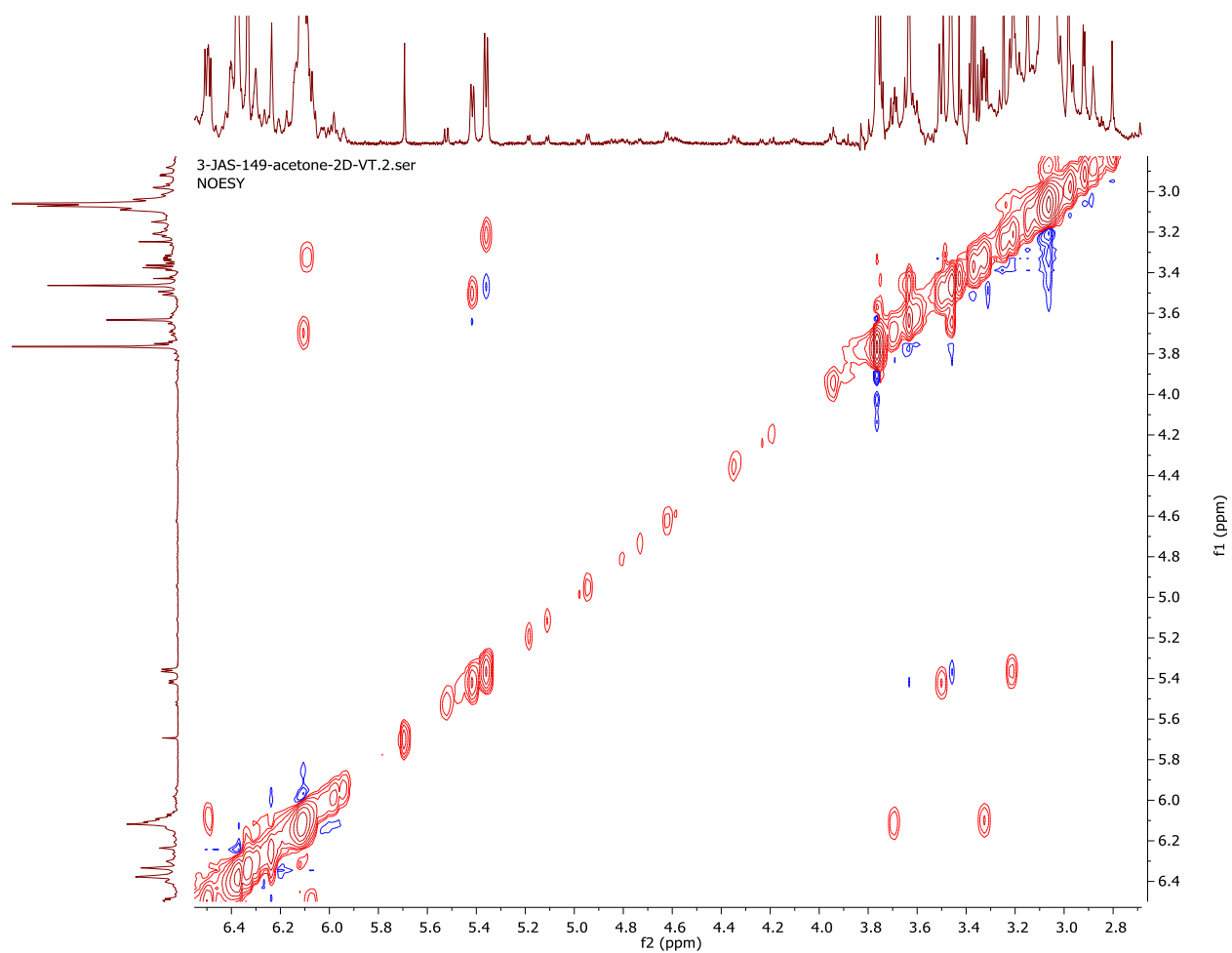
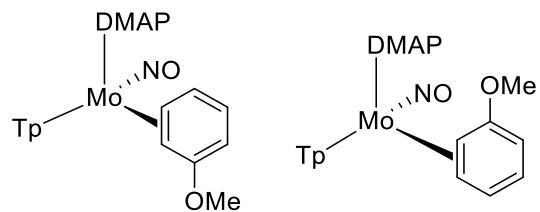
# <sup>1</sup>H NMR of 17

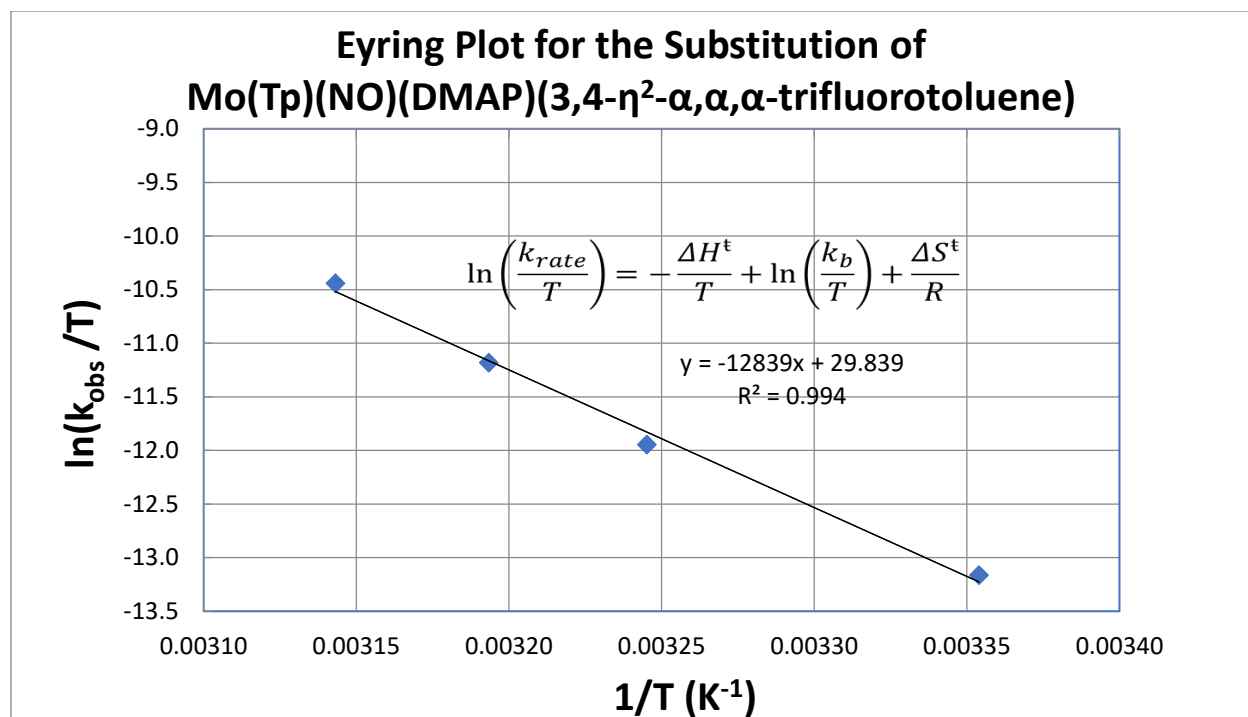


# <sup>1</sup>H NMR of 18



## NOESY of 18

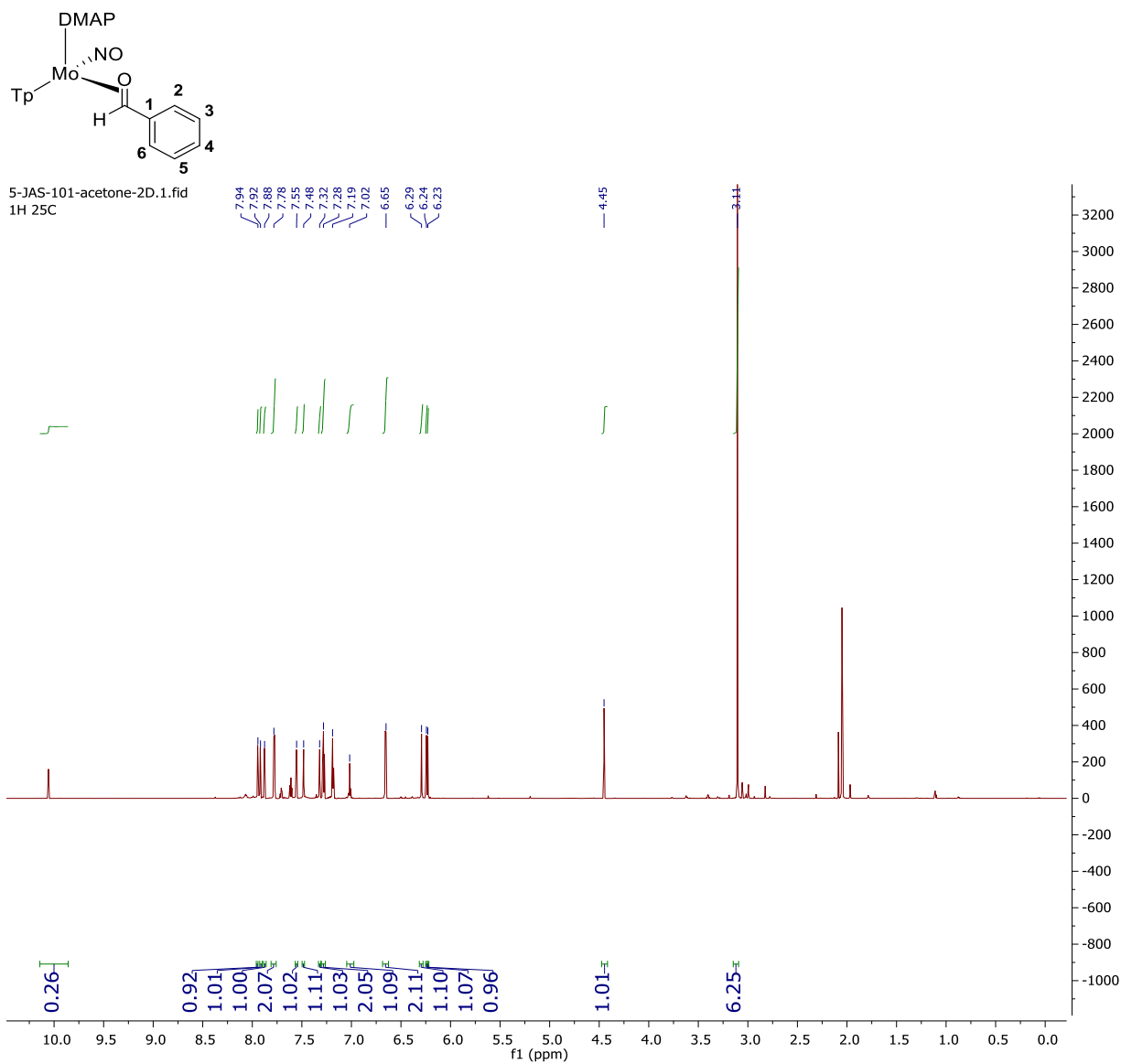




Supplemental Figure X: Eyring plot of  $\ln(k_{obs}/T)$  vs  $1/T$  where  $\Delta H^\ddagger = 25.5 \pm 1.40$  kcal/mol and  $\Delta S^\ddagger = 12.1 \pm 4.50$  eu.

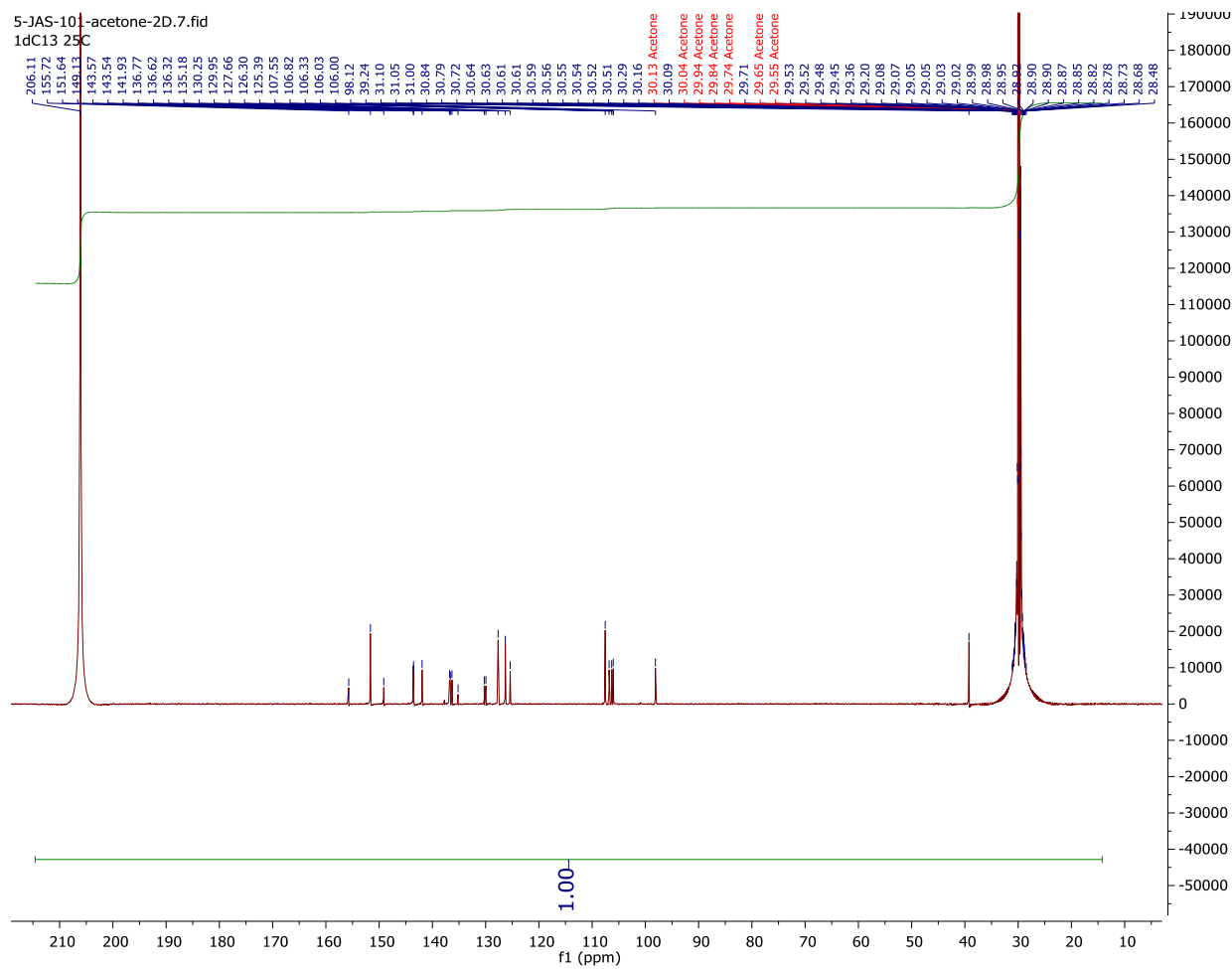
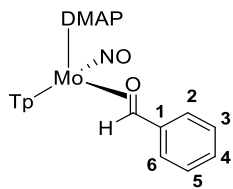
# Supporting Information for Chapter 6

## <sup>1</sup>H NMR Spectrum of 3

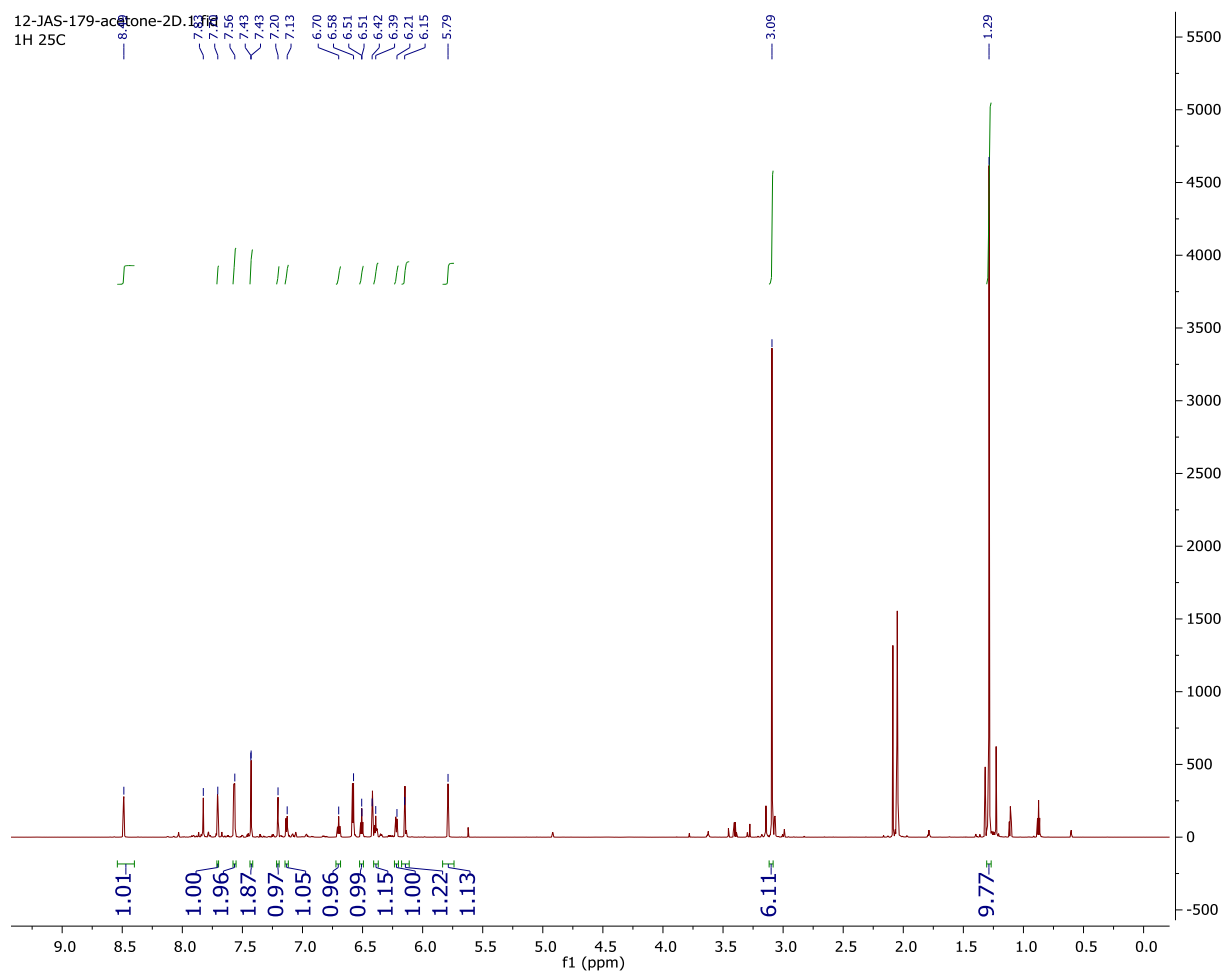
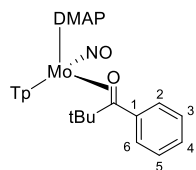


Impurity at 10.2 ppm is of free benzaldehyde ligand. Corresponding phenyl resonances observed at 7.93, 7.71 and 7.60.

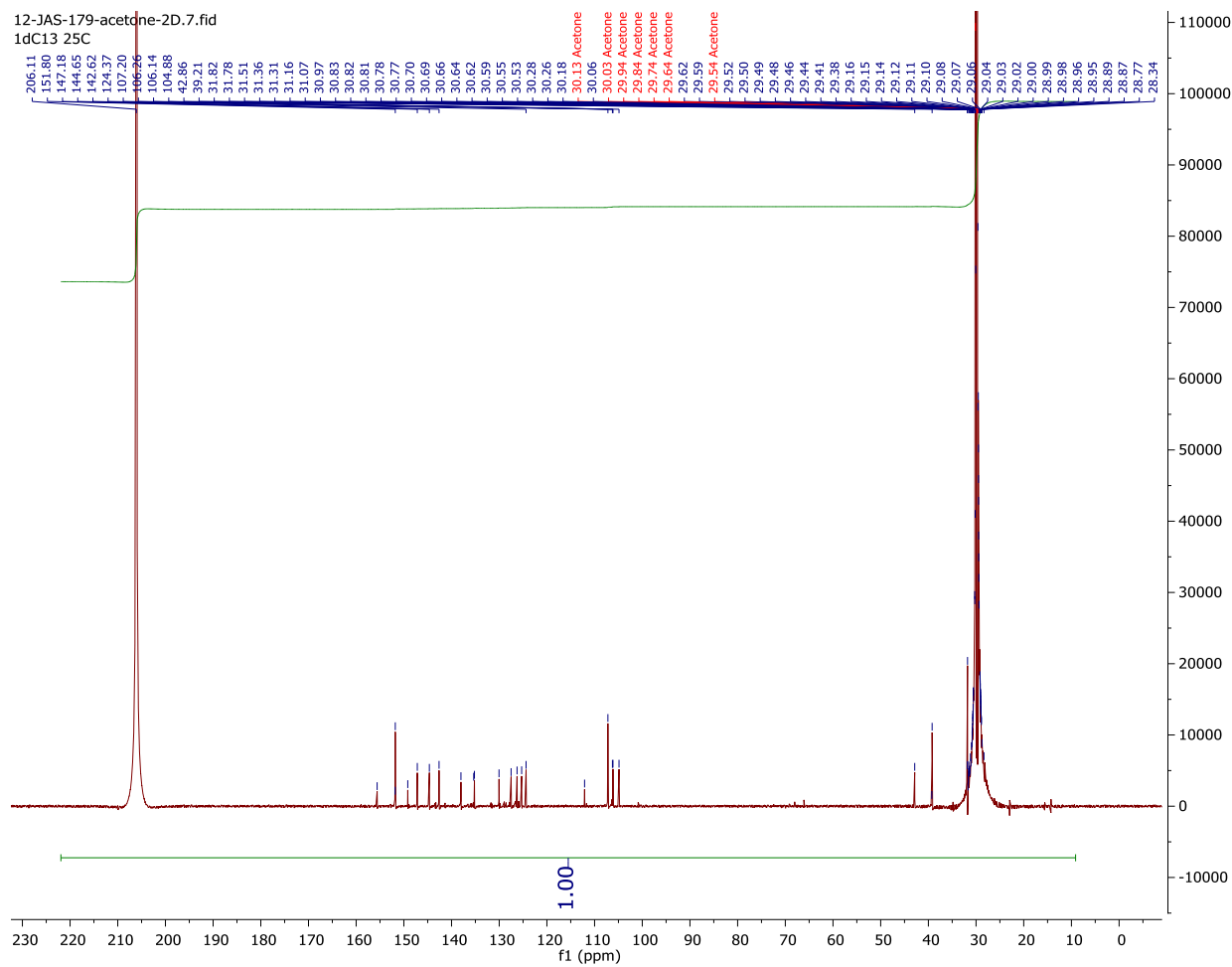
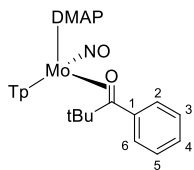
# <sup>13</sup>C{<sup>1</sup>H} NMR Spectrum of 3



# <sup>1</sup>H NMR Spectrum of 5

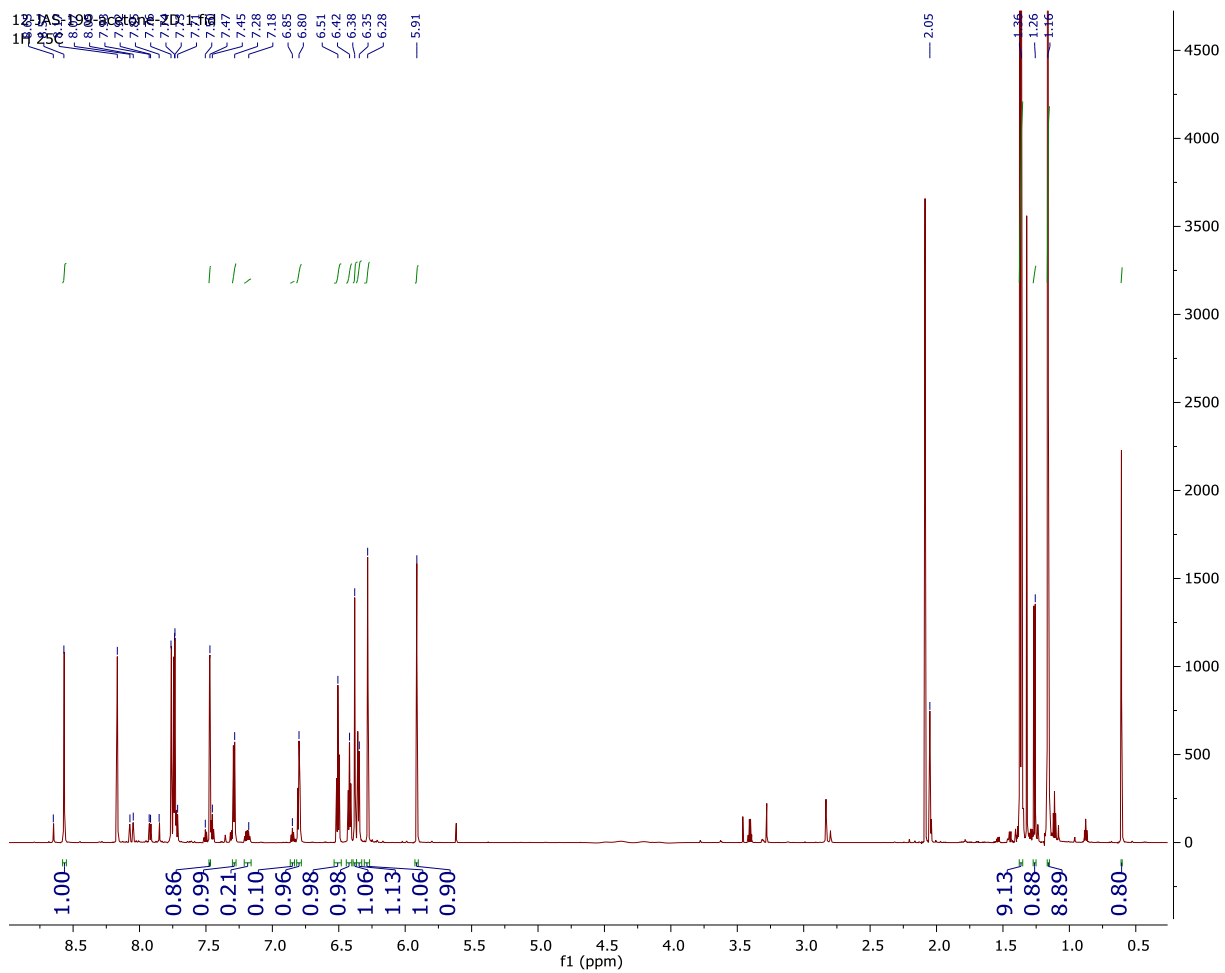
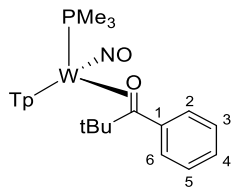


# <sup>13</sup>C{<sup>1</sup>H} NMR Spectrum of 5

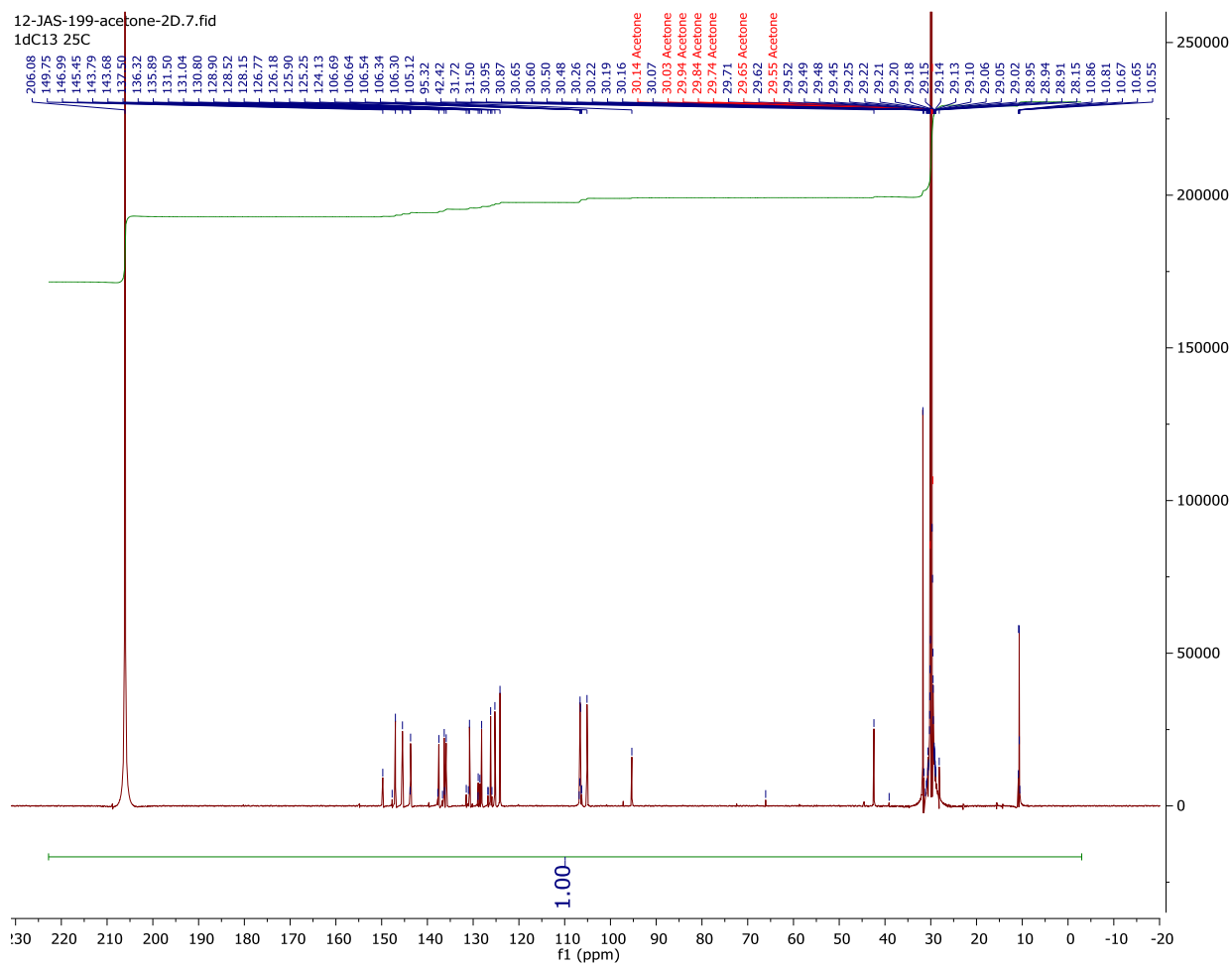
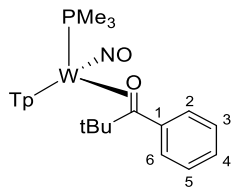




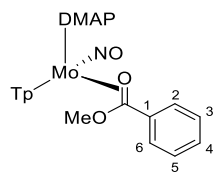
# <sup>1</sup>H NMR Spectrum of 6



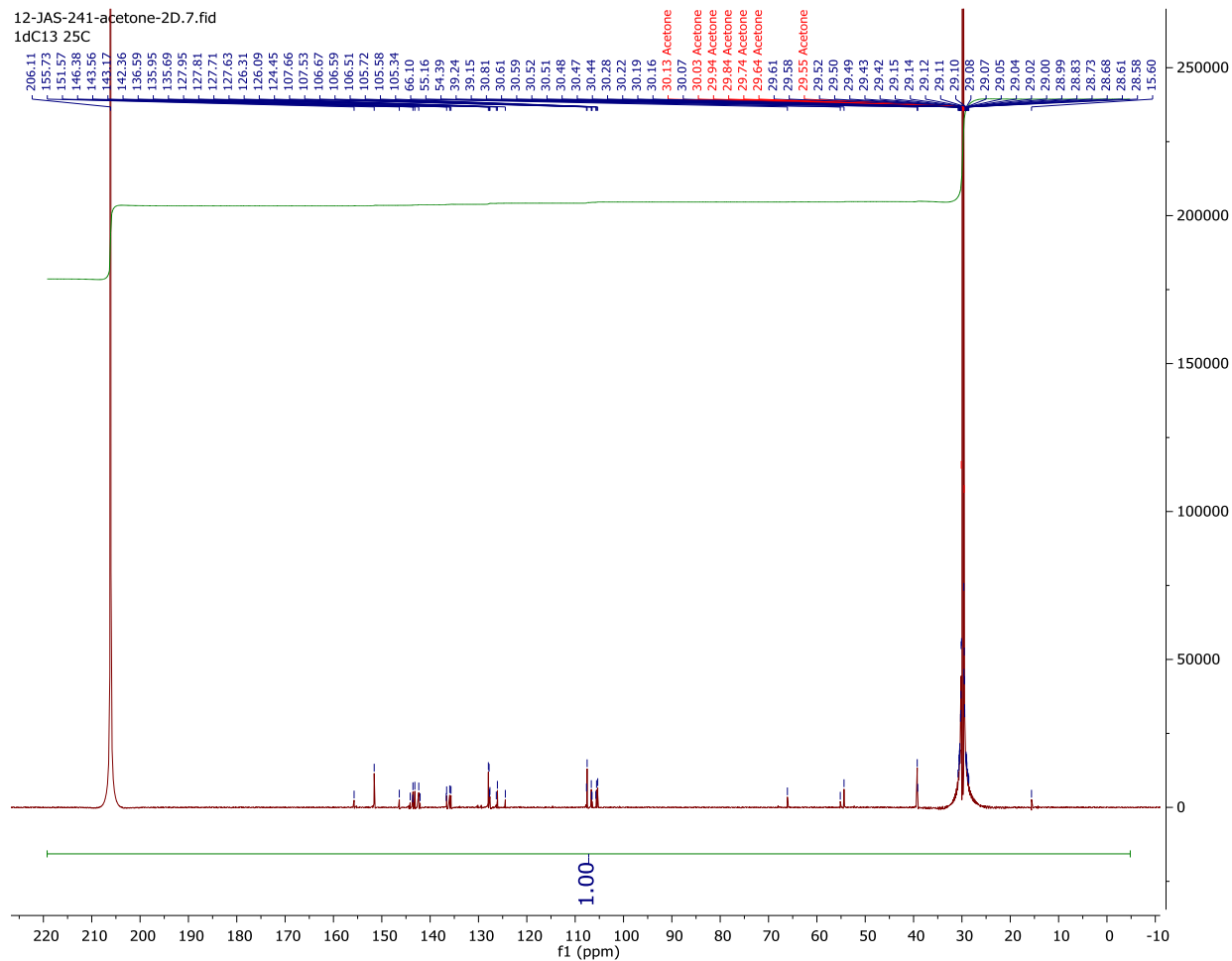
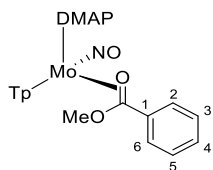
# $^{13}\text{C}\{^1\text{H}\}$ NMR Spectrum of 6



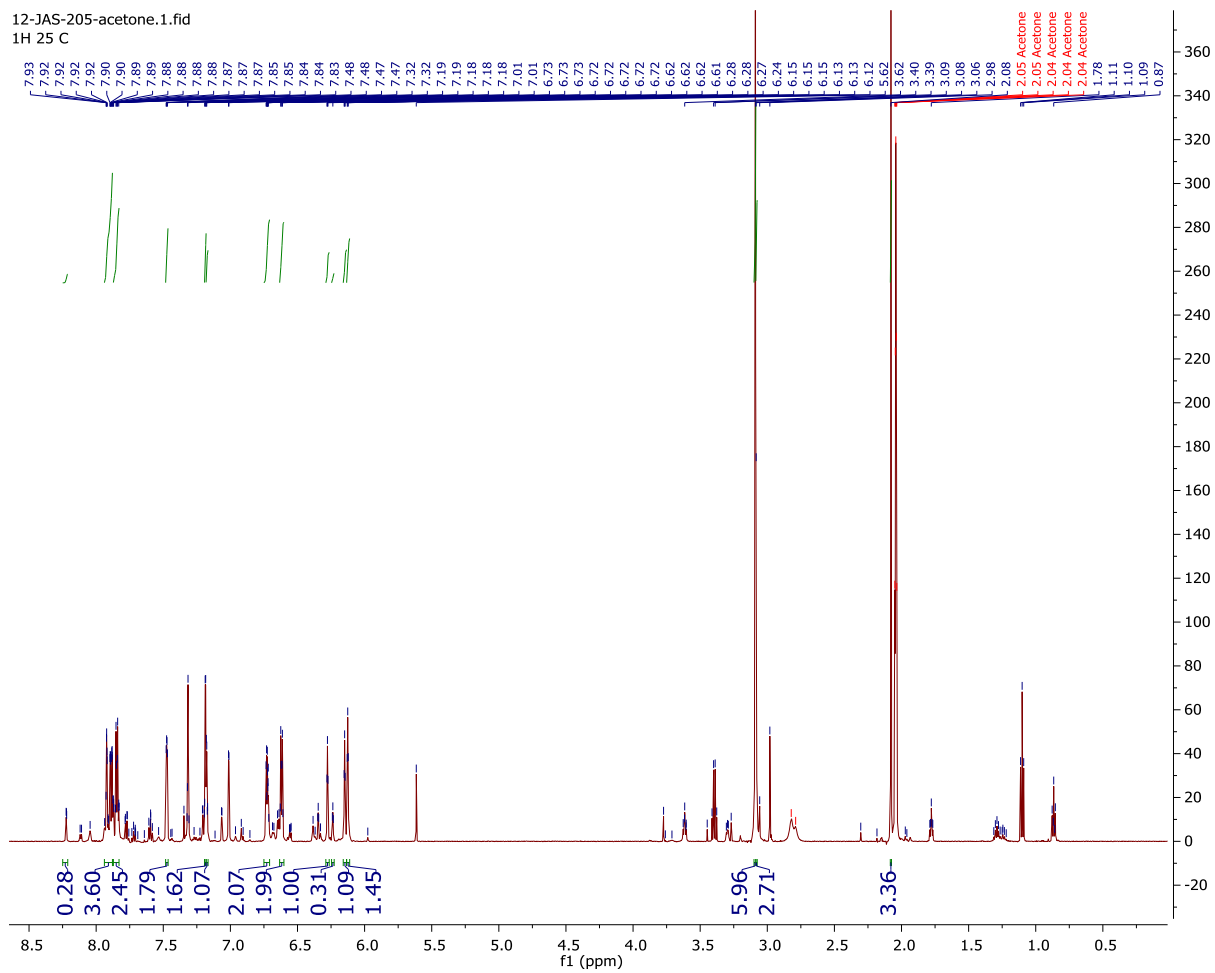
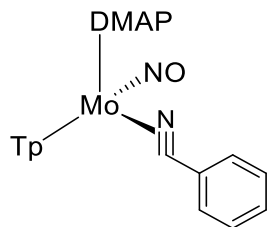
# <sup>1</sup>H NMR Spectrum of 7



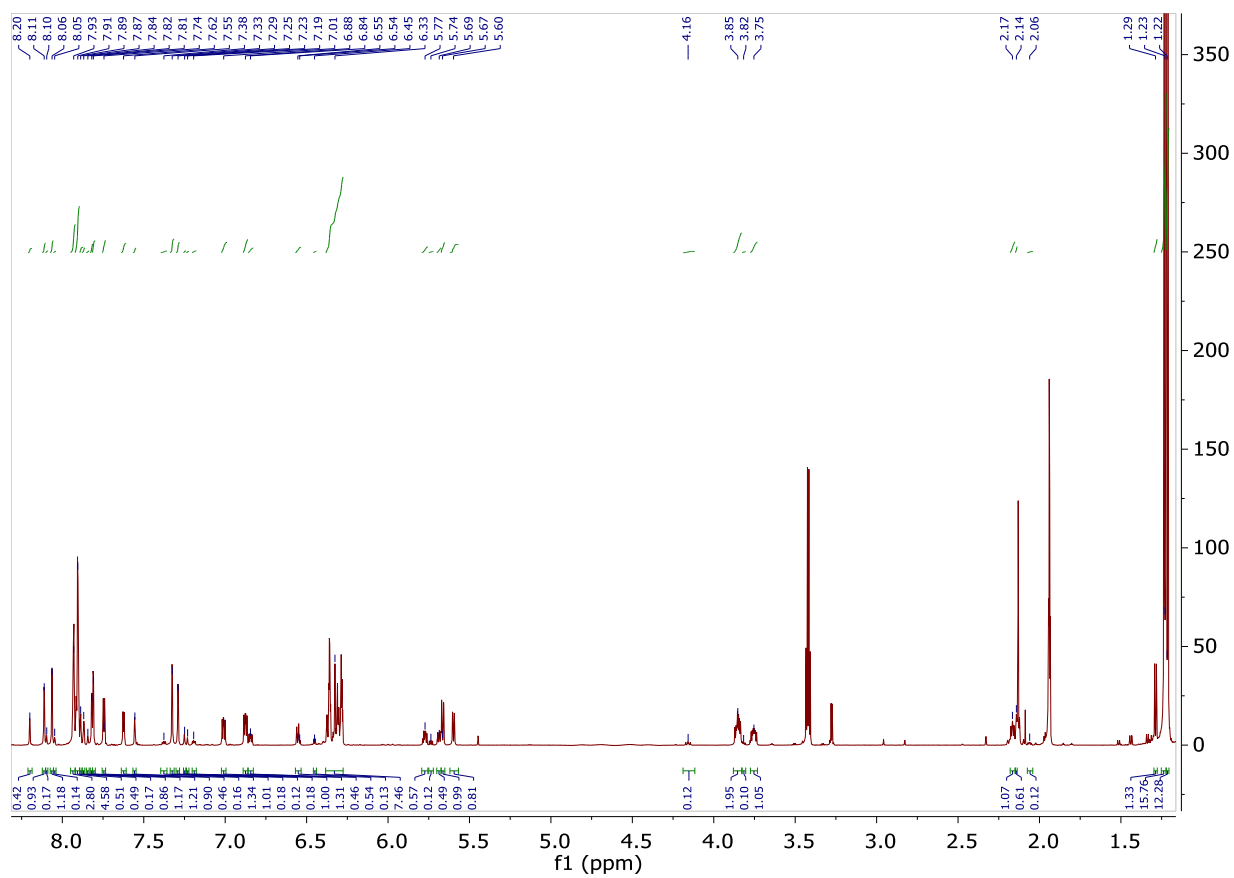
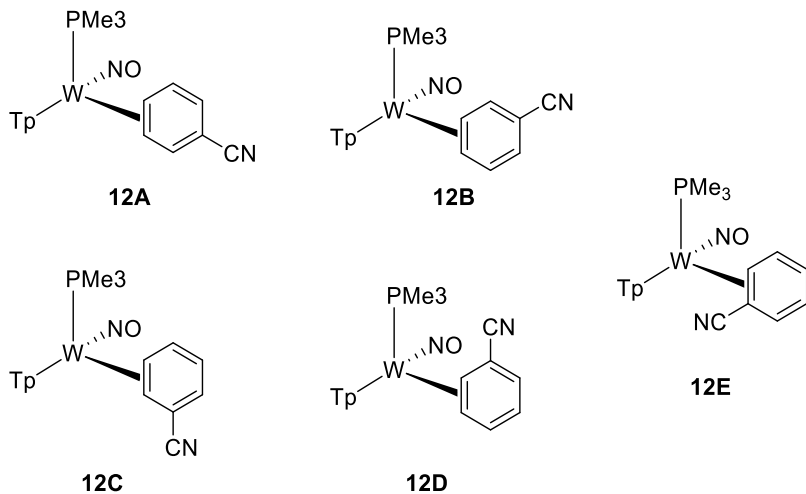
# $^{13}\text{C}\{^1\text{H}\}$ NMR Spectrum of 7



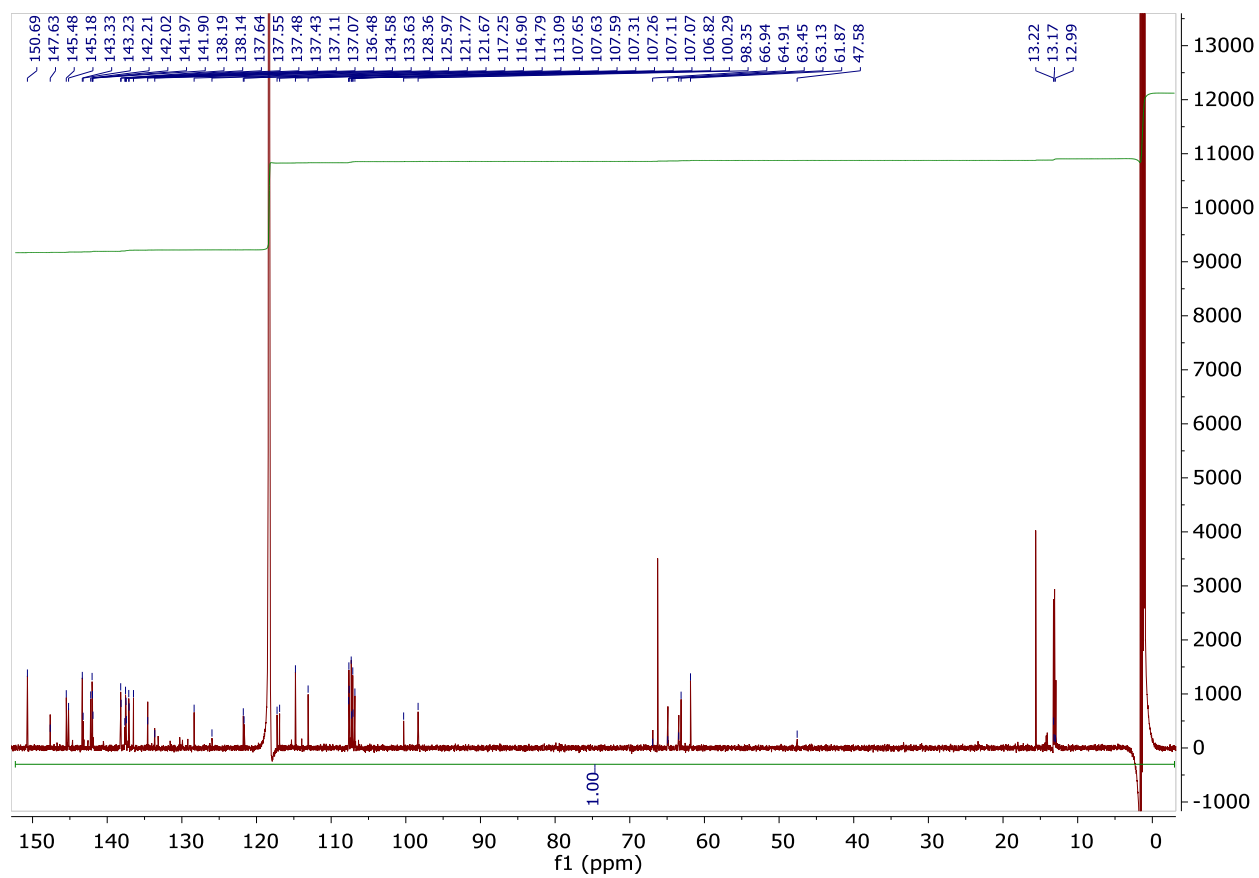
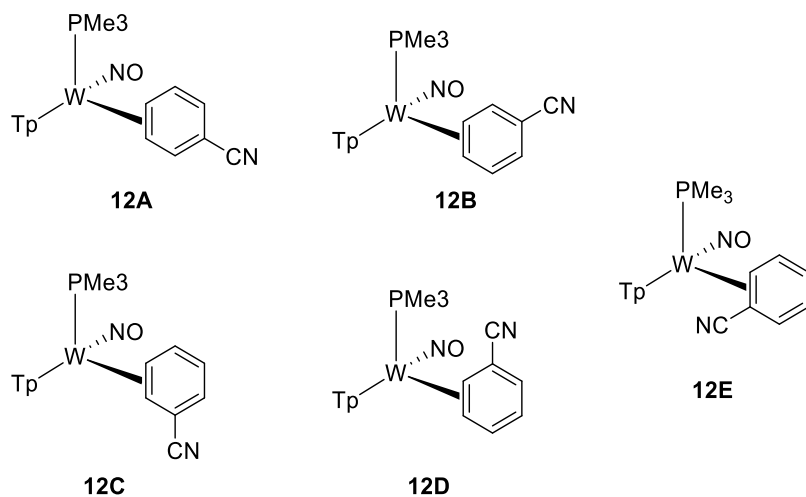
# <sup>1</sup>H NMR Spectrum of 11



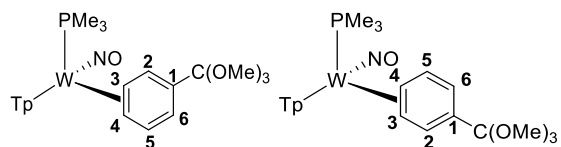
**<sup>1</sup>H NMR Spectrum of 12A 12B 12C 12D and 12E**



**$^{13}\text{C}$  { $^1\text{H}$ } NMR Spectrum of 12A 12B 12C 12D and 12E**

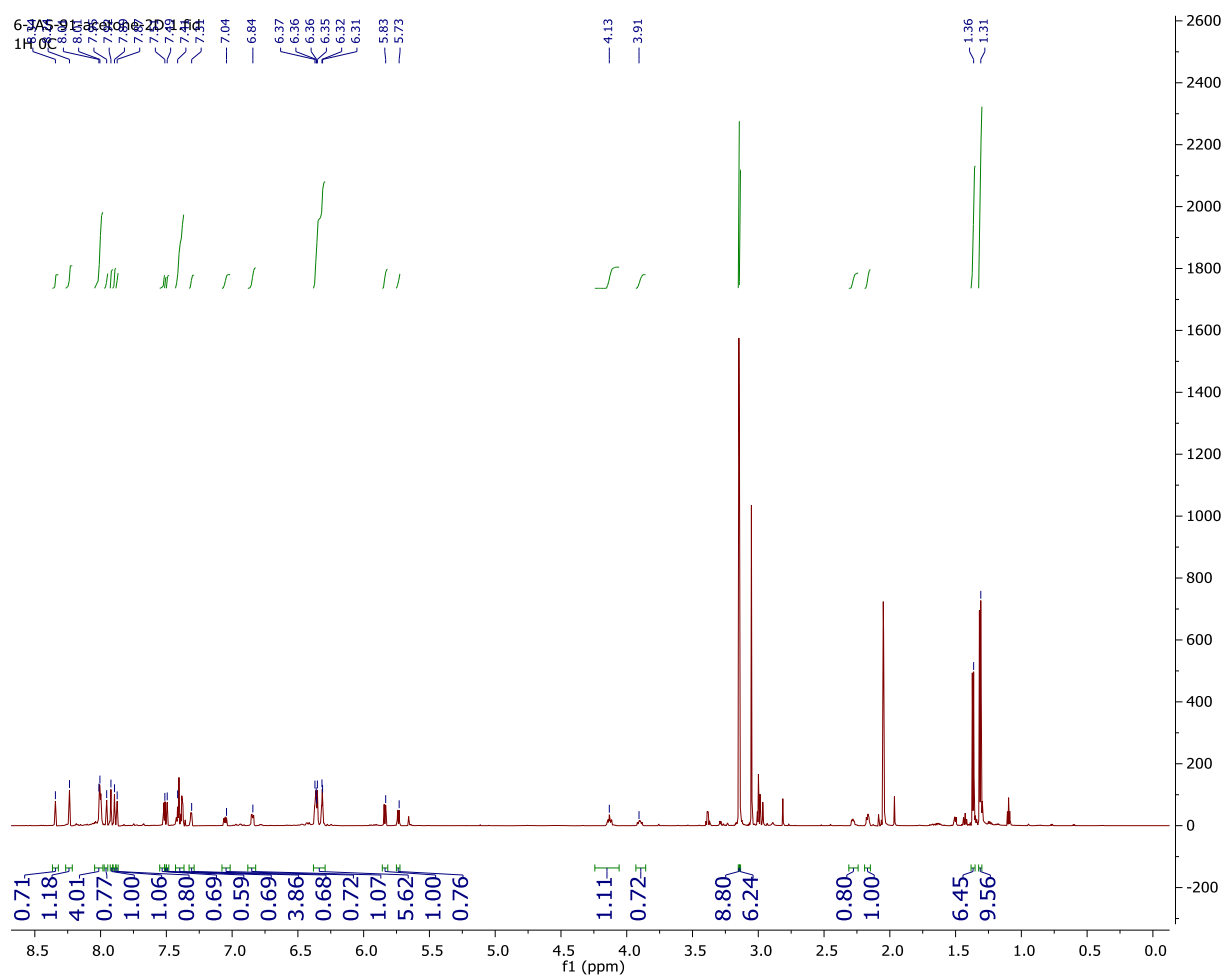


# <sup>1</sup>H NMR Spectrum of 14A and 14 B



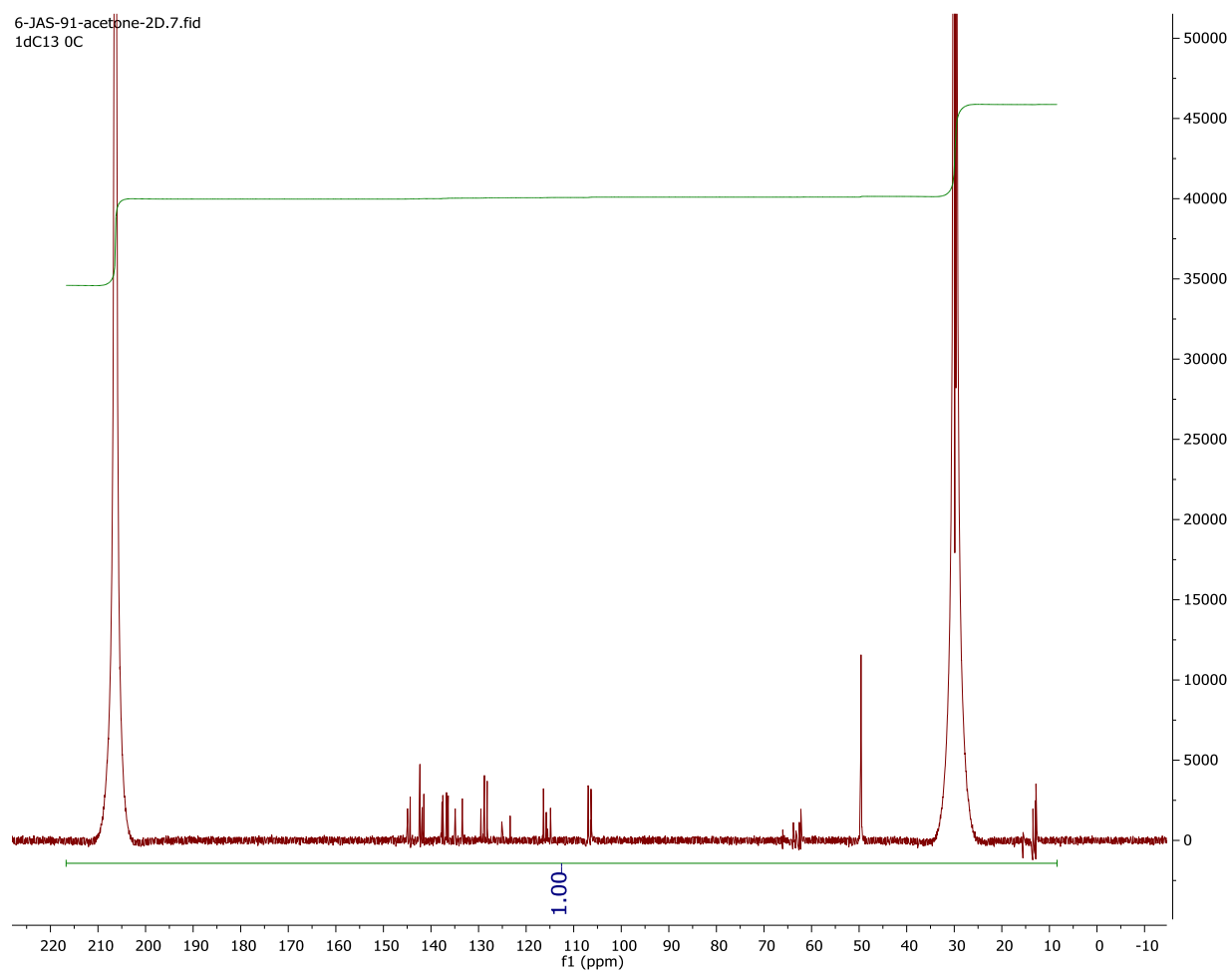
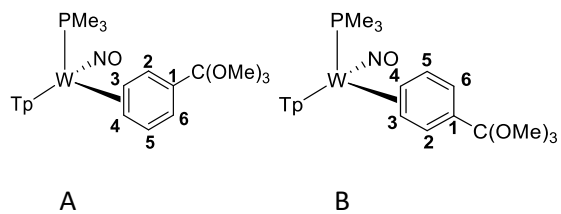
A

B



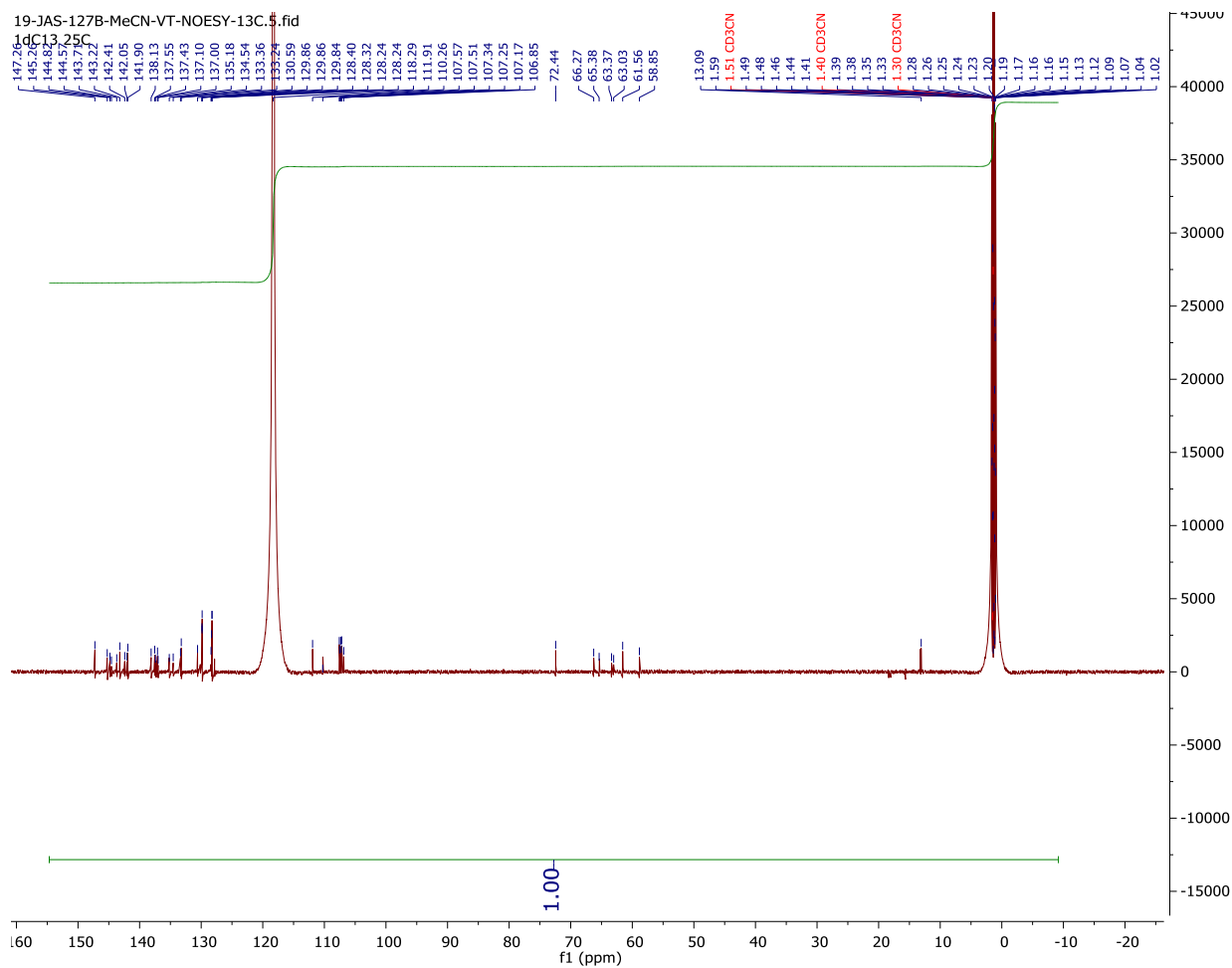
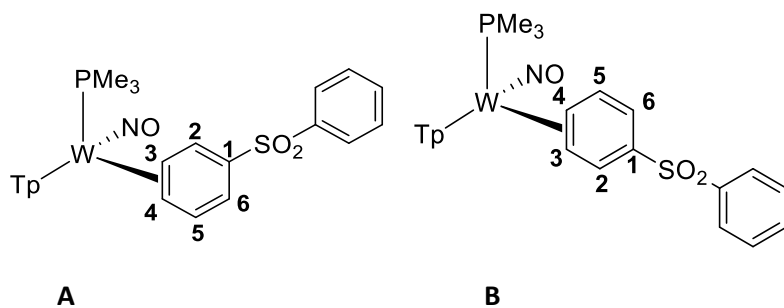


# $^{13}\text{C}\{^1\text{H}\}$ NMR Spectrum of 14A and 14 B

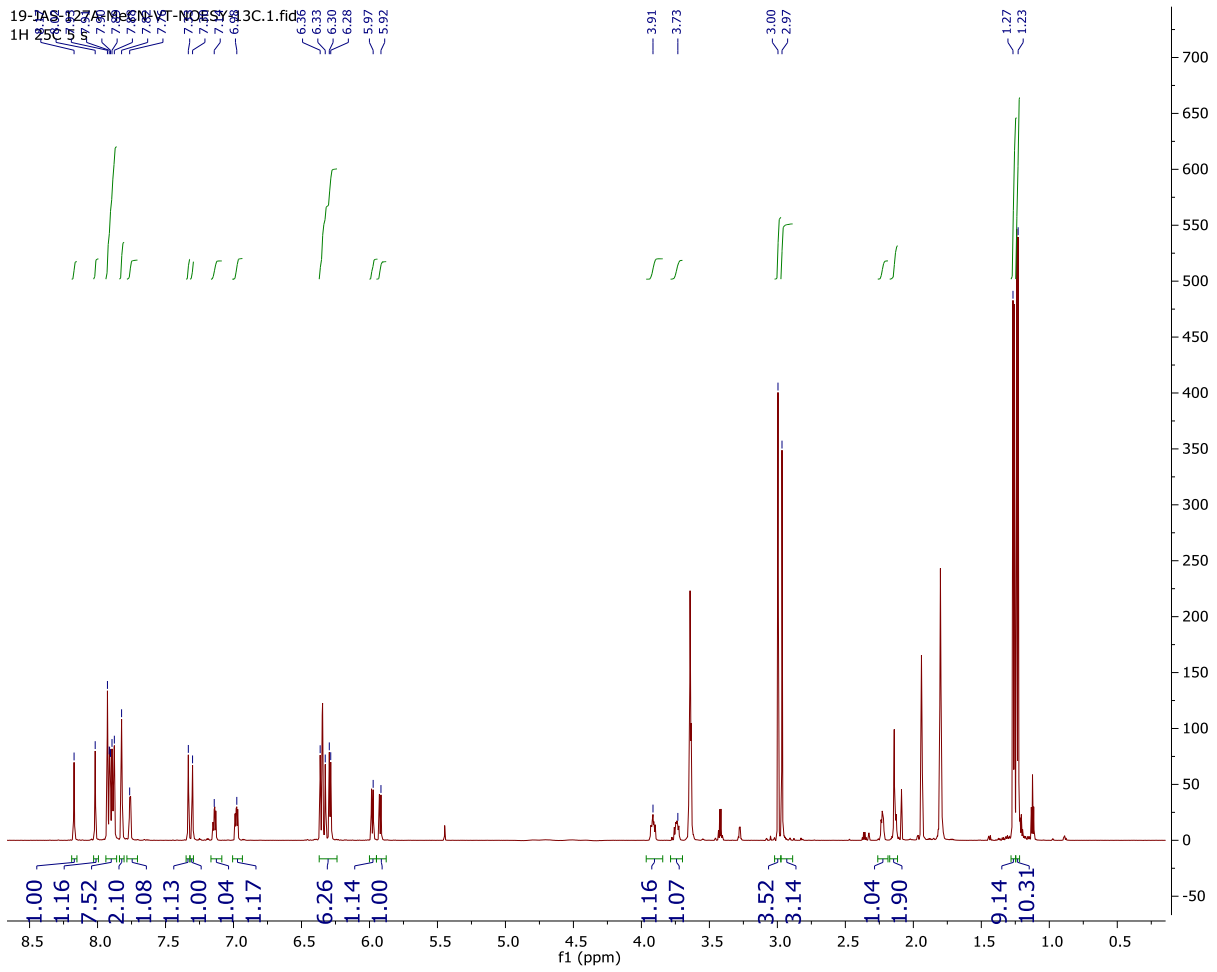
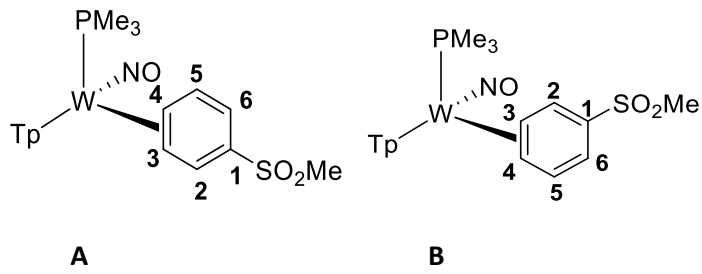




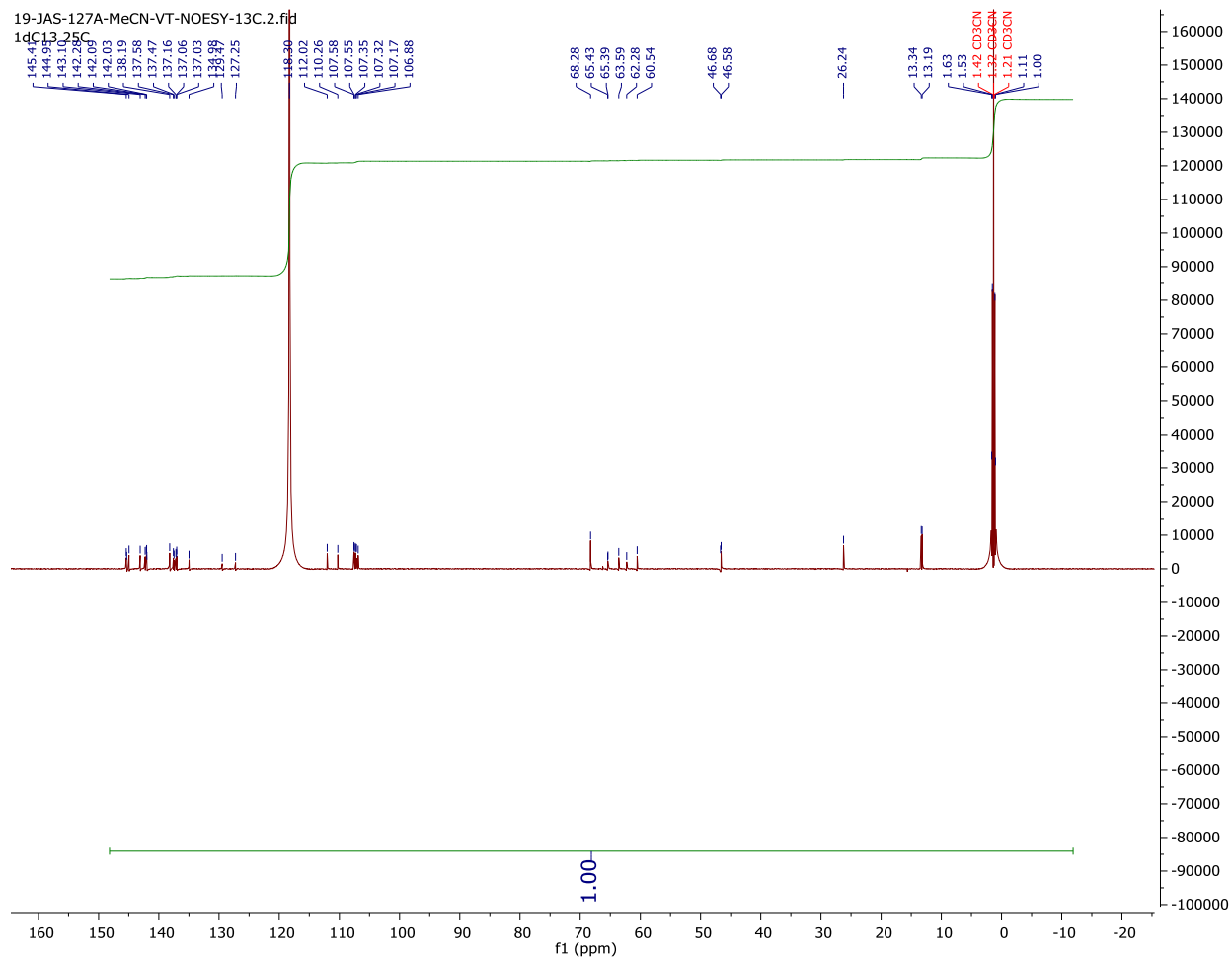
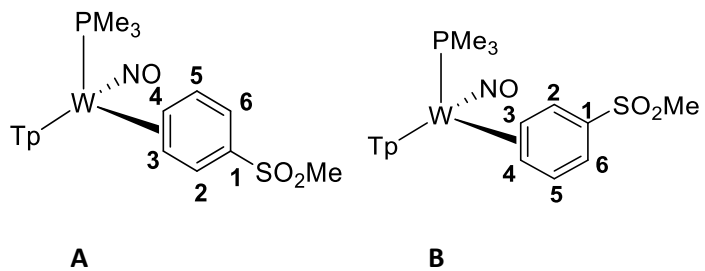
<sup>13</sup>C{<sup>1</sup>H} NMR Spectrum of 15



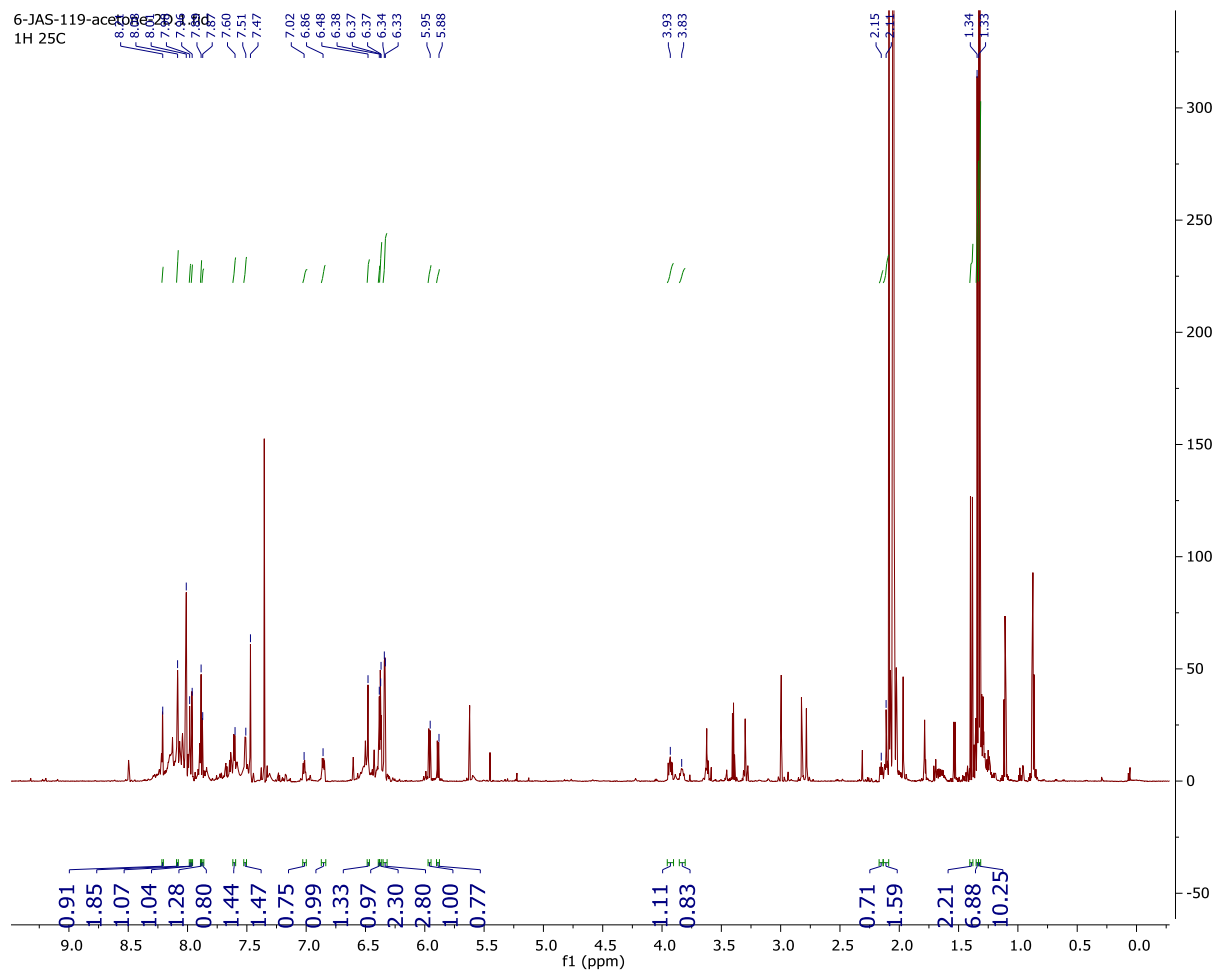
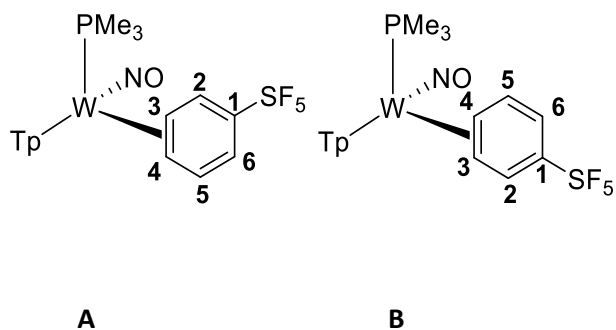
**<sup>1</sup>H NMR Spectrum of 16**



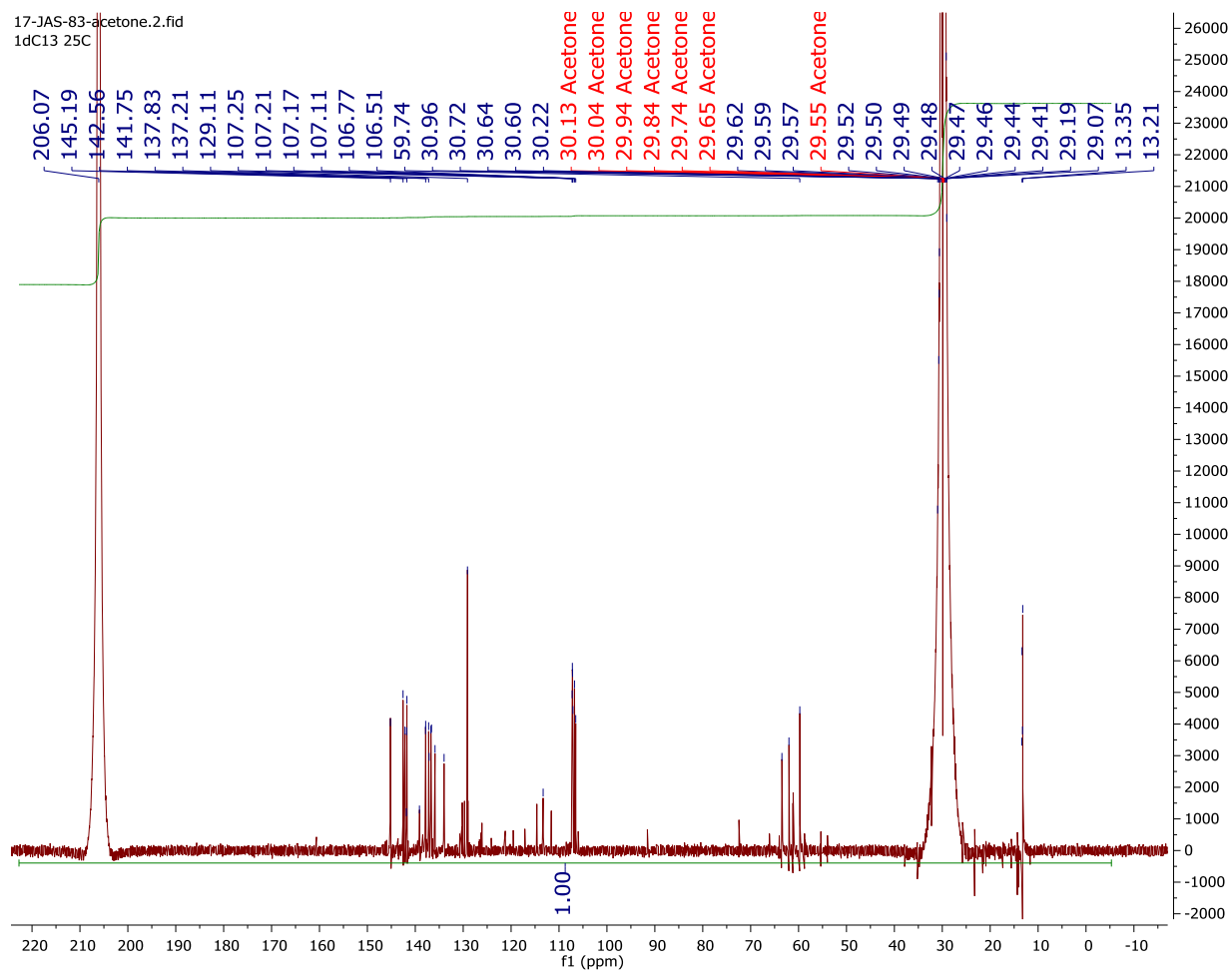
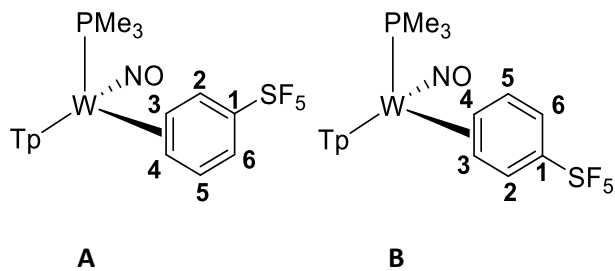
<sup>13</sup>C{<sup>1</sup>H} NMR Spectrum of 16



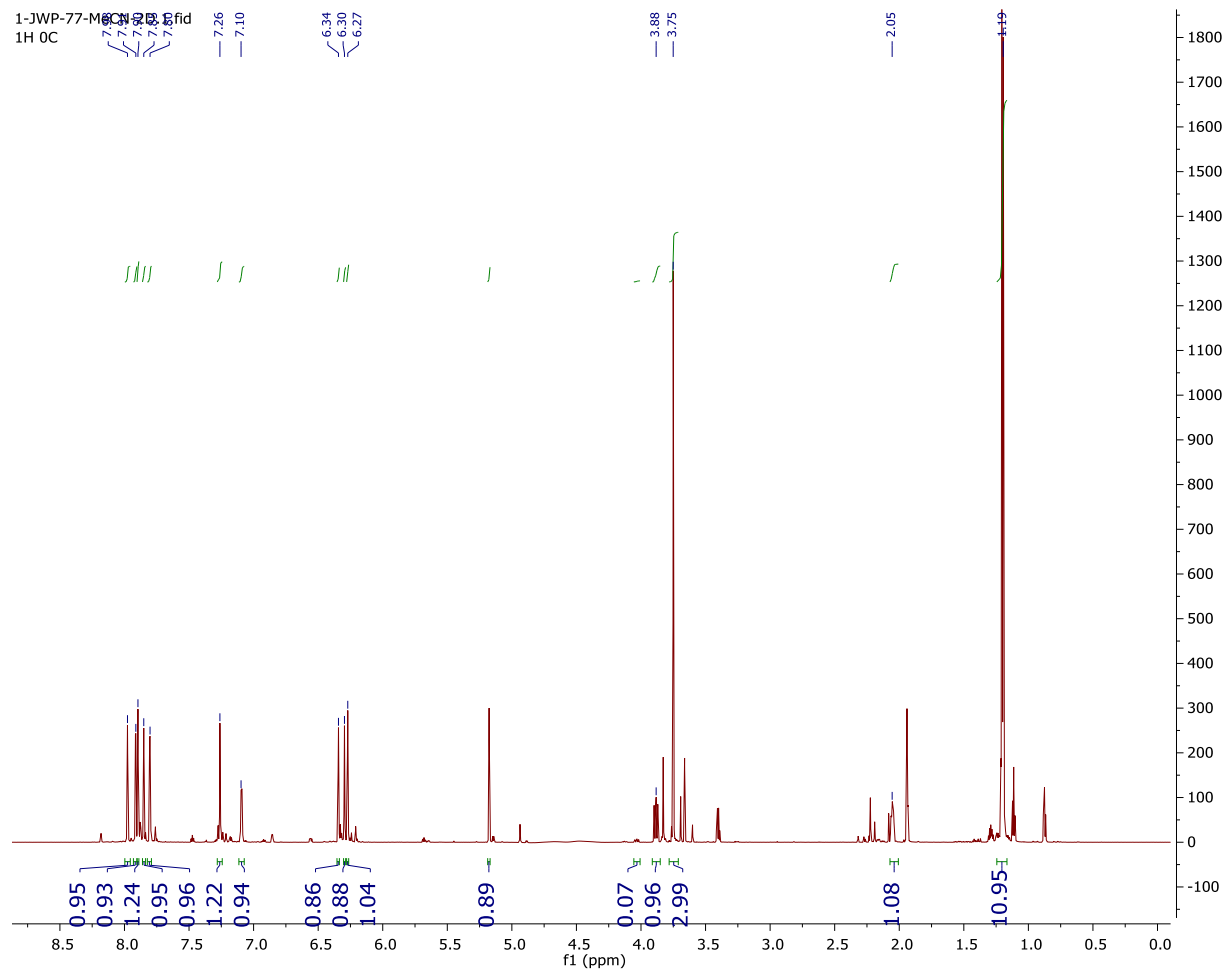
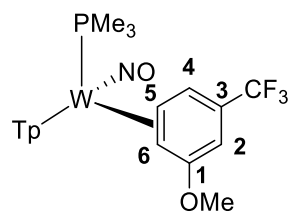
**<sup>1</sup>H NMR Spectrum of 17**



# $^{13}\text{C}\{^1\text{H}\}$ NMR Spectrum of 17

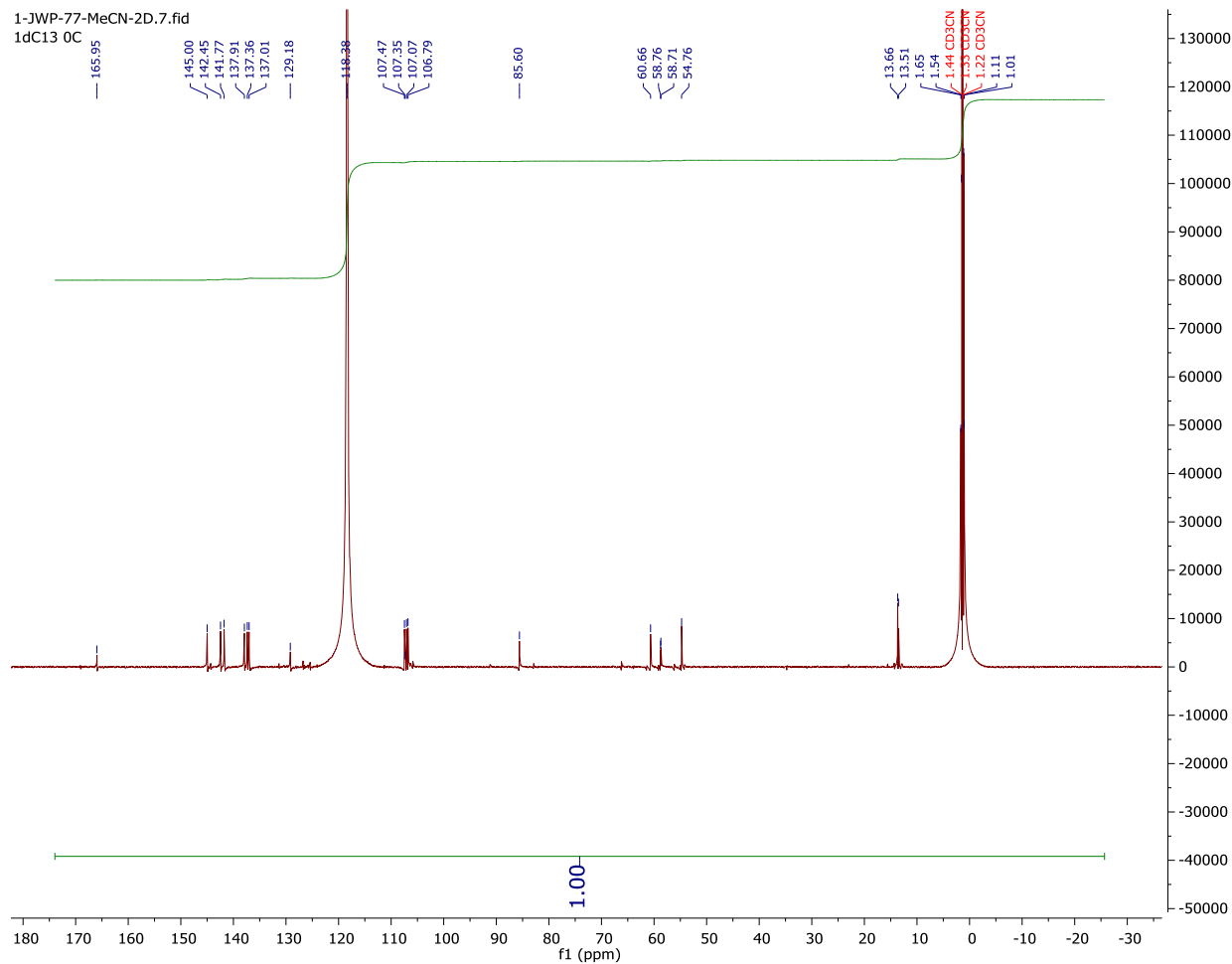
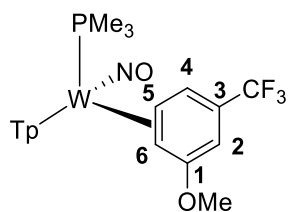


# <sup>1</sup>H NMR Spectrum of 18

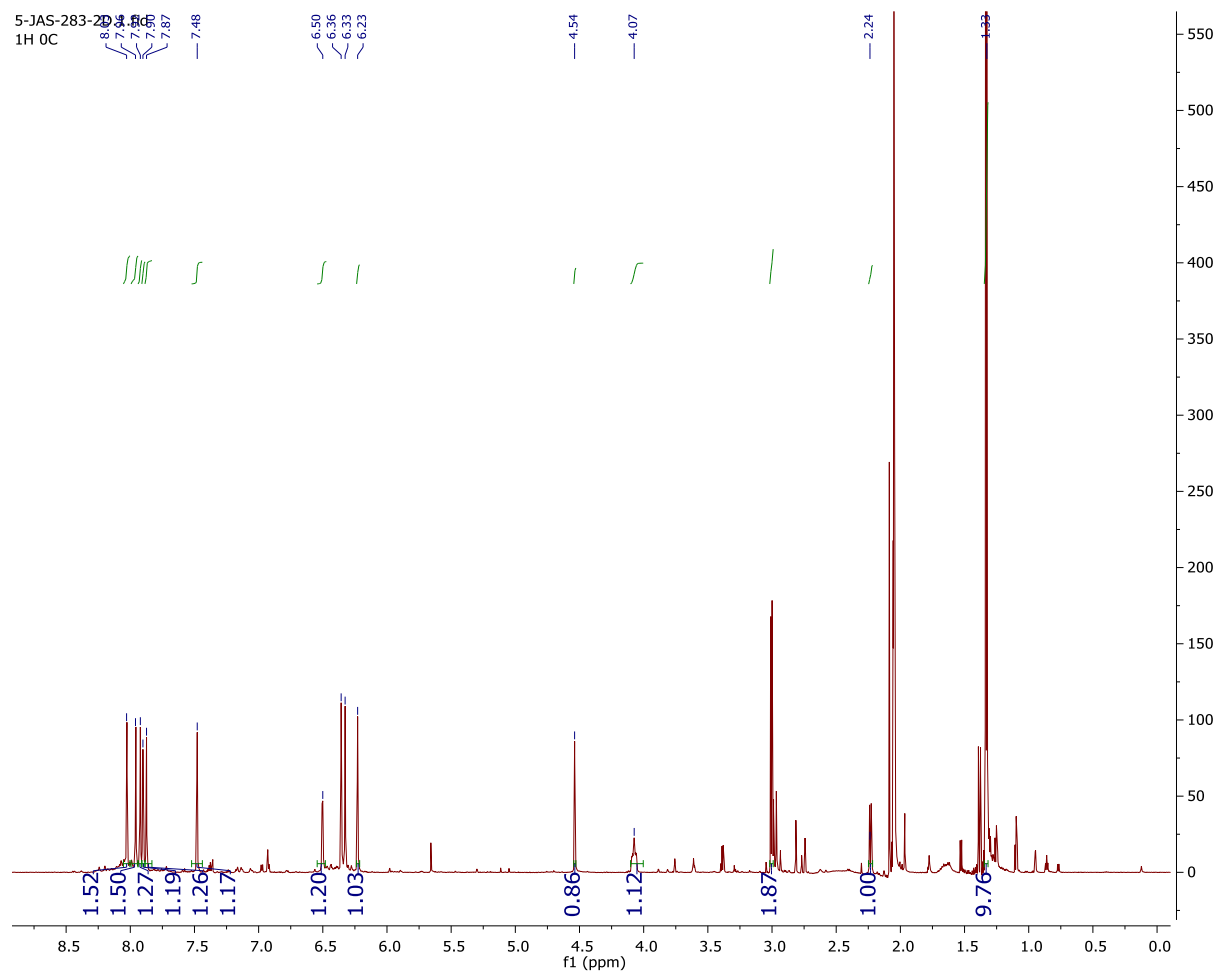
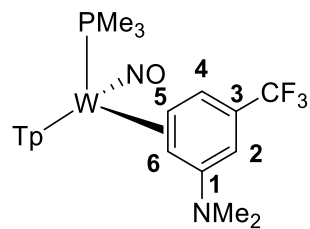




# $^{13}\text{C}\{^1\text{H}\}$ NMR Spectrum of 18

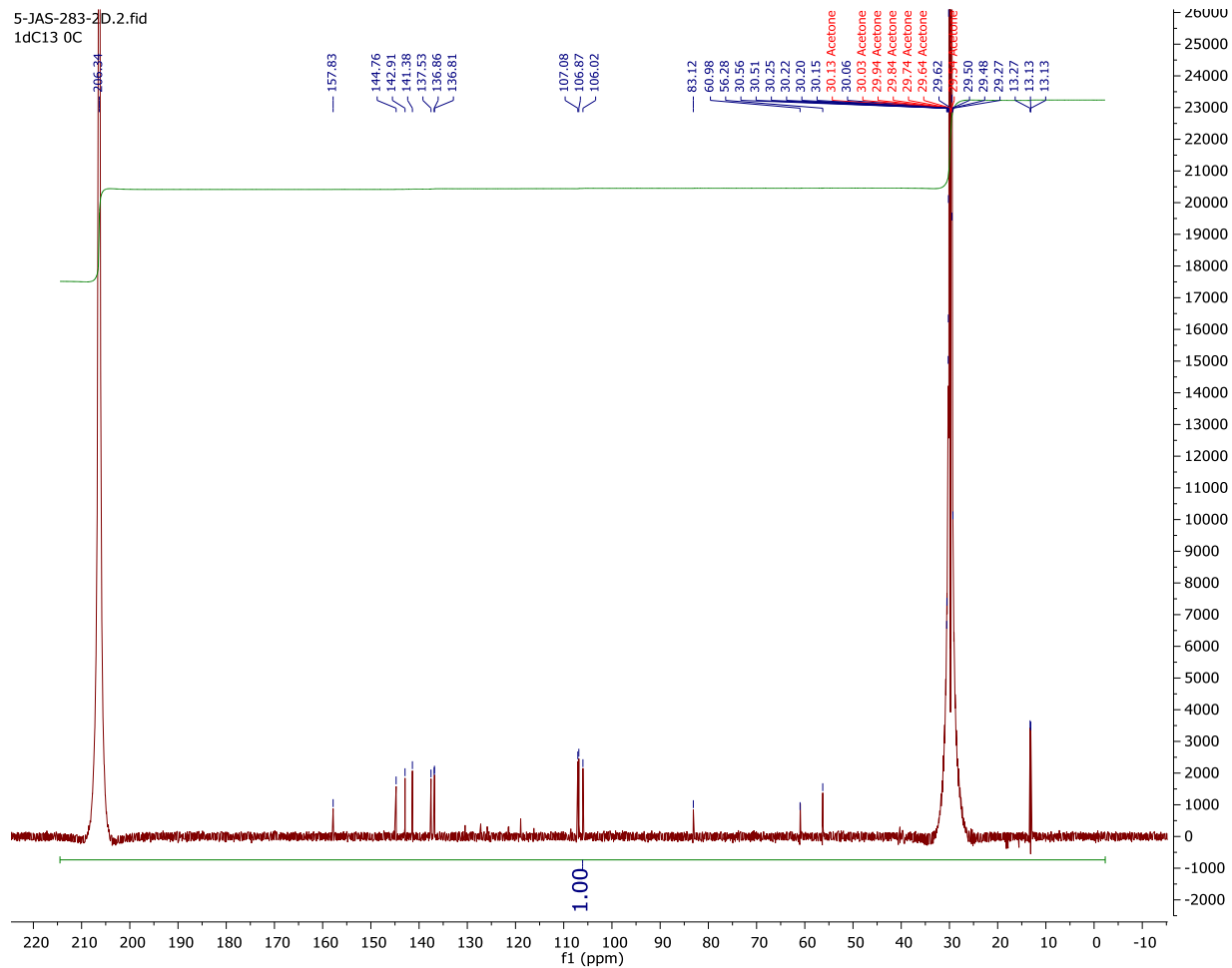
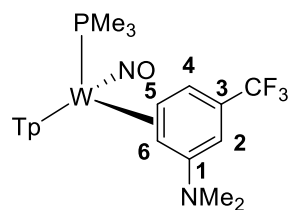


# <sup>1</sup>H NMR Spectrum of 19

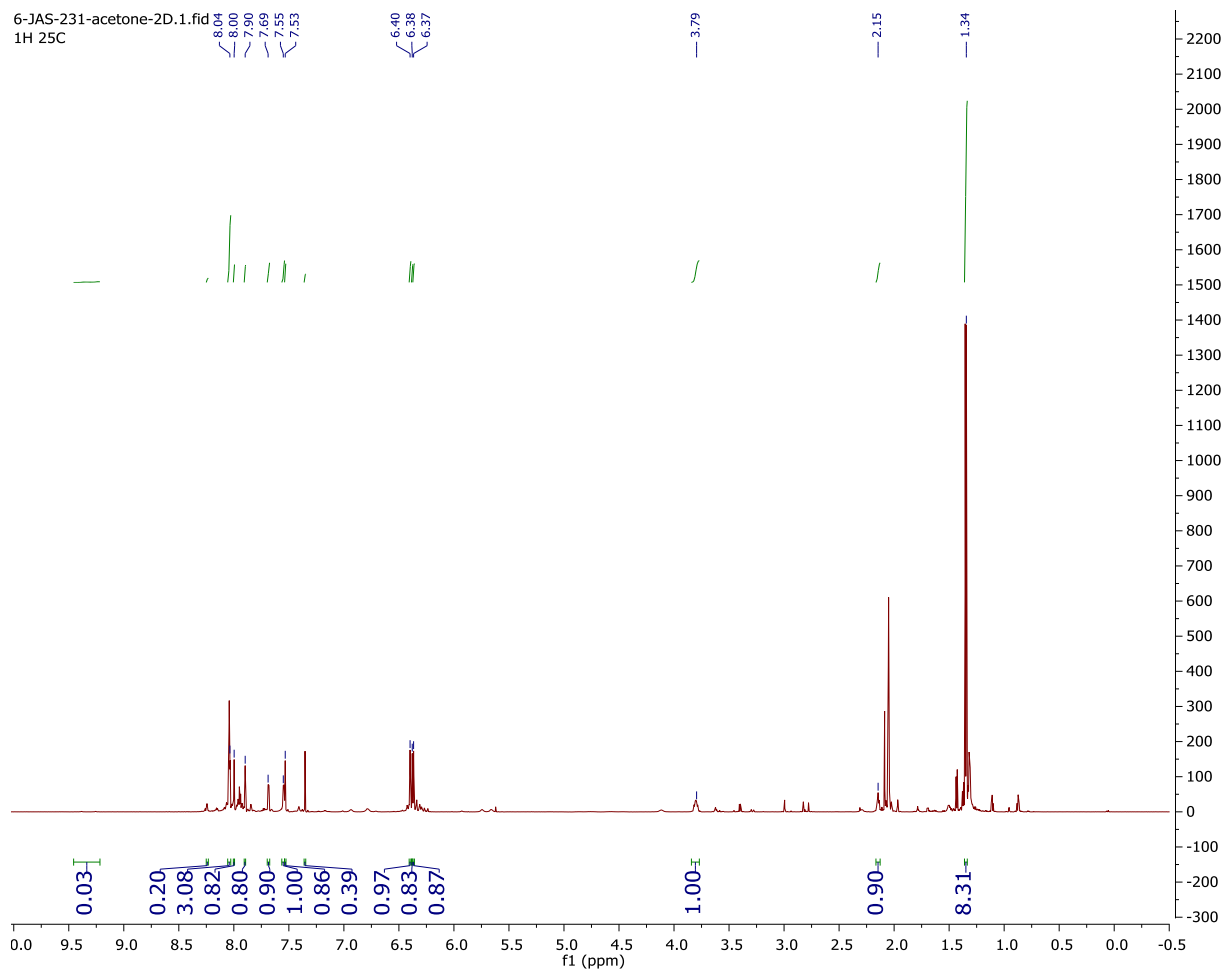
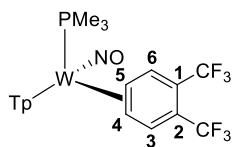


# $^{13}\text{C}\{^1\text{H}\}$ NMR Spectrum of 19

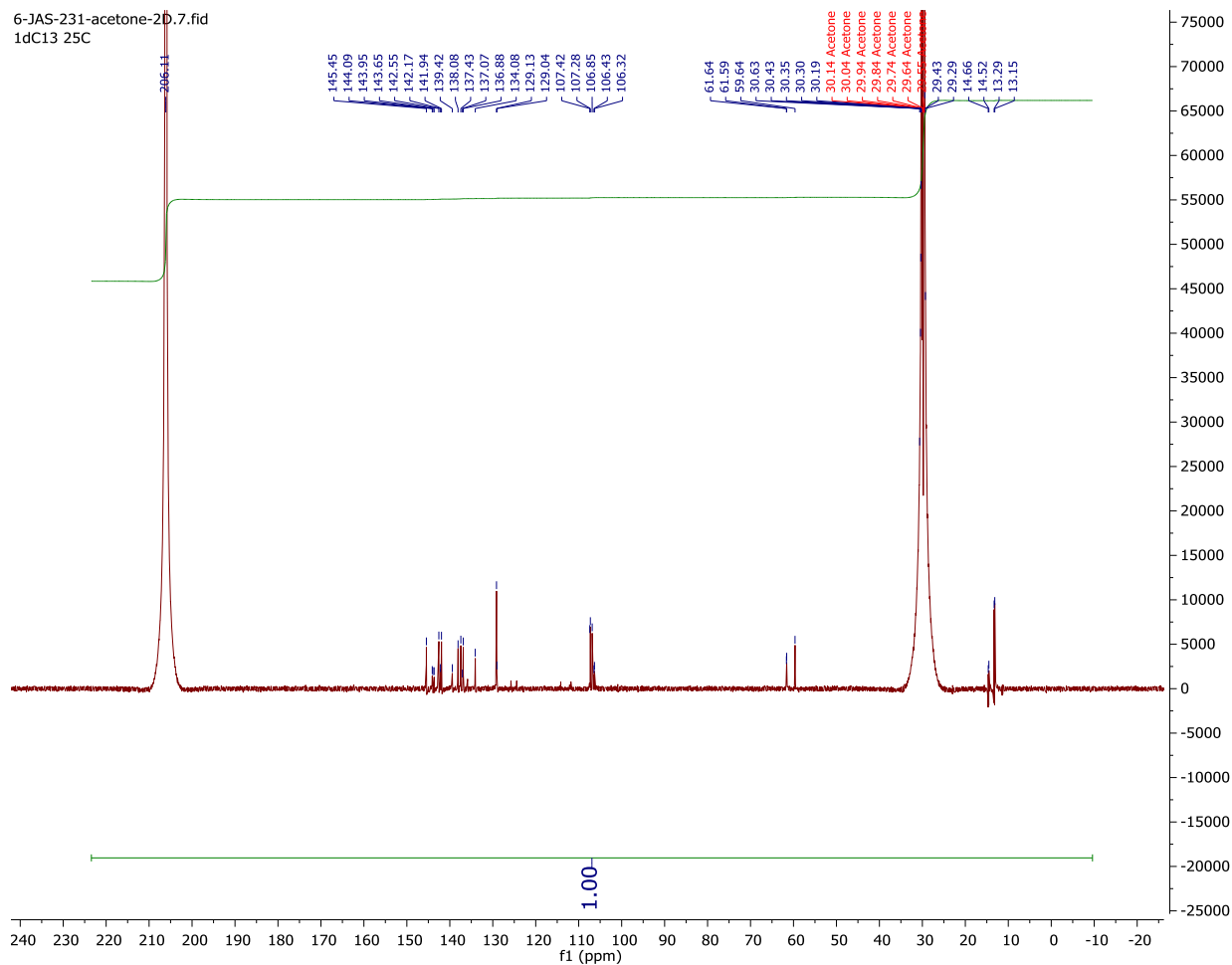
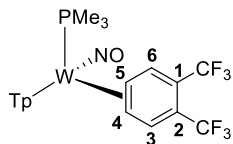
\



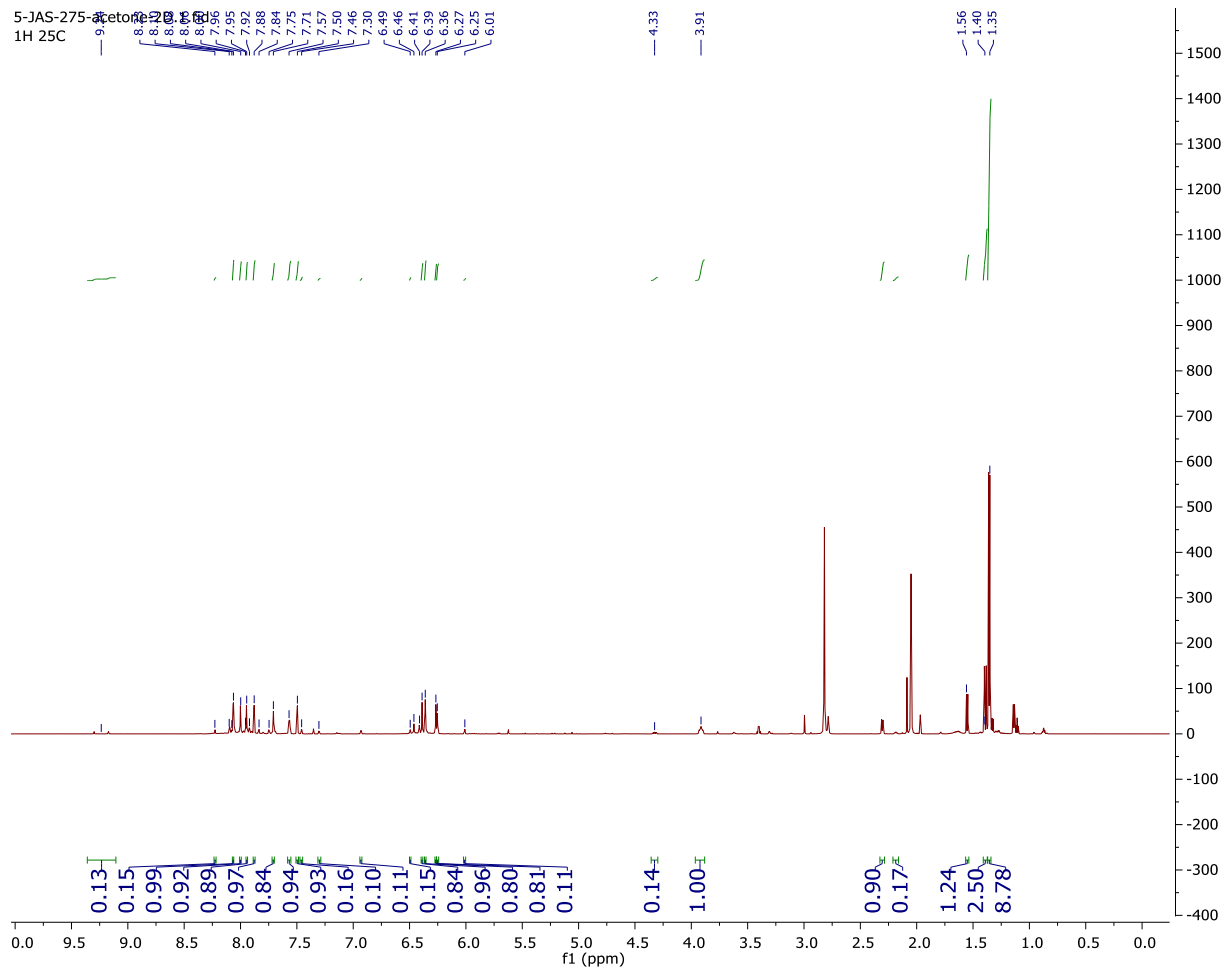
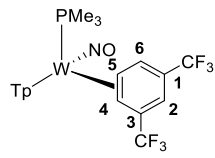
# <sup>1</sup>H NMR Spectrum of 20



# $^{13}\text{C}\{^1\text{H}\}$ NMR Spectrum of 20

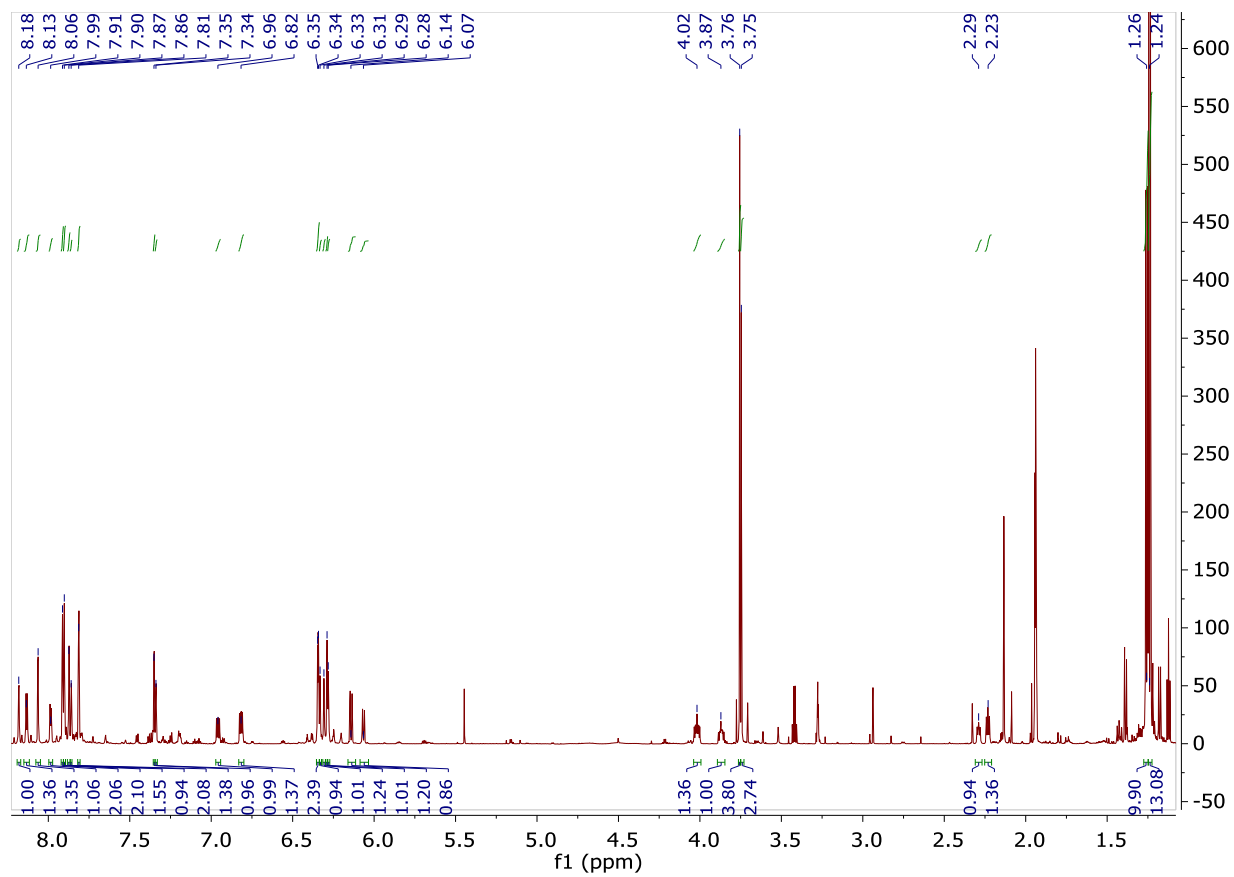
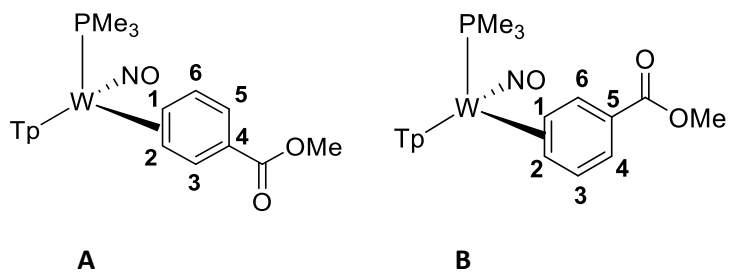


# <sup>1</sup>H NMR Spectrum of 21



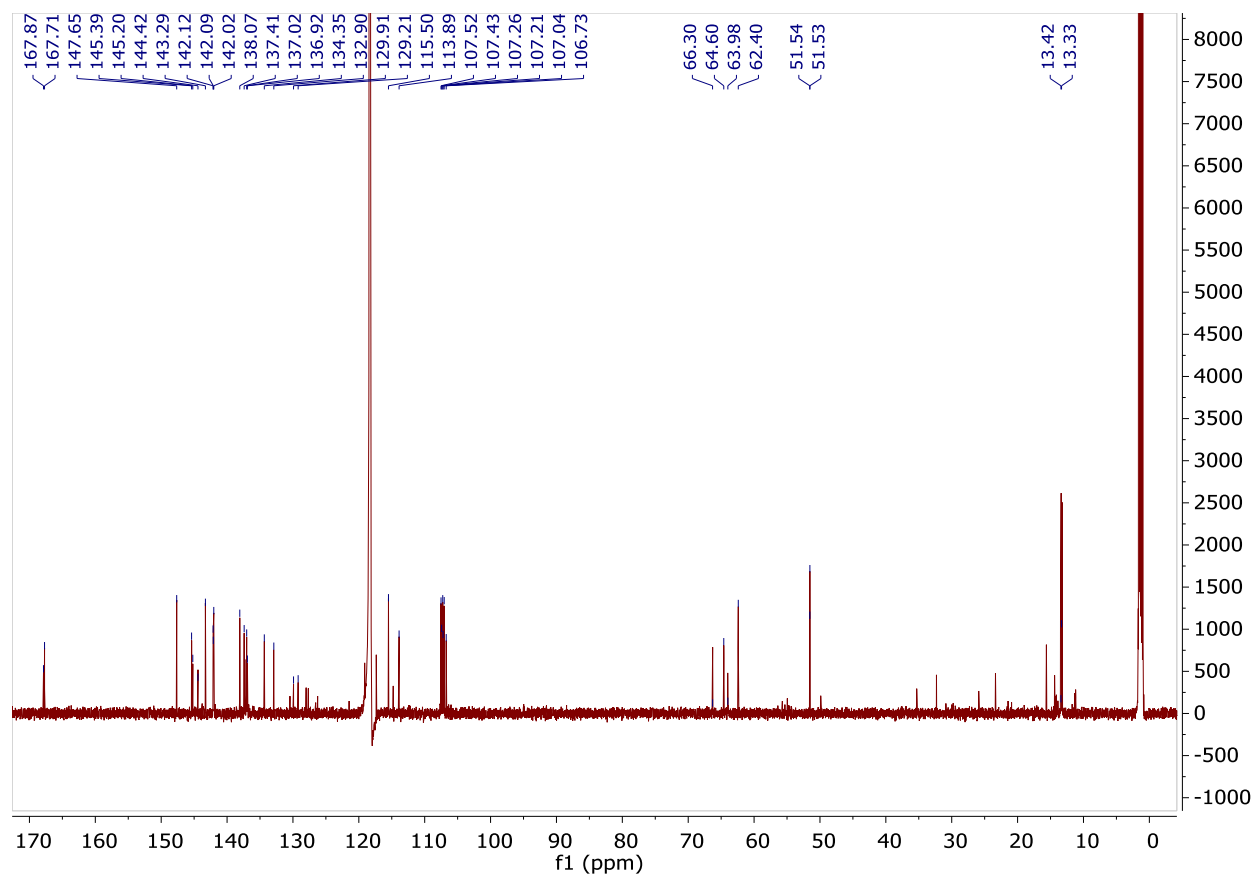
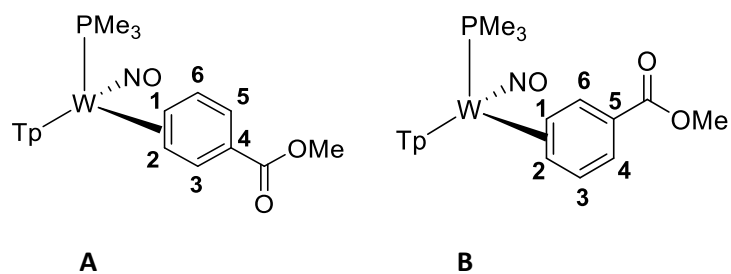


# <sup>1</sup>H NMR Spectrum of 22

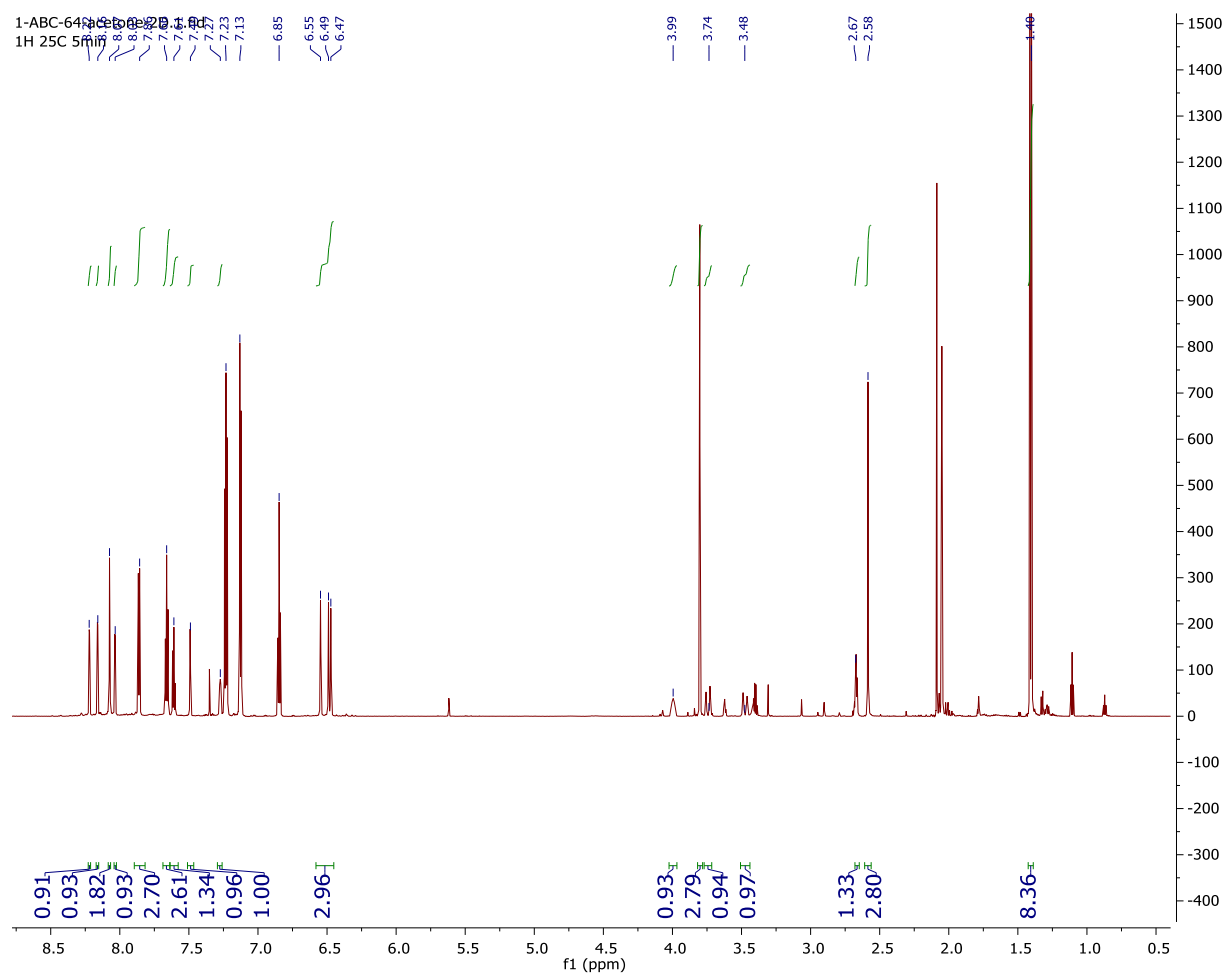
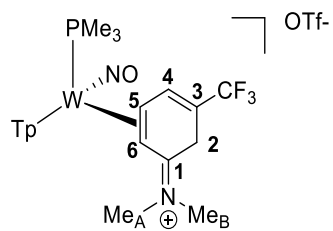




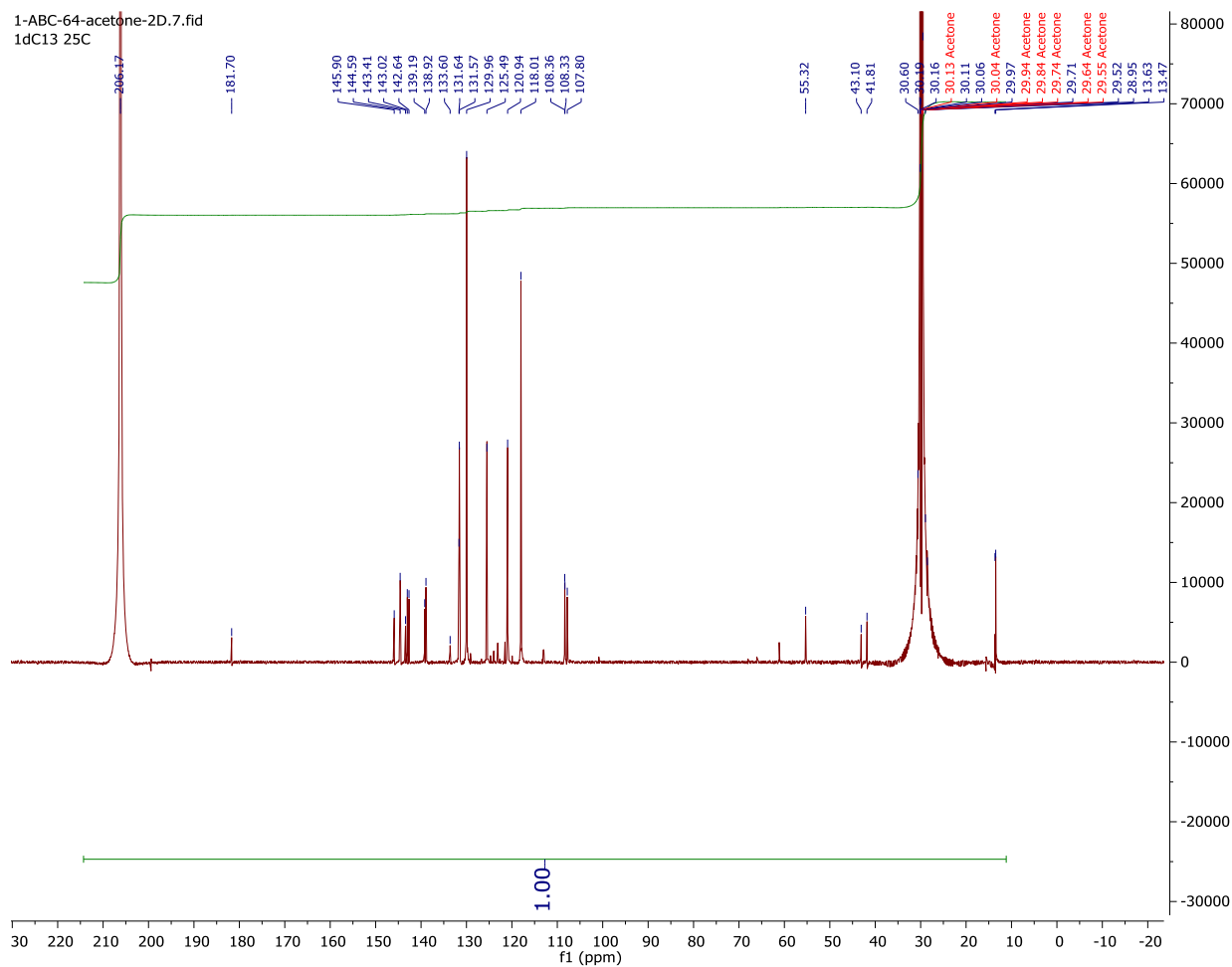
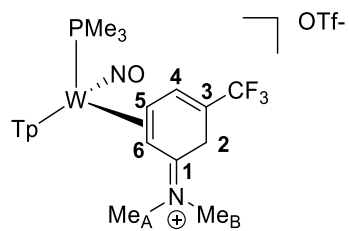
$^{13}\text{C}\{^1\text{H}\}$  NMR Spectrum of 22



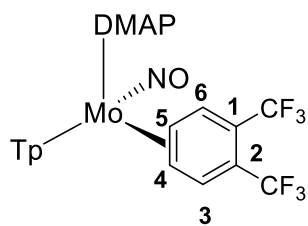
# <sup>1</sup>H NMR Spectrum of 23



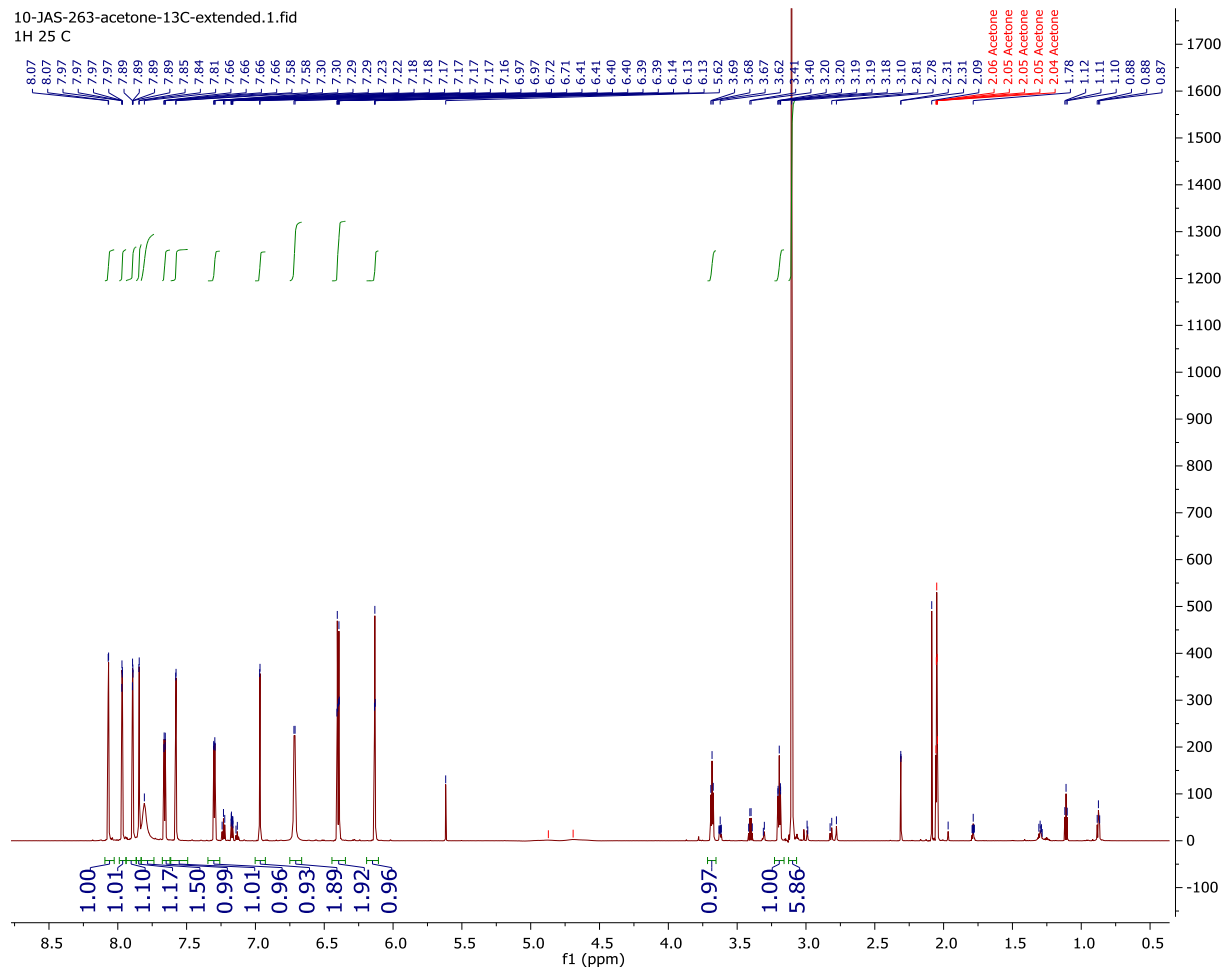
# <sup>13</sup>C{<sup>1</sup>H} NMR Spectrum of 23



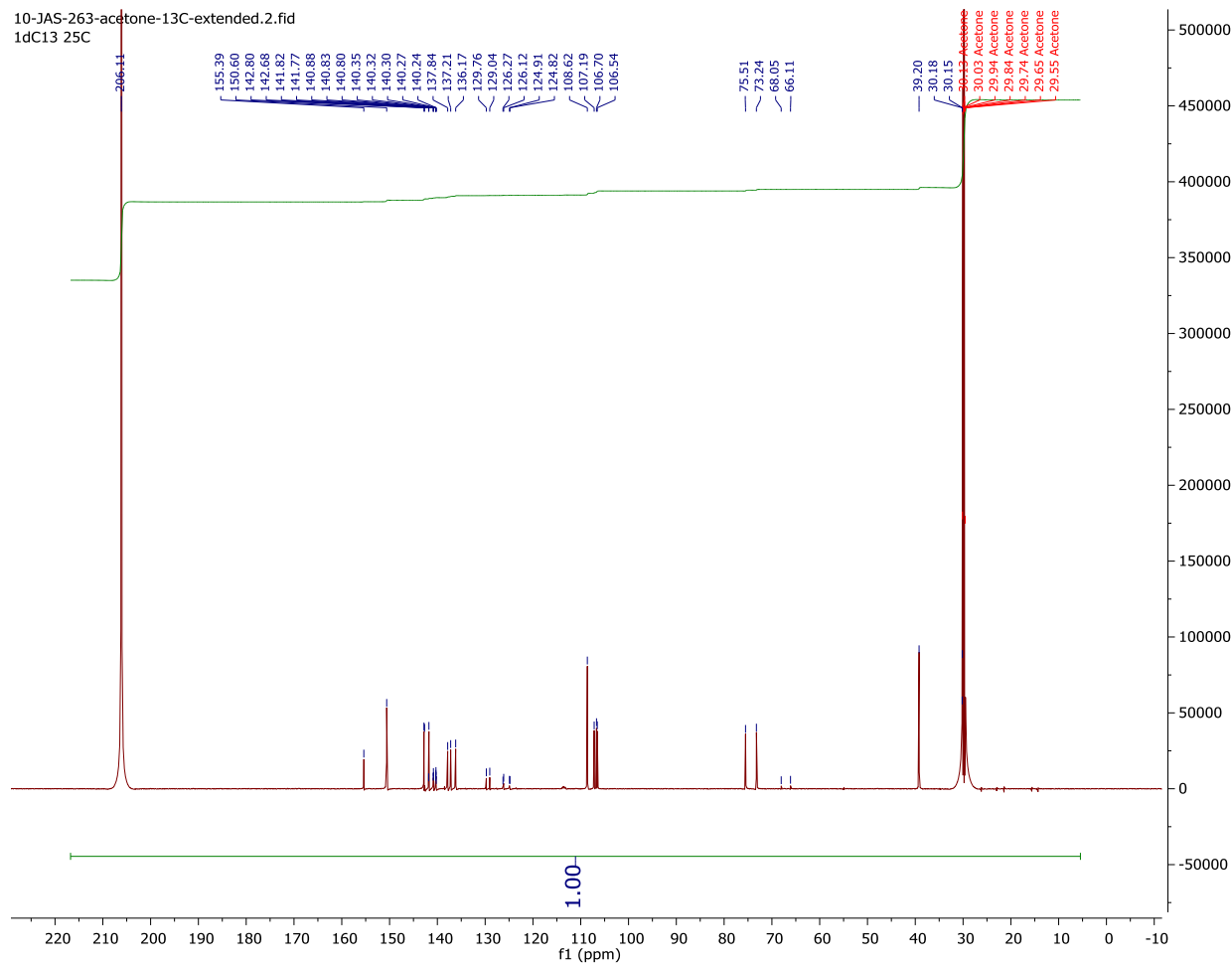
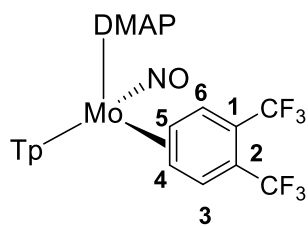
# <sup>1</sup>H NMR Spectrum of 24



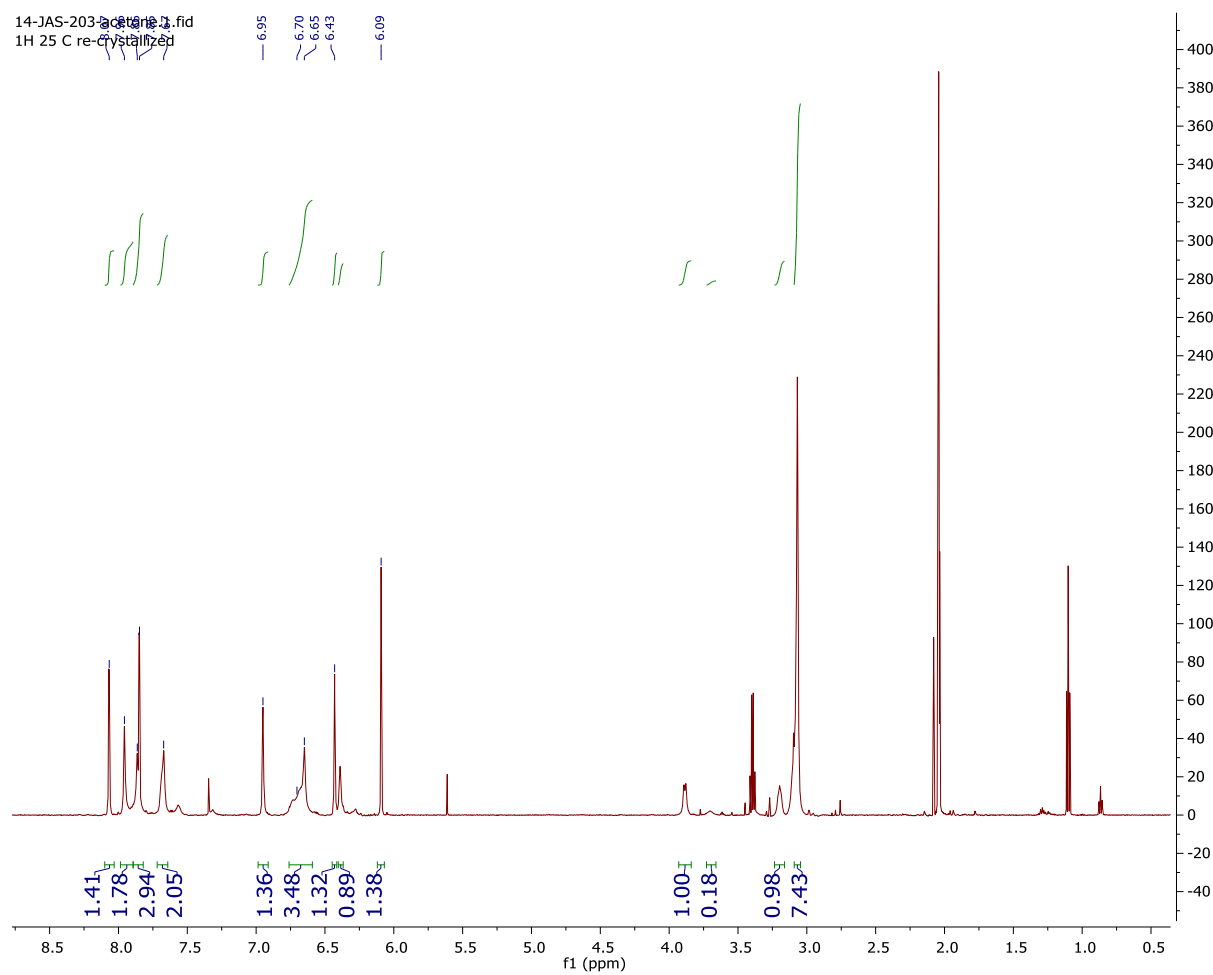
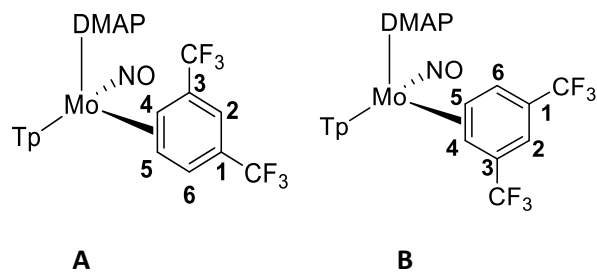
10-JAS-263-acetone-13C-extended.1.fid  
1H 25 C



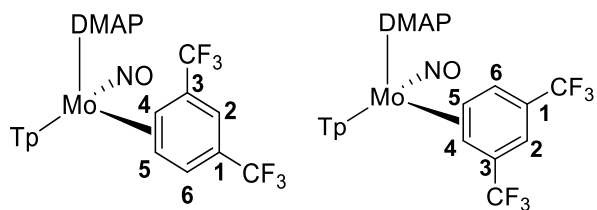
# <sup>13</sup>C{<sup>1</sup>H} NMR Spectrum of 24



# <sup>1</sup>H NMR Spectrum of 25

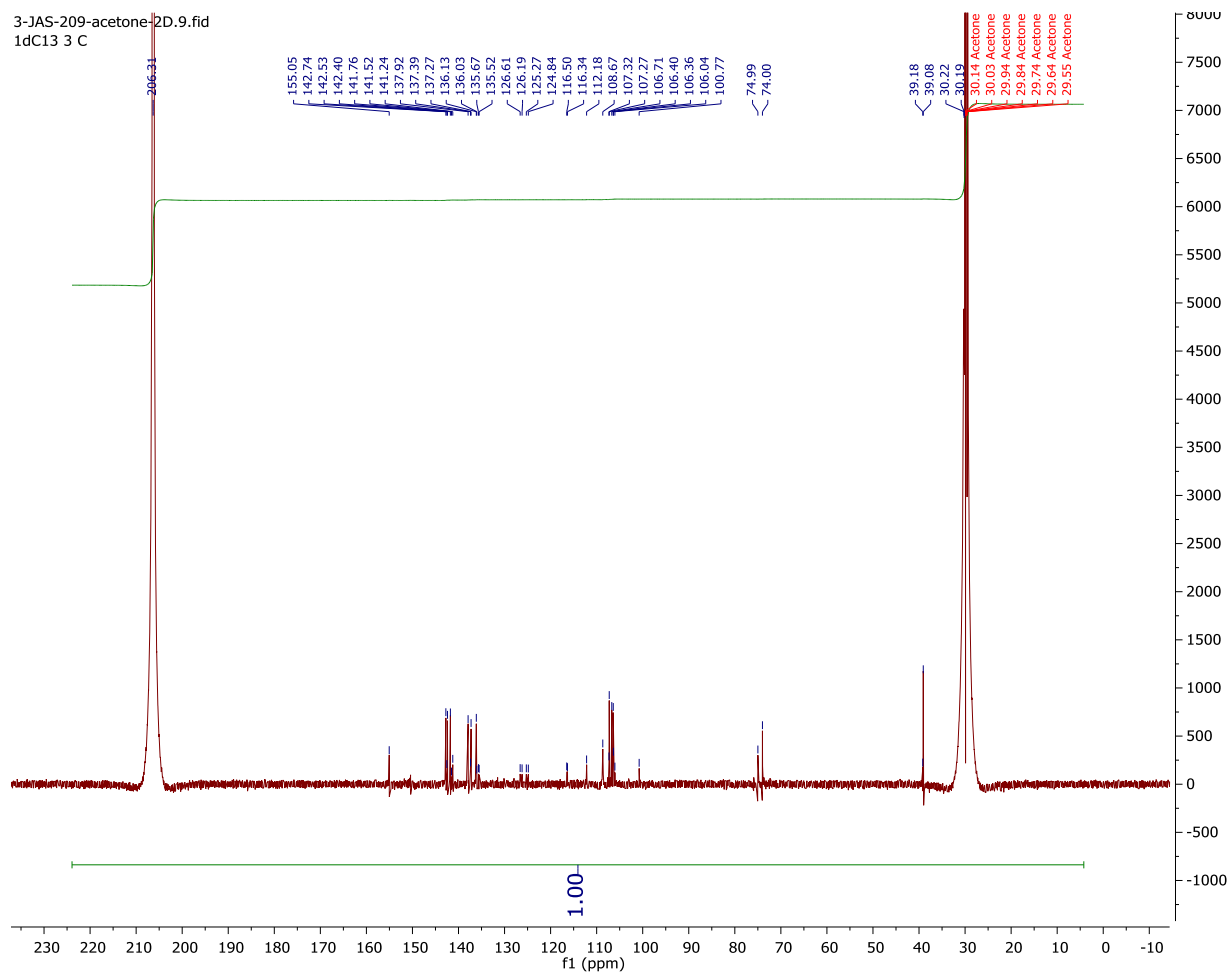


<sup>13</sup>C{<sup>1</sup>H} NMR Spectrum of 25



A

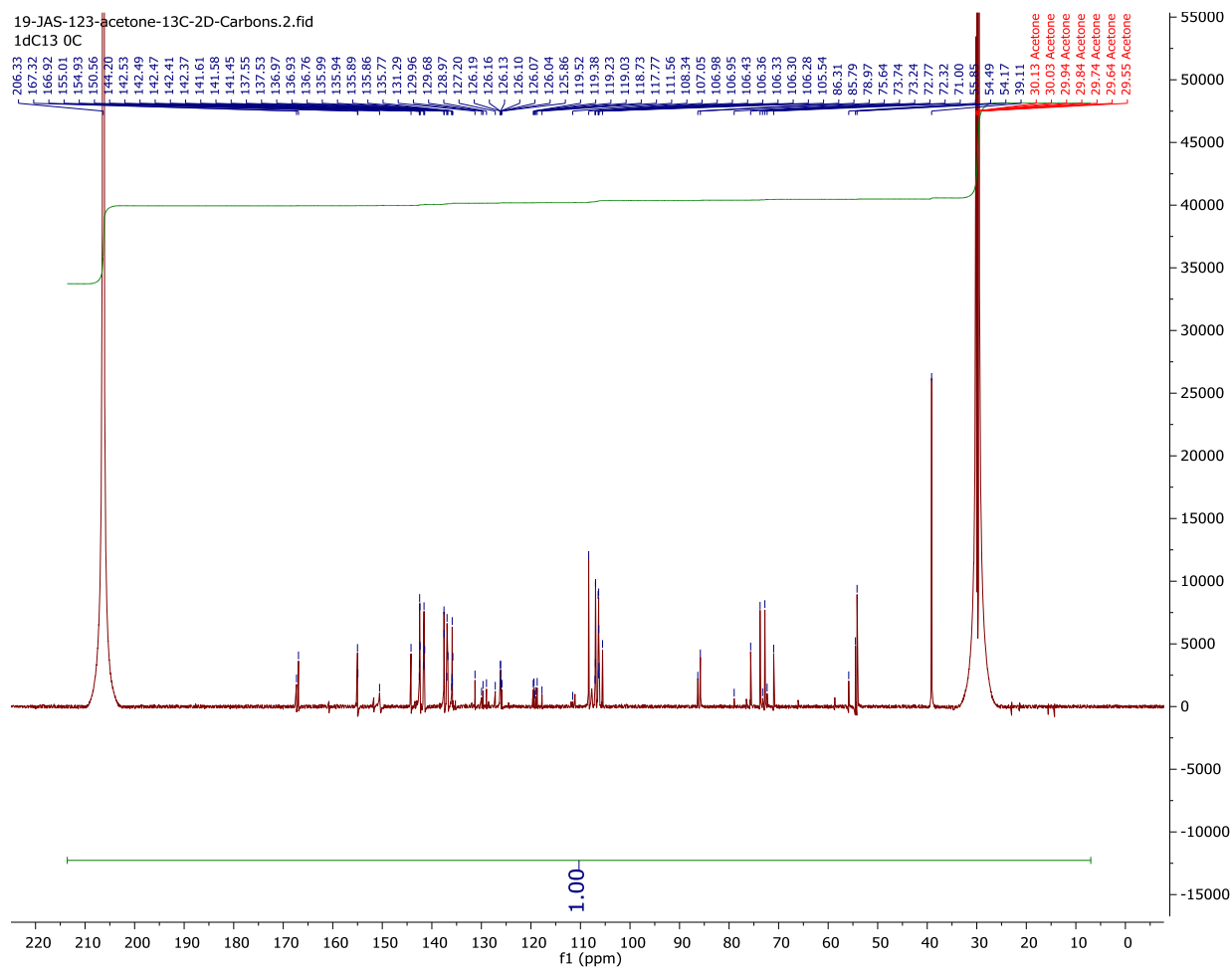
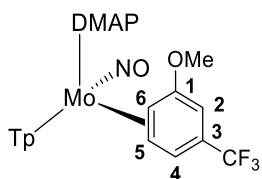
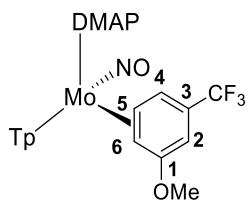
B



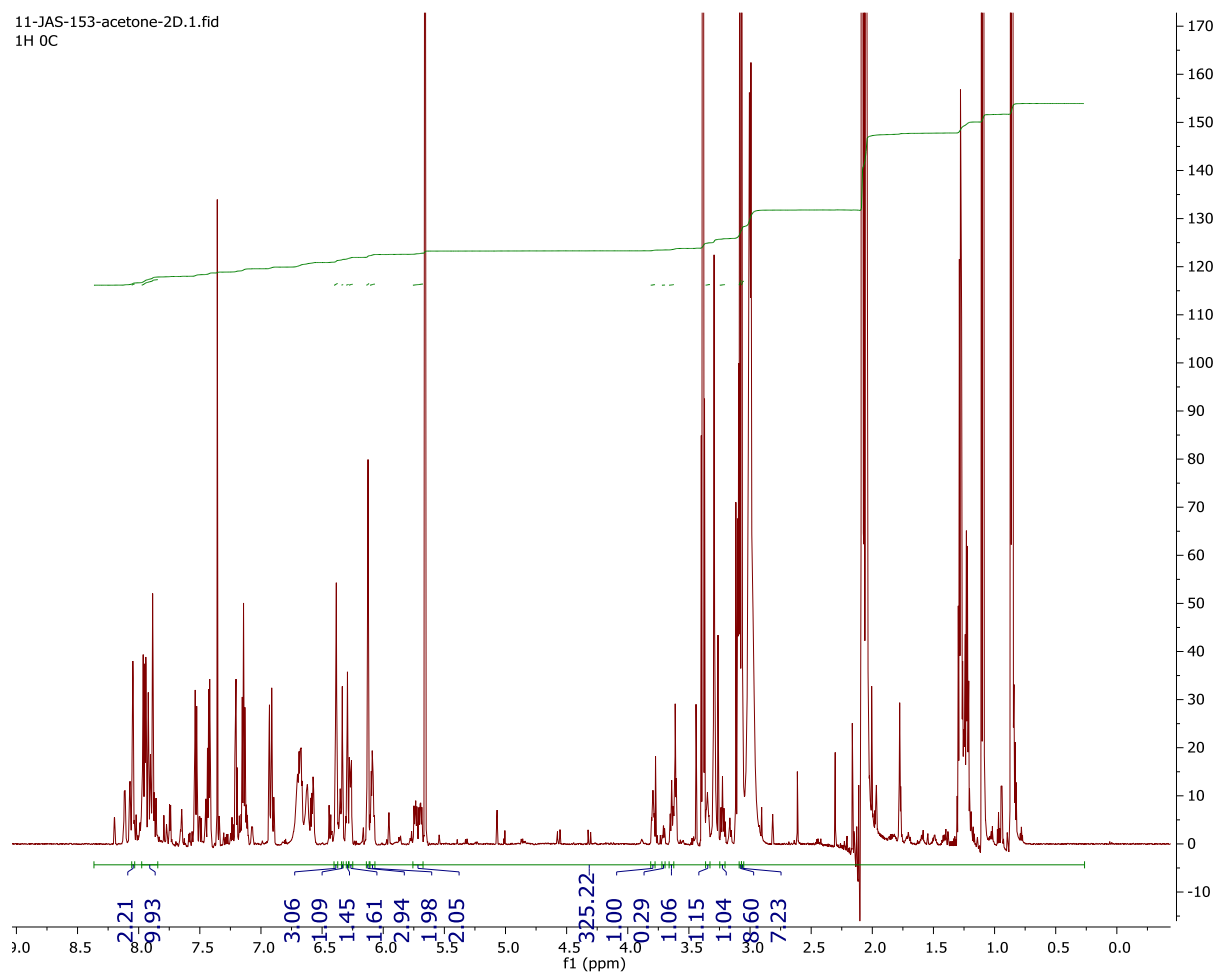
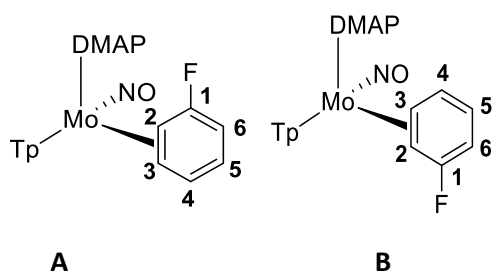




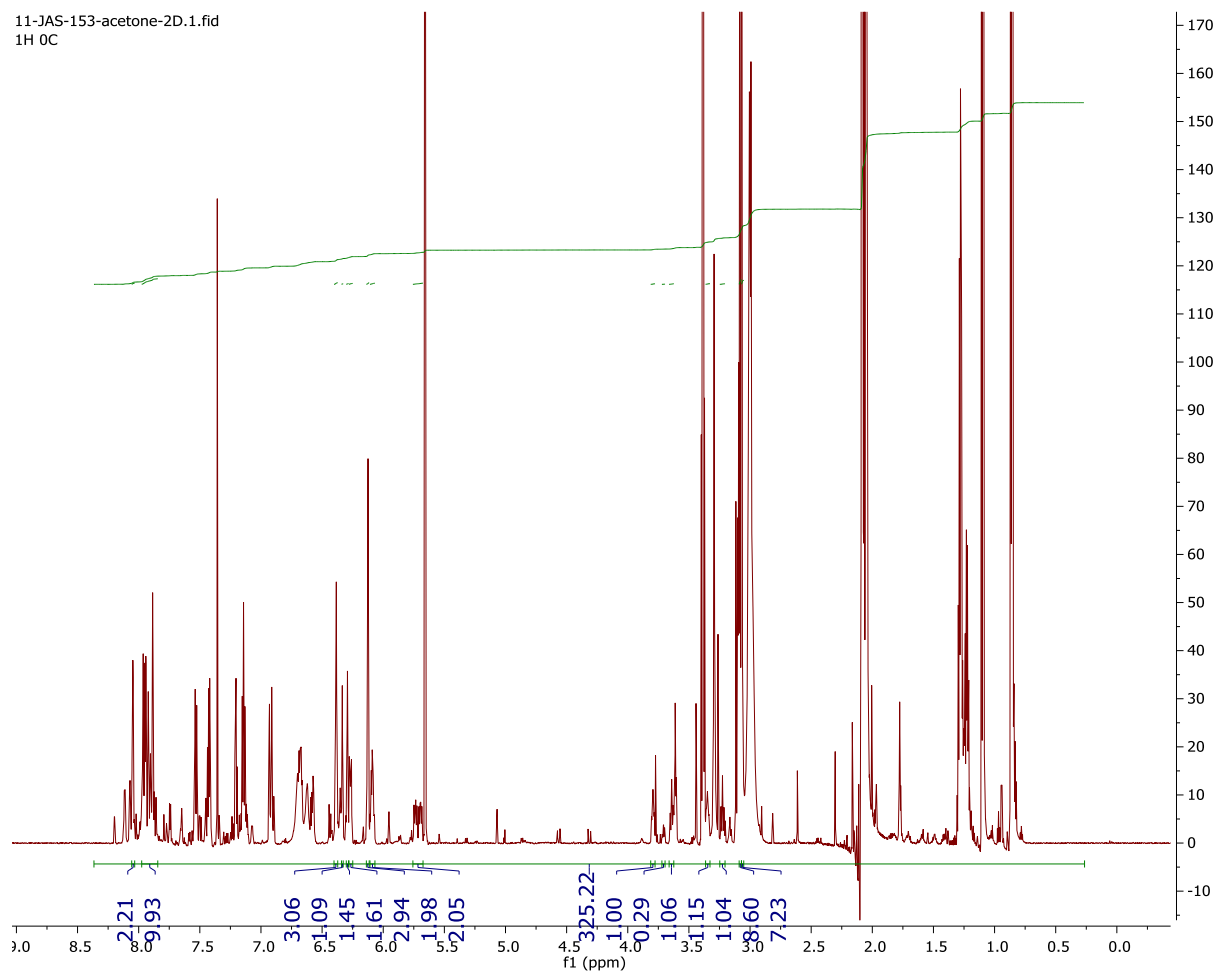
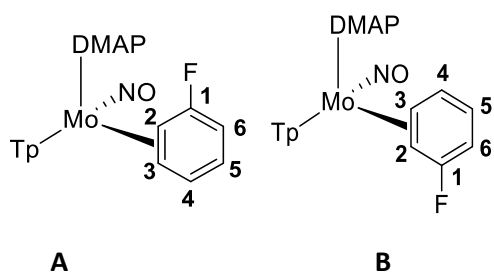
<sup>13</sup>C{<sup>1</sup>H} NMR Spectrum of 27



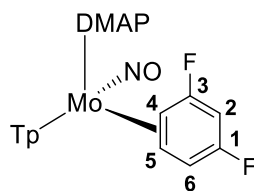
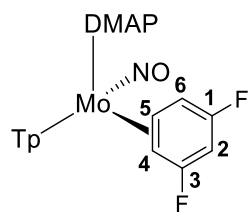
# <sup>1</sup>H NMR Spectrum of 27



# $^{13}\text{C}\{^1\text{H}\}$ NMR Spectrum of 27

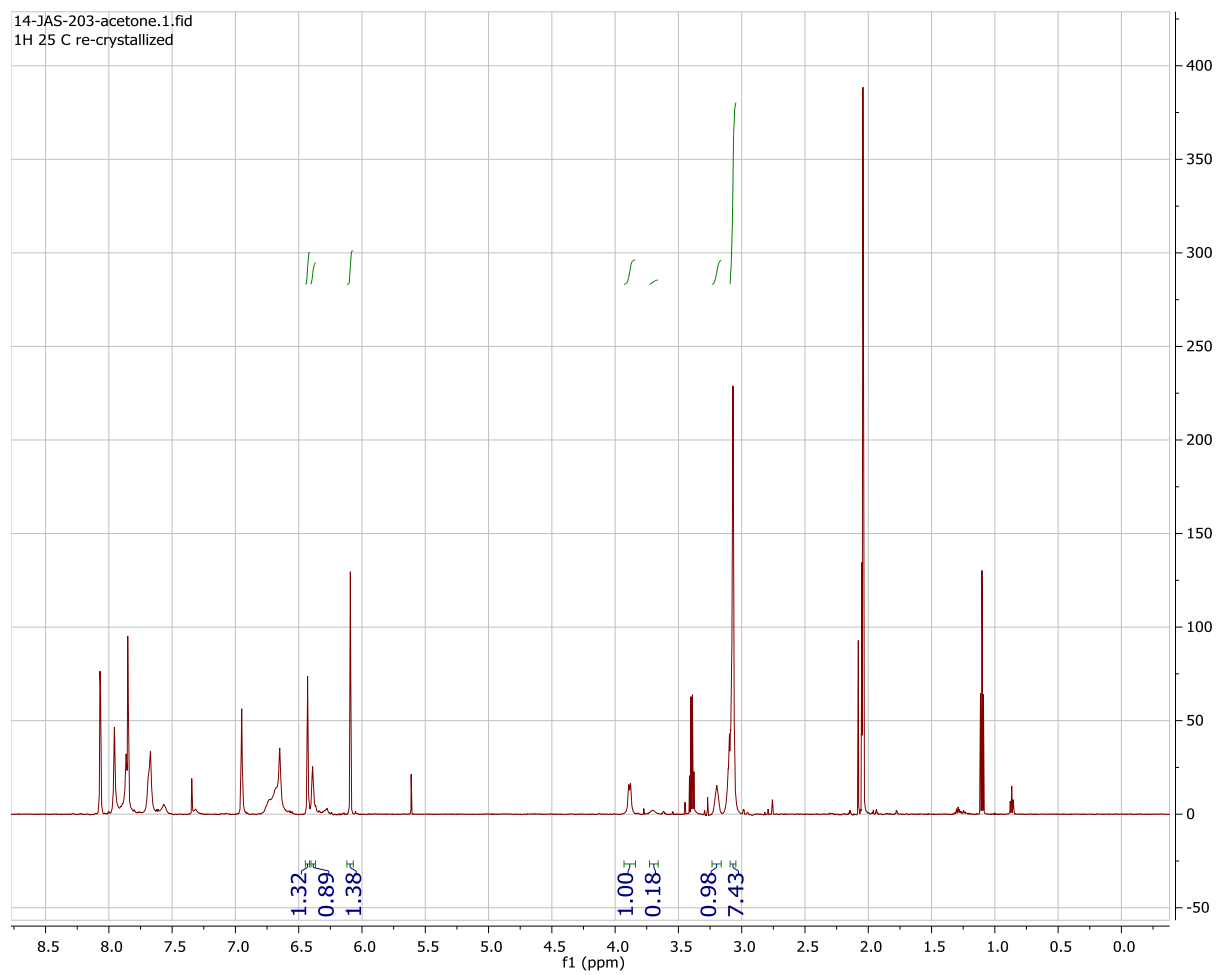


# <sup>1</sup>H NMR Spectrum of 28

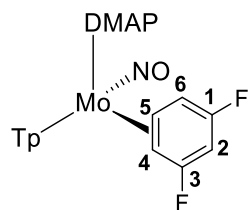


A

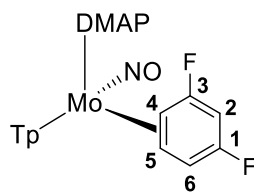
B



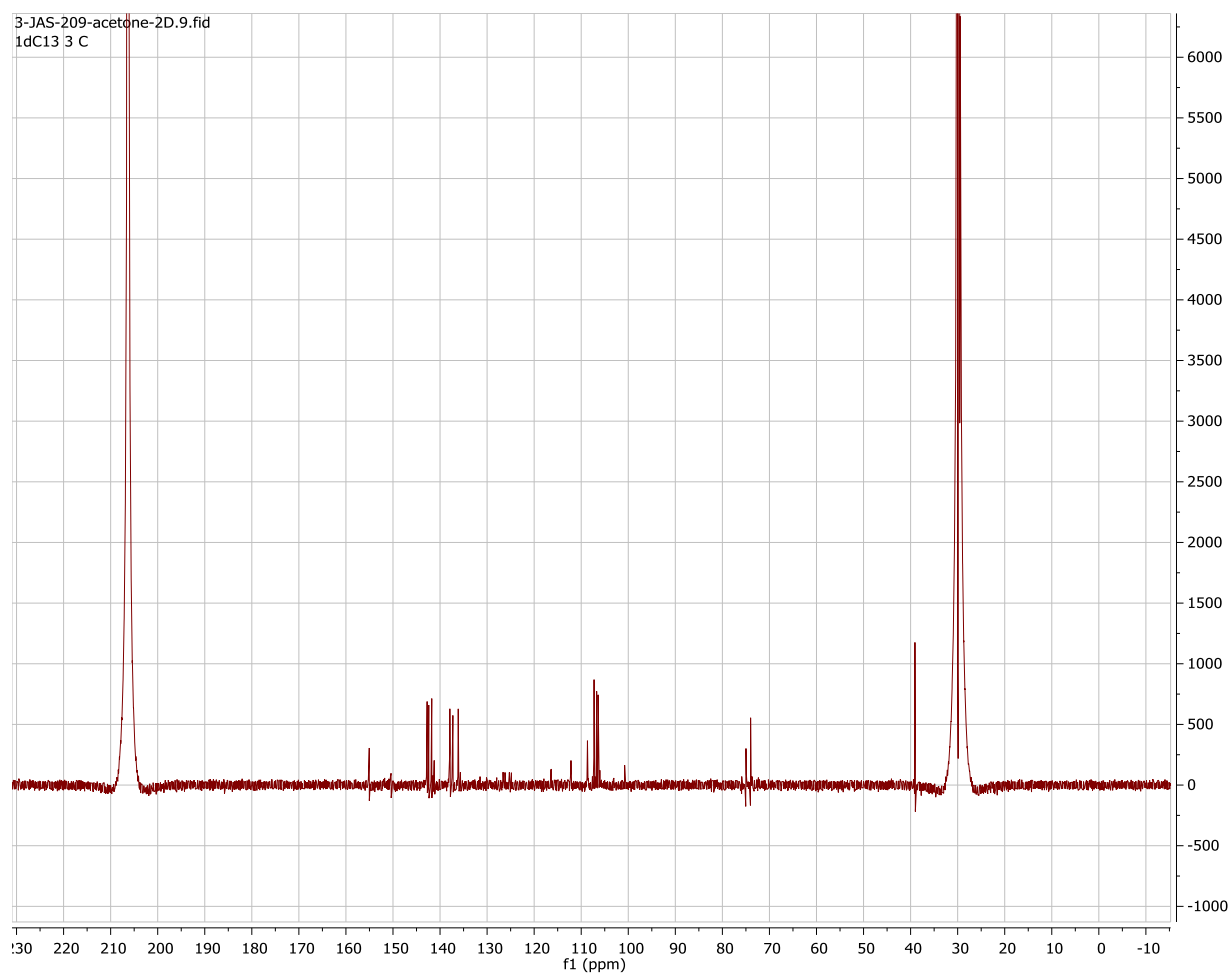
# $^{13}\text{C}\{^1\text{H}\}$ NMR Spectrum of 28



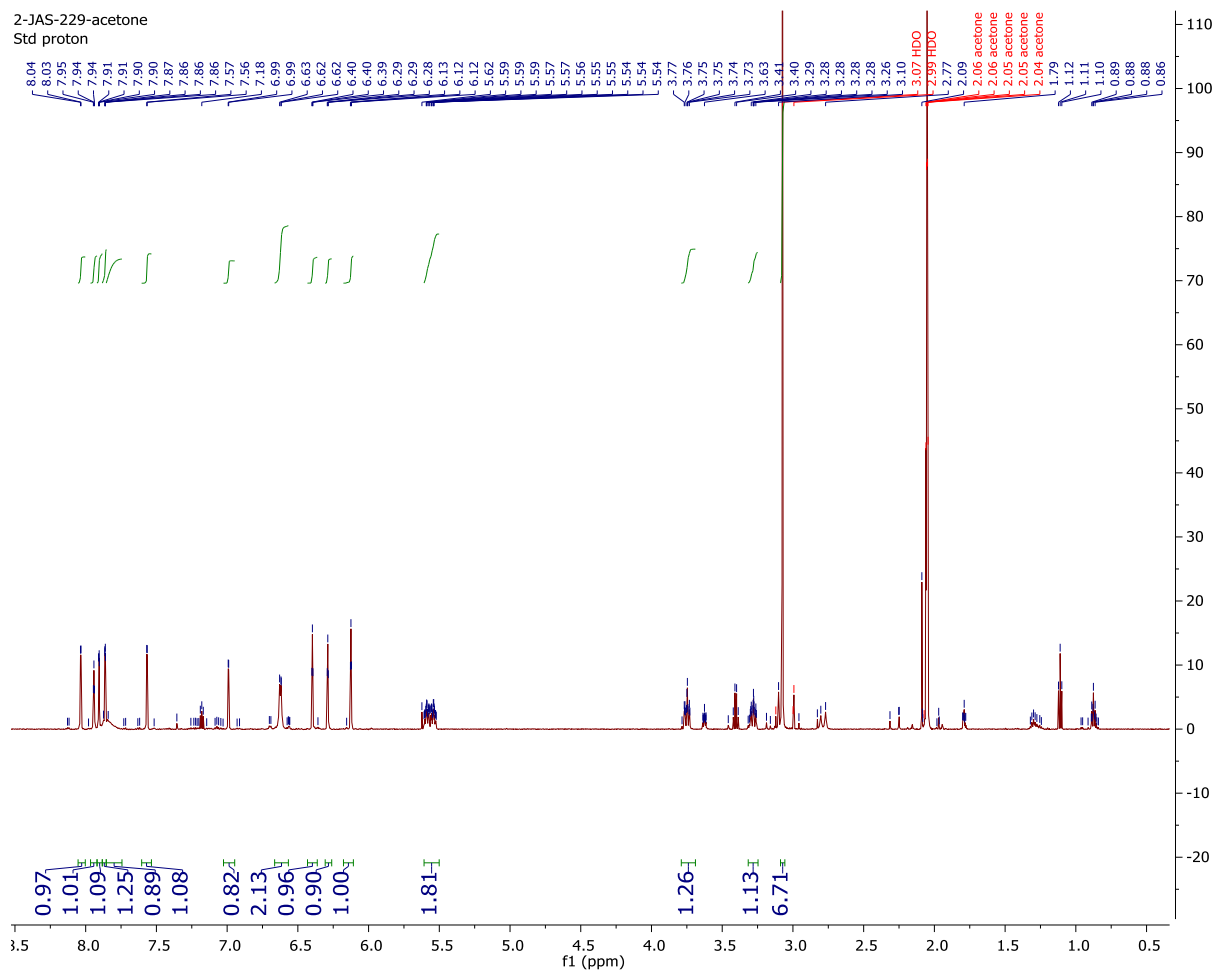
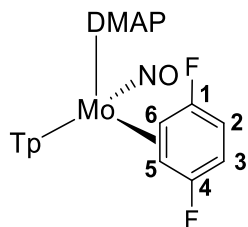
A



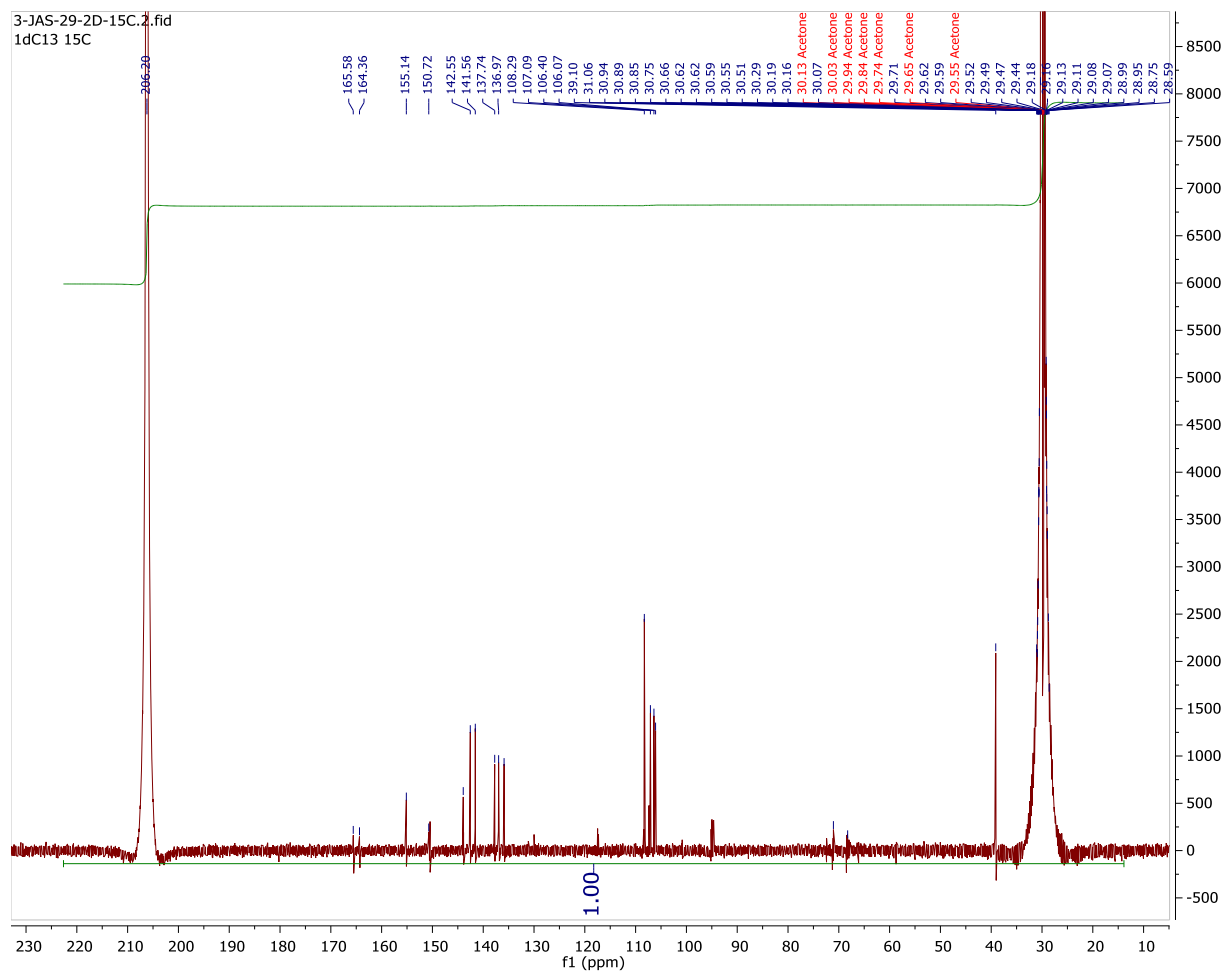
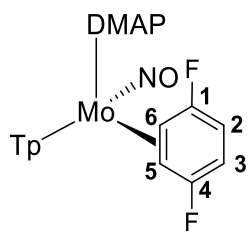
B



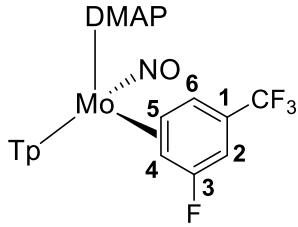
# <sup>1</sup>H NMR Spectrum of 29



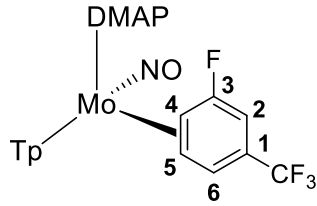
# <sup>13</sup>C{<sup>1</sup>H} NMR Spectrum of 29



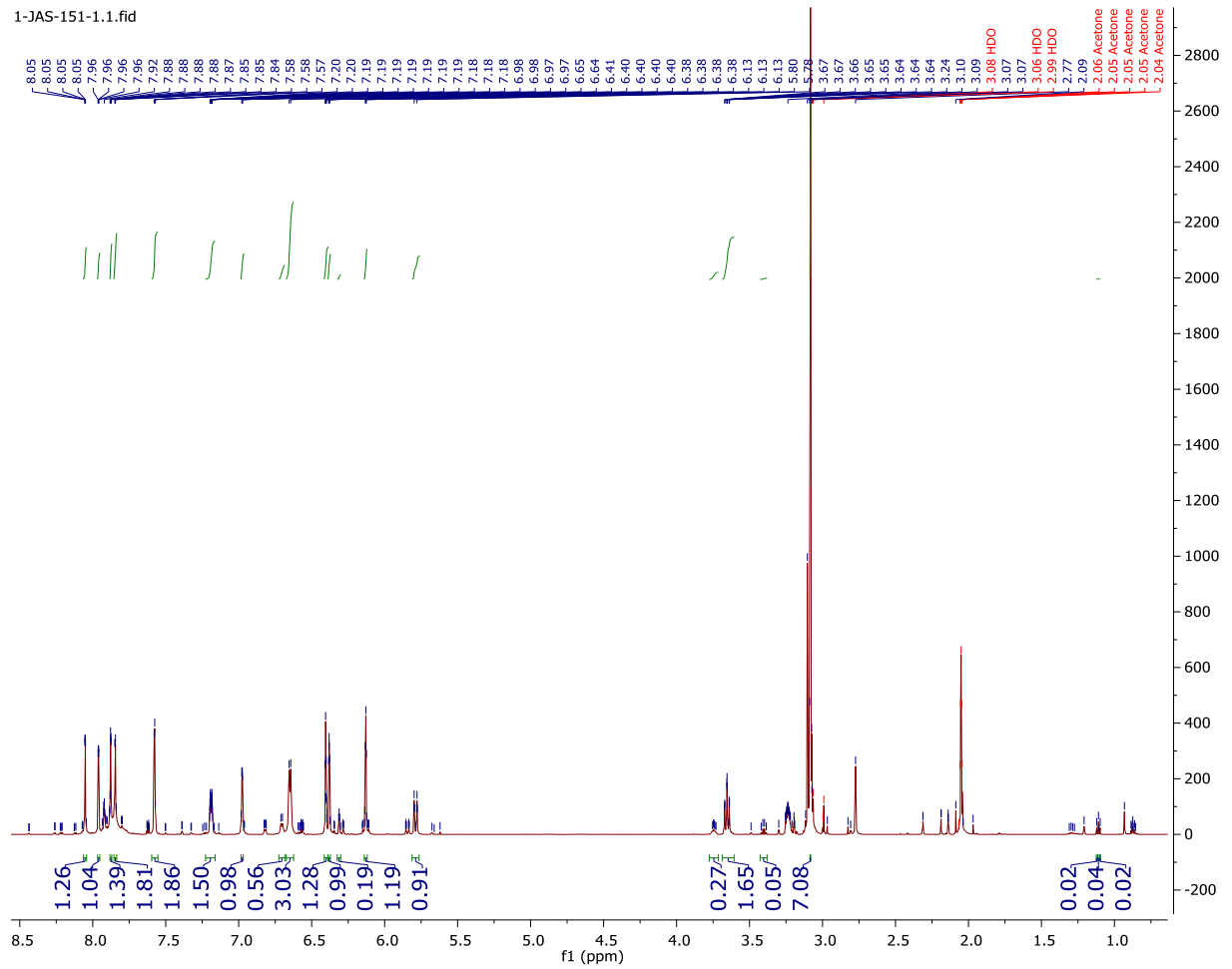
# <sup>1</sup>H NMR Spectrum of 30



30A

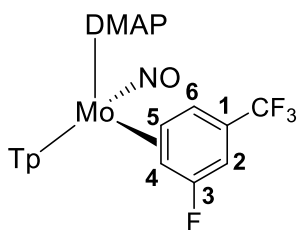


30B

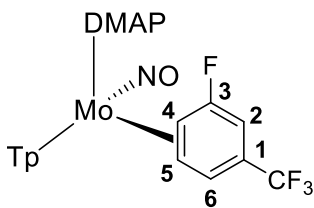




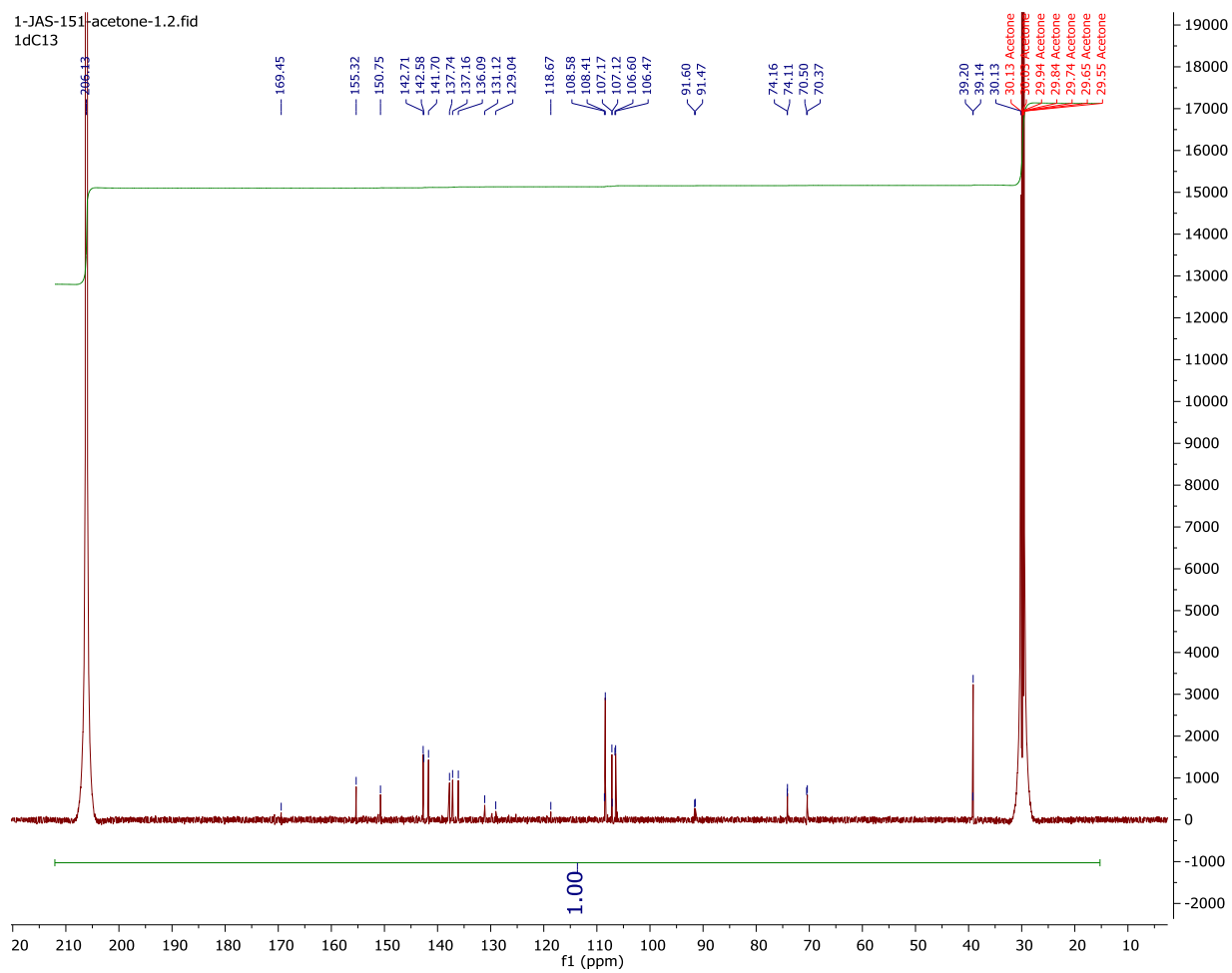
<sup>13</sup>C{<sup>1</sup>H} NMR Spectrum of 30



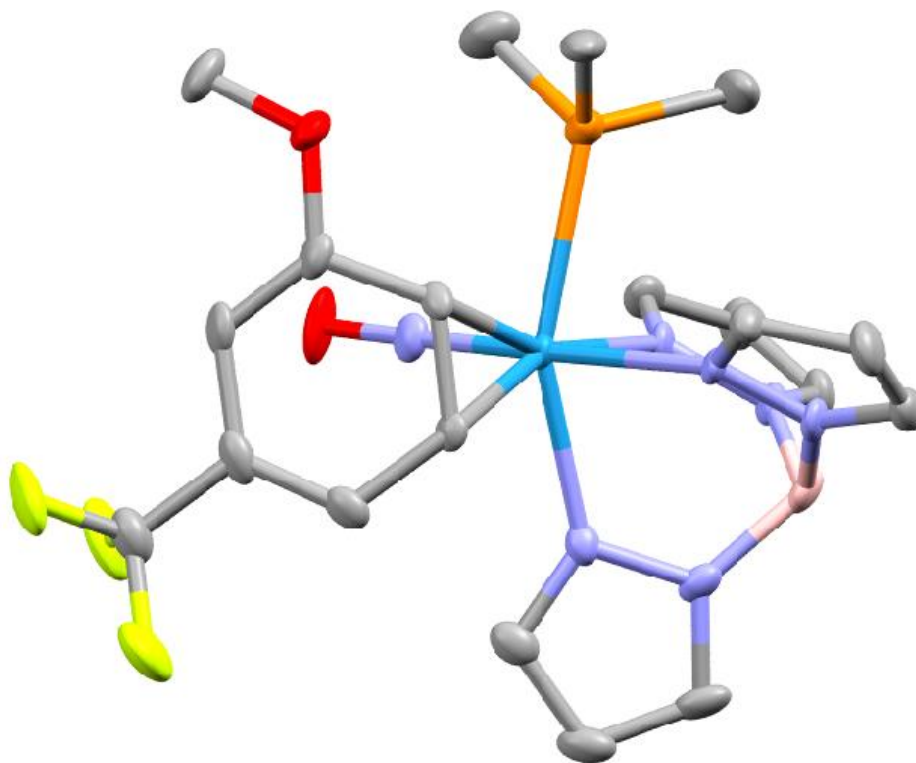
30A



30B



## Supporting Crystallographic Data for Chapter 6



### Crystal Structure Report for **Complex 18**

A **yellow rod-like** specimen of  $C_{20}H_{26}BF_3N_7O_2PW$ , approximate dimensions **0.051 mm** x **0.078 mm** x **0.097 mm**, was coated with Paratone oil and mounted on a MiTeGen MicroLoop. The X-ray intensity data were measured on a Bruker Kappa APEXII Duo system equipped with a fine-focus sealed tube ( $Mo\ K\alpha$ ,  $\lambda = 0.71073\ \text{\AA}$ ) and a graphite monochromator.

The total exposure time was 4.14 hours. The frames were integrated with the Bruker SAINT software package<sup>13</sup> using a narrow-frame algorithm. The integration of the data using a **monoclinic** unit cell yielded a total of **24648** reflections to a maximum  $\theta$  angle of **26.07°** (**0.81 Å** resolution), of which **5156**

<sup>13</sup> Bruker (2012). *Saint*; *SADABS*; *APEX3*. Bruker AXS Inc., Madison, Wisconsin, USA.

were independent (average redundancy 4.780, completeness = 99.7%,  $R_{\text{int}} = 6.92\%$ ,  $R_{\text{sig}} = 6.16\%$ ) and 3806 (73.82%) were greater than  $2\sigma(F^2)$ . The final cell constants of  $a = 11.0810(10)$  Å,  $b = 19.2009(15)$  Å,  $c = 12.4189(10)$  Å,  $\beta = 99.002(3)^\circ$ , volume = 2609.8(4) Å<sup>3</sup>, are based upon the refinement of the XYZ-centroids of 4350 reflections above  $20\sigma(I)$  with  $5.051^\circ < 2\theta < 46.30^\circ$ . Data were corrected for absorption effects using the Multi-Scan method (SADABS).<sup>1</sup> The ratio of minimum to maximum apparent transmission was 0.719. The calculated minimum and maximum transmission coefficients (based on crystal size) are 0.6670 and 0.8010.

The structure was solved and refined using the Bruker SHELXTL Software Package<sup>14</sup> within APEX3<sup>1</sup> and OLEX2,<sup>15</sup> using the space group  $P 2_1/n$ , with  $Z = 4$  for the formula unit,  $C_{20}H_{26}BF_3N_7O_2PW$ . Non-hydrogen atoms were refined anisotropically. The B-H hydrogen atom was located in the diffraction map and refined isotropically, as were the H10 and H11. All other hydrogen atoms were placed in geometrically calculated positions with  $U_{\text{iso}} = 1.2U_{\text{equiv}}$  of the parent atom ( $U_{\text{iso}} = 1.5U_{\text{equiv}}$  for methyl). The final anisotropic full-matrix least-squares refinement on  $F^2$  with 332 variables converged at  $R1 = 3.34\%$ , for the observed data and  $wR2 = 7.11\%$  for all data. The goodness-of-fit was 1.002. The largest peak in the final difference electron density synthesis was 2.808 e<sup>-</sup>/Å<sup>3</sup> and the largest hole was -0.828 e<sup>-</sup>/Å<sup>3</sup> with an RMS deviation of 0.149 e<sup>-</sup>/Å<sup>3</sup>. On the basis of the final model, the calculated density was 1.728 g/cm<sup>3</sup> and  $F(000)$ , 1328 e<sup>-</sup>.

**Table 1. Sample and crystal data for Harman\_19JAS133.**

|                             |                            |                           |
|-----------------------------|----------------------------|---------------------------|
| <b>Identification code</b>  | Harman_19JAS133            |                           |
| <b>Chemical formula</b>     | $C_{20}H_{26}BF_3N_7O_2PW$ |                           |
| <b>Formula weight</b>       | 679.11 g/mol               |                           |
| <b>Temperature</b>          | 100(2) K                   |                           |
| <b>Wavelength</b>           | 0.71073 Å                  |                           |
| <b>Crystal size</b>         | 0.051 x 0.078 x 0.097 mm   |                           |
| <b>Crystal habit</b>        | yellow rod                 |                           |
| <b>Crystal system</b>       | monoclinic                 |                           |
| <b>Space group</b>          | $P 2_1/n$                  |                           |
| <b>Unit cell dimensions</b> | $a = 11.0810(10)$ Å        | $\alpha = 90^\circ$       |
|                             | $b = 19.2009(15)$ Å        | $\beta = 99.002(3)^\circ$ |
|                             | $c = 12.4189(10)$ Å        | $\gamma = 90^\circ$       |

<sup>14</sup> Sheldrick, G. M. (2015). *Acta Cryst.* **A71**, 3-8.

<sup>15</sup> Dolomanov, O. V.; Bourhis, L. J.; Gildea, R. J.; Howard, J. A. K.; Puschmann, H. *J. Appl. Cryst.* (2009). **42**, 339-341.

|                               |                          |
|-------------------------------|--------------------------|
| <b>Volume</b>                 | 2609.8(4) Å <sup>3</sup> |
| <b>Z</b>                      | 4                        |
| <b>Density (calculated)</b>   | 1.728 g/cm <sup>3</sup>  |
| <b>Absorption coefficient</b> | 4.540 mm <sup>-1</sup>   |
| <b>F(000)</b>                 | 1328                     |

**Table 2. Data collection and structure refinement for Harman\_19JAS133.**

|  |  |
|--|--|
| <b>Diffractometer</b>                      | Bruker Kappa APEXII Duo  |
| <b>Radiation source</b>                    | fine-focus sealed tube (Mo K <sub>α</sub> , λ = 0.71073 Å)                   |
| <b>Theta range for data collection</b>     | 1.97 to 26.07°   |
| <b>Index ranges</b>                        | -13 ≤ h ≤ 13, -22 ≤ k ≤ 23, -15 ≤ l ≤ 15                                     |
| <b>Reflections collected</b>               | 24648  |
| <b>Independent reflections</b>             | 5156 [R(int) = 0.0692]   |
| <b>Coverage of independent reflections</b> | 99.7%  |
| <b>Absorption correction</b>               | Multi-Scan   |
| <b>Max. and min. transmission</b>          | 0.8010 and 0.6670  |
| <b>Structure solution technique</b>        | direct methods   |
| <b>Structure solution program</b>          | SHELXT 2014/5 (Sheldrick, 2014)  |
| <b>Refinement method</b>                   | Full-matrix least-squares on F <sup>2</sup>                                  |
| <b>Refinement program</b>                  | SHELXL-2018/3 (Sheldrick, 2018)  |
| <b>Function minimized</b>                  | Σ w(F <sub>o</sub> <sup>2</sup> - F <sub>c</sub> <sup>2</sup> ) <sup>2</sup> |
| <b>Data / restraints / parameters</b>      | 5156 / 1 / 332   |
| <b>Goodness-of-fit on F<sup>2</sup></b>    | 1.002  |
| <b>Δ/σ<sub>max</sub></b>                   | 0.001  |

|                                    |   |                              |
|------------------------------------|---|------------------------------|
| <b>Final R indices</b>             | 3806 data;<br>$I > 2\sigma(I)$  | R1 = 0.0334, wR2 =<br>0.0638 |
|                                    | all data  | R1 = 0.0608, wR2 =<br>0.0711 |
| <b>Weighting scheme</b>            | $w = 1/[\sigma^2(F_o^2) + (0.0312P)^2 + 0.8356P]$<br>where $P = (F_o^2 + 2F_c^2)/3$ |                              |
| <b>Largest diff. peak and hole</b> | 2.808 and -0.828 eÅ <sup>-3</sup>   |                              |
| <b>R.M.S. deviation from mean</b>  | 0.149 eÅ <sup>-3</sup>  |                              |

**Table 3. Atomic coordinates and equivalent isotropic atomic displacement parameters (Å<sup>2</sup>) for Harman\_19JAS133.**

U(eq) is defined as one third of the trace of the orthogonalized U<sub>ij</sub> tensor.

|    | x/a         | y/b         | z/c         | U(eq)      |
|----|-------------|-------------|-------------|------------|
| W1 | 0.72373(2)  | 0.35009(2)  | 0.51169(2)  | 0.01488(7) |
| P1 | 0.56039(15) | 0.27482(8)  | 0.40712(13) | 0.0252(4)  |
| F1 | 0.7194(4)   | 0.43769(19) | 0.9095(3)   | 0.0520(12) |
| F2 | 0.7456(4)   | 0.5421(2)   | 0.8599(3)   | 0.0549(12) |
| F3 | 0.5711(4)   | 0.5094(2)   | 0.8946(3)   | 0.0493(11) |
| O1 | 0.6964(4)   | 0.2898(2)   | 0.7294(3)   | 0.0371(12) |
| O2 | 0.3897(3)   | 0.36154(19) | 0.5662(3)   | 0.0238(9)  |
| N1 | 0.7457(4)   | 0.3901(2)   | 0.3457(3)   | 0.0178(10) |
| N2 | 0.8511(4)   | 0.3771(2)   | 0.3047(3)   | 0.0197(11) |
| N3 | 0.8440(4)   | 0.2637(2)   | 0.4772(3)   | 0.0205(11) |
| N4 | 0.9346(4)   | 0.2724(2)   | 0.4152(3)   | 0.0192(10) |
| N5 | 0.9084(4)   | 0.3951(2)   | 0.5541(3)   | 0.0181(10) |

|     | <b>x/a</b> | <b>y/b</b> | <b>z/c</b> | <b>U(eq)</b> |
|-----|------------|------------|------------|--------------|
| N6  | 0.9913(4)  | 0.3905(2)  | 0.4828(4)  | 0.0197(11)   |
| N7  | 0.7089(4)  | 0.3146(2)  | 0.6405(4)  | 0.0225(11)   |
| C1  | 0.6693(5)  | 0.4231(3)  | 0.2667(4)  | 0.0216(13)   |
| C2  | 0.7242(6)  | 0.4309(3)  | 0.1754(5)  | 0.0292(15)   |
| C3  | 0.8384(6)  | 0.4017(3)  | 0.2021(4)  | 0.0254(14)   |
| C4  | 0.8553(6)  | 0.1992(3)  | 0.5162(5)  | 0.0244(14)   |
| C5  | 0.9518(6)  | 0.1652(3)  | 0.4806(5)  | 0.0270(15)   |
| C6  | 0.0015(6)  | 0.2137(3)  | 0.4163(4)  | 0.0236(13)   |
| C7  | 0.9660(6)  | 0.4287(3)  | 0.6408(5)  | 0.0243(14)   |
| C8  | 0.0849(6)  | 0.4462(3)  | 0.6261(5)  | 0.0275(14)   |
| C9  | 0.0964(5)  | 0.4209(3)  | 0.5265(5)  | 0.0266(14)   |
| C10 | 0.6695(5)  | 0.4597(2)  | 0.5450(4)  | 0.0152(11)   |
| C11 | 0.5589(5)  | 0.4185(3)  | 0.5138(4)  | 0.0168(12)   |
| C12 | 0.4908(5)  | 0.4021(3)  | 0.6012(4)  | 0.0205(13)   |
| C13 | 0.5251(5)  | 0.4229(3)  | 0.7058(4)  | 0.0222(13)   |
| C14 | 0.6291(6)  | 0.4678(3)  | 0.7305(4)  | 0.0237(14)   |
| C15 | 0.6971(5)  | 0.4873(3)  | 0.6533(4)  | 0.0214(13)   |
| C16 | 0.6652(6)  | 0.4895(3)  | 0.8461(5)  | 0.0304(15)   |
| C17 | 0.3316(6)  | 0.3286(3)  | 0.6489(5)  | 0.0315(15)   |
| C18 | 0.4234(5)  | 0.3126(3)  | 0.3299(5)  | 0.0318(15)   |
| C19 | 0.6160(6)  | 0.2256(3)  | 0.2992(5)  | 0.0395(18)   |
| C20 | 0.5004(6)  | 0.2071(3)  | 0.4861(6)  | 0.0396(18)   |
| B1  | 0.9638(6)  | 0.3468(3)  | 0.3776(5)  | 0.0224(14)   |

**Table 4. Bond lengths (Å) for Harman\_19JAS133.**

|         |            |         |          |
|---------|------------|---------|----------|
| W1-N7   | 1.770(4)   | W1-N5   | 2.208(5) |
| W1-N3   | 2.211(4)   | W1-C10  | 2.245(5) |
| W1-N1   | 2.249(4)   | W1-C11  | 2.253(5) |
| W1-P1   | 2.5132(16) | P1-C18  | 1.815(6) |
| P1-C20  | 1.816(6)   | P1-C19  | 1.824(6) |
| F1-C16  | 1.349(7)   | F2-C16  | 1.340(7) |
| F3-C16  | 1.339(7)   | O1-N7   | 1.229(5) |
| O2-C12  | 1.377(7)   | O2-C17  | 1.442(6) |
| N1-C1   | 1.350(7)   | N1-N2   | 1.368(6) |
| N2-C3   | 1.345(7)   | N2-B1   | 1.538(8) |
| N3-C4   | 1.329(6)   | N3-N4   | 1.368(6) |
| N4-C6   | 1.348(7)   | N4-B1   | 1.553(7) |
| N5-C7   | 1.330(7)   | N5-N6   | 1.375(6) |
| N6-C9   | 1.338(7)   | N6-B1   | 1.542(8) |
| C1-C2   | 1.376(7)   | C1-H1   | 0.95     |
| C2-C3   | 1.377(8)   | C2-H2   | 0.95     |
| C3-H3   | 0.95       | C4-C5   | 1.382(8) |
| C4-H4   | 0.95       | C5-C6   | 1.396(7) |
| C5-H5   | 0.95       | C6-H6   | 0.95     |
| C7-C8   | 1.398(8)   | C7-H7   | 0.95     |
| C8-C9   | 1.353(8)   | C8-H8   | 0.95     |
| C9-H9   | 0.95       | C10-C15 | 1.434(7) |
| C10-C11 | 1.459(8)   | C10-H10 | 1.00(4)  |
| C11-C12 | 1.450(7)   | C11-H11 | 1.00(4)  |

|          |          |          |          |
|----------|----------|----------|----------|
| C12-C13  | 1.356(8) | C13-C14  | 1.434(8) |
| C13-H13  | 0.95     | C14-C15  | 1.360(8) |
| C14-C16  | 1.488(8) | C15-H15  | 0.95     |
| C17-H17A | 0.98     | C17-H17B | 0.98     |
| C17-H17C | 0.98     | C18-H18A | 0.98     |
| C18-H18B | 0.98     | C18-H18C | 0.98     |
| C19-H19A | 0.98     | C19-H19B | 0.98     |
| C19-H19C | 0.98     | C20-H20A | 0.98     |
| C20-H20B | 0.98     | C20-H20C | 0.98     |
| B1-H1A   | 1.01(5)  |          |          |

**Table 5. Bond angles (°) for Harman\_19JAS133.**

|            |            |            |            |
|------------|------------|------------|------------|
| N7-W1-N5   | 98.58(19)  | N7-W1-N3   | 91.72(17)  |
| N5-W1-N3   | 77.04(16)  | N7-W1-C10  | 97.45(19)  |
| N5-W1-C10  | 81.58(18)  | N3-W1-C10  | 157.77(19) |
| N7-W1-N1   | 177.20(17) | N5-W1-N1   | 81.69(16)  |
| N3-W1-N1   | 85.63(16)  | C10-W1-N1  | 85.35(17)  |
| N7-W1-C11  | 91.4(2)    | N5-W1-C11  | 119.44(18) |
| N3-W1-C11  | 162.53(18) | C10-W1-C11 | 37.86(19)  |
| N1-W1-C11  | 90.92(17)  | N7-W1-P1   | 94.82(16)  |
| N5-W1-P1   | 156.08(12) | N3-W1-P1   | 82.86(13)  |
| C10-W1-P1  | 116.26(15) | N1-W1-P1   | 83.99(12)  |
| C11-W1-P1  | 79.74(14)  | C18-P1-C20 | 103.0(3)   |
| C18-P1-C19 | 99.7(3)    | C20-P1-C19 | 102.7(3)   |
| C18-P1-W1  | 121.2(2)   | C20-P1-W1  | 115.3(2)   |



|             |          |            |          |
|-------------|----------|------------|----------|
| C19-P1-W1   | 112.3(2) | C12-O2-C17 | 117.1(4) |
| C1-N1-N2    | 106.9(4) | C1-N1-W1   | 132.9(4) |
| N2-N1-W1    | 120.0(3) | C3-N2-N1   | 108.7(5) |
| C3-N2-B1    | 130.2(5) | N1-N2-B1   | 120.8(4) |
| C4-N3-N4    | 106.4(4) | C4-N3-W1   | 130.9(4) |
| N4-N3-W1    | 122.4(3) | C6-N4-N3   | 110.1(4) |
| C6-N4-B1    | 129.2(5) | N3-N4-B1   | 119.2(4) |
| C7-N5-N6    | 105.5(5) | C7-N5-W1   | 133.9(4) |
| N6-N5-W1    | 120.6(3) | C9-N6-N5   | 109.7(5) |
| C9-N6-B1    | 128.6(5) | N5-N6-B1   | 121.1(4) |
| O1-N7-W1    | 178.9(5) | N1-C1-C2   | 110.0(5) |
| N1-C1-H1    | 125.0    | C2-C1-H1   | 125.0    |
| C1-C2-C3    | 105.4(5) | C1-C2-H2   | 127.3    |
| C3-C2-H2    | 127.3    | N2-C3-C2   | 109.1(5) |
| N2-C3-H3    | 125.5    | C2-C3-H3   | 125.5    |
| N3-C4-C5    | 111.0(5) | N3-C4-H4   | 124.5    |
| C5-C4-H4    | 124.5    | C4-C5-C6   | 105.2(5) |
| C4-C5-H5    | 127.4    | C6-C5-H5   | 127.4    |
| N4-C6-C5    | 107.3(5) | N4-C6-H6   | 126.3    |
| C5-C6-H6    | 126.3    | N5-C7-C8   | 110.7(5) |
| N5-C7-H7    | 124.7    | C8-C7-H7   | 124.7    |
| C9-C8-C7    | 105.0(5) | C9-C8-H8   | 127.5    |
| C7-C8-H8    | 127.5    | N6-C9-C8   | 109.1(5) |
| N6-C9-H9    | 125.5    | C8-C9-H9   | 125.5    |
| C15-C10-C11 | 119.7(5) | C15-C10-W1 | 119.7(4) |

|               |          |               |          |
|---------------|----------|---------------|----------|
| C11-C10-W1    | 71.4(3)  | C15-C10-H10   | 119.(3)  |
| C11-C10-H10   | 114.(3)  | W1-C10-H10    | 102.(3)  |
| C12-C11-C10   | 115.7(5) | C12-C11-W1    | 113.5(4) |
| C10-C11-W1    | 70.8(3)  | C12-C11-H11   | 111.(3)  |
| C10-C11-H11   | 123.(3)  | W1-C11-H11    | 118.(3)  |
| C13-C12-O2    | 124.1(5) | C13-C12-C11   | 123.5(5) |
| O2-C12-C11    | 112.4(5) | C12-C13-C14   | 118.5(5) |
| C12-C13-H13   | 120.7    | C14-C13-H13   | 120.7    |
| C15-C14-C13   | 122.0(5) | C15-C14-C16   | 120.5(6) |
| C13-C14-C16   | 117.3(5) | C14-C15-C10   | 120.0(5) |
| C14-C15-H15   | 120.0    | C10-C15-H15   | 120.0    |
| F3-C16-F2     | 105.9(5) | F3-C16-F1     | 104.8(5) |
| F2-C16-F1     | 104.7(5) | F3-C16-C14    | 113.8(5) |
| F2-C16-C14    | 114.0(5) | F1-C16-C14    | 112.7(5) |
| O2-C17-H17A   | 109.5    | O2-C17-H17B   | 109.5    |
| H17A-C17-H17B | 109.5    | O2-C17-H17C   | 109.5    |
| H17A-C17-H17C | 109.5    | H17B-C17-H17C | 109.5    |
| P1-C18-H18A   | 109.5    | P1-C18-H18B   | 109.5    |
| H18A-C18-H18B | 109.5    | P1-C18-H18C   | 109.5    |
| H18A-C18-H18C | 109.5    | H18B-C18-H18C | 109.5    |
| P1-C19-H19A   | 109.5    | P1-C19-H19B   | 109.5    |
| H19A-C19-H19B | 109.5    | P1-C19-H19C   | 109.5    |
| H19A-C19-H19C | 109.5    | H19B-C19-H19C | 109.5    |
| P1-C20-H20A   | 109.5    | P1-C20-H20B   | 109.5    |
| H20A-C20-H20B | 109.5    | P1-C20-H20C   | 109.5    |

|               |          |               |          |
|---------------|----------|---------------|----------|
| H20A-C20-H20C | 109.5    | H20B-C20-H20C | 109.5    |
| N2-B1-N6      | 109.2(5) | N2-B1-N4      | 109.7(5) |
| N6-B1-N4      | 105.6(4) | N2-B1-H1A     | 109.(3)  |
| N6-B1-H1A     | 113.(3)  | N4-B1-H1A     | 110.(3)  |

**Table 6. Torsion angles (°) for Harman\_19JAS133.**

|                 |           |                 |           |
|-----------------|-----------|-----------------|-----------|
| C1-N1-N2-C3     | -0.3(6)   | W1-N1-N2-C3     | 175.5(3)  |
| C1-N1-N2-B1     | 173.4(5)  | W1-N1-N2-B1     | -10.8(6)  |
| C4-N3-N4-C6     | -0.2(6)   | W1-N3-N4-C6     | 173.8(4)  |
| C4-N3-N4-B1     | -167.3(5) | W1-N3-N4-B1     | 6.7(6)    |
| C7-N5-N6-C9     | 0.0(5)    | W1-N5-N6-C9     | -179.5(3) |
| C7-N5-N6-B1     | 172.4(5)  | W1-N5-N6-B1     | -7.1(6)   |
| N2-N1-C1-C2     | 0.5(6)    | W1-N1-C1-C2     | -174.5(4) |
| N1-C1-C2-C3     | -0.5(6)   | N1-N2-C3-C2     | 0.0(6)    |
| B1-N2-C3-C2     | -172.9(5) | C1-C2-C3-N2     | 0.3(6)    |
| N4-N3-C4-C5     | -0.2(6)   | W1-N3-C4-C5     | -173.5(4) |
| N3-C4-C5-C6     | 0.4(7)    | N3-N4-C6-C5     | 0.4(6)    |
| B1-N4-C6-C5     | 165.9(5)  | C4-C5-C6-N4     | -0.5(7)   |
| N6-N5-C7-C8     | 0.3(6)    | W1-N5-C7-C8     | 179.7(4)  |
| N5-C7-C8-C9     | -0.5(6)   | N5-N6-C9-C8     | -0.3(6)   |
| B1-N6-C9-C8     | -172.0(5) | C7-C8-C9-N6     | 0.5(6)    |
| C15-C10-C11-C12 | -6.6(7)   | W1-C10-C11-C12  | 107.5(4)  |
| C15-C10-C11-W1  | -114.1(4) | C17-O2-C12-C13  | -12.5(7)  |
| C17-O2-C12-C11  | 165.9(5)  | C10-C11-C12-C13 | 0.1(8)    |
| W1-C11-C12-C13  | 79.2(6)   | C10-C11-C12-O2  | -178.3(4) |

|                 |           |                 |           |
|-----------------|-----------|-----------------|-----------|
| W1-C11-C12-O2   | -99.2(5)  | O2-C12-C13-C14  | -177.0(5) |
| C11-C12-C13-C14 | 4.7(8)    | C12-C13-C14-C15 | -3.1(8)   |
| C12-C13-C14-C16 | -179.6(5) | C13-C14-C15-C10 | -3.4(8)   |
| C16-C14-C15-C10 | 173.0(5)  | C11-C10-C15-C14 | 8.3(8)    |
| W1-C10-C15-C14  | -76.0(6)  | C15-C14-C16-F3  | 138.3(6)  |
| C13-C14-C16-F3  | -45.2(7)  | C15-C14-C16-F2  | 16.6(8)   |
| C13-C14-C16-F2  | -166.9(5) | C15-C14-C16-F1  | -102.5(7) |
| C13-C14-C16-F1  | 74.0(7)   | C3-N2-B1-N6     | 121.6(6)  |
| N1-N2-B1-N6     | -50.6(6)  | C3-N2-B1-N4     | -123.2(6) |
| N1-N2-B1-N4     | 64.6(6)   | C9-N6-B1-N2     | -127.0(6) |
| N5-N6-B1-N2     | 62.1(6)   | C9-N6-B1-N4     | 115.2(6)  |
| N5-N6-B1-N4     | -55.7(6)  | C6-N4-B1-N2     | 133.6(5)  |
| N3-N4-B1-N2     | -61.9(6)  | C6-N4-B1-N6     | -108.9(6) |
| N3-N4-B1-N6     | 55.5(6)   |                 |           |

**Table 7. Anisotropic atomic displacement parameters ( $\text{\AA}^2$ ) for Harman\_19JAS133.**

The anisotropic atomic displacement factor exponent takes the form: -  
 $2\pi^2 [ h^2 a^{*2} U_{11} + \dots + 2 h k a^* b^* U_{12} ]$

|    | $U_{11}$    | $U_{22}$    | $U_{33}$    | $U_{23}$    | $U_{13}$   | $U_{12}$    |
|----|-------------|-------------|-------------|-------------|------------|-------------|
| W1 | 0.01677(12) | 0.01605(11) | 0.01328(11) | 0.00009(10) | 0.00694(8) | 0.00017(12) |
| P1 | 0.0241(9)   | 0.0246(8)   | 0.0292(9)   | -0.0060(7)  | 0.0113(7)  | -0.0069(7)  |
| F1 | 0.082(3)    | 0.057(2)    | 0.0137(18)  | 0.0033(18)  | -0.002(2)  | 0.028(2)    |
| F2 | 0.078(3)    | 0.062(3)    | 0.022(2)    | -0.0148(19) | 0.001(2)   | -0.016(2)   |
| F3 | 0.052(3)    | 0.072(3)    | 0.025(2)    | -0.0182(19) | 0.0113(19) | 0.020(2)    |

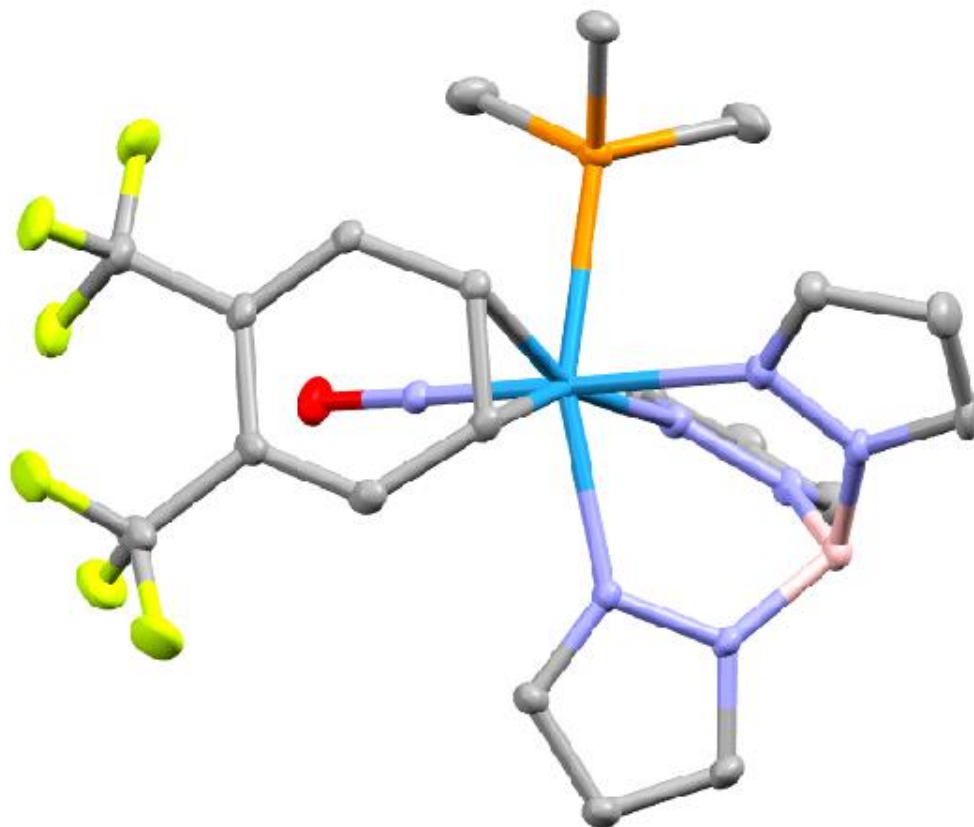
|     | <b>U<sub>11</sub></b> | <b>U<sub>22</sub></b> | <b>U<sub>33</sub></b> | <b>U<sub>23</sub></b> | <b>U<sub>13</sub></b> | <b>U<sub>12</sub></b> |
|-----|-----------------------|-----------------------|-----------------------|-----------------------|-----------------------|-----------------------|
| O1  | 0.051(3)              | 0.042(2)              | 0.025(2)              | 0.022(2)              | 0.026(2)              | 0.022(2)              |
| O2  | 0.017(2)              | 0.031(2)              | 0.025(2)              | 0.0049(17)            | 0.0072(17)            | -0.0034(18)           |
| N1  | 0.017(3)              | 0.023(2)              | 0.016(2)              | -0.002(2)             | 0.010(2)              | -0.003(2)             |
| N2  | 0.026(3)              | 0.022(2)              | 0.015(2)              | 0.0022(19)            | 0.012(2)              | -0.002(2)             |
| N3  | 0.026(3)              | 0.025(2)              | 0.013(2)              | 0.000(2)              | 0.011(2)              | 0.000(2)              |
| N4  | 0.016(3)              | 0.024(2)              | 0.019(2)              | 0.000(2)              | 0.009(2)              | 0.003(2)              |
| N5  | 0.021(3)              | 0.018(2)              | 0.015(2)              | 0.002(2)              | 0.003(2)              | 0.004(2)              |
| N6  | 0.017(3)              | 0.014(2)              | 0.030(3)              | 0.005(2)              | 0.008(2)              | 0.000(2)              |
| N7  | 0.023(3)              | 0.021(2)              | 0.025(3)              | 0.001(2)              | 0.011(2)              | 0.008(2)              |
| C1  | 0.019(3)              | 0.029(3)              | 0.016(3)              | 0.001(2)              | 0.002(3)              | -0.001(3)             |
| C2  | 0.039(4)              | 0.036(3)              | 0.014(3)              | 0.000(3)              | 0.006(3)              | 0.004(3)              |
| C3  | 0.032(4)              | 0.028(3)              | 0.018(3)              | -0.002(3)             | 0.009(3)              | -0.007(3)             |
| C4  | 0.032(4)              | 0.016(3)              | 0.027(3)              | 0.002(2)              | 0.011(3)              | -0.005(3)             |
| C5  | 0.037(4)              | 0.017(3)              | 0.031(3)              | 0.000(2)              | 0.015(3)              | 0.004(3)              |
| C6  | 0.032(4)              | 0.023(3)              | 0.018(3)              | -0.003(2)             | 0.010(3)              | 0.005(3)              |
| C7  | 0.030(4)              | 0.017(3)              | 0.024(3)              | 0.000(2)              | -0.003(3)             | 0.004(3)              |
| C8  | 0.023(4)              | 0.017(3)              | 0.040(4)              | -0.003(3)             | -0.006(3)             | -0.001(3)             |
| C9  | 0.016(3)              | 0.016(3)              | 0.047(4)              | 0.006(3)              | 0.002(3)              | -0.004(3)             |
| C10 | 0.016(3)              | 0.011(3)              | 0.019(3)              | 0.001(2)              | 0.006(2)              | 0.006(2)              |
| C11 | 0.013(3)              | 0.021(3)              | 0.015(3)              | -0.002(2)             | 0.000(2)              | 0.007(2)              |
| C12 | 0.019(3)              | 0.020(3)              | 0.025(3)              | 0.003(2)              | 0.011(3)              | 0.007(2)              |
| C13 | 0.029(4)              | 0.021(3)              | 0.019(3)              | 0.001(2)              | 0.013(3)              | 0.011(3)              |
| C14 | 0.037(4)              | 0.018(3)              | 0.017(3)              | -0.001(2)             | 0.005(3)              | 0.011(3)              |
| C15 | 0.027(4)              | 0.013(3)              | 0.023(3)              | -0.003(2)             | -0.001(3)             | 0.005(2)              |

|     | <b>U<sub>11</sub></b> | <b>U<sub>22</sub></b> | <b>U<sub>33</sub></b> | <b>U<sub>23</sub></b> | <b>U<sub>13</sub></b> | <b>U<sub>12</sub></b> |
|-----|-----------------------|-----------------------|-----------------------|-----------------------|-----------------------|-----------------------|
| C16 | 0.043(4)              | 0.027(3)              | 0.022(3)              | -0.003(3)             | 0.006(3)              | 0.008(3)              |
| C17 | 0.023(4)              | 0.040(4)              | 0.034(4)              | 0.013(3)              | 0.015(3)              | 0.002(3)              |
| C18 | 0.020(4)              | 0.045(4)              | 0.029(3)              | -0.009(3)             | 0.003(3)              | -0.014(3)             |
| C19 | 0.039(4)              | 0.037(4)              | 0.046(4)              | -0.024(3)             | 0.019(3)              | -0.012(3)             |
| C20 | 0.037(5)              | 0.026(3)              | 0.059(5)              | 0.000(3)              | 0.015(4)              | -0.009(3)             |
| B1  | 0.020(4)              | 0.025(3)              | 0.025(3)              | 0.006(3)              | 0.013(3)              | -0.002(3)             |

**Table 8. Hydrogen atomic coordinates and isotropic atomic displacement parameters ( $\text{\AA}^2$ ) for Harman\_19JAS133.**

|      | <b>x/a</b> | <b>y/b</b> | <b>z/c</b> | <b>U(eq)</b> |
|------|------------|------------|------------|--------------|
| H1   | 0.5894     | 0.4387     | 0.2732     | 0.026        |
| H2   | 0.6904     | 0.4519     | 0.1082     | 0.035        |
| H3   | 0.8985     | 0.3992     | 0.1555     | 0.031        |
| H4   | 0.8040     | 0.1791     | 0.5623     | 0.029        |
| H5   | 0.9785     | 0.1188     | 0.4966     | 0.032        |
| H6   | 1.0698     | 0.2067     | 0.3799     | 0.028        |
| H7   | 0.9313     | 0.4394     | 0.7041     | 0.029        |
| H8   | 1.1446     | 0.4705     | 0.6753     | 0.033        |
| H9   | 1.1676     | 0.4241     | 0.4930     | 0.032        |
| H10  | 0.697(5)   | 0.486(2)   | 0.483(4)   | 0.023(15)    |
| H11  | 0.502(4)   | 0.426(2)   | 0.444(3)   | 0.011(13)    |
| H13  | 0.4812     | 0.4080     | 0.7616     | 0.027        |
| H15  | 0.7628     | 0.5191     | 0.6713     | 0.026        |
| H17A | 0.2630     | 0.3001     | 0.6141     | 0.047        |

|      | <b>x/a</b> | <b>y/b</b> | <b>z/c</b> | <b>U(eq)</b> |
|------|------------|------------|------------|--------------|
| H17B | 0.3013     | 0.3643     | 0.6943     | 0.047        |
| H17C | 0.3908     | 0.2989     | 0.6945     | 0.047        |
| H18A | 0.3761     | 0.3358     | 0.3798     | 0.048        |
| H18B | 0.3739     | 0.2757     | 0.2903     | 0.048        |
| H18C | 0.4463     | 0.3466     | 0.2778     | 0.048        |
| H19A | 0.6505     | 0.2577     | 0.2508     | 0.059        |
| H19B | 0.5481     | 0.1998     | 0.2573     | 0.059        |
| H19C | 0.6792     | 0.1928     | 0.3316     | 0.059        |
| H20A | 0.5658     | 0.1743     | 0.5135     | 0.059        |
| H20B | 0.4345     | 0.1823     | 0.4398     | 0.059        |
| H20C | 0.4684     | 0.2283     | 0.5477     | 0.059        |
| H1A  | 1.035(5)   | 0.345(2)   | 0.335(4)   | 0.021(14)    |



### Crystal Structure Report for **Complex 20** in Chapter 6

A **yellow plate-like** specimen of  $C_{26}H_{29}BF_6N_7OPW$ , approximate dimensions **0.188 mm** x **0.323 mm** x **0.473 mm**, was coated with Paratone oil and mounted on a MiTeGen MicroLoop. The X-ray intensity data were measured on a Bruker Kappa APEXII Duo system equipped with a fine-focus sealed tube (Mo  $K_{\alpha}$ ,  $\lambda = 0.71073 \text{ \AA}$ ) and a graphite monochromator.

The total exposure time was 0.98 hours. The frames were integrated with the Bruker SAINT software package<sup>16</sup> using a narrow-frame algorithm. The integration of the data using an **orthorhombic** unit cell yielded a total of **61136** reflections to a maximum  $\theta$  angle of **33.15°** (**0.65 Å** resolution), of which **11727** were independent (average redundancy **5.213**, completeness = **99.9%**,  $R_{\text{int}} = 2.62\%$ ,  $R_{\text{sig}} = 2.07\%$ ) and **9802** (**83.58%**) were greater than  $2\sigma(F^2)$ . The final cell constants of  $\underline{a} = 18.9294(11) \text{ \AA}$ ,  $\underline{b} = 13.5668(8) \text{ \AA}$ ,  $\underline{c} = 23.9645(15) \text{ \AA}$ , volume = **6154.4(6) Å<sup>3</sup>**, are based upon the refinement of the XYZ-centroids of **9867** reflections above  $20 \sigma(I)$  with  $5.020^\circ < 2\theta < 66.26^\circ$ . Data were corrected for absorption effects using the

<sup>16</sup> Bruker (2012). *Saint*; *SADABS*; *APEX3*. Bruker AXS Inc., Madison, Wisconsin, USA.



Multi-Scan method (SADABS).<sup>1</sup> The ratio of minimum to maximum apparent transmission was 0.634. The calculated minimum and maximum transmission coefficients (based on crystal size) are 0.2620 and 0.5290.

The structure was solved and refined using the Bruker SHELXTL Software Package<sup>17</sup> within APEX3<sup>1</sup> and OLEX2,<sup>18</sup> using the space group *P b c a*, with *Z* = 8 for the formula unit, C<sub>26</sub>H<sub>29</sub>BF<sub>6</sub>N<sub>7</sub>OPW. Non-hydrogen atoms were refined anisotropically. Three H atoms (H1A, H10 and H11) were located in the diffraction map and refined isotropically. All other hydrogen atoms were placed in geometrically calculated positions with  $U_{iso} = 1.2U_{equiv}$  of the parent atom ( $U_{iso} = 1.5U_{equiv}$  for methyl). One molecule of benzene solvent was found to be disordered over two positions. The relative occupancies were freely refined and no constraints or restraints were used. The final anisotropic full-matrix least-squares refinement on  $F^2$  with 458 variables converged at  $R1 = 1.91\%$ , for the observed data and  $wR2 = 3.92\%$  for all data. The goodness-of-fit was 1.030. The largest peak in the final difference electron density synthesis was 0.806 e<sup>-</sup>/Å<sup>3</sup> and the largest hole was -0.695 e<sup>-</sup>/Å<sup>3</sup> with an RMS deviation of 0.087 e<sup>-</sup>/Å<sup>3</sup>. On the basis of the final model, the calculated density was 1.716 g/cm<sup>3</sup> and  $F(000)$ , 3120 e<sup>-</sup>.

**Table 1. Sample and crystal data for Harman\_16JAS17.**

|                             |  |         |
|-----------------------------|--|---------|
| <b>Identification code</b>  | Harman_16JAS17   |         |
| <b>Chemical formula</b>     | C <sub>26</sub> H <sub>29</sub> BF <sub>6</sub> N <sub>7</sub> OPW |         |
| <b>Formula weight</b>       | 795.19 g/mol   |         |
| <b>Temperature</b>          | 100(2) K   |         |
| <b>Wavelength</b>           | 0.71073 Å  |         |
| <b>Crystal size</b>         | 0.188 x 0.323 x 0.473 mm   |         |
| <b>Crystal habit</b>        | yellow plate   |         |
| <b>Crystal system</b>       | orthorhombic   |         |
| <b>Space group</b>          | <i>P b c a</i>   |         |
| <b>Unit cell dimensions</b> | a = 18.9294(11) Å  | α = 90° |
|                             | b = 13.5668(8) Å   | β = 90° |
|                             | c = 23.9645(15) Å  | γ = 90° |
| <b>Volume</b>               | 6154.4(6) Å <sup>3</sup>   |         |

<sup>17</sup> Sheldrick, G. M. (2015). *Acta Cryst.* **A71**, 3-8.

<sup>18</sup> Dolomanov, O. V.; Bourhis, L. J.; Gildea, R. J.; Howard, J. A. K.; Puschmann, H. *J. Appl. Cryst.* (2009). **42**, 339-341.

|                               |                         |
|-------------------------------|-------------------------|
| <b>Z</b>                      | 8                       |
| <b>Density (calculated)</b>   | 1.716 g/cm <sup>3</sup> |
| <b>Absorption coefficient</b> | 3.875 mm <sup>-1</sup>  |
| <b>F(000)</b>                 | 3120                    |

**Table 2. Data collection and structure refinement for Harman\_16JAS17.**

|  |  |
|--|--|
| <b>Diffractometer</b>                      | Bruker Kappa APEXII Duo  |
| <b>Radiation source</b>                    | fine-focus sealed tube (Mo K $\alpha$ , $\lambda$ = 0.71073 Å) |
| <b>Theta range for data collection</b>     | 2.01 to 33.15°   |
| <b>Index ranges</b>                        | -29 ≤ h ≤ 29, -20 ≤ k ≤ 19, -36 ≤ l ≤ 36                       |
| <b>Reflections collected</b>               | 61136  |
| <b>Independent reflections</b>             | 11727 [R(int) = 0.0262]  |
| <b>Coverage of independent reflections</b> | 99.9%  |
| <b>Absorption correction</b>               | Multi-Scan   |
| <b>Max. and min. transmission</b>          | 0.5290 and 0.2620  |
| <b>Structure solution technique</b>        | direct methods   |
| <b>Structure solution program</b>          | SHELXT 2014/5 (Sheldrick, 2014)                                |
| <b>Refinement method</b>                   | Full-matrix least-squares on F <sup>2</sup>                    |
| <b>Refinement program</b>                  | SHELXL-2018/3 (Sheldrick, 2018)                                |
| <b>Function minimized</b>                  | $\sum w(F_o^2 - F_c^2)^2$                                      |
| <b>Data / restraints / parameters</b>      | 11727 / 0 / 458  |
| <b>Goodness-of-fit on F<sup>2</sup></b>    | 1.030  |
| <b><math>\Delta/\sigma_{\max}</math></b>   | 0.012  |

|                                    |   |                              |
|------------------------------------|---|------------------------------|
| <b>Final R indices</b>             | 9802 data;<br>$I > 2\sigma(I)$  | R1 = 0.0191, wR2 =<br>0.0366 |
|                                    | all data  | R1 = 0.0282, wR2 =<br>0.0392 |
| <b>Weighting scheme</b>            | $w = 1/[\sigma^2(F_o^2) + (0.0135P)^2 + 3.8029P]$<br>where $P = (F_o^2 + 2F_c^2)/3$ |                              |
| <b>Largest diff. peak and hole</b> | 0.806 and -0.695 eÅ <sup>-3</sup>   |                              |
| <b>R.M.S. deviation from mean</b>  | 0.087 eÅ <sup>-3</sup>  |                              |

**Table 3. Atomic coordinates and equivalent isotropic atomic displacement parameters (Å<sup>2</sup>) for Harman\_16JAS17.**

U(eq) is defined as one third of the trace of the orthogonalized U<sub>ij</sub> tensor.

|    | x/a        | y/b         | z/c        | U(eq)      |
|----|------------|-------------|------------|------------|
| W1 | 0.63540(2) | 0.32903(2)  | 0.57956(2) | 0.00938(2) |
| P1 | 0.69865(2) | 0.48149(3)  | 0.54698(2) | 0.01359(7) |
| F1 | 0.44853(7) | 0.07229(8)  | 0.46628(6) | 0.0385(3)  |
| F2 | 0.55462(7) | 0.05359(8)  | 0.43673(6) | 0.0378(3)  |
| F3 | 0.47898(7) | 0.13145(9)  | 0.38666(5) | 0.0376(3)  |
| F4 | 0.53252(6) | 0.29306(8)  | 0.34031(4) | 0.0300(2)  |
| F5 | 0.61459(6) | 0.19547(8)  | 0.36958(5) | 0.0300(2)  |
| F6 | 0.63246(6) | 0.35192(9)  | 0.36630(5) | 0.0320(3)  |
| O1 | 0.69762(6) | 0.20855(9)  | 0.48690(5) | 0.0212(2)  |
| N1 | 0.59749(7) | 0.42130(9)  | 0.65161(5) | 0.0139(2)  |
| N2 | 0.61507(7) | 0.39538(10) | 0.70489(6) | 0.0152(2)  |
| N3 | 0.73094(6) | 0.31019(9)  | 0.63096(5) | 0.0132(2)  |

|     | <b>x/a</b>  | <b>y/b</b>  | <b>z/c</b> | <b>U(eq)</b> |
|-----|-------------|-------------|------------|--------------|
| N4  | 0.72849(7)  | 0.30413(10) | 0.68769(6) | 0.0155(2)    |
| N5  | 0.60462(6)  | 0.20606(9)  | 0.63601(5) | 0.0126(2)    |
| N6  | 0.61701(7)  | 0.21142(10) | 0.69202(5) | 0.0144(2)    |
| N7  | 0.67182(6)  | 0.25670(9)  | 0.52498(5) | 0.0124(2)    |
| B1  | 0.65662(10) | 0.29997(13) | 0.71755(8) | 0.0166(3)    |
| C1  | 0.56345(8)  | 0.50779(11) | 0.65546(7) | 0.0168(3)    |
| C2  | 0.55927(9)  | 0.53818(12) | 0.71091(7) | 0.0217(3)    |
| C3  | 0.59252(9)  | 0.46492(12) | 0.74077(7) | 0.0209(3)    |
| C4  | 0.79864(8)  | 0.29425(11) | 0.61635(7) | 0.0169(3)    |
| C5  | 0.83972(9)  | 0.27828(13) | 0.66371(8) | 0.0224(3)    |
| C6  | 0.79335(9)  | 0.28426(12) | 0.70802(8) | 0.0217(3)    |
| C7  | 0.57950(8)  | 0.11539(11) | 0.62610(7) | 0.0148(3)    |
| C8  | 0.57565(9)  | 0.06151(12) | 0.67566(7) | 0.0194(3)    |
| C9  | 0.59991(9)  | 0.12500(11) | 0.71635(7) | 0.0185(3)    |
| C10 | 0.52251(7)  | 0.31287(11) | 0.55345(6) | 0.0138(3)    |
| C11 | 0.55317(8)  | 0.39622(11) | 0.52320(6) | 0.0129(3)    |
| C12 | 0.56826(8)  | 0.38105(11) | 0.46447(6) | 0.0141(3)    |
| C13 | 0.55774(8)  | 0.29379(11) | 0.43811(6) | 0.0155(3)    |
| C14 | 0.52088(8)  | 0.21412(11) | 0.46741(7) | 0.0167(3)    |
| C15 | 0.50256(8)  | 0.22721(11) | 0.52161(7) | 0.0160(3)    |
| C16 | 0.50127(10) | 0.11914(13) | 0.43976(8) | 0.0259(4)    |
| C17 | 0.58383(9)  | 0.28307(12) | 0.37946(7) | 0.0212(3)    |
| C18 | 0.75921(9)  | 0.45893(13) | 0.48936(8) | 0.0244(4)    |
| C19 | 0.64975(8)  | 0.58925(11) | 0.52227(7) | 0.0186(3)    |

|      | x/a        | y/b         | z/c        | U(eq)     |
|------|------------|-------------|------------|-----------|
| C20  | 0.75336(9) | 0.53857(13) | 0.60053(8) | 0.0246(4) |
| C21  | 0.8529(10) | 0.2940(13)  | 0.3645(6)  | 0.047(4)  |
| C22  | 0.8123(6)  | 0.2133(16)  | 0.3769(4)  | 0.049(4)  |
| C23  | 0.8283(9)  | 0.1213(13)  | 0.3572(7)  | 0.053(4)  |
| C24  | 0.8868(10) | 0.1081(12)  | 0.3237(8)  | 0.048(5)  |
| C25  | 0.9281(7)  | 0.1880(14)  | 0.3110(5)  | 0.039(4)  |
| C26  | 0.9109(6)  | 0.2800(12)  | 0.3301(4)  | 0.036(3)  |
| C21A | 0.8854(13) | 0.2941(8)   | 0.3462(9)  | 0.056(5)  |
| C22A | 0.8268(12) | 0.2629(14)  | 0.3720(7)  | 0.057(6)  |
| C23A | 0.8055(11) | 0.1676(17)  | 0.3703(6)  | 0.048(4)  |
| C24A | 0.8477(12) | 0.1029(12)  | 0.3418(8)  | 0.046(4)  |
| C25A | 0.9071(11) | 0.1331(17)  | 0.3152(7)  | 0.047(6)  |
| C26A | 0.9266(8)  | 0.2299(19)  | 0.3166(8)  | 0.048(5)  |

**Table 4. Bond lengths (Å) for Harman\_16JAS17.**

|        |            |        |            |
|--------|------------|--------|------------|
| W1-N7  | 1.7747(12) | W1-N3  | 2.2030(12) |
| W1-N5  | 2.2253(13) | W1-C10 | 2.2374(14) |
| W1-N1  | 2.2500(13) | W1-C11 | 2.2534(14) |
| W1-P1  | 2.5142(4)  | P1-C18 | 1.8207(18) |
| P1-C20 | 1.8218(18) | P1-C19 | 1.8289(16) |
| F1-C16 | 1.343(2)   | F2-C16 | 1.348(2)   |
| F3-C16 | 1.351(2)   | F4-C17 | 1.357(2)   |
| F5-C17 | 1.345(2)   | F6-C17 | 1.349(2)   |
| O1-N7  | 1.2239(16) | N1-C1  | 1.3420(19) |

|          |            |          |            |
|----------|------------|----------|------------|
| N1-N2    | 1.3655(18) | N2-C3    | 1.346(2)   |
| N2-B1    | 1.545(2)   | N3-C4    | 1.3460(19) |
| N3-N4    | 1.3628(18) | N4-C6    | 1.348(2)   |
| N4-B1    | 1.538(2)   | N5-C7    | 1.3401(19) |
| N5-N6    | 1.3646(17) | N6-C9    | 1.349(2)   |
| N6-B1    | 1.543(2)   | B1-H1A   | 1.08(2)    |
| C1-C2    | 1.394(2)   | C1-H1    | 0.95       |
| C2-C3    | 1.377(2)   | C2-H2    | 0.95       |
| C3-H3    | 0.95       | C4-C5    | 1.393(2)   |
| C4-H4    | 0.95       | C5-C6    | 1.380(3)   |
| C5-H5    | 0.95       | C6-H6    | 0.95       |
| C7-C8    | 1.397(2)   | C7-H7    | 0.95       |
| C8-C9    | 1.380(2)   | C8-H8    | 0.95       |
| C9-H9    | 0.95       | C10-C15  | 1.440(2)   |
| C10-C11  | 1.463(2)   | C10-H10  | 0.94(2)    |
| C11-C12  | 1.451(2)   | C11-H11  | 0.958(19)  |
| C12-C13  | 1.357(2)   | C12-H12  | 0.95       |
| C13-C14  | 1.466(2)   | C13-C17  | 1.497(2)   |
| C14-C15  | 1.356(2)   | C14-C16  | 1.496(2)   |
| C15-H15  | 0.95       | C18-H18A | 0.98       |
| C18-H18B | 0.98       | C18-H18C | 0.98       |
| C19-H19A | 0.98       | C19-H19B | 0.98       |
| C19-H19C | 0.98       | C20-H20A | 0.98       |
| C20-H20B | 0.98       | C20-H20C | 0.98       |
| C21-C22  | 1.372(13)  | C21-C26  | 1.385(14)  |

|           |           |           |           |
|-----------|-----------|-----------|-----------|
| C21-H21   | 0.95      | C22-C23   | 1.367(13) |
| C22-H22   | 0.95      | C23-C24   | 1.380(14) |
| C23-H23   | 0.95      | C24-C25   | 1.370(14) |
| C24-H24   | 0.95      | C25-C26   | 1.369(11) |
| C25-H25   | 0.95      | C26-H26   | 0.95      |
| C21A-C22A | 1.338(18) | C21A-C26A | 1.366(13) |
| C21A-H21A | 0.95      | C22A-C23A | 1.355(14) |
| C22A-H22A | 0.95      | C23A-C24A | 1.369(16) |
| C23A-H23A | 0.95      | C24A-C25A | 1.358(16) |
| C24A-H24A | 0.95      | C25A-C26A | 1.364(15) |
| C25A-H25A | 0.95      | C26A-H26A | 0.95      |

**Table 5. Bond angles (°) for Harman\_16JAS17.**

|            |           |            |           |
|------------|-----------|------------|-----------|
| N7-W1-N3   | 91.66(5)  | N7-W1-N5   | 97.77(5)  |
| N3-W1-N5   | 77.77(5)  | N7-W1-C10  | 96.35(6)  |
| N3-W1-C10  | 158.30(5) | N5-W1-C10  | 81.17(5)  |
| N7-W1-N1   | 175.65(5) | N3-W1-N1   | 84.11(5)  |
| N5-W1-N1   | 82.37(5)  | C10-W1-N1  | 87.97(5)  |
| N7-W1-C11  | 92.87(6)  | N3-W1-C11  | 161.63(5) |
| N5-W1-C11  | 119.13(5) | C10-W1-C11 | 38.03(5)  |
| N1-W1-C11  | 90.84(5)  | N7-W1-P1   | 92.35(4)  |
| N3-W1-P1   | 83.00(3)  | N5-W1-P1   | 158.46(3) |
| C10-W1-P1  | 116.65(4) | N1-W1-P1   | 86.13(3)  |
| C11-W1-P1  | 79.05(4)  | C18-P1-C20 | 104.34(9) |
| C18-P1-C19 | 101.97(8) | C20-P1-C19 | 100.14(8) |

|           |            |           |            |
|-----------|------------|-----------|------------|
| C18-P1-W1 | 113.40(6)  | C20-P1-W1 | 113.68(6)  |
| C19-P1-W1 | 121.14(5)  | C1-N1-N2  | 106.13(12) |
| C1-N1-W1  | 133.82(11) | N2-N1-W1  | 119.77(9)  |
| C3-N2-N1  | 109.86(13) | C3-N2-B1  | 128.55(14) |
| N1-N2-B1  | 121.57(12) | C4-N3-N4  | 106.39(12) |
| C4-N3-W1  | 130.91(11) | N4-N3-W1  | 122.46(9)  |
| C6-N4-N3  | 109.98(13) | C6-N4-B1  | 129.04(14) |
| N3-N4-B1  | 119.76(12) | C7-N5-N6  | 106.51(12) |
| C7-N5-W1  | 132.33(10) | N6-N5-W1  | 120.87(9)  |
| C9-N6-N5  | 109.74(13) | C9-N6-B1  | 128.47(13) |
| N5-N6-B1  | 121.01(12) | O1-N7-W1  | 178.66(12) |
| N4-B1-N6  | 105.90(13) | N4-B1-N2  | 109.16(13) |
| N6-B1-N2  | 109.09(13) | N4-B1-H1A | 111.3(10)  |
| N6-B1-H1A | 110.4(10)  | N2-B1-H1A | 110.8(10)  |
| N1-C1-C2  | 110.58(14) | N1-C1-H1  | 124.7      |
| C2-C1-H1  | 124.7      | C3-C2-C1  | 104.84(14) |
| C3-C2-H2  | 127.6      | C1-C2-H2  | 127.6      |
| N2-C3-C2  | 108.59(15) | N2-C3-H3  | 125.7      |
| C2-C3-H3  | 125.7      | N3-C4-C5  | 110.16(15) |
| N3-C4-H4  | 124.9      | C5-C4-H4  | 124.9      |
| C6-C5-C4  | 105.24(14) | C6-C5-H5  | 127.4      |
| C4-C5-H5  | 127.4      | N4-C6-C5  | 108.23(15) |
| N4-C6-H6  | 125.9      | C5-C6-H6  | 125.9      |
| N5-C7-C8  | 110.38(14) | N5-C7-H7  | 124.8      |
| C8-C7-H7  | 124.8      | C9-C8-C7  | 104.89(14) |



|               |            |               |            |
|---------------|------------|---------------|------------|
| C9-C8-H8      | 127.6      | C7-C8-H8      | 127.6      |
| N6-C9-C8      | 108.48(14) | N6-C9-H9      | 125.8      |
| C8-C9-H9      | 125.8      | C15-C10-C11   | 117.71(13) |
| C15-C10-W1    | 118.53(10) | C11-C10-W1    | 71.58(8)   |
| C15-C10-H10   | 114.4(13)  | C11-C10-H10   | 118.6(12)  |
| W1-C10-H10    | 108.8(13)  | C12-C11-C10   | 116.68(13) |
| C12-C11-W1    | 112.84(10) | C10-C11-W1    | 70.39(8)   |
| C12-C11-H11   | 116.9(12)  | C10-C11-H11   | 118.6(12)  |
| W1-C11-H11    | 112.4(12)  | C13-C12-C11   | 123.14(14) |
| C13-C12-H12   | 118.4      | C11-C12-H12   | 118.4      |
| C12-C13-C14   | 119.36(14) | C12-C13-C17   | 118.27(14) |
| C14-C13-C17   | 122.37(14) | C15-C14-C13   | 118.95(14) |
| C15-C14-C16   | 118.28(15) | C13-C14-C16   | 122.76(15) |
| C14-C15-C10   | 123.09(14) | C14-C15-H15   | 118.5      |
| C10-C15-H15   | 118.5      | F1-C16-F2     | 105.67(14) |
| F1-C16-F3     | 105.78(15) | F2-C16-F3     | 105.36(16) |
| F1-C16-C14    | 112.48(16) | F2-C16-C14    | 113.97(15) |
| F3-C16-C14    | 112.85(14) | F5-C17-F6     | 105.98(14) |
| F5-C17-F4     | 106.05(13) | F6-C17-F4     | 104.93(14) |
| F5-C17-C13    | 113.22(14) | F6-C17-C13    | 112.18(14) |
| F4-C17-C13    | 113.79(14) | P1-C18-H18A   | 109.5      |
| P1-C18-H18B   | 109.5      | H18A-C18-H18B | 109.5      |
| P1-C18-H18C   | 109.5      | H18A-C18-H18C | 109.5      |
| H18B-C18-H18C | 109.5      | P1-C19-H19A   | 109.5      |
| P1-C19-H19B   | 109.5      | H19A-C19-H19B | 109.5      |

|                |           |                |           |
|----------------|-----------|----------------|-----------|
| P1-C19-H19C    | 109.5     | H19A-C19-H19C  | 109.5     |
| H19B-C19-H19C  | 109.5     | P1-C20-H20A    | 109.5     |
| P1-C20-H20B    | 109.5     | H20A-C20-H20B  | 109.5     |
| P1-C20-H20C    | 109.5     | H20A-C20-H20C  | 109.5     |
| H20B-C20-H20C  | 109.5     | C22-C21-C26    | 117.6(15) |
| C22-C21-H21    | 121.2     | C26-C21-H21    | 121.2     |
| C23-C22-C21    | 121.9(11) | C23-C22-H22    | 119.0     |
| C21-C22-H22    | 119.0     | C22-C23-C24    | 119.9(11) |
| C22-C23-H23    | 120.1     | C24-C23-H23    | 120.1     |
| C25-C24-C23    | 119.0(14) | C25-C24-H24    | 120.5     |
| C23-C24-H24    | 120.5     | C26-C25-C24    | 120.7(14) |
| C26-C25-H25    | 119.6     | C24-C25-H25    | 119.6     |
| C25-C26-C21    | 120.9(15) | C25-C26-H26    | 119.6     |
| C21-C26-H26    | 119.6     | C22A-C21A-C26A | 120.8(11) |
| C22A-C21A-H21A | 119.6     | C26A-C21A-H21A | 119.6     |
| C21A-C22A-C23A | 122.3(13) | C21A-C22A-H22A | 118.8     |
| C23A-C22A-H22A | 118.8     | C22A-C23A-C24A | 116.9(19) |
| C22A-C23A-H23A | 121.5     | C24A-C23A-H23A | 121.5     |
| C25A-C24A-C23A | 121.6(18) | C25A-C24A-H24A | 119.2     |
| C23A-C24A-H24A | 119.2     | C24A-C25A-C26A | 120.2(14) |
| C24A-C25A-H25A | 119.9     | C26A-C25A-H25A | 119.9     |
| C25A-C26A-C21A | 118.2(13) | C25A-C26A-H26A | 120.9     |
| C21A-C26A-H26A | 120.9     |                |           |

**Table 6. Torsion angles (°) for Harman\_16JAS17.**

|             |                 |             |                 |
|-------------|-----------------|-------------|-----------------|
| C1-N1-N2-C3 | -0.28(17)       | W1-N1-N2-C3 | 174.50(10)      |
| C1-N1-N2-B1 | -<br>178.78(14) | W1-N1-N2-B1 | -4.00(18)       |
| C4-N3-N4-C6 | -0.33(17)       | W1-N3-N4-C6 | 174.67(10)      |
| C4-N3-N4-B1 | -<br>168.86(13) | W1-N3-N4-B1 | 6.14(18)        |
| C7-N5-N6-C9 | 0.17(16)        | W1-N5-N6-C9 | -<br>174.29(10) |
| C7-N5-N6-B1 | 170.82(13)      | W1-N5-N6-B1 | -3.65(18)       |
| C6-N4-B1-N6 | -<br>110.18(17) | N3-N4-B1-N6 | 55.90(17)       |
| C6-N4-B1-N2 | 132.49(16)      | N3-N4-B1-N2 | -61.43(17)      |
| C9-N6-B1-N4 | 111.40(17)      | N5-N6-B1-N4 | -57.33(17)      |
| C9-N6-B1-N2 | -<br>131.24(16) | N5-N6-B1-N2 | 60.03(18)       |
| C3-N2-B1-N4 | -<br>118.06(17) | N1-N2-B1-N4 | 60.13(18)       |
| C3-N2-B1-N6 | 126.65(17)      | N1-N2-B1-N6 | -55.16(18)      |
| N2-N1-C1-C2 | 0.33(17)        | W1-N1-C1-C2 | -<br>173.39(11) |
| N1-C1-C2-C3 | -0.25(19)       | N1-N2-C3-C2 | 0.13(19)        |
| B1-N2-C3-C2 | 178.49(15)      | C1-C2-C3-N2 | 0.06(19)        |
| N4-N3-C4-C5 | -0.20(17)       | W1-N3-C4-C5 | -<br>174.61(11) |
| N3-C4-C5-C6 | 0.63(19)        | N3-N4-C6-C5 | 0.73(18)        |
| B1-N4-C6-C5 | 167.89(15)      | C4-C5-C6-N4 | -0.81(19)       |
| N6-N5-C7-C8 | -0.14(17)       | W1-N5-C7-C8 | 173.44(11)      |
| N5-C7-C8-C9 | 0.05(18)        | N5-N6-C9-C8 | -0.14(18)       |

|                     |                 |                     |                 |
|---------------------|-----------------|---------------------|-----------------|
| B1-N6-C9-C8         | -<br>169.89(15) | C7-C8-C9-N6         | 0.06(18)        |
| C15-C10-C11-C12     | -6.79(19)       | W1-C10-C11-C12      | 106.39(12)      |
| C15-C10-C11-W1      | -<br>113.18(13) | C10-C11-C12-C13     | -2.5(2)         |
| W1-C11-C12-C13      | 76.16(16)       | C11-C12-C13-C14     | 8.4(2)          |
| C11-C12-C13-C17     | -<br>172.25(14) | C12-C13-C14-C15     | -4.6(2)         |
| C17-C13-C14-C15     | 176.08(15)      | C12-C13-C14-C16     | 174.24(15)      |
| C17-C13-C14-C16     | -5.1(2)         | C13-C14-C15-C10     | -5.1(2)         |
| C16-C14-C15-C10     | 175.97(15)      | C11-C10-C15-C14     | 10.8(2)         |
| W1-C10-C15-C14      | -72.27(18)      | C15-C14-C16-F1      | 20.5(2)         |
| C13-C14-C16-F1      | -<br>158.39(15) | C15-C14-C16-F2      | -99.81(19)      |
| C13-C14-C16-F2      | 81.3(2)         | C15-C14-C16-F3      | 140.05(17)      |
| C13-C14-C16-F3      | -38.8(2)        | C12-C13-C17-F5      | 138.17(15)      |
| C14-C13-C17-F5      | -42.5(2)        | C12-C13-C17-F6      | 18.3(2)         |
| C14-C13-C17-F6      | -<br>162.39(14) | C12-C13-C17-F4      | -<br>100.65(17) |
| C14-C13-C17-F4      | 78.68(19)       | C26-C21-C22-C23     | 1.1(19)         |
| C21-C22-C23-C24     | -0.2(19)        | C22-C23-C24-C25     | 0.(2)           |
| C23-C24-C25-C26     | -2.(2)          | C24-C25-C26-C21     | 2.(2)           |
| C22-C21-C26-C25     | -2.2(19)        | C26A-C21A-C22A-C23A | 0.(2)           |
| C21A-C22A-C23A-C24A | 2.(2)           | C22A-C23A-C24A-C25A | -2.(3)          |
| C23A-C24A-C25A-C26A | 1.(2)           | C24A-C25A-C26A-C21A | 1.(2)           |

C22A-C21A-C26A-  
C25A -1.3(19)

**Table 7. Anisotropic atomic displacement parameters ( $\text{\AA}^2$ ) for Harman\_16JAS17.**

The anisotropic atomic displacement factor exponent takes the form: -  
 $2\pi^2 [ h^2 a^{*2} U_{11} + \dots + 2 h k a^* b^* U_{12} ]$

|    | $U_{11}$    | $U_{22}$    | $U_{33}$    | $U_{23}$    | $U_{13}$    | $U_{12}$    |
|----|-------------|-------------|-------------|-------------|-------------|-------------|
| W1 | 0.00988(2)  | 0.01025(2)  | 0.00801(2)  | -0.00033(2) | -0.00014(2) | -0.00010(2) |
| P1 | 0.01384(16) | 0.01217(16) | 0.01474(17) | 0.00092(14) | 0.00031(13) | 0.00166(13) |
| F1 | 0.0504(7)   | 0.0286(6)   | 0.0365(7)   | 0.0006(5)   | -0.0076(6)  | -0.0221(5)  |
| F2 | 0.0593(8)   | 0.0179(5)   | 0.0361(7)   | -0.0033(5)  | -0.0079(6)  | 0.0073(5)   |
| F3 | 0.0615(8)   | 0.0281(6)   | 0.0233(6)   | -0.0020(5)  | -0.0221(6)  | -0.0102(6)  |
| F4 | 0.0429(6)   | 0.0345(6)   | 0.0125(5)   | 0.0007(4)   | -0.0090(4)  | 0.0054(5)   |
| F5 | 0.0437(6)   | 0.0284(5)   | 0.0179(5)   | -0.0061(4)  | 0.0014(5)   | 0.0117(5)   |
| F6 | 0.0423(7)   | 0.0355(6)   | 0.0182(5)   | -0.0015(4)  | 0.0120(5)   | -0.0089(5)  |
| O1 | 0.0259(6)   | 0.0231(6)   | 0.0147(5)   | -0.0039(4)  | 0.0033(5)   | 0.0102(5)   |
| N1 | 0.0149(6)   | 0.0149(6)   | 0.0118(6)   | -0.0018(4)  | 0.0000(5)   | 0.0004(4)   |
| N2 | 0.0193(6)   | 0.0172(6)   | 0.0091(5)   | -0.0026(5)  | 0.0000(4)   | -0.0001(5)  |
| N3 | 0.0139(5)   | 0.0139(6)   | 0.0119(5)   | 0.0003(4)   | -0.0018(4)  | -0.0003(4)  |
| N4 | 0.0167(6)   | 0.0173(6)   | 0.0126(6)   | -0.0002(5)  | -0.0054(5)  | -0.0005(5)  |
| N5 | 0.0138(5)   | 0.0141(5)   | 0.0098(5)   | 0.0001(4)   | -0.0007(4)  | -0.0005(4)  |
| N6 | 0.0186(6)   | 0.0159(6)   | 0.0087(5)   | 0.0015(5)   | -0.0002(4)  | -0.0010(5)  |
| N7 | 0.0141(5)   | 0.0128(5)   | 0.0104(5)   | 0.0010(4)   | 0.0000(4)   | 0.0015(4)   |
| B1 | 0.0205(8)   | 0.0171(7)   | 0.0120(7)   | -0.0008(6)  | -0.0029(6)  | -0.0008(6)  |

|     | <b>U<sub>11</sub></b> | <b>U<sub>22</sub></b> | <b>U<sub>33</sub></b> | <b>U<sub>23</sub></b> | <b>U<sub>13</sub></b> | <b>U<sub>12</sub></b> |
|-----|-----------------------|-----------------------|-----------------------|-----------------------|-----------------------|-----------------------|
| C1  | 0.0173(7)             | 0.0161(7)             | 0.0168(7)             | -0.0013(6)            | 0.0020(5)             | 0.0029(5)             |
| C2  | 0.0258(8)             | 0.0211(8)             | 0.0184(8)             | -0.0061(6)            | 0.0039(6)             | 0.0042(6)             |
| C3  | 0.0256(8)             | 0.0254(8)             | 0.0117(7)             | -0.0066(6)            | 0.0010(6)             | 0.0010(6)             |
| C4  | 0.0144(6)             | 0.0154(7)             | 0.0208(8)             | 0.0010(6)             | -0.0009(5)            | 0.0007(5)             |
| C5  | 0.0143(7)             | 0.0233(8)             | 0.0297(9)             | 0.0036(7)             | -0.0064(6)            | 0.0010(6)             |
| C6  | 0.0196(7)             | 0.0233(8)             | 0.0223(8)             | 0.0011(6)             | -0.0097(6)            | -0.0006(6)            |
| C7  | 0.0170(7)             | 0.0125(6)             | 0.0150(7)             | -0.0006(5)            | -0.0006(5)            | -0.0012(5)            |
| C8  | 0.0252(8)             | 0.0151(7)             | 0.0178(7)             | 0.0020(6)             | 0.0025(6)             | -0.0036(6)            |
| C9  | 0.0243(8)             | 0.0185(7)             | 0.0126(7)             | 0.0040(5)             | 0.0016(6)             | -0.0015(6)            |
| C10 | 0.0108(6)             | 0.0190(7)             | 0.0116(6)             | 0.0008(5)             | -0.0002(5)            | -0.0003(5)            |
| C11 | 0.0124(6)             | 0.0137(6)             | 0.0126(6)             | 0.0002(5)             | -0.0012(5)            | 0.0014(5)             |
| C12 | 0.0156(6)             | 0.0154(6)             | 0.0113(6)             | 0.0023(5)             | -0.0016(5)            | 0.0013(5)             |
| C13 | 0.0189(7)             | 0.0174(7)             | 0.0102(6)             | 0.0001(5)             | -0.0019(5)            | 0.0025(5)             |
| C14 | 0.0204(7)             | 0.0147(7)             | 0.0151(7)             | 0.0005(5)             | -0.0062(6)            | -0.0023(5)            |
| C15 | 0.0137(6)             | 0.0180(7)             | 0.0164(7)             | 0.0030(6)             | -0.0034(5)            | -0.0034(5)            |
| C16 | 0.0388(10)            | 0.0186(8)             | 0.0203(8)             | 0.0012(6)             | -0.0104(7)            | -0.0056(7)            |
| C17 | 0.0298(9)             | 0.0213(8)             | 0.0127(7)             | -0.0002(6)            | -0.0015(6)            | 0.0006(6)             |
| C18 | 0.0242(8)             | 0.0212(8)             | 0.0278(9)             | 0.0045(7)             | 0.0101(7)             | -0.0001(6)            |
| C19 | 0.0206(7)             | 0.0128(6)             | 0.0224(8)             | 0.0019(6)             | -0.0010(6)            | -0.0009(5)            |
| C20 | 0.0259(8)             | 0.0176(7)             | 0.0304(9)             | 0.0017(7)             | -0.0105(7)            | -0.0063(6)            |
| C21 | 0.077(11)             | 0.039(5)              | 0.027(4)              | -0.008(4)             | -0.014(5)             | 0.019(6)              |
| C22 | 0.034(4)              | 0.086(13)             | 0.026(3)              | 0.014(8)              | 0.012(3)              | 0.011(8)              |
| C23 | 0.040(7)              | 0.061(13)             | 0.058(9)              | 0.035(8)              | -0.016(5)             | -0.021(6)             |
| C24 | 0.053(11)             | 0.035(4)              | 0.057(9)              | -0.012(5)             | -0.034(8)             | 0.017(6)              |

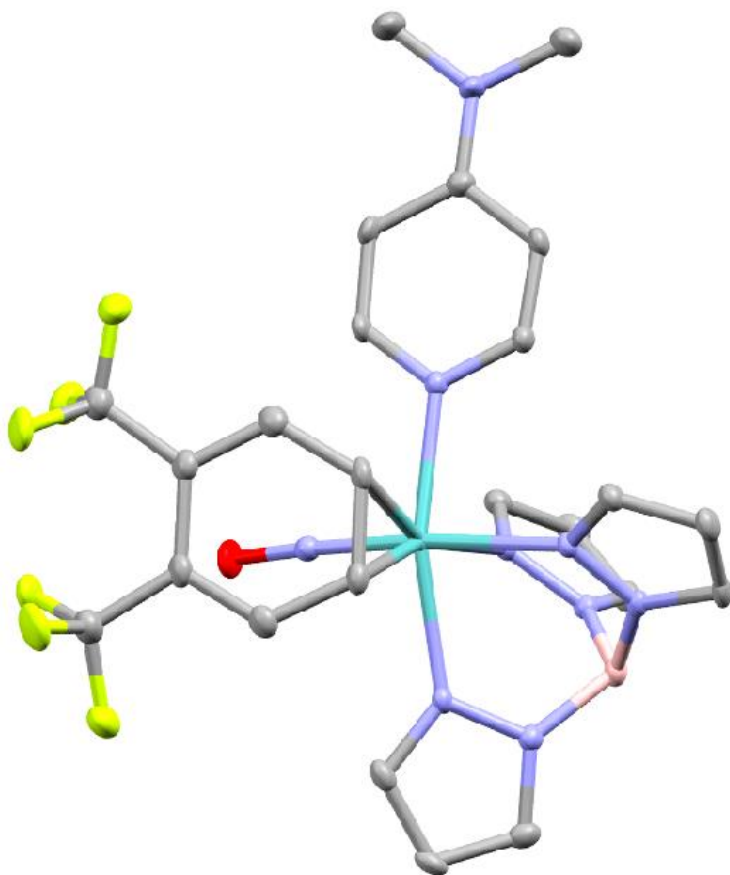
|      | <b>U<sub>11</sub></b> | <b>U<sub>22</sub></b> | <b>U<sub>33</sub></b> | <b>U<sub>23</sub></b> | <b>U<sub>13</sub></b> | <b>U<sub>12</sub></b> |
|------|-----------------------|-----------------------|-----------------------|-----------------------|-----------------------|-----------------------|
| C25  | 0.018(4)              | 0.079(12)             | 0.020(2)              | -0.006(7)             | -0.009(2)             | 0.011(7)              |
| C26  | 0.038(6)              | 0.048(7)              | 0.020(4)              | 0.013(4)              | -0.013(3)             | -0.016(5)             |
| C21A | 0.089(16)             | 0.031(4)              | 0.046(11)             | -0.001(8)             | -0.037(8)             | -0.002(10)            |
| C22A | 0.080(15)             | 0.051(10)             | 0.041(9)              | -0.020(8)             | -0.016(10)            | 0.037(8)              |
| C23A | 0.038(5)              | 0.076(13)             | 0.030(5)              | 0.019(6)              | 0.001(3)              | 0.006(6)              |
| C24A | 0.051(10)             | 0.030(3)              | 0.057(10)             | 0.009(6)              | -0.024(7)             | 0.008(6)              |
| C25A | 0.031(9)              | 0.079(18)             | 0.030(5)              | -0.023(9)             | -0.018(6)             | 0.034(8)              |
| C26A | 0.025(6)              | 0.083(14)             | 0.037(10)             | 0.023(10)             | -0.013(6)             | -0.013(10)            |

**Table 8. Hydrogen atomic coordinates and isotropic atomic displacement parameters ( $\text{\AA}^2$ ) for Harman\_16JAS17.**

|     | <b>x/a</b> | <b>y/b</b> | <b>z/c</b> | <b>U(eq)</b> |
|-----|------------|------------|------------|--------------|
| H1A | 0.6631(10) | 0.2900(13) | 0.7620(9)  | 0.017(5)     |
| H1  | 0.5448     | 0.5434     | 0.6247     | 0.02         |
| H2  | 0.5381     | 0.5966     | 0.7250     | 0.026        |
| H3  | 0.5985     | 0.4637     | 0.7801     | 0.025        |
| H4  | 0.8159     | 0.2939     | 0.5791     | 0.02         |
| H5  | 0.8891     | 0.2659     | 0.6652     | 0.027        |
| H6  | 0.8051     | 0.2758     | 0.7463     | 0.026        |
| H7  | 0.5662     | 0.0912     | 0.5904     | 0.018        |
| H8  | 0.5598     | -0.0044    | 0.6803     | 0.023        |
| H9  | 0.6039     | 0.1103     | 0.7550     | 0.022        |
| H10 | 0.4933(12) | 0.3258(15) | 0.5844(9)  | 0.027(6)     |
| H11 | 0.5405(10) | 0.4617(14) | 0.5344(9)  | 0.019(5)     |

|      | <b>x/a</b> | <b>y/b</b> | <b>z/c</b> | <b>U(eq)</b> |
|------|------------|------------|------------|--------------|
| H12  | 0.5864     | 0.4348     | 0.4435     | 0.017        |
| H15  | 0.4753     | 0.1776     | 0.5394     | 0.019        |
| H18A | 0.7936     | 0.4086     | 0.5003     | 0.037        |
| H18B | 0.7840     | 0.5201     | 0.4800     | 0.037        |
| H18C | 0.7326     | 0.4360     | 0.4568     | 0.037        |
| H19A | 0.6208     | 0.5707     | 0.4900     | 0.028        |
| H19B | 0.6831     | 0.6410     | 0.5114     | 0.028        |
| H19C | 0.6191     | 0.6137     | 0.5522     | 0.028        |
| H20A | 0.7236     | 0.5591     | 0.6319     | 0.037        |
| H20B | 0.7773     | 0.5963     | 0.5849     | 0.037        |
| H20C | 0.7886     | 0.4910     | 0.6136     | 0.037        |
| H21  | 0.8417     | 0.3573     | 0.3789     | 0.057        |
| H22  | 0.7718     | 0.2214     | 0.3999     | 0.059        |
| H23  | 0.7993     | 0.0667     | 0.3666     | 0.064        |
| H24  | 0.8983     | 0.0446     | 0.3096     | 0.058        |
| H25  | 0.9692     | 0.1794     | 0.2887     | 0.047        |
| H26  | 0.9391     | 0.3349     | 0.3197     | 0.043        |
| H21A | 0.8985     | 0.3615     | 0.3484     | 0.067        |
| H22A | 0.7992     | 0.3092     | 0.3922     | 0.068        |
| H23A | 0.7632     | 0.1467     | 0.3880     | 0.058        |
| H24A | 0.8350     | 0.0352     | 0.3407     | 0.055        |
| H25A | 0.9353     | 0.0868     | 0.2954     | 0.056        |
| H26A | 0.9677     | 0.2521     | 0.2976     | 0.058        |





### Crystal Structure Report for **Complex 24** in Chapter 6

A **orange rod-like** specimen of  $C_{24}H_{24}BF_6MoN_9O$ , approximate dimensions **0.034 mm x 0.061 mm x 0.337 mm**, was coated with Paratone oil and mounted on a MiTeGen MicroLoop. The X-ray intensity data were measured on a Bruker Kappa APEXII Duo system equipped with a fine-focus sealed tube (Mo  $K_{\alpha}$ ,  $\lambda = 0.71073 \text{ \AA}$ ) and a graphite monochromator.

The total exposure time was 5.64 hours. The frames were integrated with the Bruker SAINT software package<sup>19</sup> using a narrow-frame algorithm. The integration of the data using a **triclinic** unit cell yielded a total of **30089** reflections to a maximum  $\theta$  angle of **27.54°** (**0.77 Å** resolution), of which **6381** were independent (average redundancy **4.715**, completeness = **99.7%**,  $R_{\text{int}} = 6.75\%$ ,  $R_{\text{sig}} = 6.16\%$ ) and **5066** (**79.39%**) were greater than  $2\sigma(F^2)$ . The final cell constants of  **$a = 9.0331(6) \text{ \AA}$** ,  **$b = 11.8825(8) \text{ \AA}$** ,  **$c = 13.3782(9) \text{ \AA}$** ,  **$\alpha = 83.991(2)^\circ$** ,  **$\beta = 82.410(2)^\circ$** ,  **$\gamma = 77.201(2)^\circ$** , volume = **1383.78(16) Å<sup>3</sup>**, are based upon the refinement of the XYZ-centroids of **7982** reflections above  $20 \sigma(I)$  with  **$4.497^\circ < 2\theta < 54.98^\circ$** . Data were corrected for absorption effects using the Multi-Scan method (SADABS).<sup>1</sup> The ratio of minimum to maximum apparent transmission was **0.895**. The calculated minimum and maximum transmission coefficients (based

<sup>19</sup> Bruker (2012). *Saint*; *SADABS*; *APEX3*. Bruker AXS Inc., Madison, Wisconsin, USA.

on crystal size) are 0.8360 and 0.9810.

The structure was solved and refined using the Bruker SHELXTL Software Package<sup>20</sup> within APEX3<sup>1</sup> and OLEX2,<sup>21</sup> using the space group P -1, with Z = 2 for the formula unit, C<sub>24</sub>H<sub>24</sub>BF<sub>6</sub>MoN<sub>9</sub>O. Non-hydrogen atoms were refined anisotropically. The B-H hydrogen atom was located in the diffraction map and refined isotropically. All other hydrogen atoms were placed in geometrically calculated positions with  $U_{iso} = 1.2U_{equiv}$  of the parent atom ( $U_{iso} = 1.5U_{equiv}$  for methyl). The final anisotropic full-matrix least-squares refinement on F<sup>2</sup> with 385 variables converged at R1 = 3.88%, for the observed data and wR2 = 9.33% for all data. The goodness-of-fit was 1.023. The largest peak in the final difference electron density synthesis was 1.021 e<sup>-</sup>/Å<sup>3</sup> and the largest hole was -0.734 e<sup>-</sup>/Å<sup>3</sup> with an RMS deviation of 0.098 e<sup>-</sup>/Å<sup>3</sup>. On the basis of the final model, the calculated density was 1.621 g/cm<sup>3</sup> and F(000), 680 e<sup>-</sup>.

**Table 1. Sample and crystal data for Harman\_10JAS\_263.**

|                               |  |                |
|-------------------------------|--|----------------|
| <b>Identification code</b>    | Harman_10JAS_263   |                |
| <b>Chemical formula</b>       | C <sub>24</sub> H <sub>24</sub> BF <sub>6</sub> MoN <sub>9</sub> O |                |
| <b>Formula weight</b>         | 675.27 g/mol   |                |
| <b>Temperature</b>            | 100(2) K   |                |
| <b>Wavelength</b>             | 0.71073 Å  |                |
| <b>Crystal size</b>           | 0.034 x 0.061 x 0.337 mm   |                |
| <b>Crystal habit</b>          | orange rod   |                |
| <b>Crystal system</b>         | triclinic  |                |
| <b>Space group</b>            | P -1   |                |
| <b>Unit cell dimensions</b>   | a = 9.0331(6) Å  | α = 83.991(2)° |
|                               | b = 11.8825(8) Å   | β = 82.410(2)° |
|                               | c = 13.3782(9) Å   | γ = 77.201(2)° |
| <b>Volume</b>                 | 1383.78(16) Å <sup>3</sup>   |                |
| <b>Z</b>                      | 2  |                |
| <b>Density (calculated)</b>   | 1.621 g/cm <sup>3</sup>  |                |
| <b>Absorption coefficient</b> | 0.551 mm <sup>-1</sup>   |                |

<sup>20</sup> Sheldrick, G. M. (2015). *Acta Cryst. A* **71**, 3-8.

<sup>21</sup> Dolomanov, O. V.; Bourhis, L. J.; Gildea, R. J.; Howard, J. A. K.; Puschmann, H. *J. Appl. Cryst.* (2009). **42**, 339-341.

**F(000)** 680

**Table 2. Data collection and structure refinement for Harman\_10JAS\_263.**

|  |  |                              |
|--|--|------------------------------|
| <b>Diffractometer</b>                      | Bruker Kappa APEXII Duo  |                              |
| <b>Radiation source</b>                    | fine-focus sealed tube (Mo K $\alpha$ , $\lambda$ = 0.71073 Å) |                              |
| <b>Theta range for data collection</b>     | 1.54 to 27.54°   |                              |
| <b>Index ranges</b>                        | -11 ≤ h ≤ 11, -15 ≤ k ≤ 15, -17 ≤ l ≤ 17                       |                              |
| <b>Reflections collected</b>               | 30089  |                              |
| <b>Independent reflections</b>             | 6381 [R(int) = 0.0675]   |                              |
| <b>Coverage of independent reflections</b> | 99.7%  |                              |
| <b>Absorption correction</b>               | Multi-Scan   |                              |
| <b>Max. and min. transmission</b>          | 0.9810 and 0.8360  |                              |
| <b>Structure solution technique</b>        | direct methods   |                              |
| <b>Structure solution program</b>          | SHELXT 2014/5 (Sheldrick, 2014)                                |                              |
| <b>Refinement method</b>                   | Full-matrix least-squares on F <sup>2</sup>                    |                              |
| <b>Refinement program</b>                  | SHELXL-2018/3 (Sheldrick, 2018)                                |                              |
| <b>Function minimized</b>                  | $\Sigma w(F_o^2 - F_c^2)^2$                                    |                              |
| <b>Data / restraints / parameters</b>      | 6381 / 0 / 385   |                              |
| <b>Goodness-of-fit on F<sup>2</sup></b>    | 1.023  |                              |
| <b><math>\Delta/\sigma_{\max}</math></b>   | 0.002  |                              |
| <b>Final R indices</b>                     | 5066 data;<br>I > 2 $\sigma$ (I)                               | R1 = 0.0388, wR2 =<br>0.0856 |
|  | all data   | R1 = 0.0586, wR2 =<br>0.0933 |

|                                    |   |
|------------------------------------|---|
| <b>Weighting scheme</b>            | $w=1/[\sigma^2(F_o^2)+(0.0484P)^2]$<br>where $P=(F_o^2+2F_c^2)/3$ |
| <b>Largest diff. peak and hole</b> | 1.021 and -0.734 eÅ <sup>-3</sup>                                 |
| <b>R.M.S. deviation from mean</b>  | 0.098 eÅ <sup>-3</sup>  |

**Table 3. Atomic coordinates and equivalent isotropic atomic displacement parameters (Å<sup>2</sup>) for Harman\_10JAS\_263.**

U(eq) is defined as one third of the trace of the orthogonalized U<sub>ij</sub> tensor.

|     | <b>x/a</b> | <b>y/b</b>  | <b>z/c</b>  | <b>U(eq)</b> |
|-----|------------|-------------|-------------|--------------|
| Mo1 | 0.73324(3) | 0.59285(2)  | 0.20048(2)  | 0.01155(8)   |
| F1  | 0.7399(2)  | 0.28301(17) | 0.50758(14) | 0.0321(5)    |
| F2  | 0.9372(2)  | 0.33483(16) | 0.54578(13) | 0.0325(5)    |
| F3  | 0.9623(2)  | 0.17099(15) | 0.48406(14) | 0.0309(4)    |
| F4  | 0.7657(2)  | 0.14431(15) | 0.35421(14) | 0.0301(4)    |
| F5  | 0.9997(2)  | 0.08014(15) | 0.29606(16) | 0.0366(5)    |
| F6  | 0.8309(2)  | 0.14609(16) | 0.19404(14) | 0.0332(5)    |
| O1  | 0.5560(2)  | 0.42221(18) | 0.30316(16) | 0.0244(5)    |
| N1  | 0.8570(2)  | 0.72109(19) | 0.10522(17) | 0.0130(5)    |
| N2  | 0.7927(3)  | 0.78116(19) | 0.02310(17) | 0.0136(5)    |
| N3  | 0.5301(2)  | 0.72737(19) | 0.17014(17) | 0.0129(5)    |
| N4  | 0.5164(2)  | 0.78688(19) | 0.07791(17) | 0.0137(5)    |
| N5  | 0.7069(2)  | 0.54544(19) | 0.04875(17) | 0.0129(5)    |
| N6  | 0.6688(3)  | 0.6298(2)   | 0.97287(17) | 0.0142(5)    |
| N7  | 0.6278(3)  | 0.4936(2)   | 0.26367(17) | 0.0145(5)    |
| N8  | 0.7074(3)  | 0.6932(2)   | 0.33470(17) | 0.0137(5)    |

|     | <b>x/a</b> | <b>y/b</b> | <b>z/c</b>  | <b>U(eq)</b> |
|-----|------------|------------|-------------|--------------|
| N9  | 0.6485(3)  | 0.8892(2)  | 0.58635(18) | 0.0229(6)    |
| C1  | 0.9821(3)  | 0.7619(2)  | 0.1113(2)   | 0.0156(6)    |
| C2  | 0.9995(3)  | 0.8478(2)  | 0.0342(2)   | 0.0191(6)    |
| C3  | 0.8779(3)  | 0.8573(2)  | 0.9804(2)   | 0.0165(6)    |
| C4  | 0.4034(3)  | 0.7699(2)  | 0.2298(2)   | 0.0160(6)    |
| C5  | 0.3081(3)  | 0.8576(2)  | 0.1767(2)   | 0.0193(6)    |
| C6  | 0.3844(3)  | 0.8652(2)  | 0.0807(2)   | 0.0189(6)    |
| C7  | 0.7065(3)  | 0.4457(2)  | 0.0122(2)   | 0.0171(6)    |
| C8  | 0.6696(3)  | 0.4625(2)  | 0.9137(2)   | 0.0172(6)    |
| C9  | 0.6463(3)  | 0.5803(3)  | 0.8918(2)   | 0.0173(6)    |
| C10 | 0.9548(3)  | 0.5131(2)  | 0.2661(2)   | 0.0175(6)    |
| C11 | 0.9537(3)  | 0.4586(2)  | 0.1755(2)   | 0.0162(6)    |
| C12 | 0.9334(3)  | 0.3415(2)  | 0.1882(2)   | 0.0189(6)    |
| C13 | 0.9058(3)  | 0.2844(2)  | 0.2804(2)   | 0.0175(6)    |
| C14 | 0.9122(3)  | 0.3394(2)  | 0.3710(2)   | 0.0185(6)    |
| C15 | 0.9412(3)  | 0.4477(3)  | 0.3615(2)   | 0.0197(6)    |
| C16 | 0.8873(4)  | 0.2829(3)  | 0.4762(2)   | 0.0243(7)    |
| C17 | 0.8753(4)  | 0.1660(3)  | 0.2817(2)   | 0.0248(7)    |
| C18 | 0.6635(3)  | 0.6513(2)  | 0.4292(2)   | 0.0163(6)    |
| C19 | 0.6436(3)  | 0.7111(2)  | 0.5138(2)   | 0.0188(6)    |
| C20 | 0.6675(3)  | 0.8256(3)  | 0.5053(2)   | 0.0179(6)    |
| C21 | 0.7112(3)  | 0.8701(2)  | 0.4070(2)   | 0.0172(6)    |
| C22 | 0.7283(3)  | 0.8028(2)  | 0.3270(2)   | 0.0154(6)    |
| C23 | 0.6899(4)  | 0.0020(3)  | 0.5743(2)   | 0.0233(7)    |
| C24 | 0.6255(4)  | 0.8360(3)  | 0.6883(2)   | 0.0311(8)    |

|    | <b>x/a</b> | <b>y/b</b> | <b>z/c</b> | <b>U(eq)</b> |
|----|------------|------------|------------|--------------|
| B1 | 0.6455(4)  | 0.7578(3)  | 0.9903(2)  | 0.0153(7)    |

**Table 4. Bond lengths (Å) for Harman\_10JAS\_263.**

|         |          |         |          |
|---------|----------|---------|----------|
| Mo1-N7  | 1.757(2) | Mo1-N3  | 2.202(2) |
| Mo1-N8  | 2.217(2) | Mo1-N5  | 2.218(2) |
| Mo1-C10 | 2.264(3) | Mo1-C11 | 2.270(3) |
| Mo1-N1  | 2.274(2) | F1-C16  | 1.342(4) |
| F2-C16  | 1.343(4) | F3-C16  | 1.352(3) |
| F4-C17  | 1.340(3) | F5-C17  | 1.359(4) |
| F6-C17  | 1.348(4) | O1-N7   | 1.217(3) |
| N1-C1   | 1.339(3) | N1-N2   | 1.369(3) |
| N2-C3   | 1.349(3) | N2-B1   | 1.543(4) |
| N3-C4   | 1.338(3) | N3-N4   | 1.363(3) |
| N4-C6   | 1.339(3) | N4-B1   | 1.549(4) |
| N5-C7   | 1.329(3) | N5-N6   | 1.371(3) |
| N6-C9   | 1.345(4) | N6-B1   | 1.527(4) |
| N8-C22  | 1.350(3) | N8-C18  | 1.351(3) |
| N9-C20  | 1.358(4) | N9-C24  | 1.452(4) |
| N9-C23  | 1.456(4) | C1-C2   | 1.393(4) |
| C1-H1   | 0.95     | C2-C3   | 1.370(4) |
| C2-H2   | 0.95     | C3-H3   | 0.95     |
| C4-C5   | 1.393(4) | C4-H4   | 0.95     |
| C5-C6   | 1.379(4) | C5-H5   | 0.95     |
| C6-H6   | 0.95     | C7-C8   | 1.385(4) |

|          |          |          |          |
|----------|----------|----------|----------|
| C7-H7    | 0.95     | C8-C9    | 1.374(4) |
| C8-H8    | 0.95     | C9-H9    | 0.95     |
| C10-C15  | 1.429(4) | C10-C11  | 1.435(4) |
| C10-H10  | 0.95     | C11-C12  | 1.433(4) |
| C11-H11  | 0.95     | C12-C13  | 1.365(4) |
| C12-H12  | 0.95     | C13-C14  | 1.449(4) |
| C13-C17  | 1.490(4) | C14-C15  | 1.359(4) |
| C14-C16  | 1.506(4) | C15-H15  | 0.95     |
| C18-C19  | 1.370(4) | C18-H18  | 0.95     |
| C19-C20  | 1.414(4) | C19-H19  | 0.95     |
| C20-C21  | 1.405(4) | C21-C22  | 1.374(4) |
| C21-H21  | 0.95     | C22-H22  | 0.95     |
| C23-H23A | 0.98     | C23-H23B | 0.98     |
| C23-H23C | 0.98     | C24-H24A | 0.98     |
| C24-H24B | 0.98     | C24-H24C | 0.98     |
| B1-H1A   | 1.07(3)  |          |          |

**Table 5. Bond angles (°) for Harman\_10JAS\_263.**

|            |           |            |           |
|------------|-----------|------------|-----------|
| N7-Mo1-N3  | 94.46(9)  | N7-Mo1-N8  | 93.29(9)  |
| N3-Mo1-N8  | 79.79(8)  | N7-Mo1-N5  | 93.17(9)  |
| N3-Mo1-N5  | 81.84(8)  | N8-Mo1-N5  | 160.94(8) |
| N7-Mo1-C10 | 96.47(10) | N3-Mo1-C10 | 156.85(9) |
| N8-Mo1-C10 | 79.26(9)  | N5-Mo1-C10 | 117.75(9) |
| N7-Mo1-C11 | 94.56(10) | N3-Mo1-C11 | 161.14(9) |
| N8-Mo1-C11 | 116.15(9) | N5-Mo1-C11 | 81.15(9)  |

|             |            |            |            |
|-------------|------------|------------|------------|
| C10-Mo1-C11 | 36.90(10)  | N7-Mo1-N1  | 174.30(9)  |
| N3-Mo1-N1   | 82.56(8)   | N8-Mo1-N1  | 90.97(8)   |
| N5-Mo1-N1   | 81.62(8)   | C10-Mo1-N1 | 88.05(9)   |
| C11-Mo1-N1  | 86.96(9)   | C1-N1-N2   | 106.0(2)   |
| C1-N1-Mo1   | 135.45(19) | N2-N1-Mo1  | 118.45(16) |
| C3-N2-N1    | 109.5(2)   | C3-N2-B1   | 128.8(2)   |
| N1-N2-B1    | 121.7(2)   | C4-N3-N4   | 106.3(2)   |
| C4-N3-Mo1   | 131.54(19) | N4-N3-Mo1  | 122.14(16) |
| C6-N4-N3    | 110.0(2)   | C6-N4-B1   | 130.6(2)   |
| N3-N4-B1    | 119.4(2)   | C7-N5-N6   | 106.0(2)   |
| C7-N5-Mo1   | 133.29(19) | N6-N5-Mo1  | 120.39(16) |
| C9-N6-N5    | 109.2(2)   | C9-N6-B1   | 129.6(2)   |
| N5-N6-B1    | 121.0(2)   | O1-N7-Mo1  | 176.8(2)   |
| C22-N8-C18  | 115.1(2)   | C22-N8-Mo1 | 122.04(18) |
| C18-N8-Mo1  | 122.78(18) | C20-N9-C24 | 120.5(3)   |
| C20-N9-C23  | 119.8(2)   | C24-N9-C23 | 117.8(2)   |
| N1-C1-C2    | 110.9(3)   | N1-C1-H1   | 124.6      |
| C2-C1-H1    | 124.6      | C3-C2-C1   | 104.8(3)   |
| C3-C2-H2    | 127.6      | C1-C2-H2   | 127.6      |
| N2-C3-C2    | 108.9(2)   | N2-C3-H3   | 125.6      |
| C2-C3-H3    | 125.6      | N3-C4-C5   | 110.4(3)   |
| N3-C4-H4    | 124.8      | C5-C4-H4   | 124.8      |
| C6-C5-C4    | 104.8(2)   | C6-C5-H5   | 127.6      |
| C4-C5-H5    | 127.6      | N4-C6-C5   | 108.5(2)   |
| N4-C6-H6    | 125.7      | C5-C6-H6   | 125.7      |
| N5-C7-C8    | 111.5(3)   | N5-C7-H7   | 124.3      |



|             |            |             |           |
|-------------|------------|-------------|-----------|
| C8-C7-H7    | 124.3      | C9-C8-C7    | 104.3(3)  |
| C9-C8-H8    | 127.8      | C7-C8-H8    | 127.8     |
| N6-C9-C8    | 109.0(3)   | N6-C9-H9    | 125.5     |
| C8-C9-H9    | 125.5      | C15-C10-C11 | 119.0(3)  |
| C15-C10-Mo1 | 116.0(2)   | C11-C10-Mo1 | 71.78(15) |
| C15-C10-H10 | 120.5      | C11-C10-H10 | 120.5     |
| Mo1-C10-H10 | 82.9       | C12-C11-C10 | 116.6(3)  |
| C12-C11-Mo1 | 113.97(18) | C10-C11-Mo1 | 71.32(15) |
| C12-C11-H11 | 121.7      | C10-C11-H11 | 121.7     |
| Mo1-C11-H11 | 85.3       | C13-C12-C11 | 123.4(3)  |
| C13-C12-H12 | 118.3      | C11-C12-H12 | 118.3     |
| C12-C13-C14 | 119.0(3)   | C12-C13-C17 | 117.4(3)  |
| C14-C13-C17 | 123.5(3)   | C15-C14-C13 | 118.9(3)  |
| C15-C14-C16 | 117.7(3)   | C13-C14-C16 | 123.3(3)  |
| C14-C15-C10 | 122.6(3)   | C14-C15-H15 | 118.7     |
| C10-C15-H15 | 118.7      | F1-C16-F2   | 106.1(3)  |
| F1-C16-F3   | 106.2(2)   | F2-C16-F3   | 105.7(2)  |
| F1-C16-C14  | 113.2(2)   | F2-C16-C14  | 112.7(3)  |
| F3-C16-C14  | 112.3(3)   | F4-C17-F6   | 105.9(2)  |
| F4-C17-F5   | 105.8(2)   | F6-C17-F5   | 104.8(2)  |
| F4-C17-C13  | 113.5(3)   | F6-C17-C13  | 112.7(3)  |
| F5-C17-C13  | 113.5(3)   | N8-C18-C19  | 124.6(3)  |
| N8-C18-H18  | 117.7      | C19-C18-H18 | 117.7     |
| C18-C19-C20 | 120.0(3)   | C18-C19-H19 | 120.0     |
| C20-C19-H19 | 120.0      | N9-C20-C21  | 121.8(3)  |
| N9-C20-C19  | 122.5(3)   | C21-C20-C19 | 115.7(3)  |

|                   |           |                   |           |
|-------------------|-----------|-------------------|-----------|
| C22-C21-C20       | 119.9(3)  | C22-C21-H21       | 120.1     |
| C20-C21-H21       | 120.1     | N8-C22-C21        | 124.7(3)  |
| N8-C22-H22        | 117.6     | C21-C22-H22       | 117.6     |
| N9-C23-H23A       | 109.5     | N9-C23-H23B       | 109.5     |
| H23A-C23-<br>H23B | 109.5     | N9-C23-H23C       | 109.5     |
| H23A-C23-<br>H23C | 109.5     | H23B-C23-<br>H23C | 109.5     |
| N9-C24-H24A       | 109.5     | N9-C24-H24B       | 109.5     |
| H24A-C24-<br>H24B | 109.5     | N9-C24-H24C       | 109.5     |
| H24A-C24-<br>H24C | 109.5     | H24B-C24-<br>H24C | 109.5     |
| N6-B1-N2          | 109.5(2)  | N6-B1-N4          | 108.8(2)  |
| N2-B1-N4          | 107.6(2)  | N6-B1-H1A         | 109.6(16) |
| N2-B1-H1A         | 110.0(15) | N4-B1-H1A         | 111.4(16) |

**Table 6. Torsion angles (°) for Harman\_10JAS\_263.**

|             |                       |              |                         |
|-------------|-----------------------|--------------|-------------------------|
| C1-N1-N2-C3 | -0.1(3)               | Mo1-N1-N2-C3 | 176.35(17)              |
| C1-N1-N2-B1 | 179.4(2)              | Mo1-N1-N2-B1 | -4.1(3)                 |
| C4-N3-N4-C6 | 0.4(3)                | Mo1-N3-N4-C6 | <sup>-</sup> 178.38(18) |
| C4-N3-N4-B1 | <sup>-</sup> 179.7(2) | Mo1-N3-N4-B1 | 1.4(3)                  |
| C7-N5-N6-C9 | -0.2(3)               | Mo1-N5-N6-C9 | <sup>-</sup> 174.53(17) |
| C7-N5-N6-B1 | 175.1(2)              | Mo1-N5-N6-B1 | 0.8(3)                  |
| N2-N1-C1-C2 | 0.1(3)                | Mo1-N1-C1-C2 | <sup>-</sup> 175.45(19) |

|                     |               |                     |            |
|---------------------|---------------|---------------------|------------|
| N1-C1-C2-C3         | 0.0(3)        | N1-N2-C3-C2         | 0.1(3)     |
| B1-N2-C3-C2         | -<br>179.4(3) | C1-C2-C3-N2         | 0.0(3)     |
| N4-N3-C4-C5         | -0.5(3)       | Mo1-N3-C4-C5        | 178.18(18) |
| N3-C4-C5-C6         | 0.3(3)        | N3-N4-C6-C5         | -0.2(3)    |
| B1-N4-C6-C5         | 180.0(3)      | C4-C5-C6-N4         | -0.1(3)    |
| N6-N5-C7-C8         | 0.3(3)        | Mo1-N5-C7-C8        | 173.57(19) |
| N5-C7-C8-C9         | -0.3(3)       | N5-N6-C9-C8         | 0.0(3)     |
| B1-N6-C9-C8         | -<br>174.8(3) | C7-C8-C9-N6         | 0.1(3)     |
| C15-C10-C11-<br>C12 | 2.1(4)        | Mo1-C10-C11-<br>C12 | -108.1(2)  |
| C15-C10-C11-<br>Mo1 | 110.2(3)      | C10-C11-C12-<br>C13 | 4.4(4)     |
| Mo1-C11-C12-<br>C13 | -75.9(3)      | C11-C12-C13-<br>C14 | -6.5(4)    |
| C11-C12-C13-<br>C17 | 175.5(3)      | C12-C13-C14-<br>C15 | 1.9(4)     |
| C17-C13-C14-<br>C15 | 179.8(3)      | C12-C13-C14-<br>C16 | -178.5(3)  |
| C17-C13-C14-<br>C16 | -0.6(4)       | C13-C14-C15-<br>C10 | 4.7(4)     |
| C16-C14-C15-<br>C10 | -<br>175.0(3) | C11-C10-C15-<br>C14 | -6.7(4)    |
| Mo1-C10-C15-<br>C14 | 76.0(3)       | C15-C14-C16-<br>F1  | 103.7(3)   |
| C13-C14-C16-<br>F1  | -75.9(4)      | C15-C14-C16-<br>F2  | -16.7(4)   |
| C13-C14-C16-<br>F2  | 163.6(3)      | C15-C14-C16-<br>F3  | -136.0(3)  |

|                |           |                 |           |
|----------------|-----------|-----------------|-----------|
| C13-C14-C16-F3 | 44.4(4)   | C12-C13-C17-F4  | -140.6(3) |
| C14-C13-C17-F4 | 41.5(4)   | C12-C13-C17-F6  | -20.2(4)  |
| C14-C13-C17-F6 | 161.8(3)  | C12-C13-C17-F5  | 98.6(3)   |
| C14-C13-C17-F5 | -79.3(4)  | C22-N8-C18-C19  | -1.5(4)   |
| Mo1-N8-C18-C19 | -178.8(2) | N8-C18-C19-C20  | 0.9(5)    |
| C24-N9-C20-C21 | -170.9(3) | C23-N9-C20-C21  | -6.8(4)   |
| C24-N9-C20-C19 | 9.7(5)    | C23-N9-C20-C19  | 173.7(3)  |
| C18-C19-C20-N9 | 179.5(3)  | C18-C19-C20-C21 | 0.0(4)    |
| N9-C20-C21-C22 | -179.6(3) | C19-C20-C21-C22 | -0.1(4)   |
| C18-N8-C22-C21 | 1.4(4)    | Mo1-N8-C22-C21  | 178.7(2)  |
| C20-C21-C22-N8 | -0.6(4)   | C9-N6-B1-N2     | -127.4(3) |
| N5-N6-B1-N2    | 58.4(3)   | C9-N6-B1-N4     | 115.3(3)  |
| N5-N6-B1-N4    | -58.9(3)  | C3-N2-B1-N6     | 123.6(3)  |
| N1-N2-B1-N6    | -55.8(3)  | C3-N2-B1-N4     | -118.3(3) |
| N1-N2-B1-N4    | 62.3(3)   | C6-N4-B1-N6     | -122.7(3) |
| N3-N4-B1-N6    | 57.6(3)   | C6-N4-B1-N2     | 118.8(3)  |
| N3-N4-B1-N2    | -60.9(3)  |                 |           |

**Table 7. Anisotropic atomic displacement parameters ( $\text{\AA}^2$ ) for Harman\_10JAS\_263.**

The anisotropic atomic displacement factor exponent takes the form:  $-2\pi^2 [ h^2 a^{*2} U_{11} + \dots + 2 h k a^* b^* U_{12} ]$

|     | U <sub>11</sub> | U <sub>22</sub> | U <sub>33</sub> | U <sub>23</sub> | U <sub>13</sub> | U <sub>12</sub> |
|-----|-----------------|-----------------|-----------------|-----------------|-----------------|-----------------|
| Mo1 | 0.01429(13)     | 0.00855(12)     | 0.01224(12)     | 0.00063(8)      | 0.00021(8)      | 0.00475(8)      |
| F1  | 0.0310(11)      | 0.0381(12)      | 0.0261(10)      | 0.0054(9)       | 0.0031(8)       | -0.0122(9)      |
| F2  | 0.0522(13)      | 0.0283(11)      | 0.0219(10)      | 0.0020(8)       | -0.0136(9)      | -0.0152(9)      |
| F3  | 0.0406(11)      | 0.0171(9)       | 0.0331(11)      | 0.0103(8)       | -0.0096(9)      | -0.0042(8)      |
| F4  | 0.0429(11)      | 0.0232(10)      | 0.0272(10)      | 0.0028(8)       | 0.0029(9)       | -0.0196(9)      |
| F5  | 0.0444(12)      | 0.0127(9)       | 0.0493(13)      | 0.0008(9)       | 0.0065(10)      | 0.0005(8)       |
| F6  | 0.0534(13)      | 0.0259(10)      | 0.0257(10)      | -0.0035(8)      | -0.0028(9)      | -0.0204(9)      |
| O1  | 0.0270(12)      | 0.0239(12)      | 0.0253(12)      | 0.0055(9)       | 0.0013(9)       | 0.0174(10)      |
| N1  | 0.0147(12)      | 0.0119(12)      | 0.0135(12)      | 0.0004(9)       | -0.0012(9)      | -0.0058(9)      |
| N2  | 0.0152(12)      | 0.0116(12)      | 0.0125(11)      | 0.0011(9)       | 0.0011(9)       | -0.0025(9)      |
| N3  | 0.0146(11)      | 0.0117(12)      | 0.0134(12)      | -0.0024(9)      | -0.0005(9)      | -0.0048(9)      |
| N4  | 0.0154(12)      | 0.0133(12)      | 0.0127(11)      | -0.0002(9)      | -0.0026(9)      | -0.0038(9)      |
| N5  | 0.0142(11)      | 0.0110(11)      | 0.0136(12)      | 0.0006(9)       | 0.0004(9)       | -0.0045(9)      |
| N6  | 0.0146(12)      | 0.0155(12)      | 0.0134(12)      | -0.0001(9)      | -0.0008(9)      | -0.0059(9)      |
| N7  | 0.0162(12)      | 0.0153(12)      | 0.0125(12)      | 0.0013(10)      | -0.0009(9)      | 0.0047(10)      |
| N8  | 0.0163(12)      | 0.0134(12)      | 0.0122(11)      | 0.0000(9)       | -0.0005(9)      | -0.0056(9)      |
| N9  | 0.0417(16)      | 0.0198(13)      | 0.0095(12)      | 0.0021(10)      | 0.0008(11)      | 0.0130(12)      |
| C1  | 0.0162(14)      | 0.0141(14)      | 0.0173(14)      | 0.0014(11)      | 0.0016(11)      | 0.0054(11)      |
| C2  | 0.0200(15)      | 0.0153(15)      | 0.0226(16)      | 0.0005(12)      | 0.0027(12)      | 0.0088(12)      |

|     | <b>U<sub>11</sub></b> | <b>U<sub>22</sub></b> | <b>U<sub>33</sub></b> | <b>U<sub>23</sub></b> | <b>U<sub>13</sub></b> | <b>U<sub>12</sub></b> |
|-----|-----------------------|-----------------------|-----------------------|-----------------------|-----------------------|-----------------------|
| C3  | 0.0208(15)            | 0.0100(13)            | 0.0170(14)            | 0.0017(11)            | 0.0031(11)            | 0.0043(11)            |
| C4  | 0.0186(14)            | 0.0157(14)            | 0.0148(14)            | 0.0028(11)            | 0.0003(11)            | 0.0062(11)            |
| C5  | 0.0122(14)            | 0.0188(15)            | 0.0271(17)            | 0.0066(13)            | 0.0016(12)            | 0.0017(12)            |
| C6  | 0.0177(14)            | 0.0146(15)            | 0.0243(16)            | 0.0002(12)            | 0.0061(12)            | 0.0016(11)            |
| C7  | 0.0154(14)            | 0.0117(14)            | 0.0244(16)            | 0.0028(12)            | 0.0006(12)            | 0.0044(11)            |
| C8  | 0.0150(14)            | 0.0173(15)            | 0.0216(15)            | 0.0096(12)            | 0.0001(11)            | 0.0057(11)            |
| C9  | 0.0153(14)            | 0.0245(16)            | 0.0127(14)            | 0.0034(12)            | 0.0004(11)            | 0.0054(12)            |
| C10 | 0.0181(14)            | 0.0114(14)            | 0.0222(15)            | 0.0037(12)            | 0.0027(12)            | 0.0032(11)            |
| C11 | 0.0146(14)            | 0.0141(14)            | 0.0191(15)            | 0.0036(11)            | 0.0006(11)            | 0.0039(11)            |
| C12 | 0.0175(15)            | 0.0150(15)            | 0.0231(16)            | 0.0025(12)            | 0.0000(12)            | 0.0016(12)            |
| C13 | 0.0163(14)            | 0.0127(14)            | 0.0217(15)            | 0.0026(12)            | 0.0015(11)            | 0.0016(11)            |
| C14 | 0.0198(15)            | 0.0162(15)            | 0.0188(15)            | 0.0019(12)            | 0.0035(12)            | 0.0027(12)            |
| C15 | 0.0197(15)            | 0.0187(15)            | 0.0207(15)            | 0.0006(12)            | 0.0051(12)            | 0.0029(12)            |
| C16 | 0.0279(17)            | 0.0210(16)            | 0.0244(17)            | 0.0017(13)            | 0.0046(13)            | 0.0062(13)            |
| C17 | 0.0310(18)            | 0.0190(16)            | 0.0242(17)            | 0.0014(13)            | 0.0002(13)            | 0.0072(13)            |
| C18 | 0.0221(15)            | 0.0125(14)            | 0.0162(14)            | 0.0019(11)            | 0.0015(11)            | 0.0094(12)            |

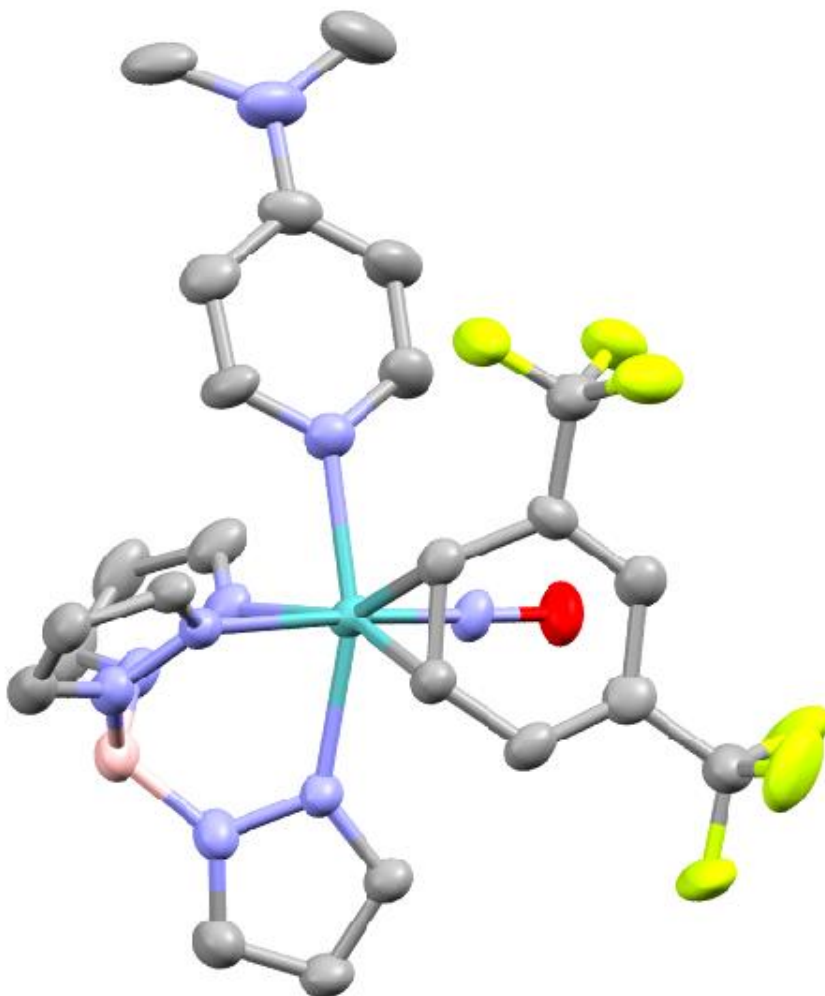
|     | U <sub>11</sub> | U <sub>22</sub> | U <sub>33</sub> | U <sub>23</sub> | U <sub>13</sub> | U <sub>12</sub> |
|-----|-----------------|-----------------|-----------------|-----------------|-----------------|-----------------|
| C19 | 0.0260(16)      | 0.0186(15)      | 0.0126(14)      | 0.0046(12)      | 0.0003(12)      | 0.0105(12)      |
| C20 | 0.0212(15)      | 0.0197(15)      | 0.0137(14)      | 0.0014(12)      | 0.0019(11)      | 0.0061(12)      |
| C21 | 0.0231(15)      | 0.0104(14)      | 0.0183(15)      | 0.0005(11)      | 0.0001(12)      | 0.0060(11)      |
| C22 | 0.0186(14)      | 0.0142(14)      | 0.0142(14)      | 0.0011(11)      | 0.0008(11)      | 0.0068(11)      |
| C23 | 0.0325(18)      | 0.0184(16)      | 0.0193(16)      | 0.0056(13)      | 0.0014(13)      | 0.0052(13)      |
| C24 | 0.054(2)        | 0.0293(18)      | 0.0135(15)      | 0.0026(13)      | 0.0002(15)      | 0.0180(16)      |
| B1  | 0.0160(16)      | 0.0129(16)      | 0.0154(16)      | 0.0016(13)      | 0.0005(12)      | 0.0024(12)      |

**Table 8. Hydrogen atomic coordinates and isotropic atomic displacement parameters (Å<sup>2</sup>) for Harman\_10JAS\_263.**

|    | x/a    | y/b    | z/c     | U(eq) |
|----|--------|--------|---------|-------|
| H1 | 1.0499 | 0.7357 | 0.1615  | 0.019 |
| H2 | 1.0784 | 0.8904 | 0.0216  | 0.023 |
| H3 | 0.8569 | 0.9090 | -0.0776 | 0.02  |
| H4 | 0.3815 | 0.7440 | 0.2987  | 0.019 |
| H5 | 0.2118 | 0.9023 | 0.2012  | 0.023 |
| H6 | 0.3493 | 0.9173 | 0.0258  | 0.023 |
| H7 | 0.7287 | 0.3723 | 0.0489  | 0.021 |
| H8 | 0.6620 | 0.4054 | -0.1290 | 0.021 |
| H9 | 0.6188 | 0.6202 | -0.1705 | 0.021 |

|      | <b>x/a</b> | <b>y/b</b> | <b>z/c</b> | <b>U(eq)</b> |
|------|------------|------------|------------|--------------|
| H10  | 0.9644     | 0.5914     | 0.2627     | 0.021        |
| H11  | 0.9659     | 0.4981     | 0.1104     | 0.019        |
| H12  | 0.9395     | 0.3015     | 0.1294     | 0.023        |
| H15  | 0.9530     | 0.4812     | 0.4206     | 0.024        |
| H18  | 0.6451     | 0.5750     | 0.4375     | 0.02         |
| H19  | 0.6138     | 0.6758     | 0.5781     | 0.023        |
| H21  | 0.7289     | 0.9465     | 0.3959     | 0.021        |
| H22  | 0.7570     | 0.8360     | 0.2615     | 0.018        |
| H23A | 0.8002     | 0.9922     | 0.5545     | 0.035        |
| H23B | 0.6627     | 1.0386     | 0.6384     | 0.035        |
| H23C | 0.6347     | 1.0510     | 0.5217     | 0.035        |
| H24A | 0.5391     | 0.7974     | 0.6941     | 0.047        |
| H24B | 0.6039     | 0.8957     | 0.7367     | 0.047        |
| H24C | 0.7179     | 0.7790     | 0.7031     | 0.047        |
| H1A  | 0.618(3)   | 0.810(2)   | -0.078(2)  | 0.017(8)     |





### Crystal Structure Report for **25A** in Chapter 6

A **red needle-like** specimen of  $C_{24}H_{24}BF_6MoN_9O$ , approximate dimensions **0.039 mm** x **0.056 mm** x **0.340 mm**, was coated with Paratone oil and mounted on a MiTeGen MicroLoop. The X-ray intensity data were measured on a Bruker Kappa APEXII Duo system equipped with a Incoatec Microfocus  $\mu S$  ( $Cu K\alpha$ ,  $\lambda = 1.54178 \text{ \AA}$ ) and a multilayer mirror monochromator.

The total exposure time was 7.87 hours. The frames were integrated with the Bruker SAINT software package<sup>22</sup> using a narrow-frame algorithm. The integration of the data using a **monoclinic** unit cell yielded a total of **16488** reflections to a maximum  $\theta$  angle of **68.39°** (**0.83 Å** resolution), of which **5075**

<sup>22</sup> Bruker (2012). *Saint*; *SADABS*; *APEX3*. Bruker AXS Inc., Madison, Wisconsin, USA.

were independent (average redundancy 3.249, completeness = 99.6%,  $R_{int} = 9.88\%$ ,  $R_{sig} = 9.63\%$ ) and 3569 (70.33%) were greater than  $2\sigma(F^2)$ . The final cell constants of  $a = 10.4814(9)$  Å,  $b = 17.2053(16)$  Å,  $c = 15.4790(13)$  Å,  $\beta = 96.511(6)^\circ$ , volume = 2773.4(4) Å<sup>3</sup>, are based upon the refinement of the XYZ-centroids of 2879 reflections above  $20\sigma(I)$  with  $7.710^\circ < 2\theta < 136.4^\circ$ . Data were corrected for absorption effects using the Multi-Scan method (SADABS).<sup>1</sup> The ratio of minimum to maximum apparent transmission was 0.799. The calculated minimum and maximum transmission coefficients (based on crystal size) are 0.3060 and 0.8420.

The structure was solved and refined using the Bruker SHELXTL Software Package<sup>23</sup> within APEX3<sup>1</sup> and OLEX2,<sup>24</sup> using the space group  $P 2_1/n$ , with  $Z = 4$  for the formula unit, C<sub>24</sub>H<sub>24</sub>BF<sub>6</sub>MoN<sub>9</sub>O. Non-hydrogen atoms were refined anisotropically. The B-H hydrogen atom was located in the diffraction map and refined isotropically. All other hydrogen atoms were placed in geometrically calculated positions with  $U_{iso} = 1.2U_{equiv}$  of the parent atom ( $U_{iso} = 1.5 U_{equiv}$  for methyl). One CF<sub>3</sub> group was found to be disordered over three positions. The relative occupancies of the three positions converged at 0.60675/0.21058/0.18243, and the constraints were used on the anisotropic displacement parameters of the disordered atoms. The final anisotropic full-matrix least-squares refinement on  $F^2$  with 406 variables converged at  $R1 = 5.48\%$ , for the observed data and  $wR2 = 14.31\%$  for all data. The goodness-of-fit was 1.005. The largest peak in the final difference electron density synthesis was 0.882 e<sup>-</sup>/Å<sup>3</sup> and the largest hole was -0.660 e<sup>-</sup>/Å<sup>3</sup> with an RMS deviation of 0.103 e<sup>-</sup>/Å<sup>3</sup>. On the basis of the final model, the calculated density was 1.617 g/cm<sup>3</sup> and  $F(000)$ , 1360 e<sup>-</sup>.

**Table 1. Sample and crystal data for Harman\_14JAS\_203.**

|                             |  |                           |
|-----------------------------|--|---------------------------|
| <b>Identification code</b>  | Harman_14JAS_203   |                           |
| <b>Chemical formula</b>     | C <sub>24</sub> H <sub>24</sub> BF <sub>6</sub> MoN <sub>9</sub> O |                           |
| <b>Formula weight</b>       | 675.27 g/mol   |                           |
| <b>Temperature</b>          | 100(2) K   |                           |
| <b>Wavelength</b>           | 1.54178 Å  |                           |
| <b>Crystal size</b>         | 0.039 x 0.056 x 0.340 mm   |                           |
| <b>Crystal habit</b>        | red needle   |                           |
| <b>Crystal system</b>       | monoclinic   |                           |
| <b>Space group</b>          | $P 2_1/n$  |                           |
| <b>Unit cell dimensions</b> | $a = 10.4814(9)$ Å   | $\alpha = 90^\circ$       |
|                             | $b = 17.2053(16)$ Å  | $\beta = 96.511(6)^\circ$ |

<sup>23</sup> Sheldrick, G. M. (2015). *Acta Cryst. A* **71**, 3-8.

<sup>24</sup> Dolomanov, O. V.; Bourhis, L. J.; Gildea, R. J.; Howard, J. A. K.; Puschmann, H. *J. Appl. Cryst.* (2009). **42**, 339-341.

|                               |                               |                     |
|-------------------------------|-------------------------------|---------------------|
|                               | $c = 15.4790(13) \text{ \AA}$ | $\gamma = 90^\circ$ |
| <b>Volume</b>                 | $2773.4(4) \text{ \AA}^3$     |                     |
| <b>Z</b>                      | 4                             |                     |
| <b>Density (calculated)</b>   | $1.617 \text{ g/cm}^3$        |                     |
| <b>Absorption coefficient</b> | $4.567 \text{ mm}^{-1}$       |                     |
| <b>F(000)</b>                 | 1360                          |                     |

**Table 2. Data collection and structure refinement for Harman\_14JAS\_203.**

|  |  |
|--|--|
| <b>Diffractometer</b>                      | Bruker Kappa APEXII Duo  |
| <b>Radiation source</b>                    | Incoatec Microfocus I $\mu$ S (Cu K $\alpha$ , $\lambda = 1.54178 \text{ \AA}$ ) |
| <b>Theta range for data collection</b>     | 3.85 to 68.39 $^\circ$   |
| <b>Index ranges</b>                        | $-12 \leq h \leq 10, -20 \leq k \leq 20, -18 \leq l \leq 18$                     |
| <b>Reflections collected</b>               | 16488  |
| <b>Independent reflections</b>             | 5075 [R(int) = 0.0988]   |
| <b>Coverage of independent reflections</b> | 99.6%  |
| <b>Absorption correction</b>               | Multi-Scan   |
| <b>Max. and min. transmission</b>          | 0.8420 and 0.3060  |
| <b>Structure solution technique</b>        | direct methods   |
| <b>Structure solution program</b>          | SHELXT 2014/5 (Sheldrick, 2014)  |
| <b>Refinement method</b>                   | Full-matrix least-squares on F $^2$  |
| <b>Refinement program</b>                  | SHELXL-2018/3 (Sheldrick, 2018)  |
| <b>Function minimized</b>                  | $\Sigma w(F_o^2 - F_c^2)^2$  |
| <b>Data / restraints / parameters</b>      | 5075 / 1 / 406   |
| <b>Goodness-of-fit on F<math>^2</math></b> | 1.005  |

|                             |   |                              |
|-----------------------------|---|------------------------------|
| $\Delta/\sigma_{\max}$      | 0.001   |                              |
| Final R indices             | 3569 data;<br>$I > 2\sigma(I)$  | R1 = 0.0548, wR2 =<br>0.1272 |
|                             | all data  | R1 = 0.0841, wR2 =<br>0.1431 |
| Weighting scheme            | $w = 1/[\sigma^2(F_o^2) + (0.0622P)^2]$<br>where $P = (F_o^2 + 2F_c^2)/3$ |                              |
| Largest diff. peak and hole | 0.882 and -0.660 eÅ <sup>-3</sup>   |                              |
| R.M.S. deviation from mean  | 0.103 eÅ <sup>-3</sup>  |                              |

**Table 3. Atomic coordinates and equivalent isotropic atomic displacement parameters (Å<sup>2</sup>) for Harman\_14JAS\_203.**

U(eq) is defined as one third of the trace of the orthogonalized U<sub>ij</sub> tensor.

|     | x/a        | y/b        | z/c        | U(eq)       |
|-----|------------|------------|------------|-------------|
| Mo1 | 0.31334(4) | 0.31761(3) | 0.61020(3) | 0.02903(14) |
| F1  | 0.2889(4)  | 0.1533(2)  | 0.3957(3)  | 0.0596(11)  |
| F2  | 0.2919(4)  | 0.0664(2)  | 0.4944(3)  | 0.0539(10)  |
| F3  | 0.4448(4)  | 0.0712(3)  | 0.4163(3)  | 0.0604(12)  |
| O1  | 0.3491(4)  | 0.1816(3)  | 0.7300(3)  | 0.0462(10)  |
| N1  | 0.3056(4)  | 0.4201(3)  | 0.5188(3)  | 0.0304(10)  |
| N2  | 0.2830(5)  | 0.4927(3)  | 0.5507(3)  | 0.0374(11)  |
| N3  | 0.1525(5)  | 0.3787(3)  | 0.6608(3)  | 0.0377(11)  |
| N4  | 0.1541(5)  | 0.4572(3)  | 0.6720(3)  | 0.0395(12)  |
| N5  | 0.4210(4)  | 0.3986(3)  | 0.7028(3)  | 0.0321(10)  |
| N6  | 0.3902(5)  | 0.4754(3)  | 0.7030(3)  | 0.0377(11)  |

|     | <b>x/a</b> | <b>y/b</b> | <b>z/c</b> | <b>U(eq)</b> |
|-----|------------|------------|------------|--------------|
| N7  | 0.3310(4)  | 0.2384(3)  | 0.6836(3)  | 0.0335(10)   |
| N8  | 0.1468(4)  | 0.2637(3)  | 0.5326(3)  | 0.0356(11)   |
| N9  | 0.7964(5)  | 0.1708(4)  | 0.4186(4)  | 0.0538(16)   |
| C1  | 0.3231(5)  | 0.4318(4)  | 0.4363(3)  | 0.0335(12)   |
| C2  | 0.3113(6)  | 0.5092(4)  | 0.4131(4)  | 0.0396(14)   |
| C3  | 0.2858(6)  | 0.5457(4)  | 0.4875(4)  | 0.0408(14)   |
| C4  | 0.0403(6)  | 0.3550(5)  | 0.6851(4)  | 0.0448(16)   |
| C5  | 0.9718(6)  | 0.4179(5)  | 0.7121(4)  | 0.0524(19)   |
| C6  | 0.0457(6)  | 0.4815(5)  | 0.7025(4)  | 0.0495(18)   |
| C7  | 0.5154(5)  | 0.3886(4)  | 0.7671(3)  | 0.0336(12)   |
| C8  | 0.5455(6)  | 0.4588(4)  | 0.8090(4)  | 0.0399(14)   |
| C9  | 0.4646(6)  | 0.5122(4)  | 0.7660(4)  | 0.0428(14)   |
| C10 | 0.5072(5)  | 0.3036(3)  | 0.5654(3)  | 0.0329(12)   |
| C11 | 0.4170(5)  | 0.2556(4)  | 0.5119(3)  | 0.0327(12)   |
| C12 | 0.4372(5)  | 0.1715(3)  | 0.5209(4)  | 0.0333(12)   |
| C13 | 0.5250(5)  | 0.1408(4)  | 0.5821(4)  | 0.0376(13)   |
| C14 | 0.6097(6)  | 0.1904(4)  | 0.6350(3)  | 0.0370(13)   |
| C15 | 0.6063(5)  | 0.2677(4)  | 0.6236(3)  | 0.0366(13)   |
| C16 | 0.3662(6)  | 0.1171(4)  | 0.4569(4)  | 0.0419(14)   |
| C17 | 0.7114(7)  | 0.1552(4)  | 0.6983(4)  | 0.0469(16)   |
| C18 | 0.0628(5)  | 0.3054(4)  | 0.4782(4)  | 0.0413(15)   |
| C19 | 0.9481(6)  | 0.2768(4)  | 0.4395(4)  | 0.0445(15)   |
| C20 | 0.9096(6)  | 0.2001(4)  | 0.4556(4)  | 0.0421(15)   |
| C21 | 0.9978(6)  | 0.1574(4)  | 0.5113(5)  | 0.0480(16)   |

|     | <b>x/a</b> | <b>y/b</b> | <b>z/c</b> | <b>U(eq)</b> |
|-----|------------|------------|------------|--------------|
| C22 | 0.1105(6)  | 0.1906(4)  | 0.5475(4)  | 0.0430(14)   |
| C23 | 0.6964(6)  | 0.2222(5)  | 0.3797(4)  | 0.0540(19)   |
| C24 | 0.7655(7)  | 0.0904(5)  | 0.4315(7)  | 0.073(3)     |
| B1  | 0.2680(8)  | 0.5051(5)  | 0.6476(5)  | 0.0425(16)   |
| F4  | 0.6743(9)  | 0.0975(8)  | 0.7432(7)  | 0.065(4)     |
| F5  | 0.8102(9)  | 0.1242(8)  | 0.6529(6)  | 0.074(3)     |
| F6  | 0.7787(19) | 0.2073(9)  | 0.7529(7)  | 0.074(6)     |
| F4A | 0.652(2)   | 0.142(2)   | 0.7793(16) | 0.065(4)     |
| F5A | 0.756(3)   | 0.088(2)   | 0.6769(17) | 0.074(3)     |
| F6A | 0.799(7)   | 0.197(3)   | 0.721(3)   | 0.074(6)     |
| F4B | 0.692(5)   | 0.080(3)   | 0.710(2)   | 0.065(4)     |
| F5B | 0.818(3)   | 0.164(3)   | 0.685(3)   | 0.074(3)     |
| F6B | 0.707(4)   | 0.194(2)   | 0.777(2)   | 0.074(6)     |

**Table 4. Bond lengths (Å) for Harman\_14JAS\_203.**

|         |          |         |          |
|---------|----------|---------|----------|
| Mo1-N7  | 1.770(5) | Mo1-N3  | 2.205(5) |
| Mo1-N8  | 2.208(5) | Mo1-N5  | 2.215(5) |
| Mo1-C10 | 2.233(5) | Mo1-C11 | 2.238(5) |
| Mo1-N1  | 2.256(5) | F1-C16  | 1.329(7) |
| F2-C16  | 1.345(7) | F3-C16  | 1.347(7) |
| O1-N7   | 1.216(6) | N1-C1   | 1.325(7) |
| N1-N2   | 1.373(7) | N2-C3   | 1.340(8) |
| N2-B1   | 1.540(8) | N3-C4   | 1.339(8) |
| N3-N4   | 1.362(7) | N4-C6   | 1.346(7) |

|         |           |         |           |
|---------|-----------|---------|-----------|
| N4-B1   | 1.532(10) | N5-C7   | 1.332(7)  |
| N5-N6   | 1.360(7)  | N6-C9   | 1.336(8)  |
| N6-B1   | 1.546(8)  | N8-C22  | 1.342(8)  |
| N8-C18  | 1.353(8)  | N9-C20  | 1.354(8)  |
| N9-C24  | 1.440(10) | N9-C23  | 1.450(10) |
| C1-C2   | 1.381(8)  | C1-H1   | 0.95      |
| C2-C3   | 1.364(9)  | C2-H2   | 0.95      |
| C3-H3   | 0.95      | C4-C5   | 1.390(10) |
| C4-H4   | 0.95      | C5-C6   | 1.358(11) |
| C5-H5   | 0.95      | C6-H6   | 0.95      |
| C7-C8   | 1.390(8)  | C7-H7   | 0.95      |
| C8-C9   | 1.370(9)  | C8-H8   | 0.95      |
| C9-H9   | 0.95      | C10-C15 | 1.435(8)  |
| C10-C11 | 1.443(8)  | C10-H10 | 0.95      |
| C11-C12 | 1.466(8)  | C11-H11 | 0.95      |
| C12-C13 | 1.352(8)  | C12-C16 | 1.498(8)  |
| C13-C14 | 1.422(9)  | C13-H13 | 0.95      |
| C14-C15 | 1.343(9)  | C14-C17 | 1.492(9)  |
| C15-H15 | 0.95      | C17-F5B | 1.17(3)   |
| C17-F6A | 1.19(6)   | C17-F4  | 1.296(12) |
| C17-F5A | 1.30(3)   | C17-F4B | 1.33(5)   |
| C17-F6  | 1.373(18) | C17-F6B | 1.40(4)   |
| C17-F5  | 1.419(12) | C17-F4A | 1.48(3)   |
| C18-C19 | 1.372(8)  | C18-H18 | 0.95      |
| C19-C20 | 1.411(9)  | C19-H19 | 0.95      |

|          |           |          |          |
|----------|-----------|----------|----------|
| C20-C21  | 1.399(10) | C21-C22  | 1.374(9) |
| C21-H21  | 0.95      | C22-H22  | 0.95     |
| C23-H23A | 0.98      | C23-H23B | 0.98     |
| C23-H23C | 0.98      | C24-H24A | 0.98     |
| C24-H24B | 0.98      | C24-H24C | 0.98     |
| B1-H1A   | 0.96(6)   |          |          |

**Table 5. Bond angles (°) for Harman\_14JAS\_203.**

|             |            |            |            |
|-------------|------------|------------|------------|
| N7-Mo1-N3   | 99.64(19)  | N7-Mo1-N8  | 92.5(2)    |
| N3-Mo1-N8   | 78.72(18)  | N7-Mo1-N5  | 93.5(2)    |
| N3-Mo1-N5   | 79.84(18)  | N8-Mo1-N5  | 158.41(18) |
| N7-Mo1-C10  | 94.8(2)    | N3-Mo1-C10 | 157.1(2)   |
| N8-Mo1-C10  | 118.48(19) | N5-Mo1-C10 | 81.63(19)  |
| N7-Mo1-C11  | 92.6(2)    | N3-Mo1-C11 | 156.74(18) |
| N8-Mo1-C11  | 81.07(19)  | N5-Mo1-C11 | 119.30(19) |
| C10-Mo1-C11 | 37.7(2)    | N7-Mo1-N1  | 176.02(19) |
| N3-Mo1-N1   | 82.86(18)  | N8-Mo1-N1  | 90.98(17)  |
| N5-Mo1-N1   | 83.88(17)  | C10-Mo1-N1 | 81.91(19)  |
| C11-Mo1-N1  | 86.11(19)  | C1-N1-N2   | 104.8(5)   |
| C1-N1-Mo1   | 136.4(4)   | N2-N1-Mo1  | 118.7(3)   |
| C3-N2-N1    | 109.7(5)   | C3-N2-B1   | 129.0(6)   |
| N1-N2-B1    | 121.1(5)   | C4-N3-N4   | 105.4(5)   |
| C4-N3-Mo1   | 133.3(5)   | N4-N3-Mo1  | 121.3(4)   |
| C6-N4-N3    | 110.7(6)   | C6-N4-B1   | 129.2(6)   |
| N3-N4-B1    | 120.1(5)   | C7-N5-N6   | 106.3(5)   |



|             |          |             |          |
|-------------|----------|-------------|----------|
| C7-N5-Mo1   | 133.0(4) | N6-N5-Mo1   | 120.6(3) |
| C9-N6-N5    | 110.0(5) | C9-N6-B1    | 128.8(5) |
| N5-N6-B1    | 120.1(5) | O1-N7-Mo1   | 175.2(4) |
| C22-N8-C18  | 115.3(5) | C22-N8-Mo1  | 121.5(4) |
| C18-N8-Mo1  | 122.3(4) | C20-N9-C24  | 119.9(7) |
| C20-N9-C23  | 120.4(6) | C24-N9-C23  | 118.7(6) |
| N1-C1-C2    | 112.3(6) | N1-C1-H1    | 123.8    |
| C2-C1-H1    | 123.8    | C3-C2-C1    | 104.1(5) |
| C3-C2-H2    | 128.0    | C1-C2-H2    | 128.0    |
| N2-C3-C2    | 109.1(6) | N2-C3-H3    | 125.5    |
| C2-C3-H3    | 125.5    | N3-C4-C5    | 110.3(7) |
| N3-C4-H4    | 124.8    | C5-C4-H4    | 124.8    |
| C6-C5-C4    | 105.9(6) | C6-C5-H5    | 127.0    |
| C4-C5-H5    | 127.0    | N4-C6-C5    | 107.6(7) |
| N4-C6-H6    | 126.2    | C5-C6-H6    | 126.2    |
| N5-C7-C8    | 110.2(6) | N5-C7-H7    | 124.9    |
| C8-C7-H7    | 124.9    | C9-C8-C7    | 105.1(5) |
| C9-C8-H8    | 127.4    | C7-C8-H8    | 127.4    |
| N6-C9-C8    | 108.3(6) | N6-C9-H9    | 125.8    |
| C8-C9-H9    | 125.8    | C15-C10-C11 | 119.7(5) |
| C15-C10-Mo1 | 118.1(4) | C11-C10-Mo1 | 71.4(3)  |
| C15-C10-H10 | 120.2    | C11-C10-H10 | 120.2    |
| Mo1-C10-H10 | 81.3     | C10-C11-C12 | 115.6(5) |
| C10-C11-Mo1 | 71.0(3)  | C12-C11-Mo1 | 118.8(4) |
| C10-C11-H11 | 122.2    | C12-C11-H11 | 122.2    |

|             |           |             |           |
|-------------|-----------|-------------|-----------|
| Mo1-C11-H11 | 81.6      | C13-C12-C11 | 122.2(5)  |
| C13-C12-C16 | 117.8(6)  | C11-C12-C16 | 119.9(5)  |
| C12-C13-C14 | 120.0(6)  | C12-C13-H13 | 120.0     |
| C14-C13-H13 | 120.0     | C15-C14-C13 | 120.9(6)  |
| C15-C14-C17 | 119.7(6)  | C13-C14-C17 | 119.2(6)  |
| C14-C15-C10 | 121.0(6)  | C14-C15-H15 | 119.5     |
| C10-C15-H15 | 119.5     | F1-C16-F2   | 105.9(5)  |
| F1-C16-F3   | 107.4(5)  | F2-C16-F3   | 103.6(5)  |
| F1-C16-C12  | 113.3(6)  | F2-C16-C12  | 112.9(5)  |
| F3-C16-C12  | 113.0(5)  | F6A-C17-F5A | 109.(3)   |
| F5B-C17-F4B | 108.(3)   | F4-C17-F6   | 109.5(9)  |
| F5B-C17-F6B | 103.(3)   | F4B-C17-F6B | 109.(2)   |
| F4-C17-F5   | 104.9(9)  | F6-C17-F5   | 101.4(10) |
| F6A-C17-F4A | 103.(3)   | F5A-C17-F4A | 106.2(18) |
| F5B-C17-C14 | 117.2(16) | F6A-C17-C14 | 115.(2)   |
| F4-C17-C14  | 115.3(7)  | F5A-C17-C14 | 116.3(12) |
| F4B-C17-C14 | 112.1(18) | F6-C17-C14  | 114.7(8)  |
| F6B-C17-C14 | 106.9(13) | F5-C17-C14  | 109.6(6)  |
| F4A-C17-C14 | 106.1(11) | N8-C18-C19  | 123.9(6)  |
| N8-C18-H18  | 118.0     | C19-C18-H18 | 118.0     |
| C18-C19-C20 | 120.8(6)  | C18-C19-H19 | 119.6     |
| C20-C19-H19 | 119.6     | N9-C20-C21  | 123.4(7)  |
| N9-C20-C19  | 121.8(7)  | C21-C20-C19 | 114.7(6)  |
| C22-C21-C20 | 120.7(7)  | C22-C21-H21 | 119.7     |
| C20-C21-H21 | 119.7     | N8-C22-C21  | 124.6(6)  |

|               |          |               |          |
|---------------|----------|---------------|----------|
| N8-C22-H22    | 117.7    | C21-C22-H22   | 117.7    |
| N9-C23-H23A   | 109.5    | N9-C23-H23B   | 109.5    |
| H23A-C23-H23B | 109.5    | N9-C23-H23C   | 109.5    |
| H23A-C23-H23C | 109.5    | H23B-C23-H23C | 109.5    |
| N9-C24-H24A   | 109.5    | N9-C24-H24B   | 109.5    |
| H24A-C24-H24B | 109.5    | N9-C24-H24C   | 109.5    |
| H24A-C24-H24C | 109.5    | H24B-C24-H24C | 109.5    |
| N4-B1-N2      | 109.5(5) | N4-B1-N6      | 107.8(5) |
| N2-B1-N6      | 108.9(5) | N4-B1-H1A     | 115.(4)  |
| N2-B1-H1A     | 110.(4)  | N6-B1-H1A     | 106.(4)  |

**Table 6. Torsion angles (°) for Harman\_14JAS\_203.**

|             |           |              |           |
|-------------|-----------|--------------|-----------|
| C1-N1-N2-C3 | 0.7(6)    | Mo1-N1-N2-C3 | 178.2(4)  |
| C1-N1-N2-B1 | -175.3(5) | Mo1-N1-N2-B1 | 2.2(7)    |
| C4-N3-N4-C6 | 0.1(6)    | Mo1-N3-N4-C6 | 179.3(4)  |
| C4-N3-N4-B1 | -178.0(5) | Mo1-N3-N4-B1 | 1.2(6)    |
| C7-N5-N6-C9 | 0.2(7)    | Mo1-N5-N6-C9 | 177.8(4)  |
| C7-N5-N6-B1 | -169.0(5) | Mo1-N5-N6-B1 | 8.6(7)    |
| N2-N1-C1-C2 | -0.7(6)   | Mo1-N1-C1-C2 | -177.5(4) |
| N1-C1-C2-C3 | 0.4(7)    | N1-N2-C3-C2  | -0.5(7)   |
| B1-N2-C3-C2 | 175.1(6)  | C1-C2-C3-N2  | 0.1(7)    |
| N4-N3-C4-C5 | -0.5(6)   | Mo1-N3-C4-C5 | -179.5(4) |
| N3-C4-C5-C6 | 0.7(7)    | N3-N4-C6-C5  | 0.4(7)    |
| B1-N4-C6-C5 | 178.3(6)  | C4-C5-C6-N4  | -0.6(7)   |
| N6-N5-C7-C8 | 0.1(6)    | Mo1-N5-C7-C8 | -177.0(4) |

|                 |            |                 |           |
|-----------------|------------|-----------------|-----------|
| N5-C7-C8-C9     | -0.4(7)    | N5-N6-C9-C8     | -0.5(7)   |
| B1-N6-C9-C8     | 167.5(6)   | C7-C8-C9-N6     | 0.6(7)    |
| C15-C10-C11-C12 | -1.3(7)    | Mo1-C10-C11-C12 | -113.6(4) |
| C15-C10-C11-Mo1 | 112.3(5)   | C10-C11-C12-C13 | 7.2(8)    |
| Mo1-C11-C12-C13 | -74.2(6)   | C10-C11-C12-C16 | -168.2(5) |
| Mo1-C11-C12-C16 | 110.4(5)   | C11-C12-C13-C14 | -5.9(8)   |
| C16-C12-C13-C14 | 169.6(5)   | C12-C13-C14-C15 | -1.9(9)   |
| C12-C13-C14-C17 | -176.1(6)  | C13-C14-C15-C10 | 7.9(8)    |
| C17-C14-C15-C10 | -177.9(5)  | C11-C10-C15-C14 | -6.1(8)   |
| Mo1-C10-C15-C14 | 77.4(6)    | C13-C12-C16-F1  | -175.5(5) |
| C11-C12-C16-F1  | 0.1(8)     | C13-C12-C16-F2  | 64.1(7)   |
| C11-C12-C16-F2  | -120.3(6)  | C13-C12-C16-F3  | -53.1(8)  |
| C11-C12-C16-F3  | 122.5(6)   | C15-C14-C17-F5B | -62.(3)   |
| C13-C14-C17-F5B | 113.(3)    | C15-C14-C17-F6A | -15.(4)   |
| C13-C14-C17-F6A | 160.(4)    | C15-C14-C17-F4  | 141.3(9)  |
| C13-C14-C17-F4  | -44.4(11)  | C15-C14-C17-F5A | -144.(2)  |
| C13-C14-C17-F5A | 30.(2)     | C15-C14-C17-F4B | 172.(2)   |
| C13-C14-C17-F4B | -13.(3)    | C15-C14-C17-F6  | 12.6(12)  |
| C13-C14-C17-F6  | -173.1(10) | C15-C14-C17-F6B | 53.(2)    |
| C13-C14-C17-F6B | -133.(2)   | C15-C14-C17-F5  | -100.6(9) |
| C13-C14-C17-F5  | 73.7(10)   | C15-C14-C17-F4A | 98.2(16)  |
| C13-C14-C17-F4A | -87.5(16)  | C22-N8-C18-C19  | -0.2(9)   |
| Mo1-N8-C18-C19  | -169.4(5)  | N8-C18-C19-C20  | 0.6(10)   |
| C24-N9-C20-C21  | -4.1(10)   | C23-N9-C20-C21  | 164.6(6)  |
| C24-N9-C20-C19  | 175.2(7)   | C23-N9-C20-C19  | -16.1(9)  |

|                |           |                 |           |
|----------------|-----------|-----------------|-----------|
| C18-C19-C20-N9 | 179.5(6)  | C18-C19-C20-C21 | -1.2(9)   |
| N9-C20-C21-C22 | -179.3(6) | C19-C20-C21-C22 | 1.4(9)    |
| C18-N8-C22-C21 | 0.5(9)    | Mo1-N8-C22-C21  | 169.8(5)  |
| C20-C21-C22-N8 | -1.2(11)  | C6-N4-B1-N2     | -119.3(6) |
| N3-N4-B1-N2    | 58.4(7)   | C6-N4-B1-N6     | 122.3(6)  |
| N3-N4-B1-N6    | -59.9(7)  | C3-N2-B1-N4     | 124.8(6)  |
| N1-N2-B1-N4    | -60.1(7)  | C3-N2-B1-N6     | -117.6(7) |
| N1-N2-B1-N6    | 57.5(8)   | C9-N6-B1-N4     | -112.9(7) |
| N5-N6-B1-N4    | 54.1(7)   | C9-N6-B1-N2     | 128.4(7)  |
| N5-N6-B1-N2    | -64.7(8)  |                 |           |

**Table 7. Anisotropic atomic displacement parameters ( $\text{\AA}^2$ ) for Harman\_14JAS\_203.**

The anisotropic atomic displacement factor exponent takes the form: -  
 $2\pi^2 [ h^2 a^{*2} U_{11} + \dots + 2 h k a^* b^* U_{12} ]$

|     | $U_{11}$  | $U_{22}$  | $U_{33}$  | $U_{23}$    | $U_{13}$    | $U_{12}$   |
|-----|-----------|-----------|-----------|-------------|-------------|------------|
| Mo1 | 0.0268(2) | 0.0349(2) | 0.0250(2) | 0.00329(19) | 0.00143(14) | 0.0000(2)  |
| F1  | 0.076(3)  | 0.046(2)  | 0.050(2)  | -0.0027(18) | -0.022(2)   | -0.006(2)  |
| F2  | 0.051(2)  | 0.052(2)  | 0.059(2)  | -0.006(2)   | 0.0060(18)  | 0.0182(19) |
| F3  | 0.049(2)  | 0.074(3)  | 0.058(2)  | -0.032(2)   | 0.0036(19)  | 0.000(2)   |
| O1  | 0.062(3)  | 0.043(2)  | 0.035(2)  | 0.011(2)    | 0.0096(19)  | 0.014(2)   |
| N1  | 0.030(2)  | 0.033(3)  | 0.028(2)  | -0.0013(19) | -0.0001(18) | 0.001(2)   |
| N2  | 0.038(3)  | 0.035(3)  | 0.038(3)  | 0.006(2)    | 0.001(2)    | 0.001(2)   |
| N3  | 0.033(2)  | 0.048(3)  | 0.031(2)  | 0.007(2)    | -0.0007(19) | 0.002(2)   |
| N4  | 0.038(3)  | 0.050(3)  | 0.029(2)  | 0.001(2)    | 0.001(2)    | 0.012(2)   |

|     | <b>U<sub>11</sub></b> | <b>U<sub>22</sub></b> | <b>U<sub>33</sub></b> | <b>U<sub>23</sub></b> | <b>U<sub>13</sub></b> | <b>U<sub>12</sub></b> |
|-----|-----------------------|-----------------------|-----------------------|-----------------------|-----------------------|-----------------------|
| N5  | 0.034(2)              | 0.035(3)              | 0.027(2)              | -0.0018(19)           | 0.0021(18)            | 0.005(2)              |
| N6  | 0.047(3)              | 0.035(3)              | 0.031(2)              | -0.003(2)             | 0.003(2)              | 0.008(2)              |
| N7  | 0.031(2)              | 0.041(3)              | 0.029(2)              | 0.006(2)              | 0.0062(18)            | 0.009(2)              |
| N8  | 0.030(2)              | 0.042(3)              | 0.035(2)              | 0.001(2)              | 0.0070(19)            | -0.003(2)             |
| N9  | 0.031(3)              | 0.070(4)              | 0.060(3)              | -0.020(3)             | 0.007(2)              | -0.011(3)             |
| C1  | 0.033(3)              | 0.038(3)              | 0.027(2)              | 0.003(2)              | -0.003(2)             | -0.007(2)             |
| C2  | 0.040(3)              | 0.046(4)              | 0.033(3)              | 0.010(3)              | 0.000(2)              | 0.001(3)              |
| C3  | 0.036(3)              | 0.040(3)              | 0.045(3)              | 0.010(3)              | -0.001(3)             | -0.004(3)             |
| C4  | 0.032(3)              | 0.072(5)              | 0.031(3)              | 0.007(3)              | 0.003(2)              | 0.004(3)              |
| C5  | 0.036(3)              | 0.085(6)              | 0.039(3)              | 0.013(3)              | 0.014(3)              | 0.021(4)              |
| C6  | 0.043(3)              | 0.075(5)              | 0.032(3)              | 0.008(3)              | 0.010(3)              | 0.029(4)              |
| C7  | 0.034(3)              | 0.041(3)              | 0.025(2)              | 0.001(2)              | 0.002(2)              | -0.001(3)             |
| C8  | 0.040(3)              | 0.048(4)              | 0.031(3)              | -0.004(3)             | -0.001(2)             | -0.002(3)             |
| C9  | 0.050(4)              | 0.038(3)              | 0.040(3)              | 0.000(3)              | 0.001(3)              | -0.003(3)             |
| C10 | 0.031(3)              | 0.037(3)              | 0.031(2)              | 0.002(2)              | 0.003(2)              | 0.000(2)              |
| C11 | 0.030(3)              | 0.043(3)              | 0.026(2)              | 0.004(2)              | 0.007(2)              | 0.001(2)              |
| C12 | 0.033(3)              | 0.034(3)              | 0.035(3)              | -0.007(2)             | 0.011(2)              | -0.005(2)             |
| C13 | 0.031(3)              | 0.043(4)              | 0.040(3)              | 0.004(3)              | 0.009(2)              | -0.001(3)             |
| C14 | 0.039(3)              | 0.049(4)              | 0.025(2)              | -0.001(3)             | 0.011(2)              | 0.000(3)              |
| C15 | 0.025(3)              | 0.055(4)              | 0.030(3)              | 0.000(3)              | 0.005(2)              | 0.003(3)              |
| C16 | 0.039(3)              | 0.050(4)              | 0.036(3)              | -0.005(3)             | 0.001(3)              | 0.000(3)              |
| C17 | 0.048(4)              | 0.045(4)              | 0.045(3)              | -0.008(3)             | -0.005(3)             | 0.003(3)              |
| C18 | 0.034(3)              | 0.059(4)              | 0.029(3)              | 0.007(3)              | -0.004(2)             | -0.010(3)             |
| C19 | 0.041(3)              | 0.062(4)              | 0.029(3)              | 0.001(3)              | 0.003(2)              | -0.005(3)             |

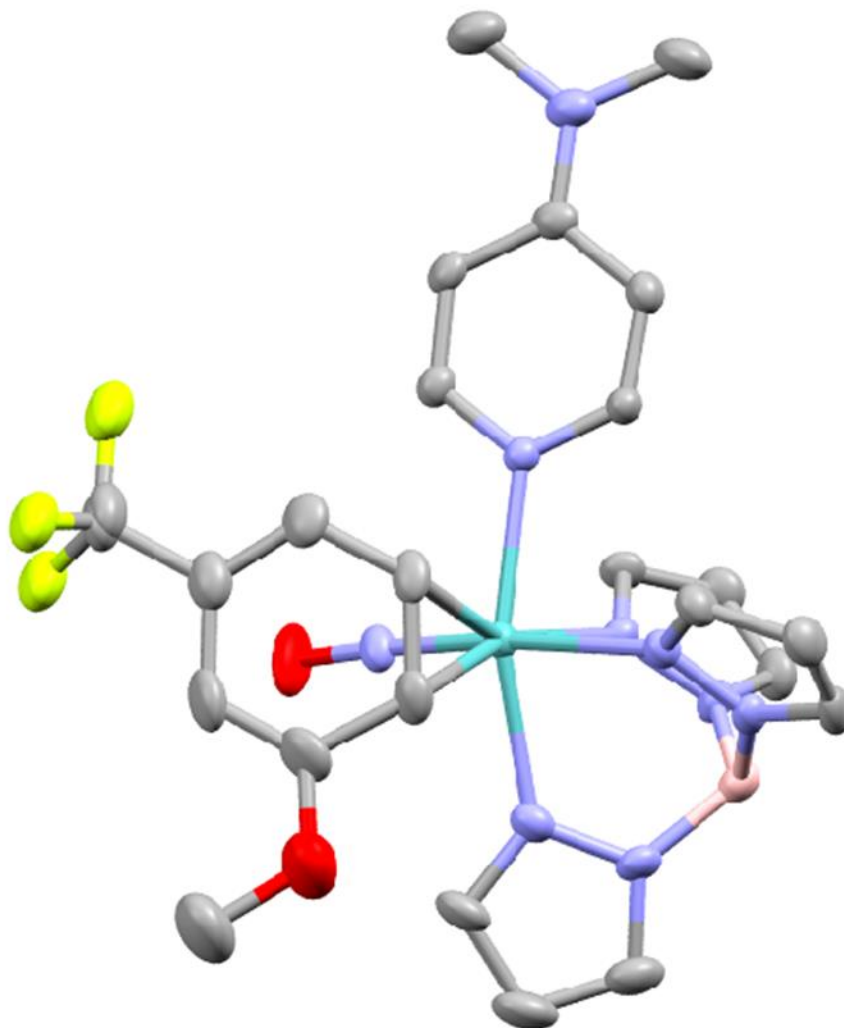
|     | <b>U<sub>11</sub></b> | <b>U<sub>22</sub></b> | <b>U<sub>33</sub></b> | <b>U<sub>23</sub></b> | <b>U<sub>13</sub></b> | <b>U<sub>12</sub></b> |
|-----|-----------------------|-----------------------|-----------------------|-----------------------|-----------------------|-----------------------|
| C20 | 0.033(3)              | 0.055(4)              | 0.041(3)              | -0.013(3)             | 0.015(3)              | -0.013(3)             |
| C21 | 0.032(3)              | 0.047(4)              | 0.066(4)              | -0.012(3)             | 0.010(3)              | -0.007(3)             |
| C22 | 0.031(3)              | 0.046(4)              | 0.054(3)              | 0.001(3)              | 0.011(3)              | -0.005(3)             |
| C23 | 0.043(3)              | 0.086(6)              | 0.032(3)              | -0.005(3)             | 0.001(3)              | -0.027(4)             |
| C24 | 0.049(4)              | 0.062(5)              | 0.108(7)              | -0.042(5)             | 0.015(4)              | -0.015(4)             |
| B1  | 0.047(4)              | 0.039(4)              | 0.040(3)              | -0.004(3)             | 0.001(3)              | 0.011(3)              |
| F4  | 0.048(5)              | 0.094(9)              | 0.048(7)              | 0.040(6)              | -0.016(6)             | -0.018(6)             |
| F5  | 0.054(4)              | 0.112(9)              | 0.059(5)              | 0.018(5)              | 0.021(4)              | 0.044(6)              |
| F6  | 0.077(9)              | 0.062(5)              | 0.070(10)             | -0.003(6)             | -0.049(11)            | -0.003(5)             |
| F4A | 0.048(5)              | 0.094(9)              | 0.048(7)              | 0.040(6)              | -0.016(6)             | -0.018(6)             |
| F5A | 0.054(4)              | 0.112(9)              | 0.059(5)              | 0.018(5)              | 0.021(4)              | 0.044(6)              |
| F6A | 0.077(9)              | 0.062(5)              | 0.070(10)             | -0.003(6)             | -0.049(11)            | -0.003(5)             |
| F4B | 0.048(5)              | 0.094(9)              | 0.048(7)              | 0.040(6)              | -0.016(6)             | -0.018(6)             |
| F5B | 0.054(4)              | 0.112(9)              | 0.059(5)              | 0.018(5)              | 0.021(4)              | 0.044(6)              |
| F6B | 0.077(9)              | 0.062(5)              | 0.070(10)             | -0.003(6)             | -0.049(11)            | -0.003(5)             |

**Table 8. Hydrogen atomic coordinates and isotropic atomic displacement parameters ( $\text{\AA}^2$ ) for Harman\_14JAS\_203.**

|    | <b>x/a</b> | <b>y/b</b> | <b>z/c</b> | <b>U(eq)</b> |
|----|------------|------------|------------|--------------|
| H1 | 0.3416     | 0.3916     | 0.3976     | 0.04         |
| H2 | 0.3191     | 0.5318     | 0.3579     | 0.048        |
| H3 | 0.2723     | 0.5999     | 0.4935     | 0.049        |
| H4 | 0.0116     | 0.3026     | 0.6841     | 0.054        |
| H5 | -0.1100    | 0.4167     | 0.7330     | 0.063        |

|      | <b>x/a</b> | <b>y/b</b> | <b>z/c</b> | <b>U(eq)</b> |
|------|------------|------------|------------|--------------|
| H6   | 0.0246     | 0.5337     | 0.7151     | 0.059        |
| H7   | 0.5562     | 0.3404     | 0.7821     | 0.04         |
| H8   | 0.6085     | 0.4678     | 0.8570     | 0.048        |
| H9   | 0.4618     | 0.5661     | 0.7789     | 0.051        |
| H10  | 0.5009     | 0.3586     | 0.5621     | 0.039        |
| H11  | 0.3490     | 0.2771     | 0.4734     | 0.039        |
| H13  | 0.5301     | 0.0860     | 0.5897     | 0.045        |
| H15  | 0.6705     | 0.2992     | 0.6545     | 0.044        |
| H18  | 0.0845     | 0.3576     | 0.4660     | 0.05         |
| H19  | -0.1061    | 0.3091     | 0.4014     | 0.053        |
| H21  | -0.0204    | 0.1048     | 0.5242     | 0.058        |
| H22  | 0.1667     | 0.1597     | 0.5858     | 0.052        |
| H23A | -0.3276    | 0.2588     | 0.4236     | 0.081        |
| H23B | -0.3789    | 0.1915     | 0.3572     | 0.081        |
| H23C | -0.2720    | 0.2512     | 0.3319     | 0.081        |
| H24A | -0.1602    | 0.0579     | 0.4228     | 0.109        |
| H24B | -0.3076    | 0.0754     | 0.3897     | 0.109        |
| H24C | -0.2568    | 0.0831     | 0.4908     | 0.109        |
| H1A  | 0.264(6)   | 0.560(4)   | 0.659(4)   | 0.038(17)    |





### Crystal Structure Report 26B in Chapter 6

A **orange block-like** specimen of  $C_{23.99}H_{27}BF_{2.97}MoN_9O_2$ , approximate dimensions **0.040** mm x **0.042** mm x **0.109** mm, was coated with Paratone oil and mounted on a MiTeGen MicroLoop. The X-ray intensity data were measured on a Bruker Kappa APEXII Duo system equipped with a fine-focus sealed tube (Cu  $K_{\alpha}$ ,  $\lambda = 1.54178$  Å) and a multi-layer mirror monochromator.

The total exposure time was 20.09 hours. The frames were integrated with the Bruker SAINT software package<sup>25</sup> using a narrow-frame algorithm. The integration of the data using a **monoclinic** unit cell yielded a total of **24768** reflections to a maximum  $\theta$  angle of **68.38°** (**0.83** Å

<sup>25</sup> Bruker (2012). *Saint*; *SADABS*; *APEX3*. Bruker AXS Inc., Madison, Wisconsin, USA.

resolution), of which 5405 were independent (average redundancy 4.582, completeness = 99.7%,  $R_{\text{int}} = 5.72\%$ ,  $R_{\text{sig}} = 4.43\%$ ) and 4774 (88.33%) were greater than  $2\sigma(F^2)$ . The final cell constants of  $a = 11.1633(7)$  Å,  $b = 19.3207(13)$  Å,  $c = 14.1736(9)$  Å,  $\beta = 105.181(4)^\circ$ , volume = 2950.3(3) Å<sup>3</sup>, are based upon the refinement of the XYZ-centroids of 8477 reflections above  $20\sigma(I)$  with  $7.919^\circ < 2\theta < 136.6^\circ$ . Data were corrected for absorption effects using the Multi-Scan method (SADABS).<sup>1</sup> The ratio of minimum to maximum apparent transmission was 0.900. The calculated minimum and maximum transmission coefficients (based on crystal size) are 0.6620 and 0.8520.

The structure was solved and refined using the Bruker SHELXTL Software Package<sup>26</sup> within APEX3<sup>1</sup> and OLEX2,<sup>27</sup> using the space group  $P 2_1/n$ , with  $Z = 4$  for the formula unit,  $C_{23.99}H_{27}BF_{2.97}MoN_9O_2$ . Non-hydrogen atoms were refined anisotropically. The B-H hydrogen atom was located in the diffraction map and refined isotropically, as were H10 and H11. All other hydrogen atoms were placed in geometrically calculated positions with  $U_{\text{iso}} = 1.2U_{\text{equiv}}$  of the parent atom ( $U_{\text{iso}} = 1.5U_{\text{equiv}}$  for methyl). The CF<sub>3</sub> group was disordered over three positions. The relative occupancies were freely refined with the sum set to 1. Constraints were used on the anisotropic displacement parameters of the disordered atoms, and restraints were used on the disordered bonds. Solvent located in the crystal lattice was severely disordered and could not be adequately modeled with or without restraints. Thus, the structure factors were modified using the PLATON SQUEEZE<sup>28</sup> technique, in order to produce a “solvate-free” structure factor set. PLATON reported a total electron density of 91 e<sup>-</sup> and total solvent accessible volume of 357 Å<sup>3</sup>. The final anisotropic full-matrix least-squares refinement on  $F^2$  with 391 variables converged at  $R1 = 3.99\%$ , for the observed data and  $wR2 = 11.30\%$  for all data. The goodness-of-fit was 1.056. The largest peak in the final difference electron density synthesis was 0.573 e<sup>-</sup>/Å<sup>3</sup> and the largest hole was -0.793 e<sup>-</sup>/Å<sup>3</sup> with an RMS deviation of 0.105 e<sup>-</sup>/Å<sup>3</sup>. On the basis of the final model, the calculated density was 1.433 g/cm<sup>3</sup> and  $F(000)$ , 1295 e<sup>-</sup>.

**Table 1. Sample and crystal data for Harman\_19JAS223.**

|                            |                                    |
|----------------------------|------------------------------------|
| <b>Identification code</b> | Harman_19JAS223                    |
| <b>Chemical formula</b>    | $C_{23.99}H_{27}BF_{2.97}MoN_9O_2$ |
| <b>Formula weight</b>      | 636.56 g/mol                       |
| <b>Temperature</b>         | 100(2) K                           |
| <b>Wavelength</b>          | 1.54178 Å                          |
| <b>Crystal size</b>        | 0.040 x 0.042 x 0.109 mm           |
| <b>Crystal habit</b>       | orange block                       |
| <b>Crystal system</b>      | monoclinic                         |

<sup>26</sup> Sheldrick, G. M. (2015). *Acta Cryst.* **A71**, 3-8.

<sup>27</sup> Dolomanov, O. V.; Bourhis, L. J.; Gildea, R. J.; Howard, J. A. K.; Puschmann, H. *J. Appl. Cryst.* (2009). **42**, 339-341.

<sup>28</sup> Spek, A. L. *Acta Crystallogr. Sect C: Struct. Chem.* **2015**, C71, 9-18.

|                               |                          |                 |
|-------------------------------|--------------------------|-----------------|
| <b>Space group</b>            | P 2 <sub>1</sub> /n      |                 |
| <b>Unit cell dimensions</b>   | a = 11.1633(7) Å         | α = 90°         |
|                               | b = 19.3207(13) Å        | β = 105.181(4)° |
|                               | c = 14.1736(9) Å         | γ = 90°         |
| <b>Volume</b>                 | 2950.3(3) Å <sup>3</sup> |                 |
| <b>Z</b>                      | 4                        |                 |
| <b>Density (calculated)</b>   | 1.433 g/cm <sup>3</sup>  |                 |
| <b>Absorption coefficient</b> | 4.130 mm <sup>-1</sup>   |                 |
| <b>F(000)</b>                 | 1295                     |                 |

**Table 2. Data collection and structure refinement for Harman\_19JAS223.**

|  |  |
|--|--|
| <b>Diffractometer</b>                      | Bruker Kappa APEXII Duo                                    |
| <b>Radiation source</b>                    | fine-focus sealed tube (Cu K <sub>α</sub> , λ = 1.54178 Å) |
| <b>Theta range for data collection</b>     | 3.96 to 68.38°   |
| <b>Index ranges</b>                        | -13 ≤ h ≤ 13, -23 ≤ k ≤ 23, -17 ≤ l ≤ 14                   |
| <b>Reflections collected</b>               | 24768  |
| <b>Independent reflections</b>             | 5405 [R(int) = 0.0572]                                     |
| <b>Coverage of independent reflections</b> | 99.7%  |
| <b>Absorption correction</b>               | Multi-Scan   |
| <b>Max. and min. transmission</b>          | 0.8520 and 0.6620  |
| <b>Structure solution technique</b>        | direct methods   |
| <b>Structure solution program</b>          | SHELXT 2014/5 (Sheldrick, 2014)                            |

|  |   |                              |
|--|---|------------------------------|
| <b>Refinement method</b>                   | Full-matrix least-squares on $F^2$  |                              |
| <b>Refinement program</b>                  | SHELXL-2018/3 (Sheldrick, 2018)   |                              |
| <b>Function minimized</b>                  | $\Sigma w(F_o^2 - F_c^2)^2$   |                              |
| <b>Data / restraints / parameters</b>      | 5405 / 40 / 391   |                              |
| <b>Goodness-of-fit on <math>F^2</math></b> | 1.056   |                              |
| $\Delta/\sigma_{\max}$                     | 0.002   |                              |
| <b>Final R indices</b>                     | 4774 data;<br>$I > 2\sigma(I)$  | R1 = 0.0399, wR2 =<br>0.1086 |
|  | all data  | R1 = 0.0455, wR2 =<br>0.1130 |
| <b>Weighting scheme</b>                    | $w = 1/[\sigma^2(F_o^2) + (0.0684P)^2 + 2.3262P]$<br>where $P = (F_o^2 + 2F_c^2)/3$ |                              |
| <b>Largest diff. peak and hole</b>         | 0.573 and -0.793 $e\text{\AA}^{-3}$   |                              |
| <b>R.M.S. deviation from mean</b>          | 0.105 $e\text{\AA}^{-3}$  |                              |

**Table 3. Atomic coordinates and equivalent isotropic atomic displacement parameters ( $\text{\AA}^2$ ) for Harman\_19JAS223.**

U(eq) is defined as one third of the trace of the orthogonalized  $U_{ij}$  tensor.

|     | <b>x/a</b> | <b>y/b</b>  | <b>z/c</b>  | <b>U(eq)</b> |
|-----|------------|-------------|-------------|--------------|
| Mo1 | 0.43368(2) | 0.68930(2)  | 0.47622(2)  | 0.01787(11)  |
| O1  | 0.5485(3)  | 0.73735(17) | 0.3208(2)   | 0.0489(8)    |
| O2  | 0.7795(3)  | 0.7520(2)   | 0.6267(3)   | 0.0626(10)   |
| N1  | 0.3521(2)  | 0.66593(14) | 0.60404(18) | 0.0211(5)    |
| N2  | 0.2767(2)  | 0.71408(15) | 0.63045(19) | 0.0227(5)    |
| N3  | 0.2480(2)  | 0.73227(14) | 0.41325(18) | 0.0202(5)    |

|     | <b>x/a</b> | <b>y/b</b>  | <b>z/c</b>  | <b>U(eq)</b> |
|-----|------------|-------------|-------------|--------------|
| N4  | 0.1862(2)  | 0.76949(15) | 0.46740(19) | 0.0237(6)    |
| N5  | 0.4606(3)  | 0.79269(15) | 0.5453(2)   | 0.0259(6)    |
| N6  | 0.3712(3)  | 0.82164(15) | 0.5827(2)   | 0.0268(6)    |
| N7  | 0.4993(2)  | 0.71622(15) | 0.3824(2)   | 0.0257(6)    |
| N8  | 0.3378(2)  | 0.59778(13) | 0.39571(18) | 0.0203(5)    |
| N9  | 0.1414(3)  | 0.43074(16) | 0.2370(2)   | 0.0315(6)    |
| C1  | 0.3613(3)  | 0.61357(19) | 0.6675(2)   | 0.0282(7)    |
| C2  | 0.2934(3)  | 0.6270(2)   | 0.7348(3)   | 0.0332(8)    |
| C3  | 0.2417(3)  | 0.69107(19) | 0.7089(3)   | 0.0301(8)    |
| C4  | 0.1711(3)  | 0.72549(17) | 0.3238(2)   | 0.0241(6)    |
| C5  | 0.0589(3)  | 0.7578(2)   | 0.3206(3)   | 0.0316(7)    |
| C6  | 0.0716(3)  | 0.7845(2)   | 0.4117(3)   | 0.0323(8)    |
| C7  | 0.5494(3)  | 0.8403(2)   | 0.5532(3)   | 0.0357(8)    |
| C8  | 0.5184(4)  | 0.9002(2)   | 0.5975(3)   | 0.0442(10)   |
| C9  | 0.4061(4)  | 0.8862(2)   | 0.6145(3)   | 0.0385(9)    |
| C10 | 0.5771(3)  | 0.60627(19) | 0.5324(3)   | 0.0286(7)    |
| C11 | 0.6207(3)  | 0.6689(2)   | 0.5840(3)   | 0.0300(7)    |
| C12 | 0.7319(3)  | 0.6997(2)   | 0.5664(3)   | 0.0380(9)    |
| C13 | 0.7844(3)  | 0.6762(2)   | 0.4959(3)   | 0.0412(9)    |
| C14 | 0.7346(4)  | 0.6159(2)   | 0.4432(3)   | 0.0388(9)    |
| C15 | 0.6396(3)  | 0.5800(2)   | 0.4632(3)   | 0.0342(8)    |
| C17 | 0.8890(5)  | 0.7859(4)   | 0.6121(5)   | 0.0721(16)   |
| C18 | 0.3714(3)  | 0.56846(17) | 0.3195(2)   | 0.0233(6)    |
| C19 | 0.3107(3)  | 0.51392(17) | 0.2658(2)   | 0.0247(6)    |
| C20 | 0.2041(3)  | 0.48507(17) | 0.2872(2)   | 0.0234(6)    |

|      | <b>x/a</b> | <b>y/b</b>  | <b>z/c</b> | <b>U(eq)</b> |
|------|------------|-------------|------------|--------------|
| C21  | 0.1664(3)  | 0.51713(18) | 0.3639(2)  | 0.0256(6)    |
| C22  | 0.2344(3)  | 0.57110(16) | 0.4142(2)  | 0.0221(6)    |
| C23  | 0.0293(4)  | 0.4049(2)   | 0.2588(3)  | 0.0429(9)    |
| C24  | 0.1876(4)  | 0.3947(2)   | 0.1634(3)  | 0.0396(9)    |
| B1   | 0.2485(4)  | 0.7837(2)   | 0.5760(3)  | 0.0256(7)    |
| F1   | 0.7316(12) | 0.5417(5)   | 0.3037(10) | 0.0555(9)    |
| F2   | 0.8250(13) | 0.6439(8)   | 0.3171(11) | 0.0555(9)    |
| F3   | 0.9073(10) | 0.5601(7)   | 0.4119(6)  | 0.0555(9)    |
| C16  | 0.7960(12) | 0.5895(7)   | 0.3680(10) | 0.0466(16)   |
| F1A  | 0.7047(11) | 0.5552(7)   | 0.2904(9)  | 0.0555(9)    |
| F2A  | 0.8582(11) | 0.6274(7)   | 0.3272(9)  | 0.0555(9)    |
| F3A  | 0.8690(11) | 0.5307(6)   | 0.4007(7)  | 0.0555(9)    |
| C16A | 0.7893(14) | 0.5839(8)   | 0.3679(11) | 0.0466(16)   |
| F1B  | 0.7750(15) | 0.5350(7)   | 0.3414(13) | 0.0555(9)    |
| F2B  | 0.805(2)   | 0.6395(12)  | 0.3038(17) | 0.0555(9)    |
| F3B  | 0.9399(12) | 0.5923(9)   | 0.4296(10) | 0.0555(9)    |
| C16B | 0.8186(14) | 0.5970(11)  | 0.3823(14) | 0.0466(16)   |

**Table 4. Bond lengths (Å) for Harman\_19JAS223.**

|         |          |         |          |
|---------|----------|---------|----------|
| Mo1-N7  | 1.756(3) | Mo1-N3  | 2.194(3) |
| Mo1-N5  | 2.210(3) | Mo1-N8  | 2.221(3) |
| Mo1-C10 | 2.259(3) | Mo1-C11 | 2.275(3) |

|          |           |          |           |
|----------|-----------|----------|-----------|
| Mo1-N1   | 2.276(3)  | O1-N7    | 1.218(4)  |
| O2-C12   | 1.341(6)  | O2-C17   | 1.448(6)  |
| N1-C1    | 1.340(4)  | N1-N2    | 1.371(4)  |
| N2-C3    | 1.347(4)  | N2-B1    | 1.541(5)  |
| N3-C4    | 1.339(4)  | N3-N4    | 1.364(4)  |
| N4-C6    | 1.347(4)  | N4-B1    | 1.539(4)  |
| N5-C7    | 1.335(5)  | N5-N6    | 1.367(4)  |
| N6-C9    | 1.349(5)  | N6-B1    | 1.534(5)  |
| N8-C22   | 1.351(4)  | N8-C18   | 1.356(4)  |
| N9-C20   | 1.356(4)  | N9-C23   | 1.454(5)  |
| N9-C24   | 1.456(5)  | C1-C2    | 1.388(5)  |
| C1-H1    | 0.95      | C2-C3    | 1.375(6)  |
| C2-H2    | 0.95      | C3-H3    | 0.95      |
| C4-C5    | 1.390(5)  | C4-H4    | 0.95      |
| C5-C6    | 1.363(5)  | C5-H5    | 0.95      |
| C6-H6    | 0.95      | C7-C8    | 1.403(6)  |
| C7-H7    | 0.95      | C8-C9    | 1.365(6)  |
| C8-H8    | 0.95      | C9-H9    | 0.95      |
| C10-C11  | 1.433(6)  | C10-C15  | 1.436(5)  |
| C10-H10  | 0.97(5)   | C11-C12  | 1.456(5)  |
| C11-H11  | 1.00(5)   | C12-C13  | 1.362(6)  |
| C13-C14  | 1.416(6)  | C13-H13  | 0.95      |
| C14-C15  | 1.358(6)  | C14-C16B | 1.478(14) |
| C14-C16A | 1.495(12) | C14-C16  | 1.501(11) |
| C15-H15  | 0.95      | C17-H17A | 0.98      |
| C17-H17B | 0.98      | C17-H17C | 0.98      |

|          |           |          |           |
|----------|-----------|----------|-----------|
| C18-C19  | 1.371(5)  | C18-H18  | 0.95      |
| C19-C20  | 1.417(5)  | C19-H19  | 0.95      |
| C20-C21  | 1.408(5)  | C21-C22  | 1.374(5)  |
| C21-H21  | 0.95      | C22-H22  | 0.95      |
| C23-H23A | 0.98      | C23-H23B | 0.98      |
| C23-H23C | 0.98      | C24-H24A | 0.98      |
| C24-H24B | 0.98      | C24-H24C | 0.98      |
| B1-H1A   | 1.00(4)   | F1-C16   | 1.363(11) |
| F2-C16   | 1.361(11) | F3-C16   | 1.359(12) |
| F1A-C16A | 1.365(13) | F2A-C16A | 1.364(12) |
| F3A-C16A | 1.360(12) | F1B-C16B | 1.364(14) |
| F2B-C16B | 1.359(14) | F3B-C16B | 1.347(13) |

**Table 5. Bond angles (°) for Harman\_19JAS223.**

|             |            |            |            |
|-------------|------------|------------|------------|
| N7-Mo1-N3   | 96.72(11)  | N7-Mo1-N5  | 91.85(12)  |
| N3-Mo1-N5   | 80.94(10)  | N7-Mo1-N8  | 95.00(12)  |
| N3-Mo1-N8   | 79.38(9)   | N5-Mo1-N8  | 159.78(10) |
| N7-Mo1-C10  | 94.55(12)  | N3-Mo1-C10 | 156.78(12) |
| N5-Mo1-C10  | 118.96(12) | N8-Mo1-C10 | 79.46(12)  |
| N7-Mo1-C11  | 93.91(13)  | N3-Mo1-C11 | 160.32(12) |
| N5-Mo1-C11  | 82.21(13)  | N8-Mo1-C11 | 116.18(12) |
| C10-Mo1-C11 | 36.84(14)  | N7-Mo1-N1  | 173.98(12) |
| N3-Mo1-N1   | 82.34(9)   | N5-Mo1-N1  | 82.13(10)  |
| N8-Mo1-N1   | 90.68(9)   | C10-Mo1-N1 | 88.44(11)  |
| C11-Mo1-N1  | 85.36(11)  | C12-O2-C17 | 117.2(4)   |



|            |            |            |          |
|------------|------------|------------|----------|
| C1-N1-N2   | 105.8(3)   | C1-N1-Mo1  | 135.1(2) |
| N2-N1-Mo1  | 119.0(2)   | C3-N2-N1   | 109.5(3) |
| C3-N2-B1   | 129.5(3)   | N1-N2-B1   | 121.0(3) |
| C4-N3-N4   | 106.9(3)   | C4-N3-Mo1  | 130.7(2) |
| N4-N3-Mo1  | 122.29(19) | C6-N4-N3   | 109.1(3) |
| C6-N4-B1   | 131.2(3)   | N3-N4-B1   | 119.6(2) |
| C7-N5-N6   | 106.7(3)   | C7-N5-Mo1  | 132.2(3) |
| N6-N5-Mo1  | 120.9(2)   | C9-N6-N5   | 109.4(3) |
| C9-N6-B1   | 129.6(3)   | N5-N6-B1   | 120.7(3) |
| O1-N7-Mo1  | 176.6(3)   | C22-N8-C18 | 115.0(3) |
| C22-N8-Mo1 | 121.7(2)   | C18-N8-Mo1 | 123.0(2) |
| C20-N9-C23 | 120.6(3)   | C20-N9-C24 | 121.0(3) |
| C23-N9-C24 | 118.3(3)   | N1-C1-C2   | 111.2(3) |
| N1-C1-H1   | 124.4      | C2-C1-H1   | 124.4    |
| C3-C2-C1   | 104.5(3)   | C3-C2-H2   | 127.7    |
| C1-C2-H2   | 127.7      | N2-C3-C2   | 109.0(3) |
| N2-C3-H3   | 125.5      | C2-C3-H3   | 125.5    |
| N3-C4-C5   | 109.6(3)   | N3-C4-H4   | 125.2    |
| C5-C4-H4   | 125.2      | C6-C5-C4   | 105.7(3) |
| C6-C5-H5   | 127.2      | C4-C5-H5   | 127.2    |
| N4-C6-C5   | 108.7(3)   | N4-C6-H6   | 125.6    |
| C5-C6-H6   | 125.6      | N5-C7-C8   | 110.0(4) |
| N5-C7-H7   | 125.0      | C8-C7-H7   | 125.0    |
| C9-C8-C7   | 105.1(3)   | C9-C8-H8   | 127.4    |
| C7-C8-H8   | 127.4      | N6-C9-C8   | 108.8(4) |
| N6-C9-H9   | 125.6      | C8-C9-H9   | 125.6    |

|                   |          |                   |           |
|-------------------|----------|-------------------|-----------|
| C11-C10-C15       | 119.1(3) | C11-C10-Mo1       | 72.20(19) |
| C15-C10-Mo1       | 115.9(2) | C11-C10-H10       | 118.(3)   |
| C15-C10-H10       | 116.(3)  | Mo1-C10-H10       | 106.(3)   |
| C10-C11-C12       | 116.6(3) | C10-C11-Mo1       | 70.96(18) |
| C12-C11-Mo1       | 119.2(2) | C10-C11-H11       | 120.(3)   |
| C12-C11-H11       | 117.(3)  | Mo1-C11-H11       | 104.(3)   |
| O2-C12-C13        | 123.1(4) | O2-C12-C11        | 114.3(4)  |
| C13-C12-C11       | 122.7(4) | C12-C13-C14       | 118.5(4)  |
| C12-C13-H13       | 120.8    | C14-C13-H13       | 120.8     |
| C15-C14-C13       | 122.0(4) | C15-C14-C16B      | 130.2(8)  |
| C13-C14-C16B      | 106.8(8) | C15-C14-C16A      | 115.2(7)  |
| C13-C14-C16A      | 122.6(7) | C15-C14-C16       | 120.1(7)  |
| C13-C14-C16       | 117.7(6) | C14-C15-C10       | 120.5(4)  |
| C14-C15-H15       | 119.8    | C10-C15-H15       | 119.8     |
| O2-C17-H17A       | 109.5    | O2-C17-H17B       | 109.5     |
| H17A-C17-<br>H17B | 109.5    | O2-C17-H17C       | 109.5     |
| H17A-C17-<br>H17C | 109.5    | H17B-C17-<br>H17C | 109.5     |
| N8-C18-C19        | 124.4(3) | N8-C18-H18        | 117.8     |
| C19-C18-H18       | 117.8    | C18-C19-C20       | 120.3(3)  |
| C18-C19-H19       | 119.9    | C20-C19-H19       | 119.9     |
| N9-C20-C21        | 121.8(3) | N9-C20-C19        | 122.7(3)  |
| C21-C20-C19       | 115.5(3) | C22-C21-C20       | 119.8(3)  |
| C22-C21-H21       | 120.1    | C20-C21-H21       | 120.1     |
| N8-C22-C21        | 125.0(3) | N8-C22-H22        | 117.5     |
| C21-C22-H22       | 117.5    | N9-C23-H23A       | 109.5     |

|               |           |               |           |
|---------------|-----------|---------------|-----------|
| N9-C23-H23B   | 109.5     | H23A-C23-H23B | 109.5     |
| N9-C23-H23C   | 109.5     | H23A-C23-H23C | 109.5     |
| H23B-C23-H23C | 109.5     | N9-C24-H24A   | 109.5     |
| N9-C24-H24B   | 109.5     | H24A-C24-H24B | 109.5     |
| N9-C24-H24C   | 109.5     | H24A-C24-H24C | 109.5     |
| H24B-C24-H24C | 109.5     | N6-B1-N4      | 108.0(3)  |
| N6-B1-N2      | 108.9(3)  | N4-B1-N2      | 109.0(3)  |
| N6-B1-H1A     | 111.(2)   | N4-B1-H1A     | 111.(2)   |
| N2-B1-H1A     | 108.(2)   | F3-C16-F2     | 104.5(10) |
| F3-C16-F1     | 106.4(10) | F2-C16-F1     | 109.0(12) |
| F3-C16-C14    | 110.5(10) | F2-C16-C14    | 109.3(11) |
| F1-C16-C14    | 116.5(10) | F3A-C16A-F2A  | 102.7(10) |
| F3A-C16A-F1A  | 102.7(11) | F2A-C16A-F1A  | 105.0(14) |
| F3A-C16A-C14  | 114.9(11) | F2A-C16A-C14  | 115.4(11) |
| F1A-C16A-C14  | 114.6(11) | F3B-C16B-F2B  | 109.6(17) |
| F3B-C16B-F1B  | 110.6(16) | F2B-C16B-F1B  | 103.3(17) |
| F3B-C16B-C14  | 115.8(13) | F2B-C16B-C14  | 112.0(17) |
| F1B-C16B-C14  | 104.8(12) |               |           |

**Table 6. Torsion angles (°) for Harman\_19JAS223.**

|             |          |              |           |
|-------------|----------|--------------|-----------|
| C1-N1-N2-C3 | 0.3(3)   | Mo1-N1-N2-C3 | -178.2(2) |
| C1-N1-N2-B1 | 177.5(3) | Mo1-N1-N2-B1 | -1.0(3)   |

|                  |           |                  |           |
|------------------|-----------|------------------|-----------|
| C4-N3-N4-C6      | 0.8(4)    | Mo1-N3-N4-C6     | -175.3(2) |
| C4-N3-N4-B1      | 177.5(3)  | Mo1-N3-N4-B1     | 1.4(4)    |
| C7-N5-N6-C9      | -0.8(4)   | Mo1-N5-N6-C9     | -175.9(2) |
| C7-N5-N6-B1      | 173.9(3)  | Mo1-N5-N6-B1     | -1.2(4)   |
| N2-N1-C1-C2      | -0.2(4)   | Mo1-N1-C1-C2     | 178.0(2)  |
| N1-C1-C2-C3      | 0.0(4)    | N1-N2-C3-C2      | -0.3(4)   |
| B1-N2-C3-C2      | -177.3(3) | C1-C2-C3-N2      | 0.2(4)    |
| N4-N3-C4-C5      | -0.6(4)   | Mo1-N3-C4-C5     | 175.1(2)  |
| N3-C4-C5-C6      | 0.2(4)    | N3-N4-C6-C5      | -0.7(4)   |
| B1-N4-C6-C5      | -176.9(3) | C4-C5-C6-N4      | 0.3(4)    |
| N6-N5-C7-C8      | 0.9(4)    | Mo1-N5-C7-C8     | 175.2(3)  |
| N5-C7-C8-C9      | -0.7(5)   | N5-N6-C9-C8      | 0.4(4)    |
| B1-N6-C9-C8      | -173.7(3) | C7-C8-C9-N6      | 0.2(4)    |
| C15-C10-C11-C12  | -3.6(5)   | Mo1-C10-C11-C12  | -113.9(3) |
| C15-C10-C11-Mo1  | 110.3(3)  | C17-O2-C12-C13   | 2.5(7)    |
| C17-O2-C12-C11   | -178.9(4) | C10-C11-C12-O2   | -170.5(3) |
| Mo1-C11-C12-O2   | 107.4(4)  | C10-C11-C12-C13  | 8.1(5)    |
| Mo1-C11-C12-C13  | -74.0(5)  | O2-C12-C13-C14   | 173.2(4)  |
| C11-C12-C13-C14  | -5.3(6)   | C12-C13-C14-C15  | -2.3(6)   |
| C12-C13-C14-C16B | -172.4(9) | C12-C13-C14-C16A | -176.9(8) |
| C12-C13-C14-C16  | -178.2(7) | C13-C14-C15-C10  | 6.6(6)    |

|                  |           |                  |            |
|------------------|-----------|------------------|------------|
| C16B-C14-C15-C10 | 174.2(11) | C16A-C14-C15-C10 | -178.3(7)  |
| C16-C14-C15-C10  | -177.6(7) | C11-C10-C15-C14  | -3.4(5)    |
| Mo1-C10-C15-C14  | 79.8(4)   | C22-N8-C18-C19   | -2.6(4)    |
| Mo1-N8-C18-C19   | -177.0(2) | N8-C18-C19-C20   | 1.1(5)     |
| C23-N9-C20-C21   | 2.0(5)    | C24-N9-C20-C21   | -174.9(3)  |
| C23-N9-C20-C19   | -177.3(3) | C24-N9-C20-C19   | 5.8(5)     |
| C18-C19-C20-N9   | -179.4(3) | C18-C19-C20-C21  | 1.3(4)     |
| N9-C20-C21-C22   | 178.6(3)  | C19-C20-C21-C22  | -2.1(4)    |
| C18-N8-C22-C21   | 1.7(5)    | Mo1-N8-C22-C21   | 176.3(2)   |
| C20-C21-C22-N8   | 0.6(5)    | C9-N6-B1-N4      | 115.6(4)   |
| N5-N6-B1-N4      | -57.9(4)  | C9-N6-B1-N2      | -126.2(4)  |
| N5-N6-B1-N2      | 60.3(4)   | C6-N4-B1-N6      | -126.4(4)  |
| N3-N4-B1-N6      | 57.8(4)   | C6-N4-B1-N2      | 115.4(4)   |
| N3-N4-B1-N2      | -60.4(4)  | C3-N2-B1-N6      | 118.5(3)   |
| N1-N2-B1-N6      | -58.2(4)  | C3-N2-B1-N4      | -123.9(3)  |
| N1-N2-B1-N4      | 59.4(4)   | C15-C14-C16-F3   | -103.2(10) |
| C13-C14-C16-F3   | 72.8(11)  | C15-C14-C16-F2   | 142.4(10)  |
| C13-C14-C16-F2   | -41.6(13) | C15-C14-C16-F1   | 18.2(15)   |

|                      |                |                      |                |
|----------------------|----------------|----------------------|----------------|
| C13-C14-C16-<br>F1   | -<br>165.8(10) | C15-C14-C16A-<br>F3A | -78.7(13)      |
| C13-C14-C16A-<br>F3A | 96.3(12)       | C15-C14-C16A-<br>F2A | 162.0(11)      |
| C13-C14-C16A-<br>F2A | -23.0(16)      | C15-C14-C16A-<br>F1A | 39.9(15)       |
| C13-C14-C16A-<br>F1A | -<br>145.0(10) | C15-C14-C16B-<br>F3B | -<br>117.6(14) |
| C13-C14-C16B-<br>F3B | 51.4(18)       | C15-C14-C16B-<br>F2B | 115.8(17)      |
| C13-C14-C16B-<br>F2B | -75.1(17)      | C15-C14-C16B-<br>F1B | 4.5(19)        |
| C13-C14-C16B-<br>F1B | 173.6(11)      |                      |                |

**Table 7. Anisotropic atomic displacement parameters ( $\text{\AA}^2$ ) for Harman\_19JAS223.**

The anisotropic atomic displacement factor exponent takes the form:  $-2\pi^2 [ h^2 a^{*2} U_{11} + \dots + 2 h k a^* b^* U_{12} ]$

|     | U <sub>11</sub> | U <sub>22</sub> | U <sub>33</sub> | U <sub>23</sub>        | U <sub>13</sub> | U <sub>12</sub>        |
|-----|-----------------|-----------------|-----------------|------------------------|-----------------|------------------------|
| Mo1 | 0.01735(15)     | 0.01986(15)     | 0.01632(15)     | 0.00226(8)             | 0.00425(10)     | 0.00066(8)             |
| O1  | 0.0569(18)      | 0.0531(18)      | 0.0513(17)      | 0.0267(14)             | 0.0399(15)      | 0.0135(14)             |
| O2  | 0.0432(17)      | 0.089(3)        | 0.055(2)        | $\bar{}$<br>0.0098(19) | 0.0127(15)      | $\bar{}$<br>0.0098(18) |
| N1  | 0.0208(12)      | 0.0244(13)      | 0.0180(12)      | 0.0007(10)             | 0.0049(10)      | $\bar{}$<br>0.0015(10) |
| N2  | 0.0221(12)      | 0.0299(15)      | 0.0167(12)      | $\bar{}$<br>0.0036(11) | 0.0059(10)      | $\bar{}$<br>0.0016(11) |
| N3  | 0.0235(12)      | 0.0203(12)      | 0.0169(12)      | -0.0009(9)             | 0.0053(10)      | 0.0012(10)             |
| N4  | 0.0212(12)      | 0.0285(14)      | 0.0214(13)      | $\bar{}$<br>0.0009(11) | 0.0055(10)      | 0.0063(11)             |

|     | <b>U<sub>11</sub></b> | <b>U<sub>22</sub></b> | <b>U<sub>33</sub></b> | <b>U<sub>23</sub></b>   | <b>U<sub>13</sub></b> | <b>U<sub>12</sub></b>   |
|-----|-----------------------|-----------------------|-----------------------|-------------------------|-----------------------|-------------------------|
| N5  | 0.0240(13)            | 0.0259(14)            | 0.0247(14)            | <sup>-</sup> 0.0004(11) | 0.0011(11)            | <sup>-</sup> 0.0040(11) |
| N6  | 0.0339(15)            | 0.0259(14)            | 0.0194(13)            | <sup>-</sup> 0.0064(11) | 0.0049(11)            | <sup>-</sup> 0.0001(12) |
| N7  | 0.0236(13)            | 0.0250(14)            | 0.0311(15)            | 0.0071(11)              | 0.0116(11)            | 0.0049(11)              |
| N8  | 0.0236(12)            | 0.0196(12)            | 0.0177(12)            | 0.0002(10)              | 0.0056(10)            | 0.0013(10)              |
| N9  | 0.0330(15)            | 0.0262(15)            | 0.0317(15)            | <sup>-</sup> 0.0060(12) | 0.0024(12)            | 0.0012(12)              |
| C1  | 0.0306(16)            | 0.0282(17)            | 0.0263(16)            | 0.0046(13)              | 0.0082(13)            | <sup>-</sup> 0.0035(13) |
| C2  | 0.0370(18)            | 0.040(2)              | 0.0242(17)            | 0.0058(14)              | 0.0108(14)            | <sup>-</sup> 0.0057(16) |
| C3  | 0.0255(16)            | 0.045(2)              | 0.0228(16)            | <sup>-</sup> 0.0045(14) | 0.0111(13)            | <sup>-</sup> 0.0063(14) |
| C4  | 0.0266(15)            | 0.0261(16)            | 0.0152(14)            | <sup>-</sup> 0.0004(12) | -0.0023(11)           | 0.0002(13)              |
| C5  | 0.0258(16)            | 0.038(2)              | 0.0261(17)            | 0.0038(14)              | -0.0014(13)           | 0.0039(14)              |
| C6  | 0.0215(15)            | 0.040(2)              | 0.0349(19)            | 0.0053(15)              | 0.0061(13)            | 0.0073(14)              |
| C7  | 0.0303(17)            | 0.0314(19)            | 0.039(2)              | <sup>-</sup> 0.0002(15) | -0.0015(15)           | <sup>-</sup> 0.0125(15) |
| C8  | 0.053(2)              | 0.031(2)              | 0.041(2)              | <sup>-</sup> 0.0058(16) | -0.0008(18)           | <sup>-</sup> 0.0156(18) |
| C9  | 0.057(2)              | 0.0291(19)            | 0.0263(18)            | <sup>-</sup> 0.0075(14) | 0.0065(16)            | <sup>-</sup> 0.0030(17) |
| C10 | 0.0242(16)            | 0.0299(18)            | 0.0334(18)            | 0.0144(14)              | 0.0102(13)            | 0.0118(13)              |
| C11 | 0.0186(15)            | 0.045(2)              | 0.0248(17)            | 0.0067(15)              | 0.0025(12)            | 0.0060(14)              |
| C12 | 0.0189(16)            | 0.047(2)              | 0.041(2)              | 0.0063(17)              | -0.0053(15)           | <sup>-</sup> 0.0016(15) |
| C13 | 0.0215(17)            | 0.053(2)              | 0.051(2)              | 0.0120(19)              | 0.0137(16)            | 0.0074(16)              |

|     | U <sub>11</sub> | U <sub>22</sub> | U <sub>33</sub> | U <sub>23</sub>            | U <sub>13</sub> | U <sub>12</sub>            |
|-----|-----------------|-----------------|-----------------|----------------------------|-----------------|----------------------------|
| C14 | 0.0319(18)      | 0.042(2)        | 0.045(2)        | 0.0122(17)                 | 0.0134(16)      | 0.0102(16)                 |
| C15 | 0.0309(17)      | 0.0335(19)      | 0.038(2)        | 0.0090(15)                 | 0.0091(15)      | 0.0144(15)                 |
| C17 | 0.047(3)        | 0.094(5)        | 0.075(4)        | -0.006(3)                  | 0.016(3)        | -0.022(3)                  |
| C18 | 0.0255(15)      | 0.0253(16)      | 0.0193(14)      | 0.0027(12)                 | 0.0064(12)      | 0.0049(13)                 |
| C19 | 0.0271(15)      | 0.0249(16)      | 0.0221(15)      | <sup>-</sup><br>0.0004(12) | 0.0064(12)      | 0.0088(13)                 |
| C20 | 0.0240(14)      | 0.0204(15)      | 0.0220(15)      | 0.0006(12)                 | -0.0008(12)     | 0.0042(12)                 |
| C21 | 0.0240(15)      | 0.0263(16)      | 0.0271(16)      | 0.0015(13)                 | 0.0078(12)      | <sup>-</sup><br>0.0001(13) |
| C22 | 0.0239(14)      | 0.0229(15)      | 0.0209(14)      | <sup>-</sup><br>0.0025(12) | 0.0082(11)      | <sup>-</sup><br>0.0011(12) |
| C23 | 0.038(2)        | 0.037(2)        | 0.048(2)        | <sup>-</sup><br>0.0088(17) | 0.0025(17)      | <sup>-</sup><br>0.0109(17) |
| C24 | 0.046(2)        | 0.0328(19)      | 0.035(2)        | <sup>-</sup><br>0.0098(16) | 0.0025(16)      | 0.0031(17)                 |
| B1  | 0.0290(18)      | 0.0270(19)      | 0.0208(17)      | <sup>-</sup><br>0.0040(14) | 0.0065(14)      | 0.0043(15)                 |
| F1  | 0.059(3)        | 0.047(3)        | 0.072(2)        | <sup>-</sup><br>0.0041(17) | 0.038(2)        | 0.0074(17)                 |
| F2  | 0.059(3)        | 0.047(3)        | 0.072(2)        | <sup>-</sup><br>0.0041(17) | 0.038(2)        | 0.0074(17)                 |
| F3  | 0.059(3)        | 0.047(3)        | 0.072(2)        | <sup>-</sup><br>0.0041(17) | 0.038(2)        | 0.0074(17)                 |
| C16 | 0.041(3)        | 0.045(4)        | 0.063(4)        | 0.004(3)                   | 0.031(3)        | 0.002(3)                   |
| F1A | 0.059(3)        | 0.047(3)        | 0.072(2)        | <sup>-</sup><br>0.0041(17) | 0.038(2)        | 0.0074(17)                 |
| F2A | 0.059(3)        | 0.047(3)        | 0.072(2)        | <sup>-</sup><br>0.0041(17) | 0.038(2)        | 0.0074(17)                 |
| F3A | 0.059(3)        | 0.047(3)        | 0.072(2)        | <sup>-</sup><br>0.0041(17) | 0.038(2)        | 0.0074(17)                 |



|      | <b>U<sub>11</sub></b> | <b>U<sub>22</sub></b> | <b>U<sub>33</sub></b> | <b>U<sub>23</sub></b> | <b>U<sub>13</sub></b> | <b>U<sub>12</sub></b> |
|------|-----------------------|-----------------------|-----------------------|-----------------------|-----------------------|-----------------------|
| C16A | 0.041(3)              | 0.045(4)              | 0.063(4)              | 0.004(3)              | 0.031(3)              | 0.002(3)              |
| F1B  | 0.059(3)              | 0.047(3)              | 0.072(2)              | -<br>0.0041(17)       | 0.038(2)              | 0.0074(17)            |
| F2B  | 0.059(3)              | 0.047(3)              | 0.072(2)              | -<br>0.0041(17)       | 0.038(2)              | 0.0074(17)            |
| F3B  | 0.059(3)              | 0.047(3)              | 0.072(2)              | -<br>0.0041(17)       | 0.038(2)              | 0.0074(17)            |
| C16B | 0.041(3)              | 0.045(4)              | 0.063(4)              | 0.004(3)              | 0.031(3)              | 0.002(3)              |

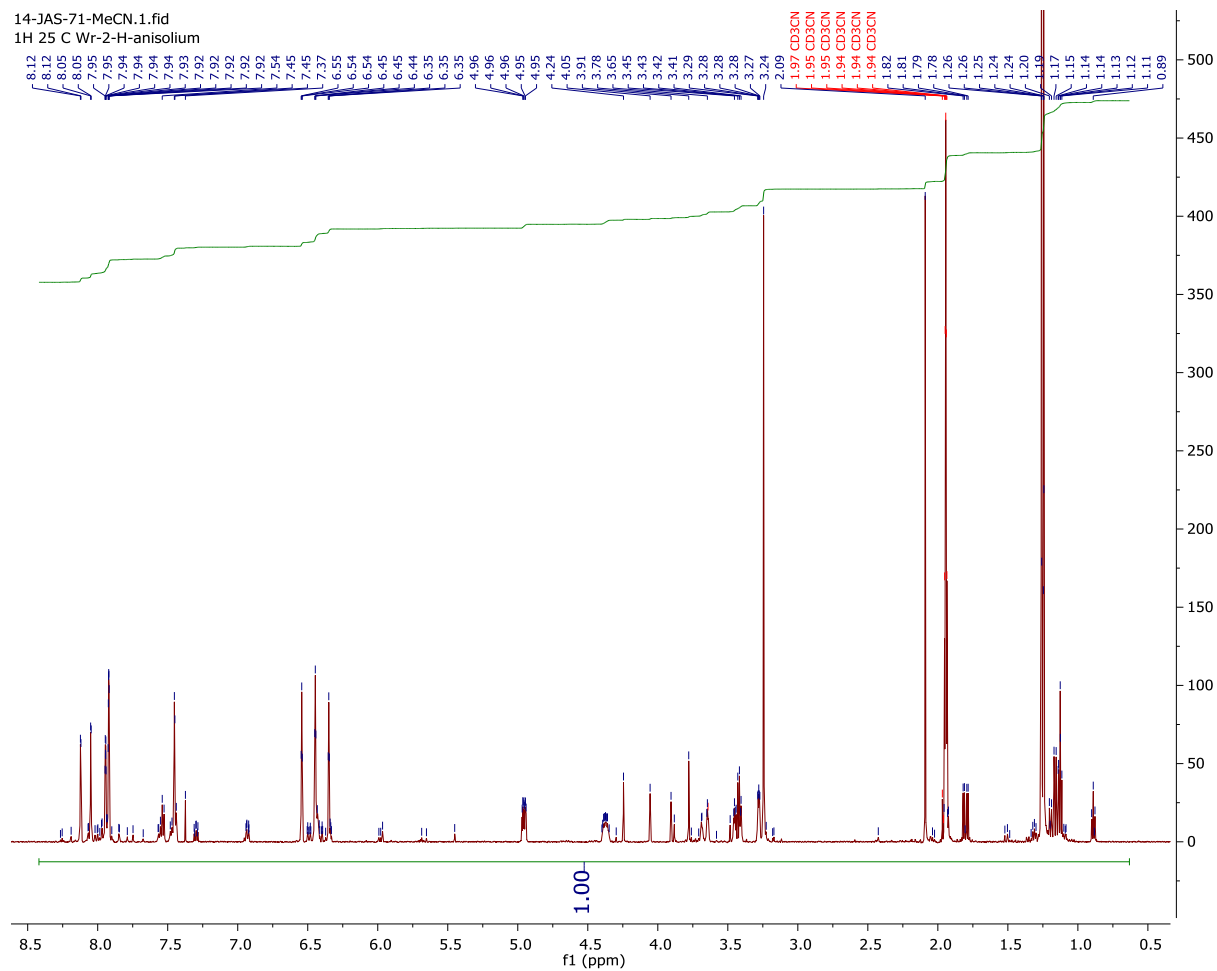
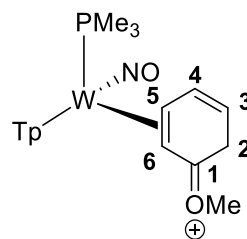
**Table 8. Hydrogen atomic coordinates and isotropic atomic displacement parameters (Å<sup>2</sup>) for Harman\_19JAS223.**

|      | <b>x/a</b> | <b>y/b</b> | <b>z/c</b> | <b>U(eq)</b> |
|------|------------|------------|------------|--------------|
| H1   | 0.4081     | 0.5726     | 0.6667     | 0.034        |
| H2   | 0.2847     | 0.5983     | 0.7871     | 0.04         |
| H3   | 0.1896     | 0.7152     | 0.7411     | 0.036        |
| H4   | 0.1902     | 0.7021     | 0.2706     | 0.029        |
| H5   | -0.0119    | 0.7607     | 0.2663     | 0.038        |
| H6   | 0.0098     | 0.8096     | 0.4325     | 0.039        |
| H7   | 0.6227     | 0.8344     | 0.5319     | 0.043        |
| H8   | 0.5655     | 0.9416     | 0.6124     | 0.053        |
| H9   | 0.3600     | 0.9169     | 0.6440     | 0.046        |
| H10  | 0.537(4)   | 0.572(3)   | 0.564(3)   | 0.045(13)    |
| H11  | 0.605(5)   | 0.678(3)   | 0.649(4)   | 0.050(14)    |
| H13  | 0.8528     | 0.6996     | 0.4824     | 0.049        |
| H15  | 0.6142     | 0.5372     | 0.4313     | 0.041        |
| H17A | 0.8723     | 0.8021     | 0.5444     | 0.108        |

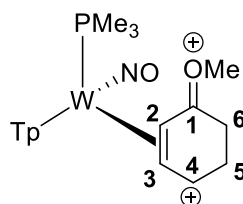
|      | <b>x/a</b> | <b>y/b</b> | <b>z/c</b> | <b>U(eq)</b> |
|------|------------|------------|------------|--------------|
| H17B | 0.9583     | 0.7530     | 0.6254     | 0.108        |
| H17C | 0.9105     | 0.8254     | 0.6567     | 0.108        |
| H18  | 0.4416     | 0.5870     | 0.3022     | 0.028        |
| H19  | 0.3403     | 0.4954     | 0.2140     | 0.03         |
| H21  | 0.0940     | 0.5015     | 0.3808     | 0.031        |
| H22  | 0.2066     | 0.5912     | 0.4658     | 0.027        |
| H23A | 0.0473     | 0.3931     | 0.3284     | 0.064        |
| H23B | 0.0003     | 0.3635     | 0.2195     | 0.064        |
| H23C | -0.0352    | 0.4406     | 0.2434     | 0.064        |
| H24A | 0.1747     | 0.4236     | 0.1048     | 0.059        |
| H24B | 0.1427     | 0.3509     | 0.1466     | 0.059        |
| H24C | 0.2764     | 0.3852     | 0.1894     | 0.059        |
| H1A  | 0.193(4)   | 0.811(2)   | 0.607(3)   | 0.030(11)    |

# Supporting Information for Chapter 7

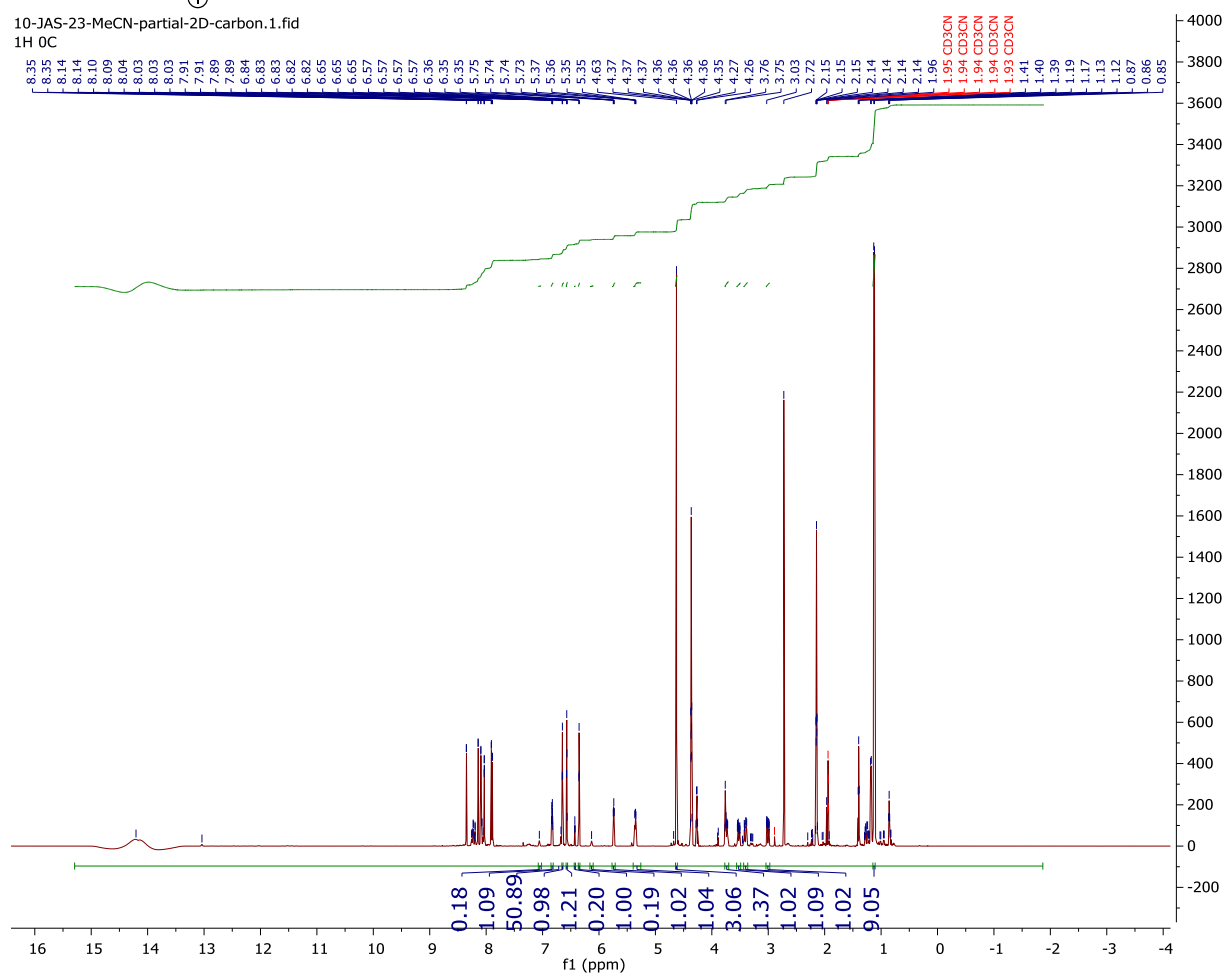
## Synthesis of $\text{W}(\text{NO})(\text{PMe}_3)(\eta^2\text{-5,6-2H-anisolum})$ (2)



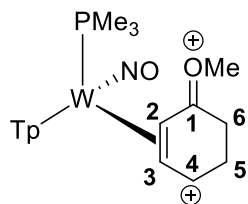
# <sup>1</sup>H NMR Spectra of 3A



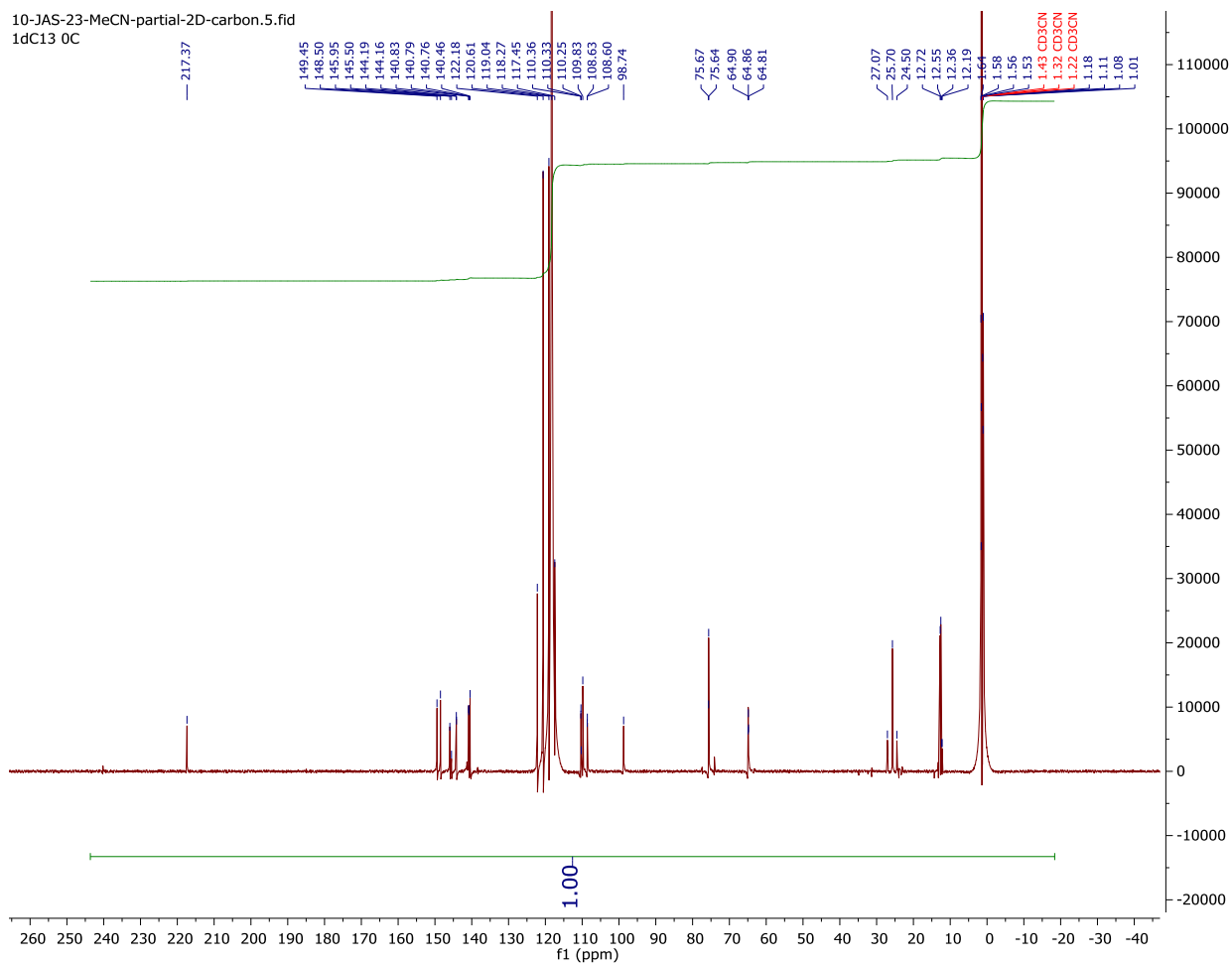
10-JAS-23-MeCN-partial-2D-carbon.1.fid  
1H OC



# $^{13}\text{C}$ $\{^1\text{H}\}$ NMR Spectra of 3A

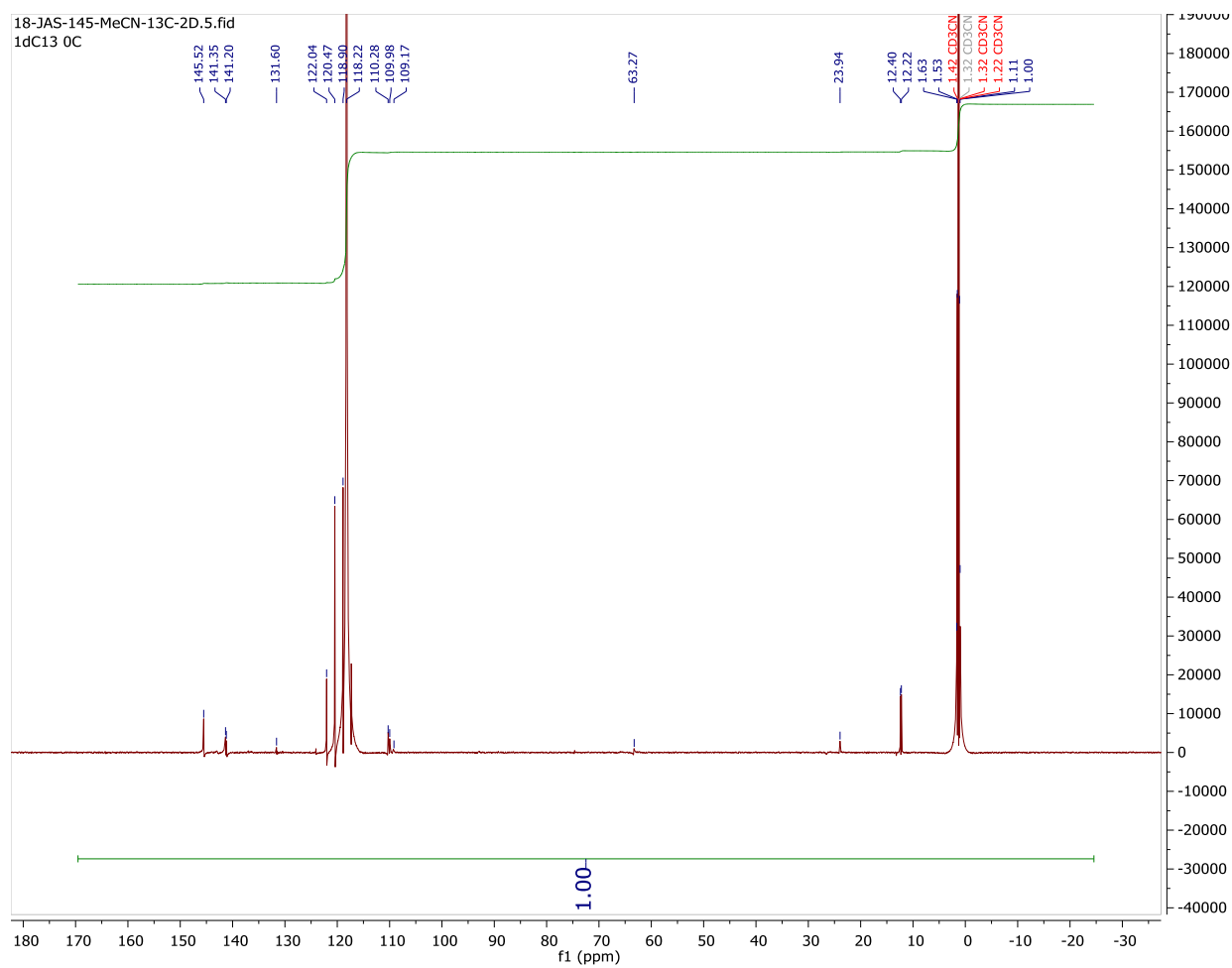
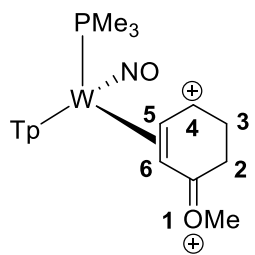


10-JAS-23-MeCN-partial-2D-carbon.5.fid  
1dC13 0C





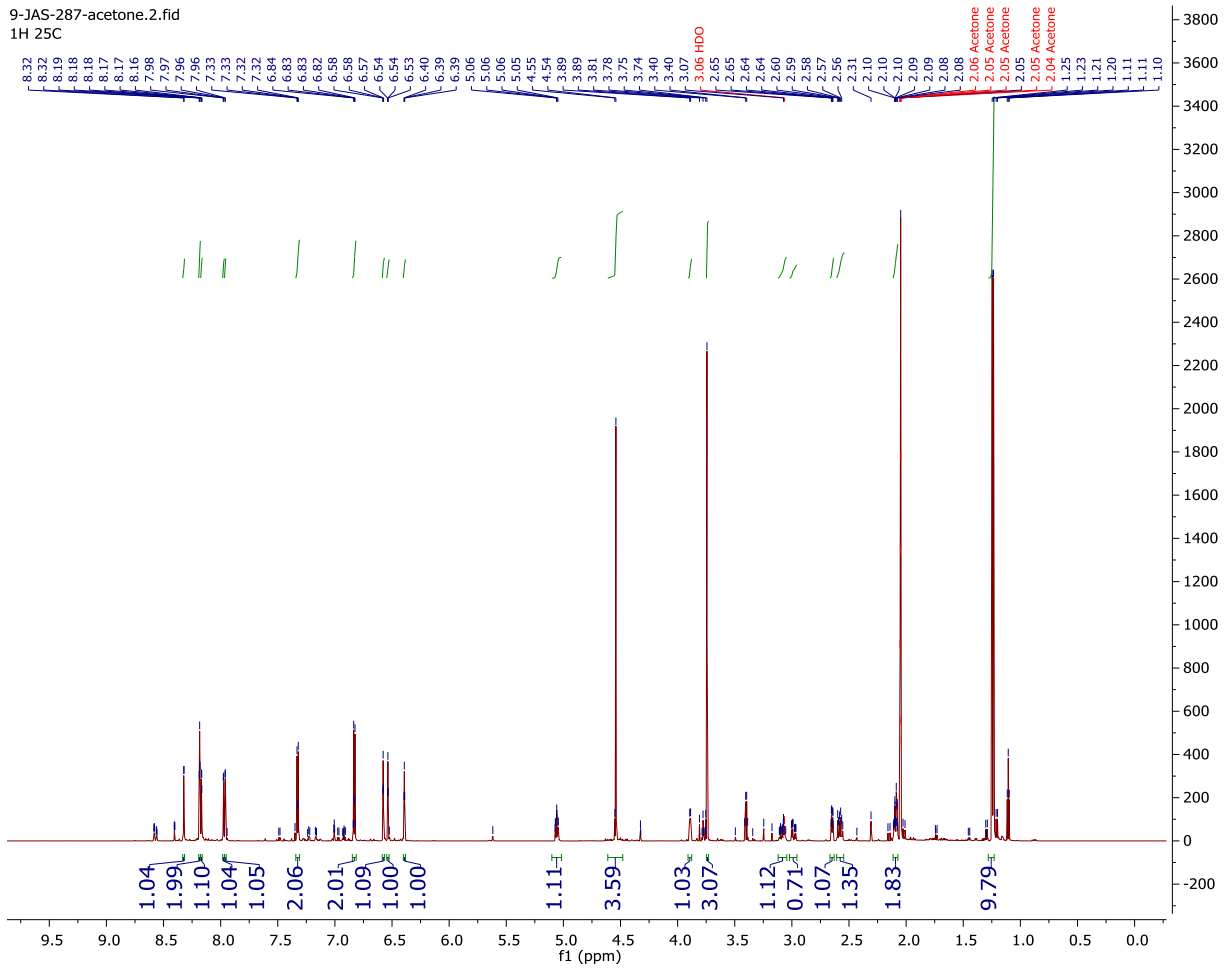
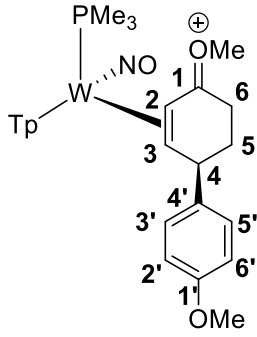
# $^{13}\text{C}$ $\{^1\text{H}\}$ NMR Spectra of 3B



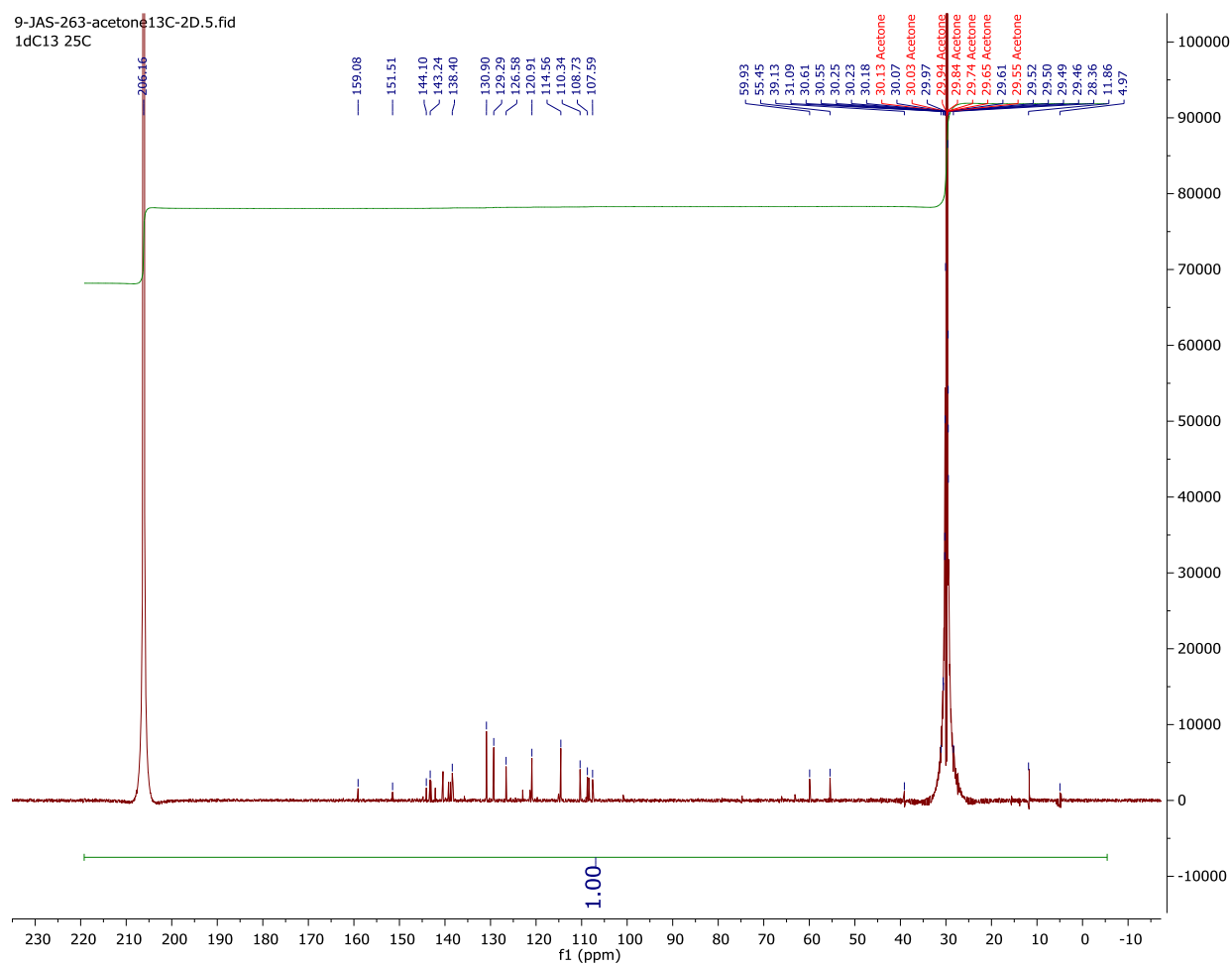
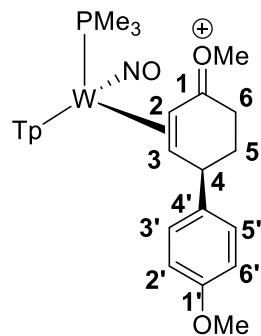




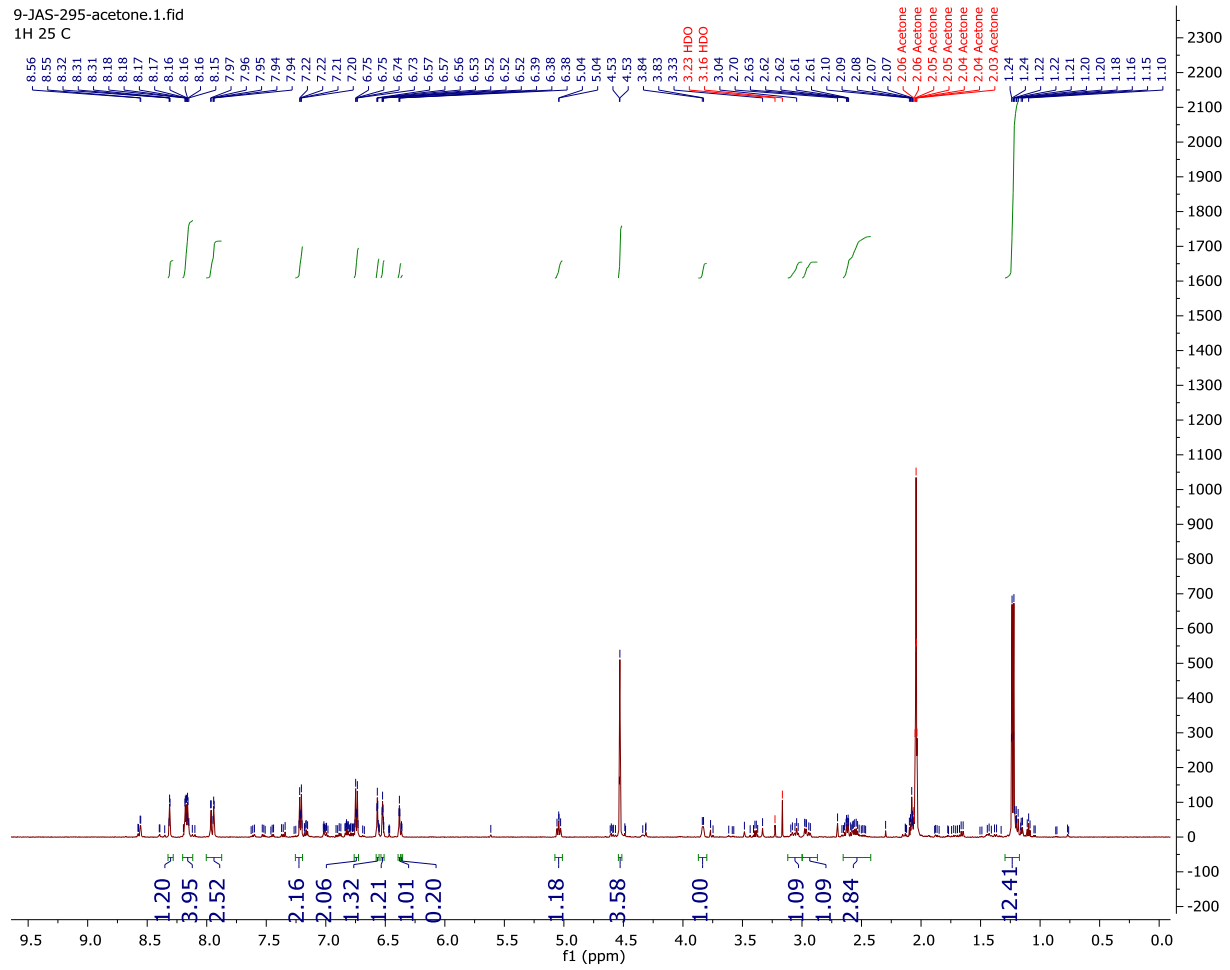
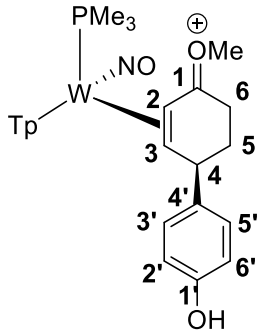
# <sup>1</sup>H NMR Spectra of 6



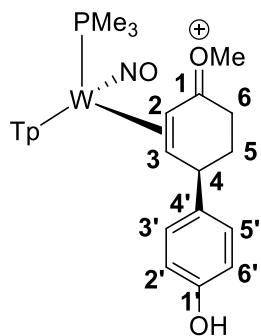
# $^{13}\text{C} \{^1\text{H}\}$ NMR Spectra of 6



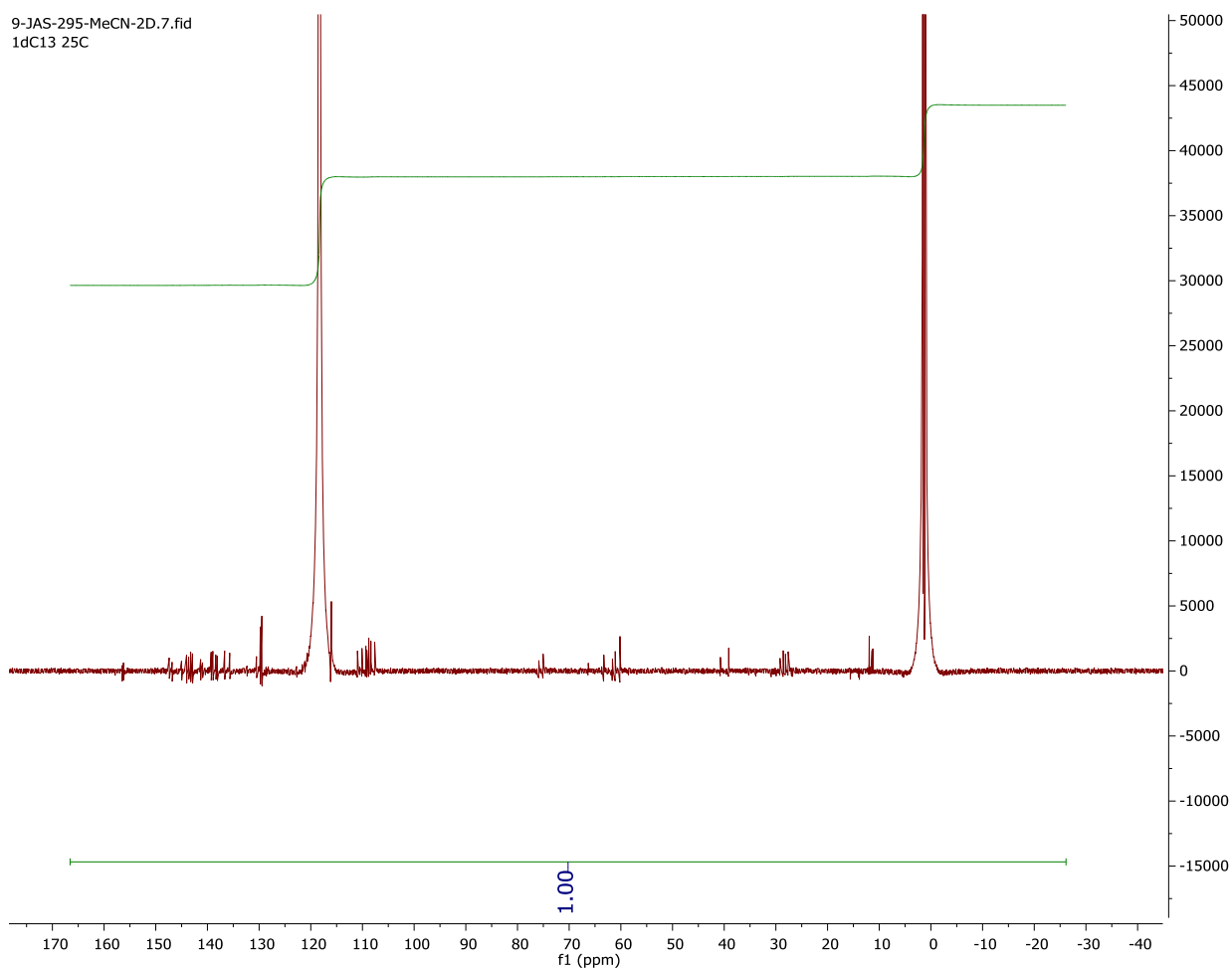
# <sup>1</sup>H NMR Spectra of 7



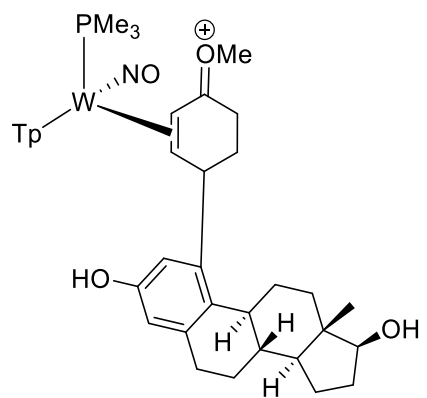
# $^{13}\text{C} \{^1\text{H}\}$ NMR Spectra of 7



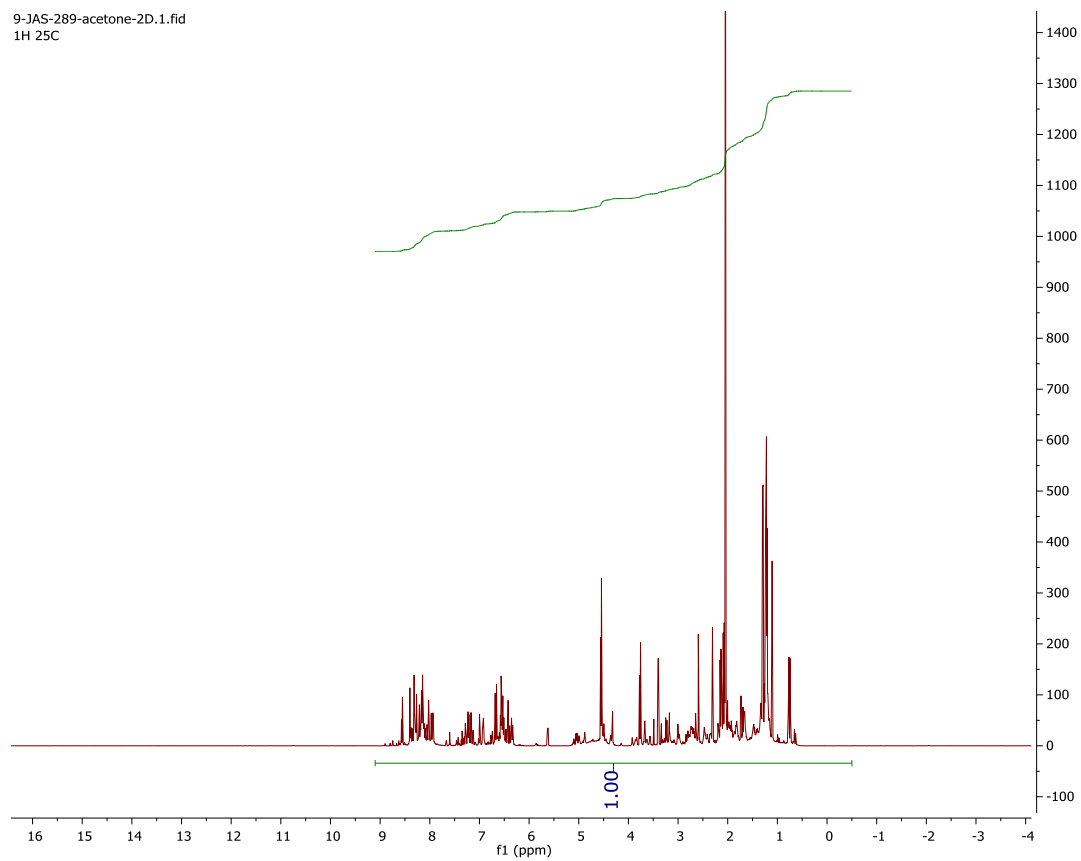
9-JAS-295-MeCN-2D.7.fid  
1dC13 25C



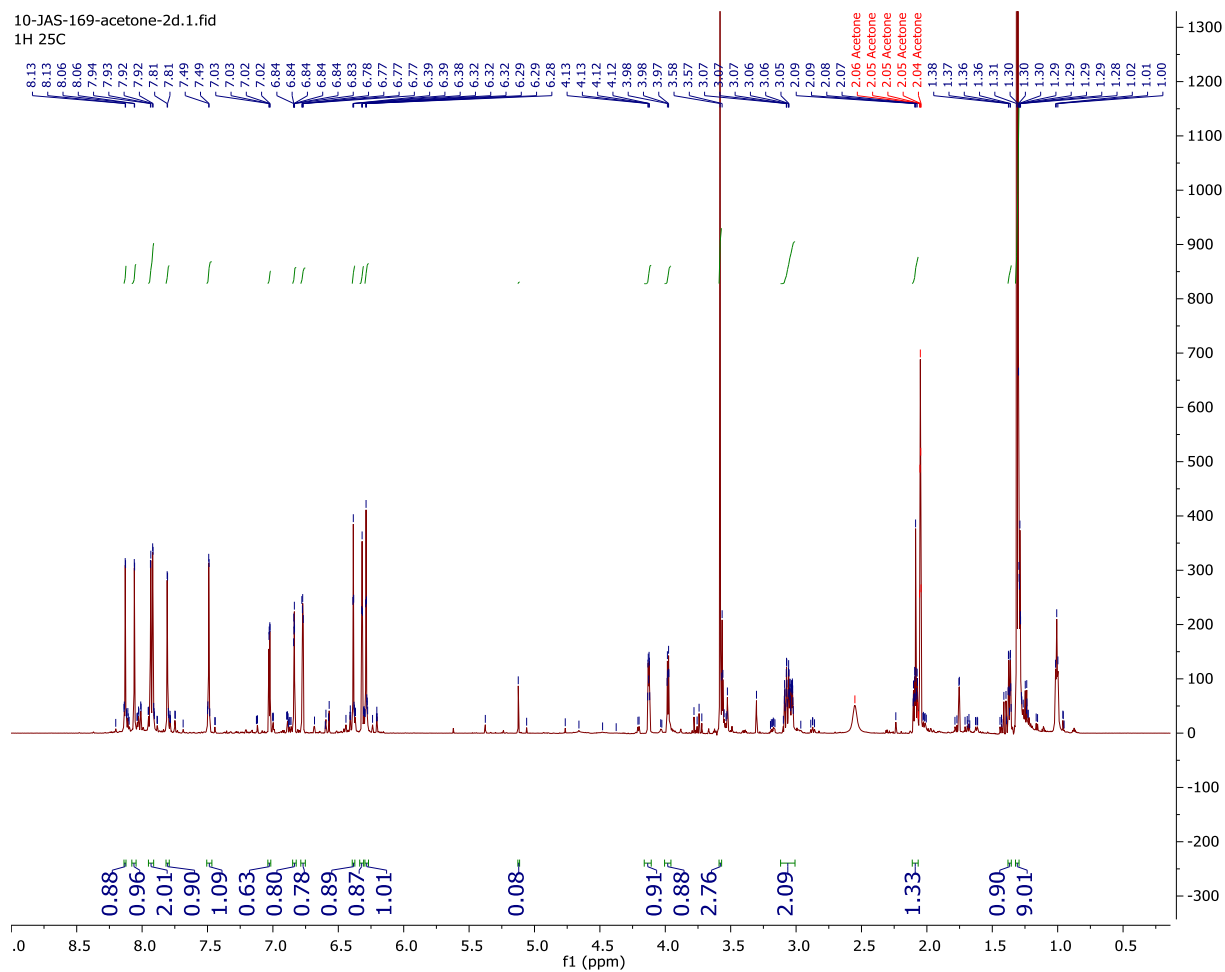
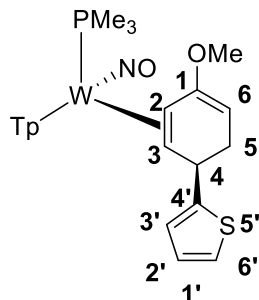
# <sup>1</sup>H NMR Spectra of 8



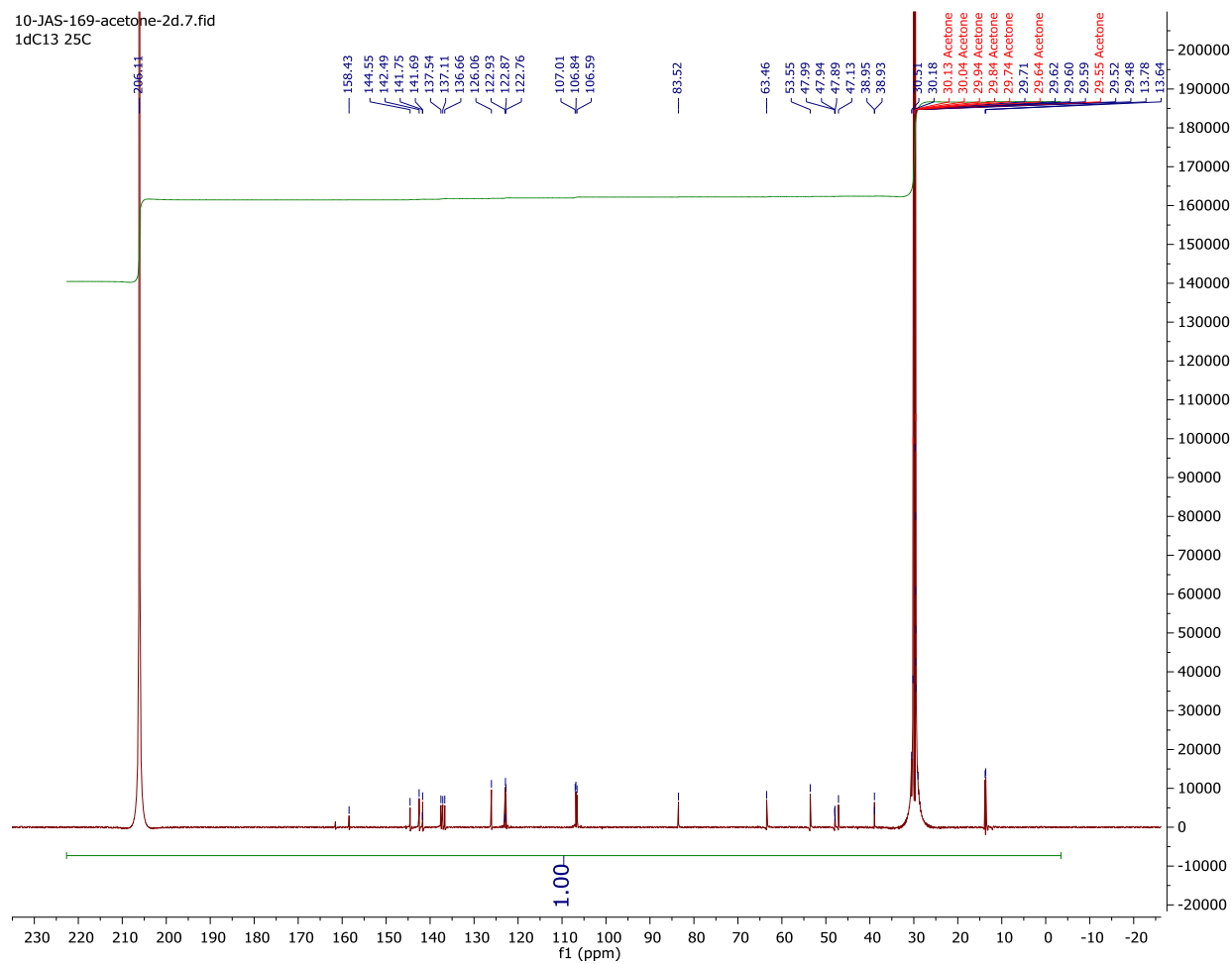
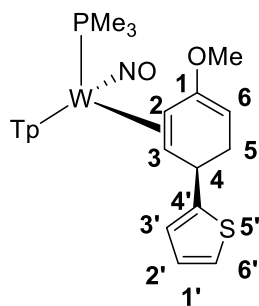
9-JAS-289-acetone-2D.1.fid  
1H 25C



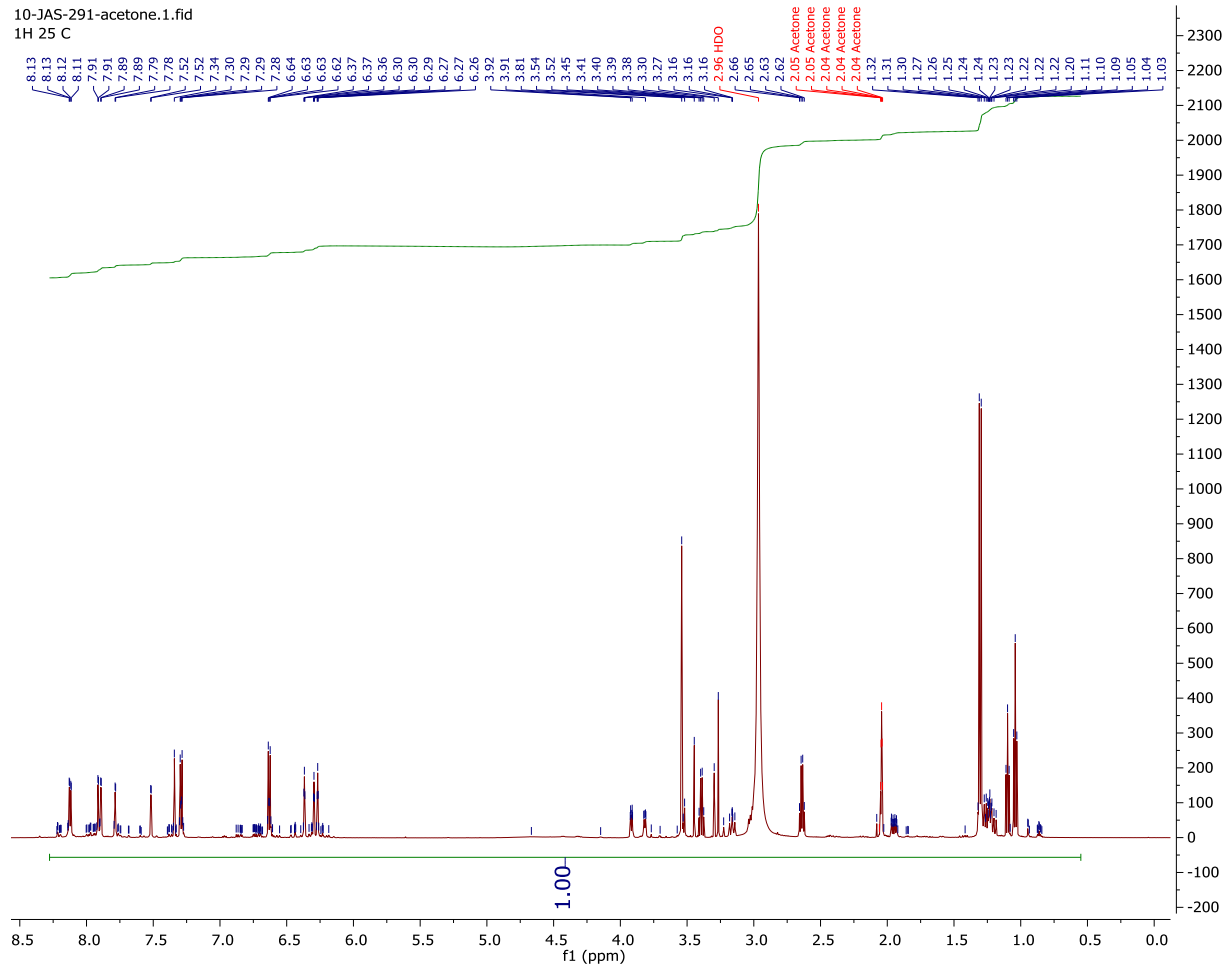
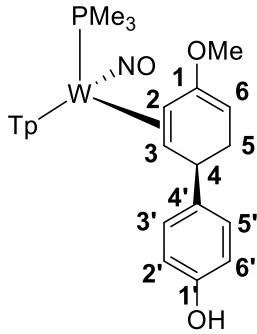
# <sup>1</sup>H NMR Spectra of 9



# $^{13}\text{C}$ $\{^1\text{H}\}$ NMR Spectra of 9

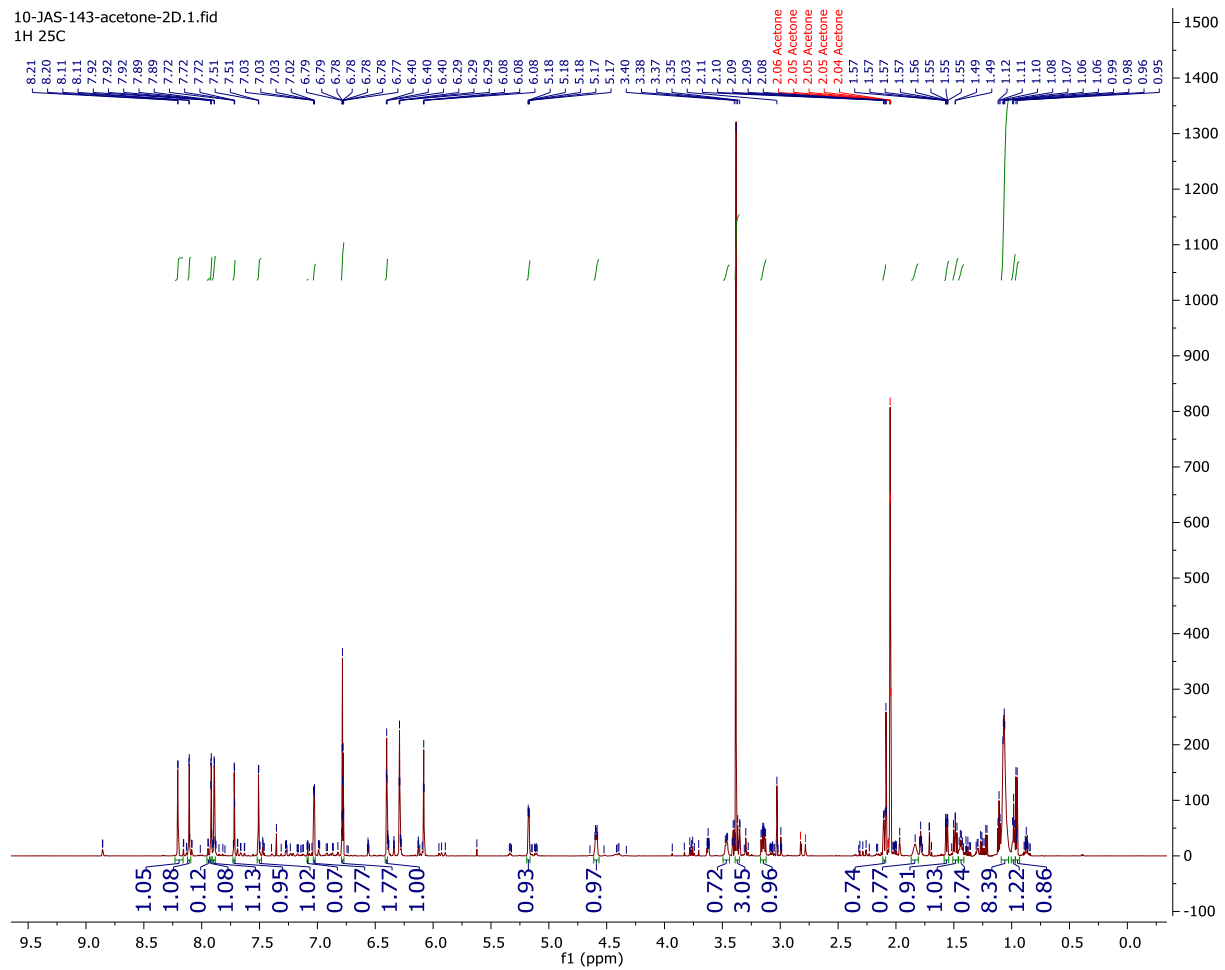
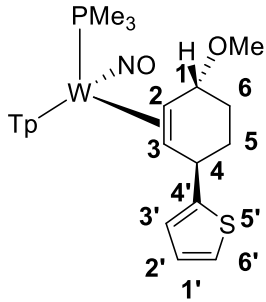


# <sup>1</sup>H NMR Spectra of 10

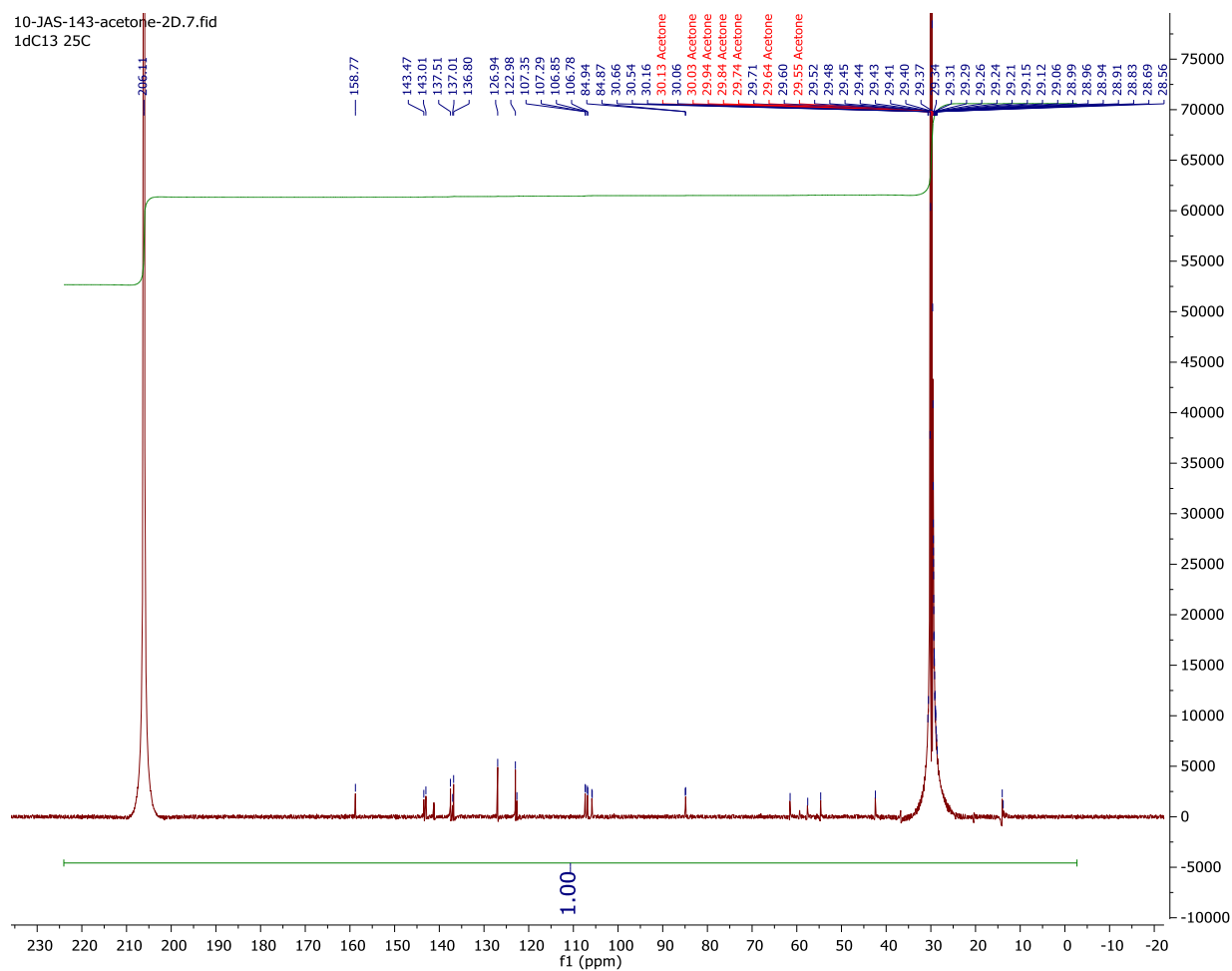
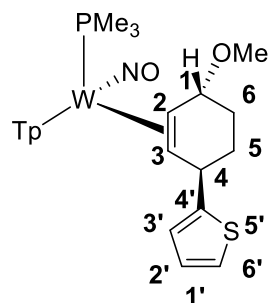




# <sup>1</sup>H NMR Spectra of 12

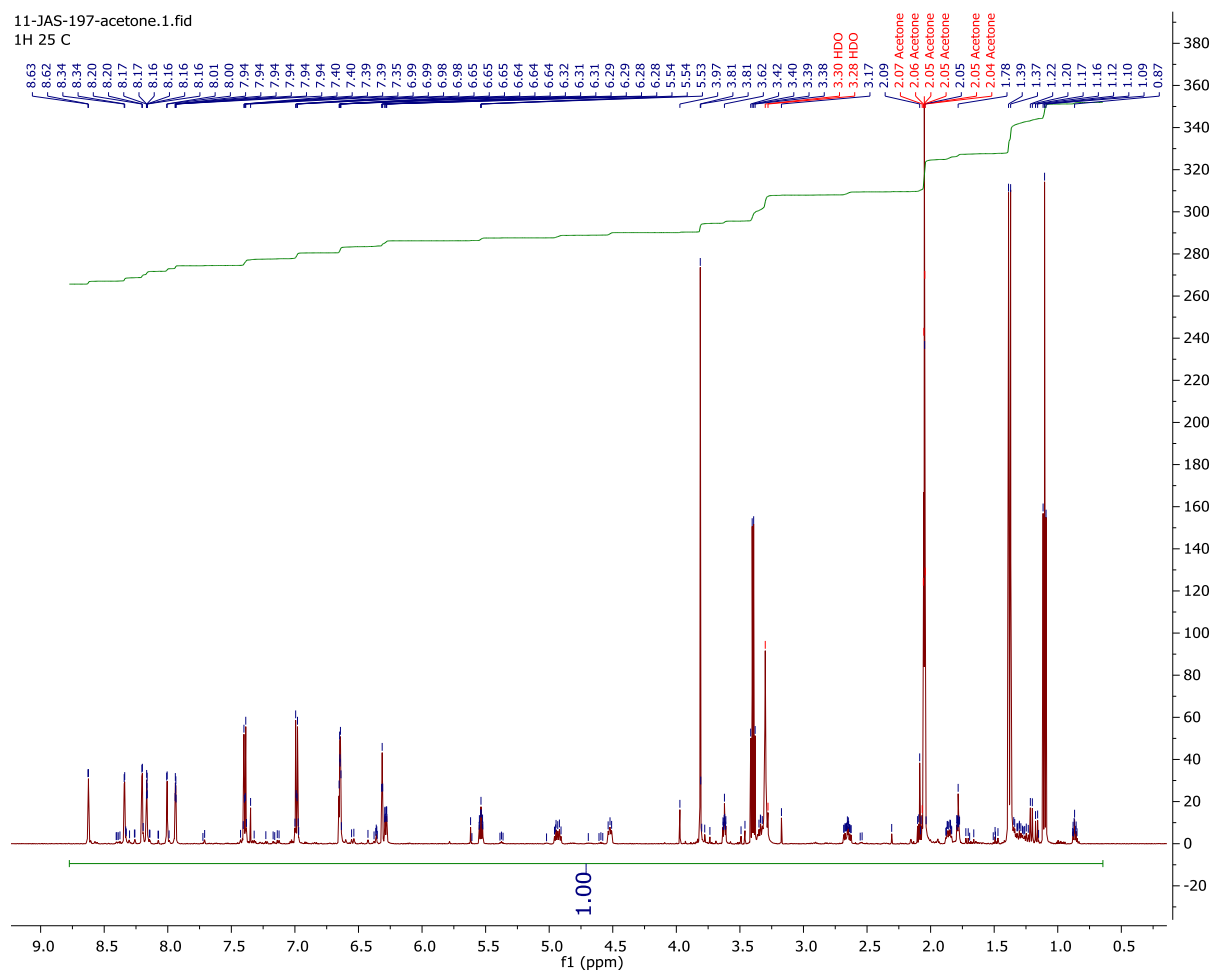
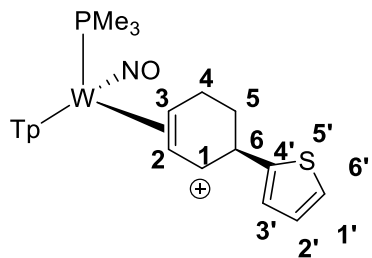


# <sup>13</sup>C {<sup>1</sup>H} NMR Spectra of 12

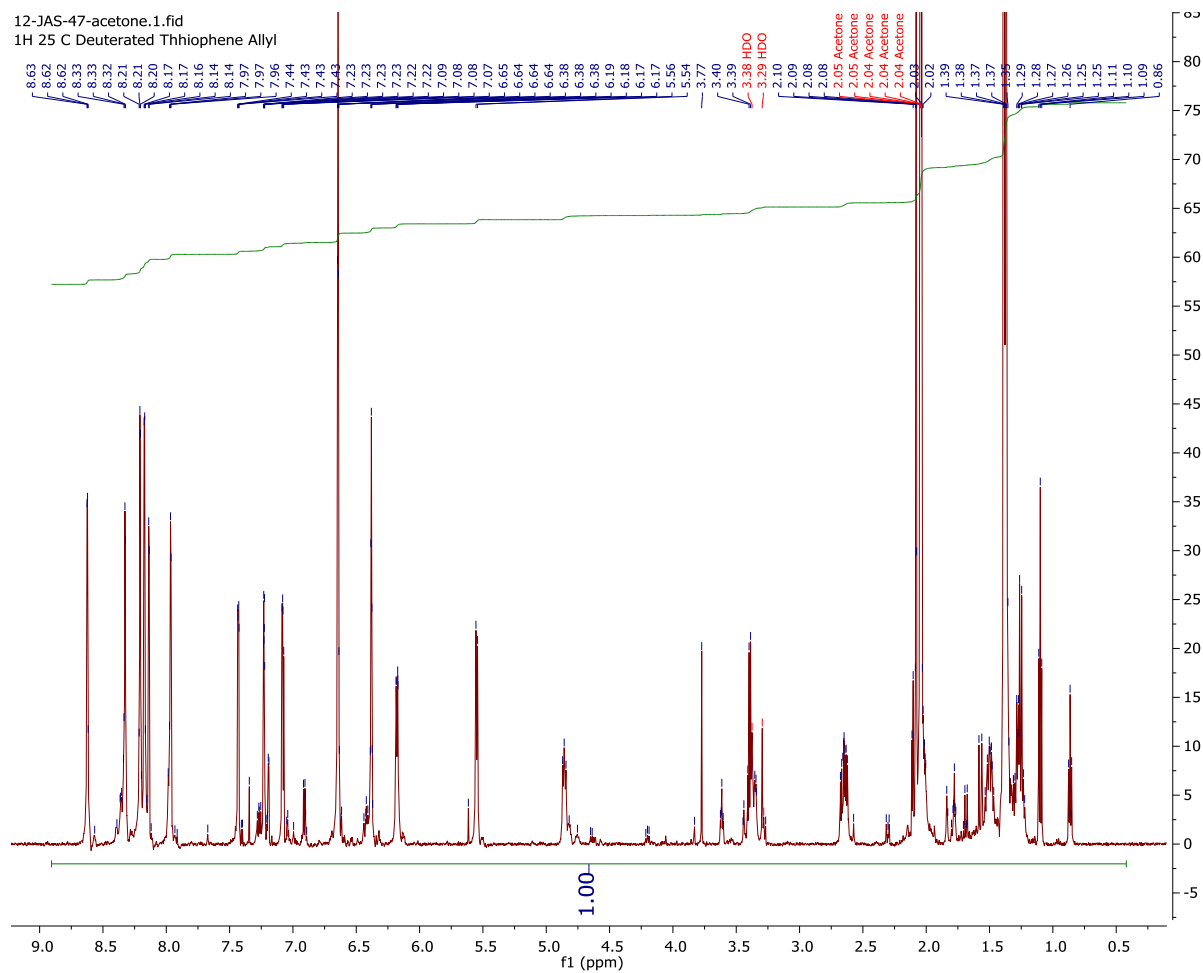
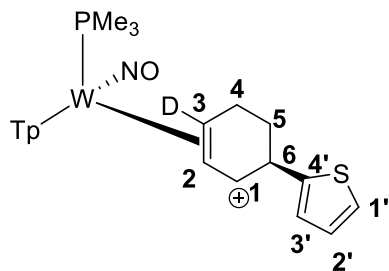




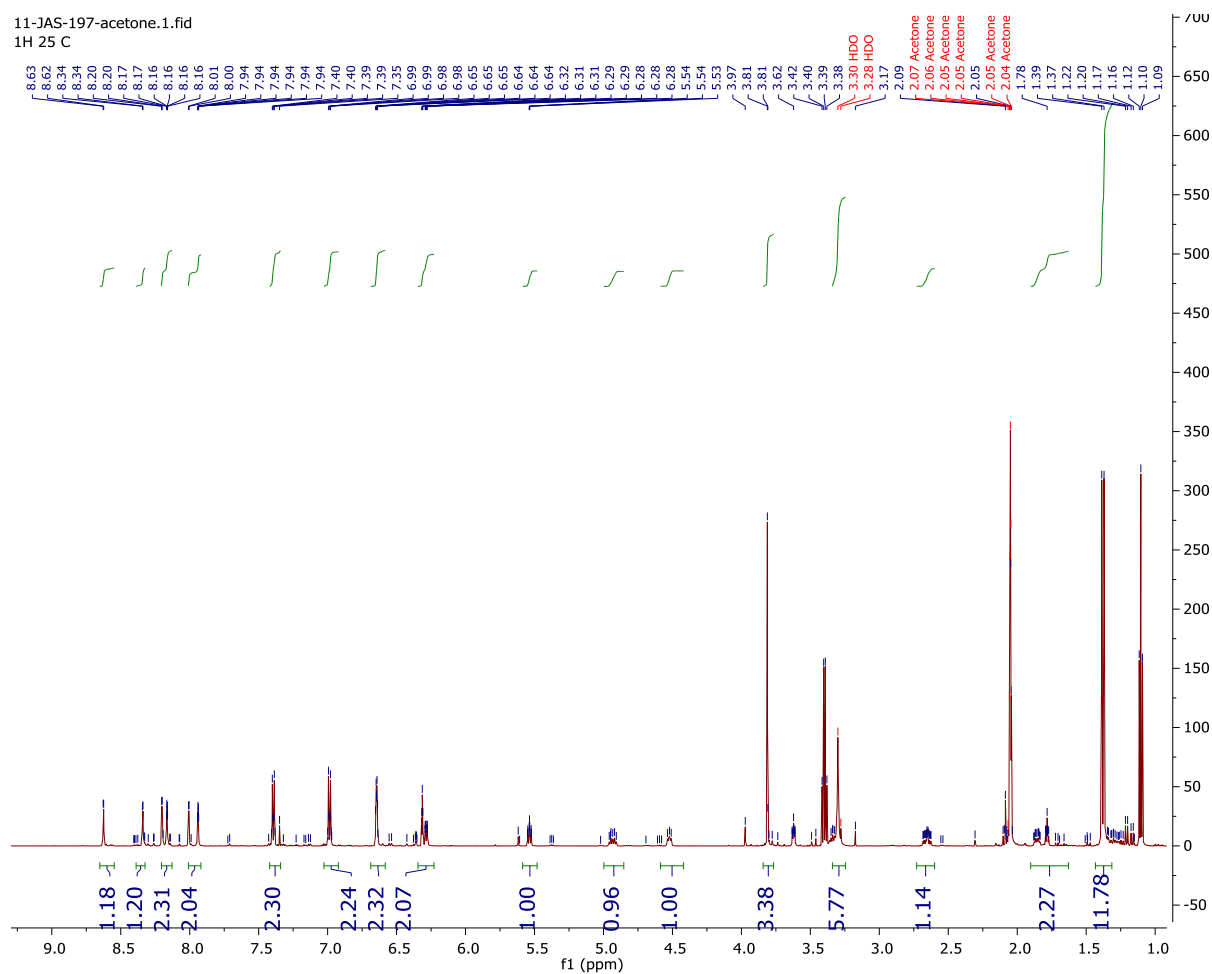
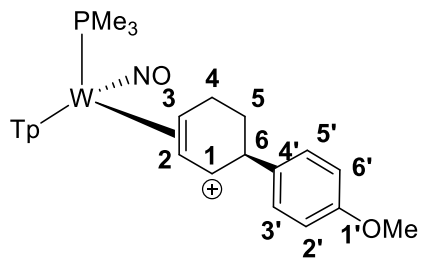
# <sup>1</sup>H NMR Spectra of 15



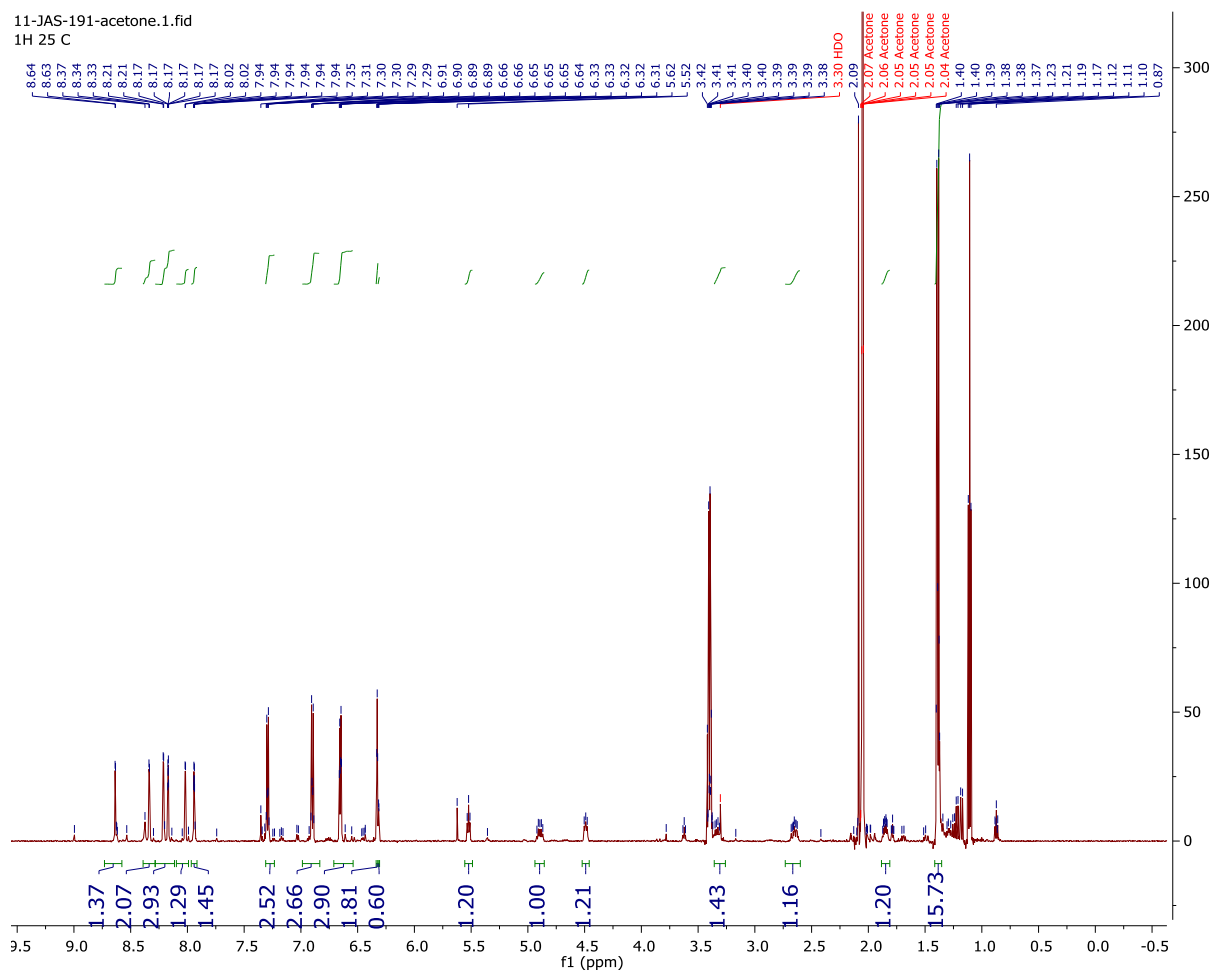
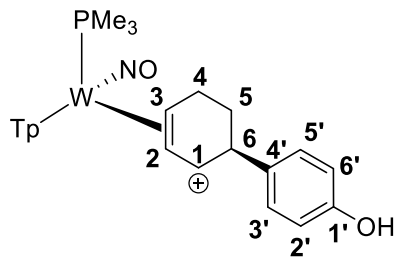
# <sup>1</sup>H NMR of 15-d1



# <sup>1</sup>H NMR Spectra of 16



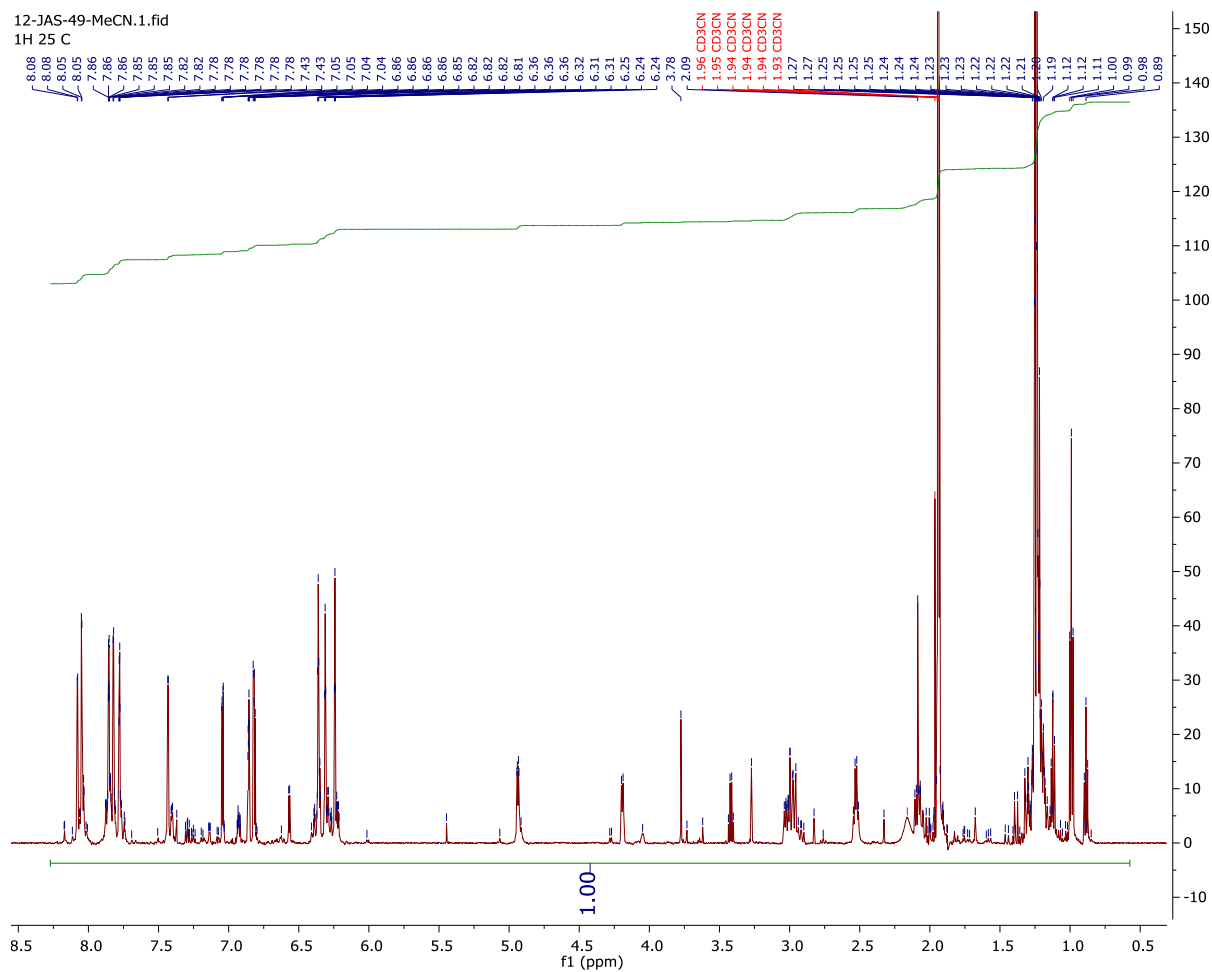
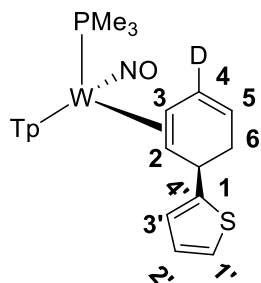
# <sup>1</sup>H NMR Spectra of 17





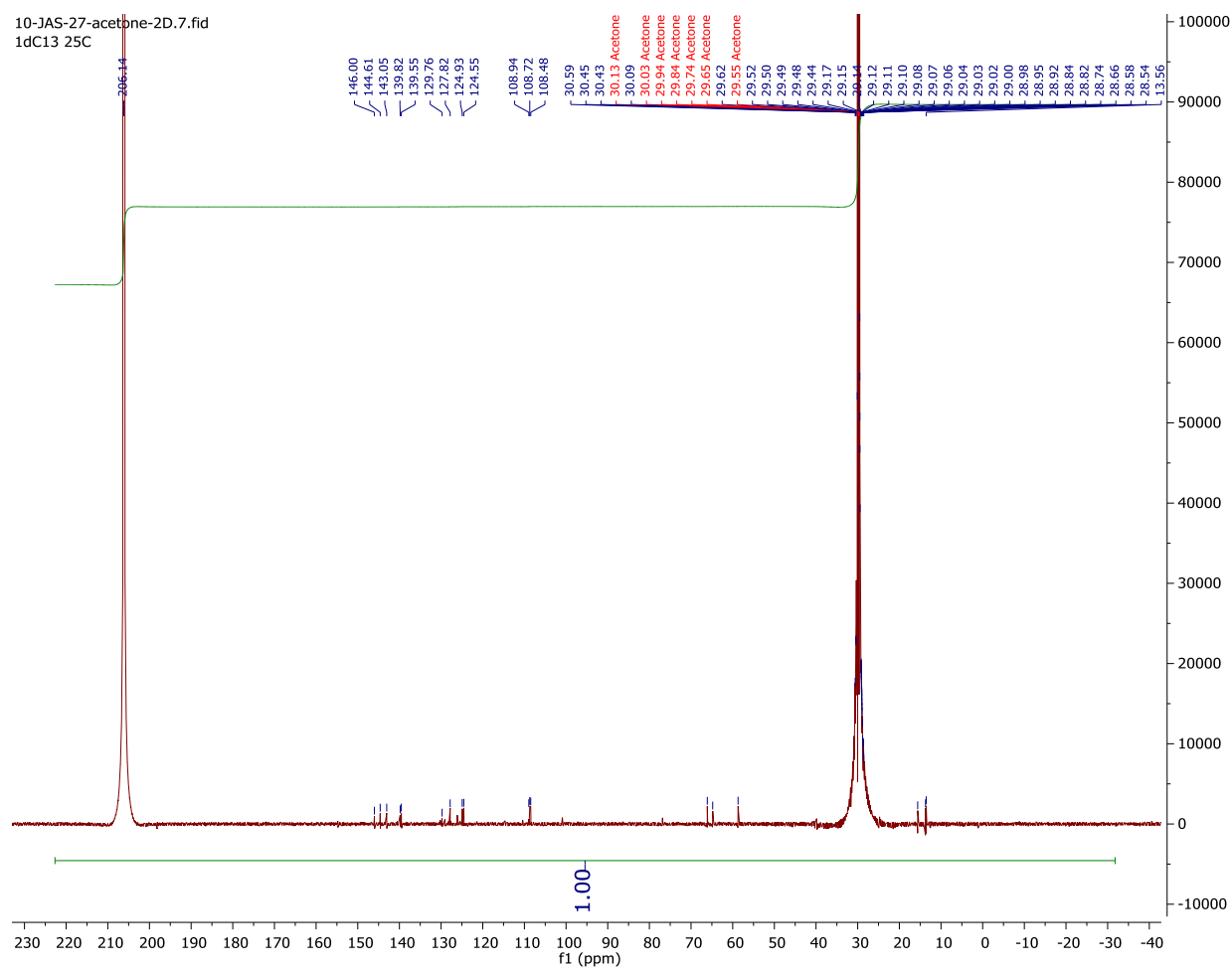
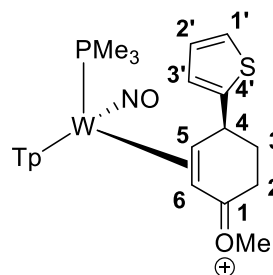


# <sup>1</sup>H NMR of 18-d1

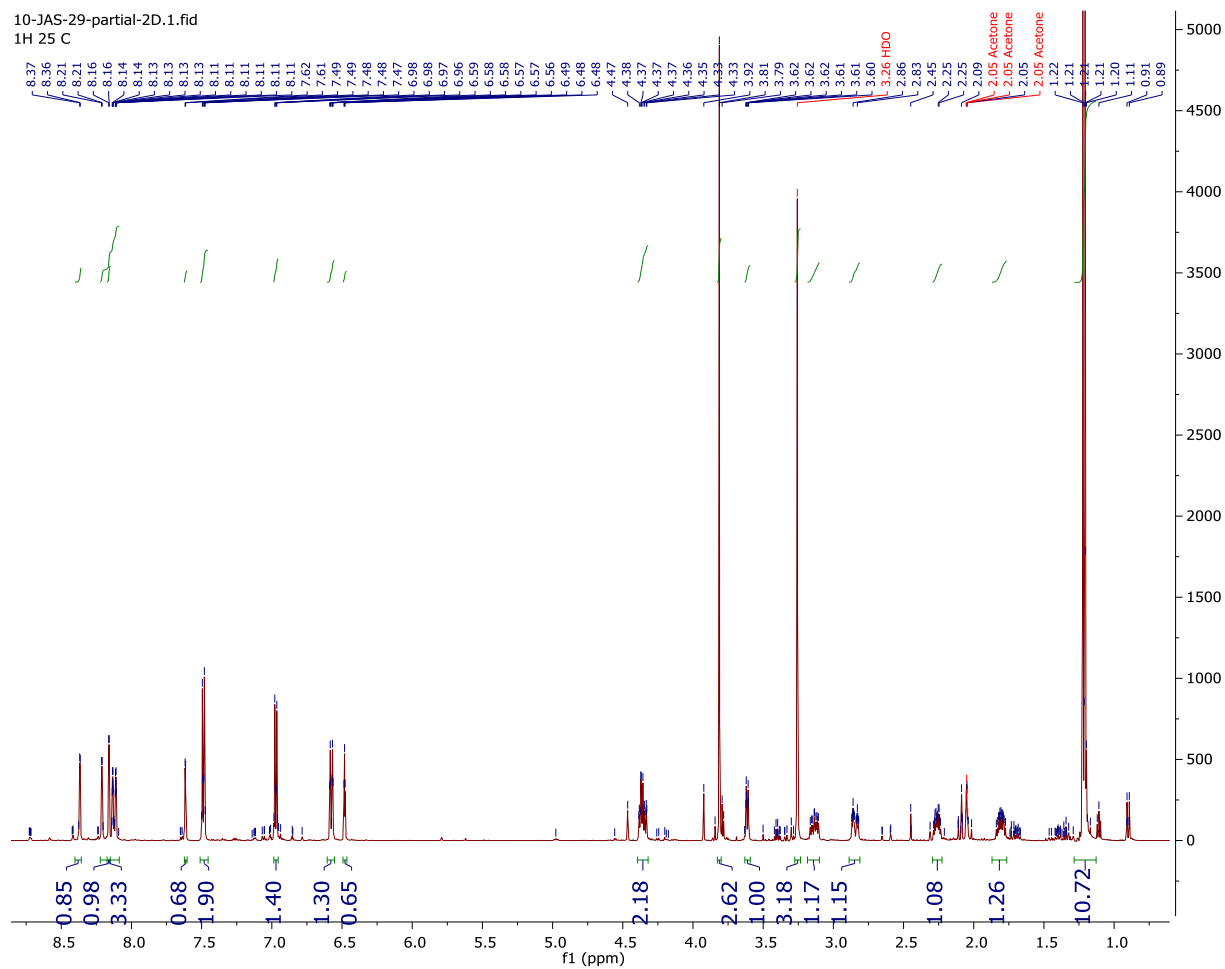
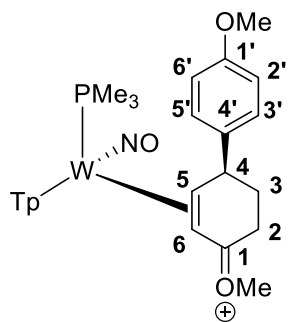




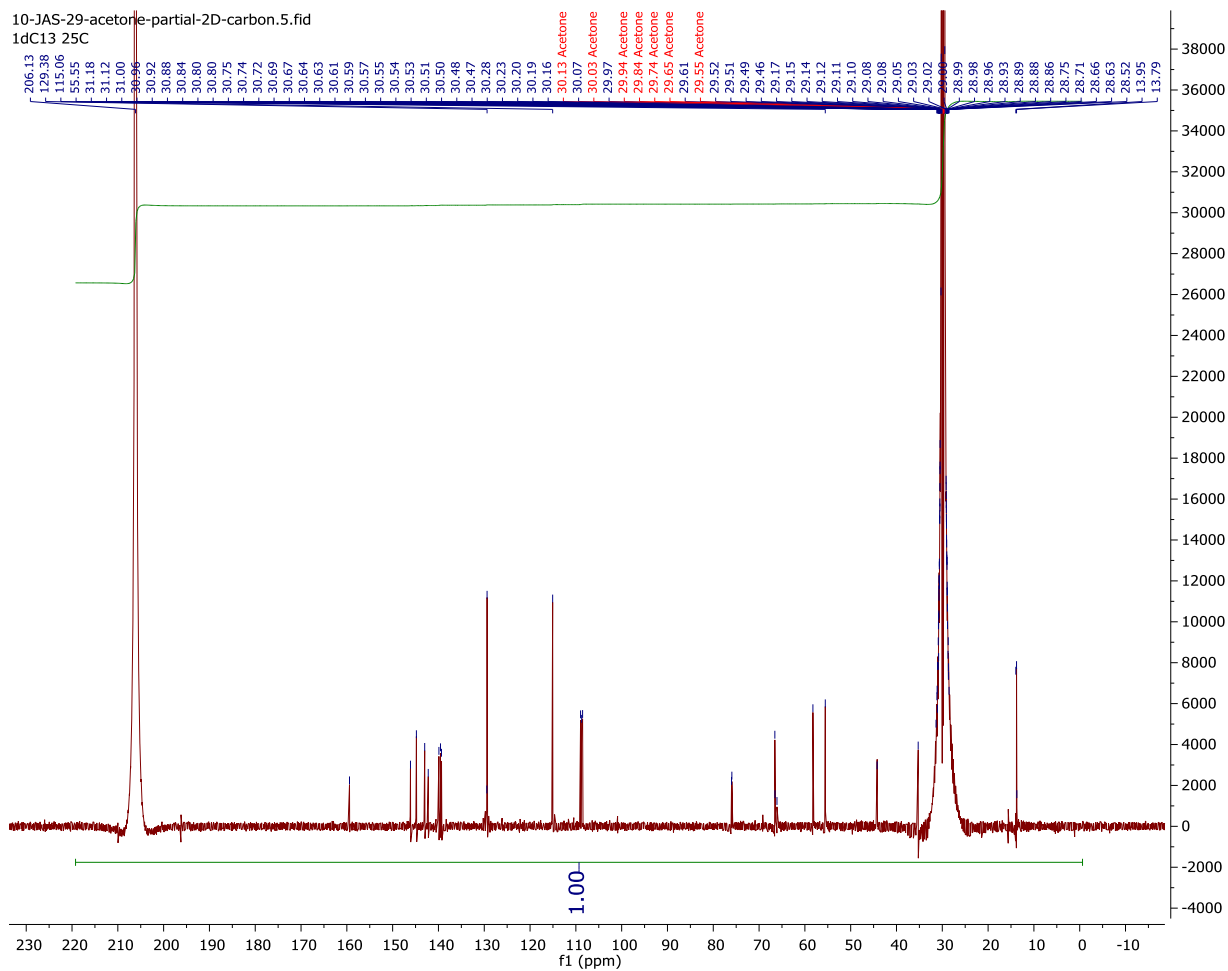
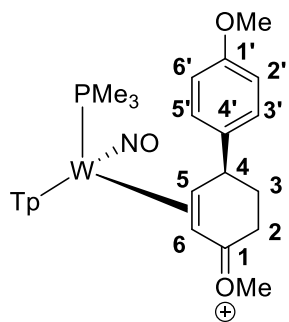
# $^{13}\text{C} \{^1\text{H}\}$ NMR Spectra of 19



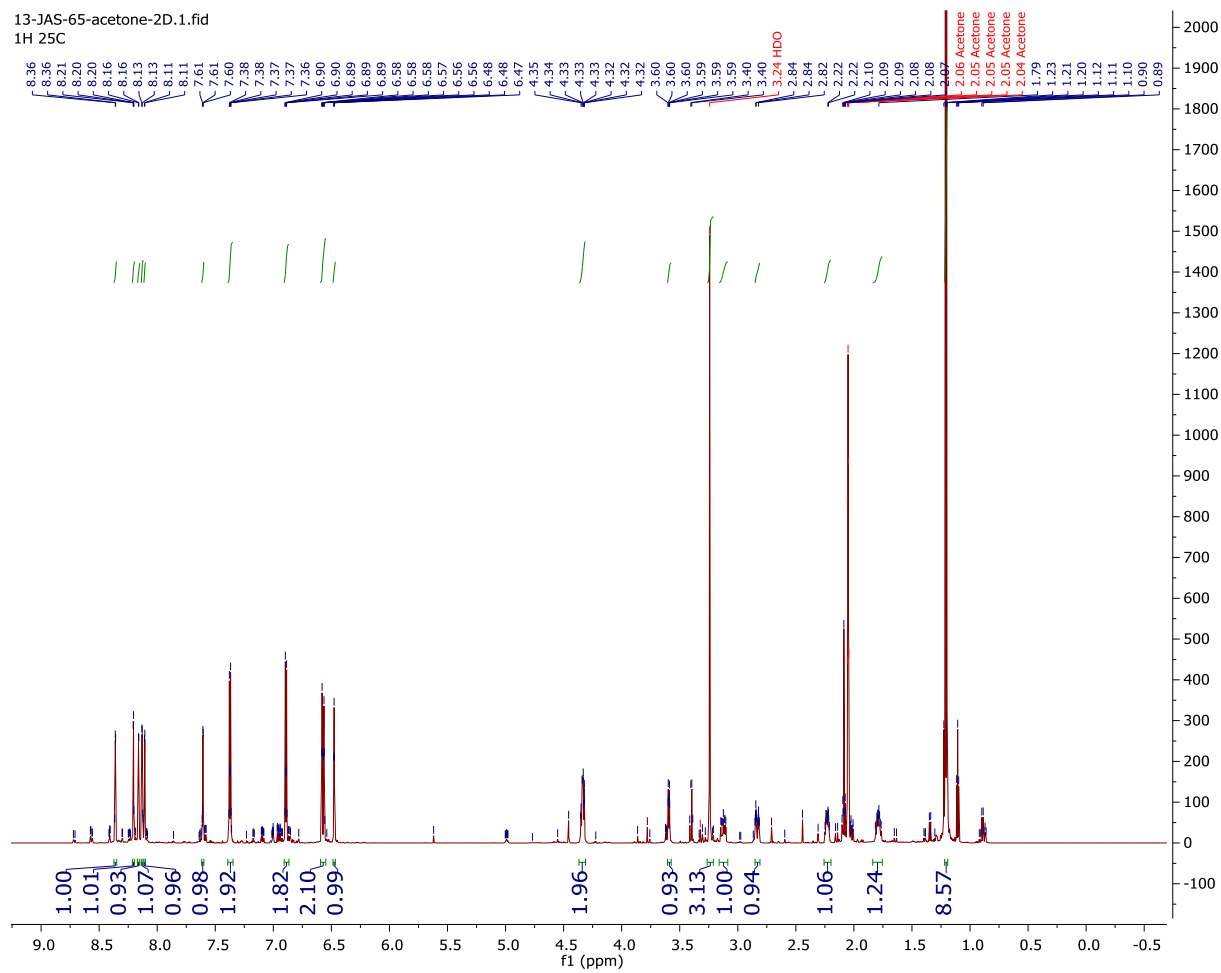
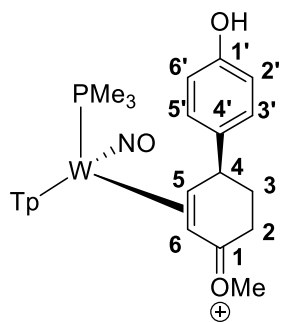
# <sup>1</sup>H NMR Spectra of 20



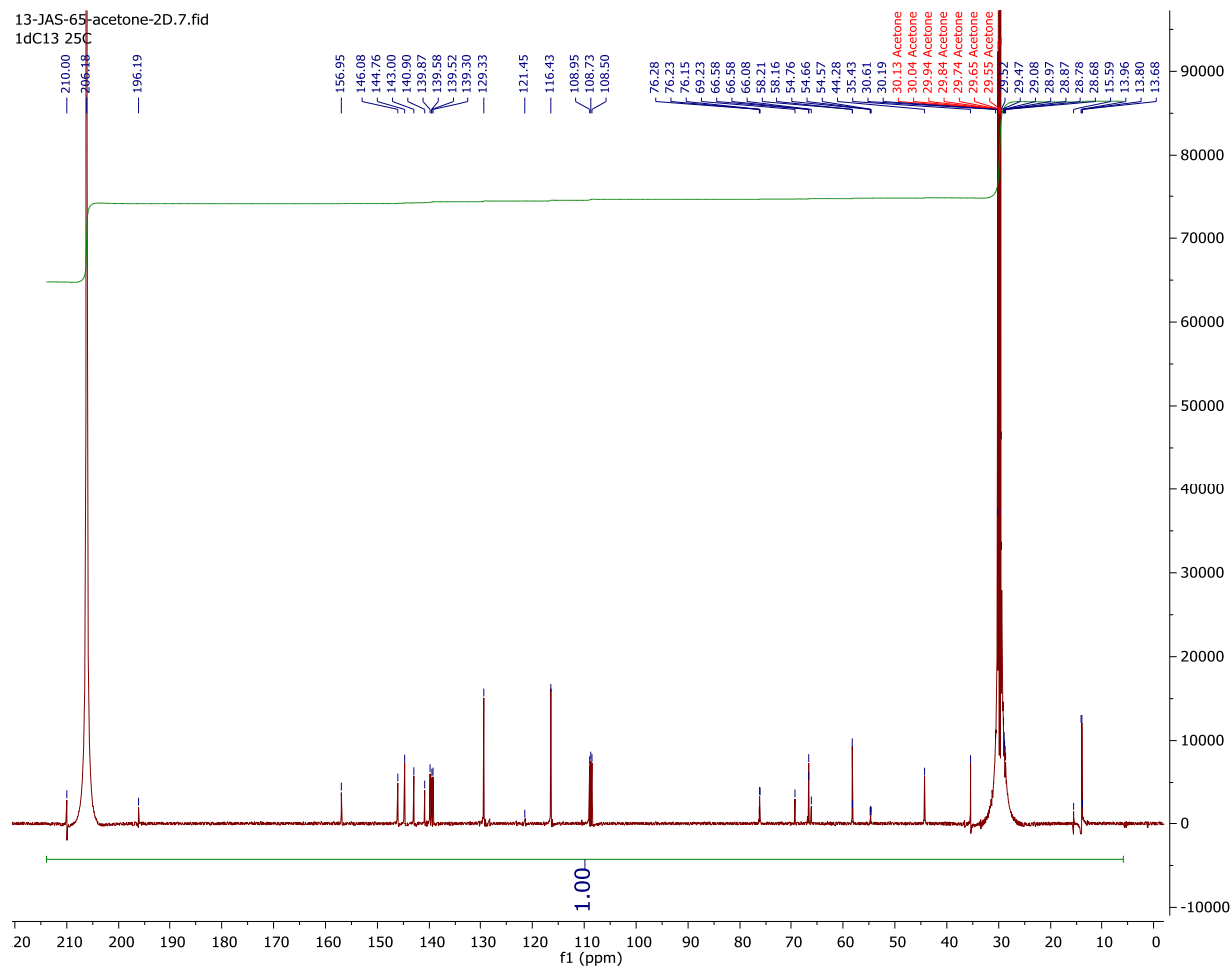
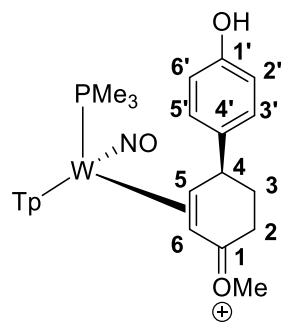
# $^{13}\text{C}$ $\{^1\text{H}\}$ NMR Spectra of 20



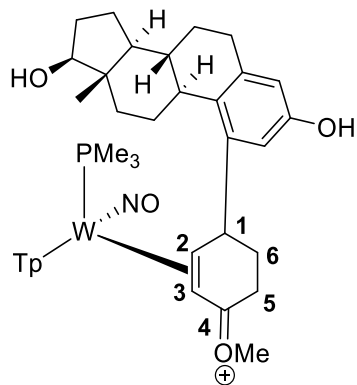
# <sup>1</sup>H NMR Spectra of 21



# <sup>13</sup>C {<sup>1</sup>H} NMR Spectra of 21

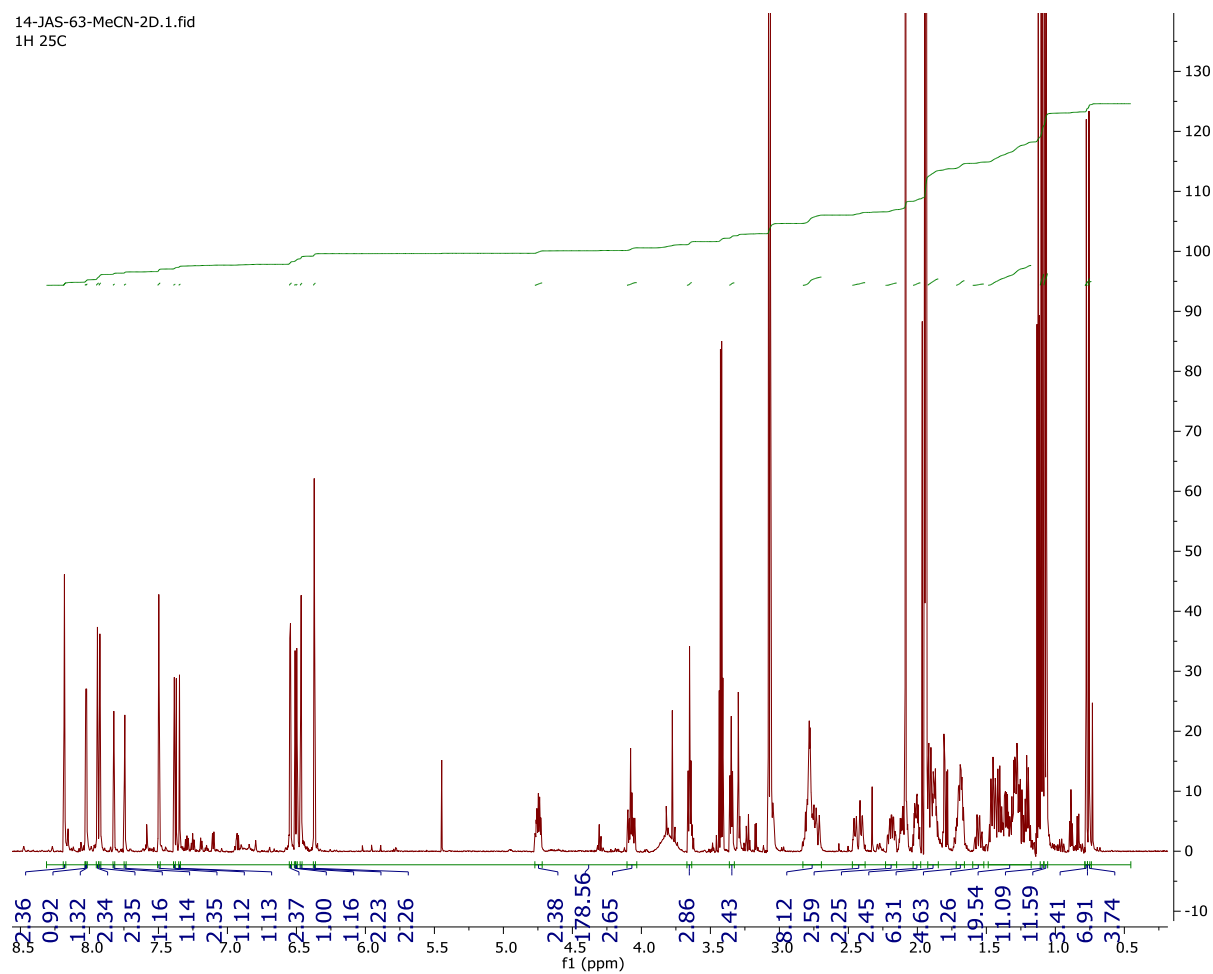


# $^{13}\text{C}\{^1\text{H}\}$ NMR Spectra of 22



WR and WS

14-JAS-63-MeCN-2D.1.fid  
1H 25C

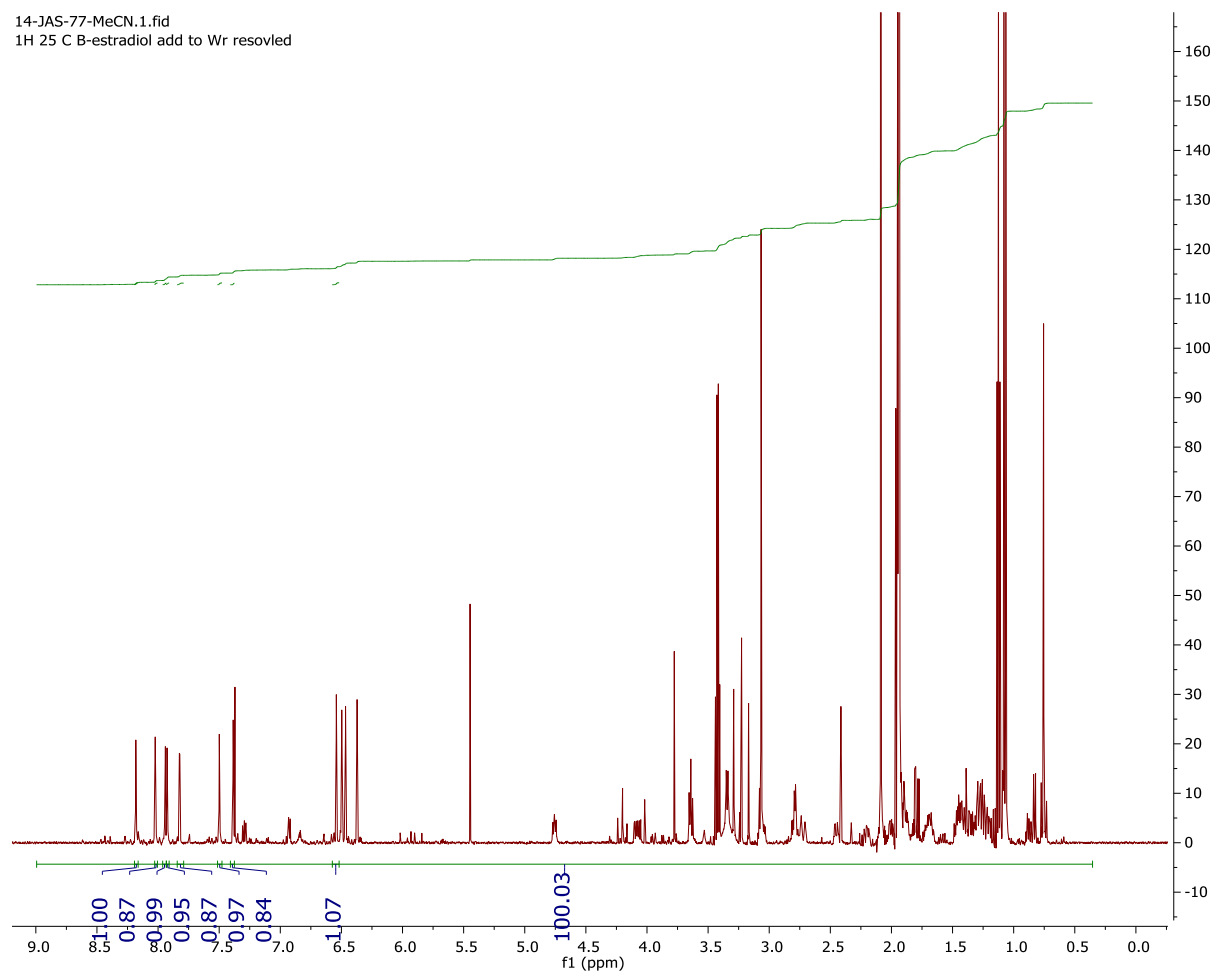




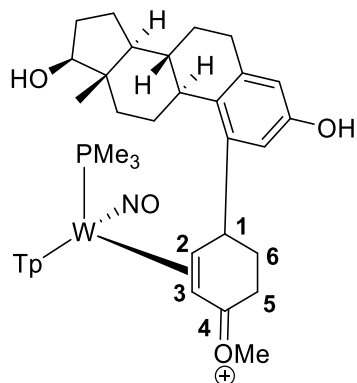
# <sup>1</sup>H NMR Spectra of 22

## ONLY WR

14-JAS-77-MeCN.1.fid  
1H 25 C B-estradiol add to Wr resolved

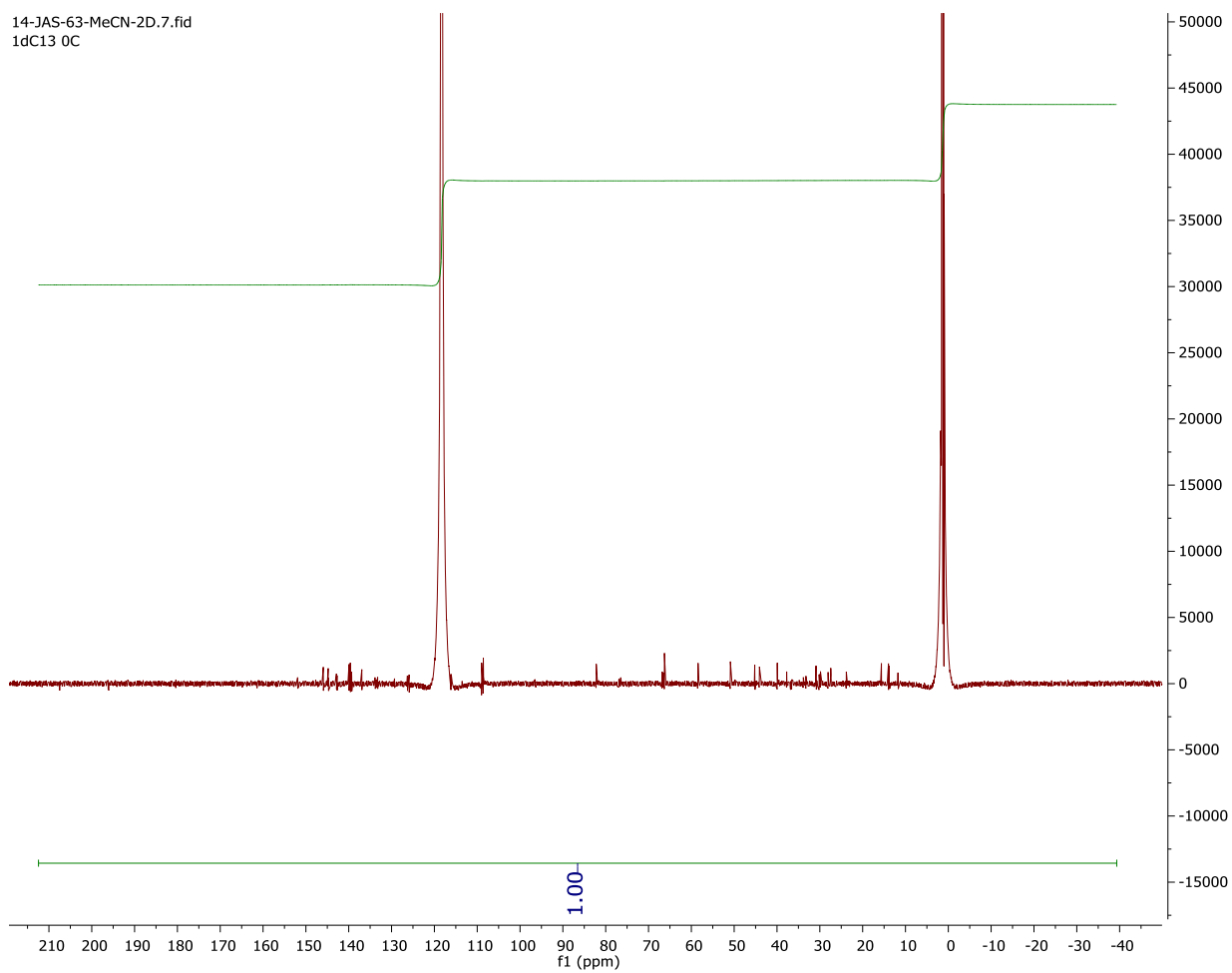


# $^{13}\text{C} \{^1\text{H}\}$ NMR Spectra of 22

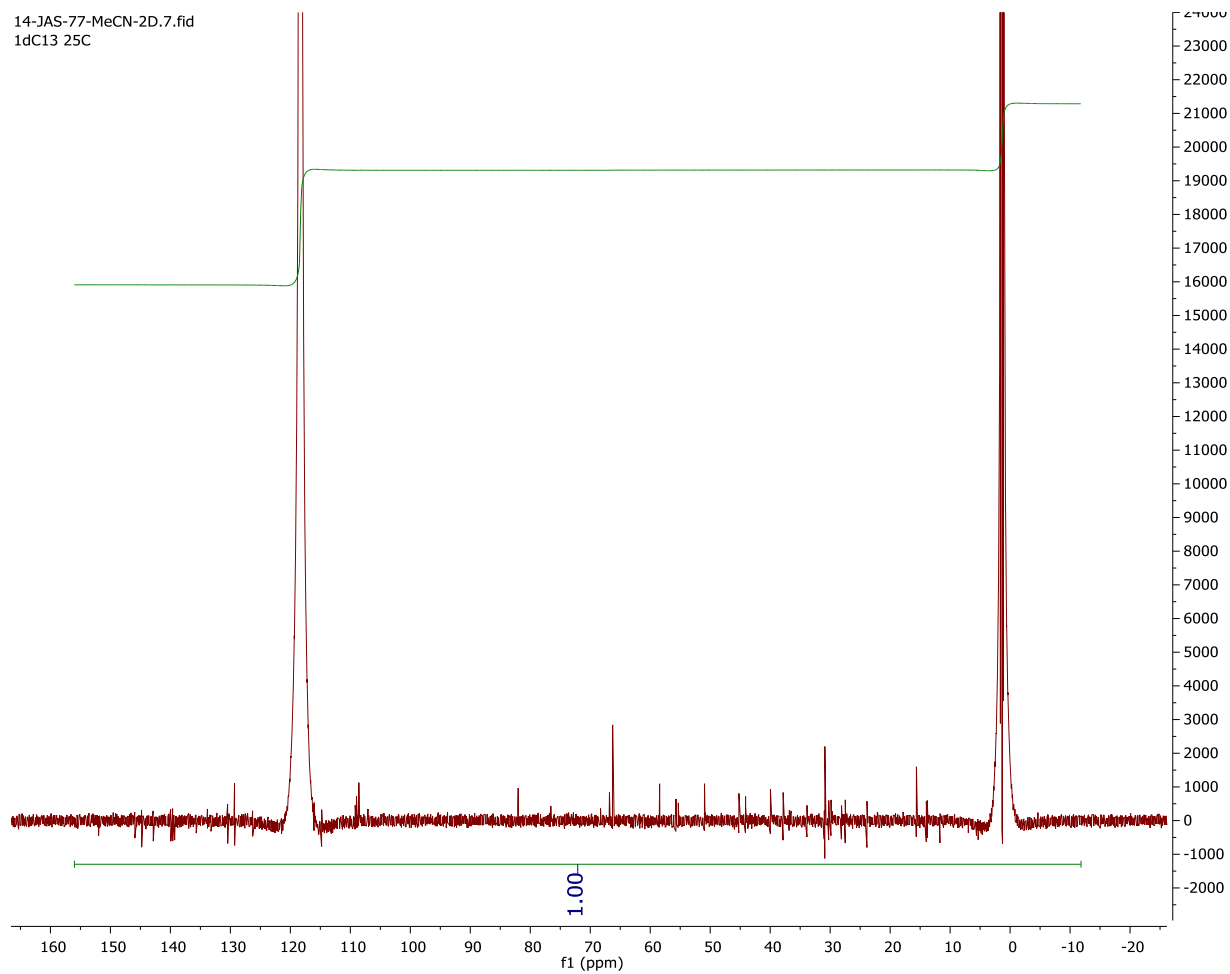
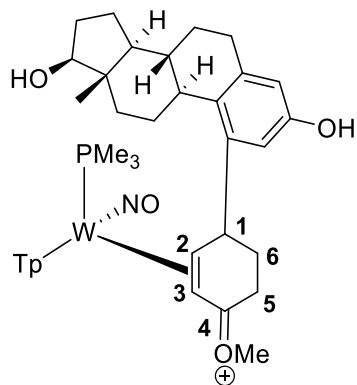


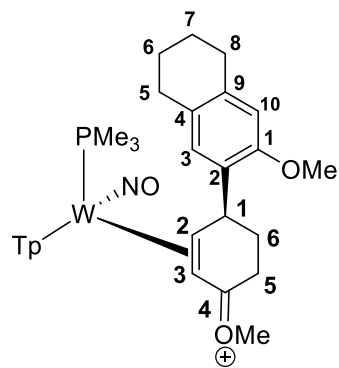
## WR and WS

14-JAS-63-MeCN-2D.7.fid  
1dC13 0C

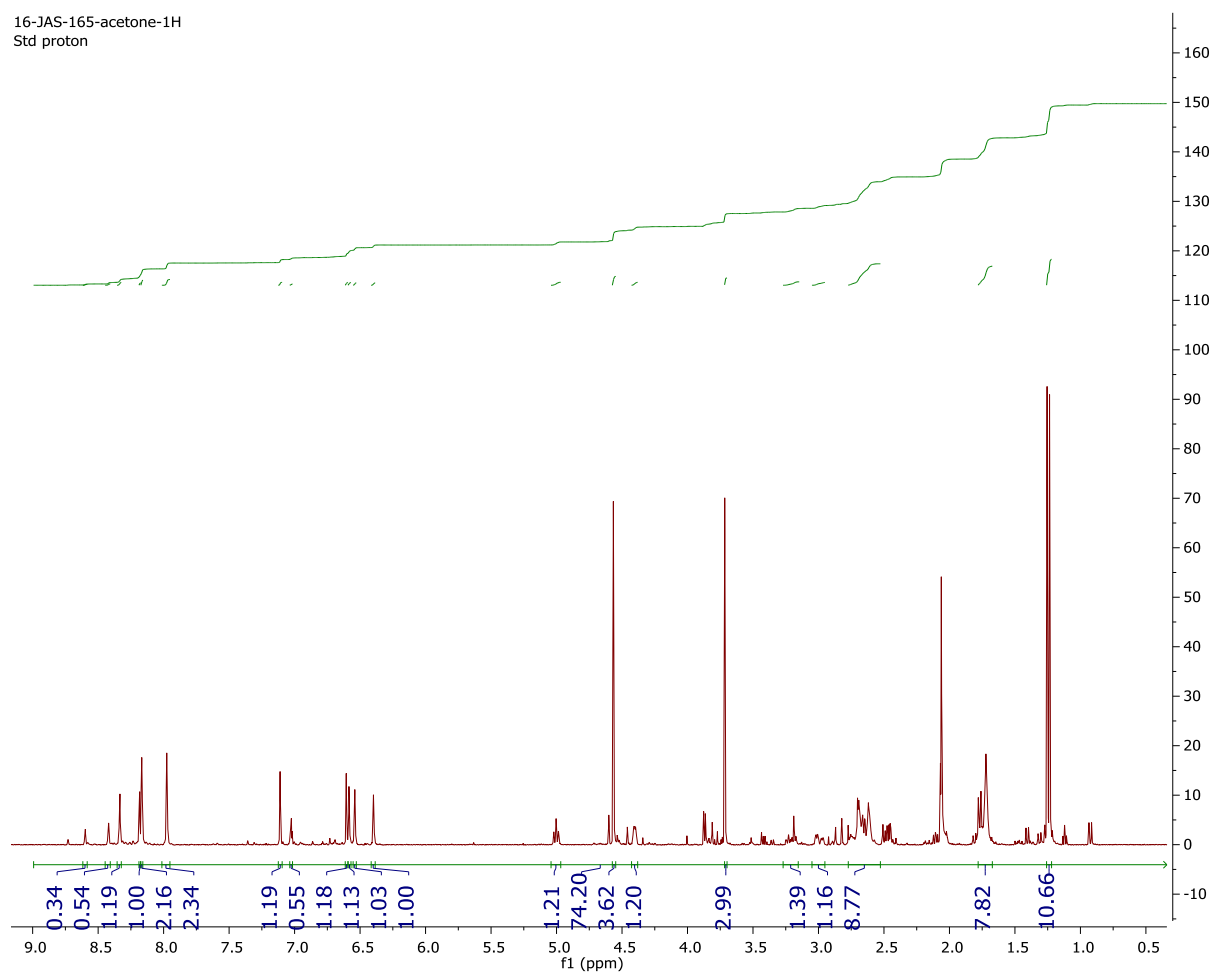


# $^{13}\text{C} \{^1\text{H}\}$ NMR Spectra of 22

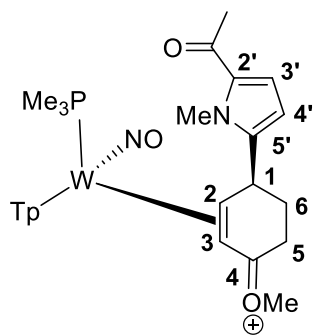




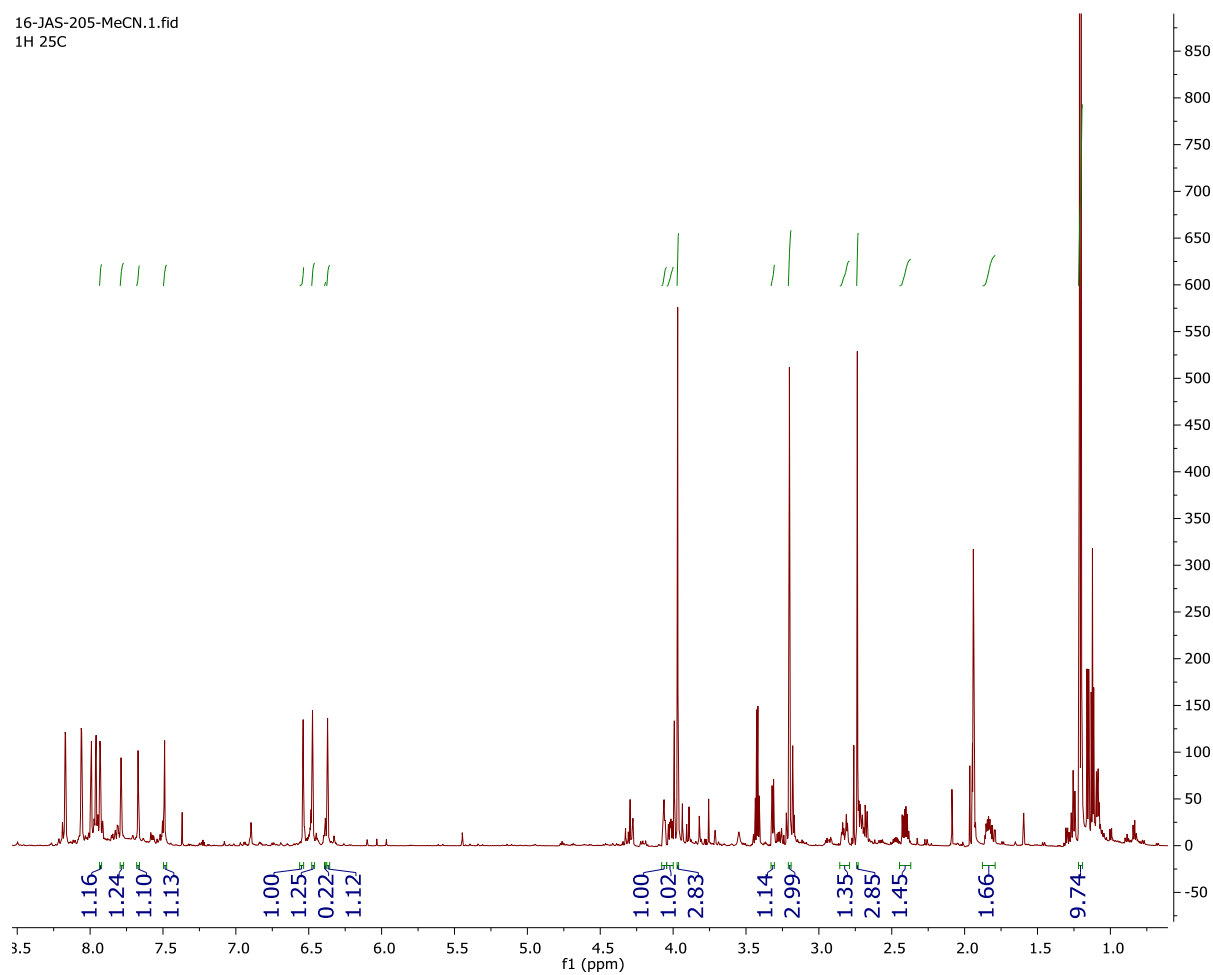
16-JAS-165-acetone-1H  
Std proton



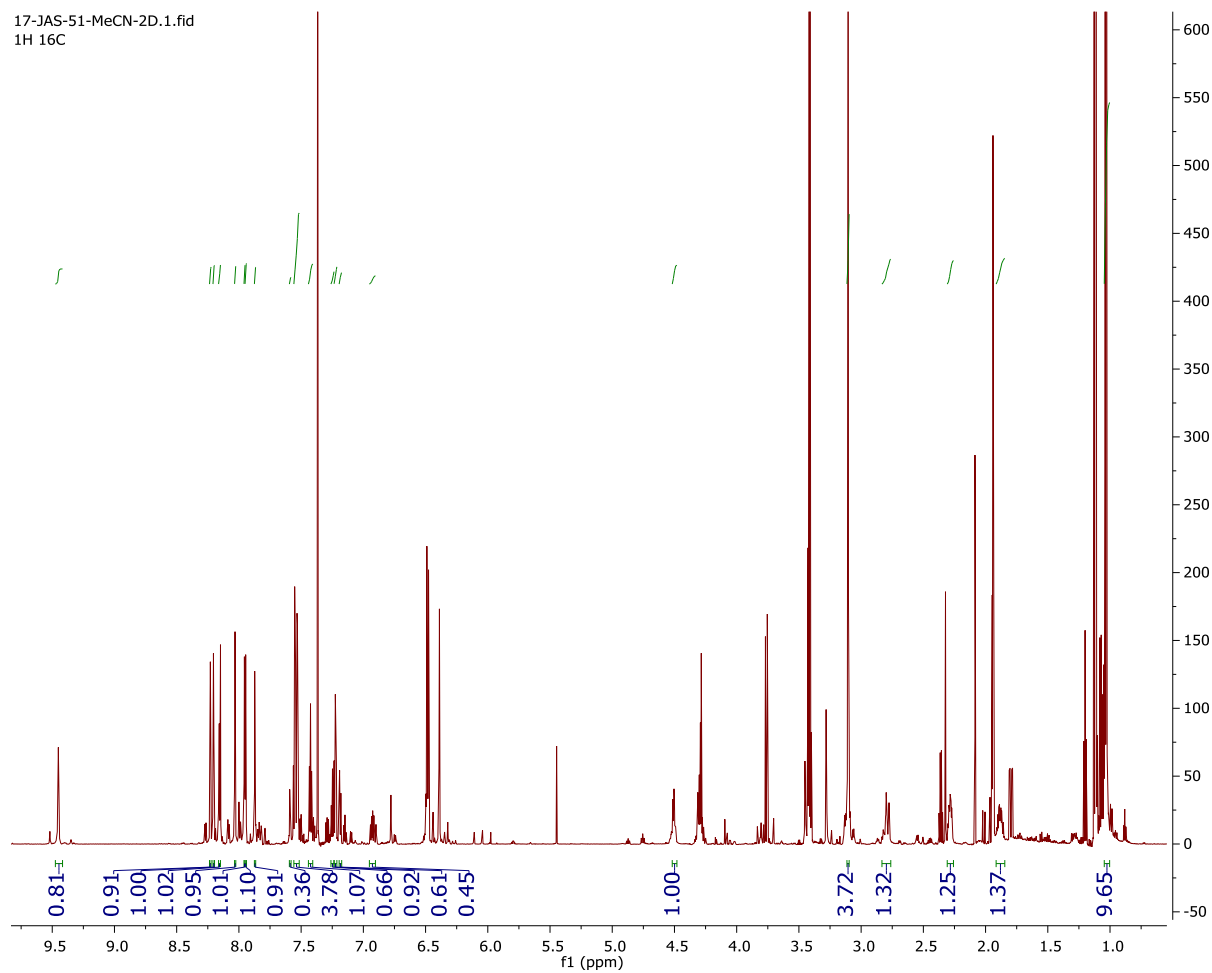
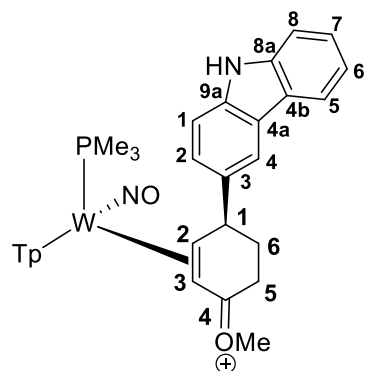
# <sup>1</sup>H NMR Spectra of 24



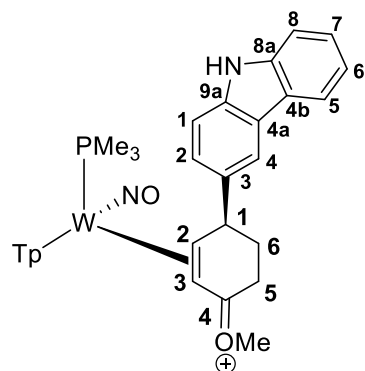
16-JAS-205-MeCN.1.fid  
1H 25C



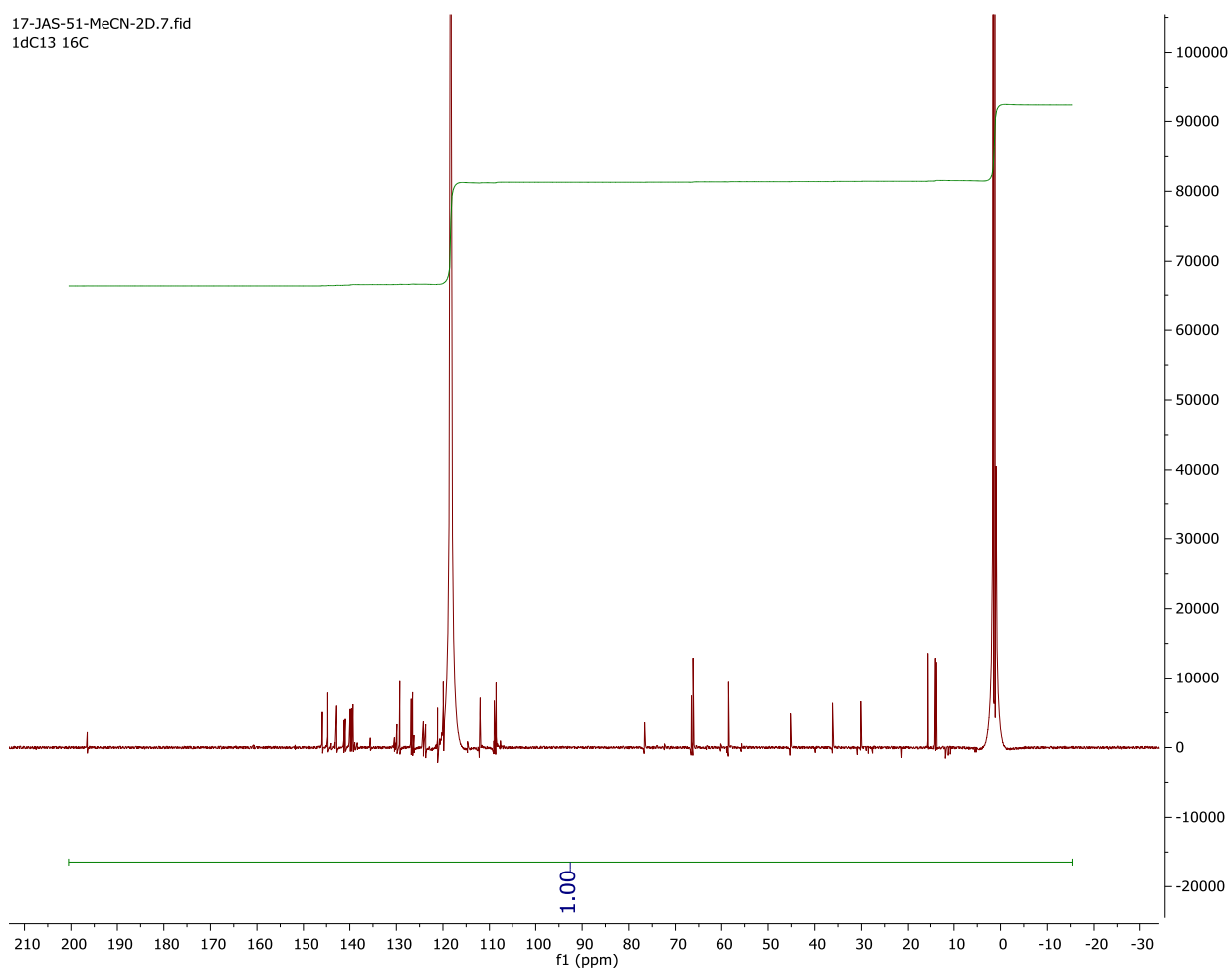
# $^{13}\text{C}\{^1\text{H}\}$ NMR Spectra of 25



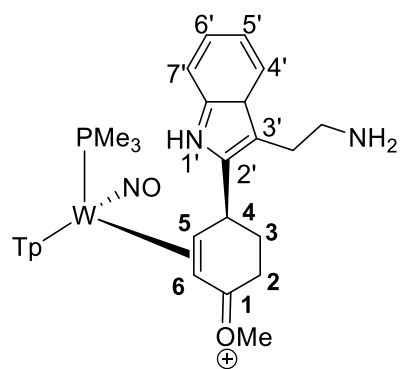
# $^{13}\text{C}$ $\{^1\text{H}\}$ NMR Spectra of 25



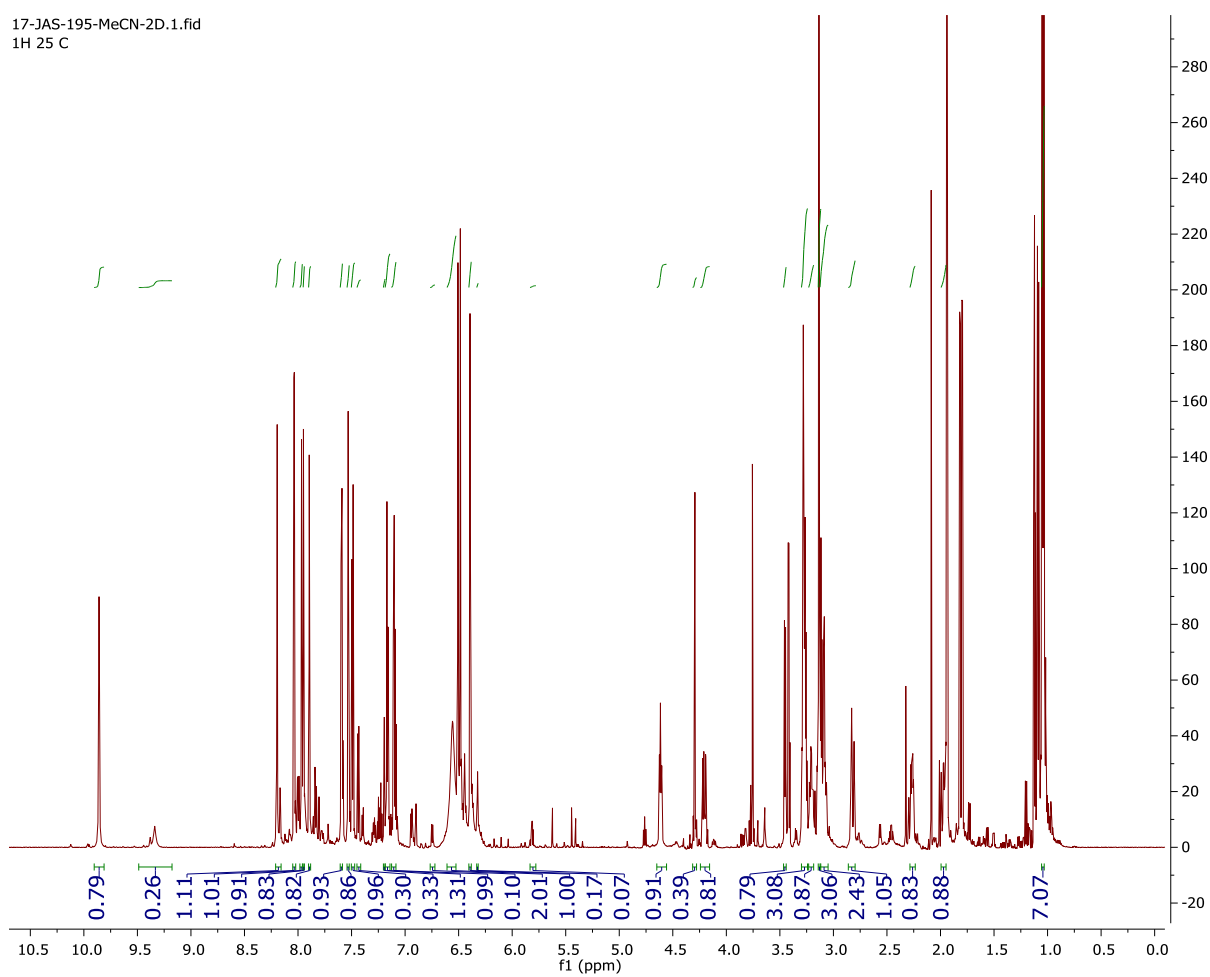
17-JAS-51-MeCN-2D.7.fid  
1dC13 16C



# <sup>1</sup>H NMR Spectra of 26

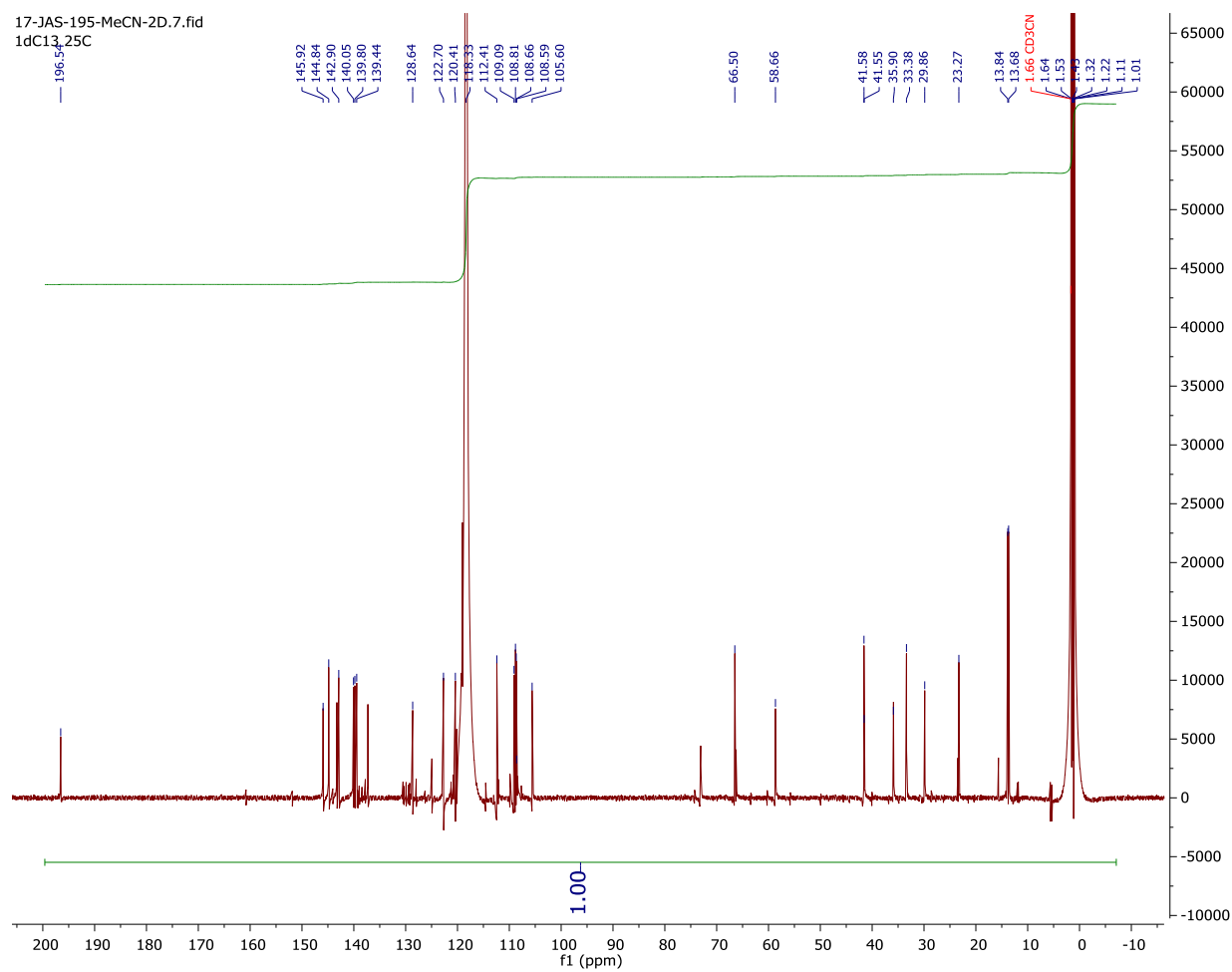
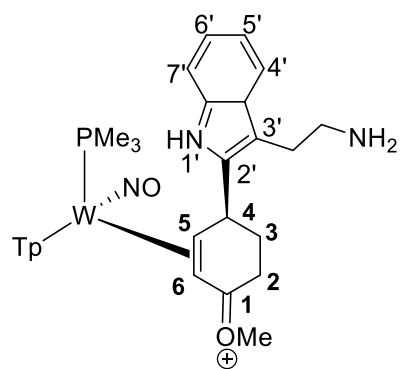


17-JAS-195-MeCN-2D.1.fid  
1H 25 C



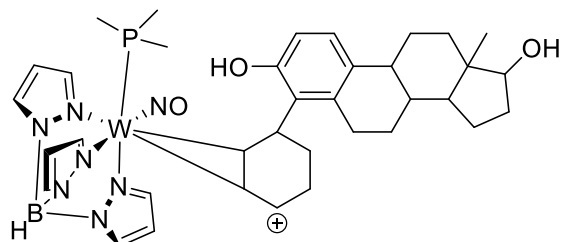


# $^{13}\text{C}$ $\{^1\text{H}\}$ NMR Spectra of 26

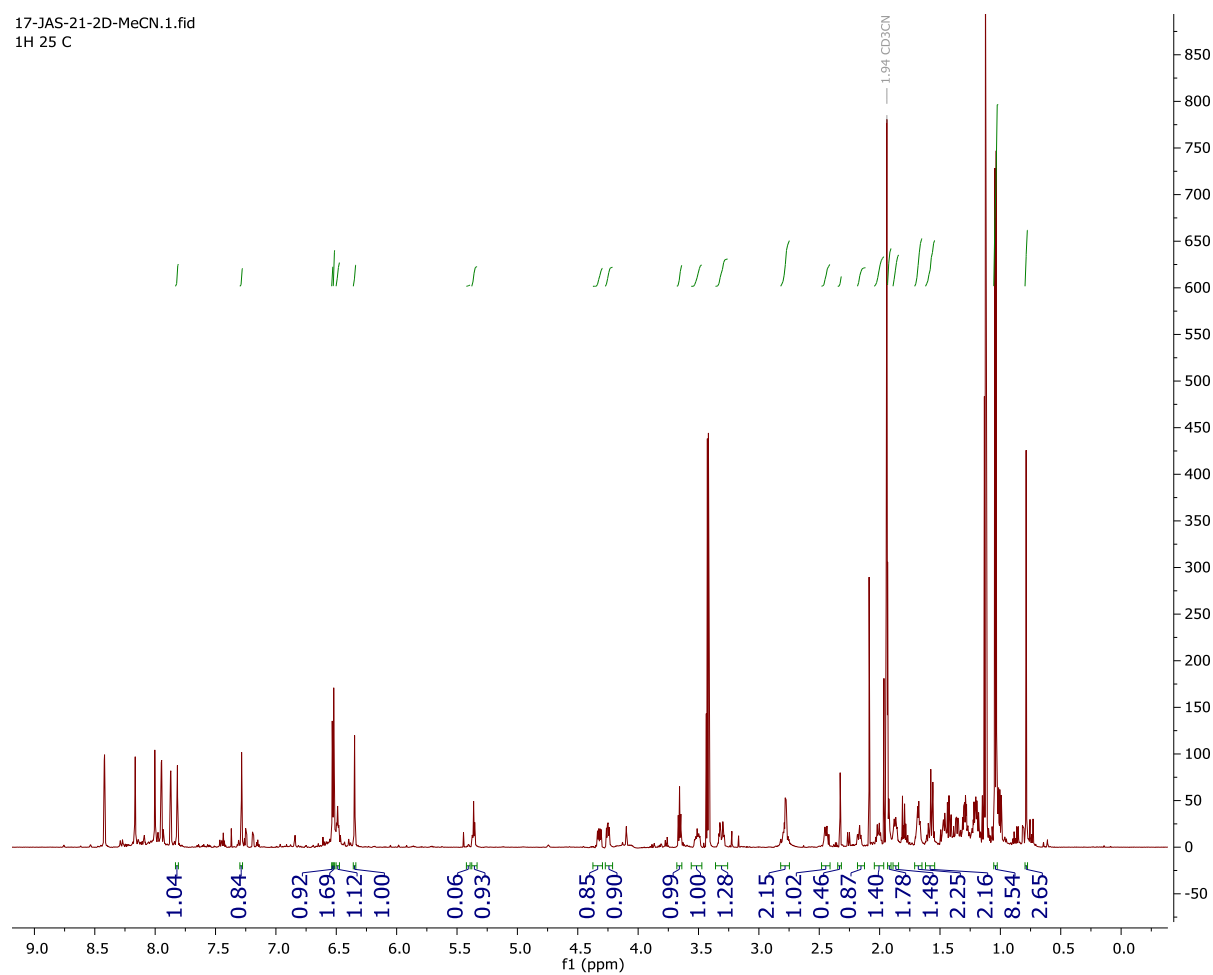


# $^{13}\text{C}$ $\{^1\text{H}\}$ NMR Spectra of 29

ONLY OF W S

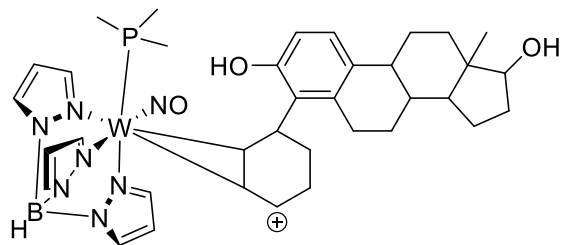


17-JAS-21-2D-MeCN.1.fid  
1H 25 C

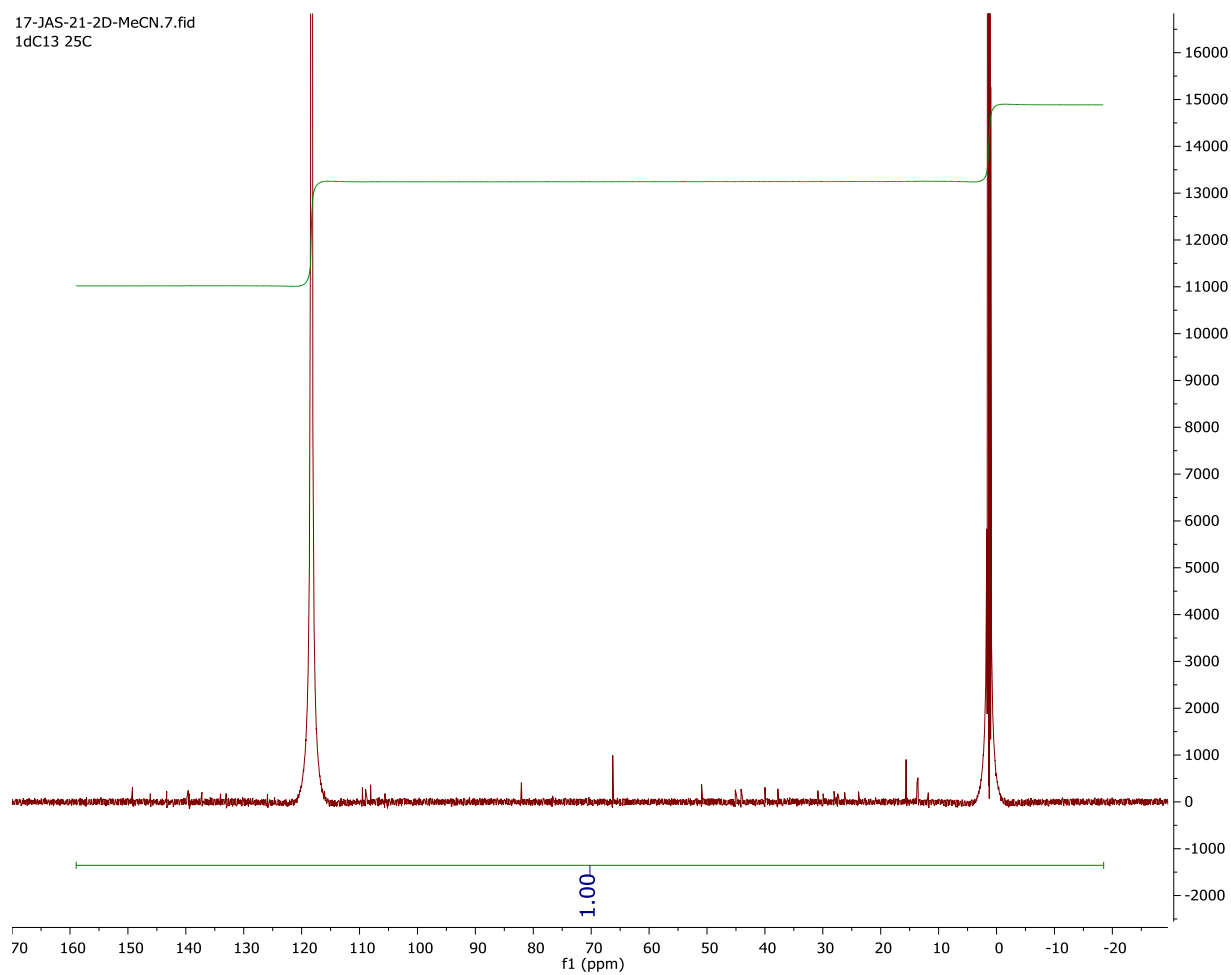


# $^{13}\text{C}$ $\{^1\text{H}\}$ NMR Spectra of 29

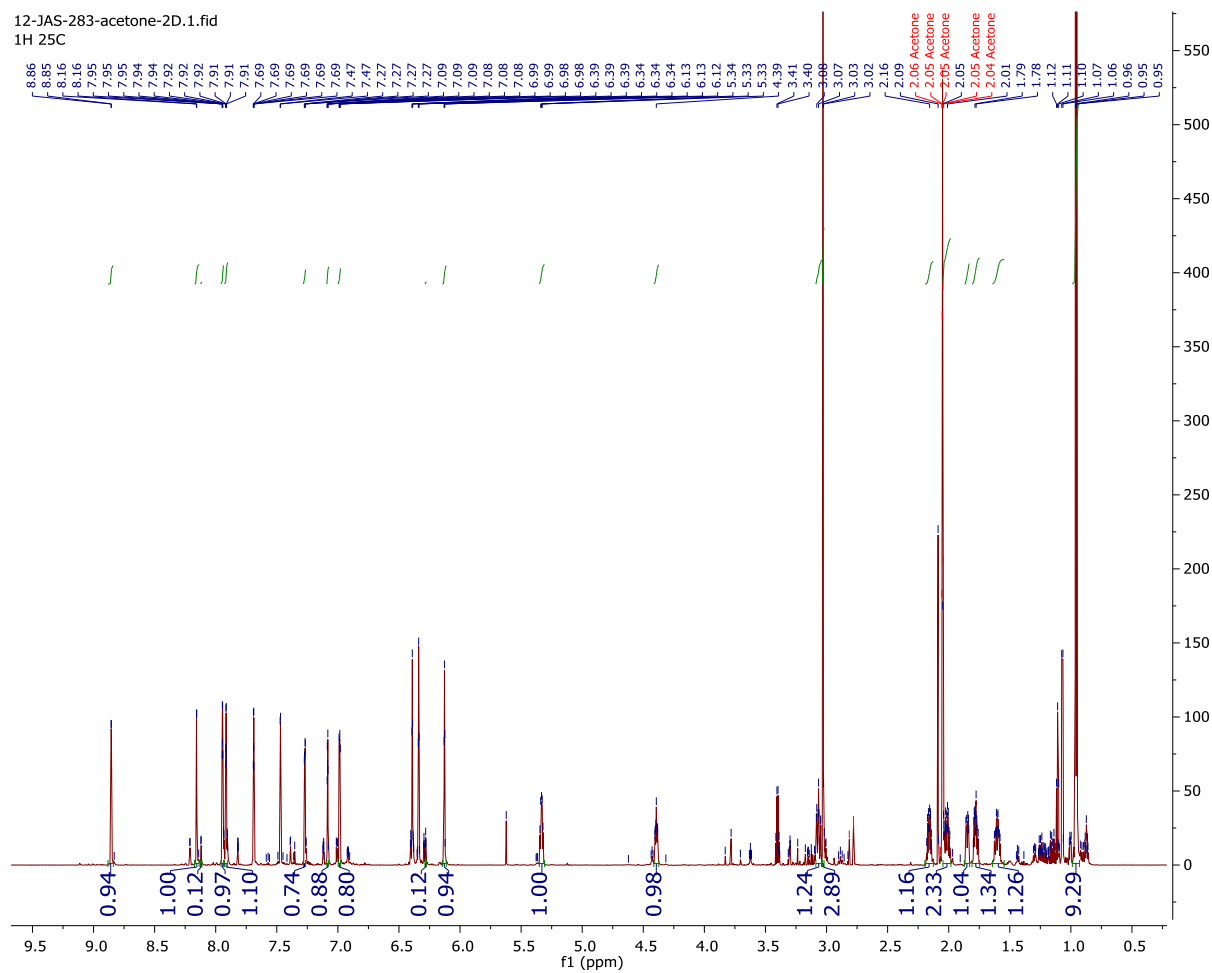
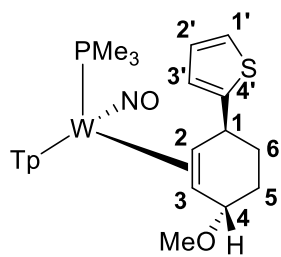
ONLY OF WS



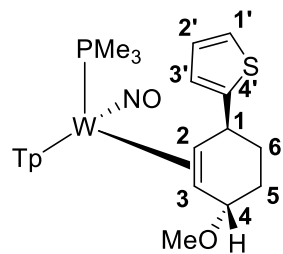
17-JAS-21-2D-MeCN.7.fid  
1dC13 25C



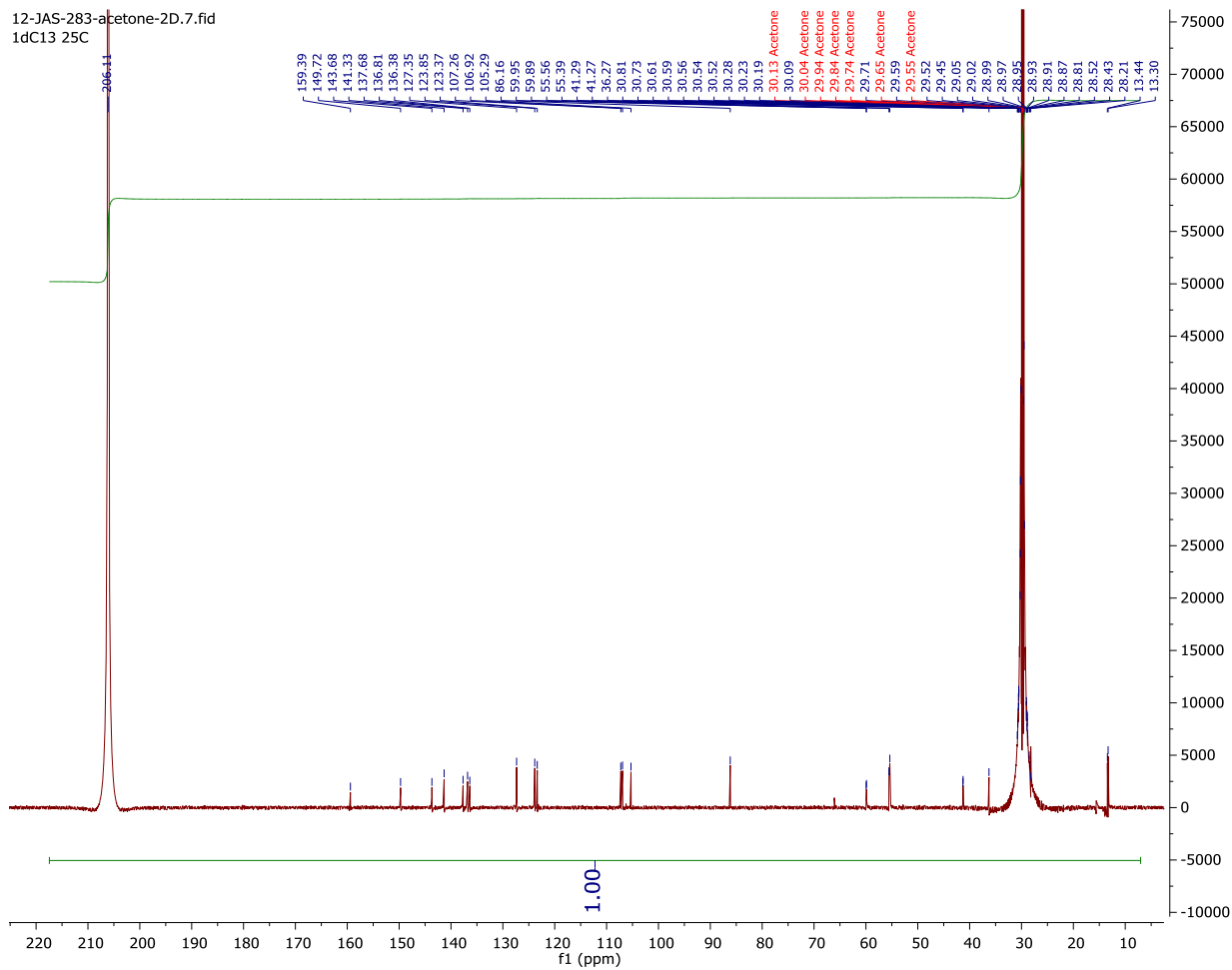
# <sup>1</sup>H NMR Spectra of 31



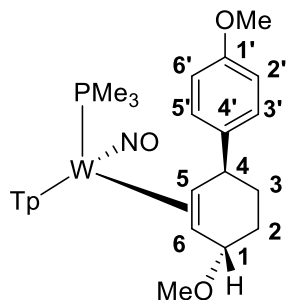
# $^{13}\text{C}$ $\{^1\text{H}\}$ NMR Spectra of 31



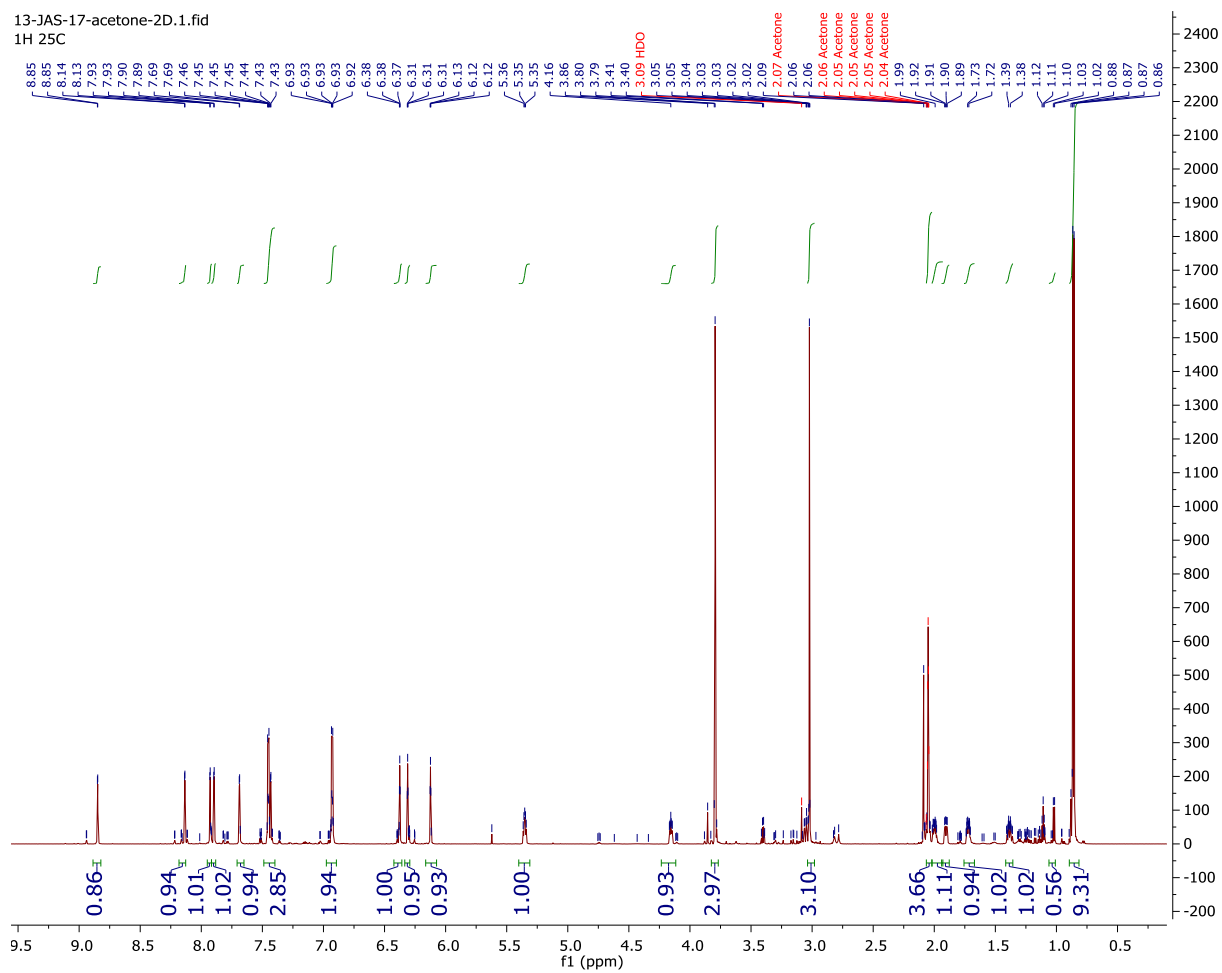
12-JAS-283-acetone-2D.7.fid  
1dC13 25C



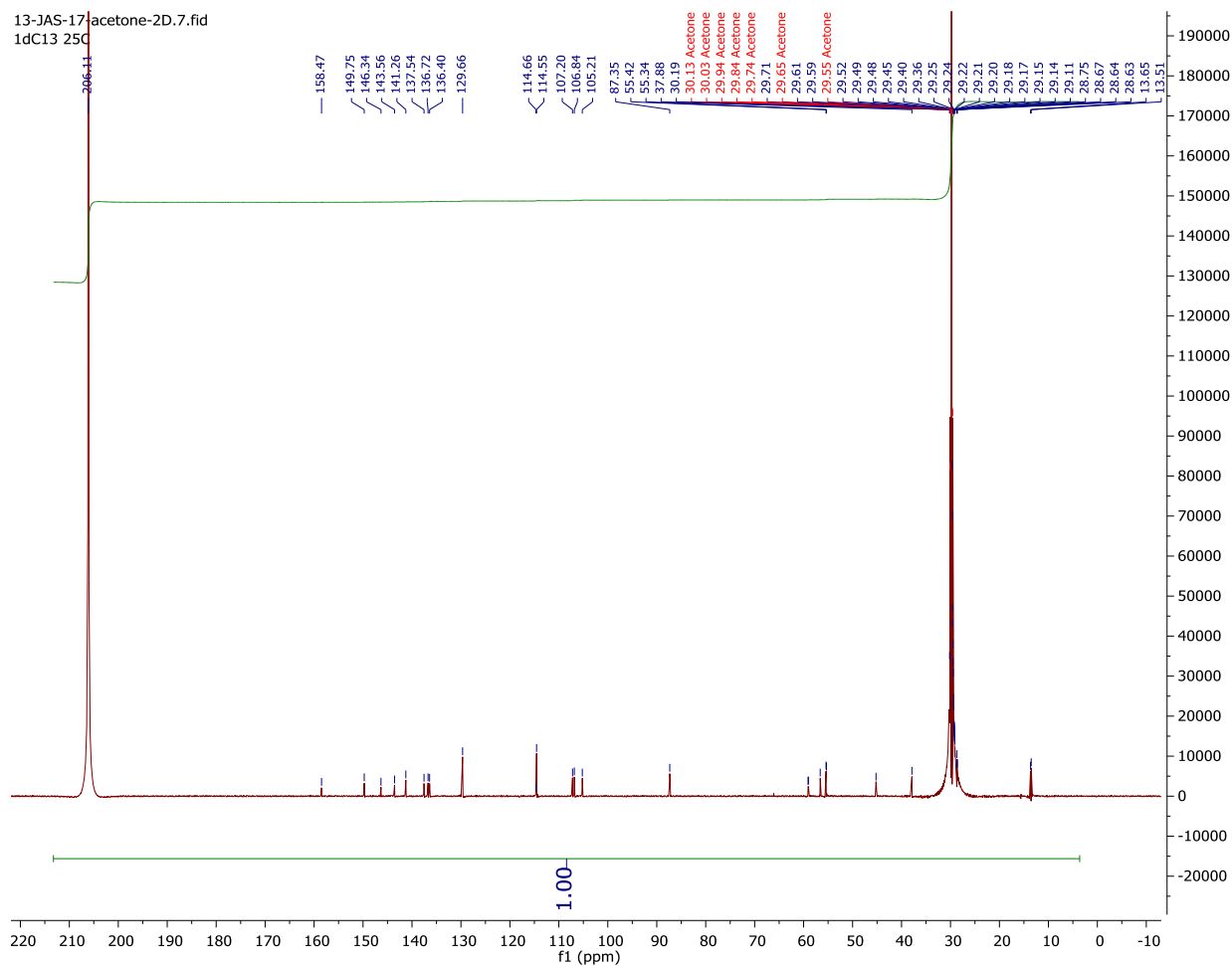
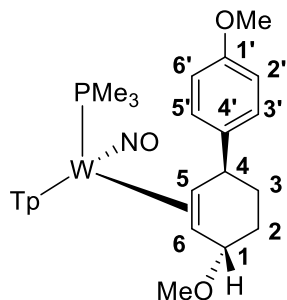
# <sup>1</sup>H NMR Spectra of 32



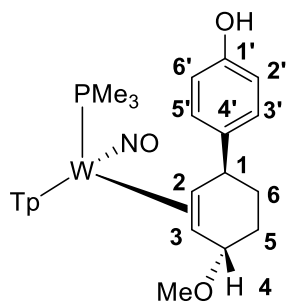
13-JAS-17-acetone-2D.1.fid  
1H 25C



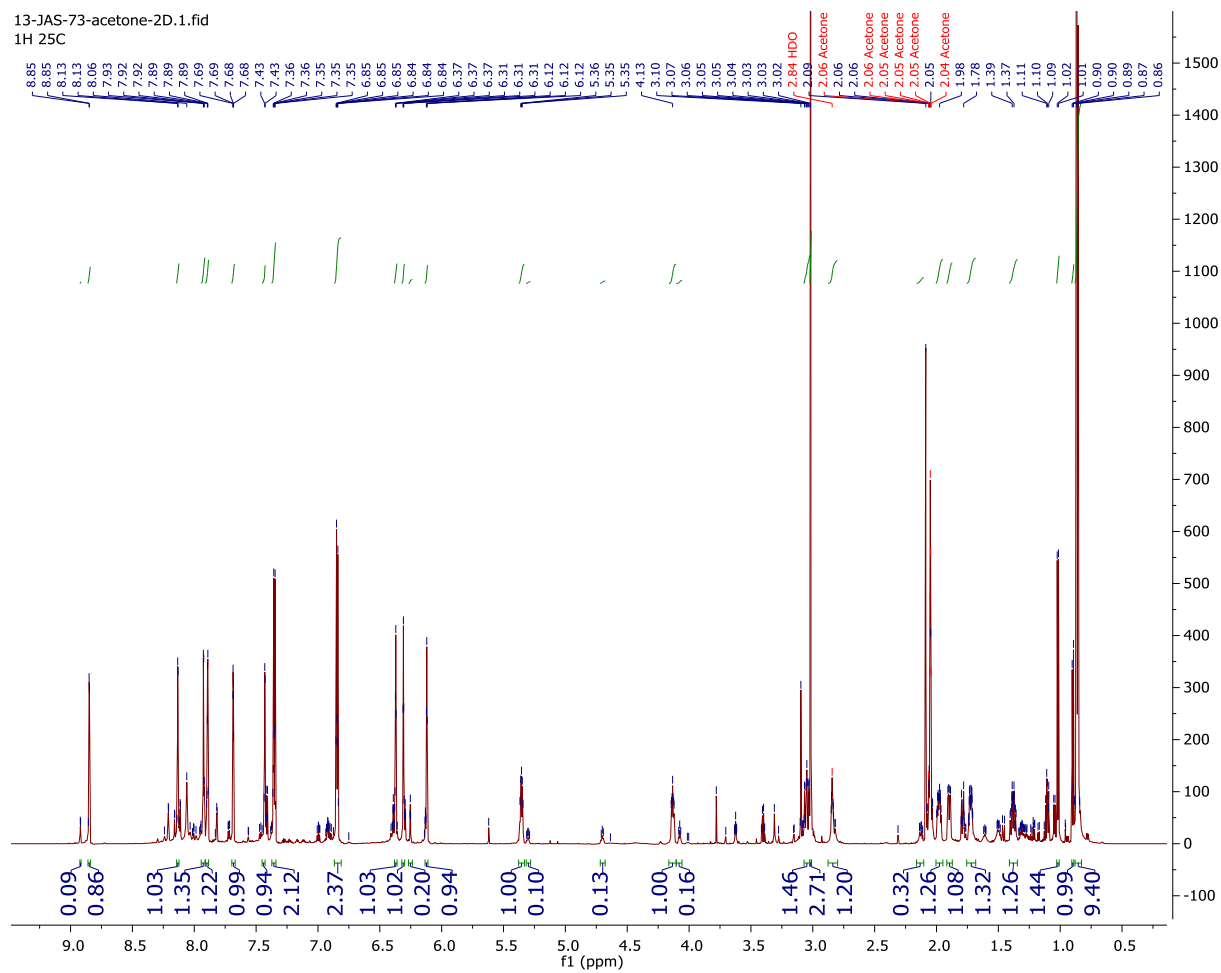
# <sup>13</sup>C {<sup>1</sup>H} NMR Spectra of 32



# <sup>1</sup>H NMR Spectra of 33

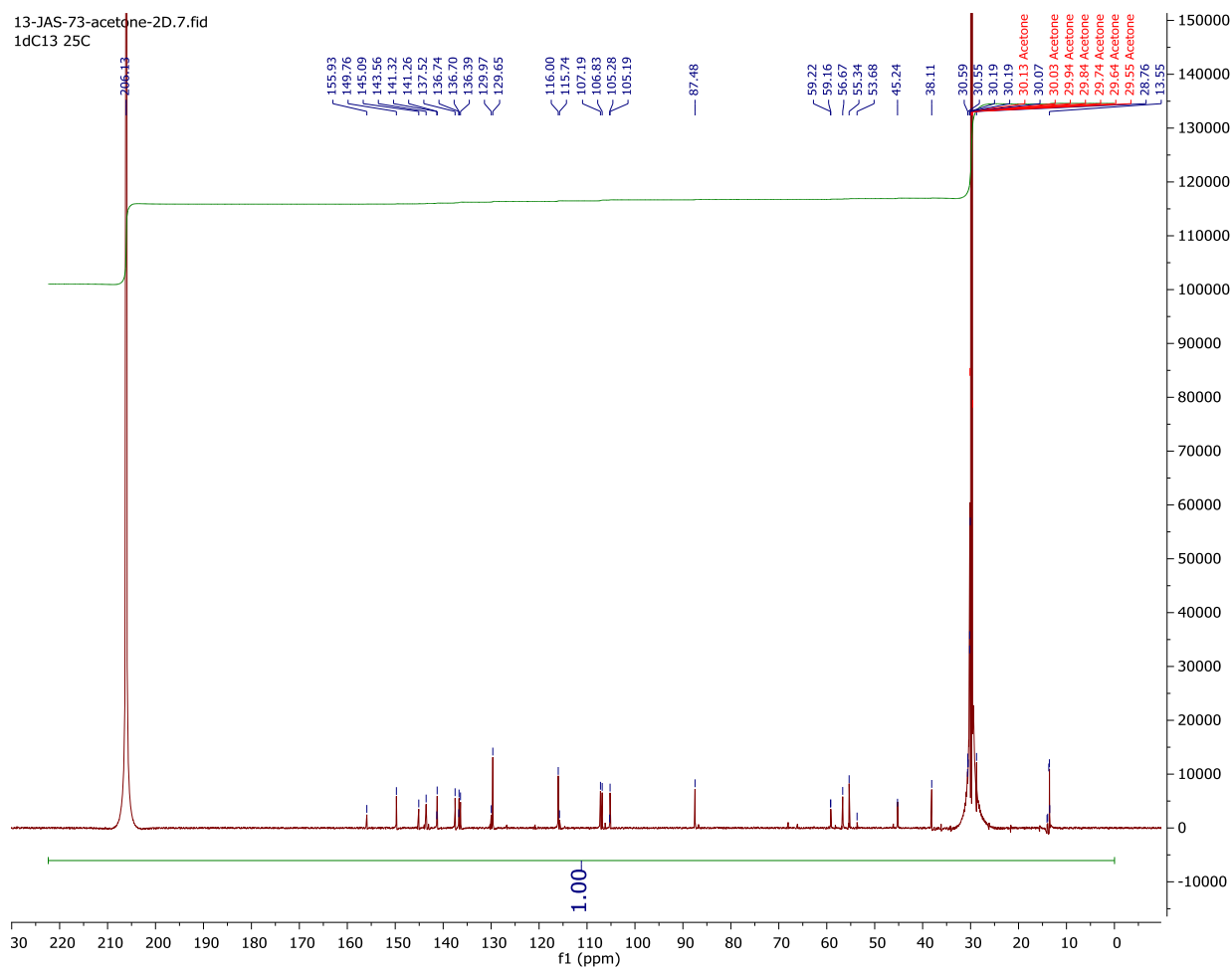
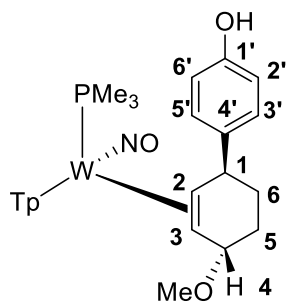


13-JAS-73-acetone-2D.1.fid  
1H 25C



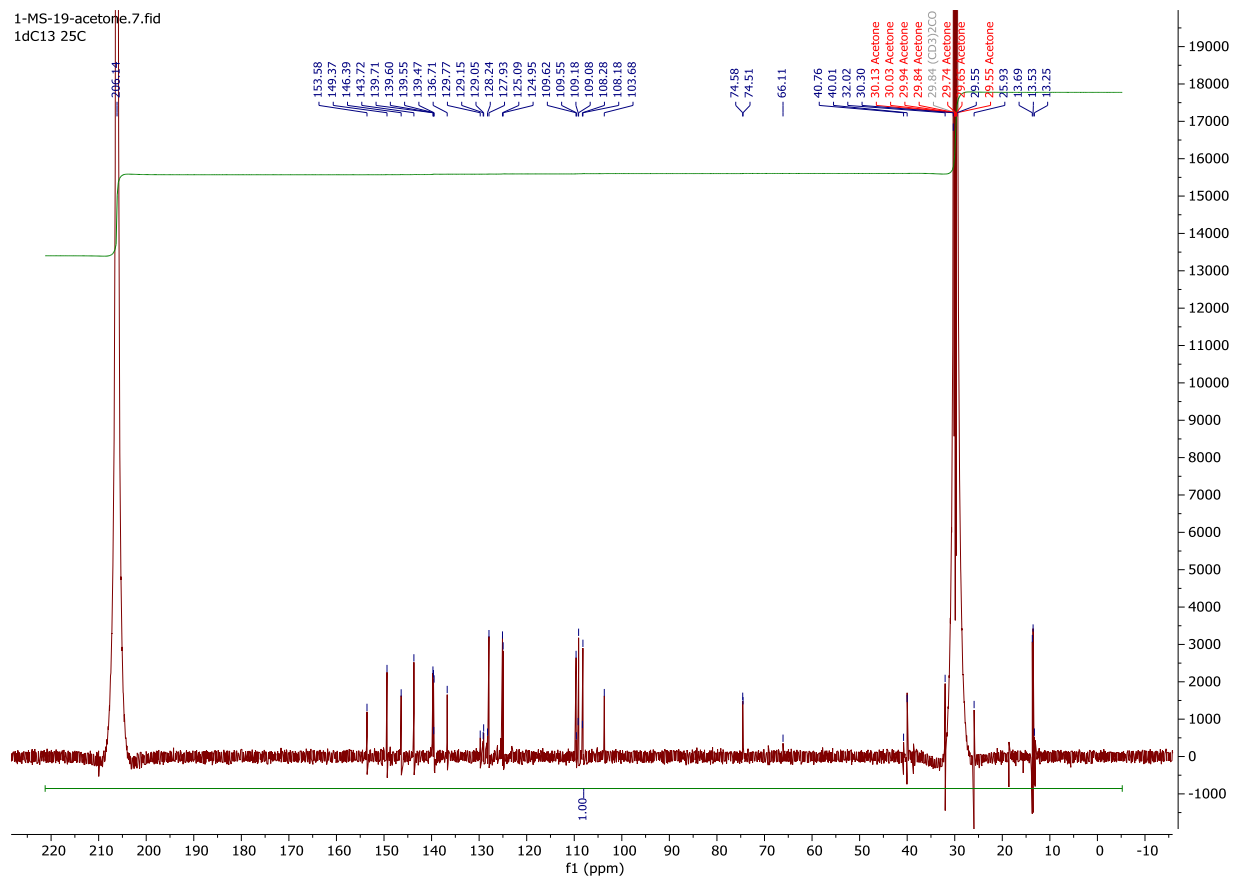
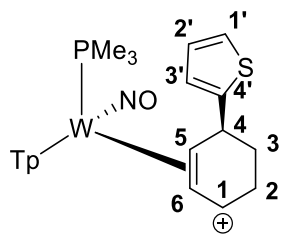


# <sup>13</sup>C {<sup>1</sup>H} NMR Spectra of 33

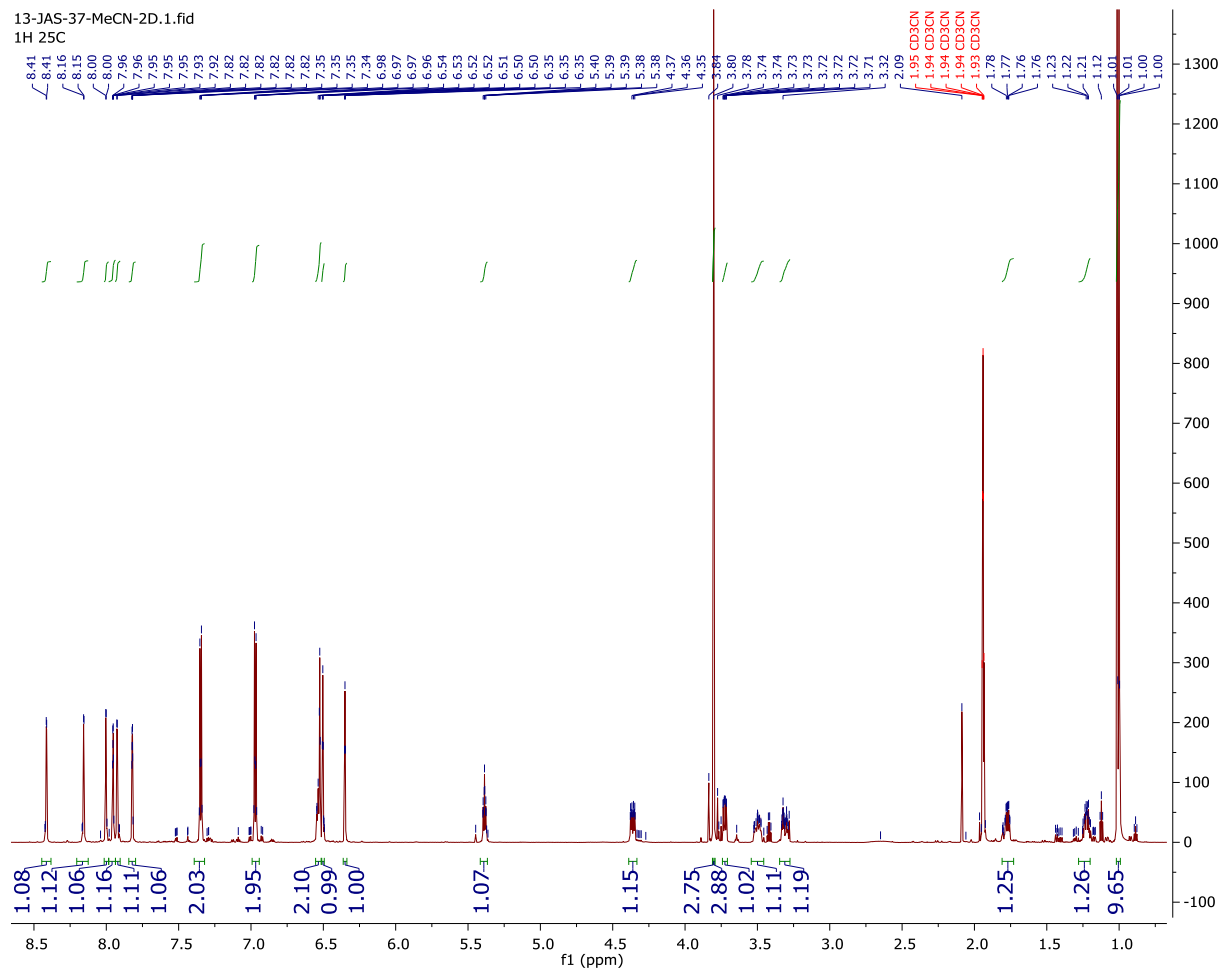
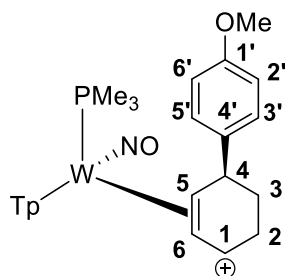




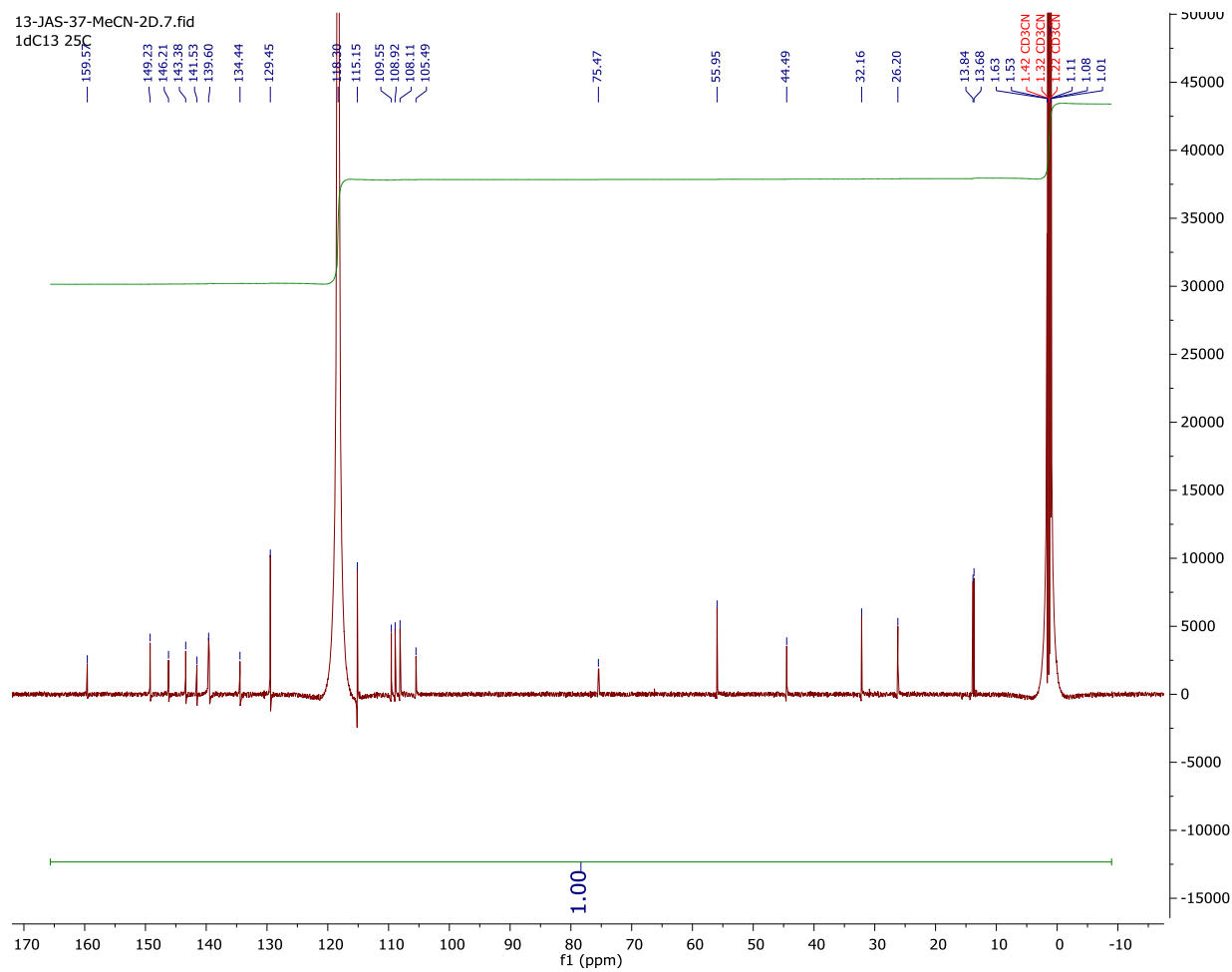
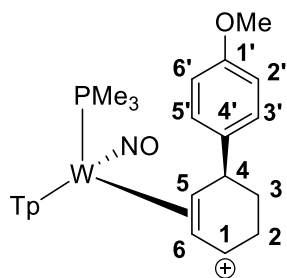
# <sup>13</sup>C {<sup>1</sup>H} NMR Spectra of 34



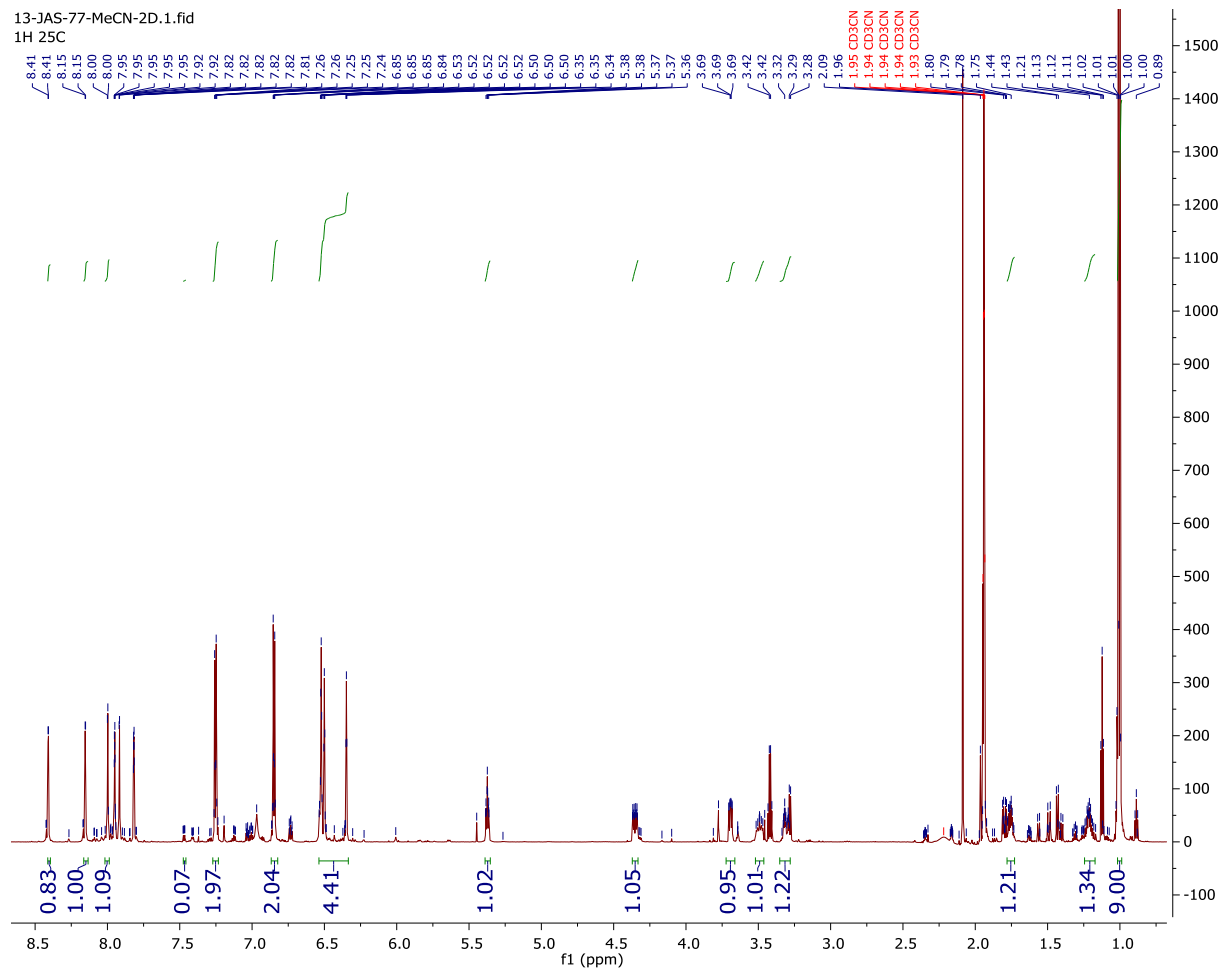
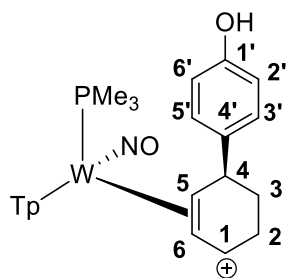
# <sup>1</sup>H NMR Spectra of 35



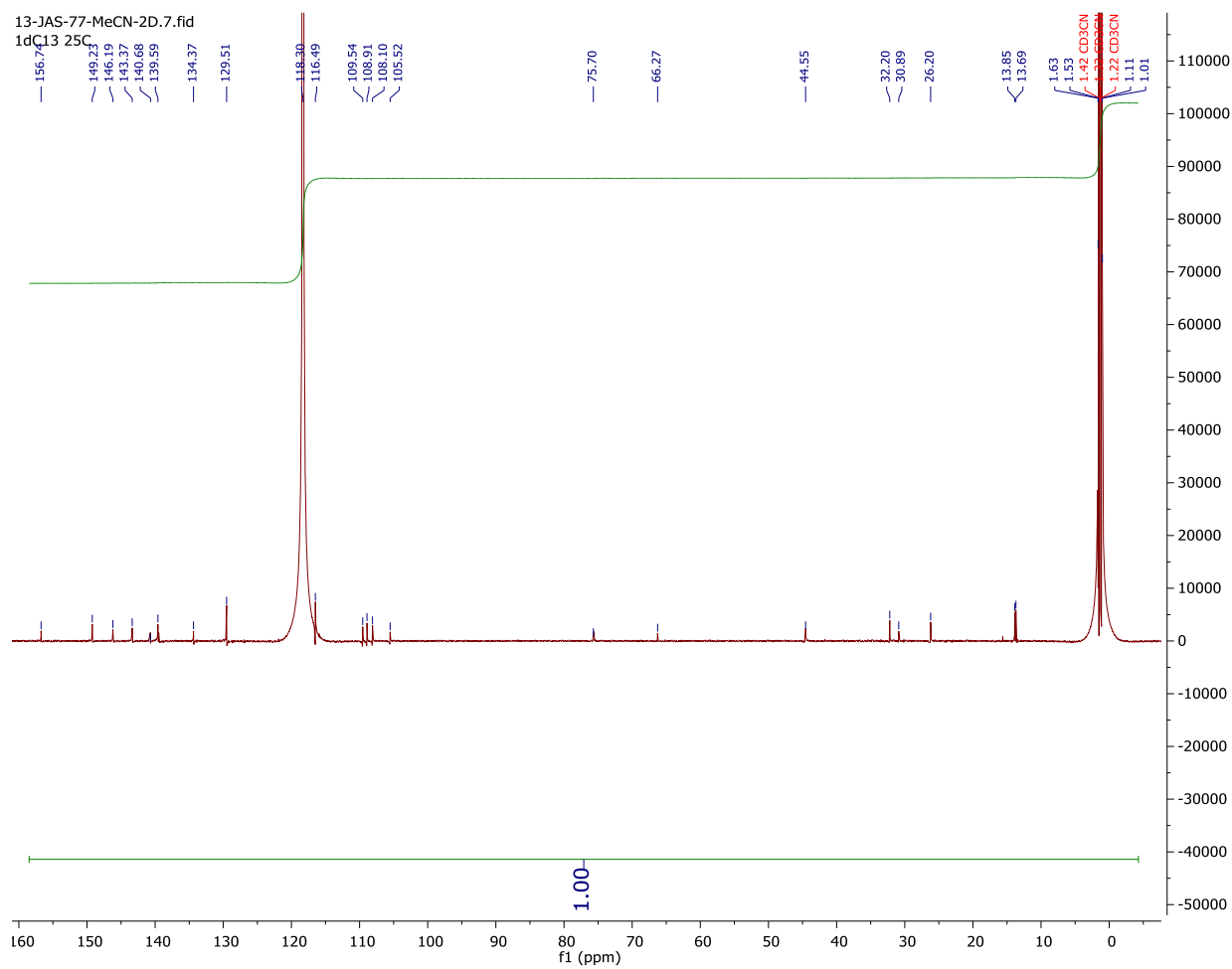
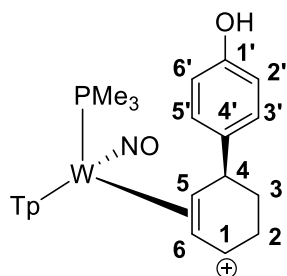
# <sup>13</sup>C {<sup>1</sup>H} NMR Spectra of 35



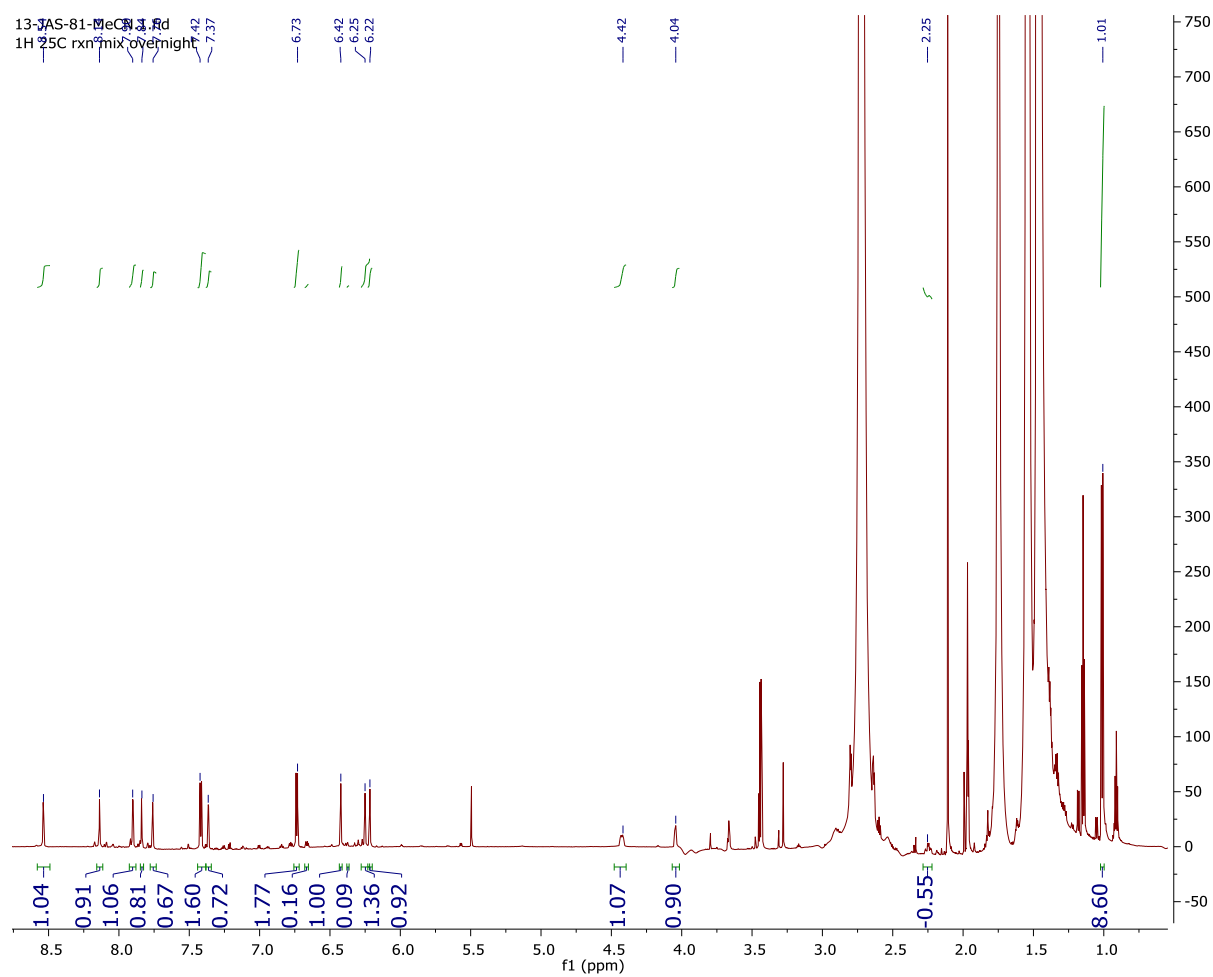
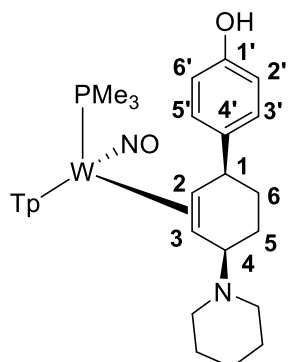
# <sup>1</sup>H NMR Spectra of 36



# $^{13}\text{C}$ $\{^1\text{H}\}$ NMR Spectra of 36

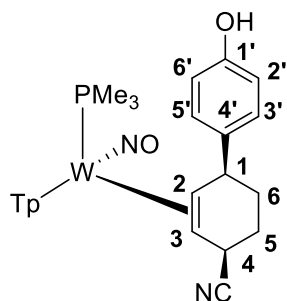


# <sup>1</sup>H NMR Spectra of 37

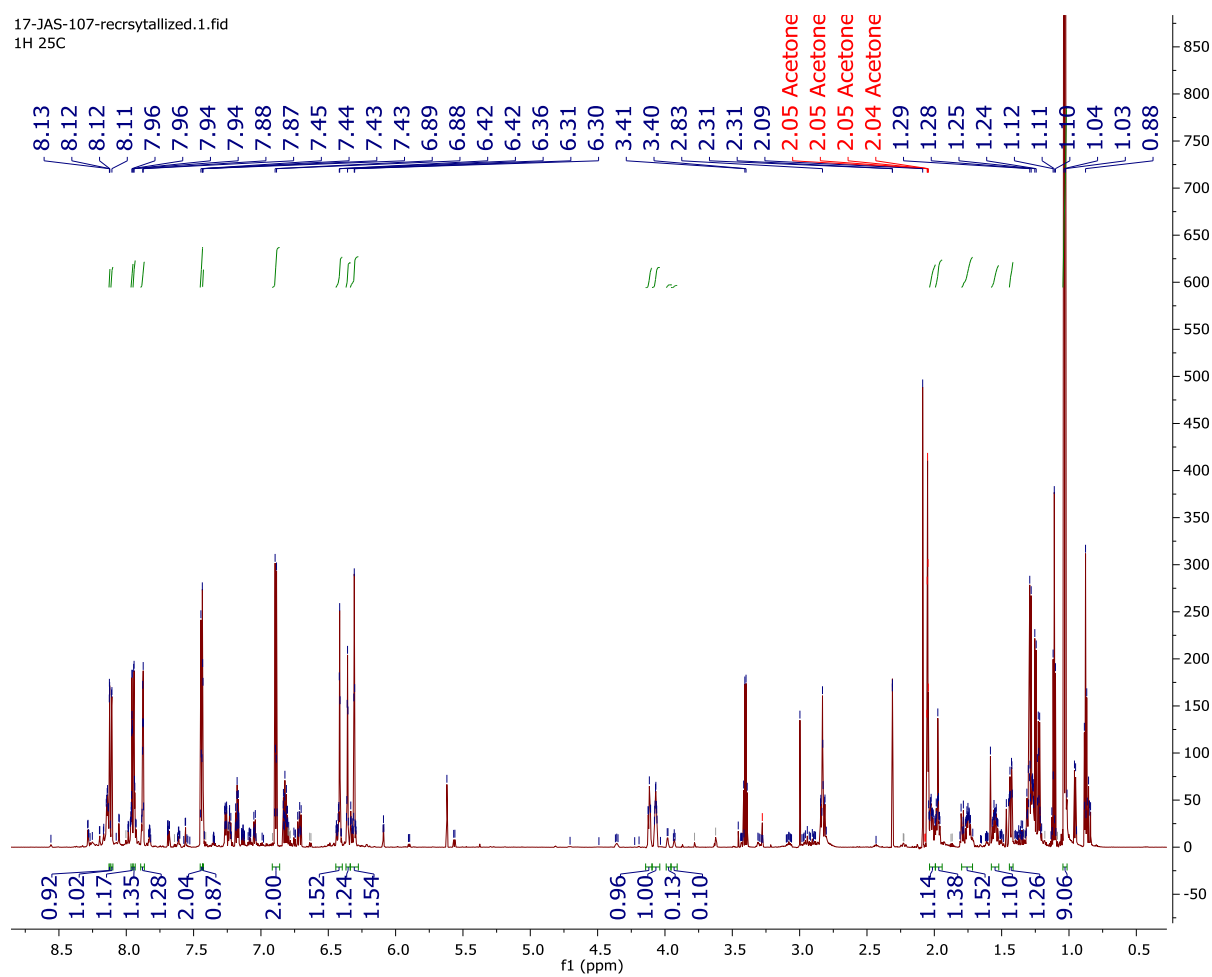




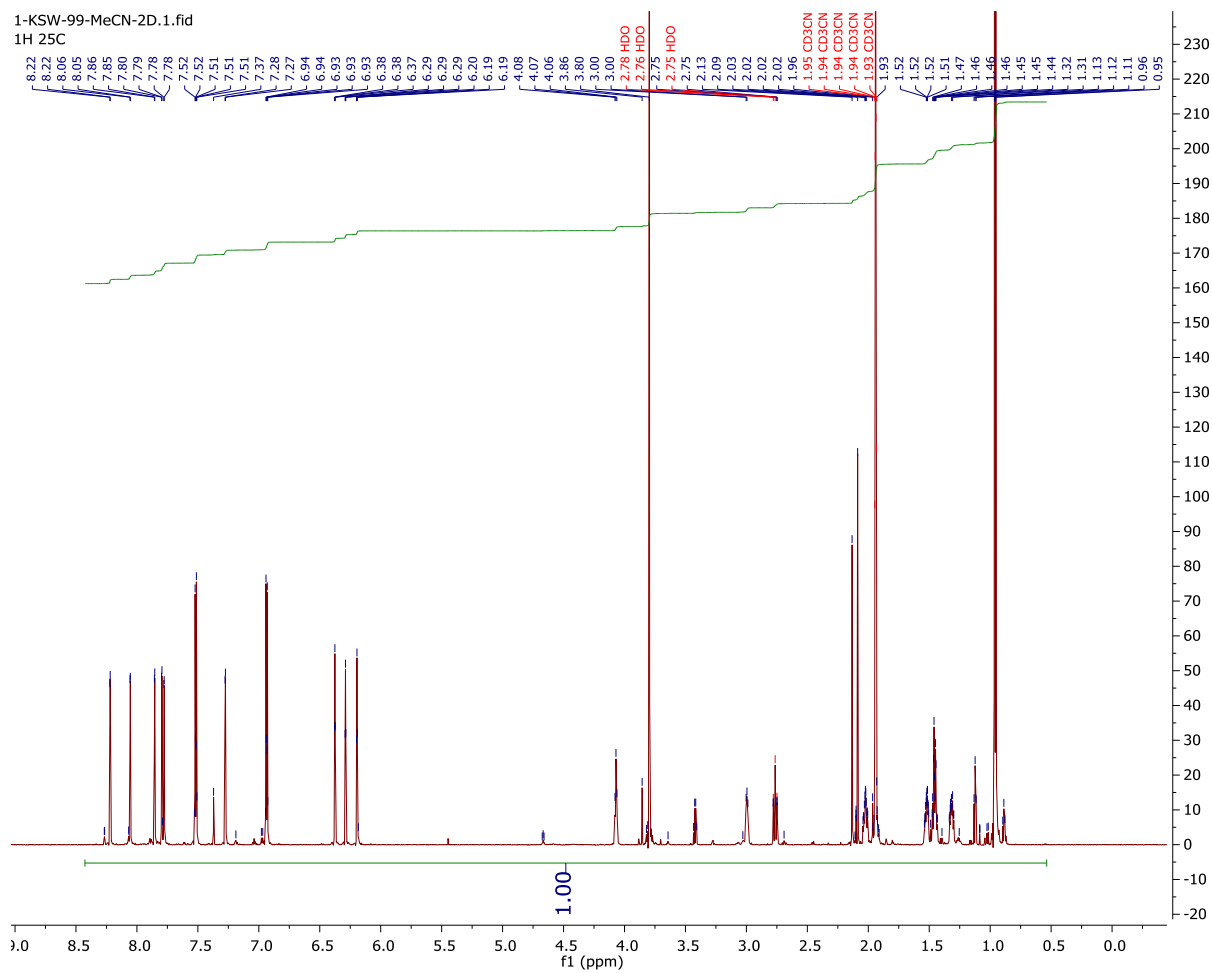
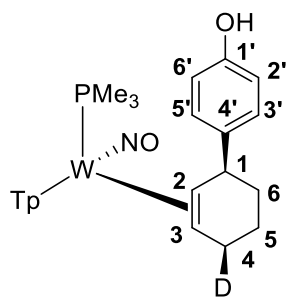
# <sup>1</sup>H NMR Spectra of 38



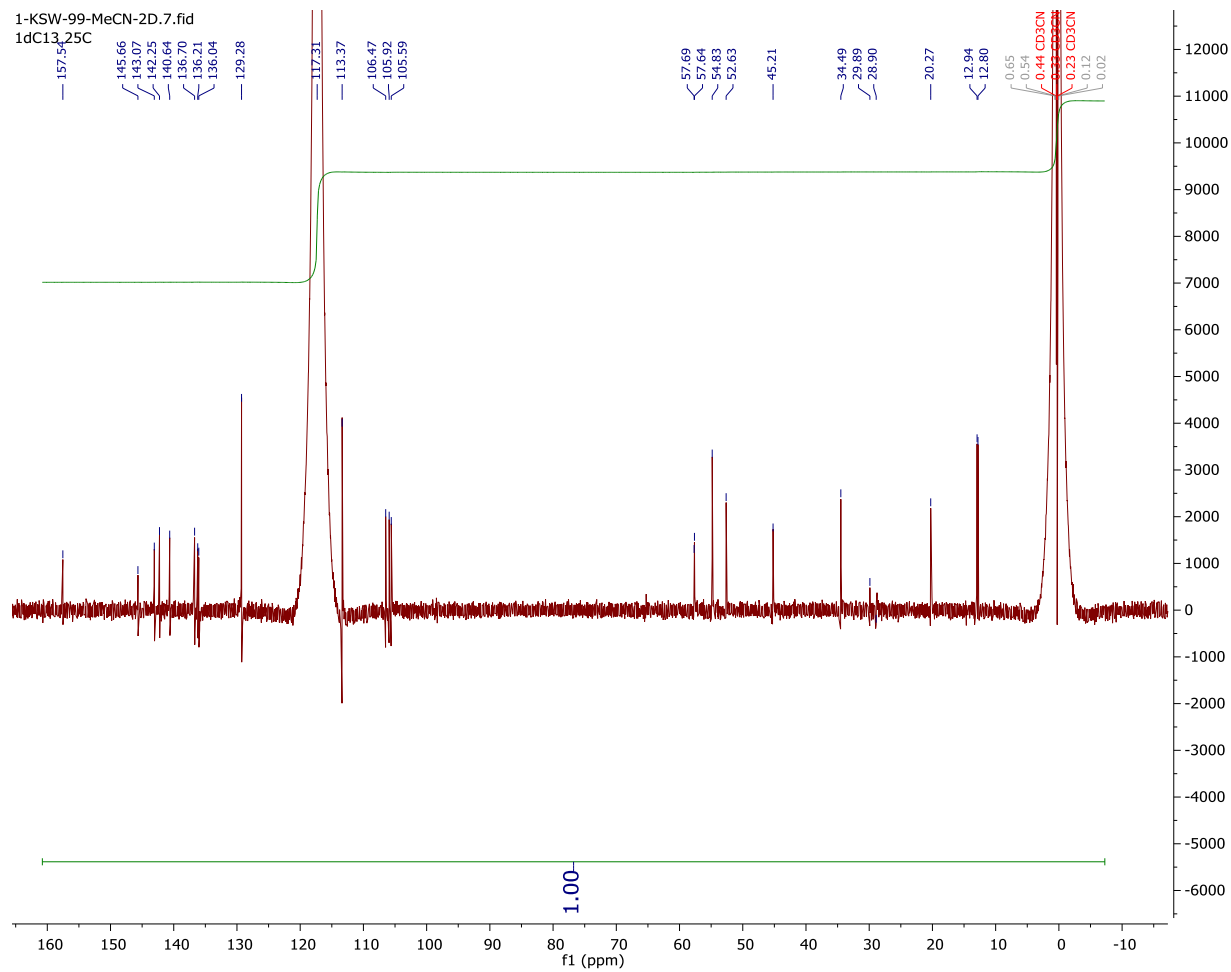
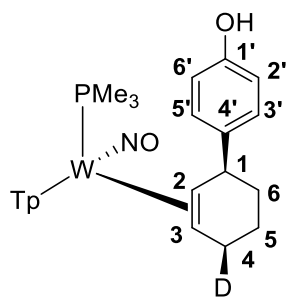
17-JAS-107-recrsytallized.1.fid  
1H 25C



# <sup>1</sup>H NMR Spectra of 39

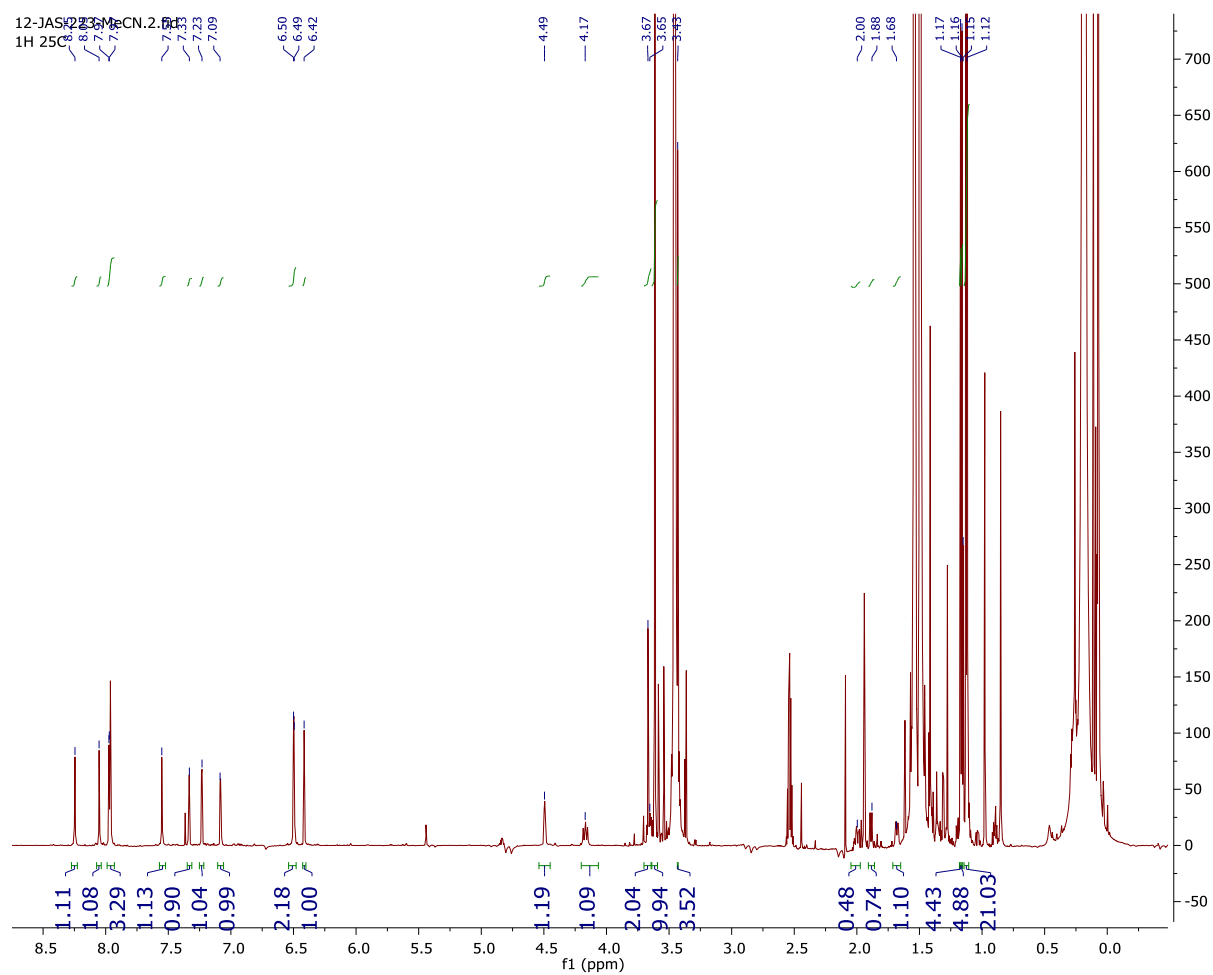
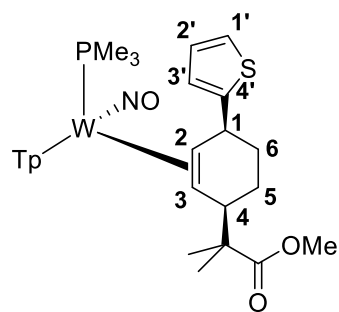


# $^{13}\text{C}$ $\{^1\text{H}\}$ NMR Spectra of 39

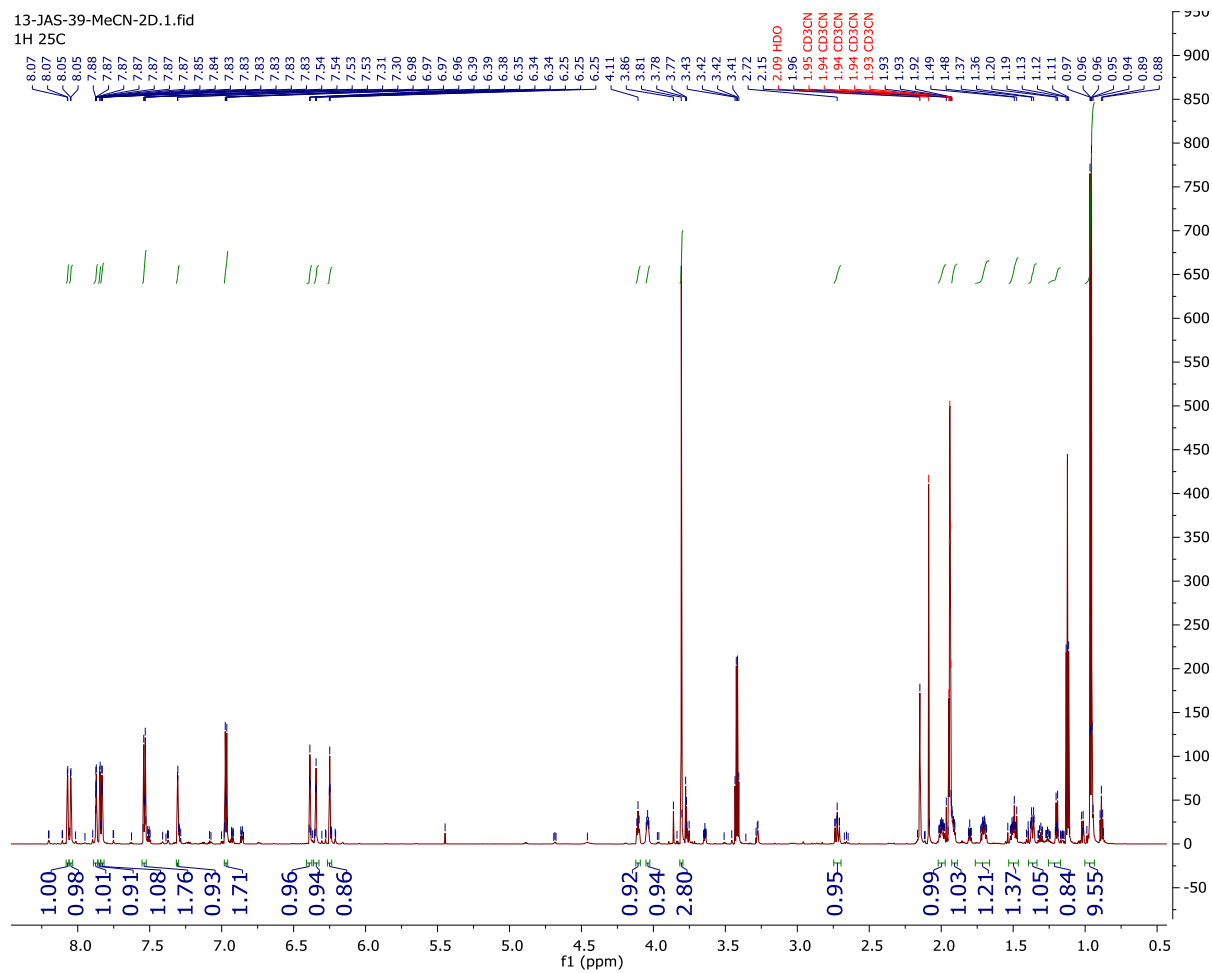
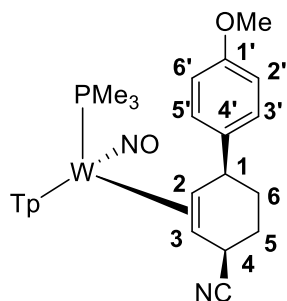




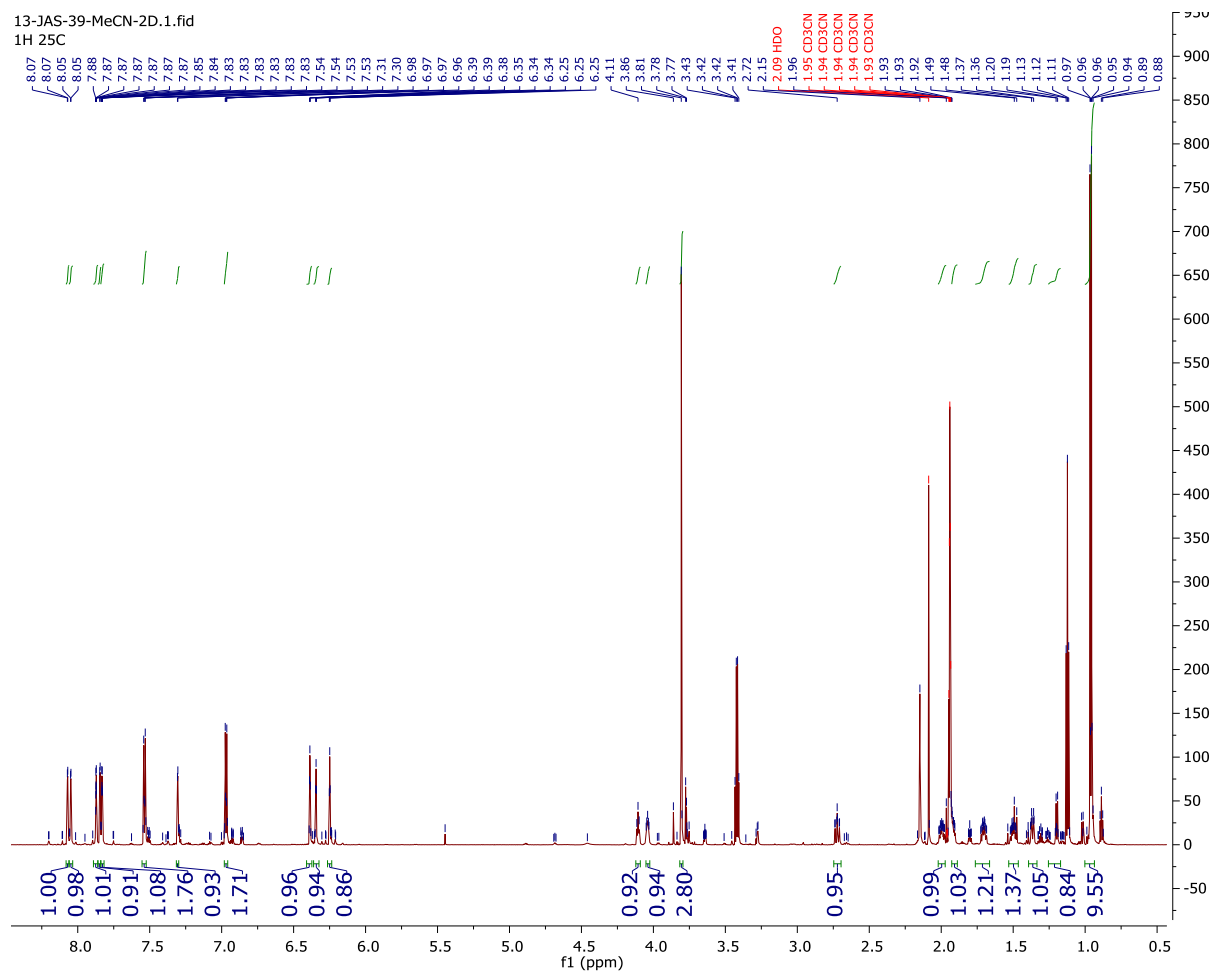
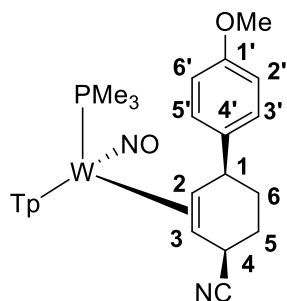
# <sup>1</sup>H NMR Spectra of 41



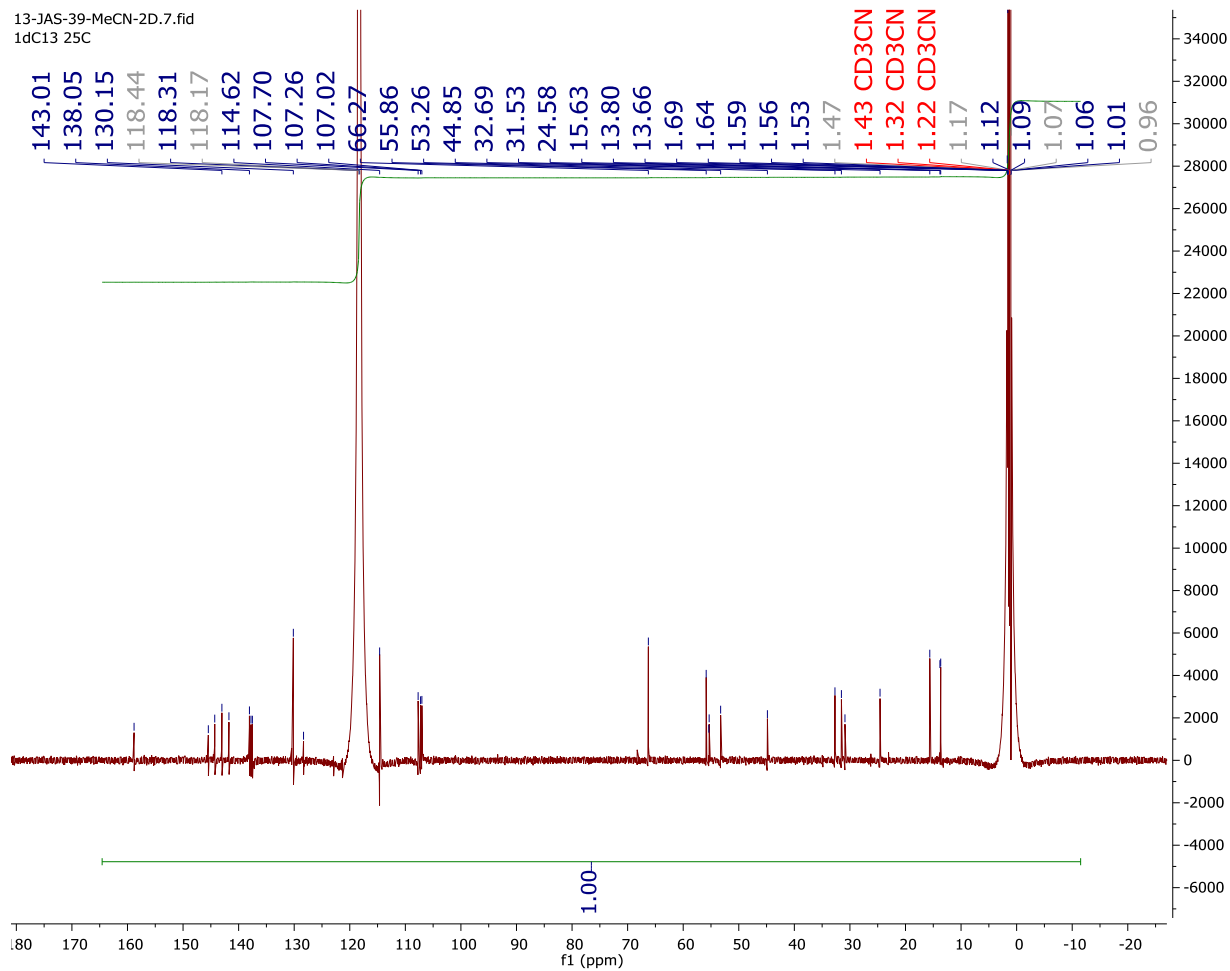
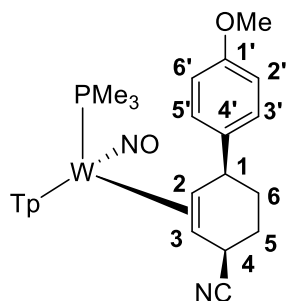
# <sup>1</sup>H NMR Spectra of 42



# <sup>13</sup>C {<sup>1</sup>H} NMR Spectra of 42

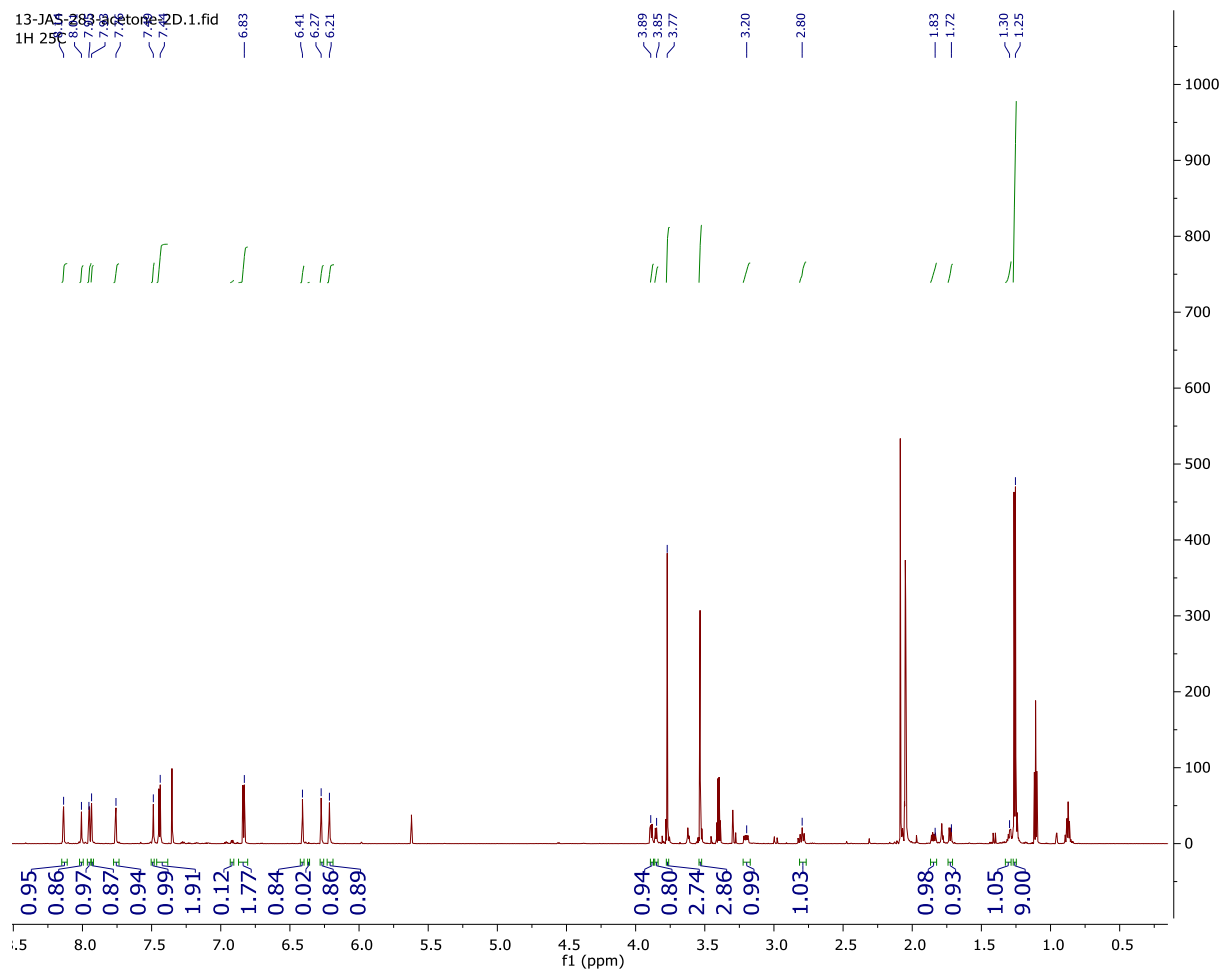
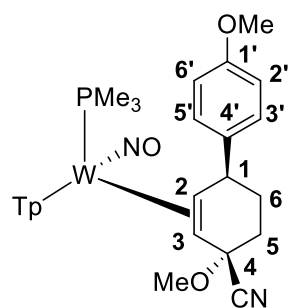


# <sup>13</sup>C {<sup>1</sup>H} NMR Spectra of 42



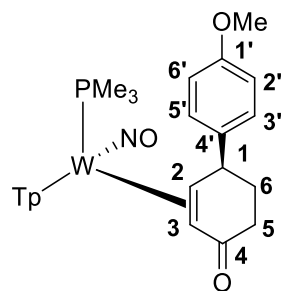


# <sup>1</sup>H NMR Spectra of 43

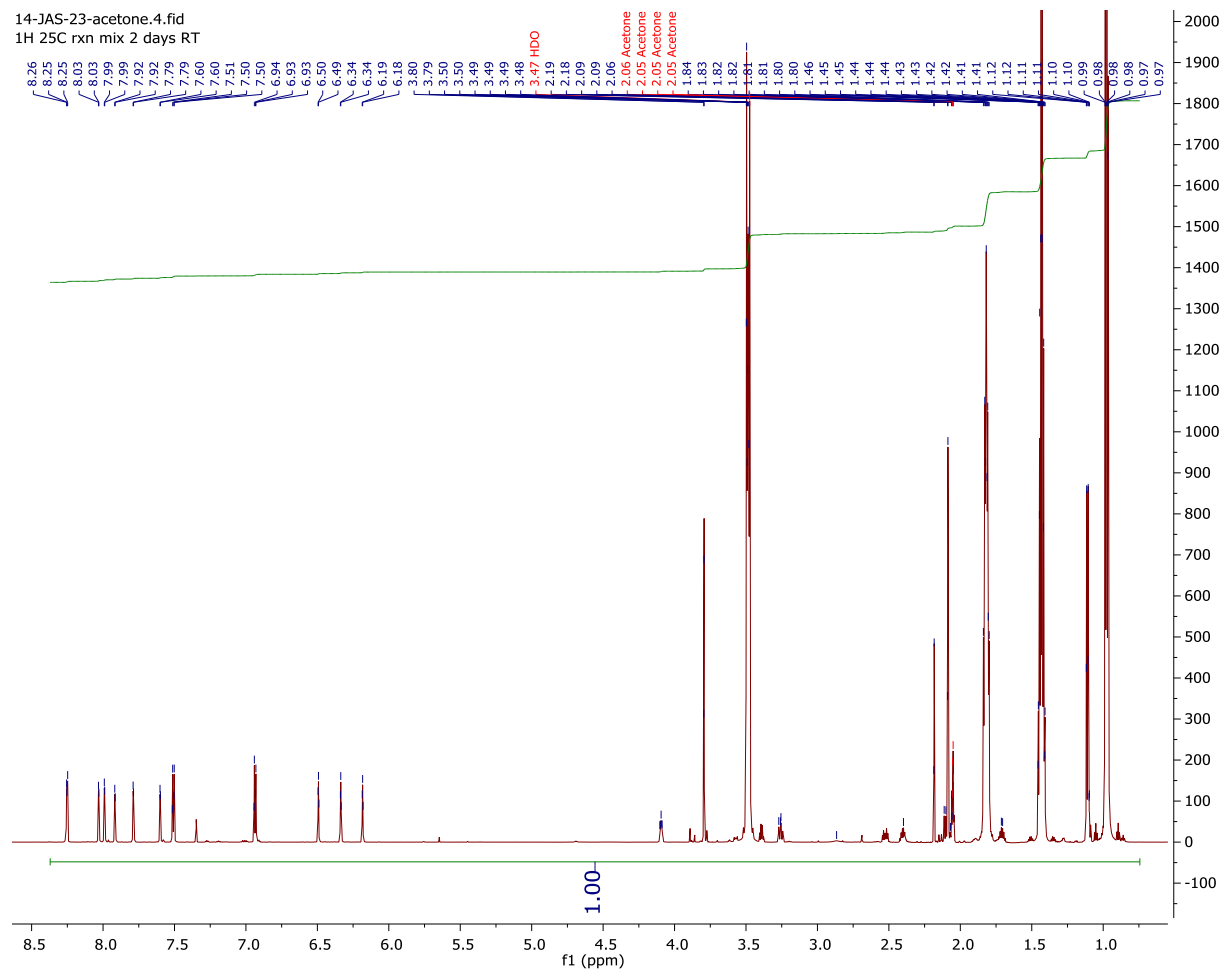




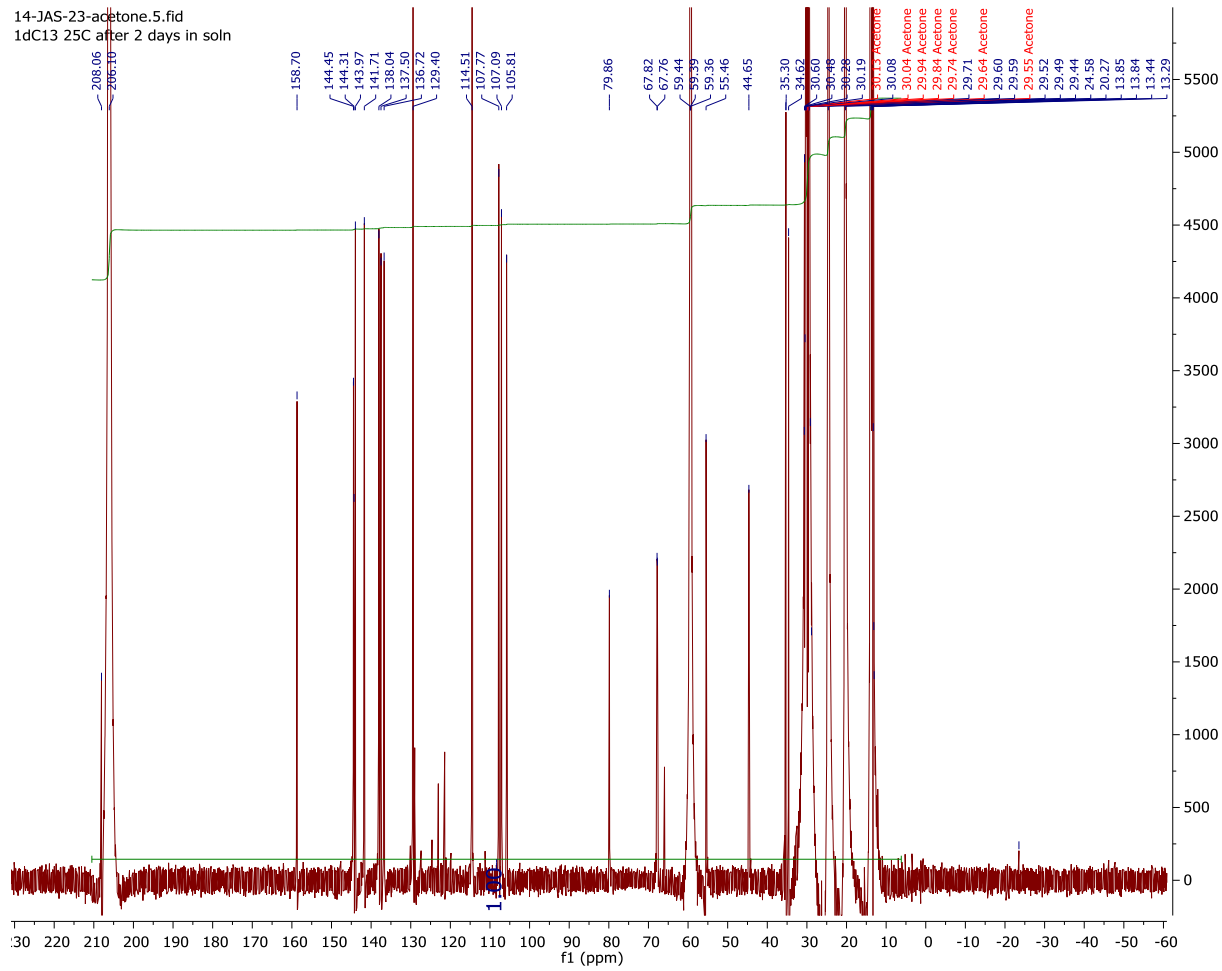
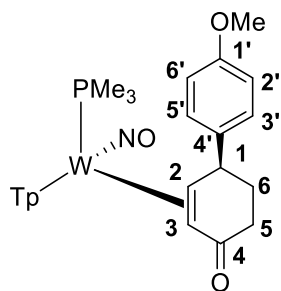
# <sup>1</sup>H NMR Spectra of 44



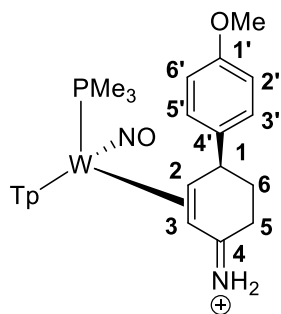
14-JAS-23-acetone.4.fid  
1H 25C rxn mix 2 days RT



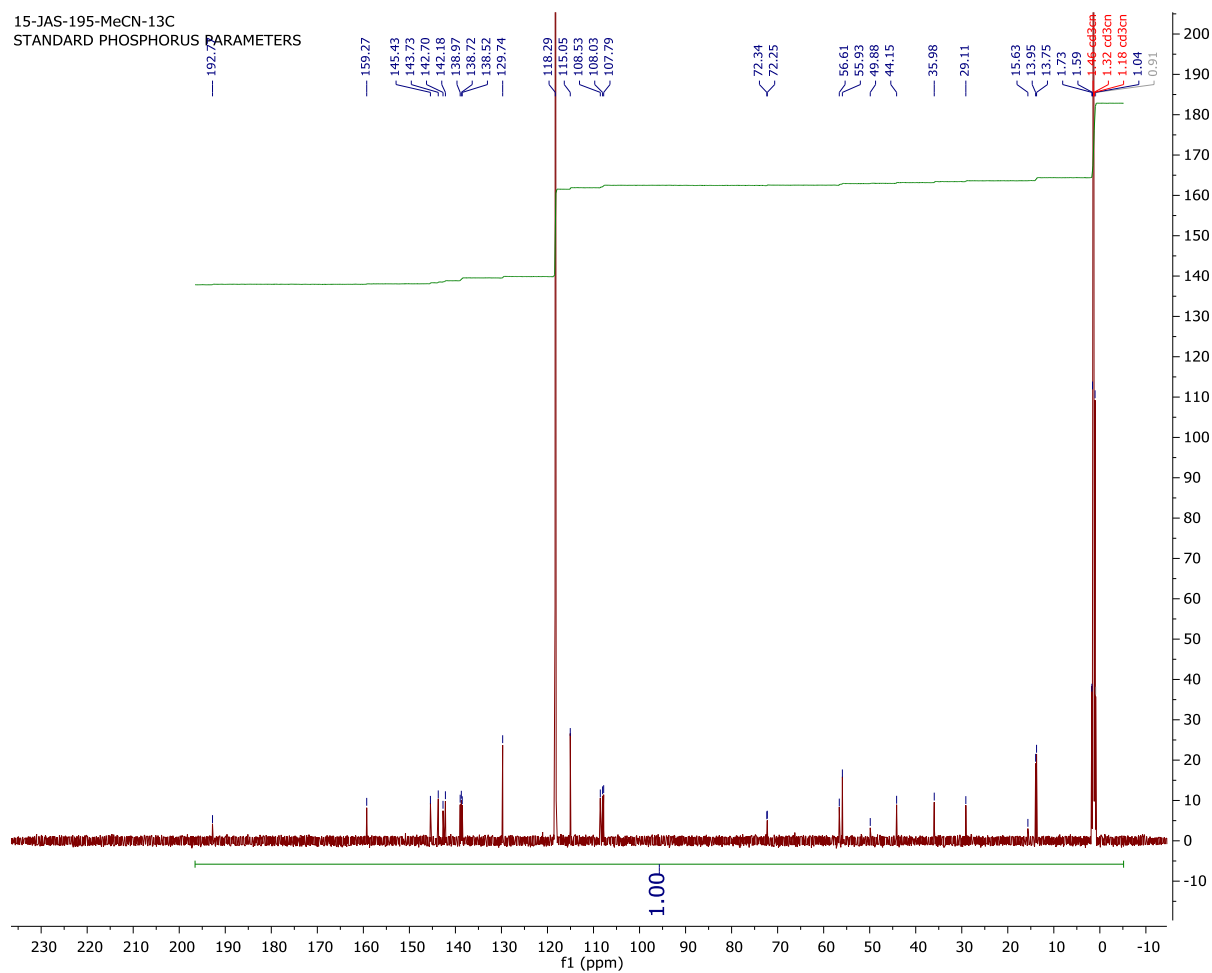
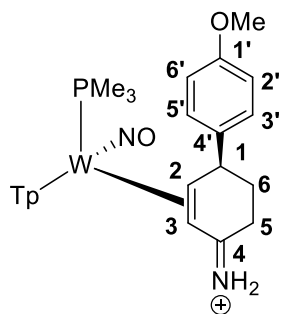
# $^{13}\text{C}$ $\{^1\text{H}\}$ NMR Spectra of 44



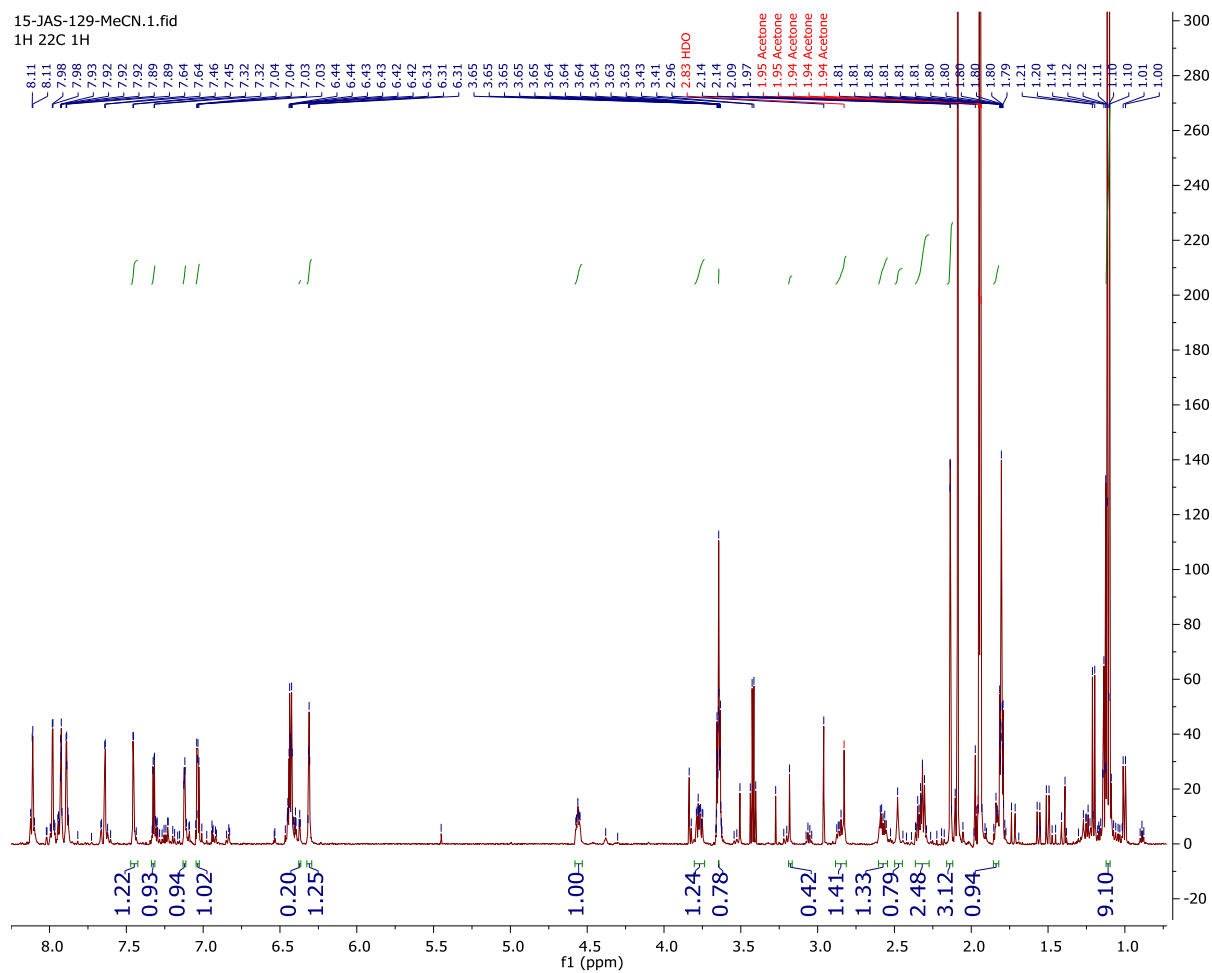
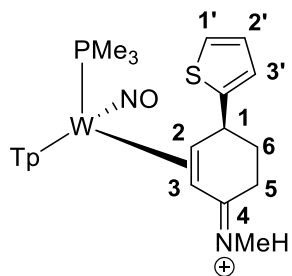
# <sup>1</sup>H NMR Spectra of 45



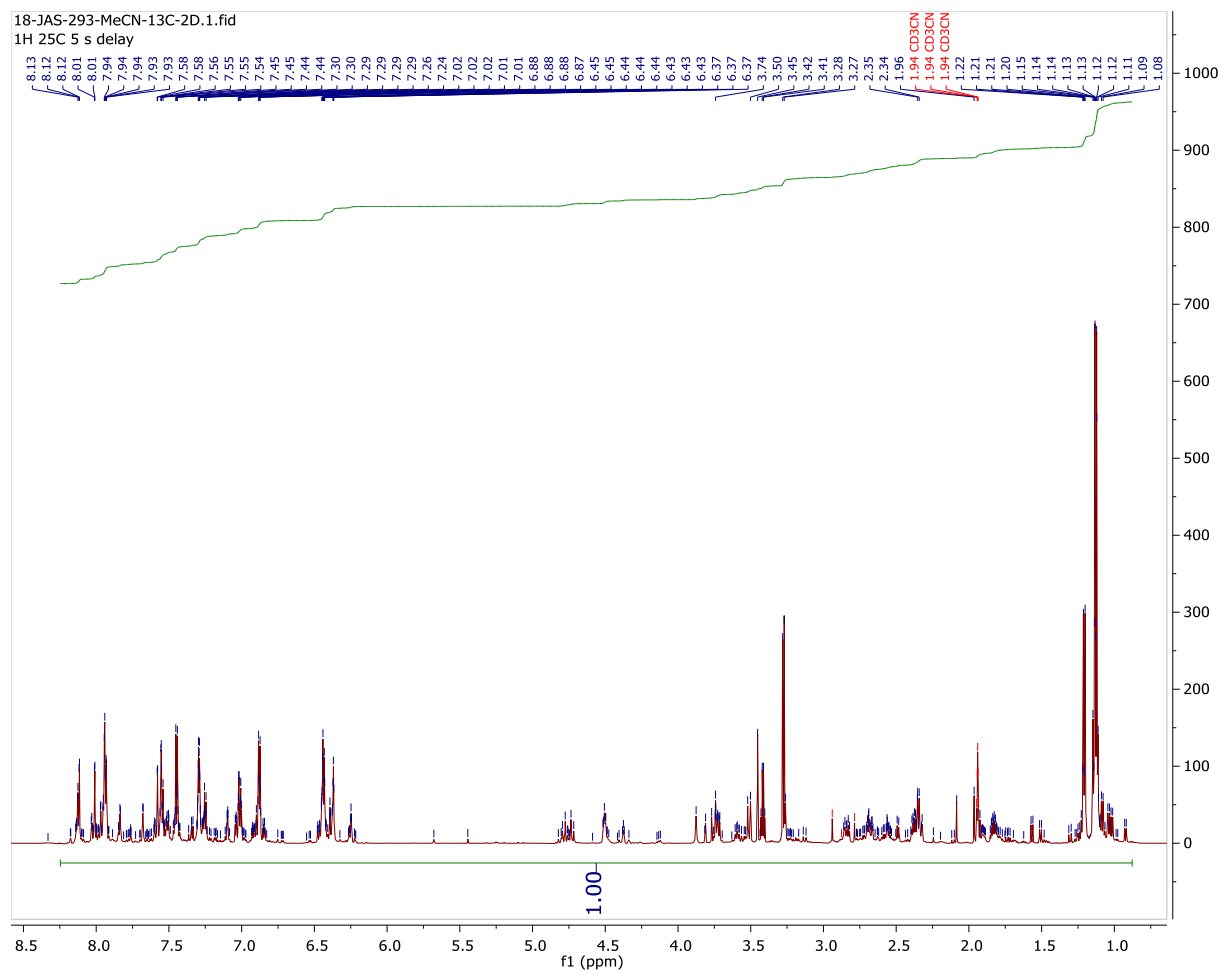
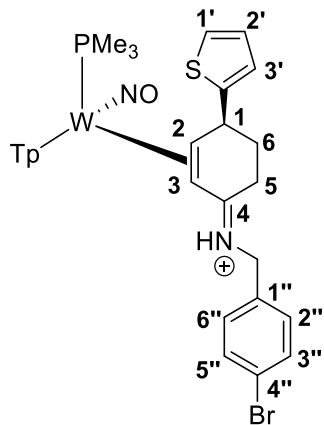
# $^{13}\text{C}$ $\{^1\text{H}\}$ NMR Spectra of 46



# {<sup>1</sup>H} NMR Spectra of 46

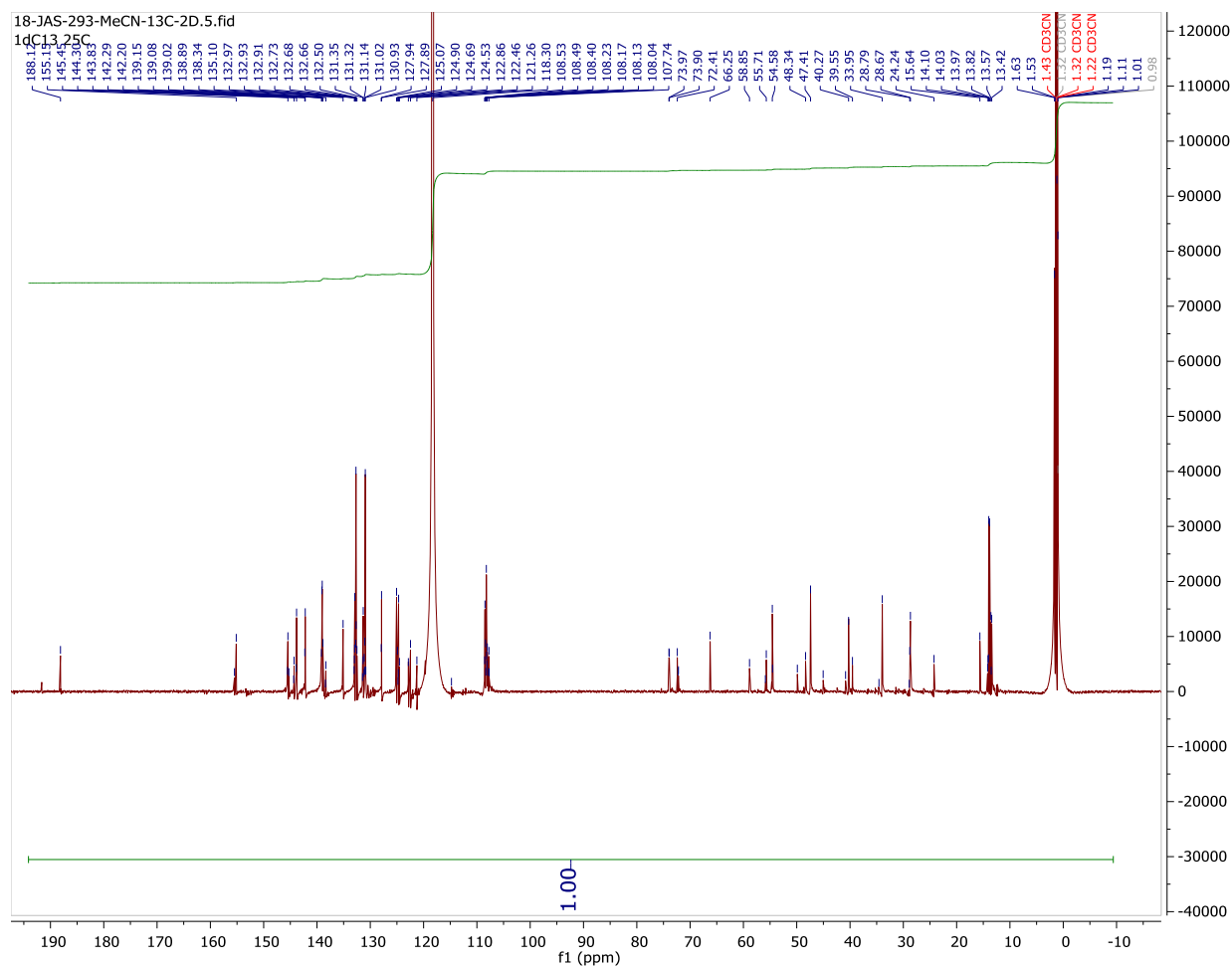
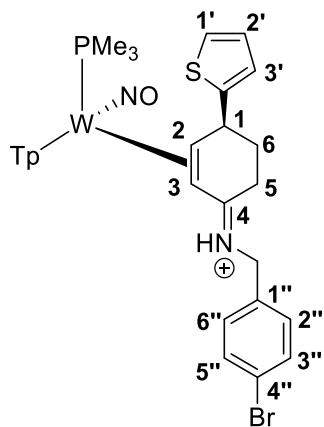


# {<sup>1</sup>H} NMR Spectra of 47

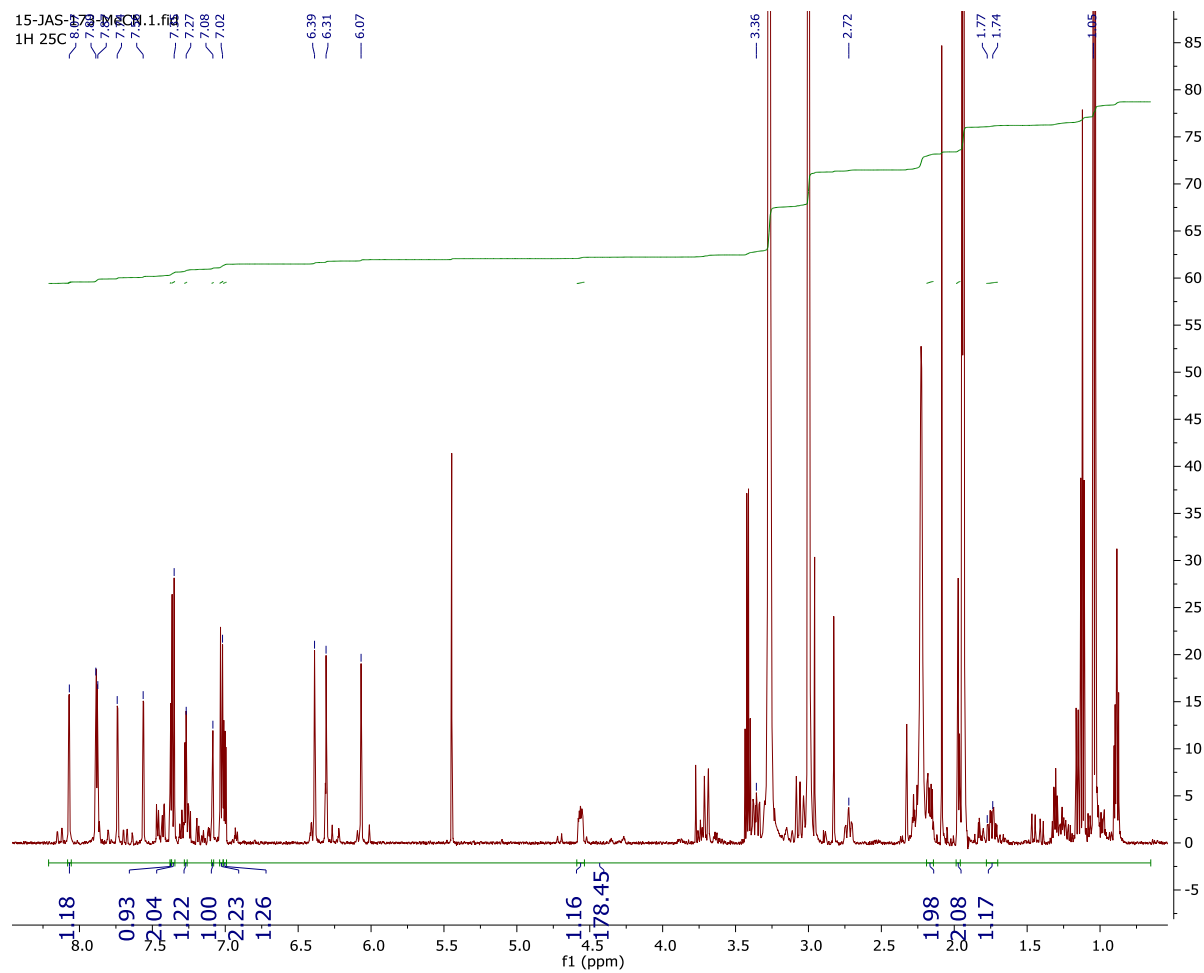
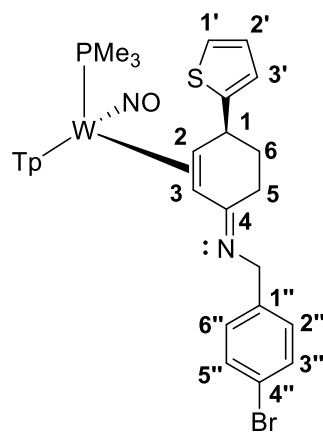




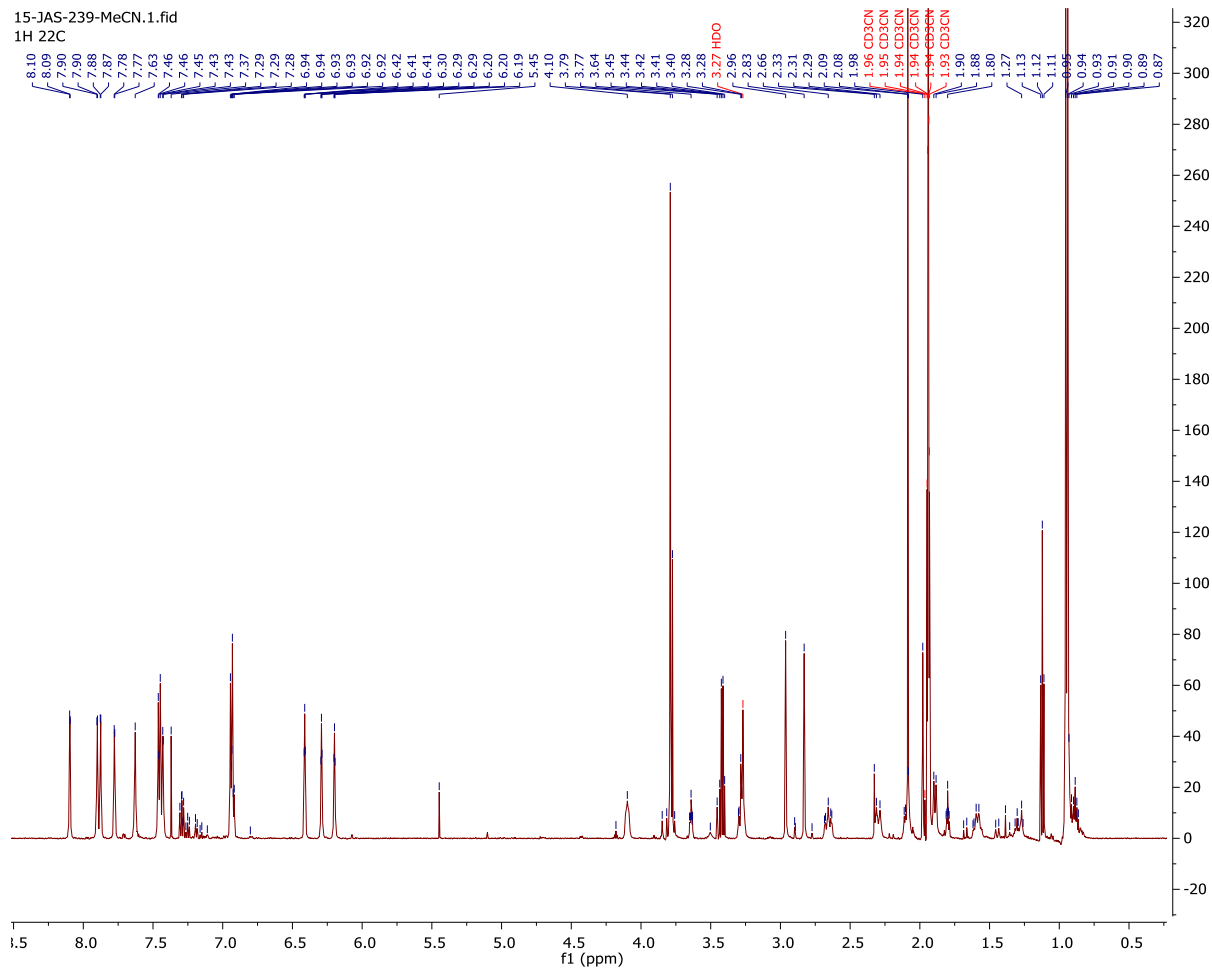
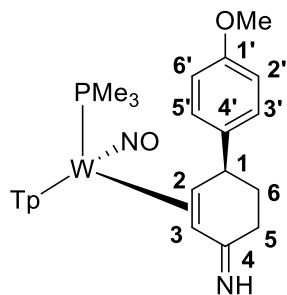
# <sup>13</sup>C {<sup>1</sup>H} NMR Spectra of 47



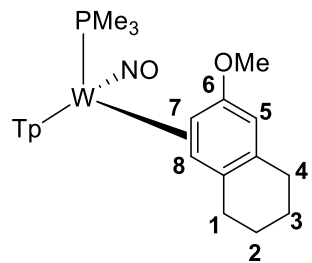
# <sup>1</sup>H NMR Spectra of 48



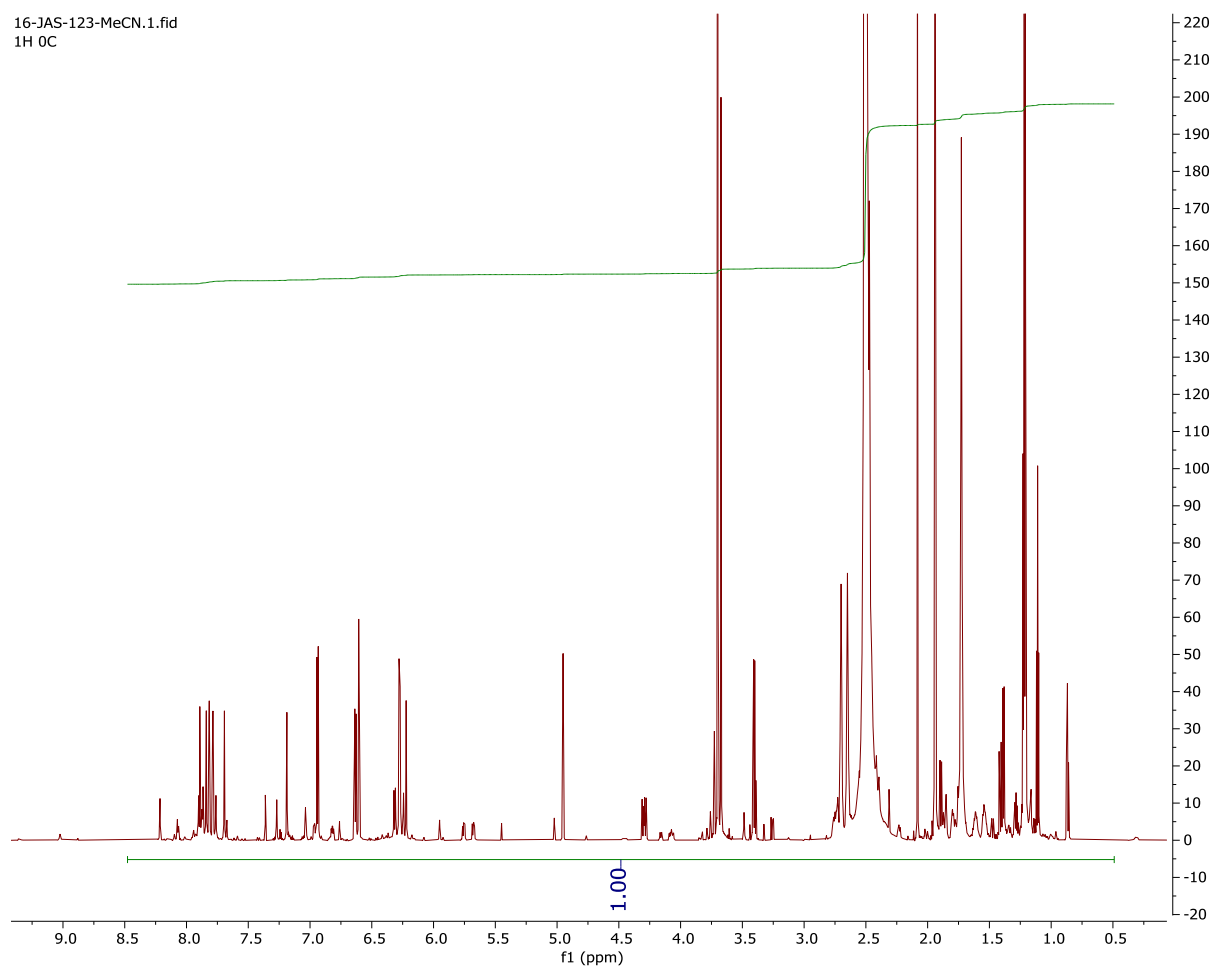
# <sup>1</sup>H NMR Spectra of 49



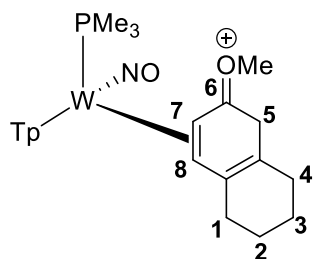
# <sup>1</sup>H NMR Spectra of 54



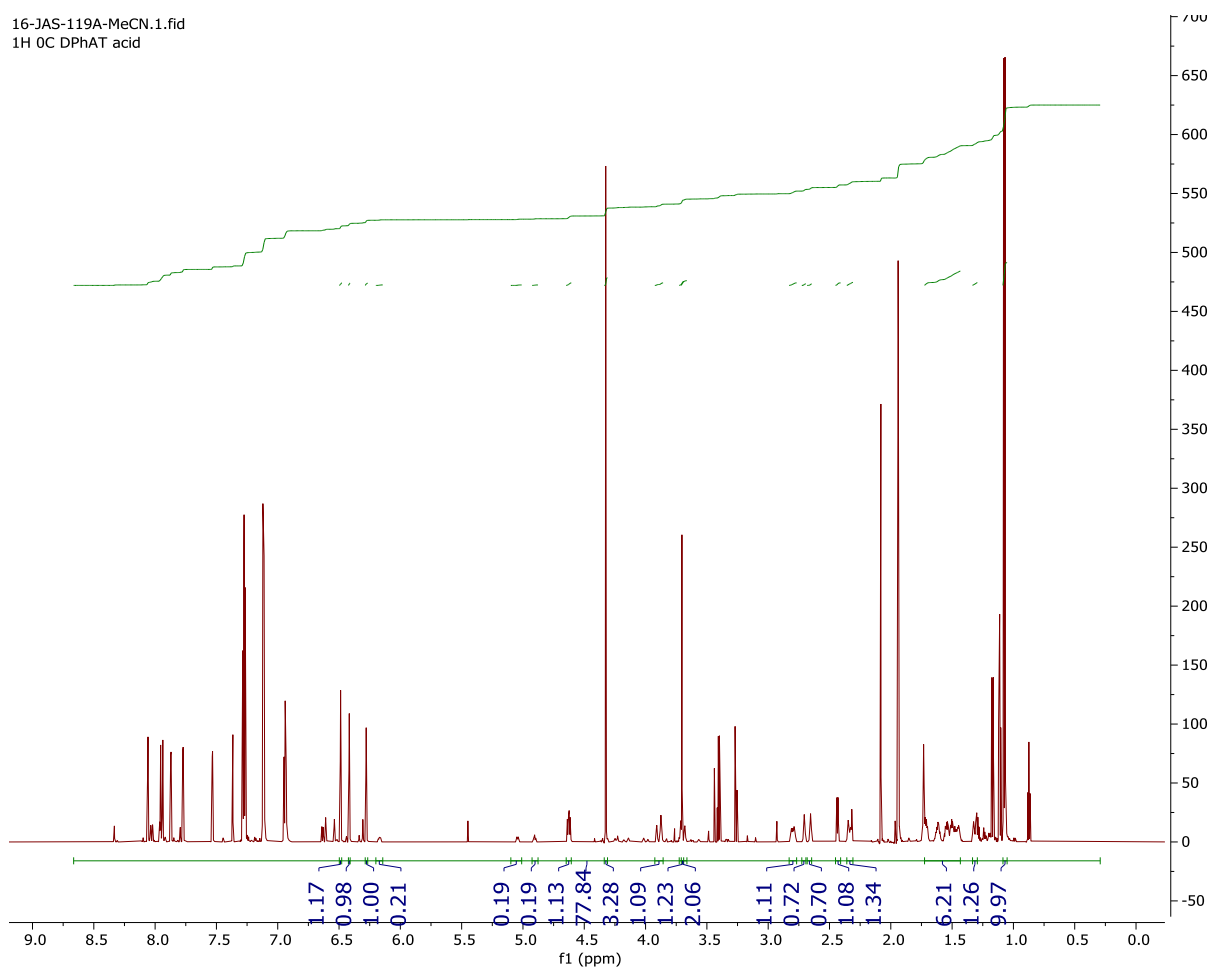
16-JAS-123-MeCN.1.fid  
1H 0C



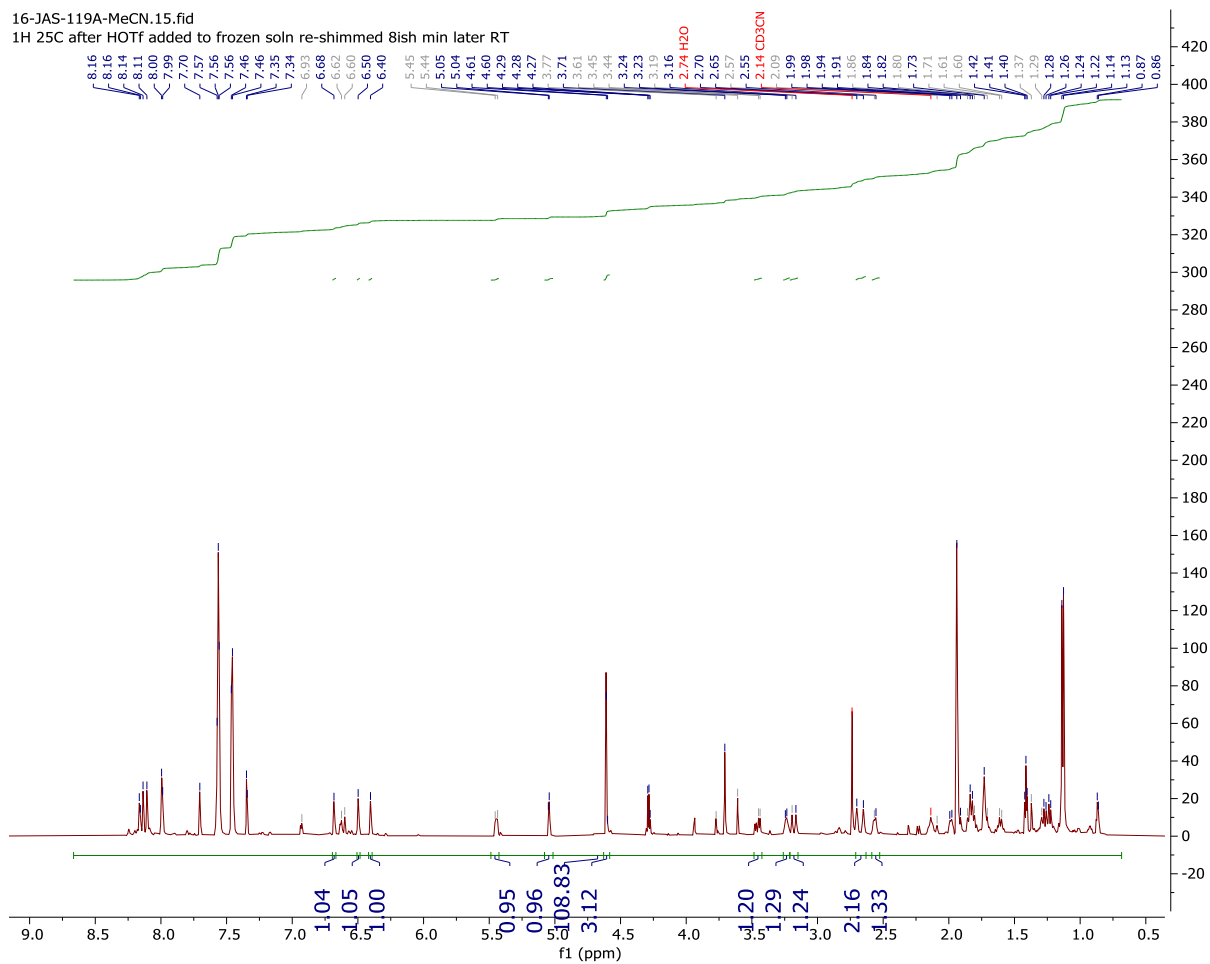
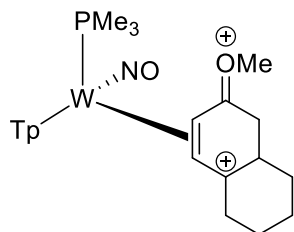
# <sup>1</sup>H NMR Spectra of 55



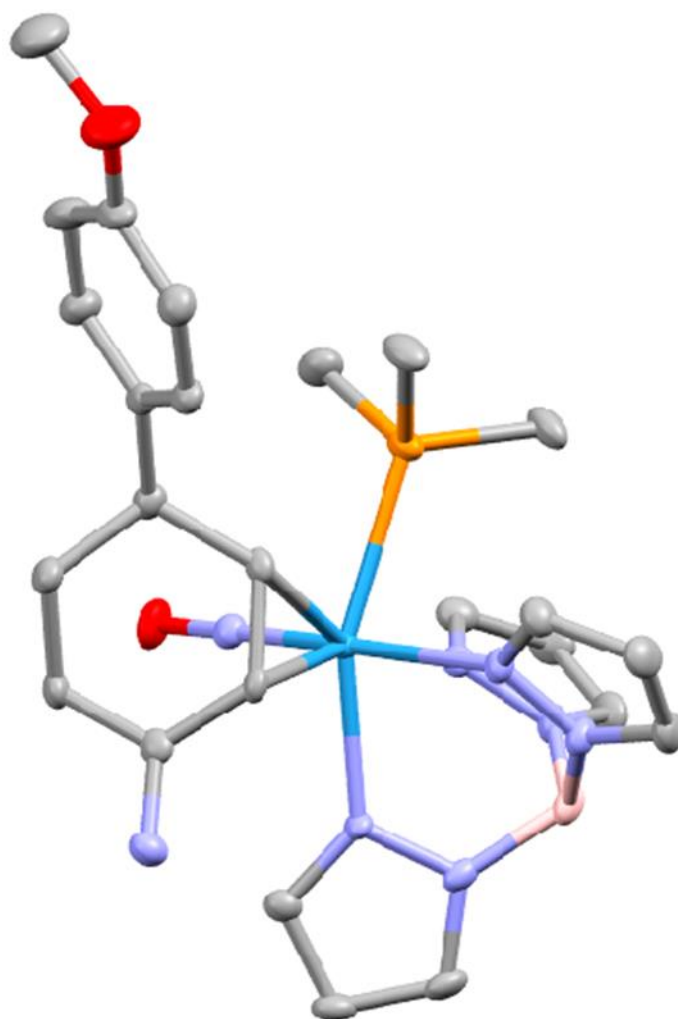
16-JAS-119A-MeCN.1.fid  
1H OC DPHAT acid



# <sup>1</sup>H NMR Spectra of 56



## Supporting Crystallographic Data for Chapter 7



Crystal Structure Report for [Harma\\_15JAS211](#)

A colorless plate-like specimen of  $C_{27}H_{39}BF_3N_8O_6PSW$ , approximate dimensions 0.031 mm x 0.212 mm x 0.213 mm, was coated with Paratone oil and mounted on a MiTeGen MicroLoop. The X-ray intensity data were measured on a Bruker Kappa APEXII Duo system equipped with a fine-focus sealed tube (Mo  $K_{\alpha}$ ,  $\lambda = 0.71073 \text{ \AA}$ ) and a graphite monochromator.

The total exposure time was 3.87 hours. The frames were integrated with the Bruker SAINT software package<sup>29</sup> using a narrow-frame algorithm. The integration of the data using a monoclinic unit cell yielded a total of 71208 reflections to a maximum  $\theta$  angle of  $28.33^\circ$  ( $0.75 \text{ \AA}$  resolution), of which 8708 were independent (average redundancy 8.177, completeness = 99.9%,  $R_{int} = 7.74\%$ ,  $R_{sig} = 4.68\%$ ) and 6849 (78.65%) were greater than  $2\sigma(F^2)$ . The final cell constants of  $a = 7.9137(6) \text{ \AA}$ ,  $b = 20.0549(15) \text{ \AA}$ ,  $c = 22.0340(16) \text{ \AA}$ ,  $\beta = 93.262(2)^\circ$ , volume =  $3491.3(5) \text{ \AA}^3$ , are based upon the refinement of the XYZ-centroids of 9847 reflections above  $20 \sigma(I)$  with  $4.464^\circ < 2\theta < 55.38^\circ$ . Data were corrected for absorption effects using the Multi-Scan method (SADABS).<sup>1</sup> The ratio of minimum to maximum apparent transmission was 0.813. The calculated minimum and maximum transmission coefficients (based on crystal size) are 0.5240 and 0.9000.

The structure was solved and refined using the Bruker SHELXTL Software Package<sup>30</sup> within APEX3<sup>1</sup> and OLEX2,<sup>31</sup> using the space group  $P 2_1/c$ , with  $Z = 4$  for the formula unit,  $C_{27}H_{39}BF_3N_8O_6PSW$ . Non-hydrogen atoms were refined anisotropically. The NH and two CH (C10 and C11) hydrogen atoms were located in the diffraction map and refined isotropically. The OH and BH hydrogen atoms were located in the diffraction map and refined isotropically with  $U_{iso} = 1.5U_{equiv}$  of the parent atoms, with a restraint was used on the O-H bond length. All other hydrogen atoms were placed in geometrically calculated positions with  $U_{iso} = 1.2U_{equiv}$  of the parent atom ( $U_{iso} = 1.5U_{equiv}$  for methyl). The final anisotropic full-matrix least-squares refinement on  $F^2$  with 460 variables converged at  $R1 = 3.37\%$ , for the observed data and  $wR2 = 6.94\%$  for all data. The goodness-of-fit was 1.022. The largest peak in the final difference electron density synthesis was  $1.472 \text{ e}^-/\text{\AA}^3$  and the largest hole was  $-1.036 \text{ e}^-/\text{\AA}^3$  with an RMS deviation of  $0.133 \text{ e}^-/\text{\AA}^3$ . On the basis of the final model, the calculated density was  $1.686 \text{ g/cm}^3$  and  $F(000)$ , 1768  $e^-$ .

**Table 1. Sample and crystal data for Harma\_15JAS211.**

|                     |                             |
|---------------------|-----------------------------|
| Identification code | Harma_15JAS211              |
| Chemical formula    | $C_{27}H_{39}BF_3N_8O_6PSW$ |
| Formula weight      | 886.35 g/mol                |
| Temperature         | 100(2) K                    |
| Wavelength          | 0.71073 $\text{\AA}$        |
| Crystal size        | 0.031 x 0.212 x 0.213 mm    |

<sup>29</sup> Bruker (2012). *Saint*; *SADABS*; *APEX3*. Bruker AXS Inc., Madison, Wisconsin, USA.

<sup>30</sup> Sheldrick, G. M. (2015). *Acta Cryst. A* **71**, 3-8.

<sup>31</sup> Dolomanov, O. V.; Bourhis, L. J.; Gildea, R. J.; Howard, J. A. K.; Puschmann, H. *J. Appl. Cryst.* (2009). **42**, 339-341.



|                               |                          |                |
|-------------------------------|--------------------------|----------------|
| <b>Crystal habit</b>          | colorless plate          |                |
| <b>Crystal system</b>         | monoclinic               |                |
| <b>Space group</b>            | P 2 <sub>1</sub> /c      |                |
| <b>Unit cell dimensions</b>   | a = 7.9137(6) Å          | α = 90°        |
|                               | b = 20.0549(15) Å        | β = 93.262(2)° |
|                               | c = 22.0340(16) Å        | γ = 90°        |
| <b>Volume</b>                 | 3491.3(5) Å <sup>3</sup> |                |
| <b>Z</b>                      | 4                        |                |
| <b>Density (calculated)</b>   | 1.686 g/cm <sup>3</sup>  |                |
| <b>Absorption coefficient</b> | 3.482 mm <sup>-1</sup>   |                |
| <b>F(000)</b>                 | 1768                     |                |

**Table 2. Data collection and structure refinement for Harma\_15JAS211.**

|  |  |
|--|--|
| <b>Diffractometer</b>                      | Bruker Kappa APEXII Duo                                    |
| <b>Radiation source</b>                    | fine-focus sealed tube (Mo K <sub>α</sub> , λ = 0.71073 Å) |
| <b>Theta range for data collection</b>     | 1.37 to 28.33°   |
| <b>Index ranges</b>                        | -10 ≤ h ≤ 10, -26 ≤ k ≤ 26, -29 ≤ l ≤ 29                   |
| <b>Reflections collected</b>               | 71208  |
| <b>Independent reflections</b>             | 8708 [R(int) = 0.0774]                                     |
| <b>Coverage of independent reflections</b> | 99.9%  |
| <b>Absorption correction</b>               | Multi-Scan   |
| <b>Max. and min. transmission</b>          | 0.9000 and 0.5240  |
| <b>Structure solution technique</b>        | direct methods   |
| <b>Structure solution program</b>          | SHELXT 2014/5 (Sheldrick, 2014)                            |

|  |   |                              |
|--|---|------------------------------|
| <b>Refinement method</b>                   | Full-matrix least-squares on $F^2$  |                              |
| <b>Refinement program</b>                  | SHELXL-2018/3 (Sheldrick, 2018)   |                              |
| <b>Function minimized</b>                  | $\Sigma w(F_o^2 - F_c^2)^2$   |                              |
| <b>Data / restraints / parameters</b>      | 8708 / 1 / 460  |                              |
| <b>Goodness-of-fit on <math>F^2</math></b> | 1.022   |                              |
| <b><math>\Delta/\sigma_{\max}</math></b>   | 0.002   |                              |
| <b>Final R indices</b>                     | 6849 data;<br>$I > 2\sigma(I)$  | R1 = 0.0337, wR2 =<br>0.0634 |
|  | all data  | R1 = 0.0541, wR2 =<br>0.0694 |
| <b>Weighting scheme</b>                    | $w = 1/[\sigma^2(F_o^2) + (0.0219P)^2 + 9.2022P]$<br>where $P = (F_o^2 + 2F_c^2)/3$ |                              |
| <b>Largest diff. peak and hole</b>         | 1.472 and -1.036 $e\text{\AA}^{-3}$   |                              |
| <b>R.M.S. deviation from mean</b>          | 0.133 $e\text{\AA}^{-3}$  |                              |

**Table 3. Atomic coordinates and equivalent isotropic atomic displacement parameters ( $\text{\AA}^2$ ) for Harma\_15JAS211.**

U(eq) is defined as one third of the trace of the orthogonalized  $U_{ij}$  tensor.

|    | x/a         | y/b         | z/c         | U(eq)      |
|----|-------------|-------------|-------------|------------|
| W1 | 0.58480(2)  | 0.20466(2)  | 0.36785(2)  | 0.01244(4) |
| S1 | 0.98813(14) | 0.30197(6)  | 0.12558(5)  | 0.0288(2)  |
| P1 | 0.48308(13) | 0.23449(5)  | 0.47107(5)  | 0.0185(2)  |
| F1 | 0.0479(4)   | 0.3815(2)   | 0.21850(15) | 0.0667(11) |
| F2 | 0.2678(3)   | 0.35602(15) | 0.17200(14) | 0.0418(7)  |
| F3 | 0.0849(4)   | 0.42556(15) | 0.13338(16) | 0.0551(9)  |

|     | <b>x/a</b> | <b>y/b</b>  | <b>z/c</b>  | <b>U(eq)</b> |
|-----|------------|-------------|-------------|--------------|
| O1  | 0.9066(4)  | 0.28258(14) | 0.38456(15) | 0.0271(7)    |
| O2  | 0.9735(4)  | 0.54098(17) | 0.42939(16) | 0.0410(9)    |
| O3  | 0.8171(4)  | 0.32613(17) | 0.12146(13) | 0.0290(7)    |
| O4  | 0.0161(5)  | 0.24606(19) | 0.16573(19) | 0.0517(10)   |
| O5  | 0.0656(4)  | 0.2972(2)   | 0.06878(16) | 0.0462(9)    |
| O6  | 0.3230(4)  | 0.17025(18) | 0.15132(16) | 0.0386(8)    |
| N1  | 0.3578(4)  | 0.13716(16) | 0.35956(15) | 0.0174(7)    |
| N2  | 0.3796(4)  | 0.06984(16) | 0.35424(16) | 0.0186(7)    |
| N3  | 0.7019(4)  | 0.12382(15) | 0.42261(14) | 0.0155(7)    |
| N4  | 0.6592(4)  | 0.05861(16) | 0.41201(16) | 0.0189(7)    |
| N5  | 0.6822(4)  | 0.13866(15) | 0.29858(14) | 0.0138(6)    |
| N6  | 0.6502(4)  | 0.07125(16) | 0.30004(15) | 0.0171(7)    |
| N7  | 0.7730(4)  | 0.25240(16) | 0.37734(15) | 0.0172(7)    |
| N8  | 0.5743(5)  | 0.26291(19) | 0.19281(16) | 0.0216(8)    |
| C1  | 0.1890(5)  | 0.1466(2)   | 0.36152(19) | 0.0210(9)    |
| C2  | 0.1039(5)  | 0.0862(2)   | 0.35722(19) | 0.0244(9)    |
| C3  | 0.2284(5)  | 0.0388(2)   | 0.35295(19) | 0.0228(9)    |
| C4  | 0.8135(5)  | 0.1242(2)   | 0.47040(18) | 0.0218(9)    |
| C5  | 0.8400(5)  | 0.0601(2)   | 0.4926(2)   | 0.0269(10)   |
| C6  | 0.7416(5)  | 0.0202(2)   | 0.4542(2)   | 0.0255(9)    |
| C7  | 0.7865(5)  | 0.1484(2)   | 0.25397(17) | 0.0181(8)    |
| C8  | 0.8218(5)  | 0.0888(2)   | 0.22521(19) | 0.0228(9)    |
| C9  | 0.7347(5)  | 0.0416(2)   | 0.25555(19) | 0.0216(9)    |
| C10 | 0.4208(5)  | 0.2917(2)   | 0.34564(17) | 0.0159(7)    |

|     | x/a       | y/b         | z/c         | U(eq)      |
|-----|-----------|-------------|-------------|------------|
| C11 | 0.4546(5) | 0.25887(18) | 0.28882(18) | 0.0139(7)  |
| C12 | 0.5670(5) | 0.28605(19) | 0.24791(18) | 0.0175(8)  |
| C13 | 0.6696(5) | 0.34634(19) | 0.26622(19) | 0.0196(8)  |
| C14 | 0.5552(5) | 0.39383(19) | 0.29869(19) | 0.0203(8)  |
| C15 | 0.4854(5) | 0.36382(19) | 0.35664(18) | 0.0181(8)  |
| C16 | 0.3486(5) | 0.41034(19) | 0.37802(17) | 0.0176(8)  |
| C17 | 0.1792(5) | 0.4037(2)   | 0.35808(19) | 0.0206(9)  |
| C18 | 0.0571(5) | 0.4475(2)   | 0.3762(2)   | 0.0248(9)  |
| C19 | 0.1039(6) | 0.5006(2)   | 0.4142(2)   | 0.0253(9)  |
| C20 | 0.2715(6) | 0.5092(2)   | 0.4340(2)   | 0.0290(10) |
| C21 | 0.3928(6) | 0.4642(2)   | 0.41559(19) | 0.0252(9)  |
| C22 | 0.0169(7) | 0.6004(3)   | 0.4626(3)   | 0.0485(15) |
| C23 | 0.6316(6) | 0.2867(2)   | 0.5157(2)   | 0.0301(10) |
| C24 | 0.2873(6) | 0.2803(2)   | 0.4775(2)   | 0.0285(10) |
| C25 | 0.4459(6) | 0.1630(2)   | 0.5196(2)   | 0.0298(11) |
| C26 | 0.1027(6) | 0.3684(3)   | 0.1650(2)   | 0.0320(11) |
| C27 | 0.3164(7) | 0.1069(3)   | 0.1801(3)   | 0.0471(14) |
| B1  | 0.5573(6) | 0.0394(2)   | 0.3525(2)   | 0.0195(10) |

**Table 4. Bond lengths (Å) for Harma\_15JAS211.**

|       |            |        |          |
|-------|------------|--------|----------|
| W1-N7 | 1.773(3)   | W1-N5  | 2.193(3) |
| W1-N3 | 2.194(3)   | W1-C10 | 2.213(4) |
| W1-N1 | 2.249(3)   | W1-C11 | 2.252(4) |
| W1-P1 | 2.5271(10) | S1-O5  | 1.428(3) |

|         |          |         |           |
|---------|----------|---------|-----------|
| S1-O3   | 1.436(3) | S1-O4   | 1.438(4)  |
| S1-C26  | 1.806(5) | P1-C24  | 1.814(4)  |
| P1-C23  | 1.820(5) | P1-C25  | 1.822(4)  |
| F1-C26  | 1.305(5) | F2-C26  | 1.330(5)  |
| F3-C26  | 1.345(6) | O1-N7   | 1.221(4)  |
| O2-C19  | 1.368(5) | O2-C22  | 1.429(6)  |
| O6-C27  | 1.422(6) | O6-H6A  | 0.854(19) |
| N1-C1   | 1.352(5) | N1-N2   | 1.367(4)  |
| N2-C3   | 1.347(5) | N2-B1   | 1.535(5)  |
| N3-C4   | 1.336(5) | N3-N4   | 1.367(4)  |
| N4-C6   | 1.347(5) | N4-B1   | 1.549(6)  |
| N5-C7   | 1.334(5) | N5-N6   | 1.376(4)  |
| N6-C9   | 1.356(5) | N6-B1   | 1.543(6)  |
| N8-C12  | 1.304(5) | N8-H8A  | 0.89(5)   |
| N8-H8B  | 0.86(5)  | C1-C2   | 1.386(6)  |
| C1-H1   | 0.95     | C2-C3   | 1.377(6)  |
| C2-H2   | 0.95     | C3-H3   | 0.95      |
| C4-C5   | 1.385(6) | C4-H4   | 0.95      |
| C5-C6   | 1.374(6) | C5-H5   | 0.95      |
| C6-H6   | 0.95     | C7-C8   | 1.388(5)  |
| C7-H7   | 0.95     | C8-C9   | 1.368(6)  |
| C8-H8   | 0.95     | C9-H9   | 0.95      |
| C10-C11 | 1.453(5) | C10-C15 | 1.549(5)  |
| C10-H10 | 1.00(4)  | C11-C12 | 1.412(5)  |
| C11-H11 | 0.93(4)  | C12-C13 | 1.499(5)  |

|          |          |          |          |
|----------|----------|----------|----------|
| C13-C14  | 1.521(5) | C13-H13A | 0.99     |
| C13-H13B | 0.99     | C14-C15  | 1.542(5) |
| C14-H14A | 0.99     | C14-H14B | 0.99     |
| C15-C16  | 1.524(5) | C15-H15  | 1.0      |
| C16-C21  | 1.393(6) | C16-C17  | 1.393(6) |
| C17-C18  | 1.382(6) | C17-H17  | 0.95     |
| C18-C19  | 1.391(6) | C18-H18  | 0.95     |
| C19-C20  | 1.383(6) | C20-C21  | 1.395(6) |
| C20-H20  | 0.95     | C21-H21  | 0.95     |
| C22-H22A | 0.98     | C22-H22B | 0.98     |
| C22-H22C | 0.98     | C23-H23A | 0.98     |
| C23-H23B | 0.98     | C23-H23C | 0.98     |
| C24-H24A | 0.98     | C24-H24B | 0.98     |
| C24-H24C | 0.98     | C25-H25A | 0.98     |
| C25-H25B | 0.98     | C25-H25C | 0.98     |
| C27-H27A | 0.98     | C27-H27B | 0.98     |
| C27-H27C | 0.98     | B1-H1A   | 1.10(5)  |

**Table 5. Bond angles (°) for Harma\_15JAS211.**

|           |            |           |            |
|-----------|------------|-----------|------------|
| N7-W1-N5  | 94.70(13)  | N7-W1-N3  | 90.50(13)  |
| N5-W1-N3  | 77.45(11)  | N7-W1-C10 | 94.50(14)  |
| N5-W1-C10 | 123.16(13) | N3-W1-C10 | 158.15(13) |
| N7-W1-N1  | 175.31(13) | N5-W1-N1  | 83.73(12)  |
| N3-W1-N1  | 84.85(12)  | C10-W1-N1 | 90.05(13)  |
| N7-W1-C11 | 100.08(14) | N5-W1-C11 | 85.22(13)  |

|            |            |            |            |
|------------|------------|------------|------------|
| N3-W1-C11  | 160.40(13) | C10-W1-C11 | 37.96(13)  |
| N1-W1-C11  | 84.22(12)  | N7-W1-P1   | 94.27(11)  |
| N5-W1-P1   | 155.74(8)  | N3-W1-P1   | 79.99(8)   |
| C10-W1-P1  | 78.43(10)  | N1-W1-P1   | 85.51(9)   |
| C11-W1-P1  | 115.24(10) | O5-S1-O3   | 114.7(2)   |
| O5-S1-O4   | 115.4(2)   | O3-S1-O4   | 114.4(2)   |
| O5-S1-C26  | 104.0(2)   | O3-S1-C26  | 103.1(2)   |
| O4-S1-C26  | 102.9(2)   | C24-P1-C23 | 101.2(2)   |
| C24-P1-C25 | 100.7(2)   | C23-P1-C25 | 104.8(2)   |
| C24-P1-W1  | 120.53(15) | C23-P1-W1  | 113.19(16) |
| C25-P1-W1  | 114.32(15) | C19-O2-C22 | 117.1(4)   |
| C27-O6-H6A | 118.(4)    | C1-N1-N2   | 105.7(3)   |
| C1-N1-W1   | 134.4(3)   | N2-N1-W1   | 119.8(2)   |
| C3-N2-N1   | 110.0(3)   | C3-N2-B1   | 129.0(3)   |
| N1-N2-B1   | 121.0(3)   | C4-N3-N4   | 106.6(3)   |
| C4-N3-W1   | 132.0(3)   | N4-N3-W1   | 121.4(2)   |
| C6-N4-N3   | 108.9(3)   | C6-N4-B1   | 130.6(4)   |
| N3-N4-B1   | 119.6(3)   | C7-N5-N6   | 106.4(3)   |
| C7-N5-W1   | 133.0(3)   | N6-N5-W1   | 120.3(2)   |
| C9-N6-N5   | 108.4(3)   | C9-N6-B1   | 129.5(3)   |
| N5-N6-B1   | 121.3(3)   | O1-N7-W1   | 177.0(3)   |
| C12-N8-H8A | 115.(3)    | C12-N8-H8B | 117.(3)    |
| H8A-N8-H8B | 127.(4)    | N1-C1-C2   | 110.7(4)   |
| N1-C1-H1   | 124.7      | C2-C1-H1   | 124.7      |
| C3-C2-C1   | 105.1(3)   | C3-C2-H2   | 127.4      |

|               |          |              |          |
|---------------|----------|--------------|----------|
| C1-C2-H2      | 127.4    | N2-C3-C2     | 108.5(4) |
| N2-C3-H3      | 125.7    | C2-C3-H3     | 125.7    |
| N3-C4-C5      | 110.7(4) | N3-C4-H4     | 124.6    |
| C5-C4-H4      | 124.6    | C6-C5-C4     | 104.7(4) |
| C6-C5-H5      | 127.7    | C4-C5-H5     | 127.7    |
| N4-C6-C5      | 109.1(4) | N4-C6-H6     | 125.5    |
| C5-C6-H6      | 125.5    | N5-C7-C8     | 111.1(4) |
| N5-C7-H7      | 124.4    | C8-C7-H7     | 124.4    |
| C9-C8-C7      | 104.6(4) | C9-C8-H8     | 127.7    |
| C7-C8-H8      | 127.7    | N6-C9-C8     | 109.4(4) |
| N6-C9-H9      | 125.3    | C8-C9-H9     | 125.3    |
| C11-C10-C15   | 118.9(3) | C11-C10-W1   | 72.5(2)  |
| C15-C10-W1    | 121.2(2) | C11-C10-H10  | 111.(3)  |
| C15-C10-H10   | 115.(3)  | W1-C10-H10   | 112.(3)  |
| C12-C11-C10   | 121.9(3) | C12-C11-W1   | 113.8(3) |
| C10-C11-W1    | 69.6(2)  | C12-C11-H11  | 113.(2)  |
| C10-C11-H11   | 120.(2)  | W1-C11-H11   | 108.(2)  |
| N8-C12-C11    | 121.3(4) | N8-C12-C13   | 119.1(4) |
| C11-C12-C13   | 119.4(3) | C12-C13-C14  | 107.7(3) |
| C12-C13-H13A  | 110.2    | C14-C13-H13A | 110.2    |
| C12-C13-H13B  | 110.2    | C14-C13-H13B | 110.2    |
| H13A-C13-H13B | 108.5    | C13-C14-C15  | 113.3(3) |
| C13-C14-H14A  | 108.9    | C15-C14-H14A | 108.9    |
| C13-C14-H14B  | 108.9    | C15-C14-H14B | 108.9    |
| H14A-C14-H14B | 107.7    | C16-C15-C14  | 108.1(3) |



|               |          |               |          |
|---------------|----------|---------------|----------|
| C16-C15-C10   | 112.7(3) | C14-C15-C10   | 111.4(3) |
| C16-C15-H15   | 108.2    | C14-C15-H15   | 108.2    |
| C10-C15-H15   | 108.2    | C21-C16-C17   | 117.7(4) |
| C21-C16-C15   | 120.0(4) | C17-C16-C15   | 122.2(4) |
| C18-C17-C16   | 121.7(4) | C18-C17-H17   | 119.2    |
| C16-C17-H17   | 119.2    | C17-C18-C19   | 119.6(4) |
| C17-C18-H18   | 120.2    | C19-C18-H18   | 120.2    |
| O2-C19-C20    | 124.9(4) | O2-C19-C18    | 114.9(4) |
| C20-C19-C18   | 120.2(4) | C19-C20-C21   | 119.4(4) |
| C19-C20-H20   | 120.3    | C21-C20-H20   | 120.3    |
| C16-C21-C20   | 121.4(4) | C16-C21-H21   | 119.3    |
| C20-C21-H21   | 119.3    | O2-C22-H22A   | 109.5    |
| O2-C22-H22B   | 109.5    | H22A-C22-H22B | 109.5    |
| O2-C22-H22C   | 109.5    | H22A-C22-H22C | 109.5    |
| H22B-C22-H22C | 109.5    | P1-C23-H23A   | 109.5    |
| P1-C23-H23B   | 109.5    | H23A-C23-H23B | 109.5    |
| P1-C23-H23C   | 109.5    | H23A-C23-H23C | 109.5    |
| H23B-C23-H23C | 109.5    | P1-C24-H24A   | 109.5    |
| P1-C24-H24B   | 109.5    | H24A-C24-H24B | 109.5    |
| P1-C24-H24C   | 109.5    | H24A-C24-H24C | 109.5    |
| H24B-C24-H24C | 109.5    | P1-C25-H25A   | 109.5    |
| P1-C25-H25B   | 109.5    | H25A-C25-H25B | 109.5    |
| P1-C25-H25C   | 109.5    | H25A-C25-H25C | 109.5    |
| H25B-C25-H25C | 109.5    | F1-C26-F2     | 107.9(4) |
| F1-C26-F3     | 105.5(4) | F2-C26-F3     | 107.0(4) |

|               |          |               |          |
|---------------|----------|---------------|----------|
| F1-C26-S1     | 113.6(3) | F2-C26-S1     | 112.4(3) |
| F3-C26-S1     | 110.1(3) | O6-C27-H27A   | 109.5    |
| O6-C27-H27B   | 109.5    | H27A-C27-H27B | 109.5    |
| O6-C27-H27C   | 109.5    | H27A-C27-H27C | 109.5    |
| H27B-C27-H27C | 109.5    | N2-B1-N6      | 109.3(3) |
| N2-B1-N4      | 108.3(3) | N6-B1-N4      | 106.5(3) |
| N2-B1-H1A     | 112.(2)  | N6-B1-H1A     | 112.(2)  |
| N4-B1-H1A     | 109.(2)  |               |          |

**Table 6. Torsion angles (°) for Harma\_15JAS211.**

|             |           |             |           |
|-------------|-----------|-------------|-----------|
| C1-N1-N2-C3 | 0.0(4)    | W1-N1-N2-C3 | 176.9(3)  |
| C1-N1-N2-B1 | -178.2(4) | W1-N1-N2-B1 | -1.3(5)   |
| C4-N3-N4-C6 | 1.6(4)    | W1-N3-N4-C6 | -176.3(3) |
| C4-N3-N4-B1 | -168.8(3) | W1-N3-N4-B1 | 13.4(4)   |
| C7-N5-N6-C9 | -0.7(4)   | W1-N5-N6-C9 | -175.3(2) |
| C7-N5-N6-B1 | 170.0(3)  | W1-N5-N6-B1 | -4.6(4)   |
| N2-N1-C1-C2 | -0.3(5)   | W1-N1-C1-C2 | -176.6(3) |
| N1-C1-C2-C3 | 0.4(5)    | N1-N2-C3-C2 | 0.3(5)    |
| B1-N2-C3-C2 | 178.3(4)  | C1-C2-C3-N2 | -0.4(5)   |
| N4-N3-C4-C5 | -2.2(4)   | W1-N3-C4-C5 | 175.4(3)  |
| N3-C4-C5-C6 | 1.9(5)    | N3-N4-C6-C5 | -0.4(5)   |
| B1-N4-C6-C5 | 168.5(4)  | C4-C5-C6-N4 | -0.9(5)   |
| N6-N5-C7-C8 | 1.0(4)    | W1-N5-C7-C8 | 174.6(3)  |
| N5-C7-C8-C9 | -0.9(5)   | N5-N6-C9-C8 | 0.2(4)    |
| B1-N6-C9-C8 | -169.6(4) | C7-C8-C9-N6 | 0.4(5)    |

|                 |           |                 |           |
|-----------------|-----------|-----------------|-----------|
| C15-C10-C11-C12 | 10.5(5)   | W1-C10-C11-C12  | -105.9(3) |
| C15-C10-C11-W1  | 116.4(3)  | C10-C11-C12-N8  | -167.8(4) |
| W1-C11-C12-N8   | 112.2(4)  | C10-C11-C12-C13 | 7.0(5)    |
| W1-C11-C12-C13  | -72.9(4)  | N8-C12-C13-C14  | 133.4(4)  |
| C11-C12-C13-C14 | -41.5(5)  | C12-C13-C14-C15 | 60.9(4)   |
| C13-C14-C15-C16 | -169.5(3) | C13-C14-C15-C10 | -45.2(4)  |
| C11-C10-C15-C16 | 130.7(4)  | W1-C10-C15-C16  | -143.3(3) |
| C11-C10-C15-C14 | 8.9(5)    | W1-C10-C15-C14  | 95.0(3)   |
| C14-C15-C16-C21 | -86.2(4)  | C10-C15-C16-C21 | 150.2(4)  |
| C14-C15-C16-C17 | 89.6(4)   | C10-C15-C16-C17 | -34.1(5)  |
| C21-C16-C17-C18 | -2.0(6)   | C15-C16-C17-C18 | -177.8(4) |
| C16-C17-C18-C19 | 1.5(6)    | C22-O2-C19-C20  | 7.2(7)    |
| C22-O2-C19-C18  | -173.1(4) | C17-C18-C19-O2  | 179.9(4)  |
| C17-C18-C19-C20 | -0.4(7)   | O2-C19-C20-C21  | 179.5(4)  |
| C18-C19-C20-C21 | -0.2(7)   | C17-C16-C21-C20 | 1.5(6)    |
| C15-C16-C21-C20 | 177.4(4)  | C19-C20-C21-C16 | -0.4(7)   |
| O5-S1-C26-F1    | 178.9(4)  | O3-S1-C26-F1    | 58.9(4)   |
| O4-S1-C26-F1    | -60.4(4)  | O5-S1-C26-F2    | -58.3(4)  |
| O3-S1-C26-F2    | -178.3(3) | O4-S1-C26-F2    | 62.4(4)   |
| O5-S1-C26-F3    | 60.8(4)   | O3-S1-C26-F3    | -59.2(4)  |
| O4-S1-C26-F3    | -178.5(3) | C3-N2-B1-N6     | 125.7(4)  |
| N1-N2-B1-N6     | -56.5(5)  | C3-N2-B1-N4     | -118.7(4) |
| N1-N2-B1-N4     | 59.1(5)   | C9-N6-B1-N2     | -130.5(4) |
| N5-N6-B1-N2     | 60.9(4)   | C9-N6-B1-N4     | 112.7(4)  |
| N5-N6-B1-N4     | -55.8(4)  | C6-N4-B1-N2     | 125.1(4)  |

N3-N4-B1-N2      -67.0(4)    C6-N4-B1-N6      -117.5(4)  
 N3-N4-B1-N6      50.4(4)

**Table 7. Anisotropic atomic displacement parameters (Å<sup>2</sup>) for Harma\_15JAS211.**

The anisotropic atomic displacement factor exponent takes the form: -  
 $2\pi^2 [ h^2 a^{*2} U_{11} + \dots + 2 h k a^* b^* U_{12} ]$

|    | <b>U<sub>11</sub></b> | <b>U<sub>22</sub></b> | <b>U<sub>33</sub></b> | <b>U<sub>23</sub></b> | <b>U<sub>13</sub></b> | <b>U<sub>12</sub></b> |
|----|-----------------------|-----------------------|-----------------------|-----------------------|-----------------------|-----------------------|
| W1 | 0.01029(7)            | 0.01180(7)            | 0.01527(7)            | 0.00009(7)            | 0.00112(5)            | 0.00099(7)            |
| S1 | 0.0205(5)             | 0.0337(6)             | 0.0322(6)             | -0.0040(5)            | 0.0023(4)             | -0.0016(5)            |
| P1 | 0.0210(5)             | 0.0184(5)             | 0.0168(5)             | 0.0023(4)             | 0.0053(4)             | 0.0064(4)             |
| F1 | 0.051(2)              | 0.107(3)              | 0.0430(19)            | -0.038(2)             | 0.0086(16)            | -0.022(2)             |
| F2 | 0.0197(13)            | 0.0467(18)            | 0.0577(19)            | 0.0001(15)            | 0.0081(13)            | 0.0019(12)            |
| F3 | 0.0460(19)            | 0.0378(18)            | 0.080(2)              | 0.0134(17)            | 0.0125(17)            | 0.0061(15)            |
| O1 | 0.0177(14)            | 0.0213(16)            | 0.0415(19)            | 0.0006(13)            | 0.0039(13)            | 0.0073(12)            |
| O2 | 0.038(2)              | 0.0343(19)            | 0.051(2)              | 0.0094(17)            | 0.0051(17)            | 0.0141(16)            |
| O3 | 0.0204(15)            | 0.0436(19)            | 0.0230(16)            | 0.0041(14)            | 0.0025(13)            | 0.0027(14)            |
| O4 | 0.035(2)              | 0.045(2)              | 0.075(3)              | 0.019(2)              | -0.001(2)             | 0.0025(18)            |
| O5 | 0.0327(18)            | 0.070(3)              | 0.037(2)              | -0.009(2)             | 0.0091(16)            | 0.0057(19)            |
| O6 | 0.038(2)              | 0.036(2)              | 0.040(2)              | 0.0019(17)            | 0.0063(17)            | 0.0012(16)            |
| N1 | 0.0150(16)            | 0.0142(16)            | 0.0232(18)            | 0.0017(13)            | 0.0015(14)            | 0.0005(13)            |

|     | <b>U<sub>11</sub></b> | <b>U<sub>22</sub></b> | <b>U<sub>33</sub></b> | <b>U<sub>23</sub></b> | <b>U<sub>13</sub></b> | <b>U<sub>12</sub></b> |
|-----|-----------------------|-----------------------|-----------------------|-----------------------|-----------------------|-----------------------|
| N2  | 0.0139(16)            | 0.0145(16)            | 0.0272(19)            | 0.0005(14)            | 0.0003(14)            | 0.0014(13)            |
| N3  | 0.0134(15)            | 0.0145(16)            | 0.0187(17)            | 0.0028(13)            | 0.0010(13)            | 0.0050(13)            |
| N4  | 0.0160(16)            | 0.0150(16)            | 0.0254(19)            | 0.0029(14)            | 0.0005(14)            | 0.0002(13)            |
| N5  | 0.0145(15)            | 0.0099(14)            | 0.0174(16)            | 0.0000(12)            | 0.0033(13)            | 0.0024(12)            |
| N6  | 0.0125(15)            | 0.0144(16)            | 0.0239(18)            | 0.0053(13)            | 0.0028(13)            | 0.0012(13)            |
| N7  | 0.0161(16)            | 0.0149(16)            | 0.0205(17)            | 0.0007(13)            | 0.0003(13)            | 0.0020(13)            |
| N8  | 0.0196(18)            | 0.026(2)              | 0.0197(19)            | 0.0004(16)            | 0.0031(15)            | 0.0015(16)            |
| C1  | 0.0136(18)            | 0.023(2)              | 0.026(2)              | 0.0024(18)            | 0.0022(16)            | 0.0016(16)            |
| C2  | 0.0127(19)            | 0.029(2)              | 0.031(3)              | 0.0006(19)            | 0.0021(17)            | 0.0050(17)            |
| C3  | 0.019(2)              | 0.022(2)              | 0.028(2)              | 0.0009(18)            | 0.0025(17)            | 0.0070(17)            |
| C4  | 0.0150(19)            | 0.028(2)              | 0.022(2)              | 0.0022(18)            | 0.0003(16)            | 0.0048(17)            |
| C5  | 0.027(2)              | 0.031(2)              | 0.022(2)              | 0.0054(19)            | 0.0034(18)            | 0.0111(19)            |
| C6  | 0.027(2)              | 0.021(2)              | 0.028(2)              | 0.0090(18)            | 0.0022(19)            | 0.0067(18)            |
| C7  | 0.0158(18)            | 0.022(2)              | 0.017(2)              | 0.0015(16)            | 0.0003(15)            | 0.0016(16)            |
| C8  | 0.020(2)              | 0.028(2)              | 0.020(2)              | 0.0085(18)            | 0.0015(17)            | 0.0055(18)            |
| C9  | 0.019(2)              | 0.020(2)              | 0.025(2)              | 0.0114(17)            | 0.0026(17)            | 0.0028(16)            |
| C10 | 0.0134(17)            | 0.0152(18)            | 0.0191(19)            | 0.0053(16)            | 0.0011(14)            | 0.0036(16)            |

|     | <b>U<sub>11</sub></b> | <b>U<sub>22</sub></b> | <b>U<sub>33</sub></b> | <b>U<sub>23</sub></b> | <b>U<sub>13</sub></b> | <b>U<sub>12</sub></b> |
|-----|-----------------------|-----------------------|-----------------------|-----------------------|-----------------------|-----------------------|
| C11 | 0.0121(17)            | 0.0105(18)            | 0.0189(19)            | 0.0022(15)            | -                     | -                     |
|     |                       |                       |                       |                       | 0.0018(15)            | 0.0007(14)            |
| C12 | 0.0161(18)            | 0.016(2)              | 0.0200(19)            | 0.0037(16)            | 0.0007(15)            | 0.0051(15)            |
| C13 | 0.021(2)              | 0.0155(19)            | 0.023(2)              | 0.0039(16)            | 0.0056(17)            | -                     |
|     |                       |                       |                       |                       |                       | 0.0033(16)            |
| C14 | 0.022(2)              | 0.0132(18)            | 0.026(2)              | 0.0014(16)            | 0.0028(17)            | 0.0006(16)            |
| C15 | 0.0174(19)            | 0.0169(19)            | 0.020(2)              | 0.0002(16)            | -                     |                       |
|     |                       |                       |                       |                       | 0.0024(16)            | 0.0013(16)            |
| C16 | 0.022(2)              | 0.0145(18)            | 0.0159(19)            | 0.0028(15)            | 0.0012(16)            | 0.0026(16)            |
| C17 | 0.023(2)              | 0.015(2)              | 0.023(2)              | 0.0014(16)            | 0.0026(17)            | 0.0024(16)            |
| C18 | 0.023(2)              | 0.022(2)              | 0.030(2)              | 0.0036(18)            | 0.0013(18)            | 0.0023(17)            |
| C19 | 0.033(2)              | 0.018(2)              | 0.025(2)              | 0.0011(17)            | 0.0081(19)            | 0.0093(18)            |
| C20 | 0.039(3)              | 0.025(2)              | 0.023(2)              | -                     |                       |                       |
|     |                       |                       |                       | 0.0067(19)            | 0.001(2)              | 0.006(2)              |
| C21 | 0.027(2)              | 0.022(2)              | 0.026(2)              | -                     | -                     |                       |
|     |                       |                       |                       | 0.0044(18)            | 0.0002(18)            | 0.0033(18)            |
| C22 | 0.057(4)              | 0.032(3)              | 0.056(4)              | -0.012(3)             | 0.009(3)              | 0.012(3)              |
| C23 | 0.040(3)              | 0.028(2)              | 0.022(2)              | -                     | -                     |                       |
|     |                       |                       |                       | 0.0037(19)            | 0.0004(19)            | 0.001(2)              |
| C24 | 0.028(2)              | 0.030(3)              | 0.028(2)              | 0.0064(19)            | 0.0115(19)            | 0.0151(19)            |
| C25 | 0.032(2)              | 0.031(2)              | 0.028(2)              | 0.012(2)              | 0.015(2)              | 0.010(2)              |
| C26 | 0.021(2)              | 0.043(3)              | 0.032(3)              | 0.000(2)              | -                     |                       |
|     |                       |                       |                       |                       | 0.0011(19)            | -0.003(2)             |
| C27 | 0.048(3)              | 0.036(3)              | 0.055(4)              | 0.004(3)              | -0.018(3)             | -0.001(3)             |
| B1  | 0.013(2)              | 0.014(2)              | 0.030(3)              | -                     | -                     | -                     |
|     |                       |                       |                       | 0.0012(18)            | 0.0019(19)            | 0.0010(17)            |

**Table 8. Hydrogen atomic coordinates and isotropic atomic displacement parameters ( $\text{\AA}^2$ ) for Harma\_15JAS211.**

|      | x/a      | y/b      | z/c        | U(eq)     |
|------|----------|----------|------------|-----------|
| H6A  | 0.234(5) | 0.194(3) | 0.150(3)   | 0.058     |
| H8A  | 0.501(6) | 0.231(2) | 0.183(2)   | 0.027(13) |
| H8B  | 0.647(6) | 0.281(2) | 0.170(2)   | 0.023(13) |
| H1   | 0.1361   | 0.1888   | 0.3653     | 0.025     |
| H2   | -0.0148  | 0.0791   | 0.3572     | 0.029     |
| H3   | 0.2108   | -0.0079  | 0.3497     | 0.027     |
| H4   | 0.8674   | 0.1630   | 0.4869     | 0.026     |
| H5   | 0.9105   | 0.0468   | 0.5268     | 0.032     |
| H6   | 0.7331   | -0.0269  | 0.4570     | 0.031     |
| H7   | 0.8309   | 0.1905   | 0.2433     | 0.022     |
| H8   | 0.8911   | 0.0822   | 0.1919     | 0.027     |
| H9   | 0.7337   | -0.0048  | 0.2468     | 0.026     |
| H10  | 0.301(6) | 0.284(2) | 0.356(2)   | 0.025(12) |
| H11  | 0.375(5) | 0.230(2) | 0.2705(18) | 0.012(10) |
| H13A | 0.7126   | 0.3682   | 0.2299     | 0.024     |
| H13B | 0.7676   | 0.3333   | 0.2936     | 0.024     |
| H14A | 0.4589   | 0.4067   | 0.2704     | 0.024     |
| H14B | 0.6194   | 0.4348   | 0.3097     | 0.024     |
| H15  | 0.5796   | 0.3624   | 0.3889     | 0.022     |
| H17  | 0.1468   | 0.3682   | 0.3314     | 0.025     |
| H18  | -0.0581  | 0.4415   | 0.3628     | 0.03      |
| H20  | 0.3037   | 0.5455   | 0.4598     | 0.035     |

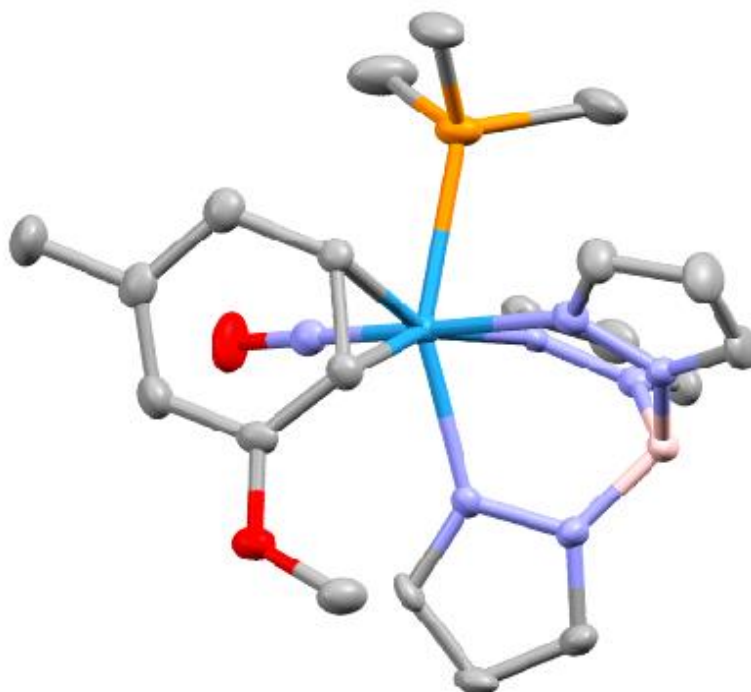
|      | x/a      | y/b       | z/c      | U(eq) |
|------|----------|-----------|----------|-------|
| H21  | 0.5080   | 0.4703    | 0.4290   | 0.03  |
| H22A | 0.0933   | 0.6275    | 0.4393   | 0.073 |
| H22B | 0.0733   | 0.5885    | 0.5018   | 0.073 |
| H22C | -0.0861  | 0.6258    | 0.4693   | 0.073 |
| H23A | 0.7410   | 0.2638    | 0.5209   | 0.045 |
| H23B | 0.5875   | 0.2951    | 0.5557   | 0.045 |
| H23C | 0.6463   | 0.3291    | 0.4947   | 0.045 |
| H24A | 0.2972   | 0.3243    | 0.4587   | 0.043 |
| H24B | 0.2650   | 0.2857    | 0.5206   | 0.043 |
| H24C | 0.1938   | 0.2557    | 0.4568   | 0.043 |
| H25A | 0.3680   | 0.1320    | 0.4980   | 0.045 |
| H25B | 0.3963   | 0.1782    | 0.5569   | 0.045 |
| H25C | 0.5535   | 0.1404    | 0.5299   | 0.045 |
| H27A | 0.2398   | 0.0775    | 0.1560   | 0.071 |
| H27B | 0.2750   | 0.1123    | 0.2209   | 0.071 |
| H27C | 0.4300   | 0.0873    | 0.1832   | 0.071 |
| H1A  | 0.553(5) | -0.015(2) | 0.349(2) | 0.029 |

**Table 9. Hydrogen bond distances (Å) and angles (°) for Harma\_15JAS211.**

|             | Donor-H   | Acceptor-H | Donor-Acceptor | Angle   |
|-------------|-----------|------------|----------------|---------|
| O6-H6A...O4 | 0.854(19) | 2.06(2)    | 2.898(5)       | 167.(6) |
| O6-H6A...O5 | 0.854(19) | 2.99(4)    | 3.677(5)       | 139.(5) |
| N8-H8A...O6 | 0.89(5)   | 1.96(5)    | 2.835(5)       | 170.(4) |



|             | Donor-H | Acceptor-H | Donor-Acceptor | Angle   |
|-------------|---------|------------|----------------|---------|
| N8-H8B...O3 | 0.86(5) | 1.99(5)    | 2.848(5)       | 177.(4) |



### Crystal Structure Report for [Harman\\_10JAS\\_137](#)

A **orange rod-like** specimen of  $C_{21}H_{30}BF_3N_7O_5PSW$ , approximate dimensions **0.046 mm** x **0.061 mm** x **0.244 mm**, was coated with Paratone oil and mounted on a MiTeGen MicroLoop. The X-ray intensity data were measured on a Bruker Kappa APEXII Duo system equipped with a graphite monochromator and a Mo  $K_{\alpha}$  fine-focus sealed tube ( $\lambda = 0.71073 \text{ \AA}$ ).

The total exposure time was 1.34 hours. The frames were integrated with the Bruker SAINT software package<sup>32</sup> using a narrow-frame algorithm. The integration of the data using an **orthorhombic** unit cell yielded a total of **29379** reflections to a maximum  $\theta$  angle of **27.91°** (**0.76 Å** resolution), of which **6959** were independent (average redundancy **4.222**, completeness = **100.0%**,  $R_{int} = 5.93\%$ ,  $R_{sig} = 5.48\%$ ) and **4912 (70.58%)** were greater than  $2\sigma(F^2)$ . The final cell constants of  $\underline{a} = 15.8379(7) \text{ \AA}$ ,  $\underline{b} = 15.8868(7) \text{ \AA}$ ,  $\underline{c} =$

<sup>32</sup> Bruker (2012). *Saint*; *SADABS*; *APEX3*. Bruker AXS Inc., Madison, Wisconsin, USA.

23.0994(12) Å, volume = 5812.1(5) Å<sup>3</sup>, are based upon the refinement of the XYZ-centroids of 4958 reflections above 20 σ(I) with 4.364° < 2θ < 54.07°. Data were corrected for absorption effects using the Multi-Scan method (SADABS).<sup>1</sup> The ratio of minimum to maximum apparent transmission was 0.769. The calculated minimum and maximum transmission coefficients (based on crystal size) are 0.4300 and 0.8310.

The structure was solved and refined using the Bruker SHELXTL Software Package<sup>33</sup> within APEX3<sup>1</sup> and OLEX2,<sup>34</sup> using the space group P b c a, with Z = 8 for the formula unit, C<sub>21</sub>H<sub>30</sub>BF<sub>3</sub>N<sub>7</sub>O<sub>5</sub>PSW. Non-hydrogen atoms were refined anisotropically. Hydrogen atoms were placed in geometrically calculated positions with  $U_{iso} = 1.2U_{equiv}$  of the parent atom ( $U_{iso} = 1.5 U_{equiv}$  for methyl), except for the B-H hydrogen atom, which was located in the diffraction map. The final anisotropic full-matrix least-squares refinement on F<sup>2</sup> with 369 variables converged at R1 = 3.30%, for the observed data and wR2 = 5.98% for all data. The goodness-of-fit was 0.996. The largest peak in the final difference electron density synthesis was 0.772 e<sup>-</sup>/Å<sup>3</sup> and the largest hole was -0.680 e<sup>-</sup>/Å<sup>3</sup> with an RMS deviation of 0.127 e<sup>-</sup>/Å<sup>3</sup>. On the basis of the final model, the calculated density was 1.772 g/cm<sup>3</sup> and F(000), 3056 e<sup>-</sup>.

**Table 1. Sample and crystal data for Harman\_10JAS\_137.**

|                             |   |         |
|-----------------------------|---|---------|
| <b>Identification code</b>  | Harman_10JAS_137  |         |
| <b>Chemical formula</b>     | C <sub>21</sub> H <sub>30</sub> BF <sub>3</sub> N <sub>7</sub> O <sub>5</sub> PSW |         |
| <b>Formula weight</b>       | 775.21 g/mol  |         |
| <b>Temperature</b>          | 150(2) K  |         |
| <b>Wavelength</b>           | 0.71073 Å   |         |
| <b>Crystal size</b>         | 0.046 x 0.061 x 0.244 mm  |         |
| <b>Crystal habit</b>        | orange rod  |         |
| <b>Crystal system</b>       | orthorhombic  |         |
| <b>Space group</b>          | P b c a   |         |
| <b>Unit cell dimensions</b> | a = 15.8379(7) Å  | α = 90° |
|                             | b = 15.8868(7) Å  | β = 90° |
|                             | c = 23.0994(12) Å   | γ = 90° |
| <b>Volume</b>               | 5812.1(5) Å <sup>3</sup>  |         |

<sup>33</sup> Sheldrick, G. M. (2015). *Acta Cryst.* **A71**, 3-8.

<sup>34</sup> Dolomanov, O. V.; Bourhis, L. J.; Gildea, R. J.; Howard, J. A. K.; Puschmann, H. *J. Appl. Cryst.* (2009). **42**, 339-341.

|                               |                         |
|-------------------------------|-------------------------|
| <b>Z</b>                      | 8                       |
| <b>Density (calculated)</b>   | 1.772 g/cm <sup>3</sup> |
| <b>Absorption coefficient</b> | 4.166 mm <sup>-1</sup>  |
| <b>F(000)</b>                 | 3056                    |

**Table 2. Data collection and structure refinement for Harman\_10JAS\_137.**

|  |   |                              |
|--|---|------------------------------|
| <b>Diffractometer</b>                      | Bruker Kappa APEXII Duo                     |                              |
| <b>Radiation source</b>                    | fine-focus sealed tube, Mo K <sub>α</sub>   |                              |
| <b>Theta range for data collection</b>     | 1.76 to 27.91°                              |                              |
| <b>Index ranges</b>                        | -20 ≤ h ≤ 20, -13 ≤ k ≤ 20, -30 ≤ l ≤ 30    |                              |
| <b>Reflections collected</b>               | 29379                                       |                              |
| <b>Independent reflections</b>             | 6959 [R(int) = 0.0593]                      |                              |
| <b>Coverage of independent reflections</b> | 100.0%                                      |                              |
| <b>Absorption correction</b>               | Multi-Scan                                  |                              |
| <b>Max. and min. transmission</b>          | 0.8310 and 0.4300                           |                              |
| <b>Structure solution technique</b>        | direct methods                              |                              |
| <b>Structure solution program</b>          | SHELXT 2014/5 (Sheldrick, 2014)             |                              |
| <b>Refinement method</b>                   | Full-matrix least-squares on F <sup>2</sup> |                              |
| <b>Refinement program</b>                  | SHELXL-2016/6 (Sheldrick, 2016)             |                              |
| <b>Function minimized</b>                  | $\sum w(F_o^2 - F_c^2)^2$                   |                              |
| <b>Data / restraints / parameters</b>      | 6959 / 0 / 369                              |                              |
| <b>Goodness-of-fit on F<sup>2</sup></b>    | 0.996                                       |                              |
| <b>Δ/σ<sub>max</sub></b>                   | 0.002                                       |                              |
| <b>Final R indices</b>                     | 4912 data;<br>I > 2σ(I)                     | R1 = 0.0330, wR2 =<br>0.0532 |

|                                    |   |                              |
|------------------------------------|---|------------------------------|
|                                    | all data  | R1 = 0.0639, wR2 =<br>0.0598 |
| <b>Weighting scheme</b>            | $w=1/[\sigma^2(F_o^2)+(0.0176P)^2+4.5596P]$<br>where $P=(F_o^2+2F_c^2)/3$ |                              |
| <b>Largest diff. peak and hole</b> | 0.772 and -0.680 eÅ <sup>-3</sup>   |                              |
| <b>R.M.S. deviation from mean</b>  | 0.127 eÅ <sup>-3</sup>  |                              |

**Table 3. Atomic coordinates and equivalent isotropic atomic displacement parameters (Å<sup>2</sup>) for Harman\_10JAS\_137.**

U(eq) is defined as one third of the trace of the orthogonalized U<sub>ij</sub> tensor.

|    | x/a         | y/b         | z/c         | U(eq)      |
|----|-------------|-------------|-------------|------------|
| W1 | 0.22393(2)  | 0.23335(2)  | 0.36872(2)  | 0.01558(5) |
| P1 | 0.23006(8)  | 0.13450(7)  | 0.28287(5)  | 0.0261(3)  |
| O1 | 0.35875(18) | 0.3491(2)   | 0.32494(15) | 0.0391(9)  |
| O2 | 0.32497(18) | 0.29994(17) | 0.51587(12) | 0.0266(7)  |
| N1 | 0.1211(2)   | 0.1473(2)   | 0.39830(15) | 0.0203(8)  |
| N2 | 0.0400(2)   | 0.1760(2)   | 0.40162(15) | 0.0202(8)  |
| N3 | 0.1296(2)   | 0.28906(19) | 0.31082(14) | 0.0186(8)  |
| N4 | 0.0457(2)   | 0.2901(2)   | 0.32580(15) | 0.0211(8)  |
| N5 | 0.1596(2)   | 0.3271(2)   | 0.42224(14) | 0.0179(7)  |
| N6 | 0.0734(2)   | 0.3260(2)   | 0.42725(14) | 0.0197(8)  |
| N7 | 0.3040(2)   | 0.3021(2)   | 0.34267(14) | 0.0208(8)  |
| C1 | 0.1170(3)   | 0.0653(3)   | 0.4125(2)   | 0.0298(11) |
| C2 | 0.0349(3)   | 0.0416(3)   | 0.4247(2)   | 0.0353(12) |
| C3 | 0.9887(3)   | 0.1132(3)   | 0.4167(2)   | 0.0303(11) |

|     | <b>x/a</b>  | <b>y/b</b>  | <b>z/c</b>  | <b>U(eq)</b> |
|-----|-------------|-------------|-------------|--------------|
| C4  | 0.1358(3)   | 0.3315(2)   | 0.26104(18) | 0.0233(10)   |
| C5  | 0.0570(3)   | 0.3599(3)   | 0.2435(2)   | 0.0308(11)   |
| C6  | 0.0026(3)   | 0.3333(3)   | 0.2853(2)   | 0.0300(11)   |
| C7  | 0.1860(3)   | 0.3964(2)   | 0.45026(18) | 0.0203(9)    |
| C8  | 0.1188(3)   | 0.4395(3)   | 0.47365(19) | 0.0265(10)   |
| C9  | 0.0488(3)   | 0.3938(3)   | 0.45805(19) | 0.0261(10)   |
| C10 | 0.3132(2)   | 0.1376(3)   | 0.40113(18) | 0.0207(9)    |
| C11 | 0.2873(3)   | 0.1866(2)   | 0.45169(17) | 0.0216(9)    |
| C12 | 0.3400(3)   | 0.2502(2)   | 0.47088(17) | 0.0214(10)   |
| C13 | 0.4227(3)   | 0.2666(3)   | 0.44515(19) | 0.0291(10)   |
| C14 | 0.4550(3)   | 0.2096(3)   | 0.40559(19) | 0.0269(10)   |
| C15 | 0.4049(3)   | 0.1405(3)   | 0.38416(19) | 0.0275(11)   |
| C16 | 0.5450(3)   | 0.2161(3)   | 0.3856(2)   | 0.0426(14)   |
| C17 | 0.2530(3)   | 0.2837(3)   | 0.55302(19) | 0.0304(11)   |
| C18 | 0.2716(3)   | 0.0285(2)   | 0.2899(2)   | 0.0366(12)   |
| C19 | 0.2902(3)   | 0.1744(3)   | 0.2224(2)   | 0.0485(15)   |
| C20 | 0.1250(3)   | 0.1116(3)   | 0.2551(2)   | 0.0408(13)   |
| B1  | 0.0196(3)   | 0.2687(3)   | 0.3880(2)   | 0.0233(10)   |
| S1  | 0.19936(7)  | 0.55614(7)  | 0.61676(5)  | 0.0276(3)    |
| F1  | 0.31386(17) | 0.48844(17) | 0.54948(12) | 0.0471(8)    |
| F2  | 0.34658(17) | 0.61050(18) | 0.57990(16) | 0.0623(10)   |
| F3  | 0.35350(18) | 0.50555(19) | 0.63762(14) | 0.0590(9)    |
| O3  | 0.16213(18) | 0.59392(17) | 0.56652(13) | 0.0283(7)    |
| O4  | 0.1709(2)   | 0.4720(2)   | 0.62875(15) | 0.0481(9)    |

|     | x/a       | y/b       | z/c         | U(eq)      |
|-----|-----------|-----------|-------------|------------|
| O5  | 0.2069(2) | 0.6109(2) | 0.66585(14) | 0.0468(10) |
| C21 | 0.3061(3) | 0.5392(3) | 0.5956(2)   | 0.0272(10) |

**Table 4. Bond lengths (Å) for Harman\_10JAS\_137.**

|        |            |        |          |
|--------|------------|--------|----------|
| W1-N7  | 1.778(3)   | W1-N5  | 2.188(3) |
| W1-N3  | 2.192(3)   | W1-C10 | 2.207(4) |
| W1-N1  | 2.233(3)   | W1-C11 | 2.288(4) |
| W1-P1  | 2.5316(11) | P1-C19 | 1.806(5) |
| P1-C18 | 1.815(4)   | P1-C20 | 1.820(5) |
| O1-N7  | 1.216(4)   | O2-C12 | 1.327(4) |
| O2-C17 | 1.450(5)   | N1-C1  | 1.345(5) |
| N1-N2  | 1.365(4)   | N2-C3  | 1.333(5) |
| N2-B1  | 1.541(6)   | N3-C4  | 1.337(5) |
| N3-N4  | 1.374(4)   | N4-C6  | 1.346(5) |
| N4-B1  | 1.532(6)   | N5-C7  | 1.344(5) |
| N5-N6  | 1.370(4)   | N6-C9  | 1.347(5) |
| N6-B1  | 1.543(5)   | C1-C2  | 1.383(6) |
| C1-H1  | 0.95       | C2-C3  | 1.365(6) |
| C2-H2  | 0.95       | C3-H3  | 0.95     |
| C4-C5  | 1.386(6)   | C4-H4  | 0.95     |
| C5-C6  | 1.360(6)   | C5-H5  | 0.95     |
| C6-H6  | 0.95       | C7-C8  | 1.376(5) |
| C7-H7  | 0.95       | C8-C9  | 1.373(6) |
| C8-H8  | 0.95       | C9-H9  | 0.95     |

|          |          |          |          |
|----------|----------|----------|----------|
| C10-C11  | 1.462(5) | C10-C15  | 1.505(6) |
| C10-H10  | 1.0      | C11-C12  | 1.382(5) |
| C11-H11  | 1.0      | C12-C13  | 1.462(6) |
| C13-C14  | 1.385(6) | C13-H13  | 0.95     |
| C14-C15  | 1.442(6) | C14-C16  | 1.501(6) |
| C15-H15A | 0.99     | C15-H15B | 0.99     |
| C16-H16A | 0.98     | C16-H16B | 0.98     |
| C16-H16C | 0.98     | C17-H17A | 0.98     |
| C17-H17B | 0.98     | C17-H17C | 0.98     |
| C18-H18A | 0.98     | C18-H18B | 0.98     |
| C18-H18C | 0.98     | C19-H19A | 0.98     |
| C19-H19B | 0.98     | C19-H19C | 0.98     |
| C20-H20A | 0.98     | C20-H20B | 0.98     |
| C20-H20C | 0.98     | B1-H1A   | 1.14(4)  |
| S1-O3    | 1.434(3) | S1-O5    | 1.434(3) |
| S1-O4    | 1.438(3) | S1-C21   | 1.780(5) |
| F1-C21   | 1.341(5) | F2-C21   | 1.351(5) |
| F3-C21   | 1.339(5) |          |          |

**Table 5. Bond angles (°) for Harman\_10JAS\_137.**

|           |            |           |            |
|-----------|------------|-----------|------------|
| N7-W1-N5  | 96.05(14)  | N7-W1-N3  | 91.82(13)  |
| N5-W1-N3  | 75.66(12)  | N7-W1-C10 | 94.62(15)  |
| N5-W1-C10 | 125.17(14) | N3-W1-C10 | 157.18(13) |
| N7-W1-N1  | 177.94(14) | N5-W1-N1  | 84.52(12)  |
| N3-W1-N1  | 86.40(12)  | C10-W1-N1 | 86.65(13)  |

|            |            |            |            |
|------------|------------|------------|------------|
| N7-W1-C11  | 99.75(15)  | N5-W1-C11  | 87.25(13)  |
| N3-W1-C11  | 160.32(13) | C10-W1-C11 | 37.92(14)  |
| N1-W1-C11  | 82.24(13)  | N7-W1-P1   | 95.07(11)  |
| N5-W1-P1   | 152.00(9)  | N3-W1-P1   | 78.38(9)   |
| C10-W1-P1  | 79.27(11)  | N1-W1-P1   | 83.56(9)   |
| C11-W1-P1  | 115.99(10) | C19-P1-C18 | 101.7(2)   |
| C19-P1-C20 | 106.3(3)   | C18-P1-C20 | 100.3(2)   |
| C19-P1-W1  | 114.12(16) | C18-P1-W1  | 121.27(16) |
| C20-P1-W1  | 111.41(16) | C12-O2-C17 | 119.9(3)   |
| C1-N1-N2   | 105.3(3)   | C1-N1-W1   | 134.7(3)   |
| N2-N1-W1   | 119.9(2)   | C3-N2-N1   | 109.8(3)   |
| C3-N2-B1   | 129.8(4)   | N1-N2-B1   | 120.4(3)   |
| C4-N3-N4   | 106.3(3)   | C4-N3-W1   | 132.8(3)   |
| N4-N3-W1   | 120.7(2)   | C6-N4-N3   | 108.7(3)   |
| C6-N4-B1   | 128.9(4)   | N3-N4-B1   | 119.6(3)   |
| C7-N5-N6   | 106.2(3)   | C7-N5-W1   | 133.3(3)   |
| N6-N5-W1   | 120.2(2)   | C9-N6-N5   | 108.8(3)   |
| C9-N6-B1   | 128.5(4)   | N5-N6-B1   | 120.6(3)   |
| O1-N7-W1   | 179.9(4)   | N1-C1-C2   | 111.0(4)   |
| N1-C1-H1   | 124.5      | C2-C1-H1   | 124.5      |
| C3-C2-C1   | 104.5(4)   | C3-C2-H2   | 127.8      |
| C1-C2-H2   | 127.8      | N2-C3-C2   | 109.4(4)   |
| N2-C3-H3   | 125.3      | C2-C3-H3   | 125.3      |
| N3-C4-C5   | 110.5(4)   | N3-C4-H4   | 124.8      |
| C5-C4-H4   | 124.8      | C6-C5-C4   | 105.2(4)   |



|               |          |               |          |
|---------------|----------|---------------|----------|
| C6-C5-H5      | 127.4    | C4-C5-H5      | 127.4    |
| N4-C6-C5      | 109.3(4) | N4-C6-H6      | 125.4    |
| C5-C6-H6      | 125.4    | N5-C7-C8      | 110.8(4) |
| N5-C7-H7      | 124.6    | C8-C7-H7      | 124.6    |
| C9-C8-C7      | 105.0(4) | C9-C8-H8      | 127.5    |
| C7-C8-H8      | 127.5    | N6-C9-C8      | 109.1(4) |
| N6-C9-H9      | 125.4    | C8-C9-H9      | 125.4    |
| C11-C10-C15   | 117.5(4) | C11-C10-W1    | 74.0(2)  |
| C15-C10-W1    | 120.6(3) | C11-C10-H10   | 113.1    |
| C15-C10-H10   | 113.1    | W1-C10-H10    | 113.1    |
| C12-C11-C10   | 118.4(4) | C12-C11-W1    | 107.3(3) |
| C10-C11-W1    | 68.1(2)  | C12-C11-H11   | 117.5    |
| C10-C11-H11   | 117.5    | W1-C11-H11    | 117.5    |
| O2-C12-C11    | 125.3(4) | O2-C12-C13    | 111.9(4) |
| C11-C12-C13   | 122.8(4) | C14-C13-C12   | 118.8(4) |
| C14-C13-H13   | 120.6    | C12-C13-H13   | 120.6    |
| C13-C14-C15   | 121.5(4) | C13-C14-C16   | 120.5(4) |
| C15-C14-C16   | 118.0(4) | C14-C15-C10   | 117.7(4) |
| C14-C15-H15A  | 107.9    | C10-C15-H15A  | 107.9    |
| C14-C15-H15B  | 107.9    | C10-C15-H15B  | 107.9    |
| H15A-C15-H15B | 107.2    | C14-C16-H16A  | 109.5    |
| C14-C16-H16B  | 109.5    | H16A-C16-H16B | 109.5    |
| C14-C16-H16C  | 109.5    | H16A-C16-H16C | 109.5    |
| H16B-C16-H16C | 109.5    | O2-C17-H17A   | 109.5    |
| O2-C17-H17B   | 109.5    | H17A-C17-H17B | 109.5    |

|               |            |               |          |
|---------------|------------|---------------|----------|
| O2-C17-H17C   | 109.5      | H17A-C17-H17C | 109.5    |
| H17B-C17-H17C | 109.5      | P1-C18-H18A   | 109.5    |
| P1-C18-H18B   | 109.5      | H18A-C18-H18B | 109.5    |
| P1-C18-H18C   | 109.5      | H18A-C18-H18C | 109.5    |
| H18B-C18-H18C | 109.5      | P1-C19-H19A   | 109.5    |
| P1-C19-H19B   | 109.5      | H19A-C19-H19B | 109.5    |
| P1-C19-H19C   | 109.5      | H19A-C19-H19C | 109.5    |
| H19B-C19-H19C | 109.5      | P1-C20-H20A   | 109.5    |
| P1-C20-H20B   | 109.5      | H20A-C20-H20B | 109.5    |
| P1-C20-H20C   | 109.5      | H20A-C20-H20C | 109.5    |
| H20B-C20-H20C | 109.5      | N4-B1-N2      | 110.3(3) |
| N4-B1-N6      | 105.7(3)   | N2-B1-N6      | 109.1(4) |
| N4-B1-H1A     | 111.(2)    | N2-B1-H1A     | 110.(2)  |
| N6-B1-H1A     | 111.(2)    | O3-S1-O5      | 114.9(2) |
| O3-S1-O4      | 114.6(2)   | O5-S1-O4      | 116.0(2) |
| O3-S1-C21     | 103.37(19) | O5-S1-C21     | 103.3(2) |
| O4-S1-C21     | 102.1(2)   | F3-C21-F1     | 106.5(3) |
| F3-C21-F2     | 105.2(4)   | F1-C21-F2     | 104.3(4) |
| F3-C21-S1     | 113.2(3)   | F1-C21-S1     | 113.3(3) |
| F2-C21-S1     | 113.4(3)   |               |          |

**Table 6. Torsion angles (°) for Harman\_10JAS\_137.**

|             |           |             |          |
|-------------|-----------|-------------|----------|
| C1-N1-N2-C3 | -0.6(5)   | W1-N1-N2-C3 | 176.2(3) |
| C1-N1-N2-B1 | -179.9(4) | W1-N1-N2-B1 | -3.0(5)  |
| C4-N3-N4-C6 | -0.3(4)   | W1-N3-N4-C6 | 175.3(3) |

|                 |           |                 |           |
|-----------------|-----------|-----------------|-----------|
| C4-N3-N4-B1     | -163.3(3) | W1-N3-N4-B1     | 12.3(4)   |
| C7-N5-N6-C9     | -0.2(4)   | W1-N5-N6-C9     | -174.7(3) |
| C7-N5-N6-B1     | 164.5(4)  | W1-N5-N6-B1     | -10.0(5)  |
| N2-N1-C1-C2     | 0.0(5)    | W1-N1-C1-C2     | -176.1(3) |
| N1-C1-C2-C3     | 0.6(6)    | N1-N2-C3-C2     | 1.0(5)    |
| B1-N2-C3-C2     | -179.8(4) | C1-C2-C3-N2     | -0.9(6)   |
| N4-N3-C4-C5     | -0.1(4)   | W1-N3-C4-C5     | -174.9(3) |
| N3-C4-C5-C6     | 0.4(5)    | N3-N4-C6-C5     | 0.6(5)    |
| B1-N4-C6-C5     | 161.5(4)  | C4-C5-C6-N4     | -0.6(5)   |
| N6-N5-C7-C8     | 0.6(4)    | W1-N5-C7-C8     | 174.1(3)  |
| N5-C7-C8-C9     | -0.7(5)   | N5-N6-C9-C8     | -0.3(5)   |
| B1-N6-C9-C8     | -163.4(4) | C7-C8-C9-N6     | 0.6(5)    |
| C15-C10-C11-C12 | 18.2(6)   | W1-C10-C11-C12  | -98.4(3)  |
| C15-C10-C11-W1  | 116.6(4)  | C17-O2-C12-C11  | 7.0(6)    |
| C17-O2-C12-C13  | -169.5(3) | C10-C11-C12-O2  | 179.8(4)  |
| W1-C11-C12-O2   | 105.8(4)  | C10-C11-C12-C13 | -4.2(6)   |
| W1-C11-C12-C13  | -78.1(4)  | O2-C12-C13-C14  | 167.3(4)  |
| C11-C12-C13-C14 | -9.3(6)   | C12-C13-C14-C15 | 7.6(6)    |
| C12-C13-C14-C16 | -169.8(4) | C13-C14-C15-C10 | 6.5(6)    |
| C16-C14-C15-C10 | -175.9(4) | C11-C10-C15-C14 | -19.5(6)  |
| W1-C10-C15-C14  | 67.5(5)   | C6-N4-B1-N2     | 135.2(4)  |
| N3-N4-B1-N2     | -65.7(4)  | C6-N4-B1-N6     | -106.9(4) |
| N3-N4-B1-N6     | 52.2(5)   | C3-N2-B1-N4     | -119.4(5) |
| N1-N2-B1-N4     | 59.7(5)   | C3-N2-B1-N6     | 124.9(4)  |
| N1-N2-B1-N6     | -56.0(5)  | C9-N6-B1-N4     | 107.5(4)  |

|              |          |              |           |
|--------------|----------|--------------|-----------|
| N5-N6-B1-N4  | -53.9(5) | C9-N6-B1-N2  | -133.8(4) |
| N5-N6-B1-N2  | 64.8(5)  | O3-S1-C21-F3 | 178.4(3)  |
| O5-S1-C21-F3 | 58.4(4)  | O4-S1-C21-F3 | -62.3(4)  |
| O3-S1-C21-F1 | -60.1(3) | O5-S1-C21-F1 | 179.9(3)  |
| O4-S1-C21-F1 | 59.1(4)  | O3-S1-C21-F2 | 58.6(4)   |
| O5-S1-C21-F2 | -61.4(4) | O4-S1-C21-F2 | 177.9(3)  |

**Table 7. Anisotropic atomic displacement parameters ( $\text{\AA}^2$ ) for Harman\_10JAS\_137.**

The anisotropic atomic displacement factor exponent takes the form: -  
 $2\pi^2 [ h^2 a^{*2} U_{11} + \dots + 2 h k a^* b^* U_{12} ]$

|    | $U_{11}$   | $U_{22}$   | $U_{33}$   | $U_{23}$   | $U_{13}$   | $U_{12}$   |
|----|------------|------------|------------|------------|------------|------------|
| W1 | 0.01777(8) | 0.01449(7) | 0.01447(7) | 0.00086(7) | 0.00077(7) | 0.00052(7) |
| P1 | 0.0382(7)  | 0.0210(6)  | 0.0191(6)  | -0.0035(4) | 0.0016(6)  | 0.0045(6)  |
| O1 | 0.0247(17) | 0.039(2)   | 0.053(2)   | 0.0152(17) | 0.0063(17) | 0.0114(15) |
| O2 | 0.0325(17) | 0.0250(16) | 0.0224(16) | 0.0047(13) | 0.0010(14) | 0.0012(14) |
| N1 | 0.0230(19) | 0.0166(18) | 0.021(2)   | 0.0009(15) | 0.0000(16) | 0.0013(15) |
| N2 | 0.0201(18) | 0.0183(19) | 0.022(2)   | 0.0032(15) | 0.0059(16) | 0.0017(15) |
| N3 | 0.0216(18) | 0.0160(18) | 0.0182(18) | 0.0058(14) | 0.0006(15) | 0.0031(14) |
| N4 | 0.0206(18) | 0.0184(19) | 0.024(2)   | 0.0041(15) | 0.0011(16) | 0.0011(14) |
| N5 | 0.0186(18) | 0.0191(18) | 0.0159(18) | 0.0002(14) | 0.0007(15) | 0.0019(14) |

|     | <b>U<sub>11</sub></b> | <b>U<sub>22</sub></b> | <b>U<sub>33</sub></b> | <b>U<sub>23</sub></b> | <b>U<sub>13</sub></b> | <b>U<sub>12</sub></b> |
|-----|-----------------------|-----------------------|-----------------------|-----------------------|-----------------------|-----------------------|
| N6  | 0.0174(18)            | 0.0192(18)            | 0.022(2)              | -<br>0.0033(15)       | 0.0057(15)            | -<br>0.0008(15)       |
| N7  | 0.0207(18)            | 0.0232(19)            | 0.0184(18)            | 0.0005(16)            | -<br>0.0018(15)       | 0.0037(15)            |
| C1  | 0.029(3)              | 0.022(2)              | 0.039(3)              | 0.005(2)              | 0.000(2)              | 0.000(2)              |
| C2  | 0.034(3)              | 0.022(3)              | 0.049(3)              | 0.007(2)              | 0.005(2)              | -0.009(2)             |
| C3  | 0.023(2)              | 0.030(3)              | 0.038(3)              | -0.003(2)             | 0.008(2)              | -0.013(2)             |
| C4  | 0.031(2)              | 0.019(2)              | 0.020(2)              | 0.0016(18)            | -0.003(2)             | -<br>0.0010(19)       |
| C5  | 0.040(3)              | 0.029(3)              | 0.024(3)              | 0.002(2)              | -0.010(2)             | 0.005(2)              |
| C6  | 0.024(2)              | 0.030(3)              | 0.036(3)              | -0.004(2)             | -0.010(2)             | 0.003(2)              |
| C7  | 0.022(2)              | 0.014(2)              | 0.024(2)              | 0.0006(18)            | -<br>0.0066(19)       | -<br>0.0067(17)       |
| C8  | 0.035(3)              | 0.020(2)              | 0.024(2)              | -<br>0.0083(19)       | -0.003(2)             | 0.004(2)              |
| C9  | 0.024(2)              | 0.027(2)              | 0.027(3)              | -0.008(2)             | 0.004(2)              | 0.0047(19)            |
| C10 | 0.023(2)              | 0.017(2)              | 0.022(2)              | 0.0019(18)            | -<br>0.0022(19)       | 0.0028(17)            |
| C11 | 0.025(2)              | 0.021(2)              | 0.019(2)              | 0.0041(17)            | -<br>0.0013(19)       | -<br>0.0013(19)       |
| C12 | 0.030(2)              | 0.019(3)              | 0.0153(19)            | 0.0014(17)            | -<br>0.0032(18)       | 0.0045(17)            |
| C13 | 0.025(2)              | 0.029(2)              | 0.034(3)              | -0.003(2)             | -0.005(2)             | -0.003(2)             |
| C14 | 0.024(2)              | 0.032(3)              | 0.024(2)              | 0.0081(19)            | -0.002(2)             | 0.0047(19)            |
| C15 | 0.028(2)              | 0.029(3)              | 0.026(3)              | 0.0052(19)            | 0.000(2)              | 0.004(2)              |
| C16 | 0.024(2)              | 0.057(4)              | 0.047(3)              | -0.007(3)             | 0.004(2)              | -0.003(2)             |
| C17 | 0.043(3)              | 0.024(3)              | 0.024(2)              | -<br>0.0008(19)       | 0.008(2)              | 0.0011(19)            |

|     | <b>U<sub>11</sub></b> | <b>U<sub>22</sub></b> | <b>U<sub>33</sub></b> | <b>U<sub>23</sub></b>   | <b>U<sub>13</sub></b>   | <b>U<sub>12</sub></b>   |
|-----|-----------------------|-----------------------|-----------------------|-------------------------|-------------------------|-------------------------|
| C18 | 0.051(3)              | 0.021(2)              | 0.037(3)              | -0.008(2)               | -0.003(3)               | 0.006(2)                |
| C19 | 0.080(4)              | 0.035(3)              | 0.030(3)              | -0.003(2)               | 0.018(3)                | 0.005(3)                |
| C20 | 0.050(3)              | 0.039(3)              | 0.034(3)              | -0.017(2)               | -0.012(3)               | 0.005(2)                |
| B1  | 0.019(2)              | 0.020(2)              | 0.030(3)              | -0.009(2)               | 0.003(2)                | -0.002(2)               |
| S1  | 0.0330(6)             | 0.0282(6)             | 0.0217(6)             | -0.0009(5)              | 0.0003(5)               | 0.0020(5)               |
| F1  | 0.0504(18)            | 0.0496(18)            | 0.0414(18)            | <sup>-</sup> 0.0112(15) | 0.0065(15)              | 0.0115(15)              |
| F2  | 0.0328(17)            | 0.0398(18)            | 0.114(3)              | 0.0066(18)              | 0.0037(18)              | <sup>-</sup> 0.0047(14) |
| F3  | 0.0551(19)            | 0.073(2)              | 0.049(2)              | <sup>-</sup> 0.0017(17) | <sup>-</sup> 0.0144(17) | 0.0335(17)              |
| O3  | 0.0296(17)            | 0.0296(17)            | 0.0258(18)            | 0.0036(14)              | <sup>-</sup> 0.0069(14) | 0.0008(14)              |
| O4  | 0.064(2)              | 0.036(2)              | 0.044(2)              | 0.0146(19)              | 0.011(2)                | <sup>-</sup> 0.0101(18) |
| O5  | 0.050(2)              | 0.058(2)              | 0.033(2)              | <sup>-</sup> 0.0215(17) | <sup>-</sup> 0.0119(17) | 0.0187(18)              |
| C21 | 0.034(3)              | 0.018(2)              | 0.030(3)              | -0.002(2)               | -0.013(2)               | 0.0061(19)              |

**Table 8. Hydrogen atomic coordinates and isotropic atomic displacement parameters (Å<sup>2</sup>) for Harman\_10JAS\_137.**

|    | <b>x/a</b> | <b>y/b</b> | <b>z/c</b> | <b>U(eq)</b> |
|----|------------|------------|------------|--------------|
| H1 | 0.1643     | 0.0285     | 0.4140     | 0.036        |
| H2 | 0.0152     | -0.0124    | 0.4361     | 0.042        |
| H3 | -0.0707    | 0.1176     | 0.4212     | 0.036        |
| H4 | 0.1869     | 0.3409     | 0.2405     | 0.028        |

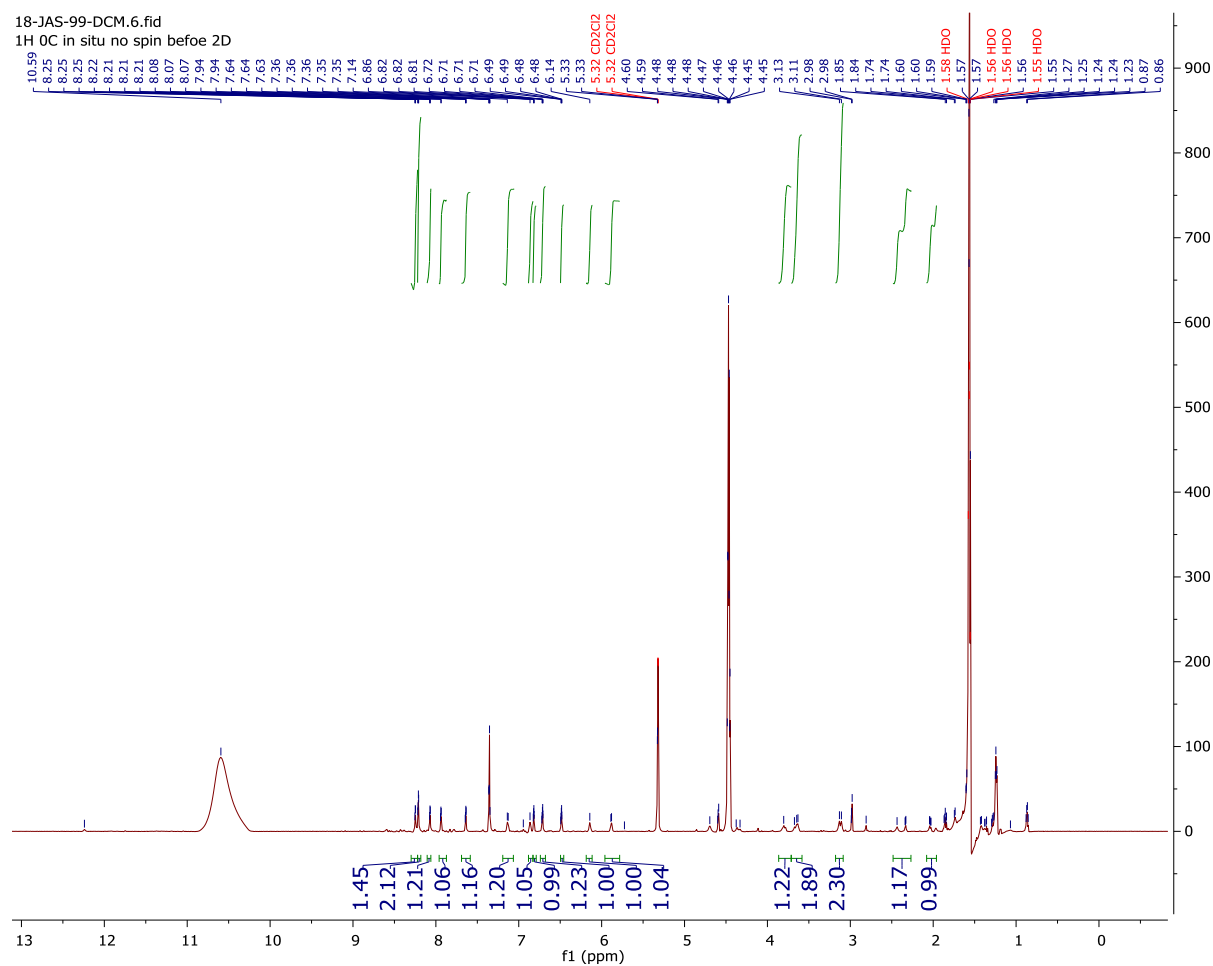
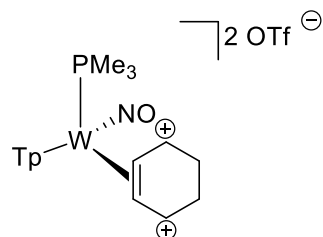
|      | <b>x/a</b> | <b>y/b</b> | <b>z/c</b> | <b>U(eq)</b> |
|------|------------|------------|------------|--------------|
| H5   | 0.0439     | 0.3912     | 0.2097     | 0.037        |
| H6   | -0.0565    | 0.3435     | 0.2857     | 0.036        |
| H7   | 0.2433     | 0.4134     | 0.4535     | 0.024        |
| H8   | 0.1204     | 0.4899     | 0.4958     | 0.032        |
| H9   | -0.0079    | 0.4077     | 0.4675     | 0.031        |
| H10  | 0.2893     | 0.0794     | 0.4008     | 0.025        |
| H11  | 0.2509     | 0.1581     | 0.4811     | 0.026        |
| H13  | 0.4538     | 0.3156     | 0.4554     | 0.035        |
| H15A | 0.4316     | 0.0875     | 0.3973     | 0.033        |
| H15B | 0.4079     | 0.1412     | 0.3414     | 0.033        |
| H16A | 0.5463     | 0.2372     | 0.3458     | 0.064        |
| H16B | 0.5715     | 0.1604     | 0.3872     | 0.064        |
| H16C | 0.5758     | 0.2550     | 0.4109     | 0.064        |
| H17A | 0.2028     | 0.2739     | 0.5292     | 0.046        |
| H17B | 0.2435     | 0.3323     | 0.5783     | 0.046        |
| H17C | 0.2642     | 0.2337     | 0.5767     | 0.046        |
| H18A | 0.3320     | 0.0312     | 0.2992     | 0.055        |
| H18B | 0.2637     | -0.0019    | 0.2534     | 0.055        |
| H18C | 0.2416     | -0.0010    | 0.3210     | 0.055        |
| H19A | 0.2684     | 0.2297     | 0.2111     | 0.073        |
| H19B | 0.2853     | 0.1355     | 0.1896     | 0.073        |
| H19C | 0.3497     | 0.1796     | 0.2335     | 0.073        |
| H20A | 0.0916     | 0.0837     | 0.2852     | 0.061        |
| H20B | 0.1295     | 0.0746     | 0.2213     | 0.061        |

|      | <b>x/a</b> | <b>y/b</b> | <b>z/c</b> | <b>U(eq)</b> |
|------|------------|------------|------------|--------------|
| H20C | 0.0973     | 0.1643     | 0.2438     | 0.061        |
| H1A  | -0.051(3)  | 0.281(2)   | 0.3945(17) | 0.028        |

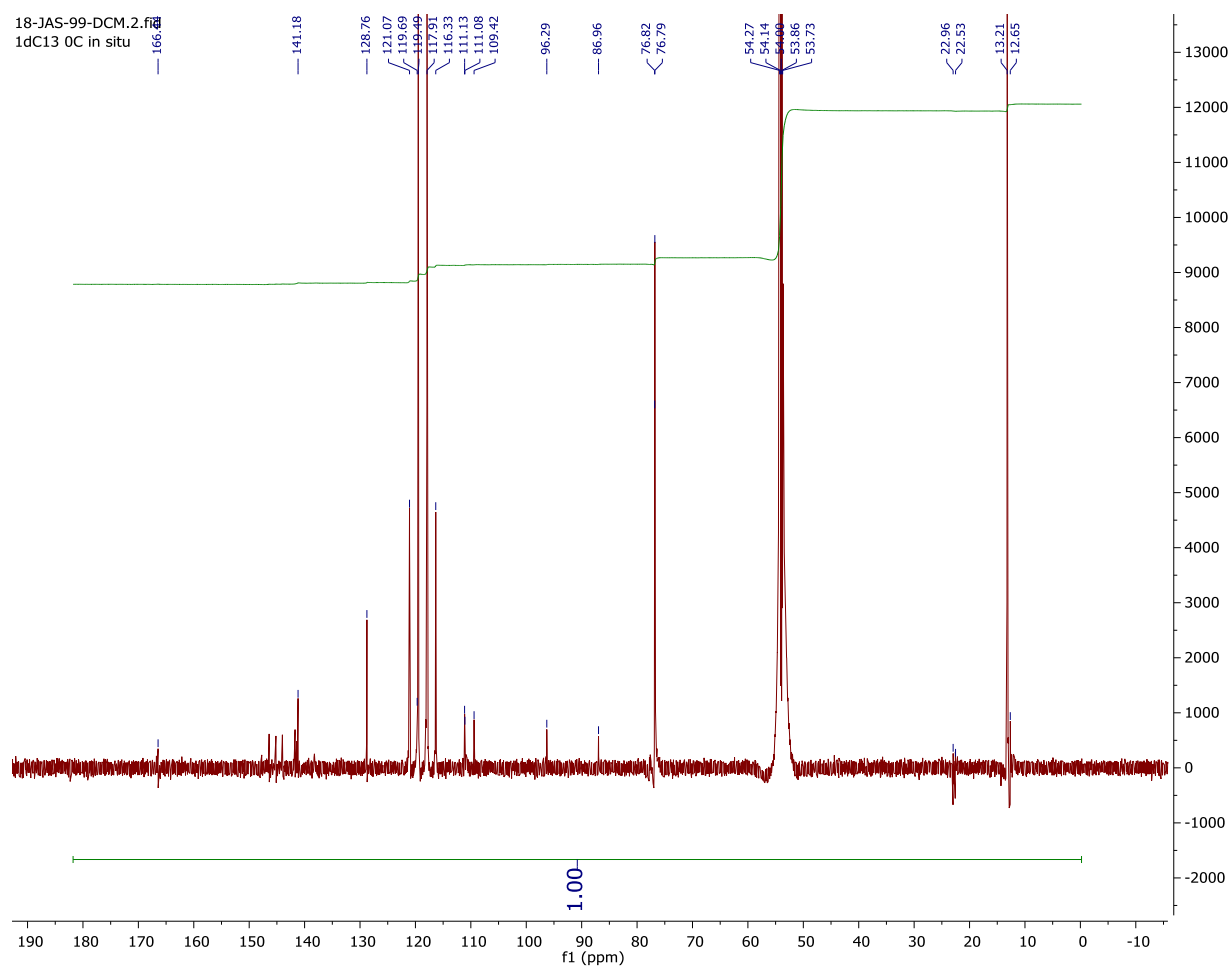
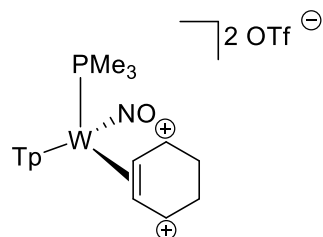


# Supporting Information for Chapter 8

## $^1\text{H}$ NMR Spectrum of 3



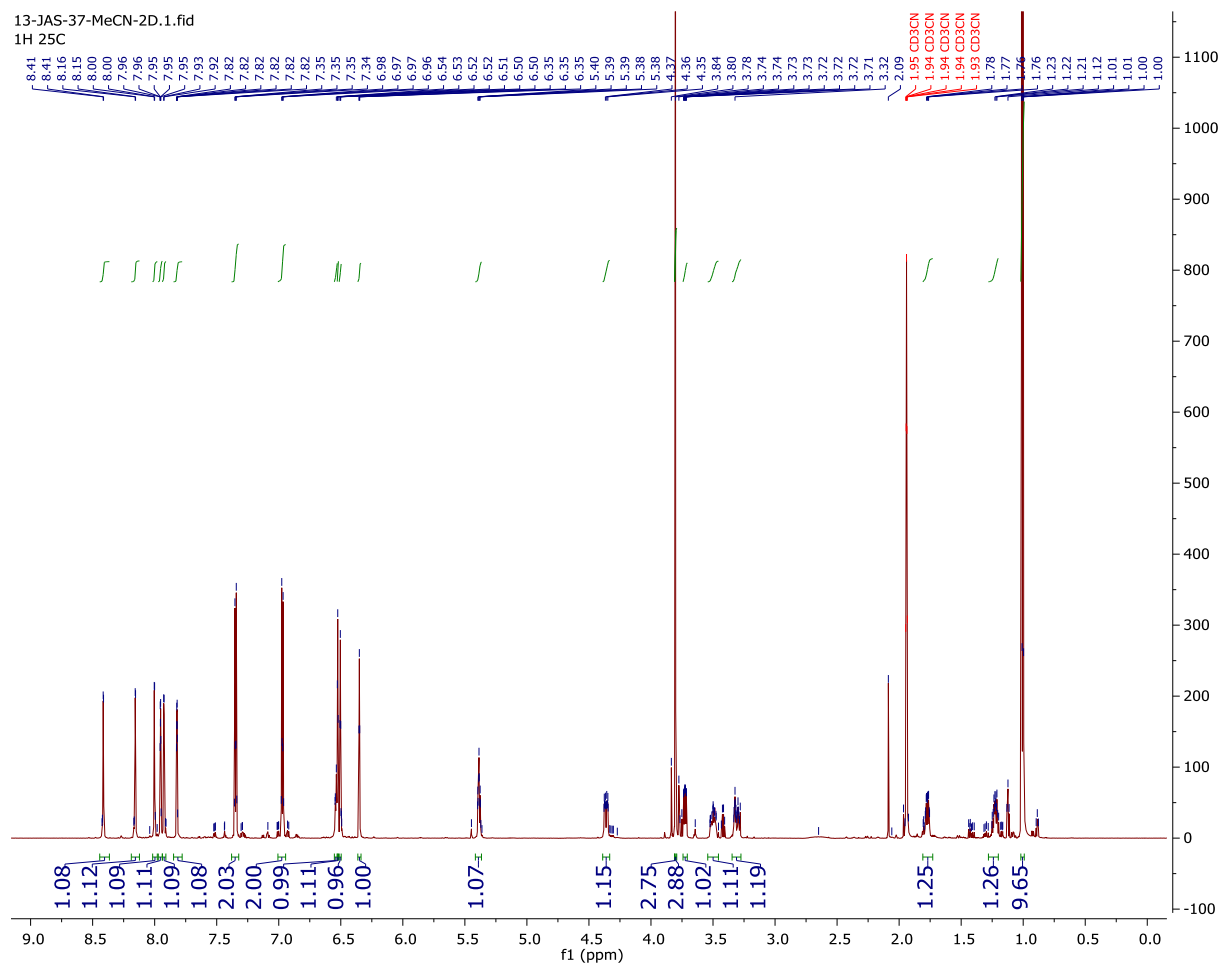
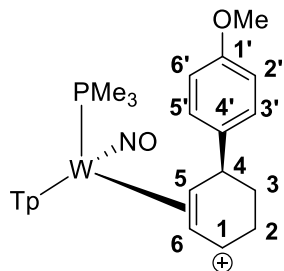
# $^{13}\text{C}\{^1\text{H}\}$ NMR Spectrum of 3



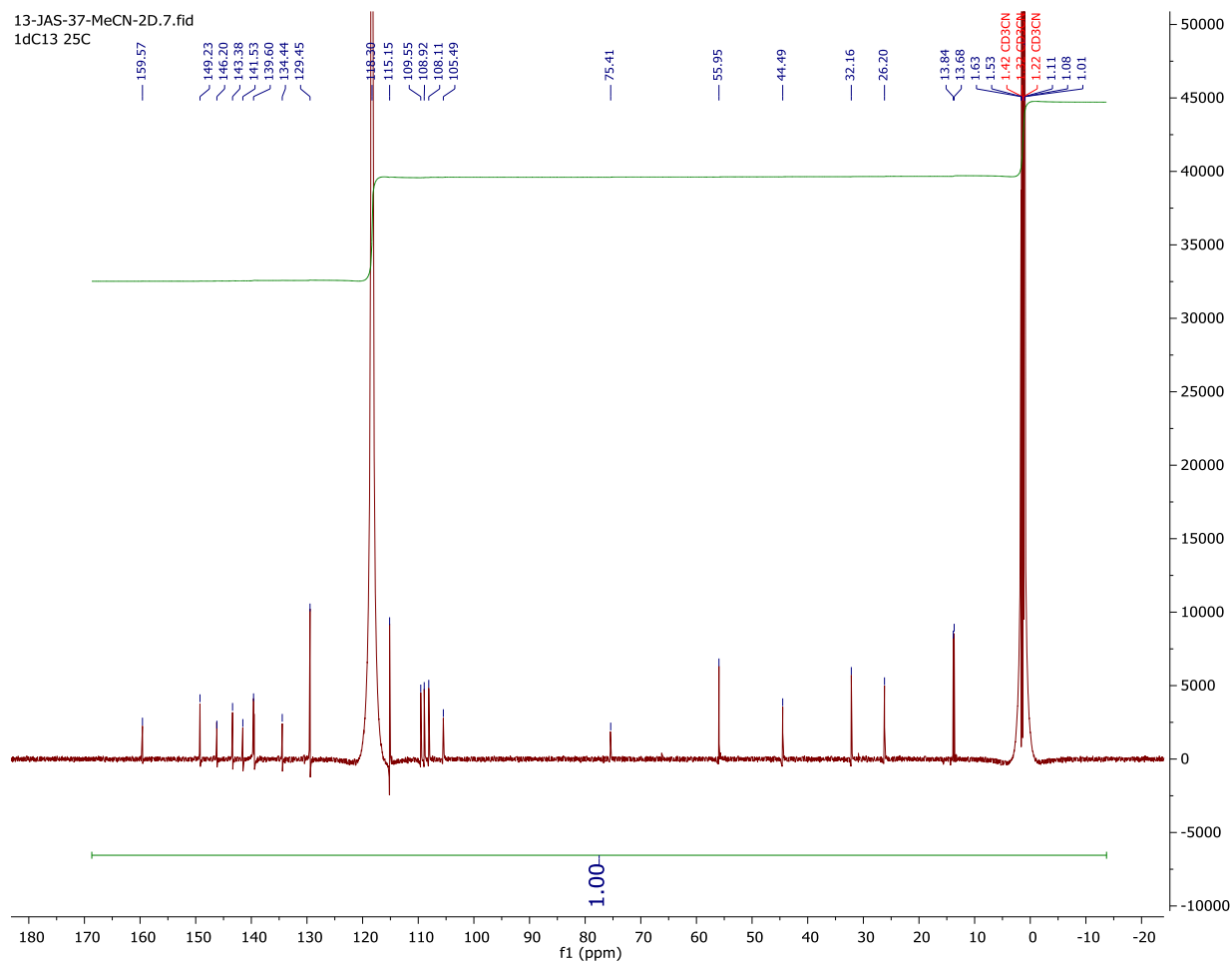
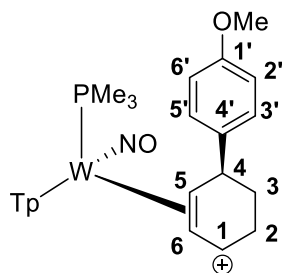




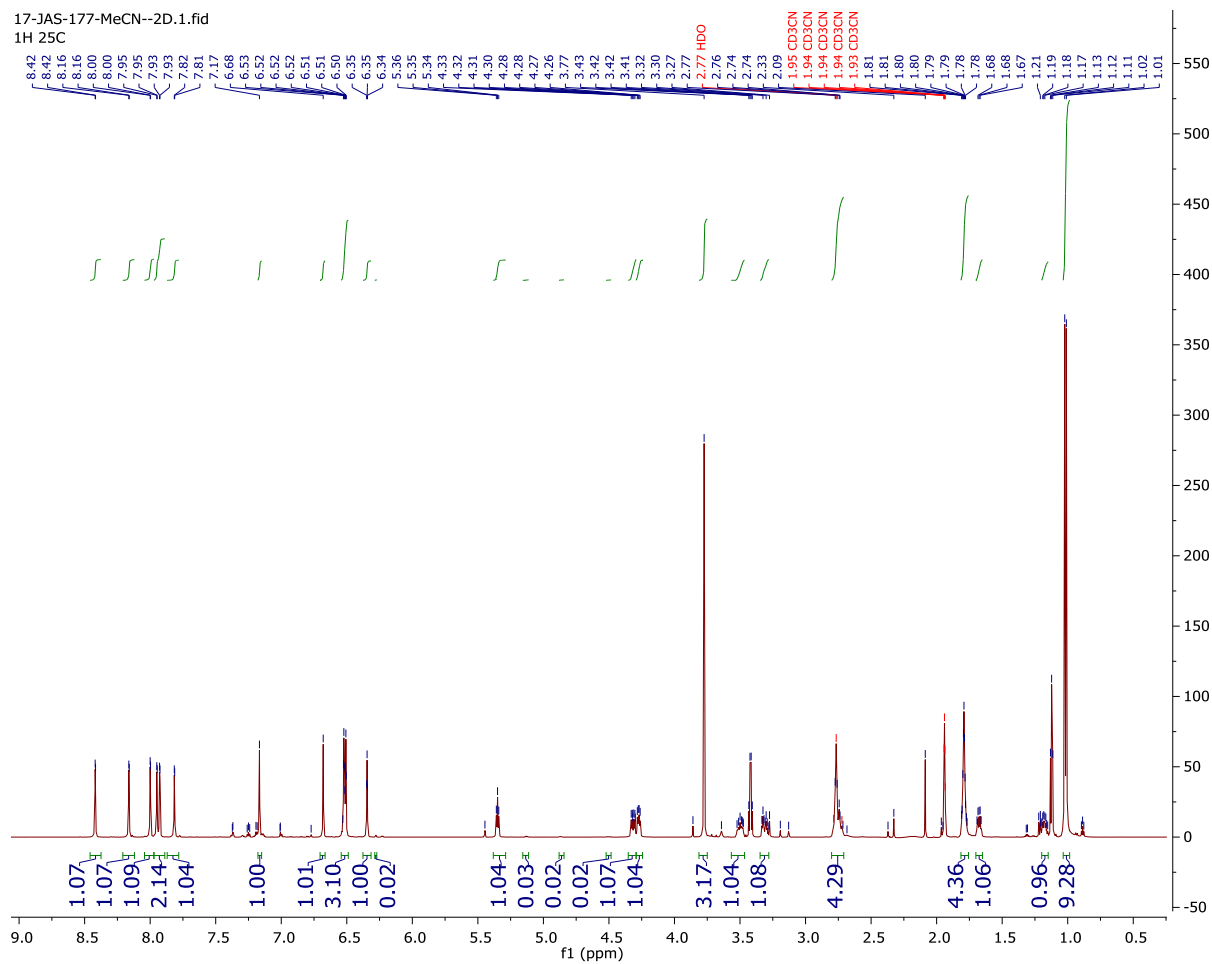
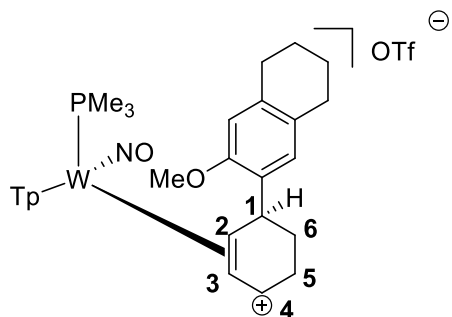
# <sup>1</sup>H NMR Spectrum of 5



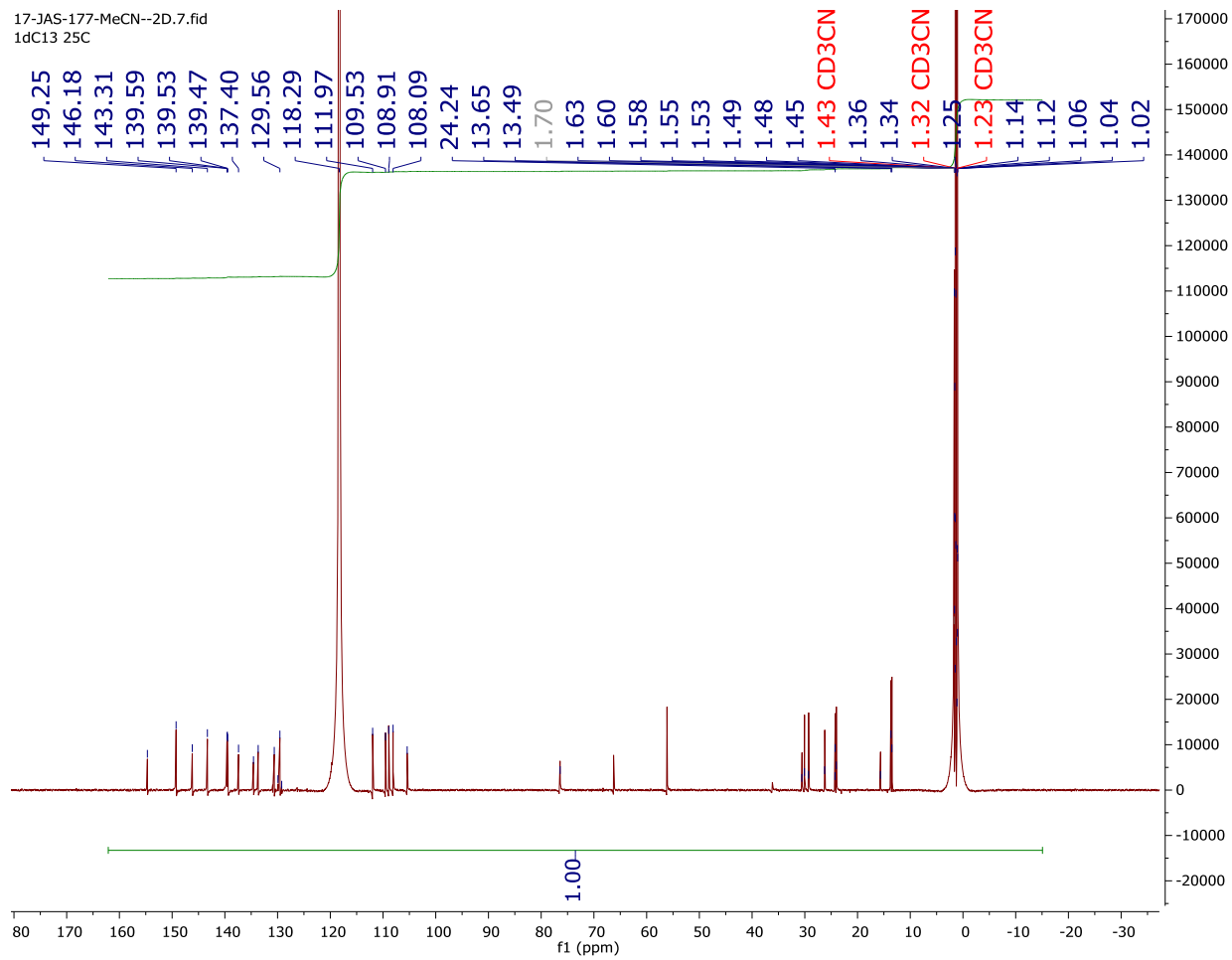
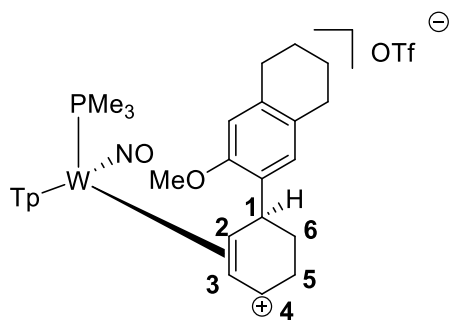
# $^{13}\text{C}\{^1\text{H}\}$ NMR Spectrum of 5



# <sup>1</sup>H NMR Spectrum of 6

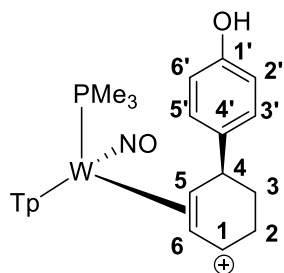


<sup>13</sup>C{<sup>1</sup>H} NMR Spectrum of 6

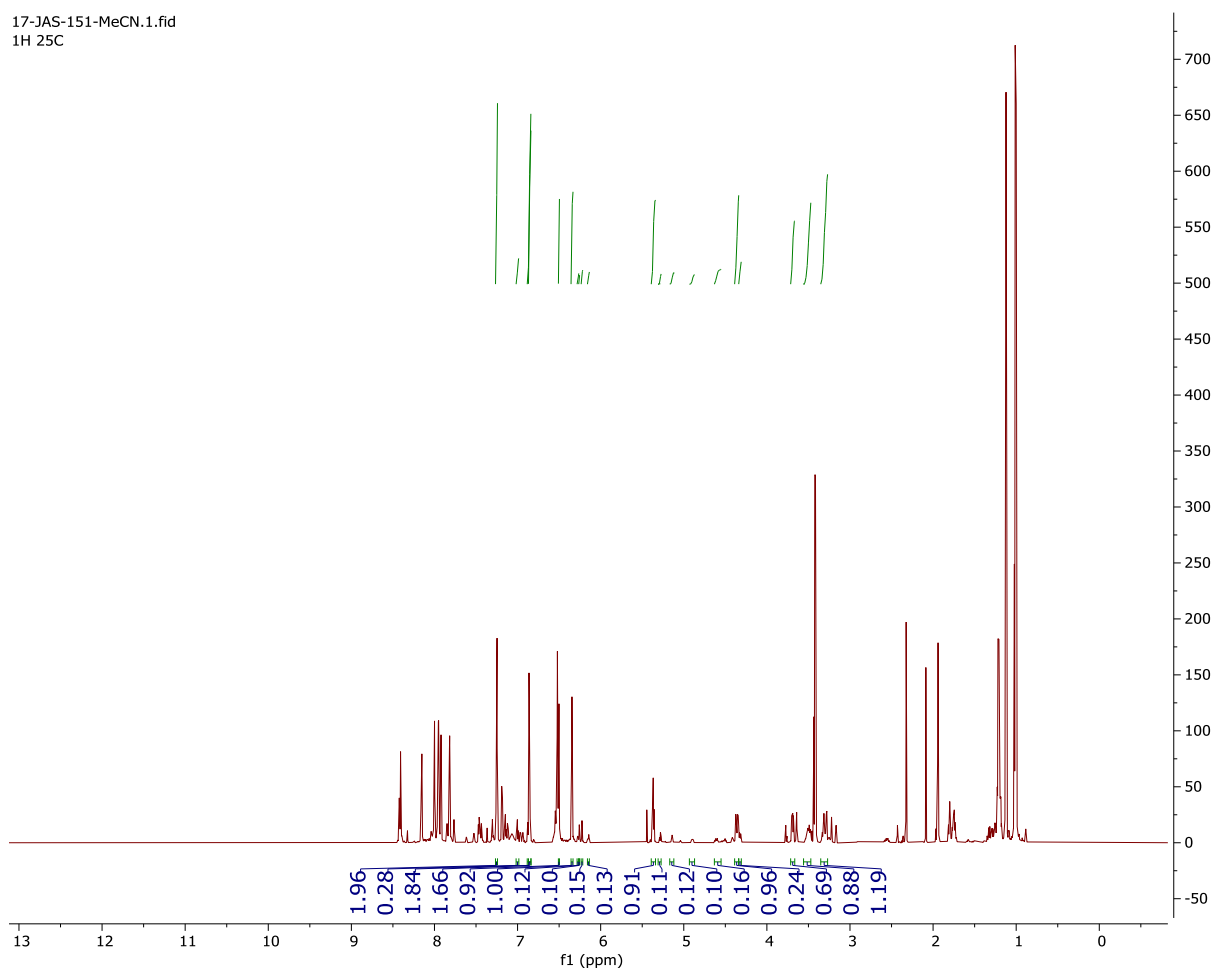




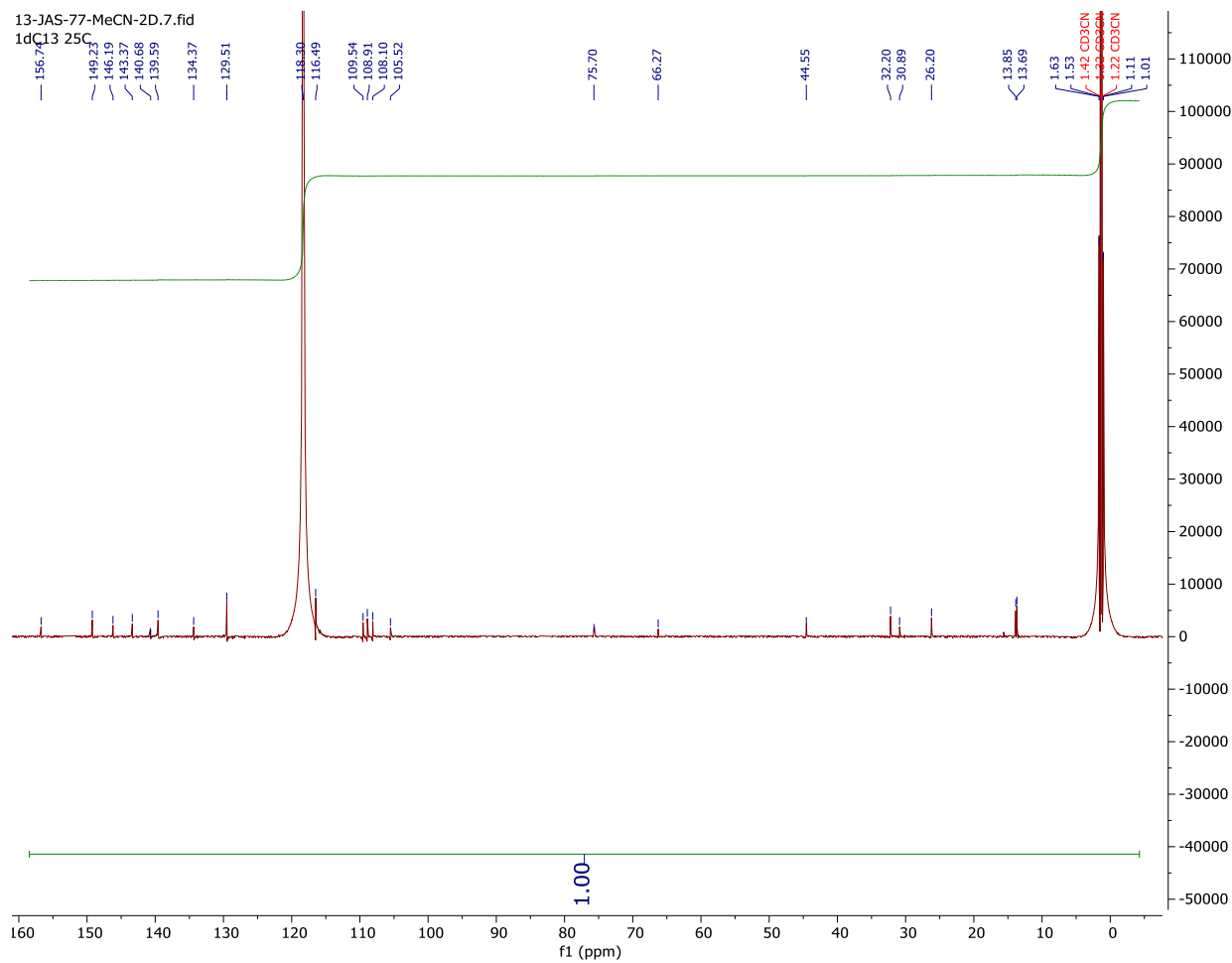
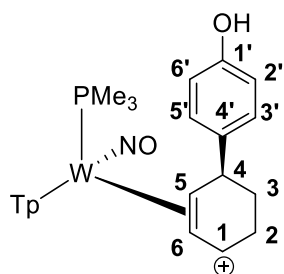
# <sup>1</sup>H NMR Spectrum of 7



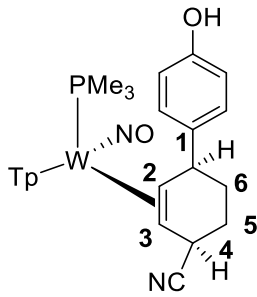
17-JAS-151-MeCN.1.fid  
1H 25C



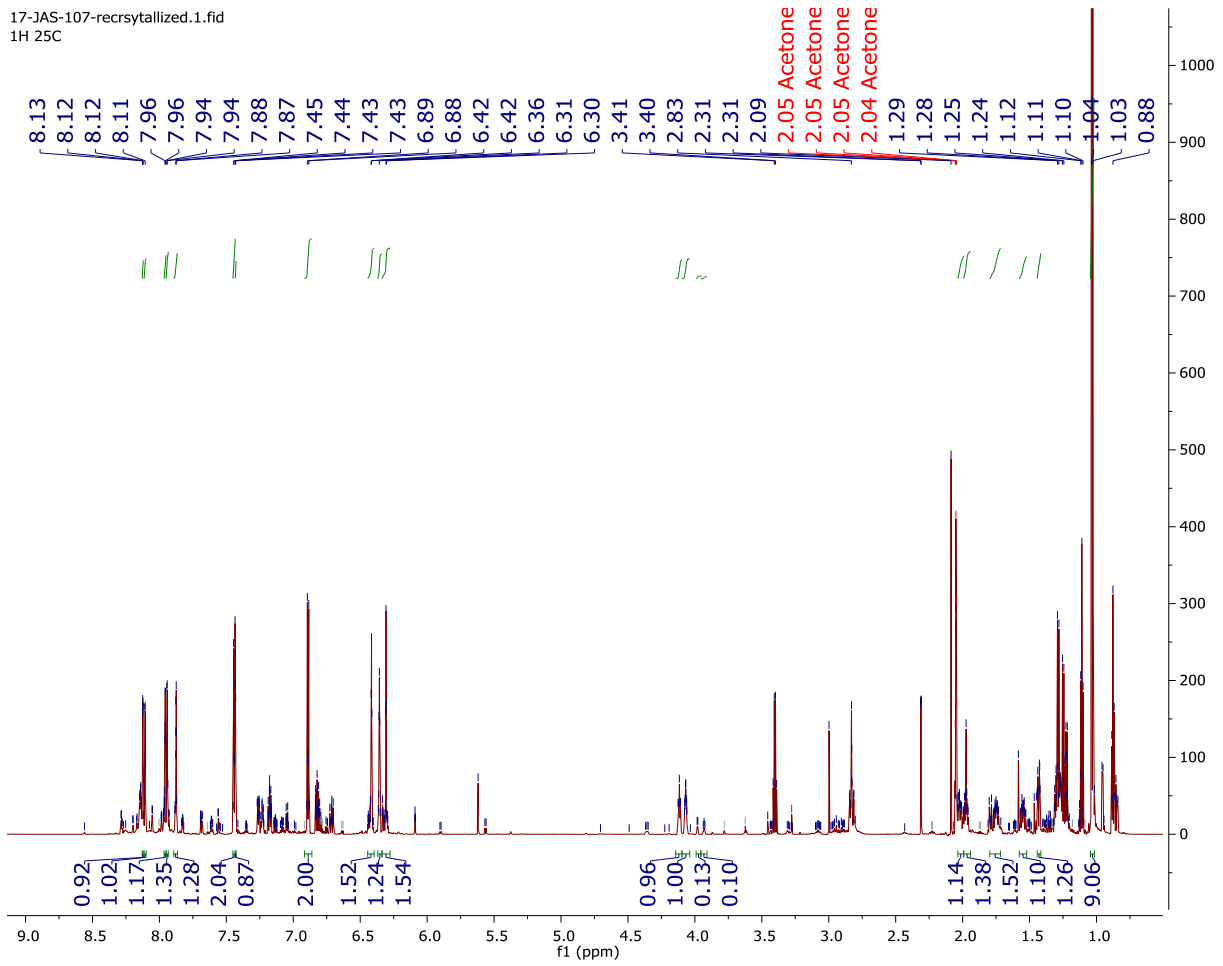
# $^{13}\text{C}\{^1\text{H}\}$ NMR Spectrum of 7



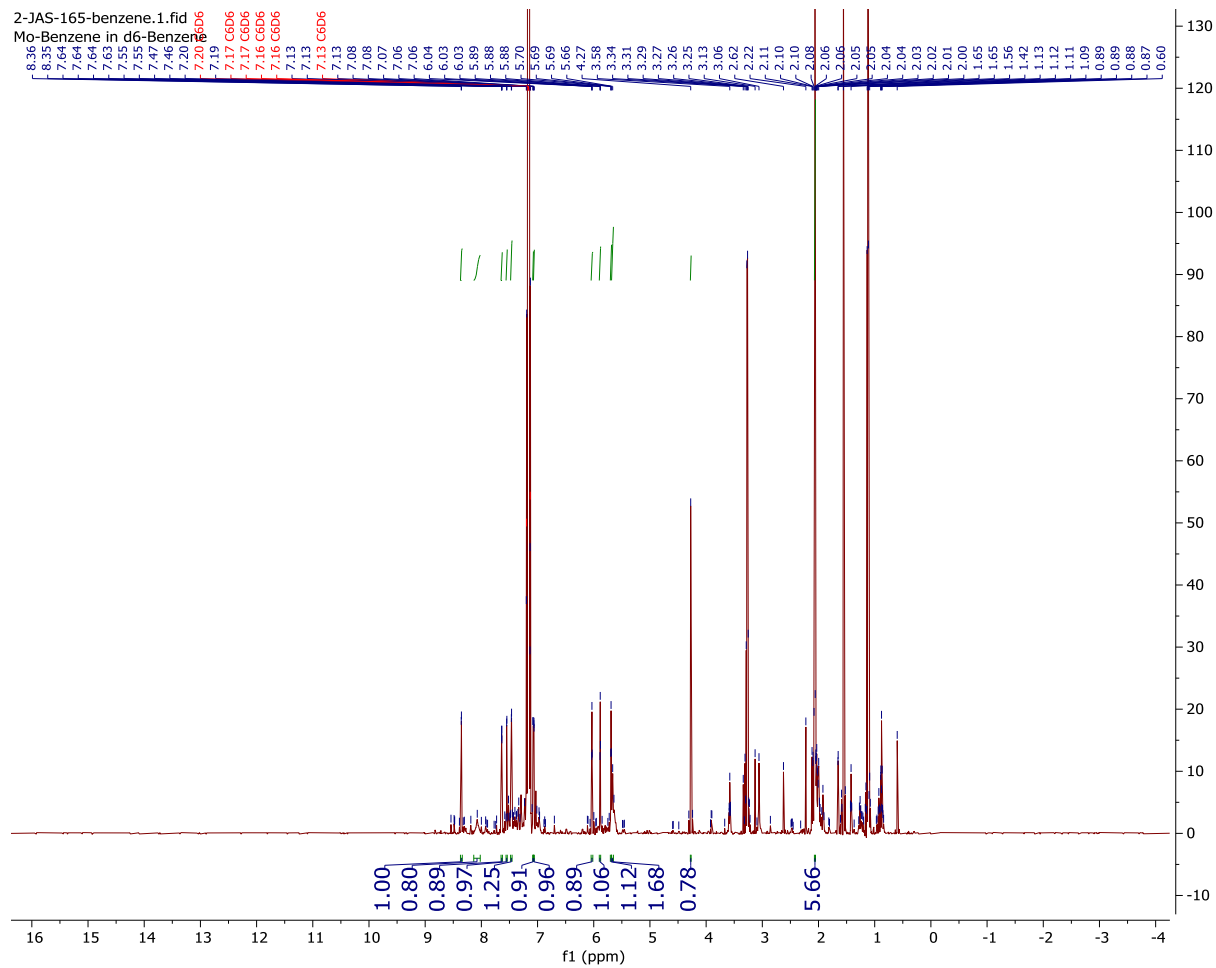
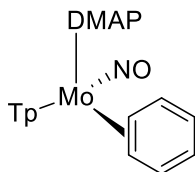
# <sup>1</sup>H NMR Spectrum of 9



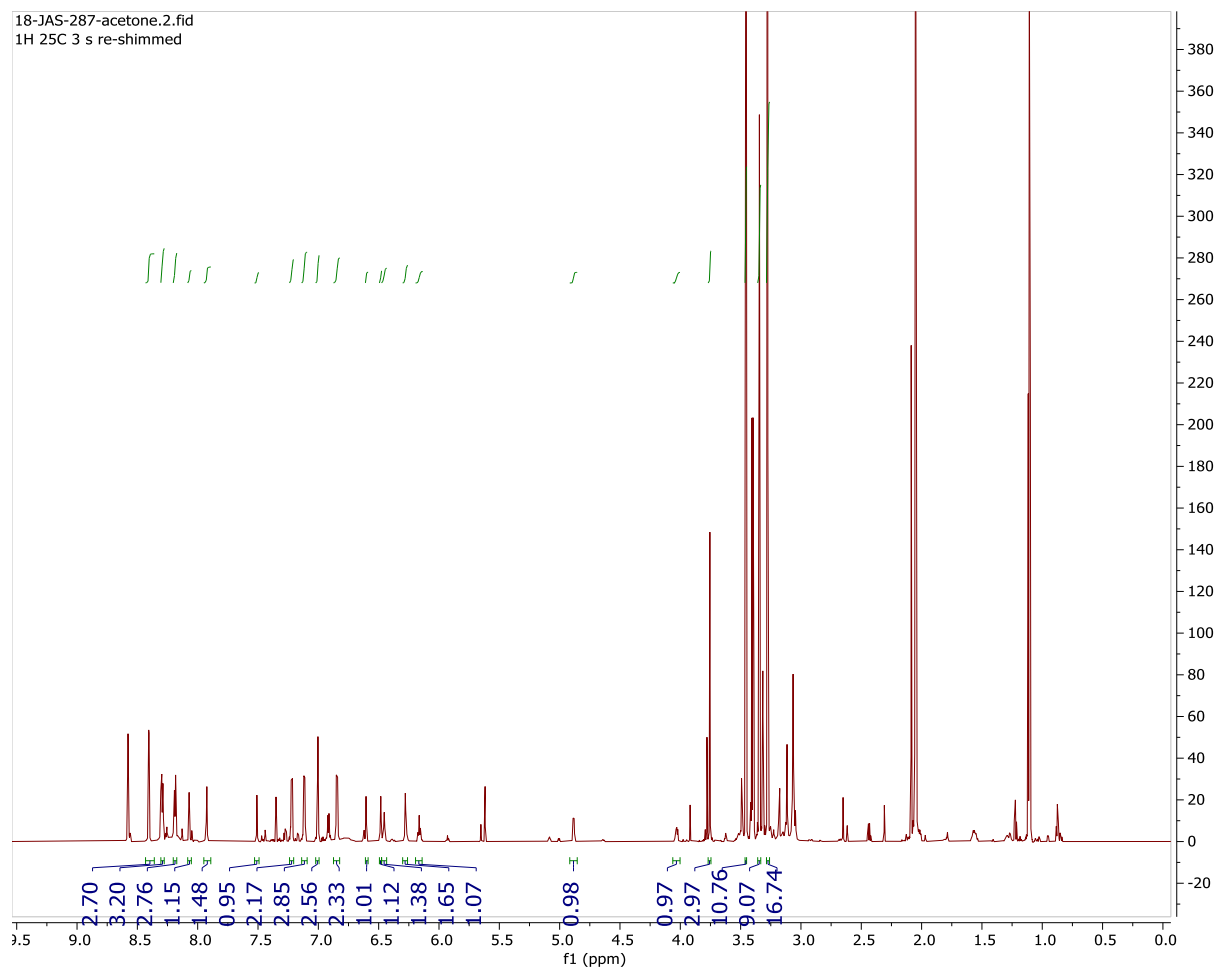
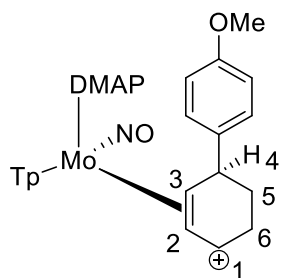
17-JAS-107-recrsyallized.1.fid  
1H 25C



# <sup>1</sup>H NMR Spectrum of 10



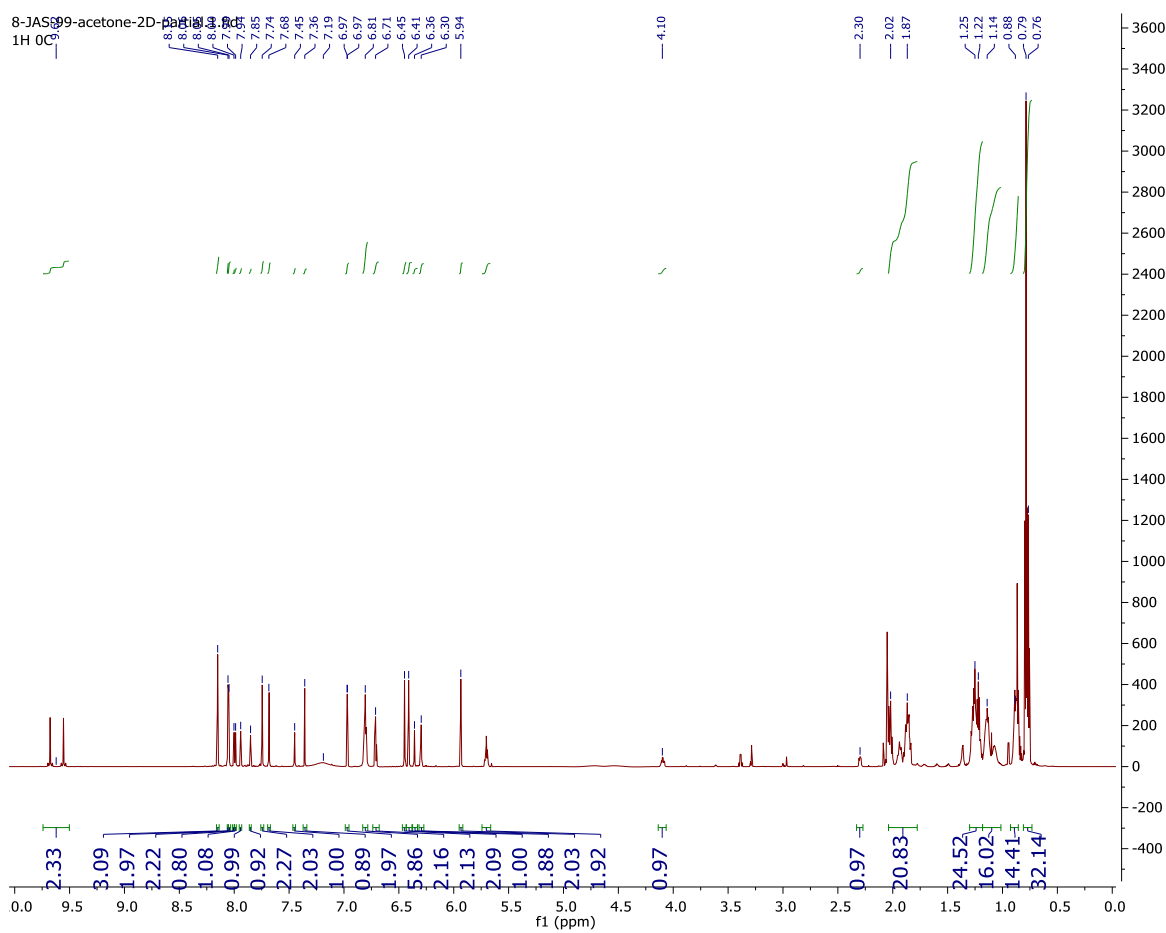
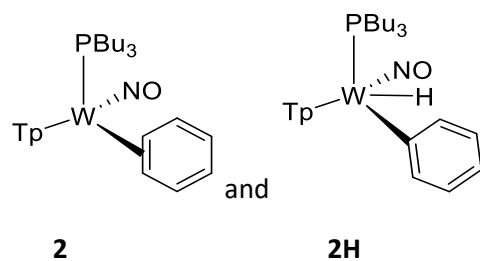
# <sup>1</sup>H NMR Spectrum of 12



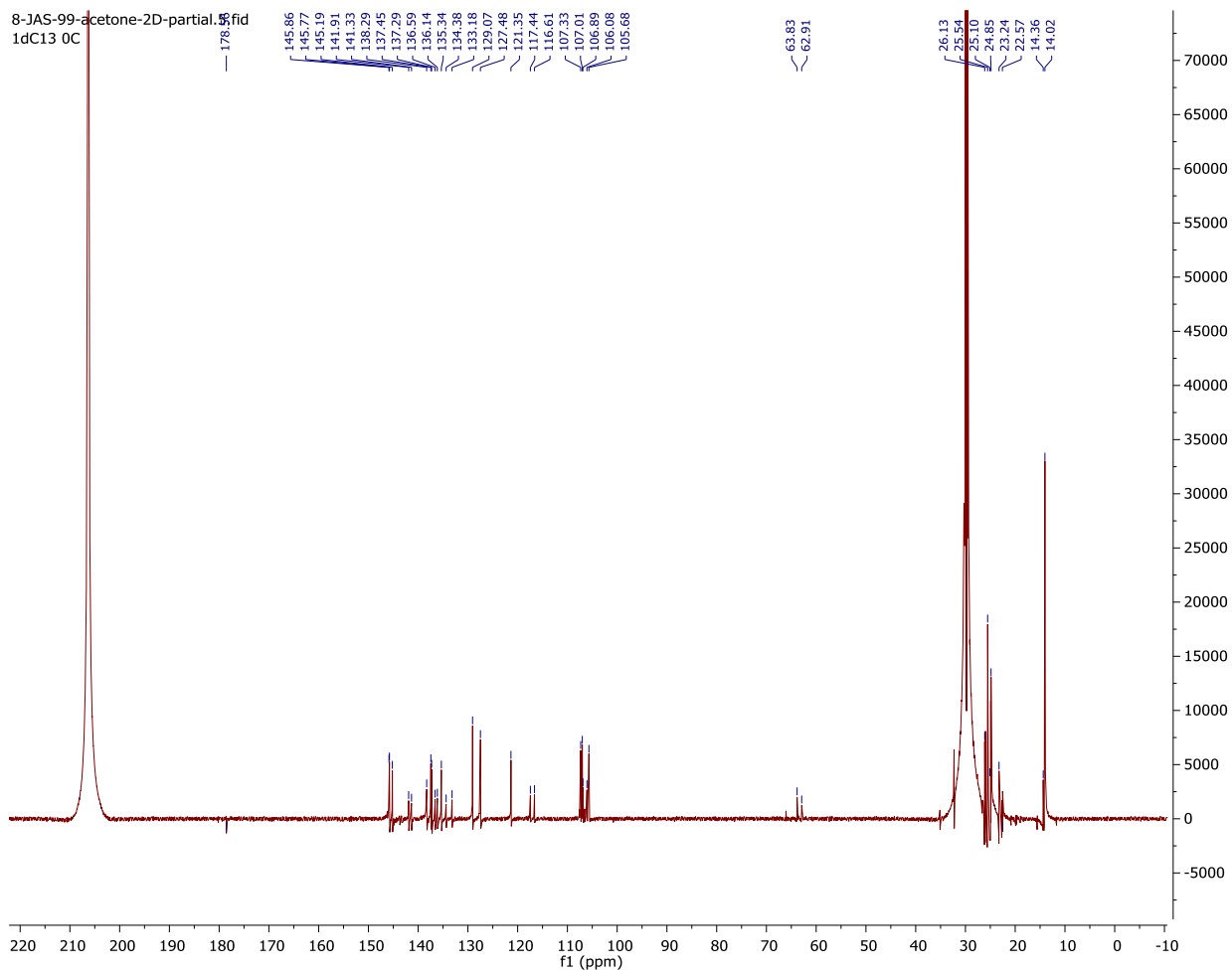
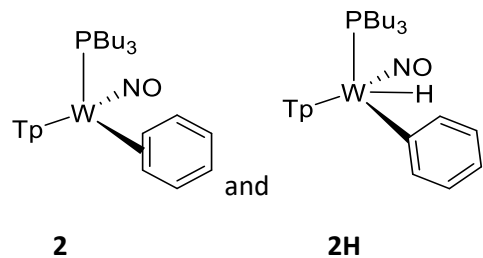
# Supporting Information for Chapter 9

## A) $^1\text{H}$ and $^{13}\text{C}$ $\{^1\text{H}\}$ NMR Spectra of Complexes

### $^1\text{H}$ NMR Spectrum of **2** and **2H**

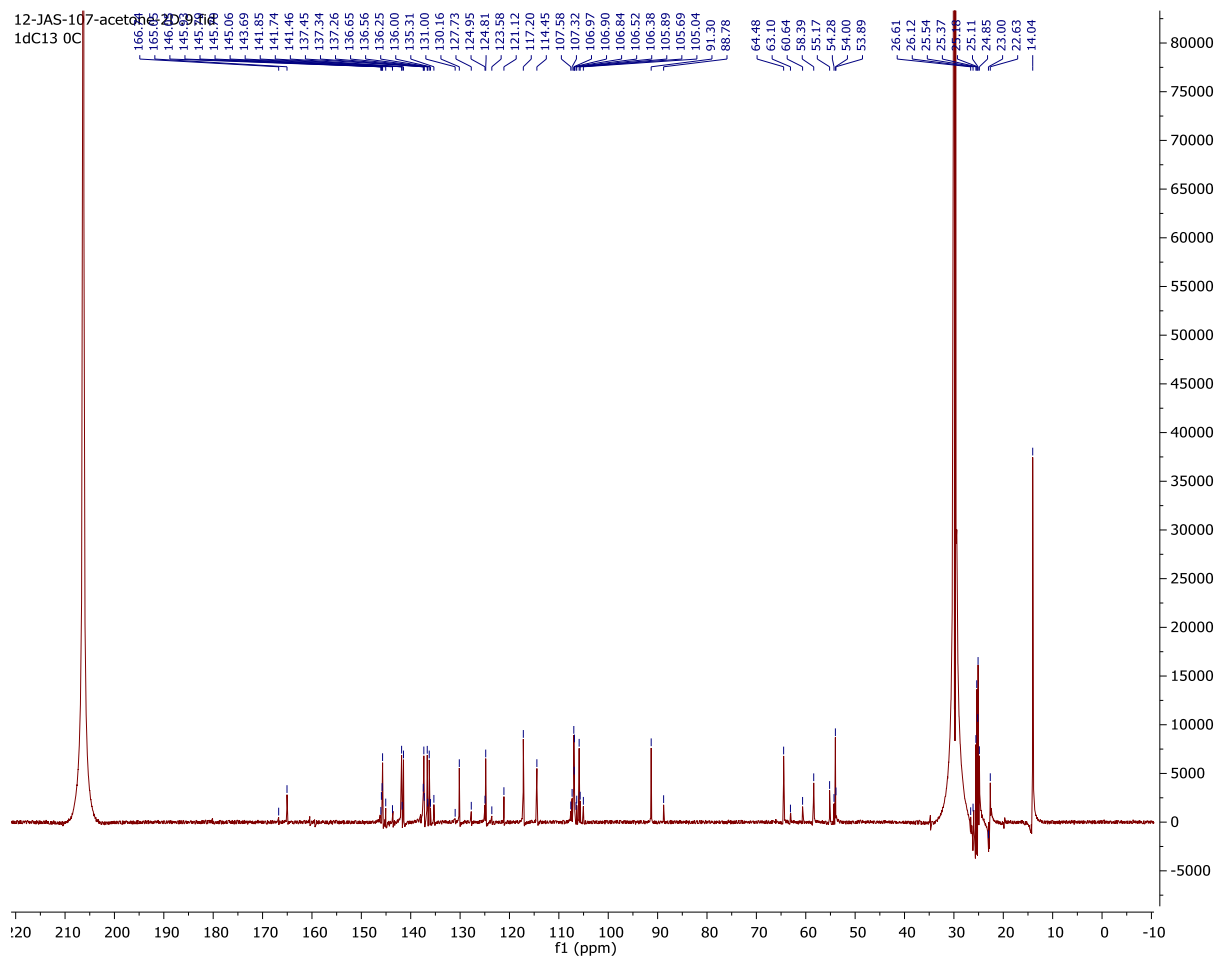
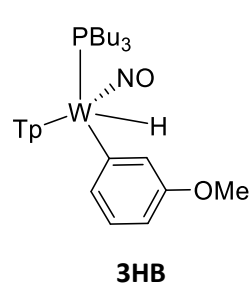
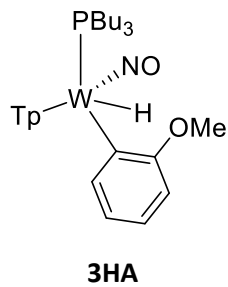
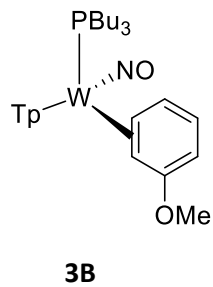
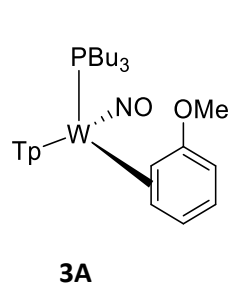


# $^{13}\text{C}\{^1\text{H}\}$ NMR Spectrum of 2 and 2H

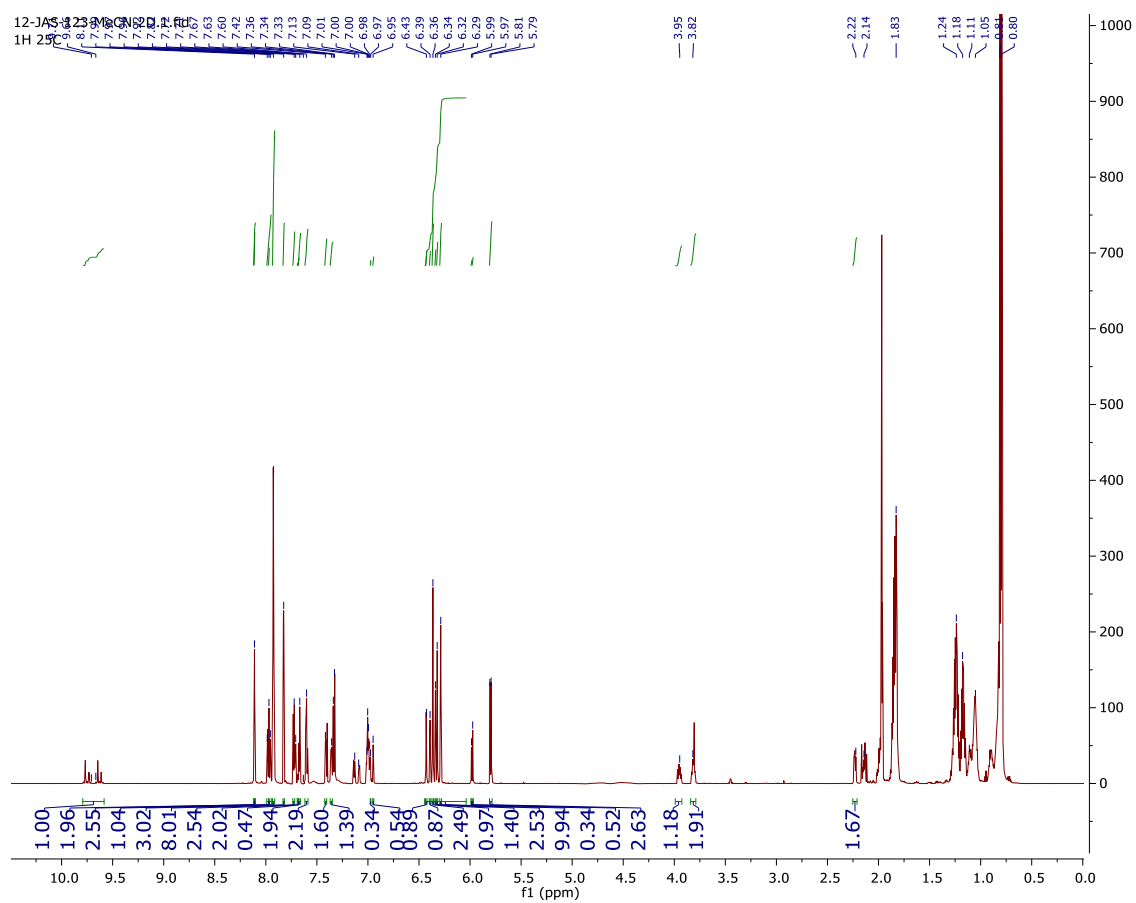
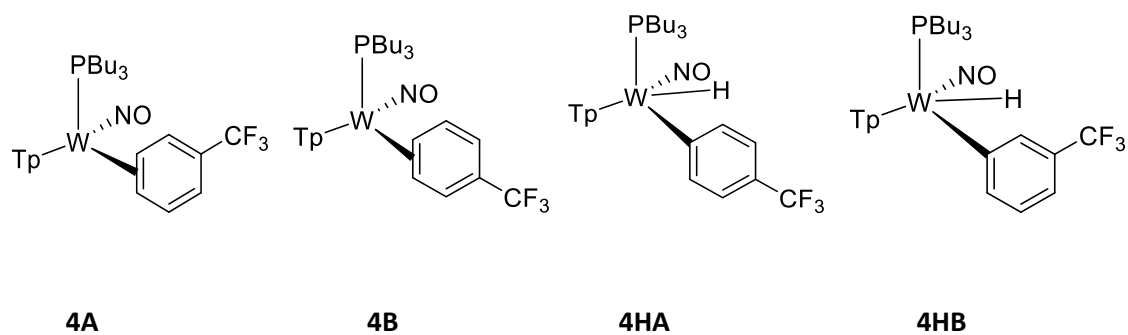




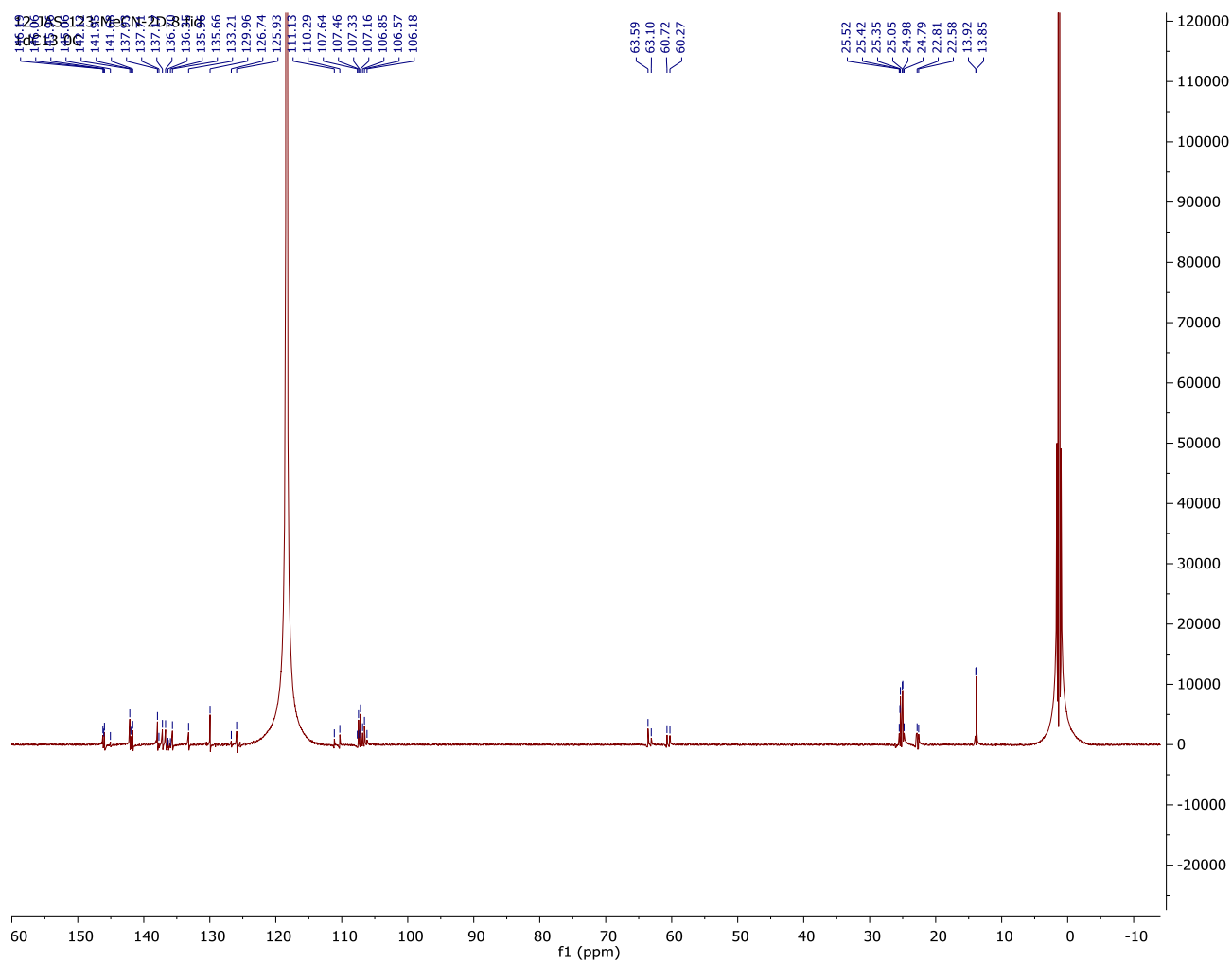
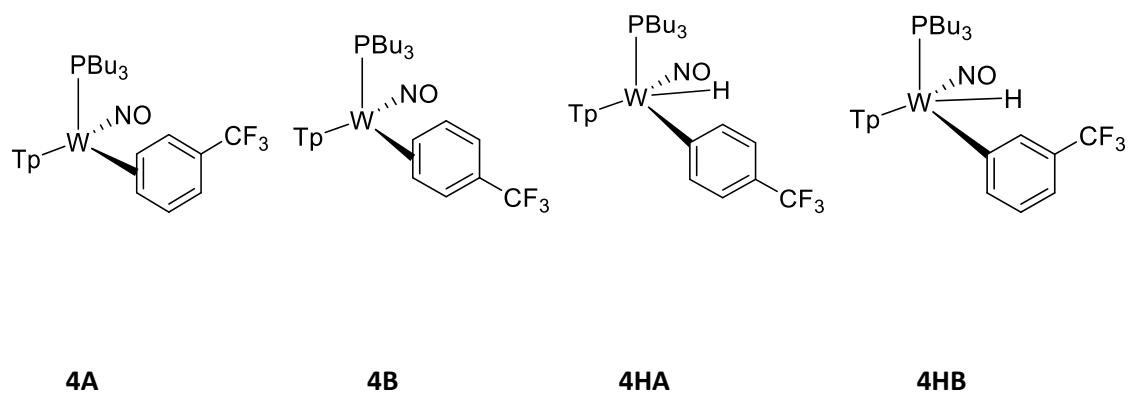




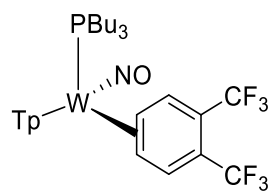
**<sup>1</sup>H NMR Spectrum of 4A and 4B and 4HA and 4HB**



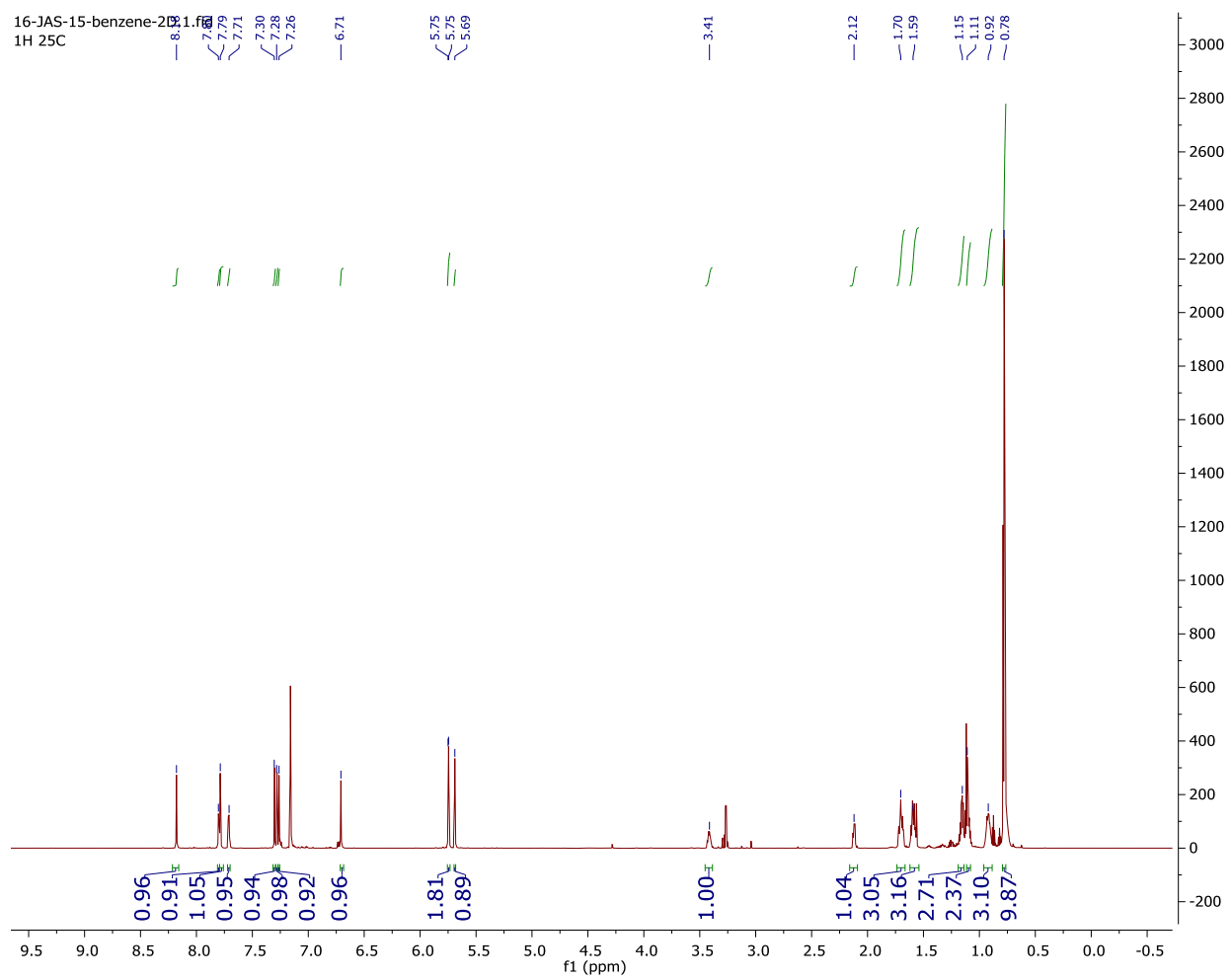
<sup>13</sup>C{<sup>1</sup>H} NMR Spectrum of 4A and 4B and 4HA and 4HB



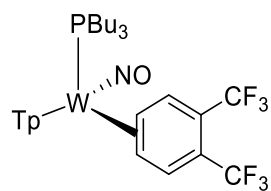
# <sup>1</sup>H NMR Spectrum of 6



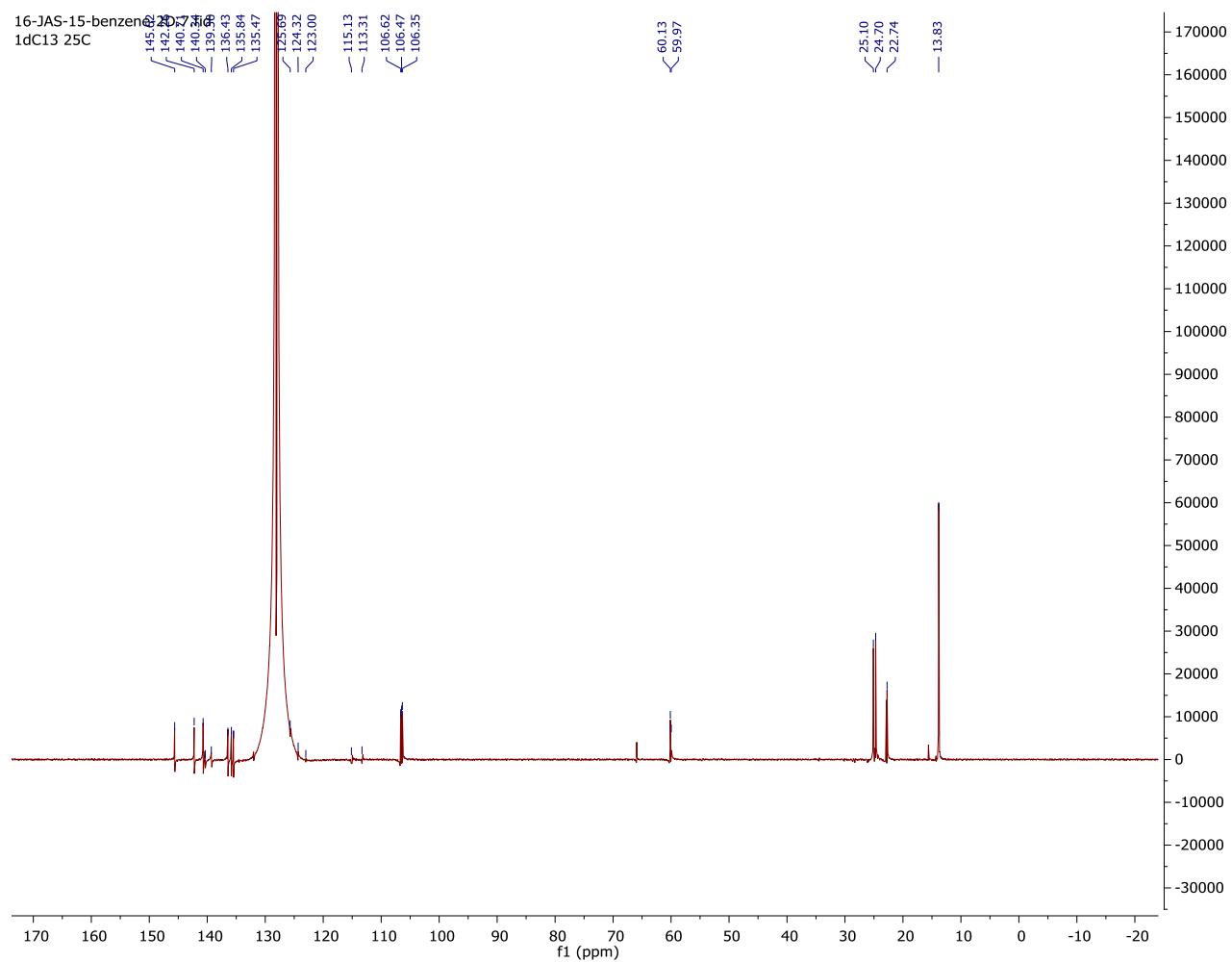
6



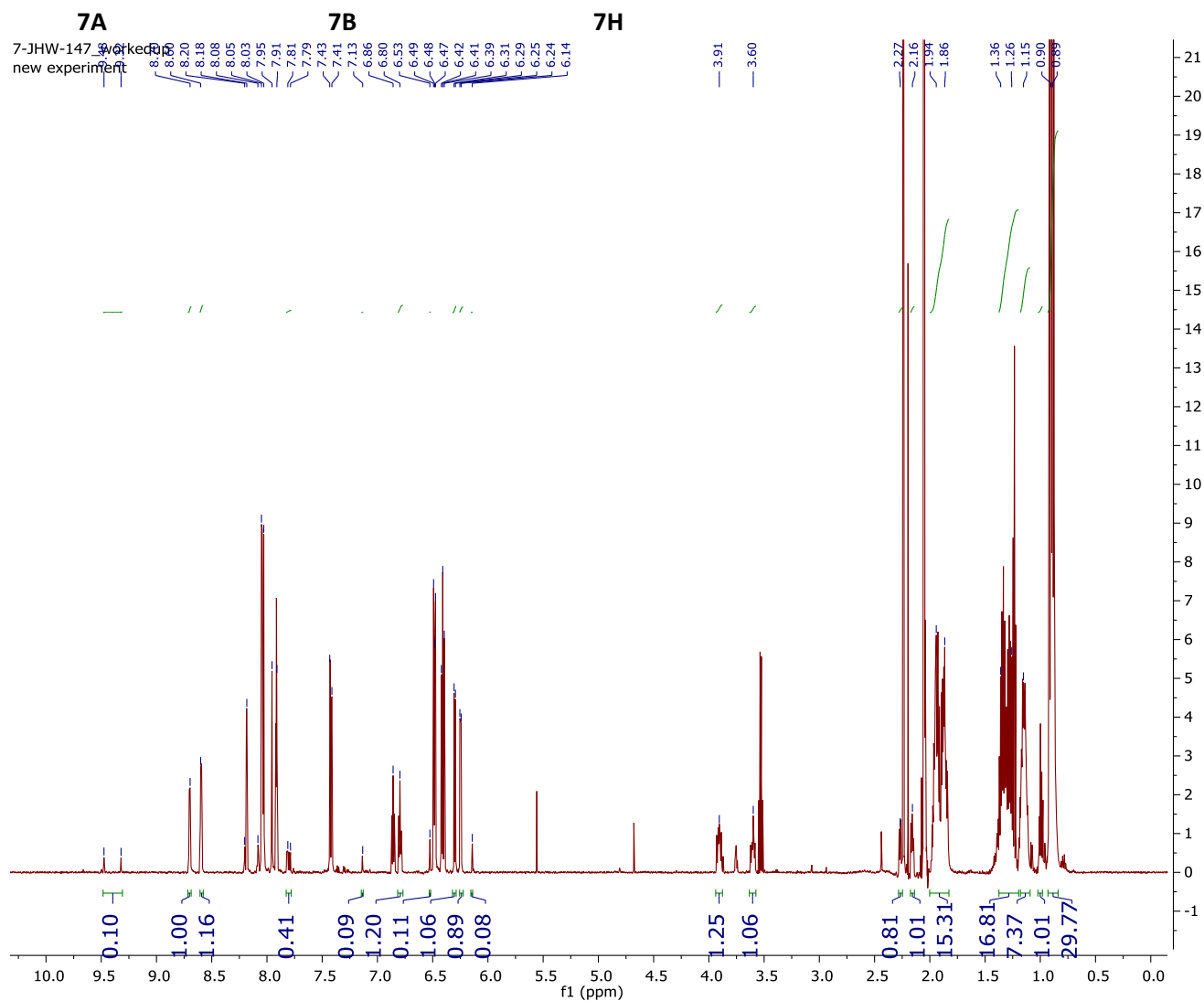
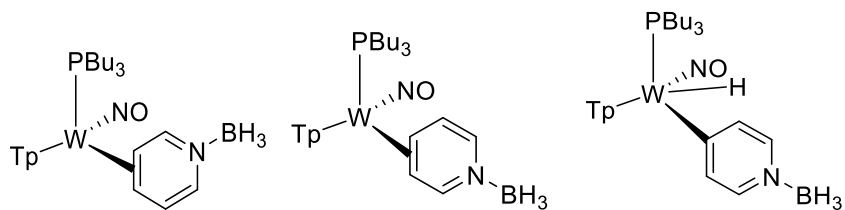
# $^{13}\text{C}\{^1\text{H}\}$ NMR Spectrum of 6



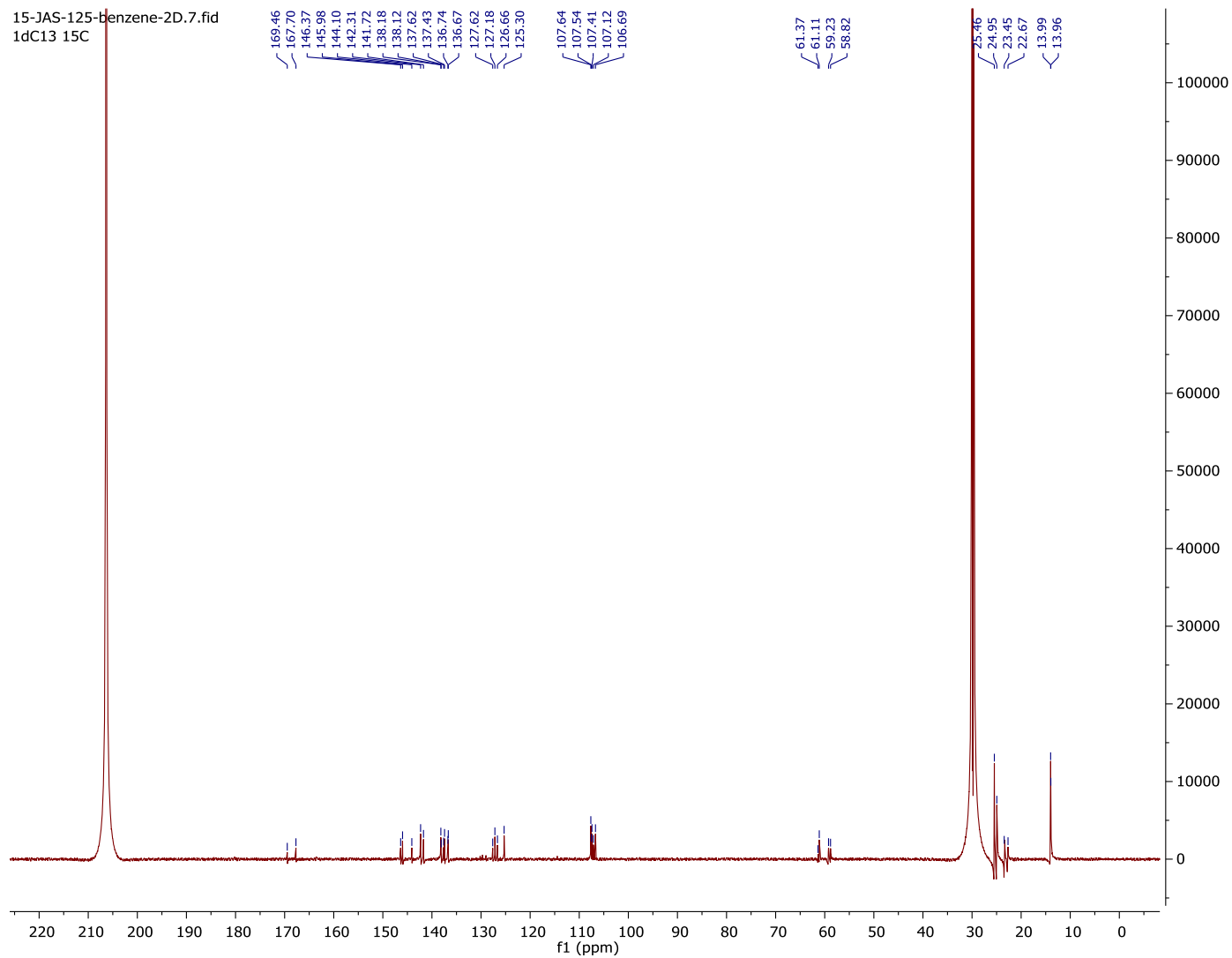
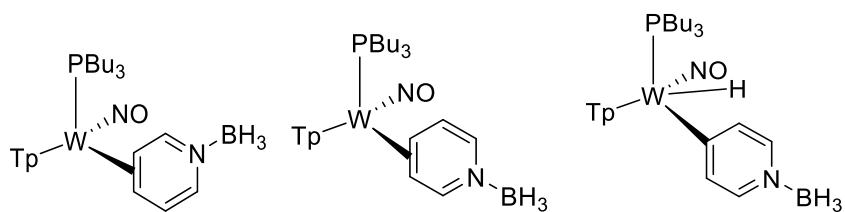
6



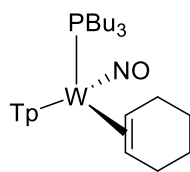
**<sup>1</sup>H NMR Spectrum of 7A and 7B and 7H**



# $^{13}\text{C}\{^1\text{H}\}$ NMR Spectrum of 7A and 7B and 7H

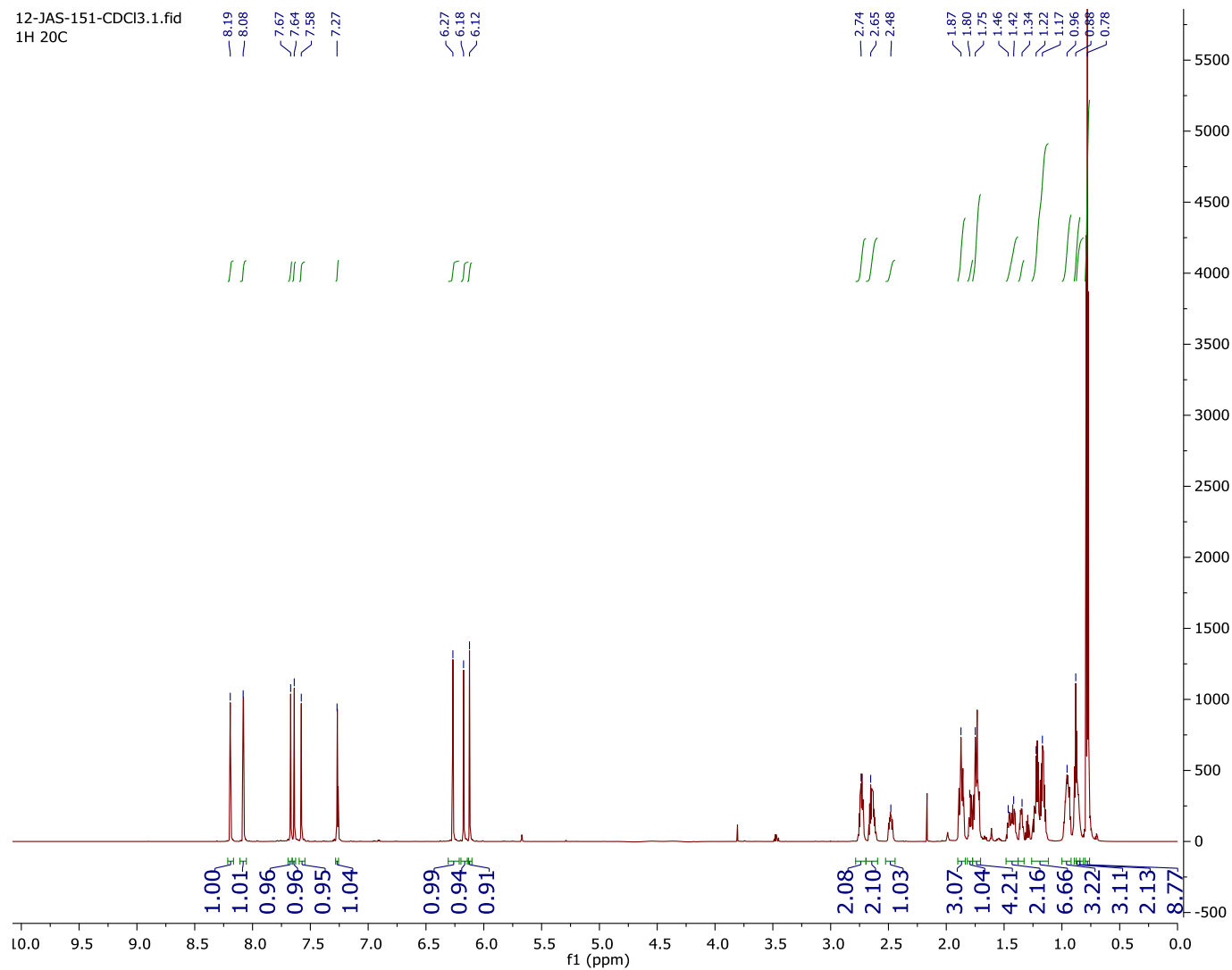


# <sup>1</sup>H NMR Spectrum of 7A and 7B and 7H



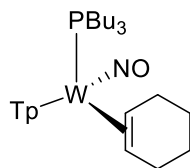
**10**

12-JAS-151-CDCl3.1.fid  
1H 20C

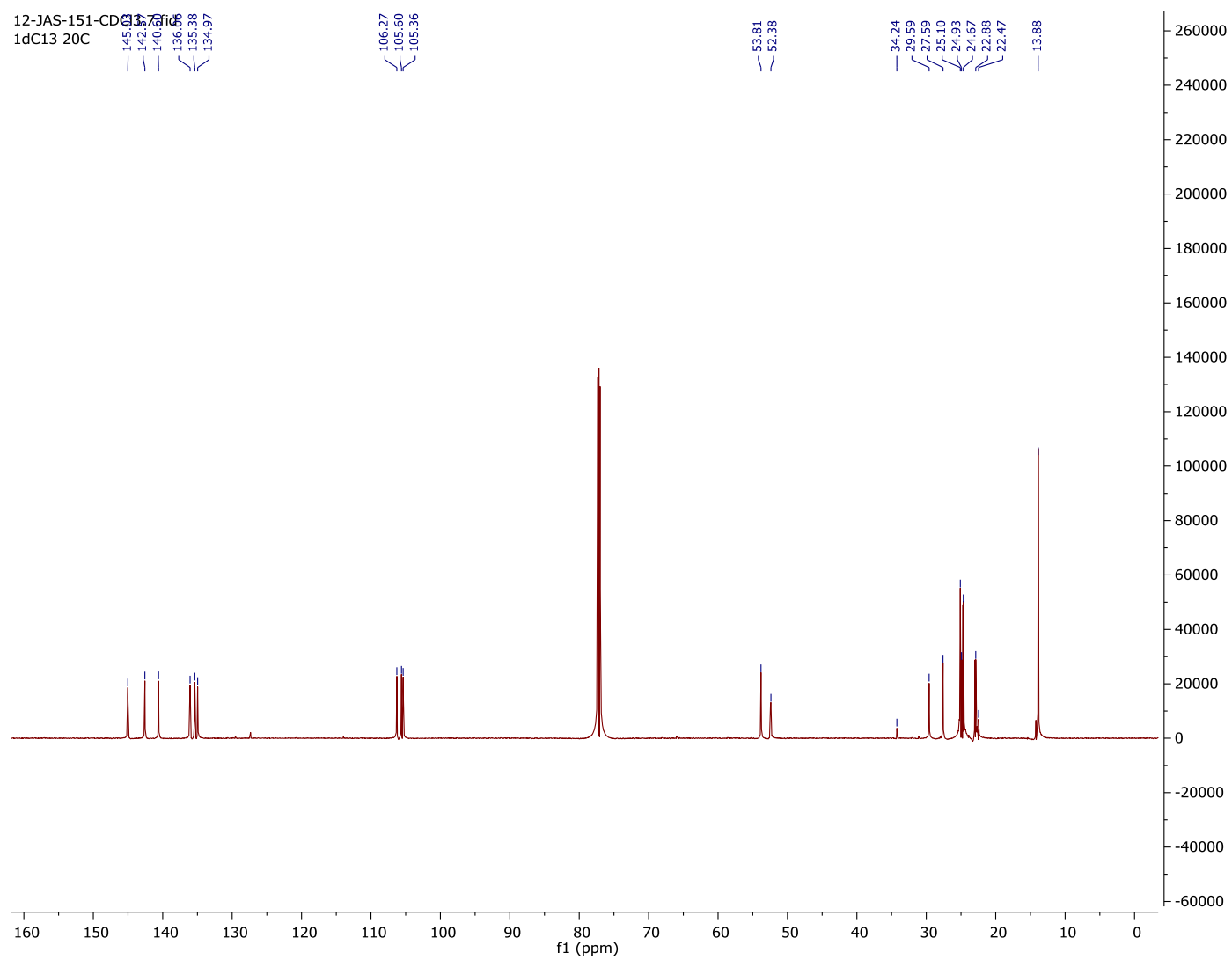




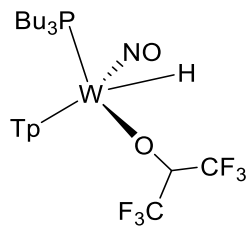
# $^{13}\text{C}\{^1\text{H}\}$ NMR Spectrum of 10



10

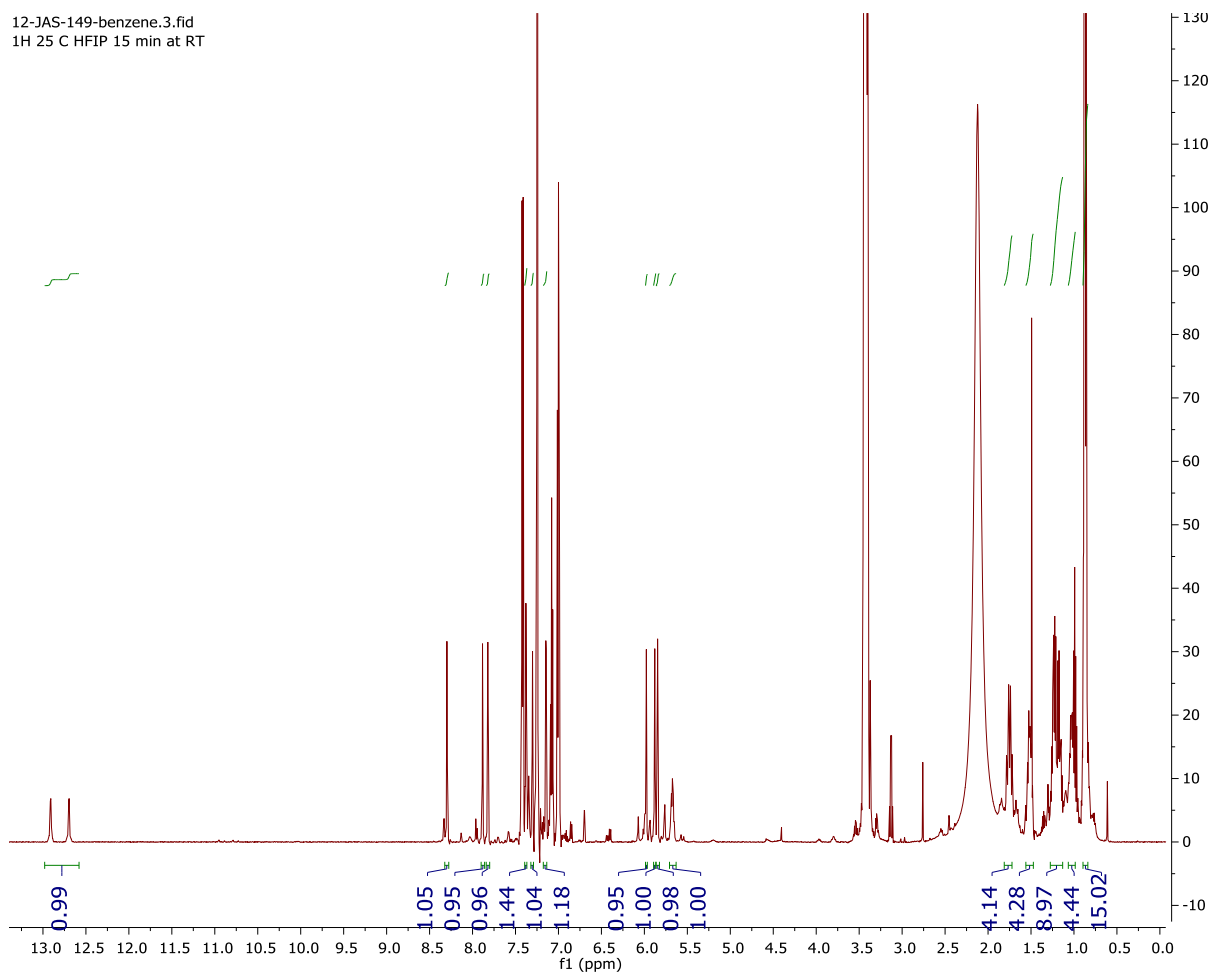


### <sup>1</sup>H NMR (*in situ*) of 11

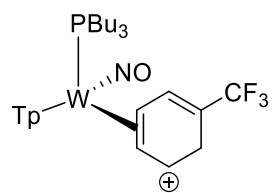


**11**

12-JAS-149-benzene.3.fid  
1H 25 C HFIP 15 min at RT

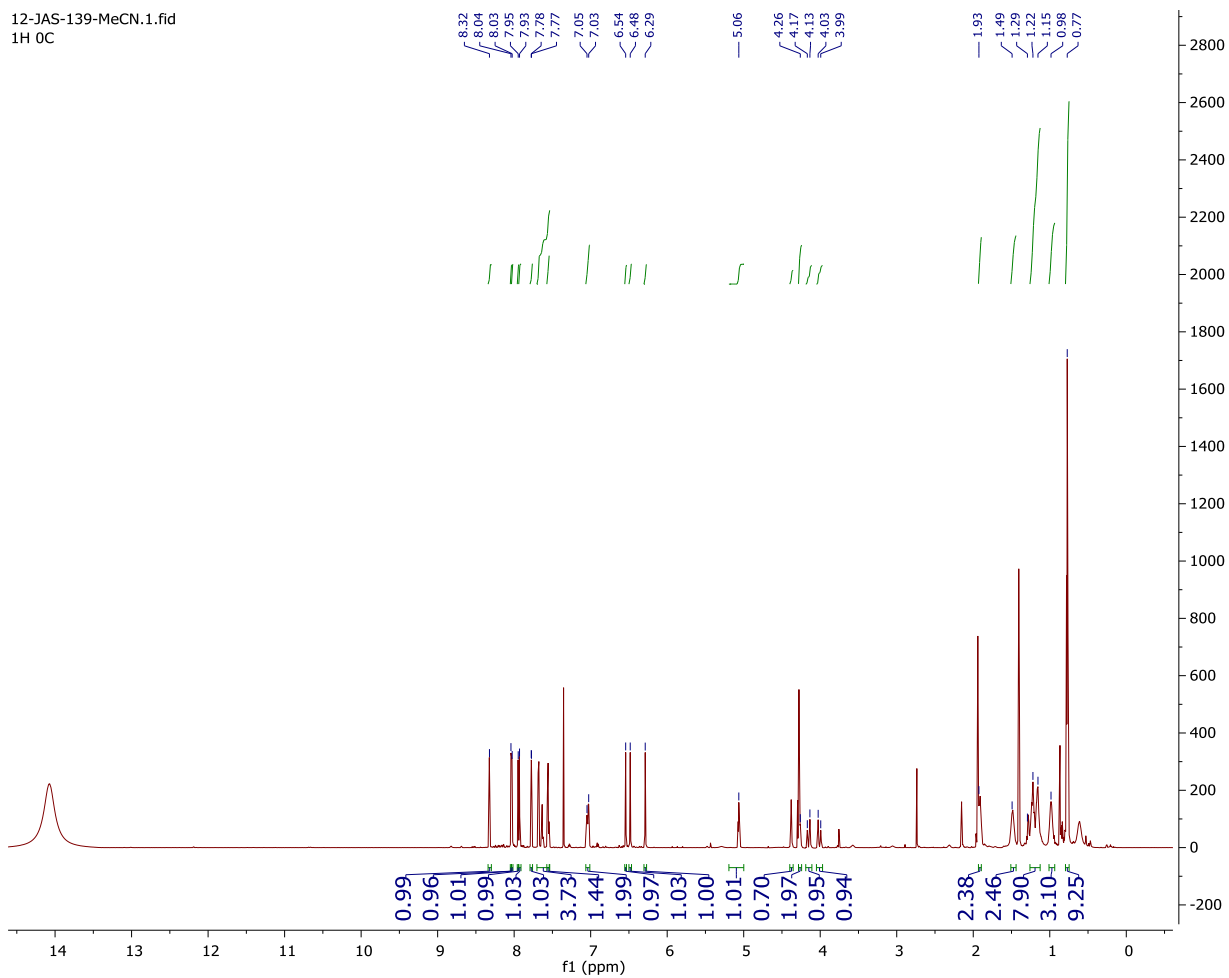


### <sup>1</sup>H NMR (*in situ*) of 12



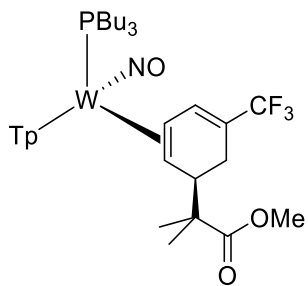
12

12-JAS-139-MeCN.1.fid  
1H OC

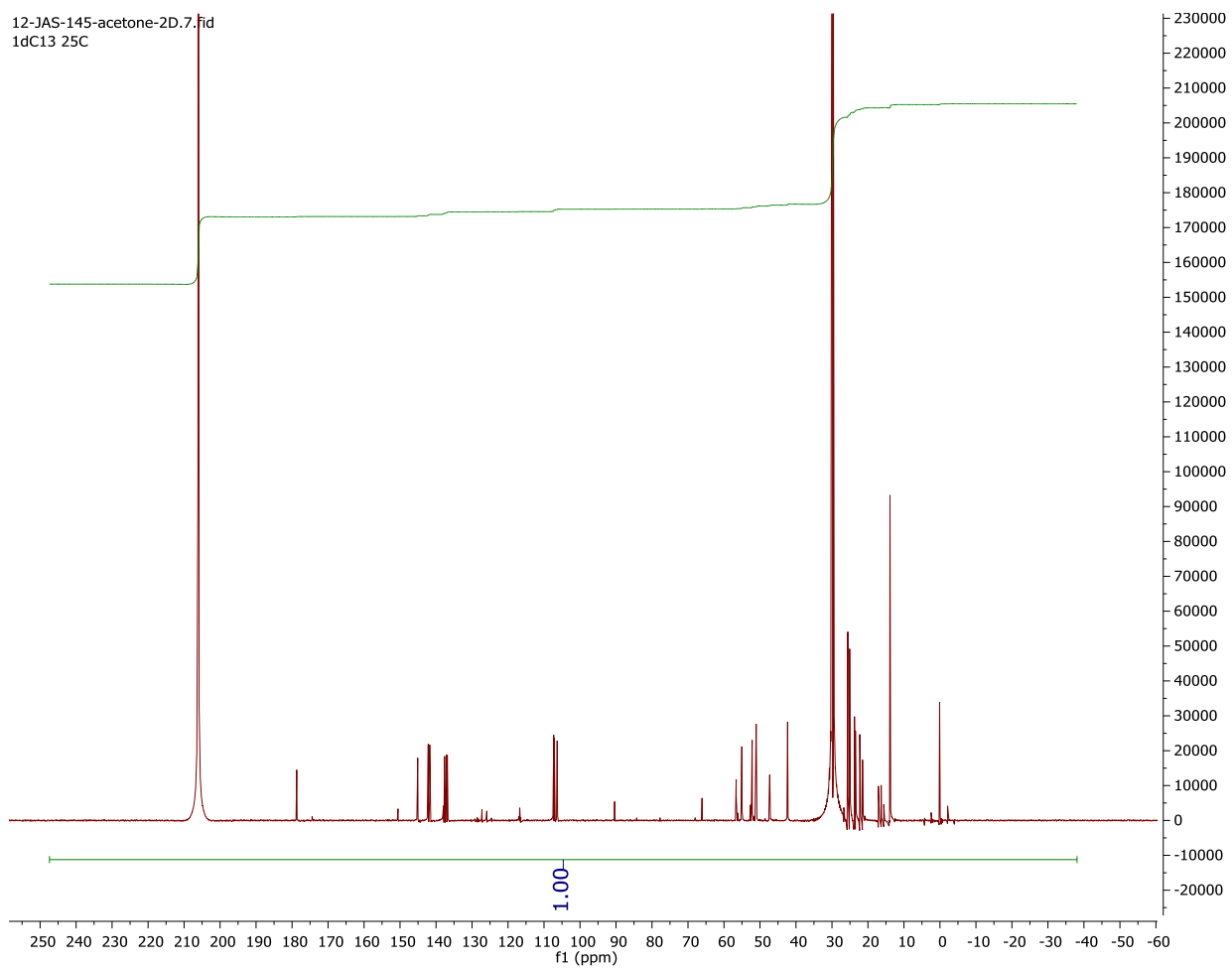




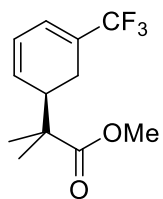
$^{13}\text{C}$   $\{^1\text{H}\}$  NMR of 13



13

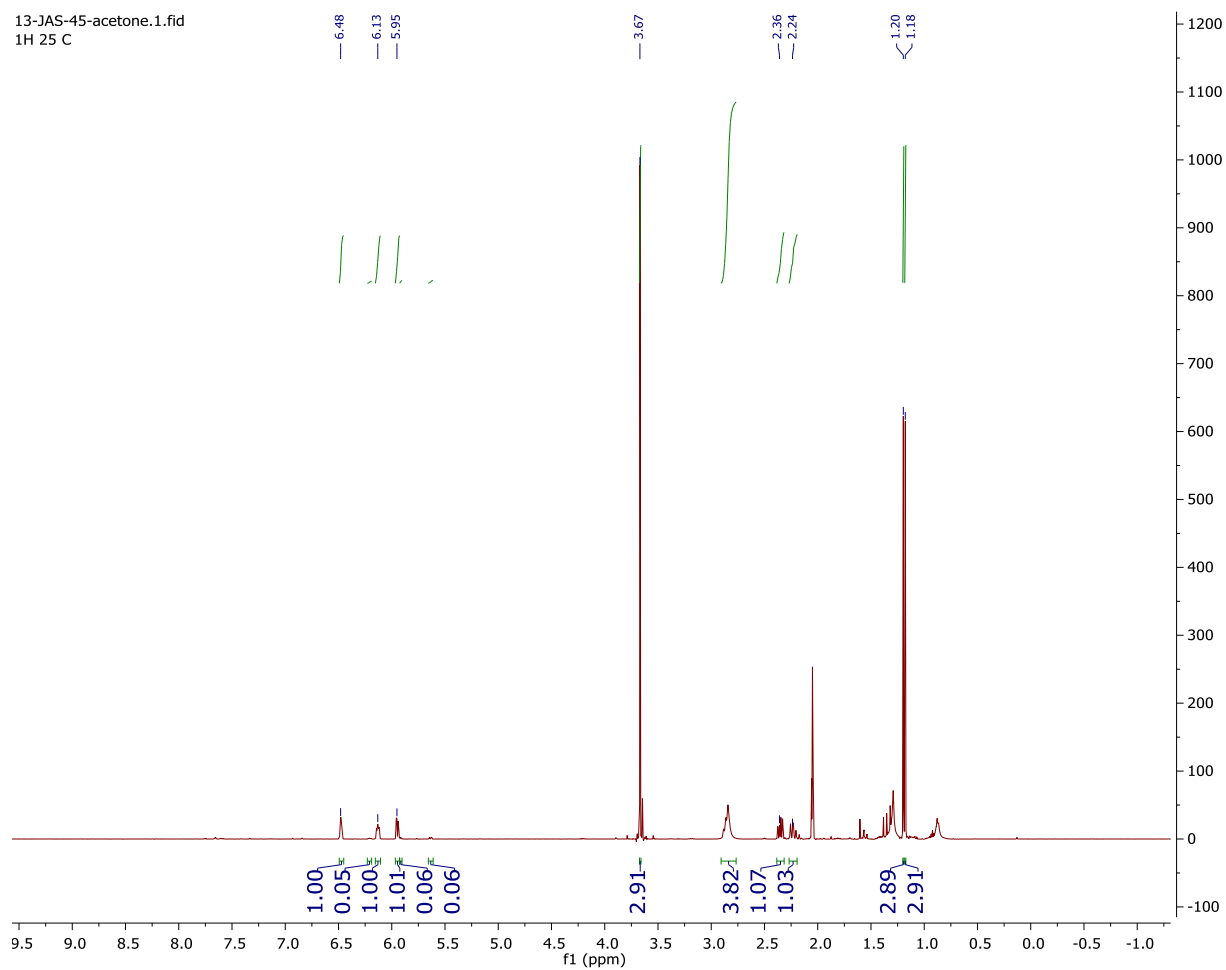


# <sup>1</sup>H NMR of 14

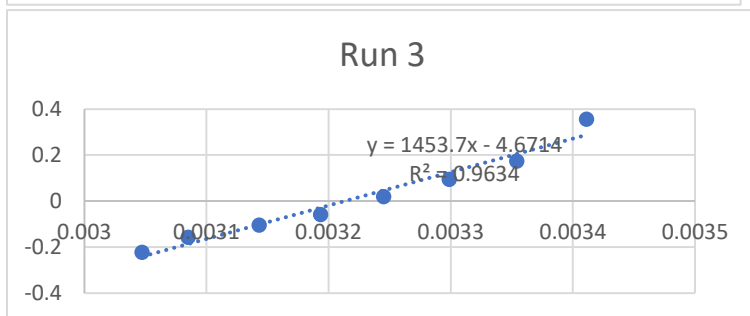
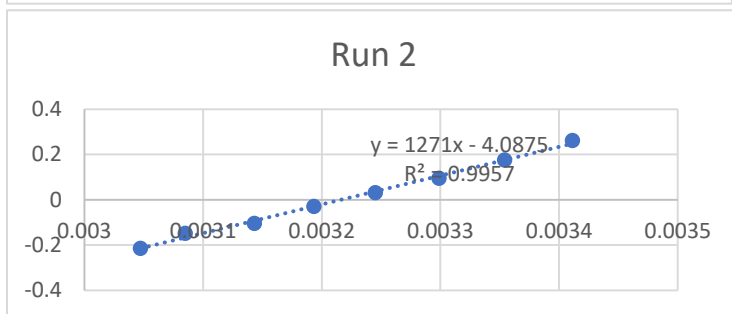
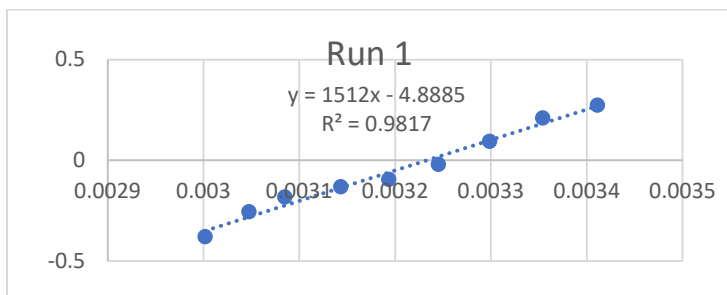
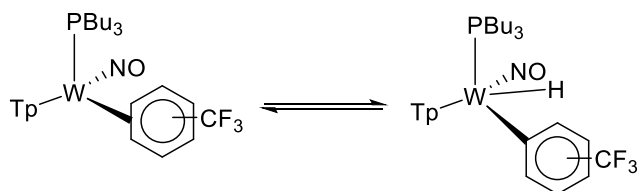


14

13-JAS-45-acetone.1.fid  
1H 25 C

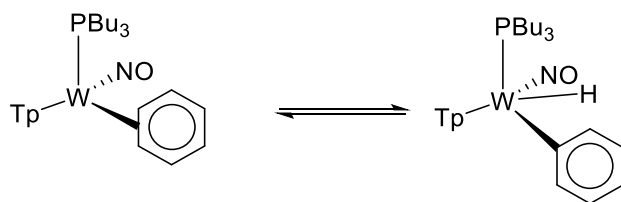


## Van't Hoff Plots for Reductive Elimination of 4 to 4H

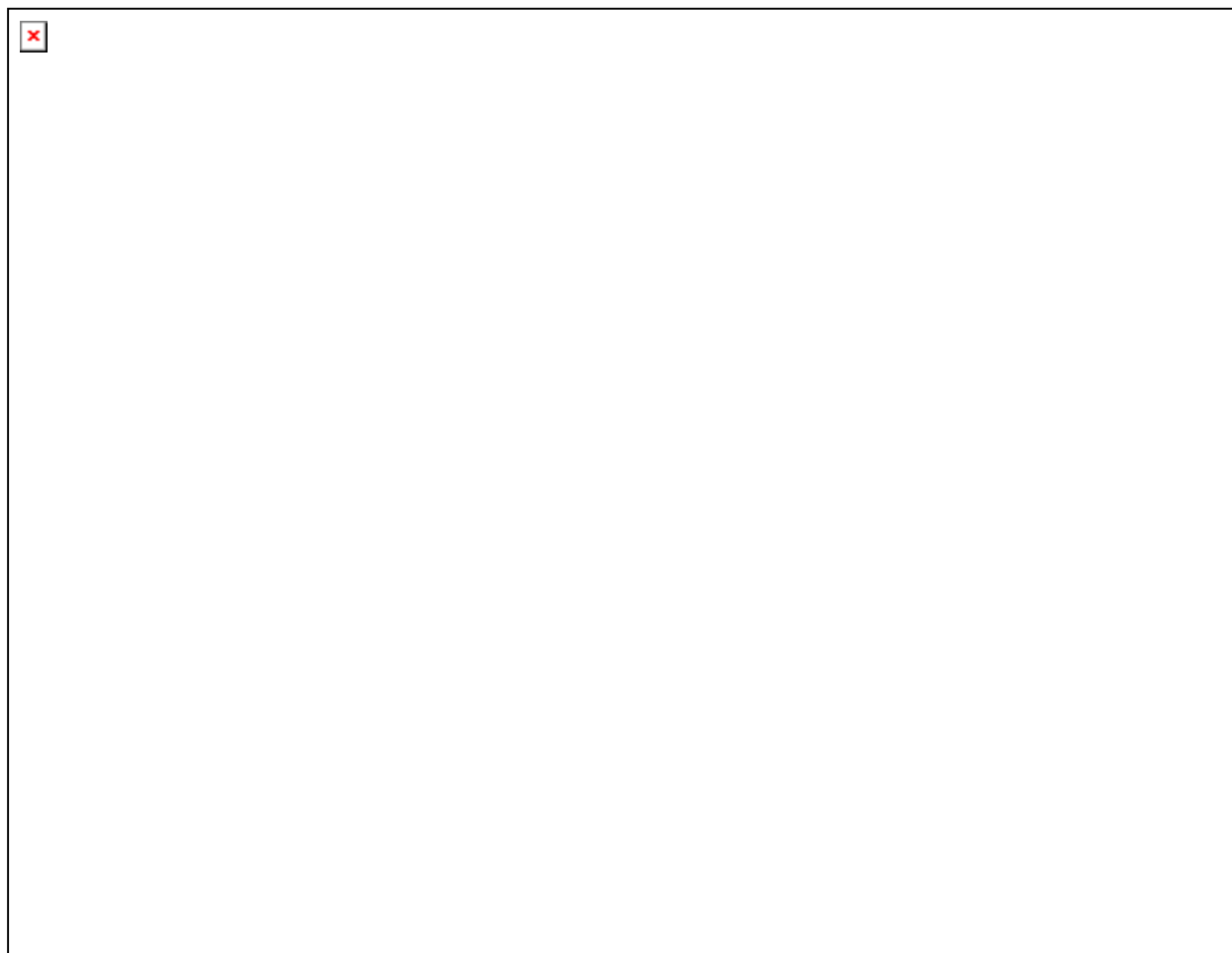


| STD Delta H | STD Delta S |
|-------------|-------------|
| 0.196694998 | 0.64856695  |
|             |             |
| AVG Delta H | AVG Delta S |
| -2.79855652 | -9.0156428  |

Figure S2B

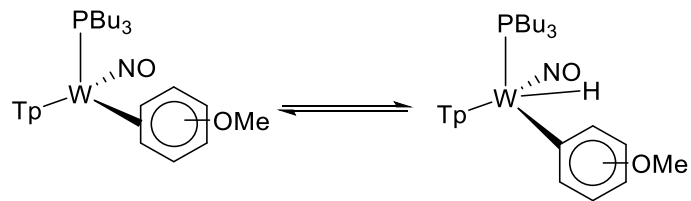


NOESY Illustrating Chemical Exchange Between **2** and **2H**

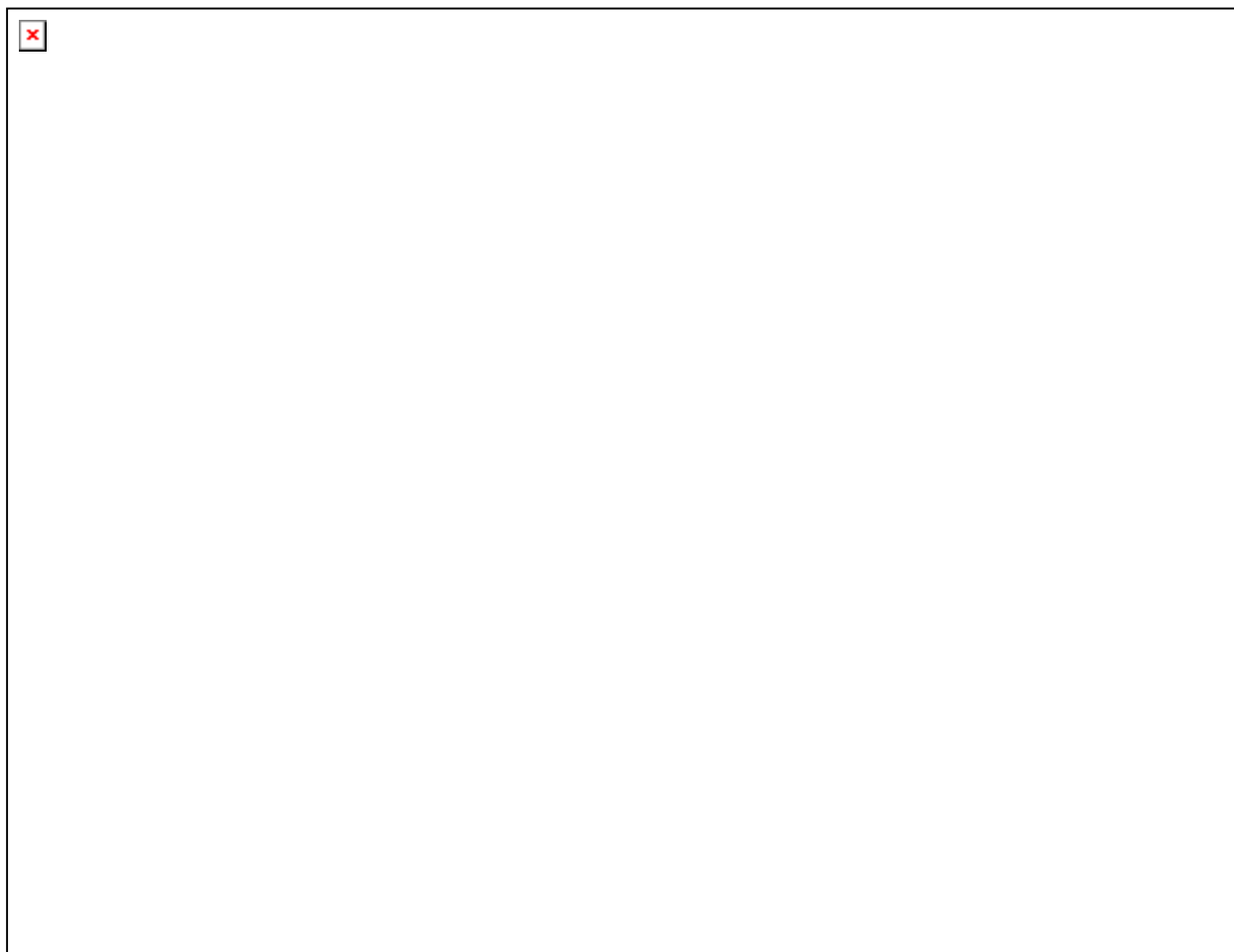


Blue off-diagonal peak resonances represent through space NOE interactions. Red off diagonal peaks show exchangeable protons between **2** and **2H** via a process that is active on the timescale of the NMR experiment.

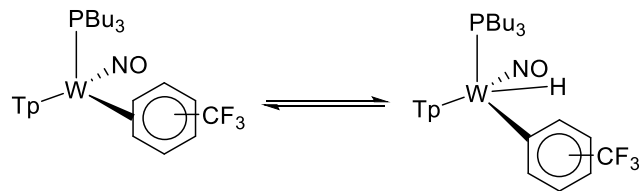




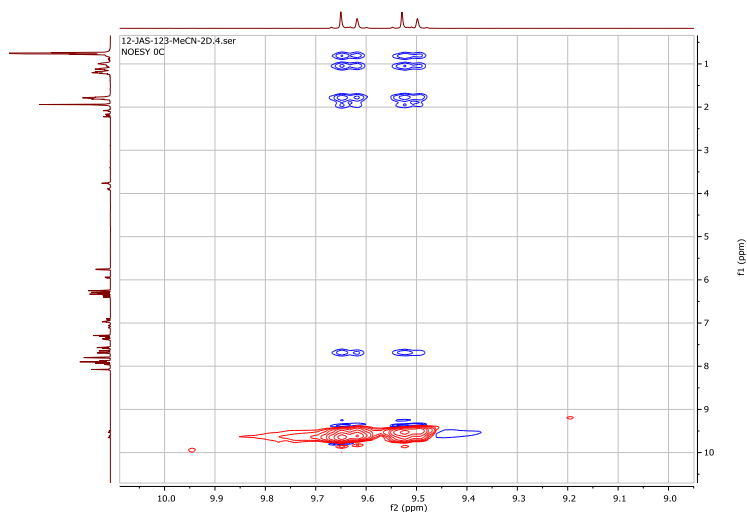
**NOESY Illustrating Chemical Exchange Between **3** and **3H****



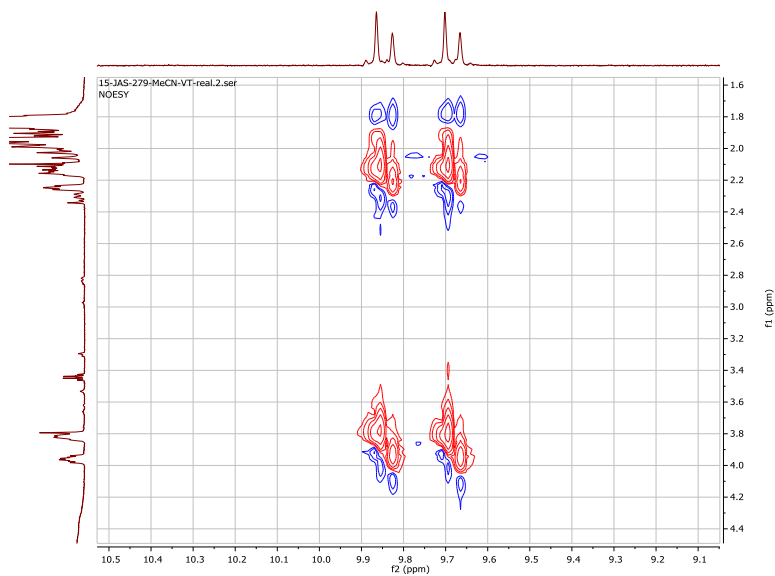
Blue off-diagonal peak resonances represent through space NOE interactions. Red off diagonal peaks show exchangeable protons between **3** and **3H** via a process that is active on the timescale of the NMR experiment.



### Variable Temperature NOESY Experiments of **4** and **4H** at 0 C



### Variable Temperature NOESY Experiments of **4** and **4H** at 50 C



Blue off-diagonal peak resonances represent through space NOE interactions. Red off diagonal peaks (bottom spectra, at 50 C) show exchangeable protons between **4** and **4H** via a process that is active on the timescale of the NMR experiment.

### C. Computational Details and Coordinates of Static Structures

**Table S1.** Thermochemical values for WTP(NO)(PMe<sub>3</sub>)-benzene. All values are given relative to structure **2** in kcal/mol.

|                      | M06/6-31g**[LANL2DZ] |      |      |      | M06/Def2-TZVPD <sup>a</sup> |
|----------------------|----------------------|------|------|------|-----------------------------|
|                      | ZPE                  | E    | H    | G    | SCF Energy                  |
| <b>2H</b>            | 3.4                  | 3.7  | 3.7  | 2.3  | 5.5                         |
| <b>TS1</b>           | 15.4                 | 15.6 | 15.6 | 13.9 | 16.3                        |
| <b>2σ</b>            | 14.0                 | 14.6 | 14.6 | 11.7 | 12.5                        |
| <b>TS2</b>           | 14.3                 | 14.5 | 14.5 | 12.7 | 15.1                        |
| <b>2</b>             | 0.0                  | 0.0  | 0.0  | 0.0  | 0.0                         |
| <b>TS3</b>           | 14.1                 | 14.5 | 14.5 | 12.1 | 15.1                        |
| <b>2π</b>            | 12.0                 | 12.8 | 12.8 | 8.0  | 11.1                        |
| <b>W-Ph rotation</b> | 12.8                 | 12.4 | 12.4 | 12.7 | -----                       |

<sup>a</sup>Geometry optimizations performed with 6-31g\*\* basis set

XYZ coordinates for static structures on the WTP(NO)(PMe<sub>3</sub>) energy surface.

#### **2H**

54

|   |             |             |             |
|---|-------------|-------------|-------------|
| W | -0.06739600 | -0.52200500 | -0.30812600 |
| N | -0.89740000 | 1.49713100  | -0.86908400 |
| C | -1.91490500 | 1.86093000  | -1.65321500 |
| N | -0.39000200 | 2.63166900  | -0.32466100 |
| C | -2.07592100 | 3.24815000  | -1.62718700 |
| H | -2.48684200 | 1.10593900  | -2.18081800 |
| C | -1.08386800 | 3.69531100  | -0.77177400 |
| B | 0.89257500  | 2.59896500  | 0.54275000  |
| H | -2.80821700 | 3.84091400  | -2.15728500 |
| H | -0.81509600 | 4.69459000  | -0.45181500 |

|   |             |             |             |
|---|-------------|-------------|-------------|
| N | 0.62857200  | 1.74964200  | 1.80151400  |
| N | 1.98116000  | 1.92258500  | -0.32463600 |
| H | 1.22517800  | 3.71035900  | 0.85082300  |
| C | 0.72367000  | 2.09895300  | 3.09729000  |
| N | 0.18786300  | 0.47190500  | 1.70032200  |
| C | 3.08501200  | 2.46289300  | -0.87398500 |
| N | 1.72396900  | 0.72502000  | -0.90306400 |
| C | 0.33413900  | 1.02040900  | 3.87374700  |
| H | 1.05762700  | 3.09185200  | 3.37240900  |
| C | 0.00473300  | 0.02725500  | 2.94926100  |
| C | 3.57321400  | 1.59185500  | -1.83294600 |
| H | 3.43453800  | 3.43595800  | -0.55139500 |
| C | 2.67507400  | 0.52178800  | -1.82045000 |
| H | 0.28918600  | 0.96497700  | 4.95232600  |
| H | -0.36700700 | -0.97782500 | 3.11509100  |
| H | 4.44527200  | 1.71876600  | -2.45891000 |
| H | 2.66539800  | -0.38032900 | -2.42192300 |
| P | 1.85054200  | -1.98554300 | 0.49300400  |
| C | 1.49023400  | -3.19036600 | 1.81591100  |
| H | 2.39831700  | -3.75014700 | 2.07075300  |
| H | 1.12739600  | -2.67242500 | 2.71012500  |
| H | 0.71655900  | -3.88606200 | 1.47413000  |
| C | 2.57349700  | -3.05443300 | -0.79828200 |
| H | 2.94652800  | -2.45611100 | -1.63564500 |
| H | 3.39847600  | -3.64531000 | -0.38226800 |
| H | 1.79698800  | -3.73174600 | -1.17149700 |
| N | -0.15268200 | -1.33114000 | -1.88338500 |
| O | -0.17843800 | -1.89157600 | -2.95588500 |
| C | 3.28398200  | -1.08627700 | 1.19341200  |
| H | 4.01340700  | -1.80521700 | 1.58553300  |

|   |             |             |             |
|---|-------------|-------------|-------------|
| H | 3.76750100  | -0.46648800 | 0.43175000  |
| H | 2.94342700  | -0.44036600 | 2.01230200  |
| C | -2.23815600 | -0.74567200 | 0.06691200  |
| C | -3.03193500 | -1.64297600 | -0.66974000 |
| C | -2.92290500 | 0.05019500  | 1.00319000  |
| C | -4.41180700 | -1.74015800 | -0.49319800 |
| H | -2.55831800 | -2.28690200 | -1.41358100 |
| C | -4.30112200 | -0.04253200 | 1.19516400  |
| H | -2.37070800 | 0.78680400  | 1.59171000  |
| C | -5.05766500 | -0.94054500 | 0.44657600  |
| H | -4.98498000 | -2.44616600 | -1.09403100 |
| H | -4.78777700 | 0.59759800  | 1.93097800  |
| H | -6.13404300 | -1.01438600 | 0.59169600  |
| H | -0.52100500 | -1.91535500 | 0.58598200  |

## TS1

54

|   |            |             |             |
|---|------------|-------------|-------------|
| W | 0.05231200 | -0.00459900 | -0.46780900 |
| P | 1.37207000 | 1.84636900  | 0.46704300  |
| C | 1.97958800 | 3.02371600  | -0.80081400 |
| H | 1.13950100 | 3.41447300  | -1.38567000 |
| H | 2.51406400 | 3.85985200  | -0.33312000 |
| H | 2.65747100 | 2.50077400  | -1.48559200 |
| C | 2.91514700 | 1.60261300  | 1.44503000  |
| H | 3.32164200 | 2.57380800  | 1.75473500  |
| H | 2.71339000 | 1.00529500  | 2.34156000  |
| H | 3.66247600 | 1.08110500  | 0.83587900  |
| C | 0.44436100 | 2.95394600  | 1.60615400  |
| H | 1.07447900 | 3.78629500  | 1.94391500  |

|   |             |             |             |
|---|-------------|-------------|-------------|
| H | -0.44038500 | 3.35585400  | 1.09942100  |
| H | 0.10876600  | 2.38335100  | 2.48063200  |
| N | 0.50101400  | 0.47290900  | -2.11427300 |
| O | 0.82895500  | 0.84512200  | -3.22980800 |
| N | -1.72821700 | 1.23736800  | -0.43643800 |
| N | -0.62298600 | -0.47320300 | 1.68136500  |
| N | -1.45176300 | -1.59771300 | -0.91803000 |
| N | -2.87911800 | 0.82446100  | 0.15519300  |
| N | -1.93953700 | -0.66070100 | 1.94243200  |
| N | -2.64362000 | -1.62569200 | -0.26880100 |
| C | -1.98660400 | 2.43065900  | -0.98815600 |
| H | -1.20267600 | 2.95890100  | -1.51942400 |
| C | -3.31342100 | 2.80192500  | -0.74891100 |
| H | -3.81398400 | 3.70775300  | -1.06167000 |
| C | -3.84124400 | 1.75487400  | -0.01689600 |
| H | -4.82970300 | 1.59915700  | 0.39733900  |
| C | -3.40010400 | -2.63680300 | -0.74099200 |
| H | -4.38652800 | -2.81807800 | -0.33181200 |
| C | -2.69081600 | -3.28873100 | -1.73350000 |
| H | -3.00499000 | -4.14235000 | -2.31802800 |
| C | -1.47501400 | -2.60114200 | -1.80311400 |
| H | -0.61486800 | -2.77682800 | -2.43972200 |
| C | -2.12050800 | -0.87849500 | 3.25726500  |
| H | -3.11531700 | -1.04563900 | 3.65181600  |
| C | -0.88663100 | -0.83747100 | 3.88461800  |
| H | -0.67387600 | -0.97523400 | 4.93551800  |
| C | 0.01769600  | -0.58029400 | 2.85168900  |
| H | 1.09582000  | -0.46788300 | 2.89150600  |
| B | -2.98241900 | -0.57105400 | 0.80578200  |
| H | -4.08864800 | -0.75149700 | 1.23957800  |

|   |            |             |             |
|---|------------|-------------|-------------|
| C | 2.28313500 | -1.29454200 | -0.29984300 |
| C | 2.70229200 | -1.90335100 | 0.88904500  |
| C | 4.05864100 | -1.99732600 | 1.18720300  |
| C | 5.00694900 | -1.51755700 | 0.28629500  |
| C | 4.59355300 | -0.96271300 | -0.92760700 |
| C | 3.24161600 | -0.86776900 | -1.23083500 |
| H | 1.95975300 | -2.29450200 | 1.58362000  |
| H | 4.37777200 | -2.45410100 | 2.12200800  |
| H | 6.06739800 | -1.59452000 | 0.51665100  |
| H | 5.33354100 | -0.60627100 | -1.64167700 |
| H | 2.91685400 | -0.43886000 | -2.17813200 |
| H | 1.23410500 | -1.57302900 | -0.66749900 |

**2σ**

54

|   |             |            |             |
|---|-------------|------------|-------------|
| W | -0.02808100 | 0.08932500 | -0.42377300 |
| P | 1.21673200  | 1.95864100 | 0.50854500  |
| C | 1.83512700  | 3.14831100 | -0.74481200 |
| H | 1.00304200  | 3.53056600 | -1.34672200 |
| H | 2.35306700  | 3.98945400 | -0.26738300 |
| H | 2.53122100  | 2.63028900 | -1.41548700 |
| C | 2.76085300  | 1.72866600 | 1.50051400  |
| H | 3.16597400  | 2.69345700 | 1.83401700  |
| H | 2.55822200  | 1.10947900 | 2.38263500  |
| H | 3.51396800  | 1.21917900 | 0.88525700  |
| C | 0.27595600  | 3.05950100 | 1.64810100  |
| H | 0.89257000  | 3.89826100 | 1.99579800  |
| H | -0.60815300 | 3.45298400 | 1.13263900  |
| H | -0.06385200 | 2.48369300 | 2.51774000  |

|   |             |             |             |
|---|-------------|-------------|-------------|
| N | 0.46199700  | 0.54892500  | -2.06821800 |
| O | 0.83106700  | 0.87892500  | -3.18811000 |
| N | -1.86360800 | 1.18421200  | -0.43843600 |
| N | -0.66089900 | -0.49601200 | 1.68211900  |
| N | -1.36511100 | -1.61639600 | -0.93762800 |
| N | -2.98647300 | 0.66235500  | 0.13075200  |
| N | -1.96358800 | -0.77962100 | 1.92580000  |
| N | -2.55747800 | -1.76156400 | -0.30461900 |
| C | -2.22035600 | 2.35589700  | -0.98558400 |
| H | -1.47631500 | 2.95969700  | -1.49261800 |
| C | -3.58114200 | 2.60098200  | -0.77088100 |
| H | -4.15452000 | 3.46175800  | -1.08631800 |
| C | -4.02548600 | 1.50889900  | -0.05212300 |
| H | -5.00107800 | 1.26677500  | 0.35077400  |
| C | -3.21530700 | -2.82986700 | -0.80122000 |
| H | -4.18672700 | -3.10501900 | -0.40882600 |
| C | -2.43823700 | -3.39918100 | -1.79363800 |
| H | -2.66804200 | -4.26820300 | -2.39468700 |
| C | -1.28826500 | -2.60319200 | -1.83896000 |
| H | -0.41021300 | -2.68893100 | -2.46989400 |
| C | -2.12509400 | -1.10782600 | 3.21976900  |
| H | -3.10619300 | -1.36353500 | 3.60111000  |
| C | -0.89241600 | -1.04281800 | 3.84894700  |
| H | -0.66919400 | -1.24474600 | 4.88722800  |
| C | -0.00817500 | -0.65545300 | 2.83948100  |
| H | 1.06219400  | -0.48401600 | 2.88430400  |
| B | -2.99384200 | -0.74240900 | 0.77013100  |
| H | -4.09092100 | -1.00819400 | 1.18363800  |
| C | 2.68487100  | -1.76118600 | -0.39427300 |
| C | 3.26439500  | -2.19477900 | 0.79641600  |



|   |            |             |             |
|---|------------|-------------|-------------|
| C | 4.57638000 | -1.83533900 | 1.09801600  |
| C | 5.30056100 | -1.03840000 | 0.21339100  |
| C | 4.71495200 | -0.59554600 | -0.97199000 |
| C | 3.40331500 | -0.95303900 | -1.27632900 |
| H | 2.69363400 | -2.81452300 | 1.48571100  |
| H | 5.03564700 | -2.17668700 | 2.02344000  |
| H | 6.32541500 | -0.75917800 | 0.44960400  |
| H | 5.28095000 | 0.03227900  | -1.65720600 |
| H | 2.93164900 | -0.59533100 | -2.19107300 |
| H | 1.64984500 | -2.03557000 | -0.63574200 |

## TS2

54

|   |             |             |             |
|---|-------------|-------------|-------------|
| W | -0.35315200 | -0.08586600 | -0.27453400 |
| N | 0.80329200  | 1.80408800  | -0.53750200 |
| C | 0.51765800  | 2.96144300  | -1.14459000 |
| N | 2.10014300  | 1.88327000  | -0.14165500 |
| C | 1.63522700  | 3.80559900  | -1.14348600 |
| H | -0.47660500 | 3.12799100  | -1.54336500 |
| C | 2.61653700  | 3.08041500  | -0.49469000 |
| B | 2.81783800  | 0.64632600  | 0.43371800  |
| H | 1.71379400  | 4.80297300  | -1.55396900 |
| H | 3.64523700  | 3.32258700  | -0.25720900 |
| N | 2.11166500  | 0.19143800  | 1.73013600  |
| N | 2.70090200  | -0.48659400 | -0.60914900 |
| H | 3.97334500  | 0.89410800  | 0.65627200  |
| C | 2.61286200  | 0.03992500  | 2.96900400  |
| N | 0.80944600  | -0.18284900 | 1.70687600  |
| C | 3.68263100  | -1.10793900 | -1.29894600 |

|   |             |             |             |
|---|-------------|-------------|-------------|
| N | 1.48681400  | -0.91031200 | -1.05188200 |
| C | 1.61094900  | -0.44605000 | 3.79216600  |
| H | 3.64711000  | 0.28751800  | 3.17463800  |
| C | 0.50248400  | -0.56878100 | 2.95110700  |
| C | 3.10078700  | -1.95182400 | -2.22532500 |
| H | 4.72139200  | -0.90245400 | -1.07173400 |
| C | 1.72418300  | -1.79528300 | -2.03112400 |
| H | 1.67451900  | -0.67761700 | 4.84623300  |
| H | -0.49865400 | -0.91627800 | 3.18249000  |
| H | 3.59860700  | -2.59736400 | -2.93572700 |
| H | 0.89366800  | -2.27740000 | -2.53437500 |
| P | -1.17460300 | -2.34086100 | 0.19739400  |
| C | -2.44706400 | -2.73743600 | 1.48115300  |
| H | -2.65577700 | -3.81494000 | 1.49419400  |
| H | -2.09361900 | -2.44041000 | 2.47614100  |
| H | -3.38066900 | -2.20274600 | 1.26845100  |
| C | -1.93592800 | -3.17040000 | -1.25254300 |
| H | -1.22950900 | -3.19141100 | -2.08984900 |
| H | -2.23132300 | -4.19753700 | -1.00496200 |
| H | -2.82143300 | -2.60753800 | -1.56988400 |
| N | -1.17167100 | -0.10077300 | -1.84848100 |
| O | -1.73148100 | -0.15078300 | -2.93150600 |
| C | -2.94726200 | 3.10967200  | -0.08716500 |
| C | -3.47783900 | 1.89142000  | -0.50592000 |
| C | -3.17109500 | 0.72044300  | 0.18981000  |
| C | -2.32611700 | 0.76211000  | 1.31095900  |
| C | -1.75660100 | 1.99274400  | 1.68716200  |
| C | -2.07643800 | 3.16054800  | 0.99964900  |
| H | -3.20264000 | 4.02321800  | -0.62099700 |
| H | -4.14443900 | 1.84935100  | -1.36442100 |

|   |             |             |             |
|---|-------------|-------------|-------------|
| H | -3.63158600 | -0.22148400 | -0.10463700 |
| H | -2.24209900 | -0.10166000 | 1.96483000  |
| H | -1.09877700 | 2.03344600  | 2.55361700  |
| H | -1.64378800 | 4.10911600  | 1.31030700  |
| C | 0.12271200  | -3.55574500 | 0.68220100  |
| H | -0.30391300 | -4.55686900 | 0.82335400  |
| H | 0.89537200  | -3.60070800 | -0.09417900 |
| H | 0.59647900  | -3.23530300 | 1.61795000  |

**2**

54

|   |             |             |             |
|---|-------------|-------------|-------------|
| W | 0.39200200  | 0.17527900  | 0.12394300  |
| N | -1.11118700 | 1.84866900  | 0.15672400  |
| C | -1.01844000 | 3.13799100  | 0.49175800  |
| N | -2.42001700 | 1.60565600  | -0.11093000 |
| C | -2.27519600 | 3.74918400  | 0.43831500  |
| H | -0.05411300 | 3.55829000  | 0.75345800  |
| C | -3.13452200 | 2.73717700  | 0.05223600  |
| B | -2.93398200 | 0.17116000  | -0.38001100 |
| H | -2.52070600 | 4.78053400  | 0.65028500  |
| H | -4.20403600 | 2.73515400  | -0.11866000 |
| N | -2.21767800 | -0.39947900 | -1.61897200 |
| N | -2.56646600 | -0.67355600 | 0.86192500  |
| H | -4.12288500 | 0.17370400  | -0.55036700 |
| C | -2.75476200 | -0.86741800 | -2.76010000 |
| N | -0.86391100 | -0.44216800 | -1.69051400 |
| C | -3.37030200 | -1.23882300 | 1.78340600  |
| N | -1.28802500 | -0.67544100 | 1.30735900  |
| C | -1.72715600 | -1.22990300 | -3.61317800 |

|   |             |             |             |
|---|-------------|-------------|-------------|
| H | -3.83016900 | -0.90287000 | -2.88346800 |
| C | -0.56422700 | -0.94010100 | -2.89659500 |
| C | -2.59609200 | -1.62889800 | 2.86251400  |
| H | -4.43669500 | -1.30951000 | 1.60767400  |
| C | -1.29746000 | -1.24262200 | 2.51854300  |
| H | -1.80793400 | -1.63790900 | -4.61090600 |
| H | 0.46989100  | -1.06475900 | -3.19694100 |
| H | -2.92517900 | -2.11413400 | 3.77078000  |
| H | -0.37233900 | -1.34611400 | 3.07503200  |
| P | 1.16289300  | -2.22557200 | 0.11351900  |
| C | 2.17621600  | -2.91030300 | -1.25278000 |
| H | 2.36587300  | -3.97328100 | -1.06048300 |
| H | 1.64183700  | -2.81754400 | -2.20484200 |
| H | 3.13623300  | -2.39123400 | -1.33281200 |
| C | 2.14351100  | -2.70085000 | 1.58192300  |
| H | 1.56862100  | -2.50409600 | 2.49353800  |
| H | 2.41198400  | -3.76366500 | 1.54693500  |
| H | 3.05726200  | -2.09588600 | 1.61552000  |
| N | 1.27490100  | 0.57945800  | 1.60185000  |
| O | 1.85084000  | 0.81883400  | 2.64374600  |
| C | 2.09203200  | 2.77872200  | -0.71224700 |
| C | 3.31022700  | 2.71476700  | -0.11537000 |
| C | 4.03276600  | 1.47089500  | -0.08293100 |
| C | 3.51303700  | 0.35901300  | -0.66374700 |
| C | 2.18239400  | 0.33796300  | -1.24707900 |
| C | 1.43422900  | 1.59916100  | -1.24244300 |
| H | 1.59843700  | 3.74372500  | -0.83441400 |
| H | 3.77642800  | 3.61431100  | 0.28397000  |
| H | 5.03108600  | 1.44488400  | 0.35175600  |
| H | 4.11998500  | -0.54659100 | -0.72552400 |

|   |             |             |             |
|---|-------------|-------------|-------------|
| H | 2.06274400  | -0.33626000 | -2.09915600 |
| H | 0.73003900  | 1.77810200  | -2.06131100 |
| C | -0.21775900 | -3.43741000 | 0.11355600  |
| H | 0.17589300  | -4.45988500 | 0.06460300  |
| H | -0.82928800 | -3.33323500 | 1.01571900  |
| H | -0.85564300 | -3.25846600 | -0.76168100 |

**TS3**

54

|   |             |             |             |
|---|-------------|-------------|-------------|
| W | 0.26109900  | 0.27031000  | -0.31680900 |
| N | 0.04513300  | -1.93474500 | -0.61305100 |
| C | 0.77749700  | -2.83830200 | -1.27511700 |
| N | -1.06421800 | -2.58342400 | -0.17270500 |
| C | 0.14403200  | -4.08690100 | -1.26556800 |
| H | 1.72372200  | -2.54437200 | -1.71560000 |
| C | -1.02143900 | -3.87835700 | -0.55249300 |
| B | -2.21454500 | -1.80230700 | 0.49333000  |
| H | 0.48944400  | -5.00938800 | -1.71176600 |
| H | -1.82646300 | -4.55240200 | -0.28627400 |
| N | -1.69799100 | -1.12162300 | 1.78045100  |
| N | -2.66986800 | -0.70533300 | -0.49300500 |
| H | -3.12972500 | -2.53844300 | 0.75169700  |
| C | -2.14233500 | -1.23739900 | 3.04453600  |
| N | -0.68220500 | -0.22575000 | 1.72474200  |
| C | -3.86394000 | -0.56221100 | -1.10977300 |
| N | -1.79662500 | 0.22849700  | -0.95690700 |
| C | -1.39704300 | -0.39408800 | 3.85132500  |
| H | -2.95730300 | -1.91152700 | 3.27824700  |
| C | -0.49731700 | 0.21620200  | 2.97444200  |
| C | -3.77031000 | 0.48227200  | -2.00910200 |

|   |             |             |             |
|---|-------------|-------------|-------------|
| H | -4.68992600 | -1.21428600 | -0.85417300 |
| C | -2.45782800 | 0.94800200  | -1.87548500 |
| H | -1.49126800 | -0.24424300 | 4.91780400  |
| H | 0.27322300  | 0.95007100  | 3.18459700  |
| H | -4.54291000 | 0.86276800  | -2.66299000 |
| H | -1.95630100 | 1.76467900  | -2.38229600 |
| P | 0.05572300  | 2.63294800  | 0.25737100  |
| C | 1.11317700  | 3.49506800  | 1.50821200  |
| H | 0.83964500  | 4.55581800  | 1.57934300  |
| H | 0.98737500  | 3.03801800  | 2.49740400  |
| H | 2.16996400  | 3.42419800  | 1.22335500  |
| C | 0.28935400  | 3.76600800  | -1.16811300 |
| H | -0.40835200 | 3.51052200  | -1.97334500 |
| H | 0.12865700  | 4.80945600  | -0.86989900 |
| H | 1.30914100  | 3.65523400  | -1.55507500 |
| N | 0.87676200  | 0.69115700  | -1.92649200 |
| O | 1.28558500  | 1.01156200  | -3.03066900 |
| C | 3.29940400  | -2.04986200 | 1.02387100  |
| C | 3.88990900  | -1.73785000 | -0.20521900 |
| C | 3.78875900  | -0.45426600 | -0.72347900 |
| C | 3.12090200  | 0.54498900  | -0.00215600 |
| C | 2.54240300  | 0.24402300  | 1.23753700  |
| C | 2.62245400  | -1.07046500 | 1.73495000  |
| H | 3.37061700  | -3.06026900 | 1.42075700  |
| H | 4.42281500  | -2.50694600 | -0.76108400 |
| H | 4.24272000  | -0.21113900 | -1.68191500 |
| H | 3.11364600  | 1.56734100  | -0.37566200 |
| H | 2.15069800  | 1.03949600  | 1.86613700  |
| H | 2.17615200  | -1.30516800 | 2.69960200  |
| C | -1.60404100 | 3.14403700  | 0.87341600  |

|   |             |            |            |
|---|-------------|------------|------------|
| H | -1.64384700 | 4.22454600 | 1.06085900 |
| H | -2.36929400 | 2.87869400 | 0.13458500 |
| H | -1.83029300 | 2.61237700 | 1.80574600 |

Energies are reported for lowest energy diastereomers. Additional diastereomers of the aryl hydride and  $\eta^2$ -benzene complex are shown below for comparison.

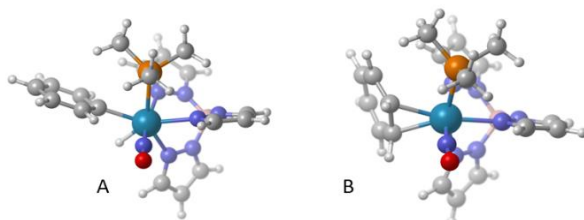


**Figure S1C.** Geometry of aryl hydride (A) and  $\eta^2$ -benzene diastereomers.

**Table S2.** Thermochemical values for WTp(NO)(PMe<sub>3</sub>)-benzene diastereomers. Values given relative to structure **2** in kcal/mol.

|          | ZPE | E   | H   | G   |
|----------|-----|-----|-----|-----|
| <b>A</b> | 9.2 | 9.4 | 9.4 | 7.9 |
| <b>B</b> | 3.0 | 3.1 | 3.1 | 2.6 |

Results from energy decomposition analysis calculations performed in QChem. Calculations were done using the ALMO-EDA (EDA2) method at the M06/6-31g\*\*[LANL2DZ] level of theory with the SMD model for implicit acetone solvation.

**Table S3.** Energy Decomposition Analysis (kcal/mol)

|                                | $\eta^2$ -benzene complex ( <b>2</b> ) | Weak coordination complex ( <b>2<math>\pi</math></b> ) |
|--------------------------------|--|--|
| Preparation                    | 0.00                                   | 0.00   |
| Solvation                      | -1.06                                  | 0.19   |
| Frozen (includes dispersion)   | 56.95                                  | -5.61  |
| Classical Frozen Decomposition |  |  |
| Electrostatics                 | -103.08                                | -4.68  |
| Pauli Repulsion                | 188.50                                 | 9.17   |
| Dispersion                     | -28.48                                 | -10.10   |
| Polarization                   | -15.45                                 | -0.76  |
| Charge Transfer                | -103.49                                | -8.29  |
| Total                          | -63.06                                 | -14.46   |

Static intermediates were located for WTP(NO)(Bu<sub>3</sub>) complex; optimization and frequency calculations were performed using M06/6-31g\*\*[LANL2DZ]. XYZ coordinates of intermediate structures are given below and thermochemical values are shown in Table S4. Experimentally, the aryl hydride was observed to exist in a 1:1 equilibrium with the  $\eta^2$ -complex; however, the computed energy difference for WTP(NO)(PMe<sub>3</sub>) did not reflect this as the computed energy gap was 3.4 kcal/mol. For WTP(NO)(Bu<sub>3</sub>), the energy gap is similar, but on the free energy surface the gap is 1.5 kcal/mol, which comes closer to representing the experimentally observed equilibrium.

**Table S4.** Thermochemical values for WTP(NO)(PBu<sub>3</sub>)-benzene intermediates, values are given relative to **2-butyl** in kcal/mol.

|  | ZPE | E | H | G |
|--|-----|---|---|---|
|--|-----|---|---|---|



|                 |      |      |      |      |
|-----------------|------|------|------|------|
| <b>2H-butyl</b> | 3.5  | 3.9  | 3.9  | 1.5  |
| <b>2σ-butyl</b> | 12.2 | 12.9 | 12.9 | 9.6  |
| <b>2-butyl</b>  | 0.0  | 0.0  | 0.0  | 0.0  |
| <b>2π-butyl</b> | 16.5 | 17.1 | 17.1 | 13.6 |

XYZ coordinated for WTP(NO)(PBu<sub>3</sub>)-benzene intermediates.

### 2H-butyl

81

|   |            |             |             |
|---|------------|-------------|-------------|
| W | 0.42371100 | 0.28171900  | -0.53924600 |
| N | 2.46035900 | -0.34046500 | -1.24709800 |
| C | 3.33470000 | 0.26041500  | -2.05794100 |
| N | 3.05141600 | -1.47423000 | -0.79621800 |
| C | 4.51178700 | -0.48722000 | -2.14115900 |
| H | 3.07786900 | 1.20385500  | -2.52645600 |
| C | 4.28453600 | -1.58208300 | -1.32519100 |
| B | 2.26345200 | -2.48525500 | 0.06808200  |
| H | 5.39977300 | -0.26445100 | -2.71608600 |
| H | 4.90687700 | -2.43593900 | -1.08684600 |
| N | 1.85245800 | -1.80675200 | 1.39113800  |
| N | 0.99280400 | -2.85423600 | -0.73174000 |
| H | 2.92323500 | -3.46383100 | 0.28917200  |
| C | 2.12693000 | -2.17760700 | 2.65523900  |
| N | 1.12316300 | -0.66362200 | 1.39395200  |
| C | 0.61378700 | -4.04320700 | -1.23498700 |

|   |             |             |             |
|---|-------------|-------------|-------------|
| N | 0.16113500  | -1.88124500 | -1.17737200 |
| C | 1.56891800  | -1.24852200 | 3.51725200  |
| H | 2.70366100  | -3.07383700 | 2.84879200  |
| C | 0.95560600  | -0.31855000 | 2.67533100  |
| C | -0.49972600 | -3.84850400 | -2.03520800 |
| H | 1.17242100  | -4.94002100 | -0.99615100 |
| C | -0.73559600 | -2.47278800 | -1.97298800 |
| H | 1.60715300  | -1.24303300 | 4.59754200  |
| H | 0.40884500  | 0.58417800  | 2.92575800  |
| H | -1.05163400 | -4.59236000 | -2.59258100 |
| H | -1.50630500 | -1.88140600 | -2.45593800 |
| N | -0.12213100 | 1.01125400  | -2.05949700 |
| O | -0.48271300 | 1.53388000  | -3.09102600 |
| C | 1.64278000  | 2.06096800  | -0.03331300 |
| C | 1.32160800  | 3.34611600  | -0.51008800 |
| C | 2.78151800  | 1.98367300  | 0.78914900  |
| C | 2.07478600  | 4.47471400  | -0.19123500 |
| H | 0.44098300  | 3.47259300  | -1.14480700 |
| C | 3.53891500  | 3.10729800  | 1.12367500  |
| H | 3.10016700  | 1.01464800  | 1.18117800  |
| C | 3.18940000  | 4.36398500  | 0.63782300  |
| H | 1.78331700  | 5.44793100  | -0.58639100 |
| H | 4.41136600  | 2.99656300  | 1.76759100  |
| H | 3.77698100  | 5.24264000  | 0.89801600  |
| H | -0.26103600 | 1.47552200  | 0.45066200  |
| P | -1.98310000 | -0.00073800 | 0.25411200  |
| C | -3.14387600 | 0.58497800  | -1.04953300 |
| H | -2.79344500 | 1.57914200  | -1.36233500 |
| H | -2.97157700 | -0.07485500 | -1.91415400 |
| C | -2.61693700 | -1.68939100 | 0.65913400  |

|   |             |             |             |
|---|-------------|-------------|-------------|
| H | -3.63208600 | -1.57236700 | 1.06684100  |
| H | -2.71614200 | -2.23576300 | -0.28969600 |
| C | -2.46833200 | 0.95279600  | 1.75865900  |
| H | -3.49650000 | 0.65332900  | 2.00155100  |
| H | -1.84135600 | 0.58128300  | 2.58165300  |
| C | -2.34354400 | 2.47819500  | 1.62485200  |
| H | -3.30883000 | 2.94266800  | 1.87486900  |
| H | -2.14363200 | 2.76707300  | 0.57951200  |
| C | -1.25939000 | 3.09123600  | 2.50274400  |
| H | -0.29270500 | 2.61682900  | 2.27101100  |
| H | -1.47134400 | 2.85817700  | 3.55776600  |
| C | -1.14103500 | 4.59177200  | 2.30552100  |
| H | -2.08089900 | 5.10357700  | 2.55223800  |
| H | -0.35046500 | 5.02403300  | 2.93008000  |
| H | -0.90129500 | 4.82889000  | 1.25962300  |
| C | -1.74184400 | -2.47377400 | 1.62702000  |
| H | -1.69042400 | -1.95389800 | 2.59724700  |
| H | -0.70999500 | -2.50874700 | 1.24851800  |
| C | -2.23099800 | -3.89825500 | 1.84432300  |
| H | -2.34703900 | -4.38965800 | 0.86548300  |
| H | -3.23349300 | -3.88112900 | 2.29813700  |
| C | -1.27185400 | -4.69658500 | 2.70989700  |
| H | -1.12081300 | -4.21310000 | 3.68456900  |
| H | -1.63173400 | -5.71524900 | 2.89444500  |
| H | -0.28625000 | -4.77413900 | 2.22881300  |
| C | -4.62331800 | 0.62592400  | -0.69500800 |
| H | -4.96762700 | -0.36788700 | -0.36928800 |
| H | -4.78927500 | 1.30428200  | 0.15652300  |
| C | -5.47490600 | 1.08770200  | -1.87060600 |
| H | -5.31186900 | 0.40963300  | -2.72208500 |

|   |             |            |             |
|---|-------------|------------|-------------|
| H | -5.12618800 | 2.07809100 | -2.20051200 |
| C | -6.95299000 | 1.14457600 | -1.52690400 |
| H | -7.55794200 | 1.47478200 | -2.37914300 |
| H | -7.32499500 | 0.15888700 | -1.21765600 |
| H | -7.13938600 | 1.84008600 | -0.69803400 |

## 2σ-butyl

81

|   |             |             |             |
|---|-------------|-------------|-------------|
| W | -0.56339300 | -0.34726600 | -0.67291200 |
| N | -0.16156400 | 0.00023800  | -2.36524000 |
| O | 0.09961600  | 0.33365300  | -3.51527800 |
| N | -2.03365300 | 1.20168600  | -0.67432900 |
| N | -1.16729900 | -0.66343600 | 1.52026700  |
| N | -2.37997900 | -1.61691500 | -0.97079200 |
| N | -3.18456700 | 1.08661400  | 0.04415400  |
| N | -2.46830000 | -0.50298500 | 1.86607800  |
| N | -3.50433000 | -1.36886100 | -0.25019100 |
| C | -2.12220800 | 2.35033600  | -1.36162800 |
| H | -1.31065300 | 2.64800000  | -2.01584500 |
| C | -3.33071200 | 2.99730100  | -1.07581900 |
| H | -3.68233100 | 3.94150400  | -1.46871900 |
| C | -3.97139900 | 2.16579200  | -0.17870000 |
| H | -4.92982700 | 2.25131800  | 0.31800500  |
| C | -4.49920500 | -2.18417700 | -0.65682800 |
| H | -5.47430900 | -2.13243900 | -0.18800700 |
| C | -4.02002100 | -2.98697400 | -1.67608700 |
| H | -4.55569200 | -3.75112300 | -2.22227000 |
| C | -2.68669700 | -2.59368700 | -1.83373700 |
| H | -1.93096400 | -2.96484300 | -2.51816300 |

|   |             |             |             |
|---|-------------|-------------|-------------|
| C | -2.61893300 | -0.69095100 | 3.18907900  |
| H | -3.59702100 | -0.60256800 | 3.64597900  |
| C | -1.38165400 | -0.98892400 | 3.73494900  |
| H | -1.14813600 | -1.19784800 | 4.76955500  |
| C | -0.50739500 | -0.96146200 | 2.64572800  |
| H | 0.56074600  | -1.14889800 | 2.61699200  |
| B | -3.53518600 | -0.21957000 | 0.78406500  |
| H | -4.62375100 | -0.13582800 | 1.28762400  |
| C | 0.65737100  | -3.38703700 | -0.27231800 |
| C | 1.22591600  | -3.95157400 | 0.87037700  |
| C | 2.60543700  | -4.11411700 | 0.94996100  |
| C | 3.42124300  | -3.69585800 | -0.10258400 |
| C | 2.85735500  | -3.11896000 | -1.23639200 |
| C | 1.47242000  | -2.96787600 | -1.32564800 |
| H | 0.58824800  | -4.27633900 | 1.69045400  |
| H | 3.04952900  | -4.57280900 | 1.83168900  |
| H | 4.50033100  | -3.82236300 | -0.03486000 |
| H | 3.49338800  | -2.79430400 | -2.05754300 |
| H | 1.02238400  | -2.53320600 | -2.21823100 |
| H | -0.42479200 | -3.28199500 | -0.35049800 |
| P | 1.25482700  | 1.16969000  | 0.00166400  |
| C | 2.54219800  | 1.30702600  | -1.32009300 |
| C | 0.79492400  | 2.95008100  | 0.27994500  |
| C | 2.25298900  | 0.90172700  | 1.54540300  |
| H | 2.94725300  | 0.28958200  | -1.44115700 |
| H | 1.98872000  | 1.51092200  | -2.24976000 |
| C | 3.67414800  | 2.30659700  | -1.13514900 |
| H | 1.70480700  | 3.53052900  | 0.49460900  |
| H | 0.39714600  | 3.32601600  | -0.67544500 |
| C | -0.22945300 | 3.15409500  | 1.38875100  |

|   |             |             |             |
|---|-------------|-------------|-------------|
| H | 2.88305700  | 1.79096200  | 1.70250300  |
| H | 1.53981400  | 0.88380500  | 2.38335100  |
| C | 3.10818800  | -0.35498100 | 1.56913600  |
| H | 3.27843400  | 3.33390500  | -1.14589600 |
| H | 4.15144300  | 2.17410400  | -0.15065700 |
| C | 4.73673400  | 2.17079400  | -2.21851100 |
| H | 0.20882700  | 2.87642500  | 2.36129700  |
| H | -1.08652000 | 2.47779500  | 1.23837300  |
| C | -0.73762000 | 4.58789500  | 1.46019700  |
| H | 3.84820400  | -0.32703500 | 0.75196200  |
| H | 2.48745800  | -1.24736400 | 1.37649500  |
| C | 3.83536300  | -0.51982700 | 2.89787700  |
| H | 4.26318500  | 2.28610700  | -3.20557200 |
| H | 5.14164000  | 1.14709100  | -2.19526200 |
| C | 5.86295500  | 3.17730500  | -2.06094100 |
| H | -1.14580800 | 4.86897600  | 0.47632300  |
| H | 0.10844600  | 5.26795700  | 1.64386800  |
| C | -1.80073000 | 4.77332400  | 2.52841300  |
| H | 3.09180200  | -0.56194100 | 3.70971700  |
| H | 4.43750700  | 0.38190700  | 3.08909300  |
| C | 4.72153700  | -1.75184900 | 2.94379900  |
| H | 6.62494000  | 3.06488800  | -2.84098500 |
| H | 5.48388100  | 4.20644900  | -2.11326300 |
| H | 6.36269200  | 3.06159900  | -1.08996900 |
| H | -1.41604300 | 4.50714500  | 3.52188300  |
| H | -2.15896800 | 5.80821200  | 2.57728200  |
| H | -2.66925500 | 4.12990000  | 2.33019700  |
| H | 5.47099100  | -1.73024100 | 2.14102900  |
| H | 5.25752200  | -1.83320000 | 3.89663300  |
| H | 4.13069300  | -2.66830000 | 2.81485500  |

**2-butyl**

81

|   |             |             |             |
|---|-------------|-------------|-------------|
| W | 0.69021200  | -0.57868100 | -0.24726200 |
| N | 2.92815900  | -0.34929200 | -0.20509900 |
| C | 3.91447500  | -1.24956000 | -0.21190800 |
| N | 3.50928800  | 0.86843700  | -0.06066000 |
| C | 5.15488200  | -0.61722300 | -0.07762700 |
| H | 3.68199000  | -2.30330000 | -0.31454800 |
| C | 4.84789500  | 0.72740600  | 0.01845800  |
| B | 2.65438000  | 2.12845400  | 0.20471500  |
| H | 6.13374200  | -1.07566100 | -0.05343000 |
| H | 5.48103700  | 1.59766200  | 0.14056900  |
| N | 1.70605100  | 2.36317200  | -0.98502200 |
| N | 1.82827600  | 1.83572200  | 1.47635300  |
| H | 3.35431500  | 3.09037100  | 0.37333000  |
| C | 1.58904800  | 3.45937100  | -1.75624300 |
| N | 0.87006100  | 1.39001900  | -1.42705200 |
| C | 1.92947600  | 2.39366400  | 2.69777800  |
| N | 1.05672700  | 0.72236300  | 1.53973300  |
| C | 0.65409200  | 3.20370400  | -2.74365600 |
| H | 2.18761200  | 4.33832300  | -1.54994300 |
| C | 0.24165800  | 1.89279700  | -2.49715200 |
| C | 1.20283400  | 1.62750800  | 3.59254200  |
| H | 2.52141700  | 3.28956900  | 2.84053300  |
| C | 0.68476000  | 0.58628300  | 2.81754800  |
| H | 0.32696400  | 3.86500500  | -3.53363900 |
| H | -0.47338400 | 1.29283500  | -3.04781700 |
| H | 1.07289100  | 1.79283800  | 4.65293900  |

|   |             |             |             |
|---|-------------|-------------|-------------|
| H | 0.05907700  | -0.24742600 | 3.11545400  |
| P | -1.78980900 | -0.09018000 | 0.14047900  |
| C | -2.85222600 | 0.29088700  | -1.32855300 |
| H | -2.31008200 | 1.01665500  | -1.95058700 |
| H | -2.90504200 | -0.63686400 | -1.91636500 |
| C | -2.67559100 | -1.51841400 | 0.90106000  |
| H | -3.76073500 | -1.35954100 | 0.81542000  |
| H | -2.42426500 | -2.38535500 | 0.27089000  |
| N | 0.61958600  | -2.06130200 | 0.71072000  |
| O | 0.57711900  | -3.08020900 | 1.37183800  |
| C | 1.81837600  | -2.88537300 | -2.18185800 |
| C | 1.08283600  | -4.01314000 | -2.00406900 |
| C | -0.35040700 | -3.93304700 | -1.91490200 |
| C | -0.97836500 | -2.73324100 | -2.01901000 |
| C | -0.24725900 | -1.48099600 | -2.10546500 |
| C | 1.21440400  | -1.56647500 | -2.17732800 |
| H | 2.89026700  | -2.96161400 | -2.36812300 |
| H | 1.56442600  | -4.98992100 | -1.99951100 |
| H | -0.93263400 | -4.85058500 | -1.84139500 |
| H | -2.06845300 | -2.70164500 | -2.07156200 |
| H | -0.74537200 | -0.69630500 | -2.67964800 |
| H | 1.74370700  | -0.80190700 | -2.75444800 |
| C | -2.16191200 | 1.32759800  | 1.26514000  |
| H | -3.24748600 | 1.37705000  | 1.43627800  |
| H | -1.70142100 | 1.10585300  | 2.23635800  |
| C | -1.61617400 | 2.64745300  | 0.73158100  |
| H | -2.16652700 | 2.95095800  | -0.17420600 |
| H | -0.57152600 | 2.50952300  | 0.41421100  |
| C | -1.65775200 | 3.77543300  | 1.75230500  |
| H | -1.17075800 | 3.43313800  | 2.67964100  |



|   |             |             |             |
|---|-------------|-------------|-------------|
| H | -2.70142300 | 4.00146200  | 2.01851600  |
| C | -0.95709900 | 5.02015200  | 1.23596600  |
| H | -1.40811400 | 5.36904200  | 0.29709300  |
| H | -0.99771500 | 5.84752300  | 1.95366900  |
| H | 0.10205500  | 4.80796500  | 1.02885400  |
| C | -2.29279000 | -1.81046300 | 2.34573900  |
| H | -2.65953600 | -1.00895600 | 3.00640900  |
| H | -1.19872500 | -1.83461900 | 2.44404600  |
| C | -2.83440400 | -3.15213800 | 2.81911700  |
| H | -2.47119700 | -3.93521300 | 2.13547500  |
| H | -3.93239300 | -3.15881800 | 2.73966400  |
| C | -2.40561400 | -3.47505500 | 4.23937600  |
| H | -2.75425100 | -2.70906000 | 4.94477100  |
| H | -2.79785700 | -4.44107800 | 4.57765600  |
| H | -1.31026500 | -3.51684100 | 4.31325100  |
| C | -4.26055500 | 0.80376500  | -1.05560600 |
| H | -4.79295700 | 0.13148200  | -0.36471400 |
| H | -4.21867600 | 1.78395800  | -0.55673800 |
| C | -5.07101000 | 0.93784900  | -2.33883600 |
| H | -5.12839000 | -0.04328600 | -2.83414900 |
| H | -4.53437200 | 1.59881200  | -3.03661100 |
| C | -6.46903400 | 1.47465900  | -2.08662000 |
| H | -7.04552600 | 1.56490900  | -3.01447100 |
| H | -7.02924500 | 0.81541800  | -1.41054400 |
| H | -6.43285300 | 2.46792500  | -1.62015400 |

### 2π-butyl

81

|   |             |             |             |
|---|-------------|-------------|-------------|
| W | -0.46168000 | -0.18609600 | -0.75494100 |
|---|-------------|-------------|-------------|

|   |             |             |             |
|---|-------------|-------------|-------------|
| N | -2.63526400 | -0.41724700 | -1.27641700 |
| C | -3.28076400 | -1.04796500 | -2.26411700 |
| N | -3.57296100 | 0.28619200  | -0.58976200 |
| C | -4.64980100 | -0.75969700 | -2.22088200 |
| H | -2.73158900 | -1.68329200 | -2.95020100 |
| C | -4.78979800 | 0.09128400  | -1.14050000 |
| B | -3.15482600 | 1.27421900  | 0.52064100  |
| H | -5.42548400 | -1.12324700 | -2.88078900 |
| H | -5.66313400 | 0.57509000  | -0.72046000 |
| N | -2.43314700 | 0.49696300  | 1.64266500  |
| N | -2.17437400 | 2.28721300  | -0.10843600 |
| H | -4.11559000 | 1.84543400  | 0.96412800  |
| C | -2.72641400 | 0.40016900  | 2.95173500  |
| N | -1.32399500 | -0.22922900 | 1.36259200  |
| C | -2.32603700 | 3.62242600  | -0.26127000 |
| N | -1.04593200 | 1.87632200  | -0.74984800 |
| C | -1.78924800 | -0.42414200 | 3.55299400  |
| H | -3.58447700 | 0.92038000  | 3.35998300  |
| C | -0.93490800 | -0.79377300 | 2.51143700  |
| C | -1.28638600 | 4.09589100  | -1.03800600 |
| H | -3.16854100 | 4.12882900  | 0.19315900  |
| C | -0.51208100 | 2.96528400  | -1.32251900 |
| H | -1.73642400 | -0.71680100 | 4.59231300  |
| H | -0.06102000 | -1.43601500 | 2.53046600  |
| H | -1.10807500 | 5.11463900  | -1.35359700 |
| H | 0.40426900  | 2.87826500  | -1.89517200 |
| N | 0.16126600  | -0.07500500 | -2.41120400 |
| O | 0.58548900  | 0.08077100  | -3.54892500 |
| C | -1.93491400 | -4.12127300 | 1.05818000  |
| C | -2.10569900 | -3.74282400 | -0.26694000 |

|   |             |             |             |
|---|-------------|-------------|-------------|
| C | -0.99470000 | -3.41244000 | -1.05026700 |
| C | 0.28628700  | -3.45654000 | -0.49681200 |
| C | 0.45360500  | -3.84336200 | 0.83690400  |
| C | -0.65184700 | -4.17640900 | 1.61056300  |
| H | -2.79919500 | -4.38308800 | 1.66519800  |
| H | -3.10330300 | -3.70710900 | -0.70124400 |
| H | -1.12219500 | -3.15233800 | -2.09960900 |
| H | 1.15319300  | -3.23133400 | -1.11740500 |
| H | 1.45372700  | -3.89241300 | 1.26683000  |
| H | -0.51873600 | -4.48183300 | 2.64651700  |
| P | 1.74249500  | 0.47925600  | 0.14268100  |
| C | 2.97378700  | 0.76113500  | -1.20926200 |
| C | 1.77079800  | 2.12337900  | 1.01655300  |
| C | 2.73302300  | -0.53739900 | 1.35662600  |
| H | 3.15177600  | -0.22547900 | -1.66398000 |
| H | 2.45792400  | 1.34410900  | -1.98555500 |
| C | 4.29355600  | 1.42080400  | -0.83370400 |
| H | 2.79177600  | 2.31590000  | 1.37790600  |
| H | 1.55399800  | 2.88582800  | 0.25311000  |
| C | 0.77093600  | 2.24774400  | 2.15589300  |
| H | 3.47542700  | 0.10693000  | 1.85212800  |
| H | 2.03398700  | -0.86276900 | 2.14221300  |
| C | 3.41303500  | -1.75032400 | 0.73900900  |
| H | 4.12293600  | 2.47299600  | -0.55864400 |
| H | 4.72991600  | 0.94226300  | 0.05780000  |
| C | 5.30696300  | 1.35897800  | -1.96913400 |
| H | 1.01847400  | 1.53198200  | 2.95777600  |
| H | -0.22993200 | 1.96474400  | 1.79861200  |
| C | 0.69359800  | 3.65113200  | 2.73934000  |
| H | 4.23211200  | -1.42779100 | 0.07638300  |

|   |             |             |             |
|---|-------------|-------------|-------------|
| H | 2.70142400  | -2.28775800 | 0.09153200  |
| C | 3.96667800  | -2.71583300 | 1.77747300  |
| H | 4.86567700  | 1.80522200  | -2.87365000 |
| H | 5.50091900  | 0.30330100  | -2.21639000 |
| C | 6.60968400  | 2.05967000  | -1.62536100 |
| H | 0.50888100  | 4.36622600  | 1.92159300  |
| H | 1.66505400  | 3.93042500  | 3.17523200  |
| C | -0.40715400 | 3.76662000  | 3.77969900  |
| H | 3.15178900  | -3.02360200 | 2.45277300  |
| H | 4.69818200  | -2.19065500 | 2.41053700  |
| C | 4.60490500  | -3.93942900 | 1.14346300  |
| H | 7.33558700  | 2.00085100  | -2.44461800 |
| H | 6.44097200  | 3.12244500  | -1.40703100 |
| H | 7.07526400  | 1.61316100  | -0.73664000 |
| H | -0.25093700 | 3.05574700  | 4.60256400  |
| H | -0.46577800 | 4.77149700  | 4.21368900  |
| H | -1.38565600 | 3.53747000  | 3.33332700  |
| H | 5.43779500  | -3.65523600 | 0.48687900  |
| H | 4.99660600  | -4.63542700 | 1.89415400  |
| H | 3.87771700  | -4.48763300 | 0.52808400  |

XYZ files for representative trajectories from each transition state can be found attached separately.

**Table S5.** Trajectory results (given as number of trajectories)

| Connection            | Total trajectories | Final structure reverse trajectory |    | Final structure forward trajectory |    |
|-----------------------|--------------------|------------------------------------|----|------------------------------------|----|
|                       |                    | 2 $\sigma$                         | N* | 2H                                 | N* |
| Trajectories from TS1 |                    |                                    |    |                                    |    |

|                           |    |           |           |           |           |           |           |           |             |           |
|---------------------------|----|-----------|-----------|-----------|-----------|-----------|-----------|-----------|-------------|-----------|
| <b>2H→TS1→2σ</b>          | 6  | 1         | 5         |           | 1         | 5         |           |           |             |           |
| <b>2→TS1→2σ</b>           | 1  | 0         | 1         |           | 0         | 1         |           |           |             |           |
| <b>Recrossing</b>         | 2  |           |           |           |           |           |           |           |             |           |
| Trajectories from TS2     |    | <b>2σ</b> | <b>2π</b> | <b>N*</b> | <b>2H</b> | <b>2σ</b> | <b>2π</b> | <b>N*</b> | <b>flip</b> |           |
| <b>2σ→TS2→2π</b>          | 15 | 5         | 7         | 3         | 1         | 8         | 3         | 2         | 1           |           |
| <b>2→TS2→2σ</b>           | 9  | 0         | 0         | 9         | 0         | 3         | 4         | 2         | 0           |           |
| <b>2→TS2→2π</b>           | 5  | 0         | 0         | 5         | 0         | 5         | 0         | 0         | 0           |           |
| <b>2H→TS2→2σ</b>          | 2  | 0         | 0         | 2         | 0         | 0         | 1         | 1         | 0           |           |
| <b>2π→TS2→dissociated</b> | 1  | 0         | 1         | 0         | 0         | 0         | 0         | 1         | 0           |           |
| <b>Recrossing</b>         | 27 |           |           |           |           |           |           |           |             |           |
| Trajectories from TS3     |    | <b>2</b>  | <b>2σ</b> | <b>2π</b> | <b>N*</b> | <b>2</b>  | <b>2σ</b> | <b>2π</b> | <b>2H</b>   | <b>N*</b> |
| <b>2σ→TS3→2π</b>          | 26 | 1         | 8         | 15        | 2         | 1         | 14        | 9         | 0           | 2         |
| <b>2→TS3→2π</b>           | 6  | 0         | 0         | 0         | 6         | 0         | 5         | 0         | 1           | 0         |
| <b>2σ→TS3→2</b>           | 2  | 0         | 0         | 0         | 2         | 0         | 0         | 0         | 0           | 2         |
| <b>2→TS3→dissociated</b>  | 1  | 0         | 0         | 0         | 1         | 0         | 0         | 0         | 0           | 1         |
| <b>Recrossing</b>         | 17 |           |           |           |           |           |           |           |             |           |

**N\*** Trajectory did not evolve after arriving at structure. Trajectories that show final structures being the same as the trajectory destination rotated such that different carbon or hydrogen atoms encountered the metal center.

**Table S6.** Thermochemical values for WTP(NO)(PMe<sub>3</sub>)-anisole with geometry optimizations and frequency calculations performed using M06/6-31g\*\*[LANL2DZ]. All values are given relative to **3B** in kcal/mol.

|                        | ZPE  | E    | H    | G    |
|------------------------|------|------|------|------|
| <b>3H</b>              |      |      |      |      |
| Ortho-PMe <sub>3</sub> | 7.9  | 8.2  | 8.2  | 7.2  |
| Meta-PMe <sub>3</sub>  | 6.1  | 6.4  | 6.4  | 4.3  |
| Para-PMe <sub>3</sub>  | 7.6  | 8.0  | 8.0  | 5.6  |
| <b>TS1</b>             |      |      |      |      |
| Ortho-PMe <sub>3</sub> | 17.5 | 17.8 | 17.8 | 16.2 |
| Meta-PMe <sub>3</sub>  | 18.1 | 18.4 | 18.4 | 15.9 |
| Para-PMe <sub>3</sub>  | 17.6 | 17.9 | 17.9 | 16.2 |
| <b>3σ</b>              |      |      |      |      |
| Ortho-PMe <sub>3</sub> | 16.4 | 17.0 | 17.0 | 13.8 |
| Meta-PMe <sub>3</sub>  | 17.2 | 18.1 | 18.1 | 13.6 |
| Para-PMe <sub>3</sub>  | 13.8 | 14.4 | 14.4 | 11.9 |
| <b>TS2</b>             |      |      |      |      |
| D-PMe <sub>3</sub>     | 14.7 | 14.8 | 14.8 | 13.2 |
| A-PMe <sub>3</sub>     | 15.1 | 15.2 | 15.2 | 13.7 |
| B-PMe <sub>3</sub>     | 15.1 | 15.4 | 15.4 | 13.9 |
| <b>3</b>               |      |      |      |      |
| C-PMe <sub>3</sub>     | 3.2  | 3.4  | 3.4  | 2.4  |
| D-PMe <sub>3</sub>     | 3.3  | 3.4  | 3.4  | 2.9  |
| B-PMe <sub>3</sub>     | 0.6  | 0.8  | 0.8  | -0.1 |
| A-PMe <sub>3</sub>     | 0.0  | 0.0  | 0.0  | 0.0  |
| <b>TS3</b>             |      |      |      |      |
| D-PMe <sub>3</sub>     | 14.5 | 14.9 | 14.9 | 12.2 |
| A-PMe <sub>3</sub>     | 13.8 | 14.0 | 14.0 | 12.6 |

|                        |      |      |      |      |
|------------------------|------|------|------|------|
| <b>3π</b>              |      |      |      |      |
| A-PMe <sub>3</sub>     | 13.0 | 13.8 | 13.8 | 10.3 |
| C-PMe <sub>3</sub>     | 14.4 | 15.2 | 15.2 | 12.1 |
| B-PMe <sub>3</sub>     | 13.1 | 13.6 | 13.6 | 10.7 |
| <b>W-Ph rotation</b>   |      |      |      |      |
| Ortho-PMe <sub>3</sub> | 23.4 | 23.3 | 23.3 | 22.1 |
| Para-PMe <sub>3</sub>  | 16.1 | 16.1 | 16.1 | 15.1 |
| Meta-PMe <sub>3</sub>  | 15.7 | 15.7 | 15.7 | 14.6 |

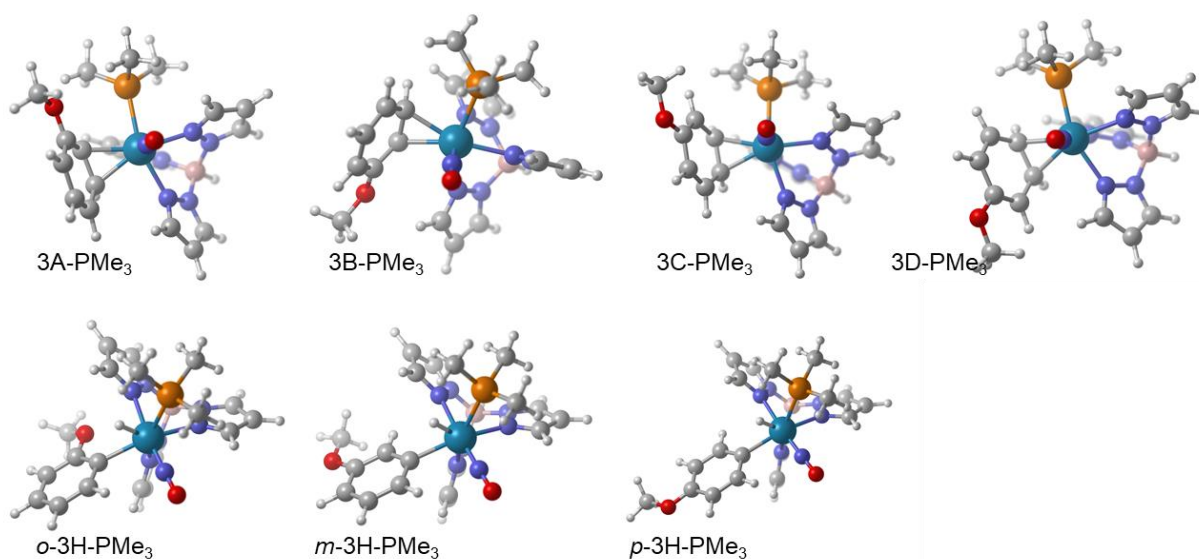


**Figure S2C.** M06 structures for structures calculated corresponding to Scheme 6.

XYZ coordinates for static structures on the WTp(NO)(PMe<sub>3</sub>)-anisole energy surface.

**o-3H**

58

|   |             |             |             |
|---|-------------|-------------|-------------|
| W | 0.21337100  | -0.62680200 | -0.24128600 |
| N | -0.86505600 | 1.08639200  | -1.22784500 |
| C | -1.87255200 | 1.13036400  | -2.10173000 |
| N | -0.59778800 | 2.36355200  | -0.86370400 |

|   |             |             |             |
|---|-------------|-------------|-------------|
| C | -2.27410800 | 2.45192600  | -2.31269000 |
| H | -2.26638000 | 0.21121900  | -2.52042900 |
| C | -1.43385400 | 3.20026000  | -1.50551400 |
| B | 0.59503300  | 2.70167600  | 0.06435000  |
| H | -3.05680200 | 2.81176400  | -2.96592500 |
| H | -1.36112300 | 4.26962300  | -1.34872200 |
| N | 0.37584500  | 2.05419300  | 1.44328300  |
| N | 1.84485400  | 2.08307100  | -0.61067400 |
| H | 0.71789600  | 3.89123900  | 0.17591800  |
| C | 0.25400900  | 2.64377000  | 2.64753000  |
| N | 0.20309300  | 0.71840700  | 1.56623000  |
| C | 2.87520400  | 2.70301300  | -1.21608000 |
| N | 1.82281200  | 0.77842200  | -0.97406200 |
| C | -0.00545900 | 1.66432900  | 3.59101800  |
| H | 0.36433900  | 3.71691600  | 2.74468600  |
| C | -0.03102600 | 0.47518800  | 2.85818700  |
| C | 3.55509300  | 1.77822700  | -1.99023900 |
| H | 3.04086800  | 3.76234100  | -1.06263100 |
| C | 2.84499300  | 0.58785000  | -1.81418900 |
| H | -0.15640000 | 1.79391800  | 4.65361800  |
| H | -0.22679600 | -0.53801700 | 3.19095100  |
| H | 4.42989500  | 1.94457300  | -2.60305600 |
| H | 3.01518900  | -0.39038300 | -2.24981000 |
| P | 2.28943700  | -1.56530200 | 0.89333900  |
| C | 2.05020300  | -2.56588500 | 2.40125200  |
| H | 3.02067800  | -2.91267500 | 2.77637100  |
| H | 1.56048300  | -1.97042600 | 3.17876700  |
| H | 1.41910600  | -3.43026100 | 2.16909600  |
| C | 3.25334400  | -2.70623200 | -0.15645600 |
| H | 3.61265200  | -2.19773900 | -1.05657700 |



|   |             |             |             |
|---|-------------|-------------|-------------|
| H | 4.11265300  | -3.09795100 | 0.40105500  |
| H | 2.60790300  | -3.53804900 | -0.46019900 |
| N | 0.42057700  | -1.70655900 | -1.63097100 |
| O | 0.61865000  | -2.45227000 | -2.56410000 |
| C | 3.51745400  | -0.33093400 | 1.46159500  |
| H | 4.32957500  | -0.84011500 | 1.99445600  |
| H | 3.93739000  | 0.22182900  | 0.61512300  |
| H | 3.03310000  | 0.37897000  | 2.14322800  |
| C | -1.93273400 | -1.21410500 | -0.02800300 |
| C | -2.37577500 | -2.43510900 | -0.55577500 |
| C | -2.94566200 | -0.39380200 | 0.52007100  |
| C | -3.71423900 | -2.83587400 | -0.56706200 |
| H | -1.63870500 | -3.10956900 | -0.99552200 |
| C | -4.29203700 | -0.77418400 | 0.52100100  |
| C | -4.67725100 | -1.99772500 | -0.02340200 |
| H | -3.99442900 | -3.79444600 | -1.00154200 |
| H | -0.06577300 | -1.88440700 | 0.89408800  |
| H | -5.72782100 | -2.28345400 | -0.01607100 |
| H | -5.04998400 | -0.12074900 | 0.94641300  |
| O | -2.55098600 | 0.80615600  | 1.03839000  |
| C | -3.52900400 | 1.76346500  | 1.35287200  |
| H | -2.99499900 | 2.67901300  | 1.62712300  |
| H | -4.18311000 | 1.97951200  | 0.49388100  |
| H | -4.15684700 | 1.46115900  | 2.20462000  |

**m-3H**

58

|   |             |             |             |
|---|-------------|-------------|-------------|
| W | 0.37251400  | -0.61251900 | -0.31066500 |
| N | -0.64721900 | 1.11094000  | -1.34497600 |

|   |             |             |             |
|---|-------------|-------------|-------------|
| C | -1.53578500 | 1.15856600  | -2.34000800 |
| N | -0.48764600 | 2.38028900  | -0.89342300 |
| C | -1.96524700 | 2.47177500  | -2.54476500 |
| H | -1.83342600 | 0.24508300  | -2.84239400 |
| C | -1.27081500 | 3.21321900  | -1.60414800 |
| B | 0.56623200  | 2.71602100  | 0.19093800  |
| H | -2.67475300 | 2.83140100  | -3.27680600 |
| H | -1.26851400 | 4.27558600  | -1.39313600 |
| N | 0.18494500  | 1.99404800  | 1.49846100  |
| N | 1.91596900  | 2.17219000  | -0.33636600 |
| H | 0.62670600  | 3.90107100  | 0.37181400  |
| C | -0.10741700 | 2.51432300  | 2.70413700  |
| N | 0.02078800  | 0.64914000  | 1.52515900  |
| C | 2.99920400  | 2.85751200  | -0.74870900 |
| N | 2.00372700  | 0.88693000  | -0.75705500 |
| C | -0.47300400 | 1.48185700  | 3.55204300  |
| H | -0.03539500 | 3.58203400  | 2.87109600  |
| C | -0.37852600 | 0.33362200  | 2.76294300  |
| C | 3.82610400  | 1.99754300  | -1.45062900 |
| H | 3.09504500  | 3.91269800  | -0.52395200 |
| C | 3.14869900  | 0.77557800  | -1.43788800 |
| H | -0.76732200 | 1.55217700  | 4.58978600  |
| H | -0.59271300 | -0.69891500 | 3.01530300  |
| H | 4.77483600  | 2.22523000  | -1.91601000 |
| H | 3.42534400  | -0.17297200 | -1.88474500 |
| P | 2.30258900  | -1.54534300 | 1.05704200  |
| C | 1.88643600  | -2.62768600 | 2.46642600  |
| H | 2.80315700  | -2.95270900 | 2.97324300  |
| H | 1.25494300  | -2.09023700 | 3.18166000  |
| H | 1.33951000  | -3.50446000 | 2.10380100  |

|   |             |             |             |
|---|-------------|-------------|-------------|
| C | 3.46540900  | -2.59188200 | 0.11601100  |
| H | 3.89994400  | -2.03731700 | -0.72152200 |
| H | 4.27169500  | -2.94378700 | 0.77094700  |
| H | 2.92091500  | -3.45615800 | -0.28109000 |
| N | 0.74588400  | -1.62373000 | -1.71896800 |
| O | 1.02569500  | -2.31997700 | -2.66840500 |
| C | 3.36873700  | -0.28887100 | 1.85666200  |
| H | 4.11668400  | -0.78675400 | 2.48554100  |
| H | 3.88171300  | 0.32239000  | 1.10706300  |
| H | 2.75148000  | 0.36520400  | 2.48515800  |
| C | -1.76405500 | -1.19494500 | -0.29097700 |
| C | -2.24169600 | -2.33277800 | -0.95911000 |
| C | -2.72259000 | -0.38412100 | 0.34522300  |
| C | -3.60319500 | -2.64149400 | -0.99382300 |
| H | -1.53940400 | -2.99322300 | -1.47027800 |
| C | -4.08366200 | -0.69249900 | 0.31755900  |
| H | -2.40019600 | 0.52622400  | 0.84816700  |
| C | -4.53319300 | -1.83242000 | -0.35578700 |
| H | -3.94476200 | -3.52862800 | -1.52709200 |
| H | -0.01704700 | -1.93628400 | 0.71059000  |
| H | -5.59834300 | -2.05486600 | -0.36858700 |
| O | -5.04714100 | 0.06260100  | 0.91339700  |
| C | -4.64121800 | 1.23903600  | 1.57591300  |
| H | -4.16166700 | 1.95172100  | 0.88826500  |
| H | -5.54657200 | 1.69630600  | 1.98343900  |
| H | -3.94652200 | 1.02796300  | 2.40245300  |

**p-3H**

58

S885

|   |             |             |             |
|---|-------------|-------------|-------------|
| W | 0.29768400  | -0.51332400 | -0.33617500 |
| N | -0.36421300 | 1.55577800  | -0.95959100 |
| C | -1.28756800 | 1.97795100  | -1.82632700 |
| N | 0.16148500  | 2.65934100  | -0.37089300 |
| C | -1.36771200 | 3.37255200  | -1.80988400 |
| H | -1.85661800 | 1.25741600  | -2.40287800 |
| C | -0.42730500 | 3.76174100  | -0.87189700 |
| B | 1.36120000  | 2.55163500  | 0.60194400  |
| H | -2.01544700 | 4.00682600  | -2.39877200 |
| H | -0.12812300 | 4.74374300  | -0.52637800 |
| N | 0.93986200  | 1.72163000  | 1.83075800  |
| N | 2.47680700  | 1.81170200  | -0.17522700 |
| H | 1.73249100  | 3.64136000  | 0.94188000  |
| C | 0.94240800  | 2.06782700  | 3.13098200  |
| N | 0.42791900  | 0.47472100  | 1.68766000  |
| C | 3.64937600  | 2.28800300  | -0.63461100 |
| N | 2.19592700  | 0.63311600  | -0.78075700 |
| C | 0.41679400  | 1.01907500  | 3.86695500  |
| H | 1.31392600  | 3.03792400  | 3.43743500  |
| C | 0.10678300  | 0.04648400  | 2.91419000  |
| C | 4.15838900  | 1.39247500  | -1.55951100 |
| H | 4.02908600  | 3.23803100  | -0.27921900 |
| C | 3.20103300  | 0.37676600  | -1.62398300 |
| H | 0.27254900  | 0.97011400  | 4.93711800  |
| H | -0.34326800 | -0.93163500 | 3.04383800  |
| H | 5.08211000  | 1.46969000  | -2.11557400 |
| H | 3.18508300  | -0.52188300 | -2.23086000 |
| P | 2.07522700  | -2.05668400 | 0.62366800  |
| C | 1.56222500  | -3.21884700 | 1.93423300  |
| H | 2.42016600  | -3.82230000 | 2.25464500  |

|   |             |             |             |
|---|-------------|-------------|-------------|
| H | 1.17266400  | -2.66724600 | 2.79647400  |
| H | 0.77512700  | -3.87744500 | 1.55217500  |
| C | 2.83117200  | -3.18074700 | -0.59996600 |
| H | 3.29789800  | -2.61294700 | -1.41125800 |
| H | 3.58922100  | -3.81037600 | -0.11862100 |
| H | 2.04853600  | -3.81928000 | -1.02513500 |
| N | 0.30636200  | -1.32258200 | -1.91338900 |
| O | 0.34346100  | -1.88379600 | -2.98539600 |
| C | 3.50265200  | -1.22267500 | 1.41245200  |
| H | 4.16205400  | -1.97234100 | 1.86627400  |
| H | 4.07183000  | -0.64288100 | 0.67859400  |
| H | 3.14070600  | -0.54476500 | 2.19540100  |
| C | -1.90570400 | -0.61326300 | -0.15512000 |
| C | -2.68567300 | -1.46377900 | -0.96205300 |
| C | -2.63228000 | 0.21909500  | 0.70773600  |
| C | -4.07472300 | -1.47963300 | -0.91912100 |
| H | -2.19050700 | -2.14048600 | -1.66131900 |
| C | -4.02927200 | 0.22084400  | 0.77892600  |
| H | -2.10190700 | 0.92690600  | 1.34952600  |
| C | -4.76088600 | -0.63572900 | -0.04193200 |
| H | -4.65292600 | -2.14317900 | -1.56127300 |
| H | -4.52907800 | 0.89697500  | 1.46897900  |
| H | -0.28714200 | -1.88606000 | 0.51368000  |
| O | -6.11940300 | -0.71973100 | -0.06384400 |
| C | -6.83564600 | 0.12748100  | 0.80521600  |
| H | -6.59532300 | -0.06894100 | 1.86014200  |
| H | -6.64564400 | 1.18929600  | 0.59166400  |
| H | -7.89640600 | -0.07993400 | 0.64194900  |

**o-TS1**

|   |             |             |             |
|---|-------------|-------------|-------------|
| W | -0.05015800 | 0.27072800  | -0.50406700 |
| P | 1.00779300  | 1.84997700  | 1.14520900  |
| C | 1.37797100  | 3.49689600  | 0.43972300  |
| H | 0.47308400  | 3.93376400  | 0.00396400  |
| H | 1.76839300  | 4.16742000  | 1.21506100  |
| H | 2.12661300  | 3.39183200  | -0.35382500 |
| C | 2.60278800  | 1.45454000  | 1.96048400  |
| H | 2.86264500  | 2.25934000  | 2.65897700  |
| H | 2.53913400  | 0.51241400  | 2.51560600  |
| H | 3.39249400  | 1.36555900  | 1.20686400  |
| C | -0.04733300 | 2.26235600  | 2.58806300  |
| H | 0.47503500  | 2.95954400  | 3.25445300  |
| H | -0.98329100 | 2.72200600  | 2.25268800  |
| H | -0.29128400 | 1.34954800  | 3.14450700  |
| N | 0.08321600  | 1.48298500  | -1.78342500 |
| O | 0.11476700  | 2.39083200  | -2.59298400 |
| N | -2.00804000 | 1.16393700  | 0.06487100  |
| N | -0.54210000 | -1.02306400 | 1.33960100  |
| N | -1.43212600 | -1.19692200 | -1.47026600 |
| N | -3.06290400 | 0.43289300  | 0.49454700  |
| N | -1.81292700 | -1.45273000 | 1.54811700  |
| N | -2.56564800 | -1.61112300 | -0.84760500 |
| C | -2.42892700 | 2.43058400  | -0.03210500 |
| H | -1.74693800 | 3.20122600  | -0.37453900 |
| C | -3.76910100 | 2.52800500  | 0.35155600  |
| H | -4.38654600 | 3.41477100  | 0.38570100  |
| C | -4.13197200 | 1.23119400  | 0.67293100  |
| H | -5.07359100 | 0.81635400  | 1.01100100  |

|   |             |             |             |
|---|-------------|-------------|-------------|
| C | -3.24471500 | -2.45210700 | -1.65086100 |
| H | -4.17650000 | -2.89157200 | -1.31654900 |
| C | -2.54478700 | -2.59244800 | -2.83596900 |
| H | -2.81067100 | -3.19468300 | -3.69348600 |
| C | -1.41464500 | -1.78819100 | -2.67001900 |
| H | -0.58784900 | -1.60650800 | -3.34705200 |
| C | -1.89213300 | -2.10837000 | 2.71960300  |
| H | -2.83643700 | -2.52336600 | 3.05008000  |
| C | -0.63801100 | -2.11393900 | 3.30570300  |
| H | -0.34964600 | -2.55784200 | 4.24832000  |
| C | 0.16871700  | -1.42186500 | 2.39991500  |
| H | 1.22791100  | -1.20303200 | 2.45449900  |
| B | -2.94410300 | -1.10388900 | 0.56243100  |
| H | -3.98124800 | -1.59431200 | 0.91924400  |
| C | 2.16726600  | -0.28846300 | -0.75031700 |
| C | 2.84662300  | -1.38132800 | -0.14498300 |
| C | 4.23765600  | -1.46059700 | -0.11364900 |
| C | 5.01515700  | -0.49089400 | -0.74829600 |
| C | 4.38451500  | 0.53674500  | -1.44084600 |
| C | 2.99492700  | 0.61889200  | -1.44904900 |
| H | 1.08326300  | -0.76551800 | -1.40477800 |
| H | 2.52339100  | 1.43322500  | -1.99860400 |
| H | 4.97071800  | 1.28494100  | -1.97201500 |
| H | 4.72632500  | -2.28799200 | 0.39458400  |
| H | 6.10018900  | -0.56483900 | -0.72049700 |
| O | 2.04783200  | -2.35152700 | 0.38181000  |
| C | 2.64725200  | -3.40746900 | 1.09394300  |
| H | 3.22614300  | -3.04075200 | 1.95510800  |
| H | 1.83274700  | -4.03970000 | 1.45871000  |
| H | 3.30665400  | -4.01342800 | 0.45619100  |

**m-TS1**

58

|   |             |             |             |
|---|-------------|-------------|-------------|
| W | 0.29166700  | -0.38593200 | -0.44276100 |
| P | -0.81323400 | -1.86729200 | 1.18718900  |
| C | -1.03646000 | -3.58292700 | 0.58098800  |
| H | -0.08064600 | -3.98936900 | 0.23349100  |
| H | -1.43968500 | -4.22552600 | 1.37341300  |
| H | -1.73304900 | -3.57952500 | -0.26573900 |
| C | -2.49963200 | -1.54244100 | 1.85713900  |
| H | -2.78689300 | -2.34771100 | 2.54520700  |
| H | -2.52717600 | -0.59258100 | 2.40342400  |
| H | -3.22585100 | -1.49782900 | 1.03750800  |
| C | 0.10644900  | -2.13307900 | 2.75823800  |
| H | -0.43496600 | -2.82088800 | 3.41987400  |
| H | 1.09873800  | -2.54659700 | 2.54598600  |
| H | 0.23921400  | -1.17351700 | 3.27298800  |
| N | 0.37314000  | -1.71558700 | -1.60950900 |
| O | 0.46417000  | -2.67156600 | -2.36135000 |
| N | 2.24955600  | -0.88798700 | 0.35886300  |
| N | 0.41118000  | 1.23559400  | 1.19794100  |
| N | 1.46679300  | 1.16851800  | -1.54233100 |
| N | 3.16064200  | 0.05962100  | 0.69719200  |
| N | 1.58812100  | 1.87331200  | 1.41468700  |
| N | 2.48202400  | 1.83173500  | -0.93163100 |
| C | 2.86023500  | -2.07297200 | 0.48914900  |
| H | 2.31881900  | -2.98552300 | 0.26514100  |
| C | 4.17859200  | -1.89728800 | 0.92103900  |
| H | 4.91689600  | -2.66156800 | 1.12018000  |



|   |             |             |             |
|---|-------------|-------------|-------------|
| C | 4.32517100  | -0.52791600 | 1.04275400  |
| H | 5.17003000  | 0.07562200  | 1.35068900  |
| C | 3.07634300  | 2.66669000  | -1.80695200 |
| H | 3.90604300  | 3.28794200  | -1.49233100 |
| C | 2.44132000  | 2.54545800  | -3.03001300 |
| H | 2.66724300  | 3.07220100  | -3.94681900 |
| C | 1.43812500  | 1.59684400  | -2.80969900 |
| H | 0.69619600  | 1.20137600  | -3.49458400 |
| C | 1.46709400  | 2.72373200  | 2.44974900  |
| H | 2.31351900  | 3.31979400  | 2.76842300  |
| C | 0.17114300  | 2.65027600  | 2.93119600  |
| H | -0.26148300 | 3.20199900  | 3.75399600  |
| C | -0.44780600 | 1.70365700  | 2.11162500  |
| H | -1.46963400 | 1.34129400  | 2.13017100  |
| B | 2.82788200  | 1.55827400  | 0.54815700  |
| H | 3.76146000  | 2.23227200  | 0.89267700  |
| C | -2.10379200 | 0.07844700  | -1.13549000 |
| C | -2.78741500 | 1.10287000  | -0.46163900 |
| C | -4.17054100 | 1.02377800  | -0.30283000 |
| C | -4.87837800 | -0.04515200 | -0.86749400 |
| C | -4.19889900 | -1.01904800 | -1.59169300 |
| C | -2.81676400 | -0.96176400 | -1.74389100 |
| H | -2.22163000 | 1.93674400  | -0.05239900 |
| H | -1.08299800 | 0.36699800  | -1.58871300 |
| H | -2.28386600 | -1.72583900 | -2.30728200 |
| H | -4.76055800 | -1.83555900 | -2.04169000 |
| H | -5.95837800 | -0.07877500 | -0.74262800 |
| O | -4.91348700 | 1.93352100  | 0.37188700  |
| C | -4.23413000 | 3.00263700  | 0.99753900  |
| H | -3.50792700 | 2.64116500  | 1.74004800  |

|   |             |            |            |
|---|-------------|------------|------------|
| H | -3.71271200 | 3.63835800 | 0.26868700 |
| H | -4.99454300 | 3.59913100 | 1.50694100 |

**p-3H**

58

|   |             |             |             |
|---|-------------|-------------|-------------|
| W | -0.28807800 | 0.08051900  | -0.52886100 |
| P | 0.66329000  | 2.07610500  | 0.66536800  |
| C | 0.94861600  | 3.51343200  | -0.43046600 |
| H | 0.03473600  | 3.75563700  | -0.98350900 |
| H | 1.26199600  | 4.38706100  | 0.15406400  |
| H | 1.73371200  | 3.26732300  | -1.15469600 |
| C | 2.25842300  | 2.00245300  | 1.56896000  |
| H | 2.48303600  | 2.99292500  | 1.98332000  |
| H | 2.20566800  | 1.28211700  | 2.39256600  |
| H | 3.06476900  | 1.70671200  | 0.88953700  |
| C | -0.43973100 | 2.76704800  | 1.95941300  |
| H | 0.04201300  | 3.61773600  | 2.45679000  |
| H | -1.38431700 | 3.10019400  | 1.51641100  |
| H | -0.66245800 | 1.99422200  | 2.70548300  |
| N | -0.17698300 | 0.93308000  | -2.07521500 |
| O | -0.13546700 | 1.59118700  | -3.09767700 |
| N | -2.29553800 | 0.97093800  | -0.16292800 |
| N | -0.66831700 | -0.78186200 | 1.57739600  |
| N | -1.59906300 | -1.64905700 | -1.08928800 |
| N | -3.29115300 | 0.30887800  | 0.47258100  |
| N | -1.91382700 | -1.19787200 | 1.91959000  |
| N | -2.69043200 | -1.96879900 | -0.34721700 |
| C | -2.80250200 | 2.14436400  | -0.55801500 |
| H | -2.17886200 | 2.84740500  | -1.09965400 |

|   |             |             |             |
|---|-------------|-------------|-------------|
| C | -4.13955900 | 2.25369400  | -0.16599500 |
| H | -4.81490500 | 3.08104300  | -0.33358600 |
| C | -4.40846600 | 1.06055700  | 0.48199300  |
| H | -5.31379100 | 0.68753100  | 0.94489700  |
| C | -3.32554900 | -3.02004400 | -0.90073500 |
| H | -4.21944200 | -3.42134100 | -0.43919400 |
| C | -2.63870600 | -3.40034300 | -2.03963000 |
| H | -2.87819800 | -4.20802500 | -2.71713000 |
| C | -1.56260100 | -2.51175700 | -2.11049000 |
| H | -0.76184400 | -2.44931400 | -2.83858800 |
| C | -1.94254600 | -1.54593400 | 3.21840900  |
| H | -2.86085200 | -1.90368000 | 3.66762500  |
| C | -0.67963500 | -1.35880400 | 3.75296300  |
| H | -0.35518300 | -1.54720100 | 4.76673800  |
| C | 0.07955300  | -0.87946300 | 2.68400300  |
| H | 1.12810000  | -0.60685700 | 2.65597400  |
| B | -3.07794600 | -1.15593500 | 0.90786600  |
| H | -4.07821100 | -1.59976800 | 1.40339500  |
| C | 1.93085200  | -0.46687700 | -0.54421800 |
| C | 2.55193200  | -1.31275000 | 0.39541500  |
| C | 3.93756600  | -1.39559200 | 0.54079300  |
| C | 4.76881400  | -0.65743700 | -0.30097900 |
| C | 4.18621200  | 0.12993800  | -1.30229000 |
| C | 2.81001000  | 0.20765400  | -1.42906700 |
| H | 1.93365000  | -1.93417700 | 1.04381900  |
| H | 0.89087400  | -1.10188000 | -1.11748500 |
| H | 2.39262300  | 0.82447800  | -2.22560700 |
| H | 4.84159400  | 0.67794000  | -1.97789800 |
| H | 4.35240900  | -2.05138100 | 1.30253600  |
| O | 6.12824200  | -0.65899500 | -0.25299000 |

|   |            |             |            |
|---|------------|-------------|------------|
| C | 6.74034000 | -1.44981900 | 0.74022900 |
| H | 7.81885700 | -1.30960200 | 0.63224300 |
| H | 6.44154800 | -1.13889100 | 1.75180000 |
| H | 6.50749900 | -2.51711900 | 0.61517600 |

**o-3σ**

58

|   |             |             |             |
|---|-------------|-------------|-------------|
| W | 0.17209200  | -0.28770600 | -0.43408200 |
| P | -0.88063400 | -2.05863700 | 0.86568400  |
| C | -1.24648900 | -3.57578500 | -0.09915000 |
| H | -0.31937100 | -3.98775600 | -0.51387200 |
| H | -1.72887900 | -4.33489800 | 0.52903700  |
| H | -1.90841900 | -3.32039400 | -0.93486800 |
| C | -2.50190600 | -1.83660800 | 1.72747100  |
| H | -2.77293100 | -2.73343200 | 2.30047500  |
| H | -2.45605700 | -0.98085100 | 2.41208600  |
| H | -3.28352200 | -1.64103900 | 0.98180000  |
| C | 0.12518400  | -2.73145500 | 2.25528700  |
| H | -0.38111000 | -3.57702200 | 2.73819900  |
| H | 1.09940400  | -3.06358800 | 1.87717700  |
| H | 0.29633200  | -1.94728100 | 3.00242400  |
| N | -0.20104900 | -1.15254200 | -1.93891100 |
| O | -0.45158900 | -1.81298200 | -2.93946600 |
| N | 2.10986900  | -1.18005000 | -0.25377000 |
| N | 0.74966000  | 0.68236100  | 1.55564200  |
| N | 1.34386600  | 1.43623700  | -1.22783700 |
| N | 3.17530500  | -0.46401300 | 0.20073600  |
| N | 2.00804400  | 1.15148100  | 1.73026900  |
| N | 2.51311900  | 1.79746500  | -0.64018000 |

|   |             |             |             |
|---|-------------|-------------|-------------|
| C | 2.57570700  | -2.39507300 | -0.57953900 |
| H | 1.89502000  | -3.14619000 | -0.96410800 |
| C | 3.95053700  | -2.47364700 | -0.33078400 |
| H | 4.60203300  | -3.32252000 | -0.48604400 |
| C | 4.28812300  | -1.23210200 | 0.17051500  |
| H | 5.23387500  | -0.83254200 | 0.51480700  |
| C | 3.05849500  | 2.83803700  | -1.30302200 |
| H | 3.99556700  | 3.26763100  | -0.97038600 |
| C | 2.22999000  | 3.16654900  | -2.36086000 |
| H | 2.37176900  | 3.95068500  | -3.09175600 |
| C | 1.16771300  | 2.26097000  | -2.26762700 |
| H | 0.28691700  | 2.15927500  | -2.89262700 |
| C | 2.11932500  | 1.72509200  | 2.94141700  |
| H | 3.06179400  | 2.15386700  | 3.25955600  |
| C | 0.89551100  | 1.63652900  | 3.58528900  |
| H | 0.64034700  | 1.99679300  | 4.57207500  |
| C | 0.07112600  | 0.97529100  | 2.67204700  |
| H | -0.97655300 | 0.70348700  | 2.75583100  |
| B | 3.04312000  | 1.02266000  | 0.58701600  |
| H | 4.10597000  | 1.46332300  | 0.93534500  |
| C | -2.82994300 | 1.00820200  | -0.88884900 |
| C | -3.48066000 | 1.65027100  | 0.16683400  |
| C | -4.75236100 | 1.21549500  | 0.56133300  |
| C | -5.35542000 | 0.15220600  | -0.09358400 |
| C | -4.70641800 | -0.50016000 | -1.14605500 |
| C | -3.44390000 | -0.06948400 | -1.53239400 |
| H | -1.83682100 | 1.33231300  | -1.21681200 |
| H | -2.90613600 | -0.57515200 | -2.33440400 |
| H | -5.18315500 | -1.33569000 | -1.65284400 |
| H | -6.34532700 | -0.17302000 | 0.22026900  |

|   |             |            |             |
|---|-------------|------------|-------------|
| H | -5.24717700 | 1.73100000 | 1.38169700  |
| O | -2.96259100 | 2.69022600 | 0.86121200  |
| C | -1.72592400 | 3.22250300 | 0.42822200  |
| H | -1.49603100 | 4.05559200 | 1.09658600  |
| H | -0.91270700 | 2.48290300 | 0.49136100  |
| H | -1.78613600 | 3.59550900 | -0.60418800 |

**m-3 $\sigma$**

58

|   |             |             |             |
|---|-------------|-------------|-------------|
| W | -0.40981700 | 0.30997100  | -0.39078300 |
| P | 0.69507800  | 1.81171500  | 1.17252600  |
| C | 0.88883100  | 3.52669400  | 0.54929000  |
| H | -0.09243500 | 3.95282300  | 0.31135200  |
| H | 1.38699500  | 4.16086700  | 1.29310300  |
| H | 1.48387500  | 3.50947900  | -0.37127800 |
| C | 2.40862600  | 1.51751000  | 1.80596100  |
| H | 2.70501500  | 2.29797600  | 2.51944700  |
| H | 2.47032400  | 0.54279400  | 2.30590700  |
| H | 3.11201500  | 1.52043400  | 0.96305300  |
| C | -0.18203500 | 2.08805900  | 2.76932100  |
| H | 0.34020800  | 2.82869000  | 3.38846400  |
| H | -1.20209000 | 2.43897400  | 2.57268200  |
| H | -0.24565100 | 1.14384700  | 3.32355400  |
| N | -0.24430700 | 1.52182800  | -1.67718500 |
| O | -0.13883000 | 2.40518600  | -2.51854200 |
| N | -2.36341900 | 0.98050400  | 0.16981500  |
| N | -0.72814300 | -1.16009500 | 1.33498700  |
| N | -1.57428500 | -1.25522200 | -1.48597300 |
| N | -3.33702900 | 0.09787100  | 0.52752900  |

|   |             |             |             |
|---|-------------|-------------|-------------|
| N | -1.93629600 | -1.74954700 | 1.49811400  |
| N | -2.65610200 | -1.83456600 | -0.90530200 |
| C | -2.92524400 | 2.19857200  | 0.18755000  |
| H | -2.32859900 | 3.06853100  | -0.06275400 |
| C | -4.27034600 | 2.11053400  | 0.56316200  |
| H | -4.97924400 | 2.91959700  | 0.67327100  |
| C | -4.48748300 | 0.76378800  | 0.77734400  |
| H | -5.37052000 | 0.22299700  | 1.09442600  |
| C | -3.23052400 | -2.70082800 | -1.76485800 |
| H | -4.10744900 | -3.26409800 | -1.46959600 |
| C | -2.51178900 | -2.68655500 | -2.94679200 |
| H | -2.70237500 | -3.26199900 | -3.84220700 |
| C | -1.48283300 | -1.76642000 | -2.71960600 |
| H | -0.68126000 | -1.44655200 | -3.37653400 |
| C | -1.89338600 | -2.60028000 | 2.53885000  |
| H | -2.77512400 | -3.16143700 | 2.82352100  |
| C | -0.61667000 | -2.57577200 | 3.07621300  |
| H | -0.24432400 | -3.13941000 | 3.92023800  |
| C | 0.07533600  | -1.65774000 | 2.28246400  |
| H | 1.10755300  | -1.32807600 | 2.34426500  |
| B | -3.09028700 | -1.42463400 | 0.51956500  |
| H | -4.08765500 | -2.01392200 | 0.84118000  |
| C | 2.66068100  | -0.56114100 | -1.34613800 |
| C | 3.50331900  | -1.31242800 | -0.52719700 |
| C | 4.77973900  | -0.82416100 | -0.23649000 |
| C | 5.19503500  | 0.40083900  | -0.77293700 |
| C | 4.33977100  | 1.13575400  | -1.58253300 |
| C | 3.05913600  | 0.66330000  | -1.87322300 |
| H | 3.15865900  | -2.26195600 | -0.12693900 |
| H | 1.65928200  | -0.94988600 | -1.57808600 |

|   |            |             |             |
|---|------------|-------------|-------------|
| H | 2.37161000 | 1.24673500  | -2.48343700 |
| H | 4.67478300 | 2.08951200  | -1.98525900 |
| H | 6.19532200 | 0.75662700  | -0.53511600 |
| O | 5.67881900 | -1.46004200 | 0.54996200  |
| C | 5.27394100 | -2.66532100 | 1.16678000  |
| H | 4.39994400 | -2.51265900 | 1.81623800  |
| H | 5.03947000 | -3.44334900 | 0.42746100  |
| H | 6.11591900 | -2.99994500 | 1.77706500  |

**p-3 $\sigma$**

58

|   |             |             |             |
|---|-------------|-------------|-------------|
| W | 0.44686000  | -0.23141800 | -0.56116100 |
| P | 1.85842700  | -1.99626000 | 0.34628300  |
| C | 3.29336400  | -2.42599300 | -0.71609700 |
| H | 3.93062400  | -1.54721300 | -0.86414200 |
| H | 3.88994400  | -3.22442300 | -0.25769700 |
| H | 2.93533900  | -2.75756400 | -1.69683900 |
| C | 1.28425200  | -3.70168200 | 0.77676600  |
| H | 2.09246300  | -4.28613600 | 1.23636600  |
| H | 0.43883100  | -3.65694800 | 1.47403700  |
| H | 0.95277400  | -4.21137500 | -0.13622800 |
| C | 2.70000300  | -1.55213300 | 1.92639900  |
| H | 3.42843700  | -2.32141200 | 2.21276600  |
| H | 3.21642000  | -0.59122600 | 1.81204400  |
| H | 1.95970500  | -1.45054200 | 2.72856600  |
| N | 1.21196900  | -0.41698800 | -2.15530600 |
| O | 1.84779100  | -0.50715700 | -3.19701900 |
| N | 1.90761200  | 1.22813600  | 0.02020700  |
| N | -0.29889600 | 0.09180100  | 1.56504000  |



|   |             |             |             |
|---|-------------|-------------|-------------|
| N | -0.74401100 | 1.63541400  | -0.94652300 |
| N | 1.57987000  | 2.27992000  | 0.82001900  |
| N | -0.37813300 | 1.34320800  | 2.07699900  |
| N | -0.72852400 | 2.65156900  | -0.04349700 |
| C | 3.20159100  | 1.37755900  | -0.29966600 |
| H | 3.68472300  | 0.64908000  | -0.94015700 |
| C | 3.72372700  | 2.52715200  | 0.30397000  |
| H | 4.73485800  | 2.90490300  | 0.23938700  |
| C | 2.66473200  | 3.06615200  | 1.00704500  |
| H | 2.59438600  | 3.95007600  | 1.62864800  |
| C | -1.38347100 | 3.72046100  | -0.54293200 |
| H | -1.47303700 | 4.62809300  | 0.04160000  |
| C | -1.84089700 | 3.40129900  | -1.80855000 |
| H | -2.40573200 | 4.02828500  | -2.48475200 |
| C | -1.41463300 | 2.08370400  | -2.01188300 |
| H | -1.56635100 | 1.43469600  | -2.86662100 |
| C | -0.88441300 | 1.29893900  | 3.32201800  |
| H | -1.01303200 | 2.21027900  | 3.89322700  |
| C | -1.15277500 | -0.02248500 | 3.64111700  |
| H | -1.56374300 | -0.40941000 | 4.56311300  |
| C | -0.76559900 | -0.73831200 | 2.50571800  |
| H | -0.80325800 | -1.80614100 | 2.31617100  |
| B | 0.11755300  | 2.54382900  | 1.24238700  |
| H | 0.04202700  | 3.55853800  | 1.88327900  |
| C | -3.21229800 | -0.84554600 | -0.54554700 |
| C | -3.53237000 | -1.53964000 | 0.61935700  |
| C | -3.00546000 | -2.81893900 | 0.82402900  |
| C | -2.14338300 | -3.39511100 | -0.09805000 |
| C | -1.80343200 | -2.68397500 | -1.25542800 |
| C | -2.35201000 | -1.42578000 | -1.49337100 |

|   |             |             |             |
|---|-------------|-------------|-------------|
| H | -4.19213500 | -1.10138400 | 1.36389600  |
| H | -3.27676200 | -3.36138800 | 1.72796300  |
| H | -1.73524200 | -4.38845500 | 0.07395500  |
| H | -2.14407100 | -0.88332300 | -2.41361300 |
| H | -1.14133400 | -3.12572900 | -1.99867800 |
| O | -3.69370800 | 0.37969500  | -0.85619200 |
| C | -4.12497400 | 1.19786500  | 0.21220300  |
| H | -4.29503300 | 2.19348100  | -0.20643000 |
| H | -5.06262300 | 0.83912000  | 0.65828000  |
| H | -3.35360900 | 1.26291000  | 0.99615000  |

**o-TS2**

58

|   |             |             |             |
|---|-------------|-------------|-------------|
| W | 0.43331700  | -0.36530300 | -0.40533200 |
| N | -1.05787300 | 1.28150900  | -0.62200000 |
| C | -2.20467400 | 1.39969800  | -1.30331200 |
| N | -0.82834000 | 2.48853300  | -0.04055900 |
| C | -2.72909900 | 2.69013000  | -1.16321600 |
| H | -2.59846900 | 0.55177200  | -1.85276500 |
| C | -1.82282500 | 3.34571500  | -0.34981000 |
| B | 0.47875800  | 2.74946000  | 0.73855700  |
| H | -3.63870000 | 3.08629600  | -1.59412300 |
| H | -1.80845600 | 4.35958500  | 0.03121200  |
| N | 0.54099300  | 1.78454900  | 1.94358500  |
| N | 1.66473700  | 2.44631700  | -0.20185500 |
| H | 0.52380900  | 3.89063300  | 1.11480300  |
| C | 0.63423500  | 2.04260900  | 3.26000500  |
| N | 0.51360800  | 0.44719400  | 1.73409900  |
| C | 2.61510600  | 3.29326100  | -0.65969800 |

|   |             |             |             |
|---|-------------|-------------|-------------|
| N | 1.81625900  | 1.22591300  | -0.78754300 |
| C | 0.66713600  | 0.83742400  | 3.94264100  |
| H | 0.66998000  | 3.06478500  | 3.61642600  |
| C | 0.58897100  | -0.13085400 | 2.93876100  |
| C | 3.39746000  | 2.62042300  | -1.57705800 |
| H | 2.66046800  | 4.31004200  | -0.28982300 |
| C | 2.86096600  | 1.32858800  | -1.62252500 |
| H | 0.73678300  | 0.68375800  | 5.01049400  |
| H | 0.58218800  | -1.21260900 | 3.02239400  |
| H | 4.24437900  | 3.00342800  | -2.12961900 |
| H | 3.17064500  | 0.46676800  | -2.20273300 |
| P | 2.24239900  | -1.87509500 | 0.18344900  |
| C | 2.01363500  | -3.40159100 | 1.20448300  |
| H | 2.96124600  | -3.94204400 | 1.33224300  |
| H | 1.62574400  | -3.13770900 | 2.19624800  |
| H | 1.29053700  | -4.06436900 | 0.71281800  |
| C | 3.11807100  | -2.59706300 | -1.26038200 |
| H | 3.51639200  | -1.79722600 | -1.89495200 |
| H | 3.94452700  | -3.24128400 | -0.93537700 |
| H | 2.41357200  | -3.18690800 | -1.85722700 |
| N | 0.48547400  | -0.90972700 | -2.09513100 |
| O | 0.60538400  | -1.23900100 | -3.26736500 |
| C | -3.63453500 | -0.79392400 | 1.20965500  |
| C | -3.86572200 | -1.13117700 | -0.12739800 |
| C | -3.03592700 | -2.05878000 | -0.76594800 |
| C | -1.97991700 | -2.63945800 | -0.07525700 |
| C | -1.73130500 | -2.29943200 | 1.25816400  |
| C | -2.56757400 | -1.37912300 | 1.88789600  |
| H | -4.26994900 | -0.07871400 | 1.72419800  |
| H | -1.34845400 | -3.37006200 | -0.57921300 |

|   |             |             |             |
|---|-------------|-------------|-------------|
| H | -0.91720600 | -2.77262500 | 1.80380000  |
| H | -2.39352000 | -1.11087800 | 2.92852300  |
| C | 3.64268300  | -1.10357900 | 1.10226400  |
| H | 4.45217400  | -1.82508200 | 1.27188400  |
| H | 4.03300200  | -0.25456800 | 0.52843000  |
| H | 3.29208800  | -0.72928200 | 2.07149100  |
| H | -3.23612700 | -2.30656900 | -1.80660100 |
| O | -4.85549600 | -0.60595900 | -0.88758400 |
| C | -5.67406300 | 0.38913300  | -0.30550500 |
| H | -5.08318500 | 1.25522100  | 0.02535900  |
| H | -6.37219500 | 0.70942500  | -1.08230000 |
| H | -6.24533900 | -0.00256500 | 0.54729000  |

#### m-TS2

58

|   |             |             |             |
|---|-------------|-------------|-------------|
| W | 0.40255000  | -0.36043200 | -0.37350200 |
| N | -0.96166000 | 1.35817700  | -0.79984400 |
| C | -2.05108200 | 1.49707800  | -1.56552300 |
| N | -0.69316200 | 2.58516000  | -0.28197900 |
| C | -2.49964900 | 2.82318300  | -1.54456400 |
| H | -2.45982000 | 0.63507000  | -2.08259300 |
| C | -1.60839200 | 3.47733100  | -0.71394300 |
| B | 0.56997800  | 2.81533100  | 0.57501200  |
| H | -3.35261400 | 3.24365900  | -2.05977900 |
| H | -1.55458900 | 4.51188600  | -0.39756400 |
| N | 0.48496800  | 1.92953100  | 1.83914600  |
| N | 1.79623900  | 2.38022900  | -0.25480700 |
| H | 0.66336600  | 3.97352200  | 0.88445400  |
| C | 0.48276400  | 2.27365200  | 3.13908200  |

|   |             |             |             |
|---|-------------|-------------|-------------|
| N | 0.39471100  | 0.58365100  | 1.71615000  |
| C | 2.83515100  | 3.13267400  | -0.68357100 |
| N | 1.90440600  | 1.11860200  | -0.75548500 |
| C | 0.38456900  | 1.11991200  | 3.89941200  |
| H | 0.55138600  | 3.31478000  | 3.42994400  |
| C | 0.33162400  | 0.08907200  | 2.95826100  |
| C | 3.63466200  | 2.35365300  | -1.49659600 |
| H | 2.92420300  | 4.16536600  | -0.37001000 |
| C | 3.01350800  | 1.09968400  | -1.50992000 |
| H | 0.35486600  | 1.03859000  | 4.97700400  |
| H | 0.25021000  | -0.98174400 | 3.11287900  |
| H | 4.54521600  | 2.64447900  | -2.00217000 |
| H | 3.30698800  | 0.18423900  | -2.01115400 |
| P | 2.08817400  | -1.92984700 | 0.42008900  |
| C | 1.73735500  | -3.32684100 | 1.58224900  |
| H | 2.65004100  | -3.89779300 | 1.79960400  |
| H | 1.33389400  | -2.94335500 | 2.52720400  |
| H | 0.99732700  | -4.00235800 | 1.13593000  |
| C | 2.93373100  | -2.85693400 | -0.91977100 |
| H | 3.38523400  | -2.16099000 | -1.63551600 |
| H | 3.71411400  | -3.51142600 | -0.51201500 |
| H | 2.19621700  | -3.46550200 | -1.45598700 |
| N | 0.51377300  | -1.02685800 | -2.01415800 |
| O | 0.65977600  | -1.46169700 | -3.14833500 |
| C | -3.73904500 | -0.88445800 | 0.46854900  |
| C | -3.72943300 | -1.44432700 | -0.81175800 |
| C | -2.76708300 | -2.40136500 | -1.13370200 |
| C | -1.83328200 | -2.82877000 | -0.19326200 |
| C | -1.86834400 | -2.28376900 | 1.09616200  |
| C | -2.80691000 | -1.31066000 | 1.42188800  |

|   |             |             |             |
|---|-------------|-------------|-------------|
| H | -1.09988000 | -3.59013800 | -0.45220200 |
| H | -1.16741700 | -2.62979800 | 1.85486800  |
| H | -2.84278700 | -0.87079600 | 2.41670400  |
| C | 3.51318000  | -1.16098500 | 1.30114000  |
| H | 4.26400600  | -1.91194600 | 1.57825800  |
| H | 3.97949500  | -0.40613100 | 0.65684700  |
| H | 3.15704400  | -0.66159400 | 2.21038500  |
| H | -2.75582200 | -2.82167200 | -2.13770600 |
| H | -4.44864100 | -1.13141300 | -1.56369600 |
| O | -4.60196900 | 0.07554600  | 0.87556700  |
| C | -5.56474500 | 0.53272600  | -0.05259600 |
| H | -6.15399600 | 1.29488200  | 0.46245100  |
| H | -5.09466300 | 0.98463500  | -0.93738000 |
| H | -6.23343400 | -0.27677900 | -0.37623400 |

**p-TS2**

58

|   |             |             |             |
|---|-------------|-------------|-------------|
| W | 0.35575600  | -0.36828000 | -0.28376200 |
| N | -1.39793900 | 0.84368900  | -0.96150500 |
| C | -2.36567300 | 0.59200200  | -1.85024700 |
| N | -1.52546200 | 2.14960500  | -0.61116000 |
| C | -3.13540300 | 1.74071100  | -2.07923500 |
| H | -2.46204400 | -0.40007600 | -2.27533000 |
| C | -2.56427900 | 2.70589100  | -1.27174900 |
| B | -0.40701700 | 2.84715600  | 0.18622000  |
| H | -3.98632900 | 1.84815600  | -2.73792200 |
| H | -2.81416700 | 3.74853500  | -1.11734200 |
| N | -0.23984500 | 2.16682400  | 1.55960100  |
| N | 0.90777900  | 2.67257100  | -0.60904800 |

|   |             |             |             |
|---|-------------|-------------|-------------|
| H | -0.65793400 | 4.01512800  | 0.32791900  |
| C | -0.36756600 | 2.69463200  | 2.79018000  |
| N | 0.15343700  | 0.87363900  | 1.64493600  |
| C | 1.67212600  | 3.61956100  | -1.19567100 |
| N | 1.38538700  | 1.43745000  | -0.91901300 |
| C | -0.04957000 | 1.72006100  | 3.72032800  |
| H | -0.66788000 | 3.72800400  | 2.91356900  |
| C | 0.27130700  | 0.60065900  | 2.94928900  |
| C | 2.67004300  | 2.99312900  | -1.91752700 |
| H | 1.44830300  | 4.66875300  | -1.04696900 |
| C | 2.45011400  | 1.62696900  | -1.71079000 |
| H | -0.04568200 | 1.80849200  | 4.79775300  |
| H | 0.57882800  | -0.38608800 | 3.27717200  |
| H | 3.45331300  | 3.45601800  | -2.50182600 |
| H | 3.00370700  | 0.77194100  | -2.08293100 |
| P | 2.42326500  | -1.31292400 | 0.61062200  |
| C | 2.49066200  | -2.45510800 | 2.06622900  |
| H | 3.52425400  | -2.77281600 | 2.25611300  |
| H | 2.11372000  | -1.95224800 | 2.96444500  |
| H | 1.87952100  | -3.34734300 | 1.88720100  |
| C | 3.36449100  | -2.31075700 | -0.60954900 |
| H | 3.56750500  | -1.71289000 | -1.50500100 |
| H | 4.31417800  | -2.65940400 | -0.18501200 |
| H | 2.76458300  | -3.17875700 | -0.90802100 |
| N | 0.54162900  | -1.20250900 | -1.83827400 |
| O | 0.66218800  | -1.75271800 | -2.91962700 |
| C | -3.28892500 | -1.97859800 | -0.15801700 |
| C | -2.76480000 | -2.98718700 | -0.97941800 |
| C | -1.48049300 | -3.47339000 | -0.81262500 |
| C | -0.68352700 | -2.95738100 | 0.22278400  |

|   |             |             |             |
|---|-------------|-------------|-------------|
| C | -1.17584300 | -1.93210000 | 1.04378600  |
| C | -2.49365400 | -1.44889500 | 0.85127000  |
| H | 0.27280600  | -3.41901500 | 0.45179500  |
| H | -0.66345400 | -1.66947400 | 1.96700800  |
| C | 3.69438000  | -0.09399300 | 1.15569500  |
| H | 4.60126400  | -0.59769100 | 1.51361400  |
| H | 3.95660300  | 0.56819400  | 0.32275800  |
| H | 3.28643300  | 0.52285200  | 1.96578800  |
| H | -1.09812600 | -4.26123700 | -1.45617800 |
| H | -3.39672500 | -3.39638000 | -1.76616000 |
| H | -4.29909900 | -1.61588400 | -0.32467000 |
| O | -2.88289800 | -0.48652200 | 1.70695600  |
| C | -4.09390300 | 0.19502900  | 1.43250000  |
| H | -4.16003100 | 1.00803800  | 2.15943400  |
| H | -4.09409000 | 0.61620800  | 0.41701000  |
| H | -4.96541000 | -0.46257500 | 1.55294000  |

### 3C

58

|   |             |            |             |
|---|-------------|------------|-------------|
| W | -0.09506600 | 0.12428800 | -0.09461100 |
| N | 1.23741000  | 1.93544100 | -0.17064600 |
| C | 1.01087800  | 3.21321200 | -0.48612800 |
| N | 2.57344300  | 1.81488600 | 0.04139700  |
| C | 2.20570300  | 3.93974500 | -0.47583000 |
| H | 0.00209600  | 3.54304200 | -0.70640000 |
| C | 3.17124100  | 3.01010800 | -0.13653200 |
| B | 3.23228800  | 0.43384800 | 0.27291400  |
| H | 2.34449700  | 4.99126900 | -0.68550300 |
| H | 4.24238000  | 3.10774200 | -0.00895000 |



|   |             |             |             |
|---|-------------|-------------|-------------|
| N | 2.62597400  | -0.21163500 | 1.53391000  |
| N | 2.89670300  | -0.43349500 | -0.96224700 |
| H | 4.42164500  | 0.54904900  | 0.39525700  |
| C | 3.25183400  | -0.63662800 | 2.64631500  |
| N | 1.28632900  | -0.38120000 | 1.66085500  |
| C | 3.71260900  | -0.91260900 | -1.92143900 |
| N | 1.60694400  | -0.55978400 | -1.35381700 |
| C | 2.29920800  | -1.10048000 | 3.53660200  |
| H | 4.33011700  | -0.57226600 | 2.72495200  |
| C | 1.08518500  | -0.91484200 | 2.87197300  |
| C | 2.93547100  | -1.37207400 | -2.97062000 |
| H | 4.78724900  | -0.87865500 | -1.79094100 |
| C | 1.62081000  | -1.11784800 | -2.56892400 |
| H | 2.45931900  | -1.50763400 | 4.52507900  |
| H | 0.08013800  | -1.13869400 | 3.21127100  |
| H | 3.27201200  | -1.81839900 | -3.89595200 |
| H | 0.68684200  | -1.31190900 | -3.08489000 |
| P | -0.63562500 | -2.33420400 | -0.07114300 |
| C | -1.50160900 | -3.12559700 | 1.33867500  |
| H | -1.59162100 | -4.20138900 | 1.14530500  |
| H | -0.93143100 | -2.98287900 | 2.26337300  |
| H | -2.50397300 | -2.70776400 | 1.47219000  |
| C | -1.65631500 | -2.88054800 | -1.48664200 |
| H | -1.15699900 | -2.62740300 | -2.42856700 |
| H | -1.83317100 | -3.96235900 | -1.45054300 |
| H | -2.61746900 | -2.35336600 | -1.45602600 |
| N | -1.08031300 | 0.43746500  | -1.52925400 |
| O | -1.73105300 | 0.60797400  | -2.54108500 |
| C | -2.01389100 | 2.53413300  | 0.84599100  |
| C | -3.24583300 | 2.36082500  | 0.30963800  |

|   |             |             |             |
|---|-------------|-------------|-------------|
| C | -3.84871100 | 1.05235700  | 0.29270300  |
| C | -3.20847400 | -0.01919800 | 0.83247100  |
| C | -1.84475100 | 0.09705300  | 1.34351200  |
| C | -1.22435500 | 1.42098100  | 1.33307000  |
| H | -1.61211800 | 3.54274300  | 0.94832100  |
| H | -3.83455200 | 3.19649300  | -0.06459200 |
| H | -3.70963400 | -0.98285400 | 0.91047000  |
| H | -1.62497200 | -0.55915600 | 2.19021900  |
| H | -0.50708100 | 1.66043800  | 2.12418300  |
| C | 0.84617100  | -3.41655500 | -0.16609200 |
| H | 0.54992600  | -4.47103500 | -0.11010300 |
| H | 1.39557800  | -3.24859100 | -1.09811800 |
| H | 1.51277000  | -3.18780200 | 0.67570100  |
| O | -5.10593100 | 1.04410000  | -0.23630600 |
| C | -5.78525500 | -0.18681700 | -0.24702200 |
| H | -5.23577200 | -0.94908600 | -0.82052900 |
| H | -5.95388300 | -0.56984800 | 0.77056700  |
| H | -6.75311100 | -0.01283900 | -0.72458600 |

### 3D

58

|   |             |             |             |
|---|-------------|-------------|-------------|
| W | -0.11268400 | -0.18187300 | -0.10475700 |
| N | 0.01231900  | 2.06481300  | -0.10512600 |
| C | -0.87517900 | 3.01687200  | -0.40318900 |
| N | 1.19165000  | 2.69057800  | 0.14270900  |
| C | -0.27665500 | 4.27971100  | -0.34344900 |
| H | -1.89733200 | 2.74362500  | -0.64124300 |
| C | 1.03632800  | 4.02304600  | 0.00521700  |
| B | 2.49843300  | 1.88949900  | 0.35186200  |

|   |             |             |             |
|---|-------------|-------------|-------------|
| H | -0.73606300 | 5.24086600  | -0.52825600 |
| H | 1.87582600  | 4.68861800  | 0.16443400  |
| N | 2.34101700  | 0.96921300  | 1.57775900  |
| N | 2.69910500  | 1.02737700  | -0.91607100 |
| H | 3.42908500  | 2.63281800  | 0.50722600  |
| C | 3.09542200  | 0.91355700  | 2.69021800  |
| N | 1.31637800  | 0.08494400  | 1.66624900  |
| C | 3.65027100  | 1.10674000  | -1.86707000 |
| N | 1.69009700  | 0.23230100  | -1.34350700 |
| C | 2.55426100  | -0.03399800 | 3.54129700  |
| H | 3.95992200  | 1.55723500  | 2.79649400  |
| C | 1.44021800  | -0.52045300 | 2.85385700  |
| C | 3.25715500  | 0.33608000  | -2.94750500 |
| H | 4.53153200  | 1.71613600  | -1.70859100 |
| C | 2.01454600  | -0.18328300 | -2.57248600 |
| H | 2.91056900  | -0.32616400 | 4.51915000  |
| H | 0.72476700  | -1.27449900 | 3.16206000  |
| H | 3.78852300  | 0.17971600  | -3.87592700 |
| H | 1.34135700  | -0.83572500 | -3.11789100 |
| P | 0.76892600  | -2.53898000 | -0.16603600 |
| C | 0.45386800  | -3.72156800 | 1.19951900  |
| H | 0.95224800  | -4.67249400 | 0.97523000  |
| H | 0.85785800  | -3.32791600 | 2.13900400  |
| H | -0.61759300 | -3.90626800 | 1.32436200  |
| C | 0.23555600  | -3.49906300 | -1.62832900 |
| H | 0.52535800  | -2.97254600 | -2.54447100 |
| H | 0.68669400  | -4.49875300 | -1.62807900 |
| H | -0.85668600 | -3.59326300 | -1.61939100 |
| N | -1.10721000 | -0.40582000 | -1.54978700 |
| O | -1.74420800 | -0.58347500 | -2.56915500 |

|   |             |             |             |
|---|-------------|-------------|-------------|
| C | -3.03854400 | 0.82446300  | 0.87146300  |
| C | -3.97285100 | 0.02187500  | 0.29553300  |
| C | -3.77114500 | -1.40266400 | 0.22101300  |
| C | -2.65484700 | -1.96553500 | 0.74311900  |
| C | -1.57866800 | -1.17401300 | 1.30981100  |
| C | -1.76687300 | 0.27411000  | 1.32669400  |
| H | -3.22735800 | 1.88427200  | 1.02642700  |
| H | -2.57092600 | -3.05387600 | 0.76419500  |
| H | -1.03861400 | -1.64834600 | 2.13284900  |
| H | -1.29273900 | 0.82915400  | 2.14271500  |
| C | 2.60179300  | -2.63426000 | -0.24476500 |
| H | 2.92902800  | -3.68079700 | -0.22216700 |
| H | 2.97744900  | -2.16261900 | -1.15870500 |
| H | 3.02902600  | -2.10772600 | 0.61849800  |
| H | -4.56910800 | -2.00610200 | -0.20832900 |
| O | -5.17800200 | 0.42782500  | -0.19738500 |
| C | -5.46447500 | 1.80238500  | -0.11726100 |
| H | -6.44319800 | 1.95207600  | -0.58062100 |
| H | -5.50660100 | 2.15075600  | 0.92546200  |
| H | -4.71734200 | 2.40499100  | -0.65655900 |

### 3B

58

|   |             |             |             |
|---|-------------|-------------|-------------|
| W | -0.13046100 | -0.27906900 | -0.16019300 |
| N | -0.42916300 | 1.94415700  | -0.30367300 |
| C | -1.41665600 | 2.68621700  | -0.80890700 |
| N | 0.57009000  | 2.79890800  | 0.03976100  |
| C | -1.06905900 | 4.04069500  | -0.79131000 |
| H | -2.32792100 | 2.20960700  | -1.14989200 |

|   |             |             |             |
|---|-------------|-------------|-------------|
| C | 0.20166400  | 4.06367600  | -0.24673000 |
| B | 1.96777500  | 2.27771900  | 0.45093800  |
| H | -1.66045600 | 4.88166700  | -1.12590200 |
| H | 0.87588400  | 4.88650200  | -0.04289000 |
| N | 1.83797300  | 1.39444300  | 1.70618900  |
| N | 2.48108100  | 1.41931100  | -0.73004400 |
| H | 2.71574300  | 3.19355800  | 0.66148200  |
| C | 2.44735200  | 1.53105200  | 2.89758800  |
| N | 0.99902400  | 0.32921100  | 1.73277300  |
| C | 3.49724500  | 1.65382800  | -1.58288100 |
| N | 1.69789000  | 0.42745500  | -1.21488900 |
| C | 1.99813000  | 0.52800000  | 3.73862600  |
| H | 3.15297700  | 2.33631500  | 3.06076500  |
| C | 1.09070900  | -0.19469500 | 2.96152200  |
| C | 3.38167900  | 0.78547500  | -2.65480700 |
| H | 4.22017700  | 2.43168100  | -1.37011100 |
| C | 2.22853900  | 0.04433200  | -2.38098700 |
| H | 2.28138300  | 0.34974300  | 4.76646600  |
| H | 0.50035400  | -1.06235400 | 3.23333000  |
| H | 4.03209900  | 0.70726200  | -3.51476400 |
| H | 1.75636300  | -0.74443100 | -2.95644000 |
| P | 1.21536100  | -2.40829900 | -0.00398600 |
| C | 0.98024700  | -3.59980700 | 1.36927400  |
| H | 1.69580800  | -4.42307000 | 1.25534800  |
| H | 1.16229700  | -3.10844300 | 2.33154700  |
| H | -0.03349400 | -4.01188700 | 1.36697100  |
| C | 1.06471300  | -3.49024700 | -1.47042900 |
| H | 1.35681000  | -2.94013400 | -2.37173800 |
| H | 1.69924100  | -4.37898600 | -1.36869900 |
| H | 0.01908600  | -3.80056600 | -1.58140600 |

|   |             |             |             |
|---|-------------|-------------|-------------|
| N | -0.86694600 | -0.71869200 | -1.70679000 |
| O | -1.29532000 | -1.01154200 | -2.80483900 |
| C | -3.28084500 | 0.09085100  | 0.49175800  |
| C | -3.99061100 | -0.88021800 | -0.15191200 |
| C | -3.47909700 | -2.22683000 | -0.15560600 |
| C | -2.32611000 | -2.55433900 | 0.47796000  |
| C | -1.49389000 | -1.54331500 | 1.11801800  |
| C | -1.97804100 | -0.16301700 | 1.08065700  |
| H | -2.01686900 | -3.59929200 | 0.53343500  |
| H | -0.97066500 | -1.87491300 | 2.01906000  |
| H | -1.74435800 | 0.49474600  | 1.92377500  |
| C | 3.02553400  | -2.12789000 | 0.13458700  |
| H | 3.54821300  | -3.08618500 | 0.24117900  |
| H | 3.41060900  | -1.60739900 | -0.74829400 |
| H | 3.22944400  | -1.51024900 | 1.01876900  |
| H | -4.07190600 | -3.00122900 | -0.64164600 |
| H | -4.95887000 | -0.67578200 | -0.60012000 |
| O | -3.71485000 | 1.36051300  | 0.70204100  |
| C | -4.94969300 | 1.72907000  | 0.12894700  |
| H | -4.93299500 | 1.62222600  | -0.96590500 |
| H | -5.77800100 | 1.12722400  | 0.52873300  |
| H | -5.11531800 | 2.77900800  | 0.38325100  |

### 3A

58

|   |             |             |             |
|---|-------------|-------------|-------------|
| W | -0.11911200 | 0.21892900  | -0.13247600 |
| P | -1.07831100 | -2.12405600 | -0.11521800 |
| O | -1.43175700 | 0.95588500  | -2.70666800 |
| N | 1.05415800  | -0.50112400 | 1.69133000  |

|   |             |             |             |
|---|-------------|-------------|-------------|
| N | 2.40682600  | -0.58341200 | 1.63943800  |
| N | 2.76466900  | -0.88844900 | -0.83903300 |
| N | 1.49608500  | -0.77460000 | -1.29738500 |
| N | 2.80760100  | 1.39273800  | 0.13369500  |
| N | 1.52905300  | 1.74883900  | -0.15336700 |
| N | -0.92631100 | 0.68684900  | -1.63535000 |
| C | 0.69202500  | -0.94826800 | 2.89991800  |
| H | -0.35409300 | -0.96712900 | 3.18455200  |
| C | 1.81339900  | -1.33199000 | 3.63855200  |
| H | 1.84257500  | -1.72908000 | 4.64349000  |
| C | 2.88207300  | -1.07958100 | 2.79605900  |
| H | 3.94783200  | -1.21114400 | 2.93717200  |
| C | 2.73325200  | -1.81825200 | -2.85178200 |
| H | 3.02877900  | -2.32014700 | -3.76256300 |
| C | 3.52678000  | -1.50918900 | -1.76046400 |
| H | 4.58150200  | -1.67285000 | -1.57637400 |
| C | 1.55466900  | 3.03832400  | -0.49899900 |
| H | 0.63340900  | 3.53969700  | -0.77294300 |
| C | 2.85985300  | 3.53646000  | -0.43197500 |
| H | 3.19825000  | 4.54049000  | -0.64727100 |
| C | 3.62134300  | 2.45558400  | -0.02741400 |
| H | 4.68436800  | 2.36040100  | 0.15727900  |
| C | 0.20663700  | -3.43531100 | -0.20507200 |
| H | -0.26093800 | -4.42415300 | -0.12501700 |
| H | 0.76629400  | -3.38077000 | -1.14397300 |
| C | -2.05323500 | -2.76416100 | 1.29944900  |
| H | -1.44362400 | -2.75389100 | 2.21022600  |
| H | -2.95044900 | -2.15811300 | 1.45259900  |
| C | -2.15970900 | -2.49602000 | -1.54215800 |
| H | -2.49898700 | -3.53880700 | -1.51825700 |

|   |             |             |             |
|---|-------------|-------------|-------------|
| H | -3.02914000 | -1.82839100 | -1.51155100 |
| B | 3.18923400  | -0.08160100 | 0.41010400  |
| H | 4.37100500  | -0.18499900 | 0.59743800  |
| C | -1.02794700 | 1.72980200  | 1.23813500  |
| H | -0.34109000 | 1.77853200  | 2.08885300  |
| C | -1.51548900 | 3.01115600  | 0.75528100  |
| H | -0.91125800 | 3.90065100  | 0.93262600  |
| C | -2.71660300 | 3.11383300  | 0.13433200  |
| H | -3.06701800 | 4.07749400  | -0.23338500 |
| C | -3.57625300 | 1.96977500  | -0.01767700 |
| C | -3.19896800 | 0.77124500  | 0.51055700  |
| C | -1.91798900 | 0.57176400  | 1.17453000  |
| H | -1.96315600 | -0.11823900 | 2.02192200  |
| H | -4.53506900 | 2.08781000  | -0.51469800 |
| C | 1.46880800  | -1.32610600 | -2.51516100 |
| H | 0.54272400  | -1.34723700 | -3.07971600 |
| H | -2.34417700 | -3.80069500 | 1.08882300  |
| H | 0.91115800  | -3.30614300 | 0.62697900  |
| H | -1.61524200 | -2.31510300 | -2.47575400 |
| O | -3.97238100 | -0.34761000 | 0.50534200  |
| C | -5.22229700 | -0.28083200 | -0.14807700 |
| H | -5.10575000 | -0.02014800 | -1.20967500 |
| H | -5.67069200 | -1.27450500 | -0.06965300 |
| H | -5.88800600 | 0.45306700  | 0.32694200  |

**o-TS3**

58

|   |             |             |             |
|---|-------------|-------------|-------------|
| W | 0.39365800  | -0.36885300 | -0.34398200 |
| N | -0.99907000 | 1.31556700  | -0.81714600 |



|   |             |             |             |
|---|-------------|-------------|-------------|
| C | -2.07928900 | 1.41726300  | -1.60076900 |
| N | -0.75956900 | 2.55767800  | -0.32282100 |
| C | -2.55218600 | 2.73522300  | -1.61490400 |
| H | -2.46687300 | 0.53658300  | -2.10251900 |
| C | -1.68426600 | 3.42392300  | -0.78756200 |
| B | 0.50678400  | 2.82973100  | 0.51615400  |
| H | -3.40580600 | 3.12805600  | -2.15058100 |
| H | -1.65223500 | 4.46649100  | -0.49561100 |
| N | 0.45698700  | 1.97293000  | 1.80286600  |
| N | 1.73001700  | 2.39946500  | -0.32272200 |
| H | 0.58303700  | 3.99624600  | 0.79771800  |
| C | 0.49442000  | 2.35375000  | 3.09192100  |
| N | 0.38958800  | 0.62183700  | 1.72121000  |
| C | 2.73137100  | 3.16770600  | -0.80920400 |
| N | 1.85886400  | 1.12693300  | -0.79029500 |
| C | 0.44694900  | 1.22067500  | 3.88732200  |
| H | 0.55315300  | 3.40397800  | 3.35059300  |
| C | 0.38259900  | 0.16209600  | 2.97807400  |
| C | 3.52709900  | 2.38719400  | -1.62448700 |
| H | 2.79951900  | 4.21206200  | -0.53106800 |
| C | 2.94354700  | 1.11605900  | -1.57951100 |
| H | 0.45787700  | 1.17022300  | 4.96713500  |
| H | 0.33372600  | -0.90526900 | 3.16570700  |
| H | 4.41152300  | 2.68819200  | -2.16901100 |
| H | 3.24688400  | 0.19455300  | -2.06354100 |
| P | 2.12633300  | -1.88985900 | 0.44286700  |
| C | 1.84230100  | -3.26342800 | 1.64972500  |
| H | 2.77315600  | -3.80987000 | 1.85256600  |
| H | 1.45864600  | -2.86525100 | 2.59692100  |
| H | 1.10368200  | -3.96388700 | 1.24055800  |

|   |             |             |             |
|---|-------------|-------------|-------------|
| C | 2.94702700  | -2.83492900 | -0.89982300 |
| H | 3.34743600  | -2.14968000 | -1.65501900 |
| H | 3.76247800  | -3.45225400 | -0.50291500 |
| H | 2.20826700  | -3.48220700 | -1.38664900 |
| N | 0.48927000  | -1.07518900 | -1.96834300 |
| O | 0.62148200  | -1.53876100 | -3.09252700 |
| C | -3.62063300 | -0.88592100 | 0.51396100  |
| C | -3.79473600 | -1.48265700 | -0.73635600 |
| C | -2.94424700 | -2.51975900 | -1.12548600 |
| C | -1.94744100 | -2.98874900 | -0.27689600 |
| C | -1.80637000 | -2.41403700 | 0.99123100  |
| C | -2.62159500 | -1.35511100 | 1.37596400  |
| H | -1.29785800 | -3.80618400 | -0.58490800 |
| H | -1.06535300 | -2.80146600 | 1.68854600  |
| H | -2.51979400 | -0.88902500 | 2.35433700  |
| C | 3.56401600  | -1.06980600 | 1.25474000  |
| H | 4.33452300  | -1.79870900 | 1.53662200  |
| H | 3.99984300  | -0.33267800 | 0.56986800  |
| H | 3.22693400  | -0.54172200 | 2.15506400  |
| H | -4.57081500 | -1.14125100 | -1.41571400 |
| H | -3.07598600 | -2.96876300 | -2.10799000 |
| O | -4.35975600 | 0.14733000  | 0.98113200  |
| C | -5.38908700 | 0.64933400  | 0.15292700  |
| H | -5.85662000 | 1.46951400  | 0.70272100  |
| H | -4.99402900 | 1.03696700  | -0.79666700 |
| H | -6.14822500 | -0.11633000 | -0.05855200 |

**m-TS3**

58

S916

|   |             |             |             |
|---|-------------|-------------|-------------|
| W | -0.08250400 | -0.03565300 | -0.17892000 |
| N | 1.11043800  | 1.82594200  | -0.48919000 |
| C | 0.80969100  | 3.02917100  | -0.99184400 |
| N | 2.45030500  | 1.82531200  | -0.26065800 |
| C | 1.95870000  | 3.82299300  | -1.08748700 |
| H | -0.21825600 | 3.26351400  | -1.24579600 |
| C | 2.97644200  | 3.01838800  | -0.61018400 |
| B | 3.17225000  | 0.53421700  | 0.18060900  |
| H | 2.03460500  | 4.83951000  | -1.44848900 |
| H | 4.03705300  | 3.20352200  | -0.49100400 |
| N | 2.60359100  | 0.07449200  | 1.54107400  |
| N | 2.87424300  | -0.55103300 | -0.87626100 |
| H | 4.35684400  | 0.72206400  | 0.26653900  |
| C | 3.21665200  | -0.10152500 | 2.72505600  |
| N | 1.28742000  | -0.21962700 | 1.65336300  |
| C | 3.74168200  | -1.17814200 | -1.70335000 |
| N | 1.59730500  | -0.88393900 | -1.21096100 |
| C | 2.27454300  | -0.52158900 | 3.64976000  |
| H | 4.27917400  | 0.08420800  | 2.82447200  |
| C | 1.08079900  | -0.57809500 | 2.92615000  |
| C | 3.01911800  | -1.92953300 | -2.60869600 |
| H | 4.80828800  | -1.03855600 | -1.57820000 |
| C | 1.68058700  | -1.71413200 | -2.26139100 |
| H | 2.43059000  | -0.75251600 | 4.69430100  |
| H | 0.08701400  | -0.86331100 | 3.25551000  |
| H | 3.40226100  | -2.55289200 | -3.40485400 |
| H | 0.77615000  | -2.11430000 | -2.70460000 |
| P | -0.87966400 | -2.28930900 | 0.34204500  |
| C | -2.03358100 | -2.73116500 | 1.71643200  |
| H | -2.18405400 | -3.81777000 | 1.76223800  |

|   |             |             |             |
|---|-------------|-------------|-------------|
| H | -1.62649000 | -2.39411100 | 2.67773900  |
| H | -2.99752300 | -2.23760400 | 1.55040200  |
| C | -1.72028900 | -3.11778200 | -1.06373200 |
| H | -1.02393500 | -3.21758100 | -1.90393200 |
| H | -2.07581300 | -4.11507600 | -0.77639000 |
| H | -2.56689300 | -2.50801200 | -1.39736400 |
| N | -1.08405700 | 0.00102500  | -1.64042100 |
| O | -1.75822800 | -0.04535600 | -2.66312800 |
| C | -2.88363100 | 3.17295800  | 0.00822100  |
| C | -3.54736200 | 1.97912000  | -0.28352600 |
| C | -3.27935900 | 0.83988800  | 0.47541300  |
| C | -2.33394000 | 0.89440400  | 1.51860500  |
| C | -1.65653000 | 2.09006900  | 1.76668800  |
| C | -1.93668800 | 3.23871900  | 1.02123100  |
| H | -2.21502700 | 0.02722700  | 2.16332900  |
| H | -0.93647200 | 2.13110100  | 2.58276400  |
| C | 0.48096200  | -3.48193900 | 0.70114500  |
| H | 0.09503600  | -4.50426300 | 0.80360300  |
| H | 1.21987000  | -3.45587100 | -0.10901200 |
| H | 0.98458500  | -3.19930500 | 1.63351000  |
| H | -4.27463900 | 1.94904400  | -1.08974700 |
| H | -3.11438900 | 4.05991200  | -0.57916000 |
| H | -1.41429900 | 4.16903500  | 1.23127900  |
| O | -3.90592400 | -0.34401600 | 0.30734400  |
| C | -4.61292900 | -0.54763300 | -0.90591100 |
| H | -3.96046300 | -0.35269100 | -1.76884800 |
| H | -4.92377500 | -1.59595200 | -0.90662800 |
| H | -5.51110900 | 0.08226100  | -0.96314300 |

o-3π

|   |             |             |             |
|---|-------------|-------------|-------------|
| W | -0.13047100 | 0.39484300  | -0.26729500 |
| N | 0.55202200  | -1.69556400 | -0.69797300 |
| C | 1.62282200  | -2.18763000 | -1.33300500 |
| N | -0.24308900 | -2.75520900 | -0.39911300 |
| C | 1.52910400  | -3.57976100 | -1.44449700 |
| H | 2.40660300  | -1.51768600 | -1.67296800 |
| C | 0.32836600  | -3.89644100 | -0.83624500 |
| B | -1.64482600 | -2.52963800 | 0.20448800  |
| H | 2.23784300  | -4.25795500 | -1.89950900 |
| H | -0.16441900 | -4.84855000 | -0.68101800 |
| N | -1.50131000 | -1.82118700 | 1.56993700  |
| N | -2.42889200 | -1.60072100 | -0.74893200 |
| H | -2.22044900 | -3.57706400 | 0.33573200  |
| C | -1.89341300 | -2.21070700 | 2.79571300  |
| N | -0.92725000 | -0.59661400 | 1.63520600  |
| C | -3.55442000 | -1.87202700 | -1.44715300 |
| N | -1.97258000 | -0.35968100 | -1.07637500 |
| C | -1.56413700 | -1.21452200 | 3.70050500  |
| H | -2.38047400 | -3.16792700 | 2.93635900  |
| C | -0.96035700 | -0.22538300 | 2.92084200  |
| C | -3.83631100 | -0.79382100 | -2.26264000 |
| H | -4.06986200 | -2.81332200 | -1.30177800 |
| C | -2.81979000 | 0.12928300  | -1.99390700 |
| H | -1.73785900 | -1.20694200 | 4.76747300  |
| H | -0.55163400 | 0.73450300  | 3.21916900  |
| H | -4.66492800 | -0.68281600 | -2.94838500 |
| H | -2.65450800 | 1.11817900  | -2.40595200 |
| P | -1.17382600 | 2.47515200  | 0.43336100  |

|   |             |             |             |
|---|-------------|-------------|-------------|
| C | -0.42428200 | 3.62161400  | 1.67704800  |
| H | -1.05450400 | 4.50672100  | 1.83720000  |
| H | -0.29205600 | 3.10647200  | 2.63665600  |
| H | 0.56050500  | 3.94795600  | 1.31854000  |
| C | -1.45455200 | 3.65912800  | -0.94206700 |
| H | -2.11392300 | 3.20997600  | -1.69348400 |
| H | -1.91178100 | 4.58617900  | -0.57451200 |
| H | -0.49849700 | 3.89111400  | -1.42404500 |
| N | 0.34814900  | 1.13759600  | -1.80463500 |
| O | 0.61870200  | 1.65310600  | -2.88364300 |
| C | 3.35595700  | -1.09261300 | 2.09518800  |
| C | 3.89682200  | -1.01113400 | 0.81949000  |
| C | 3.68983600  | 0.13276800  | 0.04091500  |
| C | 2.96069300  | 1.20714900  | 0.56144000  |
| C | 2.41541200  | 1.10609400  | 1.84597300  |
| C | 2.60539500  | -0.03882800 | 2.61619100  |
| H | 3.52258300  | -1.98931500 | 2.68856100  |
| H | 4.47417600  | -1.82980900 | 0.39441100  |
| H | 2.80899500  | 2.11544200  | -0.01730800 |
| H | 1.86439800  | 1.95350400  | 2.25156700  |
| H | 2.18490900  | -0.10482800 | 3.61701400  |
| C | -2.87272700 | 2.32783800  | 1.13219900  |
| H | -3.31017500 | 3.31659900  | 1.32055900  |
| H | -3.51047300 | 1.78096400  | 0.42729100  |
| H | -2.84460000 | 1.76838000  | 2.07442200  |
| O | 4.22576900  | 0.10334700  | -1.20184700 |
| C | 3.98398400  | 1.20515900  | -2.06186400 |
| H | 4.38602000  | 2.13768700  | -1.64337900 |
| H | 4.51220500  | 0.98408200  | -2.99241600 |
| H | 2.91273300  | 1.33201400  | -2.28085000 |

m-3π

58

|   |             |             |             |
|---|-------------|-------------|-------------|
| W | 0.34978400  | -0.36087800 | -0.37015500 |
| N | -0.99756400 | 1.41001700  | -0.54107500 |
| C | -2.15921000 | 1.61940800  | -1.17331100 |
| N | -0.62635700 | 2.60436600  | -0.00937800 |
| C | -2.54931000 | 2.95864500  | -1.05406400 |
| H | -2.65748000 | 0.79837200  | -1.67739200 |
| C | -1.54696400 | 3.54580400  | -0.30402300 |
| B | 0.74091300  | 2.75940800  | 0.69103000  |
| H | -3.43603600 | 3.42895900  | -1.45711700 |
| H | -1.41743800 | 4.56404400  | 0.04197500  |
| N | 0.79021400  | 1.81381700  | 1.91285700  |
| N | 1.83694300  | 2.33463100  | -0.30819100 |
| H | 0.90841000  | 3.89824700  | 1.03872500  |
| C | 0.96930100  | 2.09380500  | 3.21585500  |
| N | 0.64698600  | 0.47760900  | 1.74157500  |
| C | 2.83170300  | 3.08040100  | -0.84113800 |
| N | 1.83681700  | 1.09647700  | -0.87401500 |
| C | 0.94011400  | 0.90659500  | 3.92897300  |
| H | 1.10468500  | 3.11789300  | 3.54181300  |
| C | 0.73470400  | -0.07563900 | 2.95708300  |
| C | 3.48981000  | 2.32087000  | -1.78820400 |
| H | 2.99369400  | 4.09495800  | -0.49880900 |
| C | 2.83306500  | 1.08512000  | -1.77236600 |
| H | 1.05103000  | 0.77352400  | 4.99607200  |
| H | 0.64422200  | -1.15083600 | 3.07138800  |
| H | 4.33300200  | 2.61221900  | -2.39931000 |

|   |             |             |             |
|---|-------------|-------------|-------------|
| H | 3.02585000  | 0.18759700  | -2.34914100 |
| P | 2.07994100  | -1.99677000 | 0.13589700  |
| C | 1.83915300  | -3.43487800 | 1.27607800  |
| H | 2.75597400  | -4.03422400 | 1.35669200  |
| H | 1.56561300  | -3.08050700 | 2.27771300  |
| H | 1.03102100  | -4.07370800 | 0.89896700  |
| C | 2.74153100  | -2.87508700 | -1.33390200 |
| H | 3.12335100  | -2.15385700 | -2.06513300 |
| H | 3.54964800  | -3.56022300 | -1.04904000 |
| H | 1.93445700  | -3.44529100 | -1.80782000 |
| N | 0.26006300  | -0.92464700 | -2.05163700 |
| O | 0.29111700  | -1.27049500 | -3.22478100 |
| C | -3.62585900 | -0.65912400 | 1.23850300  |
| C | -3.86287100 | -1.03708200 | -0.08555100 |
| C | -3.07455900 | -2.02849700 | -0.68067000 |
| C | -2.05547900 | -2.63575900 | 0.04161000  |
| C | -1.79821300 | -2.25366500 | 1.36270100  |
| C | -2.59098700 | -1.26783800 | 1.94798900  |
| H | -4.22791400 | 0.10716700  | 1.71840200  |
| H | -1.45886900 | -3.41632700 | -0.42847900 |
| H | -1.01209700 | -2.74373700 | 1.93381000  |
| H | -2.41150700 | -0.96747600 | 2.97886800  |
| C | 3.61915800  | -1.29376700 | 0.86892300  |
| H | 4.38163900  | -2.06940300 | 1.01560100  |
| H | 4.01940700  | -0.51603800 | 0.20756400  |
| H | 3.38935000  | -0.83386300 | 1.83772800  |
| H | -3.27920200 | -2.30654900 | -1.71267700 |
| O | -4.81816800 | -0.49371900 | -0.87780000 |
| C | -5.60753100 | 0.54779900  | -0.33804600 |
| H | -6.29093400 | 0.86072800  | -1.13074500 |



|   |             |            |             |
|---|-------------|------------|-------------|
| H | -6.19497700 | 0.20623900 | 0.52518000  |
| H | -4.99129700 | 1.40672600 | -0.03592800 |

**p-3π**

58

|   |             |             |             |
|---|-------------|-------------|-------------|
| W | 0.21190900  | -0.41154800 | -0.29741300 |
| N | -0.73432400 | 1.53134600  | -0.86098100 |
| C | -1.76993400 | 1.84603800  | -1.64767800 |
| N | -0.16587200 | 2.70633200  | -0.48041500 |
| C | -1.88332700 | 3.23522800  | -1.77847300 |
| H | -2.38623200 | 1.05885100  | -2.06795200 |
| C | -0.84476600 | 3.74128500  | -1.01919700 |
| B | 1.15726300  | 2.70629800  | 0.31185700  |
| H | -2.62107500 | 3.79001600  | -2.34181000 |
| H | -0.53450000 | 4.76020200  | -0.82187800 |
| N | 0.93381400  | 1.98118700  | 1.65934700  |
| N | 2.19826000  | 1.92084300  | -0.51637000 |
| H | 1.53600800  | 3.83123900  | 0.50323200  |
| C | 1.01119800  | 2.44448800  | 2.91931000  |
| N | 0.56871500  | 0.67765200  | 1.66822600  |
| C | 3.34657500  | 2.37895500  | -1.06539000 |
| N | 1.96901000  | 0.64299500  | -0.93046000 |
| C | 0.68567100  | 1.41493200  | 3.78769100  |
| H | 1.29671200  | 3.47213400  | 3.10833200  |
| C | 0.41749100  | 0.32845200  | 2.95174600  |
| C | 3.87622700  | 1.38778400  | -1.86734000 |
| H | 3.69534600  | 3.37885400  | -0.83901800 |
| C | 2.98016700  | 0.31936500  | -1.75024300 |
| H | 0.65380500  | 1.44677800  | 4.86781500  |

|   |             |             |             |
|---|-------------|-------------|-------------|
| H | 0.12690700  | -0.68554400 | 3.20685100  |
| H | 4.78605900  | 1.42479900  | -2.45042300 |
| H | 3.01525500  | -0.66602200 | -2.20028400 |
| P | 1.59946900  | -2.22512200 | 0.54439100  |
| C | 1.06393700  | -3.46825900 | 1.80630200  |
| H | 1.87532800  | -4.16966500 | 2.04277300  |
| H | 0.75650200  | -2.96313600 | 2.73038500  |
| H | 0.20870100  | -4.03460500 | 1.41635700  |
| C | 2.20737300  | -3.36924900 | -0.75689500 |
| H | 2.74695100  | -2.81257400 | -1.53114700 |
| H | 2.87472200  | -4.12869000 | -0.33076800 |
| H | 1.35095300  | -3.86577700 | -1.22732200 |
| N | -0.01803700 | -1.24787300 | -1.84841400 |
| O | -0.13895100 | -1.82800000 | -2.91827700 |
| C | -3.57553200 | -0.20551500 | 0.25135600  |
| C | -4.07002100 | -0.94692100 | -0.82573700 |
| C | -3.68793700 | -2.27380300 | -0.99139300 |
| C | -2.82503300 | -2.88467200 | -0.08359700 |
| C | -2.34396200 | -2.14685700 | 0.99707800  |
| C | -2.70512500 | -0.80660000 | 1.16827000  |
| H | -2.53421900 | -3.92543700 | -0.21029700 |
| H | -1.70448700 | -2.62010200 | 1.74035200  |
| H | -2.33435600 | -0.25628000 | 2.02899600  |
| C | 3.17498600  | -1.66451900 | 1.31969200  |
| H | 3.80608700  | -2.51737400 | 1.60015000  |
| H | 3.72384800  | -1.02565100 | 0.61722900  |
| H | 2.95425300  | -1.07510800 | 2.21775200  |
| H | -4.07670500 | -2.83735200 | -1.83723700 |
| H | -4.74784800 | -0.46002400 | -1.52404800 |
| O | -3.99136800 | 1.07829100  | 0.33481900  |

|   |             |            |            |
|---|-------------|------------|------------|
| C | -3.43378300 | 1.89065100 | 1.34924800 |
| H | -3.83751200 | 2.89466900 | 1.19833500 |
| H | -3.71727700 | 1.53974400 | 2.35119700 |
| H | -2.33650800 | 1.93152600 | 1.27844600 |

**Table S7.** Thermochemical values for **5** and C-F activated **5** (Scheme 9) performed with M06/6-31g\*\*[LANL2DZ for W], all values relative to **5** in kcal/mol.

|                        | ZPE    | E      | H      | G      |
|------------------------|--------|--------|--------|--------|
| <b>5</b>               | 0.0    | 0.0    | 0.0    | 0.0    |
| <b>C-F activated 5</b> | -18.90 | -18.46 | -18.46 | -20.41 |

XYZ coordinates for **5** and **C-F activated 5**.

**5**

57

|   |             |             |             |
|---|-------------|-------------|-------------|
| W | 0.21053700  | 0.00820700  | -0.06179200 |
| N | 1.31635200  | 1.94985200  | -0.30772900 |
| C | 0.92725100  | 3.16956900  | -0.68813000 |
| N | 2.66549400  | 1.99672800  | -0.15652700 |
| C | 2.02767900  | 4.02592200  | -0.78257400 |
| H | -0.12117300 | 3.37243000  | -0.86634600 |
| C | 3.10985000  | 3.23705300  | -0.43796500 |
| B | 3.49073100  | 0.71647300  | 0.11280800  |
| H | 2.03223600  | 5.07046100  | -1.06113800 |
| H | 4.16687700  | 3.46416000  | -0.37306400 |
| N | 3.01928300  | 0.07882700  | 1.43312600  |
| N | 3.19976800  | -0.24785700 | -1.06140100 |
| H | 4.66261000  | 0.97107400  | 0.16838000  |

|   |             |             |             |
|---|-------------|-------------|-------------|
| C | 3.74215400  | -0.20928500 | 2.53000700  |
| N | 1.71553300  | -0.23591000 | 1.63968800  |
| C | 4.01445600  | -0.66848900 | -2.04740100 |
| N | 1.91453500  | -0.52707800 | -1.38236400 |
| C | 2.89392100  | -0.72929200 | 3.49180900  |
| H | 4.80784400  | -0.01711400 | 2.54719000  |
| C | 1.63677600  | -0.72194300 | 2.88519400  |
| C | 3.24275100  | -1.24803700 | -3.04021500 |
| H | 5.08360700  | -0.51049500 | -1.97651000 |
| C | 1.92970400  | -1.12347700 | -2.57940700 |
| H | 3.14730400  | -1.05960800 | 4.48932900  |
| H | 0.68463200  | -1.04277900 | 3.29201600  |
| H | 3.58113100  | -1.68801300 | -3.96781100 |
| H | 0.99915200  | -1.43615600 | -3.04049800 |
| P | 0.01118900  | -2.51295000 | 0.07353700  |
| C | -0.65890900 | -3.33166100 | 1.56900400  |
| H | -0.62677000 | -4.41798300 | 1.42247400  |
| H | -0.04785900 | -3.07826700 | 2.44231400  |
| H | -1.69436100 | -3.03520000 | 1.76030300  |
| C | -1.00573200 | -3.24250400 | -1.25780700 |
| H | -0.59923100 | -2.95842800 | -2.23476400 |
| H | -1.02651000 | -4.33611000 | -1.17865800 |
| H | -2.02807000 | -2.85273700 | -1.18501800 |
| N | -0.87433200 | 0.13592900  | -1.45375700 |
| O | -1.59477000 | 0.18874100  | -2.42497000 |
| C | -1.99552800 | 2.13678900  | 0.81837200  |
| C | -3.19812500 | 1.78713400  | 0.32111100  |
| C | -3.56579800 | 0.39250400  | 0.38845800  |
| C | -2.75462900 | -0.52745100 | 0.96577000  |
| C | -1.43107900 | -0.18456900 | 1.45155700  |

|   |             |             |             |
|---|-------------|-------------|-------------|
| C | -1.00812500 | 1.22140500  | 1.33358400  |
| H | -3.88447000 | 2.53622600  | -0.06496900 |
| H | -3.10748600 | -1.55092000 | 1.08452900  |
| H | -1.10581700 | -0.74583000 | 2.32972400  |
| H | -0.35794300 | 1.64189200  | 2.10617600  |
| C | 1.61732000  | -3.38790200 | -0.06914300 |
| H | 1.47044200  | -4.46484300 | 0.07580600  |
| H | 2.07190700  | -3.21882100 | -1.05031300 |
| H | 2.30216600  | -3.01258900 | 0.70213900  |
| C | -4.88749100 | 0.02166800  | -0.17390400 |
| F | -4.96488100 | 0.28712200  | -1.49275700 |
| F | -5.89053300 | 0.72204900  | 0.39392700  |
| F | -5.18691900 | -1.27520900 | -0.02276300 |
| F | -1.66526400 | 3.44450700  | 0.88123300  |

#### C-F activated 5

57

|   |             |             |             |
|---|-------------|-------------|-------------|
| W | 0.65526700  | -0.59137300 | -0.35848400 |
| N | -0.28674600 | 1.19955900  | -1.30557700 |
| C | -1.01859600 | 1.32617900  | -2.41566300 |
| N | -0.28827900 | 2.40446600  | -0.68313400 |
| C | -1.50856300 | 2.62850500  | -2.52209100 |
| H | -1.17453500 | 0.47084000  | -3.06288300 |
| C | -1.01487700 | 3.27848400  | -1.40368000 |
| B | 0.68668900  | 2.67151000  | 0.49214800  |
| H | -2.12842800 | 3.04052100  | -3.30588500 |
| H | -1.11554700 | 4.30469900  | -1.07253300 |
| N | 0.29341700  | 1.79859300  | 1.69559300  |
| N | 2.06939400  | 2.23192600  | -0.05900700 |

|   |             |             |             |
|---|-------------|-------------|-------------|
| H | 0.69276800  | 3.83162700  | 0.79388800  |
| C | -0.02918900 | 2.15657900  | 2.95208300  |
| N | 0.19138000  | 0.45527200  | 1.56382500  |
| C | 3.09589300  | 3.00937500  | -0.45246700 |
| N | 2.18757600  | 1.00914100  | -0.63360300 |
| C | -0.35059200 | 1.01372100  | 3.66575900  |
| H | -0.00857900 | 3.19865900  | 3.24612200  |
| C | -0.19812200 | -0.02814000 | 2.74836400  |
| C | 3.91548000  | 2.27469500  | -1.29212900 |
| H | 3.16089300  | 4.03609500  | -0.11405000 |
| C | 3.29267900  | 1.02861200  | -1.38629700 |
| H | -0.65625500 | 0.94719000  | 4.70044500  |
| H | -0.35174900 | -1.09451800 | 2.86577200  |
| H | 4.82646600  | 2.59739400  | -1.77599200 |
| H | 3.58203200  | 0.14969400  | -1.95128400 |
| P | 2.83402100  | -1.33929400 | 0.98022300  |
| C | 2.51080600  | -2.50443000 | 2.34631300  |
| H | 3.46115000  | -2.77660500 | 2.82101600  |
| H | 1.86040400  | -2.03446500 | 3.09170300  |
| H | 2.01835200  | -3.40158700 | 1.96510500  |
| C | 4.05872800  | -2.25110700 | -0.02440900 |
| H | 4.44637800  | -1.62234500 | -0.83279500 |
| H | 4.89649100  | -2.58544900 | 0.59959300  |
| H | 3.56807200  | -3.12561300 | -0.46758000 |
| N | 1.12604700  | -1.34649900 | -1.88405400 |
| O | 1.47872600  | -1.82727800 | -2.93340000 |
| C | 3.81147200  | -0.04318600 | 1.82350200  |
| H | 4.60419000  | -0.50906500 | 2.42124400  |
| H | 4.26907100  | 0.64029400  | 1.10117500  |
| H | 3.15507900  | 0.53006200  | 2.49013400  |

|   |             |             |             |
|---|-------------|-------------|-------------|
| C | -1.49010200 | -1.04560500 | -0.61826300 |
| C | -1.90710600 | -2.12222100 | -1.41734100 |
| C | -2.49809200 | -0.34328100 | 0.04975500  |
| C | -3.24693200 | -2.48412600 | -1.54143800 |
| H | -1.16236100 | -2.70074100 | -1.96689500 |
| C | -3.84262500 | -0.70244300 | -0.06434300 |
| H | -2.24974100 | 0.52334400  | 0.66793800  |
| C | -4.23108900 | -1.77555700 | -0.85992400 |
| H | -3.52786900 | -3.32297100 | -2.17606700 |
| H | -5.27949500 | -2.04753900 | -0.94865400 |
| C | -4.84674900 | 0.11542800  | 0.67576900  |
| F | -4.59657200 | 0.14436400  | 1.99721200  |
| F | -4.83967000 | 1.39959600  | 0.27209800  |
| F | -6.10051000 | -0.33041700 | 0.52731900  |
| F | 0.29073400  | -2.25731100 | 0.68138600  |





The total exposure time was 1.29 hours. The frames were integrated with the Bruker SAINT software package<sup>35</sup> using a narrow-frame algorithm. The integration of the data using a **monoclinic** unit cell yielded a total of **59713** reflections to a maximum  $\theta$  angle of **29.62°** (**0.72 Å** resolution), of which **7806** were independent (average redundancy **7.650**, completeness = **99.9%**,  $R_{\text{int}} = 5.53\%$ ,  $R_{\text{sig}} = 3.26\%$ ) and **6314** (**80.89%**) were greater than  $2\sigma(F^2)$ . The final cell constants of  $\underline{a} = 13.8194(13)$  Å,  $\underline{b} = 15.7357(15)$  Å,  $\underline{c} = 14.0798(13)$  Å,  $\beta = 115.166(2)^\circ$ , volume = **2771.1(5)** Å<sup>3</sup>, are based upon the refinement of the XYZ-centroids of **9853** reflections above  $20\sigma(I)$  with  $5.177^\circ < 2\theta < 59.01^\circ$ . Data were corrected for absorption effects using the Multi-Scan method (SADABS).<sup>1</sup> The ratio of minimum to maximum apparent transmission was **0.598**. The calculated minimum and maximum transmission coefficients (based on crystal size) are **0.2980** and **0.6280**.

The structure was solved and refined using the Bruker SHELXTL Software Package<sup>36</sup> within APEX3<sup>1</sup> and OLEX2,<sup>37</sup> using the space group **P 2<sub>1</sub>/n**, with  $Z = 4$  for the formula unit, **C<sub>21</sub>H<sub>37</sub>BBrN<sub>7</sub>OPW**. Non-hydrogen atoms were refined anisotropically. The B-H hydrogen atom was located in the diffraction map and refined isotropically. All other hydrogen atoms were placed in geometrically calculated positions with  $U_{\text{iso}} = 1.2U_{\text{equiv}}$  of the parent atom ( $U_{\text{iso}} = 1.5U_{\text{equiv}}$  for methyl). The relative occupancy of the disordered NO/Br substituents was freely refined, converging at a **79/21** ratio for the major and minor conformations, respectively. Constraints were used on the anisotropic displacement parameters of the NO atoms. The final anisotropic full-matrix least-squares refinement on  $F^2$  with **321** variables converged at  $R1 = 2.53\%$ , for the observed data and  $wR2 = 5.95\%$  for all data. The goodness-of-fit was **1.062**. The largest peak in the final difference electron density synthesis was **1.716 e<sup>-</sup>/Å<sup>3</sup>** and the largest hole was **-1.699 e<sup>-</sup>/Å<sup>3</sup>** with an RMS deviation of **0.138 e<sup>-</sup>/Å<sup>3</sup>**. On the basis of the final model, the calculated density was **1.700 g/cm<sup>3</sup>** and  $F(000)$ , **1396 e<sup>-</sup>**.

**Table 1. Sample and crystal data for Harman\_15JAS143.**

|                            |   |
|----------------------------|---|
| <b>Identification code</b> | Harman_15JAS143                                       |
| <b>Chemical formula</b>    | C <sub>21</sub> H <sub>37</sub> BBrN <sub>7</sub> OPW |
| <b>Formula weight</b>      | 709.11 g/mol  |
| <b>Temperature</b>         | 100(2) K  |
| <b>Wavelength</b>          | 0.71073 Å   |
| <b>Crystal size</b>        | 0.090 x 0.258 x 0.281 mm                              |
| <b>Crystal habit</b>       | green plate   |
| <b>Crystal system</b>      | monoclinic  |

<sup>35</sup> Bruker (2012). *Saint*; SADABS; APEX3. Bruker AXS Inc., Madison, Wisconsin, USA.

<sup>36</sup> Sheldrick, G. M. (2015). *Acta Cryst.* **A71**, 3-8.

<sup>37</sup> Dolomanov, O. V.; Bourhis, L. J.; Gildea, R. J.; Howard, J. A. K.; Puschmann, H. *J. Appl. Cryst.* (2009). **42**, 339-341.

|                               |                          |                 |
|-------------------------------|--------------------------|-----------------|
| <b>Space group</b>            | P 2 <sub>1</sub> /n      |                 |
| <b>Unit cell dimensions</b>   | a = 13.8194(13) Å        | α = 90°         |
|                               | b = 15.7357(15) Å        | β = 115.166(2)° |
|                               | c = 14.0798(13) Å        | γ = 90°         |
| <b>Volume</b>                 | 2771.1(5) Å <sup>3</sup> |                 |
| <b>Z</b>                      | 4                        |                 |
| <b>Density (calculated)</b>   | 1.700 g/cm <sup>3</sup>  |                 |
| <b>Absorption coefficient</b> | 5.695 mm <sup>-1</sup>   |                 |
| <b>F(000)</b>                 | 1396                     |                 |

**Table 2. Data collection and structure refinement for Harman\_15JAS143.**

|  |  |
|--|--|
| <b>Diffractometer</b>                      | Bruker Kappa APEXII Duo                                    |
| <b>Radiation source</b>                    | fine-focus sealed tube (Mo K <sub>α</sub> , λ = 0.71073 Å) |
| <b>Theta range for data collection</b>     | 1.73 to 29.62°   |
| <b>Index ranges</b>                        | -19 ≤ h ≤ 19, -21 ≤ k ≤ 21, -19 ≤ l ≤ 19                   |
| <b>Reflections collected</b>               | 59713  |
| <b>Independent reflections</b>             | 7806 [R(int) = 0.0553]                                     |
| <b>Coverage of independent reflections</b> | 99.9%  |
| <b>Absorption correction</b>               | Multi-Scan   |
| <b>Max. and min. transmission</b>          | 0.6280 and 0.2980  |
| <b>Structure solution technique</b>        | direct methods   |
| <b>Structure solution program</b>          | SHELXT 2014/5 (Sheldrick, 2014)                            |
| <b>Refinement method</b>                   | Full-matrix least-squares on F <sup>2</sup>                |
| <b>Refinement program</b>                  | SHELXL-2017/1 (Sheldrick, 2017)                            |

|  |   |                              |
|--|---|------------------------------|
| <b>Function minimized</b>                | $\Sigma w(F_o^2 - F_c^2)^2$   |                              |
| <b>Data / restraints / parameters</b>    | 7806 / 0 / 321  |                              |
| <b>Goodness-of-fit on F<sup>2</sup></b>  | 1.062   |                              |
| <b><math>\Delta/\sigma_{\max}</math></b> | 0.004   |                              |
| <b>Final R indices</b>                   | 6314 data;<br>I > 2 $\sigma$ (I)  | R1 = 0.0253, wR2 =<br>0.0518 |
|  | all data  | R1 = 0.0430, wR2 =<br>0.0595 |
| <b>Weighting scheme</b>                  | w=1/[ $\sigma^2(F_o^2)+(0.0177P)^2+5.6437P$ ]<br>where P=(F <sub>o</sub> <sup>2</sup> +2F <sub>c</sub> <sup>2</sup> )/3 |                              |
| <b>Largest diff. peak and hole</b>       | 1.716 and -1.699 eÅ <sup>-3</sup>   |                              |
| <b>R.M.S. deviation from mean</b>        | 0.138 eÅ <sup>-3</sup>  |                              |

**Table 3. Atomic coordinates and equivalent isotropic atomic displacement parameters (Å<sup>2</sup>) for Harman\_15JAS143.**

U(eq) is defined as one third of the trace of the orthogonalized U<sub>ij</sub> tensor.

|    | <b>x/a</b>  | <b>y/b</b>  | <b>z/c</b>  | <b>U(eq)</b> |
|----|-------------|-------------|-------------|--------------|
| W1 | 0.80430(2)  | 0.50507(2)  | 0.67953(2)  | 0.01292(4)   |
| P1 | 0.77227(6)  | 0.52937(5)  | 0.49129(6)  | 0.01743(16)  |
| N1 | 0.92158(19) | 0.61030(15) | 0.74418(19) | 0.0132(5)    |
| N2 | 0.9118(2)   | 0.66743(15) | 0.8124(2)   | 0.0159(5)    |
| N3 | 0.69252(19) | 0.60167(15) | 0.6804(2)   | 0.0157(5)    |
| N4 | 0.7177(2)   | 0.65661(16) | 0.7634(2)   | 0.0178(5)    |
| N5 | 0.83471(19) | 0.49274(15) | 0.84370(19) | 0.0151(5)    |
| N6 | 0.84557(19) | 0.56250(16) | 0.9047(2)   | 0.0167(5)    |

|     | <b>x/a</b> | <b>y/b</b>  | <b>z/c</b> | <b>U(eq)</b> |
|-----|------------|-------------|------------|--------------|
| C1  | 0.0009(2)  | 0.63855(19) | 0.7219(2)  | 0.0159(6)    |
| C2  | 0.0414(2)  | 0.7148(2)   | 0.7737(2)  | 0.0201(6)    |
| C3  | 0.9826(2)  | 0.73073(19) | 0.8304(3)  | 0.0205(6)    |
| C4  | 0.5919(2)  | 0.6212(2)   | 0.6126(3)  | 0.0221(7)    |
| C5  | 0.5534(3)  | 0.6886(2)   | 0.6500(3)  | 0.0263(7)    |
| C6  | 0.6350(3)  | 0.7090(2)   | 0.7457(3)  | 0.0241(7)    |
| C7  | 0.8511(2)  | 0.4246(2)   | 0.9055(3)  | 0.0192(6)    |
| C8  | 0.8734(3)  | 0.4499(2)   | 0.0071(3)  | 0.0223(7)    |
| C9  | 0.8695(2)  | 0.5374(2)   | 0.0036(3)  | 0.0202(6)    |
| C10 | 0.8264(3)  | 0.4439(2)   | 0.4408(3)  | 0.0218(7)    |
| C11 | 0.7773(3)  | 0.3563(2)   | 0.4410(3)  | 0.0215(7)    |
| C12 | 0.8404(3)  | 0.2846(2)   | 0.4214(3)  | 0.0330(9)    |
| C13 | 0.7903(4)  | 0.1972(2)   | 0.4165(4)  | 0.0379(10)   |
| C14 | 0.6296(3)  | 0.5335(2)   | 0.3993(3)  | 0.0232(7)    |
| C15 | 0.6002(3)  | 0.5249(2)   | 0.2833(3)  | 0.0327(9)    |
| C16 | 0.4776(3)  | 0.5303(3)   | 0.2175(3)  | 0.0355(9)    |
| C17 | 0.4429(4)  | 0.5045(3)   | 0.1058(3)  | 0.0456(11)   |
| C18 | 0.8295(3)  | 0.6254(2)   | 0.4613(3)  | 0.0247(7)    |
| C19 | 0.7927(3)  | 0.7073(2)   | 0.4941(3)  | 0.0271(8)    |
| C20 | 0.8560(3)  | 0.7860(2)   | 0.4906(3)  | 0.0366(10)   |
| C21 | 0.8533(4)  | 0.8045(3)   | 0.3840(4)  | 0.0709(19)   |
| B1  | 0.8291(3)  | 0.6526(2)   | 0.8573(3)  | 0.0169(7)    |
| Br1 | 0.96793(4) | 0.41317(3)  | 0.70745(4) | 0.01690(13)  |
| O1  | 0.6217(3)  | 0.3802(2)   | 0.5878(3)  | 0.0253(8)    |

|      | x/a         | y/b         | z/c         | U(eq)     |
|------|-------------|-------------|-------------|-----------|
| N7   | 0.6992(3)   | 0.4281(2)   | 0.6262(3)   | 0.0153(6) |
| Br1A | 0.65721(17) | 0.39873(13) | 0.63298(19) | 0.0231(6) |
| O1A  | 0.9864(12)  | 0.3885(10)  | 0.7028(13)  | 0.0253(8) |
| N7A  | 0.9149(12)  | 0.4341(9)   | 0.6964(10)  | 0.0153(6) |

**Table 4. Bond lengths (Å) for Harman\_15JAS143.**

|        |           |         |           |
|--------|-----------|---------|-----------|
| W1-N7  | 1.792(4)  | W1-N7A  | 1.825(17) |
| W1-N3  | 2.171(2)  | W1-N5   | 2.175(3)  |
| W1-N1  | 2.223(2)  | W1-Br1A | 2.496(2)  |
| W1-P1  | 2.5236(9) | W1-Br1  | 2.5695(5) |
| P1-C10 | 1.824(3)  | P1-C18  | 1.836(3)  |
| P1-C14 | 1.843(3)  | N1-C1   | 1.338(4)  |
| N1-N2  | 1.364(3)  | N2-C3   | 1.343(4)  |
| N2-B1  | 1.541(4)  | N3-C4   | 1.346(4)  |
| N3-N4  | 1.374(4)  | N4-C6   | 1.345(4)  |
| N4-B1  | 1.546(4)  | N5-C7   | 1.339(4)  |
| N5-N6  | 1.362(3)  | N6-C9   | 1.347(4)  |
| N6-B1  | 1.542(4)  | C1-C2   | 1.392(4)  |
| C1-H1  | 0.95      | C2-C3   | 1.382(5)  |
| C2-H2  | 0.95      | C3-H3   | 0.95      |
| C4-C5  | 1.386(5)  | C4-H4   | 0.95      |
| C5-C6  | 1.377(5)  | C5-H5   | 0.95      |
| C6-H6  | 0.95      | C7-C8   | 1.388(5)  |
| C7-H7  | 0.95      | C8-C9   | 1.377(5)  |

|          |          |          |          |
|----------|----------|----------|----------|
| C8-H8    | 0.95     | C9-H9    | 0.95     |
| C10-C11  | 1.537(4) | C10-H10A | 0.99     |
| C10-H10B | 0.99     | C11-C12  | 1.521(5) |
| C11-H11A | 0.99     | C11-H11B | 0.99     |
| C12-C13  | 1.529(5) | C12-H12A | 0.99     |
| C12-H12B | 0.99     | C13-H13A | 0.98     |
| C13-H13B | 0.98     | C13-H13C | 0.98     |
| C14-C15  | 1.512(5) | C14-H14A | 0.99     |
| C14-H14B | 0.99     | C15-C16  | 1.549(5) |
| C15-H15A | 0.99     | C15-H15B | 0.99     |
| C16-C17  | 1.492(6) | C16-H16A | 0.99     |
| C16-H16B | 0.99     | C17-H17A | 0.98     |
| C17-H17B | 0.98     | C17-H17C | 0.98     |
| C18-C19  | 1.528(5) | C18-H18A | 0.99     |
| C18-H18B | 0.99     | C19-C20  | 1.528(5) |
| C19-H19A | 0.99     | C19-H19B | 0.99     |
| C20-C21  | 1.514(6) | C20-H20A | 0.99     |
| C20-H20B | 0.99     | C21-H21A | 0.98     |
| C21-H21B | 0.98     | C21-H21C | 0.98     |
| B1-H1A   | 1.10(3)  | O1-N7    | 1.231(5) |
| O1A-N7A  | 1.19(2)  |          |          |

**Table 5. Bond angles (°) for Harman\_15JAS143.**

|          |           |           |          |
|----------|-----------|-----------|----------|
| N7-W1-N3 | 91.33(13) | N7A-W1-N3 | 170.5(4) |
| N7-W1-N5 | 98.08(13) | N7A-W1-N5 | 92.0(4)  |

|            |            |             |            |
|------------|------------|-------------|------------|
| N3-W1-N5   | 82.68(9)   | N7-W1-N1    | 174.00(12) |
| N7A-W1-N1  | 88.7(4)    | N3-W1-N1    | 82.68(9)   |
| N5-W1-N1   | 81.58(9)   | N7A-W1-Br1A | 99.6(4)    |
| N3-W1-Br1A | 88.22(8)   | N5-W1-Br1A  | 89.26(8)   |
| N1-W1-Br1A | 167.81(8)  | N7-W1-P1    | 85.05(12)  |
| N7A-W1-P1  | 89.6(4)    | N3-W1-P1    | 95.31(7)   |
| N5-W1-P1   | 176.30(7)  | N1-W1-P1    | 95.10(7)   |
| Br1A-W1-P1 | 93.80(6)   | N7-W1-Br1   | 100.83(10) |
| N3-W1-Br1  | 167.19(7)  | N5-W1-Br1   | 91.57(6)   |
| N1-W1-Br1  | 85.16(6)   | P1-W1-Br1   | 89.77(2)   |
| C10-P1-C18 | 103.25(16) | C10-P1-C14  | 104.20(16) |
| C18-P1-C14 | 104.23(15) | C10-P1-W1   | 112.32(11) |
| C18-P1-W1  | 117.79(11) | C14-P1-W1   | 113.63(12) |
| C1-N1-N2   | 106.4(2)   | C1-N1-W1    | 132.8(2)   |
| N2-N1-W1   | 120.41(18) | C3-N2-N1    | 109.8(3)   |
| C3-N2-B1   | 130.0(3)   | N1-N2-B1    | 120.1(2)   |
| C4-N3-N4   | 105.8(2)   | C4-N3-W1    | 132.8(2)   |
| N4-N3-W1   | 121.45(18) | C6-N4-N3    | 109.9(3)   |
| C6-N4-B1   | 130.0(3)   | N3-N4-B1    | 120.1(2)   |
| C7-N5-N6   | 107.0(2)   | C7-N5-W1    | 131.7(2)   |
| N6-N5-W1   | 121.19(18) | C9-N6-N5    | 109.2(2)   |
| C9-N6-B1   | 130.1(3)   | N5-N6-B1    | 120.7(2)   |
| N1-C1-C2   | 110.5(3)   | N1-C1-H1    | 124.8      |
| C2-C1-H1   | 124.8      | C3-C2-C1    | 104.8(3)   |
| C3-C2-H2   | 127.6      | C1-C2-H2    | 127.6      |

|               |          |               |          |
|---------------|----------|---------------|----------|
| N2-C3-C2      | 108.5(3) | N2-C3-H3      | 125.8    |
| C2-C3-H3      | 125.8    | N3-C4-C5      | 110.6(3) |
| N3-C4-H4      | 124.7    | C5-C4-H4      | 124.7    |
| C6-C5-C4      | 105.3(3) | C6-C5-H5      | 127.3    |
| C4-C5-H5      | 127.3    | N4-C6-C5      | 108.4(3) |
| N4-C6-H6      | 125.8    | C5-C6-H6      | 125.8    |
| N5-C7-C8      | 110.0(3) | N5-C7-H7      | 125.0    |
| C8-C7-H7      | 125.0    | C9-C8-C7      | 105.2(3) |
| C9-C8-H8      | 127.4    | C7-C8-H8      | 127.4    |
| N6-C9-C8      | 108.6(3) | N6-C9-H9      | 125.7    |
| C8-C9-H9      | 125.7    | C11-C10-P1    | 114.0(2) |
| C11-C10-H10A  | 108.8    | P1-C10-H10A   | 108.8    |
| C11-C10-H10B  | 108.8    | P1-C10-H10B   | 108.8    |
| H10A-C10-H10B | 107.7    | C12-C11-C10   | 112.1(3) |
| C12-C11-H11A  | 109.2    | C10-C11-H11A  | 109.2    |
| C12-C11-H11B  | 109.2    | C10-C11-H11B  | 109.2    |
| H11A-C11-H11B | 107.9    | C11-C12-C13   | 113.1(3) |
| C11-C12-H12A  | 109.0    | C13-C12-H12A  | 109.0    |
| C11-C12-H12B  | 109.0    | C13-C12-H12B  | 109.0    |
| H12A-C12-H12B | 107.8    | C12-C13-H13A  | 109.5    |
| C12-C13-H13B  | 109.5    | H13A-C13-H13B | 109.5    |
| C12-C13-H13C  | 109.5    | H13A-C13-H13C | 109.5    |
| H13B-C13-H13C | 109.5    | C15-C14-P1    | 118.2(3) |
| C15-C14-H14A  | 107.8    | P1-C14-H14A   | 107.8    |
| C15-C14-H14B  | 107.8    | P1-C14-H14B   | 107.8    |



|               |           |               |           |
|---------------|-----------|---------------|-----------|
| H14A-C14-H14B | 107.1     | C14-C15-C16   | 111.4(3)  |
| C14-C15-H15A  | 109.3     | C16-C15-H15A  | 109.3     |
| C14-C15-H15B  | 109.3     | C16-C15-H15B  | 109.3     |
| H15A-C15-H15B | 108.0     | C17-C16-C15   | 113.3(4)  |
| C17-C16-H16A  | 108.9     | C15-C16-H16A  | 108.9     |
| C17-C16-H16B  | 108.9     | C15-C16-H16B  | 108.9     |
| H16A-C16-H16B | 107.7     | C16-C17-H17A  | 109.5     |
| C16-C17-H17B  | 109.5     | H17A-C17-H17B | 109.5     |
| C16-C17-H17C  | 109.5     | H17A-C17-H17C | 109.5     |
| H17B-C17-H17C | 109.5     | C19-C18-P1    | 113.2(2)  |
| C19-C18-H18A  | 108.9     | P1-C18-H18A   | 108.9     |
| C19-C18-H18B  | 108.9     | P1-C18-H18B   | 108.9     |
| H18A-C18-H18B | 107.8     | C18-C19-C20   | 113.9(3)  |
| C18-C19-H19A  | 108.8     | C20-C19-H19A  | 108.8     |
| C18-C19-H19B  | 108.8     | C20-C19-H19B  | 108.8     |
| H19A-C19-H19B | 107.7     | C21-C20-C19   | 114.5(3)  |
| C21-C20-H20A  | 108.6     | C19-C20-H20A  | 108.6     |
| C21-C20-H20B  | 108.6     | C19-C20-H20B  | 108.6     |
| H20A-C20-H20B | 107.6     | C20-C21-H21A  | 109.5     |
| C20-C21-H21B  | 109.5     | H21A-C21-H21B | 109.5     |
| C20-C21-H21C  | 109.5     | H21A-C21-H21C | 109.5     |
| H21B-C21-H21C | 109.5     | N2-B1-N6      | 108.6(2)  |
| N2-B1-N4      | 106.6(3)  | N6-B1-N4      | 108.5(2)  |
| N2-B1-H1A     | 111.4(18) | N6-B1-H1A     | 109.9(18) |
| N4-B1-H1A     | 111.7(18) | O1-N7-W1      | 175.3(3)  |

O1A-N7A-W1 177.0(14)

**Table 6. Torsion angles (°) for Harman\_15JAS143.**

|                 |           |                 |             |
|-----------------|-----------|-----------------|-------------|
| C1-N1-N2-C3     | 1.1(3)    | W1-N1-N2-C3     | -172.3(2)   |
| C1-N1-N2-B1     | -178.0(3) | W1-N1-N2-B1     | 8.6(3)      |
| C4-N3-N4-C6     | -0.8(3)   | W1-N3-N4-C6     | -179.0(2)   |
| C4-N3-N4-B1     | -179.7(3) | W1-N3-N4-B1     | 2.1(3)      |
| C7-N5-N6-C9     | 0.6(3)    | W1-N5-N6-C9     | -176.68(19) |
| C7-N5-N6-B1     | -178.6(3) | W1-N5-N6-B1     | 4.1(3)      |
| N2-N1-C1-C2     | -1.3(3)   | W1-N1-C1-C2     | 171.0(2)    |
| N1-C1-C2-C3     | 0.9(4)    | N1-N2-C3-C2     | -0.6(4)     |
| B1-N2-C3-C2     | 178.5(3)  | C1-C2-C3-N2     | -0.2(4)     |
| N4-N3-C4-C5     | 1.1(3)    | W1-N3-C4-C5     | 179.0(2)    |
| N3-C4-C5-C6     | -0.9(4)   | N3-N4-C6-C5     | 0.3(4)      |
| B1-N4-C6-C5     | 179.0(3)  | C4-C5-C6-N4     | 0.4(4)      |
| N6-N5-C7-C8     | -0.4(3)   | W1-N5-C7-C8     | 176.4(2)    |
| N5-C7-C8-C9     | 0.1(4)    | N5-N6-C9-C8     | -0.5(3)     |
| B1-N6-C9-C8     | 178.6(3)  | C7-C8-C9-N6     | 0.3(4)      |
| C18-P1-C10-C11  | -171.3(2) | C14-P1-C10-C11  | -62.6(3)    |
| W1-P1-C10-C11   | 60.8(2)   | P1-C10-C11-C12  | -167.5(3)   |
| C10-C11-C12-C13 | -177.5(3) | C10-P1-C14-C15  | -41.9(3)    |
| C18-P1-C14-C15  | 66.1(3)   | W1-P1-C14-C15   | -164.4(2)   |
| P1-C14-C15-C16  | -179.7(3) | C14-C15-C16-C17 | -168.1(3)   |
| C10-P1-C18-C19  | 178.5(2)  | C14-P1-C18-C19  | 69.8(3)     |
| W1-P1-C18-C19   | -57.1(3)  | P1-C18-C19-C20  | 168.2(2)    |

|                 |          |             |           |
|-----------------|----------|-------------|-----------|
| C18-C19-C20-C21 | 58.5(5)  | C3-N2-B1-N6 | -126.7(3) |
| N1-N2-B1-N6     | 52.3(3)  | C3-N2-B1-N4 | 116.6(3)  |
| N1-N2-B1-N4     | -64.5(3) | C9-N6-B1-N2 | 120.2(3)  |
| N5-N6-B1-N2     | -60.8(3) | C9-N6-B1-N4 | -124.3(3) |
| N5-N6-B1-N4     | 54.7(3)  | C6-N4-B1-N2 | -120.1(3) |
| N3-N4-B1-N2     | 58.6(3)  | C6-N4-B1-N6 | 123.2(3)  |
| N3-N4-B1-N6     | -58.2(3) |             |           |

**Table 7. Anisotropic atomic displacement parameters ( $\text{\AA}^2$ ) for Harman\_15JAS143.**

The anisotropic atomic displacement factor exponent takes the form: -  
 $2\pi^2 [ h^2 a^{*2} U_{11} + \dots + 2 h k a^* b^* U_{12} ]$

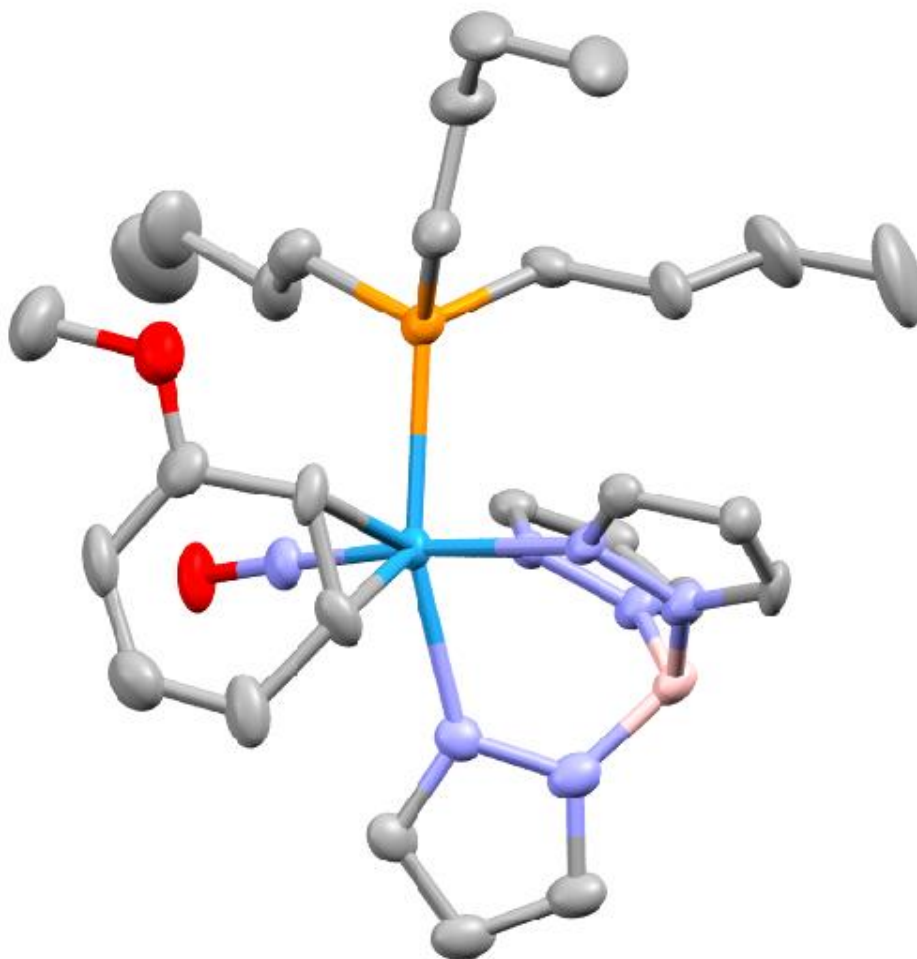
|    | $U_{11}$   | $U_{22}$   | $U_{33}$   | $U_{23}$    | $U_{13}$   | $U_{12}$    |
|----|------------|------------|------------|-------------|------------|-------------|
| W1 | 0.01230(5) | 0.01183(5) | 0.01405(6) | 0.00062(5)  | 0.00504(4) | -0.00105(4) |
| P1 | 0.0158(4)  | 0.0183(3)  | 0.0148(4)  | 0.0003(3)   | 0.0032(3)  | -0.0043(3)  |
| N1 | 0.0133(11) | 0.0126(10) | 0.0120(12) | -0.0017(9)  | 0.0037(10) | 0.0005(9)   |
| N2 | 0.0167(12) | 0.0142(11) | 0.0178(13) | -0.0017(10) | 0.0083(10) | -0.0013(9)  |
| N3 | 0.0147(12) | 0.0143(11) | 0.0201(13) | 0.0032(10)  | 0.0094(11) | 0.0010(9)   |
| N4 | 0.0153(12) | 0.0153(11) | 0.0239(14) | 0.0017(10)  | 0.0095(11) | 0.0016(9)   |
| N5 | 0.0146(11) | 0.0159(11) | 0.0147(12) | 0.0002(10)  | 0.0062(9)  | -0.0007(9)  |
| N6 | 0.0148(12) | 0.0203(12) | 0.0152(13) | -0.0007(10) | 0.0064(10) | -0.0026(10) |
| C1 | 0.0146(13) | 0.0229(14) | 0.0112(14) | -0.0017(11) | 0.0064(11) | -0.0019(11) |
| C2 | 0.0184(15) | 0.0237(15) | 0.0185(16) | -0.0029(12) | 0.0080(13) | -0.0090(12) |
| C3 | 0.0208(15) | 0.0165(14) | 0.0236(17) | -0.0038(12) | 0.0087(13) | -0.0081(12) |
| C4 | 0.0153(14) | 0.0237(15) | 0.0243(17) | 0.0083(13)  | 0.0057(13) | 0.0006(12)  |
| C5 | 0.0172(15) | 0.0257(16) | 0.039(2)   | 0.0100(15)  | 0.0146(15) | 0.0079(13)  |

|      | <b>U<sub>11</sub></b> | <b>U<sub>22</sub></b> | <b>U<sub>33</sub></b> | <b>U<sub>23</sub></b> | <b>U<sub>13</sub></b> | <b>U<sub>12</sub></b> |
|------|-----------------------|-----------------------|-----------------------|-----------------------|-----------------------|-----------------------|
| C6   | 0.0215(16)            | 0.0184(14)            | 0.037(2)              | 0.0045(14)            | 0.0173(15)            | 0.0052(12)            |
| C7   | 0.0172(14)            | 0.0181(14)            | 0.0225(16)            | 0.0061(12)            | 0.0086(13)            | 0.0014(11)            |
| C8   | 0.0182(15)            | 0.0306(17)            | 0.0164(16)            | 0.0096(13)            | 0.0057(13)            | 0.0031(13)            |
| C9   | 0.0156(14)            | 0.0302(16)            | 0.0144(15)            | 0.0001(13)            | 0.0061(12)            | -0.0021(12)           |
| C10  | 0.0216(16)            | 0.0255(16)            | 0.0193(16)            | -0.0029(13)           | 0.0095(13)            | -0.0050(12)           |
| C11  | 0.0219(16)            | 0.0230(15)            | 0.0206(16)            | -0.0016(13)           | 0.0100(13)            | -0.0030(12)           |
| C12  | 0.035(2)              | 0.0285(18)            | 0.048(2)              | -0.0058(17)           | 0.0297(19)            | -0.0030(15)           |
| C13  | 0.053(3)              | 0.0245(18)            | 0.052(3)              | -0.0065(17)           | 0.037(2)              | -0.0025(17)           |
| C14  | 0.0185(15)            | 0.0206(14)            | 0.0206(17)            | 0.0021(13)            | -0.0011(13)           | -0.0046(12)           |
| C15  | 0.036(2)              | 0.0301(18)            | 0.0201(17)            | -0.0022(14)           | 0.0006(15)            | 0.0034(15)            |
| C16  | 0.031(2)              | 0.037(2)              | 0.028(2)              | -0.0003(16)           | 0.0033(16)            | 0.0037(16)            |
| C17  | 0.038(2)              | 0.045(2)              | 0.035(2)              | -0.0069(19)           | -0.0023(18)           | 0.0128(19)            |
| C18  | 0.0273(17)            | 0.0272(16)            | 0.0161(16)            | 0.0023(13)            | 0.0059(14)            | -0.0105(14)           |
| C19  | 0.0193(15)            | 0.0220(16)            | 0.0298(19)            | 0.0105(14)            | 0.0006(14)            | -0.0019(12)           |
| C20  | 0.0217(17)            | 0.0249(17)            | 0.049(2)              | 0.0100(17)            | 0.0014(17)            | -0.0053(14)           |
| C21  | 0.053(3)              | 0.076(4)              | 0.053(3)              | 0.041(3)              | -0.007(2)             | -0.039(3)             |
| B1   | 0.0179(16)            | 0.0151(15)            | 0.0204(18)            | -0.0007(13)           | 0.0106(14)            | -0.0017(12)           |
| Br1  | 0.0151(2)             | 0.0158(2)             | 0.0176(2)             | -0.00053(16)          | 0.00474(16)           | 0.00230(15)           |
| O1   | 0.0200(18)            | 0.0242(17)            | 0.027(2)              | -0.0030(15)           | 0.0060(15)            | -0.0093(14)           |
| N7   | 0.0119(15)            | 0.0163(15)            | 0.0163(17)            | 0.0040(13)            | 0.0046(13)            | -0.0032(14)           |
| Br1A | 0.0157(11)            | 0.0182(9)             | 0.0306(12)            | 0.0032(8)             | 0.0051(9)             | -0.0037(7)            |
| O1A  | 0.0200(18)            | 0.0242(17)            | 0.027(2)              | -0.0030(15)           | 0.0060(15)            | -0.0093(14)           |
| N7A  | 0.0119(15)            | 0.0163(15)            | 0.0163(17)            | 0.0040(13)            | 0.0046(13)            | -0.0032(14)           |

**Table 8. Hydrogen atomic coordinates and isotropic atomic displacement parameters ( $\text{\AA}^2$ ) for Harman\_15JAS143.**

|      | x/a    | y/b    | z/c    | U(eq) |
|------|--------|--------|--------|-------|
| H1   | 1.0262 | 0.6105 | 0.6771 | 0.019 |
| H2   | 1.0970 | 0.7486 | 0.7707 | 0.024 |
| H3   | 0.9909 | 0.7784 | 0.8746 | 0.025 |
| H4   | 0.5527 | 0.5928 | 0.5479 | 0.026 |
| H5   | 0.4854 | 0.7150 | 0.6168 | 0.032 |
| H6   | 0.6331 | 0.7528 | 0.7913 | 0.029 |
| H7   | 0.8479 | 0.3673 | 0.8831 | 0.023 |
| H8   | 0.8882 | 0.4146 | 1.0664 | 0.027 |
| H9   | 0.8817 | 0.5739 | 1.0614 | 0.024 |
| H10A | 0.8142 | 0.4579 | 0.3680 | 0.026 |
| H10B | 0.9046 | 0.4407 | 0.4837 | 0.026 |
| H11A | 0.7751 | 0.3472 | 0.5096 | 0.026 |
| H11B | 0.7029 | 0.3550 | 0.3860 | 0.026 |
| H12A | 0.9139 | 0.2846 | 0.4781 | 0.04  |
| H12B | 0.8454 | 0.2954 | 0.3543 | 0.04  |
| H13A | 0.7175 | 0.1966 | 0.3603 | 0.057 |
| H13B | 0.7879 | 0.1850 | 0.4837 | 0.057 |
| H13C | 0.8334 | 0.1538 | 0.4023 | 0.057 |
| H14A | 0.5924 | 0.4878 | 0.4191 | 0.028 |
| H14B | 0.6005 | 0.5882 | 0.4102 | 0.028 |
| H15A | 0.6265 | 0.4697 | 0.2700 | 0.039 |
| H15B | 0.6354 | 0.5706 | 0.2613 | 0.039 |

|      | <b>x/a</b> | <b>y/b</b> | <b>z/c</b> | <b>U(eq)</b> |
|------|------------|------------|------------|--------------|
| H16A | 0.4419     | 0.4932     | 0.2498     | 0.043        |
| H16B | 0.4539     | 0.5893     | 0.2196     | 0.043        |
| H17A | 0.3658     | 0.5137     | 0.0670     | 0.068        |
| H17B | 0.4591     | 0.4442     | 0.1027     | 0.068        |
| H17C | 0.4811     | 0.5386     | 0.0744     | 0.068        |
| H18A | 0.9084     | 0.6220     | 0.4975     | 0.03         |
| H18B | 0.8090     | 0.6274     | 0.3848     | 0.03         |
| H19A | 0.7991     | 0.7003     | 0.5664     | 0.033        |
| H19B | 0.7163     | 0.7167     | 0.4473     | 0.033        |
| H20A | 0.8273     | 0.8359     | 0.5131     | 0.044        |
| H20B | 0.9314     | 0.7785     | 0.5418     | 0.044        |
| H21A | 0.7792     | 0.8140     | 0.3330     | 0.106        |
| H21B | 0.8830     | 0.7561     | 0.3615     | 0.106        |
| H21C | 0.8958     | 0.8554     | 0.3884     | 0.106        |
| H1A  | 0.837(3)   | 0.700(2)   | 0.918(3)   | 0.018(9)     |



### Crystal Structure Report for **Complex 3** in Chapter 9

A **yellow rod-like** specimen of  $C_{28}H_{45}BN_7O_2PW$ , approximate dimensions **0.046 mm** x **0.070 mm** x **0.358 mm**, was coated with Paratone oil and mounted on a MiTeGen MicroLoop. The X-ray intensity data were measured on a Bruker Kappa APEXII Duo system equipped with a fine-focus sealed tube (Mo  $K_{\alpha}$ ,  $\lambda = 0.71073 \text{ \AA}$ ) and a graphite monochromator.

The total exposure time was 2.33 hours. The frames were integrated with the Bruker SAINT software package<sup>38</sup> using a narrow-frame algorithm. The integration of the data using a **trigonal** unit cell yielded a total of **43412** reflections to a maximum  $\theta$  angle of **26.49°** (**0.80 Å** resolution), of which **7471** were independent (average redundancy **5.811**, completeness = **99.6%**,  $R_{int} = 9.73\%$ ,  $R_{sig} = 7.87\%$ ) and **5360** (**71.74%**) were greater than  $2\sigma(F^2)$ . The final cell constants of  $\underline{a} = 41.3100(19) \text{ \AA}$ ,  $\underline{b} = 41.3100(19) \text{ \AA}$ ,  $\underline{c} = 11.032(3) \text{ \AA}$ , volume = **16304.5 Å<sup>3</sup>**, are based upon the refinement of the XYZ-centroids of **6013** reflections above  $20 \sigma(I)$  with  $5.217^\circ < 2\theta < 44.14^\circ$ . Data were corrected for absorption effects using the Multi-Scan method (SADABS).<sup>1</sup> The ratio of minimum to maximum apparent transmission was **0.746**. The

<sup>38</sup> Bruker (2012). *Saint*; *SADABS*; *APEX3*. Bruker AXS Inc., Madison, Wisconsin, USA.

calculated minimum and maximum transmission coefficients (based on crystal size) are 0.5562 and 0.7454.

The structure was solved and refined using the Bruker SHELXTL Software Package<sup>39</sup> within APEX3<sup>1</sup> and OLEX2,<sup>40</sup> using the space group R -3, with Z = 18 for the formula unit, C<sub>28</sub>H<sub>45</sub>BN<sub>7</sub>O<sub>2</sub>PW. Non-hydrogen atoms were refined anisotropically. The B-H, C10 and C11 hydrogen atoms were located in the diffraction map and refined isotropically with  $U_{iso} = 1.2U_{equiv}$  of the parent atom and restraints on the C-H bond lengths. All other hydrogen atoms were placed in geometrically calculated positions with  $U_{iso} = 1.2U_{equiv}$  of the parent atom ( $U_{iso} = 1.5U_{equiv}$  for methyl). Two of the three terminal methyl groups of the butyl substituents were found to be disordered over two positions. The relative occupancies of the disordered site were freely refined. Constraints were used on the anisotropic displacement parameters of the disordered atoms, and the disordered bonds needed restraints. Disordered pentane solvent was located in the crystal, but it could not be adequately modeled with or without restraints. Thus, the structure factors were modified using the PLATON SQUEEZE<sup>41</sup> technique, in order to produce a “solvate-free” structure factor set. PLATON reported a total electron density of 660 e<sup>-</sup> and total solvent accessible volume of 2294 Å<sup>3</sup>. The final anisotropic full-matrix least-squares refinement on F<sup>2</sup> with 384 variables converged at R1 = 4.72%, for the observed data and wR2 = 9.62% for all data. The goodness-of-fit was 1.008. The largest peak in the final difference electron density synthesis was 1.733 e<sup>-</sup>/Å<sup>3</sup> and the largest hole was -2.422 e<sup>-</sup>/Å<sup>3</sup> with an RMS deviation of 0.140 e<sup>-</sup>/Å<sup>3</sup>. On the basis of the final model, the calculated density was 1.352 g/cm<sup>3</sup> and F(000), 6696 e<sup>-</sup>.

**Table 1. Sample and crystal data for Harman\_15JAS155b.**

|                             |   |         |
|-----------------------------|---|---------|
| <b>Identification code</b>  | Harman_15JAS155b  |         |
| <b>Chemical formula</b>     | C <sub>28</sub> H <sub>45</sub> BN <sub>7</sub> O <sub>2</sub> PW |         |
| <b>Formula weight</b>       | 737.34 g/mol  |         |
| <b>Temperature</b>          | 100(2) K  |         |
| <b>Wavelength</b>           | 0.71073 Å   |         |
| <b>Crystal size</b>         | 0.046 x 0.070 x 0.358 mm  |         |
| <b>Crystal habit</b>        | yellow rod  |         |
| <b>Crystal system</b>       | trigonal  |         |
| <b>Space group</b>          | R -3  |         |
| <b>Unit cell dimensions</b> | a = 41.3100(19) Å   | α = 90° |

<sup>39</sup> Sheldrick, G. M. (2015). *Acta Cryst.* **A71**, 3-8.

<sup>40</sup> Dolomanov, O. V.; Bourhis, L. J.; Gildea, R. J.; Howard, J. A. K.; Puschmann, H. *J. Appl. Cryst.* (2009). **42**, 339-341.

<sup>41</sup> Spek, A. L. *Acta Crystallogr. Sect C: Struct. Chem.* **2015**, *C71*, 9-18.



|                               |                               |                      |
|-------------------------------|-------------------------------|----------------------|
|                               | $b = 41.3100(19) \text{ \AA}$ | $\beta = 90^\circ$   |
|                               | $c = 11.032(3) \text{ \AA}$   | $\gamma = 120^\circ$ |
| <b>Volume</b>                 | 16304.(5) $\text{\AA}^3$      |                      |
| <b>Z</b>                      | 18                            |                      |
| <b>Density (calculated)</b>   | 1.352 $\text{g/cm}^3$         |                      |
| <b>Absorption coefficient</b> | 3.264 $\text{mm}^{-1}$        |                      |
| <b>F(000)</b>                 | 6696                          |                      |

**Table 2. Data collection and structure refinement for Harman\_15JAS155b.**

|  |   |
|--|---|
| <b>Diffractometer</b>                      | Bruker Kappa APEXII Duo   |
| <b>Radiation source</b>                    | fine-focus sealed tube (Mo $K_\alpha$ , $\lambda = 0.71073 \text{ \AA}$ ) |
| <b>Theta range for data collection</b>     | 1.71 to 26.49°  |
| <b>Index ranges</b>                        | -50 ≤ h ≤ 51, -51 ≤ k ≤ 51, -13 ≤ l ≤ 13                                  |
| <b>Reflections collected</b>               | 43412   |
| <b>Independent reflections</b>             | 7471 [R(int) = 0.0973]  |
| <b>Coverage of independent reflections</b> | 99.6%   |
| <b>Absorption correction</b>               | Multi-Scan  |
| <b>Max. and min. transmission</b>          | 0.7454 and 0.5562   |
| <b>Structure solution technique</b>        | direct methods  |
| <b>Structure solution program</b>          | SHELXT 2014/5 (Sheldrick, 2014)   |
| <b>Refinement method</b>                   | Full-matrix least-squares on $F^2$  |
| <b>Refinement program</b>                  | SHELXL-2018/3 (Sheldrick, 2018)   |
| <b>Function minimized</b>                  | $\sum w(F_o^2 - F_c^2)^2$   |
| <b>Data / restraints / parameters</b>      | 7471 / 6 / 384  |

|  |   |
|--|---|
| <b>Goodness-of-fit on F<sup>2</sup></b>  | 1.008   |
| <b><math>\Delta/\sigma_{\max}</math></b> | 0.002   |
| <b>Final R indices</b>                   | 5360 data; $l > 2\sigma(l)$ R1 = 0.0472, wR2 = 0.0867                                 |
|  | all data R1 = 0.0811, wR2 = 0.0962  |
| <b>Weighting scheme</b>                  | $w = 1/[\sigma^2(F_o^2) + (0.0348P)^2 + 117.4176P]$<br>where $P = (F_o^2 + 2F_c^2)/3$ |
| <b>Largest diff. peak and hole</b>       | 1.733 and -2.422 eÅ <sup>-3</sup>   |
| <b>R.M.S. deviation from mean</b>        | 0.140 eÅ <sup>-3</sup>  |

**Table 3. Atomic coordinates and equivalent isotropic atomic displacement parameters (Å<sup>2</sup>) for Harman\_15JAS155b.**

U(eq) is defined as one third of the trace of the orthogonalized U<sub>ij</sub> tensor.

|    | x/a         | y/b         | z/c         | U(eq)      |
|----|-------------|-------------|-------------|------------|
| W1 | 0.21312(2)  | 0.29250(2)  | 0.51790(2)  | 0.02179(8) |
| P1 | 0.15343(4)  | 0.22970(5)  | 0.51201(14) | 0.0264(4)  |
| O1 | 0.21361(13) | 0.30080(13) | 0.7877(3)   | 0.0376(12) |
| O2 | 0.11782(14) | 0.28705(14) | 0.6062(4)   | 0.0439(12) |
| B1 | 0.2832(2)   | 0.2943(2)   | 0.3593(6)   | 0.0278(16) |
| N1 | 0.21991(12) | 0.28870(13) | 0.3165(4)   | 0.0228(11) |
| N2 | 0.25088(13) | 0.28805(14) | 0.2738(4)   | 0.0261(12) |
| N3 | 0.24144(13) | 0.25936(13) | 0.5332(4)   | 0.0219(11) |
| N4 | 0.26863(13) | 0.26355(14) | 0.4550(4)   | 0.0264(12) |
| N5 | 0.27282(14) | 0.33548(14) | 0.5051(4)   | 0.0254(12) |

|     | <b>x/a</b>  | <b>y/b</b>  | <b>z/c</b> | <b>U(eq)</b> |
|-----|-------------|-------------|------------|--------------|
| N6  | 0.29676(14) | 0.33168(14) | 0.4277(4)  | 0.0292(12)   |
| N7  | 0.21265(14) | 0.29730(14) | 0.6776(4)  | 0.0296(12)   |
| C1  | 0.19973(17) | 0.28628(16) | 0.2193(5)  | 0.0243(14)   |
| C2  | 0.21689(16) | 0.28394(17) | 0.1142(5)  | 0.0271(14)   |
| C3  | 0.24891(18) | 0.28513(17) | 0.1537(5)  | 0.0309(15)   |
| C4  | 0.23872(16) | 0.23480(16) | 0.6169(5)  | 0.0248(13)   |
| C5  | 0.26463(17) | 0.22351(17) | 0.5937(6)  | 0.0322(15)   |
| C6  | 0.28303(17) | 0.24260(17) | 0.4922(6)  | 0.0307(15)   |
| C7  | 0.29422(18) | 0.36782(17) | 0.5656(5)  | 0.0282(15)   |
| C8  | 0.33093(18) | 0.38440(19) | 0.5266(6)  | 0.0365(17)   |
| C9  | 0.33150(18) | 0.36131(18) | 0.4404(6)  | 0.0332(16)   |
| C10 | 0.2077(2)   | 0.34209(18) | 0.4648(5)  | 0.0315(16)   |
| C11 | 0.17086(18) | 0.31173(19) | 0.4846(5)  | 0.0294(15)   |
| C12 | 0.15253(19) | 0.3158(2)   | 0.5933(6)  | 0.0351(16)   |
| C13 | 0.1701(2)   | 0.3467(2)   | 0.6666(6)  | 0.0410(18)   |
| C14 | 0.2051(2)   | 0.3773(2)   | 0.6330(7)  | 0.0439(18)   |
| C15 | 0.2236(2)   | 0.3770(2)   | 0.5364(6)  | 0.0422(18)   |
| C16 | 0.0992(2)   | 0.2874(2)   | 0.7173(6)  | 0.061(2)     |
| C17 | 0.12820(19) | 0.21416(19) | 0.6568(6)  | 0.0367(16)   |
| C18 | 0.1490(2)   | 0.2071(2)   | 0.7578(6)  | 0.0424(18)   |
| C19 | 0.1263(3)   | 0.1942(2)   | 0.8739(6)  | 0.062(2)     |
| C20 | 0.1456(3)   | 0.1853(3)   | 0.9745(8)  | 0.096(4)     |
| C21 | 0.11611(17) | 0.22353(18) | 0.4066(6)  | 0.0348(16)   |
| C22 | 0.08316(19) | 0.1839(2)   | 0.3872(7)  | 0.0471(19)   |

|      | x/a         | y/b         | z/c        | U(eq)      |
|------|-------------|-------------|------------|------------|
| C23  | 0.05561(18) | 0.1813(2)   | 0.2919(7)  | 0.048(2)   |
| C25  | 0.15920(18) | 0.18960(17) | 0.4712(6)  | 0.0331(15) |
| C26  | 0.1735(2)   | 0.19142(18) | 0.3422(6)  | 0.0357(16) |
| C27  | 0.1809(3)   | 0.1598(2)   | 0.3116(7)  | 0.061(2)   |
| C24  | 0.0704(3)   | 0.1852(4)   | 0.1661(9)  | 0.058(3)   |
| C28  | 0.1952(4)   | 0.1614(4)   | 0.1810(9)  | 0.081(4)   |
| C24A | 0.0300(6)   | 0.1395(5)   | 0.2601(19) | 0.058(3)   |
| C28A | 0.1399(6)   | 0.1247(7)   | 0.303(2)   | 0.081(4)   |

**Table 4. Bond lengths (Å) for Harman\_15JAS155b.**

|        |            |        |          |
|--------|------------|--------|----------|
| W1-N7  | 1.774(5)   | W1-N3  | 2.207(5) |
| W1-N5  | 2.208(5)   | W1-C10 | 2.246(6) |
| W1-N1  | 2.255(5)   | W1-C11 | 2.280(6) |
| W1-P1  | 2.5334(17) | P1-C17 | 1.839(6) |
| P1-C25 | 1.843(6)   | P1-C21 | 1.845(6) |
| O1-N7  | 1.221(6)   | O2-C12 | 1.336(8) |
| O2-C16 | 1.450(8)   | B1-N4  | 1.526(8) |
| B1-N2  | 1.546(8)   | B1-N6  | 1.548(9) |
| B1-H1A | 1.08(6)    | N1-C1  | 1.331(7) |
| N1-N2  | 1.376(6)   | N2-C3  | 1.329(7) |
| N3-C4  | 1.334(7)   | N3-N4  | 1.357(6) |
| N4-C6  | 1.337(7)   | N5-C7  | 1.353(7) |
| N5-N6  | 1.374(7)   | N6-C9  | 1.349(8) |
| C1-C2  | 1.387(8)   | C1-H1  | 0.95     |

|          |           |          |           |
|----------|-----------|----------|-----------|
| C2-C3    | 1.370(8)  | C2-H2    | 0.95      |
| C3-H3    | 0.95      | C4-C5    | 1.389(8)  |
| C4-H4    | 0.95      | C5-C6    | 1.362(8)  |
| C5-H5    | 0.95      | C6-H6    | 0.95      |
| C7-C8    | 1.384(9)  | C7-H7    | 0.95      |
| C8-C9    | 1.355(9)  | C8-H8    | 0.95      |
| C9-H9    | 0.95      | C10-C11  | 1.425(9)  |
| C10-C15  | 1.479(9)  | C10-H10  | 0.95(2)   |
| C11-C12  | 1.472(8)  | C11-H11  | 0.96(2)   |
| C12-C13  | 1.373(9)  | C13-C14  | 1.415(10) |
| C13-H13  | 0.95      | C14-C15  | 1.315(9)  |
| C14-H14  | 0.95      | C15-H15  | 0.95      |
| C16-H16A | 0.98      | C16-H16B | 0.98      |
| C16-H16C | 0.98      | C17-C18  | 1.523(9)  |
| C17-H17A | 0.99      | C17-H17B | 0.99      |
| C18-C19  | 1.519(9)  | C18-H18A | 0.99      |
| C18-H18B | 0.99      | C19-C20  | 1.517(11) |
| C19-H19A | 0.99      | C19-H19B | 0.99      |
| C20-H20A | 0.98      | C20-H20B | 0.98      |
| C20-H20C | 0.98      | C21-C22  | 1.534(9)  |
| C21-H21A | 0.99      | C21-H21B | 0.99      |
| C22-C23  | 1.514(9)  | C22-H22A | 0.99      |
| C22-H22B | 0.99      | C23-C24  | 1.493(11) |
| C23-C24A | 1.550(15) | C23-H23A | 0.99      |
| C23-H23B | 0.99      | C23-H23C | 0.99      |

|           |           |           |           |
|-----------|-----------|-----------|-----------|
| C23-H23D  | 0.99      | C25-C26   | 1.529(8)  |
| C25-H25A  | 0.99      | C25-H25B  | 0.99      |
| C26-C27   | 1.519(9)  | C26-H26A  | 0.99      |
| C26-H26B  | 0.99      | C27-C28   | 1.546(11) |
| C27-C28A  | 1.589(18) | C27-H27A  | 0.99      |
| C27-H27B  | 0.99      | C27-H27C  | 0.99      |
| C27-H27D  | 0.99      | C24-H24A  | 0.98      |
| C24-H24B  | 0.98      | C24-H24C  | 0.98      |
| C28-H28A  | 0.98      | C28-H28B  | 0.98      |
| C28-H28C  | 0.98      | C24A-H24D | 0.98      |
| C24A-H24E | 0.98      | C24A-H24F | 0.98      |
| C28A-H28D | 0.98      | C28A-H28E | 0.98      |
| C28A-H28F | 0.98      |           |           |

**Table 5. Bond angles (°) for Harman\_15JAS155b.**

|           |            |            |            |
|-----------|------------|------------|------------|
| N7-W1-N3  | 91.85(19)  | N7-W1-N5   | 92.5(2)    |
| N3-W1-N5  | 77.20(17)  | N7-W1-C10  | 98.4(2)    |
| N3-W1-C10 | 155.6(2)   | N5-W1-C10  | 80.2(2)    |
| N7-W1-N1  | 174.3(2)   | N3-W1-N1   | 84.79(16)  |
| N5-W1-N1  | 82.25(17)  | C10-W1-N1  | 83.1(2)    |
| N7-W1-C11 | 93.9(2)    | N3-W1-C11  | 164.5(2)   |
| N5-W1-C11 | 116.8(2)   | C10-W1-C11 | 36.7(2)    |
| N1-W1-C11 | 90.53(18)  | N7-W1-P1   | 94.62(17)  |
| N3-W1-P1  | 85.02(13)  | N5-W1-P1   | 161.03(13) |
| C10-W1-P1 | 115.95(18) | N1-W1-P1   | 89.70(12)  |

|            |           |            |          |
|------------|-----------|------------|----------|
| C11-W1-P1  | 80.20(18) | C17-P1-C25 | 101.8(3) |
| C17-P1-C21 | 102.2(3)  | C25-P1-C21 | 101.4(3) |
| C17-P1-W1  | 115.3(2)  | C25-P1-W1  | 115.4(2) |
| C21-P1-W1  | 118.4(2)  | C12-O2-C16 | 114.8(6) |
| N4-B1-N2   | 109.6(5)  | N4-B1-N6   | 106.8(5) |
| N2-B1-N6   | 108.5(5)  | N4-B1-H1A  | 113.(3)  |
| N2-B1-H1A  | 110.(3)   | N6-B1-H1A  | 109.(3)  |
| C1-N1-N2   | 106.0(5)  | C1-N1-W1   | 134.8(4) |
| N2-N1-W1   | 119.2(3)  | C3-N2-N1   | 109.1(5) |
| C3-N2-B1   | 129.2(5)  | N1-N2-B1   | 121.3(5) |
| C4-N3-N4   | 106.6(5)  | C4-N3-W1   | 130.9(4) |
| N4-N3-W1   | 122.3(3)  | C6-N4-N3   | 109.3(5) |
| C6-N4-B1   | 129.4(5)  | N3-N4-B1   | 120.1(5) |
| C7-N5-N6   | 105.5(5)  | C7-N5-W1   | 132.7(4) |
| N6-N5-W1   | 121.7(4)  | C9-N6-N5   | 109.4(5) |
| C9-N6-B1   | 130.2(5)  | N5-N6-B1   | 119.6(5) |
| O1-N7-W1   | 177.7(4)  | N1-C1-C2   | 110.9(5) |
| N1-C1-H1   | 124.6     | C2-C1-H1   | 124.6    |
| C3-C2-C1   | 104.5(5)  | C3-C2-H2   | 127.8    |
| C1-C2-H2   | 127.8     | N2-C3-C2   | 109.5(5) |
| N2-C3-H3   | 125.2     | C2-C3-H3   | 125.2    |
| N3-C4-C5   | 110.0(5)  | N3-C4-H4   | 125.0    |
| C5-C4-H4   | 125.0     | C6-C5-C4   | 104.9(5) |
| C6-C5-H5   | 127.5     | C4-C5-H5   | 127.5    |
| N4-C6-C5   | 109.1(6)  | N4-C6-H6   | 125.5    |

|               |          |               |          |
|---------------|----------|---------------|----------|
| C5-C6-H6      | 125.5    | N5-C7-C8      | 110.4(6) |
| N5-C7-H7      | 124.8    | C8-C7-H7      | 124.8    |
| C9-C8-C7      | 105.7(6) | C9-C8-H8      | 127.2    |
| C7-C8-H8      | 127.2    | N6-C9-C8      | 109.1(6) |
| N6-C9-H9      | 125.5    | C8-C9-H9      | 125.5    |
| C11-C10-C15   | 122.3(6) | C11-C10-W1    | 73.0(3)  |
| C15-C10-W1    | 123.5(4) | C11-C10-H10   | 115.(4)  |
| C15-C10-H10   | 117.(4)  | W1-C10-H10    | 96.(4)   |
| C10-C11-C12   | 114.1(6) | C10-C11-W1    | 70.4(3)  |
| C12-C11-W1    | 115.9(4) | C10-C11-H11   | 122.(4)  |
| C12-C11-H11   | 116.(4)  | W1-C11-H11    | 109.(4)  |
| O2-C12-C13    | 126.6(6) | O2-C12-C11    | 111.7(6) |
| C13-C12-C11   | 121.6(6) | C12-C13-C14   | 120.3(6) |
| C12-C13-H13   | 119.8    | C14-C13-H13   | 119.8    |
| C15-C14-C13   | 122.9(7) | C15-C14-H14   | 118.5    |
| C13-C14-H14   | 118.5    | C14-C15-C10   | 117.8(7) |
| C14-C15-H15   | 121.1    | C10-C15-H15   | 121.1    |
| O2-C16-H16A   | 109.5    | O2-C16-H16B   | 109.5    |
| H16A-C16-H16B | 109.5    | O2-C16-H16C   | 109.5    |
| H16A-C16-H16C | 109.5    | H16B-C16-H16C | 109.5    |
| C18-C17-P1    | 115.2(5) | C18-C17-H17A  | 108.5    |
| P1-C17-H17A   | 108.5    | C18-C17-H17B  | 108.5    |
| P1-C17-H17B   | 108.5    | H17A-C17-H17B | 107.5    |
| C19-C18-C17   | 111.9(6) | C19-C18-H18A  | 109.2    |
| C17-C18-H18A  | 109.2    | C19-C18-H18B  | 109.2    |



|               |          |               |           |
|---------------|----------|---------------|-----------|
| C17-C18-H18B  | 109.2    | H18A-C18-H18B | 107.9     |
| C20-C19-C18   | 113.1(7) | C20-C19-H19A  | 109.0     |
| C18-C19-H19A  | 109.0    | C20-C19-H19B  | 109.0     |
| C18-C19-H19B  | 109.0    | H19A-C19-H19B | 107.8     |
| C19-C20-H20A  | 109.5    | C19-C20-H20B  | 109.5     |
| H20A-C20-H20B | 109.5    | C19-C20-H20C  | 109.5     |
| H20A-C20-H20C | 109.5    | H20B-C20-H20C | 109.5     |
| C22-C21-P1    | 118.0(5) | C22-C21-H21A  | 107.8     |
| P1-C21-H21A   | 107.8    | C22-C21-H21B  | 107.8     |
| P1-C21-H21B   | 107.8    | H21A-C21-H21B | 107.1     |
| C23-C22-C21   | 114.0(6) | C23-C22-H22A  | 108.8     |
| C21-C22-H22A  | 108.8    | C23-C22-H22B  | 108.8     |
| C21-C22-H22B  | 108.8    | H22A-C22-H22B | 107.7     |
| C24-C23-C22   | 112.6(7) | C22-C23-C24A  | 107.7(10) |
| C24-C23-H23A  | 109.1    | C22-C23-H23A  | 109.1     |
| C24-C23-H23B  | 109.1    | C22-C23-H23B  | 109.1     |
| H23A-C23-H23B | 107.8    | C22-C23-H23C  | 110.2     |
| C24A-C23-H23C | 110.2    | C22-C23-H23D  | 110.2     |
| C24A-C23-H23D | 110.2    | H23C-C23-H23D | 108.5     |
| C26-C25-P1    | 113.8(4) | C26-C25-H25A  | 108.8     |
| P1-C25-H25A   | 108.8    | C26-C25-H25B  | 108.8     |
| P1-C25-H25B   | 108.8    | H25A-C25-H25B | 107.7     |
| C27-C26-C25   | 113.8(6) | C27-C26-H26A  | 108.8     |
| C25-C26-H26A  | 108.8    | C27-C26-H26B  | 108.8     |
| C25-C26-H26B  | 108.8    | H26A-C26-H26B | 107.7     |

|                |          |                |           |
|----------------|----------|----------------|-----------|
| C26-C27-C28    | 114.1(7) | C26-C27-C28A   | 102.7(12) |
| C26-C27-H27A   | 108.7    | C28-C27-H27A   | 108.7     |
| C26-C27-H27B   | 108.7    | C28-C27-H27B   | 108.7     |
| H27A-C27-H27B  | 107.6    | C26-C27-H27C   | 111.2     |
| C28A-C27-H27C  | 111.2    | C26-C27-H27D   | 111.2     |
| C28A-C27-H27D  | 111.2    | H27C-C27-H27D  | 109.1     |
| C23-C24-H24A   | 109.5    | C23-C24-H24B   | 109.5     |
| H24A-C24-H24B  | 109.5    | C23-C24-H24C   | 109.5     |
| H24A-C24-H24C  | 109.5    | H24B-C24-H24C  | 109.5     |
| C27-C28-H28A   | 109.5    | C27-C28-H28B   | 109.5     |
| H28A-C28-H28B  | 109.5    | C27-C28-H28C   | 109.5     |
| H28A-C28-H28C  | 109.5    | H28B-C28-H28C  | 109.5     |
| C23-C24A-H24D  | 109.5    | C23-C24A-H24E  | 109.5     |
| H24D-C24A-H24E | 109.5    | C23-C24A-H24F  | 109.5     |
| H24D-C24A-H24F | 109.5    | H24E-C24A-H24F | 109.5     |
| C27-C28A-H28D  | 109.5    | C27-C28A-H28E  | 109.5     |
| H28D-C28A-H28E | 109.5    | C27-C28A-H28F  | 109.5     |
| H28D-C28A-H28F | 109.5    | H28E-C28A-H28F | 109.5     |

**Table 6. Torsion angles (°) for Harman\_15JAS155b.**

|             |           |             |          |
|-------------|-----------|-------------|----------|
| C1-N1-N2-C3 | -0.3(6)   | W1-N1-N2-C3 | 179.0(4) |
| C1-N1-N2-B1 | 173.8(5)  | W1-N1-N2-B1 | -7.0(7)  |
| N4-B1-N2-C3 | -125.3(6) | N6-B1-N2-C3 | 118.5(7) |
| N4-B1-N2-N1 | 62.0(7)   | N6-B1-N2-N1 | -54.2(7) |
| C4-N3-N4-C6 | -1.6(6)   | W1-N3-N4-C6 | 174.4(4) |

|                 |           |                 |           |
|-----------------|-----------|-----------------|-----------|
| C4-N3-N4-B1     | -170.3(5) | W1-N3-N4-B1     | 5.7(7)    |
| N2-B1-N4-C6     | 132.5(6)  | N6-B1-N4-C6     | -110.2(7) |
| N2-B1-N4-N3     | -61.3(7)  | N6-B1-N4-N3     | 56.0(7)   |
| C7-N5-N6-C9     | -0.8(6)   | W1-N5-N6-C9     | -178.5(4) |
| C7-N5-N6-B1     | 169.7(5)  | W1-N5-N6-B1     | -8.0(6)   |
| N4-B1-N6-C9     | 113.7(6)  | N2-B1-N6-C9     | -128.2(6) |
| N4-B1-N6-N5     | -54.5(6)  | N2-B1-N6-N5     | 63.5(6)   |
| N2-N1-C1-C2     | 0.2(6)    | W1-N1-C1-C2     | -178.9(4) |
| N1-C1-C2-C3     | 0.0(7)    | N1-N2-C3-C2     | 0.2(7)    |
| B1-N2-C3-C2     | -173.2(6) | C1-C2-C3-N2     | -0.1(7)   |
| N4-N3-C4-C5     | 0.9(6)    | W1-N3-C4-C5     | -174.6(4) |
| N3-C4-C5-C6     | 0.1(7)    | N3-N4-C6-C5     | 1.8(7)    |
| B1-N4-C6-C5     | 169.1(6)  | C4-C5-C6-N4     | -1.2(7)   |
| N6-N5-C7-C8     | 0.5(6)    | W1-N5-C7-C8     | 177.8(4)  |
| N5-C7-C8-C9     | 0.0(7)    | N5-N6-C9-C8     | 0.8(7)    |
| B1-N6-C9-C8     | -168.3(6) | C7-C8-C9-N6     | -0.5(7)   |
| C15-C10-C11-C12 | -9.0(8)   | W1-C10-C11-C12  | 110.4(5)  |
| C15-C10-C11-W1  | -119.3(6) | C16-O2-C12-C13  | -7.5(9)   |
| C16-O2-C12-C11  | 174.5(5)  | C10-C11-C12-O2  | 178.7(5)  |
| W1-C11-C12-O2   | -102.4(5) | C10-C11-C12-C13 | 0.6(9)    |
| W1-C11-C12-C13  | 79.5(7)   | O2-C12-C13-C14  | -171.6(6) |
| C11-C12-C13-C14 | 6.1(10)   | C12-C13-C14-C15 | -4.5(11)  |
| C13-C14-C15-C10 | -3.7(10)  | C11-C10-C15-C14 | 10.8(9)   |
| W1-C10-C15-C14  | -79.3(8)  | C25-P1-C17-C18  | 61.7(6)   |
| C21-P1-C17-C18  | 166.2(5)  | W1-P1-C17-C18   | -64.0(6)  |

|                 |           |                  |           |
|-----------------|-----------|------------------|-----------|
| P1-C17-C18-C19  | -179.8(5) | C17-C18-C19-C20  | 177.4(7)  |
| C17-P1-C21-C22  | -62.7(6)  | C25-P1-C21-C22   | 42.2(6)   |
| W1-P1-C21-C22   | 169.5(4)  | P1-C21-C22-C23   | -175.5(5) |
| C21-C22-C23-C24 | 73.5(9)   | C21-C22-C23-C24A | 166.2(10) |
| C17-P1-C25-C26  | 169.8(5)  | C21-P1-C25-C26   | 64.6(5)   |
| W1-P1-C25-C26   | -64.6(5)  | P1-C25-C26-C27   | 175.9(5)  |
| C25-C26-C27-C28 | 179.8(8)  | C25-C26-C27-C28A | 71.4(12)  |

**Table 7. Anisotropic atomic displacement parameters ( $\text{\AA}^2$ ) for Harman\_15JAS155b.**

The anisotropic atomic displacement factor exponent takes the form: -  
 $2\pi^2 [ h^2 a^{*2} U_{11} + \dots + 2 h k a^* b^* U_{12} ]$

|    | $U_{11}$    | $U_{22}$    | $U_{33}$    | $U_{23}$    | $U_{13}$    | $U_{12}$    |
|----|-------------|-------------|-------------|-------------|-------------|-------------|
| W1 | 0.02418(15) | 0.02693(16) | 0.01933(12) | 0.00115(11) | 0.00093(11) | 0.01657(13) |
| P1 | 0.0231(9)   | 0.0314(10)  | 0.0271(8)   | 0.0015(7)   | 0.0001(7)   | 0.0153(8)   |
| O1 | 0.056(3)    | 0.061(3)    | 0.015(2)    | -0.004(2)   | -0.002(2)   | 0.044(3)    |
| O2 | 0.047(3)    | 0.057(3)    | 0.036(3)    | -0.003(2)   | 0.000(2)    | 0.032(3)    |
| B1 | 0.021(4)    | 0.037(5)    | 0.025(4)    | 0.005(3)    | 0.004(3)    | 0.014(4)    |
| N1 | 0.017(3)    | 0.028(3)    | 0.024(3)    | 0.001(2)    | 0.001(2)    | 0.012(2)    |
| N2 | 0.022(3)    | 0.033(3)    | 0.024(3)    | 0.004(2)    | 0.004(2)    | 0.015(2)    |
| N3 | 0.022(3)    | 0.023(3)    | 0.018(2)    | -0.001(2)   | -0.001(2)   | 0.009(2)    |
| N4 | 0.022(3)    | 0.033(3)    | 0.028(3)    | 0.003(2)    | 0.003(2)    | 0.016(3)    |
| N5 | 0.029(3)    | 0.029(3)    | 0.020(2)    | 0.003(2)    | -0.007(2)   | 0.016(3)    |
| N6 | 0.024(3)    | 0.035(3)    | 0.027(3)    | 0.009(2)    | -0.002(2)   | 0.014(3)    |
| N7 | 0.033(3)    | 0.037(3)    | 0.028(3)    | -0.003(2)   | 0.001(2)    | 0.024(3)    |

|     | <b>U<sub>11</sub></b> | <b>U<sub>22</sub></b> | <b>U<sub>33</sub></b> | <b>U<sub>23</sub></b> | <b>U<sub>13</sub></b> | <b>U<sub>12</sub></b> |
|-----|-----------------------|-----------------------|-----------------------|-----------------------|-----------------------|-----------------------|
| C1  | 0.026(3)              | 0.025(3)              | 0.026(3)              | 0.006(3)              | 0.000(3)              | 0.016(3)              |
| C2  | 0.027(4)              | 0.032(4)              | 0.021(3)              | 0.000(3)              | 0.000(3)              | 0.015(3)              |
| C3  | 0.036(4)              | 0.036(4)              | 0.027(3)              | 0.003(3)              | 0.014(3)              | 0.024(3)              |
| C4  | 0.020(3)              | 0.024(3)              | 0.028(3)              | 0.000(3)              | -0.003(3)             | 0.009(3)              |
| C5  | 0.026(4)              | 0.026(4)              | 0.044(4)              | 0.005(3)              | -0.010(3)             | 0.012(3)              |
| C6  | 0.027(4)              | 0.033(4)              | 0.044(4)              | -0.001(3)             | 0.001(3)              | 0.024(3)              |
| C7  | 0.037(4)              | 0.031(4)              | 0.016(3)              | 0.003(3)              | -0.006(3)             | 0.016(3)              |
| C8  | 0.031(4)              | 0.038(4)              | 0.029(4)              | 0.012(3)              | -0.007(3)             | 0.009(3)              |
| C9  | 0.024(4)              | 0.035(4)              | 0.036(4)              | 0.010(3)              | -0.005(3)             | 0.012(3)              |
| C10 | 0.053(5)              | 0.028(4)              | 0.023(3)              | -0.001(3)             | -0.007(3)             | 0.027(4)              |
| C11 | 0.037(4)              | 0.052(5)              | 0.016(3)              | 0.002(3)              | 0.001(3)              | 0.035(4)              |
| C12 | 0.031(4)              | 0.047(4)              | 0.037(4)              | 0.006(3)              | 0.001(3)              | 0.027(4)              |
| C13 | 0.062(5)              | 0.062(5)              | 0.023(3)              | -0.011(3)             | -0.005(3)             | 0.049(5)              |
| C14 | 0.052(5)              | 0.042(5)              | 0.048(5)              | -0.008(4)             | -0.010(4)             | 0.031(4)              |
| C15 | 0.065(5)              | 0.059(5)              | 0.029(4)              | -0.005(3)             | -0.008(3)             | 0.051(5)              |
| C16 | 0.057(5)              | 0.093(7)              | 0.037(4)              | 0.003(4)              | 0.010(4)              | 0.042(5)              |
| C17 | 0.037(4)              | 0.038(4)              | 0.037(4)              | 0.009(3)              | 0.006(3)              | 0.020(4)              |
| C18 | 0.058(5)              | 0.042(4)              | 0.030(4)              | 0.010(3)              | 0.012(3)              | 0.028(4)              |
| C19 | 0.089(7)              | 0.071(6)              | 0.033(4)              | 0.018(4)              | 0.014(4)              | 0.045(6)              |
| C20 | 0.140(10)             | 0.080(7)              | 0.056(6)              | 0.021(5)              | 0.001(6)              | 0.047(7)              |
| C21 | 0.030(4)              | 0.043(4)              | 0.032(4)              | -0.001(3)             | 0.000(3)              | 0.019(3)              |
| C22 | 0.028(4)              | 0.049(5)              | 0.054(5)              | -0.001(4)             | -0.005(3)             | 0.011(4)              |
| C23 | 0.023(4)              | 0.055(5)              | 0.060(5)              | -0.012(4)             | -0.011(3)             | 0.015(4)              |
| C25 | 0.027(4)              | 0.028(4)              | 0.039(4)              | -0.005(3)             | -0.008(3)             | 0.010(3)              |

|      | <b>U<sub>11</sub></b> | <b>U<sub>22</sub></b> | <b>U<sub>33</sub></b> | <b>U<sub>23</sub></b> | <b>U<sub>13</sub></b> | <b>U<sub>12</sub></b> |
|------|-----------------------|-----------------------|-----------------------|-----------------------|-----------------------|-----------------------|
| C26  | 0.045(4)              | 0.036(4)              | 0.037(4)              | -0.008(3)             | -0.003(3)             | 0.029(4)              |
| C27  | 0.085(7)              | 0.044(5)              | 0.064(5)              | -0.021(4)             | -0.011(5)             | 0.041(5)              |
| C24  | 0.040(6)              | 0.082(9)              | 0.044(6)              | -0.024(6)             | -0.015(5)             | 0.023(6)              |
| C28  | 0.147(13)             | 0.106(11)             | 0.033(6)              | -0.023(6)             | -0.014(7)             | 0.096(10)             |
| C24A | 0.040(6)              | 0.082(9)              | 0.044(6)              | -0.024(6)             | -0.015(5)             | 0.023(6)              |
| C28A | 0.147(13)             | 0.106(11)             | 0.033(6)              | -0.023(6)             | -0.014(7)             | 0.096(10)             |

**Table 8. Hydrogen atomic coordinates and isotropic atomic displacement parameters ( $\text{\AA}^2$ ) for Harman\_15JAS155b.**

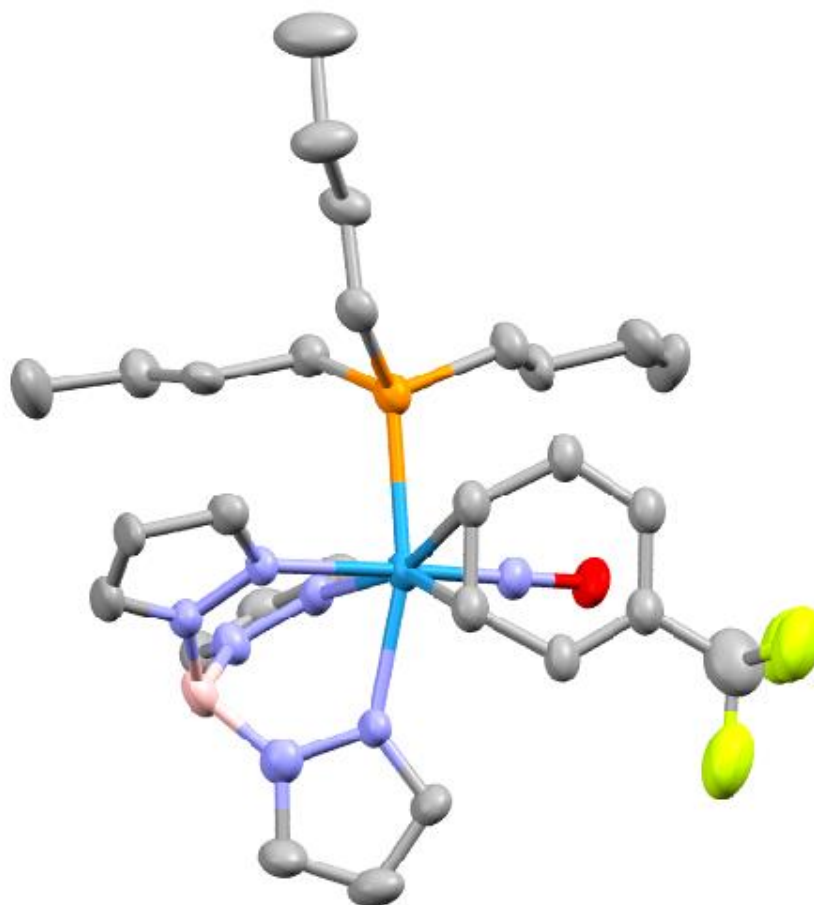
|     | <b>x/a</b> | <b>y/b</b> | <b>z/c</b> | <b>U(eq)</b> |
|-----|------------|------------|------------|--------------|
| H1A | 0.3061(16) | 0.2958(16) | 0.307(5)   | 0.033        |
| H1  | 0.1767     | 0.2862     | 0.2215     | 0.029        |
| H2  | 0.2084     | 0.2820     | 0.0331     | 0.033        |
| H3  | 0.2669     | 0.2840     | 0.1030     | 0.037        |
| H4  | 0.2216     | 0.2263     | 0.6826     | 0.03         |
| H5  | 0.2686     | 0.2062     | 0.6388     | 0.039        |
| H6  | 0.3029     | 0.2412     | 0.4539     | 0.037        |
| H7  | 0.2853     | 0.3777     | 0.6263     | 0.034        |
| H8  | 0.3515     | 0.4072     | 0.5544     | 0.044        |
| H9  | 0.3529     | 0.3653     | 0.3961     | 0.04         |
| H10 | 0.2169(16) | 0.3442(17) | 0.385(3)   | 0.038        |
| H11 | 0.1547(14) | 0.2976(14) | 0.419(4)   | 0.035        |
| H13 | 0.1586     | 0.3476     | 0.7403     | 0.049        |
| H14 | 0.2157     | 0.3991     | 0.6824     | 0.053        |

|      | <b>x/a</b> | <b>y/b</b> | <b>z/c</b> | <b>U(eq)</b> |
|------|------------|------------|------------|--------------|
| H15  | 0.2464     | 0.3985     | 0.5134     | 0.051        |
| H16A | 0.0945     | 0.3084     | 0.7156     | 0.091        |
| H16B | 0.1152     | 0.2901     | 0.7868     | 0.091        |
| H16C | 0.0754     | 0.2639     | 0.7244     | 0.091        |
| H17A | 0.1222     | 0.2333     | 0.6848     | 0.044        |
| H17B | 0.1042     | 0.1908     | 0.6424     | 0.044        |
| H18A | 0.1550     | 0.1878     | 0.7311     | 0.051        |
| H18B | 0.1729     | 0.2304     | 0.7740     | 0.051        |
| H19A | 0.1212     | 0.2140     | 0.9021     | 0.075        |
| H19B | 0.1019     | 0.1717     | 0.8564     | 0.075        |
| H20A | 0.1470     | 0.1630     | 0.9526     | 0.144        |
| H20B | 0.1314     | 0.1806     | 1.0499     | 0.144        |
| H20C | 0.1709     | 0.2065     | 0.9860     | 0.144        |
| H21A | 0.1059     | 0.2393     | 0.4357     | 0.042        |
| H21B | 0.1277     | 0.2335     | 0.3266     | 0.042        |
| H22A | 0.0930     | 0.1674     | 0.3633     | 0.057        |
| H22B | 0.0698     | 0.1745     | 0.4650     | 0.057        |
| H23A | 0.0323     | 0.1569     | 0.2995     | 0.057        |
| H23B | 0.0494     | 0.2012     | 0.3067     | 0.057        |
| H23C | 0.0691     | 0.1955     | 0.2187     | 0.057        |
| H23D | 0.0405     | 0.1920     | 0.3235     | 0.057        |
| H25A | 0.1769     | 0.1883     | 0.5288     | 0.04         |
| H25B | 0.1348     | 0.1663     | 0.4803     | 0.04         |
| H26A | 0.1549     | 0.1908     | 0.2844     | 0.043        |

|      | <b>x/a</b> | <b>y/b</b> | <b>z/c</b> | <b>U(eq)</b> |
|------|------------|------------|------------|--------------|
| H26B | 0.1969     | 0.2155     | 0.3313     | 0.043        |
| H27A | 0.1574     | 0.1357     | 0.3229     | 0.073        |
| H27B | 0.1995     | 0.1605     | 0.3693     | 0.073        |
| H27C | 0.1955     | 0.1564     | 0.3762     | 0.073        |
| H27D | 0.1944     | 0.1645     | 0.2336     | 0.073        |
| H24A | 0.0950     | 0.2079     | 0.1607     | 0.087        |
| H24B | 0.0532     | 0.1870     | 0.1089     | 0.087        |
| H24C | 0.0728     | 0.1634     | 0.1462     | 0.087        |
| H28A | 0.2045     | 0.1438     | 0.1733     | 0.121        |
| H28B | 0.2155     | 0.1868     | 0.1635     | 0.121        |
| H28C | 0.1747     | 0.1546     | 0.1235     | 0.121        |
| H24D | 0.0445     | 0.1304     | 0.2158     | 0.087        |
| H24E | 0.0092     | 0.1365     | 0.2095     | 0.087        |
| H24F | 0.0202     | 0.1250     | 0.3349     | 0.087        |
| H28D | 0.1338     | 0.1104     | 0.3783     | 0.121        |
| H28E | 0.1388     | 0.1088     | 0.2349     | 0.121        |
| H28F | 0.1219     | 0.1332     | 0.2891     | 0.121        |



**x/a      y/b      z/c      U(eq)**



### Crystal Structure Report for **Complex 4** in Chapter 9

A **yellow plate-like** specimen of  $C_{33}H_{53}BF_3N_7OPW$ , approximate dimensions **0.045 mm x 0.115 mm x 0.181 mm**, was coated with Paratone oil and mounted on a MiTeGen MicroLoop. The X-ray intensity data were measured on a Bruker Kappa APEXII Duo system equipped with a fine-focus sealed tube (Mo  $K_{\alpha}$ ,  $\lambda = 0.71073 \text{ \AA}$ ) and a graphite monochromator.

The total exposure time was 4.53 hours. The frames were integrated with the Bruker SAINT software package<sup>42</sup> using a narrow-frame algorithm. The integration of the data using a **monoclinic** unit cell yielded a total of **39059** reflections to a maximum  $\theta$  angle of **26.48°** (**0.80 Å** resolution), of which **7689** were independent (average redundancy **5.080**, completeness = **99.0%**,  $R_{int} = 15.17\%$ ,  $R_{sig} = 15.52\%$ ) and **4437** (**57.71%**) were greater than  $2\sigma(F^2)$ . The final cell constants of  $\underline{a} = 14.2625(18) \text{ \AA}$ ,  $\underline{b} = 24.790(3) \text{ \AA}$ ,  $\underline{c} = 10.7573(12) \text{ \AA}$ ,  $\beta = 99.653(3)^\circ$ , volume = **3749.6(8) Å<sup>3</sup>**, are based upon the refinement of the XYZ-centroids of **7340** reflections above  $20 \sigma(I)$  with  $4.406^\circ < 2\theta < 49.81^\circ$ . Data were corrected for absorption effects using the Multi-Scan method (SADABS).<sup>1</sup> The ratio of minimum to maximum apparent transmission was **0.713**. The calculated minimum and maximum transmission coefficients (based on

<sup>42</sup> Bruker (2012). *Saint*; *SADABS*; *APEX3*. Bruker AXS Inc., Madison, Wisconsin, USA.

crystal size) are 0.5970 and 0.8700.

The structure was solved and refined using the Bruker SHELXTL Software Package<sup>43</sup> within APEX3<sup>1</sup> and OLEX2,<sup>44</sup> using the space group  $P 2_1/c$ , with  $Z = 4$  for the formula unit,  $C_{33}H_{53}BF_3N_7OPW$ . Non-hydrogen atoms were refined anisotropically. Hydrogen atoms were placed in geometrically calculated positions with  $U_{iso} = 1.2U_{equiv}$  of the parent atom ( $U_{iso} = 1.5U_{equiv}$  for methyl). The trifluorotoluene ring was found to be disordered over two positions. The relative occupancies of the two positions was freely refined. Constraints were used on the bond lengths and anisotropic displacement parameters of the disordered atoms. The final anisotropic full-matrix least-squares refinement on  $F^2$  with 404 variables converged at  $R1 = 5.40\%$ , for the observed data and  $wR2 = 14.35\%$  for all data. The goodness-of-fit was 0.962. The largest peak in the final difference electron density synthesis was  $2.579 e^-/\text{\AA}^3$  and the largest hole was  $-1.182 e^-/\text{\AA}^3$  with an RMS deviation of  $0.170 e^-/\text{\AA}^3$ . On the basis of the final model, the calculated density was  $1.499 \text{ g/cm}^3$  and  $F(000)$ , 1716  $e^-$ .

**Table 1. Sample and crystal data for Harman\_15JAS145.**

|                             |                              |                           |
|-----------------------------|------------------------------|---------------------------|
| <b>Identification code</b>  | Harman_15JAS145              |                           |
| <b>Chemical formula</b>     | $C_{33}H_{53}BF_3N_7OPW$     |                           |
| <b>Formula weight</b>       | 846.45 g/mol                 |                           |
| <b>Temperature</b>          | 100(2) K                     |                           |
| <b>Wavelength</b>           | 0.71073 $\text{\AA}$         |                           |
| <b>Crystal size</b>         | 0.045 x 0.115 x 0.181 mm     |                           |
| <b>Crystal habit</b>        | yellow plate                 |                           |
| <b>Crystal system</b>       | monoclinic                   |                           |
| <b>Space group</b>          | $P 2_1/c$                    |                           |
| <b>Unit cell dimensions</b> | $a = 14.2625(18) \text{\AA}$ | $\alpha = 90^\circ$       |
|                             | $b = 24.790(3) \text{\AA}$   | $\beta = 99.653(3)^\circ$ |
|                             | $c = 10.7573(12) \text{\AA}$ | $\gamma = 90^\circ$       |
| <b>Volume</b>               | $3749.6(8) \text{\AA}^3$     |                           |
| <b>Z</b>                    | 4                            |                           |

<sup>43</sup> Sheldrick, G. M. (2015). *Acta Cryst. A* **71**, 3-8.

<sup>44</sup> Dolomanov, O. V.; Bourhis, L. J.; Gildea, R. J.; Howard, J. A. K.; Puschmann, H. *J. Appl. Cryst.* (2009). **42**, 339-341.

|                        |                         |
|------------------------|-------------------------|
| Density (calculated)   | 1.499 g/cm <sup>3</sup> |
| Absorption coefficient | 3.174 mm <sup>-1</sup>  |
| F(000)                 | 1716                    |

**Table 2. Data collection and structure refinement for Harman\_15JAS145.**

|                                     |  |
|-------------------------------------|--|
| Diffractometer                      | Bruker Kappa APEXII Duo  |
| Radiation source                    | fine-focus sealed tube (Mo K <sub>α</sub> , λ = 0.71073 Å)                   |
| Theta range for data collection     | 1.67 to 26.48°   |
| Index ranges                        | -17<=h<=17, -30<=k<=31, -13<=l<=12   |
| Reflections collected               | 39059  |
| Independent reflections             | 7689 [R(int) = 0.1517]   |
| Coverage of independent reflections | 99.0%  |
| Absorption correction               | Multi-Scan   |
| Max. and min. transmission          | 0.8700 and 0.5970  |
| Structure solution technique        | direct methods   |
| Structure solution program          | SHELXT 2014/5 (Sheldrick, 2014)  |
| Refinement method                   | Full-matrix least-squares on F <sup>2</sup>                                  |
| Refinement program                  | SHELXL-2018/3 (Sheldrick, 2018)  |
| Function minimized                  | Σ w(F <sub>o</sub> <sup>2</sup> - F <sub>c</sub> <sup>2</sup> ) <sup>2</sup> |
| Data / restraints / parameters      | 7689 / 15 / 404  |
| Goodness-of-fit on F <sup>2</sup>   | 0.962  |
| Δ/σ <sub>max</sub>                  | 0.001  |
| Final R indices                     | 4437 data; R1 = 0.0540, wR2 =<br>l>2σ(l) 0.1129                              |

all data R1 = 0.1205, wR2 = 0.1435

**Weighting scheme**  $w=1/[\sigma^2(F_o^2)]$   
where  $P=(F_o^2+2F_c^2)/3$

**Largest diff. peak and hole** 2.579 and -1.182 eÅ<sup>-3</sup>

**R.M.S. deviation from mean** 0.170 eÅ<sup>-3</sup>

**Table 3. Atomic coordinates and equivalent isotropic atomic displacement parameters (Å<sup>2</sup>) for Harman\_15JAS145.**

U(eq) is defined as one third of the trace of the orthogonalized U<sub>ij</sub> tensor.

|    | x/a         | y/b        | z/c        | U(eq)       |
|----|-------------|------------|------------|-------------|
| W1 | 0.32867(3)  | 0.61907(2) | 0.53222(3) | 0.02954(13) |
| P1 | 0.20662(18) | 0.54532(9) | 0.5009(2)  | 0.0327(6)   |
| O1 | 0.3304(5)   | 0.6169(2)  | 0.8110(5)  | 0.0437(16)  |
| N1 | 0.3265(5)   | 0.6236(3)  | 0.3234(6)  | 0.0288(16)  |
| N2 | 0.2986(5)   | 0.6700(3)  | 0.2602(6)  | 0.0344(18)  |
| N3 | 0.2019(5)   | 0.7150(3)  | 0.4048(6)  | 0.0323(17)  |
| N4 | 0.2085(5)   | 0.6772(3)  | 0.4978(6)  | 0.0302(16)  |
| N5 | 0.3728(5)   | 0.7330(3)  | 0.4285(7)  | 0.0376(18)  |
| N6 | 0.4007(5)   | 0.6984(3)  | 0.5272(6)  | 0.0330(17)  |
| N7 | 0.3298(5)   | 0.6180(3)  | 0.6971(7)  | 0.0334(17)  |
| C1 | 0.3410(6)   | 0.5872(4)  | 0.2360(8)  | 0.036(2)    |
| C2 | 0.3236(7)   | 0.6107(3)  | 0.1153(8)  | 0.037(2)    |
| C3 | 0.2975(7)   | 0.6621(4)  | 0.1352(8)  | 0.043(2)    |
| C4 | 0.1388(6)   | 0.6856(3)  | 0.5634(8)  | 0.035(2)    |

|     | <b>x/a</b> | <b>y/b</b> | <b>z/c</b> | <b>U(eq)</b> |
|-----|------------|------------|------------|--------------|
| C5  | 0.0839(7)  | 0.7289(3)  | 0.5104(9)  | 0.044(2)     |
| C6  | 0.1273(7)  | 0.7466(3)  | 0.4129(9)  | 0.040(2)     |
| C7  | 0.4686(7)  | 0.7227(3)  | 0.6068(8)  | 0.037(2)     |
| C8  | 0.4872(7)  | 0.7727(4)  | 0.5589(9)  | 0.048(3)     |
| C9  | 0.4268(7)  | 0.7776(4)  | 0.4471(9)  | 0.045(3)     |
| C17 | 0.0820(6)  | 0.5652(4)  | 0.4408(8)  | 0.039(2)     |
| C18 | 0.0696(6)  | 0.5885(3)  | 0.3049(8)  | 0.040(2)     |
| C19 | 0.9754(7)  | 0.6188(4)  | 0.2740(9)  | 0.046(2)     |
| C20 | 0.9590(9)  | 0.6390(5)  | 0.1357(10) | 0.076(4)     |
| C21 | 0.2216(7)  | 0.4887(3)  | 0.3935(8)  | 0.038(2)     |
| C22 | 0.1439(7)  | 0.4470(3)  | 0.3710(9)  | 0.043(2)     |
| C23 | 0.1659(8)  | 0.3998(4)  | 0.2896(11) | 0.058(3)     |
| C24 | 0.0851(9)  | 0.3581(4)  | 0.2728(12) | 0.080(4)     |
| C25 | 0.1982(7)  | 0.5114(3)  | 0.6500(7)  | 0.039(2)     |
| C26 | 0.1432(7)  | 0.5417(3)  | 0.7384(8)  | 0.044(2)     |
| C27 | 0.1576(8)  | 0.5161(4)  | 0.8680(8)  | 0.050(3)     |
| C28 | 0.1016(8)  | 0.5457(4)  | 0.9567(8)  | 0.058(3)     |
| C29 | 0.7810(16) | 0.7434(7)  | 0.947(2)   | 0.170(9)     |
| C30 | 0.6900(14) | 0.7581(8)  | 0.873(2)   | 0.147(7)     |
| C31 | 0.6611(14) | 0.8095(7)  | 0.904(2)   | 0.152(8)     |
| C32 | 0.7053(13) | 0.8586(7)  | 0.8671(18) | 0.128(6)     |
| C33 | 0.6789(15) | 0.8736(6)  | 0.7380(17) | 0.145(8)     |
| B1  | 0.2862(8)  | 0.7211(4)  | 0.3295(10) | 0.041(3)     |
| F1  | 0.5457(7)  | 0.5788(4)  | 0.9874(8)  | 0.0902(18)   |

|      | x/a        | y/b        | z/c        | U(eq)      |
|------|------------|------------|------------|------------|
| F2   | 0.6491(7)  | 0.6218(4)  | 0.8962(8)  | 0.0902(18) |
| F3   | 0.6648(7)  | 0.5389(4)  | 0.9230(8)  | 0.0902(18) |
| C10  | 0.4190(10) | 0.5440(6)  | 0.5349(12) | 0.0361(12) |
| C11  | 0.4788(11) | 0.5919(6)  | 0.5498(11) | 0.0361(12) |
| C12  | 0.5407(9)  | 0.5995(5)  | 0.6703(11) | 0.0361(12) |
| C13  | 0.5375(9)  | 0.5661(5)  | 0.7676(11) | 0.0361(12) |
| C14  | 0.4800(9)  | 0.5198(4)  | 0.7533(10) | 0.0361(12) |
| C15  | 0.4281(9)  | 0.5064(5)  | 0.6401(11) | 0.0361(12) |
| C16  | 0.5957(10) | 0.5760(5)  | 0.8874(14) | 0.075(5)   |
| F1A  | 0.468(3)   | 0.4575(14) | 0.860(3)   | 0.0902(18) |
| F2A  | 0.603(3)   | 0.5043(16) | 0.938(3)   | 0.0902(18) |
| F3A  | 0.467(3)   | 0.5370(15) | 0.962(3)   | 0.0902(18) |
| C10A | 0.434(3)   | 0.5445(19) | 0.547(3)   | 0.0361(12) |
| C11A | 0.483(4)   | 0.5916(18) | 0.530(3)   | 0.0361(12) |
| C12A | 0.548(3)   | 0.6126(13) | 0.629(4)   | 0.0361(12) |
| C13A | 0.564(2)   | 0.5866(15) | 0.745(3)   | 0.0361(12) |
| C14A | 0.514(3)   | 0.5395(15) | 0.762(3)   | 0.0361(12) |
| C15A | 0.450(3)   | 0.5185(14) | 0.663(4)   | 0.0361(12) |
| C16A | 0.510(3)   | 0.5073(16) | 0.879(5)   | 0.075(5)   |

**Table 4. Bond lengths (Å) for Harman\_15JAS145.**

|       |          |        |           |
|-------|----------|--------|-----------|
| W1-N7 | 1.771(7) | W1-C11 | 2.222(15) |
| W1-N4 | 2.223(7) | W1-N6  | 2.223(7)  |
| W1-N1 | 2.244(6) | W1-C10 | 2.261(15) |

|          |           |          |           |
|----------|-----------|----------|-----------|
| W1-C11A  | 2.31(5)   | W1-C10A  | 2.37(5)   |
| W1-P1    | 2.508(2)  | P1-C25   | 1.833(8)  |
| P1-C21   | 1.852(9)  | P1-C17   | 1.854(9)  |
| O1-N7    | 1.224(8)  | N1-C1    | 1.344(10) |
| N1-N2    | 1.362(8)  | N2-C3    | 1.357(10) |
| N2-B1    | 1.495(12) | N3-C6    | 1.336(11) |
| N3-N4    | 1.363(9)  | N3-B1    | 1.565(12) |
| N4-C4    | 1.328(10) | N5-C9    | 1.344(11) |
| N5-N6    | 1.371(9)  | N5-B1    | 1.518(13) |
| N6-C7    | 1.326(10) | C1-C2    | 1.407(11) |
| C1-H1    | 0.95      | C2-C3    | 1.355(12) |
| C2-H2    | 0.95      | C3-H3    | 0.95      |
| C4-C5    | 1.393(12) | C5-C6    | 1.377(12) |
| C5-H5    | 0.95      | C6-H6    | 0.95      |
| C7-C8    | 1.384(12) | C7-H7    | 0.95      |
| C8-C9    | 1.363(12) | C8-H8    | 0.95      |
| C9-H9    | 0.95      | C17-C18  | 1.553(11) |
| C17-H17A | 0.99      | C17-H17B | 0.99      |
| C18-C19  | 1.526(12) | C18-H18A | 0.99      |
| C18-H18B | 0.99      | C19-C20  | 1.550(13) |
| C19-H19A | 0.99      | C19-H19B | 0.99      |
| C20-H20A | 0.98      | C20-H20B | 0.98      |
| C20-H20C | 0.98      | C21-C22  | 1.505(12) |
| C21-H21A | 0.99      | C21-H21B | 0.99      |
| C22-C23  | 1.524(12) | C22-H22A | 0.99      |



|          |           |          |           |
|----------|-----------|----------|-----------|
| C22-H22B | 0.99      | C23-C24  | 1.537(13) |
| C23-H23A | 0.99      | C23-H23B | 0.99      |
| C24-H24A | 0.98      | C24-H24B | 0.98      |
| C24-H24C | 0.98      | C25-C26  | 1.528(12) |
| C25-H25A | 0.99      | C25-H25B | 0.99      |
| C26-C27  | 1.513(11) | C26-H26A | 0.99      |
| C26-H26B | 0.99      | C27-C28  | 1.531(13) |
| C27-H27A | 0.99      | C27-H27B | 0.99      |
| C28-H28A | 0.98      | C28-H28B | 0.98      |
| C28-H28C | 0.98      | C29-C30  | 1.45(2)   |
| C29-H29A | 0.98      | C29-H29B | 0.98      |
| C29-H29C | 0.98      | C30-C31  | 1.40(2)   |
| C30-H30A | 0.99      | C30-H30B | 0.99      |
| C31-C32  | 1.458(19) | C31-H31A | 0.99      |
| C31-H31B | 0.99      | C32-C33  | 1.43(2)   |
| C32-H32A | 0.99      | C32-H32B | 0.99      |
| C33-H33A | 0.98      | C33-H33B | 0.98      |
| C33-H33C | 0.98      | B1-H1A   | 1.0       |
| F1-C16   | 1.388(12) | F2-C16   | 1.363(12) |
| F3-C16   | 1.356(12) | C10-C15  | 1.454(14) |
| C10-C11  | 1.456(15) | C10-H10  | 0.95      |
| C11-C12  | 1.453(15) | C11-H11  | 0.95      |
| C12-C13  | 1.341(15) | C12-H12  | 0.95      |
| C13-C14  | 1.403(15) | C13-C16  | 1.432(19) |
| C14-C15  | 1.356(15) | C14-H14  | 0.95      |

|           |           |           |           |
|-----------|-----------|-----------|-----------|
| C15-H15   | 0.95      | F1A-C16A  | 1.375(17) |
| F2A-C16A  | 1.369(17) | F3A-C16A  | 1.376(17) |
| C10A-C11A | 1.39      | C10A-C15A | 1.39      |
| C10A-H10A | 0.95      | C11A-C12A | 1.39      |
| C11A-H11A | 0.95      | C12A-C13A | 1.39      |
| C12A-H12A | 0.95      | C13A-C14A | 1.39      |
| C13A-H13A | 0.95      | C14A-C15A | 1.39      |
| C14A-C16A | 1.50(6)   | C15A-H15A | 0.95      |

**Table 5. Bond angles (°) for Harman\_15JAS145.**

|            |           |              |            |
|------------|-----------|--------------|------------|
| N7-W1-C11  | 93.6(4)   | N7-W1-N4     | 93.1(3)    |
| C11-W1-N4  | 156.3(4)  | N7-W1-N6     | 96.3(3)    |
| C11-W1-N6  | 80.1(4)   | N4-W1-N6     | 76.6(3)    |
| N7-W1-N1   | 178.0(3)  | C11-W1-N1    | 87.2(3)    |
| N4-W1-N1   | 85.4(2)   | N6-W1-N1     | 82.0(2)    |
| N7-W1-C10  | 93.8(4)   | C11-W1-C10   | 37.9(4)    |
| N4-W1-C10  | 163.3(4)  | N6-W1-C10    | 117.7(4)   |
| N1-W1-C10  | 88.1(4)   | N7-W1-C11A   | 99.1(7)    |
| N4-W1-C11A | 154.1(10) | N6-W1-C11A   | 79.3(11)   |
| N1-W1-C11A | 81.8(7)   | N7-W1-C10A   | 91.3(10)   |
| N4-W1-C10A | 168.3(8)  | N6-W1-C10A   | 113.6(11)  |
| N1-W1-C10A | 90.4(10)  | C11A-W1-C10A | 34.5(7)    |
| N7-W1-P1   | 90.8(2)   | C11-W1-P1    | 115.3(4)   |
| N4-W1-P1   | 87.23(18) | N6-W1-P1     | 162.65(19) |
| N1-W1-P1   | 90.51(18) | C10-W1-P1    | 77.4(4)    |

|            |           |            |          |
|------------|-----------|------------|----------|
| C11A-W1-P1 | 115.2(12) | C10A-W1-P1 | 81.9(10) |
| C25-P1-C21 | 103.3(4)  | C25-P1-C17 | 103.2(4) |
| C21-P1-C17 | 100.9(4)  | C25-P1-W1  | 111.3(3) |
| C21-P1-W1  | 119.1(3)  | C17-P1-W1  | 117.1(3) |
| C1-N1-N2   | 106.6(6)  | C1-N1-W1   | 133.5(6) |
| N2-N1-W1   | 119.7(5)  | C3-N2-N1   | 109.0(7) |
| C3-N2-B1   | 129.4(7)  | N1-N2-B1   | 121.1(7) |
| C6-N3-N4   | 108.3(7)  | C6-N3-B1   | 131.7(8) |
| N4-N3-B1   | 118.8(7)  | C4-N4-N3   | 108.5(7) |
| C4-N4-W1   | 129.6(6)  | N3-N4-W1   | 121.6(5) |
| C9-N5-N6   | 108.4(7)  | C9-N5-B1   | 130.0(8) |
| N6-N5-B1   | 121.2(7)  | C7-N6-N5   | 107.5(7) |
| C7-N6-W1   | 132.6(6)  | N5-N6-W1   | 119.8(5) |
| O1-N7-W1   | 179.5(7)  | N1-C1-C2   | 110.1(8) |
| N1-C1-H1   | 124.9     | C2-C1-H1   | 124.9    |
| C3-C2-C1   | 104.7(8)  | C3-C2-H2   | 127.6    |
| C1-C2-H2   | 127.6     | C2-C3-N2   | 109.6(8) |
| C2-C3-H3   | 125.2     | N2-C3-H3   | 125.2    |
| N4-C4-C5   | 108.8(8)  | C6-C5-C4   | 105.3(8) |
| C6-C5-H5   | 127.3     | C4-C5-H5   | 127.3    |
| N3-C6-C5   | 109.0(8)  | N3-C6-H6   | 125.5    |
| C5-C6-H6   | 125.5     | N6-C7-C8   | 109.4(8) |
| N6-C7-H7   | 125.3     | C8-C7-H7   | 125.3    |
| C9-C8-C7   | 106.1(8)  | C9-C8-H8   | 127.0    |
| C7-C8-H8   | 127.0     | N5-C9-C8   | 108.6(8) |

|               |          |               |       |
|---------------|----------|---------------|-------|
| N5-C9-H9      | 125.7    | C8-C9-H9      | 125.7 |
| C18-C17-P1    | 112.2(6) | C18-C17-H17A  | 109.2 |
| P1-C17-H17A   | 109.2    | C18-C17-H17B  | 109.2 |
| P1-C17-H17B   | 109.2    | H17A-C17-H17B | 107.9 |
| C19-C18-C17   | 110.2(8) | C19-C18-H18A  | 109.6 |
| C17-C18-H18A  | 109.6    | C19-C18-H18B  | 109.6 |
| C17-C18-H18B  | 109.6    | H18A-C18-H18B | 108.1 |
| C18-C19-C20   | 110.7(8) | C18-C19-H19A  | 109.5 |
| C20-C19-H19A  | 109.5    | C18-C19-H19B  | 109.5 |
| C20-C19-H19B  | 109.5    | H19A-C19-H19B | 108.1 |
| C19-C20-H20A  | 109.5    | C19-C20-H20B  | 109.5 |
| H20A-C20-H20B | 109.5    | C19-C20-H20C  | 109.5 |
| H20A-C20-H20C | 109.5    | H20B-C20-H20C | 109.5 |
| C22-C21-P1    | 117.5(6) | C22-C21-H21A  | 107.9 |
| P1-C21-H21A   | 107.9    | C22-C21-H21B  | 107.9 |
| P1-C21-H21B   | 107.9    | H21A-C21-H21B | 107.2 |
| C21-C22-C23   | 113.7(8) | C21-C22-H22A  | 108.8 |
| C23-C22-H22A  | 108.8    | C21-C22-H22B  | 108.8 |
| C23-C22-H22B  | 108.8    | H22A-C22-H22B | 107.7 |
| C22-C23-C24   | 111.2(9) | C22-C23-H23A  | 109.4 |
| C24-C23-H23A  | 109.4    | C22-C23-H23B  | 109.4 |
| C24-C23-H23B  | 109.4    | H23A-C23-H23B | 108.0 |
| C23-C24-H24A  | 109.5    | C23-C24-H24B  | 109.5 |
| H24A-C24-H24B | 109.5    | C23-C24-H24C  | 109.5 |
| H24A-C24-H24C | 109.5    | H24B-C24-H24C | 109.5 |

|               |           |               |       |
|---------------|-----------|---------------|-------|
| C26-C25-P1    | 115.8(6)  | C26-C25-H25A  | 108.3 |
| P1-C25-H25A   | 108.3     | C26-C25-H25B  | 108.3 |
| P1-C25-H25B   | 108.3     | H25A-C25-H25B | 107.4 |
| C27-C26-C25   | 111.2(7)  | C27-C26-H26A  | 109.4 |
| C25-C26-H26A  | 109.4     | C27-C26-H26B  | 109.4 |
| C25-C26-H26B  | 109.4     | H26A-C26-H26B | 108.0 |
| C26-C27-C28   | 111.7(8)  | C26-C27-H27A  | 109.3 |
| C28-C27-H27A  | 109.3     | C26-C27-H27B  | 109.3 |
| C28-C27-H27B  | 109.3     | H27A-C27-H27B | 108.0 |
| C27-C28-H28A  | 109.5     | C27-C28-H28B  | 109.5 |
| H28A-C28-H28B | 109.5     | C27-C28-H28C  | 109.5 |
| H28A-C28-H28C | 109.5     | H28B-C28-H28C | 109.5 |
| C30-C29-H29A  | 109.5     | C30-C29-H29B  | 109.5 |
| H29A-C29-H29B | 109.5     | C30-C29-H29C  | 109.5 |
| H29A-C29-H29C | 109.5     | H29B-C29-H29C | 109.5 |
| C31-C30-C29   | 112.(2)   | C31-C30-H30A  | 109.3 |
| C29-C30-H30A  | 109.3     | C31-C30-H30B  | 109.3 |
| C29-C30-H30B  | 109.3     | H30A-C30-H30B | 107.9 |
| C30-C31-C32   | 122.5(19) | C30-C31-H31A  | 106.7 |
| C32-C31-H31A  | 106.7     | C30-C31-H31B  | 106.7 |
| C32-C31-H31B  | 106.7     | H31A-C31-H31B | 106.6 |
| C33-C32-C31   | 115.4(17) | C33-C32-H32A  | 108.4 |
| C31-C32-H32A  | 108.4     | C33-C32-H32B  | 108.4 |
| C31-C32-H32B  | 108.4     | H32A-C32-H32B | 107.5 |
| C32-C33-H33A  | 109.5     | C32-C33-H33B  | 109.5 |

|                |           |                |           |
|----------------|-----------|----------------|-----------|
| H33A-C33-H33B  | 109.5     | C32-C33-H33C   | 109.5     |
| H33A-C33-H33C  | 109.5     | H33B-C33-H33C  | 109.5     |
| N2-B1-N5       | 111.3(8)  | N2-B1-N3       | 109.9(8)  |
| N5-B1-N3       | 105.2(7)  | N2-B1-H1A      | 110.1     |
| N5-B1-H1A      | 110.1     | N3-B1-H1A      | 110.1     |
| C15-C10-C11    | 117.5(10) | C15-C10-W1     | 120.9(9)  |
| C11-C10-W1     | 69.6(7)   | C15-C10-H10    | 121.2     |
| C11-C10-H10    | 121.2     | W1-C10-H10     | 80.8      |
| C12-C11-C10    | 117.4(10) | C12-C11-W1     | 118.0(9)  |
| C10-C11-W1     | 72.5(7)   | C12-C11-H11    | 121.3     |
| C10-C11-H11    | 121.3     | W1-C11-H11     | 80.7      |
| C13-C12-C11    | 121.4(11) | C13-C12-H12    | 119.3     |
| C11-C12-H12    | 119.3     | C12-C13-C14    | 121.0(11) |
| C12-C13-C16    | 120.4(13) | C14-C13-C16    | 118.6(11) |
| C15-C14-C13    | 121.3(11) | C15-C14-H14    | 119.4     |
| C13-C14-H14    | 119.4     | C14-C15-C10    | 120.4(10) |
| C14-C15-H15    | 119.8     | C10-C15-H15    | 119.8     |
| F3-C16-F2      | 100.0(12) | F3-C16-F1      | 105.0(11) |
| F2-C16-F1      | 105.0(11) | F3-C16-C13     | 115.0(11) |
| F2-C16-C13     | 116.0(11) | F1-C16-C13     | 114.3(12) |
| C11A-C10A-C15A | 120.0     | C11A-C10A-W1   | 70.5(18)  |
| C15A-C10A-W1   | 115.(2)   | C11A-C10A-H10A | 120.0     |
| C15A-C10A-H10A | 120.0     | W1-C10A-H10A   | 84.8      |
| C10A-C11A-C12A | 120.0     | C10A-C11A-W1   | 75.0(18)  |
| C12A-C11A-W1   | 113.(2)   | C10A-C11A-H11A | 120.0     |

|                |         |                |         |
|----------------|---------|----------------|---------|
| C12A-C11A-H11A | 120.0   | W1-C11A-H11A   | 82.3    |
| C13A-C12A-C11A | 120.0   | C13A-C12A-H12A | 120.0   |
| C11A-C12A-H12A | 120.0   | C14A-C13A-C12A | 120.0   |
| C14A-C13A-H13A | 120.0   | C12A-C13A-H13A | 120.0   |
| C13A-C14A-C15A | 120.0   | C13A-C14A-C16A | 130.(3) |
| C15A-C14A-C16A | 109.(3) | C14A-C15A-C10A | 120.0   |
| C14A-C15A-H15A | 120.0   | C10A-C15A-H15A | 120.0   |
| F2A-C16A-F1A   | 113.(4) | F2A-C16A-F3A   | 104.(4) |
| F1A-C16A-F3A   | 110.(4) | F2A-C16A-C14A  | 104.(3) |
| F1A-C16A-C14A  | 115.(4) | F3A-C16A-C14A  | 110.(3) |

**Table 6. Torsion angles (°) for Harman\_15JAS145.**

|             |           |             |           |
|-------------|-----------|-------------|-----------|
| C1-N1-N2-C3 | -0.9(9)   | W1-N1-N2-C3 | -176.3(6) |
| C1-N1-N2-B1 | -173.4(8) | W1-N1-N2-B1 | 11.2(10)  |
| C6-N3-N4-C4 | -0.3(9)   | B1-N3-N4-C4 | 168.7(8)  |
| C6-N3-N4-W1 | -175.1(5) | B1-N3-N4-W1 | -6.1(10)  |
| C9-N5-N6-C7 | 2.1(10)   | B1-N5-N6-C7 | -170.9(8) |
| C9-N5-N6-W1 | -179.9(6) | B1-N5-N6-W1 | 7.1(10)   |
| N2-N1-C1-C2 | 0.9(9)    | W1-N1-C1-C2 | 175.4(6)  |
| N1-C1-C2-C3 | -0.5(10)  | C1-C2-C3-N2 | -0.1(10)  |
| N1-N2-C3-C2 | 0.6(10)   | B1-N2-C3-C2 | 172.3(9)  |
| N3-N4-C4-C5 | 1.5(10)   | W1-N4-C4-C5 | 175.8(5)  |
| N4-C4-C5-C6 | -2.1(10)  | N4-N3-C6-C5 | -1.0(10)  |
| B1-N3-C6-C5 | -168.1(9) | C4-C5-C6-N3 | 1.9(10)   |
| N5-N6-C7-C8 | -1.6(10)  | W1-N6-C7-C8 | -179.3(6) |

|                 |           |                 |                |
|-----------------|-----------|-----------------|----------------|
| N6-C7-C8-C9     | 0.6(11)   | N6-N5-C9-C8     | -1.8(11)       |
| B1-N5-C9-C8     | 170.5(9)  | C7-C8-C9-N5     | 0.8(11)        |
| C25-P1-C17-C18  | -172.6(6) | C21-P1-C17-C18  | -66.0(7)       |
| W1-P1-C17-C18   | 64.9(6)   | P1-C17-C18-C19  | -163.7(6)      |
| C17-C18-C19-C20 | -176.2(8) | C25-P1-C21-C22  | 59.7(8)        |
| C17-P1-C21-C22  | -46.8(8)  | W1-P1-C21-C22   | -176.4(6)      |
| P1-C21-C22-C23  | -175.6(7) | C21-C22-C23-C24 | 178.7(9)       |
| C21-P1-C25-C26  | -153.8(7) | C17-P1-C25-C26  | -49.1(8)       |
| W1-P1-C25-C26   | 77.3(7)   | P1-C25-C26-C27  | -168.3(7)      |
| C25-C26-C27-C28 | -179.1(8) | C29-C30-C31-C32 | 73.(3)         |
| C30-C31-C32-C33 | 76.(3)    | C3-N2-B1-N5     | -<br>120.4(10) |
| N1-N2-B1-N5     | 50.4(11)  | C3-N2-B1-N3     | 123.4(9)       |
| N1-N2-B1-N3     | -65.8(10) | C9-N5-B1-N2     | 126.7(10)      |
| N6-N5-B1-N2     | -62.0(11) | C9-N5-B1-N3     | -<br>114.3(10) |
| N6-N5-B1-N3     | 57.1(10)  | C6-N3-B1-N2     | -131.5(9)      |
| N4-N3-B1-N2     | 62.5(10)  | C6-N3-B1-N5     | 108.6(10)      |
| N4-N3-B1-N5     | -57.4(9)  | C15-C10-C11-C12 | -2.1(15)       |
| W1-C10-C11-C12  | 113.0(11) | C15-C10-C11-W1  | -<br>115.1(10) |
| C10-C11-C12-C13 | -5.3(16)  | W1-C11-C12-C13  | 78.5(13)       |
| C11-C12-C13-C14 | 5.6(17)   | C11-C12-C13-C16 | -<br>176.8(12) |
| C12-C13-C14-C15 | 2.0(17)   | C16-C13-C14-C15 | -<br>175.7(11) |
| C13-C14-C15-C10 | -9.7(17)  | C11-C10-C15-C14 | 9.4(16)        |



|                         |                |                         |                |
|-------------------------|----------------|-------------------------|----------------|
| W1-C10-C15-C14          | -72.2(14)      | C12-C13-C16-F3          | -<br>113.1(13) |
| C14-C13-C16-F3          | 64.6(16)       | C12-C13-C16-F2          | 3.0(17)        |
| C14-C13-C16-F2          | -<br>179.3(10) | C12-C13-C16-F1          | 125.4(12)      |
| C14-C13-C16-F1          | -56.9(15)      | C15A-C10A-C11A-<br>C12A | 0              |
| W1-C10A-C11A-<br>C12A   | 108.(2)        | C15A-C10A-C11A-<br>W1   | -108.(2)       |
| C10A-C11A-C12A-<br>C13A | 0              | W1-C11A-C12A-<br>C13A   | 85.6(19)       |
| C11A-C12A-C13A-<br>C14A | 0              | C12A-C13A-C14A-<br>C15A | 0              |
| C12A-C13A-C14A-<br>C16A | -173.(4)       | C13A-C14A-C15A-<br>C10A | 0              |
| C16A-C14A-C15A-<br>C10A | 174.(3)        | C11A-C10A-C15A-<br>C14A | 0              |
| W1-C10A-C15A-<br>C14A   | -81.1(18)      | C13A-C14A-C16A-<br>F2A  | -45.(4)        |
| C15A-C14A-C16A-<br>F2A  | 142.(3)        | C13A-C14A-C16A-<br>F1A  | -169.(3)       |
| C15A-C14A-C16A-<br>F1A  | 18.(4)         | C13A-C14A-C16A-<br>F3A  | 66.(4)         |
| C15A-C14A-C16A-<br>F3A  | -108.(3)       |                         |                |

**Table 7. Anisotropic atomic displacement parameters ( $\text{\AA}^2$ ) for Harman\_15JAS145.**

The anisotropic atomic displacement factor exponent takes the form: -  
 $2\pi^2 [ h^2 a^{*2} U_{11} + \dots + 2 h k a^* b^* U_{12} ]$

|     | <b>U<sub>11</sub></b> | <b>U<sub>22</sub></b> | <b>U<sub>33</sub></b> | <b>U<sub>23</sub></b> | <b>U<sub>13</sub></b> | <b>U<sub>12</sub></b> |
|-----|-----------------------|-----------------------|-----------------------|-----------------------|-----------------------|-----------------------|
| W1  | 0.0341(2)             | 0.03326(19)           | 0.0216(2)             | 0.00146(17)           | 0.00573(14)           | 0.00329(19)           |
| P1  | 0.0409(15)            | 0.0328(12)            | 0.0256(13)            | 0.0017(10)            | 0.0092(10)            | 0.0036(11)            |
| O1  | 0.061(5)              | 0.050(4)              | 0.019(3)              | -0.006(3)             | 0.004(3)              | -0.001(3)             |
| N1  | 0.037(4)              | 0.031(4)              | 0.019(4)              | 0.000(3)              | 0.007(3)              | 0.001(3)              |
| N2  | 0.040(5)              | 0.034(4)              | 0.027(4)              | 0.003(3)              | 0.000(3)              | -0.002(3)             |
| N3  | 0.037(5)              | 0.030(4)              | 0.030(4)              | 0.005(3)              | 0.007(3)              | 0.004(3)              |
| N4  | 0.025(4)              | 0.038(4)              | 0.027(4)              | 0.001(3)              | 0.003(3)              | 0.000(3)              |
| N5  | 0.036(5)              | 0.045(5)              | 0.033(4)              | -0.001(4)             | 0.010(4)              | 0.001(4)              |
| N6  | 0.040(5)              | 0.037(4)              | 0.022(4)              | 0.001(3)              | 0.005(3)              | -0.005(3)             |
| N7  | 0.034(4)              | 0.035(4)              | 0.029(4)              | 0.003(3)              | -0.001(3)             | 0.003(3)              |
| C1  | 0.040(6)              | 0.040(5)              | 0.029(5)              | 0.000(4)              | 0.011(4)              | -0.004(4)             |
| C2  | 0.059(7)              | 0.038(6)              | 0.015(4)              | 0.003(4)              | 0.008(4)              | -0.008(4)             |
| C3  | 0.053(7)              | 0.051(6)              | 0.024(5)              | 0.011(4)              | 0.003(4)              | -0.009(5)             |
| C4  | 0.034(6)              | 0.037(5)              | 0.036(5)              | -0.009(4)             | 0.009(4)              | 0.004(4)              |
| C5  | 0.034(6)              | 0.037(5)              | 0.059(7)              | -0.011(5)             | 0.006(5)              | 0.001(4)              |
| C6  | 0.045(6)              | 0.029(5)              | 0.043(6)              | 0.000(4)              | -0.004(5)             | 0.010(4)              |
| C7  | 0.043(6)              | 0.037(5)              | 0.031(5)              | -0.009(4)             | 0.004(4)              | 0.000(4)              |
| C8  | 0.050(7)              | 0.044(6)              | 0.053(7)              | -0.017(5)             | 0.017(5)              | -0.016(5)             |
| C9  | 0.060(7)              | 0.031(5)              | 0.045(6)              | -0.005(5)             | 0.009(5)              | -0.005(5)             |
| C17 | 0.043(6)              | 0.042(5)              | 0.032(5)              | -0.001(4)             | 0.008(4)              | -0.004(4)             |
| C18 | 0.045(6)              | 0.030(5)              | 0.043(6)              | 0.004(4)              | 0.005(5)              | -0.012(4)             |
| C19 | 0.052(7)              | 0.042(5)              | 0.043(6)              | 0.005(5)              | 0.006(5)              | 0.007(5)              |
| C20 | 0.075(9)              | 0.082(8)              | 0.063(8)              | 0.038(7)              | -0.014(6)             | -0.007(7)             |
| C21 | 0.036(6)              | 0.044(5)              | 0.038(5)              | 0.006(4)              | 0.014(4)              | -0.001(4)             |

|     | <b>U<sub>11</sub></b> | <b>U<sub>22</sub></b> | <b>U<sub>33</sub></b> | <b>U<sub>23</sub></b> | <b>U<sub>13</sub></b> | <b>U<sub>12</sub></b> |
|-----|-----------------------|-----------------------|-----------------------|-----------------------|-----------------------|-----------------------|
| C22 | 0.055(7)              | 0.032(5)              | 0.047(6)              | -0.004(4)             | 0.021(5)              | -0.003(5)             |
| C23 | 0.050(7)              | 0.046(6)              | 0.080(8)              | -0.024(6)             | 0.021(6)              | -0.007(5)             |
| C24 | 0.082(10)             | 0.050(6)              | 0.117(11)             | -0.037(7)             | 0.042(8)              | -0.019(7)             |
| C25 | 0.052(7)              | 0.038(5)              | 0.029(5)              | 0.004(4)              | 0.012(4)              | 0.002(4)              |
| C26 | 0.063(7)              | 0.043(5)              | 0.027(5)              | 0.008(4)              | 0.010(5)              | -0.002(5)             |
| C27 | 0.063(8)              | 0.051(6)              | 0.038(6)              | 0.009(5)              | 0.016(5)              | -0.011(5)             |
| C28 | 0.052(7)              | 0.094(8)              | 0.028(6)              | -0.001(5)             | 0.009(5)              | -0.012(6)             |
| C29 | 0.15(2)               | 0.133(16)             | 0.21(2)               | 0.038(15)             | -0.019(17)            | 0.047(15)             |
| C30 | 0.124(19)             | 0.125(16)             | 0.21(2)               | 0.040(16)             | 0.068(16)             | 0.014(13)             |
| C31 | 0.139(19)             | 0.075(11)             | 0.24(2)               | -0.007(14)            | 0.028(15)             | -0.022(12)            |
| C32 | 0.129(17)             | 0.112(13)             | 0.148(18)             | 0.011(13)             | 0.041(13)             | -0.025(12)            |
| C33 | 0.22(2)               | 0.092(12)             | 0.110(15)             | -0.024(11)            | -0.020(14)            | -0.042(12)            |
| B1  | 0.047(8)              | 0.039(6)              | 0.038(7)              | 0.015(5)              | 0.010(5)              | 0.005(5)              |
| F1  | 0.089(4)              | 0.111(4)              | 0.062(3)              | -0.005(3)             | -0.013(3)             | 0.023(3)              |
| F2  | 0.089(4)              | 0.111(4)              | 0.062(3)              | -0.005(3)             | -0.013(3)             | 0.023(3)              |
| F3  | 0.089(4)              | 0.111(4)              | 0.062(3)              | -0.005(3)             | -0.013(3)             | 0.023(3)              |
| C10 | 0.039(3)              | 0.039(3)              | 0.030(3)              | 0.003(2)              | 0.004(2)              | 0.010(2)              |
| C11 | 0.039(3)              | 0.039(3)              | 0.030(3)              | 0.003(2)              | 0.004(2)              | 0.010(2)              |
| C12 | 0.039(3)              | 0.039(3)              | 0.030(3)              | 0.003(2)              | 0.004(2)              | 0.010(2)              |
| C13 | 0.039(3)              | 0.039(3)              | 0.030(3)              | 0.003(2)              | 0.004(2)              | 0.010(2)              |
| C14 | 0.039(3)              | 0.039(3)              | 0.030(3)              | 0.003(2)              | 0.004(2)              | 0.010(2)              |
| C15 | 0.039(3)              | 0.039(3)              | 0.030(3)              | 0.003(2)              | 0.004(2)              | 0.010(2)              |
| C16 | 0.088(13)             | 0.066(10)             | 0.076(11)             | -0.002(9)             | 0.023(9)              | 0.028(9)              |
| F1A | 0.089(4)              | 0.111(4)              | 0.062(3)              | -0.005(3)             | -0.013(3)             | 0.023(3)              |

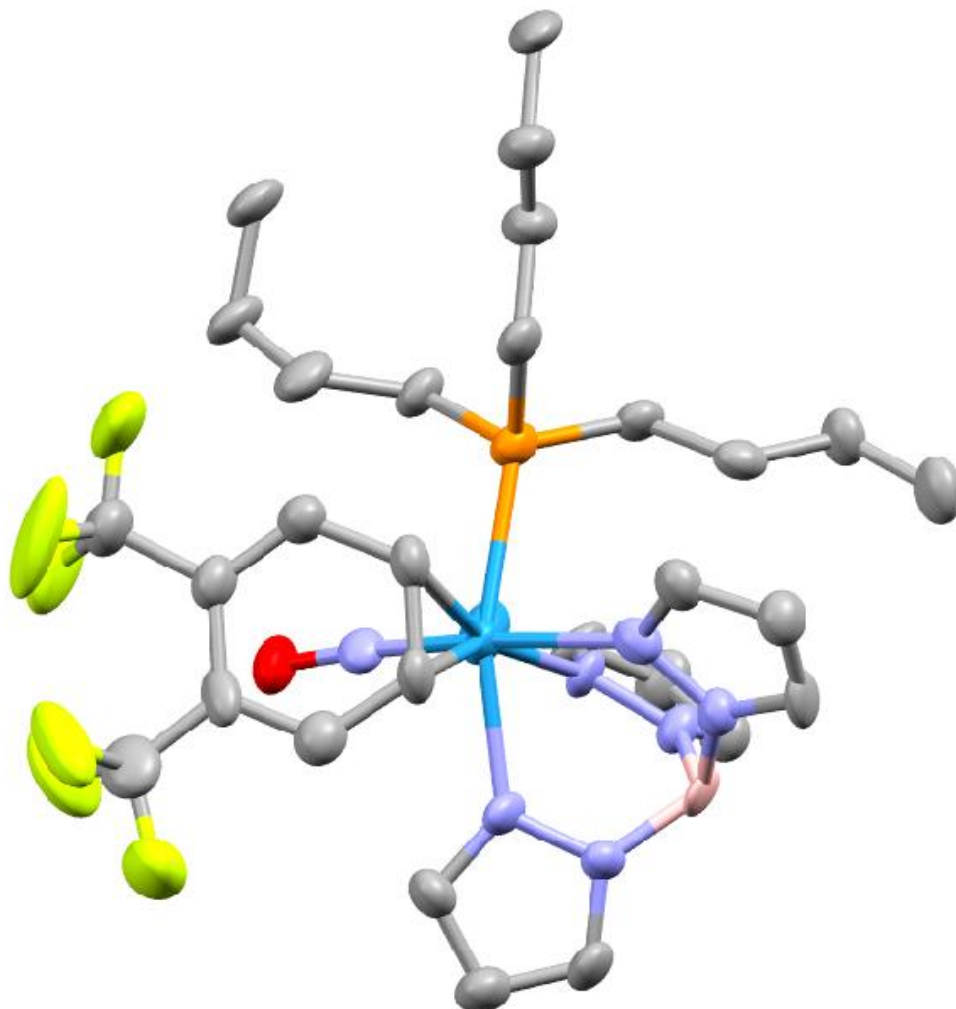
|      | <b>U<sub>11</sub></b> | <b>U<sub>22</sub></b> | <b>U<sub>33</sub></b> | <b>U<sub>23</sub></b> | <b>U<sub>13</sub></b> | <b>U<sub>12</sub></b> |
|------|-----------------------|-----------------------|-----------------------|-----------------------|-----------------------|-----------------------|
| F2A  | 0.089(4)              | 0.111(4)              | 0.062(3)              | -0.005(3)             | -0.013(3)             | 0.023(3)              |
| F3A  | 0.089(4)              | 0.111(4)              | 0.062(3)              | -0.005(3)             | -0.013(3)             | 0.023(3)              |
| C10A | 0.039(3)              | 0.039(3)              | 0.030(3)              | 0.003(2)              | 0.004(2)              | 0.010(2)              |
| C11A | 0.039(3)              | 0.039(3)              | 0.030(3)              | 0.003(2)              | 0.004(2)              | 0.010(2)              |
| C12A | 0.039(3)              | 0.039(3)              | 0.030(3)              | 0.003(2)              | 0.004(2)              | 0.010(2)              |
| C13A | 0.039(3)              | 0.039(3)              | 0.030(3)              | 0.003(2)              | 0.004(2)              | 0.010(2)              |
| C14A | 0.039(3)              | 0.039(3)              | 0.030(3)              | 0.003(2)              | 0.004(2)              | 0.010(2)              |
| C15A | 0.039(3)              | 0.039(3)              | 0.030(3)              | 0.003(2)              | 0.004(2)              | 0.010(2)              |
| C16A | 0.088(13)             | 0.066(10)             | 0.076(11)             | -0.002(9)             | 0.023(9)              | 0.028(9)              |

**Table 8. Hydrogen atomic coordinates and isotropic atomic displacement parameters ( $\text{\AA}^2$ ) for Harman\_15JAS145.**

|      | <b>x/a</b> | <b>y/b</b> | <b>z/c</b> | <b>U(eq)</b> |
|------|------------|------------|------------|--------------|
| H1   | 0.3603     | 0.5509     | 0.2533     | 0.043        |
| H2   | 0.3290     | 0.5941     | 0.0372     | 0.044        |
| H3   | 0.2810     | 0.6885     | 0.0714     | 0.052        |
| H5   | 0.0284     | 0.7431     | 0.5361     | 0.052        |
| H6   | 0.1075     | 0.7766     | 0.3599     | 0.048        |
| H7   | 0.4996     | 0.7081     | 0.6846     | 0.045        |
| H8   | 0.5329     | 0.7983     | 0.5964     | 0.057        |
| H9   | 0.4233     | 0.8076     | 0.3916     | 0.054        |
| H17A | 0.0402     | 0.5334     | 0.4413     | 0.047        |
| H17B | 0.0618     | 0.5927     | 0.4978     | 0.047        |
| H18A | 0.1228     | 0.6133     | 0.2978     | 0.048        |

|      | <b>x/a</b> | <b>y/b</b> | <b>z/c</b> | <b>U(eq)</b> |
|------|------------|------------|------------|--------------|
| H18B | 0.0709     | 0.5588     | 0.2439     | 0.048        |
| H19A | -0.0241    | 0.6500     | 0.3317     | 0.055        |
| H19B | -0.0774    | 0.5947     | 0.2868     | 0.055        |
| H20A | 0.0106     | 0.6635     | 0.1235     | 0.114        |
| H20B | -0.1019    | 0.6582     | 0.1176     | 0.114        |
| H20C | -0.0421    | 0.6082     | 0.0786     | 0.114        |
| H21A | 0.2290     | 0.5042     | 0.3108     | 0.046        |
| H21B | 0.2818     | 0.4701     | 0.4274     | 0.046        |
| H22A | 0.0844     | 0.4645     | 0.3298     | 0.052        |
| H22B | 0.1329     | 0.4329     | 0.4535     | 0.052        |
| H23A | 0.2258     | 0.3824     | 0.3295     | 0.069        |
| H23B | 0.1749     | 0.4135     | 0.2059     | 0.069        |
| H24A | 0.0727     | 0.3467     | 0.3557     | 0.12         |
| H24B | 0.1036     | 0.3268     | 0.2270     | 0.12         |
| H24C | 0.0274     | 0.3743     | 0.2249     | 0.12         |
| H25A | 0.1674     | 0.4759     | 0.6305     | 0.047        |
| H25B | 0.2634     | 0.5046     | 0.6953     | 0.047        |
| H26A | 0.1650     | 0.5797     | 0.7459     | 0.053        |
| H26B | 0.0746     | 0.5417     | 0.7025     | 0.053        |
| H27A | 0.2262     | 0.5167     | 0.9043     | 0.06         |
| H27B | 0.1369     | 0.4780     | 0.8602     | 0.06         |
| H28A | 0.1220     | 0.5835     | 0.9645     | 0.087        |
| H28B | 0.1135     | 0.5286     | 1.0399     | 0.087        |
| H28C | 0.0336     | 0.5441     | 0.9225     | 0.087        |

|      | <b>x/a</b> | <b>y/b</b> | <b>z/c</b> | <b>U(eq)</b> |
|------|------------|------------|------------|--------------|
| H29A | 0.7990     | 0.7072     | 0.9223     | 0.255        |
| H29B | 0.8295     | 0.7694     | 0.9314     | 0.255        |
| H29C | 0.7760     | 0.7435     | 1.0365     | 0.255        |
| H30A | 0.6950     | 0.7572     | 0.7821     | 0.176        |
| H30B | 0.6415     | 0.7313     | 0.8872     | 0.176        |
| H31A | 0.6671     | 0.8104     | 0.9972     | 0.182        |
| H31B | 0.5924     | 0.8122     | 0.8700     | 0.182        |
| H32A | 0.6889     | 0.8886     | 0.9202     | 0.153        |
| H32B | 0.7752     | 0.8540     | 0.8854     | 0.153        |
| H33A | 0.7120     | 0.9069     | 0.7221     | 0.218        |
| H33B | 0.6966     | 0.8447     | 0.6841     | 0.218        |
| H33C | 0.6100     | 0.8795     | 0.7190     | 0.218        |
| H1A  | 0.2737     | 0.7519     | 0.2689     | 0.049        |
| H10  | 0.3755     | 0.5375     | 0.4593     | 0.043        |
| H11  | 0.4775     | 0.6172     | 0.4832     | 0.043        |
| H12  | 0.5844     | 0.6287     | 0.6804     | 0.043        |
| H14  | 0.4774     | 0.4974     | 0.8243     | 0.043        |
| H15  | 0.3976     | 0.4723     | 0.6294     | 0.043        |
| H10A | 0.3900     | 0.5301     | 0.4790     | 0.043        |
| H11A | 0.4729     | 0.6094     | 0.4506     | 0.043        |
| H12A | 0.5818     | 0.6448     | 0.6175     | 0.043        |
| H13A | 0.6078     | 0.6010     | 0.8129     | 0.043        |
| H15A | 0.4160     | 0.4863     | 0.6744     | 0.043        |



### Crystal Structure Report for **Complex 6** in Chapter 9

A **yellow block-like** specimen of  $C_{29}H_{41}BF_6N_7OPW$ , approximate dimensions **0.070 mm** x **0.131 mm** x **0.136 mm**, was coated with Paratone oil and mounted on a MiTeGen MicroLoop. The X-ray intensity data were measured on a Bruker Kappa APEXII CCD system equipped with a fine-focus sealed tube (Mo  $K_{\alpha}$ ,  $\lambda = 0.71073 \text{ \AA}$ ) and a graphite monochromator.

The total exposure time was 9.00 hours. A three-component twin was identified using CELL\_NOW.<sup>45</sup> Starting with 2409 reflections, 1500 reflections were fit to the first domain, 1233 to the second domain (656 exclusively), and 590 to the third domain (251 exclusively) with 2 unindexed reflection remaining. The second domain was oriented at a  $3.5^{\circ}$  rotation about the real axis  $-0.086 \ 0.029 \ 1.000$ . The twin law was  $0.998 \ 0.066 \ -0.026 / -0.055 \ 1.001 \ -0.003 / 0.001 \ 0.006 \ 0.998$ . The third domain was oriented at a  $9.1^{\circ}$  rotation about the real axis  $-0.062 \ -0.360 \ 1.00$  and its twin law was  $0.989 \ -0.165 \ 0.019 / 0.164 \ 0.981 \ 0.007 / 0.066 \ -0.016 \ 1.004$ . The frames were integrated with the Bruker SAINT

<sup>45</sup> Sheldrick, G. M. (2008). *Cell\_now*, version 2008/4. Georg-August-Universität Göttingen, Göttingen, Germany

software package<sup>46</sup> using a narrow-frame algorithm. The integration of the data using a triclinic unit cell yielded a total of 6702 reflections to a maximum  $\theta$  angle of 25.60° (0.82 Å resolution), and 4391 (65.52%) were greater than  $2\sigma(F^2)$ . The final cell constants of  $a = 11.465(2)$  Å,  $b = 11.7033(18)$  Å,  $c = 13.760(2)$  Å,  $\alpha = 66.976(4)^\circ$ ,  $\beta = 89.730(4)^\circ$ ,  $\gamma = 88.613(4)^\circ$ , volume = 1698.7(5) Å<sup>3</sup>, are based upon the refinement of the XYZ-centroids of 9945 reflections above  $20\sigma(I)$  with  $4.781^\circ < 2\theta < 44.03^\circ$ . Data were corrected for absorption effects using the Multi-Scan method (TWINABS).<sup>2</sup> The ratio of minimum to maximum apparent transmission was 0.681. The calculated minimum and maximum transmission coefficients (based on crystal size) are 0.6460 and 0.7910.

The structure was solved and refined using the Bruker SHELXTL Software Package<sup>47</sup> within APEX3<sup>2</sup> and OLEX2,<sup>48</sup> using the space group P -1, with Z = 2 for the formula unit, C<sub>29</sub>H<sub>41</sub>BF<sub>6</sub>N<sub>7</sub>OPW. The structure was refined as a two-component twin on HKLF5 data, with the BASF for the twin domains refining to 0.43072 and 0.12709. Non-hydrogen atoms were refined anisotropically. Hydrogen atoms were placed in geometrically calculated positions with  $U_{iso} = 1.2U_{equiv}$  of the parent atom ( $1.5U_{equiv}$  for methyl). Two independent sites of disorder were identified. Their relative occupancies were freely refined. Constraints were used on the anisotropic displacement parameters of the disordered C atoms, and restraints were used on the disordered C-C bonds. The final anisotropic full-matrix least-squares refinement on F<sup>2</sup> with 429 variables converged at R1 = 7.01%, for the observed data and wR2 = 15.23% for all data. The goodness-of-fit was 1.045. The largest peak in the final difference electron density synthesis was 2.328 e<sup>-</sup>/Å<sup>3</sup> and the largest hole was -1.054 e<sup>-</sup>/Å<sup>3</sup> with an RMS deviation of 0.236 e<sup>-</sup>/Å<sup>3</sup>. On the basis of the final model, the calculated density was 1.649 g/cm<sup>3</sup> and F(000), 840 e<sup>-</sup>.

**Table 1. Sample and crystal data for Harman\_16JAS\_15.**

|                            |  |
|----------------------------|--|
| <b>Identification code</b> | Harman_16JAS_15  |
| <b>Chemical formula</b>    | C <sub>29</sub> H <sub>41</sub> BF <sub>6</sub> N <sub>7</sub> OPW |
| <b>Formula weight</b>      | 843.32 g/mol   |
| <b>Temperature</b>         | 100(2) K   |
| <b>Wavelength</b>          | 0.71073 Å  |
| <b>Crystal size</b>        | 0.070 x 0.131 x 0.136 mm   |
| <b>Crystal habit</b>       | yellow block   |
| <b>Crystal system</b>      | triclinic  |
| <b>Space group</b>         | P -1   |

<sup>46</sup> Bruker (2012). *Saint*; *SADABS*; *APEX3*. Bruker AXS Inc., Madison, Wisconsin, USA.

<sup>47</sup> Sheldrick, G. M. (2015). *Acta Cryst. A* **71**, 3-8.

<sup>48</sup> Dolomanov, O. V.; Bourhis, L. J.; Gildea, R. J.; Howard, J. A. K.; Puschmann, H. *J. Appl. Cryst.* (2009). **42**, 339-341.



|                               |                          |                            |
|-------------------------------|--------------------------|----------------------------|
| <b>Unit cell dimensions</b>   | a = 11.465(2) Å          | $\alpha = 66.976(4)^\circ$ |
|                               | b = 11.7033(18) Å        | $\beta = 89.730(4)^\circ$  |
|                               | c = 13.760(2) Å          | $\gamma = 88.613(4)^\circ$ |
| <b>Volume</b>                 | 1698.7(5) Å <sup>3</sup> |                            |
| <b>Z</b>                      | 2                        |                            |
| <b>Density (calculated)</b>   | 1.649 g/cm <sup>3</sup>  |                            |
| <b>Absorption coefficient</b> | 3.515 mm <sup>-1</sup>   |                            |
| <b>F(000)</b>                 | 840                      |                            |

**Table 2. Data collection and structure refinement for Harman\_16JAS\_15.**

|  |  |
|--|--|
| <b>Diffractometer</b>                      | Bruker Kappa APEXII CCD  |
| <b>Radiation source</b>                    | fine-focus sealed tube (Mo K $\alpha$ , $\lambda = 0.71073$ Å) |
| <b>Theta range for data collection</b>     | 1.61 to 25.60°   |
| <b>Reflections collected</b>               | 6702   |
| <b>Coverage of independent reflections</b> | 98.1%  |
| <b>Absorption correction</b>               | Multi-Scan   |
| <b>Max. and min. transmission</b>          | 0.7910 and 0.6460  |
| <b>Structure solution technique</b>        | direct methods   |
| <b>Structure solution program</b>          | SHELXT 2014/5 (Sheldrick, 2014)                                |
| <b>Refinement method</b>                   | Full-matrix least-squares on F <sup>2</sup>                    |
| <b>Refinement program</b>                  | SHELXL-2018/3 (Sheldrick, 2018)                                |
| <b>Function minimized</b>                  | $\Sigma w(F_o^2 - F_c^2)^2$                                    |
| <b>Data / restraints / parameters</b>      | 6702 / 1 / 429   |
| <b>Goodness-of-fit on F<sup>2</sup></b>    | 1.045  |

|                                    |   |                              |
|------------------------------------|---|------------------------------|
| <b>Final R indices</b>             | 4391 data;<br>$I > 2\sigma(I)$  | R1 = 0.0701, wR2 =<br>0.1267 |
|                                    | all data  | R1 = 0.1363, wR2 =<br>0.1523 |
| <b>Weighting scheme</b>            | $w = 1/[\sigma^2(F_o^2) + 0.7825P]$<br>where $P = (F_o^2 + 2F_c^2)/3$ |                              |
| <b>Largest diff. peak and hole</b> | 2.328 and -1.054 eÅ <sup>-3</sup>                                     |                              |
| <b>R.M.S. deviation from mean</b>  | 0.236 eÅ <sup>-3</sup>  |                              |

**Table 3. Atomic coordinates and equivalent isotropic atomic displacement parameters (Å<sup>2</sup>) for Harman\_16JAS\_15.**

U(eq) is defined as one third of the trace of the orthogonalized U<sub>ij</sub> tensor.

|    | <b>x/a</b> | <b>y/b</b> | <b>z/c</b> | <b>U(eq)</b> |
|----|------------|------------|------------|--------------|
| W1 | 0.6127(2)  | 0.6583(2)  | 0.2214(3)  | 0.0258(7)    |
| P1 | 0.7637(2)  | 0.4868(3)  | 0.3213(2)  | 0.0385(7)    |
| F1 | 0.4252(7)  | 0.2224(7)  | 0.2574(8)  | 0.108(3)     |
| F2 | 0.2844(9)  | 0.2867(8)  | 0.1485(6)  | 0.117(4)     |
| F3 | 0.2796(8)  | 0.3118(8)  | 0.2878(7)  | 0.095(3)     |
| F4 | 0.1744(6)  | 0.5049(10) | 0.0401(9)  | 0.117(4)     |
| F5 | 0.1585(7)  | 0.5163(10) | 0.1885(8)  | 0.113(3)     |
| F6 | 0.1768(7)  | 0.6778(9)  | 0.0500(9)  | 0.111(4)     |
| O1 | 0.4118(6)  | 0.5369(7)  | 0.3618(6)  | 0.055(2)     |
| N1 | 0.7490(7)  | 0.7659(8)  | 0.1136(6)  | 0.035(2)     |
| N2 | 0.7742(7)  | 0.8840(8)  | 0.1047(7)  | 0.036(2)     |
| N3 | 0.6815(7)  | 0.7448(7)  | 0.3294(6)  | 0.032(2)     |

|     | <b>x/a</b> | <b>y/b</b> | <b>z/c</b> | <b>U(eq)</b> |
|-----|------------|------------|------------|--------------|
| N4  | 0.7286(7)  | 0.8580(7)  | 0.2904(7)  | 0.034(2)     |
| N5  | 0.5211(7)  | 0.8372(7)  | 0.1717(6)  | 0.035(2)     |
| N6  | 0.5787(7)  | 0.9451(7)  | 0.1537(6)  | 0.032(2)     |
| N7  | 0.4981(7)  | 0.5834(8)  | 0.3075(7)  | 0.037(2)     |
| C1  | 0.8213(8)  | 0.7456(11) | 0.0437(9)  | 0.044(3)     |
| C2  | 0.8913(9)  | 0.8469(11) | 0.9926(9)  | 0.044(3)     |
| C3  | 0.8581(8)  | 0.9313(11) | 0.0310(8)  | 0.039(3)     |
| C4  | 0.6919(10) | 0.7050(10) | 0.4335(9)  | 0.045(3)     |
| C5  | 0.7445(10) | 0.7888(11) | 0.4629(9)  | 0.051(3)     |
| C6  | 0.7664(9)  | 0.8858(11) | 0.3685(9)  | 0.044(3)     |
| C7  | 0.4068(9)  | 0.8669(11) | 0.1662(9)  | 0.045(3)     |
| C8  | 0.3906(10) | 0.9913(10) | 0.1459(9)  | 0.053(3)     |
| C9  | 0.5009(9)  | 0.0367(10) | 0.1397(9)  | 0.045(3)     |
| C10 | 0.5975(9)  | 0.5477(10) | 0.1221(8)  | 0.041(3)     |
| C11 | 0.5307(8)  | 0.6618(10) | 0.0741(8)  | 0.040(3)     |
| C12 | 0.4065(10) | 0.6598(11) | 0.0662(9)  | 0.047(3)     |
| C13 | 0.3449(9)  | 0.5537(11) | 0.1116(10) | 0.045(3)     |
| C14 | 0.4110(10) | 0.4384(10) | 0.1629(9)  | 0.043(3)     |
| C15 | 0.5291(9)  | 0.4352(10) | 0.1643(8)  | 0.043(3)     |
| C16 | 0.3516(11) | 0.3154(12) | 0.2131(11) | 0.056(3)     |
| C17 | 0.2202(12) | 0.5638(14) | 0.1000(12) | 0.063(4)     |
| C18 | 0.8900(9)  | 0.5382(9)  | 0.3740(8)  | 0.039(3)     |
| C19 | 0.9547(8)  | 0.6467(10) | 0.2913(8)  | 0.040(3)     |
| C20 | 0.0603(9)  | 0.6870(11) | 0.3363(9)  | 0.044(3)     |

|      | x/a        | y/b        | z/c        | U(eq)    |
|------|------------|------------|------------|----------|
| C21  | 0.1104(10) | 0.8038(12) | 0.2555(10) | 0.056(3) |
| C22  | 0.8344(9)  | 0.3994(9)  | 0.2505(8)  | 0.042(3) |
| C23  | 0.9171(10) | 0.2911(11) | 0.3125(10) | 0.054(3) |
| C24  | 0.9637(10) | 0.2226(10) | 0.2459(10) | 0.052(3) |
| C25  | 0.0445(10) | 0.1155(10) | 0.3095(11) | 0.062(4) |
| C26  | 0.7129(9)  | 0.3672(9)  | 0.4442(8)  | 0.042(3) |
| C27  | 0.6202(10) | 0.2799(10) | 0.4305(9)  | 0.052(3) |
| C28  | 0.5942(10) | 0.1739(9)  | 0.5351(9)  | 0.050(2) |
| C29  | 0.6875(14) | 0.0751(13) | 0.5623(13) | 0.050(2) |
| B1   | 0.7093(10) | 0.9424(11) | 0.1722(10) | 0.037(3) |
| W1A  | 0.6185(14) | 0.6480(18) | 0.253(3)   | 0.060(4) |
| C29A | 0.527(3)   | 0.070(3)   | 0.532(3)   | 0.050(2) |

**Table 4. Bond lengths (Å) for Harman\_16JAS\_15.**

|        |           |        |           |
|--------|-----------|--------|-----------|
| W1-N7  | 1.768(9)  | W1-N5  | 2.176(8)  |
| W1-N1  | 2.200(9)  | W1-C11 | 2.223(11) |
| W1-C10 | 2.228(11) | W1-N3  | 2.254(9)  |
| W1-P1  | 2.571(4)  | P1-C26 | 1.827(10) |
| P1-C18 | 1.838(11) | P1-C22 | 1.840(11) |
| P1-W1A | 2.39(2)   | F1-C16 | 1.308(14) |
| F2-C16 | 1.322(14) | F3-C16 | 1.305(14) |
| F4-C17 | 1.378(14) | F5-C17 | 1.332(15) |
| F6-C17 | 1.324(15) | O1-N7  | 1.239(10) |
| N1-C1  | 1.353(13) | N1-N2  | 1.377(11) |

|          |           |          |           |
|----------|-----------|----------|-----------|
| N1-W1A   | 2.41(3)   | N2-C3    | 1.356(12) |
| N2-B1    | 1.532(15) | N3-C4    | 1.326(13) |
| N3-N4    | 1.346(10) | N3-W1A   | 1.98(3)   |
| N4-C6    | 1.317(13) | N4-B1    | 1.551(14) |
| N5-C7    | 1.342(12) | N5-N6    | 1.373(10) |
| N5-W1A   | 2.31(3)   | N6-C9    | 1.333(13) |
| N6-B1    | 1.518(13) | N7-W1A   | 1.625(17) |
| C1-C2    | 1.390(14) | C1-H1    | 0.95      |
| C2-C3    | 1.337(15) | C2-H2    | 0.95      |
| C3-H3    | 0.95      | C4-C5    | 1.354(14) |
| C4-H4    | 0.95      | C5-C6    | 1.377(15) |
| C5-H5    | 0.95      | C6-H6    | 0.95      |
| C7-C8    | 1.379(15) | C7-H7    | 0.95      |
| C8-C9    | 1.373(15) | C8-H8    | 0.95      |
| C9-H9    | 0.95      | C10-C11  | 1.440(15) |
| C10-C15  | 1.462(14) | C10-W1A  | 2.52(3)   |
| C10-H10  | 0.95      | C11-C12  | 1.430(14) |
| C11-W1A  | 2.60(4)   | C11-H11  | 0.95      |
| C12-C13  | 1.365(15) | C12-H12  | 0.95      |
| C13-C17  | 1.436(16) | C13-C14  | 1.450(16) |
| C14-C15  | 1.353(14) | C14-C16  | 1.509(15) |
| C15-H15  | 0.95      | C18-C19  | 1.539(13) |
| C18-H18A | 0.99      | C18-H18B | 0.99      |
| C19-C20  | 1.527(14) | C19-H19A | 0.99      |
| C19-H19B | 0.99      | C20-C21  | 1.509(15) |

|           |           |           |           |
|-----------|-----------|-----------|-----------|
| C20-H20A  | 0.99      | C20-H20B  | 0.99      |
| C21-H21A  | 0.98      | C21-H21B  | 0.98      |
| C21-H21C  | 0.98      | C22-C23   | 1.529(15) |
| C22-H22A  | 0.99      | C22-H22B  | 0.99      |
| C23-C24   | 1.523(16) | C23-H23A  | 0.99      |
| C23-H23B  | 0.99      | C24-C25   | 1.513(15) |
| C24-H24A  | 0.99      | C24-H24B  | 0.99      |
| C25-H25A  | 0.98      | C25-H25B  | 0.98      |
| C25-H25C  | 0.98      | C26-C27   | 1.554(15) |
| C26-H26A  | 0.99      | C26-H26B  | 0.99      |
| C27-C28   | 1.522(15) | C27-H27A  | 0.99      |
| C27-H27B  | 0.99      | C28-C29A  | 1.47(2)   |
| C28-C29   | 1.492(16) | C28-H28A  | 0.99      |
| C28-H28B  | 0.99      | C28-H28C  | 0.99      |
| C28-H28D  | 0.99      | C29-H29A  | 0.98      |
| C29-H29B  | 0.98      | C29-H29C  | 0.98      |
| B1-H1A    | 1.0       | C29A-H29D | 0.98      |
| C29A-H29E | 0.98      | C29A-H29F | 0.98      |

**Table 5. Bond angles (°) for Harman\_16JAS\_15.**

|           |         |            |          |
|-----------|---------|------------|----------|
| N7-W1-N5  | 91.6(3) | N7-W1-N1   | 175.3(4) |
| N5-W1-N1  | 83.9(3) | N7-W1-C11  | 96.8(4)  |
| N5-W1-C11 | 81.0(4) | N1-W1-C11  | 83.8(3)  |
| N7-W1-C10 | 94.9(4) | N5-W1-C10  | 118.8(4) |
| N1-W1-C10 | 88.4(4) | C11-W1-C10 | 37.7(4)  |

|            |           |            |           |
|------------|-----------|------------|-----------|
| N7-W1-N3   | 93.7(4)   | N5-W1-N3   | 75.6(3)   |
| N1-W1-N3   | 84.0(3)   | C11-W1-N3  | 154.6(4)  |
| C10-W1-N3  | 163.0(3)  | N7-W1-P1   | 93.3(3)   |
| N5-W1-P1   | 157.6(3)  | N1-W1-P1   | 90.4(2)   |
| C11-W1-P1  | 120.0(3)  | C10-W1-P1  | 82.6(3)   |
| N3-W1-P1   | 82.3(2)   | C26-P1-C18 | 98.7(5)   |
| C26-P1-C22 | 104.4(5)  | C18-P1-C22 | 101.8(5)  |
| C26-P1-W1A | 109.9(8)  | C18-P1-W1A | 111.7(6)  |
| C22-P1-W1A | 126.6(10) | C26-P1-W1  | 115.5(4)  |
| C18-P1-W1  | 115.3(4)  | C22-P1-W1  | 118.4(4)  |
| C1-N1-N2   | 104.1(8)  | C1-N1-W1   | 134.6(8)  |
| N2-N1-W1   | 121.2(6)  | C1-N1-W1A  | 137.8(8)  |
| N2-N1-W1A  | 117.4(7)  | C3-N2-N1   | 109.6(8)  |
| C3-N2-B1   | 130.0(9)  | N1-N2-B1   | 120.3(8)  |
| C4-N3-N4   | 105.6(8)  | C4-N3-W1A  | 125.3(12) |
| N4-N3-W1A  | 129.0(12) | C4-N3-W1   | 133.2(7)  |
| N4-N3-W1   | 121.1(6)  | C6-N4-N3   | 109.7(8)  |
| C6-N4-B1   | 129.9(9)  | N3-N4-B1   | 119.1(8)  |
| C7-N5-N6   | 106.1(8)  | C7-N5-W1   | 131.3(7)  |
| N6-N5-W1   | 121.9(6)  | C7-N5-W1A  | 130.8(8)  |
| N6-N5-W1A  | 119.6(7)  | C9-N6-N5   | 109.3(8)  |
| C9-N6-B1   | 129.0(9)  | N5-N6-B1   | 120.6(7)  |
| O1-N7-W1A  | 170.9(16) | O1-N7-W1   | 175.0(8)  |
| N1-C1-C2   | 111.6(11) | N1-C1-H1   | 124.2     |
| C2-C1-H1   | 124.2     | C3-C2-C1   | 104.9(10) |

|             |           |             |           |
|-------------|-----------|-------------|-----------|
| C3-C2-H2    | 127.5     | C1-C2-H2    | 127.5     |
| C2-C3-N2    | 109.7(10) | C2-C3-H3    | 125.2     |
| N2-C3-H3    | 125.2     | N3-C4-C5    | 112.0(10) |
| N3-C4-H4    | 124.0     | C5-C4-H4    | 124.0     |
| C4-C5-C6    | 103.6(10) | C4-C5-H5    | 128.2     |
| C6-C5-H5    | 128.2     | N4-C6-C5    | 109.1(10) |
| N4-C6-H6    | 125.4     | C5-C6-H6    | 125.4     |
| N5-C7-C8    | 110.3(10) | N5-C7-H7    | 124.8     |
| C8-C7-H7    | 124.8     | C9-C8-C7    | 105.2(10) |
| C9-C8-H8    | 127.4     | C7-C8-H8    | 127.4     |
| N6-C9-C8    | 109.0(10) | N6-C9-H9    | 125.5     |
| C8-C9-H9    | 125.5     | C11-C10-C15 | 115.3(9)  |
| C11-C10-W1  | 70.9(6)   | C15-C10-W1  | 117.3(7)  |
| C11-C10-W1A | 77.1(10)  | C15-C10-W1A | 112.2(9)  |
| C11-C10-H10 | 122.4     | C15-C10-H10 | 122.4     |
| W1-C10-H10  | 82.9      | C12-C11-C10 | 120.4(9)  |
| C12-C11-W1  | 120.0(7)  | C10-C11-W1  | 71.3(6)   |
| C12-C11-W1A | 117.6(8)  | C10-C11-W1A | 70.3(7)   |
| C12-C11-H11 | 119.8     | C10-C11-H11 | 119.8     |
| W1-C11-H11  | 79.6      | C13-C12-C11 | 122.7(11) |
| C13-C12-H12 | 118.7     | C11-C12-H12 | 118.7     |
| C12-C13-C17 | 117.5(12) | C12-C13-C14 | 117.4(10) |
| C17-C13-C14 | 125.0(11) | C15-C14-C13 | 121.6(10) |
| C15-C14-C16 | 116.7(10) | C13-C14-C16 | 121.6(10) |
| C14-C15-C10 | 122.4(10) | C14-C15-H15 | 118.8     |



|               |           |               |           |
|---------------|-----------|---------------|-----------|
| C10-C15-H15   | 118.8     | F3-C16-F1     | 105.2(12) |
| F3-C16-F2     | 102.6(10) | F1-C16-F2     | 107.5(12) |
| F3-C16-C14    | 112.9(11) | F1-C16-C14    | 112.8(10) |
| F2-C16-C14    | 114.8(11) | F6-C17-F5     | 105.1(11) |
| F6-C17-F4     | 100.7(12) | F5-C17-F4     | 102.0(11) |
| F6-C17-C13    | 115.6(12) | F5-C17-C13    | 116.5(12) |
| F4-C17-C13    | 114.9(10) | C19-C18-P1    | 114.1(7)  |
| C19-C18-H18A  | 108.7     | P1-C18-H18A   | 108.7     |
| C19-C18-H18B  | 108.7     | P1-C18-H18B   | 108.7     |
| H18A-C18-H18B | 107.6     | C20-C19-C18   | 113.3(9)  |
| C20-C19-H19A  | 108.9     | C18-C19-H19A  | 108.9     |
| C20-C19-H19B  | 108.9     | C18-C19-H19B  | 108.9     |
| H19A-C19-H19B | 107.7     | C21-C20-C19   | 110.8(9)  |
| C21-C20-H20A  | 109.5     | C19-C20-H20A  | 109.5     |
| C21-C20-H20B  | 109.5     | C19-C20-H20B  | 109.5     |
| H20A-C20-H20B | 108.1     | C20-C21-H21A  | 109.5     |
| C20-C21-H21B  | 109.5     | H21A-C21-H21B | 109.5     |
| C20-C21-H21C  | 109.5     | H21A-C21-H21C | 109.5     |
| H21B-C21-H21C | 109.5     | C23-C22-P1    | 118.1(8)  |
| C23-C22-H22A  | 107.8     | P1-C22-H22A   | 107.8     |
| C23-C22-H22B  | 107.8     | P1-C22-H22B   | 107.8     |
| H22A-C22-H22B | 107.1     | C24-C23-C22   | 112.5(10) |
| C24-C23-H23A  | 109.1     | C22-C23-H23A  | 109.1     |
| C24-C23-H23B  | 109.1     | C22-C23-H23B  | 109.1     |
| H23A-C23-H23B | 107.8     | C25-C24-C23   | 111.3(10) |

|               |           |               |           |
|---------------|-----------|---------------|-----------|
| C25-C24-H24A  | 109.4     | C23-C24-H24A  | 109.4     |
| C25-C24-H24B  | 109.4     | C23-C24-H24B  | 109.4     |
| H24A-C24-H24B | 108.0     | C24-C25-H25A  | 109.5     |
| C24-C25-H25B  | 109.5     | H25A-C25-H25B | 109.5     |
| C24-C25-H25C  | 109.5     | H25A-C25-H25C | 109.5     |
| H25B-C25-H25C | 109.5     | C27-C26-P1    | 115.0(8)  |
| C27-C26-H26A  | 108.5     | P1-C26-H26A   | 108.5     |
| C27-C26-H26B  | 108.5     | P1-C26-H26B   | 108.5     |
| H26A-C26-H26B | 107.5     | C28-C27-C26   | 111.4(10) |
| C28-C27-H27A  | 109.4     | C26-C27-H27A  | 109.4     |
| C28-C27-H27B  | 109.4     | C26-C27-H27B  | 109.4     |
| H27A-C27-H27B | 108.0     | C29A-C28-C27  | 117.7(17) |
| C29-C28-C27   | 110.7(10) | C29-C28-H28A  | 109.5     |
| C27-C28-H28A  | 109.5     | C29-C28-H28B  | 109.5     |
| C27-C28-H28B  | 109.5     | H28A-C28-H28B | 108.1     |
| C29A-C28-H28C | 107.9     | C27-C28-H28C  | 107.9     |
| C29A-C28-H28D | 107.9     | C27-C28-H28D  | 107.9     |
| H28C-C28-H28D | 107.2     | C28-C29-H29A  | 109.5     |
| C28-C29-H29B  | 109.5     | H29A-C29-H29B | 109.5     |
| C28-C29-H29C  | 109.5     | H29A-C29-H29C | 109.5     |
| H29B-C29-H29C | 109.5     | N6-B1-N2      | 110.4(9)  |
| N6-B1-N4      | 105.6(8)  | N2-B1-N4      | 108.8(9)  |
| N6-B1-H1A     | 110.6     | N2-B1-H1A     | 110.6     |
| N4-B1-H1A     | 110.6     | N7-W1A-N3     | 109.9(18) |
| N7-W1A-N5     | 90.6(8)   | N3-W1A-N5     | 78.1(6)   |

|                |           |                |           |
|----------------|-----------|----------------|-----------|
| N7-W1A-P1      | 104.4(13) | N3-W1A-P1      | 93.3(14)  |
| N5-W1A-P1      | 164.6(7)  | N7-W1A-N1      | 158.(2)   |
| N3-W1A-N1      | 85.1(6)   | N5-W1A-N1      | 76.5(10)  |
| P1-W1A-N1      | 90.2(5)   | N7-W1A-C10     | 88.6(11)  |
| N3-W1A-C10     | 161.6(10) | N5-W1A-C10     | 103.3(17) |
| P1-W1A-C10     | 80.8(5)   | N1-W1A-C10     | 77.6(11)  |
| N7-W1A-C11     | 87.1(14)  | N3-W1A-C11     | 144.7(14) |
| N5-W1A-C11     | 70.8(12)  | P1-W1A-C11     | 112.7(9)  |
| N1-W1A-C11     | 72.0(12)  | C10-W1A-C11    | 32.6(6)   |
| C28-C29A-H29D  | 109.5     | C28-C29A-H29E  | 109.5     |
| H29D-C29A-H29E | 109.5     | C28-C29A-H29F  | 109.5     |
| H29D-C29A-H29F | 109.5     | H29E-C29A-H29F | 109.5     |

**Table 6. Torsion angles (°) for Harman\_16JAS\_15.**

|              |            |              |           |
|--------------|------------|--------------|-----------|
| C1-N1-N2-C3  | 0.6(10)    | W1-N1-N2-C3  | -177.9(6) |
| W1A-N1-N2-C3 | 173.2(11)  | C1-N1-N2-B1  | 179.9(9)  |
| W1-N1-N2-B1  | 1.4(11)    | W1A-N1-N2-B1 | -7.4(14)  |
| C4-N3-N4-C6  | 0.1(11)    | W1A-N3-N4-C6 | -176.2(9) |
| W1-N3-N4-C6  | -177.5(6)  | C4-N3-N4-B1  | -168.0(9) |
| W1A-N3-N4-B1 | 15.7(13)   | W1-N3-N4-B1  | 14.4(11)  |
| C7-N5-N6-C9  | 1.1(11)    | W1-N5-N6-C9  | -170.9(7) |
| W1A-N5-N6-C9 | -159.9(12) | C7-N5-N6-B1  | 169.6(9)  |
| W1-N5-N6-B1  | -2.4(11)   | W1A-N5-N6-B1 | 8.5(15)   |
| N2-N1-C1-C2  | 0.6(11)    | W1-N1-C1-C2  | 178.8(7)  |
| W1A-N1-C1-C2 | -169.7(15) | N1-C1-C2-C3  | -1.5(12)  |

|                 |            |                 |            |
|-----------------|------------|-----------------|------------|
| C1-C2-C3-N2     | 1.8(12)    | N1-N2-C3-C2     | -1.6(11)   |
| B1-N2-C3-C2     | 179.2(10)  | N4-N3-C4-C5     | -0.2(12)   |
| W1A-N3-C4-C5    | 176.3(9)   | W1-N3-C4-C5     | 177.0(7)   |
| N3-C4-C5-C6     | 0.2(13)    | N3-N4-C6-C5     | 0.0(12)    |
| B1-N4-C6-C5     | 166.5(10)  | C4-C5-C6-N4     | -0.1(13)   |
| N6-N5-C7-C8     | -0.5(12)   | W1-N5-C7-C8     | 170.5(8)   |
| W1A-N5-C7-C8    | 157.6(15)  | N5-C7-C8-C9     | -0.3(13)   |
| N5-N6-C9-C8     | -1.4(12)   | B1-N6-C9-C8     | -168.5(10) |
| C7-C8-C9-N6     | 1.0(13)    | C15-C10-C11-C12 | -2.5(15)   |
| W1-C10-C11-C12  | -114.4(10) | W1A-C10-C11-C12 | -111.2(10) |
| C15-C10-C11-W1  | 111.9(9)   | C15-C10-C11-W1A | 108.7(10)  |
| C10-C11-C12-C13 | 6.4(16)    | W1-C11-C12-C13  | -78.4(12)  |
| W1A-C11-C12-C13 | -75.9(13)  | C11-C12-C13-C17 | 178.7(10)  |
| C11-C12-C13-C14 | -4.6(16)   | C12-C13-C14-C15 | -1.1(16)   |
| C17-C13-C14-C15 | 175.3(11)  | C12-C13-C14-C16 | -178.4(11) |
| C17-C13-C14-C16 | -2.0(18)   | C13-C14-C15-C10 | 5.0(16)    |
| C16-C14-C15-C10 | -177.6(11) | C11-C10-C15-C14 | -3.0(15)   |
| W1-C10-C15-C14  | 77.6(12)   | W1A-C10-C15-C14 | 82.7(13)   |
| C15-C14-C16-F3  | 123.2(12)  | C13-C14-C16-F3  | -59.3(16)  |
| C15-C14-C16-F1  | 4.1(17)    | C13-C14-C16-F1  | -178.5(11) |
| C15-C14-C16-F2  | -119.6(12) | C13-C14-C16-F2  | 57.9(16)   |
| C12-C13-C17-F6  | -3.1(17)   | C14-C13-C17-F6  | -179.5(11) |
| C12-C13-C17-F5  | -127.3(13) | C14-C13-C17-F5  | 56.3(16)   |
| C12-C13-C17-F4  | 113.6(14)  | C14-C13-C17-F4  | -62.8(18)  |
| C26-P1-C18-C19  | -177.4(8)  | C22-P1-C18-C19  | 75.8(8)    |

|                 |           |                  |            |
|-----------------|-----------|------------------|------------|
| W1A-P1-C18-C19  | -61.8(12) | W1-P1-C18-C19    | -53.7(8)   |
| P1-C18-C19-C20  | -179.3(8) | C18-C19-C20-C21  | -172.5(9)  |
| C26-P1-C22-C23  | -45.3(9)  | C18-P1-C22-C23   | 57.0(9)    |
| W1A-P1-C22-C23  | -174.3(8) | W1-P1-C22-C23    | -175.4(7)  |
| P1-C22-C23-C24  | 176.6(8)  | C22-C23-C24-C25  | -179.6(9)  |
| C18-P1-C26-C27  | -167.6(8) | C22-P1-C26-C27   | -62.9(9)   |
| W1A-P1-C26-C27  | 75.5(11)  | W1-P1-C26-C27    | 68.8(9)    |
| P1-C26-C27-C28  | 173.0(8)  | C26-C27-C28-C29A | -167.8(17) |
| C26-C27-C28-C29 | -78.9(13) | C9-N6-B1-N2      | -136.0(10) |
| N5-N6-B1-N2     | 58.1(11)  | C9-N6-B1-N4      | 106.6(11)  |
| N5-N6-B1-N4     | -59.3(11) | C3-N2-B1-N6      | 122.0(10)  |
| N1-N2-B1-N6     | -57.2(11) | C3-N2-B1-N4      | -122.5(10) |
| N1-N2-B1-N4     | 58.3(11)  | C6-N4-B1-N6      | -114.3(11) |
| N3-N4-B1-N6     | 51.1(11)  | C6-N4-B1-N2      | 127.2(10)  |
| N3-N4-B1-N2     | -67.4(11) |                  |            |

**Table 7. Anisotropic atomic displacement parameters ( $\text{\AA}^2$ ) for Harman\_16JAS\_15.**

The anisotropic atomic displacement factor exponent takes the form: -  
 $2\pi^2 [ h^2 a^{*2} U_{11} + \dots + 2 h k a^* b^* U_{12} ]$

|    | $U_{11}$   | $U_{22}$   | $U_{33}$   | $U_{23}$   | $U_{13}$   | $U_{12}$   |
|----|------------|------------|------------|------------|------------|------------|
| W1 | 0.0291(8)  | 0.0219(7)  | 0.0230(10) | -0.0048(6) | 0.0062(6)  | -0.0045(4) |
| P1 | 0.0439(17) | 0.0273(16) | 0.0388(17) | 0.0068(14) | 0.0085(13) | 0.0026(12) |
| F1 | 0.089(6)   | 0.040(5)   | 0.168(10)  | -0.009(5)  | -0.015(6)  | -0.023(4)  |
| F2 | 0.192(9)   | 0.113(8)   | 0.045(5)   | -0.021(5)  | -0.002(5)  | -0.117(7)  |

|     | <b>U<sub>11</sub></b> | <b>U<sub>22</sub></b> | <b>U<sub>33</sub></b> | <b>U<sub>23</sub></b> | <b>U<sub>13</sub></b> | <b>U<sub>12</sub></b> |
|-----|-----------------------|-----------------------|-----------------------|-----------------------|-----------------------|-----------------------|
| F3  | 0.130(7)              | 0.081(6)              | 0.078(6)              | -0.031(5)             | 0.059(5)              | -0.063(5)             |
| F4  | 0.044(5)              | 0.165(10)             | 0.210(11)             | -0.148(10)            | 0.017(6)              | -0.013(5)             |
| F5  | 0.060(5)              | 0.177(10)             | 0.104(7)              | -0.058(7)             | 0.042(5)              | -0.014(6)             |
| F6  | 0.059(5)              | 0.074(7)              | 0.176(10)             | -0.023(6)             | -0.016(6)             | 0.004(5)              |
| O1  | 0.050(5)              | 0.043(5)              | 0.070(6)              | -0.020(4)             | 0.025(4)              | -0.017(4)             |
| N1  | 0.034(5)              | 0.045(6)              | 0.031(5)              | -0.020(5)             | -0.004(4)             | 0.004(4)              |
| N2  | 0.033(5)              | 0.035(5)              | 0.037(5)              | -0.012(4)             | 0.001(4)              | -0.006(4)             |
| N3  | 0.044(5)              | 0.020(5)              | 0.029(5)              | -0.004(4)             | 0.008(4)              | -0.012(4)             |
| N4  | 0.043(5)              | 0.029(5)              | 0.030(5)              | -0.012(4)             | 0.008(4)              | -0.010(4)             |
| N5  | 0.038(5)              | 0.021(5)              | 0.040(5)              | -0.003(4)             | 0.014(4)              | -0.005(4)             |
| N6  | 0.033(5)              | 0.026(5)              | 0.031(5)              | -0.003(4)             | 0.002(4)              | 0.002(4)              |
| N7  | 0.042(5)              | 0.032(5)              | 0.042(5)              | -0.021(4)             | 0.010(4)              | -0.001(4)             |
| C1  | 0.035(6)              | 0.047(8)              | 0.045(7)              | -0.013(6)             | -0.001(5)             | -0.002(5)             |
| C2  | 0.044(7)              | 0.048(8)              | 0.037(7)              | -0.014(6)             | 0.008(5)              | -0.008(6)             |
| C3  | 0.032(6)              | 0.046(7)              | 0.030(6)              | -0.003(6)             | 0.011(5)              | -0.018(5)             |
| C4  | 0.074(8)              | 0.017(6)              | 0.035(7)              | 0.000(5)              | 0.014(6)              | -0.004(5)             |
| C5  | 0.073(8)              | 0.049(8)              | 0.034(7)              | -0.019(6)             | -0.004(6)             | -0.014(6)             |
| C6  | 0.047(7)              | 0.048(8)              | 0.039(7)              | -0.020(6)             | -0.002(6)             | -0.006(5)             |
| C7  | 0.031(6)              | 0.048(8)              | 0.050(8)              | -0.014(6)             | -0.002(5)             | 0.001(5)              |
| C8  | 0.056(8)              | 0.034(7)              | 0.060(8)              | -0.007(6)             | 0.002(6)              | 0.004(6)              |
| C9  | 0.052(7)              | 0.024(6)              | 0.048(7)              | -0.002(5)             | 0.001(6)              | -0.008(5)             |
| C10 | 0.032(6)              | 0.046(7)              | 0.044(7)              | -0.015(6)             | 0.004(5)              | -0.011(5)             |
| C11 | 0.033(6)              | 0.044(7)              | 0.035(6)              | -0.006(5)             | 0.005(5)              | -0.014(5)             |
| C12 | 0.054(7)              | 0.045(7)              | 0.043(7)              | -0.018(6)             | 0.008(6)              | -0.005(6)             |

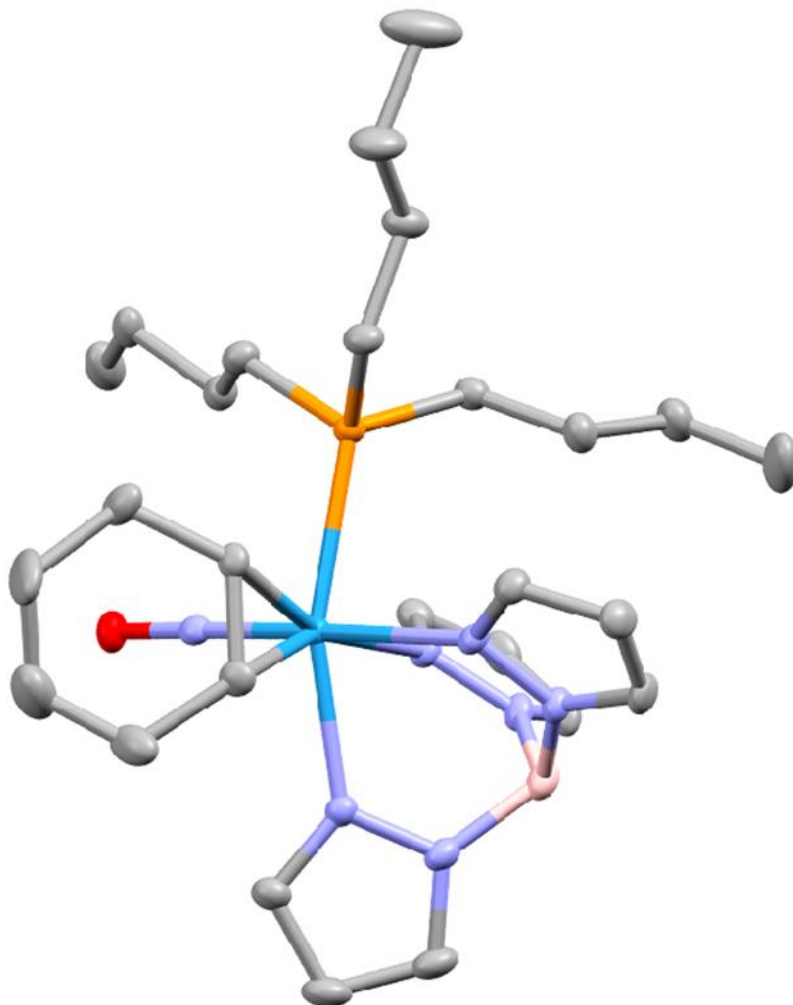
|      | <b>U<sub>11</sub></b> | <b>U<sub>22</sub></b> | <b>U<sub>33</sub></b> | <b>U<sub>23</sub></b> | <b>U<sub>13</sub></b> | <b>U<sub>12</sub></b> |
|------|-----------------------|-----------------------|-----------------------|-----------------------|-----------------------|-----------------------|
| C13  | 0.035(6)              | 0.058(8)              | 0.064(8)              | -0.045(7)             | 0.010(6)              | -0.015(6)             |
| C14  | 0.048(7)              | 0.038(7)              | 0.040(7)              | -0.013(6)             | 0.011(5)              | -0.011(5)             |
| C15  | 0.045(7)              | 0.035(7)              | 0.042(7)              | -0.010(6)             | 0.000(5)              | -0.003(5)             |
| C16  | 0.057(8)              | 0.042(8)              | 0.062(9)              | -0.013(7)             | 0.005(7)              | -0.012(7)             |
| C17  | 0.070(10)             | 0.065(10)             | 0.075(10)             | -0.050(9)             | 0.010(8)              | -0.006(8)             |
| C18  | 0.044(6)              | 0.026(6)              | 0.040(7)              | -0.004(5)             | -0.001(5)             | 0.003(5)              |
| C19  | 0.038(6)              | 0.038(7)              | 0.039(7)              | -0.010(5)             | 0.005(5)              | 0.010(5)              |
| C20  | 0.037(6)              | 0.051(8)              | 0.042(7)              | -0.015(6)             | -0.006(5)             | -0.010(5)             |
| C21  | 0.045(7)              | 0.070(9)              | 0.056(8)              | -0.026(7)             | -0.006(6)             | -0.017(6)             |
| C22  | 0.046(7)              | 0.026(6)              | 0.042(7)              | -0.001(5)             | 0.004(5)              | -0.008(5)             |
| C23  | 0.049(7)              | 0.037(7)              | 0.072(9)              | -0.017(7)             | 0.001(6)              | 0.006(6)              |
| C24  | 0.055(8)              | 0.033(7)              | 0.060(8)              | -0.011(6)             | -0.001(6)             | 0.005(6)              |
| C25  | 0.057(8)              | 0.026(7)              | 0.105(11)             | -0.027(7)             | 0.005(7)              | 0.001(6)              |
| C26  | 0.056(7)              | 0.024(6)              | 0.041(7)              | -0.006(5)             | 0.008(5)              | -0.009(5)             |
| C27  | 0.072(8)              | 0.028(6)              | 0.058(8)              | -0.020(6)             | 0.014(6)              | -0.002(6)             |
| C28  | 0.071(7)              | 0.019(5)              | 0.052(6)              | -0.004(4)             | 0.014(5)              | -0.004(4)             |
| C29  | 0.071(7)              | 0.019(5)              | 0.052(6)              | -0.004(4)             | 0.014(5)              | -0.004(4)             |
| B1   | 0.045(7)              | 0.017(6)              | 0.037(7)              | 0.002(6)              | 0.012(6)              | -0.015(5)             |
| W1A  | 0.067(4)              | 0.050(4)              | 0.074(11)             | -0.034(6)             | 0.031(5)              | -0.021(3)             |
| C29A | 0.071(7)              | 0.019(5)              | 0.052(6)              | -0.004(4)             | 0.014(5)              | -0.004(4)             |

**Table 8. Hydrogen atomic coordinates and isotropic atomic displacement parameters ( $\text{\AA}^2$ ) for Harman\_16JAS\_15.**

|      | <b>x/a</b> | <b>y/b</b> | <b>z/c</b> | <b>U(eq)</b> |
|------|------------|------------|------------|--------------|
| H1   | 0.8239     | 0.6713     | 0.0311     | 0.053        |
| H2   | 0.9499     | 0.8545     | -0.0584    | 0.053        |
| H3   | 0.8886     | 1.0122     | 0.0098     | 0.047        |
| H4   | 0.6656     | 0.6269     | 0.4816     | 0.054        |
| H5   | 0.7621     | 0.7823     | 0.5323     | 0.061        |
| H6   | 0.8030     | 0.9608     | 0.3609     | 0.052        |
| H7   | 0.3457     | 0.8103     | 0.1750     | 0.054        |
| H8   | 0.3186     | 1.0360     | 0.1379     | 0.064        |
| H9   | 0.5189     | 1.1200     | 0.1274     | 0.054        |
| H10  | 0.6803     | 0.5458     | 0.1261     | 0.05         |
| H11  | 0.5692     | 0.7389     | 0.0476     | 0.048        |
| H12  | 0.3652     | 0.7354     | 0.0278     | 0.057        |
| H15  | 0.5689     | 0.3569     | 0.1938     | 0.051        |
| H18A | 0.8632     | 0.5635     | 0.4313     | 0.047        |
| H18B | 0.9455     | 0.4670     | 0.4053     | 0.047        |
| H19A | 0.9810     | 0.6220     | 0.2335     | 0.048        |
| H19B | 0.8998     | 0.7185     | 0.2606     | 0.048        |
| H20A | 1.0366     | 0.7020     | 0.3997     | 0.053        |
| H20B | 1.1207     | 0.6197     | 0.3579     | 0.053        |
| H21A | 1.1311     | 0.7898     | 0.1917     | 0.084        |
| H21B | 1.1803     | 0.8255     | 0.2846     | 0.084        |
| H21C | 1.0523     | 0.8718     | 0.2376     | 0.084        |
| H22A | 0.7722     | 0.3667     | 0.2196     | 0.05         |
| H22B | 0.8787     | 0.4589     | 0.1910     | 0.05         |



|      | <b>x/a</b> | <b>y/b</b> | <b>z/c</b> | <b>U(eq)</b> |
|------|------------|------------|------------|--------------|
| H23A | 0.9835     | 0.3230     | 0.3394     | 0.065        |
| H23B | 0.8753     | 0.2320     | 0.3742     | 0.065        |
| H24A | 0.8975     | 0.1907     | 0.2187     | 0.062        |
| H24B | 1.0063     | 0.2811     | 0.1846     | 0.062        |
| H25A | 1.0713     | 0.0718     | 0.2652     | 0.093        |
| H25B | 1.0027     | 0.0580     | 0.3707     | 0.093        |
| H25C | 1.1119     | 0.1474     | 0.3336     | 0.093        |
| H26A | 0.7810     | 0.3159     | 0.4823     | 0.051        |
| H26B | 0.6795     | 0.4083     | 0.4890     | 0.051        |
| H27A | 0.5474     | 0.3283     | 0.4016     | 0.062        |
| H27B | 0.6490     | 0.2453     | 0.3795     | 0.062        |
| H28A | 0.5889     | 0.2062     | 0.5917     | 0.06         |
| H28B | 0.5181     | 0.1382     | 0.5303     | 0.06         |
| H28C | 0.6696     | 0.1398     | 0.5707     | 0.06         |
| H28D | 0.5515     | 0.2093     | 0.5800     | 0.06         |
| H29A | 0.6926     | 0.0431     | 0.5063     | 0.075        |
| H29B | 0.6686     | 0.0073     | 0.6293     | 0.075        |
| H29C | 0.7624     | 0.1099     | 0.5690     | 0.075        |
| H1A  | 0.7375     | 1.0279     | 0.1566     | 0.044        |
| H29D | 0.5287     | 0.0715     | 0.4605     | 0.075        |
| H29E | 0.4462     | 0.0783     | 0.5523     | 0.075        |
| H29F | 0.5615     | -0.0083    | 0.5816     | 0.075        |



### Crystal Structure Report for **Complex 10** in Chapter 9

A **colorless block-like** specimen of  $C_{27}H_{47}BN_7OPW$ , approximate dimensions **0.108 mm** x **0.120 mm** x **0.266 mm**, was coated with Paratone oil and mounted on a MiTeGen MicroLoop. The X-ray intensity data were measured on a Bruker Kappa APEXII Duo system equipped with a fine-focus sealed tube (Mo  $K_{\alpha}$ ,  $\lambda = 0.71073 \text{ \AA}$ ) and a graphite monochromator.

The total exposure time was 1.42 hours. The frames were integrated with the Bruker SAINT software package<sup>49</sup> using a narrow-frame algorithm. The integration of the data using a **monoclinic** unit cell yielded a total of **36706** reflections to a maximum  $\theta$  angle of **29.62°** (**0.72 \AA** resolution), of which **8741** were independent (average redundancy **4.199**, completeness = **100.0%**,  $R_{int} = 4.21\%$ ,  $R_{sig} = 4.04\%$ ) and **7026** (**80.38%**) were greater than  $2\sigma(F^2)$ . The final cell constants of  $\underline{a} = 11.9475(5) \text{ \AA}$ ,  $\underline{b} = 15.6261(6) \text{ \AA}$ ,  $\underline{c} = 16.6514(8) \text{ \AA}$ ,  $\beta = 94.1280(10)^\circ$ , volume = **3100.6(2) \AA^3**, are based upon the refinement of the XYZ-centroids of **9958** reflections above  $20 \sigma(I)$  with  $4.825^\circ < 2\theta < 57.78^\circ$ . Data were corrected for absorption effects using the Multi-Scan method (SADABS).<sup>1</sup> The ratio of minimum to maximum apparent

<sup>49</sup> Bruker (2012). *Saint*; *SADABS*; *APEX3*. Bruker AXS Inc., Madison, Wisconsin, USA.

transmission was 0.825. The calculated minimum and maximum transmission coefficients (based on crystal size) are 0.4310 and 0.6840.

The structure was solved and refined using the Bruker SHELXTL Software Package<sup>50</sup> within APEX3<sup>1</sup> and OLEX2,<sup>51</sup> using the space group  $P 2_1/n$ , with  $Z = 4$  for the formula unit,  $C_{27}H_{47}BN_7OPW$ . Non-hydrogen atoms were refined anisotropically. Hydrogen atoms were placed in geometrically calculated positions with  $U_{iso} = 1.2U_{equiv}$  of the parent atom ( $U_{iso} = 1.5U_{equiv}$  for methyl), except for the B-H hydrogen atom which was found in the diffraction map and refined isotropically. The final anisotropic full-matrix least-squares refinement on  $F^2$  with 350 variables converged at  $R1 = 2.66\%$ , for the observed data and  $wR2 = 5.38\%$  for all data. The goodness-of-fit was 1.018. The largest peak in the final difference electron density synthesis was  $1.742 e^-/\text{\AA}^3$  and the largest hole was  $-1.069 e^-/\text{\AA}^3$  with an RMS deviation of  $0.117 e^-/\text{\AA}^3$ . On the basis of the final model, the calculated density was  $1.524 \text{ g/cm}^3$  and  $F(000)$ , 1440  $e^-$ .

**Table 1. Sample and crystal data for Harman\_12JAS151.**

|                             |                              |                             |
|-----------------------------|------------------------------|-----------------------------|
| <b>Identification code</b>  | Harman_12JAS151              |                             |
| <b>Chemical formula</b>     | $C_{27}H_{47}BN_7OPW$        |                             |
| <b>Formula weight</b>       | 711.34 g/mol                 |                             |
| <b>Temperature</b>          | 100(2) K                     |                             |
| <b>Wavelength</b>           | 0.71073 Å                    |                             |
| <b>Crystal size</b>         | 0.108 x 0.120 x 0.266 mm     |                             |
| <b>Crystal habit</b>        | colorless block              |                             |
| <b>Crystal system</b>       | monoclinic                   |                             |
| <b>Space group</b>          | $P 2_1/n$                    |                             |
| <b>Unit cell dimensions</b> | $a = 11.9475(5) \text{ \AA}$ | $\alpha = 90^\circ$         |
|                             | $b = 15.6261(6) \text{ \AA}$ | $\beta = 94.1280(10)^\circ$ |
|                             | $c = 16.6514(8) \text{ \AA}$ | $\gamma = 90^\circ$         |
| <b>Volume</b>               | $3100.6(2) \text{ \AA}^3$    |                             |
| <b>Z</b>                    | 4                            |                             |
| <b>Density (calculated)</b> | $1.524 \text{ g/cm}^3$       |                             |

<sup>50</sup> Sheldrick, G. M. (2015). *Acta Cryst.* **A71**, 3-8.

<sup>51</sup> Dolomanov, O. V.; Bourhis, L. J.; Gildea, R. J.; Howard, J. A. K.; Puschmann, H. *J. Appl. Cryst.* (2009). **42**, 339-341.

|                               |                        |
|-------------------------------|------------------------|
| <b>Absorption coefficient</b> | 3.809 mm <sup>-1</sup> |
| <b>F(000)</b>                 | 1440                   |

**Table 2. Data collection and structure refinement for Harman\_12JAS151.**

|  |  |                              |
|--|--|------------------------------|
| <b>Diffractometer</b>                      | Bruker Kappa APEXII Duo  |                              |
| <b>Radiation source</b>                    | fine-focus sealed tube (Mo K $\alpha$ , $\lambda$ = 0.71073 Å) |                              |
| <b>Theta range for data collection</b>     | 1.79 to 29.62°   |                              |
| <b>Index ranges</b>                        | -16 ≤ h ≤ 16, -20 ≤ k ≤ 21, -23 ≤ l ≤ 23                       |                              |
| <b>Reflections collected</b>               | 36706  |                              |
| <b>Independent reflections</b>             | 8741 [R(int) = 0.0421]   |                              |
| <b>Coverage of independent reflections</b> | 100.0%   |                              |
| <b>Absorption correction</b>               | Multi-Scan   |                              |
| <b>Max. and min. transmission</b>          | 0.6840 and 0.4310  |                              |
| <b>Structure solution technique</b>        | direct methods   |                              |
| <b>Structure solution program</b>          | SHELXT 2014/5 (Sheldrick, 2014)                                |                              |
| <b>Refinement method</b>                   | Full-matrix least-squares on F <sup>2</sup>                    |                              |
| <b>Refinement program</b>                  | SHELXL-2017/1 (Sheldrick, 2017)                                |                              |
| <b>Function minimized</b>                  | $\sum w(F_o^2 - F_c^2)^2$                                      |                              |
| <b>Data / restraints / parameters</b>      | 8741 / 0 / 350   |                              |
| <b>Goodness-of-fit on F<sup>2</sup></b>    | 1.018  |                              |
| <b><math>\Delta/\sigma_{\max}</math></b>   | 0.001  |                              |
| <b>Final R indices</b>                     | 7026 data;<br>I > 2 $\sigma$ (I)                               | R1 = 0.0266, wR2 =<br>0.0498 |

|                                    |   |                              |
|------------------------------------|---|------------------------------|
|                                    | all data  | R1 = 0.0420, wR2 =<br>0.0538 |
| <b>Weighting scheme</b>            | $w=1/[\sigma^2(F_o^2)+(0.0197P)^2+2.2979P]$<br>where $P=(F_o^2+2F_c^2)/3$ |                              |
| <b>Largest diff. peak and hole</b> | 1.742 and -1.069 eÅ <sup>-3</sup>   |                              |
| <b>R.M.S. deviation from mean</b>  | 0.117 eÅ <sup>-3</sup>  |                              |

**Table 3. Atomic coordinates and equivalent isotropic atomic displacement parameters (Å<sup>2</sup>) for Harman\_12JAS151.**

U(eq) is defined as one third of the trace of the orthogonalized U<sub>ij</sub> tensor.

|    | x/a         | y/b         | z/c         | U(eq)       |
|----|-------------|-------------|-------------|-------------|
| W1 | 0.38821(2)  | 0.35662(2)  | 0.31092(2)  | 0.01262(3)  |
| P1 | 0.19677(6)  | 0.31790(4)  | 0.35684(4)  | 0.01524(14) |
| O1 | 0.32820(17) | 0.54236(12) | 0.28583(12) | 0.0208(4)   |
| N1 | 0.44200(18) | 0.21977(14) | 0.33597(14) | 0.0150(5)   |
| N2 | 0.52982(19) | 0.20288(14) | 0.39114(14) | 0.0178(5)   |
| N3 | 0.43397(19) | 0.37434(14) | 0.44218(14) | 0.0163(5)   |
| N4 | 0.5203(2)   | 0.33051(14) | 0.48206(14) | 0.0186(5)   |
| N5 | 0.57267(19) | 0.37691(13) | 0.31587(14) | 0.0152(5)   |
| N6 | 0.64340(19) | 0.33492(14) | 0.37006(15) | 0.0192(5)   |
| N7 | 0.35171(18) | 0.46574(14) | 0.29582(13) | 0.0151(5)   |
| C1 | 0.4035(2)   | 0.14332(17) | 0.31008(17) | 0.0194(5)   |
| C2 | 0.4657(2)   | 0.07760(18) | 0.34783(19) | 0.0227(6)   |
| C3 | 0.5443(2)   | 0.11809(18) | 0.39823(19) | 0.0219(6)   |
| C4 | 0.3943(2)   | 0.42767(18) | 0.49641(17) | 0.0196(6)   |

|     | <b>x/a</b> | <b>y/b</b>  | <b>z/c</b>  | <b>U(eq)</b> |
|-----|------------|-------------|-------------|--------------|
| C5  | 0.4529(3)  | 0.41828(18) | 0.57080(17) | 0.0228(6)    |
| C6  | 0.5324(3)  | 0.35685(18) | 0.55952(17) | 0.0224(6)    |
| C7  | 0.6354(2)  | 0.43238(19) | 0.27818(18) | 0.0211(6)    |
| C8  | 0.7475(2)  | 0.4271(2)   | 0.3082(2)   | 0.0278(7)    |
| C9  | 0.7485(2)  | 0.36474(19) | 0.3660(2)   | 0.0256(7)    |
| C10 | 0.3000(2)  | 0.31315(18) | 0.19429(16) | 0.0172(6)    |
| C11 | 0.4172(2)  | 0.32719(19) | 0.18430(17) | 0.0193(6)    |
| C12 | 0.4557(3)  | 0.3887(2)   | 0.1214(2)   | 0.0333(8)    |
| C13 | 0.3738(3)  | 0.4538(2)   | 0.0947(3)   | 0.0473(10)   |
| C14 | 0.2590(3)  | 0.4197(2)   | 0.0792(2)   | 0.0443(10)   |
| C15 | 0.2132(3)  | 0.3713(2)   | 0.14948(18) | 0.0263(7)    |
| C16 | 0.1144(2)  | 0.23250(18) | 0.30464(18) | 0.0203(6)    |
| C17 | 0.0102(2)  | 0.2010(2)   | 0.3452(2)   | 0.0255(7)    |
| C18 | 0.9270(3)  | 0.1563(2)   | 0.2875(2)   | 0.0350(8)    |
| C19 | 0.8252(3)  | 0.1229(2)   | 0.3283(3)   | 0.0545(13)   |
| C20 | 0.0938(2)  | 0.40546(18) | 0.34831(18) | 0.0199(6)    |
| C21 | 0.1194(2)  | 0.48438(17) | 0.40065(18) | 0.0197(6)    |
| C22 | 0.0281(2)  | 0.55228(17) | 0.38862(18) | 0.0214(6)    |
| C23 | 0.0568(3)  | 0.63236(19) | 0.4375(2)   | 0.0306(7)    |
| C24 | 0.1930(2)  | 0.28554(18) | 0.46289(17) | 0.0194(6)    |
| C25 | 0.2631(3)  | 0.20627(18) | 0.48664(18) | 0.0227(6)    |
| C26 | 0.2750(3)  | 0.1918(2)   | 0.57750(19) | 0.0293(7)    |
| C27 | 0.3483(3)  | 0.1145(3)   | 0.6000(2)   | 0.0473(10)   |
| B1  | 0.5979(3)  | 0.2752(2)   | 0.4335(2)   | 0.0210(7)    |

**Table 4. Bond lengths (Å) for Harman\_12JAS151.**

|          |           |          |          |
|----------|-----------|----------|----------|
| W1-N7    | 1.773(2)  | W1-C11   | 2.210(3) |
| W1-N5    | 2.222(2)  | W1-N3    | 2.232(2) |
| W1-C10   | 2.247(3)  | W1-N1    | 2.263(2) |
| W1-P1    | 2.5366(7) | P1-C20   | 1.839(3) |
| P1-C16   | 1.839(3)  | P1-C24   | 1.841(3) |
| O1-N7    | 1.238(3)  | N1-C1    | 1.340(3) |
| N1-N2    | 1.370(3)  | N2-C3    | 1.340(4) |
| N2-B1    | 1.535(4)  | N3-C4    | 1.340(3) |
| N3-N4    | 1.369(3)  | N4-C6    | 1.352(3) |
| N4-B1    | 1.539(4)  | N5-C7    | 1.332(3) |
| N5-N6    | 1.360(3)  | N6-C9    | 1.346(4) |
| N6-B1    | 1.537(4)  | C1-C2    | 1.391(4) |
| C1-H1    | 0.95      | C2-C3    | 1.368(4) |
| C2-H2    | 0.95      | C3-H3    | 0.95     |
| C4-C5    | 1.386(4)  | C4-H4    | 0.95     |
| C5-C6    | 1.373(4)  | C5-H5    | 0.95     |
| C6-H6    | 0.95      | C7-C8    | 1.398(4) |
| C7-H7    | 0.95      | C8-C9    | 1.368(4) |
| C8-H8    | 0.95      | C9-H9    | 0.95     |
| C10-C11  | 1.439(4)  | C10-C15  | 1.532(4) |
| C10-H10  | 1.0       | C11-C12  | 1.517(4) |
| C11-H11  | 1.0       | C12-C13  | 1.459(5) |
| C12-H12A | 0.99      | C12-H12B | 0.99     |

|          |          |          |          |
|----------|----------|----------|----------|
| C13-C14  | 1.478(5) | C13-H13A | 0.99     |
| C13-H13B | 0.99     | C14-C15  | 1.527(5) |
| C14-H14A | 0.99     | C14-H14B | 0.99     |
| C15-H15A | 0.99     | C15-H15B | 0.99     |
| C16-C17  | 1.539(4) | C16-H16A | 0.99     |
| C16-H16B | 0.99     | C17-C18  | 1.503(4) |
| C17-H17A | 0.99     | C17-H17B | 0.99     |
| C18-C19  | 1.527(5) | C18-H18A | 0.99     |
| C18-H18B | 0.99     | C19-H19A | 0.98     |
| C19-H19B | 0.98     | C19-H19C | 0.98     |
| C20-C21  | 1.528(4) | C20-H20A | 0.99     |
| C20-H20B | 0.99     | C21-C22  | 1.525(4) |
| C21-H21A | 0.99     | C21-H21B | 0.99     |
| C22-C23  | 1.519(4) | C22-H22A | 0.99     |
| C22-H22B | 0.99     | C23-H23A | 0.98     |
| C23-H23B | 0.98     | C23-H23C | 0.98     |
| C24-C25  | 1.531(4) | C24-H24A | 0.99     |
| C24-H24B | 0.99     | C25-C26  | 1.526(4) |
| C25-H25A | 0.99     | C25-H25B | 0.99     |
| C26-C27  | 1.522(5) | C26-H26A | 0.99     |
| C26-H26B | 0.99     | C27-H27A | 0.98     |
| C27-H27B | 0.98     | C27-H27C | 0.98     |
| B1-H1A   | 1.08(3)  |          |          |

**Table 5. Bond angles (°) for Harman\_12JAS151.**



|            |            |            |            |
|------------|------------|------------|------------|
| N7-W1-C11  | 96.81(11)  | N7-W1-N5   | 95.81(9)   |
| C11-W1-N5  | 80.90(9)   | N7-W1-N3   | 93.44(9)   |
| C11-W1-N3  | 156.37(10) | N5-W1-N3   | 76.92(8)   |
| N7-W1-C10  | 94.18(10)  | C11-W1-C10 | 37.66(10)  |
| N5-W1-C10  | 118.51(9)  | N3-W1-C10  | 161.91(9)  |
| N7-W1-N1   | 176.71(9)  | C11-W1-N1  | 85.25(10)  |
| N5-W1-N1   | 81.97(8)   | N3-W1-N1   | 83.71(8)   |
| C10-W1-N1  | 89.02(9)   | N7-W1-P1   | 93.11(7)   |
| C11-W1-P1  | 116.40(8)  | N5-W1-P1   | 159.43(6)  |
| N3-W1-P1   | 84.09(6)   | C10-W1-P1  | 79.13(7)   |
| N1-W1-P1   | 88.24(6)   | C20-P1-C16 | 99.85(13)  |
| C20-P1-C24 | 102.47(13) | C16-P1-C24 | 101.82(13) |
| C20-P1-W1  | 114.33(10) | C16-P1-W1  | 119.62(9)  |
| C24-P1-W1  | 116.08(9)  | C1-N1-N2   | 105.8(2)   |
| C1-N1-W1   | 134.18(18) | N2-N1-W1   | 119.96(16) |
| C3-N2-N1   | 109.7(2)   | C3-N2-B1   | 128.8(2)   |
| N1-N2-B1   | 121.4(2)   | C4-N3-N4   | 106.0(2)   |
| C4-N3-W1   | 131.55(19) | N4-N3-W1   | 122.40(17) |
| C6-N4-N3   | 109.6(2)   | C6-N4-B1   | 130.2(3)   |
| N3-N4-B1   | 119.2(2)   | C7-N5-N6   | 106.4(2)   |
| C7-N5-W1   | 131.70(19) | N6-N5-W1   | 121.54(17) |
| C9-N6-N5   | 109.7(2)   | C9-N6-B1   | 128.4(3)   |
| N5-N6-B1   | 121.0(2)   | O1-N7-W1   | 178.8(2)   |
| N1-C1-C2   | 110.7(3)   | N1-C1-H1   | 124.7      |
| C2-C1-H1   | 124.7      | C3-C2-C1   | 104.9(2)   |

|               |           |              |            |
|---------------|-----------|--------------|------------|
| C3-C2-H2      | 127.6     | C1-C2-H2     | 127.6      |
| N2-C3-C2      | 109.0(3)  | N2-C3-H3     | 125.5      |
| C2-C3-H3      | 125.5     | N3-C4-C5     | 110.8(3)   |
| N3-C4-H4      | 124.6     | C5-C4-H4     | 124.6      |
| C6-C5-C4      | 105.2(2)  | C6-C5-H5     | 127.4      |
| C4-C5-H5      | 127.4     | N4-C6-C5     | 108.4(3)   |
| N4-C6-H6      | 125.8     | C5-C6-H6     | 125.8      |
| N5-C7-C8      | 110.5(3)  | N5-C7-H7     | 124.8      |
| C8-C7-H7      | 124.8     | C9-C8-C7     | 104.7(3)   |
| C9-C8-H8      | 127.6     | C7-C8-H8     | 127.6      |
| N6-C9-C8      | 108.7(3)  | N6-C9-H9     | 125.7      |
| C8-C9-H9      | 125.7     | C11-C10-C15  | 118.9(3)   |
| C11-C10-W1    | 69.76(15) | C15-C10-W1   | 120.03(19) |
| C11-C10-H10   | 113.7     | C15-C10-H10  | 113.7      |
| W1-C10-H10    | 113.7     | C10-C11-C12  | 121.5(3)   |
| C10-C11-W1    | 72.59(15) | C12-C11-W1   | 127.1(2)   |
| C10-C11-H11   | 110.2     | C12-C11-H11  | 110.2      |
| W1-C11-H11    | 110.2     | C13-C12-C11  | 115.0(3)   |
| C13-C12-H12A  | 108.5     | C11-C12-H12A | 108.5      |
| C13-C12-H12B  | 108.5     | C11-C12-H12B | 108.5      |
| H12A-C12-H12B | 107.5     | C12-C13-C14  | 113.3(3)   |
| C12-C13-H13A  | 108.9     | C14-C13-H13A | 108.9      |
| C12-C13-H13B  | 108.9     | C14-C13-H13B | 108.9      |
| H13A-C13-H13B | 107.7     | C13-C14-C15  | 115.1(3)   |
| C13-C14-H14A  | 108.5     | C15-C14-H14A | 108.5      |

|               |       |               |          |
|---------------|-------|---------------|----------|
| C13-C14-H14B  | 108.5 | C15-C14-H14B  | 108.5    |
| H14A-C14-H14B | 107.5 | C14-C15-C10   | 113.5(3) |
| C14-C15-H15A  | 108.9 | C10-C15-H15A  | 108.9    |
| C14-C15-H15B  | 108.9 | C10-C15-H15B  | 108.9    |
| H15A-C15-H15B | 107.7 | C17-C16-P1    | 116.6(2) |
| C17-C16-H16A  | 108.2 | P1-C16-H16A   | 108.2    |
| C17-C16-H16B  | 108.2 | P1-C16-H16B   | 108.2    |
| H16A-C16-H16B | 107.3 | C18-C17-C16   | 112.7(3) |
| C18-C17-H17A  | 109.0 | C16-C17-H17A  | 109.0    |
| C18-C17-H17B  | 109.0 | C16-C17-H17B  | 109.0    |
| H17A-C17-H17B | 107.8 | C17-C18-C19   | 112.7(3) |
| C17-C18-H18A  | 109.1 | C19-C18-H18A  | 109.1    |
| C17-C18-H18B  | 109.1 | C19-C18-H18B  | 109.1    |
| H18A-C18-H18B | 107.8 | C18-C19-H19A  | 109.5    |
| C18-C19-H19B  | 109.5 | H19A-C19-H19B | 109.5    |
| C18-C19-H19C  | 109.5 | H19A-C19-H19C | 109.5    |
| H19B-C19-H19C | 109.5 | C21-C20-P1    | 116.8(2) |
| C21-C20-H20A  | 108.1 | P1-C20-H20A   | 108.1    |
| C21-C20-H20B  | 108.1 | P1-C20-H20B   | 108.1    |
| H20A-C20-H20B | 107.3 | C22-C21-C20   | 112.0(2) |
| C22-C21-H21A  | 109.2 | C20-C21-H21A  | 109.2    |
| C22-C21-H21B  | 109.2 | C20-C21-H21B  | 109.2    |
| H21A-C21-H21B | 107.9 | C23-C22-C21   | 111.8(3) |
| C23-C22-H22A  | 109.3 | C21-C22-H22A  | 109.3    |
| C23-C22-H22B  | 109.3 | C21-C22-H22B  | 109.3    |

|               |           |               |           |
|---------------|-----------|---------------|-----------|
| H22A-C22-H22B | 107.9     | C22-C23-H23A  | 109.5     |
| C22-C23-H23B  | 109.5     | H23A-C23-H23B | 109.5     |
| C22-C23-H23C  | 109.5     | H23A-C23-H23C | 109.5     |
| H23B-C23-H23C | 109.5     | C25-C24-P1    | 114.8(2)  |
| C25-C24-H24A  | 108.6     | P1-C24-H24A   | 108.6     |
| C25-C24-H24B  | 108.6     | P1-C24-H24B   | 108.6     |
| H24A-C24-H24B | 107.5     | C26-C25-C24   | 112.7(2)  |
| C26-C25-H25A  | 109.0     | C24-C25-H25A  | 109.0     |
| C26-C25-H25B  | 109.0     | C24-C25-H25B  | 109.0     |
| H25A-C25-H25B | 107.8     | C27-C26-C25   | 111.8(3)  |
| C27-C26-H26A  | 109.2     | C25-C26-H26A  | 109.2     |
| C27-C26-H26B  | 109.2     | C25-C26-H26B  | 109.2     |
| H26A-C26-H26B | 107.9     | C26-C27-H27A  | 109.5     |
| C26-C27-H27B  | 109.5     | H27A-C27-H27B | 109.5     |
| C26-C27-H27C  | 109.5     | H27A-C27-H27C | 109.5     |
| H27B-C27-H27C | 109.5     | N2-B1-N6      | 109.4(2)  |
| N2-B1-N4      | 109.6(2)  | N6-B1-N4      | 106.1(2)  |
| N2-B1-H1A     | 109.5(16) | N6-B1-H1A     | 111.6(16) |
| N4-B1-H1A     | 110.6(16) |               |           |

**Table 6. Torsion angles (°) for Harman\_12JAS151.**

|             |           |             |            |
|-------------|-----------|-------------|------------|
| C1-N1-N2-C3 | 0.2(3)    | W1-N1-N2-C3 | 177.86(19) |
| C1-N1-N2-B1 | 178.8(2)  | W1-N1-N2-B1 | -3.6(3)    |
| C4-N3-N4-C6 | 0.2(3)    | W1-N3-N4-C6 | 177.03(18) |
| C4-N3-N4-B1 | -169.3(2) | W1-N3-N4-B1 | 7.6(3)     |

|                 |            |                 |             |
|-----------------|------------|-----------------|-------------|
| C7-N5-N6-C9     | 0.4(3)     | W1-N5-N6-C9     | -173.85(18) |
| C7-N5-N6-B1     | 170.7(2)   | W1-N5-N6-B1     | -3.5(3)     |
| N2-N1-C1-C2     | -0.1(3)    | W1-N1-C1-C2     | -177.3(2)   |
| N1-C1-C2-C3     | 0.0(3)     | N1-N2-C3-C2     | -0.2(3)     |
| B1-N2-C3-C2     | -178.6(3)  | C1-C2-C3-N2     | 0.1(3)      |
| N4-N3-C4-C5     | -0.6(3)    | W1-N3-C4-C5     | -177.08(19) |
| N3-C4-C5-C6     | 0.8(3)     | N3-N4-C6-C5     | 0.3(3)      |
| B1-N4-C6-C5     | 168.2(3)   | C4-C5-C6-N4     | -0.7(3)     |
| N6-N5-C7-C8     | -0.4(3)    | W1-N5-C7-C8     | 172.98(19)  |
| N5-C7-C8-C9     | 0.3(3)     | N5-N6-C9-C8     | -0.2(3)     |
| B1-N6-C9-C8     | -169.7(3)  | C7-C8-C9-N6     | -0.1(3)     |
| C15-C10-C11-C12 | -9.4(4)    | W1-C10-C11-C12  | -123.3(3)   |
| C15-C10-C11-W1  | 113.9(2)   | C10-C11-C12-C13 | 22.1(4)     |
| W1-C11-C12-C13  | -69.2(4)   | C11-C12-C13-C14 | -44.0(5)    |
| C12-C13-C14-C15 | 55.0(5)    | C13-C14-C15-C10 | -40.9(4)    |
| C11-C10-C15-C14 | 18.1(4)    | W1-C10-C15-C14  | 100.3(3)    |
| C20-P1-C16-C17  | -65.7(3)   | C24-P1-C16-C17  | 39.4(3)     |
| W1-P1-C16-C17   | 168.84(19) | P1-C16-C17-C18  | 159.5(2)    |
| C16-C17-C18-C19 | 178.5(3)   | C16-P1-C20-C21  | 166.8(2)    |
| C24-P1-C20-C21  | 62.3(2)    | W1-P1-C20-C21   | -64.2(2)    |
| P1-C20-C21-C22  | -179.8(2)  | C20-C21-C22-C23 | -177.1(2)   |
| C20-P1-C24-C25  | 174.2(2)   | C16-P1-C24-C25  | 71.2(2)     |
| W1-P1-C24-C25   | -60.5(2)   | P1-C24-C25-C26  | 169.3(2)    |
| C24-C25-C26-C27 | -178.0(3)  | C3-N2-B1-N6     | 123.2(3)    |
| N1-N2-B1-N6     | -55.1(3)   | C3-N2-B1-N4     | -120.9(3)   |

|             |          |             |           |
|-------------|----------|-------------|-----------|
| N1-N2-B1-N4 | 60.8(3)  | C9-N6-B1-N2 | -131.6(3) |
| N5-N6-B1-N2 | 59.9(3)  | C9-N6-B1-N4 | 110.2(3)  |
| N5-N6-B1-N4 | -58.2(3) | C6-N4-B1-N2 | 130.1(3)  |
| N3-N4-B1-N2 | -63.0(3) | C6-N4-B1-N6 | -111.9(3) |
| N3-N4-B1-N6 | 55.1(3)  |             |           |

**Table 7. Anisotropic atomic displacement parameters ( $\text{\AA}^2$ ) for Harman\_12JAS151.**

The anisotropic atomic displacement factor exponent takes the form: -  
 $2\pi^2 [ h^2 a^{*2} U_{11} + \dots + 2 h k a^* b^* U_{12} ]$

|    | $U_{11}$   | $U_{22}$   | $U_{33}$   | $U_{23}$   | $U_{13}$   | $U_{12}$   |
|----|------------|------------|------------|------------|------------|------------|
| W1 | 0.01320(5) | 0.01290(5) | 0.01158(5) | 0.00148(5) | 0.00043(3) | 0.00038(5) |
| P1 | 0.0142(3)  | 0.0156(3)  | 0.0159(3)  | -0.0020(3) | 0.0010(3)  | 0.0000(3)  |
| O1 | 0.0274(11) | 0.0136(10) | 0.0209(11) | 0.0010(8)  | -0.0009(9) | 0.0031(8)  |
| N1 | 0.0136(11) | 0.0162(11) | 0.0148(11) | -0.0014(9) | -0.0018(9) | 0.0018(9)  |
| N2 | 0.0200(12) | 0.0143(11) | 0.0184(12) | -0.0007(9) | 0.0031(10) | 0.0027(9)  |
| N3 | 0.0171(11) | 0.0174(12) | 0.0142(11) | -0.0019(9) | -0.0011(9) | 0.0006(9)  |
| N4 | 0.0223(12) | 0.0169(11) | 0.0158(12) | 0.0002(9)  | 0.0050(10) | 0.0005(10) |
| N5 | 0.0158(11) | 0.0150(11) | 0.0149(11) | -0.0023(8) | 0.0011(9)  | 0.0012(9)  |
| N6 | 0.0157(11) | 0.0175(12) | 0.0238(13) | -0.0034(9) | 0.0027(10) | 0.0021(9)  |
| N7 | 0.0137(11) | 0.0181(12) | 0.0132(11) | -0.0020(9) | -0.0011(9) | -0.0012(9) |
| C1 | 0.0187(14) | 0.0184(13) | 0.0205(13) | 0.0044(13) | 0.0018(11) | 0.0007(12) |

|     | <b>U<sub>11</sub></b> | <b>U<sub>22</sub></b> | <b>U<sub>33</sub></b> | <b>U<sub>23</sub></b> | <b>U<sub>13</sub></b> | <b>U<sub>12</sub></b> |
|-----|-----------------------|-----------------------|-----------------------|-----------------------|-----------------------|-----------------------|
| C2  | 0.0262(15)            | 0.0131(14)            | 0.0286(16)            | 0.0022(12)            | 0.0012(13)            | 0.0008(12)            |
| C3  | 0.0238(15)            | 0.0164(14)            | 0.0249(16)            | 0.0020(11)            | 0.0030(12)            | 0.0066(11)            |
| C4  | 0.0233(14)            | 0.0167(14)            | 0.0191(14)            | 0.0047(11)            | 0.0025(11)            | 0.0040(12)            |
| C5  | 0.0352(17)            | 0.0196(15)            | 0.0139(14)            | 0.0051(11)            | 0.0031(12)            | 0.0044(13)            |
| C6  | 0.0331(16)            | 0.0192(14)            | 0.0138(12)            | 0.0003(12)            | 0.0068(11)            | 0.0046(13)            |
| C7  | 0.0197(14)            | 0.0225(15)            | 0.0216(15)            | 0.0031(12)            | 0.0054(12)            | 0.0013(12)            |
| C8  | 0.0182(14)            | 0.0313(17)            | 0.0345(18)            | 0.0077(14)            | 0.0062(13)            | 0.0065(13)            |
| C9  | 0.0139(13)            | 0.0282(17)            | 0.0343(17)            | 0.0067(14)            | 0.0013(12)            | 0.0003(12)            |
| C10 | 0.0211(14)            | 0.0180(14)            | 0.0121(13)            | 0.0018(10)            | 0.0017(11)            | 0.0001(11)            |
| C11 | 0.0211(14)            | 0.0239(14)            | 0.0131(13)            | 0.0035(11)            | 0.0026(11)            | 0.0001(12)            |
| C12 | 0.0319(18)            | 0.049(2)              | 0.0185(16)            | 0.0002(14)            | 0.0003(14)            | 0.0129(16)            |
| C13 | 0.053(2)              | 0.046(2)              | 0.045(2)              | 0.0151(19)            | 0.019(2)              | 0.0071(19)            |
| C14 | 0.048(2)              | 0.044(2)              | 0.037(2)              | 0.0180(17)            | 0.0224(18)            | 0.0057(18)            |
| C15 | 0.0235(15)            | 0.0380(19)            | 0.0169(14)            | 0.0023(13)            | 0.0016(12)            | 0.0080(13)            |
| C16 | 0.0168(14)            | 0.0229(15)            | 0.0211(15)            | 0.0055(12)            | 0.0002(11)            | 0.0026(11)            |

|     | <b>U<sub>11</sub></b> | <b>U<sub>22</sub></b> | <b>U<sub>33</sub></b> | <b>U<sub>23</sub></b>   | <b>U<sub>13</sub></b>   | <b>U<sub>12</sub></b>   |
|-----|-----------------------|-----------------------|-----------------------|-------------------------|-------------------------|-------------------------|
| C17 | 0.0191(14)            | 0.0243(16)            | 0.0338(18)            | <sup>-</sup> 0.0061(13) | 0.0061(13)              | <sup>-</sup> 0.0040(12) |
| C18 | 0.0234(16)            | 0.038(2)              | 0.043(2)              | <sup>-</sup> 0.0114(16) | 0.0032(15)              | <sup>-</sup> 0.0103(15) |
| C19 | 0.034(2)              | 0.048(2)              | 0.085(3)              | -0.037(2)               | 0.028(2)                | <sup>-</sup> 0.0192(18) |
| C20 | 0.0160(14)            | 0.0229(15)            | 0.0208(15)            | <sup>-</sup> 0.0021(11) | 0.0014(11)              | 0.0023(11)              |
| C21 | 0.0200(14)            | 0.0195(14)            | 0.0195(14)            | <sup>-</sup> 0.0007(11) | 0.0007(11)              | 0.0015(11)              |
| C22 | 0.0260(15)            | 0.0213(15)            | 0.0174(14)            | 0.0021(11)              | 0.0054(12)              | 0.0063(12)              |
| C23 | 0.0398(19)            | 0.0225(17)            | 0.0309(17)            | 0.0018(13)              | 0.0124(15)              | 0.0073(14)              |
| C24 | 0.0188(14)            | 0.0215(14)            | 0.0181(14)            | <sup>-</sup> 0.0010(11) | 0.0023(11)              | <sup>-</sup> 0.0020(11) |
| C25 | 0.0270(16)            | 0.0208(15)            | 0.0206(15)            | 0.0027(12)              | 0.0033(12)              | 0.0020(12)              |
| C26 | 0.0331(18)            | 0.0300(17)            | 0.0257(17)            | 0.0073(13)              | 0.0080(14)              | 0.0025(14)              |
| C27 | 0.054(2)              | 0.056(2)              | 0.032(2)              | 0.0206(18)              | 0.0095(18)              | 0.018(2)                |
| B1  | 0.0206(16)            | 0.0195(16)            | 0.0219(17)            | <sup>-</sup> 0.0013(13) | <sup>-</sup> 0.0056(13) | 0.0026(13)              |

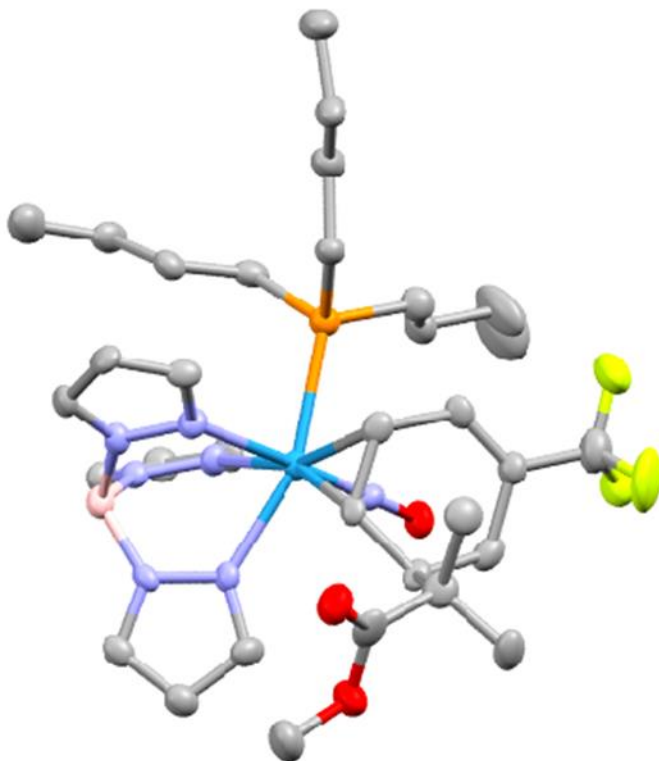
**Table 8. Hydrogen atomic coordinates and isotropic atomic displacement parameters (Å<sup>2</sup>) for Harman\_12JAS151.**

|    | <b>x/a</b> | <b>y/b</b> | <b>z/c</b> | <b>U(eq)</b> |
|----|------------|------------|------------|--------------|
| H1 | 0.3422     | 0.1351     | 0.2713     | 0.023        |
| H2 | 0.4559     | 0.0177     | 0.3403     | 0.027        |
| H3 | 0.6000     | 0.0906     | 0.4327     | 0.026        |
| H4 | 0.3341     | 0.4667     | 0.4853     | 0.024        |



|      | <b>x/a</b> | <b>y/b</b> | <b>z/c</b> | <b>U(eq)</b> |
|------|------------|------------|------------|--------------|
| H5   | 0.4406     | 0.4479     | 0.6192     | 0.027        |
| H6   | 0.5867     | 0.3363     | 0.5994     | 0.027        |
| H7   | 0.6078     | 0.4702     | 0.2367     | 0.025        |
| H8   | 0.8092     | 0.4595     | 0.2921     | 0.033        |
| H9   | 0.8128     | 0.3457     | 0.3979     | 0.031        |
| H10  | 0.2782     | 0.2514     | 0.1940     | 0.021        |
| H11  | 0.4571     | 0.2712     | 0.1809     | 0.023        |
| H12A | 0.5248     | 0.4177     | 0.1437     | 0.04         |
| H12B | 0.4754     | 0.3553     | 0.0740     | 0.04         |
| H13A | 0.3975     | 0.4806     | 0.0448     | 0.057        |
| H13B | 0.3730     | 0.4990     | 0.1364     | 0.057        |
| H14A | 0.2581     | 0.3807     | 0.0323     | 0.053        |
| H14B | 0.2078     | 0.4679     | 0.0645     | 0.053        |
| H15A | 0.1485     | 0.3361     | 0.1289     | 0.032        |
| H15B | 0.1855     | 0.4133     | 0.1880     | 0.032        |
| H16A | 0.0898     | 0.2531     | 0.2500     | 0.024        |
| H16B | 0.1645     | 0.1829     | 0.2982     | 0.024        |
| H17A | 0.0342     | 0.1612     | 0.3894     | 0.031        |
| H17B | -0.0269    | 0.2505     | 0.3691     | 0.031        |
| H18A | -0.0353    | 0.1077     | 0.2624     | 0.042        |
| H18B | -0.0987    | 0.1966     | 0.2441     | 0.042        |
| H19A | -0.2281    | 0.0972     | 0.2878     | 0.082        |
| H19B | -0.2110    | 0.1705     | 0.3547     | 0.082        |
| H19C | -0.1505    | 0.0798     | 0.3685     | 0.082        |

|      | <b>x/a</b> | <b>y/b</b> | <b>z/c</b> | <b>U(eq)</b> |
|------|------------|------------|------------|--------------|
| H20A | 0.0858     | 0.4241     | 0.2914     | 0.024        |
| H20B | 0.0203     | 0.3823     | 0.3617     | 0.024        |
| H21A | 0.1266     | 0.4670     | 0.4580     | 0.024        |
| H21B | 0.1920     | 0.5091     | 0.3872     | 0.024        |
| H22A | 0.0181     | 0.5675     | 0.3308     | 0.026        |
| H22B | -0.0438    | 0.5286     | 0.4048     | 0.026        |
| H23A | 0.1301     | 0.6541     | 0.4239     | 0.046        |
| H23B | 0.0596     | 0.6186     | 0.4950     | 0.046        |
| H23C | -0.0006    | 0.6761     | 0.4251     | 0.046        |
| H24A | 0.2200     | 0.3339     | 0.4975     | 0.023        |
| H24B | 0.1140     | 0.2743     | 0.4741     | 0.023        |
| H25A | 0.2275     | 0.1553     | 0.4603     | 0.027        |
| H25B | 0.3387     | 0.2127     | 0.4666     | 0.027        |
| H26A | 0.3083     | 0.2433     | 0.6042     | 0.035        |
| H26B | 0.1997     | 0.1831     | 0.5974     | 0.035        |
| H27A | 0.4204     | 0.1204     | 0.5759     | 0.071        |
| H27B | 0.3106     | 0.0623     | 0.5797     | 0.071        |
| H27C | 0.3611     | 0.1112     | 0.6587     | 0.071        |
| H1A  | 0.665(2)   | 0.2482(18) | 0.4725(19) | 0.021(8)     |



### Crystal Structure Report for **Complex 13 in Chapter 9**

A **yellow plate-like** specimen of  $C_{69}H_{110}B_2F_6N_{14}O_7P_2W_2$ , approximate dimensions **0.041 mm x 0.066 mm x 0.103 mm**, was coated with Paratone oil and mounted on a MiTeGen MicroLoop. The X-ray intensity data were measured on a Bruker Kappa APEXII Duo system equipped with a fine-focus sealed tube (Mo  $K_{\alpha}$ ,  $\lambda = 0.71073 \text{ \AA}$ ) and a graphite monochromator.

The total exposure time was 12.38 hours. The frames were integrated with the Bruker SAINT software package<sup>52</sup> using a narrow-frame algorithm. The integration of the data using a **triclinic** unit cell yielded a total of **60372** reflections to a maximum  $\theta$  angle of **25.73°** (**0.82 Å** resolution), of which **15595** were independent (average redundancy **3.871**, completeness = **99.6%**,  $R_{\text{int}} = 10.12\%$ ,  $R_{\text{sig}} = 11.81\%$ ) and **9468** (**60.71%**) were greater than  $2\sigma(F^2)$ . The final cell constants of  $\underline{a} = 13.1384(15) \text{ \AA}$ ,  $\underline{b} = 14.6742(17) \text{ \AA}$ ,  $\underline{c} = 21.777(3) \text{ \AA}$ ,  $\alpha = 97.443(4)^\circ$ ,  $\beta = 93.751(4)^\circ$ ,  $\gamma = 97.774(4)^\circ$ , volume = **4110.1(8) Å<sup>3</sup>**, are based upon the refinement of the XYZ-centroids of **9207** reflections above  $20 \sigma(I)$  with  $4.400^\circ < 2\theta < 44.25^\circ$ . Data were corrected for absorption effects using the Multi-Scan method (SADABS).<sup>1</sup> The ratio of minimum to maximum apparent transmission was **0.877**. The calculated minimum and maximum transmission coefficients (based on crystal size) are **0.7540** and **0.8900**.

<sup>52</sup> Bruker (2012). *Saint*; *SADABS*; *APEX3*. Bruker AXS Inc., Madison, Wisconsin, USA.

The structure was solved and refined using the Bruker SHELXTL Software Package<sup>53</sup> within APEX3<sup>1</sup> and OLEX2,<sup>54</sup> using the space group **P -1**, with **Z = 2** for the formula unit, **C<sub>69</sub>H<sub>110</sub>B<sub>2</sub>F<sub>6</sub>N<sub>14</sub>O<sub>7</sub>P<sub>2</sub>W<sub>2</sub>**. Non-hydrogen atoms were refined anisotropically. The B-H, C10 and C43 hydrogen atoms were located in the diffraction map and refined isotropically with  $U_{iso} = 1.2U_{equiv}$  of the parent atom. All other hydrogen atoms were placed in geometrically calculated positions with  $U_{iso} = 1.2U_{equiv}$  of the parent atom ( $U_{iso} = 1.5U_{equiv}$  for methyl). The relative occupancies of the disordered atoms were freely refined. Constraints were used on the anisotropic displacement parameters of the disordered atoms, and the disordered bonds needed restraints. Disordered acetone solvent was located in the crystal, but it could not be adequately modeled with or without restraints. Thus, the structure factors were modified using the PLATON SQUEEZE<sup>55</sup> technique, in order to produce a “solvate-free” structure factor set. PLATON reported a total electron density of 63 e<sup>-</sup> and total solvent accessible volume of 186 Å<sup>3</sup>. The final anisotropic full-matrix least-squares refinement on F<sup>2</sup> with **984** variables converged at **R1 = 4.89%**, for the observed data and **wR2 = 10.16%** for all data. The goodness-of-fit was **0.990**. The largest peak in the final difference electron density synthesis was **1.715 e<sup>-</sup>/Å<sup>3</sup>** and the largest hole was **-1.315 e<sup>-</sup>/Å<sup>3</sup>** with an RMS deviation of **0.157 e<sup>-</sup>/Å<sup>3</sup>**. On the basis of the final model, the calculated density was **1.465 g/cm<sup>3</sup>** and F(000), **1840 e<sup>-</sup>**.

**Table 1. Sample and crystal data for Harman\_16JAS235.**

|                             |   |                |
|-----------------------------|---|----------------|
| <b>Identification code</b>  | Harman_16JAS235   |                |
| <b>Chemical formula</b>     | C <sub>69</sub> H <sub>110</sub> B <sub>2</sub> F <sub>6</sub> N <sub>14</sub> O <sub>7</sub> P <sub>2</sub> W <sub>2</sub> |                |
| <b>Formula weight</b>       | 1812.96 g/mol   |                |
| <b>Temperature</b>          | 100(2) K  |                |
| <b>Wavelength</b>           | 0.71073 Å   |                |
| <b>Crystal size</b>         | 0.041 x 0.066 x 0.103 mm  |                |
| <b>Crystal habit</b>        | yellow plate  |                |
| <b>Crystal system</b>       | triclinic   |                |
| <b>Space group</b>          | P -1  |                |
| <b>Unit cell dimensions</b> | a = 13.1384(15) Å   | α = 97.443(4)° |
|                             | b = 14.6742(17) Å   | β = 93.751(4)° |
|                             | c = 21.777(3) Å   | γ = 97.774(4)° |

<sup>53</sup> Sheldrick, G. M. (2015). *Acta Cryst.* **A71**, 3-8.

<sup>54</sup> Dolomanov, O. V.; Bourhis, L. J.; Gildea, R. J.; Howard, J. A. K.; Puschmann, H. *J. Appl. Cryst.* (2009). **42**, 339-341.

<sup>55</sup> Spek, A. L. *Acta Crystallogr. Sect C: Struct. Chem.* **2015**, C71, 9-18.

|                               |                          |
|-------------------------------|--------------------------|
| <b>Volume</b>                 | 4110.1(8) Å <sup>3</sup> |
| <b>Z</b>                      | 2                        |
| <b>Density (calculated)</b>   | 1.465 g/cm <sup>3</sup>  |
| <b>Absorption coefficient</b> | 2.905 mm <sup>-1</sup>   |
| <b>F(000)</b>                 | 1840                     |

**Table 2. Data collection and structure refinement for Harman\_16JAS235.**

|  |  |
|--|--|
| <b>Diffractometer</b>                      | Bruker Kappa APEXII Duo  |
| <b>Radiation source</b>                    | fine-focus sealed tube (Mo K <sub>α</sub> , λ = 0.71073 Å)                   |
| <b>Theta range for data collection</b>     | 1.41 to 25.73°   |
| <b>Index ranges</b>                        | -16 ≤ h ≤ 14, -17 ≤ k ≤ 17, -26 ≤ l ≤ 26                                     |
| <b>Reflections collected</b>               | 60372  |
| <b>Independent reflections</b>             | 15595 [R(int) = 0.1012]  |
| <b>Coverage of independent reflections</b> | 99.6%  |
| <b>Absorption correction</b>               | Multi-Scan   |
| <b>Max. and min. transmission</b>          | 0.8900 and 0.7540  |
| <b>Structure solution technique</b>        | direct methods   |
| <b>Structure solution program</b>          | SHELXT 2014/5 (Sheldrick, 2014)  |
| <b>Refinement method</b>                   | Full-matrix least-squares on F <sup>2</sup>                                  |
| <b>Refinement program</b>                  | SHELXL-2018/3 (Sheldrick, 2018)  |
| <b>Function minimized</b>                  | Σ w(F <sub>o</sub> <sup>2</sup> - F <sub>c</sub> <sup>2</sup> ) <sup>2</sup> |
| <b>Data / restraints / parameters</b>      | 15595 / 21 / 984   |
| <b>Goodness-of-fit on F<sup>2</sup></b>    | 0.990  |
| <b>Δ/σ<sub>max</sub></b>                   | 0.001  |

|                                    |   |                              |
|------------------------------------|---|------------------------------|
| <b>Final R indices</b>             | 9468 data;<br>$I > 2\sigma(I)$  | R1 = 0.0489, wR2 =<br>0.0858 |
|                                    | all data  | R1 = 0.1082, wR2 =<br>0.1016 |
| <b>Weighting scheme</b>            | $w = 1/[\sigma^2(F_o^2) + (0.0363P)^2]$<br>where $P = (F_o^2 + 2F_c^2)/3$ |                              |
| <b>Largest diff. peak and hole</b> | 1.715 and -1.315 eÅ <sup>-3</sup>   |                              |
| <b>R.M.S. deviation from mean</b>  | 0.157 eÅ <sup>-3</sup>  |                              |

**Table 3. Atomic coordinates and equivalent isotropic atomic displacement parameters (Å<sup>2</sup>) for Harman\_16JAS235.**

U(eq) is defined as one third of the trace of the orthogonalized U<sub>ij</sub> tensor.

|    | x/a         | y/b         | z/c        | U(eq)      |
|----|-------------|-------------|------------|------------|
| W1 | 0.89010(2)  | 0.87305(2)  | 0.81089(2) | 0.02123(9) |
| W2 | 0.29371(2)  | 0.19735(2)  | 0.66672(2) | 0.02438(9) |
| P1 | 0.90645(14) | 0.70139(13) | 0.80316(8) | 0.0248(4)  |
| P2 | 0.18071(16) | 0.32442(14) | 0.67748(9) | 0.0310(5)  |
| F1 | 0.5207(4)   | 0.6339(4)   | 0.7369(2)  | 0.0664(16) |
| F2 | 0.5250(3)   | 0.7343(3)   | 0.6733(2)  | 0.0495(13) |
| F3 | 0.4253(3)   | 0.7428(4)   | 0.7462(2)  | 0.0751(18) |
| F4 | 0.5010(5)   | 0.5172(4)   | 0.8345(2)  | 0.085(2)   |
| F5 | 0.6460(5)   | 0.4625(5)   | 0.8356(3)  | 0.114(3)   |
| F6 | 0.5273(4)   | 0.4059(4)   | 0.8874(2)  | 0.0822(19) |
| O1 | 0.8017(4)   | 0.8465(3)   | 0.6781(2)  | 0.0310(13) |
| O2 | 0.6475(4)   | 0.0655(4)   | 0.9733(2)  | 0.0414(14) |

|     | <b>x/a</b> | <b>y/b</b> | <b>z/c</b> | <b>U(eq)</b> |
|-----|------------|------------|------------|--------------|
| O3  | 0.6634(4)  | 0.1373(4)  | 0.8893(2)  | 0.0388(13)   |
| O4  | 0.2866(4)  | 0.1798(3)  | 0.8016(2)  | 0.0356(13)   |
| O7  | 0.2453(4)  | 0.2630(4)  | 0.9878(2)  | 0.0475(15)   |
| N1  | 0.9775(4)  | 0.8950(4)  | 0.9062(2)  | 0.0247(14)   |
| N2  | 0.0755(4)  | 0.9421(4)  | 0.9144(2)  | 0.0231(14)   |
| N3  | 0.0436(4)  | 0.8852(4)  | 0.7743(3)  | 0.0249(14)   |
| N4  | 0.1292(4)  | 0.9401(4)  | 0.8049(2)  | 0.0221(14)   |
| N5  | 0.9413(4)  | 0.0262(4)  | 0.8240(2)  | 0.0227(14)   |
| N6  | 0.0385(4)  | 0.0651(4)  | 0.8506(2)  | 0.0207(14)   |
| N7  | 0.8352(4)  | 0.8577(4)  | 0.7336(3)  | 0.0219(13)   |
| N8  | 0.2824(4)  | 0.2021(4)  | 0.5627(2)  | 0.0301(15)   |
| N9  | 0.2331(5)  | 0.1268(4)  | 0.5230(3)  | 0.0334(16)   |
| N10 | 0.1434(4)  | 0.1064(4)  | 0.6482(2)  | 0.0226(14)   |
| N11 | 0.1150(4)  | 0.0498(4)  | 0.5935(2)  | 0.0258(14)   |
| N12 | 0.3343(5)  | 0.0564(4)  | 0.6362(3)  | 0.0319(16)   |
| N13 | 0.2872(5)  | 0.0037(4)  | 0.5818(3)  | 0.0329(16)   |
| N14 | 0.2933(4)  | 0.1889(4)  | 0.7465(3)  | 0.0256(14)   |
| C1  | 0.9621(5)  | 0.8607(5)  | 0.9602(3)  | 0.0249(17)   |
| C2  | 0.0482(5)  | 0.8867(5)  | 0.0015(3)  | 0.0268(17)   |
| C3  | 0.1177(5)  | 0.9372(5)  | 0.9711(3)  | 0.0239(17)   |
| C4  | 0.0715(5)  | 0.8555(5)  | 0.7178(3)  | 0.0270(18)   |
| C5  | 0.1720(5)  | 0.8895(5)  | 0.7114(3)  | 0.0321(19)   |
| C6  | 0.2071(5)  | 0.9438(5)  | 0.7675(3)  | 0.0295(18)   |
| C7  | 0.8950(6)  | 0.0981(5)  | 0.8122(3)  | 0.0288(18)   |

|     | <b>x/a</b> | <b>y/b</b> | <b>z/c</b> | <b>U(eq)</b> |
|-----|------------|------------|------------|--------------|
| C8  | 0.9590(5)  | 0.1815(5)  | 0.8305(3)  | 0.0300(18)   |
| C9  | 0.0490(6)  | 0.1572(5)  | 0.8541(3)  | 0.0267(18)   |
| C10 | 0.7475(5)  | 0.8168(5)  | 0.8543(3)  | 0.0254(18)   |
| C11 | 0.7546(5)  | 0.9170(5)  | 0.8548(3)  | 0.0223(16)   |
| C12 | 0.6647(5)  | 0.9552(5)  | 0.8229(3)  | 0.0239(17)   |
| C13 | 0.6148(5)  | 0.8873(5)  | 0.7656(3)  | 0.0304(19)   |
| C14 | 0.6030(5)  | 0.7871(5)  | 0.7743(3)  | 0.0265(17)   |
| C15 | 0.6655(5)  | 0.7568(5)  | 0.8149(3)  | 0.0256(18)   |
| C16 | 0.5210(6)  | 0.7247(7)  | 0.7344(4)  | 0.043(2)     |
| C17 | 0.5840(6)  | 0.9791(6)  | 0.8718(3)  | 0.033(2)     |
| C18 | 0.5457(6)  | 0.9004(5)  | 0.9077(3)  | 0.037(2)     |
| C19 | 0.4891(5)  | 0.0106(6)  | 0.8394(3)  | 0.036(2)     |
| C20 | 0.6348(5)  | 0.0620(6)  | 0.9179(4)  | 0.0320(19)   |
| C21 | 0.7074(6)  | 0.2206(6)  | 0.9300(4)  | 0.051(2)     |
| C22 | 0.0378(5)  | 0.6723(5)  | 0.7950(3)  | 0.0273(18)   |
| C23 | 0.1150(5)  | 0.7102(5)  | 0.8499(3)  | 0.0280(18)   |
| C24 | 0.2232(5)  | 0.6971(5)  | 0.8378(4)  | 0.034(2)     |
| C25 | 0.3009(6)  | 0.7300(6)  | 0.8944(4)  | 0.049(2)     |
| C26 | 0.8309(5)  | 0.6275(5)  | 0.7375(3)  | 0.0324(19)   |
| C27 | 0.8726(6)  | 0.6297(5)  | 0.6735(3)  | 0.0343(19)   |
| C28 | 0.8035(8)  | 0.5677(6)  | 0.6229(4)  | 0.066(3)     |
| C29 | 0.8465(9)  | 0.5643(8)  | 0.5598(4)  | 0.096(4)     |
| C30 | 0.8678(5)  | 0.6428(5)  | 0.8693(3)  | 0.0257(17)   |
| C31 | 0.8979(6)  | 0.5465(5)  | 0.8734(4)  | 0.0342(19)   |



|     | <b>x/a</b> | <b>y/b</b> | <b>z/c</b> | <b>U(eq)</b> |
|-----|------------|------------|------------|--------------|
| C32 | 0.8640(6)  | 0.5078(5)  | 0.9310(3)  | 0.0343(19)   |
| C33 | 0.9048(6)  | 0.4188(5)  | 0.9406(4)  | 0.045(2)     |
| C34 | 0.3129(6)  | 0.2671(6)  | 0.5269(3)  | 0.043(2)     |
| C35 | 0.2814(6)  | 0.2346(6)  | 0.4648(4)  | 0.050(3)     |
| C36 | 0.2315(6)  | 0.1471(7)  | 0.4642(4)  | 0.049(3)     |
| C37 | 0.0664(5)  | 0.0914(5)  | 0.6847(3)  | 0.0245(17)   |
| C38 | 0.9878(5)  | 0.0263(5)  | 0.6530(3)  | 0.0304(18)   |
| C39 | 0.0213(6)  | 0.0007(5)  | 0.5956(3)  | 0.0314(19)   |
| C40 | 0.3992(6)  | 0.0066(6)  | 0.6596(4)  | 0.038(2)     |
| C41 | 0.3960(7)  | 0.9198(6)  | 0.6211(4)  | 0.051(2)     |
| C42 | 0.3260(7)  | 0.9225(6)  | 0.5731(4)  | 0.048(2)     |
| C43 | 0.4186(6)  | 0.3214(6)  | 0.6731(4)  | 0.034(2)     |
| C44 | 0.4604(5)  | 0.2353(5)  | 0.6655(3)  | 0.0329(19)   |
| C45 | 0.5447(5)  | 0.2190(7)  | 0.7131(4)  | 0.048(2)     |
| C46 | 0.5318(6)  | 0.2732(7)  | 0.7791(4)  | 0.058(3)     |
| C47 | 0.5057(6)  | 0.3681(6)  | 0.7784(4)  | 0.046(2)     |
| C48 | 0.4518(6)  | 0.3872(6)  | 0.7298(3)  | 0.041(2)     |
| C49 | 0.5440(8)  | 0.4389(8)  | 0.8323(4)  | 0.059(3)     |
| C55 | 0.1465(6)  | 0.3567(5)  | 0.7571(3)  | 0.035(2)     |
| C56 | 0.2325(7)  | 0.4046(5)  | 0.8040(3)  | 0.041(2)     |
| C57 | 0.1973(8)  | 0.4311(6)  | 0.8685(4)  | 0.058(3)     |
| C58 | 0.2844(8)  | 0.4777(6)  | 0.9155(4)  | 0.067(3)     |
| C59 | 0.0499(6)  | 0.2952(6)  | 0.6373(3)  | 0.038(2)     |
| C60 | 0.0450(6)  | 0.2770(6)  | 0.5671(4)  | 0.044(2)     |

|      | <b>x/a</b> | <b>y/b</b> | <b>z/c</b> | <b>U(eq)</b> |
|------|------------|------------|------------|--------------|
| C61  | 0.9364(6)  | 0.2528(7)  | 0.5348(5)  | 0.060(3)     |
| C63  | 0.2255(6)  | 0.4361(5)  | 0.6512(4)  | 0.044(2)     |
| C64  | 0.1591(8)  | 0.5120(5)  | 0.6548(4)  | 0.066(3)     |
| C67  | 0.3392(7)  | 0.2711(6)  | 0.9891(3)  | 0.036(2)     |
| C68  | 0.3926(6)  | 0.2091(6)  | 0.9462(3)  | 0.042(2)     |
| C69  | 0.4055(6)  | 0.3431(6)  | 0.0342(4)  | 0.047(2)     |
| B1   | 0.1184(7)  | 0.0026(6)  | 0.8661(4)  | 0.027(2)     |
| B2   | 0.1964(6)  | 0.0356(7)  | 0.5468(4)  | 0.031(2)     |
| O5   | 0.664(2)   | 0.196(3)   | 0.5620(10) | 0.040(7)     |
| O6   | 0.6023(15) | 0.0748(12) | 0.6087(9)  | 0.047(2)     |
| C50  | 0.6473(14) | 0.2174(17) | 0.6783(11) | 0.038(3)     |
| C51  | 0.693(3)   | 0.3172(17) | 0.671(2)   | 0.042(4)     |
| C52  | 0.7367(18) | 0.175(2)   | 0.7088(14) | 0.053(4)     |
| C53  | 0.644(2)   | 0.1677(15) | 0.6109(13) | 0.038(3)     |
| C54  | 0.581(2)   | 0.0172(19) | 0.5490(14) | 0.067(4)     |
| C62  | 0.8854(12) | 0.3381(13) | 0.5425(9)  | 0.063(7)     |
| C65  | 0.2218(16) | 0.5902(10) | 0.6273(10) | 0.092(4)     |
| C66  | 0.1740(16) | 0.6721(12) | 0.6281(8)  | 0.092(4)     |
| O5A  | 0.6853(12) | 0.1950(12) | 0.5908(6)  | 0.055(4)     |
| O6A  | 0.6610(6)  | 0.0958(5)  | 0.6596(4)  | 0.047(2)     |
| C50A | 0.6561(8)  | 0.2562(8)  | 0.6980(6)  | 0.038(3)     |
| C51A | 0.6740(14) | 0.3519(8)  | 0.6761(9)  | 0.042(4)     |
| C52A | 0.7384(9)  | 0.2477(10) | 0.7499(6)  | 0.053(4)     |
| C53A | 0.6699(9)  | 0.1844(9)  | 0.6438(7)  | 0.038(3)     |

|      | x/a        | y/b        | z/c        | U(eq)    |
|------|------------|------------|------------|----------|
| C54A | 0.6759(11) | 0.0229(9)  | 0.6112(7)  | 0.067(4) |
| C62A | 0.9317(17) | 0.2465(15) | 0.4656(9)  | 0.081(9) |
| C65A | 0.197(2)   | 0.6129(11) | 0.6553(12) | 0.092(4) |
| C66A | 0.255(2)   | 0.623(2)   | 0.6032(12) | 0.092(4) |

**Table 4. Bond lengths (Å) for Harman\_16JAS235.**

|        |           |        |           |
|--------|-----------|--------|-----------|
| W1-N7  | 1.761(6)  | W1-C11 | 2.208(6)  |
| W1-N3  | 2.210(5)  | W1-N5  | 2.232(6)  |
| W1-C10 | 2.258(7)  | W1-N1  | 2.269(5)  |
| W1-P1  | 2.542(2)  | W2-N14 | 1.759(6)  |
| W2-C44 | 2.189(7)  | W2-N10 | 2.210(5)  |
| W2-N12 | 2.234(6)  | W2-C43 | 2.263(7)  |
| W2-N8  | 2.271(5)  | W2-P2  | 2.533(2)  |
| P1-C26 | 1.824(7)  | P1-C30 | 1.835(7)  |
| P1-C22 | 1.847(7)  | P2-C55 | 1.838(7)  |
| P2-C63 | 1.840(8)  | P2-C59 | 1.846(8)  |
| F1-C16 | 1.341(10) | F2-C16 | 1.358(9)  |
| F3-C16 | 1.354(9)  | F4-C49 | 1.344(11) |
| F5-C49 | 1.332(11) | F6-C49 | 1.371(10) |
| O1-N7  | 1.242(6)  | O2-C20 | 1.200(8)  |
| O3-C20 | 1.359(9)  | O3-C21 | 1.441(9)  |
| O4-N14 | 1.232(6)  | O7-C67 | 1.221(9)  |
| N1-C1  | 1.352(8)  | N1-N2  | 1.366(7)  |
| N2-C3  | 1.335(8)  | N2-B1  | 1.548(10) |

|          |           |          |           |
|----------|-----------|----------|-----------|
| N3-C4    | 1.343(8)  | N3-N4    | 1.369(7)  |
| N4-C6    | 1.348(8)  | N4-B1    | 1.543(10) |
| N5-C7    | 1.331(8)  | N5-N6    | 1.383(7)  |
| N6-C9    | 1.331(8)  | N6-B1    | 1.533(10) |
| N8-C34   | 1.345(9)  | N8-N9    | 1.368(8)  |
| N9-C36   | 1.352(9)  | N9-B2    | 1.527(11) |
| N10-C37  | 1.340(8)  | N10-N11  | 1.360(7)  |
| N11-C39  | 1.346(8)  | N11-B2   | 1.539(9)  |
| N12-C40  | 1.316(9)  | N12-N13  | 1.386(8)  |
| N13-C42  | 1.355(9)  | N13-B2   | 1.531(10) |
| C1-C2    | 1.377(9)  | C1-H1    | 0.95      |
| C2-C3    | 1.359(9)  | C2-H2A   | 0.95      |
| C3-H3    | 0.95      | C4-C5    | 1.369(9)  |
| C4-H4    | 0.95      | C5-C6    | 1.384(10) |
| C5-H5    | 0.95      | C6-H6    | 0.95      |
| C7-C8    | 1.384(10) | C7-H7    | 0.95      |
| C8-C9    | 1.368(10) | C8-H8    | 0.95      |
| C9-H9    | 0.95      | C10-C15  | 1.448(10) |
| C10-C11  | 1.458(10) | C10-H10  | 0.93(6)   |
| C11-C12  | 1.538(9)  | C11-H11  | 1.0       |
| C12-C13  | 1.539(10) | C12-C17  | 1.592(9)  |
| C12-H12  | 1.0       | C13-C14  | 1.495(10) |
| C13-H13A | 0.99      | C13-H13B | 0.99      |
| C14-C15  | 1.328(9)  | C14-C16  | 1.469(10) |
| C15-H15  | 0.95      | C17-C20  | 1.520(11) |

|          |           |          |           |
|----------|-----------|----------|-----------|
| C17-C18  | 1.525(10) | C17-C19  | 1.547(10) |
| C18-H18A | 0.98      | C18-H18B | 0.98      |
| C18-H18C | 0.98      | C19-H19A | 0.98      |
| C19-H19B | 0.98      | C19-H19C | 0.98      |
| C21-H21A | 0.98      | C21-H21B | 0.98      |
| C21-H21C | 0.98      | C22-C23  | 1.512(9)  |
| C22-H22A | 0.99      | C22-H22B | 0.99      |
| C23-C24  | 1.496(9)  | C23-H23A | 0.99      |
| C23-H23B | 0.99      | C24-C25  | 1.530(10) |
| C24-H24A | 0.99      | C24-H24B | 0.99      |
| C25-H25A | 0.98      | C25-H25B | 0.98      |
| C25-H25C | 0.98      | C26-C27  | 1.532(9)  |
| C26-H26A | 0.99      | C26-H26B | 0.99      |
| C27-C28  | 1.501(10) | C27-H27A | 0.99      |
| C27-H27B | 0.99      | C28-C29  | 1.516(11) |
| C28-H28A | 0.99      | C28-H28B | 0.99      |
| C29-H29A | 0.98      | C29-H29B | 0.98      |
| C29-H29C | 0.98      | C30-C31  | 1.531(9)  |
| C30-H30A | 0.99      | C30-H30B | 0.99      |
| C31-C32  | 1.511(9)  | C31-H31A | 0.99      |
| C31-H31B | 0.99      | C32-C33  | 1.510(10) |
| C32-H32A | 0.99      | C32-H32B | 0.99      |
| C33-H33A | 0.98      | C33-H33B | 0.98      |
| C33-H33C | 0.98      | C34-C35  | 1.391(10) |
| C34-H34  | 0.95      | C35-C36  | 1.359(11) |

|          |           |          |           |
|----------|-----------|----------|-----------|
| C35-H35  | 0.95      | C36-H36  | 0.95      |
| C37-C38  | 1.388(9)  | C37-H37  | 0.95      |
| C38-C39  | 1.376(9)  | C38-H38  | 0.95      |
| C39-H39  | 0.95      | C40-C41  | 1.424(11) |
| C40-H40  | 0.95      | C41-C42  | 1.355(11) |
| C41-H41  | 0.95      | C42-H42  | 0.95      |
| C43-C44  | 1.439(10) | C43-C48  | 1.468(11) |
| C43-H43  | 1.12(7)   | C44-C45  | 1.531(10) |
| C44-H44  | 1.0       | C45-C50A | 1.562(11) |
| C45-C46  | 1.583(12) | C45-C50  | 1.589(17) |
| C45-H45  | 1.0       | C45-H45A | 1.0       |
| C46-C47  | 1.480(12) | C46-H46A | 0.99      |
| C46-H46B | 0.99      | C47-C48  | 1.316(11) |
| C47-C49  | 1.475(12) | C48-H48  | 0.95      |
| C55-C56  | 1.503(10) | C55-H55A | 0.99      |
| C55-H55B | 0.99      | C56-C57  | 1.528(10) |
| C56-H56A | 0.99      | C56-H56B | 0.99      |
| C57-C58  | 1.510(12) | C57-H57A | 0.99      |
| C57-H57B | 0.99      | C58-H58A | 0.98      |
| C58-H58B | 0.98      | C58-H58C | 0.98      |
| C59-C60  | 1.514(10) | C59-H59A | 0.99      |
| C59-H59B | 0.99      | C60-C61  | 1.524(11) |
| C60-H60A | 0.99      | C60-H60B | 0.99      |
| C61-C62  | 1.494(17) | C61-C62A | 1.50(2)   |
| C61-H61A | 0.99      | C61-H61B | 0.99      |

|           |           |           |           |
|-----------|-----------|-----------|-----------|
| C61-H61C  | 0.99      | C61-H61D  | 0.99      |
| C63-C64   | 1.503(10) | C63-H63A  | 0.99      |
| C63-H63B  | 0.99      | C64-C65A  | 1.496(15) |
| C64-C65   | 1.530(13) | C64-H64A  | 0.99      |
| C64-H64B  | 0.99      | C64-H64C  | 0.99      |
| C64-H64D  | 0.99      | C67-C69   | 1.485(11) |
| C67-C68   | 1.495(10) | C68-H68A  | 0.98      |
| C68-H68B  | 0.98      | C68-H68C  | 0.98      |
| C69-H69A  | 0.98      | C69-H69B  | 0.98      |
| C69-H69C  | 0.98      | B1-H1A    | 1.01(7)   |
| B2-H2     | 1.19(6)   | O5-C53    | 1.22(2)   |
| O6-C53    | 1.393(18) | O6-C54    | 1.44(3)   |
| C50-C51   | 1.538(17) | C50-C53   | 1.55(2)   |
| C50-C52   | 1.549(16) | C51-H51A  | 0.98      |
| C51-H51B  | 0.98      | C51-H51C  | 0.98      |
| C52-H52A  | 0.98      | C52-H52B  | 0.98      |
| C52-H52C  | 0.98      | C54-H54A  | 0.98      |
| C54-H54B  | 0.98      | C54-H54C  | 0.98      |
| C62-H62A  | 0.98      | C62-H62B  | 0.98      |
| C62-H62C  | 0.98      | C65-C66   | 1.428(13) |
| C65-H65A  | 0.99      | C65-H65B  | 0.99      |
| C66-H66A  | 0.98      | C66-H66B  | 0.98      |
| C66-H66C  | 0.98      | O5A-C53A  | 1.211(15) |
| O6A-C53A  | 1.379(12) | O6A-C54A  | 1.444(13) |
| C50A-C53A | 1.514(17) | C50A-C51A | 1.534(13) |

|           |           |           |           |
|-----------|-----------|-----------|-----------|
| C50A-C52A | 1.542(12) | C51A-H51D | 0.98      |
| C51A-H51E | 0.98      | C51A-H51F | 0.98      |
| C52A-H52D | 0.98      | C52A-H52E | 0.98      |
| C52A-H52F | 0.98      | C54A-H54D | 0.98      |
| C54A-H54E | 0.98      | C54A-H54F | 0.98      |
| C62A-H62D | 0.98      | C62A-H62E | 0.98      |
| C62A-H62F | 0.98      | C65A-C66A | 1.417(15) |
| C65A-H65C | 0.99      | C65A-H65D | 0.99      |
| C66A-H66D | 0.98      | C66A-H66E | 0.98      |
| C66A-H66F | 0.98      |           |           |

**Table 5. Bond angles (°) for Harman\_16JAS235.**

|            |            |            |           |
|------------|------------|------------|-----------|
| N7-W1-C11  | 96.6(2)    | N7-W1-N3   | 88.2(2)   |
| C11-W1-N3  | 158.7(2)   | N7-W1-N5   | 99.5(2)   |
| C11-W1-N5  | 81.9(2)    | N3-W1-N5   | 76.8(2)   |
| N7-W1-C10  | 97.3(3)    | C11-W1-C10 | 38.1(2)   |
| N3-W1-C10  | 161.7(2)   | N5-W1-C10  | 119.1(2)  |
| N7-W1-N1   | 173.9(2)   | C11-W1-N1  | 89.1(2)   |
| N3-W1-N1   | 85.7(2)    | N5-W1-N1   | 78.8(2)   |
| C10-W1-N1  | 88.7(2)    | N7-W1-P1   | 91.03(18) |
| C11-W1-P1  | 116.44(18) | N3-W1-P1   | 84.10(16) |
| N5-W1-P1   | 157.83(15) | C10-W1-P1  | 78.3(2)   |
| N1-W1-P1   | 88.66(15)  | N14-W2-C44 | 96.9(3)   |
| N14-W2-N10 | 90.6(2)    | C44-W2-N10 | 156.4(3)  |
| N14-W2-N12 | 97.3(2)    | C44-W2-N12 | 81.3(3)   |



|            |           |            |            |
|------------|-----------|------------|------------|
| N10-W2-N12 | 75.6(2)   | N14-W2-C43 | 98.1(3)    |
| C44-W2-C43 | 37.7(3)   | N10-W2-C43 | 162.2(3)   |
| N12-W2-C43 | 118.3(3)  | N14-W2-N8  | 175.8(2)   |
| C44-W2-N8  | 87.1(2)   | N10-W2-N8  | 85.1(2)    |
| N12-W2-N8  | 82.0(2)   | C43-W2-N8  | 85.9(2)    |
| N14-W2-P2  | 91.13(19) | C44-W2-P2  | 119.2(2)   |
| N10-W2-P2  | 82.74(15) | N12-W2-P2  | 156.81(17) |
| C43-W2-P2  | 81.6(2)   | N8-W2-P2   | 88.03(16)  |
| C26-P1-C30 | 102.5(3)  | C26-P1-C22 | 102.9(3)   |
| C30-P1-C22 | 102.0(3)  | C26-P1-W1  | 115.1(3)   |
| C30-P1-W1  | 116.6(2)  | C22-P1-W1  | 115.6(2)   |
| C55-P2-C63 | 104.3(4)  | C55-P2-C59 | 99.2(3)    |
| C63-P2-C59 | 101.5(4)  | C55-P2-W2  | 114.2(3)   |
| C63-P2-W2  | 118.9(3)  | C59-P2-W2  | 116.1(3)   |
| C20-O3-C21 | 115.5(6)  | C1-N1-N2   | 105.2(5)   |
| C1-N1-W1   | 134.7(5)  | N2-N1-W1   | 119.4(4)   |
| C3-N2-N1   | 110.0(5)  | C3-N2-B1   | 128.0(6)   |
| N1-N2-B1   | 121.4(6)  | C4-N3-N4   | 105.5(5)   |
| C4-N3-W1   | 130.3(5)  | N4-N3-W1   | 123.6(4)   |
| C6-N4-N3   | 109.9(5)  | C6-N4-B1   | 129.2(6)   |
| N3-N4-B1   | 119.3(5)  | C7-N5-N6   | 104.9(6)   |
| C7-N5-W1   | 133.3(5)  | N6-N5-W1   | 121.8(4)   |
| C9-N6-N5   | 110.0(6)  | C9-N6-B1   | 129.6(6)   |
| N5-N6-B1   | 120.2(6)  | O1-N7-W1   | 176.6(5)   |
| C34-N8-N9  | 106.1(6)  | C34-N8-W2  | 134.1(5)   |

|             |          |             |          |
|-------------|----------|-------------|----------|
| N9-N8-W2    | 119.7(4) | C36-N9-N8   | 109.2(6) |
| C36-N9-B2   | 129.7(7) | N8-N9-B2    | 120.9(6) |
| C37-N10-N11 | 106.5(5) | C37-N10-W2  | 130.7(5) |
| N11-N10-W2  | 122.8(4) | C39-N11-N10 | 110.1(5) |
| C39-N11-B2  | 129.6(6) | N10-N11-B2  | 118.8(5) |
| C40-N12-N13 | 106.3(6) | C40-N12-W2  | 133.2(5) |
| N13-N12-W2  | 120.5(5) | C42-N13-N12 | 109.1(6) |
| C42-N13-B2  | 130.2(7) | N12-N13-B2  | 120.1(6) |
| O4-N14-W2   | 175.8(5) | N1-C1-C2    | 110.5(6) |
| N1-C1-H1    | 124.8    | C2-C1-H1    | 124.8    |
| C3-C2-C1    | 105.5(6) | C3-C2-H2A   | 127.3    |
| C1-C2-H2A   | 127.3    | N2-C3-C2    | 108.9(6) |
| N2-C3-H3    | 125.6    | C2-C3-H3    | 125.6    |
| N3-C4-C5    | 111.5(6) | N3-C4-H4    | 124.3    |
| C5-C4-H4    | 124.3    | C4-C5-C6    | 105.2(6) |
| C4-C5-H5    | 127.4    | C6-C5-H5    | 127.4    |
| N4-C6-C5    | 108.0(6) | N4-C6-H6    | 126.0    |
| C5-C6-H6    | 126.0    | N5-C7-C8    | 111.5(7) |
| N5-C7-H7    | 124.2    | C8-C7-H7    | 124.2    |
| C9-C8-C7    | 104.8(7) | C9-C8-H8    | 127.6    |
| C7-C8-H8    | 127.6    | N6-C9-C8    | 108.8(7) |
| N6-C9-H9    | 125.6    | C8-C9-H9    | 125.6    |
| C15-C10-C11 | 118.5(7) | C15-C10-W1  | 118.7(5) |
| C11-C10-W1  | 69.1(4)  | C15-C10-H10 | 119.(4)  |
| C11-C10-H10 | 114.(4)  | W1-C10-H10  | 108.(4)  |

|               |          |               |          |
|---------------|----------|---------------|----------|
| C10-C11-C12   | 118.5(6) | C10-C11-W1    | 72.8(4)  |
| C12-C11-W1    | 126.5(4) | C10-C11-H11   | 111.2    |
| C12-C11-H11   | 111.2    | W1-C11-H11    | 111.2    |
| C11-C12-C13   | 111.0(6) | C11-C12-C17   | 109.9(5) |
| C13-C12-C17   | 112.6(6) | C11-C12-H12   | 107.7    |
| C13-C12-H12   | 107.7    | C17-C12-H12   | 107.7    |
| C14-C13-C12   | 114.7(6) | C14-C13-H13A  | 108.6    |
| C12-C13-H13A  | 108.6    | C14-C13-H13B  | 108.6    |
| C12-C13-H13B  | 108.6    | H13A-C13-H13B | 107.6    |
| C15-C14-C16   | 122.4(7) | C15-C14-C13   | 121.1(7) |
| C16-C14-C13   | 116.5(7) | C14-C15-C10   | 123.4(7) |
| C14-C15-H15   | 118.3    | C10-C15-H15   | 118.3    |
| F1-C16-F3     | 106.4(7) | F1-C16-F2     | 105.4(7) |
| F3-C16-F2     | 103.2(7) | F1-C16-C14    | 115.3(7) |
| F3-C16-C14    | 113.0(7) | F2-C16-C14    | 112.5(7) |
| C20-C17-C18   | 108.7(6) | C20-C17-C19   | 106.1(6) |
| C18-C17-C19   | 108.2(6) | C20-C17-C12   | 107.8(6) |
| C18-C17-C12   | 115.2(6) | C19-C17-C12   | 110.5(5) |
| C17-C18-H18A  | 109.5    | C17-C18-H18B  | 109.5    |
| H18A-C18-H18B | 109.5    | C17-C18-H18C  | 109.5    |
| H18A-C18-H18C | 109.5    | H18B-C18-H18C | 109.5    |
| C17-C19-H19A  | 109.5    | C17-C19-H19B  | 109.5    |
| H19A-C19-H19B | 109.5    | C17-C19-H19C  | 109.5    |
| H19A-C19-H19C | 109.5    | H19B-C19-H19C | 109.5    |
| O2-C20-O3     | 121.4(7) | O2-C20-C17    | 126.8(8) |

|               |          |               |          |
|---------------|----------|---------------|----------|
| O3-C20-C17    | 111.8(6) | O3-C21-H21A   | 109.5    |
| O3-C21-H21B   | 109.5    | H21A-C21-H21B | 109.5    |
| O3-C21-H21C   | 109.5    | H21A-C21-H21C | 109.5    |
| H21B-C21-H21C | 109.5    | C23-C22-P1    | 115.0(5) |
| C23-C22-H22A  | 108.5    | P1-C22-H22A   | 108.5    |
| C23-C22-H22B  | 108.5    | P1-C22-H22B   | 108.5    |
| H22A-C22-H22B | 107.5    | C24-C23-C22   | 113.3(6) |
| C24-C23-H23A  | 108.9    | C22-C23-H23A  | 108.9    |
| C24-C23-H23B  | 108.9    | C22-C23-H23B  | 108.9    |
| H23A-C23-H23B | 107.7    | C23-C24-C25   | 113.6(6) |
| C23-C24-H24A  | 108.8    | C25-C24-H24A  | 108.8    |
| C23-C24-H24B  | 108.8    | C25-C24-H24B  | 108.8    |
| H24A-C24-H24B | 107.7    | C24-C25-H25A  | 109.5    |
| C24-C25-H25B  | 109.5    | H25A-C25-H25B | 109.5    |
| C24-C25-H25C  | 109.5    | H25A-C25-H25C | 109.5    |
| H25B-C25-H25C | 109.5    | C27-C26-P1    | 117.0(5) |
| C27-C26-H26A  | 108.0    | P1-C26-H26A   | 108.0    |
| C27-C26-H26B  | 108.0    | P1-C26-H26B   | 108.0    |
| H26A-C26-H26B | 107.3    | C28-C27-C26   | 112.5(6) |
| C28-C27-H27A  | 109.1    | C26-C27-H27A  | 109.1    |
| C28-C27-H27B  | 109.1    | C26-C27-H27B  | 109.1    |
| H27A-C27-H27B | 107.8    | C27-C28-C29   | 113.3(8) |
| C27-C28-H28A  | 108.9    | C29-C28-H28A  | 108.9    |
| C27-C28-H28B  | 108.9    | C29-C28-H28B  | 108.9    |
| H28A-C28-H28B | 107.7    | C28-C29-H29A  | 109.5    |

|               |          |               |          |
|---------------|----------|---------------|----------|
| C28-C29-H29B  | 109.5    | H29A-C29-H29B | 109.5    |
| C28-C29-H29C  | 109.5    | H29A-C29-H29C | 109.5    |
| H29B-C29-H29C | 109.5    | C31-C30-P1    | 118.3(5) |
| C31-C30-H30A  | 107.7    | P1-C30-H30A   | 107.7    |
| C31-C30-H30B  | 107.7    | P1-C30-H30B   | 107.7    |
| H30A-C30-H30B | 107.1    | C32-C31-C30   | 112.6(6) |
| C32-C31-H31A  | 109.1    | C30-C31-H31A  | 109.1    |
| C32-C31-H31B  | 109.1    | C30-C31-H31B  | 109.1    |
| H31A-C31-H31B | 107.8    | C33-C32-C31   | 113.7(6) |
| C33-C32-H32A  | 108.8    | C31-C32-H32A  | 108.8    |
| C33-C32-H32B  | 108.8    | C31-C32-H32B  | 108.8    |
| H32A-C32-H32B | 107.7    | C32-C33-H33A  | 109.5    |
| C32-C33-H33B  | 109.5    | H33A-C33-H33B | 109.5    |
| C32-C33-H33C  | 109.5    | H33A-C33-H33C | 109.5    |
| H33B-C33-H33C | 109.5    | N8-C34-C35    | 110.2(7) |
| N8-C34-H34    | 124.9    | C35-C34-H34   | 124.9    |
| C36-C35-C34   | 105.4(7) | C36-C35-H35   | 127.3    |
| C34-C35-H35   | 127.3    | N9-C36-C35    | 109.0(7) |
| N9-C36-H36    | 125.5    | C35-C36-H36   | 125.5    |
| N10-C37-C38   | 109.9(6) | N10-C37-H37   | 125.1    |
| C38-C37-H37   | 125.1    | C39-C38-C37   | 105.8(6) |
| C39-C38-H38   | 127.1    | C37-C38-H38   | 127.1    |
| N11-C39-C38   | 107.7(6) | N11-C39-H39   | 126.1    |
| C38-C39-H39   | 126.1    | N12-C40-C41   | 110.8(7) |
| N12-C40-H40   | 124.6    | C41-C40-H40   | 124.6    |

|               |           |               |           |
|---------------|-----------|---------------|-----------|
| C42-C41-C40   | 104.6(8)  | C42-C41-H41   | 127.7     |
| C40-C41-H41   | 127.7     | C41-C42-N13   | 109.2(8)  |
| C41-C42-H42   | 125.4     | N13-C42-H42   | 125.4     |
| C44-C43-C48   | 118.2(7)  | C44-C43-W2    | 68.4(4)   |
| C48-C43-W2    | 124.4(5)  | C44-C43-H43   | 121.(4)   |
| C48-C43-H43   | 109.(4)   | W2-C43-H43    | 111.(4)   |
| C43-C44-C45   | 119.6(7)  | C43-C44-W2    | 74.0(4)   |
| C45-C44-W2    | 127.3(5)  | C43-C44-H44   | 110.4     |
| C45-C44-H44   | 110.4     | W2-C44-H44    | 110.4     |
| C44-C45-C50A  | 113.5(7)  | C44-C45-C46   | 110.0(7)  |
| C50A-C45-C46  | 105.0(8)  | C44-C45-C50   | 106.8(10) |
| C46-C45-C50   | 127.6(11) | C44-C45-H45   | 103.2     |
| C46-C45-H45   | 103.2     | C50-C45-H45   | 103.2     |
| C44-C45-H45A  | 109.4     | C50A-C45-H45A | 109.4     |
| C46-C45-H45A  | 109.4     | C47-C46-C45   | 115.0(7)  |
| C47-C46-H46A  | 108.5     | C45-C46-H46A  | 108.5     |
| C47-C46-H46B  | 108.5     | C45-C46-H46B  | 108.5     |
| H46A-C46-H46B | 107.5     | C48-C47-C49   | 122.4(10) |
| C48-C47-C46   | 119.6(8)  | C49-C47-C46   | 118.1(8)  |
| C47-C48-C43   | 124.6(9)  | C47-C48-H48   | 117.7     |
| C43-C48-H48   | 117.7     | F5-C49-F4     | 108.0(9)  |
| F5-C49-F6     | 103.7(8)  | F4-C49-F6     | 106.0(8)  |
| F5-C49-C47    | 112.1(9)  | F4-C49-C47    | 114.6(8)  |
| F6-C49-C47    | 111.7(8)  | C56-C55-P2    | 116.8(5)  |
| C56-C55-H55A  | 108.1     | P2-C55-H55A   | 108.1     |

|               |           |               |           |
|---------------|-----------|---------------|-----------|
| C56-C55-H55B  | 108.1     | P2-C55-H55B   | 108.1     |
| H55A-C55-H55B | 107.3     | C55-C56-C57   | 113.6(7)  |
| C55-C56-H56A  | 108.8     | C57-C56-H56A  | 108.8     |
| C55-C56-H56B  | 108.8     | C57-C56-H56B  | 108.8     |
| H56A-C56-H56B | 107.7     | C58-C57-C56   | 113.2(8)  |
| C58-C57-H57A  | 108.9     | C56-C57-H57A  | 108.9     |
| C58-C57-H57B  | 108.9     | C56-C57-H57B  | 108.9     |
| H57A-C57-H57B | 107.7     | C57-C58-H58A  | 109.5     |
| C57-C58-H58B  | 109.5     | H58A-C58-H58B | 109.5     |
| C57-C58-H58C  | 109.5     | H58A-C58-H58C | 109.5     |
| H58B-C58-H58C | 109.5     | C60-C59-P2    | 115.6(5)  |
| C60-C59-H59A  | 108.4     | P2-C59-H59A   | 108.4     |
| C60-C59-H59B  | 108.4     | P2-C59-H59B   | 108.4     |
| H59A-C59-H59B | 107.4     | C59-C60-C61   | 114.8(7)  |
| C59-C60-H60A  | 108.6     | C61-C60-H60A  | 108.6     |
| C59-C60-H60B  | 108.6     | C61-C60-H60B  | 108.6     |
| H60A-C60-H60B | 107.5     | C62-C61-C60   | 108.1(11) |
| C62A-C61-C60  | 114.3(11) | C62-C61-H61A  | 110.1     |
| C60-C61-H61A  | 110.1     | C62-C61-H61B  | 110.1     |
| C60-C61-H61B  | 110.1     | H61A-C61-H61B | 108.4     |
| C62A-C61-H61C | 108.7     | C60-C61-H61C  | 108.7     |
| C62A-C61-H61D | 108.7     | C60-C61-H61D  | 108.7     |
| H61C-C61-H61D | 107.6     | C64-C63-P2    | 120.5(6)  |
| C64-C63-H63A  | 107.2     | P2-C63-H63A   | 107.2     |
| C64-C63-H63B  | 107.2     | P2-C63-H63B   | 107.2     |

|               |           |               |           |
|---------------|-----------|---------------|-----------|
| H63A-C63-H63B | 106.8     | C65A-C64-C63  | 125.0(14) |
| C63-C64-C65   | 104.1(9)  | C63-C64-H64A  | 110.9     |
| C65-C64-H64A  | 110.9     | C63-C64-H64B  | 110.9     |
| C65-C64-H64B  | 110.9     | H64A-C64-H64B | 109.0     |
| C65A-C64-H64C | 106.1     | C63-C64-H64C  | 106.1     |
| C65A-C64-H64D | 106.1     | C63-C64-H64D  | 106.1     |
| H64C-C64-H64D | 106.3     | O7-C67-C69    | 121.2(8)  |
| O7-C67-C68    | 121.8(8)  | C69-C67-C68   | 117.0(7)  |
| C67-C68-H68A  | 109.5     | C67-C68-H68B  | 109.5     |
| H68A-C68-H68B | 109.5     | C67-C68-H68C  | 109.5     |
| H68A-C68-H68C | 109.5     | H68B-C68-H68C | 109.5     |
| C67-C69-H69A  | 109.5     | C67-C69-H69B  | 109.5     |
| H69A-C69-H69B | 109.5     | C67-C69-H69C  | 109.5     |
| H69A-C69-H69C | 109.5     | H69B-C69-H69C | 109.5     |
| N6-B1-N4      | 106.2(6)  | N6-B1-N2      | 108.1(6)  |
| N4-B1-N2      | 109.7(6)  | N6-B1-H1A     | 113.(4)   |
| N4-B1-H1A     | 111.(4)   | N2-B1-H1A     | 109.(4)   |
| N9-B2-N13     | 109.4(6)  | N9-B2-N11     | 110.3(7)  |
| N13-B2-N11    | 106.9(6)  | N9-B2-H2      | 112.(3)   |
| N13-B2-H2     | 107.(3)   | N11-B2-H2     | 111.(3)   |
| C53-O6-C54    | 119.(2)   | C51-C50-C53   | 101.(2)   |
| C51-C50-C52   | 106.(3)   | C53-C50-C52   | 100.(2)   |
| C51-C50-C45   | 109.(2)   | C53-C50-C45   | 120.7(18) |
| C52-C50-C45   | 117.8(17) | C50-C51-H51A  | 109.5     |
| C50-C51-H51B  | 109.5     | H51A-C51-H51B | 109.5     |



|                |           |                |           |
|----------------|-----------|----------------|-----------|
| C50-C51-H51C   | 109.5     | H51A-C51-H51C  | 109.5     |
| H51B-C51-H51C  | 109.5     | C50-C52-H52A   | 109.5     |
| C50-C52-H52B   | 109.5     | H52A-C52-H52B  | 109.5     |
| C50-C52-H52C   | 109.5     | H52A-C52-H52C  | 109.5     |
| H52B-C52-H52C  | 109.5     | O5-C53-O6      | 118.(3)   |
| O5-C53-C50     | 133.(3)   | O6-C53-C50     | 109.2(19) |
| O6-C54-H54A    | 109.5     | O6-C54-H54B    | 109.5     |
| H54A-C54-H54B  | 109.5     | O6-C54-H54C    | 109.5     |
| H54A-C54-H54C  | 109.5     | H54B-C54-H54C  | 109.5     |
| C61-C62-H62A   | 109.5     | C61-C62-H62B   | 109.5     |
| H62A-C62-H62B  | 109.5     | C61-C62-H62C   | 109.5     |
| H62A-C62-H62C  | 109.5     | H62B-C62-H62C  | 109.5     |
| C66-C65-C64    | 113.7(14) | C66-C65-H65A   | 108.8     |
| C64-C65-H65A   | 108.8     | C66-C65-H65B   | 108.8     |
| C64-C65-H65B   | 108.8     | H65A-C65-H65B  | 107.7     |
| C65-C66-H66A   | 109.5     | C65-C66-H66B   | 109.5     |
| H66A-C66-H66B  | 109.5     | C65-C66-H66C   | 109.5     |
| H66A-C66-H66C  | 109.5     | H66B-C66-H66C  | 109.5     |
| C53A-O6A-C54A  | 116.2(10) | C53A-C50A-C51A | 107.7(10) |
| C53A-C50A-C52A | 106.0(10) | C51A-C50A-C52A | 111.3(12) |
| C53A-C50A-C45  | 100.4(9)  | C51A-C50A-C45  | 117.8(10) |
| C52A-C50A-C45  | 112.4(9)  | C50A-C51A-H51D | 109.5     |
| C50A-C51A-H51E | 109.5     | H51D-C51A-H51E | 109.5     |
| C50A-C51A-H51F | 109.5     | H51D-C51A-H51F | 109.5     |
| H51E-C51A-H51F | 109.5     | C50A-C52A-H52D | 109.5     |

|                |           |                |           |
|----------------|-----------|----------------|-----------|
| C50A-C52A-H52E | 109.5     | H52D-C52A-H52E | 109.5     |
| C50A-C52A-H52F | 109.5     | H52D-C52A-H52F | 109.5     |
| H52E-C52A-H52F | 109.5     | O5A-C53A-O6A   | 118.6(15) |
| O5A-C53A-C50A  | 129.1(13) | O6A-C53A-C50A  | 112.3(11) |
| O6A-C54A-H54D  | 109.5     | O6A-C54A-H54E  | 109.5     |
| H54D-C54A-H54E | 109.5     | O6A-C54A-H54F  | 109.5     |
| H54D-C54A-H54F | 109.5     | H54E-C54A-H54F | 109.5     |
| C61-C62A-H62D  | 109.5     | C61-C62A-H62E  | 109.5     |
| H62D-C62A-H62E | 109.5     | C61-C62A-H62F  | 109.5     |
| H62D-C62A-H62F | 109.5     | H62E-C62A-H62F | 109.5     |
| C66A-C65A-C64  | 108.6(18) | C66A-C65A-H65C | 110.0     |
| C64-C65A-H65C  | 110.0     | C66A-C65A-H65D | 110.0     |
| C64-C65A-H65D  | 110.0     | H65C-C65A-H65D | 108.3     |
| C65A-C66A-H66D | 109.5     | C65A-C66A-H66E | 109.5     |
| H66D-C66A-H66E | 109.5     | C65A-C66A-H66F | 109.5     |
| H66D-C66A-H66F | 109.5     | H66E-C66A-H66F | 109.5     |

**Table 6. Torsion angles (°) for Harman\_16JAS235.**

|               |           |              |           |
|---------------|-----------|--------------|-----------|
| C1-N1-N2-C3   | -0.5(7)   | W1-N1-N2-C3  | -172.2(4) |
| C1-N1-N2-B1   | -172.1(6) | W1-N1-N2-B1  | 16.3(8)   |
| C4-N3-N4-C6   | 0.3(7)    | W1-N3-N4-C6  | -171.1(5) |
| C4-N3-N4-B1   | 167.0(6)  | W1-N3-N4-B1  | -4.4(8)   |
| C7-N5-N6-C9   | -0.3(7)   | W1-N5-N6-C9  | -178.8(4) |
| C7-N5-N6-B1   | -175.2(6) | W1-N5-N6-B1  | 6.2(7)    |
| C34-N8-N9-C36 | -1.6(8)   | W2-N8-N9-C36 | 177.0(5)  |

|                 |           |                 |           |
|-----------------|-----------|-----------------|-----------|
| C34-N8-N9-B2    | 174.3(6)  | W2-N8-N9-B2     | -7.1(8)   |
| C37-N10-N11-C39 | 0.4(8)    | W2-N10-N11-C39  | 178.3(4)  |
| C37-N10-N11-B2  | -167.3(6) | W2-N10-N11-B2   | 10.6(8)   |
| C40-N12-N13-C42 | -0.6(8)   | W2-N12-N13-C42  | 178.9(5)  |
| C40-N12-N13-B2  | 172.0(6)  | W2-N12-N13-B2   | -8.5(8)   |
| N2-N1-C1-C2     | 0.8(7)    | W1-N1-C1-C2     | 170.5(5)  |
| N1-C1-C2-C3     | -0.7(8)   | N1-N2-C3-C2     | 0.1(8)    |
| B1-N2-C3-C2     | 170.9(6)  | C1-C2-C3-N2     | 0.4(8)    |
| N4-N3-C4-C5     | 0.1(8)    | W1-N3-C4-C5     | 170.7(5)  |
| N3-C4-C5-C6     | -0.5(9)   | N3-N4-C6-C5     | -0.6(8)   |
| B1-N4-C6-C5     | -165.6(7) | C4-C5-C6-N4     | 0.7(8)    |
| N6-N5-C7-C8     | -0.1(7)   | W1-N5-C7-C8     | 178.2(4)  |
| N5-C7-C8-C9     | 0.5(8)    | N5-N6-C9-C8     | 0.6(7)    |
| B1-N6-C9-C8     | 174.9(6)  | C7-C8-C9-N6     | -0.7(7)   |
| C15-C10-C11-C12 | 10.5(9)   | W1-C10-C11-C12  | 122.7(5)  |
| C15-C10-C11-W1  | -112.2(6) | C10-C11-C12-C13 | -33.7(8)  |
| W1-C11-C12-C13  | 55.4(7)   | C10-C11-C12-C17 | 91.5(7)   |
| W1-C11-C12-C17  | -179.5(5) | C11-C12-C13-C14 | 40.7(8)   |
| C17-C12-C13-C14 | -82.9(7)  | C12-C13-C14-C15 | -26.5(9)  |
| C12-C13-C14-C16 | 155.1(6)  | C16-C14-C15-C10 | 179.3(6)  |
| C13-C14-C15-C10 | 1.0(10)   | C11-C10-C15-C14 | 7.6(10)   |
| W1-C10-C15-C14  | -72.9(8)  | C15-C14-C16-F1  | -7.0(10)  |
| C13-C14-C16-F1  | 171.4(6)  | C15-C14-C16-F3  | 115.7(8)  |
| C13-C14-C16-F3  | -65.9(9)  | C15-C14-C16-F2  | -127.9(8) |
| C13-C14-C16-F2  | 50.5(9)   | C11-C12-C17-C20 | 68.7(7)   |

|                 |           |                  |           |
|-----------------|-----------|------------------|-----------|
| C13-C12-C17-C20 | -167.0(6) | C11-C12-C17-C18  | -52.8(8)  |
| C13-C12-C17-C18 | 71.4(8)   | C11-C12-C17-C19  | -175.7(6) |
| C13-C12-C17-C19 | -51.5(8)  | C21-O3-C20-O2    | -1.2(10)  |
| C21-O3-C20-C17  | 176.8(6)  | C18-C17-C20-O2   | 2.7(10)   |
| C19-C17-C20-O2  | 118.9(8)  | C12-C17-C20-O2   | -122.7(7) |
| C18-C17-C20-O3  | -175.1(6) | C19-C17-C20-O3   | -59.0(7)  |
| C12-C17-C20-O3  | 59.4(8)   | C26-P1-C22-C23   | -169.3(5) |
| C30-P1-C22-C23  | -63.3(6)  | W1-P1-C22-C23    | 64.3(5)   |
| P1-C22-C23-C24  | -171.5(5) | C22-C23-C24-C25  | -176.5(6) |
| C30-P1-C26-C27  | -155.6(6) | C22-P1-C26-C27   | -50.0(6)  |
| W1-P1-C26-C27   | 76.7(6)   | P1-C26-C27-C28   | -179.0(6) |
| C26-C27-C28-C29 | -176.5(8) | C26-P1-C30-C31   | 66.5(6)   |
| C22-P1-C30-C31  | -39.8(6)  | W1-P1-C30-C31    | -166.8(5) |
| P1-C30-C31-C32  | 178.3(5)  | C30-C31-C32-C33  | -172.4(6) |
| N9-N8-C34-C35   | 1.3(9)    | W2-N8-C34-C35    | -177.0(5) |
| N8-C34-C35-C36  | -0.6(10)  | N8-N9-C36-C35    | 1.3(9)    |
| B2-N9-C36-C35   | -174.2(8) | C34-C35-C36-N9   | -0.5(10)  |
| N11-N10-C37-C38 | -1.0(8)   | W2-N10-C37-C38   | -178.6(5) |
| N10-C37-C38-C39 | 1.1(8)    | N10-N11-C39-C38  | 0.3(8)    |
| B2-N11-C39-C38  | 166.2(7)  | C37-C38-C39-N11  | -0.8(8)   |
| N13-N12-C40-C41 | -0.2(8)   | W2-N12-C40-C41   | -179.6(5) |
| N12-C40-C41-C42 | 0.9(9)    | C40-C41-C42-N13  | -1.3(9)   |
| N12-N13-C42-C41 | 1.3(9)    | B2-N13-C42-C41   | -170.4(7) |
| C48-C43-C44-C45 | -5.7(9)   | W2-C43-C44-C45   | -124.2(6) |
| C48-C43-C44-W2  | 118.5(6)  | C43-C44-C45-C50A | -87.5(10) |

|                  |                |                 |                |
|------------------|----------------|-----------------|----------------|
| W2-C44-C45-C50A  | -179.3(7)      | C43-C44-C45-C46 | 29.9(9)        |
| W2-C44-C45-C46   | -61.9(9)       | C43-C44-C45-C50 | -<br>112.2(12) |
| W2-C44-C45-C50   | 156.0(11)      | C44-C45-C46-C47 | -41.7(9)       |
| C50A-C45-C46-C47 | 80.9(9)        | C50-C45-C46-C47 | 90.4(14)       |
| C45-C46-C47-C48  | 30.2(11)       | C45-C46-C47-C49 | -148.2(7)      |
| C49-C47-C48-C43  | 175.1(7)       | C46-C47-C48-C43 | -3.2(12)       |
| C44-C43-C48-C47  | -10.2(11)      | W2-C43-C48-C47  | 71.8(10)       |
| C48-C47-C49-F5   | -<br>109.2(11) | C46-C47-C49-F5  | 69.2(11)       |
| C48-C47-C49-F4   | 14.4(13)       | C46-C47-C49-F4  | -167.3(8)      |
| C48-C47-C49-F6   | 135.0(9)       | C46-C47-C49-F6  | -46.7(12)      |
| C63-P2-C55-C56   | -63.4(7)       | C59-P2-C55-C56  | -167.8(6)      |
| W2-P2-C55-C56    | 68.0(6)        | P2-C55-C56-C57  | 178.6(6)       |
| C55-C56-C57-C58  | 179.1(7)       | C55-P2-C59-C60  | 171.8(6)       |
| C63-P2-C59-C60   | 65.1(7)        | W2-P2-C59-C60   | -65.4(6)       |
| P2-C59-C60-C61   | 179.9(6)       | C59-C60-C61-C62 | 70.0(11)       |
| C59-C60-C61-C62A | 172.9(11)      | C55-P2-C63-C64  | -53.5(8)       |
| C59-P2-C63-C64   | 49.2(7)        | W2-P2-C63-C64   | 177.9(6)       |
| P2-C63-C64-C65A  | 158.8(14)      | P2-C63-C64-C65  | -<br>178.4(11) |
| C9-N6-B1-N4      | -117.9(7)      | N5-N6-B1-N4     | 55.9(7)        |
| C9-N6-B1-N2      | 124.4(7)       | N5-N6-B1-N2     | -61.8(8)       |
| C6-N4-B1-N6      | 106.6(8)       | N3-N4-B1-N6     | -57.2(8)       |
| C6-N4-B1-N2      | -136.9(7)      | N3-N4-B1-N2     | 59.4(8)        |
| C3-N2-B1-N6      | -121.6(7)      | N1-N2-B1-N6     | 48.3(8)        |

|                        |                |                        |                |
|------------------------|----------------|------------------------|----------------|
| C3-N2-B1-N4            | 123.0(7)       | N1-N2-B1-N4            | -67.1(8)       |
| C36-N9-B2-N13          | 120.2(8)       | N8-N9-B2-N13           | -54.8(8)       |
| C36-N9-B2-N11          | -122.5(8)      | N8-N9-B2-N11           | 62.5(8)        |
| C42-N13-B2-N9          | -124.5(8)      | N12-N13-B2-N9          | 64.6(8)        |
| C42-N13-B2-N11         | 116.1(8)       | N12-N13-B2-N11         | -54.8(9)       |
| C39-N11-B2-N9          | 130.2(8)       | N10-N11-B2-N9          | -64.9(8)       |
| C39-N11-B2-N13         | -111.0(8)      | N10-N11-B2-N13         | 54.0(9)        |
| C44-C45-C50-C51        | 76.(3)         | C46-C45-C50-C51        | -57.(3)        |
| C44-C45-C50-C53        | -41.(2)        | C46-C45-C50-C53        | -<br>174.2(15) |
| C44-C45-C50-C52        | -163.(2)       | C46-C45-C50-C52        | 63.(3)         |
| C54-O6-C53-O5          | -2.(4)         | C54-O6-C53-C50         | 173.(2)        |
| C51-C50-C53-O5         | -4.(4)         | C52-C50-C53-O5         | -113.(4)       |
| C45-C50-C53-O5         | 117.(3)        | C51-C50-C53-O6         | -179.(3)       |
| C52-C50-C53-O6         | 73.(2)         | C45-C50-C53-O6         | -58.(3)        |
| C63-C64-C65-C66        | -<br>178.0(17) | C44-C45-C50A-<br>C53A  | -73.5(10)      |
| C46-C45-C50A-<br>C53A  | 166.2(8)       | C44-C45-C50A-<br>C51A  | 43.0(15)       |
| C46-C45-C50A-<br>C51A  | -77.3(13)      | C44-C45-C50A-<br>C52A  | 174.2(10)      |
| C46-C45-C50A-<br>C52A  | 53.9(12)       | C54A-O6A-C53A-<br>O5A  | 2.9(18)        |
| C54A-O6A-C53A-<br>C50A | -<br>178.4(10) | C51A-C50A-C53A-<br>O5A | -4.7(19)       |
| C52A-C50A-C53A-<br>O5A | -<br>123.9(15) | C45-C50A-C53A-<br>O5A  | 119.0(15)      |

|                    |           |                    |          |
|--------------------|-----------|--------------------|----------|
| C51A-C50A-C53A-O6A | 176.7(11) | C52A-C50A-C53A-O6A | 57.5(12) |
| C45-C50A-C53A-O6A  | -59.6(11) | C63-C64-C65A-C66A  | 53.(3)   |

**Table 7. Anisotropic atomic displacement parameters ( $\text{\AA}^2$ ) for Harman\_16JAS235.**

The anisotropic atomic displacement factor exponent takes the form: -  
 $2\pi^2 [ h^2 a^{*2} U_{11} + \dots + 2 h k a^* b^* U_{12} ]$

|    | $U_{11}$    | $U_{22}$    | $U_{33}$    | $U_{23}$    | $U_{13}$    | $U_{12}$    |
|----|-------------|-------------|-------------|-------------|-------------|-------------|
| W1 | 0.02198(18) | 0.02594(19) | 0.01647(17) | 0.00382(14) | 0.00702(13) | 0.00256(14) |
| W2 | 0.02528(19) | 0.0305(2)   | 0.01758(18) | 0.00472(14) | 0.00720(13) | 0.00092(15) |
| P1 | 0.0257(11)  | 0.0277(12)  | 0.0222(11)  | 0.0044(9)   | 0.0072(8)   | 0.0045(9)   |
| P2 | 0.0414(13)  | 0.0299(12)  | 0.0242(11)  | 0.0090(9)   | 0.0104(9)   | 0.0055(10)  |
| F1 | 0.068(4)    | 0.047(4)    | 0.075(4)    | 0.018(3)    | -0.024(3)   | -0.018(3)   |
| F2 | 0.055(3)    | 0.060(3)    | 0.030(3)    | 0.008(2)    | -0.005(2)   | -0.003(2)   |
| F3 | 0.025(3)    | 0.123(5)    | 0.070(4)    | -0.001(3)   | 0.000(3)    | 0.000(3)    |
| F4 | 0.123(5)    | 0.063(4)    | 0.052(4)    | 0.006(3)    | -0.015(3)   | -0.034(4)   |
| F5 | 0.089(5)    | 0.162(7)    | 0.061(4)    | 0.010(4)    | -0.021(3)   | -0.074(5)   |
| F6 | 0.095(4)    | 0.104(5)    | 0.034(3)    | 0.020(3)    | -0.013(3)   | -0.033(4)   |
| O1 | 0.031(3)    | 0.039(3)    | 0.020(3)    | 0.001(2)    | 0.001(2)    | -0.001(2)   |
| O2 | 0.036(3)    | 0.059(4)    | 0.031(3)    | 0.008(3)    | 0.007(3)    | 0.009(3)    |
| O3 | 0.045(3)    | 0.034(3)    | 0.034(3)    | 0.005(3)    | 0.002(3)    | -0.003(3)   |
| O4 | 0.049(3)    | 0.039(3)    | 0.018(3)    | 0.008(2)    | 0.012(2)    | -0.002(3)   |
| O7 | 0.044(4)    | 0.052(4)    | 0.048(4)    | 0.010(3)    | 0.021(3)    | 0.002(3)    |
| N1 | 0.026(3)    | 0.033(4)    | 0.016(3)    | 0.005(3)    | 0.004(3)    | 0.004(3)    |

|     | <b>U<sub>11</sub></b> | <b>U<sub>22</sub></b> | <b>U<sub>33</sub></b> | <b>U<sub>23</sub></b> | <b>U<sub>13</sub></b> | <b>U<sub>12</sub></b> |
|-----|-----------------------|-----------------------|-----------------------|-----------------------|-----------------------|-----------------------|
| N2  | 0.020(3)              | 0.029(4)              | 0.020(3)              | 0.001(3)              | 0.006(3)              | 0.002(3)              |
| N3  | 0.018(3)              | 0.032(4)              | 0.026(3)              | 0.005(3)              | 0.007(3)              | 0.005(3)              |
| N4  | 0.023(3)              | 0.027(4)              | 0.018(3)              | 0.007(3)              | 0.005(3)              | 0.004(3)              |
| N5  | 0.023(3)              | 0.029(4)              | 0.015(3)              | 0.002(3)              | 0.002(3)              | 0.002(3)              |
| N6  | 0.025(3)              | 0.020(4)              | 0.015(3)              | 0.002(3)              | 0.004(3)              | -0.003(3)             |
| N7  | 0.022(3)              | 0.026(4)              | 0.021(4)              | 0.008(3)              | 0.004(3)              | 0.006(3)              |
| N8  | 0.029(4)              | 0.045(4)              | 0.012(3)              | 0.001(3)              | 0.002(3)              | -0.006(3)             |
| N9  | 0.038(4)              | 0.042(4)              | 0.017(4)              | -0.005(3)             | 0.009(3)              | -0.003(3)             |
| N10 | 0.020(3)              | 0.031(4)              | 0.013(3)              | -0.008(3)             | -0.002(2)             | 0.000(3)              |
| N11 | 0.021(3)              | 0.033(4)              | 0.020(3)              | -0.002(3)             | 0.005(3)              | -0.004(3)             |
| N12 | 0.028(4)              | 0.041(4)              | 0.026(4)              | -0.001(3)             | 0.009(3)              | 0.004(3)              |
| N13 | 0.033(4)              | 0.042(4)              | 0.023(4)              | 0.001(3)              | 0.011(3)              | 0.005(3)              |
| N14 | 0.030(4)              | 0.025(4)              | 0.020(3)              | 0.005(3)              | 0.004(3)              | -0.001(3)             |
| C1  | 0.029(4)              | 0.029(4)              | 0.022(4)              | 0.009(3)              | 0.015(3)              | 0.008(3)              |
| C2  | 0.032(4)              | 0.035(5)              | 0.016(4)              | 0.008(3)              | 0.001(3)              | 0.010(4)              |
| C3  | 0.022(4)              | 0.027(4)              | 0.021(4)              | -0.001(3)             | 0.000(3)              | -0.001(3)             |
| C4  | 0.033(4)              | 0.030(5)              | 0.015(4)              | -0.004(3)             | 0.008(3)              | -0.001(3)             |
| C5  | 0.032(5)              | 0.041(5)              | 0.027(4)              | 0.011(4)              | 0.019(4)              | 0.004(4)              |
| C6  | 0.022(4)              | 0.036(5)              | 0.032(5)              | 0.009(4)              | 0.014(3)              | 0.003(3)              |
| C7  | 0.023(4)              | 0.034(5)              | 0.034(5)              | 0.012(4)              | 0.011(3)              | 0.009(4)              |
| C8  | 0.031(5)              | 0.029(5)              | 0.031(5)              | 0.004(4)              | 0.011(4)              | 0.004(4)              |
| C9  | 0.031(4)              | 0.027(5)              | 0.022(4)              | 0.001(3)              | 0.012(3)              | 0.000(3)              |
| C10 | 0.024(4)              | 0.038(5)              | 0.017(4)              | 0.004(4)              | 0.010(3)              | 0.008(3)              |
| C11 | 0.024(4)              | 0.030(5)              | 0.011(4)              | 0.004(3)              | 0.004(3)              | 0.000(3)              |



|     | <b>U<sub>11</sub></b> | <b>U<sub>22</sub></b> | <b>U<sub>33</sub></b> | <b>U<sub>23</sub></b> | <b>U<sub>13</sub></b> | <b>U<sub>12</sub></b> |
|-----|-----------------------|-----------------------|-----------------------|-----------------------|-----------------------|-----------------------|
| C12 | 0.022(4)              | 0.037(5)              | 0.015(4)              | 0.011(3)              | 0.006(3)              | 0.004(3)              |
| C13 | 0.023(4)              | 0.047(5)              | 0.025(4)              | 0.012(4)              | 0.007(3)              | 0.010(4)              |
| C14 | 0.025(4)              | 0.034(5)              | 0.020(4)              | 0.003(3)              | 0.005(3)              | 0.003(3)              |
| C15 | 0.027(4)              | 0.030(5)              | 0.020(4)              | -0.002(3)             | 0.012(3)              | 0.002(3)              |
| C16 | 0.035(5)              | 0.061(7)              | 0.033(5)              | 0.004(5)              | 0.004(4)              | 0.002(5)              |
| C17 | 0.034(5)              | 0.045(5)              | 0.022(4)              | 0.006(4)              | 0.013(4)              | 0.007(4)              |
| C18 | 0.034(5)              | 0.048(6)              | 0.035(5)              | 0.012(4)              | 0.021(4)              | 0.008(4)              |
| C19 | 0.023(4)              | 0.047(5)              | 0.035(5)              | -0.008(4)             | 0.004(4)              | 0.011(4)              |
| C20 | 0.023(4)              | 0.047(6)              | 0.030(5)              | 0.000(4)              | 0.010(4)              | 0.019(4)              |
| C21 | 0.045(5)              | 0.046(6)              | 0.057(6)              | -0.001(5)             | 0.001(5)              | -0.001(4)             |
| C22 | 0.032(4)              | 0.023(4)              | 0.030(4)              | 0.009(3)              | 0.013(3)              | 0.006(3)              |
| C23 | 0.033(4)              | 0.024(4)              | 0.028(4)              | 0.005(3)              | 0.009(3)              | 0.000(3)              |
| C24 | 0.027(4)              | 0.035(5)              | 0.046(5)              | 0.011(4)              | 0.017(4)              | 0.010(4)              |
| C25 | 0.035(5)              | 0.046(6)              | 0.067(6)              | 0.004(5)              | 0.009(5)              | 0.009(4)              |
| C26 | 0.034(5)              | 0.038(5)              | 0.027(4)              | 0.004(4)              | 0.011(3)              | 0.005(4)              |
| C27 | 0.039(5)              | 0.034(5)              | 0.027(4)              | -0.002(4)             | 0.004(4)              | 0.000(4)              |
| C28 | 0.107(8)              | 0.052(6)              | 0.026(5)              | -0.009(4)             | 0.005(5)              | -0.026(6)             |
| C29 | 0.118(10)             | 0.110(10)             | 0.044(7)              | -0.013(7)             | 0.019(6)              | -0.021(8)             |
| C30 | 0.025(4)              | 0.025(4)              | 0.028(4)              | 0.005(3)              | 0.005(3)              | 0.005(3)              |
| C31 | 0.032(5)              | 0.031(5)              | 0.042(5)              | 0.010(4)              | 0.009(4)              | 0.004(4)              |
| C32 | 0.032(4)              | 0.038(5)              | 0.033(5)              | 0.013(4)              | -0.001(4)             | 0.000(4)              |
| C33 | 0.051(6)              | 0.034(5)              | 0.049(6)              | 0.014(4)              | -0.005(4)             | 0.006(4)              |
| C34 | 0.045(5)              | 0.062(6)              | 0.019(4)              | 0.013(4)              | 0.012(4)              | -0.012(4)             |
| C35 | 0.053(6)              | 0.071(7)              | 0.021(5)              | 0.012(4)              | 0.009(4)              | -0.022(5)             |

|     | <b>U<sub>11</sub></b> | <b>U<sub>22</sub></b> | <b>U<sub>33</sub></b> | <b>U<sub>23</sub></b> | <b>U<sub>13</sub></b> | <b>U<sub>12</sub></b> |
|-----|-----------------------|-----------------------|-----------------------|-----------------------|-----------------------|-----------------------|
| C36 | 0.041(5)              | 0.082(8)              | 0.020(5)              | -0.001(5)             | 0.012(4)              | -0.006(5)             |
| C37 | 0.030(4)              | 0.019(4)              | 0.026(4)              | 0.008(3)              | 0.010(3)              | 0.002(3)              |
| C38 | 0.018(4)              | 0.037(5)              | 0.036(5)              | 0.016(4)              | 0.003(3)              | -0.006(3)             |
| C39 | 0.034(5)              | 0.031(5)              | 0.026(4)              | 0.001(4)              | 0.000(4)              | 0.000(4)              |
| C40 | 0.030(5)              | 0.054(6)              | 0.032(5)              | 0.003(4)              | 0.002(4)              | 0.012(4)              |
| C41 | 0.053(6)              | 0.049(6)              | 0.058(6)              | 0.006(5)              | 0.018(5)              | 0.024(5)              |
| C42 | 0.047(6)              | 0.041(6)              | 0.057(6)              | -0.006(5)             | 0.024(5)              | 0.017(4)              |
| C43 | 0.032(5)              | 0.037(5)              | 0.030(5)              | 0.012(4)              | 0.010(4)              | -0.010(4)             |
| C44 | 0.028(4)              | 0.042(5)              | 0.031(5)              | 0.016(4)              | 0.009(4)              | -0.005(4)             |
| C45 | 0.023(5)              | 0.069(7)              | 0.055(6)              | 0.031(5)              | 0.004(4)              | -0.008(4)             |
| C46 | 0.035(5)              | 0.081(8)              | 0.055(7)              | 0.028(6)              | -0.005(4)             | -0.016(5)             |
| C47 | 0.049(5)              | 0.053(6)              | 0.028(5)              | 0.014(4)              | -0.006(4)             | -0.027(5)             |
| C48 | 0.038(5)              | 0.055(6)              | 0.026(5)              | 0.012(4)              | 0.004(4)              | -0.015(4)             |
| C49 | 0.066(7)              | 0.073(8)              | 0.028(6)              | 0.003(5)              | -0.009(5)             | -0.018(6)             |
| C55 | 0.054(5)              | 0.037(5)              | 0.019(4)              | 0.006(4)              | 0.016(4)              | 0.013(4)              |
| C56 | 0.077(6)              | 0.027(5)              | 0.022(4)              | 0.004(4)              | 0.022(4)              | 0.009(4)              |
| C57 | 0.112(8)              | 0.036(6)              | 0.033(5)              | 0.014(4)              | 0.026(5)              | 0.017(6)              |
| C58 | 0.130(10)             | 0.042(6)              | 0.030(5)              | 0.005(5)              | 0.013(6)              | 0.010(6)              |
| C59 | 0.051(5)              | 0.034(5)              | 0.037(5)              | 0.019(4)              | 0.015(4)              | 0.014(4)              |
| C60 | 0.033(5)              | 0.059(6)              | 0.041(5)              | 0.018(5)              | -0.001(4)             | 0.010(4)              |
| C61 | 0.039(6)              | 0.072(8)              | 0.070(7)              | 0.031(6)              | -0.009(5)             | -0.003(5)             |
| C63 | 0.055(6)              | 0.042(6)              | 0.036(5)              | 0.020(4)              | 0.005(4)              | -0.002(4)             |
| C64 | 0.139(10)             | 0.031(6)              | 0.036(6)              | 0.018(4)              | 0.007(6)              | 0.025(6)              |
| C67 | 0.046(6)              | 0.038(5)              | 0.025(5)              | 0.013(4)              | 0.007(4)              | 0.003(4)              |

|      | <b>U<sub>11</sub></b> | <b>U<sub>22</sub></b> | <b>U<sub>33</sub></b> | <b>U<sub>23</sub></b> | <b>U<sub>13</sub></b> | <b>U<sub>12</sub></b> |
|------|-----------------------|-----------------------|-----------------------|-----------------------|-----------------------|-----------------------|
| C68  | 0.044(5)              | 0.046(6)              | 0.031(5)              | 0.003(4)              | -0.004(4)             | -0.001(4)             |
| C69  | 0.056(6)              | 0.041(6)              | 0.041(5)              | 0.001(4)              | 0.000(4)              | 0.005(4)              |
| B1   | 0.024(5)              | 0.035(6)              | 0.023(5)              | 0.007(4)              | 0.006(4)              | 0.001(4)              |
| B2   | 0.023(5)              | 0.051(6)              | 0.015(5)              | -0.007(4)             | 0.000(4)              | 0.001(4)              |
| O5   | 0.036(14)             | 0.066(16)             | 0.027(16)             | 0.027(16)             | 0.019(13)             | 0.018(11)             |
| O6   | 0.055(6)              | 0.031(5)              | 0.057(6)              | 0.001(4)              | 0.027(4)              | 0.009(4)              |
| C50  | 0.020(4)              | 0.040(6)              | 0.060(8)              | 0.018(6)              | 0.014(4)              | 0.005(4)              |
| C51  | 0.035(9)              | 0.023(10)             | 0.066(8)              | 0.003(10)             | 0.023(6)              | -0.008(8)             |
| C52  | 0.029(6)              | 0.069(10)             | 0.067(10)             | 0.029(7)              | 0.005(6)              | 0.006(7)              |
| C53  | 0.020(4)              | 0.040(6)              | 0.060(8)              | 0.018(6)              | 0.014(4)              | 0.005(4)              |
| C54  | 0.081(10)             | 0.032(7)              | 0.089(11)             | -0.005(7)             | 0.061(8)              | 0.002(7)              |
| C62  | 0.037(11)             | 0.066(14)             | 0.108(17)             | 0.054(12)             | 0.034(11)             | 0.031(10)             |
| C65  | 0.158(12)             | 0.064(8)              | 0.088(11)             | 0.050(7)              | 0.078(8)              | 0.066(8)              |
| C66  | 0.158(12)             | 0.064(8)              | 0.088(11)             | 0.050(7)              | 0.078(8)              | 0.066(8)              |
| O5A  | 0.073(10)             | 0.059(8)              | 0.041(9)              | 0.015(9)              | 0.029(9)              | 0.014(7)              |
| O6A  | 0.055(6)              | 0.031(5)              | 0.057(6)              | 0.001(4)              | 0.027(4)              | 0.009(4)              |
| C50A | 0.020(4)              | 0.040(6)              | 0.060(8)              | 0.018(6)              | 0.014(4)              | 0.005(4)              |
| C51A | 0.035(9)              | 0.023(10)             | 0.066(8)              | 0.003(10)             | 0.023(6)              | -0.008(8)             |
| C52A | 0.029(6)              | 0.069(10)             | 0.067(10)             | 0.029(7)              | 0.005(6)              | 0.006(7)              |
| C53A | 0.020(4)              | 0.040(6)              | 0.060(8)              | 0.018(6)              | 0.014(4)              | 0.005(4)              |
| C54A | 0.081(10)             | 0.032(7)              | 0.089(11)             | -0.005(7)             | 0.061(8)              | 0.002(7)              |
| C62A | 0.099(18)             | 0.061(15)             | 0.071(17)             | 0.002(12)             | -0.061(13)            | 0.011(13)             |
| C65A | 0.158(12)             | 0.064(8)              | 0.088(11)             | 0.050(7)              | 0.078(8)              | 0.066(8)              |
| C66A | 0.158(12)             | 0.064(8)              | 0.088(11)             | 0.050(7)              | 0.078(8)              | 0.066(8)              |

**Table 8. Hydrogen atomic coordinates and isotropic atomic displacement parameters ( $\text{\AA}^2$ ) for Harman\_16JAS235.**

|      | x/a      | y/b      | z/c      | U(eq) |
|------|----------|----------|----------|-------|
| H1   | 0.9006   | 0.8239   | 0.9683   | 0.03  |
| H2A  | 1.0570   | 0.8723   | 1.0427   | 0.032 |
| H3   | 1.1852   | 0.9646   | 0.9875   | 0.029 |
| H4   | 1.0272   | 0.8160   | 0.6862   | 0.032 |
| H5   | 1.2096   | 0.8782   | 0.6761   | 0.039 |
| H6   | 1.2742   | 0.9778   | 0.7779   | 0.035 |
| H7   | 0.8266   | 1.0928   | 0.7937   | 0.035 |
| H8   | 0.9437   | 1.2422   | 0.8274   | 0.036 |
| H9   | 1.1091   | 1.1991   | 0.8703   | 0.032 |
| H10  | 0.769(5) | 0.799(5) | 0.892(3) | 0.031 |
| H11  | 0.7745   | 0.9510   | 0.8976   | 0.027 |
| H12  | 0.6934   | 1.0144   | 0.8081   | 0.029 |
| H13A | 0.5459   | 0.9034   | 0.7543   | 0.036 |
| H13B | 0.6572   | 0.8961   | 0.7303   | 0.036 |
| H15  | 0.6558   | 0.6924   | 0.8184   | 0.031 |
| H18A | 0.5099   | 0.8475   | 0.8786   | 0.056 |
| H18B | 0.4982   | 0.9218   | 0.9374   | 0.056 |
| H18C | 0.6046   | 0.8812   | 0.9302   | 0.056 |
| H19A | 0.5122   | 1.0577   | 0.8133   | 0.053 |
| H19B | 0.4472   | 1.0370   | 0.8709   | 0.053 |
| H19C | 0.4477   | 0.9571   | 0.8135   | 0.053 |

|      | <b>x/a</b> | <b>y/b</b> | <b>z/c</b> | <b>U(eq)</b> |
|------|------------|------------|------------|--------------|
| H21A | 0.7205     | 1.2720     | 0.9056     | 0.076        |
| H21B | 0.7724     | 1.2108     | 0.9511     | 0.076        |
| H21C | 0.6592     | 1.2358     | 0.9609     | 0.076        |
| H22A | 1.0337     | 0.6038     | 0.7878     | 0.033        |
| H22B | 1.0637     | 0.6962     | 0.7576     | 0.033        |
| H23A | 1.1121     | 0.7773     | 0.8611     | 0.034        |
| H23B | 1.0952     | 0.6789     | 0.8859     | 0.034        |
| H24A | 1.2443     | 0.7316     | 0.8035     | 0.041        |
| H24B | 1.2251     | 0.6304     | 0.8241     | 0.041        |
| H25A | 1.3700     | 0.7199     | 0.8833     | 0.073        |
| H25B | 1.2818     | 0.6948     | 0.9283     | 0.073        |
| H25C | 1.3005     | 0.7963     | 0.9079     | 0.073        |
| H26A | 0.8239     | 0.5626     | 0.7464     | 0.039        |
| H26B | 0.7609     | 0.6453     | 0.7350     | 0.039        |
| H27A | 0.8803     | 0.6942     | 0.6639     | 0.041        |
| H27B | 0.9418     | 0.6099     | 0.6748     | 0.041        |
| H28A | 0.7357     | 0.5900     | 0.6201     | 0.08         |
| H28B | 0.7923     | 0.5041     | 0.6340     | 0.08         |
| H29A | 0.7969     | 0.5251     | 0.5285     | 0.143        |
| H29B | 0.9115     | 0.5384     | 0.5614     | 0.143        |
| H29C | 0.8591     | 0.6273     | 0.5487     | 0.143        |
| H30A | 0.8970     | 0.6840     | 0.9078     | 0.031        |
| H30B | 0.7918     | 0.6373     | 0.8689     | 0.031        |
| H31A | 0.8665     | 0.5034     | 0.8362     | 0.041        |

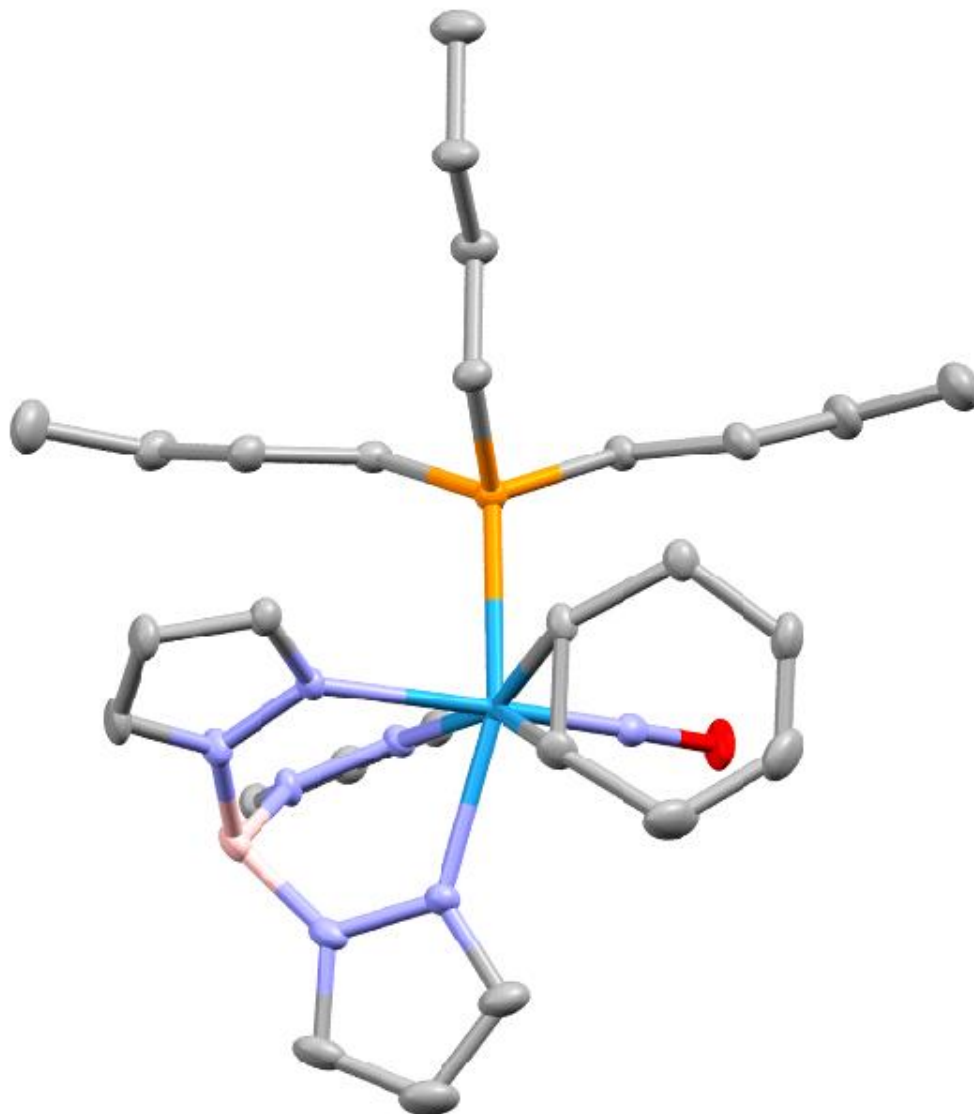
|      | <b>x/a</b> | <b>y/b</b> | <b>z/c</b> | <b>U(eq)</b> |
|------|------------|------------|------------|--------------|
| H31B | 0.9737     | 0.5504     | 0.8734     | 0.041        |
| H32A | 0.8874     | 0.5550     | 0.9677     | 0.041        |
| H32B | 0.7877     | 0.4962     | 0.9282     | 0.041        |
| H33A | 0.8802     | 0.3711     | 0.9051     | 0.067        |
| H33B | 0.8803     | 0.3978     | 0.9787     | 0.067        |
| H33C | 0.9803     | 0.4299     | 0.9444     | 0.067        |
| H34  | 0.3505     | 0.3266     | 0.5419     | 0.051        |
| H35  | 0.2925     | 0.2668     | 0.4301     | 0.06         |
| H36  | 0.2006     | 0.1067     | 0.4282     | 0.059        |
| H37  | 0.0657     | 0.1210     | 0.7261     | 0.029        |
| H38  | -0.0760    | 0.0039     | 0.6678     | 0.036        |
| H39  | -0.0151    | -0.0437    | 0.5632     | 0.038        |
| H40  | 0.4424     | 0.0258     | 0.6970     | 0.046        |
| H41  | 0.4344     | -0.1290    | 0.6277     | 0.062        |
| H42  | 0.3072     | -0.1251    | 0.5387     | 0.057        |
| H43  | 0.409(5)   | 0.361(5)   | 0.633(3)   | 0.04         |
| H44  | 0.4815     | 0.2217     | 0.6223     | 0.04         |
| H45  | 0.5248     | 0.1525     | 0.7185     | 0.058        |
| H45A | 0.5394     | 0.1510     | 0.7158     | 0.058        |
| H46A | 0.4770     | 0.2366     | 0.7986     | 0.07         |
| H46B | 0.5968     | 0.2774     | 0.8056     | 0.07         |
| H48  | 0.4330     | 0.4477     | 0.7316     | 0.049        |
| H55A | 0.0929     | 0.3979     | 0.7553     | 0.043        |
| H55B | 0.1153     | 0.2996     | 0.7724     | 0.043        |

|      | <b>x/a</b> | <b>y/b</b> | <b>z/c</b> | <b>U(eq)</b> |
|------|------------|------------|------------|--------------|
| H56A | 0.2650     | 0.4615     | 0.7889     | 0.049        |
| H56B | 0.2855     | 0.3631     | 0.8072     | 0.049        |
| H57A | 0.1452     | 0.4735     | 0.8655     | 0.07         |
| H57B | 0.1638     | 0.3744     | 0.8834     | 0.07         |
| H58A | 0.3374     | 0.4370     | 0.9180     | 0.101        |
| H58B | 0.2579     | 0.4901     | 0.9564     | 0.101        |
| H58C | 0.3146     | 0.5365     | 0.9028     | 0.101        |
| H59A | 0.0148     | 0.2393     | 0.6524     | 0.045        |
| H59B | 0.0108     | 0.3469     | 0.6494     | 0.045        |
| H60A | 0.0840     | 0.2253     | 0.5549     | 0.052        |
| H60B | 0.0797     | 0.3329     | 0.5519     | 0.052        |
| H61A | -0.0606    | 0.2308     | 0.4901     | 0.072        |
| H61B | -0.1033    | 0.2027     | 0.5536     | 0.072        |
| H61C | -0.0953    | 0.1925     | 0.5458     | 0.072        |
| H61D | -0.1054    | 0.3005     | 0.5510     | 0.072        |
| H63A | 0.2920     | 0.4619     | 0.6753     | 0.053        |
| H63B | 0.2405     | 0.4224     | 0.6073     | 0.053        |
| H64A | 0.1465     | 0.5326     | 0.6985     | 0.08         |
| H64B | 0.0920     | 0.4909     | 0.6303     | 0.08         |
| H64C | 0.1058     | 0.4945     | 0.6194     | 0.08         |
| H64D | 0.1226     | 0.5079     | 0.6930     | 0.08         |
| H68A | 0.4412     | 0.1798     | 0.9705     | 0.062        |
| H68B | 0.4302     | 0.2459     | 0.9181     | 0.062        |
| H68C | 0.3415     | 0.1610     | 0.9218     | 0.062        |

|      | <b>x/a</b> | <b>y/b</b> | <b>z/c</b> | <b>U(eq)</b> |
|------|------------|------------|------------|--------------|
| H69A | 0.3628     | 0.3859     | 1.0545     | 0.07         |
| H69B | 0.4571     | 0.3778     | 1.0121     | 0.07         |
| H69C | 0.4403     | 0.3132     | 1.0655     | 0.07         |
| H1A  | 1.188(5)   | 1.039(5)   | 0.884(3)   | 0.033        |
| H2   | 0.165(4)   | -0.025(4)  | 0.506(3)   | 0.018(16)    |
| H51A | 0.6438     | 0.3440     | 0.6454     | 0.063        |
| H51B | 0.7575     | 0.3165     | 0.6510     | 0.063        |
| H51C | 0.7064     | 0.3548     | 0.7121     | 0.063        |
| H52A | 0.7438     | 0.1962     | 0.7537     | 0.08         |
| H52B | 0.8010     | 0.1962     | 0.6911     | 0.08         |
| H52C | 0.7217     | 0.1075     | 0.7011     | 0.08         |
| H54A | 0.5377     | 0.0463     | 0.5215     | 0.1          |
| H54B | 0.5460     | -0.0441    | 0.5544     | 0.1          |
| H54C | 0.6465     | 0.0102     | 0.5306     | 0.1          |
| H62A | -0.1285    | 0.3529     | 0.5861     | 0.095        |
| H62B | -0.1796    | 0.3273     | 0.5161     | 0.095        |
| H62C | -0.0690    | 0.3902     | 0.5304     | 0.095        |
| H65A | 0.2902     | 0.6065     | 0.6510     | 0.111        |
| H65B | 0.2330     | 0.5673     | 0.5839     | 0.111        |
| H66A | 0.1988     | 0.7149     | 0.6662     | 0.138        |
| H66B | 0.0990     | 0.6554     | 0.6270     | 0.138        |
| H66C | 0.1912     | 0.7023     | 0.5918     | 0.138        |
| H51D | 0.6215     | 0.3549     | 0.6426     | 0.063        |
| H51E | 0.7426     | 0.3619     | 0.6609     | 0.063        |



|      | <b>x/a</b> | <b>y/b</b> | <b>z/c</b> | <b>U(eq)</b> |
|------|------------|------------|------------|--------------|
| H51F | 0.6692     | 0.4002     | 0.7110     | 0.063        |
| H52D | 0.7429     | 0.3009     | 0.7827     | 0.08         |
| H52E | 0.8054     | 0.2467     | 0.7327     | 0.08         |
| H52F | 0.7192     | 0.1901     | 0.7674     | 0.08         |
| H54D | 0.6152     | 0.0095     | 0.5810     | 0.1          |
| H54E | 0.6854     | -0.0333    | 0.6296     | 0.1          |
| H54F | 0.7370     | 0.0428     | 0.5902     | 0.1          |
| H62D | -0.0605    | 0.3091     | 0.4539     | 0.121        |
| H62E | -0.1349    | 0.2120     | 0.4475     | 0.121        |
| H62F | -0.0125    | 0.2142     | 0.4501     | 0.121        |
| H65C | 0.1386     | 0.6482     | 0.6533     | 0.111        |
| H65D | 0.2414     | 0.6377     | 0.6942     | 0.111        |
| H66D | 0.2868     | 0.6876     | 0.6052     | 0.138        |
| H66E | 0.2096     | 0.6043     | 0.5650     | 0.138        |
| H66F | 0.3095     | 0.5829     | 0.6035     | 0.138        |



### Crystal Structure Report for [Harman\\_12JAS\\_159](#)

A [colorless block-like](#) specimen of  $C_{33}H_{51}BN_7OPW$ , approximate dimensions  $0.074$  mm x  $0.090$  mm x  $0.251$  mm, was coated with Paratone oil and mounted on a MiTeGen MicroLoop. The X-ray intensity data were measured on a Bruker Kappa APEXII Duo system equipped with a fine-focus sealed tube (Mo  $K_{\alpha}$ ,  $\lambda = 0.71073$  Å) and a graphite monochromator.

The total exposure time was 2.40 hours. The frames were integrated with the Bruker SAINT software package<sup>56</sup> using a narrow-frame algorithm. The integration of the data using a [triclinic](#) unit cell yielded a total of [35024](#) reflections to a maximum  $\theta$  angle of  $29.62^{\circ}$  ( $0.72$  Å resolution), of which [9750](#) were independent (average redundancy [3.592](#), completeness =  $100.0\%$ ,  $R_{int} = 5.82\%$ ,  $R_{sig} = 6.29\%$ ) and [7981](#) ( $81.86\%$ ) were greater than  $2\sigma(F^2)$ . The final cell constants of  $\underline{a} = 10.2939(9)$  Å,  $\underline{b} = 12.5693(11)$  Å,  $\underline{c} =$

<sup>56</sup> Bruker (2012). *Saint*; *SADABS*; *APEX3*. Bruker AXS Inc., Madison, Wisconsin, USA.

14.6205(13) Å,  $\alpha = 102.900(2)^\circ$ ,  $\beta = 103.194(2)^\circ$ ,  $\gamma = 101.886(2)^\circ$ , volume = 1728.2(3) Å<sup>3</sup>, are based upon the refinement of the XYZ-centroids of 9427 reflections above 20  $\sigma(I)$  with  $4.414^\circ < 2\theta < 52.41^\circ$ . Data were corrected for absorption effects using the Multi-Scan method (SADABS).<sup>1</sup> The ratio of minimum to maximum apparent transmission was 0.788. The calculated minimum and maximum transmission coefficients (based on crystal size) are 0.4800 and 0.7860.

The structure was solved and refined using the Bruker SHELXTL Software Package<sup>57</sup> within APEX3<sup>1</sup> and OLEX2,<sup>58</sup> using the space group P -1, with Z = 2 for the formula unit, C<sub>33</sub>H<sub>51</sub>BN<sub>7</sub>OPW. Non-hydrogen atoms were refined anisotropically. Hydrogen atoms were placed in geometrically calculated positions with  $U_{iso} = 1.2U_{equiv}$  of the parent atom ( $U_{iso} = 1.5 U_{equiv}$  for methyl), except for the B-H hydrogen atom. It was located in the diffraction map and refined isotropically. The final anisotropic full-matrix least-squares refinement on F<sup>2</sup> with 404 variables converged at R1 = 3.11%, for the observed data and wR2 = 6.39% for all data. The goodness-of-fit was 1.005. The largest peak in the final difference electron density synthesis was 1.184 e<sup>-</sup>/Å<sup>3</sup> and the largest hole was -1.685 e<sup>-</sup>/Å<sup>3</sup> with an RMS deviation of 0.148 e<sup>-</sup>/Å<sup>3</sup>. On the basis of the final model, the calculated density was 1.513 g/cm<sup>3</sup> and F(000), 800 e<sup>-</sup>.

**Table 1. Sample and crystal data for Harman\_12JAS\_159.**

|                             |   |                             |
|-----------------------------|---|-----------------------------|
| <b>Identification code</b>  | Harman_12JAS_159                                    |                             |
| <b>Chemical formula</b>     | C <sub>33</sub> H <sub>51</sub> BN <sub>7</sub> OPW |                             |
| <b>Formula weight</b>       | 787.43 g/mol  |                             |
| <b>Temperature</b>          | 100(2) K  |                             |
| <b>Wavelength</b>           | 0.71073 Å   |                             |
| <b>Crystal size</b>         | 0.074 x 0.090 x 0.251 mm                            |                             |
| <b>Crystal habit</b>        | colorless block                                     |                             |
| <b>Crystal system</b>       | triclinic   |                             |
| <b>Space group</b>          | P -1  |                             |
| <b>Unit cell dimensions</b> | a = 10.2939(9) Å                                    | $\alpha = 102.900(2)^\circ$ |
|                             | b = 12.5693(11) Å                                   | $\beta = 103.194(2)^\circ$  |
|                             | c = 14.6205(13) Å                                   | $\gamma = 101.886(2)^\circ$ |
| <b>Volume</b>               | 1728.2(3) Å <sup>3</sup>                            |                             |

<sup>57</sup> Sheldrick, G. M. (2015). *Acta Cryst.* A71, 3-8.

<sup>58</sup> Dolomanov, O. V.; Bourhis, L. J.; Gildea, R. J.; Howard, J. A. K.; Puschmann, H. *J. Appl. Cryst.* (2009). 42, 339-341.

|                               |                         |
|-------------------------------|-------------------------|
| <b>Z</b>                      | 2                       |
| <b>Density (calculated)</b>   | 1.513 g/cm <sup>3</sup> |
| <b>Absorption coefficient</b> | 3.425 mm <sup>-1</sup>  |
| <b>F(000)</b>                 | 800                     |

**Table 2. Data collection and structure refinement for Harman\_12JAS\_159.**

|  |  |
|--|--|
| <b>Diffractometer</b>                      | Bruker Kappa APEXII Duo  |
| <b>Radiation source</b>                    | fine-focus sealed tube (Mo K <sub>α</sub> , λ = 0.71073 Å)                   |
| <b>Theta range for data collection</b>     | 1.49 to 29.62°   |
| <b>Index ranges</b>                        | -14 ≤ h ≤ 14, -17 ≤ k ≤ 17, -20 ≤ l ≤ 20                                     |
| <b>Reflections collected</b>               | 35024  |
| <b>Independent reflections</b>             | 9750 [R(int) = 0.0582]   |
| <b>Coverage of independent reflections</b> | 100.0%   |
| <b>Absorption correction</b>               | Multi-Scan   |
| <b>Max. and min. transmission</b>          | 0.7860 and 0.4800  |
| <b>Structure solution technique</b>        | direct methods   |
| <b>Structure solution program</b>          | SHELXT 2014/5 (Sheldrick, 2014)  |
| <b>Refinement method</b>                   | Full-matrix least-squares on F <sup>2</sup>                                  |
| <b>Refinement program</b>                  | SHELXL-2017/1 (Sheldrick, 2017)  |
| <b>Function minimized</b>                  | Σ w(F <sub>o</sub> <sup>2</sup> - F <sub>c</sub> <sup>2</sup> ) <sup>2</sup> |
| <b>Data / restraints / parameters</b>      | 9750 / 0 / 404   |
| <b>Goodness-of-fit on F<sup>2</sup></b>    | 1.005  |
| <b>Δ/σ<sub>max</sub></b>                   | 0.001  |

|                                    |   |                              |
|------------------------------------|---|------------------------------|
| <b>Final R indices</b>             | 7981 data;<br>$I > 2\sigma(I)$  | R1 = 0.0311, wR2 =<br>0.0589 |
|                                    | all data  | R1 = 0.0504, wR2 =<br>0.0639 |
| <b>Weighting scheme</b>            | $w = 1/[\sigma^2(F_o^2) + (0.0280P)^2]$<br>where $P = (F_o^2 + 2F_c^2)/3$ |                              |
| <b>Largest diff. peak and hole</b> | 1.184 and -1.685 eÅ <sup>-3</sup>   |                              |
| <b>R.M.S. deviation from mean</b>  | 0.148 eÅ <sup>-3</sup>  |                              |

**Table 3. Atomic coordinates and equivalent isotropic atomic displacement parameters (Å<sup>2</sup>) for Harman\_12JAS\_159.**

U(eq) is defined as one third of the trace of the orthogonalized U<sub>ij</sub> tensor.

|    | x/a        | y/b        | z/c         | U(eq)       |
|----|------------|------------|-------------|-------------|
| W1 | 0.46277(2) | 0.25543(2) | 0.27425(2)  | 0.01173(4)  |
| P1 | 0.47076(8) | 0.39382(7) | 0.17391(6)  | 0.01380(16) |
| O1 | 0.7260(2)  | 0.2140(2)  | 0.23843(18) | 0.0262(6)   |
| N1 | 0.2472(3)  | 0.2680(2)  | 0.27753(18) | 0.0139(5)   |
| N2 | 0.1364(3)  | 0.1743(2)  | 0.23501(19) | 0.0160(6)   |
| N3 | 0.3546(3)  | 0.1277(2)  | 0.13017(18) | 0.0133(5)   |
| N4 | 0.2234(3)  | 0.0621(2)  | 0.10787(18) | 0.0150(5)   |
| N5 | 0.3916(3)  | 0.0941(2)  | 0.31050(19) | 0.0163(6)   |
| N6 | 0.2578(3)  | 0.0289(2)  | 0.27099(19) | 0.0173(6)   |
| N7 | 0.6219(3)  | 0.2351(2)  | 0.25898(18) | 0.0164(6)   |
| C1 | 0.1946(3)  | 0.3514(3)  | 0.3143(2)   | 0.0161(6)   |
| C2 | 0.0525(3)  | 0.3123(3)  | 0.2969(2)   | 0.0208(7)   |

|     | <b>x/a</b> | <b>y/b</b> | <b>z/c</b> | <b>U(eq)</b> |
|-----|------------|------------|------------|--------------|
| C3  | 0.0199(3)  | 0.2004(3)  | 0.2466(2)  | 0.0205(7)    |
| C4  | 0.4017(3)  | 0.0938(3)  | 0.0531(2)  | 0.0174(7)    |
| C5  | 0.2994(3)  | 0.0071(3)  | 0.9801(2)  | 0.0169(7)    |
| C6  | 0.1887(3)  | 0.9885(3)  | 0.0179(2)  | 0.0183(7)    |
| C7  | 0.4580(4)  | 0.0378(3)  | 0.3641(2)  | 0.0251(8)    |
| C8  | 0.3669(4)  | 0.9383(3)  | 0.3618(3)  | 0.0302(9)    |
| C9  | 0.2426(4)  | 0.9354(3)  | 0.3021(2)  | 0.0257(8)    |
| C10 | 0.5405(3)  | 0.4173(3)  | 0.3965(2)  | 0.0158(6)    |
| C11 | 0.5280(4)  | 0.3218(3)  | 0.4355(2)  | 0.0196(7)    |
| C12 | 0.6568(4)  | 0.3052(3)  | 0.5003(3)  | 0.0315(9)    |
| C13 | 0.7900(4)  | 0.3660(3)  | 0.4875(2)  | 0.0291(8)    |
| C14 | 0.8013(4)  | 0.4553(3)  | 0.4538(2)  | 0.0239(8)    |
| C15 | 0.6817(3)  | 0.5029(3)  | 0.4249(2)  | 0.0185(7)    |
| C16 | 0.3379(3)  | 0.3460(3)  | 0.0538(2)  | 0.0172(7)    |
| C17 | 0.1899(3)  | 0.3416(3)  | 0.0561(2)  | 0.0198(7)    |
| C18 | 0.0855(4)  | 0.2760(3)  | 0.9571(2)  | 0.0230(7)    |
| C19 | 0.9397(4)  | 0.2868(3)  | 0.9525(3)  | 0.0303(9)    |
| C20 | 0.6264(3)  | 0.4152(3)  | 0.1311(2)  | 0.0172(7)    |
| C21 | 0.7650(3)  | 0.4826(3)  | 0.2075(2)  | 0.0188(7)    |
| C22 | 0.8867(3)  | 0.4856(3)  | 0.1644(3)  | 0.0239(8)    |
| C23 | 0.0219(4)  | 0.5668(3)  | 0.2351(3)  | 0.0328(9)    |
| C24 | 0.4514(3)  | 0.5361(3)  | 0.2219(2)  | 0.0157(6)    |
| C25 | 0.4613(4)  | 0.6158(3)  | 0.1570(2)  | 0.0216(7)    |
| C26 | 0.4409(4)  | 0.7302(3)  | 0.2030(2)  | 0.0221(7)    |

|     | x/a       | y/b       | z/c       | U(eq)     |
|-----|-----------|-----------|-----------|-----------|
| C27 | 0.4507(4) | 0.8100(3) | 0.1382(3) | 0.0287(8) |
| B1  | 0.1556(4) | 0.0582(3) | 0.1916(3) | 0.0179(8) |
| C28 | 0.1996(7) | 0.1107(6) | 0.5242(5) | 0.086(2)  |
| C29 | 0.1690(9) | 0.1934(6) | 0.5920(5) | 0.109(3)  |
| C30 | 0.1593(7) | 0.1710(5) | 0.6829(5) | 0.080(2)  |
| C31 | 0.1626(7) | 0.0738(6) | 0.7058(5) | 0.083(2)  |
| C32 | 0.1786(8) | 0.9818(7) | 0.6330(5) | 0.110(3)  |
| C33 | 0.1968(7) | 0.0037(7) | 0.5479(5) | 0.094(2)  |

**Table 4. Bond lengths (Å) for Harman\_12JAS\_159.**

|        |           |        |          |
|--------|-----------|--------|----------|
| W1-N7  | 1.764(3)  | W1-C11 | 2.208(3) |
| W1-N3  | 2.222(2)  | W1-N5  | 2.231(3) |
| W1-C10 | 2.242(3)  | W1-N1  | 2.268(2) |
| W1-P1  | 2.5140(8) | P1-C24 | 1.838(3) |
| P1-C20 | 1.839(3)  | P1-C16 | 1.847(3) |
| O1-N7  | 1.240(3)  | N1-C1  | 1.340(4) |
| N1-N2  | 1.368(4)  | N2-C3  | 1.343(4) |
| N2-B1  | 1.528(5)  | N3-C4  | 1.344(4) |
| N3-N4  | 1.354(3)  | N4-C6  | 1.348(4) |
| N4-B1  | 1.546(4)  | N5-C7  | 1.336(4) |
| N5-N6  | 1.365(4)  | N6-C9  | 1.344(4) |
| N6-B1  | 1.543(5)  | C1-C2  | 1.388(4) |
| C1-H1  | 0.95      | C2-C3  | 1.365(5) |
| C2-H2  | 0.95      | C3-H3  | 0.95     |

|          |          |          |          |
|----------|----------|----------|----------|
| C4-C5    | 1.390(4) | C4-H4    | 0.95     |
| C5-C6    | 1.376(4) | C5-H5    | 0.95     |
| C6-H6    | 0.95     | C7-C8    | 1.389(5) |
| C7-H7    | 0.95     | C8-C9    | 1.363(5) |
| C8-H8    | 0.95     | C9-H9    | 0.95     |
| C10-C11  | 1.435(4) | C10-C15  | 1.524(4) |
| C10-H10  | 1.0      | C11-C12  | 1.525(5) |
| C11-H11  | 1.0      | C12-C13  | 1.500(5) |
| C12-H12A | 0.99     | C12-H12B | 0.99     |
| C13-C14  | 1.317(5) | C13-H13  | 0.95     |
| C14-C15  | 1.493(5) | C14-H14  | 0.95     |
| C15-H15A | 0.99     | C15-H15B | 0.99     |
| C16-C17  | 1.522(4) | C16-H16A | 0.99     |
| C16-H16B | 0.99     | C17-C18  | 1.524(4) |
| C17-H17A | 0.99     | C17-H17B | 0.99     |
| C18-C19  | 1.521(5) | C18-H18A | 0.99     |
| C18-H18B | 0.99     | C19-H19A | 0.98     |
| C19-H19B | 0.98     | C19-H19C | 0.98     |
| C20-C21  | 1.534(4) | C20-H20A | 0.99     |
| C20-H20B | 0.99     | C21-C22  | 1.523(4) |
| C21-H21A | 0.99     | C21-H21B | 0.99     |
| C22-C23  | 1.528(5) | C22-H22A | 0.99     |
| C22-H22B | 0.99     | C23-H23A | 0.98     |
| C23-H23B | 0.98     | C23-H23C | 0.98     |
| C24-C25  | 1.531(4) | C24-H24A | 0.99     |



|          |          |          |          |
|----------|----------|----------|----------|
| C24-H24B | 0.99     | C25-C26  | 1.523(4) |
| C25-H25A | 0.99     | C25-H25B | 0.99     |
| C26-C27  | 1.530(5) | C26-H26A | 0.99     |
| C26-H26B | 0.99     | C27-H27A | 0.98     |
| C27-H27B | 0.98     | C27-H27C | 0.98     |
| B1-H1A   | 1.08(4)  | C28-C29  | 1.407(8) |
| C28-C33  | 1.458(9) | C28-H28  | 0.95     |
| C29-C30  | 1.439(9) | C29-H29  | 0.95     |
| C30-C31  | 1.343(9) | C30-H30  | 0.95     |
| C31-C32  | 1.451(9) | C31-H31  | 0.95     |
| C32-C33  | 1.377(8) | C32-H32  | 0.95     |
| C33-H33  | 0.95     |          |          |

**Table 5. Bond angles (°) for Harman\_12JAS\_159.**

|           |            |            |            |
|-----------|------------|------------|------------|
| N7-W1-C11 | 98.22(12)  | N7-W1-N3   | 88.96(10)  |
| C11-W1-N3 | 156.00(11) | N7-W1-N5   | 96.71(11)  |
| C11-W1-N5 | 81.20(11)  | N3-W1-N5   | 75.21(9)   |
| N7-W1-C10 | 99.86(12)  | C11-W1-C10 | 37.62(12)  |
| N3-W1-C10 | 162.59(10) | N5-W1-C10  | 118.09(10) |
| N7-W1-N1  | 173.78(10) | C11-W1-N1  | 87.61(11)  |
| N3-W1-N1  | 84.82(9)   | N5-W1-N1   | 81.98(9)   |
| C10-W1-N1 | 86.07(10)  | N7-W1-P1   | 90.13(9)   |
| C11-W1-P1 | 118.73(9)  | N3-W1-P1   | 83.91(7)   |
| N5-W1-P1  | 157.86(7)  | C10-W1-P1  | 81.11(8)   |
| N1-W1-P1  | 88.95(7)   | C24-P1-C20 | 106.04(15) |

|            |            |            |            |
|------------|------------|------------|------------|
| C24-P1-C16 | 100.56(14) | C20-P1-C16 | 98.65(14)  |
| C24-P1-W1  | 120.39(10) | C20-P1-W1  | 113.14(11) |
| C16-P1-W1  | 115.22(11) | C1-N1-N2   | 105.4(2)   |
| C1-N1-W1   | 134.7(2)   | N2-N1-W1   | 119.87(18) |
| C3-N2-N1   | 109.9(3)   | C3-N2-B1   | 128.5(3)   |
| N1-N2-B1   | 121.4(2)   | C4-N3-N4   | 106.6(2)   |
| C4-N3-W1   | 130.1(2)   | N4-N3-W1   | 123.10(18) |
| C6-N4-N3   | 109.7(2)   | C6-N4-B1   | 129.4(3)   |
| N3-N4-B1   | 118.5(2)   | C7-N5-N6   | 106.3(3)   |
| C7-N5-W1   | 132.6(2)   | N6-N5-W1   | 121.06(19) |
| C9-N6-N5   | 109.4(3)   | C9-N6-B1   | 129.3(3)   |
| N5-N6-B1   | 120.7(3)   | O1-N7-W1   | 173.3(2)   |
| N1-C1-C2   | 111.0(3)   | N1-C1-H1   | 124.5      |
| C2-C1-H1   | 124.5      | C3-C2-C1   | 104.9(3)   |
| C3-C2-H2   | 127.6      | C1-C2-H2   | 127.6      |
| N2-C3-C2   | 108.8(3)   | N2-C3-H3   | 125.6      |
| C2-C3-H3   | 125.6      | N3-C4-C5   | 110.2(3)   |
| N3-C4-H4   | 124.9      | C5-C4-H4   | 124.9      |
| C6-C5-C4   | 104.9(3)   | C6-C5-H5   | 127.6      |
| C4-C5-H5   | 127.6      | N4-C6-C5   | 108.6(3)   |
| N4-C6-H6   | 125.7      | C5-C6-H6   | 125.7      |
| N5-C7-C8   | 110.3(3)   | N5-C7-H7   | 124.9      |
| C8-C7-H7   | 124.9      | C9-C8-C7   | 105.2(3)   |
| C9-C8-H8   | 127.4      | C7-C8-H8   | 127.4      |
| N6-C9-C8   | 108.8(3)   | N6-C9-H9   | 125.6      |

|               |           |              |          |
|---------------|-----------|--------------|----------|
| C8-C9-H9      | 125.6     | C11-C10-C15  | 118.8(3) |
| C11-C10-W1    | 69.89(17) | C15-C10-W1   | 126.2(2) |
| C11-C10-H10   | 111.8     | C15-C10-H10  | 111.8    |
| W1-C10-H10    | 111.8     | C10-C11-C12  | 119.5(3) |
| C10-C11-W1    | 72.48(17) | C12-C11-W1   | 122.9(2) |
| C10-C11-H11   | 112.1     | C12-C11-H11  | 112.1    |
| W1-C11-H11    | 112.1     | C13-C12-C11  | 113.7(3) |
| C13-C12-H12A  | 108.8     | C11-C12-H12A | 108.8    |
| C13-C12-H12B  | 108.8     | C11-C12-H12B | 108.8    |
| H12A-C12-H12B | 107.7     | C14-C13-C12  | 122.6(3) |
| C14-C13-H13   | 118.7     | C12-C13-H13  | 118.7    |
| C13-C14-C15   | 122.3(3)  | C13-C14-H14  | 118.9    |
| C15-C14-H14   | 118.9     | C14-C15-C10  | 114.0(3) |
| C14-C15-H15A  | 108.7     | C10-C15-H15A | 108.7    |
| C14-C15-H15B  | 108.7     | C10-C15-H15B | 108.7    |
| H15A-C15-H15B | 107.6     | C17-C16-P1   | 116.1(2) |
| C17-C16-H16A  | 108.3     | P1-C16-H16A  | 108.3    |
| C17-C16-H16B  | 108.3     | P1-C16-H16B  | 108.3    |
| H16A-C16-H16B | 107.4     | C16-C17-C18  | 111.7(3) |
| C16-C17-H17A  | 109.3     | C18-C17-H17A | 109.3    |
| C16-C17-H17B  | 109.3     | C18-C17-H17B | 109.3    |
| H17A-C17-H17B | 107.9     | C19-C18-C17  | 112.7(3) |
| C19-C18-H18A  | 109.1     | C17-C18-H18A | 109.1    |
| C19-C18-H18B  | 109.1     | C17-C18-H18B | 109.1    |
| H18A-C18-H18B | 107.8     | C18-C19-H19A | 109.5    |

|               |       |               |          |
|---------------|-------|---------------|----------|
| C18-C19-H19B  | 109.5 | H19A-C19-H19B | 109.5    |
| C18-C19-H19C  | 109.5 | H19A-C19-H19C | 109.5    |
| H19B-C19-H19C | 109.5 | C21-C20-P1    | 117.5(2) |
| C21-C20-H20A  | 107.9 | P1-C20-H20A   | 107.9    |
| C21-C20-H20B  | 107.9 | P1-C20-H20B   | 107.9    |
| H20A-C20-H20B | 107.2 | C22-C21-C20   | 112.2(3) |
| C22-C21-H21A  | 109.2 | C20-C21-H21A  | 109.2    |
| C22-C21-H21B  | 109.2 | C20-C21-H21B  | 109.2    |
| H21A-C21-H21B | 107.9 | C21-C22-C23   | 112.6(3) |
| C21-C22-H22A  | 109.1 | C23-C22-H22A  | 109.1    |
| C21-C22-H22B  | 109.1 | C23-C22-H22B  | 109.1    |
| H22A-C22-H22B | 107.8 | C22-C23-H23A  | 109.5    |
| C22-C23-H23B  | 109.5 | H23A-C23-H23B | 109.5    |
| C22-C23-H23C  | 109.5 | H23A-C23-H23C | 109.5    |
| H23B-C23-H23C | 109.5 | C25-C24-P1    | 116.9(2) |
| C25-C24-H24A  | 108.1 | P1-C24-H24A   | 108.1    |
| C25-C24-H24B  | 108.1 | P1-C24-H24B   | 108.1    |
| H24A-C24-H24B | 107.3 | C26-C25-C24   | 112.4(3) |
| C26-C25-H25A  | 109.1 | C24-C25-H25A  | 109.1    |
| C26-C25-H25B  | 109.1 | C24-C25-H25B  | 109.1    |
| H25A-C25-H25B | 107.9 | C25-C26-C27   | 112.5(3) |
| C25-C26-H26A  | 109.1 | C27-C26-H26A  | 109.1    |
| C25-C26-H26B  | 109.1 | C27-C26-H26B  | 109.1    |
| H26A-C26-H26B | 107.8 | C26-C27-H27A  | 109.5    |
| C26-C27-H27B  | 109.5 | H27A-C27-H27B | 109.5    |

|               |           |               |           |
|---------------|-----------|---------------|-----------|
| C26-C27-H27C  | 109.5     | H27A-C27-H27C | 109.5     |
| H27B-C27-H27C | 109.5     | N2-B1-N6      | 108.9(3)  |
| N2-B1-N4      | 110.2(3)  | N6-B1-N4      | 106.2(3)  |
| N2-B1-H1A     | 111.1(18) | N6-B1-H1A     | 110.5(19) |
| N4-B1-H1A     | 109.8(18) | C29-C28-C33   | 115.3(6)  |
| C29-C28-H28   | 122.3     | C33-C28-H28   | 122.3     |
| C28-C29-C30   | 117.4(7)  | C28-C29-H29   | 121.3     |
| C30-C29-H29   | 121.3     | C31-C30-C29   | 126.3(6)  |
| C31-C30-H30   | 116.8     | C29-C30-H30   | 116.8     |
| C30-C31-C32   | 117.6(6)  | C30-C31-H31   | 121.2     |
| C32-C31-H31   | 121.2     | C33-C32-C31   | 117.1(7)  |
| C33-C32-H32   | 121.4     | C31-C32-H32   | 121.4     |
| C32-C33-C28   | 125.6(7)  | C32-C33-H33   | 117.2     |
| C28-C33-H33   | 117.2     |               |           |

**Table 6. Torsion angles (°) for Harman\_12JAS\_159.**

|             |           |             |           |
|-------------|-----------|-------------|-----------|
| C1-N1-N2-C3 | -0.4(3)   | W1-N1-N2-C3 | 179.2(2)  |
| C1-N1-N2-B1 | -175.0(3) | W1-N1-N2-B1 | 4.6(4)    |
| C4-N3-N4-C6 | -0.3(3)   | W1-N3-N4-C6 | -176.4(2) |
| C4-N3-N4-B1 | 163.8(3)  | W1-N3-N4-B1 | -12.4(4)  |
| C7-N5-N6-C9 | 1.3(3)    | W1-N5-N6-C9 | 178.3(2)  |
| C7-N5-N6-B1 | -170.4(3) | W1-N5-N6-B1 | 6.6(4)    |
| N2-N1-C1-C2 | 0.6(3)    | W1-N1-C1-C2 | -179.0(2) |
| N1-C1-C2-C3 | -0.5(4)   | N1-N2-C3-C2 | 0.1(4)    |
| B1-N2-C3-C2 | 174.2(3)  | C1-C2-C3-N2 | 0.2(4)    |

|                 |           |                 |           |
|-----------------|-----------|-----------------|-----------|
| N4-N3-C4-C5     | 1.0(3)    | W1-N3-C4-C5     | 176.7(2)  |
| N3-C4-C5-C6     | -1.3(4)   | N3-N4-C6-C5     | -0.5(4)   |
| B1-N4-C6-C5     | -162.3(3) | C4-C5-C6-N4     | 1.1(4)    |
| N6-N5-C7-C8     | -1.7(4)   | W1-N5-C7-C8     | -178.2(2) |
| N5-C7-C8-C9     | 1.5(4)    | N5-N6-C9-C8     | -0.3(4)   |
| B1-N6-C9-C8     | 170.4(3)  | C7-C8-C9-N6     | -0.7(4)   |
| C15-C10-C11-C12 | -2.8(4)   | W1-C10-C11-C12  | 118.4(3)  |
| C15-C10-C11-W1  | -121.1(3) | C10-C11-C12-C13 | -21.1(5)  |
| W1-C11-C12-C13  | 66.3(4)   | C11-C12-C13-C14 | 23.6(5)   |
| C12-C13-C14-C15 | -0.5(5)   | C13-C14-C15-C10 | -24.3(5)  |
| C11-C10-C15-C14 | 25.2(4)   | W1-C10-C15-C14  | -60.1(4)  |
| C24-P1-C16-C17  | -59.5(3)  | C20-P1-C16-C17  | -167.7(2) |
| W1-P1-C16-C17   | 71.6(3)   | P1-C16-C17-C18  | -166.7(2) |
| C16-C17-C18-C19 | -170.5(3) | C24-P1-C20-C21  | 62.1(3)   |
| C16-P1-C20-C21  | 165.8(3)  | W1-P1-C20-C21   | -72.0(3)  |
| P1-C20-C21-C22  | 175.2(2)  | C20-C21-C22-C23 | 171.3(3)  |
| C20-P1-C24-C25  | 48.5(3)   | C16-P1-C24-C25  | -53.8(3)  |
| W1-P1-C24-C25   | 178.5(2)  | P1-C24-C25-C26  | 178.8(2)  |
| C24-C25-C26-C27 | -179.9(3) | C3-N2-B1-N6     | -118.1(3) |
| N1-N2-B1-N6     | 55.4(4)   | C3-N2-B1-N4     | 125.7(3)  |
| N1-N2-B1-N4     | -60.8(4)  | C9-N6-B1-N2     | 127.4(3)  |
| N5-N6-B1-N2     | -62.7(3)  | C9-N6-B1-N4     | -113.9(3) |
| N5-N6-B1-N4     | 56.0(4)   | C6-N4-B1-N2     | -134.1(3) |
| N3-N4-B1-N2     | 65.4(4)   | C6-N4-B1-N6     | 108.0(4)  |
| N3-N4-B1-N6     | -52.5(4)  | C33-C28-C29-C30 | 9.1(11)   |

C28-C29-C30-C31 -7.3(12) C29-C30-C31-C32 0.6(11)  
 C30-C31-C32-C33 3.5(11) C31-C32-C33-C28 -0.9(12)  
 C29-C28-C33-C32 -5.7(12)

**Table 7. Anisotropic atomic displacement parameters ( $\text{\AA}^2$ ) for Harman\_12JAS\_159.**

The anisotropic atomic displacement factor exponent takes the form: -  
 $2\pi^2 [ h^2 a^{*2} U_{11} + \dots + 2 h k a^* b^* U_{12} ]$

|    | $U_{11}$   | $U_{22}$   | $U_{33}$   | $U_{23}$   | $U_{13}$   | $U_{12}$   |
|----|------------|------------|------------|------------|------------|------------|
| W1 | 0.01053(6) | 0.01359(6) | 0.01074(6) | 0.00310(4) | 0.00280(4) | 0.00322(4) |
| P1 | 0.0155(4)  | 0.0144(4)  | 0.0114(4)  | 0.0033(3)  | 0.0038(3)  | 0.0044(3)  |
| O1 | 0.0121(12) | 0.0314(15) | 0.0365(15) | 0.0053(12) | 0.0106(11) | 0.0096(11) |
| N1 | 0.0123(13) | 0.0153(14) | 0.0134(12) | 0.0037(10) | 0.0038(10) | 0.0023(11) |
| N2 | 0.0124(13) | 0.0164(14) | 0.0170(13) | 0.0004(11) | 0.0052(11) | 0.0025(11) |
| N3 | 0.0136(13) | 0.0116(13) | 0.0143(13) | 0.0023(10) | 0.0053(10) | 0.0023(11) |
| N4 | 0.0100(13) | 0.0170(14) | 0.0153(13) | 0.0032(11) | 0.0023(10) | 0.0007(11) |
| N5 | 0.0183(14) | 0.0154(14) | 0.0158(13) | 0.0061(11) | 0.0049(11) | 0.0039(12) |
| N6 | 0.0216(15) | 0.0123(14) | 0.0184(14) | 0.0029(11) | 0.0097(12) | 0.0028(12) |
| N7 | 0.0166(14) | 0.0135(14) | 0.0162(13) | 0.0038(11) | 0.0015(11) | 0.0019(11) |
| C1 | 0.0159(16) | 0.0186(17) | 0.0129(15) | 0.0031(12) | 0.0034(12) | 0.0051(13) |
| C2 | 0.0144(16) | 0.0261(19) | 0.0206(17) | 0.0015(14) | 0.0068(13) | 0.0066(14) |
| C3 | 0.0098(15) | 0.0268(19) | 0.0226(17) | 0.0029(14) | 0.0054(13) | 0.0036(14) |
| C4 | 0.0178(16) | 0.0184(17) | 0.0191(16) | 0.0055(13) | 0.0081(13) | 0.0084(14) |
| C5 | 0.0196(17) | 0.0186(17) | 0.0107(14) | 0.0009(12) | 0.0033(13) | 0.0055(14) |
| C6 | 0.0175(16) | 0.0143(16) | 0.0172(16) | 0.0001(13) | 0.0004(13) | 0.0017(13) |

|     | <b>U<sub>11</sub></b> | <b>U<sub>22</sub></b> | <b>U<sub>33</sub></b> | <b>U<sub>23</sub></b> | <b>U<sub>13</sub></b> | <b>U<sub>12</sub></b> |
|-----|-----------------------|-----------------------|-----------------------|-----------------------|-----------------------|-----------------------|
| C7  | 0.038(2)              | 0.0214(19)            | 0.0188(17)            | 0.0069(14)            | 0.0064(15)            | 0.0143(17)            |
| C8  | 0.051(3)              | 0.022(2)              | 0.0196(18)            | 0.0102(15)            | 0.0092(17)            | 0.0109(18)            |
| C9  | 0.041(2)              | 0.0167(18)            | 0.0220(18)            | 0.0071(14)            | 0.0168(17)            | 0.0039(16)            |
| C10 | 0.0146(16)            | 0.0164(17)            | 0.0122(15)            | 0.0022(12)            | 0.0034(12)            | 0.0025(13)            |
| C11 | 0.0246(18)            | 0.0220(18)            | 0.0100(15)            | 0.0036(13)            | 0.0047(13)            | 0.0028(15)            |
| C12 | 0.044(2)              | 0.027(2)              | 0.0160(17)            | 0.0075(15)            | 0.0040(16)            | 0.0061(18)            |
| C13 | 0.0247(19)            | 0.035(2)              | 0.0202(18)            | 0.0017(16)            | 0.0058(15)            | 0.0119(17)            |
| C14 | 0.0145(17)            | 0.032(2)              | 0.0195(17)            | 0.0017(15)            | 0.0009(13)            | 0.0058(15)            |
| C15 | 0.0187(17)            | 0.0210(18)            | 0.0118(15)            | 0.0004(13)            | 0.0032(13)            | 0.0028(14)            |
| C16 | 0.0233(17)            | 0.0136(16)            | 0.0117(15)            | 0.0021(12)            | 0.0015(13)            | 0.0040(14)            |
| C17 | 0.0227(18)            | 0.0198(18)            | 0.0136(15)            | 0.0034(13)            | 0.0008(13)            | 0.0050(14)            |
| C18 | 0.0260(19)            | 0.0223(19)            | 0.0160(16)            | 0.0029(14)            | 0.0011(14)            | 0.0075(15)            |
| C19 | 0.0231(19)            | 0.033(2)              | 0.0250(19)            | 0.0017(16)            | 0.0032(15)            | 0.0061(17)            |
| C20 | 0.0173(16)            | 0.0183(17)            | 0.0172(16)            | 0.0051(13)            | 0.0074(13)            | 0.0047(14)            |
| C21 | 0.0188(17)            | 0.0178(17)            | 0.0189(16)            | 0.0039(13)            | 0.0074(13)            | 0.0019(14)            |
| C22 | 0.0199(18)            | 0.029(2)              | 0.0268(19)            | 0.0109(15)            | 0.0122(15)            | 0.0049(16)            |
| C23 | 0.024(2)              | 0.035(2)              | 0.039(2)              | 0.0140(18)            | 0.0107(17)            | 0.0024(18)            |
| C24 | 0.0202(16)            | 0.0149(16)            | 0.0128(15)            | 0.0034(12)            | 0.0046(13)            | 0.0068(13)            |
| C25 | 0.0292(19)            | 0.0199(18)            | 0.0187(16)            | 0.0069(14)            | 0.0094(14)            | 0.0090(15)            |
| C26 | 0.031(2)              | 0.0167(17)            | 0.0215(17)            | 0.0062(14)            | 0.0091(15)            | 0.0093(15)            |
| C27 | 0.042(2)              | 0.023(2)              | 0.0280(19)            | 0.0119(16)            | 0.0148(17)            | 0.0134(18)            |



|     | <b>U<sub>11</sub></b> | <b>U<sub>22</sub></b> | <b>U<sub>33</sub></b> | <b>U<sub>23</sub></b> | <b>U<sub>13</sub></b> | <b>U<sub>12</sub></b> |
|-----|-----------------------|-----------------------|-----------------------|-----------------------|-----------------------|-----------------------|
| B1  | 0.0143(18)            | 0.0155(19)            | 0.0231(19)            | 0.0041(15)            | 0.0085(15)            | 0.0002(15)            |
| C28 | 0.089(5)              | 0.106(6)              | 0.070(4)              | 0.019(4)              | 0.044(4)              | 0.023(4)              |
| C29 | 0.175(8)              | 0.052(4)              | 0.100(6)              | 0.016(4)              | 0.063(6)              | 0.009(5)              |
| C30 | 0.102(5)              | 0.059(4)              | 0.073(4)              | 0.010(3)              | 0.045(4)              | -0.006(4)             |
| C31 | 0.088(5)              | 0.085(5)              | 0.068(4)              | 0.013(4)              | 0.039(4)              | -0.007(4)             |
| C32 | 0.139(7)              | 0.181(8)              | 0.094(5)              | 0.088(6)              | 0.081(5)              | 0.117(7)              |
| C33 | 0.104(6)              | 0.152(7)              | 0.070(4)              | 0.050(5)              | 0.047(4)              | 0.082(6)              |

**Table 8. Hydrogen atomic coordinates and isotropic atomic displacement parameters ( $\text{\AA}^2$ ) for Harman\_12JAS\_159.**

|      | <b>x/a</b> | <b>y/b</b> | <b>z/c</b> | <b>U(eq)</b> |
|------|------------|------------|------------|--------------|
| H1   | 0.2477     | 0.4273     | 0.3479     | 0.019        |
| H2   | -0.0087    | 0.3542     | 0.3158     | 0.025        |
| H3   | -0.0703    | 0.1494     | 0.2235     | 0.025        |
| H4   | 0.4919     | 0.1247     | 0.0491     | 0.021        |
| H5   | 0.3047     | -0.0311    | -0.0823    | 0.02         |
| H6   | 0.1024     | -0.0669    | -0.0140    | 0.022        |
| H7   | 0.5538     | 0.0624     | 0.3989     | 0.03         |
| H8   | 0.3869     | -0.1161    | 0.3948     | 0.036        |
| H9   | 0.1591     | -0.1231    | 0.2851     | 0.031        |
| H10  | 0.4654     | 0.4554     | 0.4029     | 0.019        |
| H11  | 0.4478     | 0.3110     | 0.4634     | 0.024        |
| H12A | 0.6586     | 0.3324     | 0.5697     | 0.038        |
| H12B | 0.6502     | 0.2232     | 0.4855     | 0.038        |

|      | <b>x/a</b> | <b>y/b</b> | <b>z/c</b> | <b>U(eq)</b> |
|------|------------|------------|------------|--------------|
| H13  | 0.8693     | 0.3391     | 0.5043     | 0.035        |
| H14  | 0.8885     | 0.4908     | 0.4478     | 0.029        |
| H15A | 0.6901     | 0.5330     | 0.3688     | 0.022        |
| H15B | 0.6868     | 0.5671     | 0.4801     | 0.022        |
| H16A | 0.3640     | 0.3971     | 0.0145     | 0.021        |
| H16B | 0.3399     | 0.2692     | 0.0193     | 0.021        |
| H17A | 0.1808     | 0.4199     | 0.0747     | 0.024        |
| H17B | 0.1693     | 0.3051     | 0.1065     | 0.024        |
| H18A | 0.1157     | 0.3043     | -0.0947    | 0.028        |
| H18B | 0.0839     | 0.1949     | -0.0562    | 0.028        |
| H19A | -0.1239    | 0.2406     | -0.1114    | 0.045        |
| H19B | -0.0606    | 0.3663     | -0.0387    | 0.045        |
| H19C | -0.0901    | 0.2603     | 0.0045     | 0.045        |
| H20A | 0.6355     | 0.3396     | 0.1001     | 0.021        |
| H20B | 0.6107     | 0.4542     | 0.0794     | 0.021        |
| H21A | 0.7613     | 0.5611     | 0.2344     | 0.023        |
| H21B | 0.7796     | 0.4478     | 0.2622     | 0.023        |
| H22A | 0.8653     | 0.5090     | 0.1036     | 0.029        |
| H22B | 0.8991     | 0.4083     | 0.1468     | 0.029        |
| H23A | 1.0984     | 0.5600     | 0.2068     | 0.049        |
| H23B | 1.0398     | 0.5477     | 0.2974     | 0.049        |
| H23C | 1.0140     | 0.6448     | 0.2465     | 0.049        |
| H24A | 0.3602     | 0.5272     | 0.2352     | 0.019        |
| H24B | 0.5234     | 0.5732     | 0.2855     | 0.019        |

|      | <b>x/a</b> | <b>y/b</b> | <b>z/c</b> | <b>U(eq)</b> |
|------|------------|------------|------------|--------------|
| H25A | 0.5534     | 0.6279     | 0.1450     | 0.026        |
| H25B | 0.3902     | 0.5797     | 0.0929     | 0.026        |
| H26A | 0.5121     | 0.7663     | 0.2670     | 0.026        |
| H26B | 0.3489     | 0.7181     | 0.2150     | 0.026        |
| H27A | 0.3766     | 0.7769     | 0.0763     | 0.043        |
| H27B | 0.5408     | 0.8211     | 0.1249     | 0.043        |
| H27C | 0.4408     | 0.8833     | 0.1720     | 0.043        |
| H1A  | 0.058(4)   | -0.006(3)  | 0.164(2)   | 0.023(9)     |
| H28  | 0.2206     | 0.1236     | 0.4670     | 0.104        |
| H29  | 0.1552     | 0.2613     | 0.5783     | 0.131        |
| H30  | 0.1497     | 0.2308     | 0.7314     | 0.096        |
| H31  | 0.1548     | 0.0654     | 0.7675     | 0.1          |
| H32  | 0.1765     | -0.0903    | 0.6435     | 0.132        |
| H33  | 0.2086     | -0.0561    | 0.5005     | 0.113        |